Volume 189 Number 1

THE BIOLOGICAL BULLETIN

AUGUST, 1995

Published by the Marine Biological Laboratory

THE
BIOLOGICAL BULLETIN

PUBLISHED BY
THE MARINE BIOLOGICAL LABORATORY

AUGUST, 1995

Printed and Issued by
LANCASTER PRESS, Inc.
3575 HEMPLAND ROAD
LANCASTER, PA

THE BIOLOGICAL BULLETIN

THE BIOLOGICAL BULLETIN is published six times a year by the Marine Biological Laboratory, MBL Street, Woods Hole, Massachusetts 02543.

Subscriptions and similar matter should be addressed to Subscription Manager, THE BIOLOGICAL BULLETIN, Marine Biological Laboratory, Woods Hole, Massachusetts 02543. Single numbers, $37.50. Subscription per volume (three issues), $92.50 ($185.00 per year for six issues).

Communications relative to manuscripts should be sent to Michael J. Greenberg, Editor-in-Chief, or Pamela L. Clapp, Managing Editor, at the Marine Biological Laboratory, Woods Hole, Massachusetts 02543. Telephone: (508) 548-3705, ext. 428. FAX: 508-540-6902. E-mail: pclapp@hoh.mbl.edu.

THE BIOLOGICAL BULLETIN is indexed in bibliographic services including *Index Medicus* and MEDLINE, *Chemical Abstracts*, *Current Contents*, and *CABS (Current Awareness in Biological Sciences)*.
Printed on acid free paper,
effective with Volume 180, Issue 1, 1991.

POSTMASTER: Send address changes to THE BIOLOGICAL BULLETIN, Marine Biological Laboratory, Woods Hole, MA 02543.

Second-class postage paid at Woods Hole, MA, and additional mailing offices.
ISSN 0006-3185

INSTRUCTIONS TO AUTHORS

The Biological Bulletin accepts outstanding original research reports of general interest to biologists throughout the world. Papers are usually of intermediate length (10–40 manuscript pages). A limited number of solicited review papers may be accepted after formal review. A paper will usually appear within four months after its acceptance.

Very short, especially topical papers (less than 9 manuscript pages including tables, figures, and bibliography) will be published in a separate section entitled "Research Notes." A Research Note in *The Biological Bulletin* follows the format of similar notes in *Nature*. It should open with a summary paragraph of 150 to 200 words comprising the introduction and the conclusions. The rest of the text should continue on without subheadings, and there should be no more than 30 references. References should be referred to in the text by number, and listed in the Literature Cited section in the order that they appear in the text. Unlike references in *Nature*, references in the Research Notes section should conform in punctuation and arrangement to the style of recent issues of *The Biological Bulletin*. Materials and Methods should be incorporated into appropriate figure legends. See the article by Lohmann *et al.* (October 1990, Vol. **179**: 214–218) for sample style. A Research Note will usually appear within two months after its acceptance.

The Editorial Board requests that regular manuscripts conform to the requirements set below; those manuscripts that do not conform will be returned to authors for correction before review.

1. ***Manuscripts.*** Manuscripts, including figures, should be submitted in triplicate. (Xerox copies of photographs are not acceptable for review purposes.) The submission letter accompanying the manuscript should include a telephone number, a FAX number, and (if possible) an E-mail address for the corresponding author. The original manuscript must be typed in no smaller than 12 pitch or 10 point, using double spacing (*including* figure legends, footnotes, bibliography, etc.) on one side of 16- or 20-lb. bond paper, 8½ by 11 inches. Please, no right justification. Manuscripts should be proofread carefully and errors corrected legibly in black ink. Pages should be numbered consecutively. Margins on all sides should be at least 1 inch (2.5 cm). Manuscripts should conform to the *Council of Biology Editors Style Manual*, 5th Edition (Council of Biology Editors, 1983) and to American spelling. Unusual abbreviations should be kept to a minimum and should be spelled out on first reference as well as defined in a footnote on the title page. Manuscripts should be divided into the following components: Title page, Abstract (of no more than 200 words), Introduction, Materials and Methods, Results, Discussion, Acknowledgments, Literature Cited, Tables, and Figure Legends. In addition, authors should supply a list of words and phrases under which the article should be indexed.

2. ***Title page.*** The title page consists of a condensed title or running head of no more than 35 letters and spaces, the manuscript title, authors' names and appropriate addresses, and footnotes listing present addresses, acknowledgments or contribution numbers, and explanation of unusual abbreviations.

3. ***Figures.*** The dimensions of the printed page, 7 by 9 inches, should be kept in mind in preparing figures for publication. We recommend that figures be about 1½ times the linear dimensions of the final printing desired, and that the ratio of the largest to the smallest letter or number and of the thickest to the thinnest line not exceed 1:1.5. Explanatory matter generally should be included in legends, although axes should always be identified on the illustration itself. Figures should be prepared for reproduction as either line cuts or halftones. Figures to be reproduced as line cuts should be unmounted glossy photographic reproductions or drawn in black ink on white paper, good-quality tracing cloth or plastic, or blue-lined coordinate paper. Those to be reproduced as halftones should be mounted on board, with both designating numbers or letters and scale

bars affixed directly to the figures. All figures should be numbered in consecutive order, with no distinction between text and plate figures. The author's name and an arrow indicating orientation should appear on the reverse side of all figures.

4. ***Tables, footnotes, figure legends, etc.*** Authors should follow the style in a recent issue of *The Biological Bulletin* in preparing table headings, figure legends, and the like. Because of the high cost of setting tabular material in type, authors are asked to limit such material as much as possible. Tables, with their headings and footnotes, should be typed on separate sheets, numbered with consecutive Roman numerals, and placed after the Literature Cited. Figure legends should contain enough information to make the figure intelligible separate from the text. Legends should be typed double spaced, with consecutive Arabic numbers, on a separate sheet at the end of the paper. Footnotes should be limited to authors' current addresses, acknowledgments or contribution numbers, and explanation of unusual abbreviations. All such footnotes should appear on the title page. Footnotes are not normally permitted in the body of the text.

5. ***Literature cited.*** In the text, literature should be cited by the Harvard system, with papers by more than two authors cited as Jones *et al.*, 1980. Personal communications and material in preparation or in press should be cited in the text only, with author's initials and institutions, unless the material has been formally accepted and a volume number can be supplied. The list of references following the text should be headed Literature Cited, and must be typed double spaced on separate pages, conforming in punctuation and arrangement to the style of recent issues of *The Biological Bulletin*. Citations should include complete titles and inclusive pagination. Journal abbreviations should normally follow those of the U. S. A. Standards Institute (USASI), as adopted by BIOLOGICAL ABSTRACTS and CHEMICAL ABSTRACTS, with the minor differences set out below. The most generally useful list of biological journal titles is that published each year by BIOLOGICAL ABSTRACTS (BIOSIS List of Serials; the most recent issue). Foreign authors, and others who are accustomed to using THE WORLD LIST OF SCIENTIFIC PERIODICALS, may find a booklet published by the Biological Council of the U.K. (obtainable from the Institute of Biology, 41 Queen's Gate, London, S.W.7, England, U.K.) useful, since it sets out the WORLD LIST abbreviations for most biological journals with notes of the USASI abbreviations where these differ. CHEMICAL ABSTRACTS publishes quarterly supplements of additional abbreviations. The following points of reference style for THE BIOLOGICAL BULLETIN differ from USASI (or modified WORLD LIST) usage:

A. Journal abbreviations, and book titles, all underlined (for *italics*)

B. All components of abbreviations with initial capitals (not as European usage in WORLD LIST *e.g., J. Cell. Comp. Physiol.* NOT *J. cell. comp. Physiol.*)

C. *All* abbreviated components must be followed by a period, whole word components *must not* (*i.e., J. Cancer Res.*)

D. Space between all components (*e.g., J. Cell. Comp. Physiol.*, not *J.Cell.Comp.Physiol.*)

E. Unusual words in journal titles should be spelled out in full, rather than employing new abbreviations invented by the author. For example, use *Rit Visindafjélags Islendinga* without abbreviation.

F. All single word journal titles in full (*e.g., Veliger, Ecology, Brain*).

G. The order of abbreviated components should be the same as the word order of the complete title (*i.e., Proc.* and *Trans.* placed where they appear, not transposed as in some BIOLOGICAL ABSTRACTS listings).

H. A few well-known international journals in their preferred forms rather than WORLD LIST or USASI usage (*e.g., Nature, Science, Evolution* NOT *Nature, Lond., Science, N.Y.; Evolution, Lancaster, Pa.*)

6. ***Reprints, page proofs, and charges.*** Authors receive their first 100 reprints (without covers) free of charge. Additional reprints may be ordered at time of publication and normally will be delivered about two to three months after the issue date. Authors (or delegates for foreign authors) will receive page proofs of articles shortly before publication. They will be charged the current cost of printers' time for corrections to these (other than corrections of printers' or editors' errors). Other than these charges for authors' alterations, *The Biological Bulletin* does not have page charges.

Reference: *Biol. Bull.* **189**: 1–5. (August, 1995)

A Short Story of Aequorin

OSAMU SHIMOMURA

Marine Biological Laboratory, Woods Hole, Massachusetts 02543

Discovery of Aequorin

One day in the fall of 1960, shortly after my arrival at Princeton from Japan, Dr. Frank Johnson showed me a small jar containing a spoonful of white powder. He explained that the powder was a freeze dried "squeezate" made from the luminous jellyfish *Aequorea*, and that it would emit light when mixed with water. He asked me if I would be interested in studying the bioluminescence of this jellyfish. The powder did not emit any light when moistened. But I was quite impressed by Dr. Johnson's description of the brilliant luminescence of live jellyfish and the great abundance of specimens around Friday Harbor, Washington. So my response was a definite "yes." My experience in bioluminescence research at the time was meager and limited to only the luminescent system of the ostracod *Cypridina*. I imagined, vaguely, that the jellyfish would probably contain a kind of luciferin and a luciferase, possibly with one of the cofactors, such as ATP, FMN, or NADH, like the fireflies, luminous bacteria, and *Cypridina* that were known at that time.

In the early summer of 1961, we traveled from Princeton to Friday Harbor in Dr. Johnson's station wagon, which he had newly purchased for the excursion. The car was fully loaded with necessary equipment and chemicals, including a MacNichol integrating photometer of gigantic size (a two-foot cube), and four travelers (my wife and Yo Saiga, an assistant, came along) with all of their baggage on the roof. It took us seven days to the West Coast, through Chicago and Glacier National Park. Dr. Johnson was the only driver throughout the trip, driving 12 hours a day with an admirable toughness.

Upon arrival at the Friday Harbor Laboratories, we were welcomed by Dr. Robert Fernald, Director of the Lab. We set up our work space in Lab 1, a small building consisting of two rooms, and we started to work. There were three other scientists in the room, and one of them was Dr. Dixy Lee Ray, future governor of Washington State, who was always accompanied by a dog, her well-known trademark. The laboratory area was a sanctuary prohibited to common dogs, but she declared that the animal was her assistant, not a dog.

The jellyfish were abundant. A constant stream of floating jellyfish passed along the side of the lab dock every morning and evening, riding with the current caused by the tide. We carefully scooped up the jellyfish into buckets, one by one, using a shallow dip-net. The specimens of *Aequorea* are shaped like hemispherical umbrellas and are nearly transparent. An average specimen measures 3–4 inches in diameter and weighs about 50 g. The light organs—about 100 granules—are distributed evenly along the edge of the umbrella. Thus, the margin of the umbrella containing light organs could be easily cut off with a pair of scissors, yielding a thin strip called a "ring." When the rings obtained from 20–30 jellyfish were squeezed through a rayon gauze, a liquid called "squeezate" was obtained. The squeezate was only dimly luminescent, but when it was diluted with water, the luminescence increased significantly for a period of 5–10 minutes, as the granular light organs were cytolyzed.

We tried to extract luminescent substance from the squeezate by every thinkable method, but all failed; and we ran out of ideas after only a few days of work. Convinced that the cause of our failure was the luciferin-luciferase hypothesis that dominated our thinking, I suggested to Dr. Johnson that we should forget the idea of extracting luciferin and luciferase and, instead, try to isolate the luminescent substance whatever it might be. I was, however, unable to convince him. He did not agree with my idea, which had neither theoretical backing nor experimental support. Because of the disagreement on the experimental procedure, I started to work alone at one side of a table while, on the other side, Dr. Johnson and his assistant Yo Saiga continued their efforts to extract a luciferin by grinding luminous tissues with sand. It was an awkward situation.

Received 23 March 1995; accepted 5 June 1995.

The basic principle of isolating a bioluminescent substance is to extract it from the tissue under conditions that reversibly inhibit luminescence, or that cause a selective inactivation, consumption, or removal of a component necessary for light emission. In the case of a luciferin-luciferase system, for example, the luciferin is usually extracted with methanol, which stops luminescence by inactivating the luciferase. And the luciferase can be obtained from an aqueous extract after the luciferin has been exhausted by several minutes of spontaneous luminescence reactions. If a cofactor is involved in light emission, its removal or exhaustion can cause a reversible inhibition of luminescence, as in the case of the firefly bioluminescence system that requires ATP as the cofactor.

In the case of the jellyfish *Aequorea*, however, the presumed lack of luciferin and luciferase severely limited the range of techniques usable for the extraction of the light-emitting principle. I did believe that jellyfish luminescence requires molecular oxygen like all other known bioluminescence systems (later proved to be incorrect!), but we had no other information about the luminescence system or cofactor requirements. In an effort to find a way to extract the luminescent principle, I tried to inhibit the luminescence of the squeezate by using the anaerobic conditions that were created by vacuum or by the addition of reducing agents, but nothing worked. The results forced me to assume that the jellyfish system, like that of *Cypridina*, requires a very low oxygen tension—a level less than that attainable in my evacuated container. Furthermore, all of the known enzymatic cofactors, such as ATP, FMN, and DPNH, showed no effect on the luminescence when added. Finally, the only recourse was to try various chemicals available in the stockroom of the Lab, with the hope that one would reversibly inhibit the luminescence. This was clearly an approach that relied entirely on good luck, and I was not surprised when all of my efforts failed. I was conceptually exhausted, and could not come up with one further idea.

I spent the next several days soul-searching, trying to imagine the reaction that occurs in luminescing jellyfish and searching for a way to extract the luminescent principle. I often meditated on a drifting rowboat under the clear summer sky. Friday Harbor in summer, at that time, was quiet and peaceful, differing from the present-day scene that is almost saturated with busy pleasure boats and noisy seaplanes. A rowboat always has the right of way over one with a motor, so nobody disturbed my drifting vessel; even large ferries saved me a wide berth. Thus, meditation afloat was safe, but if I fell asleep and the boat was carried away by the tidal current, then I had to row for a long time to get back to the Lab.

One afternoon on the boat, a thought suddenly struck me—a thought so simple that I should have had it much sooner: "Even if a luciferin-luciferase system is not involved in the jellyfish luminescence, another enzyme or protein is very probably involved directly in the light-emitting reaction. If so, the activity of this enzyme or protein can probably be altered by a pH change, at least to some extent. Indeed, there might be a certain level of acidity at which an enzyme or protein could be reversibly inactivated."

I immediately went back to the lab and made a squeezate. Then, I mixed a small portion of the squeezate with acidified water containing various amounts of acetic acid. The resultant mixtures at pH 6.0 and pH 5.0 were clearly luminous, but at pH 4.0, I saw no luminescence. I filtered off the liquid from the rest of squeezate and mixed the solid part, containing the granules of light organs, with water of pH 4.0. After the mixture was filtered, the filtrate, now free of cells and debris, was nearly dark, but it regained its luminescence upon neutralization with a small amount of sodium bicarbonate. Indeed, the experiment showed that the luminescent substance of the jellyfish can be extracted.

But my real surprise came in the next moment, when I added a small amount of seawater to the solution and saw that its light became explosively strong. The experiment showed that some component of seawater activates the luminescence. Because the composition of seawater is known, I quickly discovered that the activator is Ca^{2+}. The discovery of Ca^{2+} as the activator in turn suggested that EDTA should serve as a better inhibitor of luminescence than acidification during the extraction of the light-emitting principle. On the basis of these data, we devised a method of extracting the light-emitting principle.

With a workable procedure in hand for extracting the luminescent principle, our next task was to catch and process as many jellyfish as possible. We would collect jellyfish from 6 to 8 AM, then after a quick breakfast, we would cut rings from the jellyfish until noon. We devoted all afternoon to the extraction. After dinner, we again collected jellyfish from 6:30 to 8:30 PM, and the catch was kept in an aquarium to be processed next day together with the catch of the next morning. We soon found that the bottleneck of the operation was the step of cutting rings with scissors, which is a delicate and very slow process. Even after considerable practice, it took more than 1 minute to cut one jellyfish ring, and 3 hours of work by four persons could not produce more than 500 rings. To increase productivity, we hired several high school girls, trained them, and paid them 2 cents for each ring they cut. We also decided to buy jellyfish from the kids of scientists living on the campus, paying a penny for each jellyfish. This job provided dual benefits, the fun of catching jellyfish and of earning money. I remember a 6- or 7-year-old girl who grossed more than 10 dollars in 2 days (probably with parental help). Unfortunately, just when our operation was in full swing, the jellyfish suddenly

vanished from the area. Thus, we extracted and processed only about 10,000 specimens of *Aequorea* that summer.

We returned to Princeton with the jellyfish extract packed in dry ice, and then began to purify the light-emitting principle from the extract by repeated chromatography on various kinds of large columns. It was a long process, and the utmost care was required to prevent the luminescence activity from being lost, which could be brought about by many causes. We completed the purification in early 1962, obtaining about 5 mg of the light-emitting principle. The substance was found to be a protein with a molecular weight about 20,000, and it emitted light when a trace of Ca^{2+} was added—whether in the presence or absence of oxygen, to our astonishment. We named the protein "aequorin" after the genus name of the jellyfish. Aequorin is an extraordinary protein containing a large amount of energy that can be released when calcium is added; thus it resembles a charged battery that releases the energy when short-circuited. The system was so unusual that some biochemistry professors expressed their skepticism. After 30 years of discovery, however, the importance of aequorin and its use as a calcium probe are firmly established in biochemistry and physiology. The word "aequorin" now can be found in various common dictionaries.

The Town Dock

In 1962, using the methods that had worked in the previous year, we obtained an additional amount of aequorin and began to study various aspects of the molecule, including its application in the measurement of calcium ions. We also wanted to know the mechanism of the luminescence reaction and the structure of the light-emitting chromophore. But our efforts to achieve these goals were soon blocked by an insuperable difficulty. When various methods were used to break down the molecules of aequorin, the first step of the reaction was always an intramolecular chemical change; so it was impossible to isolate intact chromophores. We therefore decided to postpone further study on the light-emitting mechanism.

In 1967, Ridgway and Ashley reported their observation, with the aid of microinjected aequorin, of transient Ca^{2+} signals in single muscle fibers of the barnacle. It was the first report on the use of aequorin in studying intracellular calcium, and it was soon followed by hundreds of papers. Because the importance of aequorin was now evident, we wanted to study the chemistry of the luminescence reaction. Although the structure of the native light-emitting chromophore seemed intractable, I thought that the structure of the chromophore after the luminescence reaction could be determined. For a structural study of the chromophore, I estimated that 100–200 mg of pure aequorin would be needed in a single experiment. About 50,000 jellyfish (2.5 tons) would be needed to produce this amount of aequorin. But to process 50,000 jellyfish in one summer, we would have to collect and cut at least 3000 of the animals each day, allowing for days of bad weather and poor fishing. This was a workload that could not be accomplished by collecting jellyfish at the lab dock and cutting ring with scissors at a rate of one ring per minute.

We resumed the jellyfish operation at Friday Harbor in the summer of 1967, not anticipating that it would continue for the next 20 years. To collect more jellyfish, we expanded our fishing ground beyond the lab dock, adding the Chevron dock (a small commercial pier), the town dock (public pier), and the shipyard (a covered boat storage), and we used a car to move around and to transport the buckets of jellyfish. When the current carried the stream of jellyfish far beyond the docks, we also used rowboats to collect jellyfish, a tricky activity that occasionally caused a collector to fall into very cold seawater. The Chevron dock was our favorite place during the first 2–3 years, because there was a part of it where a large number of jellyfish would stack up on an early morning tide. We had to be careful, however, not to make noise that might awaken sleeping people on the boats.

The town dock was very small—almost nonexistent—in the late '60s; but then it was rapidly expanded. By 1975, the dock had been extended far enough into the bay to intersect with the main jellyfish stream, and it then became a highly favorable spot for fishing. Indeed, the town dock with its large sign saying "Port of Friday Harbor" became our main fishing ground, and the collection became much easier than before. We harvested jellyfish every morning and evening. The collectors were usually my wife, our son and daughter, a couple of assistants, and me. Dr. and Mrs. Johnson also helped for the first several years. Because the jellyfish are nearly transparent in seawater, they cannot easily be seen with untrained eyes. Our children were only 3–4 years old when they began collecting jellyfish with specially made short nets; they had become as efficient as an average adult by the age of 8; and through high school they continued to be great helpers in my project.

Before beginning a collection, we filled buckets about half-full with seawater and placed them strategically along the edge of pier, then gathered jellyfish until the buckets were completely full. When a dense stream of animals was passing the dock, we could collect at a rate of 5–10 jellyfish per minute. When all the buckets were filled, we poured off some water to about 80% capacity, and then covered each bucket with a plastic bag to prevent seawater from spilling during transportation. The buckets—each crammed with about 100 jellyfish in very little water—were then packed into the trunk of a car (which could accommodate 12 buckets) and rushed to the lab. More

buckets were usually transported to the lab on a Boston Whaler by one of the assistants. Once at the lab, and before any rings were cut, the jellyfish were kept in aquaria to revive. In this manner, we were able to collect an average of 3000–4000 jellyfish each day at the town dock.

The town dock was very good for jellyfish fishing, but there were some problems. Often we found too many boats at the dockside; this decreased the open space where we could collect jellyfish. When the loading area, located halfway along the main dock, was fully occupied, we had to carry the heavy buckets of jellyfish all the way to our car, which would be parked more than 200 yards away. The biggest problem, however, was that there were too many boat people who asked us questions. "What are you doing?" "What are you collecting?" "How do you use them?" Almost every passerby felt obliged to ask us a question while we were busily collecting. Most people were satisfied by our simple reply: "These are for scientific research." Some people persisted until they had received a complete explanation of our research.

I cannot forget a funny exchange that took place one early morning. An old lady poked her head out from the window of a small boat, looked at the jellyfish on my net, and asked me, "How do you cook them?"

I answered, "We don't cook those jellyfish."

She gazed at me distastefully, "Do you eat them raw?" and her head disappeared.

"No! We don't eat them!" But my reply was too late.

The Jellyfish Factory

Cutting the jellyfish rings with scissors was impossibly slow; we could not produce the amount of aequorin that we needed using this technique. This problem was solved primarily by Dr. Johnson. He constructed the first model of a jellyfish-cutting machine in the summer of 1967; it was essentially a strip of wire screen that worked like a grater. An average jellyfish has about 100 light organs the size of poppy seeds located under the edge of its umbrella. By sliding the jellyfish over the screen, we hoped that the light organs would be scraped off the body and collected in a tray under the screen. We found, however, that the light organs were not scraped off by the wire screen. The next version of the cutting machine had a strip of coarse sandpaper over which seawater flowed slowly; the sandpaper was connected to one end of the first version. When jellyfish were slid down—first over the sandpaper, then the screen—most of the light organs were indeed scraped off. But the material accumulated in the tray contained an excessive amount of slime, and the quality of the material was much poorer than that of the hand-cut rings. Thus, the manufacture of a machine based on the principle of a grater was abandoned.

Dr. Johnson next purchased two circular meat-slicing blades (10″ diameter) at a local hardware store and began to build a cutting machine; this project took the next two summers to complete. The basic plan was to install a meat-slicing blade perpendicular to a black Lucite board, and with the blade slowly rotating, cut the ring off the jellyfish. The motor from a small laboratory shaker was used to rotate the blade. The jellyfish were rotated with a hand tool called a "peg," a small disk with several short nails on one side and a 2-inch-long, stick-shaped handle attached in the center on the other side. A jellyfish on the Lucite board was grasped by the nails of the disk and rotated by the stick, which was held between the index finger and thumb. The setup worked, at least in principle.

A number of improvements were made over the next two years. A razor blade was installed at the edge of the Lucite board; the razor blade and the rotating circular blade were in contact each other on their flat sides and the jellyfish was cut at the intersection of the two cutting edges. It made cutting so sharp and smooth that the jellyfish might not even feel that their rings were being cut off. To make the rotation of jellyfish easy, a seawater outlet was installed near the center of the board to lubricate its surface. An ice bath was installed to cool the ring reservoir; this prevented a loss of activity from the rings and also served as a preparation for the extraction process. In the summer of 1969, the quality of the machine-cut rings finally surpassed that of the hand-cut ones. We therefore set up two cutting machines and used them, thereafter, to cut all of the jellyfish.

With machines that could cut rings at 10 times the speed of a hand-cutter, and with a sufficient supply of jellyfish, our mode of operation had to be changed. We needed a large working space, and we also did not want to disturb other researchers with our messy, smelly, and noisy experimental processes. Fortunately, we were assigned to use the Gear Locker, a small, isolated building that had been used for storage in the past. Two large tanks installed outside the building were used for temporary storage of collected jellyfish.

Ring cutting was probably the most important step in determining the quality and yield of purified aequorin. Cutting too thick would increase the amount of impurities. Cutting too thin would decrease the yield because some of the light organs were cut through and destroyed. Therefore, we always assigned the best workers to do this job. Of the many excellent helpers we had in our jellyfish operation, I remember particularly three girls who worked for many summers and cut rings extremely skillfully and fast: Debby Nash, Liz Illg, and Laura Norris; the first was from the town and the other two were daughters of biology professors.

Our jellyfish cutting usually began at 11 AM. A counting person would put 80 jellyfish into each bucket, already half-full of seawater, and would then take the buckets to the cutters. Two cutters cut the jellyfish with the machines

that were installed side-by-side: the cutter would place a jellyfish onto the cutting board, quickly rotate it with a peg to spread out the edge of the umbrella where the light organs are located, and then—pushing the jellyfish to the cutting blade while simultaneously rotating the jellyfish quickly—cut off the rings, all in less than 5 seconds. The rings would fall automatically into the ice-cold reservoir, and the ringless jellyfish body was slid down into a waste bucket. These buckets, each filled with about 200 spent jellyfish, were carried to the nearest seashore about 50 yard away, called by us "jellyfish cliff," and dumped onto the rocks below. The heaps of jellyfish bodies, several thousands of them, were carried away by the next high tide.

The process of extracting aequorin from rings began at 2 PM; it was carried out by a team of two persons. The extraction was done in batches of 480 rings (*i.e.*, six buckets). The first person would drain the rings on a nylon gauze, then mix the drained rings with a cold EDTA solution saturated with ammonium sulfate. The rings shrank quickly and were also desensitized by the salt. They were cut with scissors into pieces 1–2 inches long, then stirred with a cake mixer for 10 minutes to dislodge the granular light organs from the tissue. The mixture was squeezed through a nylon gauze to remove the shrunken ring tissue, and then the turbid liquid obtained was filtered on a Buchner funnel using some Celite. The filter cake, containing the light organs, was given to the second person, who was responsible for the rest of the extraction process. The second person put the filter cake into a 2-liter flask containing cold EDTA solution (1 liter), then shook the flask vigorously to extract aequorin from the light organs into the EDTA solution. Finally, the mixture was filtered through a large Buchner funnel, and the filtrate containing aequorin was saturated with ammonium sulfate to precipitate the protein. The first person in the team would start a new batch of rings every 20 minutes, and the second person's work would also take 20 minutes. Thus, 3360 jellyfish rings could be extracted in about 2 hours and 40 minutes.

The precipitates of crude aequorin were purified at our laboratory in Princeton. The purification was done in several steps of column chromatography, mainly by Sephadex gel filtration and DEAE-cellulose chromatography, all at 0°C. It was indeed a lengthy, time-consuming process, notwithstanding the fact that aequorin should be purified as quickly as possible because it is constantly decomposing through spontaneous weak luminescence, even in the presence of a high concentration of EDTA. To purify an extract of 50,000 jellyfish, which contains a large amount of total protein, chromatography had to be repeated 30 times for only the first gel filtration step, and the total number of chromatography runs required for complete purification was more than 60. An extract of 50,000 jellyfish yielded only 150–200 mg of purified aequorin in the early '70s, but as the techniques improved, the yield gradually increased, exceeding 500 mg by 1980. Since 1975, all of the steps in the purification have been done by my wife, Akemi, who is highly knowledgeable in handling aequorin.

The purified aequorin was used in various studies of luminescence in our laboratory. Thus, the chemical structure of the light-emitter was determined in 1973. Then the structure of the aequorin chromophore "coelenterazine" was elucidated and the regeneration of spent aequorin into active aequorin was accomplished, both in 1975. The molecular characterization of various aequorin isoforms was reported in 1986. The improved forms of aequorin—"semisynthetic aequorins" with widely different calcium sensitivities—were produced in 1988–1989. Purified aequorin has also been supplied to hundreds of cell biologists and physiologists who study intracellular calcium, leading to many important findings about intracellular calcium. Aequorin was cloned in 1985 by two groups simultaneously, one in Georgia and another in Japan. With the recent progress in molecular genetics, studies involving recombinant aequorin are now flourishing.

Acknowledgments

Our work on aequorin was initiated by Dr. Frank H. Johnson, and developed with support and encouragement from many individuals. I thank all the people who helped directly or indirectly with this project. The work was made possible by the excellent facilities of the Friday Harbor Laboratories, University of Washington, and of Princeton University, and was financially supported by research grants from the National Science Foundation and the National Institutes of Health.

Literature Cited

Ridgway, E. B., and C. C. Ashley. 1967. Calcium transients in single muscle fibers. *Biochem. Biophys. Res. Commun.* **29**: 229–234.

Reference: *Biol. Bull.* **189:** 6–12. (August, 1995)

Fine Structure of Spermatozoa of the Hagfish *Eptatretus burgeri* (Agnatha)[1]

SACHIKO MORISAWA

Biological Laboratory, St. Marianna University, School of Medicine, 2-16-1 Sugao, Miyamae, Kawasaki 216, Japan

Abstract. Live motile spermatozoa of the hagfish *Eptatretus burgeri* were obtained for the first time, and their fine structure was examined. The spermatozoon is characterized by an extremely long midpiece. Two of the four midpiece mitochondria are extensively elongated and extend through almost the entire length of the tail. The acrosome contains electron-dense and less dense materials in two different compartments. Amorphous subacrosomal material lies between the acrosome and the nucleus. No distinct perforatorium rod or filamentous structure was observed within the subacrosomal material. Two centrioles lie almost end to end in the nuclear fossa near the posterior end of the nucleus. The structure of the acrosomal complex in the hagfish, which is quite different from that in the lamprey, was compared to that of other chordates with respect to its function in sperm-egg interaction and phylogeny.

Introduction

The reproductive life of the lamprey has been studied extensively (Kille, 1960; Nicander *et al.*, 1968), but little is known about reproduction, especially fertilization, in hagfish (Dean, 1899; Walvig, 1963; Gorbman, 1983). The structures of the testes and spermatozoa of hagfish have been described in *Myxine glutinosa*, *Bdellostoma burgeri*, and *B. stouti* (Walvig, 1963); *M. glutinosa* (Nicander, 1970); *E. burgeri* (Patzner, 1977, 1982); *Paramyxine atami* (Patzner, 1982); and *E. stouti* (Gorbman, 1990). Electron micrographical studies on the formation and structure of hagfish spermatozoa in *Myxine circifrons*, *M.* sp., *Eptatretus stoutii*, *E. deani*, and *E.* sp. were performed by Jespersen (1975). Because of difficulties in catching mature hagfish males alive (Walvig, 1963; Jespersen, 1975; Patzner, 1982), there had been few studies describing live and motile spermatozoa (Patzner, 1982).

In the sea near the Misaki Marine Biological Station in the Kanagawa Prefecture of Japan, the hagfish species *Eptatretus burgeri* migrates from depths of 50-100 m to the shore (10–12 m deep) between November and June (Kobayashi *et al.*, 1972); in contrast, most other hagfish species inhabit the deeper sea throughout the year (Adam and Strahan, 1963; Jespersen, 1975). *Eptatretus burgeri* is thought to breed in October, while living in deep water (Kobayashi *et al.*, 1972; Patzner, 1977, 1978).

By catching hagfish from the shore and keeping them in an aquarium (Fernholm, 1975; Ooka-Souda *et al.*, 1985), we were able to obtain males with mature spermatozoa and to investigate for the first time the ultrastructural details of these motile spermatozoa. Because the phylogeny, as well as the fertilization, of living agnathans (hagfish and lampreys) has attracted much attention from biologists (Brodal and Fänge, 1963; Hardisty, 1979), we compared these sperm to those of other chordates.

Materials and Methods

Males of the hagfish *Eptatretus burgeri*, 45–60 cm in body length, were caught in July in Sagami Bay near the Misaki Marine Biological Station in Kanagawa Prefecture, Japan. They were kept in a seawater tank (15°C) without food under controlled light (light 0700–1900) until they were used for experiments between September and December in the same year. After an animal was anesthesized with 0.5% 3-aminobenzoic acid ethyl ester (MS222, Sankyo Pharmaceut., Tokyo), its abdomen was opened to remove the testis. Actively motile spermatozoa were

[1] This article is dedicated to the late professor Dr. J. C. Dan who introduced the author to biological science.

Received 22 February 1994; accepted 5 June 1995.

obtained when pieces of the posterior portion of the testis were immersed in seawater.

For transmission electron microscopy (TEM), small pieces of testis with mature spermatozoa were fixed for 1 h with 2% glutaraldehyde in 0.1 *M* phosphate buffer (pH 7.4), and postfixed with 1% osmium tetroxide in the same buffer for 1 h. Dehydration in a graded alcohol series, followed by propylene oxide, and infiltration with Epon were performed using an automatic electron microscopy processor (REM-20B, Sakura, Tokyo). All procedures were done at room temperature. Thin sections were obtained using diamond knives, stained with uranyl acetate and lead citrate, and then examined with an electron microscope (JEOL100 or JEM-1200EX, JEOL Ltd., Tokyo).

For scanning electron microscopy (SEM), a testis was minced and spermatozoa were released onto a sheet of filter paper. Sperm on the paper were fixed in 2% glutaraldehyde in 70% seawater, followed by postfixation with 2% osmium tetroxide in 2.5% $NaHCO_3$. Samples were critical-point dried and examined using a scanning electron microscope (US4, JEOL Ltd., Tokyo).

Results

Macroscopic aspects of testis

Four male hagfish kept in the laboratory had mature testes between late September and early October in 1992. The testis appeared as a single nodular, spiral structure, longitudinally located along the right side of the mesentery as described in *E. burgeri* (Patzner, 1982) and in other hagfish (Walvig, 1963; Gorbman, 1990). Toward December, after the breeding season, the testis became thinner.

Motility and light microscopic aspects of sperm

When a small piece of mature testis was immersed in seawater, many spermatozoa were released from the testis and exhibited active forward motility for about 10 min. Motile spermatozoa could be obtained during late October in some fish. The number of spermatozoa with normal ultrastructure decreased in November. Thus, the hagfish kept in the laboratory had mature spermatozoa at about the same time as their natural breeding period.

The sperm head and tail could be identified with a light microscope. They were about 10 μm and 35–40 μm in length, respectively. These were almost the same as those observed by Walvig (1963). After active swimming in seawater for about 5 min, some spermatozoa stuck to the glass surface with the tip of their heads, rotating their tails freely. Some spermatozoa had shortened tails with a knot near the end of the tail. Heads of some spermatozoa were bent backward, and they swam with their heads pointing backward.

Fine structure of spermatozoa

Figure 1 is a scanning electron micrograph of an *E. burgeri* spermatozoon. The head is 8–10 μm in length and about 0.5 and 1.2 μm wide at the anterior and posterior regions, respectively. The acrosome is at the anterior end of the sperm head (Figs. 2 and 3a). The outer acrosomal membrane is in close approximation with the overlying plasma membrane at the posterior 1/2–2/3 of the acrosome (Fig. 3a). The inner acrosomal membrane covers a conspicuous subacrosomal material into which the apex of the nucleus projects, and the double structure of the nuclear membranes is indistinct in this area. The acrosomal contents are tightly packed in the anterior region of the acrosome (Fig. 3b), but somewhat loosely packed

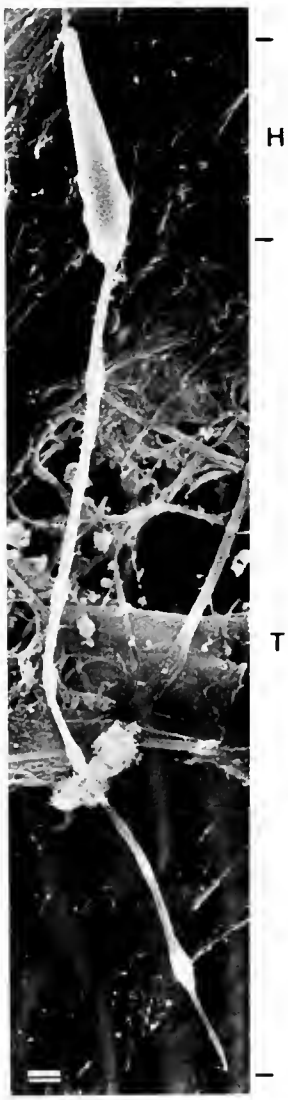

Figure 1. A scanning electron micrograph of an *Eptatretus burgeri* spermatozoon. H, head (acrosomal and nuclear regions); T, tail (midpiece and end piece). Bar = 1 μm.

Figure 2. An electron micrograph of the longitudinal section of the sperm head. A, acrosomal region; N, nucleus. Bar = 1 μm.

in the posterior region (Fig. 3c,d). The subacrosomal material between the acrosome and the nucleus is almost homogeneous in electron density. Neither a distinct perforatorium rod nor filamentous structures are detected within the subacrosomal material.

The nucleus increases its thickness posteriorly (Fig. 2). In the posterior lateral surface of the sperm head is a small fossa in which two centrioles are located almost end to end (Fig. 4a). The axoneme has the ordinary 9 + 2 arrangement of doublets (Fig. 4e,f).

Four mitochondria encircle the axoneme at the base of the flagellum (Fig. 4c), each arranged longitudinally (Fig. 4a). Two of them are extensively elongated and extend almost along the entire length of the axoneme (Fig. 4d,e). Most cross sections of the midpiece exhibit a 9 + 2 arrangement of axonemal doublets flanked by two mitochondria (Fig. 4e). Axonemes without associated mitochondria or with only one mitochondrion are observed only in sections near the posterior end of the tail (Fig. 4f).

The unique feature of the *E. burgeri* spermatozoon is the two extremely elongated mitochondria that run parallel with the axoneme throughout nearly the entire length of the tail. Figure 5 diagrams the structure of various regions of the *E. burgeri* spermatozoon.

Discussion

Spermatozoa of species that exhibit external fertilization, including common fishes, usually have a few mitochondria in the short midpiece surrounding the centrioles and the 9 + 2 axoneme without accessory structures in the flagellum. The sperm midpiece in many species with internal fertilization [*e.g.*, mammals (Phillips, 1977) and viviparous teleosts (Grier, 1975)] has a long mitochondrial sheath or a long cytoplasmic sleeve that contains many separate mitochondria. Hagfish sperm have four mitochondria, but two of them extend nearly the entire length of the tail, forming a long midpiece, as in spermatozoa of species with internal fertilization.

The acrosomal vesicle of protochordate spermatozoa is either ovoid, as in the urochordate *Oikopleura* (Holland *et al.*, 1988), or cap-shaped, as in the cephalochordate *Branchiostoma* (Baccetti *et al.*, 1972), and a distinct ac-

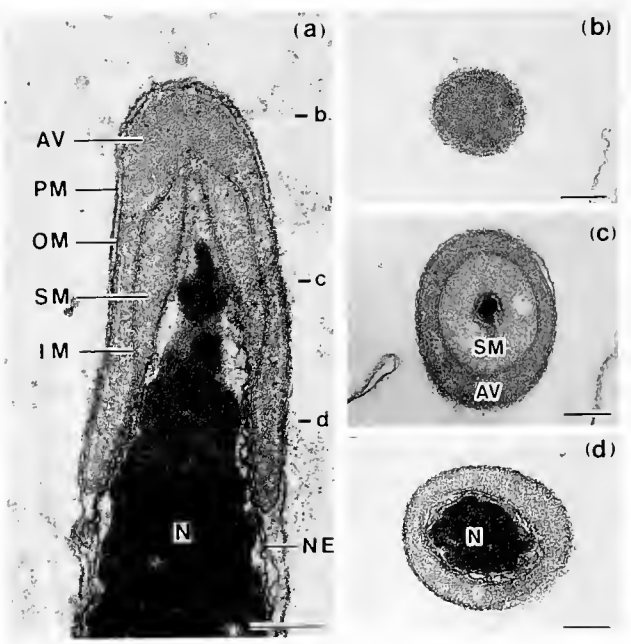

Figure 3. Longitudinal (a) and cross sections (b–d) of the acrosomal region. Labels -b, -c, and -d in figure (a) indicate the levels of sections shown in b, c, and d, respectively. Acrosomal vesicle (AV) and the underlying subacrosomal material (SM) cover the anterior end of the nucleus (N). IM, inner acrosomal membrane; NE, nuclear envelope; OM, outer acrosomal membrane; PM, plasma membrane. Each bar = 200 nm.

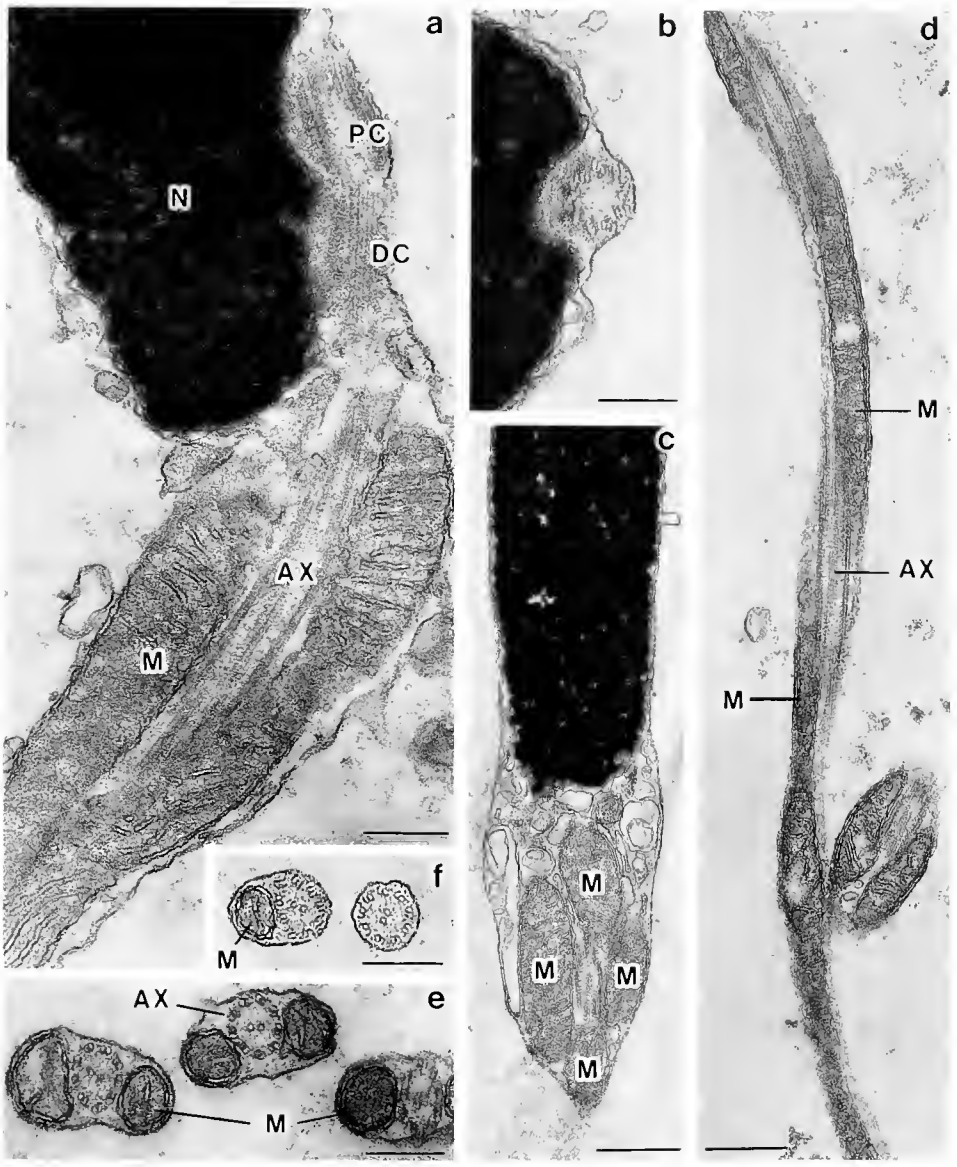

Figure 4. Longitudinal and cross sections of various regions of the tail. (a) The base of a flagellum. The proximal centriole (PC) and distal centriole (DC) lie almost longitudinally. Elongated mitochondria (M) are arranged along the axoneme (AX). (b) A cross section through a centriole. (c) An oblique section through the base of a flagellum. Four mitochondria encircle the axoneme. (d) A longitudinal section of the winding and twisting flagellum. Two long mitochondria flank the axoneme. (e) Cross sections of three flagellae. Two mitochondria flank the axoneme in the plane of two central singlets. (f) Cross sections of flagellae through near endpiece (left) and endpiece (right). Note that the axoneme without mitochondria has incomplete doublets. Bar = 250 nm (in a, b, e, f) and 500 nm (in c, d).

rosomal process is produced *de novo* following the acrosomal exocytosis at the anterior end of the sperm (Holland *et al.*, 1988). Spermatozoa of vertebrates such as amphibians (Yoshizaki and Katagiri, 1982; Fig. 6c), reptiles (Furieri, 1970; Fig. 6d), birds (Okamura and Nishiyama, 1978; Fig. 6e), and mammals (Yanagimachi and Noda, 1970; Fig. 6f) have a cap-shaped acrosomal vesicle and underlying subacrosomal material, which cover the anterior portion of the nucleus. The exocytosis of the acrosomal vesicle occurs at several points, and a new acrosomal process does not protrude (Yanagimachi and Usui, 1974; Okamura and Nishiyama, 1978; Yoshizaki and Katagiri, 1982).

A variety of acrosomal structures are found in fish spermatozoa. The lamprey, which is a cyclostome, has spermatozoa that carry a spherical acrosomal vesicle at

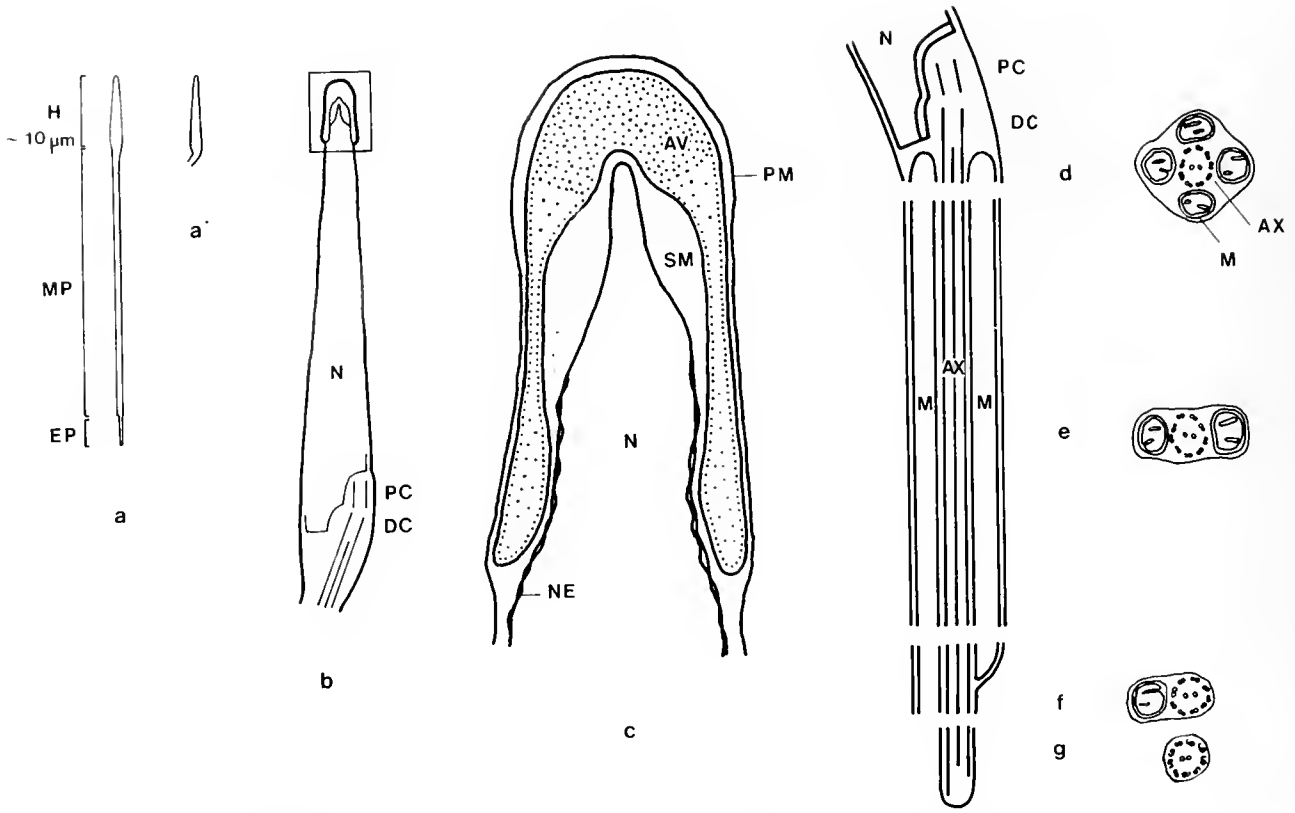

Figure 5. Schematic drawings of the *Eptatretus burgeri* spermatozoon. (a) Whole view at low magnification; a, surface view; a', side view of the head. (b) Head and regions. (c) Acrosomal region indicated by a rectangle in the figure b. (d–g) A longitudinal and cross section of the flagellum. AV, acrosomal vesicle; AX, axoneme; DC, distal centriole; EP, endpiece; H, head; M, mitochondria; MP, midpiece; N, nucleus; NE, nuclear envelope; PC, proximal centriole; PM, plasma membrane; SM, subacrosomal material.

the anterior end of their heads, subacrosomal material between the acrosome and the nucleus, and a long perforatorium rod through the nucleus (Follenius, 1965; Stanley, 1967; Nicander and Sjöden, 1971; Jaana and Yamamoto, 1981) (see Fig. 6b). When the sperm reach the outer chorion of the egg during fertilization (Nicander and Sjöden, 1971), or when they are exposed to fixatives (Jaana and Yamamoto, 1981), a long acrosomal process is formed. Spermatozoa of the elasmobranch *Squalus suckleyi*, a species that has internal fertilization, have a cap-shaped acrosomal vesicle and a subacrosomal rod (Stanley, 1971). Spermatozoa of the sturgeon, *Acipenser transmontanus*, which have a scalloped and cap-shaped acrosomal vesicle and filamentous structure in the subacrosomal material and in the canals through the nucleus, form an acrosomal process upon the acrosome reaction (Cherr and Clark, 1984). In Holostei (Afzelius, 1978) and Teleostei (Mattei, 1970), spermatozoa lack an acrosome. In hagfish, the acrosomal vesicle of the spermatozoa covers the protrusion of the nucleus with underlying subacrosomal material (Figs. 3, 6). In our preliminary experiments, the acrosomal exocytosis of the *Eptatretus burgeri* sperm occurred not only at the apical point of the sperm head but at several points, and was not followed by conspicuous formation of a long process. Such features are common in the spermatozoa of higher animals. The role of the acrosomal complex of the hagfish spermatozoa remains to be studied.

The acrosome reaction occurs inside or on the surface of the egg envelope to allow sperm penetration. In the case of external fertilization in teleosts, spermatozoa reach the egg plasma membrane through a narrow micropyle that has been perforated in the chorion; the sperm lack an acrosome. Lamprey eggs have a two-layered chorion (Afzelius *et al.*, 1968) that has no micropyle (Kille, 1960); the sperm penetrate the chorion with the acrosome reaction (Nicander and Sjöden, 1971). Sturgeon eggs have numerous micropyles, and the sperm form an acrosomal process (Cherr and Clark, 1984). In hagfish eggs, one micropyle with an outer opening diameter of 4.2 μm, 4.7 μm, or 4 μm in *Myxine glutinosa* (Kosmath *et al.*, 1981), *Eptatretus burgeri* (Kosmath *et al.*, 1981), or *E. stouti* (Koch *et al.*, 1993), respectively, is perforated at the animal pole through the thick and hard chorion. Inasmuch as

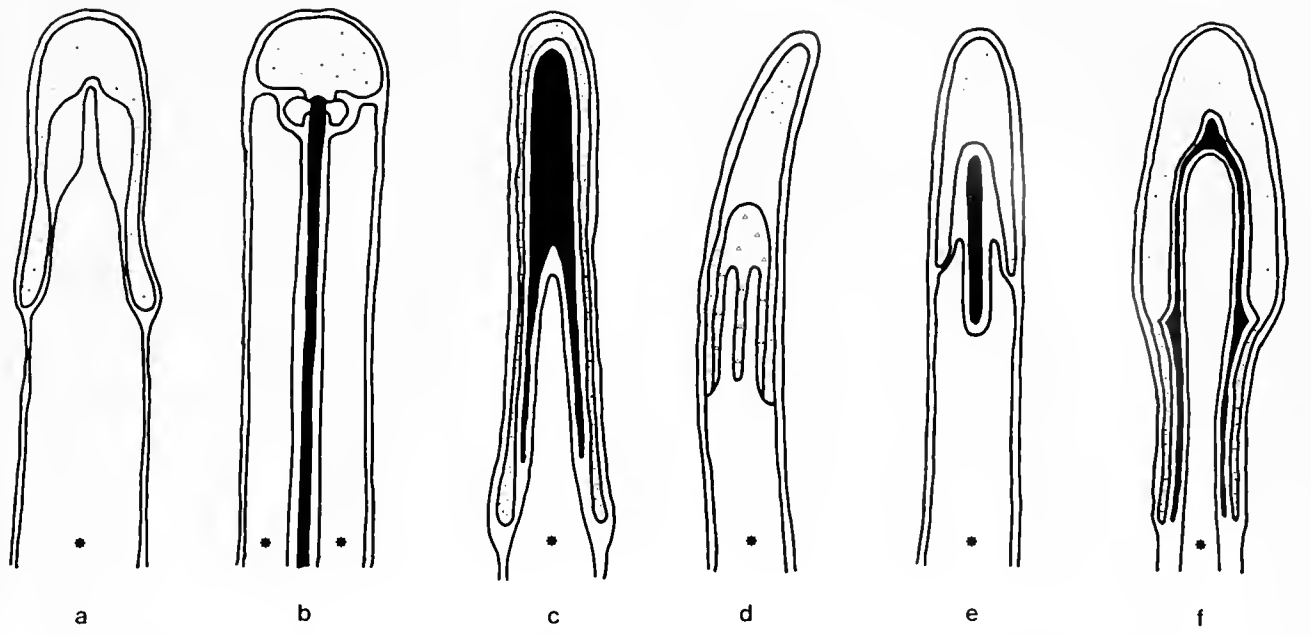

Figure 6. Comparison of the acrosomal region of the spermatozoa of various vertebrates. (a) Agnathans (*Eptatretus burgeri*); (b) agnathans (*Lampetra planeri*); (c) amphibians (*Bufo bufo japonicus*); (d) reptiles (*Chelonia* sp.); (e) birds (*Gallus gallus*); (f) mammals (*Mesocricetus auratus*). b–f were redrawn from Stanley (1967), Yoshizaki and Katagiri (1982), Furieri (1970), Okamura and Nishiyama (1978), Yanagimachi and Noda (1970), respectively. Acrosomal vesicle, spotted; perforatorium (subzonal material), shaded; nucleus, *; inner acrosomal cap with granular substance (Furieri, 1970), triangles.

the head of the hagfish spermatozoon is 2.5–3 μm wide in *M. glutinosa* (Walvig, 1963), about 1.2 μm wide (see Results) and 1.5 μm wide (Walvig, 1963) in *E. burgeri*, and about 1.5 μm wide (Jespersen, 1975) and 2.5–3 μm wide (Koch *et al.*, 1993) in *E. stouti*, the spermatozoa could access the egg surface directly. Judging by the features of the anterior portion of the spermatozoa and the micropyle, the relationship between sperm and egg in hagfish may differ from those in lampreys and teleosts. The exocytosis of the acrosomal vesicle at several points in hagfish (our preliminary observation) as seen in higher vertebrates may be different from the acrosome reaction in sturgeon. The relationship between the existence of egg micropyle and no acrosome in spermatozoa has been considered in teleosts having external fertilization (Baccetti and Afzelius, 1976). In hagfish and sturgeon, however, gametes have both structures, although the mode of fertilization in hagfish is still unknown. The structure of the micropyle in hagfish and sturgeon should be studied in detail to understand the role of these structures in fertilization.

The hagfish has a phylogenetically interesting position in the Chordata. Analysis of sperm function—for example, the interaction between sperm and egg during fertilization and the acrosome reaction—would contribute to an understanding of both the mode and the phylogenical aspects of fertilization in hagfish.

Acknowledgments

The author is indebted to Prof. R. Yanagimachi, University of Hawaii, for revising the original manuscript. She thanks Prof. M. Morisawa, Misaki Marine Biological Station, University of Tokyo, Dr. S. Ooka-Souda, Atomi College, and Dr. N. Usui, Teikyo University, for their valuable advice. She also thanks Dr. H. Kabasawa, Keikyu Aburatubo Marine Park, and the staff of the MMBS for providing the material, and the staff of the Central Facility of Electron Microscopy, St. Marianna University, for technical assistance. This work was supported in part by a Grant-in-Aid for Scientific Research from the Ministry of Education, Science and Culture, No. 06839024.

Literature Cited

Adam, H., and R. Strahan. 1963. Systematics and geographical distribution of Myxinoids. Pp. 1–8 in *The Biology of Myxine*, A. Brodal and R. Fänge, eds. Universitetsforlaget, Oslo.

Afzelius, B. A. 1978. Fine structure of the garfish spermatozoon. *J Ultrastruct. Res.* **64:** 309–314.

Afzelius, B. A., L. Nicander, and I. Sjöden. 1968. Fine structure of egg envelopes and the activation changes of cortical alveoli in the river

lamprey, *Lampetra [illegible] attilis*. *J. Embryol. Exp. Morph.* **19:** 311–318.

Baccetti, B., and [illegible]fzelius, B. A. 1976. *The Biology of the Sperm Cell.* S. Karger, Basel.

Baccetti, B., [illegible] G. Burrini, and R. Dallai. 1972. The spermatozoon of *Branchiostoma lanceolatum* L. *J. Morph.* **136:** 211–226.

Brodal, A., and R. Fange. 1963. *The Biology of Myxine.* Universitetsforlaget, Oslo.

Cherr, G. N., and W. H. Clark. 1984. An acrosome reaction in sperm from the white sturgeon, *Acipenser transmontanus*. *J. Exp. Zool.* **232:** 129–139.

Dean, B. 1899. On the embryology of *Bdellostoma stouti*. A general account of myxinoid development from the egg and segmentation to hatching. *Festschr. Carl von Kupffer, Jena* Pp. 221–276.

Fernholm, B. 1975. Ovulation and eggs of the hagfish *Eptatretus burgeri*. *Acta Zool. (Stockholm)* **56:** 199–204.

Follenius, E. 1965. Particularites de structure des spermatozoides de *Lampetra planeri*. *J. Ultrastruct. Res.* **13:** 459–468.

Furieri, P. 1970. Sperm morphology in some reptiles. Pp. 115–131 in *Comparative Spermatology*, B. Baccetti, ed. Academic Press, New York.

Gorbman, A. 1983. Reproduction in cyclostome fishes and its regulation. Pp. 1–29 in *Fish Physiology*, vol. IXA, W. S. Hoar, D. J. Randall and E. M. Donaldson, eds. Academic Press, New York.

Gorbman, A. 1990. Sex differentiation in the hagfish *Eptatretus stouti*. *Gen. Comparative Endocrinol.* **77:** 309–323.

Grier, H. J. 1975. Spermiogenesis in the teleost *Gambusia affinis* with particular reference to the role played by microtubules. *Cell Tissue Res.* **165:** 89–102.

Hardisty, M. W. 1979. *Biology of the Cyclostomes* Chapman & Hall, London.

Holland, L. Z., G. Gorsky, and R. Fenaux. 1988. Fertilization in *Oikopleura dioica* (Tunicata; Appendicularia): acrosome reaction, cortical reaction and sperm-egg fusion. *Zoomorphology* **108:** 229–243.

Jaana, H., and T. S. Yamamoto. 1981. The ultrastructure of spermatozoa with a note on the formation of the acrosomal filament in the lamprey, *Lampetra japonica*. *Jpn. J. Ichthyol.* **28:** 135–147.

Jespersen, A. 1975. Fine structure of spermiogenesis in eastern pacific species of hagfish (Myxinidae). *Acta Zool. (Stockholm)* **56:** 189–198.

Kille, R. A. 1960. Fertilization of the lamprey egg. *Exp. Cell Res.* **20:** 12–27.

Kobayashi, H., T. Ichikawa, H. Suzuki, and M. Sekimoto. 1972. Seasonal migration of the hagfish, *Eptatretus burgeri*. *Jpn. J. Ichthyol.* **19:** 191–194.

Koch, E. A., R. H. Spitzer, R. B. Pithawalla, F. A. Castillos III, and L. J. Wilson. 1993. The hagfish oocyte at late stages of oogenesis: structural and metabolic events at the micropylar region. *Tissue Cell* **25:** 259–273.

Kosmath, L., R. A. Patzner, and H. Adam. 1981. The fine structure of the micropyles of the eggs of *Myxine glutinosa* and *Eptatretus burgeri* (Cyclostomata). *Zool. Ans. Jena* **206:** 273–278.

Mattei, X. 1970. Spermiogenese comparee des poissons. Pp. 57–69 in *Comparative Spermatology*, B. Baccetti, ed. Academic Press, New York.

Nicander, L. 1970. Comparative studies on the fine structure of vertebrate spermatozoa. Pp. 47–56 in *Comparative Spermatology*, B. Baccetti, ed. Academic Press, New York.

Nicander, L., and I. Sjöden. 1971. An electron microscopical study on the acrosomal complex and its role in fertilization in the river lamprey, *Lampetra fluviatilis*. *J. Submicrosc. Cytol.* **3:** 309–317.

Nicander, L., B. A. Afzelius, and I. Sjöden. 1968. Fine structure and early fertilization changes of the animal pole in eggs of the river lamprey, *Lampetra fluviatilis*. *J. Embryol. Exp. Morphol.* **19:** 319–326.

Okamura, F., and H. Nishiyama. 1978. The passage of spermatozoa through the vitelline membrane in the domestic fowl, *Gallus gallus*. *Cell Tissue Res.* **188:** 497–508.

Ooka-Souda, S., H. Kabasawa, and S. Kinoshita. 1985. Circadian rhythms in locomotor activity in the hagfish, *Eptatretus burgeri*, and the effect of reversal of light-dark cycle. *Zool. Sci.* **2:** 749–754.

Patzner, R. A. 1977. Cyclical changes in the testis of the hagfish *Eptatretus burgeri* (Cyclostomata). *Acta Zool. (Stockholm)* **58:** 223–226.

Patzner, R. A. 1978. Cyclical changes in the ovary of the hagfish *Eptatretus burgeri* (Cyclostomata). *Acta Zool. (Stockholm).* **59:** 57–61.

Patzner, R. A. 1982. Die reproduktion der myxinoiden. Ein vergleich von *Myxine glutinosa* und *Eptatretus burgeri*. *Zool. Anz., Jena.* **208:** 132–144.

Phillips, D. M. 1977. Mitochondrial disposition in mammalian spermatozoa. *J. Ultrastruct. Res.* **58:** 144–154.

Stanley, H. P. 1967. The fine structure of spermatozoa in the lamprey *Lampetra planeri*. *J. Ultrastruct. Res.* **58:** 144–154.

Stanley, H. P. 1971. Fine structure of spermiogenesis in the elasmobranch fish *Squalus suckleyi* II. Late stages of differentiation and structure of the mature spermatozoon. *J. Ultrastruct. Res.* **36:** 103–118.

Walvig, F. 1963. The gonad and the formation of the sexual cells. Pp. 530–580 in *The Biology of Myxine*, A. Brodal and R. Fänge, eds, Universitetsforlaget, Oslo.

Yanagimachi, R., and Y. D. Noda. 1970. Fine structure of the hamster sperm head. *Am. J. Anat.* **128:** 367–388.

Yanagimachi, R., and N. Usui. 1974. Calcium dependence of the acrosome reaction and activation of guinea pig spermatozoa. *Exp. Cell Res.* **89:** 161–174.

Yoshizaki, N., and C. Katagiri. 1982. Acrosome reaction in sperm of the toad, *Bufo bufo japonicus*. *Gamete Res.* **6:** 343–352.

Reference: *Biol. Bull.* **189**: 13–21. (August, 1995)

Oxidase Activity Associated with the Elevation of the Penaeoid Shrimp Hatching Envelope

PATRICIA S. GLAS[1], JEFFREY D. GREEN[2], AND JOHN W. LYNN[1,*]

[1]*Louisiana State University, Department of Zoology and Physiology, Baton Rouge, Louisiana 70803; and* [2]*Louisiana State University—Medical School, Department of Anatomy, New Orleans, Louisiana 70112*

Abstract. When penaeoid shrimp spawn into seawater, the ova elevate a hatching envelope (HE) within 30–50 min. By 60 min after spawning, the bilayered HE is completely formed. In other animal systems, peroxidatic enzymes are responsible for the hardening of the extra-embryonic coat. In this study, observations are made consistent with the involvement of an oxidase in the assembly of the shrimp HE. As observed by electron microscopy, eggs of *Sicyonia ingentis* and *Trachypenaeus similis* spawned in seawaters containing peroxidase inhibitors had abnormally assembled HEs compared to control eggs in seawater. Dihydrotetramethylrosamine, an oxidase-sensitive fluorescent dye, supravitally stained the cortex of *S. ingentis* eggs at the time of initial HE formation. The HE fluoresced from elevation (40–50 min postspawn in *S. ingentis*) until 60–70 min postspawn. By first cleavage (90–120 min postspawn), HE staining was no longer visible, although staining persisted in the egg cortex. In eggs treated with the peroxidase inhibitors 3-amino-1,2,4-triazole or sodium sulfite, the egg cortex fluoresced, but no fluorescence appeared in the HE before, during, or after its elevation.

Introduction

Formation of extracellular egg coats has been the subject of studies especially in frogs (for review, Schmell *et al.*, 1983), sea urchins (for review, Schuel, 1978, 1985; Kay and Shapiro, 1985), and crustaceans. The crab and lobster egg coats were described by Goudeau and her colleagues (Goudeau and Becker, 1982; Goudeau and Lachaise, 1980, 1983; Talbot and Goudeau, 1988), and Pillai and Clark (1987, 1988, 1990) described the elevation and formation of the hatching envelope of the penaeid shrimp *Sicyonia ingentis*.

The presence of an ovoperoxidase enzyme has been demonstrated as crucial in the assembly of the sea urchin fertilization envelope (FE) (Kay and Shapiro, 1985, for review). Peroxidases catalyze reactions in which hydrogen peroxide serves as a substrate that, when bound to peroxidase, oxidizes other substances much more rapidly than alone (Kiernan, 1990). Ovoperoxidase in sea urchins forms a complex with the protein proteoliaisin and is incorporated into the FE as it catalyzes di- and tri-tyrosine linkages. This hardens the sea urchin FE mechanically so that it is resistant to sperm proteases and environmental stress. Extra-embryonic coat assembly involving di- and tri-tyrosine linkages mediated by an ovoperoxidase-proteoliaisin complex has been described in detail (for review, Kay and Shapiro, 1985, 1987; Weidman *et al.*, 1985, 1987; Somers *et al.*, 1989). In fish, Kudo *et al.* (1988) demonstrated a peroxidatic reaction in the fertilized fish egg chorion. This is believed to be part of the hardening reaction in the chorion necessary to provide a microenvironment for the developing embryo (Kudo and Inoue, 1986, 1989; Kudo and Teshima, 1991; Kudo, 1992).

These peroxidatic reactions were visualized by substrate localization using 3,3-diaminobenzidine (DAB) (Daems *et al.*, 1964; Katsura and Tominaga, 1974; Klebanoff *et al.*, 1979; Kudo *et al.*, 1988; Green *et al.*, 1990). Ovoperoxidase inhibitors such as 3-amino-1,2,4-triazole (ATA) or sodium sulfite have been used to prevent normal assembly of sea urchin FE (Veron *et al.*, 1977; Showman and Foerder, 1979). In the presence of inhibitors, lack of incorporation of the ovoperoxidase enzyme is implicated

Received 16 September 1994; accepted 24 May 1995.

* Author to whom correspondence should be addressed.

Abbreviations: 3-amino-1,2,4-triazole (ATA); 3,3-diaminobenzidine (DAB); artificial seawater (ASW); hatching envelope (HE); scanning electron microscopy (SEM); transmission electron microscopy (TEM); fertilization envelope (FE); dihydrotetramethylrosamine (DHTMR); perivitelline space (PVS).

by an absence of DAB precipitation staining (Katsura and Tominaga, 1974; Klebanoff *et al.*, 1979; Green *et al.*, 1990). Although ovoperoxidase has been demonstrated in the cortical granules in mammals, other enzymes are believed to account for the change in zona pellucida permeability during the zona reaction (Wasserman, 1987; Bleil and Wasserman, 1980).

In eggs of the penaeoid shrimp *Sicyonia ingentis* and *Trachypenaeus similis*, the hatching envelope (HE) is elevated 30–50 min after spawning in seawater. This elevation is the result of exocytosis of at least two distinct types of cortical vesicles in *S. ingentis* (Pillai and Clark 1988; 1990) and *T. similis* (Lynn *et al.*, 1991; Glas, 1994). Assembly results in an HE with a thin, electron-dense outer layer and a thick, more electron-translucent inner core. When peroxidase inhibitors were added to the spawning media, abnormal hatching envelopes elevated (Lynn *et al.*, 1993) indicating that a peroxidatic reaction may be necessary for normal HE assembly. However, attempts to localize a peroxidase with DAB did not show significant staining. This apparently conflicting evidence suggests the presence of an oxidatic enzyme, but not necessarily ovoperoxidase.

Materials and Methods

Gamete collection

Animals were collected as previously described by Pillai *et al.* (1988) and Lynn *et al.* (1991, 1992, 1993). Eggs were collected in 70 × 50 mm crystallizing dishes containing artificial seawater (ASW) (Cavanaugh, 1956). The dishes were gently swirled for 10 min postspawning to prevent clumping of the eggs.

Inhibitor and localization substrates

The peroxidase inhibitors ATA or sodium sulfite were added to dishes of eggs in ASW 10 min after spawning to give a final concentration of 100 μM ATA (Lynn *et al.*, 1993) or 20 mM sodium sulfite in seawater. Hatching envelope elevation was monitored with light microscopy.

Samples for light microscopy were removed from the spawning dishes at intervals to correct for temperature changes from the microscope light. Transmission electron microscopy (TEM) samples were removed and processed by fixation, osmication, dehydration (Lynn *et al.*, 1992), infiltration, and embedding in modified Spurr's resin (Spurr, 1969). Sections were double stained with uranyl acetate and lead citrate (Venable and Coggeshall, 1965). Scanning electron microscopy (SEM) samples were processed through dehydration, then critical-point dried, sputter-coated, and viewed.

For fluorescent localization of enzyme activity, a peroxidase-sensitive, rhodamine analog dye, dihydrotetramethylrosamine (DHTMR) (Molecular Probes, D-638), was added directly to spawning dishes containing *S. ingentis* eggs. The dye was in an aqueous stock solution of 2 mg/ml of which 100 μl per 100 ml egg suspension was used. An FITC filter cube with excitation at 485 nm and transmission at 510 nm was used to observe eggs for fluorescence.

Localization of peroxidase activity with DAB as a substrate was performed as described by Klebanoff *et al.* (1979). Samples were removed from the spawning dish and washed in a solution of 0.1 M TRIS–0.45 M NaCl, pH 8.0, to remove salts that might interfere with the reaction. The wash solution was replaced with a reaction solution (2 mg/ml of 3,3-diaminobenzidine, 0.01% H_2O_2 in 0.1 M Tris–0.45 M NaCl, pH 8.0), and the reaction was allowed to proceed for 10 min. The reaction was stopped by the addition of two times the volume of 5.0% glutaraldehyde/1.6% formaldehyde fixative in 0.1 M Tris-buffer, pH 8.0. Samples were then processed for TEM. Both stained and unstained sections were observed.

Permeability of the hatching envelope

To ascertain permeability of the HE, fluorescently tagged dextrans (500 μg/ml egg suspension) (Sigma) were added to the ASW and ATA seawater media after the hatching envelope was visible. Eggs were observed with epifluoresence until 90 min postspawn. A flow-through chamber was used on an inverted microscope to allow changing the solution without agitating the eggs. Dextrans of 4400, 10,000, 40,000, 76,000, and 155,000 molecular weight, conjugated to fluorescein isothiocyanate (FITC-dextran) or tetramethylrhodamine isothiocyanate (TRITC-dextran) probes were used. Eggs were incubated in the presence of the dextran at room temperature. Eggs were transferred to a flow-through chamber, which was purged two times with seawater. The eggs were observed for the absence of fluorescence within the perivitelline space (PVS) by using FITC or TRITC excitation and barrier filters on a Nikon diaphot inverted microscope. Dye exclusion was indicated by decreased fluorescence compared to the medium outside the hatching envelope in the PVS when eggs were observed at an equatorial focus.

Enzyme assays

Enzyme assays were performed on supernatants from the spawned eggs to detect ovoperoxidase secretion from the egg. The guaiacol assay was used as described by Deits *et al.* (1984) with 28 mM guaiacol, 1.0 mM H_2O_2, and 50–500 μl supernatant from settled eggs in the spawning dishes. Supernatant from a dish with spawned eggs was assayed at 10, 30, 45, and 60 min postspawn. Protein assays were as described by Lowry *et al.* (1951).

Results

Historical descriptions

For clarity, a brief description of hatching envelope (HE) formation in *S. ingentis* and *T. similis* is reiterated here. Eggs spawned from penaeoid shrimp release a jelly coat upon contact with seawater (Pillai and Clark, 1987; Lynn *et al.*, 1991). The first cortical vesicle exocytosis occurs about 30–35 min postspawn in *S. ingentis*, and the products interact with a surface coat to form the outer, electron-dense layer of the HE (Pillai and Clark, 1988). The HE is elevated by 40–50 min postspawn. HE elevation is reported to be independent of fertilization (Clark *et al.*, 1980; Pillai and Clark, 1987). In *T. similis*, the first exocytosis also occurs about 30 min postspawn. However, the second exocytosis follows more rapidly so that the HE is elevated by 40 min postspawn (Glas, 1994). Formation of the first polar body occurs 5 to 10 min before the HE is apparent. The second polar body appears at 30–45 min postspawn beneath the elevating HE, and both polar bodies remain throughout HE elevation. During this period, granular material is observed accumulating in the PVS. At 90 min postspawn, the HE is refractile and an expansive PVS is visible. Transmission electron micrographs reveal an HE with a distinct bilayered appearance.

The criteria for successful assembly and elevation of the HE were based on the morphology of the envelope. These included the continued elevation of the HE without collapse and a bilayered appearance. The extra-embryonic envelopes remain around the zygote until the time of hatching, about 24 h later.

Assessment of peroxidase activity

In *S. ingentis* eggs spawned into ASW, a distinct PVS was visible at 75 min postspawn (Fig. 1), separating the oolemma from the elevated HE. With TEM, the HE appeared as a well-formed structure with flocculent material juxtaposed on the interior of an electron-dense outer layer. Remnants of the jelly layer remained outside the HE (Fig. 2). Materials within the PVS were seen in close association with the oolemma or the thickening HE. With higher magnification, the bilayered configuration of the HE was evident as a distinct electron-dense outer layer and a flocculent, more electron-translucent inner layer (Fig. 3). The exterior of the egg envelope had no noticeable ridges or marks.

S. ingentis eggs treated with ATA elevated HEs by 45 min postspawn. Envelope elevation in these samples often preceded that in the control samples by 5 min, and initial elevation was frequently greater than in control egg HEs. At 75 min postspawn, inhibitor-treated eggs had envelopes that were more refractile and less birefringent than the control eggs, and the envelopes often collapsed to the oolemma (Fig. 4). The envelopes were very fragile, were often wrinkled and folded, and were easily removed (Lynn *et al.*, 1993; Glas, 1994). Transmission electron micrographs of envelopes and eggs of ATA-treated samples revealed no significant differences between control and treated eggs in the appearance of the PVS or the release of cortical vesicles (compare Figs. 2 and 5). HEs of eggs in ATA, however, showed a dense outer layer, but the more electron-translucent layer was absent or poorly developed (Fig. 6). This resulted in a thinner envelope than seen in the controls (Figs. 3 and 6).

In *S. ingentis*, even at 75 min postspawn, definitive DAB localization was absent in the hatching envelope in ASW (data not shown). The intense black precipitant indicative of peroxidase activity in other systems such as the sea urchin FE was not present (see Klebanoff *et al.*, 1979). Similarly, DAB staining was also not apparent in the elevated HE of *T. similis* eggs.

In *T. similis* eggs, the HE appeared as a distinct refractile coat around the egg by 40 min postspawn and remained so at 90 min postspawn (Fig. 7). The intact HE prevented observation of the oolemma in scanning electron micrographs (Fig. 8). Handling and dehydration techniques caused the envelope to collapse, so that large folds in the HE were observed with SEM. At higher magnifications, small ridge-like contours on the exterior of the envelope were visible. These ridges were arranged in distinctive polygonal patterns encompassing areas of smooth envelope (Fig. 9).

In transmission electron micrographs of *T. similis* eggs at 90 min postspawn, the HE appeared as a bilayered structure (Fig. 10). The ridge-like contours seen with SEM correlated with cone-shaped protrusions of electron-dense material (Fig. 10). This material appeared continuous with the electron-dense outer layer of the hatching envelope. A flocculent, less electron-dense layer formed interiorly to the outer layer, and was three to four times the thickness of the outer dense layer (Fig. 10).

T. similis eggs treated with 100 μm ATA at 10 min postspawn elevated HEs about 30–35 min postspawn. By 90 min postspawn, eggs incubated in ATA had envelopes that appeared less refractile (Fig. 11). Frequently, the granular material observed in the PVS was coarser and more abundant than in control eggs. When 90-min-postspawn eggs were observed with SEM, a ridge-like pattern was distinguishable (Fig. 12), but was much less prominent (Fig. 13) than in the control eggs (Fig. 9).

At 90 min postspawn, eggs treated with ATA appeared to have a thinner HE that consisted of the electron-dense layer (Fig. 14) with the flocculent, more electron-translucent layer absent or greatly reduced when examined with TEM. The inhibitor-treated HEs often folded on themselves, so that, in section, the ridges sometimes appeared to be on the "inside" of the envelope (Fig. 14).

When *S. ingentis* eggs were treated with the oxidase-sensitive fluorescent dye dihydrotetramethylrosamine

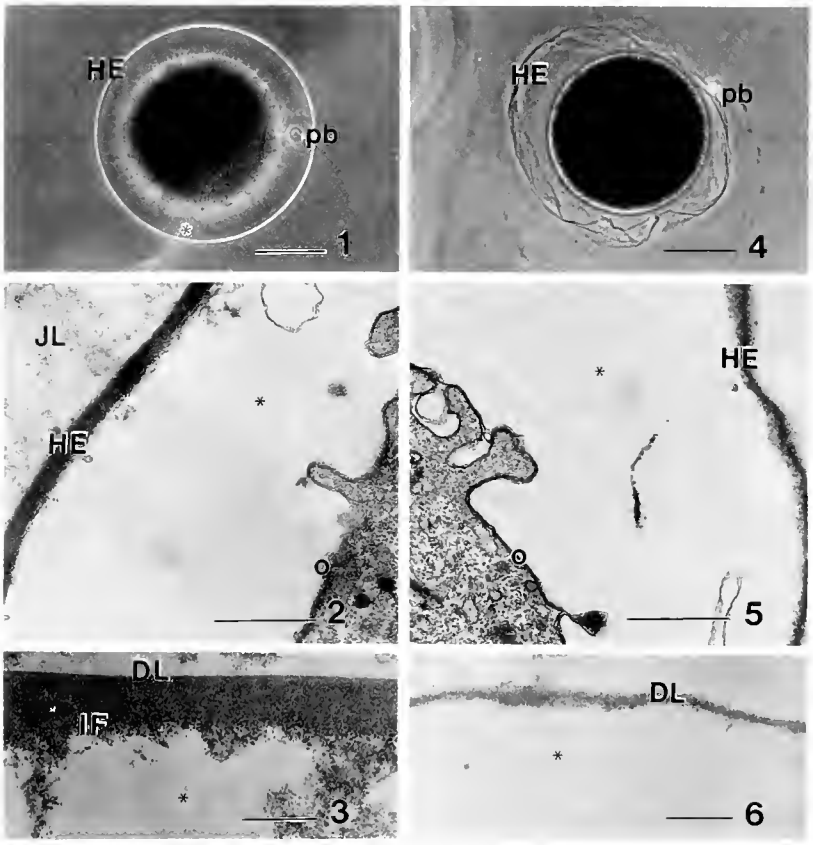

Figures 1–6. *Sicyonia ingentis* eggs. HE, hatching envelope; PVS, perivitelline space; ATA, 3-amino-1,2,4-triazole.

Figure 1. With phase microscopy, eggs in artificial seawater show a distinctive refractile HE surrounding the PVS (*). The second polar body (pb) is visible within the PVS. Bar equals 100 μm.

Figure 2. With transmission electron microscopy, eggs in artificial seawater show the jelly layer (JL) outside of the HE (HE). The PVS (*), separating the HE and oolemma (O), contains materials that may be added to the HE. Bar equals 1 μm.

Figure 3. At higher magnification, the bilayered structure of the HE is apparent. The outer dense layer (DL) forms a smooth exterior while the inner flocculent layer (IF) appears to be incorporating more material from the PVS (*). Bar equals 0.25 μm.

Figure 4. Eggs in 3-amino-1,2,4-triazole (ATA) seawater have HEs (HE) that often collapse. The first polar body (pb) is visible outside of the collapsed HE. Bar equals 100 μm.

Figure 5. With transmission electron microscopy, eggs in ATA seawater show HEs (HE) that do not have the structural bilayered appearance of those in control eggs. The inner electron translucent layer is missing. The PVS (*) separates the oolemma (O) from the HE. Bar equals 1 μm.

Figure 6. Higher magnification shows that the ATA-treated HEs are thinner and do not appear to have the flocculent inner layer attached to the dense layer (DL). Bar equals 0.25 μm.

(DHTMR) (Whitaker *et al.*, 1991), no fluorescence was visible in the egg before HE elevation. Sperm attached to the egg surface were visibly fluorescent (Fig. 15a, b). A fluorescent band appeared in the cortex of the egg as the HE became visible (Fig. 16a, b). A thin, fluorescent outline of the HE appeared after HE elevation. The HE fluorescence intensified briefly and remained in the region of the newly elevated HE until about 60 min postspawn (Fig. 17a, b). By the two-cell stage, the fluorescence in the HE was no longer detectable (Fig. 18a, b).

The cortex of eggs incubated in ATA was fluorescent immediately before HE elevation, as in controls. However, unlike the controls (Figs. 15a, b; 16a, b; 17a, b), eggs in ATA showed no fluorescence associated with the HE during and after elevation (Fig. 19a, b).

Eggs incubated in another peroxidase inhibitor, sodium sulfite, showed no cortical fluorescence immediately before HE elevation. Continued monitoring showed no fluorescence by 60 min postspawn in the elevated HE (Fig. 20a, b).

Hatching envelope permeability

S. ingentis eggs were incubated with fluorescently labeled dextrans of a range of sizes to examine the perme-

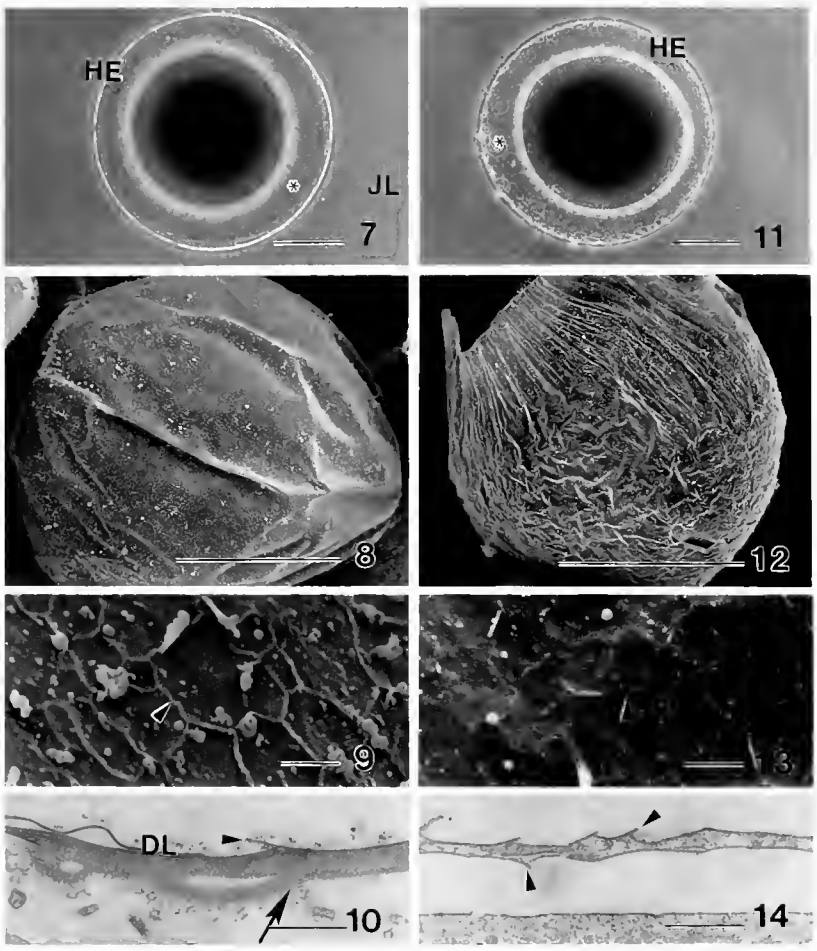

Figures 7–14. *Trachypenaeus similis* eggs. HE, hatching envelope; PVS, perivitelline space; ATA, 3-amino-1,2,4-triazole.

Figure 7. Eggs in artificial seawater show a jelly layer (JL) outside of the refractile HE (HE) that surrounds the PVS (*). Bar equals 100 μm.

Figure 8. Scanning electron microscopy shows the HE covering the developing zygote to act as an environmental barrier. The HE collapses during processing, resulting in some wrinkling of the envelope. Bar equals 100 μm.

Figure 9. Higher magnification of the HE shows an exterior series of ridges (arrowhead) not seen in *Sicyonia ingentis* egg HEs. The ridges form octagonal patterns on the surface of the HE. Bar equals 1 μm.

Figure 10. Transmission electron microscopy shows the distinct bilayered HE with the ridges appearing to be constructed of the electron-dense material (DL). The arrowhead indicates a ridge now seen in cross section. Note the ring material in the PVS associated with the flocculent inner layer (large arrow). The flocculent layer is three to four times the thickness of the outer dense layer. Bar equals 0.5 μm.

Figure 11. Phase microscopy of an egg in ATA shows a less refractile HE (HE) surrounding the PVS (*). Bar equals 100 μm.

Figure 12. Scanning electron microscopy of an egg in ATA seawater shows an egg with more folds than in ASW. The collapse of the HE causes the envelope to be folded on itself. Bar equals 100 μm.

Figure 13. At higher magnification, the ridges (arrowhead) are not as prominent as in the control eggs. The height of the ridges appears lower than in normal eggs. Bar equals 1 μm.

Figure 14. Transmission electron microscopy shows that the envelope is folded so that ridges (arrowheads) appear to be on the interior and exterior of the HE. The electron-dense layer is present, but the electron-translucent layer is greatly reduced. Bar equals 0.5 μm.

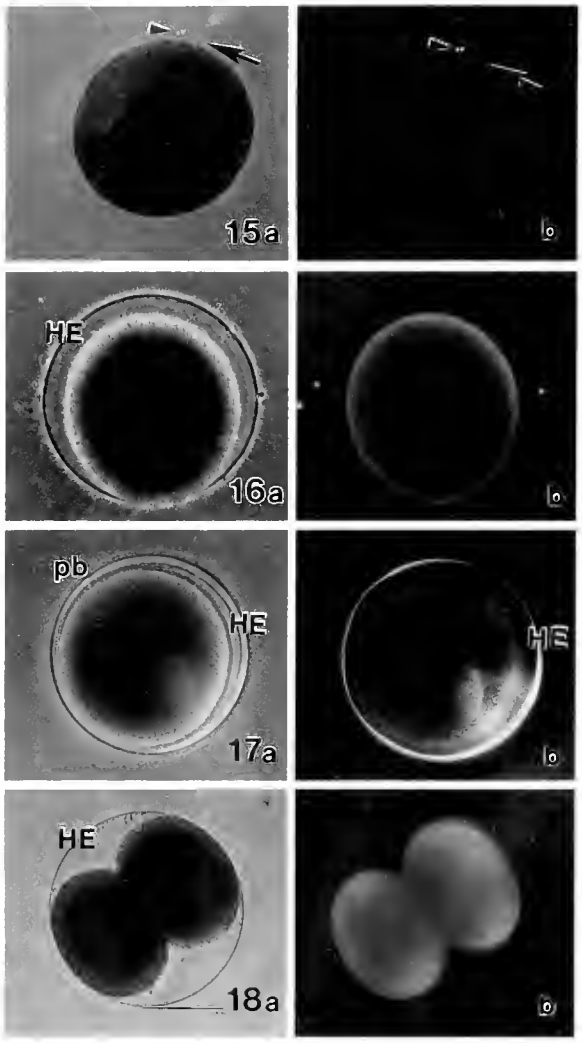

Figures 15–18. A time series of *Sicyonia ingentis* eggs in artificial seawater shows the elevation of the hatching envelope (HE) under light microscopy (a) and labeling of the HE with an oxidase sensitive fluorescent dye, dihydrotetramethylrosamine (b).

Figure 15. (a) Normal egg before elevation at 35 min postspawn. Two sperm are visible on the exterior of the egg (arrowhead). Arrow indicates first polar body. (b) No fluorescence is visible in the cortex; however, the sperm are fluorescent (arrowhead). The first polar body (arrow) can also be seen.

Figure 16. At 47 min postspawn, the HE has begun to lift from the oolemma. (a) The HE (HE) is separating from the oolemma and has extranumerary sperm on its exterior. (b) The cortex can be seen to react with DHTMR.

Figure 17. By 60 min postspawn, the HE is fully formed. (a) A normal HE (HE) with the second polar body (pb) visible in the perivitelline space. (b) The HE fluoresces brightly, as does the cortex of the egg. The polar body does not fluoresce.

Figure 18. At 100 min postspawn, the two-cell stage can be seen. (a) The cells are visible within the elevated HE (HE). (b) The cortex still fluoresces, but the HE does not. Bar equals 100 μm.

ability of the HE (Table 1). Based on the relative fluorescent intensity inside *vs.* outside the PVS at an equatorial focus, both the control and ATA-treated eggs had fluorescent dextrans within the PVS when incubated with the 4400 KDa sugar. When incubated with the 10,000 KDa dextran, the ATA-treated eggs contained fluorescent dextrans within the PVS, but eggs in ASW did not. The entry of the dextrans was variable in the ATA-treated eggs with 40,000 and 76,000 Da dextrans, although the control eggs revealed no fluorescent dextrans within the PVS (Table 1). Even though extreme care was used, the presence of high molecular weight fluorescent dextrans in the PVS of ATA-treated eggs may have been due to damage of the envelope allowing the dextrans to enter the PVS.

Enzyme assays

A spectrophotometric assay using the colorometric substrate guaiacol (Foerder and Shapiro, 1977) failed to indicate peroxidase activity in the supernatant within 3 min at 10, 30, 45, or 60 min postspawn. These time points encompass the period before, during, and after HE elevation.

Discussion

Histochemical localization and identification of peroxidase using DAB staining is well documented (Kay and

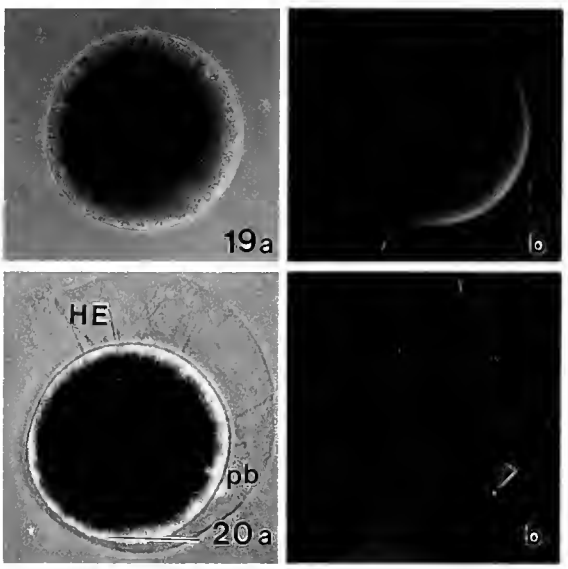

Figure 19. *Sicyonia ingentis* eggs were treated with the peroxidase inhibitor 3-amino-1,2,4-triazole and then incubated with DHTMR. (a) In the inhibitor, the eggs elevate the hatching envelope (HE), which then frequently collapses back to the egg surface. (b) With DHTMR, the cortex can be seen to fluoresce weakly on one side of the egg and is not consistent with fluorescence in the HE (compare with same time point of controls in Fig. 17a, b).

Figure 20. *Sicyonia ingentis* eggs were also treated with sodium sulfite, a peroxidase inhibitor, and then incubated with DHTMR. (a) The hatching envelope (HE) is elevated, but collapses around the egg as seen with light microscopy. The second polar body (pb) is visible. (b) Fluorescent microscopy shows no labeling of the HE or cortex although the sperm shows fluorescence (arrowhead). Bar equals 100 μm.

Table I

Presence of fluorescent dextrans in the perivitelline space after hatching envelope elevation

Molecular weight	Control (artificial seawater)	Treated (3-amino-1,2,4-triazole + seawater)
4,400	−, ½+ ½−	+,+
10,000	−	+
40,000	−	−
76,000	−,−,−	−,+,−
155,000	−,−	+,−

Each score represents a separate trial of 10 or more visibly undamaged eggs.

+ not excluded from the perivitelline space; − excluded from the perivitelline space.

½+ 50% had fluorescence in the perivitelline space; ½− 50% excluded fluorescence.

Shapiro, 1985, for review; Kiernan, 1990; Green *et al.*, 1990). These studies report intense black staining as indicative of the peroxidase reaction in sea urchin eggs and mammalian tissue. DAB staining due to peroxidatic activity has been reported in the FEs of the sea urchins *Hemicentrotus pulcherrimus, Temnopleurus toreumaticus, Strongylocentrotus purpuratus,* and *Lytechinus pictus* (Katsura and Tominaga, 1974; Klebanoff *et al.*, 1979; Green *et al.*, 1990). Using DAB, Kudo *et al.* (1988) also demonstrated peroxidase activity in the vitelline envelope of unfertilized fish eggs and in the chorion and micropylar region of fertilized fish eggs. In addition, DAB reactivity remains detectable over an extended time (Klebanoff *et al.*, 1979; Kay and Shapiro, 1985, for review; Green *et al.*, 1990). Heavy precipitation indicative of peroxidase activity was not visualized in the HE of eggs from either *S. ingentis* or *T. similis* by using the DAB methodology. Staining was not observed at any of the time points sampled (30, 45, 75, or 90 minutes postspawn).

The peroxidase inhibitors ATA and sodium sulfite are believed to interfere with tyrosine cross-linking by oxidative inhibition of the enzyme or enzymes responsible for FE elevation and transformation (Kay and Shapiro, 1985, for review; Kay and Shapiro, 1987; Lynn *et al.*, 1988; Green *et al.*, 1990). Inhibitor-treated sea urchin eggs have FEs that are thinner and less refractile than the normal envelopes. Treatment of penaeid shrimp eggs with the peroxidase inhibitors ATA and sodium sulfite results in "soft" HEs that are less refractile and tend to collapse. The morphology of the envelope shows a thinner envelope that lacks the bilayered appearance. These inhibitors are not detrimental to the development of the shrimp egg (Lynn *et al.*, 1993).

In contrast, interference by "peroxidase" inhibitors with normal HE assembly is also implicated by changes in HE permeability as exhibited by fluorescently labeled dextrans. In these experiments, the HE is more permeable to substances of 10,000 and 40,000 kDa in peroxidase-inhibited medium than in artificial seawater. The variability of exclusion in the higher ranges may be due to other influences including time of dextran addition, damage to the envelopes, or possibly, whether fertilization had taken place. Variation due to damage of the envelopes was minimized by developing a system with minimum handling of the eggs. Further implications of differences in HE permeability due to sperm interaction were not considered during this study since envelope elevation and formation were previously reported to be independent of fertilization (Pillai and Clark, 1987).

The paradox of these findings resulted in the use of a fluorescent probe, dihydrotetramethylrosamine (DHTMR), a rhodamine analog. DHTMR reacts with oxidizable substrates and is pH independent in its absorption and emission (Whitaker *et al.*, 1991). Whitaker *et al.* (1991) describe this compound as a neutral, lipophilic substrate for horseradish peroxidase and hydrogen peroxide. An advantage of the dye is that it can be used with *in vitro* preparations, thereby eliminating the use of fixatives and the accompanying interference by aldehyde groups. The cytoplasm of spawned eggs placed in this dye fluoresces, indicating the presence of an oxidative capacity. Similar fluorescence is reported in mammalian and protozoan systems in relation to phagocytosis and the immune response (Whitaker *et al.*, 1991). The dye reaction in shrimp eggs may be indicative of several reactions. These reactions could include a peroxidase, a hydroxide, or superoxide-based change that may correspond to the "respiratory burst" in sea urchin eggs (Turner *et al.*, 1985; Heinecke and Shapiro, 1989; Epel, 1990, for review) or respiratory activity associated with mitochondria. Thus, it appears that DHTMR may react with one or more substrates in the shrimp egg, but the substrate cannot be defined as ovoperoxidase. In shrimp, bound sperm also fluoresced, a result in keeping with observations by Lindsay and Clark (1992) of a pH (hydroxide) change involved in sperm acrosomal filament formation. It is unclear why all sperm that were attached to eggs did not fluoresce, but there did not appear to be any correlation to the fertilizing sperm. Since this was not the main point of this study, further investigations will be required to resolve this interesting phenomenon.

Comparison of the amino acid composition of the sea urchin FE (Foerder and Shapiro, 1977) with the amino acid composition of the shrimp HE (Pillai and Clark, 1990) reveals that the relative abundance of tyrosine residues is considerably lower in the shrimp HE than in the sea urchin FE. Because tyrosine is a major substrate for ovoperoxidase activity, lack of an abundant supply may suggest there is not a major role for an ovoperoxidase in shrimp eggs. Assays for the di- and tri-tyrosine components in the shrimp HE have not been performed.

Sufficient ovoperoxidase is released by sea urchin eggs to allow quantitative analysis of the supernatant (Deits *et al.*, 1984; Green *et al.*, 1990). In peneaoid shrimp, however, if an ovoperoxidase is released following spawning, the quantities are insufficient to detect between spawning and 90 minutes postspawn. Although HE assembly could be acting as a barrier to release into the supernatant, we do not believe this is the case for two reasons. First, multiple time points were used for the assay and included times before, during, and after the HE assembly was "complete." Second, the relative permeability of the assembled envelope allows molecules of at least 10,000 Da through, as demonstrated by the dextran experiments. It is very likely that even larger molecules would pass the envelope prior to the final "tanning" process. An alternative explanation might be that the enzyme is bound so tightly to the assembling envelope that none escapes. Although this is possible, it is inconsistent with the reports in other systems and contradictory to the results of the DAB assays, which failed to demonstrate localization in the HE.

Ovoperoxidase from sea urchins is reported to have oxidoreductase activity requiring Mn^{+2} ions and certain phenols related to the respiratory burst (Turner *et al.*, 1985; 1986; 1988; Heinecke and Shapiro, 1989). Phenol oxidase in crustaceans oxidizes diphenols to the corresponding quinones that react in the tanning of crustacean exoskeletons to cross-link proteins within the chitin matrix (Stevenson, 1985). Perhaps the oxidase of the shrimp embryo is a closer analog of phenol oxidase than of ovoperoxidase. Pillai and Clark (1990) report that carbohydrates similar to those found in chitin are abundant in the peneaoid hatching envelope. Lectin-binding assays demonstrate the presence of oligosaccharides, especially mannose and *N*-acetylglucosamine, in the HE (Pillai and Clark, 1990; Lin, 1992; Glas, 1994). These sugars are the major components of chitin. A phenol-oxidase-driven cross-linkage of carbohydrates within the HE would be consistent with the presence of an oxidase. The action of such an enzyme is also consistent with the thinner HE in the presence of the oxidase inhibitors ATA and sodium sulfite.

Thus, an oxidase is probably involved, as indicated by the morphology of the HE after exposure to the peroxidase inhibitors ATA and sodium sulfite and the staining with DHTMR. The active enzyme is not similar to the ovoperoxidase identified in the sea urchin, as shown by the lack of localization with DAB or quantitation by the guaiacol assay; neither does the enzyme appear to be analogous to the enzyme that stimulates the peroxidatic reaction in fish fertilization. Nevertheless, a peroxidase-inhibitor-sensitive enzyme is involved with the assembly of the penaeoid HE. Further identification of such an active enzyme is required for a full understanding of the mechanisms responsible for HE assembly, elevation, and function.

Acknowledgments

The authors would like to express their appreciation to Dr. Wallis Clark, Jr., and his students at University of California, Bodega Marine Laboratory, for procurement of the *Sicyonia ingentis* and use of laboratory space. We are also grateful to Jim Hanifen and his colleagues at Louisiana Department of Wildlife and Fisheries for providing the *Trachypenaeus similis*. We thank Becky Demler, Ron Bouchard, Cindy Henk, and Dr. Sharon Matthews of the Louisiana State University Life Sciences Microscopy Facility for their assistance. Research supported by Louisiana Sea Grant #NA89-AA-D-SG226 project #R/SA-1 to JWL and JDG and Sigma Xi Grant-in-Aid of Research to PSG.

Literature Cited

Bleil, J. D., and P. M. Wasserman. 1980. Mammalian sperm and egg interaction: identification of a glycoprotein in mouse egg zonae pellucidae possessing receptor activity for sperm. *Cell* **20:** 873–882.

Cavanaugh, G. M. (Ed). 1956. *Formulae and Methods of the Marine Biological Laboratory Chemical Room,* 6th ed. Marine Biological Laboratory, Woods Hole, MA. P. 55.

Clark, W. H., Jr., J. W. Lynn, A. I. Yudin, and H. O. Persyn. 1980. Morphology of the cortical reaction in the eggs of *Penaeus aztecus*. *Biol. Bull.* **158:** 175–186.

Daems, W. Th., M. Van Der Ploeg, J.-P. Perslin, and P. Van Duijn. 1964. Demonstration with the electron microscope of injected peroxidase in rat liver cells. *Histochemie* **3:** 561–564.

Deits, T., M. Farrance, E. S. Kay, L. Medill, E. E. Turner, P. J. Weidman, and B. M. Shapiro. 1984. Purification and properties of ovoperoxidase, the enzyme responsible for hardening the fertilization membrane of the sea urchin egg. *J. Biol. Chem.* **259:** 13525–13533.

Epel, D. 1990. The initiation of development at fertilization. *Cell Differ. Devel.* **29:** 1–12.

Foerder, C. A., and B. M. Shapiro. 1977. Release of ovoperoxidase from sea urchin eggs hardens the fertilization membrane with tyrosine crosslinks. *Proc. Natl. Acad. Sci. USA* **74:** 4214–4218.

Glas, P. S. 1994. Elevation of the hatching envelope in penaeidea shrimp: morphology and assembly. Ph.D. Dissertation. Louisiana State University, Baton Rouge, LA. 113 pp.

Goudeau, M., and J. Becker. 1982. Fertilization in a crab. II. Cytological aspects of the cortical reaction and fertilization envelope elaboration. *Tissue & Cell* **14:** 273–282.

Goudeau, M., and F. Lachaise. 1980. Fine structure and secretion of the capsule enclosing the embryo in a crab (*Carcinus maenas* (L.)). *Tissue & Cell* **12:** 287–308.

Goudeau, M., and F. Lachaise. 1983. Structure of the egg funiculus and deposition of embryonic envelopes in a crab. *Tissue & Cell* **15:** 47–62.

Green, J. D., P. S. Glas, S.-D. Cheng, and J. W. Lynn. 1990. Fertilization envelope assembly in sea urchin eggs inseminated in chloride-deficient sea water: II. Biochemical effects. *Mol. Reprod. Dev.* **25:** 177–185.

Heinecke, J. W., and B. M. Shapiro. 1989. Respiratory burst oxidase of fertilization. *Proc. Natl. Acad. Sci. USA* **86:** 1259–1263.

Katsura, S., and A. Tominaga. 1974. Peroxidatic activity of catalase in the cortical granules of sea urchin eggs. *Dev. Biol.* **40:** 292–297.

Kay, E. S., and B. M. Shapiro. 1985. The formation of the fertilization membrane of the sea urchin egg. Pp. 45–80 in *Biology of Fertilization*, Vol. 3, C. B. Metz and A. Monroy, eds. Academic Press, Orlando, FL.

Kay, E. S., and B. M. Shapiro. 1987. Ovoperoxidase assembly into the sea urchin fertilization envelope and dityrosine crosslinking. *Dev Biol.* **121:** 325–334.

Kiernan, J. A. 1990. *Histological and Histochemical Methods: Theory and Practice.* Pergamon Press, Oxford.

Klebanoff, S. J., C. A. Foerder, E. M. Eddy, and B. M. Shapiro. 1979. Metabolic similarities between fertilization and phagocytosis: conservation of a peroxidatic mechanism. *J Exp. Med.* **149:** 938–953.

Kudo, S., and M. Inoue. 1986. A bactericidal effect of fertilization envelope extract from fish eggs. *Zool. Sci. (Tokyo)* **3:** 323–329.

Kudo, S., A. Sato, and M. Inoue. 1988. Chorionic peroxidase activity in eggs of the fish *Tribolodon hakonensis*. *J Exp. Zool.* **245:** 63–70.

Kudo, S., and M. Inoue. 1989. Bactericidal action of fertilization envelope extract from eggs of the fish *Cyprinus carpio* and *Plecoglossus altivelis*. *J. Exp. Zool.* **250:** 219–228.

Kudo, S., and C. Teshima. 1991. Enzymes activities and antifungal action of fertilization envelope extract from fish eggs. *J. Exp. Zool.* **259:** 392–398.

Kudo, S. 1992. Enzymatic basis for protection of fish embryos by the fertilization envelope. *Experientia* **48:** 277–281.

Lin, Q. 1992. Assembly of the embryonic envelopes in the marine shrimp *Sicyonia ingentis:* morphology and lectin binding affinities. M. S. Thesis. Louisiana State University, Baton Rouge, LA. 100 pp.

Lindsay, L. L., and W. H. Clark. 1992. Protease-induced formation of the sperm acrosomal filament. *Dev. Growth Differ.* **43:** 189–197.

Lowry, O. H., N. J. Rosenbrough, A. L. Farr, and R. J. Randall. 1951. Protein measurement with the folin phenol reagent. *J Biol. Chem.* **193:** 265–275.

Lynn, J. W., R. L. Goddard, P. Glas, and J. D. Green. 1988. Fertilization envelope assembly in sea urchin eggs inseminated in Cl^- deficient sea water: I. Morphological effects. *Gam Res.* **21:** 135–149.

Lynn, J. W., M. C. Pillai, P. S. Glas, and J. D. Green. 1991. Comparative morphology and physiology of egg activation in selected penaeoidea. Pp. 47–64 in *Frontiers in Shrimp Research*, M. A. Davidson and W. J. Dougherty, eds. Elsevier Science Publishers, Amsterdam.

Lynn, J. W., P. S. Glas, and J. D. Green. 1992. Assembly of the hatching envelope around the eggs of *Trachypenaeus similis* and *Sicyonia ingentis* in a low sodium environment. *Biol. Bull.* **183:** 84–93.

Lynn, J. W., P. S. Glas, P. L. Hertzler, W. H. Clark, Jr., and J. D. Green. 1993. Manipulations of shrimp embryos: a viable technique for the removal of the hatching envelope. *J World Aquacult. Soc.* **24:** 1–5.

Pillai, M. C., and W. H. Clark, Jr. 1987. Oocyte activation in the marine shrimp, *Sicyonia ingentis*. *J. Exp. Zool.* **244:** 325–329.

Pillai, M. C., and W. H. Clark, Jr. 1988. Hatching envelope formation in shrimp (*Sicyonia ingentis*) ova: origin and sequential exocytosis of cortical vesicles. *Tissue & Cell* **20:** 941–952.

Pillai, M. C., and W. H. Clark, Jr. 1990. Development of cortical vesicles in *Sicyonia ingentis* ova: their heterogeneity and role in elaboration of the hatching envelope. *Mol. Reprod Dev.* **26:** 78–89.

Pillai, M. C., F. J. Griffin, and W. H. Clark, Jr. 1988. Induced spawning of the decapod crustacean *Sicyonia ingentis*. *Biol Bull.* **174:** 181–185.

Schuel, H. 1978. Secretory functions of egg cortical granules in fertilization and development: a critical review. *Gam. Res.* **1:** 299–382.

Schuel, H. 1985. Functions of egg cortical granules. Pp. 1–43 in *Biology of Fertilization*, C. B. Metz and A. Monroy, eds. Academic Press, Orlando, FL.

Schmell, E. D., B. J. Gulyas, and J. L. Hedrick. 1983. Egg surface changes during fertilization and the molecular mechanism of the block to polyspermy. Pp. 365–413 in *Mechanisms and Control of Animal Fertilization*, J. F. Hartman, ed. Academic Press, New York.

Showman, R. M., and C. A. Foerder. 1979. Removal of the fertilization membrane of sea urchin embryos employing aminotriazole. *Exp. Cell Res.* **120:** 253–255.

Stevenson, R. J. 1985. Dynamics of the integument. Pp. 1–42 in *Integuments, Pigments, and Hormonal Processes*, D. E. Bliss and L. H. Mantel, eds. Academic Press, Orlando, FL.

Somers, C. E., D. E. Battaglia, and B. M. Shapiro. 1989. Localization and developmental fate of ovoperoxidase and proteoliaisin, two proteins involved in fertilization envelope assembly. *Dev. Biol.* **131:** 226–235.

Spurr, A. R. 1969. A low-viscosity epoxy resin embedding media for electron microscopy. *J Ultrastruct. Res.* **26:** 31–43.

Talbot, P., and M. Goudeau. 1988. A complex cortical reaction leads to formation of the fertilization envelope in the lobster, *Homarus*. *Gam. Res.* **19:** 1–18.

Turner, E., L. J. Hager, and B. M. Shapiro. 1988. Ovothiol replaces glutathione peroxidase as a hydrogen peroxide scavenger in sea urchin eggs. *Science* **242:** 939–941.

Turner, E., R. Klevit, P. B. Hopkins, and B. M. Shapiro. 1986. Ovothiol: a novel thiohistidine compound from sea urchin eggs that confers NAD(P) H-O_2 oxidoreductase activity on ovoperoxidase. *J. Biol. Chem.* **261:** 13056–13063.

Turner, E., C. E. Somers, and B. M. Shapiro. 1985. The relationship between a novel NAD(P) H oxidase activity of ovoperoxidase and the CN^--resistant respiratory burst that follows fertilization of sea urchin eggs. *J Biol Chem* **260:** 13163–13171.

Venable, J. H., and R. Coggeshall. 1965. A simplified lead citrate stain for use in electron microscopy. *J. Cell Biol.* **25:** 407.

Veron, M., C. A. Foerder, E. M. Eddy, and B. M. Shapiro. 1977. Sequential biochemical and morphological events during assembly of the fertilization membrane of the sea urchin. *Cell* **10:** 321–328.

Wasserman, P. M. 1987. The biology and chemistry of fertilization. *Science* **235:** 553–560.

Weidman, P. J., E. S. Kay, and B. M. Shapiro. 1985. Assembly of the sea urchin fertilization membrane: isolation of proteoliaisin, a calcium-dependent ovoperoxidase binding protein. *J Cell Biol.* **100:** 938–946.

Weidman, P. J., D. C. Teller, and B. M. Shapiro. 1987. Purification and characterization of proteoliaisin, a coordinating protein in fertilization envelope assembly. *J Biol. Chem* **262:** 15076–15084.

Whitaker, J. E., P. L. Moore, R. P. Haugland, and R. P. Haugland. 1991. Dihydrotetramethylrosamine: a long wavelength, fluorogenic peroxidase substrate evaluated *in vitro* and in a model phagocyte. *Bioch. Biophys Res Comm.* **175:** 387–393.

Reference: *Biol. Bull* **189**: 22–28. (August, 1995)

Sensitivity of Metabolic Rate, Growth, and Fecundity of Tadpole Shrimp *Triops longicaudatus* to Environmental Variation

DAVID A. SCHOLNICK

University of Colorado, Department of E.P.O. Biology, Boulder, Colorado 80309

Abstract. The influence of fluctuations of ambient oxygen tensions and temperature on the rate of oxygen consumption ($\dot{V}O_2$) was determined for the tadpole shrimp, *Triops longicaudatus*. $\dot{V}O_2$ was oxygen dependent up to 185 torr P_{O_2}, and Q_{10} for oxygen consumption between 20° and 30°C was 1.9. From these results it was estimated that oxygen consumption increases more than 1100 $\mu l \cdot g^{-1} \cdot h^{-1}$ in *T. longicaudatus* for typical diurnal changes in temperature and oxygen in desert ephemeral pools. Elevated $\dot{V}O_2$ may be coupled with increased growth rate and fecundity, because these characteristics were highly sensitive to changes in ambient temperature and oxygen tension. Depressing mean daily temperatures by 2.3°C significantly decreased body mass, whereas hyperoxia (200 torr) significantly increased growth compared to that of animals raised under hypoxic conditions (70 torr). Fecundity was dependent on animal mass and ambient oxygen tension. Thus, for a 22-day season, one *T. longicaudatus* female could produce 30 more eggs per 10 torr increase in oxygen tension and 43 more eggs per 1°C change in mean daily temperature. These results indicate that there are selective pressures for metabolic sensitivity to the high temperature–high oxygen conditions of the ephemeral environments inhabited by *T. longicaudatus*.

Introduction

Tadpole shrimp (*Triops longicaudatus* LeConte) are primitive branchiopod crustaceans that face extreme environmental conditions in the ephemeral desert pools that they inhabit. These pools are characterized by large diurnal oscillations (greater than 200 torr O_2 per day) in the dissolved gasses produced by the photosynthesis and metabolism of their biota, and by large and rapid fluctuations in water temperature (greater than 15°C per day; Scholnick, 1994). In addition, pool water may persist for as little as 10 days during the summer when evaporation rates are high. As a result, species such as *T. longicaudatus*, which survive dry periods as dormant eggs, must complete their life cycles rapidly while experiencing extreme environmental fluctuations.

Metabolic control in tadpole shrimp presents a unique problem because of the need for rapid development in a variable environment. Only a few physiological studies have been conducted on tadpole shrimp. Horne (1971) and Scott and Grigarick (1979) reported that *Triops* eggs do not hatch until temperatures are greater than 14°C. Hillyard and Vinegar (1972) reported that oxygen consumption in immature *T. longicaudatus* was three times more sensitive to temperature than in adults. In another species of tadpole shrimp (*Lepidurus lemmoni*), metabolism was sensitive to changes in ambient oxygen tensions (Eriksen and Brown, 1980). Therefore, it is unclear what effects simultaneous fluctuations of both oxygen and temperature have on the metabolism, growth, and reproductive success of tadpole shrimp inhabiting desert ephemeral pools.

This investigation examines the influence of simultaneous fluctuations in oxygen and temperature, which occur naturally in desert ephemeral habitats, on rates of oxygen uptake in *Triops longicaudatus*. The effects of these fluctuations on growth and fecundity were also examined.

Materials and Methods

Specimens of *Triops longicaudatus* LeConte were hatched from and raised with rehydrated soils collected from four previously studied ephemeral pools near Moab,

Received 29 September 1994, accepted 26 May 1995.

Utah (Scholnick, 1994). Soils containing eggs from the four pools were mixed and randomly subsampled for different treatments. Animals were raised in plastic tubs (70 × 50 × 13 cm) or 10-gallon glass aquaria under cycles of temperature (18°–32°C) and light (12L:12D) to simulate summer conditions. Diets consisted of naturally occurring protozoa and algae of rehydrated soils, supplemented with commercially purchased live *Tubifex*.

Metabolic measurements

Respiration rates ($\dot{V}O_2$, microliters of oxygen consumed per gram wet weight per hour, standardized to STP) were determined for oxygen tensions of 77, 127, and 185 torr at 20°, 25°, and 30°C. $\dot{V}O_2$ values were determined in a temperature-equilibrated flow-through system. The system consisted of an elevated 4.5-l water reservoir that was equilibrated with different partial pressures of O_2 and used as a pressure head to maintain constant flow. Flow was measured volumetrically and regulated by the height of the reservoir and the diameter of the tubes. Flow rates were set between 6.5 and 8 $ml \cdot min^{-1}$, depending on animal size and temperature, and were held constant throughout each experiment (less than 0.1 ml change over 5 h). The oxygen content of the water was measured with an Orion oxygen meter and probe (#840 Orion Research, Boston) fitted with a 0.5-ml flow-through cell and a stir bar. Voltage output was connected to a personal computer through an analog-to-digital converter and sampled every 20 s. A 133-ml animal chamber was suspended in a water bath equipped with a thermostat and was continually stirred with an enclosed stir bar to ensure mixing. Water was collected downstream and pumped back to the reservoir with a water pump. A series of valves made it possible to measure the oxygen content of the incurrent water (water coming directly from the reservoir) or the excurrent water (water coming directly from animal chamber) without disrupting flow.

Animals of similar masses (mean of 364 ± 10.5 mg ranging from 290 to 440 mg) were given 1 h to adjust to the temperature and oxygen tensions of the chamber before measurements began. Animals were selected from simulated pools at predetermined times when oxygen and temperature levels were similar to experimental conditions. $\dot{V}O_2$ was measured for individual animals, and each animal was measured only once. Measurement periods ranged from 3 to 4 h for each animal at a given temperature and P_{O_2}.

The design of the animal chamber and oxygen sampling system conformed to the principles of a single-chamber system as defined in Frappell *et al.* (1989). In this system, the time constant for the washout of oxygen for the animal chamber and from the electrode chamber ($\tau_1 + \tau_2$) was 24 min, while the time constant for the electrode circuit alone (τ_2) was less than 2 min. Because τ_2 was reasonably small with respect to ($\tau_1 + \tau_2$) the system could be considered a single chamber in which $\tau_2 = 0$.

Measurements of growth

Growth rates of *T. longicaudatus* under natural conditions were determined in four study pools near Moab, Utah, during the summer of 1993. Animals were individually caught in a small sieve, blotted dry through the sieve, and weighed. Animals were held in a beaker containing pool water until all animals were weighed. Wet weight was determined daily by weighing 10 to 20 animals from each pool on an Ohaus portable balance (#CT 10-3, Florham, Park, NJ).

The influence of temperature on growth rate was determined, as described above, in laboratory-simulated ephemeral pools where the average temperature was either 25.7° or 23.4°C. For the high-temperature condition (mean = 25.7°C), temperatures were cycled between 19° and 31°C by using heat lamps; the average temperature change was $0.85°C \cdot h^{-1}$. For the low-temperature condition (mean = 23.4°C), temperature fluctuated from 19° to 29°C; average temperature change was $0.65°C \cdot h^{-1}$. Animals were hatched at treatment temperature cycles, and growth rates were determined from daily measurements of wet weight. Average oxygen partial pressure of 125 ± 2 torr was maintained in each treatment by vigorously bubbling air into each tank. Temperature treatments were replicated five times with 4–5 animals in each tank at the beginning of the experiment.

Sensitivity of growth to oxygen was determined from animals raised in laboratory-simulated pools as described above at 200 ± 5 and 70 ± 7 torr P_{O_2} by either continually bubbling 100% oxygen or 13% oxygen, remainder nitrogen. Temperature was cycled in a manner identical to the low-temperature condition described above, and growth rates were determined by changes in wet weight per day. Oxygen treatments were replicated five times with 3–5 animals in each tank at the beginning of the experiment. Animals were hatched at treatment temperature cycles and growth rates were determined from daily measurements of wet weight.

Fecundity

Animals were raised in simulated ephemeral pools where temperature and light were cycled at 125 or 200 torr O_2 as described above. Fecundity, or egg production, was determined by chilling gravid animals (eggs were visible in brood pouches) to 8°C. When animals became hypothermic, the brood pouches opened and the eggs were released. All eggs released per female were collected and counted. Brood pouches were checked to ensure that all eggs had been liberated. This procedure resulted in zero

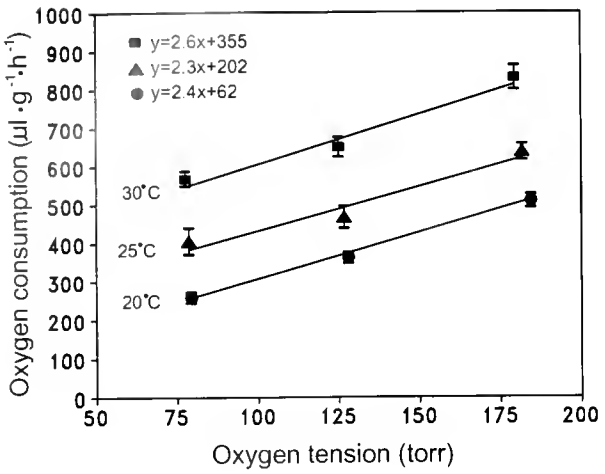

Figure 1. Mean oxygen consumption (microliters of oxygen per gram wet weight per hour) at different oxygen tensions for *Triops longicaudatus*. Values presented are means ± SEM. Lines represent linear regressions with r^2 greater than 0.7 in all cases.

adult mortality. However, egg viability appeared to be severely compromised as a result of the "forced" release. Attempts to dry and rehydrate eggs were unsuccessful.

Statistics and calculations

An analysis of covariance was applied to the mean weights for each treatment group to determine statistical differences between growth rates. ANCOVA was weighted by the number of individuals in each tank to account for uncontrollable differences in animal number. Higher sample size was assumed to be a more accurate predictor of mean population mass and was therefore given more weight in the analysis. A probability of ≤0.05 was considered statistically significant.

Sensitivity of oxygen consumption to change in temperature, Q_{10}, was calculated by using the general formula:

$$Q_{10} = (M_2/M_1)^{10/(T_2-T_1)}$$

where M_2 and M_1 are metabolic rates at the higher (T_2) and lower (T_1) temperatures, respectively.

In order to reduce mass-specific effects, animals of similar masses were chosen for metabolic measurements. Because mass did not vary significantly between treatment groups ($p < 0.05$ ANOVA), $\dot{V}O_2$ ($\mu l \cdot g^{-1} \cdot h^{-1}$) was determined by dividing oxygen consumption by wet mass.

Results

Rates of oxygen consumption ($\dot{V}O_2$) in *Triops longicaudatus* are sensitive to changes in ambient temperature and oxygen (Fig. 1). Temperature sensitivity, or Q_{10}, at 125 torr was 1.85 between 20° and 30°C, 1.82 between 20° and 25°C, and 1.92 between 25° and 30°C. There was a positive linear relationship between $\dot{V}O_2$ and oxygen tension throughout the physiological range. Temperature had very little effect on oxygen sensitivity. The average change in $\dot{V}O_2$ per torr oxygen tension was 2.5 $\mu l \cdot g^{-1} \cdot h^{-1}$.

Changes in $\dot{V}O_2$ for oxygen and temperature fluctuations typical of diurnal cycles in desert pools (Scholnick, 1994) were predicted from the metabolic responses presented in Figure 1. Metabolic rates were estimated to increase more than sixfold during a typical diurnal cycle (Fig. 2) when temperature and oxygen vary between 18° and 32.5°C and 60 and 226 torr, respectively. Therefore, animals could experience a change in $\dot{V}O_2$ as great as 1100 $\mu l \cdot g^{-1} \cdot h^{-1}$ during a single 6-h diurnal period. Growth rates in the field ranged from 97.7 to 44.7 mg · day^{-1} between pools (Fig. 3). The average growth rate for field animals was 53 mg · day^{-1}, similar to the rate of about 57 mg · day^{-1} for animals raised in the laboratory (Fig. 4). Depressing the mean daily temperatures by 2.3°C resulted in a significant decrease in body mass ($p < 0.02$ ANCOVA; Fig. 4). On average, animals raised at the higher temperature cycle weighed over 80 mg more than those raised at the low temperature cycle after 5 days of age. At day 9, about the time when egg laying is initiated, body mass was 27% greater for animals raised at the higher average daily temperature.

Animals raised under hyperoxic conditions (200 torr) grew significantly faster (an increase of more than twofold until day 20) and were significantly larger ($p < 0.01$ ANCOVA) at every age over 5 days than animals raised under hypoxic conditions (70 torr; Fig. 5). The results for the

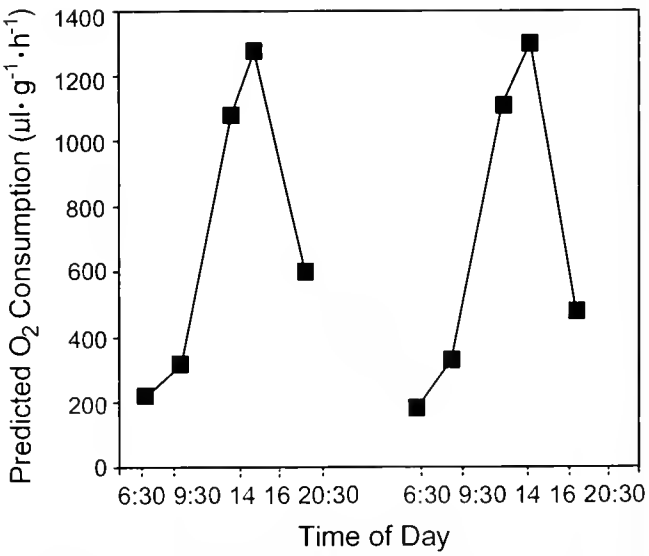

Figure 2. Predicted change in oxygen consumption rates (microliters per gram per hour) for *Triops longicaudatus* for typical diurnal fluctuations in oxygen and temperature measured in the field (Scholnick, 1994). Changes in oxygen consumption rates are based on temperature and oxygen sensitivity presented in Figure 1.

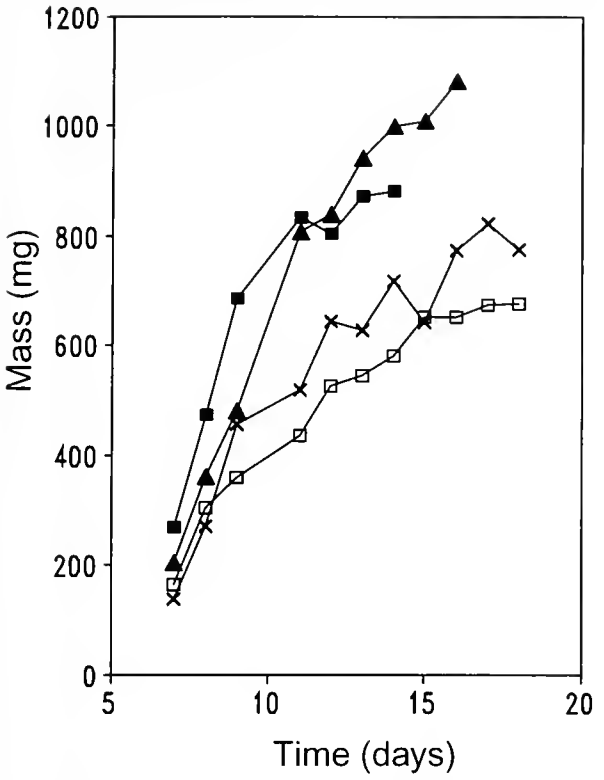

Figure 3. Growth rates for *Triops longicaudatus* from four desert pools near Moab, Utah, during the summer months of 1993. Each point represents an average wet mass of 10–20 animals in each pool.

oxygen and temperature treatments were statistically identical whether the entire growth curve (linearized using log time) or only the linear portion of the curve was used.

There was a positive linear relationship between number of eggs and wet mass (Fig. 6). At a PO_2 of 200 torr, the brood pouches of an 800-mg animal contained an average of 50 more eggs than those of a 300-mg animal. Rearing temperature (mean cyclic temperature of either 25.7° or 23.4°C) had no effect on the relationship between body mass and egg number. The slope of the regression line for animals raised at elevated ambient oxygen tensions (200 torr) was significantly greater than that of the regression line for animals raised at oxygen saturation (125 torr O_2; $p < 0.01$ ANCOVA).

Small changes in temperature or oxygen dramatically change the estimate of total number of eggs laid in one season (Table 1). Based on the independent influence of temperature or oxygen on body mass (Figs. 4 and 5) and the relationship between body mass and fecundity (Fig. 6), an increase of 2°–3°C in average diurnal temperature was calculated to increase fecundity by about 99 eggs over a 22-day period. This estimate assumes that animals produce one brood every 3 days (estimated from Ahl, 1983) and the first brood is produced at a wet weight of 200 mg (Fig. 6; Table 1). Animals experiencing hyperoxic conditions could produce 378 more eggs over a 22-day season than animals raised under hypoxic conditions at the lower average daily temperature (Table 1).

Discussion

The results presented in this study indicate that *Triops longicaudatus* maintains a high degree of metabolic sensitivity despite the wide range of environmental conditions in its natural habitat. The net effect of temperature and oxygen sensitivity is to increase oxygen consumption during the day when temperature and oxygen tensions are high. Development and fecundity are related to PO_2 and temperature, and hence to elevated $\dot{V}O_2$. Shortened development time and increased fecundity are critical for successful completion of life cycles in ephemeral environments.

Branchiopods are primitive crustaceans that are often prominent in ephemeral systems (Hessler *et al.*, 1982).

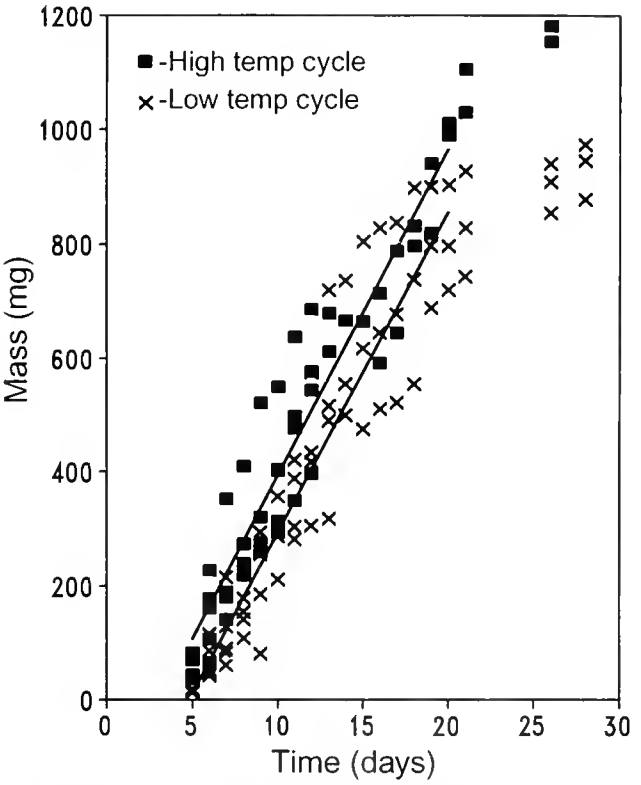

Figure 4. Effect of cyclic temperature regimes on growth rate of *Triops longicaudatus*. Each point represents the mean wet mass of all animals raised in a single pool (see Materials and Methods for details). Squares represent mean wet mass for animals raised at a mean temperature of 25.7°C, cycled between 19° and 31°C ($y = 57.7x - 190.7$, $r^2 = 0.91$). Crosses represent mean wet mass for animals raised at a mean temperature of 23.4°C, cycled between 19° and 29°C ($y = 56.8x - 271.3$, $r^2 = 0.89$). Positions of regression lines were significantly different ($p < 0.02$).

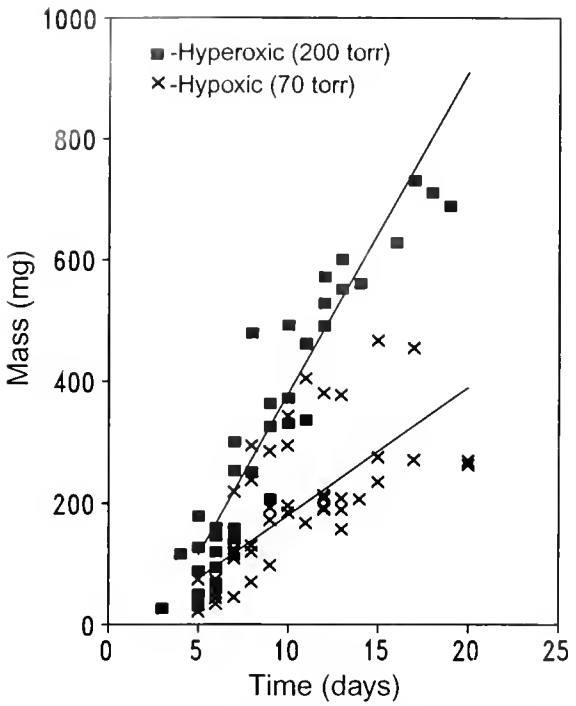

Figure 5. Effect of oxygen tension on growth rate of *Triops longicaudatus* Each point represents the mean mass of all individuals in a single pool (see Materials and Methods for details). Squares represent mean wet mass for animals raised at constant hyperoxia (200 torr). Crosses represent mean wet mass for animals raised at constant hypoxia (70 torr). Slopes of lines are significantly different (ANCOVA $p < 0.01$).

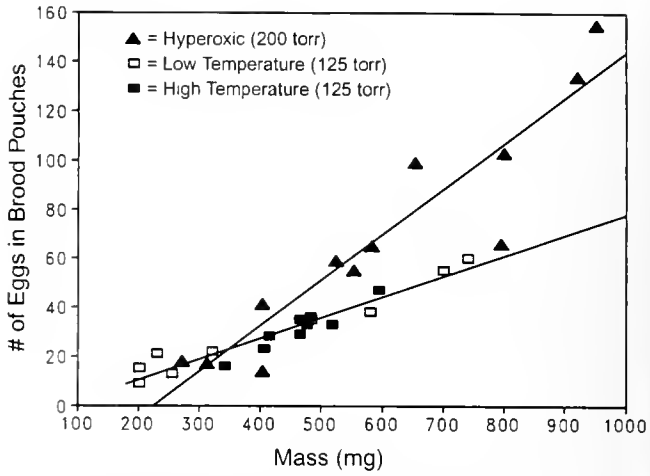

Figure 6. Relationship between mass and fecundity for *Triops longicaudatus* Triangles represent animals raised at constant hyperoxic conditions (200 torr) and a mean temperature of 25.7°C, cycled between 19° and 31°C. Open squares represent animals raised at a mean temperature of 23.4°C (cycled between 19° and 29°C), and closed squares represent animals raised at mean temperature of 25.7°C (cycled between 19° and 31°C) and normoxia. Regression lines are for all data at 125 torr and animals raised at hyperoxia. Slope of hyperoxic line is significantly different than temperature line (ANCOVA $p < 0.05$).

The two extant genera of Notostraca (*Triops* and *Lepidurus*) exhibit an extremely high degree of morphological stasis (Fryer, 1985). The specific adaptations these species use may have evolved quite early and remained relatively unchanged throughout geologic time. Of the two genera, *Triops* prefers warm habitats, whereas *Lepidurus* prefers cooler regions and more permanent pools (Fryer, 1988). Eriksen and Brown (1980) determined that $\dot{V}O_2$ in *Lepidurus lemmoni* is dependent upon both oxygen (35% decrease in $\dot{V}O_2$ from saturation to critical O_2) and temperature (Q_{10} ranging from 2.1 to 2.7 from 18°–28°C). In addition, Shtcherbakov and Muragina (1953) reported a Q_{10} of 2.2 at 15°C for *Triops cancriformis*, and Hillyard and Vinegar (1972) reported a lower Q_{10} of 1.55 between 26° and 30°C for *T. longicaudatus*, although it is unclear what oxygen tensions were used to measure metabolic rate. The relatively high temperature sensitivity of the Notostraca suggests that diurnal fluctuations in temperature, even in vernal pools where oscillations may be less extreme (Wiggins *et al.*, 1980), may be essential to elevate metabolism and thus increase rates of growth and reproduction.

Many crustaceans from environments that regularly experience large fluctuations of oxygen and temperature are known to regulate oxygen consumption (see Taylor, 1988, for a review). Numerous mechanisms, including increasing ventilation volume and changing heart rate, pH, or the oxygen-transporting properties of the blood, have been shown to aid in the regulation of oxygen uptake. Thus, metabolic independence appears to be adaptive for many crustaceans. The results presented here suggest the opposite—that there are strong selection pressures on *T. longicaudatus* to maintain metabolic sensitivity in predictably high temperature–high oxygen environments.

Lowering the average ambient temperature by 2.3°C significantly decreased the body mass of the tadpole shrimp but did not change rate of growth except early in life (<5 days). This result suggests that temperature sensitivity before adulthood may be critical. Hillyard and

Table I

Estimated fecundity of a single female T. longicaudatus *over a 22-day season*

	Day first clutch oviposited	Cumulative no. of eggs laid
High temp. cycle (25.7°C)	7	287
Low temp. cycle (23.4°C)	8	188
Hyperoxic (200 torr)	7	452
Hypoxic (70 torr)	11	74

Assuming one clutch oviposited every 3 days (estimated from Ahl, 1983) and first clutch oviposited at 200 mg wet mass (Fig. 5).

Vinegar (1972) reported that, between 26° and 30°C, *T. longicaudatus* oxygen consumption rates were almost three times more temperature-sensitive in immature animals than in adult animals. Therefore, temperature sensitivity in *Triops* may be elevated immediately after hatching, when pools have recently filled and temperature fluctuations are reduced (Scholnick, 1994).

Unlike changes in temperature, changes in ambient oxygen tensions affect growth rate throughout the life of the animal. This result is not surprising considering the large metabolic oxygen sensitivity exhibited by *T. longicaudatus*. The dependence of metabolism on oxygen tension, even above saturation, suggests that oxygen diffusion is limiting $\dot{V}O_2$ throughout the physiological range of the animal. Although an extracellular hemoglobin with a relatively high affinity for oxygen has been described for *T. longicaudatus* (P_{50} = 6.8 at pH = 7 and 22°–23°C; Horne and Beyenbach, 1971), the unspecialized respiratory structures (bulbous epipodite, Fryer, 1988; and entire abdominal phyllopod) in this primitive crustacean—unlike the specialized respiratory structures in more advanced crustacea—appear to be inadequate for adjusting oxygen delivery at variable oxygen tensions. In view of the high degree of morphological stasis exhibited by tadpole shrimp (Fryer, 1985) and the possible reproductive advantages of maintaining oxygen sensitivity, the selection pressure for more specialized respiratory structures is probably low.

T. longicaudatus does not appear to fit the typical pattern of an active oxygen conformer (for reviews see Herreid, 1980; Prosser, 1991). $\dot{V}O_2$ in *T. longicaudatus* is highly dependent on ambient oxygen tensions well above oxygen saturation. Therefore, $\dot{V}O_2$ is seemingly influenced by ambient oxygen tension at all oxygen tensions within this species' physiological range. Few studies have examined the physiological effects of hyperoxia; however, ventilation was found to decrease in both crayfish (Massabuau *et al.*, 1984) and lugworm (Toulmond and Tchernigovtzeff, 1984) in response to an increase in oxygen. In the few decapod crustaceans studied, $\dot{V}O_2$ remains independent of oxygen tensions above saturation (Dejours and Beekenkamp, 1977; Jouve-Duhamel and Truchot, 1983). *T. longicaudatus* apparently does not stabilize $\dot{V}O_2$ against hyperoxia. Furthermore, predawn measurements of oxygen in ephemeral desert pools (Scholnick, 1994) indicate that partial pressures of oxygen typically do not drop below 40 torr and should therefore not have a large negative effect on $\dot{V}O_2$.

Growth in *T. longicaudatus* is dependent on high temperature. In addition, growth and survivorship are strongly influenced by the large fluctuations of temperature and oxygen that are characteristic of these habitats (Horne, 1971; Scholnick, 1994). Horne (1971) and Scott and Grigarick (1979) found that *T. longicaudatus* eggs did not hatch until temperatures were greater than 14°C and that the rates of hatching were highest above 22°C (Takahashi, 1977). Additionally, Scott and Grigarick (1978) reported high mortality rates and slow growth rates (about 9 times lower growth rates than those reported in this study) for animals raised at 25° or 30°C compared to those raised under diurnal oscillations, as in this study. Therefore, hatching, growth rate, and survivorship in *T. longicaudatus* all appear to be extremely dependent on the high temperature conditions characteristic of ephemeral desert pools.

A small change in average daily temperature or oxygen tension has a large effect on the total number of eggs that can be laid in a season. Calculations based on differences in mass indicate that over a 22-day season an individual can produce about 30 more eggs in response to an increase of 1°C in mean temperature. In addition, a 10-torr increase in ambient oxygen results in production of about 43 more eggs during a 22-day season. Therefore, small changes in temperature, oxygen, or both between seasons can dramatically affect fecundity and reproductive success. The dependence of initial oviposition times on temperature and oxygen would exaggerate this effect when rainfall is limited and seasons are compressed. Ahl (1991) and Seaman *et al.* (1991) reported a similar relationship between carapace length and fecundity for the tadpole shrimp *Lepidurus packardi* and *Triops granarius*, respectively. Although it was not possible to measure egg viability, a change in viability would be unlikely to offset the large effect of oxygen and temperature on fecundity. Food for tadpole shrimp is abundant in ephemeral pools (Dodson, 1987), suggesting that the limiting factor in these environments is not food availability but the time necessary to complete the life cycle.

The results from this investigation suggest that metabolic sensitivity in high temperature–high oxygen environments enhances the reproductive success of *Triops longicaudatus*. Shortened development times and increased fecundity are critical for success in ephemeral environments. Because $\dot{V}O_2$ is associated with aerobic energy metabolism and appears to be diffusion-limited in *Triops longicaudatus*, the combination of hyperoxia and high temperature may engender a higher rate of energy metabolism and in turn a higher growth and reproductive output. Thus, there appear to be reproductive advantages for metabolic sensitivity to the hot, hyperoxic conditions in the ephemeral pools inhabited by *Triops longicaudatus*.

Acknowledgments

The author is grateful to Dr. G. K. Snyder for valuable advice and comments on the manuscript. This work was supported in part by National Science Foundation Grant DCB8818647 to G. K. Snyder.

Literature Cited

Ahl, J. S. 1983. The reproductive biology and the availability of eggs to oversummer in the tadpole shrimp, *Lepidurus packardi*. Thesis, California State University, Chico. 21 pp.

Ahl, J. S. 1991. Factors affecting contributions of the tadpole shrimp, *Lepidurus packardi*, to its oversummering egg reserves. *Hydrobiologia* **212**:137–143.

Dejours, P., and H. Beekenkamp. 1977. Crayfish respiration as a function of oxygenation. *Respir. Physiol.* **30**:241–251.

Dodson, S. I. 1987. Animal assemblages in temporary desert rock pools: aspects of the ecology of *Dasyhelea sublettei* (Diptera: Ceratopogonidae). *J. North Am. Benthol. Soc.* **6**:65–71.

Eriksen, C. H., and R. J. Brown. 1980. Comparative respiratory physiology and ecology of phyllopod crustacea. III. Notostraca. *Crustaceana* **39**:22–32.

Frappell, P. B., H. A. Blevin, and R. V. Baudinett. 1989. Understanding respirometry chambers: what goes in must come out. *J. Theor. Biol.* **138**:479–485.

Fryer, G. 1985. Structure and habits of living branchiopod crustaceans and their bearing on the interpretation of fossil forms. *Trans. R. Soc. Edinb.* **76**:103–113.

Fryer, G. 1988. Studies on the functional morphology and biology of the Notostraca (Crustacea: Branchiopoda). *Philos. Trans. R. Soc. Lond. B* **321**:27–124.

Herreid, C. F. 1980. Hypoxia in invertebrates. *Comp. Biochem. Physiol. A* **67**:311–320.

Hessler, R. R., B. Marcotte, W. Newman, and R. Maddocks. 1982. Evolution within the crustacea. Pp. 150–179 in *The Biology of Crustacea*, Vol 1, L. Abele, ed. Academic Press, New York.

Hillyard, S. D., and A. Vinegar. 1972. Respiration and thermal tolerance of the phyllopod crustacean *Triops longicaudatus* and *Thamnocephalus platyurus* inhabiting desert ephemeral ponds. *Physiol. Zool.* **45**:189–196.

Horne, F. R. 1971. Some effects of temperature and oxygen concentration on phyllopod ecology. *Ecology* **52**:343–347.

Horne, F. R., and K. W. Beyenbach. 1971. Physiological properties of hemoglobin in the branchiopod crustacean *Triops*. *Am. J. Physiol.* **220**:1875–1880.

Jouve-Duhamel, A., and J. P. Truchot. 1983. Ventilation in the shore crab *Carcinus maenas* (L.) as a function of ambient oxygen and carbon dioxide: field and laboratory studies. *J. Exp. Mar. Biol. Ecol.* **70**:281–296.

Massabuau, J. C., P. Dejours, and Y. Sakakibara. 1984. Ventilatory CO_2 drive in the crayfish: influence of oxygen consumption level and water oxygenation. *J. Comp. Physiol. B* **154**:65–72.

Prosser, C. L. 1991. *Environmental and Metabolic Animal Physiology*. Wiley-Liss, New York, pp. 409–411.

Scholnick, D. A. 1994. Seasonal variation and diurnal fluctuations in ephemeral desert pools. *Hydrobiologia* **294**:111–116.

Scott, S. R., and A. A. Grigarick. 1978. Observations on the biology and rearing of the tadpole shrimp *Triops longicaudatus* (LeConte) (Notostraca: Triopsidae). *Wasmann J. Biol.* **36**:116–126.

Scott, S. R., and A. A. Grigarick. 1979. Laboratory studies of factors affecting egg hatch of *Triops longicaudatus* (LeConte) (Notostraca: Triopsidae). *Hydrobiologia* **63**:145–152.

Seaman, M. T., D. J. Kok, J. J. von Schlichting, and A. J. Kruger. 1991. Natural growth and reproduction in *Triops granarius* (Lucas) (Crustacea: Notostraca). *Hydrobiologia* **212**:87–94.

Shtcherbakov, A. P., and T. Muragina. 1953. Intensity of respiration in *Apus cancriformis* Schaff. *Zool. Zhur.* **32**:844–947.

Takahashi, F. 1977. Pioneer life of the tadpole shrimps, *Triops*, spp. (Notostraca: Triopsidae). *Appl. Entomol. Zool.* **12**:104–117.

Taylor, A. C. 1988. The ecophysiology of decapods in the rock pool environment. Pp. 227–261 in *Aspects of Decapod Crustacean Biology*, A. A. Finchman and P. S. Rainbow, eds. Clarendon Press, Oxford.

Toulmond, A., and C. Tchernigovtzeff. 1984. Ventilation and respiratory gas exchanges of the lugworm *Arenicola marina* (L.) as functions of ambient P_{O_2} (20–700). *Respir. Physiol.* **57**:349–363.

Wiggins, G. B., R. J. Mackay, and I. M. Smith. 1980. Evolutionary and ecological strategies of animals in annual temporary pools. *Archiv. Hydrobiol. Suppl.* **58**:97–206.

Reference: *Biol. Bull* **189**: 29–35. (August, 1995)

Microfilament Contraction Promotes Rounding of Tunic Slices: An Integumentary Defense System in the Colonial Ascidian *Aplidium yamazii*

EUICHI HIROSE[1] AND TERUHISA ISHII[2]

[1]*Biological Laboratory, College of Agriculture and Veterinary Medicine, Nihon University, Fujisawa, Kanagawa 252, Japan; and* [2]*Shimoda Marine Research Center, University of Tsukuba, Shimoda, Shizuoka 415, Japan*

Abstract. In *Aplidium yamazii*, when a slice of a live colony (approximately 0.5 mm thick) was incubated in seawater for 12 h, the slice became a round tunic fragment. This tunic rounding was inhibited by freezing of the slices, incubation with Ca^{2+}-Mg^{2+}-free seawater, or addition of cytochalasin B. Staining of microfilaments in the slices with phalloidin-FITC showed the existence of a cellular network in the tunic. Contraction of this cellular network probably promotes rounding of the tunic slice. In electron microscopic observations, a new tunic cuticle regenerated at the surface of the round tunic fragments; the tunic cuticle did not regenerate in newly sliced specimens nor in specimens in which rounding was experimentally inhibited.

Based on these results, an integumentary defense system is proposed in this species as follows. (1) When the colony is wounded externally, contraction of the cellular network promotes tunic contraction around the wound. (2) The wound is almost closed by tunic contraction. (3) Tunic contraction increases the density of the filamentous components of the tunic at the wound, and it may accelerate the regeneration of tunic cuticle there.

Introduction

The integumentary tissues of metazoans commonly function to protect the body from a hostile environment and as a transporting surface, and they display various structures. Some of these tissues have a keratinous, collagenous, or chitinous cuticle, and some have a ciliated surface or a mucous layer. The body of urochordates (tunicates) is usually covered with a leathery or gelatinous matrix called the tunic. The tunic is a peculiar integumentary tissue in metazoans for the following two reasons. First, the tunic contains cellulosic fibers that link proteins (De Leo *et al.*, 1977; Van Daele *et al.*, 1992). Second, live free cells, called tunic cells, are distributed within the tunic, which is thus a mesenchyme-like tissue. In ascidians, the tunic cells are involved in various biological functions, such as phagocytic activity (De Leo *et al.*, 1981; Hirose *et al.*, 1994a), conduction of impulses (Mackie and Singla, 1987), and bioluminescence (Aoki *et al.*, 1989). Because it is unique, investigations on tunic morphology and functions may lend perspective to our understanding of integumentary and mesenchymal tissues.

Aplidium yamazii is a colonial ascidian (Polyclinidae, Aplousobranchia) with a gelatinous, transparent tunic in which elongated forms of zooids are embedded separately from each other. The tunic is overlaid by a thin cuticle, and the cuticular surface has numerous minute protrusions, each about 60 nm in height (Hirose *et al.*, 1990). The tunic cuticle has a dense structure that is probably an effective barrier to the invasion of microorganisms into the tunic. Various kinds of tunic cells are distributed in the tunic of this species (Hirose *et al.*, 1994b), and no colonial vascular network (tunic vessels) connects the zooids. When tunic slices are incubated in seawater, they spontaneously round up to form tunic balls. This phenomenon is presumed to represent the mechanism by which external injuries of the tunic are healed. In this study, we examine the mechanism of rounding of the slices and discuss its functions as an integumentary defense system of this tissue.

Received 18 November 1994; accepted 23 May 1995.

Materials and Methods

Animals

The colonies of *Aplidium yamazii* were collected in Nabeta Bay, Shimoda (Shizuoka Prefecture, Japan). They were temporarily kept in running seawater in the laboratory or reared in a culture box immersed in Nabeta Bay. *A. yamazii* forms a relatively flat colony, about 2 to 3 mm thick, spreading on a flat substratum; its rod-shaped zooids are embedded separately in a common tunic (Fig. 1).

Tunic rounding assay

Colonies were transversely sliced with a razor blade into pieces that were 0.5 mm thick or less (*e.g.*, 7 × 2 × 0.5 mm). The tunic slices (Hirose *et al.*, 1994a) were composed of tunic, tunic cells, and small fragments of zooids; many of the zooid fragments were washed out. The fresh tunic slices were placed in a plastic petri dish filled with filtered seawater (FSW) or artificial seawater (ASW), and were incubated overnight at 17° to 20°C. During the incubation, each specimen shrank and became a single tunic ball.

Video recording of tunic rounding

The tunic slices were put in a 100-ml beaker filled with FSW (16°–18°C), and the process of tunic rounding was recorded with a time-lapse videocassette recorder (AG-6010; National, Osaka, Japan) and a video camera (WV-1800; National) equipped with a 55-mm macro lens (Micro-Nikkor; Nikon, Tokyo). Recording was performed at about 1/60 of the actual speed. The time course of transformation was analyzed by hourly measurements of the length of the longest diagonal line that could be drawn within the profile of the rounding specimens.

Tunic rounding assay under experimental conditions

Some of the slices were frozen at −20°C, thawed at room temperature, and then incubated in ASW.

Live slices were incubated in three kinds of experimental media: Ca^{2+}-Mg^{2+}-free artificial seawater (CMF-ASW), various concentrations of colchicine-ASW, and various concentrations of cytochalasin B-ASW. Because cytochalasin B was dissolved in dimethylsulfoxide (DMSO) before dilution in ASW, the assay was also carried out in 1% DMSO-ASW as a control. All media also contained penicillin (100 IU/ml) and streptomycin (1 μg/ml).

Staining with phalloidin-fluorescein isothiocyanate (FITC)

Microfilaments were visualized in colony slices by labeling with phalloidin-FITC. The specimens were fixed with 3.5% formaldehyde in Ca^{2+}-free artificial seawater (CF-ASW) for 10 min, made permeable with 0.1% Triton X-100 in CF-ASW for 5 min, and washed with phosphate-buffered saline (PBS). They were incubated with 1 μg/ml phalloidin-FITC in PBS for 30 min and then were rinsed extensively with PBS. Some fixed specimens were embedded in O.C.T. compound so that cryostat sections could be made. Sections that were 20 μm thick were stained with 2 μg/ml phalloidin-FITC in PBS for 30 min and rinsed with PBS. These specimens were observed under a microscope equipped with epifluorescence and Nomarski differential interference contrast optics.

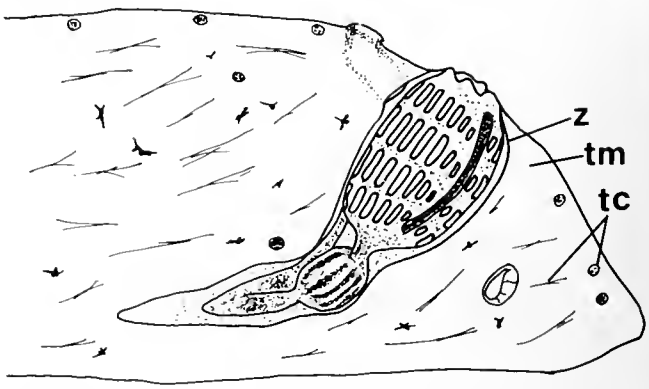

Figure 1. Schematic drawing showing the frontal section of a colony. A zooid (z) is embedded in the tunic matrix (tm). Tunic cells (tc) are distributed throughout the tunic. There are no blood vessels in the tunic.

Chemicals

ASW, CF-ASW, and CMF-ASW were obtained from Jamarine Lab., Osaka, Japan. Colchicine, cytochalasin B, and phalloidin-FITC were from Sigma Chemical Co., St. Louis, Missouri. O.C.T. compound was from Miles Inc., Naperville, Illinois.

Electron microscopy

The specimens were fixed in 2.5% glutaraldehyde-ASW or 2.5% glutaraldehyde-0.1 *M* cacodylate-0.45 *M* sucrose (pH 7.4). They were rinsed with the same buffer, postfixed in 1% osmium tetroxide-0.1 *M* cacodylate (pH 7.4), and dehydrated through graded ethanol. For scanning electron microscopy (SEM), the specimens were dried in a critical-point dryer, coated with Au-Pd, and examined in a Hitachi S-570 scanning electron microscope at 20 kV. For transmission electron microscopy (TEM), the dehydrated specimens were cleared with *n*-butyl glycidyl ether and embedded in low-viscosity epoxy resins. Thin sections were stained with uranyl acetate and lead citrate and were examined in a Hitachi HS-9 transmission electron microscope.

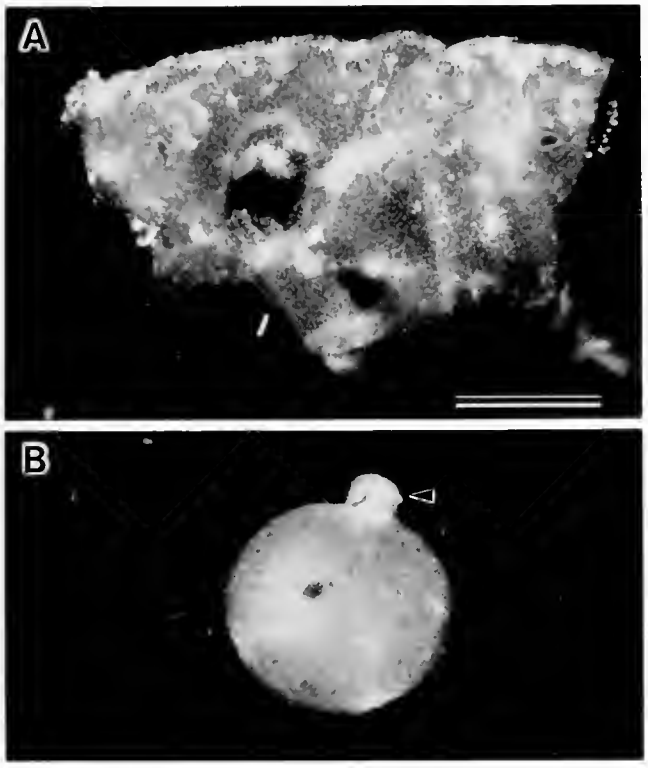

Figure 2. A freshly cut tunic slice (A) and a rounding tunic specimen after incubation in FSW for 24 h (B). Arrowhead indicates a zooid fragment extruded from the tunic ball. Magnifications of these two figure parts are the same. Scale bar = 1 mm.

Results

Freshly cut tunic slices were basically thin rectangular pieces of tunic (Fig. 2A), and each of them rounded up into an elastic tunic ball after incubation in ASW (Fig. 2B). The tunic ball was completely filled with tunic matrix, and no hollows remained. During the incubation, some of the zooid fragments were pushed out from the rounding tunic specimens, and the others were packed inside the tunic ball, but rounding occurred even if every zooid fragment in a tunic slice was lost. Tunic rounding, therefore, did not depend on the presence of zooids or zooid fragments. The size of a tunic ball depended on the initial size of the slice and the quantity of zooid fragments that were lost during rounding. For instance, tunic slices of about 2.5 × 5 × 0.5 mm transformed to tunic balls of 2 to 2.7 mm in diameter. In a few cases, one tunic slice would round up into two or three balls connected to each other by thin strands of tunic material, or a tunic slice deformed into a rodlike or irregularly shaped mass of tunic. Within a tunic ball or deformed tunic mass, the tunic cells were alive and some were motile. Noticeable tunic rounding began 4 to 5 h after a slice was prepared, and proceeded gradually for about 20 h; typical time courses are shown in Figure 3.

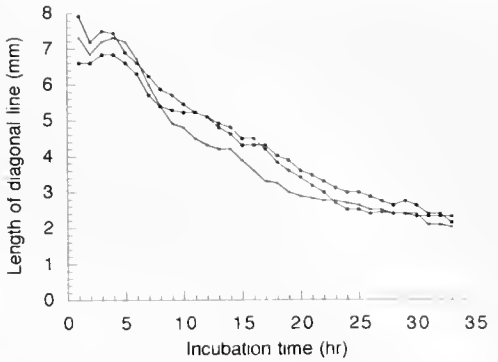

Figure 3. Time course of rounding of the tunic slices. The length of the longest diagonal line was measured in three specimens every hour during the incubation in FSW.

Table I shows the results of the tunic rounding assay under experimental conditions. In ASW (control), most of the tunic slices became tunic balls; those that did not form balls stuck on the surface of the petri dishes and rounding or deformation of the tunic partially occurred in the periphery or in some small areas in these slices. Tunic slices that were frozen and thawed did not round up, and the hardness and shapes of these tunic slices were almost unchanged (Fig. 4A). Tunic rounding was completely inhibited in CMF-ASW, and the tunic slices were transformed into disorganized soft gel (Fig. 4B). These specimens were so soft that they were easily taken to bits by handling with forceps. Cytochalasin B also inhibited the rounding, with 1 μg/ml of cytochalasin B being enough for complete inhibition. These tunic slices became softer than either new or frozen slices, and they were swollen to some extent (Fig. 4C). Because tunic rounding normally occurred in 1% DMSO-ASW, the small amount of DMSO

Table I

Rounding of colony slices under experimental conditions

Medium[a]	Concentration	No. of specimens	No. of rounding specimens (%)
ASW (control)		224	213 (95)
Freeze treatment		67	0 (0)
CMF-ASW		49	0 (0)
Cytochalasin B-ASW	5 μg/ml	95	0 (0)
	1 μg/ml	67	0 (0)
	0.5 μg/ml	18	13 (72)
	0.3 μg/ml	18	10 (56)
	0.1 μg/ml	37	32 (86)
DMSO-ASW	1%	56	51 (91)
Colchicine-ASW	10 μg/ml	30	28 (93)
	100 μg/ml	47	42 (89)

[a] ASW = artificial seawater; CMF-ASW = Ca^{2+}-Mg^{2+}-free artificial seawater; DMSO = dimethylsulfoxide.

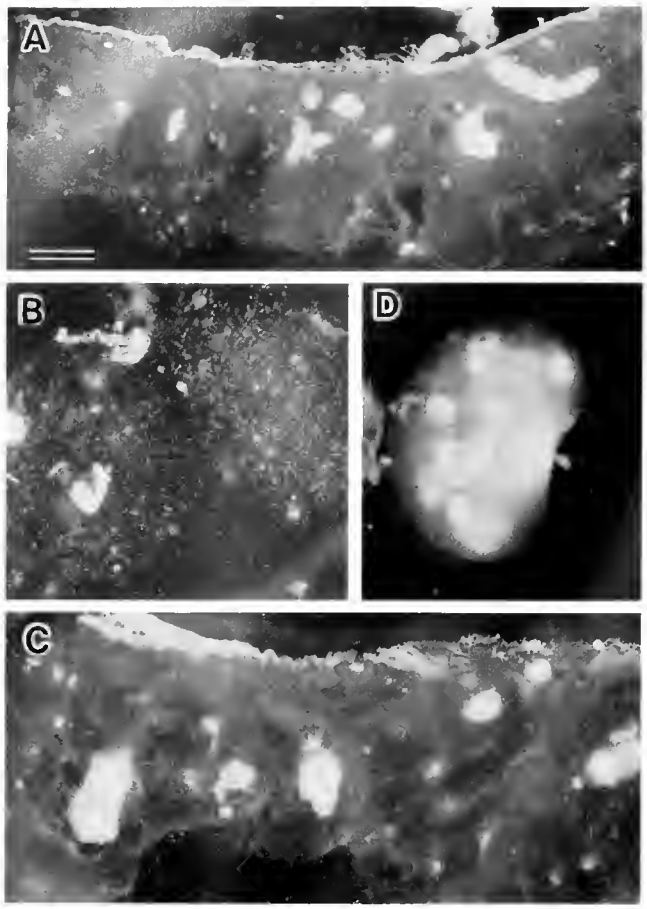

Figure 4. Tunic slices assayed under experimental conditions after a 24-h incubation: frozen and thawed once (A), incubated in Ca^{2+}-Mg^{2+}-free-ASW (B), incubated in cytochalasin B-ASW (5 μg/ml) (C), incubated in colchicine-ASW (10 μg/ml) (D). Tunic rounding occurred only in D. The slice was transformed into disorganized soft gel in B. Magnifications are the same for all parts of this figure. Scale bar = 1 mm.

contained in cytochalasin B-ASW did not have an inhibitory effect (see Table I). Colchicine did not inhibit tunic rounding even in high concentrations (Fig. 4D).

The inhibitory effects on rounding by cytochalasin B suggest that microfilaments promote tunic rounding. Microfilaments in the tunic slices were visualized by labeling with phalloidin-FITC, which stained cellular microfilaments of tunic cells, particularly their filopodia. In *A. yamazii*, a type of tunic cell, called an elongated tunic cell, extended long cellular processes that were stained extensively with phalloidin-FITC. The elongated tunic cells appeared to form a cellular network by contacting each other with their cellular processes (Hirose *et al.*, 1994b) (Fig. 5A). But, this cellular network disappeared in tunic slices that had been incubated in CMF-ASW (Fig. 5B) or cytochalasin B-ASW (Fig. 5C). In these specimens, most of the tunic cells were almost spherical, with shortened filopodia or none at all. Cryostat sections were prepared from pieces of the colony (Fig. 5D) and rounding tunic balls (Fig. 5E). The cells were distributed rather uniformly in the tunics of colony pieces. After rounding, the number of tunic cells and filamentous materials increased significantly in cortical area of the specimens.

SEM observation of a fresh slice reveals the tunic matrix consisting of fine filamentous materials that densely intertwine; the surface of the slice has a sponge-like structure (Fig. 6A). After some rounding, a dense, sheetlike material covered the surface of the tunic ball, so the filamentous materials were not exposed (Fig. 6B); and TEM observation disclosed an electron-dense, thin layer covering the tunic matrix (Fig. 6C). This thin layer is a regenerating tunic cuticle. The ascidian tunic is always overlaid by a cuticle that entirely covers the matrix. In *A. yamazii*, the intact tunic cuticle has protrusions of about 60 nm (Hirose *et al.*, 1990) (Fig. 6D), and tiny protrusions were also found in the regenerating cuticle of the rounding tunic (Fig. 6C, arrows). Under experimental conditions in which the tunic did not round, the cuticle did not regenerate, and the filamentous materials remained exposed. In tunic slices that were frozen and thawed once, the surface structures were almost the same as those of freshly sliced specimens (Fig. 6E). In the tunic slices incubated in CMF-ASW or cytochalasin B-ASW (Fig. 6, F and G), the filamentous materials of the tunic were loosely packed in comparison with newly sliced specimens.

Discussion

Tunic slices of *Aplidium yamazii* gradually round up in seawater, usually becoming round tunic masses within 24 h. In other words, the superficial area of the specimen is minimized by rounding. Because tunic slices that had been frozen did not round, live tunic cells are probably necessary for rounding. Tunic rounding was also inhibited by cytochalasin B, which suggests that microfilaments are involved in the process. Phalloidin-FITC staining allowed visualization of the distribution of microfilaments in the tunic slices, and it revealed a network of tunic cells interconnected by their long filopodia. We deduce that tunic rounding is promoted by contraction of this cellular network in the tunic; that is, the network contracts, carrying with it the surrounding gelatinous tunic matrix. As shown in Figure 5E, the number of tunic cells and filamentous materials increase in the cortical area of the tunic ball. This suggests that shrinkage of the tunic occurs in the cortical area, and that the contraction of the cellular network probably promotes this tunic shrinkage. The complete inhibition of rounding in CMF-ASW may be caused by the disappearance of the cellular network (Fig. 5B). In contrast to microfilaments, microtubules are probably not essential for tunic rounding, because high concentrations of colchicine were not inhibitory.

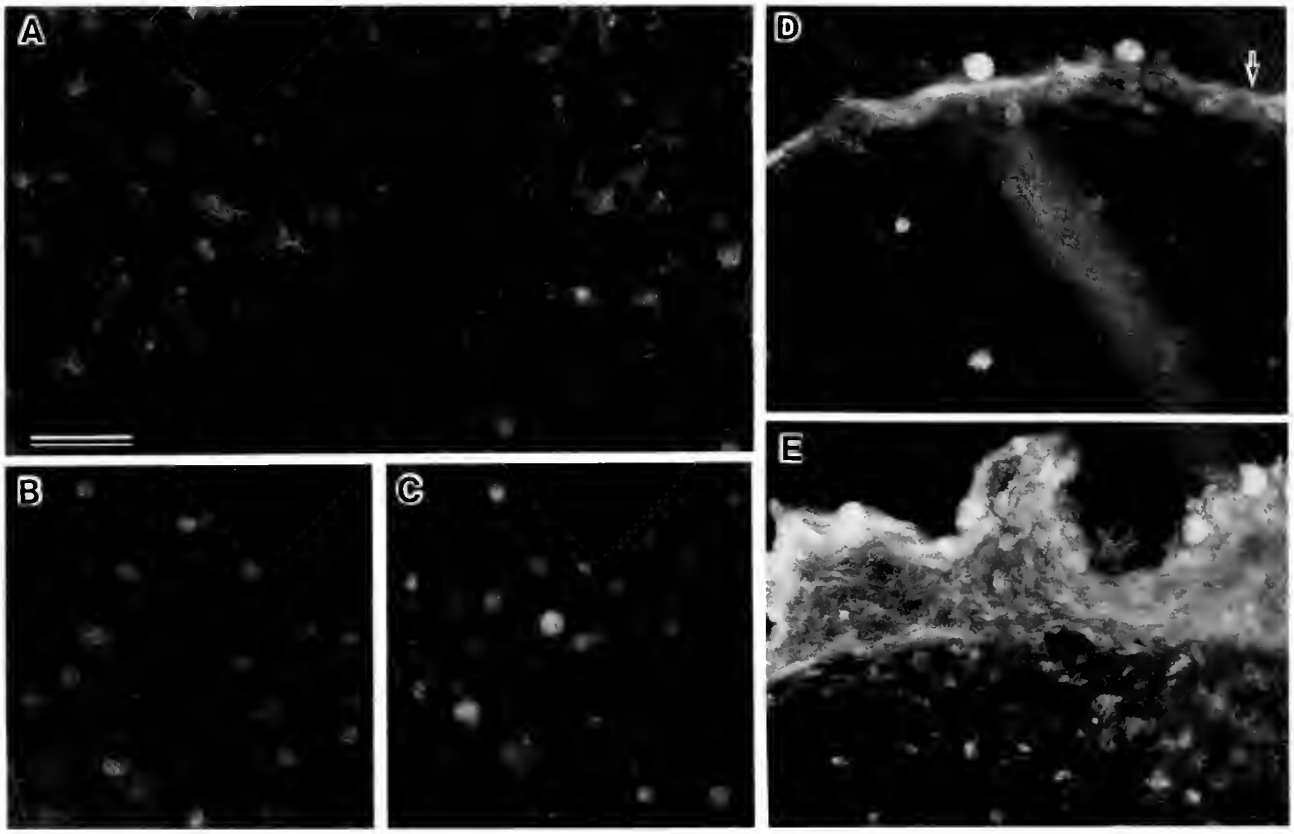

Figure 5. Microfilaments in the tunic specimens stained with phalloidin-FITC. In a newly sliced tunic, elongated tunic cells extending filopodia form a cellular network (A). The cellular network has disappeared in the tunic slices incubated in Ca^{2+}-Mg^{2+}-free-ASW (B), or incubated in cytochalasin B-ASW (10 μg/ml) (C). Cryostat sections of colony pieces (D) and rounding tunic balls (E), showing cortical area of the specimens. Arrow indicates tunic cuticle. Magnifications are the same for all parts of this figure. Scale bar = 50 μm.

The tunic cells forming the network have been described as "elongated tunic cells" (Hirose *et al.*, 1994b) and probably correspond to the "myocytes" described in *Diplosoma* species (Mackie and Singla, 1987). The myocytes also form a network in the tunic, and the net of myocytes itself is supposed to conduct impulses that trigger its contraction, according to electrophysiological studies (Mackie and Singla, 1987). Elongated forms of tunic cells were also reported in *Leptoclinides echinatus* (Hirose, 1992), although it is uncertain whether they form a network. On the other hand, similar types of tunic cells or tunic cell network have not been described in other colonial ascidians that have colonial vascular networks in the tunic, such as *Clavelina miniata* (Aoki *et al.*, 1989), *Perophora viridis* (Deck *et al.*, 1966), and *Botryllus* and *Botrylloides* species (Zaniolo, 1981; Hirose *et al.*, 1991). Although the epidermal cells of the vascular network show contractility (Mukai *et al.*, 1978) and impulse conductivity (Mackie and Singla, 1983), the tunic cell network may be uniquely developed in some colonial species that lack a colonial vascular network.

The fine-structure study revealed that the tunic cuticle, a thin, electron-dense layer, had regenerated in the rounding tunic ball and covered the entire surface. In contrast, the tunic cuticle was lacking and filamentous tunic materials were exposed at the surface of newly sliced tunic and in the specimens in which tunic rounding was inhibited. Rounding (or tunic shrinkage at the cortical area) may be necessary for cuticle regeneration at the exposed surface of the tunic.

Like newly sliced tunics, frozen specimens were gelatinous, and the filamentous tunic materials were intertwined densely at the surface. When the slices were incubated in CMF-ASW or cytochalasin B-SW, the specimens became much softer than newly sliced tunic or frozen specimens; moreover, the filamentous materials of the tunic were loosely packed, and the cellular network in the tunic was not present. The cellular network of elongated tunic cells may also be important for maintaining

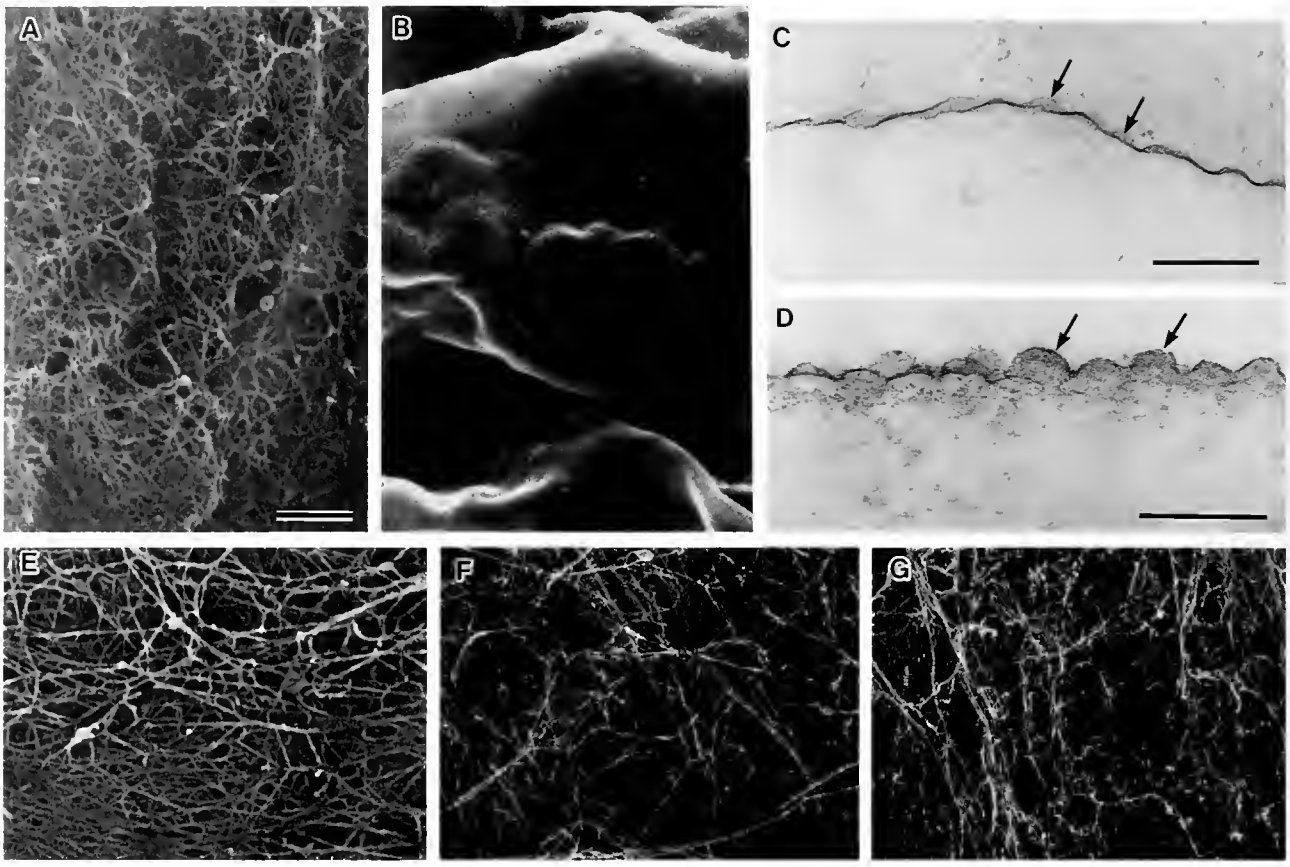

Figure 6. SEM (A, B, E, F, and G) and TEM (C and D) observation of tunic slices assayed under experimental conditions: newly sliced surface of the tunic (A), surface of rounding tunic (B and C), tunic cuticle of intact tunic (D), surface of tunic slice frozen and thawed once (E), tunic slice incubated in Ca^{2+}-Mg^{2+}-free-ASW (F), tunic slices incubated in cytochalasin B-ASW (10 μg/ml) (G). All SEM micrographs are at the same magnification. Arrows indicate some minute protrusions of the tunic cuticle. Scale bars = 1 μm in A, 0.2 μm in C and D.

tension in the tunic and the organization of the tunic filaments.

Tunic rounding is presumed to represent the healing mechanism that is initiated when the exterior of the tunic is injured. We propose the following integumentary defense system in the *A. yamazii* tunic. When the colony is externally wounded, contraction of the network of elongated tunic cells promotes contraction of the tunic around the wound. Tunic contraction almost closes the wound, and it minimizes the exposed area that lacks tunic cuticle. At the same time, tunic contraction increases the density of the filamentous components of the tunic at the wound, and it may accelerate the regeneration of tunic cuticle so as to cover the exposed surface of the wound. The tunic cuticle has a dense structure that is effective in preventing the invasion of microorganisms. Tunic rounding is, however, a slow process in which noticeable rounding begins 4–5 h after production of a slice, so this phenomenon may not be an effective defensive mechanism in the early stages after an injury. If, in *A. yamazii*, microorganisms invade through the wounded part before the completion of cuticle regeneration, phagocytic tunic cells might be expected to phagocytize those invaders (Hirose *et al.*, 1994a). This integumentary defense system is unique among metazoans, and it appears to be especially suited to the organization of this species, which has a large amount of tunic outside the epidermis and no vascular network in the tunic. In this system, the contractile cellular network in the tunic may work like the dermal or epidermal muscle does in other metazoans.

Acknowledgments

This study was supported in part by grants from Nihon University and from the Ministry of Education, Science and Culture of Japan (#07456092). Most of this study was performed at Shimoda Marine Research Center (SMRC), University of Tsukuba, and we are grateful to

the staff of SMRC, particularly Dr. Y. Saito, for providing facilities. We also thank anonymous referees for their valuable comments. The present study includes contribution No. 583 from SMRC.

Literature Cited

Aoki, M., K. Hashimoto, and H. Watanabe. 1989. The intrinsic origin of bioluminescence in the ascidian, *Clavelina miniata*. *Biol. Bull.* **176:** 57–62.

Deck, J. D., E. D. Hay, and J.-P. Revel. 1966. Fine structure and origin of the tunic of *Perophora viridis*. *J. Morphol.* **120:** 267–280.

De Leo, G., E. Patricolo, and G. D'Ancona Lunetta. 1977. Studies on the fibrous components of the test of *Ciona intestinalis* Linaeus. I. Cellulose-like polysaccharide. *Acta Zool. (Stockh.)* **58:** 135–141.

De Leo, G., E. Patricolo, and G. Frittita. 1981. Fine structure of the tunic of *Ciona intestinalis* L. II. Tunic morphology, cell distribution and their functional importance. *Acta Zool.* **62:** 259–271.

Hirose, E. 1992. Tunic cells in *Leptoclinides echinatus* (Didemnidae, Ascidiacea): An application of scanning electron microscopy for paraffin embedding specimens. *Hiyoshi Rev. Natur. Sci. Keio Univ.* **11:** 5–8.

Hirose, E., Y. Saito, K. Hashimoto, and H. Watanabe. 1990. Minute protrusions of the cuticle: Fine surface structures of the tunic in ascidians. *J. Morphol.* **204:** 67–73.

Hirose, E., Y. Saito, and H. Watanabe. 1991. Tunic cell morphology and classification in botryllid ascidians. *Zool. Sci.* **8:** 951–958.

Hirose, E., T. Ishii, Y. Saito, and Y. Taneda. 1994a. Phagocytic activity of tunic cells in the compound ascidian *Aplidium yamazii* (Polyclinidae, Aplousobranchia). *Zool. Sci* **11:** 203–208.

Hirose, E., T. Ishii, Y. Saito, and Y. Taneda. 1994b. Seven types of tunic cells in the colonial ascidian *Aplidium yamazii* (Polyclinidae, Aplousobranchia): Morphology, classification and possible functions. *Zool. Sci.* **11:** 737–743.

Mackie, G. O., and C. L. Singla. 1983. Coordination of compound ascidians by epithelial conduction in the colonial blood vessels. *Biol. Bull.* **165:** 209–220.

Mackie, G. O., and C. L. Singla. 1987. Impulse propagation and contraction in the tunic of a compound ascidian. *Biol. Bull.* **173:** 188–204.

Mukai, H., K. Sugimoto, and Y. Taneda. 1978. Comparative studies on the circulatory system of the compound ascidians *Botryllus*, *Botrylloides* and *Symplegma*. *J. Morphol.* **157:** 49–77.

Yan Daele Y., J.-F. Revol, F. Gaill, and G. Goffinet. 1992. Characterization and supramolecular architecture of the cellulose-protein fibrils in the tunic of the sea peach (*Halocynthia papillosa*, Ascidiacea, Urochordata). *Biol. Cell* **76:** 87–96.

Zaniolo, G. 1981. Histology of the ascidian *Botryllus schlosseri* tunic: In particular, the test cell. *Boll. Zool.* **48:** 169–178.

Reference: *Biol. Bull.* **189:** 36–41. (August, 1995)

Life Histories and Senescence of *Botryllus schlosseri* (Chordata, Ascidiacea) in Monterey Bay

NANETTE E. CHADWICK-FURMAN[1,*] AND IRVING L. WEISSMAN[2]

[1]*Hopkins Marine Station of Stanford University, Pacific Grove, California 93950; and* [2]*Department of Pathology, Stanford University Medical School, Stanford, California 94305*

Abstract. The colonial ascidian *Botryllus schlosseri* is a model organism for research on invertebrate histocompatibility, development, and evolutionary biology. Nonetheless, the basic life history of Pacific Ocean populations of the species remains unknown. We determined field rates of growth, reproduction, and senescence in four cohorts of *B. schlosseri* colonies in Monterey Bay, California. Colonies grew exponentially as juveniles and reached sizes of up to 1400 zooids within 69 days. After a juvenile phase lasting at least 49 days, the colonies began to reproduce sexually. Each zooid produced up to 10 clutches, each with a maximum of 5 eggs, resulting in very high fecundity of up to 8000 eggs per colony. Following a short period (maximum 70 days) of continuous sexual reproduction, colonies abruptly senesced and died while still bearing a full clutch of eggs. Senescence progressed through four distinct stages over 1–2 weeks, and inevitably led to the simultaneous death of all zooids in the colony. Although senescence was the main cause of mortality, some colonies died as a result of predation or undetermined causes. Certain life history traits varied significantly between cohorts that settled at different times of year. For example, lifespans in the field varied from about 3 months for spring to 8 months for fall-born colonies, but the lifetime fecundity of colonies did not vary between cohorts. The morphologies and life histories of colonies monitored in the field and reported here differed from those of colonies cultured previously in the laboratory.

Introduction

The colonial ascidian *Botryllus schlosseri* Pallas is widely employed in studies on invertebrate alloimmunity (reviewed by Weissman *et al.*, 1990; Rinkevich, 1992; Sabbadin *et al.* 1992), development (Milkman, 1967; Mukai and Watanabe, 1976; Rinkevich *et al.*, 1992; Lauzon *et al.*, 1993), and evolutionary ecology (Grosberg, 1988; Harvell and Grosberg, 1988; Buss, 1990). Most of this research has been conducted under laboratory conditions. Life histories of *B. schlosseri* colonies in the field are known for some populations in the Atlantic Ocean (Grave, 1933; Grosberg, 1988) and Mediterranean Sea (Brunetti, 1974). The life histories of Pacific Ocean populations are, however, little known, despite their extensive use in laboratory investigations (Scofield *et al.*, 1982; Rinkevich and Weissman, 1987; Lauzon *et al.*, 1933, and references therein) (Carwile, 1989). *B. schlosseri* was probably introduced to the Pacific Ocean sometime during the last century as one of the fouling organisms on wooden-hulled vessels or concomitant with the culture of Atlantic oysters, which transferred whole organisms and their encrusting communities from the Atlantic to the Pacific Ocean (Carlton, 1987; Hewitt, 1993). Recent morphological and genetic studies indicate that *B. schlosseri* at Woods Hole (Atlantic Ocean) and Monterey (Pacific Ocean) are the same species (Boyd *et al.*, 1990). Results of laboratory cultures from both of the latter populations have been used to infer evolutionary processes in nature (Harvell and Grosberg, 1988; Weissman *et al.*, 1990; Rinkevich, 1992, and references therein). Thus, it becomes important to understand the life history patterns of *B. schlosseri* from different populations and under different culture conditions.

We present here the life histories of *B. schlosseri* colonies growing under field conditions in Monterey Bay, California. We describe patterns of growth, sexual reproduction, and senescence in cohorts that settled at four times of year. We then compare these field life histories

Received 14 September 1993; accepted 5 June 1995.

*Present address: Interuniversity Institute for Marine Sciences, P.O. Box 469, Eilat, Israel.

with those of laboratory-cultured colonies from the same population.

Materials and Methods

We conducted the present study during 1990–1991 in the Monterey Municipal Marina, Monterey County, California (36° 37.4'N, 121° 54'W). Surface seawater temperatures varied from 11.4°C in January to 16.5°C in August (E. C. Haderlie, pers. comm.). This site is described in detail by Haderlie and Donat (1978) and Carwile (1989). Colonies of *Botryllus schlosseri* grow on docks, floats, and pilings throughout the marina and seasonally dominate the fouling community (pers. obs., N. E. Chadwick-Furman). Colonies of *B. schlosseri* sexually reproduce throughout the year at Monterey; sexual generations overlap and cohorts are not discrete (Carwile, 1989).

To determine life history patterns, we monitored cohorts of *B. schlosseri* that settled at four arbitrarily chosen dates: 19 May 1990, 3 July 1990, 15 October 1990, and 25 January 1991. To obtain each cohort, we collected 10 large colonies from wooden pilings at 0–1 m depth in the marina, transported them to Hopkins Marine Station of Stanford University, and maintained them in flowing seawater at ambient temperature. We secured the colonies with string to glass plates and placed them vertically in aquaria, with an empty plate facing each colony. Within a few days, they released swimming larvae that rapidly settled and metamorphosed into sessile zooids on the facing plates. We then isolated each newly settled zooid on a separate 5.0 × 7.5 cm glass plate, and allowed it to firmly attach during 1 week in the laboratory. For each cohort, we transplanted at least 25 newly settled, isolated zooids to the marina field site.

In the marina, we placed the zooids in wooden racks and hung them face down from floating docks at 0.5–1.0 m depth (after Brunetti, 1974; Boyd *et al.*, 1986; Grosberg, 1988). Sessile organisms colonized the racks and formed a fouling community around the experimental plates (see Carwile, 1989, for community description). No epibionts were observed to settle on individuals of *B. schlosseri*.

At each sample interval, every 4–7 days, we observed the growing colonies in the laboratory and then returned them to the field within a few hours (for details of methods, see Brunetti, 1974; Grosberg, 1988). They showed no adverse effects of handling (see also Milkman, 1967). To avoid effects of crowding on colony growth, we removed all other organisms from the plates during each sample interval (after Brunetti and Copello, 1978; Grosberg, 1988). Colonies grew over both sides of the plates, but did not fill all of the space provided. About every 7 days, depending on the time of year, all the zooids in each colony passed through an asexual growth cycle (hereafter termed "cycle"). During each cycle, the zooids produced buds, then shrank and were replaced by their buds, which formed a new asexual generation of zooids in each colony. The replacement of zooids during each cycle in *Botryllus* is described in detail by Mukai and Watanabe (1976) and Grosberg (1988). Here we report colony age in terms of both the number of cycles and the days since settlement (after Brunetti and Copello, 1978; Grosberg, 1988).

During each sample interval, we determined the number of zooids, number of eggs, cycle stage (see Mukai and Watanabe, 1976), and the general condition of each colony. In colonies of less than 800 zooids, we counted zooid number directly. For larger colonies, zooid number was estimated by placing a grid over the colony surface, counting all zooids under a single grid-square (1.5 × 1.8 cm), and multiplying by the number of squares occupied by the entire colony (maximum = 12). To determine the number of eggs per colony, we visually estimated the number of eggs per zooid, then multiplied by the total number of zooids. Eggs were observed from the exterior of whole, undissected colonies.

The causes of mortality were determined by analyzing colony morphology. In senescing colonies, the entire organism deteriorated in distinct stages during the 1–2 weeks preceding death (Brunetti, 1974; Rinkevich *et al.*, 1992). Colonies that senesced left behind a residue of decaying tissue that distinguished them from colonies killed by other agents. In cases of predation, colonies showed localized lesions and then sections of dead tissue that increased in area for several weeks before the complete consumption of the colony by predators.

Results

Morphology and growth

In the Monterey Marina, members of all cohorts of *Botryllus schlosseri* exhibited the same general morphology. Colonies were flat and roughly circular to oval in outline. Their zooids were closely packed, with almost no space between adjacent zooids or systems (circular groups of zooids). Each colony formed a compact disk that did not fragment.

Juvenile colonies in all cohorts grew exponentially (Fig. 1). Colonies that settled in May grew significantly faster than those in all other cohorts (Fig. 2A, Table I) and reached a size of up to 1400 zooids in 69 days. Members of the July and October cohorts grew the slowest, at rates that did not differ significantly (Fig. 2a, Table I). Colonies that settled during October and January delayed their exponential growth until the spring months (Fig. 1). Some colonies reduced their growth rates after commencing sexual reproduction (Fig. 1). In addition, 15.6% of all colonies (N = 122) shrank slightly (by 15.2% + 11.1% in zooid number, x + SD) during the 2 weeks preceding

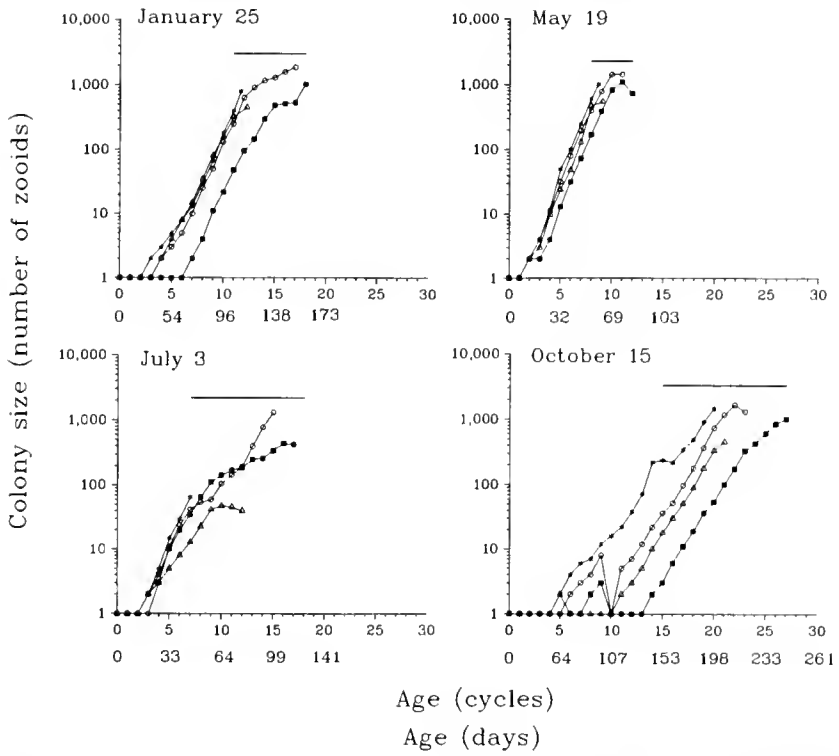

Figure 1. Growth, reproduction and lifespan in four cohorts of the colonial ascidian *Botryllus schlosseri* in Monterey Bay. For clarity, growth curves are presented for only four colonies per settlement date (out of >25 original); they represent the extremes of those that survived to reproduce in each cohort: the smallest in final size (triangle), largest in final size (circle), shortest-lived (asterisk), and longest-lived (square). Horizontal bars indicate the period of sexual reproduction for the entire cohort. Note that colony size is plotted on a logarithmic scale.

death. The only other lapse in exponential growth occurred when members of the October cohort were attacked by an unknown predator during cycles 5–15 (Fig. 1).

Sexual reproduction

After a period of exponential somatic growth, the colonies entered sexual reproduction. The May and July cohorts reached sexual maturity the earliest, at ages that did not differ significantly (Fig. 2b, Table I). The minimum age at sexual maturity was 49 days (7 cycles). Members of the October cohort began to reproduce when significantly older than other cohorts (Table I, Fig. 2b). They overwintered as small juveniles and postponed reproduction until spring, at a minimum age of 153 days (15 cycles) (Fig. 1).

The size at which colonies began to reproduce varied widely (range = 38 to 1297 zooids) but did not differ significantly between most cohorts (Table I). Colonies that settled in July reproduced at the smallest sizes; those in January and May at the largest (Fig. 2c). Due to differences in growth rate, some cohorts matured at similar sizes but widely different ages (compare May and July cohorts, Fig. 2b and c).

Most zooids in each colony produced eggs continuously throughout the period of sexual reproduction. The duration of reproduction extended for 7–70 days (1–10 cycles), with one clutch of eggs produced during each cycle. Some cohorts produced significantly more clutches than did others (Table I). Each zooid contained up to five eggs per cycle, although most zooids produced only one to two eggs per cycle (Fig. 2d). Colonies did not interrupt clutch production or reduce the number of eggs per zooid as they aged; mature colonies still contained a full clutch of eggs when they died.

Lifetime fecundity was very high (maximum = about 8000 eggs). Such high fecundity was possible because of the large number of zooids in adult colonies and their ability to produce multiple clutches. Lifetime fecundity did not differ significantly between colonies that settled at different times of year (Table I, Fig. 2f).

Longevity and survivorship

Colonies grown in the field at Monterey had short, subannual lifespans. Maximum lifespan ranged from almost 3 months (82 days) in the May cohort, to just over 8 months (247 days) in the October cohort (Fig. 3).

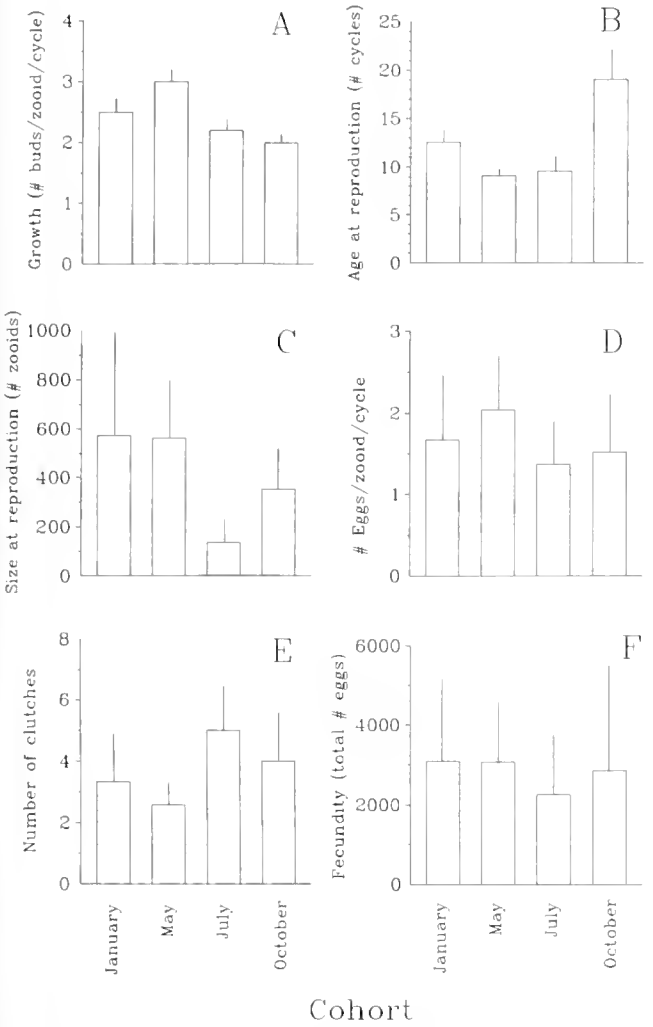

Figure 2. Variation in six life-history traits among four cohorts of the colonial ascidian *Botryllus schlosseri* in Monterey Bay. Error bars: positive standard deviations of the means.

The percentage of colonies that survived to first reproduction was high in most cohorts (Fig. 3). Colonies that settled in October had lower survivorship to maturity than did the other three cohorts. An undetermined predator began to attack members of the October cohort during cycle 5. Mortality increased gradually, and by the 15th cycle, only 21% of the cohort remained (Fig. 3). Nevertheless, the remaining October colonies all eventually reproduced sexually and lived longer than those of any other cohort (Figs. 1 and 3). In all cohorts, survivorship decreased rapidly after commencement of sexual reproduction, and all colonies then died within 10 cycles (Fig. 3).

Senescence caused most of the mortality in field-raised colonies (54.9% of colonies, $N = 122$). After a period of continuous sexual reproduction, colonies passed through four stages of degeneration, as previously described for *B. schlosseri* (Brunetti, 1974; Rinkevich *et al.*, 1992). First, blood vessels narrowed and blood flow slowed. Then, the zooids shrank and became densely pigmented. In the third stage, circular systems (groups) of zooids were disconnected and became disorganized. In the fourth and final stage, the protective tunic softened and disintegrated, and all of the tissue died. A film of tunic material persisted for at least 1 week after death, and marked the former extent of the colony. Senescence was not reversible. In all cases, the initial stages of senescence led to the death of the entire colony within 1–2 weeks. Some colonies senesced while still in the juvenile stage, at an age of at least 70 days (= 10 cycles), and died without reproducing sexually. The occurrence and timing of senescence did not appear to be related to the position of the colonies in the racks or to other extrinsic factors.

Other agents of mortality included predation (12.3% of colonies, $N = 122$, described above), and undetermined causes of death early in life (32.8%, $N = 122$). In the latter case, small juvenile colonies suddenly disappeared from the field site without showing any previous signs of damage.

Discussion

We demonstrate here that *Botryllus schlosseri* colonies raised in the field at Monterey have characteristic morphologies, which are readily distinguishable from those of colonies grown under laboratory conditions. In the field, isolated colonies are rounded and compact (Brunetti, 1974; Grosberg, 1988; Carwile, 1989; this paper). In con-

Table I

Tukey-Kramer multiple comparisons test for differences in life history traits between cohorts of the ascidian Botryllus schlosseri *grown in Monterey Bay, California, during 1990–1991*

Life-history trait	Cohort*			
Growth rate (#buds/zooid/cycle)	Jan	May	Jul	Oct
Age at 1st reprod. (# cycles)	Jan	May	Jul	Oct
Size at 1st reprod. (# zooids)	May	Jan	Oct	Jul
Number of eggs/zooid/clutch	May	Jan	Oct	Jul
Clutch number	Jan	May	Oct	Jul
Fecundity (total # eggs/colony)	Jan	May	Jul	Oct

* Cohorts that did not differ significantly ($p > 0.05$) are conjointly underlined. See text for details.

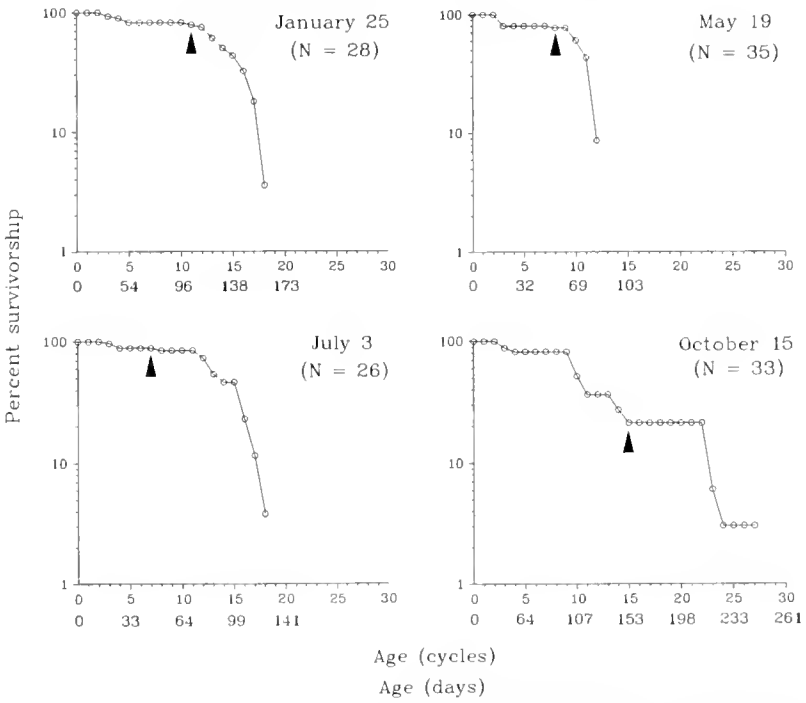

Figure 3. Survivorship curves of the colonial ascidian *Botryllus schlosseri* in Monterey Bay. Presented are four cohorts, each settled at the date shown. Arrows indicate the beginning of sexual reproduction in each cohort. Note that survivorship is plotted on a logarithmic scale.

trast, colonies grown in the laboratory tend to branch and produce extensions along the substratum; these extensions may fragment into subcolonies (Rinkevich and Weissman, 1987; N. E. Chadwick-Furman, pers. obs.).

In addition, the life history patterns of colonies in the field seem to differ from those in the laboratory. Members of all field cohorts at Monterey exhibited the same general features: rapid growth, short and intense reproduction, short lifespan, and senescence soon after reaching maturity (Figs. 1–3). In contrast, Monterey colonies raised in the laboratory have been observed to grow slowly or shrink over many months, to cease reproduction long before death, and to live for more than 2 years (Boyd *et al.*, 1986; Rinkevich and Weissman, 1987; Rinkevich *et al.*, 1992). Also in Mediterranean populations, the same life history differences are exhibited between field- and laboratory-raised colonies (Brunetti, 1974; Brunetti and Copello, 1978).

Several factors may be responsible for these differences. Under laboratory conditions, water motion is slower, and particulate food is less varied and abundant than for *B. schlosseri* populations in the field (Milkman, 1967; Brunetti and Copello, 1978; Carwile, 1989). In addition, the absence of natural grazers in the laboratory may lead to the formation of a fouling film that inhibits the attachment and growth of colonies (Boyd *et al.*, 1986; N. E. Chadwick-Furman, pers. obs.). Laboratory culture is important for the maintenance of genetically defined stocks that are employed in histocompatibility studies and other investigations (reviewed in Sabbadin *et al.*, 1992; Rinkevich *et al.*, 1992). Laboratory culture at summer temperatures also allows continued production of experimental tissues during the winter when field colonies in Monterey slow their growth (Boyd *et al.*, 1986). Unfortunately, however, the life history traits exhibited by laboratory cultures, including patterns of growth, reproduction, and longevity, may not reflect the evolutionary or ecological processes that act upon *B. schlosseri* in nature.

In the field at Monterey, life history variation between cohorts is probably related to seasonal environmental cycles. Factors known to correlate with such variation in other field populations of *B. schlosseri* include water temperature and particulate food concentration (Millar, 1971; Brunetti, 1974). In the present study, we observed slowed growth and delayed reproduction of young colonies during the winter months when temperature and planktonic food levels are at their annual minima in Monterey Bay (Haderlie and Donat, 1978; Boyd *et al.*, 1986; Carwile, 1989, and references therein). The colonies began to grow exponentially and reproduce sexually in the spring to summer when the above two factors reach their annual maxima. In some localities, *B. schlosseri* colonies completely cease sexual reproduction during the winter when temperatures fall below 11°C (Millar, 1971). At Monterey,

however, sea temperature remains above 11°C all year, so mature colonies continue to produce eggs even during January (see Methods).

The present study had several weaknesses. Although colonies were cultured in the sea, they did not grow under completely natural conditions. The periodic removal of competitors may have led to inflated rates of growth and reproduction. Thus, values reported here are probably maximal in the absence of space competition. Also, we did not monitor colonies immediately following natural settlement in the field. Thus, survival rates are probably inflated because we did not determine natural mortality rates during the first 1–2 weeks of life. Finally, we conducted our study in an artificial habitat, on a non-native population of *B. schlosseri*. As such, the life histories presented here are not those of a natural field population. Members of this species probably have been introduced over much of their current range, possibly from native populations in the Mediterranean Sea (Carlton, 1987; Hewitt, 1993). Indeed, a weakness of most life history studies on this species is that they have been conducted on introduced populations or in manmade fouling environments, or both (Millar, 1971; Brunetti, 1974; Grosberg, 1988; Carwile, 1989).

In spite of the above drawbacks, the data presented here give the most complete picture to date of life histories and morphologies of Pacific Ocean populations of *B. schlosseri*. The life histories of Monterey Bay colonies are quite similar to those of iteroparous colonies at Woods Hole in the western Atlantic (Grave, 1933; Grosberg, 1988), and at the Venice Lagoon in the Mediterranean (Brunetti, 1974).

We present here the first description of senescence in the field for Monterey *B. schlosseri*. Our observations confirm that senescence progresses under field conditions through essentially the same stages as in the laboratory, and takes about 1–2 weeks (Brunetti and Copello, 1978; Rinkevich *et al.*, 1992). Senescence appears to be controlled intrinsically, as inferred from the synchronized death of segregated laboratory clones (Rinkevich *et al.*, 1992). The specific factors that regulate the timing and initiation of senescence in *B. schlosseri*, and in other ascidians, remain unknown.

Acknowledgments

We thank the staff of Hopkins Marine Station and the Pathology Department of Stanford University Medical School, especially Kathi Ishizuka, Karla Palmeri, and Margaret Finney. The manuscript benefitted from extensive comments by Richard Grosberg, Robert Lauzon, Baruch Rinkevich, and anonymous reviewers. This project was supported by a Frederick B. Bang Grant from the American Association of Immunologists and a postdoctoral fellowship from the National Cancer Institute (PHS Grant Number CA09302, DHHS) to N. E. C.-F., and by USPHS grants to I. L. W.

Literature Cited

Boyd, H. C., S. K. Brown, J. A. Harp, and I. L. Weissman. 1986. Growth and sexual maturation of laboratory-cultured Monterey *Botryllus schlosseri*. *Biol. Bull.* **170:** 91–109.

Boyd, H. C., I. L. Weissman, and Y. Saito. 1990. Morphologic and genetic verification that Monterey *Botryllus* and Woods Hole *Botryllus* are the same species. *Biol. Bull.* **178:** 239–250.

Brunetti, R. 1974. Observations on the life cycle of *Botryllus schlosseri* (Pallas) (Ascidiacea) in the Venetian lagoon. *Boll. Zool.* **41:** 225–251.

Brunetti, R., and M. Copello. 1978. Growth and senescence in colonies of *Botryllus schlosseri* (Pallas) (Ascidiacea). *Boll. Zool.* **45:** 359–364.

Buss, L. W. 1990. Competition within and between encrusting clonal invertebrates. *Trends Ecol. Evol.* **11:** 352–356.

Carlton, J. T. 1987. Patterns of transoceanic marine biological invasions in the Pacific Ocean. *Bull. Mar. Sci.* **41:** 452–465.

Carwile, A. H. 1989. Settlement of larvae, colony growth and longevity in three species of ascidians and the effect on the species composition of a marine fouling community. Ph.D. dissertation, University of California at Los Angeles, 229 pp.

Grave, B. H. 1933. Rate of growth, age at sexual maturity, and duration of life of certain sessile organisms, at Woods Hole, MA. *Biol. Bull.* **65:** 375–386.

Grosberg, R. K. 1988. Life-history variation within a population of the colonial ascidian *Botryllus schlosseri*. I. The genetic and environmental control of seasonal variation. *Evolution* **42:** 900–920.

Haderlie, E. C., and W. Donat. 1978. Wharf piling fauna and flora in Monterey Harbor, California. *Veliger* **21:** 45–69.

Harvell, C. D., and R. K. Grosberg. 1988. The timing of sexual maturity in clonal animals. *Ecology* **69:** 1855–1864.

Hewitt, C. L. 1993. Marine biological invasions: the distributional ecology and interactions between native and introduced encrusting organisms. Ph. D. dissertation, University of Oregon, 301 pp.

Lauzon, R. J., C. W. Patton, and I. L. Weissman. 1993. A morphological and immunohistochemical study of programmed cell death in *Botryllus schlosseri* (Tunicata, Ascidiacea). *Cell Tiss. Res.* **272:** 115–127.

Milkman, R. 1967. Genetic and developmental studies on *Botryllus schlosseri*. *Biol. Bull.* **132:** 229–243.

Millar, R. H. 1971. The biology of ascidians. *Adv. Mar. Biol.* **9:** 1–100.

Mukai, H., and H. Watanabe. 1976. Studies on the formation of germ cells in a compound ascidian *Botryllus primigenus* Oka. *J. Morph.* **148:** 337–362.

Rinkevich, B., and I. L. Weissman. 1987. A long-term study on fused subclones in the ascidian *Botryllus schlosseri*: the resorption phenomenon (Protochordata: Tunicata). *J. Zool. (Lond.)* **213:** 717–733.

Rinkevich, B. 1992. Aspects of the incompatibility nature in botryllid ascidians. *Anim. Biol.* **1:** 17–28.

Rinkevich, B., R. J. Lauzon, B. W. M. Brown, and I. L. Weissman. 1992. Evidence for a programmed life span in a colonial protochordate. *Proc. Nat'l. Acad. Sci. USA* **89:** 3546–3550.

Sabbadin, A., G. Zaniolo, and L. Ballarin. 1992. Genetic and cytological aspects of histocompatibility in ascidians. *Boll. Zool.* **59:** 167–173.

Scofield, V. L., J. M. Schlumpberger, L. A. West, and I. L. Weissman. 1982. Protochordate allorecognition is controlled by an MHC-like gene system. *Nature* **295:** 499–502.

Weissman, I. L., Y. Saito, and B. Rinkevich. 1990. Allorecognition histocompatibility in a protochordate species: is the relationship to MHC semantic or structural? *Immunol. Rev.* **113:** 227–241.

Reference: *Biol. Bull* **189**: 42–48. (August, 1995)

The Interaction of Photoperiod and Temperature in Diapause Timing: A Copepod Example

NELSON G. HAIRSTON, JR., AND COLLEEN M. KEARNS

Section of Ecology and Systematics, Cornell University, Ithaca, New York 14853

Abstract. In many organisms, photoperiod and temperature are thought to be the most significant token cues for seasonally timed life history events, including diapause in arthropods. A common pattern in many species of terrestrial insects and several copepod species is the existence of a critical daylength on one side of which the animals do not enter diapause and on the other side of which they do. Temperature plays a secondary role as modifier of the critical daylength. In some species, however, including the freshwater copepod *Diaptomus sanguineus*, the fraction of females making subitaneous eggs (eggs that hatch immediately) undergoes a very gradual transition as daylength changes over the natural range of photoperiods experienced in nature. Here we show that temperature is as important as photoperiod in cuing diapause timing in a population of *D. sanguineus* living in Bullhead Pond, Rhode Island. When ecologically relevant photoperiod and temperature cues are provided in the laboratory, the copepods rapidly switch from producing subitaneous eggs to producing diapausing eggs in a way that is typical of the seasonal switch seen in the pond. We provide a graphical model that illustrates how copepod sensitivities to photoperiod and temperature interact to produce an abrupt transition, and we discuss how natural selection should act on *D. sanguineus* diapause response to produce the variation in diapause timing seen within and between natural populations.

Introduction

An organism that times its life history to seasonal variations in its habitat must be able to detect some component of the environment that indicates time of year. To this end, many plants and animals perceive and respond to daylength (or change in daylength) as a cue for such phenological events as leafing-out, flowering, and seed set in plants (Harper, 1977; Begon *et al.*, 1990), diapause and dispersal in insects (Tauber *et al.*, 1986), and hibernation, molting, or migration in various vertebrates (Hairston, 1994). Other features of the environment (*e.g.*, temperature, resource availability; Danilevskii, 1965; Tauber *et al.*, 1986) can also play a role, but are typically thought to be less important because they are less reliable seasonal indicators. For example, photoperiod is the most common environmental factor cuing the onset of diapause in temperate-zone insect populations, and temperature is typically seen as one of several possible modifiers of the photoperiod response (Lees, 1955; Danilevskii, 1965; Beck, 1980; Tauber *et al.*, 1986). A common pattern for insects that overwinter in diapause is response to a critical photoperiod below which essentially all individuals in a population enter diapause and above which no individuals enter diapause (*e.g.*, Kogure, 1933; Tauber and Tauber, 1981, Tauber *et al.*, 1986). Temperature affects the timing of diapause by altering the critical photoperiod: as temperature declines, the photoperiod that induces diapause increases (Danilevskii, 1965; Tauber *et al.*, 1986). Other effects of temperature on diapause induction in insects include determination of whether any photoperiod response exists and alteration of photoperiod responses due to changes in temperature or due to diel thermoperiod (Tauber *et al.*, 1986; Eizaguirre *et al.*, 1994).

The reason typically given for photoperiod primacy is that daylength is the most reliable predictor of seasonal changes, and so most insects living in seasonal environments have evolved a means of sensing this cue (Lees, 1955; Tauber *et al.*, 1986). This argument holds especially true for terrestrial habitats in which brief periods of unseasonable warming or cooling could send a false signal about time in the season. In contrast, animals living in large-volume aquatic habitats (lakes and the oceans) are buffered from short-term temperature fluctuations by the

Received 6 January 1995; accepted 4 May 1995.

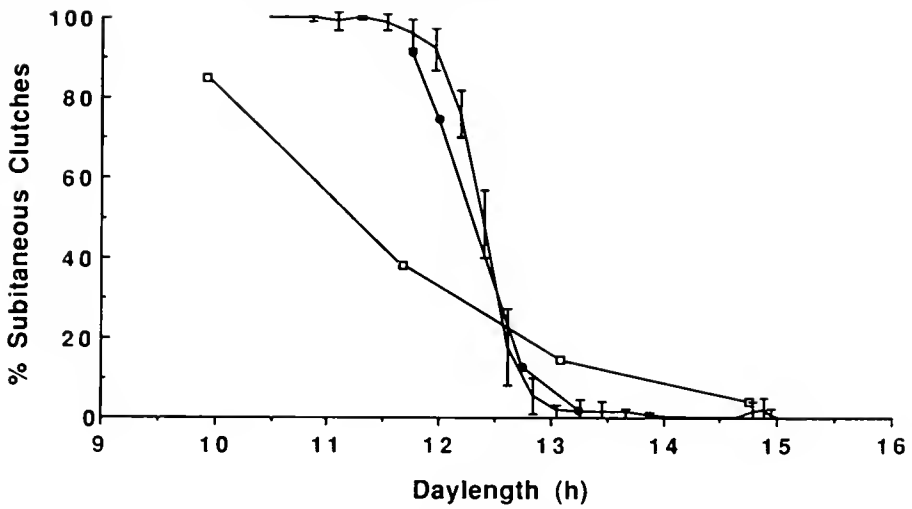

Figure 1. The timing of the switch from production of subitaneous (immediately hatching) eggs to diapausing eggs by *Diaptomus sanguineus* from Bullhead Pond, Rhode Island. The continuous line connecting error bars shows the mean trajectory over 9 years (± 95% CI) for copepods in the lake, expressed as a function of photoperiod on the date that the animals were collected. The line connecting individual open data points shows the photoperiod response of females reared in the laboratory at 9°C (from Hairston and Olds, 1986). The line connecting closed data points shows the photoperiod response of females reared at the temperatures prevailing at the daylengths indicated (this study).

thermal inertia of water. The temperature of the medium in which they live is a more reliable indicator of the passing of the seasons than is the case on land. We might expect, then, that temperature plays a more significant role in regulating timing of diapause in aquatic animals than in their terrestrial counterparts. Among pelagic copepods, significant temperature modification of photoperiod response has been found in every instance investigated, both for cyclopoid copepods with a late-instar diapause (Watson and Smallman, 1971; Alekseev, 1990) and for calanoid copepods with egg diapause (Marcus, 1982; Walton, 1985; Hairston *et al.*, 1990; Ban, 1992). Furthermore, Alekseev (1990) has pointed out that the effect of temperature in delaying critical photoperiod is about twice as great in pelagic copepods (0.65 hours per C°) as it is in terrestrial insects (0.3 hours per C°).

An enhanced effect on critical photoperiod is only one way in which temperature might be expected to influence the timing of diapause. In some species, diapause response to changing photoperiod can be gradual rather than a distinct threshold (Tauber *et al.*, 1986). In this instance the temperature-photoperiod interaction must be somewhat different. An opportunity to explore such an interaction was presented by the data available on the timing and control of diapause in a population of *Diaptomus sanguineus*, a small (*ca.* 1 mm), herbivorous, obligately sexual, freshwater copepod. This population is found in Bullhead Pond, a small Rhode Island lake that has a surface area of 2.4 ha and a maximum depth of 4 m. While active during winter these copepods make subitaneous (immediately hatching) eggs (Hairston and Munns, 1984); in early spring they switch to making diapausing eggs, and they continue to do so until they are eliminated in late spring or early summer by sunfish predation. Nine years of data on the timing of the switch to diapause show that most females make the transition during a relatively brief 3-week period between 10 March and 10 April (Fig. 1). The timing of the switch is apparently an adaptation to avoid an annual springtime increase in fish predation (Hairston and Munns, 1984; Hairston and Walton, 1986; Hairston and Dillon, 1990). The phenological pattern shown in Figure 1 looks superficially like a typical critical photoperiod response. However, when the copepods are reared in the laboratory at a range of photoperiods, and at a single water temperature (9°C) approximating that in the lake at the time of the switch to diapause, the transition from production of subitaneous eggs to diapausing eggs is very gradual (Fig. 1; Hairston and Olds, 1986). This experiment suggests that the copepods in the lake require a more complex signal than photoperiod alone to achieve not only the appropriate mean timing, but also the observed rate, of transition from subitaneous to diapausing eggs.

In laboratory and field studies of *D. sanguineus*, Hairston *et al.* (1990) showed that temperature has a striking effect on the timing of diapause, but their data are inadequate to reveal the nature of the temperature-photoperiod interaction in cuing diapause timing. Here we provide evidence that temperature and photoperiod acting together are sufficient to effect the rapid transition, as ob-

served in Bullhead Pond, from subitaneous to diapausing eggs. We suggest a graphical depiction of the *D. sanguineus* diapause response that illustrates how its graded reaction to photoperiod alone can result in a distinct seasonal phenology when combined with temperature. The resulting model is intented as a description of the interaction of the two cues in effecting diapause timing, not as a deeper mechanistic explanation of its physiological basis.

Materials and Methods

Our objective was to test the hypothesis that photoperiod and temperature are together sufficient to cue *D. sanguineus* to make subitaneous or diapausing eggs in a pattern consistent with the seasonal phenology observed in Bullhead Pond. For testing, we chose four photoperiod-temperature combinations that span the range of dates at which copepods in the lake switched between the two egg types. Our choice of conditions was based on the average distribution of switch dates in Bullhead Pond for 9 years (Fig. 1; Hairston, 1987; Hairston and De Stasio, 1988; Hairston, unpub. data), and lie ± 1.5 and ± 2.5 standard deviations from the mean switch date (= Julian day 85, 26 March). The standard deviation of switch date is about 7 days (Hairston and Dillon, 1990), so temperature and photoperiod conditions mimicked Julian days 67.5 (8 March), 74.5 (15 March), 95.5 (5 April), and 102.5 (12 April). Temperatures at these times were established using averages of 11 years of *in situ* pond measurements (using linear extrapolation between measurement dates), and these values were paired with the photoperiods obtained from standard tables. Photoperiod-temperature combinations (L:D × °C) were set up in four controlled environment chambers as follows: 11.75:12.25 × 4.3, 12.00:12.00 × 6.0, 12.75:11.25 × 8.0, and 13.25:10.75 × 10.5. Photoperiods were established at the 15-min increment nearest to that for the chosen date, with illumination provided by daylight fluorescent lamps (17–38 $\mu mol \cdot s^{-1} \cdot m^{-2}$ depending upon location within the growth chamber); temperatures were maintained ± 0.5 C°.

Live fifth-instar copepodids of *D. sanguineus* were collected from Bullhead Pond on 2 March 1993. We mated 144 females in 125-ml glass jars (one female and two males per jar) at 8:16 L:D photoperiod and 4.8°C (*i.e.*, short-day and cold conditions to ensure that all clutches produced were subitaneous; see Hairston and Olds, 1986, 1987). The copepods were fed laboratory-cultured *Chlamydomonas* sp. every few days. From these matings we obtained 121 ovigerous females over a period of 17 days. An additional 82 ovigerous females were obtained over the same time period from the stock 20-l carboy of copepods in which the plankton were transported from Bullhead Pond. As egg-carrying females were found, they were distributed evenly among the four environmental treatments. When egg clutches hatched, the nauplii were placed in 250-ml glass jars, one family per jar, and again fed *Chlamydomonas*. As these animals reached copepodid stage, their diet was supplemented with *Euglena gracilis*. Mature males and females were taken from separate families within each environmental treatment and mated as previously described. Individual ovigerous females from these laboratory-reared cultures were isolated in 7-ml wells of 12-well plastic tissue culture plates and monitored daily for hatching. Based on established procedure (Hairston and Munns, 1984; Hairston and Olds, 1984, 1986), eggs hatching within 2 weeks (warm temperatures) or 4 weeks (cold temperatures) of laying were scored as subitaneous, and those that had not hatched by this time were scored as diapausing eggs.

Results

In each of the four environmental conditions, between 207 and 356 female copepods were reared from nauplius to ovigerous adult (Table I), although in the two lower temperature treatments a substantial fraction of the egg sacs produced were nonviable (*i.e.*, eggs turned grey and decomposed). The fractions of egg sacs that were either subitaneous or diapausing were calculated relative to the total number of viable sacs (Table I). Because the nature of the nonviable egg sacs could not be determined, we make the null assumption that viability was independent of egg type.

A plot of percent subitaneous clutches produced at each of the treatment conditions as a function of daylength (Fig. 1) shows that photoperiod and temperature together produce a diapause phenology remarkably similar to that observed in the wild. The fit is much better—both in mean timing and in the rapidity of the population switch to diapause—than that found previously for photoperiod alone (Hairston and Olds, 1986).

Table I

Photoperiod and temperature combinations under which diapause response was determined for Diaptomus sanguineus *(reasons for condition chosen given in the text), the total number of egg clutches produced (one clutch per female), the number of viable clutches, and the percentages of viable clutches that were either subitaneous or diapausing*

Treatment		Clutches		%	%
Daylength (h)	Temp. (°C)	Total	Viable	Subitaneous clutches	Diapausing clutches
11.75	4.3	356	265	91.3	8.7
12.00	6.0	293	121	74.7	25.6
12.75	8.0	245	243	12.8	87.2
13.25	10.5	207	203	2.0	98.0

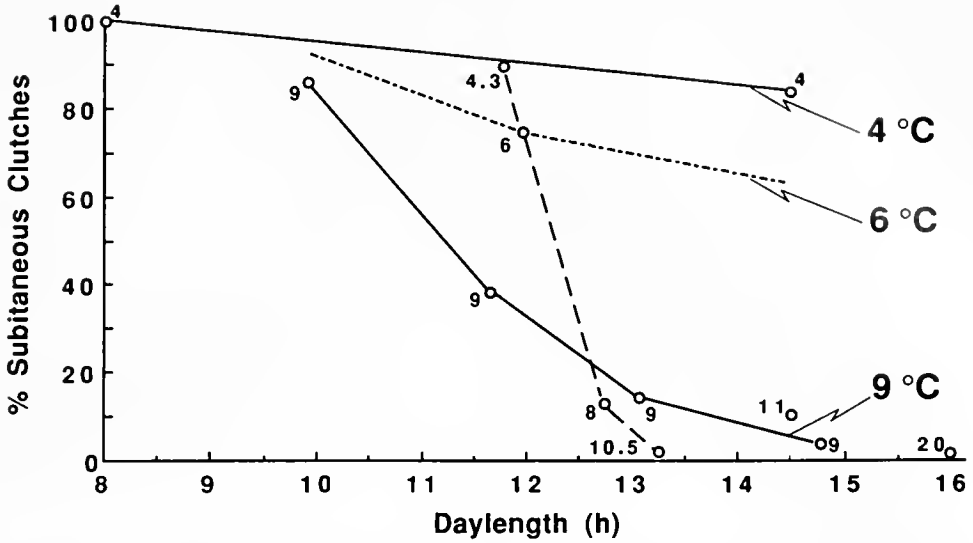

Figure 2. The fraction of subitaneous eggs (versus diapausing eggs) produced by *Diaptomus sanguineus* when reared in the laboratory at different combinations of photoperiod and temperature. The data, taken from three previous studies (Hairston and Olds, 1986, 1987; Hairston *et al.*, 1990) and the current investigation, show distinct diapause responses to daylength at different temperatures. Solid lines connect values from experiments at equal temperatures (4°C and 9°C). The dotted 6°C line is a hypothetical relationship based on the single 6°C point and the 4°C and 9°C lines. The dashed line connects the four photoperiod-temperature treatments reported here and thus shows the trajectory of diapause phenology of *D. sanguineus* as photoperiod and temperature increase during spring in Bullhead Pond, Rhode Island.

Discussion

For *Diaptomus sanguineus* in Bullhead Pond, the gradual effect of photoperiod at a constant temperature (Hairston and Olds, 1986, see Fig. 1) is converted into a discrete seasonal timing of diapause by the addition of a thermal cue. Similar to our result, those of Marcus (1982) show a gradual shift from subitaneous to diapausing egg production as a function of photoperiod for the calanoid copepod *Labidocera aestiva*, despite a seasonal transition to diapause in nature that is quite discrete (Marcus, 1979). In her study, however, temperature had a weaker effect on the diapause response than we have observed for *D. sanguineus*. Our result contrasts with the photoperiod-dominated pattern seen in many insect species (Danilevskii, 1965; Tauber *et al.*, 1986) and in several previous studies of diapause in pelagic copepods. Photoperiod plays a primary role in the switch to diapausing eggs in the calanoid copepod *Eurytemora affinis* (Ban, 1992) and in the late-instar diapause of the cyclopoid copepods *Diacyclops navus* (Watson and Smallman, 1971) and *Metacyclops minutus* (Alekseev, 1990). Copepod density can also act as a significant modifier of the photoperiod cue (*E. affinis*, Ban, 1992; *M. minutus*, Alekseev, 1990); and in *Diaptomus birgei*, photoperiod is only a secondary factor in cuing diapause (Walton, 1985).

How does temperature sensitivity convert a gradual photoperiod response into a relatively discrete seasonal switch to diapause for the *D. sanguineus* population? An answer emerges when we plot, in a single figure (Fig. 2), all of the available data for *D. sanguineus* diapause response at a range of photoperiods and temperatures (Hairston and Olds, 1986, 1987; Hairston *et al.*, 1990; this study). In this plot, the slope of the line relating the percentage of subitaneous clutches to the daylength is much shallower at 4°C than at 9°C. The single data point at 6°C is intermediate between these two lines, and we conjecture that a 6°C line would have an intermediate slope. Data points at higher temperatures (*i.e.*, 8–11°C) are variable, but uniformly give low values for the percentage of subitaneous clutches. The dashed line in Figure 2 shows what happens as both temperature and photoperiod change early in the season in Bullhead Pond. At short photoperiods, when water temperatures are 4°C or below, the copepods make subitaneous eggs. As spring comes on, not only does photoperiod increase, but so does temperature; thus the appropriate daylength-response shifts from the 4°C line to the 6°C line to the 9°C line, and so on. The result is the relatively discrete seasonal switch to production of diapausing eggs seen in Bullhead Pond. Note also that the data in Figure 2 could be expressed equally well by plotting the percentage of subitaneous clutches against temperature, with lines of equal photoperiod radiating from the upper left-hand corner. The photoperiod-temperature interaction would be still apparent.

Our depiction of the response of *D. sanguineus* to combined photoperiod and thermal cues (Fig. 2) illustrates only the phenotypes expressed by the copepods when exposed to environments of differing photoperiod and temperature combinations. Behind this response surface lies the physiological mechanisms by which the copepods detect daylength (or nightlength) and temperature and then react by producing the appropriate egg type.

Two alternative photoperiodic clock mechanisms have received substantial attention in the entomological literature. The circadian oscillator model posits an internal pacemaker of intrinsic period, which is then either compared (physiologically) to the environment (*i.e.*, photoperiod) or drives other, "slave," oscillators whose phases are differentially altered by the environment (Pittendrigh, 1981; Saunders, 1982; Gillanders and Saunders, 1992). The hourglass model hypothesizes the production of some chemical substance that accumulates incrementally during the dark (or the light) phase of a light-dark cycle, up to some critical threshold (Lees, 1973; Skopik and Bowen, 1976; Veerman *et al.*, 1988). Some recent studies have emphasized models that have an underlying oscillator but can exhibit hourglass-like behavior (*e.g.*, Vas Nunes *et al.*, 1991). In addition to providing a mechanism for critical photoperiod response, each model provides a mechanism for the influence of temperature in shifting critical photoperiod earlier or later in the season (Pittendrigh *et al.*, 1991; Vas Nunes *et al.*, 1991; Kimura and Masaki, 1993). The conversion, in *D. sanguineus*, of a graded photoperiod response to a much sharper seasonal phenology by the addition of a thermal cue results simply from a rightward shift (towards longer photoperiods) of the diapause response curve under low temperatures and a leftward shift (towards shorter photoperiods) under high temperatures (Fig. 3; explained in detail below). Because both clock models could, in principle, accommodate this behavior, the data presented here do not permit us to distinguish between the two alternatives. Nevertheless, experiments designed to determine the photoperiodic clock mechanism in this copepod should provide essential clues for understanding both the range of expression of diapause response by *D. sanguineus* to different environments and the possible constraints on the genetic covariance structure of sensitivity to photoperiod and thermal cues (*i.e.*, how selection on copepod sensitivity of diapause expression to photoperiod might influence trait sensitivity to temperature).

The pattern of photoperiod-temperature response proposed here does not in fact differ radically from typical thermal alteration of critical photoperiod. Figure 3A shows a family of hypothetical critical daylength responses modified by temperature that would produce a spring switch from production of subitaneous to diapausing eggs by a pelagic copepod species. If the lake temperature increased with lengthening photoperiod according to the patterns listed in Figure 3E, the copepods would make subitaneous eggs until the threshold photoperiod and temperature combination that induced a complete switch to diapausing eggs was reached. Figure 3B shows critical response curves more typical of many insect species in which the transition to diapause is not rectilinear but somewhat graded, with a thermal effect on critical photoperiod of 0.3 h per C° (*c.f.*, Danilevskii, 1965, pp. 114–115). Tracking the environment of Figure 3E produces a seasonal switch to diapause more rapid than that seen along any constant temperature line, though not as rapid as that seen in Figure 3A. In contrast to these two patterns, the photoperiod response lines for different temperatures in Figure 2 radiate from 100% subitaneous clutches at short photoperiod (*i.e.*, there is no temperature effect at short daylength). Suppose now that these lines of constant temperature reconverge at long photoperiods on 0% subitaneous clutches (100% diapause), as illustrated in Figure 3C. Tracking the Figure 3E environment again produces a seasonal switch to diapause, just as seen in Figure 2. The differences between each of these three patterns lie in the steepness of the slopes of the photoperiod responses. It is not difficult, however, to envision any one pattern being derived from one of the others through a simple change in how rapidly diapause responds to photoperiod at each temperature.

A gradual transition from production of subitaneous eggs to diapausing eggs in a single population implies that individual females must respond differently to any given photoperiod-temperature combination (*i.e.*, some fraction make subitaneous eggs while the others make diapausing eggs). For *D. sanguineus*, we know that there is significant heritable variation for diapause response at 13 h of light and 9°C in the laboratory (Hairston and Dillon, 1990). If the model in Figures 2 and 3C is an accurate representation of the sensitivity of the copepods' diapause response to temperature and photoperiod, it provides a means of envisioning how natural selection might act on this genetic variation to alter the timing of diapause in natural populations. For example, 500 m from Bullhead Pond lies Little Bullhead Pond. In 1979, the *D. sanguineus* population in this pond switched to diapause in late March, the same time as the population in Bullhead Pond. In 1981, a drought dried Little Bullhead Pond and killed all of the fish, thus removing the principal selection force maintaining the March diapause date. The pond refilled in 1982, and by 1983 the mean timing of diapause had moved to late April, apparently as a response to the altered selection regime (Hairston and Walton, 1986; Hairston and De Stasio, 1988). Bullhead Pond, which is deeper than Little Bullhead Pond, did not dry, no fish were killed, and the timing of diapause in that population changed little between 1979 and 1983 (Hairston and Walton, 1986;

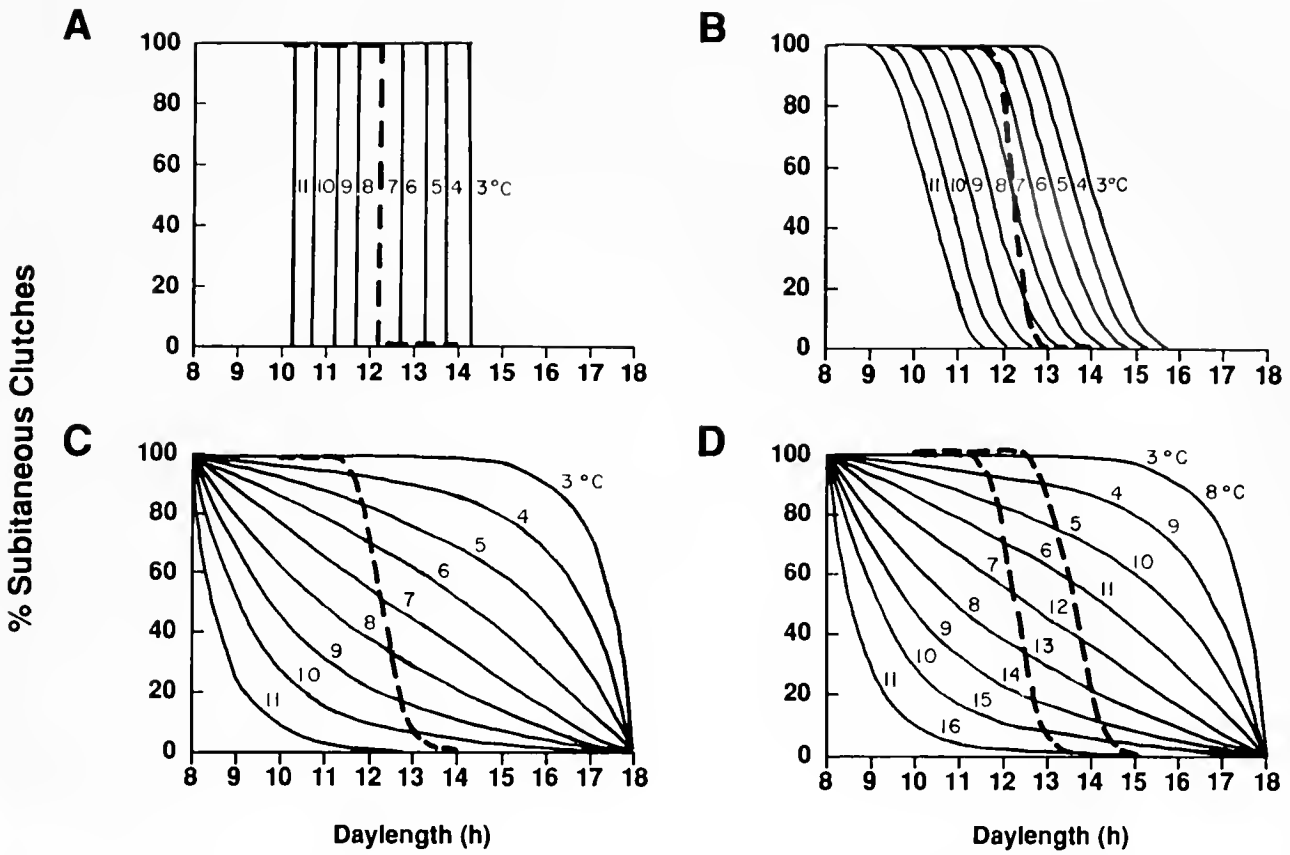

E

Date	Feb	1	10	21	Mar	6	18	29	Apr	10	20	May	5	20
Daylight (h)		10	10.5	11		11.5	12	12.5		13	13.5		14	14.5
Temp (°C)		3	3	3		4	6	8		10	11		13	18

Figure 3. Three patterns of springtime diapause responses under varying combinations of photoperiod and temperature. (A) Strict critical-photoperiod response with thermal effect. (B) Critical-photoperiod response with a graded transition from 100% non-diapause to 100% diapause covering a photoperiod range of about 2 h and a temperature delay of 1.5 h per 1°C, as is typical of many insects. (C) Gradual transition from 100% non-diapause to 100% diapause with lengthening daylength as seen for *D. sanguineus* (Fig. 2), but with the added assumption that all animals produce diapausing eggs at long photoperiods independent of temperature. (D) Same graph as in C, but with response line relabeled to show the effect of selection for later diapause. (E) Springtime pattern of increasing photoperiod and temperature typical of Bullhead Pond, Rhode Island (see Table I). These values are used in A, B, and C to illustrate projected diapause phenologies. In each case the mean switch to diapause occurs at 12.3 h daylength and 7°C.

Hairston and Dillon, 1990). What features of the photoperiod and temperature responses of the Little Bullhead Pond populations were altered by selection to produce the change in diapause phenology? For diapause timing to be heritable, the hypothetical temperature-specific photoperiod-response lines in Figures 2 and 3C must vary depending upon genotype. That is, for some genotypes the lines lie above the population mean, and for others the lines lie below the mean. Directional selection for later diapause would simply move the population mean response lines upward (as in Figure 3D). The effect is a joint one on both thermal and photoperiodic responses of the copepods: at a given temperature, the slope of the response to change in daylength is shallower, but also, at a given photoperiod, the position of each of the isothermal lines is raised. With the new temperature-specific photoperiod-response lines, the timing of diapause shifts to later in the season (Figure 3D).

Populations of *D. sanguineus* living in different lakes and ponds exhibit both distinct photoperiod responses

under controlled laboratory conditions (Hairston and Olds, 1986, 1987) and distinct seasonal diapause phenologies in the field (Hairston and Olds, 1984; Hairston *et al.*, 1985). Both the mean timing of diapause and the temporal pattern of the switch from subitaneous to diapausing eggs vary between populations. In ephemeral pools, water depths and temperatures fluctuate depending upon local rainfall, leading to a decoupling of temperature and photoperiod as predictors of time in the season. Here, *D. sanguineus* can show late-season reversals to subitaneous egg production (Hairston and Olds, 1987). The graphical model developed here provides a framework for investigating the genetic covariance structure underlying such interpopulation variation in diapause responses to photoperiod and to temperature, and how this structure differs to produce the variety of diapause phenologies observed in nature.

Acknowledgments

We thank C. Tauber, M. Tauber, S. Ellner, L. Polishchuck, and N. Hairston, Sr., for helpful discussions, and K. Batson for technical assistance. This research was supported by National Science Foundation grant BSR-9118894 to NGH and S. Ellner.

Literature Cited

Alekseev, V. 1990. *Crustaceans Diapause: Ecological and Physiological Aspects.* Nauka, Moscow. 143 pp.

Ban, S. 1992. Seasonal distribution, abundance and viability of diapause eggs of *Eurytemora affinis* (Copepoda: Calanoida) in the sediment of Lake Ohnuma, Hokkaido. *Bull. Plankton Soc. Jpn.* **39:** 41–48.

Beck, S. 1980. *Insect Photoperiodism.* Academic Press, New York. 387 pp.

Begon, M., J. L. Harper, and C. R. Townsend. 1990. Ecology: Individuals, Populations and Communities. Blackwell, Boston. 945 pp.

Danilevskii, A. S. 1965. *Photoperiodism and Seasonal Development of Insects.* Oliver and Boyd, Edinburgh. 283 pp.

Eizaguirre, M., C. López, L. Asín, and R. Albajes. 1994. Thermoperiodism, photoperiodism and sensitive stage in the diapause induction of *Sesamia nonagrioides* (Lepidoptera: Noctuidae). *J. Insect Physiol.* **44:** 113–119.

Gillanders, S. W., and D. S. Saunders. 1992. A coupled pacemaker-slave model for the insect photoperiodic clock: interpretation of ovarian diapause data in *Drosophila melanogaster*. *Biol. Cybern.* **67:** 451–459.

Hairston, N. G., Jr. 1987. Diapause as a predator-avoidance adaptation. Pp. 281–290 in *Predation. Direct and Indirect Impacts on Aquatic Communities*, W. C. Kerfoot and A. Sih, eds. Univ. Press of New England, Hanover, NH.

Hairston, N. G., Jr., and B. T. De Stasio, Jr. 1988. Rate of evolution slowed by a dormant propagule pool. *Nature* **336:** 239–242.

Hairston, N. G., Jr., and T. A. Dillon. 1990. Fluctuating selection and response in a population of freshwater copepods. *Evolution* **44:** 1796–1805.

Hairston, N. G., Jr., and W. R. Munns, Jr. 1984. The timing of copepod diapause as an evolutionarily stable strategy. *Am. Nat.* **123:** 733–751.

Hairston, N. G., Jr., and E. J. Olds. 1984. Population differences in the timing of diapause: adaptation in a spatially heterogeneous environment. *Oecologia* **61:** 42–48.

Hairston, N. G., Jr., and E. J. Olds. 1986. Partial photoperiodic control of diapause in three populations of the freshwater copepod *Diaptomus sanguineus*. *Biol. Bull.* **171:** 135–142.

Hairston, N. G., Jr., and E. J. Olds. 1987. Population differences in the timing of diapause: a test of hypotheses. *Oecologia* **71:** 339–344.

Hairston, N. G., Jr., and W. E. Walton. 1986. Rapid evolution of a life history trait. *Proc. Natl. Acad. Sci. USA* **83:** 4831–4833.

Hairston, N. G., Jr., T. A. Dillon, and B. T. De Stasio, Jr. 1990. A field test for the cues of diapause in a freshwater copepod. *Ecology* **71:** 2218–2223.

Hairston, N. G., Jr., E. J. Olds, and W. R. Munns, Jr. 1985. Bet-hedging and environmentally cued diapause strategies of diaptomid copepods. *Int. Ver. Theor. Angew. Limnol. Verh.* **22:** 3170–3177.

Hairston, N. G., Sr. 1994. *Vertebrate Zoology: An Experimental Field Approach.* Cambridge Univ. Press, Cambridge. 347 pp.

Harper, J. L. 1977. *Population Biology of Plants.* Academic Press, New York. 892 pp.

Kimura, Y., and S. Masaki. 1993. Hourglass and oscillator expression of photoperiodic diapause response in the cabbage moth *Mamestra brassicae*. *Physiol. Entomol.* **18:** 240–246.

Kogure, M. 1933. The influence of light and temperature on certain characters of the silkworm, *Bombyx mori*. *J. Seric. Sci. Jpn.* **4:** 1–93.

Lees, A. D. 1955. *The Physiology of Diapause in Arthropods.* Cambridge Univ. Press, Cambridge. 151 pp.

Lees, A. D. 1973. Photoperiodic time measurement in the aphid *Megoura viciae*. *J. Insect Physiol.* **19:** 2279–2316.

Marcus, N. H. 1979. On the population biology and nature of diapause of *Labidocera aestiva* (Copepods: Calanoida). *Biol. Bull.* **157:** 297–305.

Marcus, N. H. 1982. Photoperiodic and temperature regulation of diapause in *Labidocera aestiva*. *Biol. Bull.* **162:** 45–52.

Pittendrigh, C. S. 1981. Circadian organization and the photoperiodic phenomena. Pp. 1–35 in *Biological Clocks in Seasonal Reproductive Cycles*, B. K. Follett and D. E. Follett, eds. Wiley, New York.

Pittendrigh, C. S., W. T. Kyner, and T. Takamura. 1991. The amplitude of circadian oscillations: temperature dependence, latitudinal clines and the photoperiodic time measurement. *J. Biol. Rhythms* **6:** 299–313.

Saunders, D. S. 1982. *Insect Clocks.* 2nd ed. Pergamon Press, New York. 409 pp.

Skopik, S. D., and M. F. Bowen. 1976. Insect photoperiodism: an hourglass measures photoperiodic time in *Ostrinia nubilalis*. *J. Comp. Physiol.* **111:** 249–259.

Tauber, C. A., and M. J. Tauber. 1981. Insect seasonal cycles: genetics and evolution. *Ann. Rev. Ecol. Syst.* **12:** 281–308.

Tauber, M. J., C. A. Tauber, and S. Masaki. 1986. *Seasonal Adaptations of Insects.* Oxford Univ. Press, New York. 411 pp.

Vas Nunes, M., R. D. Lewis, and D. S. Saunders. 1991. A coupled oscillator feedback system as a model for the photoperiodic clock in insects and mites. II. Simulations of photoperiodic responses. *J. Theor. Biol.* **152:** 299–317.

Veerman, A., M. Beekman, and R. L. Veenendaal. 1988. Photoperiodic induction of diapause in the large white butterfly, *Pieris brassicae*: evidence for hourglass time measurement. *J. Insect Physiol.* **34:** 1063–1069.

Walton, W. E. 1985. Factors regulating the reproductive phenology of *Onychodiaptomus birgei* (Copepoda: Calanoida). *Limnol. Oceanogr.* **30:** 167–179.

Watson, N. H., and B. N. Smallman. 1971. The role of photoperiod and temperature in the induction and termination of an arrested development in two species of freshwater cyclopoid copepods. *Can. J. Zool.* **49:** 855–862.

Reference: *Biol. Bull.* **189**: 49–58. (August, 1995)

Process-Specific Recruitment Cues in Marine Sedimentary Systems

SARAH A. WOODIN, SARA M. LINDSAY, AND DAVID S. WETHEY

Department of Biological Sciences, University of South Carolina, Columbia, South Carolina 29208

Abstract. In marine sediments, many of the processes associated with high post-settlement mortality of infauna have similar effects on the sediment surface. In most cases the original sediment surface is either removed, buried, or mixed with subsurface sediment. The experiments reported here tested the ability of new juvenile infauna to discriminate between undisturbed and recently disturbed sediment surfaces (*i.e.*, subsurface sediment exposed).

Recently settled juveniles of two polychaete species (*Nereis vexillosa* and *Arenicola cristata*) and one bivalve species (*Mercenaria mercenaria*) were exposed to simulated erosional and mixing events as well as to fresh feces, burrow tailings, and feeding tracks. Where the disturbance buried or removed several millimeters of the sediment surface, the time to initiate burrowing or the percentage of individuals failing to burrow increased significantly over times and percentages for juveniles on undisturbed surfaces. In all cases the results were consistent with the hypothesis that new juveniles reject (or are significantly slower to burrow into) disturbed sediment surfaces, if the disturbance is less than several hours old. For example, 51% of nereid juveniles did not burrow when placed on subsurface sediments, whereas 100% burrowed into surface sediments; their average burrowing time on surface sediments was 29.3 s compared with 109.7 s on fecal mounds of arenicolid polychaetes or 106.1 s on burrow tailings of thalassinid crustaceans. Individuals that did not indicate acceptance of a sediment surface by burrowing were all rapidly eroded from the surface in the presence of flow. Erosion of nonburrowing individuals occurred within 90 s of initiation of flow. Burrowing individuals were not eroded. The decision as to the acceptability of a sediment was made within 30 s. These data imply that the new juveniles are utilizing cues associated with a process, the disturbance of surface sediments, in addition to the species-specific cues described elsewhere.

Received 12 December 1994; accepted 2 May 1995.

Contribution Number 1051 of the Belle W. Baruch Institute for Marine and Coastal Research.

Introduction

Recruitment is of fundamental importance to community structure because it is the foundation upon which all subsequent interactions within the community take place. When recruitment fails, organisms do not have the opportunity to interact as adults (Underwood and Denley, 1984). Therefore, the often substantial variation in success of recruitment (Loosanoff, 1964; Wethey, 1985; Feller *et al.*, 1992) can profoundly influence the dynamics of adult populations. Two major classes of processes combine to determine the eventual recruitment success of species with planktonic larvae, assuming that competent larvae are in the plankton. First, larval transport on geographic and local scales can determine how many larvae actually reach a site and are retained (Boicourt, 1982; Cameron and Rumrill, 1982; Kendall *et al.*, 1982; Levin, 1984; Jonsson *et al.*, 1991). Only larvae that arrive on the bottom have an opportunity to exercise a behavioral choice of substratum (Highsmith, 1982; Butman *et al.*, 1988). Second, mortality and emigration occurring during or after settlement and metamorphosis can determine the success of the larvae that settle (Sellmer, 1967; Muus, 1973; Sigurdson *et al.*, 1976; Bell and Coull, 1980; Brenchley, 1981; Levin, 1981; Wilson, 1981; Watzin, 1983; Luckenbach, 1984; Connell, 1985; Wethey, 1985; Elmgren *et al.*, 1986; Woodin, 1986; Eyster and Pechenik, 1987; Walters, 1992). Thus, both presettlement and postsettlement events are involved in recruitment.

The literature on recruitment is dominated by two types of papers, those on mortality and those on larval choice. This dichotomy is interesting because the mortality literature is primarily directed toward elucidating how var-

ious postsettlement factors cause greater mortality, *i.e.*, on negative influences. The literature on choice, if it were parallel, would be on cues by which new recruits avoid sites that have characteristics associated with high mortality. Instead, most of the choice literature is directed toward identification of positive, species-specific cues that are associated with the presence of either prey (Hadfield, 1984; Morse and Morse, 1984) or mates (Highsmith, 1982; Crisp, 1984). We would argue that given the cues associated with high mortality and the characteristics of recruits that allow them to recognize such cues, there would be strong selection for retention of individuals with such traits (for examples of larvae with such traits see Johnson and Strathmann, 1989, and Grosberg, 1981).

A characteristic common to the majority of the mortality sources for new juveniles in sediments, such as predation, erosion, and deposition, is that these mortality sources alter the sediment surface either by removing it or by covering it with a layer of subsurface or a mixed surface-subsurface. A testable deduction consistent with our proposed selection regime, then, is that new recruits distinguish between recently disturbed and undisturbed sediment surfaces. The experiments described here were designed to test this hypothesis. We confined ourselves to sediments that are stable and rarely move as bedload (for events characteristic of more mobile habitats, see Emerson and Grant, 1991). We defined the disruptions of interest to be those that either covered the original surface of the sediment or removed at least 3–5 mm vertically. Biotic erosional forces, such as tellinid bivalve feeding, and physical erosion can easily remove at least this much sediment. We also asked whether the behavior of new juveniles on disturbed surfaces is likely to result in rates of recruitment that are reduced compared with those on undisturbed surfaces.

Materials and Methods

Background information on infauna

New juveniles of infaunal bivalves and polychaetes were used to contrast the responses of taxa that can burrow as new juveniles (the polychaetes) and those that cannot (the bivalves). The use of new juveniles rather than settling larvae also avoids the potentially serious problem of differentiating between competent larvae and incompetent larvae of similar size and appearance (Bachelet *et al.*, 1992). Bivalves and polychaetes are quite different at the initiation of metamorphosis. For example, bivalves have a shell at settlement but usually cannot burrow for a week or more after metamorphosis begins (Belding, 1930; Carriker, 1961; Gustafson and Reid, 1986). Polychaetes lack a shell but can burrow at this developmental stage (Wilson, 1952; Roe, 1975). Bivalves generally cannot emigrate from a habitat by swimming off the bottom once their velum has been lost; they can, however, both crawl and use water currents to waft away from a site after erosion off the bottom sediment (Sigurdsson *et al.*, 1976; Sastry, 1979). Many polychaete juveniles can crawl, waft, and actively swim away from a site, even after they metamorphose (*e.g.*, Roe, 1975). The important point of similarity is that sediment-dwelling juveniles of both taxa can crawl away as well as waft away. Thus rejection of a site may occur at the juvenile as well as the larval stage.

In all experiments, we used juveniles that had initiated metamorphosis less than one week before they were tested. The polychaetes were *Nereis vexillosa*, a nereid, and *Arenicola cristata*, an arenicolid. These larvae are lecithotrophic and were not fed. The juveniles of both species were fed *Isochrysis galbana* T-ISO strain as well as a mixture of diatom species. *Nereis* is common near the University of Washington Friday Harbor Laboratories on San Juan Island, Washington. Females lay egg masses containing hundreds of eggs (Johnson, 1943). *Arenicola* also lays egg masses that are initially attached to the bottom. Egg masses of both species were collected in the field and transported to the laboratory, where they were placed in individual micro-airlifts (Strathmann, 1987) until the larvae hatched at four to five setigers (*Nereis*) or three to four setigers (*Arenicola*). Swimming larvae were cultured in 11-cm-i.d. glass culture dishes. When the larvae develop six setigers, at a length of about 500 μm for *Nereis* and about 600 μm for *Arenicola*, the larvae will burrow and build tubes in acceptable sediments. Both polychaete species actively reject some sediments by either initiating a crawling sequence or standing perpendicular to the sediment surface, attached only by a mucus thread. In flowing water such individuals are easily eroded off their attachment point (see below). Sediments into which the recruits did not burrow within the observation period were classified as unacceptable.

The bivalve species used in these experiments was *Mercenaria mercenaria*. Late pediveligers of *Mercenaria* were cultured in the laboratory with stirring and fed *Isochrysis galbana* T-ISO strain until settlement and initiation of metamorphosis. The individuals of *Mercenaria* averaged 0.307 mm (SD = 0.035) in length. New spat of *Mercenaria* do not penetrate the sediments and burrow; rather they nestle into the substratum to about half the length of the shell, position themselves with the hinge down, and gape slightly (Carriker, 1961). Initiation time for spat was defined as the time at which the foot of the individual penetrated the sediment surface and the shell was pulled down. In some types of sediments the spat fail to show this nestling behavior: instead they remain on the surface, typically resting on one valve or sometimes actively crawling across the sediment without any evidence of movement of the hinge and shell below the sediment sur-

face. Sediments eliciting such behaviors were classified as unacceptable.

Behavioral observations

Glass dishes with a 1.5- to 2-cm layer of test sediment on the bottom, covered by a layer of seawater 2 cm deep, were used for observations. Individual juveniles were gently pipetted into the water column and allowed to drift onto the sediment surface. Individuals that contacted the sediment surface forcefully, landed on a sand grain larger than their length, or (for the worms) landed in any position other than their ventral surface were not used in the analyses. Timing of responses to the sediments began when the individual made contact with the sediment surface. A dissecting microscope was used to monitor individuals continuously from their arrival on the sediment surface until they disappeared below the surface (polychaetes) or nestled in among the surface sediments and began to feed (bivalves), or until the designated observation period expired. The length of the observation period depended upon the species (*Nereis*, 5 min; *Mercenaria*, 6 min; *Arenicola*, 7 min) and was set to a minimum of 10× the mean time individuals took to initiate burrowing in preliminary observations. In the experiments with *Nereis* and *Mercenaria*, 4 to 10 individuals were separately added to each dish or core. To avoid the possibility of interactions, individuals that landed within 2 cm of another animal were not used.

Experimental sediments

Experimental sediments were collected in the field and immediately transported to the laboratory. Sediments were collected as two types: surface sediments (the top 1- to 2-mm-thick layer) and subsurface sediments (the 1- to 2-mm-thick layer exposed after removal of the top 4 to 5 mm). In the field, the surface sediments were collected with a paint scraper. Areas of disturbance such as fecal mounds, burrow scrapings, tubes, and feeding traces were avoided. Subsurface sediments were collected by removing the top 4 to 5 mm of sediment and then collecting the next 1 to 2 mm with a paint scraper. In field-processed sediments, each type of sediment was collected and placed in a 11-cm-i.d. glass dish, creating a layer 1.5 to 2.0 cm deep. Once in the laboratory, each dish was filled with seawater to a depth of at least 2 cm. Dishes were stored floating in a seawater table and were used within 2 h. In addition, we used several other types of sediments: fresh feces of arenicolid polychaetes (*Abarenicola pacifica*), fresh burrow scrapings of thalassinid crustaceans (*Upogebia pugettensis*), 1:1 mixtures by volume of surface and subsurface sediments, and sediments that had been reworked physically by storm events. All were used within 2 h of collection, including the 1:1 mixtures that were made from field-collected sediments.

Juvenile *Nereis* were also tested on sediments containing active macrofauna. Sediments from False Bay were defaunated by freezing, thawing, and refreezing, then rinsed thoroughly with seawater and sieved on a 0.5-mm mesh. Cores (7 cm × 6 cm i.d.) of defaunated sediment were either innoculated with known numbers and species of macrofauna or left as controls. After two weeks, juvenile *Nereis* were exposed to the surfaces of each type. Within the macrofauna-addition cores, the juveniles were added to the feeding areas of the macrofauna (half of the tested cores) as well as to sites outside of the feeding areas (remainder of the macrofauna-addition cores). The macrofauna used were three species of spionid polychaete (*Spio* sp., *Rhynchospio glutaeus*, and *Pygospio elegans*) and a tellinid bivalve (*Macoma nasuta*).

Several sites were used for sediment collection. In all cases adults of the species to be tested were common at the collection site. For *Nereis vexillosa* the sites were a semiprotected fine sandflat, False Bay, Washington (48°29′ N: 123°04′ W, median grain size 0.18 mm, silt-clay 10%) and a more enclosed bay with a mud-gravel sediment mixture, Snug Harbor, Washington (48°34′ N, 123°10′ W, median grain size 1.66 mm, silt-clay 6%). For *Arenicola cristata* and *Mercenaria mercenaria* the sites were medium- to fine-grained sandflats on the landward side of Pawleys Island, South Carolina (33°24′ N, 79°8′ W, median grain size 0.39 mm, silt-clay 0.05%) and at Oyster Landing, North Inlet, South Carolina (33°20′ N, 79°12′ W, median grain size 0.38 mm, silt-clay 0%). The numbers of replicates per treatment differed among experiments and are given in the Results section.

All experiments on *Nereis vexillosa* were run in June 1990 at the Friday Harbor Laboratories. The controls were run on every day of the experiment, and each experimental treatment was run on most days. The experiments on *Arenicola cristata* were run in July 1992. Those on *Mercenaria mercenaria* were run in May 1991. Controls were always alternated with experimental sediments to ensure that the juveniles were still responsive.

Flume observations and design

A rectangular pipe flume, 1.3 × 10 cm in cross section and 1.26 m in length, was fitted with a 2.5 × 2.5 cm sediment box 0.8 m from the inlet. Honeycomb material (5-mm cells, 11 cm long) was used as a flow straightener in the inlet. A hot film flow sensor (TSI 1231W) was flush-mounted 0.5 cm upstream from the test section. The sensor was calibrated in the wall of a cylindrical pipe. The flume geometry is scaled up from the larval flume used by Eckman *et al.* (1990) in their studies of barnacle cyprids. Rectangular pipe flow was turbulent, with boundary

layer growth from the top, bottom, and sides of the flume. The test section was small enough that flow characteristics varied by no more than 10% over its area. The flow near the sediment surface can be summarized by the boundary shear velocity u_*, which is a measure of the turbulent momentum transfer from the water to the sediment, and is calculated from the covariance between the vertical (v) and horizontal (u) velocity fluctuations:

$$u_* = \sqrt{\text{cov}\,(u.v)}$$

In our flow treatments the boundary shear velocity was approximately 1.0 cm s^{-1}, which is close to the critical erosion condition for sediments in False Bay (critical erosion u_* = 1.2 cm s^{-1}: Miller and Sternberg, 1988). In our flow treatments, which are typical of tidal flows, surface sand grains wiggled and surface floc was eroded. In storms with 15-cm waves, u_* can be 3.5 cm s^{-1} or higher, and large amounts of sediment are resuspended (Miller and Sternberg, 1988).

Individual juveniles were introduced to the flume through an opening about 1 cm upstream of the test section. As in the still-water dish experiments, individuals were timed from the moment of initial contact with the sediment surface. A dissecting microscope with a video camera was used to observe the behavior of six-setiger *Nereis* juveniles on sediments of three types: surface sediments of False Bay origin; clean, not previously seawater-aged, foundry sand; and surface sediments of False Bay origin contaminated with the dibromobenzyl alcohol produced by the terebellid polychaete *Thelepus crispus*. Contaminated sediments resulted from introducing *T. crispus* into the sediments for a minimum of 48 h (for concentration data as well as extraction details, see Woodin *et al.*, 1993). Such sediments are known to be rejected by juveniles of *Nereis* in both the field and the laboratory (Woodin *et al.*, 1993). In most cases, juveniles were observed in still and flowing water.

Statistical analysis

All experiments were analyzed using PC SAS version 6.04 (SAS Institute, Cary, NC). The data were of two types: (a) times to initiation of burrowing or nestling and (b) percentages of juveniles per dish accepting or rejecting the sediment. In the first case only individuals that initiated burrowing or nestling were used. The burrowing times were analyzed by analysis of variance (*Arenicola*) or nested analysis of variance with dishes nested under treatment (*Nereis* and *Mercenaria*). If a large number of the individuals failed to initiate burrowing, making the number of observations per dish per treatment highly unbalanced, then the analysis was done on the average time to initiation of burrowing for each dish. In these cases, the analysis was not nested. Simultaneous comparisons among treatments were made with the Tukey's studentized range test. All data were examined for normality and homogeneity of variance and transformed if necessary. The analyses and transformations used are indicated for each experiment below. The percentage burrowing data for the nereid juveniles were normalized using an arcsine square root transformation and analyzed by analysis of variance followed by an *a posteriori* Tukey's studentized range test, except for the data from Snug Harbor. Those data were non-normal with unequal variances per treatment, so the data were analyzed by separate Fisher's exact tests using a conservative probability of 0.01. For the data on *Mercenaria* and *Arenicola* juveniles where only two treatments were involved, a Fisher's exact test was used.

Results

Juveniles on field-collected sediment

When sediment from a semiprotected fine sand site (False Bay, WA) was used, juveniles of *Nereis vexillosa* clearly differentiated between surface and subsurface layers; 100% burrowed into surface sediments and 51% burrowed into subsurface sediments (Table I: False Bay—Calm). The same was true for 1:1 mixtures by volume of surface and subsurface sediments; 25% failed to burrow within the 5-min observation period. In contrast, the rejection rates were only 12% and 14% for freshly collected burrow cleanout sediments of thalassinid crustaceans (burrow tailings) and arenicolid polychaete feces, respectively. The percentages of juveniles rejecting the sediment were significantly greater for the subsurface and 1:1 mixture treatments than for the surface, feces, and burrow tailings (ANOVA, arcsine square root transformation: df = 4, 19; MSE = 0.0599; $F = 6.39$; $p < 0.005$; multiple comparison tests: Table I). For individuals that did burrow, times to initiate burrowing were significantly shorter on undisturbed surface sediments than on all treatments including naturally disturbed sediments (ANOVA, reciprocal transformation of average times per dish: df = 4, 19; MSE = 0.00017; $F = 6.10$, $p < 0.005$) (Table I: False Bay—Calm).

The surface *versus* subsurface trials were repeated with juveniles of *Nereis* in a mud-gravel mixed sediment (Snug Harbor, WA). The results were similar to those for the fine sand habitat (False Bay, WA). One hundred percent of the nereid juveniles burrowed into the surface sediments, but only 50% burrowed into the subsurface sediments. For individuals that did burrow, times to initiate burrowing were significantly shorter in all treatments other than the subsurface sediments (Table I: Snug Harbor) (ANOVA, average times per dish: df = 3, 6; MSE = 79.53; $F = 40.29$, $p < 0.0005$). Because of resuspension problems,

Table I

Responses of nereid juveniles to selected sediment types: Part A, rejection percentages by dish; Part B, initiation times in seconds of individuals that burrowed

Part A. Percentage of Individuals That Did Not Burrow

	False Bay—Calm		False Bay—Storm		Snug Harbor—Calm	
Sediment	*N*	Reject	*N*	Reject	*N*	Reject
Surface	45	0 (0) A	10	0 (0) A	40	0 (0) A
Subsurface	31	51 (12) B	8	0 (0) A	30	50 (26.5) B
1:1 mix	39	25 (7) B	NA	NA	NA	NA
Feces	50	14 (8) A	NA	NA	21	0 (0) A
Bur. tailings	50	12 (6) A	NA	NA	20	0 (0) A

Part B. Initiation Times (s) of Individuals That Burrowed

	False Bay—Calm		False Bay—Storm		Snug Harbor—Calm	
Sediment	*N*	Init. (s)	*N*	Init. (s)	*N*	Init. (s)
Surface	45	29.3 (3.8) A	10	58.4 (21.6) A	40	15.3 (3.8) A
Subsurface	15	126.6 (11.0) B	8	41.8 (6.8) A	15	97.8 (5.9) B
1:1 mix	30	117.6 (25.7) B	NA	NA	NA	NA
Feces	43	109.7 (19.5) B	NA	NA	21	25.2 (10.3) A
Bur. tailings	44	106.1 (24.3) B	NA	NA	20	31.6 (3.5) A

'1:1 mix' are volumetric mixtures of surface and subsurface sediments; 'feces' are fresh feces of the polychaete *Abarenicola pacifica*; 'bur. tailings' are fresh burrow cleanouts of the thalassinid crustacean *Upogebia pugettensis*. 'Reject' is the mean percentage of individuals per dish which did not burrow. 'Init. (s)' is the time in seconds to initiation of burrowing into the sediment. These are means and standard errors of individuals by dish. 'NA' means not available. Letters after each number indicate the results of *a posteriori* Tukey's studentized range tests ($p \leq 0.05$) for that column category, with the exception of the percent rejection data for Snug Harbor, which are Fisher's exact tests. Numbers with the same letter within a column are not significantly different from one another. False Bay is a semiprotected, muddy sand site, while the sediment at Snug Harbor is a protected mud-gravel mixture. 'False Bay—Storm' are results from False Bay sediments following a windstorm that caused whitecaps within the bay. '*N*' is total number of juveniles used in that treatment.

we were unable to make satisfactory 1:1 mixtures of the sediments at this site.

The results for time to initiate burrowing for the juveniles of *Arenicola cristata* were similar to those for *Nereis vexillosa*. The time to initiate burrowing was significantly longer for juveniles on subsurface sediments than on surface sediments (ANOVA, log transformed times: df = 1, 21; MSE = 0.0497; $F = 26.97$; $p < 0.0001$) (Table IIB). The percentage burrowing into each treatment was equivalent: 93% burrowed into surface sediments; 86% burrowed into subsurface sediments.

New juveniles (spat) of *Mercenaria mercenaria* clearly differentiated between surface and subsurface sediments, both in mud and sand (Table IIA). The initiation times were significantly shorter on surface sediments than on subsurface sediments (nested ANOVA, log base 10 transformed data: df = 1, 4; MSE = 0.064; $F = 39.4$; $p < 0.005$) (Table IIA). Correspondingly, for both mud and sand sediment combined, 100% nestled into surface sediments, but only 40% to 50% nestled into subsurface sediments (Table IIA). The initiation times were not significantly different between mud and sand sediments (nested ANOVA, log base 10 transformed data: df = 1, 24; MSE = 3.13; $F = 0.08$; $p = 0.78$). Particle size appears to be much less important than whether the sediment is from the surface or the subsurface.

Storm-mixed sediments

At one of our sites, False Bay, storms have been observed to resuspend and transport surface sediment layers at a rate of 16 mg cm^{-2} s^{-1} (average sediment flux rate without regard to direction) and 5.4 mg cm^{-2} s^{-1} (deposition or vertical sediment flux rate) (Miller and Sternberg, 1988). When a storm occurred during these experiments, we collected surface and subsurface sediments and exposed the nereid juveniles to them. As expected under these conditions—surface and subsurface sediments thoroughly mixed to a depth of several centimeters—there was no significant difference in time to initiate burrowing on surface compared with subsurface sediments (Table I: False Bay—Storm: nested ANOVA: df = 1, 6; MSE = 1578.48; $F = 0.65$; $p = 0.45$). One hundred percent of the nereid juveniles burrowed into the surface and the subsurface sediments. This result is quite different from that obtained with 1:1 mixtures of sediment in which subsurface sediment was mixed with surface sediment without the agitation and aeration typical of storm-induced sediment mixing.

Feeding traces

Juvenile *Nereis* were also tested on sediments containing active macrofauna: the spionid polychaetes *Spio* sp., *Rhynchospio glutaeus*, and *Pygospio elegans* and the tellinid bivalve *Macoma nasuta*. Individuals of each species were introduced into separate cores of defaunated sediment and maintained in the laboratory in running seawater for two weeks before use. Only cores with obvious feces after the two-week incubation were used. Controls were cores without added fauna; these control cores were also maintained in running seawater in the laboratory for two weeks before use. Although 100% of the nereid juveniles burrowed in all treatments, times to initiate burrowing were significantly different among the treatments (nested ANOVA on log transformed data: df = 7, 16; MSE = 0.0883; $F = 18.76$; $p < 0.0001$). The feeding traces of *Macoma* caused a significant increase in time to initiation of burrowing (Table IIIA). Of the species tested, *Macoma* is the infaunal organism with the deepest feeding

Table II

Times in seconds to initiate nestling or burrowing into the sediment ('Init. Time') by juveniles of Mercenaria mercenaria *and* Arenicola cristata

Sediment	Type	*N*	Init. Time	*N*	Perc. Reject
Mercenaria mercenaria	Surface	10	35.7 (7.7) A	10	0 (0) A
Mud	Subsurface	5	156.6 (35.5) B	10	50 (50) B
Muddy sand	Surface	10	21.7 (6.7) A	10	0 (0) A
	Subsurface	6	128.4 (7.1) B	10	40 (20) B
Arenicola cristata	Surface	13	41.4 (6.4) A	14	7 A
Muddy sand	Subsurface	12	133.9 (23.2) B	14	14 A

Percentage of the individuals that did not nestle or burrow within the observation period ('Perc. Reject'). Letters after each number indicate the results of *a posteriori* Tukey's studentized range tests ($p \leq 0.05$) for initiation times in seconds ('Init. Time') or a Fisher's exact test for percentage rejecting the sediment ('Perc. Reject'). Numbers with the same letter are not significantly different from one another. '*N*' is number of juveniles in that treatment. Means and standard errors are for individuals by dish for *Mercenaria mercenaria* and by treatment for *Arenicola cristata*.

traces: 2 to 5 mm compared with 1 mm or less for the spionid polychaetes.

Times to burrow were significantly greater on recent feeding traces than in adjacent areas (nested ANOVA on log transformed data: df = 3, 32; MSE = 0.1132; $F = 5.33$; $p < 0.01$) (Table IIIB). The distances between sites of different types on a single core surface were 3 cm or less, showing that differentiation can occur on small spatial scales.

Table III

Times in seconds ('Init. Time') for juveniles of Nereis vexillosa *to initiate burrowing*

Macrofauna	Type of Location	Init. Time	*N*
Part A.			
Spio (P)	Control	7.3 (0.7) A	15
	Feeding	8.3 (1.0) A	15
Pygospio (P)	Control	15.1 (3.4) A	15
	Feeding	7.3 (1.6) A	16
Rhynchospio (P)	Control	10.4 (2.7) A	15
	Feeding	10.7 (2.0) A	17
Macoma (B)	Control	14.6 (1.9) A	20
	Feeding	59.5 (19.6) B	22
Part B.			
Macoma (B)	Outside recent disturb.	24.5 (6.8) A	17
	New feeding areas	59.5 (19.6) B	22

Means and standard errors of initiation times by core. Part A. Results from core surfaces with known macrofauna present, feeding areas only ('feeding') or from surfaces of cores held in the same tank but without macrofaunal additions ('control'). Part B. Results for cores with *Macoma*, different locations within the same core. All cores with *Macoma* added but sites designated as recently disturbed or undisturbed. Recently disturbed sites were areas of recent feeding activity by *Macoma*. The surface floc layer was missing and the feeding traces were clearly defined. Letters in parentheses after the species indicate taxon: 'P' polychaete and 'B' bivalve. Letters after each number indicate the results of *a posteriori* Tukey's studentized range tests ($p \leq 0.05$) for that column category within that section of the table. '*N*' is total number of juveniles used in that treatment.

Flow versus *no-flow conditions*

In the flume with surface sediments as the test substrate, times to initiate burrowing by *Nereis* juveniles were similar for still water and flow treatments (Table IV: Burrowed: Init.), and burrowing individuals were not eroded from such surfaces. All but 3 of 17 juveniles successfully burrowed in the flow treatment; all burrowed without flow (Table IV). In the flow treatment, flow was initiated as soon as the individual appeared to reach the sediment surface. The three that were eroded blew off at 2, 3, and 135 s. The first two probably had not made contact with the sediment surface before flow was initiated.

Observations were also made on individuals placed onto sediments likely to be unacceptable to the nereid juveniles: clean foundry sands and sediment contaminated with the bromobenzyl alcohol of *Thelepus crispus* (Woodin *et al.*, 1993). The nereids did not burrow immediately on either of these sediments; in contrast, on uncontaminated surface sediments, the nereid juveniles burrowed on average within 11 s both with and without flow (Table IV). To ensure that individuals had made contact with the sediment surface in the treatments with foundry sand and with contaminated sediments, flow was not initiated until at least 20 s after the juveniles made contact with the sediments. Individuals remaining on the surface for more than 40 s were eroded within 2 min in all but 3 of 17 cases. One of the three eventually burrowed (at 210 s), while the other two eroded off. Times to erosion once flow was initiated are given in Table IV. On average, individuals were eroded in less than 80 s with flow (Table IV: Erosion Time in Flow).

Discussion

Surfaces of sedimentary habitats are dynamic landscapes, changing in response to both biotic and physical forces. Currents, winds, and waves can mix, resuspend, transport, move as bedload, and deposit sediments, al-

Table IV

Responses of nereid juveniles to selected sediment types in the flume

	Burrowed		Eroded			
	N	Init. (s)	*N*	Seconds	Erosion time in flow	Perc. reject
Surface Sed.						
No flow	7	9.8 (14.7) A	0	NA	NA	0 A
Flow	14	10.4 (5.8) A	3	46.7 (76.5)	46.7 (76.5)	17.6 A
All with Flow						
Surface sed.	14	10.4 (5.8)	3	46.7 (76.5) A	46.7 (76.5) A	17.6 A
Foundry sand	0		8	170.1 (135.3) B	80.7 (96.8) A	100 B
Thelepus sed.	1	210	9	51.3 (17.5) AB	15.9 (15.2) A	90.0 B

'Burrowed' means those individuals that burrowed into the sediment. 'Init. (s)' is the time in seconds to initiation of burrowing into the sediment. 'Eroded' is the time in seconds from contact with the sediment surface to erosion and includes both time with and without flow. 'Erosion Time in Flow' is the time in seconds from initiation of flow to erosion off the surface. 'Perc. Reject' is the percentage of the individuals that did not burrow. '*N*' is the number of juveniles per category of a treatment. 'NA' means not available. For example, in the no-flow treatment for surface sediments, 7 juveniles burrowed, none were eroded, and 0% rejected the sediment. Letters after each number indicate the results of *a posteriori* Tukey's studentized range tests ($p \leq 0.05$) for that column category with the exception of 'Perc. Reject', which are results of Fisher's exact tests. Numbers with the same letter within a column are not significantly different from one another at the 0.05 level. Means and standard deviations are given.

tering the landscape (Miller and Sternberg, 1988). Biotic events such as predator excavations, surface deposit feeding, pit feeding, burrowing, and defecation also shape the sediment surface (Hughes, 1969; Rhoads and Young, 1970; Brenchley, 1981; Grant, 1983; Smith *et al.*, 1986; Nowell *et al.*, 1984; Posey, 1986; Krager and Woodin, 1993). Many of these events require a response from the infauna. Sediment deposition, whether biotic or physical in origin, can result in a period of burrowing and reestablishment or even in the death of the infauna (Gallucci and Kawaratani, 1975; Nichols *et al.*, 1978; Turk and Risk, 1981; Wilson, 1981).

Recently settled juveniles of infauna are particularly susceptible to a number of these surface-associated processes. Feeding by surface deposit-feeders, such as spionid polychaetes and tellinid bivalves, can result in spatial partitioning of large individuals (Holme, 1950; Levin, 1981) or mortality of small ones (Wilson, 1980; Levin, 1981; Elmgren *et al.*, 1986; Hines *et al.*, 1989; Olafsson, 1989). Sediment deposition can also increase rates of mortality for juveniles (Wilson, 1981; Brenchley, 1982; Posey, 1986). These biotic and physical events have similar effects on the original sediment surface, causing either burial or removal of the original surface. Given this commonality of effect on surfaces and on mortality rates, selection should favor those recruits capable of (a) distinguishing between recently disturbed (exposed subsurface sediments) and undisturbed surfaces and (b) emigrating from sites with disturbance. The data presented here show clearly that new juveniles of two polychaete species and a bivalve species can distinguish between recently disturbed and undisturbed sediment surfaces and modify their behavior accordingly. In all cases, burrowing times are significantly greater on recently disturbed surfaces than on undisturbed surfaces (Tables I to III); in some cases, rates of complete rejection, where the juvenile did not burrow, are higher on disturbed surfaces (Tables I and II). This was true for simulated erosional events (surface compared with subsurface: Tables I and II), as well as for simulated mixing (surface compared with 1:1 mix: Table I). Time to acceptance was also significantly longer for new juveniles offered fresh feces or burrow tailings than for those given undisturbed surface sediments (Table I). Finally, exposure to feeding traces made by large infauna such as the tellinid bivalve *Macoma nasuta* caused significant increases in burrowing times (Table III). All of these results are consistent with the hypothesis that juveniles distinguish between undisturbed and recently disturbed sediment surfaces, whether the disturbance is depositional or erosional, physical or biotic. A corollary of this hypothesis is that there is a selective advantage to individuals able to distinguish between recently disturbed and undisturbed sediment surfaces. This does not, of course, mean that the currently undisturbed site will remain undisturbed, either by biotic or physical forces (Wilson, 1981; Krager and Woodin, 1993).

When disturbed sediments were accepted by the juveniles, times to initiation of burrowing or nestling were significantly (4- to 5-fold) longer than in undisturbed sediments (Tables I and II). Under these conditions, juveniles remained on the sediment surface for 1.5 to 2 min or more. Such behaviors can increase the probability of erosion. Our flume data clearly indicate that individuals that did not burrow were eroded (Table IV). None of the individuals that burrowed was eroded. All but 3 of the 17 individuals that did not burrow within 40 s of contacting

the bottom were eroded within 2 min of initiation of flow. On average, erosion of individuals from the surface occurred in less than 80 s after initiation of flow. Flow in these experiments had an average boundary shear velocity of 1.0 cm s^{-1}, which is much less than storm conditions (False Bay, WA: u_* = 3.5 cm s^{-1} or more: Miller and Sternberg, 1988) and is comparable to conditions for maximum flood tidal flows [Oyster Landing, SC: u_*: 0.7 to 1.0 cm s^{-1} (Palmer and Gust, 1985; Wethey *et al.*, unpub. data)] in these habitats or for small-amplitude waves (Denny and Shibata, 1989). Thus our flume results are a highly conservative estimate of the probability of erosion. Interestingly, the temporal spacing between small-amplitude waves typical of these habitats and likely to cause erosion is of the same order of magnitude as the time necessary to initiate burrowing (Pond and Pickard, 1983; Denny, 1988; Miller and Sternberg, 1988).

Travel by erosion or wafting is a well-known phenomenon (Sigurdsson *et al.*, 1976; Sastry, 1979) and may also help explain some of the results of Butman and her collaborators on the effect of still water and flow conditions on larval settlement selectivity (*e.g.*, Snelgrove *et al.*, 1993). Some species show more settlement selectivity with flow than without (*Mulinia lateralis*: Grassle *et al.*, 1992b), whereas other species are relatively insensitive to the presence or absence of water motion (*Capitella* sp. 1: Butman and Grassle, 1992; Grassle *et al.*, 1992a). For species that rely on erosion from the surface to transport them short distances, such as the nereid juveniles used in these experiments, the no-flow treatment would result in lowered rates of emigration and thus less apparent selectivity.

Larvae and new juveniles are known to reject other habitats on the basis of chemical cues (see review by Pawlik, 1992), although the literature on negative settlement cues is not extensive. In all of these cases, the compound that causes rejection is intimately associated with the organism and is produced by that organism or a symbiont. For example, the terebellid polychaete *Thelepus crispus* releases a brominated aromatic compound into the sediments surrounding its tube, and this inhibits the recruitment of *Nereis vexillosa* (Woodin *et al.*, 1993). To date, all the reported negative responses are to organism-specific cues (Pawlik, 1992). In the data reported here, the negative response is to a process-specific event, disruption of the surface sediments either by removal or burial (Tables I to III). A process-specific cue is distinctly different from an organism-specific cue. For example, although a number of organisms have bioactive compounds that deter settlement, these compounds vary greatly in their effectiveness on different taxa, and the effect of the compound is typically limited to the surface of the organism itself or the immediately surrounding area (Pawlik, 1992; Woodin *et al.*, 1993). With process-specific cues, the effect is confined to the area affected by the process, which can be physical or biotic, and is thus not limited to the distribution or abundance or even the habitat of a given taxon. Given the mortality associated with sediments that are disturbed, the selective advantage accrued to individuals able to differentiate between disturbed and undisturbed habitats and vary emigration rates in response is potentially enormous.

Acknowledgments

Dr. Mark Luckenbach kindly provided late pediveliger *Mercenaria mercenaria* larvae. The Director of the Friday Harbor Laboratories gave us research space and access to research sites. The Snug Harbor Resort allowed us to use their property as a research site. The Director of the Belle W. Baruch Institute for Marine and Coastal Research allowed us access to research sites. E. R. W. Wethey collected egg masses and provided field assistance. C. Richmond, M. Grove, J. Hilbish, L. Levin, W. H. Wilson, R. Zimmer-Faust, and two anonymous reviewers made valuable comments on the manuscript. S. M. Lindsay was supported by an NSF graduate research fellowship. This research was supported by NSF grant OCE-8900212 to S. A. Woodin and ONR grant N00014-82-K-0645 and NSF grant OCE-86-00531 to D. S. Wethey.

Literature Cited

Bachelet, G., C. A. Butman, C. M. Webb, V. R. Starczak, and P. V. R. Snelgrove. 1992. Non-selective settlement of *Mercenaria mercenaria* (L.) larvae in short-term, still-water, laboratory experiments. *J. Exp. Mar. Biol. Ecol.* **161:** 241–280.

Belding, D. L. 1930. The soft-shelled clam fishery of Massachusetts. *Mass. Marine Fisheries Ser.* **No. 1:** 1–65.

Bell, S. S., and B. C. Coull. 1980. Experimental evidence for a model of juvenile macrofauna-meiofauna interactions. Pp. 179–194 in *Marine Benthic Dynamics*, Belle W. Baruch Library in Marine Science, No. 11, K. R. Tenore and B. C. Coull, eds. University of South Carolina Press, Columbia.

Boicourt, W. C. 1982. Estuarine larval retention mechanisms on two scales. Pp. 445–457 in *Estuarine Comparisons*, V. S. Kennedy, ed. Academic Press, New York.

Brenchley, G. A. 1981. Disturbance and community structure: an experimental study of bioturbation in marine soft-bottom environments. *J. Mar. Res.* **39:** 767–790.

Brenchley, G. A. 1982. Mechanisms of spatial competition in marine soft bottom communities. *J. Exp. Mar. Biol. Ecol.* **60:** 17–33.

Butman, C. A., and J. P. Grassle. 1992. Active habitat selection by *Capitella* sp. 1 larvae. I. Two-choice experiments in still water and flume flows. *J. Mar. Res.* **50:** 669–715.

Butman, C. A., J. P. Grassle, and C. M. Webb. 1988. Substrate choices made by marine larvae settling in still water and in a flume flow. *Nature* **333:** 771–773.

Cameron, R. A., and S. S. Rumrill. 1982. Larval abundance and recruitment of the sand dollar *Dendraster excentricus* in Monterey Bay, California, USA. *Mar. Biol.* **71:** 197–202.

Carriker, M. R. 1961. Interrelation of functional morphology, behavior, and autecology in early stages of the bivalve *Mercenaria mercenaria*. *J. Elisha Mitchell Sci. Soc.* **77:** 168–241.

Connell, J. H. 1985. Variation and persistence of rocky shore populations. Pp. 57–69 in *The Ecology of Rocky Coasts*, P. G. Moore and R. Seed, eds. Hodder and Stoughton, Sevenoaks, Kent, UK.

Crisp, D. J. 1984. Overview of research on marine invertebrate larvae, 1940–1980. Pp. 103–126 in *Marine Biodeterioration: an Interdisciplinary Study*, J. D. Costlow and R. C. Tipper, eds. Naval Institute Press, Annapolis, MD.

Denny, M. W. 1988. *Biology and the Mechanics of the Wave Swept Environment.* Princeton University Press, Princeton. 329 pp.

Denny, M. W., and M. F. Shibata. 1989. Consequences of surf-zone turbulence for settlement and external fertilization. *Am. Nat.* **134:** 859–889.

Eckman, J. E., W. B. Savidge, and T. F. Gross. 1990. The relationship between duration of attachment of *Balanus amphitrite* cyprids to a surface and drag forces associated with detachment. *Mar. Biol.* **107:** 111–118.

Elmgren, R., S. Ankar, B. Marteleur, and G. Ejdung. 1986. Adult interference with postlarvae in soft sediments: the *Pontoporeia-Macoma* example. *Ecology* **67:** 827–836.

Emerson, C. W., and J. Grant. 1991. The control of soft-shell clam (*Mya arenaria*) recruitment on intertidal sandflats by bedload sediment transport. *Limnol. Oceanogr.* **36:** 1288–1300.

Eyster, L. S., and J. A. Pechenik. 1987. Attachment of *Mytilus edulis* L. larvae on algal and byssal filaments is enhanced by water agitation. *J. Exp. Mar. Biol. Ecol.* **114:** 99–110.

Feller, R. J., S. E. Stancyk, B. C. Coull, and D. G. Edwards. 1992. Recruitment of polychaetes and bivalves: long-term assessment of predictability in a soft-bottom habitat. *Mar. Ecol. Prog. Ser.* **87:** 227–238.

Gallucci, V., and R. K. Kawaratani. 1975. Mortality of *Transennella tantilla* due to burial. *J. Fish. Res. Board Can.* **32:** 1637–1640.

Grant, J. 1983. The relative magnitude of biological and physical sediment reworking in an intertidal community. *J. Mar. Res.* **41:** 673–689.

Grassle, J. P., C. A. Butman, and S. W. Mills. 1992a. Active habitat selection by *Capitella* sp. I. larvae. II. Multiple-choice experiments in still water and flume flows. *J. Mar. Res.* **50:** 717–743.

Grassle, J. P., P. V. R. Snelgrove, and C. A. Butman. 1992b. Larval habitat choice in still water and flume flows in the opportunistic bivalve *Mulinia lateralis*. *Neth. J. Sea Res.* **30:** 33–44.

Grosberg, R. K. 1981. Competitive ability influences habitat choice in marine invertebrates. *Nature* **290:** 700–702.

Gustafson, R. G., and R. G. B. Reid. 1986. Development of the pericalymma larva of *Solemya reidi* (Bivalvia: Cryptodonta: Solemyidae) as revealed by light microscopy. *Mar. Biol.* **93:** 411–427.

Hadfield, M. G. 1984. Settlement requirements of molluscan larvae: new data on chemical and genetic roles. *Aquaculture* **39:** 283–298.

Highsmith, R. C. 1982. Induced settlement and metamorphosis of sand dollar (*Dendraster excentricus*) larvae in predator-free sites: adult sand dollar beds. *Ecology* **63:** 329–337.

Hines, A. H., M. H. Posey, and P. J. Haddon. 1989. Effects of adult suspension- and deposit-feeding bivalves on recruitment of estuarine infauna. *Veliger* **32:** 109–119.

Holme, N. A. 1950. Population dispersion in *Tellina tenuis* Da Costa. *J. Mar. Biol. Ass. U.K.* **29:** 267–280.

Hughes, R. N. 1969. A study of feeding in *Scrobicularia plana*. *J. Mar Biol. Ass. U.K.* **49:** 805–823.

Johnson, L. E., and R. R. Strathmann. 1989. Settling barnacle larvae avoid substrata previously occupied by a mobile predator. *J. Exp Mar. Biol. Ecol.* **128:** 87–103.

Johnson, M. W. 1943. Studies on the life history of the marine annelid *Nereis vexillosa*. *Biol. Bull.* **84:** 106–114.

Jonsson, P. R., C. Andre, and M. Lindegarth. 1991. Swimming behaviour of marine bivalve larvae in a flume boundary-layer flow: Evidence for near-bottom confinement. *Mar. Ecol. Prog. Ser.* **79:** 67–76.

Kendall, M. A., T. S. Bowman, P. Williamson, and J. R. Lewis. 1982. Settlement patterns, density and stability in the barnacle *Balanus balanoides*. *Neth. J. Sea Res.* **16:** 119–126.

Krager, D. C., and S. A. Woodin. 1993. Spatial persistence and sediment disturbance of an arenicolid polychaete. *Limnol. Oceanogr.* **38:** 509–520.

Levin, L. A. 1981. Dispersion, feeding behavior and competition in two spionid polychaetes. *J. Mar. Res.* **39:** 99–117.

Levin, L. A. 1984. Life history and dispersal patterns in a dense infaunal polychaete assemblage: community structure and response to disturbance. *Ecology* **65:** 1185–1200.

Loosanoff, V. L. 1964. Variations in time and intensity of setting of the starfish *Asterias forbesi* in Long Island Sound during a twenty-five year period. *Biol. Bull.* **126:** 423–439.

Luckenbach, M. 1984. Settlement and early post-settlement survival in the recruitment of *Mulinia lateralis* (Bivalvia). *Mar. Biol. Prog. Ser.* **17:** 245–250.

Miller, D. C., and R. W. Sternberg. 1988. Field measurements of the fluid and sediment-dynamic environment of a benthic deposit feeder. *J. Mar. Res.* **46:** 771–796.

Morse, A. N., and D. E. Morse. 1984. Recruitment and metamorphosis of *Haliotis* larvae induced by molecules uniquely available at the surfaces of crustose red algae. *J. Exp. Mar. Biol. Ecol.* **75:** 191–215.

Muus, K. 1973. Settling, growth and mortality of young bivalves in the Oresund. *Ophelia* **12:** 79–116.

Nichols, J. A., G. T. Rowe, C. H. Clifford, and R. A. Young. 1978. *In situ* experiments on the burial of marine invertebrates. *J. Sed. Pet.* **48:** 419–425.

Nowell, A. R. M., P. A. Jumars, and K. Fauchald. 1984. The foraging strategy of a subtidal and deep-sea deposit feeder. *Limnol. Oceanogr.* **29:** 645–649.

Olafsson, E. B. 1989. Contrasting influences of suspension-feeding and deposit-feeding populations of *Macoma balthica* on infaunal recruitment. *Mar. Ecol. Prog. Ser.* **55:** 171–179.

Palmer, M. A., and G. Gust. 1985. Dispersal of meiofauna in a turbulent tidal creek. *J. Mar. Res.* **43:** 179–210.

Pawlik, J. R. 1992. Chemical ecology of the settlement of benthic marine invertebrates. *Oceanogr. Mar. Biol. Annu. Rev.* **30:** 272–335.

Posey, M. H. 1986. Changes in a benthic community associated with dense beds of a burrowing deposit feeder, *Callianassa californiensis*. *Mar. Ecol. Prog. Ser.* **31:** 15–22.

Pond, S., and G. L. Pickard. 1983. *Introductory Dynamical Oceanography.* Pergamon Press, Oxford. 329 pp.

Rhoads, D. C., and D. K. Young. 1970. The influence of deposit feeding organisms on sediment stability and community trophic structure. *J. Mar. Res.* **28:** 150–178.

Roe, P. 1975. Aspects of life history and of territorial behavior in young individuals of *Platynereis bicanaliculata* and *Nereis vexillosa* (Annelida, Polychaeta). *Pac. Sci.* **29:** 341–348.

Sastry, A. N. 1979. Pelecypoda (excluding Ostreidae). Pp. 113–292 in *Reproduction of Marine Invertebrates*, Vol. 5, *Molluscs: Pelecypods and Lesser Classes*, A. C. Giese and J. S. Pearse, eds. Academic Press, New York.

Sellmer, G. P. 1967. Functional morphology and ecological life history of the gem clam, *Gemma gemma* (Eulamellibranchia: Veneridae). *Malacologia* **5:** 137–223.

Sigurdsson, J. B., C. W. Titman, and P. A. Davies. 1976. The dispersal of young post-larval bivalve molluscs by byssus threads. *Nature* **262:** 386–387.

Smith, C. R., P. A. Jumars, and D. J. DeMaster. 1986. *In situ* studies of megafaunal mounds indicate rapid sediment turnover and community response at the deep-sea floor. *Nature* **323:** 251–253.

Snelgrove, P. V. R., C. A. Butman, and J. P. Grassle. 1993. Hydrodynamic enhancement of larval settlement in the bivalve *Mulinia lateralis* (Say) and the polychaete *Capitella* sp. I in microdepositional environments. *J. Exp. Mar. Biol. Ecol.* **168:** 71–109.

Strathmann, M. F. 1987. *Reproduction and Development of Marine Invertebrates of the Northern Pacific Coast.* University of Washington Press, Seattle.

Turk, T. R., and M. J. Risk. 1981. Effect of sedimentation on infaunal invertebrate populations of Cobequid Bay, Bay of Fundy. *Can. J. Fish. Aquat. Sci.* **38:** 642–648.

Underwood, A. J., and E. J. Denley. 1984. Paradigms, explanations, and generalizations in models for the structure of intertidal communities on rocky shores. Pp. 151–180 in *Ecological Communities: Conceptual Issues and the Evidence,* D. R. Strong, Jr., D. Simberloff, L. G. Abele, and A. B. Thistle, eds. Princeton University Press, Princeton.

Walters, L. J. 1992. Field settlement locations on subtidal marine hard substrata. Is active larval exploration involved? *Limnol. Oceanogr.* **37:** 1101–1107.

Watzin, M. C. 1983. The effects of meiofauna on settling macrofauna: Meiofauna may structure macrofaunal communities. *Oecologia* **59:** 163–166.

Wethey, D. S. 1985. Local and regional variation in settlement and survival in the littoral barnacle *Semibalanus balanoides* (L.): patterns and consequences. Pp. 194–202 in *The Ecology of Rocky Coasts,* P. G. Moore and R. Seed, eds. Hodder and Stoughton, Sevenoaks, Kent, UK.

Wilson, D. P. 1952. The influence of the nature of the substratum on the metamorphosis of the larvae of marine animals, especially the larvae of *Ophelia bicornis* Savigny. *Ann. Inst. Oceanogr.* **27:** 49–156.

Wilson, W. H., Jr. 1980. A laboratory investigation of the effects of a terebellid polychaete on the survivorship of nereid polychaete larvae. *J. Exp. Mar. Biol. Ecol.* **46:** 73–80.

Wilson, W. H., Jr. 1981. Sediment-mediated interactions in a densely populated infaunal assemblage: the effects of the polychaete *Abarenicola pacifica*. *J. Mar. Res.* **39:** 735–748.

Woodin, S. A. 1986. Settlement of infauna: larval choice? *Bull. Mar. Sci.* **39:** 401–407.

Woodin, S. A., R. L. Marinelli, and D. E. Lincoln. 1993. Allelochemical inhibition of recruitment in a sedimentary assemblage. *J. Chem. Ecol.* **19:** 517–530.

Reference: *Biol. Bull.* **189:** 59–68. (August, 1995)

Functional Significance of Varices in the Muricid Gastropod *Ceratostoma foliatum*

THOMAS H. CAREFOOT AND DEBORAH A. DONOVAN

Department of Zoology, University of British Columbia, Vancouver, Canada V6T 1Z4

Abstract. Functional significance of varices in the muricid gastropod *Ceratostoma foliatum* was investigated from the standpoints of (1) frequency of landing in the two upside-down orientations after short vertical falls of less than five body lengths through seawater and energy costs of righting from these upside-down positions, and (2) scaling relationships of varix areas with other body dimensions. Field manipulations showed that *C. foliatum* occupied habitats that mostly permit short falls of less than five body lengths upon dislodgment, as might occur during predation by fish. After short vertical falls in the laboratory, animals landed 48% of the time on their aperture sides (upright), 15% on their right sides (on right and middle varices), and 37% on their left sides (on left and middle varices). These frequencies differed significantly from the expected frequencies calculated on the basis of the percentage circumference delineated by each varix pair (50%, 31%, and 19%, respectively). Righting from the right-side orientation was slower and four times more energetically costly than from the left-side orientation, underscoring the advantage conferred by animals, if not landing in the upright position after short falls, preferentially landing on their left sides. Removal of individual varices showed that the large, right varix is most influential in producing this "destabilization." Landings are biased to the side from which rightings are easiest due to a combination of the location of center of mass within the left side of the main body whorl and the broad right varix possibly acting as an upward-trailing vane.

Morphometric relationships of shell length, live weight, varix areas, aperture dimensions, and labial spine (tooth) length were investigated over a wide range of body sizes in an attempt to infer varix function. Aperture area scaled allometrically with length. Right-, middle-, and left-varix areas also grew relatively larger as the animals increased in length. In contrast, combined varix areas around the aperture increased in direct proportion with aperture area, forming a broad shelf surrounding the aperture. We infer from this that, in addition to their effects on landing orientation from both long and short vertical falls, the varices of *C. foliatum* may function to protect the aperture, and thus protect the soft body parts that protrude from it during feeding and locomotion.

Received 17 October 1994; accepted 1 May 1995.

Introduction

The function of shell ornamentation in prosobranch gastropods has intrigued scientists for decades. Shell ornamentation is most well-developed in the family Muricidae, where it consists of ridgings, or varices, elaborated from thickenings of the outermost shell edge during growth. In the adult leafy hornmouth snail, *Ceratostoma foliatum*, three such varices predominate (Fig. 1). The newest varix is the right one. New varices are added in growth spurts, which causes the varices to shift position, with the present right one coming to occupy a new middle position, and the present middle one becoming a new left varix.

The precise function of shell sculpturing in *C. foliatum* and other muricid gastropods is not known, although suggestions include (1) stabilizing the shell in shifting substratum; (2) aiding in feeding; (3) supporting or protecting sensory structures; (4) perceiving vibration; (5) protecting the snail from predators; (6) strengthening the shell (as seen for thicker-shelled *Nucella lapillus*, which withstand predatory attacks by crabs better than thinner-shelled varieties); and (7) in *C. foliatum*, destabilizing the falling orientation such that landing is more often in the aperture-down position (Ebling *et al.*, 1964; Kitching *et al.*, 1966; Carter, 1967; Fotheringham, 1971; Spight and Lyons, 1974; Palmer, 1977; Vermeij, 1974, 1979, pers. com.;

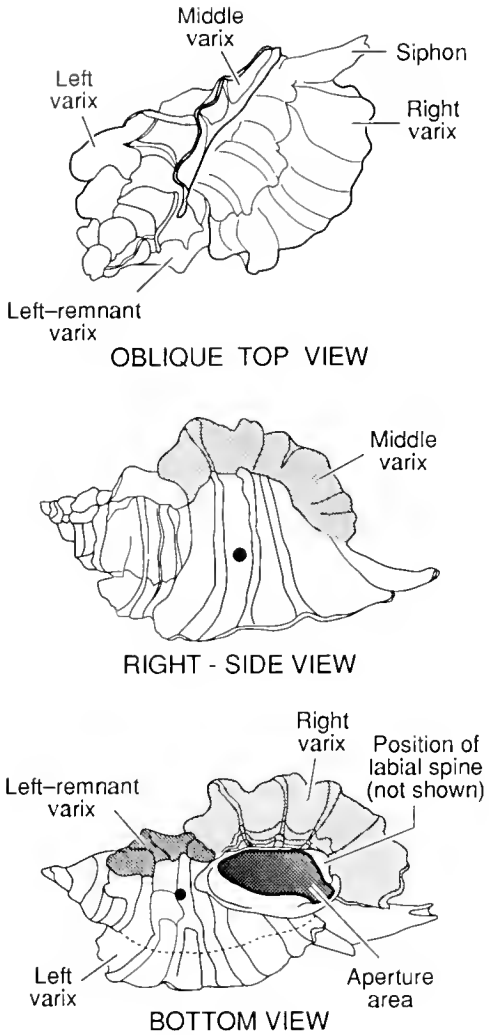

Figure 1. *Top:* Oblique plan view of *Ceratostoma foliatum* to show varix arrangement. *Middle* and *bottom:* Views from the right side and bottom, respectively, to show areas of right-, left-, middle-, and left-remnant varices, and aperture, as measured for allometry. The dots indicate the location of center of mass in a live but withdrawn animal.

Morris *et al.*, 1980). Other possible paradigms are (8) camouflaging the snail (reminiscent of the shell debris employed by the carrier shell, *Xenophora conchyliophora*); (9) reducing or preventing rolling in currents; and (10) increasing apparent size to deter predators.

The problem for molluscan functional morphologists is that few of these hypotheses are testable. Even the elegant demonstration by Palmer (1977) that the middle varix of *C. foliatum* (see Fig. 1) acts to destabilize the animal's orientation during falling, causing it to land aperture down, is open to question.

First, the requirement for a falling distance of at least 10 body-lengths to ensure 35%–70% landing success (aperture down) would rarely be satisfied in *C. foliatum's* rock- and seaweed-strewn natural habitat. Our field observations (shown later) suggest that few individuals of this species occupy positions that permit even five body-lengths of free-fall to the bottom. Most would bump, roll, or slide, even from near-vertical slopes.

Second, Palmer suggests that kelp greenling prey upon *C. foliatum* by dislodging the snails and consuming their feet when they are exposed during righting. However, we have been unable, using the precipitin test of Pickavance (1970), to identify the presence of *C. foliatum* antigens in the stomach contents of 42 kelp greenling fish coexisting with *C. foliatum*. This is despite positive responses from stomach contents of kelp greenling experimentally fed on *C. foliatum*, and a robust response of *C. foliatum* antisera (induced in rabbits) to *C. foliatum* antigen preparations in control tests (unpub. data). *C. foliatum* lives most commonly in the low intertidal and subtidal regions to a depth of 30 m and feeds predominantly on barnacles and bivalves (Spight *et al.*, 1974; Spight and Lyons, 1974; Kent, 1981). Although little is known of its natural biology, its principal predators might be seastars, such as the large, fast-moving sunflower star, *Pycnopodia helianthoides*, rather than fish. If this is the case, dislodgment due to predation is less likely.

Third, although this by no means discounts a destabilizing function for the middle varix of *C. foliatum*, the fact that many other muricids have tri-radiate varices of spines rather than blades suggests that other selective factors are operating.

Finally, if the primary function of varices in *C. foliatum* is to provide a large right varix for protection or stability during locomotion and feeding, then the destabilizing function of the middle varix might be only secondarily important.

Two features of *C. foliatum's* growth are relevant to this introduction of varix function. First, the varices are produced relatively rapidly. Spight and Lyons (1974) recorded varix production about once per year in older animals, each one taking 1–2 months for completion. Our *in situ* scuba observations indicate that varix growth must be as rapid, or more so, in the field. We have only once observed a partially formed varix, indicating that varices are produced in growth spurts of extremely short duration or that they are produced secretively. In either case, it is clear that a fully formed varix is vital to the well-being of the animal. Second, the three-varix morphology of the adult snail is not typical of its entire life. While young (<25 mm), the snail produces multiple axial ribs, up to 7–10 per whorl. This changes to a three-varix pattern in the adult, suggesting that the three-varix morphology, whatever its function, is more important in older stages.

Palmer (1977) constructed his argument for varix function in *C. foliatum* around the premise that, on dislodgment and subsequent free-fall, it would be advantageous for the snail to land upright. He was not concerned

with landing orientations other than upright, yet the other two landing orientations occurred with 43%–100% frequency, depending on height of fall, in his study (Palmer, 1977). Lacking any other information, similar values could be predicted from falls of the bump-and-roll type. Based on shell shape and angle of the varices (Fig. 2a), and discounting for the present any varix or center of mass influence on falling, an animal that landed randomly might be expected to land 50% of the time on its right and left varices (*i.e.*, upright), 31% on its right and middle varices (right-side posture), and 19% on its middle and left varices (left-side posture).

Two implications derive from these considerations, both of which focus on the advantages of landing in a left-side orientation over a right-side orientation. First, an animal should be able to right itself more readily, that is more quickly and with less energy expenditure, from the smaller-angled left-side orientation (Fig. 2c) than from the larger-angled right-side one (Fig. 2b). This is because the foot has a shorter reach to gain purchase on the substratum. In contrast, from the proposed less-favorable landing position (Fig. 2b), the foot must reach further and the shell be levered through a greater angle to right it. Note that righting from the "easy" orientation exposes the foot to lesser risk of predation than from the "hard" orientation. The second implication is that relative varix height affects the ability of the animal to right itself due to the change in the angles the animal experiences in relation to the substratum (Fig. 2b, c). Thus, a larger middle varix relative to the other varices favors the righting process from both easy and hard orientations by decreasing the distance that the foot must traverse. By the same token, a larger right varix impedes righting from the hard orientation by increasing the distance of foot extension. However, because a large right varix is required to produce eventually a large middle varix, any such argument of effect of relative varix sizes from the hard orientation is self-defeating.

Palmer's (1977) interest was in the destabilizing effect of the middle varix during falls mainly in excess of 10 body lengths in height. We are interested here in dislodgment effects from heights less than this, and especially in the energetic consequences of the animal landing and having to right from the left- and right-side orientations. We are also interested in the relationship of varix areas to other body dimensions, in particular to aperture area, since three varices combine to form a broad shelf surrounding the aperture, which may provide either protection or stabilization (Fig. 1, bottom). Hypotheses to be tested are (1) that landing orientations, other than ones ending with the animal upright, will favor the "easy" side, despite the smaller circumference occupied by this side; and (2) that righting times from the "easy" posture will be shorter than from the "hard" and, correlatively, that energy expenditure will be less. Additionally, morphometric relationships of various shell structures are investigated and interpreted in an attempt to infer varix function.

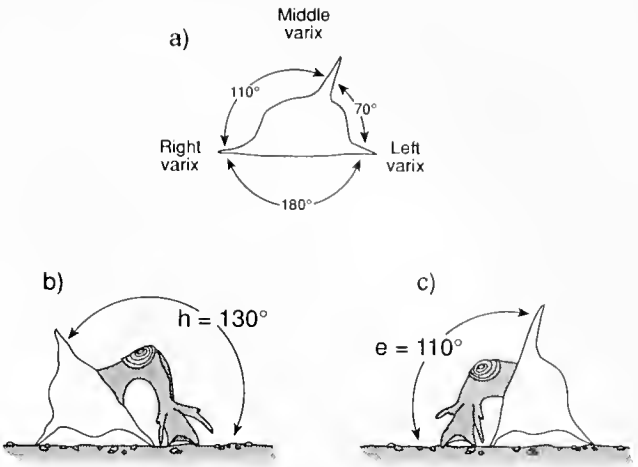

Figure 2. Schematic representation of varices and shell-righting postures in *Ceratostoma foliatum*, from head-on views. (a) Extent of circumference occupied by each varix-pair (110° is equivalent to 31% of the circumference; 70° to 19%). (b) Righting from the "hard" right-side landing orientation (resting on the middle and right varices). The angle "h" denotes the extent of traverse of the foot during righting from the "hard" orientation (130°). (c) Righting from the "easy" left-side landing orientation (resting on the middle and left varices). The angle "e" denotes the extent of traverse of the foot during righting from the "easy" orientation (110°).

Materials and Methods

Collection of animals

Animals were collected from subtidal locations in Barkley Sound, on the west coast of Vancouver Island, and in Telegraph Cove, West Vancouver, British Columbia. They were brought to the University of British Columbia and held in tanks supplied with recirculated seawater. Barnacle-encrusted rocks and mussels were provided as sources of food.

Field tests of falling distances

One hundred snails were selected at random during scuba dives at depths of 3–10 m along a 200-m section of Barkley Sound shoreline characterized by large boulders and rock walls. Each snail was manually dislodged and its unimpeded vertical falling distance recorded. The divers moved from habitat to habitat, selecting and testing the first individual of *Ceratostoma foliatum* seen in each. This procedure allowed a variety of habitats to be sampled, such as sloping and vertical rock walls and overhangs. Length of each snail was recorded to determine falling

distance relative to body length (apex to tip of siphonal canal).

VO_2 and righting times

VO_2 (oxygen consumption in microliters of oxygen per hour) of individual animals was measured in a closed respirometry system by means of a polarographic oxygen electrode coupled with a DATACAN data acquisition and analysis program (SABLE Systems Ltd., Salt Lake City). A stir-bar in the chamber ensured continuous and thorough mixing. Temperature was maintained at 12°C, the same as in the holding tanks. Respirometers were made of clear plastic and varied in size (85, 120, and 700 cm^3) for use with different-sized animals. The snails were placed in an aperture-down position in the chamber and allowed to rest for 20 min while the system equilibrated. Oxygen consumption was then measured for 20 min to establish a resting VO_2. A narrow-gauge wire hook inserted into the chamber through a small hole in the top was used to flip each snail randomly to either its right ("hard") side or its left ("easy") side. It took less than 5–10 s to flip a snail onto its side. The snails were observed as they righted themselves and times of the following specific events were recorded: (1) appearance of the snail's foot from under the operculum, (2) attachment of the snail's foot to the bottom of the chamber, and (3) completion of righting, as defined by the settling of the shell onto the back of the snail. Righting time was measured as the time from first appearance of the snail's foot to when the shell settled over the back of the snail. Oxygen consumption was recorded during the righting episode. After the 20-min rest period, the snail was flipped onto its other side and the procedure repeated. Three VO_2 values were generated for each animal from this procedure: (1) normal upright resting VO_2 (snails that crawled in the chamber were not tested), (2) VO_2 when righting from the easy orientation, and (3) VO_2 when righting from the hard orientation.

VO_2's were multiplied by righting times from each upside-down orientation to give absolute cost in microliters of oxygen for each righting episode. Costs in microliters of oxygen were converted to joules by multiplying by an oxycalorific coefficient (Q_{ox}) of 21.10 $mJ \cdot \mu l\ O_2^{-1}$, representing an accepted value for catabolism of carbohydrate (Elliot and Davison, 1975). This value was chosen because most gastropods rely on glycogen stores for energy during activity (Carefoot, 1987).

Landing frequencies

To determine the frequency of landing in each of the three orientations, upright, left side (easy), and right side (hard), 137 snails of varying size were dropped in aquaria with seawater depths about 5 times the length of the snail. We chose this depth because (1) we did not wish to invoke the destabilizing effect of the middle varix, shown by Palmer (1977) to occur at depths greater than 10 bodylengths, and (2) we believed from our field observations that short falls, or bump-and-roll falls, would be most commonly experienced by snails in the field. Each snail was held just below the water surface and released. Release positions were random. Each snail was tested 10 times and the average landing frequency calculated. After this, the length of each snail was measured.

In another series of experiments to test the effect of varix removal on landing frequency, snails were dropped 20 times from random release positions and their landing orientations noted, then dropped 20 more times after removal of a single varix. Varices were removed by grinding them down flush with the shell surface with a rotary grinder. Fifty snails were used for each of the three treatments, or 150 snails total. A given landing orientation was calculated as the mean percentage of 50 animals each dropped 20 times. Before-and-after comparisons were done on arcsine-transformed percentage values using either paired Student's t tests or Wilcoxon signed-rank tests, depending on whether the data were normally distributed.

Varix angles and righting angles

A protractor was used to measure the angles between varices shown in Figure 2a. To standardize the measurements, the middle of the protractor was aligned with the siphon and upward-facing middle varix. Angles through which a snail's foot had to traverse during righting from the two upside-down landing positions shown in Figure 2b and 2c were also measured with a protractor. In this case, the middle of the protractor was aligned with the upward-facing varix in each position. The angles were determined for 88 shells ranging in length from 25–82 mm.

Center of mass

Center of mass with the snail in the withdrawn position was ascertained by suspending five live snails of varying sizes (16–37 g) from threads attached at about midpoint in their right and middle varix edges, and from a point near the siphon. Each snail was suspended in seawater successively from each of the three positions. Centers of mass were estimated from the point of intersection of the three lines generated by following the visual extensions of the threads from which the animals were hung down into the body of the snail. Penciled reference marks on the shells were used to help assess the point of intersection of the three lines. Changes in center of mass on removal of varices were estimated in the same way, except that hanging positions were adjusted depending on which varix was being removed.

Morphometry

The following morphometric measurements on perfect, uneroded *C. foliatum* shells were made: areas of the three main varices and left-remnant varix (described below), aperture area, aperture length, total shell length including siphon, labial spine (tooth) length, and live body weight (measured in air with the animal retracted into its shell). The left-remnant varix constitutes a remnant of the previous left varix that abuts on the current right varix to form a combined right-shelf area of larger dimension (see Fig. 1, bottom). This abutment is often not perfect, yet visual analysis of many shells suggests that the animal may use this remnant as a guide to where to terminate growth of each new varix. The end result of the juxtaposition of these two varices, and the surface area of the left varix, is a broad shelf surrounding the aperture.

The labial spine projects downward from the anterior-right aperture margin. It is an extension of a shallow collar that borders the aperture on the right-hand side. It is this collar that ultimately extends during growth to form the new right varix, and the spine remnant can be seen embedded in the upper surface of each preceding varix. Its function may be to anchor the snail during feeding, as surmised for other gastropods (Paine, 1966). Spine length was defined as the magnitude of its extension above the rim of the collar.

Varix and aperture areas were determined by drawing their outlines at 8-power magnification using a Leitz drawing tube, then analyzing with a SIGMA-SCAN area-measurement software system (Jandel Scientific, California).

Allometric or isometric relationships between the morphological features were investigated with standard least-squares linear regressions calculated on log-transformed values for several combinations of variables. The slope (b) of a regression is often underestimated due to error in measurements of the independent variable (LaBarbera, 1989). To compensate for this underestimation, reliability ratios (k) were calculated (as described below) and the log-log transformed slope (b) was multiplied by k^{-1} to produce a corrected log-log slope (β) (Fuller, 1987; Harvey and Pagel, 1991; Johnson and Koehl, 1994). To calculate k for length measurements, the lengths of 10 shells were measured three times. The first set of values was regressed on the second set of values, the first on the third, and the second on the third. The mean r for these regressions was used as the value of k. To calculate k for area measurements, the areas of 10 circles were calculated in two ways: (1) from measured radii, and (2) using the SIGMA-SCAN software system described above. The values of the two sets of data were regressed and the resulting r was used as the value of k. β was then tested against the predicted slope for isometry for each scaling relationship using a t test.

Results

Field tests of falling distances of 100 snails encountered in random sampling of rocky subtidal habitats showed that 18 resided on horizontal surfaces from which falling did not occur, 28 resided on inclines from which a bump-and-roll response without free-fall occurred, 28 resided on inclines from which bump-and-roll responses followed by free-fall occurred, and 26 resided on vertical slopes from which only free-fall occurred. Of the 54 animals that experienced free-fall, 40 (74%) fell less than 5 body lengths, while the remaining 14 (26%) fell more than 5 body lengths. However, no animal fell further than 8.4 body lengths. Thus, most of the specimens sampled occupied rocky habitats from which only a short unimpeded vertical fall was possible, while the rest did not experience free-fall.

Righting times from the right-side (hard) orientation were significantly greater than from the left-side (easy) orientation ($W = 681$, $p < 0.001$, Wilcoxon signed-rank test; Fig. 3). A 10-g animal took 6.3 min to right from the hard orientation and 2.9 min from the easy orientation.

Significant differences were shown between all VO_2 rates ($p < 0.001$, Friedman repeated measures ANOVA) and the data segregated into three statistically homogeneous subgroups representing each activity (Newman-Keuls test, $p < 0.05$; Fig. 4).

Righting costs (mJ) from the hard orientation were 4-fold greater than from the easy orientation (expressed in

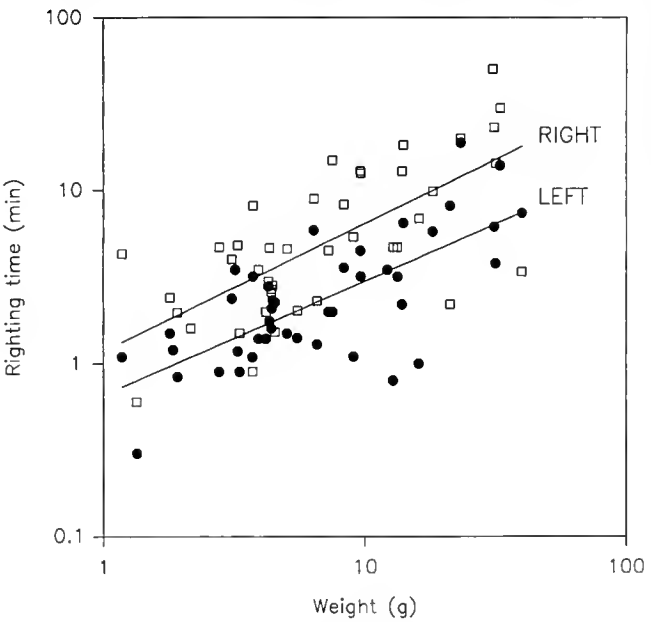

Figure 3. Righting times from right ("hard") and left ("easy") landing orientations in *Ceratostoma foliatum* as a function of body weight (including shell). Regression statistics are, for RIGHT: $\log Y = 0.0626 + 0.7382 \log X$, $r^2 = 0.494$, $n = 43$ and, for LEFT: $\log Y = -0.1830 + 0.6495 \log X$, $r^2 = 0.494$, $n = 43$.

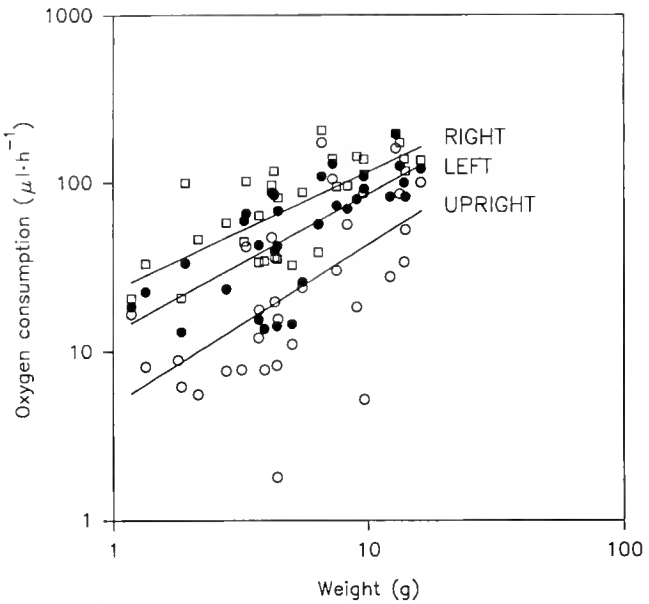

Figure 4. Rates of oxygen consumption during righting from the right ("hard") and left ("easy") orientation compared with that in the upright (resting) orientation as a function of body weight (including shell) in *Ceratostoma foliatum*. Regression statistics are for RIGHT: $\log Y = 1.381 + 0.665 \log X$, $r^2 = 0.522$, $n = 32$; for LEFT: $\log Y = 1.092 + 0.814 \log X$, $r^2 = 0.529$, $n = 32$; and for UPRIGHT: $\log Y = 0.688 + 0.919 \log X$, $r^2 = 0.349$, $n = 33$.

Table I for an equivalent 10-g animal). The higher costs from the right side are explained by the greater angle (130°) through which the foot must traverse to gain a purchase on the substratum, as compared with that of the left side (110°). These angles are constant through a wide weight range (1–41 g, $n = 88$) and variances are small: right-side angle = 130° ± 4 SD, left-side angle = 110° ± 5 SD. It should be noted that these righting angles do not correspond directly with the varix angles depicted in Figure 2a because, as the shell lies on its side, the angle is determined by the relative heights of the varix-pair and the different balance points of the shell on these varices.

A summary of landing frequencies when dropped through seawater of depths of five body lengths (Table II) indicates that the animals landed in a pattern that differed significantly from that expected based on the proportion of circumference delineated by each varix-pair ($\chi^2 = 20.9$, $p < 0.001$). Thus, although the right-side varix-pair occupied 31% of the circumference (see Fig. 2a), the animals landed on it only 15% of the time. The left-side varix-pair, from which righting was easiest, occupied only 19% of the circumference, but was landed on 37% of the time. The aperture-down landing position occurred 48% of the time, conforming closely to the 50% circumference that it represented.

The reason for the disproportionate landings on the left-side varix-pair becomes clear when the snail's center of mass is known. When representative-sized snails were suspended from threads attached to their individual varices, points of intersection were located within the largest, most recent whorl, slightly to the left of the longitudinal axis of the snail, and about midway between the aperture and the top of the main body whorl (see Fig. 1). Thus, the tendency during falling was for the shell to rotate to its most stable orientation, with the center of mass downwards. This falling orientation was probably aided and further stabilized by the broad right varix, which presumably acted as a rudder as it trailed. Thus, most animals not landing aperture down actually landed on the left-side varix pair from which subsequent righting was easiest.

Removal of the varices affected this landing pattern as follows (Table III). Right-varix removal caused the animals to land significantly more on their right sides and significantly less on their left sides and upright. Middle-varix removal led to a similar pattern of landing, but with even greater frequency of landings on the right side. In contrast, left-varix removal greatly increased the probability of landing upright at the expense of both left-side and right-side landings. Varix removal was accompanied by shifts in center of mass: right-varix removal produced a slight shift dorsally, middle-varix removal produced a slight shift ventrally, and left-varix removal produced a slight shift to the right.

There was no relationship between landing orientation and length in *C. foliatum* (t values all < 1.52, p values all > 0.135, t test of significance of regression; Zar, 1984).

Table I

Righting costs of Ceratostoma foliatum *(n = 34) from the right-side ("hard") and left-side ("easy") orientations*

Orientation	Angle (°)	Regression equation	r^2	Righting cost (mJ) for 10-g animal
Right-side ("hard")	130	$\log Y = 0.969 + 1.447 \log X$	0.703	261
Left-side ("easy")	110	$\log Y = 0.557 + 1.265 \log X$	0.606	66

The angle is the degree through which the snail's foot must traverse during righting from each orientation. Righting cost is the product of rate of energy expenditure and total righting time. The regression equations were generated by regressing the log transformation of energy needed to right (mJ) against the log transformation of body weight including shell (g). Righting costs were calculated for a 10-g animal from the regression equations.

Table II

Landing frequencies of Ceratostoma foliatum *(n = 137) onto the right side, the left side, and the normal aperture-down position*

Orientation	Mean landing frequency % ± 1 SD	% circumference occupied by each varix-pair
Aperture-down (right and left varix pair)	48 ± 19	50
Right-side (right and middle varix pair)	15 ± 16	31
Left-side (left and middle varix pair)	37 ± 17	19

Each snail was dropped 10 times in an aquarium tank with a seawater depth of 5 body lengths. These data were combined into a grand aggregate for all animals, from which the landing percentage values were calculated. Percentage circumference data were taken from Figure 2.

Regression analyses on log-log transformed data showed that there were significant relationships between most shell-parts as well as body weight and shell-parts (Table IV). Right-, middle-, and left-varix areas scaled allometrically to shell length (corrected log-log slopes equal to 2.15, 2.38, and 2.38 respectively; all significantly greater than 2.0, $t = 2.72$, 5.78, and 5.22, respectively, p all < 0.01), as did aperture area ($\beta = 2.24$, significantly different than 2.0, $t = 6.24$, $p < 0.001$). Of interest was the fact that right-varix area scaled to shell length with a constant log-log slope of 2.15 (Fig. 5a). Thus, animals of the largest size recorded here (82 mm shell length) were producing new varices in a constant allometric proportion to length. Combined varix area (right, left, and left-remnant varices) increased linearly with aperture area. The log-log slope of the regression of right-varix area compared to aperture area ($\beta = 0.93$, $r^2 = 0.918$) differed significantly from 1.0 ($t = 2.24$, $p < 0.05$), but when the left-varix and left varix-remnant areas were successively added to the right-varix area (the three components combine to produce a flat shelf surrounding the aperture), progressive improvements in fit were seen: right + left *vs.* aperture: $\beta = 0.96$, $r^2 = 0.931$ and right + left + left-remnant *vs.* aperture: $\beta = 0.98$, $r^2 = 0.941$. The addition of the left varix and the left-remnant varix also changed the log-log slopes of the lines in a progressive manner such that they no longer differed significantly from 1.0 (right + left *vs.* aperture: $t = 1.58$, $p > 0.10$ and right + left + left-remnant *vs.* aperture: $t = 0.81$, $p > 0.20$). This shows that as the aperture grows in size in *C. foliatum*, so the shelf surrounding it grows in proportional scale, with the best fit being realized when all three shelf components are included.

To ensure that our two populations from Barkley Sound and Telegraph Cove did not differ in any respect of morphometry, we compared log-log slopes and, if necessary, intercepts of regression lines for each morphometric comparison generated independently for each population. In no instance was a significant difference shown (all comparisons: $t < 1.96$, $p > 0.05$, tests of slope and intercept differences; Zar, 1984).

Labial-spine length scaled allometrically to body length ($\beta = 1.87$, significantly different than 1.0, $t = 12.67$, $p < 0.001$; Table IV). There was no indication in our data of any break in this relationship, at least over the size range represented by our collection (25–82 mm length).

Discussion

Several notable findings have arisen from this study. First, aerobic righting costs from the right-side, or hard, orientation are significantly greater than aerobic costs from the left-side, or easy, orientation. This was expected in view of the greater angle that the foot must traverse, requiring a greater period of time and a greater absolute need for oxygen. Also in accordance with our prediction was that landings after short vertical falls were preferen-

Table III

Landing frequencies of Ceratostoma foliatum *after removal of single varices*

Following removal of	Landing orientation (%)					
	Upright	Right	Left	Upright *vs.* upright	Right *vs.* right	Left *vs.* left
Right varix	33	44	23	$t = 3.16$	$t = 11.21$	$t = 5.65$
Control	44	16	40	$p = 0.003$	$p < 0.001$	$p < 0.001$
Middle varix	16	73	11	$t = 12.03$	$t = 20.93$	$t = 8.96$
Control	48	13	39	$p < 0.001$	$p < 0.001$	$p < 0.001$
Left varix	85	6	9	$t = 12.05$	$W = 431$	$t = 13.59$
Control	50	13	37	$p < 0.001$	$p < 0.001$	$p < 0.001$

Drops were in seawater of 5 body-length depth. $N = 50$ snails for each treatment, with 20 drops for each snail before (control) and after removal of varix. Values presented are mean percentage landings in each orientation for 20 drops for each of 50 animals, tested intact (control) and then following removal of a single varix. t: paired t test; W: Wilcoxon signed-rank test.

Table IV

Scaling relationships of shell and body parts of Ceratostoma foliatum *(n = 88)*

Relationship (Y vs. X)	log$a$	b	r^2	k	β	Predicted slope for isometry
weight *vs.* shell length	−3.829	2.83	0.984	0.999	2.83*	3
aperture area *vs.* shell length	−3.599	2.24	0.975	0.999	2.24*	2
labial spine length *vs.* shell length	−2.808	1.87	0.882	0.999	1.87*	1
right-varix area *vs.* shell length	−3.099	2.15	0.946	0.999	2.15*	2
middle-varix area *vs.* shell length	−3.707	2.38	0.938	0.999	2.38*	2
left-varix area *vs.* shell length	−3.860	2.38	0.925	0.999	2.38*	2
right-varix area *vs.* aperture area	0.358	0.93	0.918	0.999	0.93*	1
right + left varix area *vs.* aperture area	0.511	0.96	0.931	0.999	0.96	1
right + left + left remnant varix area *vs.* aperture area	0.550	0.98	0.941	0.999	0.98	1

Regression statistics are for the equation $\log Y = \log a + b \log X$. β is the corrected slope calculated by multiplying b by the reliability ratio, k (see text for explanation).

* Indicates that corrected log-log slope (β) differs significantly from the predicted slope for isometry, p all < 0.05.

tially on the left-side varix-pair, which offered the smaller angle for the foot to traverse.

Our data suggest that it is the presence of the right varix that most contributes to this result. Its effects are both through its potential vanelike influence and through its large size (weight). In the absence of the right varix the animal lands more on its right, or more vulnerable, side, probably because the trailing-edge stabilizing function of the broad right varix is missing (see Table III). Now the animal falls with the middle and left varices trailing upwards in winglike fashion, but rotated slightly clockwise by an accompanying dorsalward shift in center of mass. This produces a bias towards a right-side landing. In the absence of the middle varix the animal falls with center of gravity down (aperture up), with right and left varices extending outwards, and lands on the main body whorl. On impact, the imbalanced weight of the right varix tends to roll the animal onto its right side, even from landing orientations that, in the presence of the middle varix, would have resulted in a left-side posture. Thus, 73% of landings with the middle varix absent are on the right side. The slight ventral shift in center of mass on removal of the middle varix was not enough to affect this falling orientation. A similar falling orientation is produced in the absence of the left varix. Now the animal falls with center of mass downwards, stabilized by the right and middle varices, which project out in winglike fashion. However, because of the disproportionate weight of the right-varix, this falling orientation is not perfectly symmetrical; rather, it is skewed somewhat to a right-side-down orientation, perhaps aided by a slight shift to the right in center of mass on removal of the varix. Thus, mostly aperture-down landings result. Where this skewing is less, landing is still mostly on the main body whorl previously occupied by the left varix, and the heavy weight of the right varix rolls the animal onto its aperture. Thus, 85% of landings in the absence of the left varix lead to an upright position. In all cases where a varix was absent, subsequent landing orientation was greatly influenced by the two trailing varices, especially the right one in its presence. Whereas Palmer (1977) attributed a slight, but significant, destabilizing effect of the middle varix, leading to more upright landings from falls of 10 body lengths or greater, we show that the right varix is mainly responsible for the type of "destabilizing" event recorded here. Obviously these functions are inter-related, as the right varix ultimately becomes the middle one.

Based on these considerations, then, the optimal shell design (ignoring other possible varix functions) would be to have only right and middle varices, and not a left varix. But, because of the way the snails grow, varices can only be partially removed after they are laid down. Thus, the method of growth constrains *C. foliatum* to a less-than-optimal shell shape with respect to the feature of landing orientation after falling.

Our morphometric analyses failed to indicate the diminution of growth that was noted for San Juan Island, Washington, populations of *C. foliatum* by Spight and Lyons (1974) and Spight *et al.* (1974). These authors suggested that growth stops in mature snails, with the animals subsequently appearing to shrink in size as the varices, siphon, and spire erode. Our data indicate that animals are still adding undiminished right varices up to 82 mm length; but, as this is also equivalent to the largest size recorded by Spight and colleagues, it may represent a maximum for the species in this geographical area. Furthermore, the allometry of labial spine size to body length was consistent over the complete size range (25–82 mm length) found in our populations. There was no break discernible in the relationship corresponding to the spine reaching its "mature" form at 60 mm body length; a break

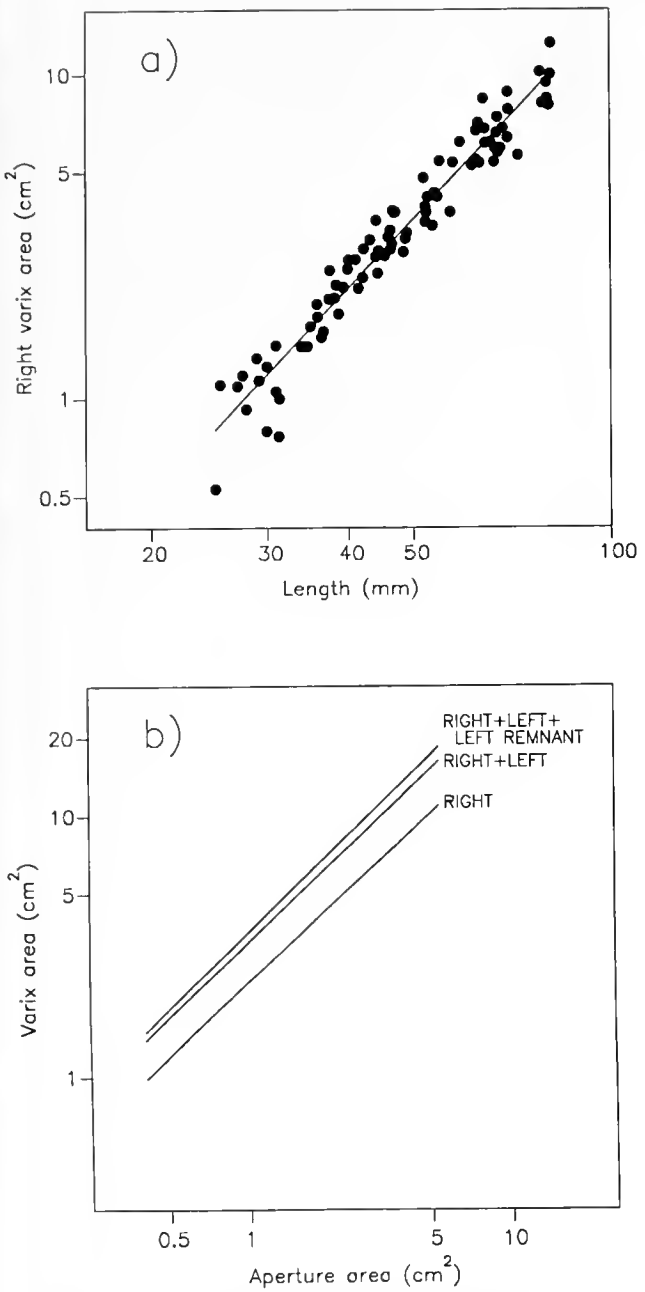

Figure 5. (a) Right-varix area as a function of shell length in *Ceratostoma foliatum*. (b) Areas of various varix combinations around the aperture plotted against aperture area in *C. foliatum*. The combined right + left + left-remnant varix area represents the flat shelf that surrounds the aperture. Regression statistics for the relationships are given in Table IV. $N = 88$ for each regression.

was noted for San Juan populations of *C. foliatum* by Spight and Lyons (1974).

Despite the attractiveness of a dual destabilizing-effect theory for the function of the varices during falls—that is, that the right one leads to preferential landing on the easy side during short falls and the middle one to preferential upright landings during long falls—the truth is probably that the varices serve multiple functions. Our inclination on viewing *C. foliatum*, and from our morphometry data, is to believe that the extended platform surrounding the aperture formed from the combined right and left varices could serve for protection of the soft parts during feeding and locomotion or, as suggested by Palmer (1977), for providing a stable platform during drilling of its prey. These ideas are supported by the juxtaposition of the previous left-varix remnant with the present right varix, which increases this area. In fact, we showed that the combined right-, left-, and left remnant-varix areas scaled isometrically with aperture area ($\beta = 0.98$), suggesting a related function.

Such hypotheses of protection and stability are testable, and could provide provocative areas for future work, especially if incorporated into a larger comparative study. Several other muricid species (in the genera *Ceratostoma* and *Pteropurpura*) on Pacific Ocean coasts have tri-varix morphology similar to that of *C. foliatum*. Most are large (4–8 cm) and all are carnivorous, but data on their habitat preferences and other aspects of their biology are scanty. A comparison of varix morphometries of a few of these species relative to aperture areas, combined with tests of their susceptibility to nipping or enveloping predators and their stability in currents, could lead to further insights on optimal shell design in gastropod molluscs.

Acknowledgments

We thank Jo Wieruszewski for help with the morphometric measurements; Patricia Lee, Joseph West, and Jeffrey Fleming for other technical help; Steve Land for assistance in scuba collections; and Andy Spencer, Director of the Bamfield Marine Station, and his staff for logistical support during collection of animals. Barbara Taylor, Steve Pennings, and A. Richard Palmer gave helpful comments on the manuscript. The work was supported by a Natural Science and Engineering Research Council (NSERC) grant to T. Carefoot and a University Graduate Fellowship to D. Donovan.

Literature Cited

Carefoot, T. H. 1987. Gastropoda. Pp. 89–72 in *Animal Energetics. Vol. 2. Bivalvia through Reptilia*, T. J. Pandian and F. J. Vernberg, eds. Academic Press, San Diego.

Carter, R. M. 1967. The shell ornament of *Hysteroconcha* and *Hecuba* (Bivalvia): a test case for inferential functional morphology. *Veliger* **10**:59–71.

Ebling, F. J., J. A. Kitching, L. Muntz, and C. M. Taylor. 1964. The ecology of Lough Ine. XIII. Experimental observations of the destruction of *Mytilus edulis* and *Nucella lapillus* by crabs. *J. Anim. Ecol.* **33**:73–82.

Elliott, J. M., and W. Davison. 1975. Energy equivalents of oxygen consumption in animal energetics. *Oecologia* **19**:195–201.

Fotheringham, N. 1971. Field identification of crab predation on *Shaskyus festivus* and *Ocenebra poulsoni* (Prosobranchia: Muricidae). *Veliger* **14**:204.

Fuller, W. A. 1987. *Measurement Error Models.* John Wiley and Sons, New York.

Harvey, P. H., and M. D. Pagel. 1991. *The Comparative Method in Evoluttonary Biology.* Oxford University Press, Oxford.

Johnson, A. S., and M. A. R. Koehl. 1991. Maintenance of dynamic strain similarity and environmental stress factor in different flow habitats: thallus allometry and material properties of giant kelp. *J Exp. Biol.* **195**:381–410.

Kent, B. W. 1981. Feeding and food preferences of the muricid gastropod *Ceratostoma foliatum*. *Nautilus* **95**:38–42.

Kitching, J. A., L. Muntz, and F. J. Ebling. 1966. The ecology of Lough Ine. XV. The ecological significance of shell and body forms in *Nucella*. *J Anim. Ecol* **35**:113–126.

LaBarbera, M. 1989. Analyzing body size as a factor in ecology and evolution. *Ann Rev Ecol Syst.* **20**:97–117.

Morris, R. H., D. P. Abbott, and E. C. Haderlie. 1980. *Ceratostoma foliatum.* Pp. 275–276 in *Intertidal Invertebrates of California.* Stanford University Press, Stanford, CA.

Paine, R. T. 1966. Function of labial spines, composition of diets, and size of certain marine gastropods. *Veliger* **9**:17–24.

Palmer, A. R. 1977. Function of shell sculpture in marine gastropods: hydrodynamic destabilization in *Ceratostoma foliatum*. *Science* **197**: 1293–1295.

Pickavance, J. R. 1970. A new approach to the immunological analysis of invertebrate diets. *J. Anim. Ecol* **39**:715–724.

Spight, T. M., C. Birkeland, and A. Lyons. 1974. Life histories of large and small murexes (Prosobranchia: Muricidae). *Mar. Biol.* **24**:229–242.

Spight, T. M., and A. Lyons. 1974. Development and functions of the shell sculpture of the marine snail *Ceratostoma foliatum*. *Mar Biol.* **24**:77–83.

Vermeij, G. J. 1974. Marine faunal dominance and molluscan shell form. *Evolution* **28**:656–664.

Vermeij, G. J. 1979. Shell architecture and causes of death of Micronesian reef snails. *Evolution* **33**:686–696.

Zar, J. H. 1984. *Biostatistical Analysis* Prentice-Hall, Englewood Cliffs, NJ.

Marine Biological Laboratory Woods Hole Massachusetts

Ninety-Seventh Report for the Year 1994 One-Hundred and Sixth Year

Officers of the Corporation

Sheldon J. Segal, *Chairman of the Board of Trustees*
Robert E. Mainer, *Vice Chairman of the Board of Trustees*
James D. Ebert, *President of the Corporation*
John E. Burris, *Director and Chief Executive Officer*
Robert D. Manz, *Treasurer*
Neil Jacobs, *Clerk of the Corporation*

Contents

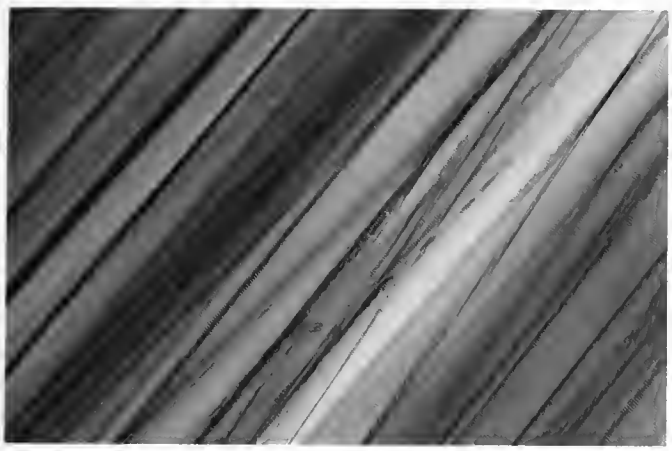

Report of the Director and Chief Executive Officer

In 1994, the Decennial Review Committee, which has met every decade since 1924 to comprehensively evaluate the Marine Biological Laboratory, examined the full range of Laboratory activities, including summer and year-round research and education programs. I am pleased to say that its final report, prepared under the chairmanship of Malcolm Steinberg of Princeton University, was thorough and positive. It affirms that the MBL continues to be a valuable part of biological research in the U.S. and the world.

"The socioscientific ethos generated by the amalgam of knowledge, drive, and free scientific exchange that continues to characterize it has served to make the MBL the most important center of its kind in the world. This spectacularly successful enterprise is the product of a unique blend of historical accidents and good sense . . . the ultimate scientific watering hole, bringing together the most distinguished minds in the biological sciences in an environment where free interaction is possible."
—1994 Report of the Decennial Review Committee

Year-Round Scientific Activities

The Ecosystems Center is one of many scientific "watering holes" at the Marine Biological Laboratory. The largest of the year-round laboratories, the Center is one of the premier facilities in the world for investigating the functioning of terrestrial and aquatic ecosystems and the effects of human activities on those systems. Research projects currently underway include the study of global change and the carbon balance of Arctic ecosystems, land use change and soil processes in the Amazon River Basin, and a study on the effects of land use and the introduction of organic matter to estuarine ecosystems. Some of the estuarine research was conducted locally in Plum Island Sound north of Boston and in Waquoit Bay here on Cape Cod.

In 1994, researchers at the Ecosystems Center pioneered the use of a stable isotope of nitrogen (^{15}N) to follow the pathway of this important element in undisturbed ecosystems. Senior Scientist Bruce Peterson added ammonium-^{15}N to an Arctic river continuously for three weeks to trace how fast nitrogen moved from the water into algae, then into grazing insects and eventually into predatory fish. These rates were then used to test a mathematical model of the entire stream system. Associate Scientist Knute Nadelhoffer used both ammonium-and nitrate-^{15}N to study what happened to the nitrogen added to forests of New England from acid rain. Most of the added nitrogen remains in the soil. Scientists from the Ecosystems Center incorporate results from these and other studies into ecosystem models of carbon and nitrogen dynamics. One of these models, called the Terrestrial Ecosystem Model, is now part of an MIT-centered integrated assessment model that also deals with the atmosphere, the oceans, and the global economy. This large model is used to address global change issues.

Investigators in the Architectural Dynamics in Living Cells Program conduct research at the molecular and cellular level at the interface of anatomy and physiology. They use advanced instrumentation to image real-time cellular events occurring in living cells. The report of the Decennial Review Committee stated that "MBL Distinguished Scientist Dr. Shinya Inoué's work has produced a true revolution in the analysis of the living, functioning cell, marrying the best available light-microscopic techniques with the most sophisticated image analysis approaches, utilizing both video and computer graphics at an exquisite level of performance." During the summer of 1994, Program investigators collaborated with Rand Fellow Ted Salmon (University of North Carolina, Chapel Hill) and Nikon Fellow Andrew Murray (University of California, San Francisco). While in Woods Hole, Salmon and Murray successfully attached

chromosomes (derived from sperm in the egg extract) to microtubules assembled in frog egg extract, and, for the first time, experimentally got them to go through anaphase movement outside of a living cell. These exciting events were recorded as 4-D sequences in collaboration with Ted Inoué of Universal Imaging Corporation. In the fall of 1994, the Program also welcomed two visiting investigators from Japan, Dr. Rieko Arimoto of Nikon, Inc., and Dr. Keisuke Suzuki of the Olympus Corporation.

The Molecular Evolution Program, directed by Dr. Mitchell Sogin, is another resident laboratory where scientists gather, often over a computer monitor, to share information. The Program has helped to advance the field of molecular evolution by using molecular techniques to calibrate the evolution of organisms and their genes. Using measures of similarity for ribosomal RNAs, investigators measure genetic differences between members of the same species or reconstruct phylogenies for organisms that span the largest evolutionary distances. Drs. Sogin, Hinkle, and collaborators' studies on the stable co-evolution of attine ants and their fungi over 50 million years suggests that preservation of biodiversity may require maintenance of both members of a symbiotic partnership. This work was published in 1994 in the journal *Science*, and featured subsequently in *The New York Times* and the local press.

Postdoctoral Research Associate Hilary Morrison in the Molecular Evolution laboratory (photo by Richard Howard).

Senior Scientist Osamu Shimomura (photo by Linda Golder/MBL).

The Calcium Patterning Program, under the direction of Senior Scientist Lionel F. Jaffe and Assistant Scientist Andrew L. Miller, continues to advance the study of the role played by calcium in a wide range of fundamental cell processes. The Program uses a group of bioluminescent proteins, acquorins, that emit light when in contact with calcium for their studies. Aequorin, which was first purified by MBL Senior Scientist Osamu Shimomura in the 1960s, is produced in a species of jellyfish. Throughout 1994, Program investigators continued their work with the slime mold *Dictyostelium*, which they use as a simple model for studying the development of multicellular organisms. In a paper just published by the journal *Development*, Miller and Jaffe and their colleagues documented the cellular calcium patterns throughout the life cycle of the slime mold. This is an important first step to understanding the role that calcium plays in switching on or off various genes within the organism. Collaborations are currently underway with scientists at Massachusetts General Hospital, the University of Pennsylvania, and Cornell University to pursue this research in other animal and plant models.

The National Vibrating Probe Facility, directed by Associate Scientist Peter J. S. Smith, develops and makes available techniques for measuring, non-invasively, the movement of ions across cell membranes. In 1994, Facility investigators were successful in their attempts to measure the small steady-state calcium fluxes from isolated neurons in culture. This has opened up new areas of research into the regulation of calcium and second messengers. Two new probes are currently in development at the Facility. The BioKelvin probe is being designed to measure the weak

ion fields that exist around tissue in a gaseous environment. Investigators plan to use this new machine in the study of skin. The second instrument currently in development is a vibrating oxygen probe, which Facility investigators intend to use in the study of cell respiration.

In September of 1994, the Boston University Marine Program kicked off a year-long celebration of its 25th anniversary. Since it began in 1969, BUMP has grown from a small graduate program into one of the strongest undergraduate and graduate programs in marine biology in the country. In 1994 BUMP enrolled 60 undergraduates and 33 masters and doctoral candidates who studied with 8 teaching and 9 research faculty.

The year-round research program at the MBL expanded in 1994 with the addition of two new programs. In the fall the MBL welcomed the Laboratory of Cell Communication, led by Drs. Werner Loewenstein and Birgit Rose. Investigators in this Laboratory study the membrane channel built into junctions between cells that provides one of the most basic forms of intercellular communication in organs and tissues. They also examine feedback loops in normal and abnormal cell proliferation, which is important in cancer research. The MBL also received an award from NASA to establish the Center for Advanced Studies in the Space Life Sciences. This new Center will review and study a variety of life science areas, with special attention on how gravity influences biological processes.

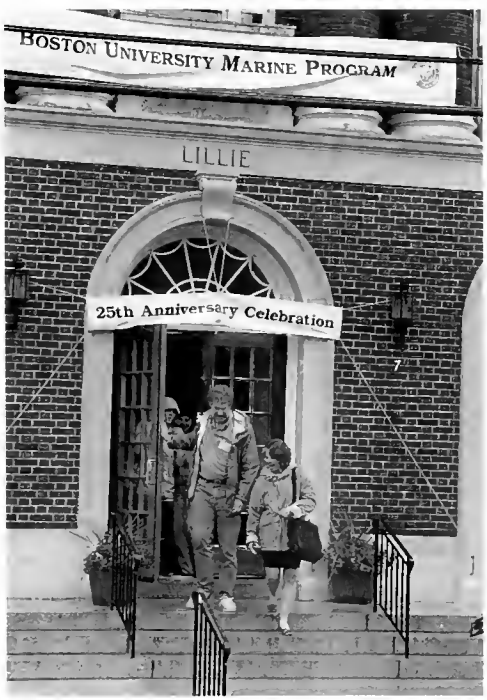

BUMP celebrates its 25th Anniversary (photo by Boston University Photo Services).

The Marine Resources Center

The Marine Resources Center (MRC), now in operation for two years, continues to supply healthy animals for biological and biomedical research and education. The seawater system is monitored daily to provide readings on temperature, nutrients, and dissolved gases. A variety of research projects involve the use of this facility.

- The clam, *Mulinia*, is being raised in the MRC's mariculture room. This clam, a close relative of the extensively studied surf clam, *Spisula*, is easy to maintain and culture. It is also useful as a model in the study of the cellular and molecular biology of cell division. These studies are important for learning more about diseases such as cancer, where cells divide without adequate control.
- Ecosystems Center scientists are analyzing oxygen uptake from the water overlying sediments to measure bacterial and animal respiration in subtidal muds from Boston Harbor and Massachusetts Bay. The data are part of an environmental impact assessment on the proposed sewage outfall pipe. Center scientists moved their project from the Homestead building to the MRC to take advantage of the running, filtered, and temperature-controlled seawater available there.
- In a cooperative effort with a local commercial scallop producer, approximately 250,000,000 scallop "spat" were produced from about 1,200 mature scallops conditioned by overfeeding, an accelerated light/dark cycle, and exposure to a computer-controlled regime of increasing seawater temperatures. Animals spawned early in the year gained more than two months additional growing/maturation time ahead of feral stocks.
- This past year, MBL scientists began collaborating with the Nantucket Research and Education Foundation to improve the health of cultured scallops and to develop genetic markers to trace their dispersion patterns in order to gauge the success of mariculture efforts.

In 1994 the MRC continued to win accolades. In May the project received "High Honors" in *R & D Magazine's* Laboratory of the Year competition; in September, Facilities Manager Richard Cutler accepted the American Institute of Plant Engineers' FAME Award of Excellence on behalf of the MBL; and in October Tsoi/Kobus, the architectural firm that designed the MRC, was awarded one of eleven awards

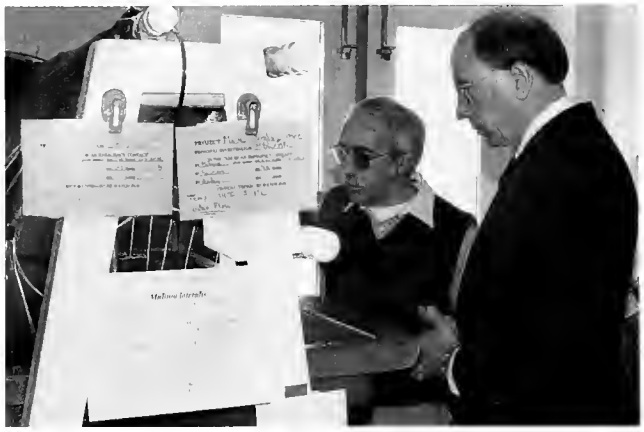

Associate Scientist Alan Kuzirian shows Congressman Gerry Studds Mulinia cultures in the MRC (photo by Mark Dornblaser/MBL).

in the Top Quality Urban Waterfront Projects category sponsored by the Waterfront Center organization in Washington, DC. Most recently, the MBL received the Construction Industry Liaison Group "Owner Recognition Award" at the Build Boston Design and Construction Industry Convention.

The MBL was fortunate to receive a total of $1 million from the Clowes Fund and the Lakian Foundation to help recruit a leading scientist to establish an independent research program and direct research services provided by the MRC. As I prepare this report, a group of applicants for this position is being interviewed by our Search Committee.

Summer Research Activities

From August 15 to 17, MBL scientists gathered in the Lillie Auditorium for the Laboratory's annual General Scientific Meetings. Last year more than 60 investigators and students presented their summer's research at the meeting. Topics ranged from cell division to comparative biology to neurobiology to phytoplankton dynamics. Fifty-one of those presentations were published as Short Reports in the October issue of the MBL's journal, *The Biological Bulletin.*

The two short reports submitted by Peter Armstrong (University of California, Davis) and James Quigley (SUNY, Stony Brook) were recognized by *The Biological Bulletin* as the issue's Featured Articles. During the summer of 1994, Armstrong and Quigley and their co-workers found evidence that two protein molecules found in the blood of horseshoe crabs—limulin and α_2-macroglobulin—play key roles in the innate immune systems of invertebrates. Their work suggests that limulin both recognizes and destroys invading microbes, and that α_2-macroglobulin appears to be the regulator of that cell-destruction system.

Research performed by Yale University Professor Walter Boron and colleagues last summer at the MBL was recently described in an article published in the journal *Nature.* In that article, Boron and colleagues documented a novel technique that they developed for studying the transport of bicarbonate across cell membranes using the squid giant axon. This technique involves rapidly mixing two solutions to produce an out-of-equilibrium solution with virtually any combination of pH, carbon dioxide, and bicarbonate levels. Boron's work resulted in the identification of a new mechanism for bicarbonate transport, a potassium/bicarbonate transporter. This work could be significant for understanding human diseases in which acid-base balance is important, including epilepsy and stroke, respiratory and renal disorders, cancer, and heart disease.

The results of research from many summer laboratories saw publication in a number of other journals. The 1994 work of Rodolfo Llinás (NYU) and his colleagues was published in the December issue of the *Proceedings of the National Academy of Science;* an article by Antionio Giuditta (University of Naples) and co-authors appeared in the *Journal of Neurochemistry;* and Robert Paul Malchow (University of Illinois), Haohua Qian (Harvard University), and Harris Ripps (University of Illinois) published an article in the December 1994 issue of the *Journal of General Physiology.* Many other articles based on MBL summer research appeared in *The Journal of Biological Chemistry, Cell Motility and the Cytoskeleton, the Journal of Cell Science,* the *Journal of Cell Biology,* the *Journal of Neurophysiology, Neuroscience Letters,*

Joe DeGiorgis dissects a squid giant axon.

Summer investigator Robert Palazzo examines a surf clam.

Biophysical Journal, Biomembrane Electrochemistry, the *Journal of Neuroscience, Glia,* and *Brain Research Bulletin.* A partial list of articles published in 1994 by year-round and summer MBL scientists appears at the end of this Annual Report.

Educational Programs

The MBL's strong commitment to teaching the scientific method in an interdisciplinary and highly motivated research environment represents the apex of training efforts in the life sciences.

"Long regarded as jewels in the crown of U.S. graduate education in the biological sciences, [MBL] courses have retained their superb quality. Many outstanding scientists pay tribute to them as landmarks in their own education . . . Students in these courses receive state-of-the-art training that cannot be obtained at their home institution—or indeed any other institution of higher learning in the world. This is made possible by the intense, total immersion-in-science approach that results from having a large faculty, drawn from around the world, who interact on an almost 24 hour-a-day basis providing the student with conceptual and practical training . . . the additional availability of the most up-to-date equipment provides access to the latest and even breaking technologies."
—1994 Report of the Decennial Review Committee

While preparing this report, I learned that the Howard Hughes Medical Institute will award the MBL $2 million to support four years of summer courses, from 1996 to 1999. "The courses at the MBL are so consistently excellent that scientists are always eager to enroll," said Joseph G. Perpich, M.D., J.D., HHMI's vice president for grants and special programs. The MBL is indeed grateful to the Howard Hughes Medical Institute for its continued support of these remarkable courses.

The summer of 1994 marked the final year of a five-year tenure as directors for John Breznak and Martin Dworkin of the Microbial Diversity course, Ron Calabrese and Martha Constantine-Paton of the Neural Systems & Behavior course, and Irwin Levitan and Leonard Kaczmarek of the Neurobiology course. The efforts of these retiring course directors are greatly appreciated; each director served his or her course and the Laboratory with dedication and enthusiasm. Ron Calabrese and Irwin Levitan will continue to serve the Laboratory as co-chairs of the newly formed Education Committee, which replaces the MBL's Instruction Committee. The new Committee reports directly to the Science Council on all educational matters.

Summer Fellowships and Scholarships

The MBL Summer Research Fellowship and Scholarship Programs provided funding for 150 individuals last summer. Fellowship awards to support independent research totaled nearly $157,000, a

Senior Scientist Mitchell Sogin teaching the Molecular Evolution Workshop at the MBL.

$26,000 increase over 1993. Students attending MBL courses were awarded more than $357,000 in scholarships last summer.

Twelve young scientists were awarded Grass fellowships in Neurophysiology at the MBL last summer. The Program, which is sponsored by the Grass Foundation, has been held at the MBL for over 40 years, offering young neuroscientists an opportunity to do independent research, often for the first time in their careers.

Nine minority graduate students from around the country participated in the 7th annual Minority Fellowship Program (MFP) at the MBL during the summer of 1994. The Program, sponsored by a grant from the National Institute of Mental Health, is designed to unite pre-doctoral neuroscience students from underrepresented ethnic groups with postdoctoral fellows and members of the MFP scientific board. Students participating in this month-long program gain scientific "survival skills," including increased skills in writing, delivering oral scientific presentations, and career development techniques.

The Science Writing Fellowships Program completed its ninth successful year, enrolling 13 journalists from a variety of print and broadcast media last summer. The Program, which fosters a better-informed and more interactive dialogue between scientists and science writers to provide the public with improved information about the life sciences, has now trained over 100 journalists.

MBL Trustees

We were fortunate to welcome three new Trustees to the Board in 1994. They are: Dr. Darcy Brisbane Kelley of the Department of Biological Sciences at Columbia University, Dr. Laurie Landeau of Listowel, Inc., and Dr. Burton J. Lee, III of Intracel Corporation.

Dr. Kelley is a former co-director of the MBL's Neural Systems & Behavior Course. She is also professor and chair of the Department of Biological Sciences at Columbia University. Dr. Kelley received her A.B. from Barnard College and her Ph.D. from Rockefeller University.

Dr. Lee is a member of the MBL's Council of Visitors. He received his B.A. from Yale University and his M.D. from Columbia University. Dr. Lee served as President Bush's physician during Mr. Bush's term in the White House, and was a member of the White House Task Force on Infant Mortality and the Presidential Drug Advisory Council. He now serves as Chairman of the Board of Intracel Corporation in Cambridge, MA.

Dr. Landeau is also a member of the MBL's Council of Visitors and serves as an associate director of the AQUAVET Program held annually at the Laboratory. She is General Manager of Listowel, Inc., and the President of the Marinetics, Inc., a firm that researches and develops disease-resistant shellfish for culture. Dr. Landeau holds an MBA and a VMD from the University of Pennsylvania.

MBL Trustee and Harvard University neurobiologist Edward Kravitz recently completed his term on the MBL Board. Ed has served several terms on the Board and has been, and continues to be, a strong supporter of the Laboratory's programs for young scientists. His contributions to the Laboratory were recognized with appreciation at the February 1995 meeting of the MBL Board of Trustees.

The MBL/WHOI Library

The Library continued its evolution from the traditional role of exclusively providing information in print into electronic document delivery services. We were the nation's first library to mount commercial CD-ROMs on the Internet, and we negotiated various novel distribution arrangements for our collection through the National Library of Medicine, Elsevier Publishing Corporation, and Readmore Subscription Agency. Much of this development has been possible through grants from Howard Hughes Medical Institute, the Andrew W. Mellon Foundation and the Bay Foundation. The Library remains, however, a vital

A student examines journals in the MBL/WHOI Library (photo by Richard Howard).

resource for access to a complete and up-to-date book and print journal collection. Roger Stoddard of the Houghton Library at Harvard University reviewed the collection in 1994 and stated that it was "breath-taking in its comprehensiveness of coverage and completeness of holdings."

Renovations, Restorations, and Recycling

The renovation of the Crane wing of the Lillie Building was completed in 1994. Renovations included the removal of asbestos and the installation of an HVAC system throughout the wing, which has resulted in a much improved working environment for our Lillie Laboratory scientists and staff.

If the MBL's 1994 water and sewer bill is any indication, our conservation efforts are paying off. Thanks to fewer aspirators in the laboratories, the conversion of the Whitman seawater chiller from fresh to salt water, the installation of water-saver toilets and shower heads in the dorms, better facility maintenance, and fewer coldwave room chillers in the Lillie building, the MBL's water and sewer bill dropped dramatically—from $152,630 in 1991 to $86,917 in 1994.

All MBL renovation projects, whether large or small, are first evaluated with an eye towards conservation. A good example of this effort is the replacement last year of windows in the Homestead building, funded at a cost of $23,000 by the local Colonial Gas company. The installation of those energy-efficient windows has netted the MBL an annual savings of approximately $5,000 in gas usage. Ecosystems Center personnel are also enjoying a more comfortable working environment.

Special Events, Symposia, and Conferences

The MBL held its first annual Poster Session last June to promote scientific exchange among students, faculty, fellows, and established summer and year-round MBL investigators. The event was a great success: 45 posters were presented by year-round and summer scientists on topics ranging from the control of the cell cycle in early embryos to protein synthesis in the squid axon and nerve endings. Over 250 members of the MBL community gathered to review the posters and attend a reception that followed in the Meigs Room. Another Poster Session is scheduled for the summer of 1995.

The Tokyo String Quartet returned to the MBL last July for another spectacular Lillie Auditorium concert. The quartet played to a full house, and the elegant post-concert candlelight dinner on the Swope Terrace made for a memorable evening. The Quartet will perform again at the MBL this coming summer.

In September the MBL sponsored its first annual symposium in marine biotechnology titled "Biomaterials from the Sea." The symposium was designed to provide scientific and technical insights into the exciting area of marine biomaterials. Seventy-five individuals from the worlds of science, business, investment, and policy participated in the meeting. The second annual marine biotechnology symposium will be held on September 22, 1995.

The Marine Biological Laboratory also provided conference and housing services for over 40 scientific meetings, departmental retreats, and conferences last year, which attracted an additional 3800 scientists and students to Woods Hole. For the first time in the history of the Laboratory, MBL housing and dining revenues surpassed the $1 million mark in 1994.

MBL Head Mail Clerk Bob Illgen recycles.

Ecosystems Center Co-Director Jerry Melillo greets participants in the GCTE conference held at the MBL last spring

In Closing

As I've become more familiar and involved with the MBL's multi-faceted research and educational programs during my tenure here, I marvel at this century-old Laboratory's ability to reinvent itself in the face of rapid and broad-based change. I close with a statement from a student in one of last summer's courses. It resonates with my feelings about the MBL:

"I feel like Woods Hole is to scientists what Paris is to artists. It's a special place where people with similar interests roam together to feed and grow off of other people's ideas and ultimately create something greater than anyone could ever do alone. It was wonderful to be in such a community, to be able to discuss ideas with some of the greatest minds . . . For a student starting out in science it was the best thing I could ever do. And it seemed for the old pros a great opportunity to remember why they got into the field and to get a little enthusiasm from the students."

—John E. Burris

Report of the Treasurer

In 1994 our financial performance was marked by continued success in operating funds, in financial stabilization of the MBL's physical plant, and in a decreased value of our invested portfolios.

Operating Funds

The MBL's Unrestricted Operating Funds ended the year with a surplus of $513,900, the General Fund showed a surplus of $347,811, and the Housing and Dining Auxiliary Fund had a surplus of $166,089. Mandatory transfers to repay debt principal amounted to $69,010; $104,984 was used to fund capital acquisitions; and $359,000 was transferred to the renewals and replacement fund for future capital investment ($235,000 to the General Renewals and Replacement Fund and $124,000 to the Housing Renewals and Replacement funds). While the amount of the transfers to the Renewals and Replacement funds was slightly less than in 1993, it is still a significant amount and demonstrates the Laboratory's commitment to one of the Trustees' long-standing goals: Reinvesting in the physical plant infrastructure of the MBL.

In 1994 funding of research and education programs both increased over 1993. The former grew from $5,727,323 to $5,900,614, and the latter from $1,538,190 to $1,702,345. Equally encouraging is the stabilization of the summer research program rentals, which have increased almost 5% over 1993. The Boston University Marine Program has expanded as well, and has provided increased revenues for the MBL.

The financial operating environment of the MBL continues to improve, and as we look forward to 1995, we have every reason to believe we will build on that record of stability and measured growth.

Endowment Funds

The success that we enjoyed in operating funds was not duplicated in our endowment funds. In fact, the endowment fund market values decreased in 1994, primarily due to the poor performance of our investment portfolios. This matter has concerned us for the past several years, and the Finance and Investment Committee spent much of the past year reviewing and evaluating our current investment strategies and management. In December, the Committee decided to change radically our approach and diversify our investments and investment managers (this was implemented in early 1995).

In making this change, we have concluded that the investment climate for the future is far more complex than it has been in the recent past. We therefore need to diversify our endowment by using a balance of specialized managers if we are to improve our performance for long-term growth.

For the future, the task remains clear: Build the necessary overall financial support base that will provide stability and enhance the MBL's research and education programs. During the past several years, we have done so in our operating funds. For 1995 and the years ahead, we will concentrate our efforts in establishing a system of investment management that will duplicate our recent success in our operating monies and provide additional financial support for our research and education programs.

—Robert D. Manz

Financial Statements

Coopers &Lybrand

certified public accountants

REPORT OF INDEPENDENT ACCOUNTANTS

To the Board of Trustees of
Marine Biological Laboratory
Woods Hole, Massachusetts

We have audited the accompanying balance sheet of Marine Biological Laboratory (the "Laboratory") as of December 31, 1994 and the related statement of support, revenues, expenses and changes in fund balances for the year then ended. We previously audited and reported upon the financial statements of the Laboratory for the year ended December 31, 1993, for which condensed statements are presented for comparative purposes only. These financial statements are the responsibility of the Laboratory's management. Our responsibility is to express an opinion on these financial statements based on our audit.

We conducted our audit in accordance with generally accepted auditing standards. Those standards require that we plan and perform the audit to obtain reasonable assurance about whether the financial statements are free of material misstatement. An audit includes examining, on a test basis, evidence supporting the amounts and disclosures in the financial statements. An audit also includes assessing the accounting principles used and significant estimates made by management, as well as evaluating the overall financial statement presentation. We believe that our audit provides a reasonable basis for our opinion.

In our opinion, the financial statements referred to above present fairly, in all material respects, the financial position of Marine Biological Laboratory at December 31, 1994, and its support, revenues, expenses and changes in fund balances for the year then ended in conformity with generally accepted accounting principles.

Our audit was conducted for the purpose of forming an opinion on the basic financial statements taken as a whole. The supplemental schedules of support, revenues, expenses and changes in fund balances for current funds (Schedule I), endowment funds (Schedule II) and plant funds (Schedule III) as of December 31, 1994 are presented for purposes of additional analysis and are not a required part of the basic financial statements. Such information has been subjected to the auditing procedures applied in the audit of the basic financial statements and, in our opinion, is fairly stated, in all material respects, in relation to the basic financial statements taken as a whole.

Boston, Massachusetts
April 20, 1995

Coopers & Lybrand

MARINE BIOLOGICAL LABORATORY

BALANCE SHEETS

December 31, 1994
(with comparative totals for 1993)

ASSETS	1994	1993
Cash	$ 582,333	$ 580,165
Restricted cash	6,869	9,354
Investments, at market (Note C)	2,864,732	3,427,321
Accounts receivable, net of allowance for doubtful accounts of $10,000 in 1994 and 1993	809,216	804,955
Receivables due for costs incurred on grants and contracts	1,014,323	906,011
Other assets	455,008	421,392
Total current assets	5,732,481	6,149,198
Restricted cash (Note E)	—	54,847
Investments, at market (Notes C and D)	20,115,871	20,257,186
Deposits with trustee (Note F)	—	492,852
Fixed assets (Note B):		
Land	689,661	689,661
Buildings	31,138,144	29,403,841
Equipment	3,316,335	3,120,483
Construction in progress	49,387	1,148,917
	35,193,527	34,362,902
Less accumulated depreciation	(13,124,465)	(11,884,268)
	22,069,062	22,478,634
Total assets	$47,917,414	$49,432,717

LIABILITIES AND FUND BALANCES	1994	1993
Current portion of long-term debt (Note F)	$ 79,010	$ 69,010
Current obligations held under capital leases (Note E)	28,014	—
Accounts payable and accrued expenses	1,811,037	1,489,146
Deferred income	246,746	240,672
Total current liabilities	2,164,807	1,798,828
Accounts payable	—	218,050
Annuities payable (Note B)	785,096	157,359
Long-term debt (Note F)	2,396,671	2,475,680
Obligations held under capital leases (Note E)	44,687	—
Deferred support (Note G)	2,991,470	3,796,864
Total long-term liabilities	6,217,924	6,647,953
Commitments and contingencies (Note E)		
Total liabilities	8,382,731	8,446,781
Current unrestricted fund balances	35,443	32,097
Annuity fund balance	551,450	70,115
Endowment fund balances:		
Quasi-endowment unrestricted	553,379	595,694
Endowment, income for unrestricted purposes	3,666,240	3,876,604
Endowment, income for restricted purposes	9,055,124	9,547,900
Quasi-endowment restricted	5,506,459	5,907,490
Total endowment funds	18,781,202	19,927,688
Plant fund balances:		
Unrestricted	19,452,623	19,869,320
Repairs and replacement reserve	664,578	546,838
Restricted	49,387	539,878
Total plant funds	20,166,588	20,956,036
Total liabilities and fund balances	$47,917,414	$49,432,717

The accompanying notes are an integral part of the financial statements.

MARINE BIOLOGICAL LABORATORY

STATEMENT OF SUPPORT, REVENUES, EXPENSES AND CHANGES IN FUND BALANCES

for the year ended December 31, 1994
(with appropriate totals for 1993)

	Current Funds									
	Unrestricted						Plant Fund			
	Operating Fund	Auxiliary Enterprises Fund	Total	Restricted Fund	Annuity Fund	Endowment Fund	Unrestricted	Restricted	1994 Total All Funds	1993 Total All Funds
SUPPORT AND REVENUES:										
Grant reimbursements of direct costs				$5,388,844					$ 5,388,844	$ 5,565,338
Grant for capital additions								$185,087	185,087	1,450,632
Recovery of indirect costs	$3,700,412		$3,700,412						3,700,412	3,711,139
Tuition				577,365					577,365	611,700
Fee for services	1,342,754	$2,107,719	3,450,473	101,219					3,551,692	3,481,304
Investment income	453,507		453,507	496,870	$ 20,646			1,566	972,589	968,729
	5,496,673	2,107,719	7,604,392	6,564,298	20,646			186,653	14,375,989	15,788,842
Gifts	581,554		581,554	1,328,616	455,327	$ 175,630		58,000	2,599,127	5,254,237
Change in deferred support (Note G)	559,476		559,476	237,087	36,398				832,961	(278,601)
	1,141,030		1,141,030	1,565,703	491,725	175,630		58,000	3,432,088	4,975,636
Miscellaneous revenue	116,867		116,867	658,864					775,731	498,823
Total support and revenues	6,754,570	2,107,719	8,862,289	8,788,865	512,371	175,630		244,653	18,583,808	21,263,301
EXPENSES:										
Research				5,900,614					5,900,614	5,727,323
Instruction				1,702,345					1,702,345	1,538,190
Scholarships, fellowships and stipends				465,824					465,824	447,454
Services	2,013,091	1,756,808	3,769,899	331,105					4,101,004	3,956,295
Administration	2,469,813	184,822	2,654,635						2,654,635	2,577,112
Plant operations	1,923,855		1,923,855	156,592			215,260		2,295,707	1,922,606
Depreciation							1,224,994		1,224,994	1,183,814
Other				241,733	20,175				261,908	248,253
Total expenses	6,406,759	1,941,630	8,348,389	8,798,213	20,175		1,440,254		18,607,031	17,601,047
Excess (deficit) of support and revenue over expenses before gain on investments	347,811	166,089	513,900	(9,348)	492,196	175,630	(1,440,254)	244,653	(23,223)	3,662,254
Net realized gain (loss) on investments				93,184	(4,490)	1,441,106			1,529,800	1,057,581
Net unrealized gain (loss) on investments				(143,698)	(6,371)	(2,807,761)			(2,957,830)	(101,100)
Total gain (loss) on investments				(50,514)	(10,861)	(1,366,655)			(1,428,030)	956,481
Transfers	(344,465)	(166,089)	(510,554)	59,862		44,539	1,141,297	(735,144)	—	—
Net change in fund balances	3,346	—	3,345	—	481,335	(1,146,486)	(298,957)	(490,491)	(1,451,253)	4,618,735
Fund balances, beginning of year	32,097	—	32,097	—	70,115	19,927,688	20,416,158	539,878	40,985,936	36,367,201
Fund balances, end of year	$ 35,443	—	$ 35,443	—	$551,450	$18,781,202	20,117,201	$ 49,387	$39,534,683	$40,985,936

The accompanying notes are an integral part of the financial statements.

Marine Biological Laboratory

Notes to Financial Statements

A. *Purpose of the Laboratory:*

The purpose of Marine Biological Laboratory (the "Laboratory") is to establish and maintain a laboratory or station for scientific study and investigations, and a school for instruction in biology and natural history.

B. *Significant Accounting Policies:*

Basis of Presentation—Fund Accounting

In order to ensure observance of limitations and restrictions placed on the use of resources available to the Laboratory, the accounts of the Laboratory are maintained in accordance with the principles of fund accounting. This is the procedure by which resources are classified into separate funds in accordance with specified activities or objectives. Separate accounts are maintained for each fund; however, in the accompanying financial statements, funds that have similar characteristics have been combined into fund groups. Accordingly, all financial transactions have been recorded and reported by fund group.

Externally restricted funds may only be utilized in accordance with the purposes established by the donor or grantor of such funds. However, the Laboratory has full control over the utilization of unrestricted funds. Restricted gifts, grants, and other restricted support are accounted for in the appropriate restricted funds. Restricted current funds are reported as revenue as the related costs are incurred (see Note G).

Endowment funds are subject to restrictions which require that the principal be invested in perpetuity. Related investment income is available for use for restricted or unrestricted purposes by the Laboratory depending on donor restrictions. Quasi-endowment funds have been established by the Laboratory for the same purposes as endowment funds; however, the principal of these funds may be expended for various restricted and unrestricted purposes at the direction of the Trustees.

Fixed Assets

Land, buildings and equipment purchased by the Laboratory are recorded at cost. Donated fixed assets are recorded at fair market value at the date of the gift. Depreciation is computed using the straight-line method, beginning the month after the asset is placed in service, over the asset's estimated useful life. Estimated useful lives are generally three to five years for equipment and 20 to 40 years for buildings and improvements. When assets are sold or retired, the cost and accumulated depreciation are removed from the accounts and any resulting gain or loss is included in income for the period.

Contracts and Grants

Revenues associated with contracts and grants are recognized in the statement of support, revenues, expenses and changes in fund balances as the related costs are incurred (see Note G). Reimbursement of indirect costs relating to government contracts and grants is based on negotiated indirect cost rates. Any over or underrecovery of indirect costs is recognized through future adjustments of indirect cost rates.

Investments

Investments purchased by the Laboratory are carried at market value. Money market securities are carried at cost plus accrued interest, which approximates market value. Donated investments are recorded at fair market value at the date of the gift. For determination of gain or loss upon disposal of investments, cost is determined based on the first-in, first-out method.

The Laboratory is the beneficiary of certain investments reported in the endowment funds which are held in trust by others. The Laboratory's continuing right to these funds is subject to review every 10 years by an independent committee. The committee met in 1994 and determined that MBL was still eligible to remain as beneficiary of the trusts for another 10 years. The market values of such investments are $4,595,615 and $4,873,242 at December 31, 1994 and 1993, respectively. The income on these investments totaled $193,359 and $226,702 in 1994 and 1993, respectively.

Investment Income and Distribution

The Laboratory follows the accrual basis of accounting except that investment income is recorded on a cash basis. The difference between such basis and the accrual basis does not have a material effect on the determination of investment income earned on a year-to-year basis.

Investment income includes income from a pooled investment account, which income is allocated to the participating funds on the market value unit basis (Note D).

Annuities Payable

Amounts due to donors in connection with gift annuities are determined based on remainder value calculations, as of December 31, 1994 with varied assumptions of rates of return and payout terms.

Tax-Exempt Status

The Laboratory is exempt from federal income tax under Section 501(c)3 of the Internal Revenue Code.

Professional Standards

For the fiscal year ending December 31, 1995, the Laboratory will adopt Statement of Financial Accounting Standards (SFAS) No. 116, Accounting for Contributions Received and Made, and SFAS No. 117, Financial Statements of Not-for-Profit Organizations, and will apply these standards on a retroactive basis. SFAS No. 117 establishes standards for external financial reporting by not-for-profit organizations and requires that resources be classified for accounting and reporting purposes into three net asset categories (unrestricted, temporarily restricted and permanently restricted) according to externally (donor) imposed restrictions. SFAS No. 116 requires that unconditional promises to give (pledges) be recorded as receivables and revenues and requires the organization to distinguish between contributions received for each net asset category in accordance with donor imposed restrictions. Outstanding pledges as of December 31, 1994 are disclosed in Note I.

C. *Investments:*

The following is a summary of the cost and market value of investments at December 31, 1994 and 1993:

	Market		*Cost*	
	1994	*1993*	*1994*	*1993*
Certificates of deposit	$ 50,173	$ 48,483	$ 50,173	$ 48,483
Money market securities	1,877,731	4,822,875	1,877,731	4,822,875
U.S. Government securities	1,057,616	—	1,047,615	—
Corporate fixed income	12,248,905	9,706,380	12,598,467	8,824,824
Common stocks	7,732,931	9,093,522	7,428,618	7,052,496
Real estate	13,247	13,247	13,247	13,247
Total investments	22,980,603	$23,684,507	$23,015,851	$20,761,925

Investments by fund group and related portfolios for the years ended December 31, 1994 and 1993 are as follows:

	Market		*Cost*	
	1994	*1993*	*1994*	*1993*
Current Funds				
Certificates of deposit	$ 50,173	$ 48,483	$ 50,173	$ 48,483
Money market securities	1,000,000	2,000,000	1,000,000	2,000,000
S.T.A.R. Fund	1,019,462	—	1,041,641	—
Instruction Fund	795,097	1,378,838	886,250	1,339,557
Total	2,864,732	3,427,321	2,978,064	3,388,040
Long-Term Funds				
Endowment and quasi-endowment				
General endowment trust fund	3,636,845	3,855,724	3,445,228	3,135,652
Library endowment trust fund	958,770	1,017,518	923,305	807,175
Ecosystem funds	4,388,463	4,829,277	4,363,838	4,029,966
Pooled funds	9,782,000	10,343,724	9,949,252	9,187,655
Other Funds:				
Annuity Fund	1,336,546	197,696	1,342,917	200,190
Real Estate	13,247	13,247	13,247	13,247
Total	20,115,871	20,257,186	20,037,787	17,373,885
Total investments	$22,980,603	$23,684,507	$23,015,851	$20,761,925

D. *Accounting for Pooled Investments*

Certain endowment fund assets are pooled for investment purposes. Investment income from the pooled investment account is allocated on the market value unit basis, and each endowment fund subscribes to or disposes of units on the basis of the market value per unit at the beginning of the calendar quarter within which the transaction takes place. The unit participation of the funds at December 31, 1994 and 1993 is as follows:

	1994	*1993*
Quasi-endowment unrestricted	4,342	4,342
Quasi-endowment restricted	8,773	8,771
Endowment, income for restricted purposes	65,524	62,158
Endowment, income for unrestricted purposes	229	152
Total	76,868	75,423

Pooled investment activity on a per-unit basis was as follows:

	1994	*1993*
Unit value at beginning of year	$137.18	$128.66
Unit value at end of year	127.43	137.18
Increase in realized and unrealized appreciation	(9.57)	8.52
Net income earned on pooled investments	5.53	4.52
Total return on pooled investments	$ (4.22)	$ 13.04

E. *Commitment and Contingencies:*

Capital Leases

As of December 31, 1994 the Laboratory had capital leases for office equipment. Interest rates on the obligation are between 1.55% and 6.63%. The future minimum lease payments as of December 31, 1994 are as follows:

1995	$28,014
1996	26,789
1997	14,458
1998	3,440
	$72,701

F. *Long-Term Debt:*

Long-term debt at December 31, 1994 amounted to $2,475,681. The aggregate amount of principal due for each of the next five fiscal years and thereafter is as follows:

1995	$ 79,010
1996	76,671
1997	80,000
1998	85,000
1999	90,000
Thereafter	2,065,000
	2,475,681
Less current portion	79,010
Total	$2,396,671

In 1992, the Laboratory issued $1,100,000 Massachusetts Industrial Finance Authority (MIFA) Series 1992A Bonds and $1,500,000 MIFA Series 1992B. These bonds pay varying annual interest rates ranging from 3.48% to 6.63%. Interest expense on this debt totaled $151,354 for the year ended December 31, 1994. The Series 1992 A and B Bonds mature on December 1, 2012 and are collateralized by a first mortgage on certain Laboratory property.

The agreements related to these Bonds subject the Laboratory to certain covenants and restrictions. Under the most restrictive covenant of this debt, the Laboratory's operating surplus (before transfers), interest, expense and transfers from the quasi-endowment for debt service must equal or exceed all debt service payments. The Laboratory was in compliance with these covenants and restrictions at December 31, 1994.

G. *Restricted Current Funds Deferred Support:*

The Laboratory defers revenue on current restricted funds until the related costs are incurred. Amounts received in excess of expenses are recorded as deferred support. The following summarizes the activity of the deferred support account:

	1994	*1993*
Balance at beginning of year	$3,796,864	$3,518,263
Additions:		
Gifts, endowment income and grants received	7,983,471	8,509,929
Net unrealized gains (losses)	(143,698)	(58,026)
Net realized gains	93,184	155,460
Transfers	59,862	21,223
Deductions:		
Funds expended under gifts and grants	8,798,213	8,349,985
Transfers	—	—
Balance at end of year	$2,991,470	$3,796,864

Deferred restricted gifts of $559,476 and $527,945 were expended in 1994 and 1993, respectively, for the support of indirect costs attributable to the Laboratory's instruction programs.

H. *Retirement Plan*

The Laboratory participates in the defined contribution pension plan of TIAA-CREF (the "Plan"). The Plan is available to permanent employees that have completed two years of service. Under the Plan, the Laboratory contributes 10% of total compensation for each participant. Contributions amounted to $525,918 in 1994 and $507,324 in 1993.

I. *Pledges:*

As of December 31, 1994, the Laboratory has outstanding pledges of $1,746,331 of which $1,713,731 is restricted (unaudited). These pledges are scheduled to be paid over the next three years in the amounts of $1,016,600, $434,731, and $295,000, respectively. As required by SFAS No. 116, pledges will be included in the financial statements for the year ended December 31, 1995 (Note B).

J. *Interfund Borrowings:*

Current unrestricted fund interfund borrowings at December 31 are as follows:

	1994	*1993*
Due from restricted education funds	—	$ 31,098
Due from (to) restricted endowment fund	$ 15,126	(6,445)
Due from restricted quasi-endowment funds	—	125,000
Total	$ 15,126	$ 149,653

K. *Postretirement Benefits.*

On November 20, 1993, the Laboratory adopted Statement No. 106, "Employers' Accounting for Postretirement Benefits Other Than Pensions," for the year beginning January 1, 1994. This new standard requires employers to accrue, during the years that the employee renders the necessary service, the expected cost of benefits to be provided during retirement.

The Laboratory's policy is that all current retirees and certain eligible employees who retire prior to June 1, 1994 will continue to receive postretirement health benefits. The remaining current employees will receive benefits; however, those benefits will be limited as defined by the Plan. Employees hired on or after January 1, 1995 will not be eligible to participate in the postretirement medical benefit plan.

Accumulated postretirement benefit obligations at the date of adoption:	
1993 accumulated postretirement benefit obligation	$1,736,447
Net postretirement benefits for 1994 include:	
Service cost (benefits earned during period)	$ 54,494
Interest cost (on projected benefit obligation)	135,459
Actual return on plan assets	(3,032)
Net amortization and deferral	86,918
Net postretirement benefits cost	$273,839

Below is a reconciliation of the funded status of the Plan at December 31, 1994:	
Accumulated benefit obligation	
Retirees and dependents	$1,195,739
Fully eligible active participants	242,279
Other active participants	401,951
Total	1,839,969
Market value of plan assets	190,601
Assets less than obligations	1,649,368
Unrecognized prior service cost (credit)	—
Unrecognized net (gain) loss	96
Unrecognized transition obligation	1,649,625
Prepaid postretirement benefit cost	$ 161

The health care cost trend rate assumptions used in determining the projected benefit obligation begins at 10.0% in 1994 and gradually decreases to 6% in the year 2004 and thereafter. The effect of raising the assumed health care cost trend rate by one percentage point in each year would be to increase the accumulated postretirement benefit obligation as of December 31, 1994 by $167,767 and to increase the aggregate of the service and interest cost components of net periodic postretirement benefit cost for the year then ended by $15,780. The discount rate used in determining the accumulated postretirement benefit obligation is 8.0%, and the expected return on plan assets was 8.0%. During 1994, the Laboratory contributed $274,000 to fund the Trust for these postretirement benefits.

MARINE BIOLOGICAL LABORATORY

STATEMENT OF SUPPORT, REVENUES, EXPENSES AND CHANGES IN FUND BALANCES

CURRENT FUNDS

for the year ended December 31, 1994

	Current Unrestricted Funds				
	Operating Fund	*Auxiliary Enterprises Fund*	*Total*	*Current Restricted Fund*	*Total*
SUPPORT AND REVENUE:					
Grant reimbursements of direct costs				$5,388,844	$5,388,844
Recovery of indirect costs	$3,700,412		$3,700,412		3,700,412
Tuition				577,365	577,365
Fees for services:					
Dormitories		$1,077,395	1,077,395		1,077,395
Dining hall		1,030,324	1,030,324		1,030,324
Library	486,287		486,287		486,287
Scientific journals	241,169		241,169	44,500	285,669
Research services	430,341		430,341	56,719	487,060
Marine resources	184,957		184,957		184,957
Investment income	453,507		453,507	496,870	950,377
Miscellaneous revenue	116,867		116,867	658,864	775,731
Gifts	581,554		581,554	1,328,616	1,910,170
Change in deferred support	559,476		559,476	237,087	796,563
Total support and revenues	6,754,570	2,107,719	8,862,289	8,788,865	17,651,154
EXPENSES:					
Research				5,900,614	5,900,614
Instruction				1,702,345	1,702,345
Scholarships, fellowships and stipends				465,824	465,824
Services:					
Dormitories		831,866	831,866		831,866
Dining hall		924,942	924,942		924,942
Library	837,480		837,480	120,711	958,191
Scientific journals	192,549		192,549	48,282	240,831
Research services	540,055		540,055	153,026	693,081
Marine resources	443,007		443,007	9,086	452,093
Administration:					
Administration	2,013,705	184,822	2,198,527		2,198,527
Sponsored projects administration	456,108		456,108		456,108
Plant operations	1,923,855		1,923,855	156,592	2,080,447
Other			—	241,733	241,733
Total expenses	6,406,759	1,941,630	8,348,389	8,798,213	17,146,602
Excess (deficit) of support and revenues over expenses before gain on investments	347,811	166,089	513,900	(9,348)	504,552
Net unrealized gain (loss) on investments			—	93,184	93,184
Net realized (loss) on investments			—	(143,698)	(143,698)
Net gain on investments			—	(50,514)	(50,514)
TRANSFERS AMONG FUNDS:					
Debt services	(29,010)	(40,000)	(69,010)		(69,010)
Acquisition of fixed assets	(102,895)	(2,089)	(104,984)		(104,984)
Repairs and replacement	(235,000)	(124,000)	(359,000)		(359,000)
Endowment transfer				150,000	150,000
Capitalization of income				(180,916)	(180,916)
Other	22,440		22,440	90,778	113,218
Total transfers among funds	(344,465)	(166,089)	(510,554)	59,862	(450,692)
Net change in fund balances	3,346	—	3,346	—	3,346
Fund balances, beginning of year	32,097		32,097		32,097
Fund balances, end of year	$ 35,443		$ 35,443		$ 35,443

SCHEDULE II

MARINE BIOLOGICAL LABORATORY

STATEMENT OF SUPPORT, REVENUES, EXPENSES AND CHANGES IN FUND BALANCES

ENDOWMENT FUNDS

for the year ended December 31, 1994

	Unrestricted	*Restricted*				
	Quasi-Endowment	*Income for Unrestricted Purposes*	*Income for Restricted Purposes*	*Quasi-Endowment*	*Total Restricted*	*Total*
SUPPORT AND REVENUES:						
Gifts		$ 10,000	$ 165,380	$ 250	$ 175,630	$ 175,630
Total support and revenues		10,000	165,380	250	175,630	175,630
Net realized gain on investments	$ 33,689	310,755	599,012	497,650	1,407,417	1,441,106
Net unrealized gain (loss) on investments	(76,004)	(531,119)	(1,270,791)	(929,847)	(2,731,757)	(2,807,761)
Net gain (loss) on investments	(42,315)	(220,364)	(671,779)	(432,197)	(1,324,340)	(1,366,655)
TRANSFERS AMONG FUNDS:						
Capitalization of income	0	0	0	180,916	180,916	180,916
Endowment transfers	0	0	0	(150,000)	(150,000)	(150,000)
Other transfers	0	0	13,623	0	13,623	13,623
Total transfers among funds	0	0	13,623	30,916	44,539	44,539
Net change in fund balances	(42,315)	(210,364)	(492,776)	(401,031)	(1,104,171)	(1,146,486)
Fund balances, beginning of year	595,694	3,876,604	9,547,900	5,907,490	19,331,994	19,927,688
Fund balances, end of year	$ 553,379	$ 3,666,240	$ 9,055,124	$ 5,506,459	$18,227,823	$18,781,202

SCHEDULE III

MARINE BIOLOGICAL LABORATORY

STATEMENT OF SUPPORT, REVENUES, EXPENSES AND CHANGES IN FUND BALANCES

PLANT FUNDS

for the year ended December 31, 1994

	Unrestricted				
	Unrestricted	*Repairs and Replacements Reserve*	*Total Unrestricted*	*Restricted*	*Total*
SUPPORT AND REVENUES:					
Grant for capital additions				$ 185,087	$ 185,087
Investment income				1,566	1,566
Gifts				58,000	58,000
Other revenue					
Total support and revenues				244,653	244,653
EXPENSES:					
Depreciation	$ 1,224,994		$ 1,224,994		1,224,994
Plant operations		$ 215,260	215,260		215,260
Total expenses	1,224,994	215,260	1,440,254	0	1,440,254
Excess (deficit) of support and revenues over expenses	(1,224,994)	(215,260)	(1,440,254)	244,653	(1,195,601)
TRANSFERS AMONG FUNDS:					
Debt service	69,010		69,010		69,010
Acquisition of fixed assets	104,984		104,984		104,984
Capital additions	634,303		634,303	(634,303)	—
Other transfers	0	333,000	333,000	(100,841)	232,159
Total transfers among funds	808,297	333,000	1,141,297	(735,144)	406,153
Net change in fund balances	(416,697)	117,740	(298,957)	(490,491)	(789,448)
Fund balances, beginning of year	19,869,320	546,838	20,416,158	539,878	20,956,036
Fund balances, end of year	$19,452,623	$ 664,578	$20,117,201	$ 49,387	$20,166,588

Report of the Librarian

During 1994 the MBL/WHOI Library implemented systems to protect our holdings. Recognizing the Library's need to provide information, service, and a comfortable and safe working environment for its users, the Trustees and the members of the Joint Library Committee agreed that it must adopt ways to protect both the collection and its users. Traditionally, the Library's doors have been open 24 hours a day, 365 days a year. Beginning in 1995, patrons will still be allowed that same access to the collection but by means of a card access security system during non-staffed hours. I am pleased to report that the system was successfully installed, tested and placed on-line on February 1, 1995. The new MBL/WHOI Library access card is available free of charge to all MBL corporation members and year-round staff. Others wishing to use the Library may purchase readerships which will assure them access to the collection after hours.

The Journal Collection

We were able to maintain our level of journal subscriptions in 1994. However, next year we will again need to reduce the number of journals to which we subscribe to allow us to purchase new journals that meet changing research needs. The cost of journals has skyrocketed in recent years. During the past eight years, journal subscription rates have increased 108%, while our serials budget has increased only 36% during that same time. The current forecast for journal subscription prices in FY96 is an overall increase of 13.1% based on a 33% North American 67% European title split. Because most of the MBL's journals come from European publishers, our increase will be even higher, meaning that it will not be financially possible to maintain our collection at the current level.

Overcrowded stacks are another area of concern. Six years ago, surveys showed that the Library would be filled to capacity in 1995. Although this will not occur, the Library is terribly overcrowded. In the coming year we will begin planning for off-site storage of a portion of the collection.

The combined forces of subscription costs, space needs, and a large increase in our student user population have led to the creation of a new service model for article delivery. Easy access article delivery services are now available from the Library's electronic menu, table of contents, and on-line document ordering and delivery. Interlibrary photo duplication via the Internet or Fax are also available.

During the past year the Library automated serial management and binding and negotiated a favorable agreement with a new subscription agency, the Readmore Company. Joe DeVeer, Serials Librarian,

Monograph and Serial Costs in ARL Libraries, 1986-1993

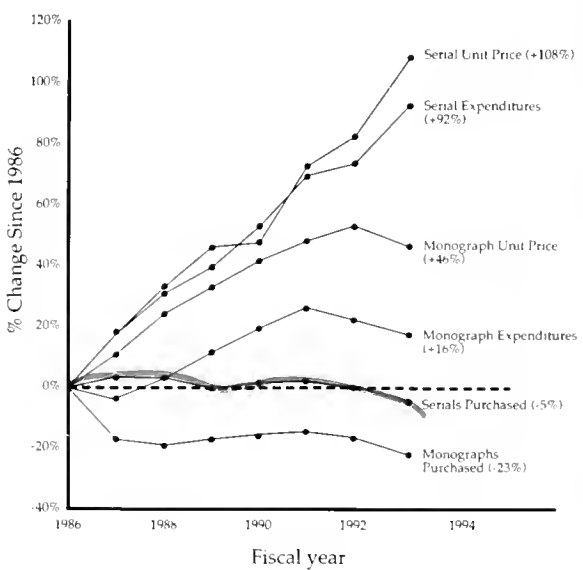

and Maggie Rioux, Systems Librarian, were instrumental in effecting a smooth transition.

A contract was signed with UnCover, a multi-disciplinary organization supplying journal articles and tables of contents. This service makes accessible 19,000+ journal titles on-line. The system is customized such that users can easily identify articles in journals owned by either MBL/WHOI Library or the Boston Library Consortium. An automatic table of contents service initiated with this same company provides up to 50 different table of contents on the day of publication from titles selected by the user. All of these transactions take place over the Internet minimizing delivery time and costs.

The Book Collection

Over the last year a new gift policy that was developed in collaboration with both WHOI and MBL development offices enabled us to acquire resources that added value to our collection and reduced costs and processing time. Detailed lists and bibliographies supplied by the donors enable Library staff to assess the collection before handling.

The donation of a major gift collection, the success of the Book Fair, and the guidance of the Library Coordinators for Book Acquisitions resulted in enhanced book acquisitions in subject areas, including molecular biology and environmental sciences, that required strengthening and additional support.

The Volunteers

Last year former WHOI Research Librarian Carol Winn, who retired in 1994, joined Dr. and Mrs. Robert Huettner as a volunteer in the Archives. A portion of the rare book collection is now available for local and national access due to the automation efforts of this trio. Programs for groups and visitors to the Archives were conducted, and more than 25 rare books—some dating back to the 1600s—were restored, rebound, and deacidified. The Huettners also began a program to raise funds for the restoration of rare books in memory of departed members of the MBL community. This year 20 books were rebound as part of this program. In the main collection, Arthur Voorhis continues to care for and mend the monographs.

In the Data Library at McLean, Mr. William Dunkle, who retired as Data Librarian/Archivist in 1994, provided assistance in the Data Library and Archives while focusing primarily on the Map/Chart and Photo collections. In particular, he has been largely responsible for WHOI's acquisition of the Bowdoin Collection of historical maps. These maps, circa 1840–1870, will be a valuable addition to the existing historical map and chart collection. Mr. Garfield Arthur continues his volunteer role in evaluating the dive videos including generating machine-searchable log shots which are widely referenced by members of the community.

The Archives, Preservation, and Rare Books Collection

Last March, at the request of the Joint MBL/WHOI Library Trustees Committee, Dr. Robert Stoddard (Houghton Library Harvard University) provided us with an assessment of the Archive and rare book collections. He wrote "This [collection] is a powerful arsenal for historical studies and programs that could not be duplicated anywhere." Mr. Stoddard's report was shared with the trustees of both institutions. The Committee agreed that his assessment "forces us to develop a plan to fulfill our shared accountability and responsibility for providing access to this national treasure and for its preservation and conservation." As a first step in developing such a plan the Librarian has engaged Ralph Titcomb, rare book appraiser, to assess the financial value of the rare book collection.

A new exhibit, *Women of Science at Woods Hole—The Middle Years*, was prepared and is now available on the MBL/WHOI Web server along with its predecessor, *Women of Science at Woods Hole—The Early Years*. The Leuckart Charts have all been scanned and loaded on the Library's Web Home Page and are proving to be a popular resource. The Library also supplied research papers and co-sponsored a talk at the Clark Laboratory last November by Dr. Gary Weir, Naval Historian, Navy Museum, "Finding a Niche, Columbus Iselin, and mobilizing Oceanography for War."

Cooperative Relationships

Two new reciprocal borrowing and photo duplication agreements with the Scripps Institution of Oceanography in California and the Institute of Ocean Science in the UK give us access to new journal resources oceans apart and bring the number of resource sharing agreements we have to 82 libraries. To assure the continued support of core journals in chemistry and neuroscience, the Library has entered into an agreement with members of the Boston Library Consortium to maintain selected titles. These cooperative arrangements will become increasingly important as the economic climate and copyright rules for scientific publications become progressively more restrictive.

The Library entered into a second agreement with the UnCover company to become a supplier of documents. Our unique captive collection of journals makes us a perfect candidate for this type of resource sharing. UnCover financed the establishment of Library office space and personnel to meet the demands of the service, and the Library receives compensation for each article shared from our collection.

The Electronic Library

The MBL/WHOI Library is on the Internet via its World Wide Web home page at **html://www.mbl.edu/html/LIBRARY/libweb.html** and through the Library gopher. New CD-ROMS on fish, water resources, Arctic literature, and marine research, and our UnCover Reveal Table of Contents service as well as automated article request and delivery at a reduced rate are available on the Library network.

The physical relocation of our local library utility and on-line catalog, CLAMS, from WHOI to Hyannis has resulted in a continuing disruption in access and a crisis in service for both patrons and staff. The Library is currently seeking a permanent, reliable long-term solution to our predicament.

WHOI Branch Libraries

The WHOI branch libraries underwent a re-engineering process by a team of scientists charged "to examine the current WHOI library services and to make recommendations for improvement in these services while maintaining or reducing overall costs." The time and effort expended by the team and Library staff were enormous and the results are currently under consideration by the WHOI Directorate. The Joint Library Committee, staff and department heads have all been invited to comment on the final report, and the results will be available in the spring of 1995. The Library has also changed its reporting schedule and now reports to the Associate Director for Education and Dean of Graduate Studies, John Farrington.

Library Instruction

New classes were developed to introduce the scientific community to the World Wide Web browsing tools. Classes were conducted on a weekly basis in the National Library of Medicine (NLM) computer Lab in Loeb, and Connecting Point (a local computer vendor) rented space for teaching basic courses on Windows, Word, Excel, and Lotus to the scientific community. The NLM's Medical Informatics course was held here again in 1994 and numerous sessions were conducted throughout the year. Four groups of Elderhostel classes were taught how to "surf" the Internet and search the National Library of Medicine's resources using Grateful Med. David Remsen and Cathy Norton again participated in the cooperative teaching effort with Northern Arizona University's Summer of Science Program, which brought 20 Native Americans and minority students and teachers to the MBL for a two-week experience using local marsh environmental models and the computer lab to enhance their science skills.

Library Trustees

The Joint MBL/WHOI Trustees' Library Planning Committee delivered a second report to the Trustees of the MBL in February and to WHOI in May on management's progress on their earlier recommendations and proposed inter-institutional development priorities to address goals that cannot be met without new funding. The Library Trustees' priorities for capital outlay include (1) the installation of a heating, ventilation, and air-conditioning system and improved lighting in the stacks, (2a) the purchase of computer equipment for the library network, (2b) rare book restoration, and (3) digitization of the video/film archives. The development of policies and procedures for a joint development effort of the two institutions was also highlighted in the report.

—Catherine Norton

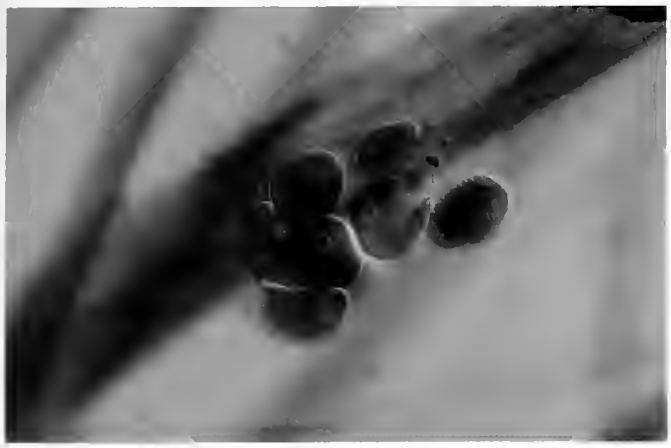

Educational Programs

Summer Courses

Biology of Parasitism (June 12–August 13)

Director
Steven Hajduk, University of Alabama, Birmingham

Course Faculty
John Boothroyd, Stanford University
Jean Feagin, Seattle Biomedical Research Institute
Fred Finkelman, Uniformed Services University of the Health Service
Patricia Johnson, University of California School of Medicine, Los Angeles
Keith Joiner, Yale University School of Medicine
Richard Komuniecki, University of Toledo
Richard Locksley, University of California, San Francisco
Steven Reiner, University of California, San Francisco
Buddy Ullman, Oregon Health Sciences University
Joseph F. Urban, United States Department of Agriculture

Teaching Assistants
Thomas Allen, Seattle Biomedical Research Institute
Con Beckers, Yale University School of Medicine
Peter Bradley, University of California, Los Angeles
Francisca Diaz, University of Toledo
Mark Drew, Seattle Biomedical Research Institute
Michele Klingbeil, University of Toledo
Allen J. LeBlanc, Jr., University of Alabama, Birmingham
Suzanne Morris, Uniformed Services University of the Health Sciences
Anthony Sinai, Yale University School of Medicine

Laboratory Assistants
Curtis Maier, University of Alabama, Birmingham
Victoria Pollard, University of Alabama, Birmingham

Students
Billy Apola, National Museums of Kenya, Kenya
Hani Atamna, Hebrew University, Israel
Leonard Basco, University of Paris, France
Barbara Davids, University of Wisconsin, Madison
Sócrates Herrera Valencia, Universidad del Valle, Colombia
Laura Knoll, Washington University
Susan Little, University of Georgia
Stephen Manale, Louisiana State University
Deborah Schechtman, Weizmann Institute of Science, Israel
Andrea Smith, University of Alabama, Birmingham
Martine Soete, INSERM, France
Andrea Torres-Perez, Stanford University
Henri van der Heyde, University of Wisconsin, Madison
Fred van Leeuwen, Netherlands Cancer Institute, The Netherlands
Ulrike Zelck, University of Hamburg, Germany
Xiaonong Zhou, Jiangsu Institute of Parasitic Diseases, China

Embryology (June 15–July 29)

Directors
Eric H. Davidson, California Institute of Technology
Michael Levine, University of California, San Diego
David McClay, Duke University

Course Faculty
Mariann Bienz, Medical Research Council, Cambridge
Marianne Bronner-Fraser, University of California, Irvine
R. Andrew Cameron, California Institute of Technology
Lois Edgar, University of Colorado
Scott E. Fraser, California Institute of Technology
Janet Heasman, University of Minnesota School of Medicine
Alexander D. Johnson, University of California, San Francisco
Andrew McMahon, Harvard University
Noriyuki Satoh, Kyoto University, Japan
Christopher C. Wylie, University of Minnesota School of Medicine

Teaching Assistants
Kristin B. Artinger, University of California, Irvine
Andres Collazo, California Institute of Technology
Susan Gray, University of California, San Diego
Carmen Kirchhamer, California Institute of Technology
Carole LaBonne, Harvard University
Catriona Logan, Duke University
Yusuke Marikawa, Kyoto University, Japan
Jorg Muller, Medical Research Council, Cambridge, UK
Jos Raats, The Wellcome/CRC Institute, UK
Kimberly Van Auken, University of Colorado
Robert Zeller, California Institute of Technology

Administrator
Jane Rigg, California Institute of Technology

Course Assistants
Courtney Horman, Wesleyan University
Aaron Sloboda, Skidmore College

Course Coordinator
Linda Huffer, Marine Biological Laboratory

Students
Catherine Brennan, University of Southern California
Melchiorre Cervello, Instituto di biologia dello Sviluppo, Italy
Anna Di Gregorio, Stazione Zoologica A. Dohrn, Italy
Shigeki Fujiwara, Kochi University, Japan
Martin Garcia-Castro, University of Cambridge, UK
Wendy Gerber, University of Texas, Austin
Xiaohua Gong, Scripps Research Institute
Maneesha Inamdar, Tata Institute of Fundamental Research, India
Boris Kablar, University of Pisa, Italy
Karla Knobel, University of Utah
Matthew Kourakis, University of Chicago
Julie Kuhlman, Cornell Medical College
Elizabeth Laxson, University of Wisconsin, Madison
Radma Mahmood, Guy's Hospital, London, UK
Daniel Martinez, University of California, Irvine
Michael McGrew, Boston University
Ivan Moskowitz, University of Wisconsin, Madison
Craig Nelson, Harvard University
Annette Neubüser, Max-Planck-Institute of Immunobiology, Germany
Sandra Nicola, Carol Davila University of Medicine, Romania
Lennart Olsson, Uppsala University, Sweden
Kevin Peterson, University of California, Los Angeles
Stephan Schneider, Max-Planck-Institute for Developmental Biology, Germany
Eliza Shah, Harvard University
Melissa Shirley, Case Western Reserve University

Microbial Diversity (June 12–July 28)

Directors
John Breznak, Michigan State University
Martin Dworkin, University of Minnesota

Faculty
Yehuda Cohen, Hebrew University, Israel
Jorg Overmann, Universität Oldenburg, Germany

Teaching Assistants
Joseph P. Calabrese, West Virginia University
Susan Childers, University of Connecticut
John D'Elia, University of Illinois
Magdalena Martinez-Canamero, University of Southern California
Michael Renner, Michigan State University

Course Coordinator
Richard M. Behmlander, Michigan State University

Laboratory Assistant
Jessica L. Breznak

Students
Frédéric Ampe, INSA, France
Michael Cerio, University of Connecticut
Mark DeSouza, University of South Carolina
Ilka Faath, University of Bonn, Germany
Daniel Ferber, University of Illinois
Georg Jander, Harvard Medical School
Kathleen Londry, University of Oklahoma
Sarah McHatton, University of California, Davis
Ute Müh, Philipps Universität Marburg
Julie Olson, University of North Carolina, Chapel Hill
Mary Rothermich, University of Massachusetts
James Scott, Center for Great Lakes Studies
Antonius Suwanto, Bogor Agricultural University, Indonesia
Debra Tumbula, University of Georgia
Marc van der Maarel, University of Groningen, Germany
Paula van Schie, Rutgers University
Madeline Vargas, University of Connecticut
Shiri Venezia, Tel Aviv University, Israel
David Westenberg, Dartmouth College
Dinesh Yernool, Rutgers University

Neural Systems & Behavior (June 12–August 5)

Directors
Ronald L. Calabrese, Emory University
Martha Constantine-Paton, Yale University

Faculty
Larry Abott, Brandeis University
Alexander Borst, Max-Planck-Institüt für Biologische, Germany
Thomas Carew, Yale University
Holly Cline, Cold Spring Harbor Laboratory
Elizabeth Debski, University of Kentucky
Patsy Dickinson, Bowdoin College
Robert Douglas, University of British Columbia, Canada
Douglas L. Falls, Harvard Medical School
Cole Gilbert, Cornell University
Richard Levine, University of Arizona
Christine Li, Boston University
Robert Malinow, Cold Spring Harbor Laboratory
Pierre Meyrand, University of Bordeaux, France
Michael Nusbaum, University of Alabama, Birmingham
Bruce O'Gara, Barnard College
Martin Shankland, Harvard Medical School
Darrell R. Stokes, Emory University
Janis Weeks, University of Oregon
Angela Wenning, Universität Konstanz, Germany

Scholars-in-Residence
Ron Hoy, Cornell University
Darcy Kelley, Columbia University
Eduardo Macagno, Columbia University

Teaching Assistants
Syd Cash, Columbia University
Melissa Coleman, University of Alabama, Birmingham
Jennifer Cummings, University of California, San Francisco
John F. Dalton, Emory University
Yang Dan, Columbia University
Juergen Haag, Max-Planck-Institüt für Biologische Kybernetik, Germany

Neal A. Hessler, Cold Spring Harbor Laboratory
Zachary Mainen, University of California, San Diego
Farzan Nadim, Emory University
Laurie Nelson, Boston University
Andrea Novicki, University of Oregon
Oystein Olsen, Emory University
Glen Prusky, University of Lethbridge, Canada
James Weimann, Stanford University
Anne West, Harvard Medical School
Sonia Witte, Cold Spring Harbor Laboratory

Students
John Allison, Vanderbilt Medical School
Curtis Anderson, Northern Arizona University
Michael Berry, Harvard University
James Contos, University of California, San Diego
Amanda Edmiston, University of Colorado
Ruth Empson, University of Koln, Germany
Sarah Farris, University of Illinois, Urbana-Champaign
Lynn Hodges, University of California, Los Angeles
Patricio Huerta, Brandeis University
Douglas Ikelheimer, Columbia University
Patricia Janak, University of California, Berkeley
Ole Kjaerulff, Copenhagen University, Denmark
Dawn Konrad, University of Washington
Mildred Morales, Albert Einstein College of Medicine
Sowmyalakshmi Rasika, Rockefeller University
Kimberly Scearce, Columbia University
Stefan Schuster, Max-Planck-Institüt für Biologische Kybernetik, Germany
Karel Svoboda, Harvard University
James Williams, University of California, San Diego
Bettina Winckler, Columbia University

Neurobiology (June 12–August 13)

Directors
Leonard Kaczmarek, Yale University School of Medicine
Irwin Levitan, Brandeis University

Course Faculty
Hannelore Asmussen, University of Virginia Medical School
Gary Banker, University of Virginia Medical School
Judith Drazba, National Institutes of Health
Keith Elmslie, Tulane University Medical Center
Richard Horn, Jefferson Medical College
Stephen Jones, Case Western Reserve University
Bechara Kachar, National Institutes of Health
Julie Kauer, Duke University School of Medicine
Richard Kramer, University of Miami
Diane Lipscombe, Brown University
John Marshall, Yale University School of Medicine
Carol Ann Mason, Columbia University College of Physicians & Surgeons
Andrew I. Matus, Friedrich Miescher Institute, Germany
Sally Moody, The George Washington University
Angus Nairn, Rockefeller University
Marina Picciotto, The Pasteur Institute, France
Thomas Reese, National Institutes of Health
Peter Reinhart, Duke University Medical Center
Talvinder Sihra, Royal Free Hospital School of Medicine, UK
Carolyn Smith, National Institutes of Health
Leslie Vosshall, Columbia University

Course Assistant
Ethan Treistman, University of North Carolina, Chapel Hill

Students
Max Boakye, National Institutes of Health
Michale Fee, AT&T Bell Laboratories
Jonathan Gale, Bristol University, UK
Paul Huynh, Albert Einstein College of Medicine
Peter Kloppenburg, ARLDN, Tucson
Carol Koenigsberger, Mayo Graduate School
Zhixin Lin, Brown University
David Molea, University of Washington
Kazunori Nakajima, RIKEN, Japan
Teresa Nick, Yale University
Christophe Pouzat, Laboratoire de Neurobiologie, ENS, France
Claudia Wiedemann, Friedrich-Miescher Institüt, Germany

Physiology (June 12–July 23)

Director
Mark S. Mooseker, Yale University
Karen Yeow, University of Manitoba, Canada

Course Faculty
Steven Block, Princeton University
William Busa, Johns Hopkins University
Richard Cheney, Yale University
Laura Davis, Duke University Medical Center
Stuart Feinstein, University of California, Santa Barbara
Kathleen Foltz, University of California, Santa Barbara
Mary Lou Guerinot, Dartmouth College
Leah Haimo, University of California, Riverside
C. Robertson McClung, Dartmouth College
Michael Mendelsohn, New England Medical Center
Robert E. Palazzo, University of Kansas
Roger D. Sloboda, Dartmouth College
Margaret A. Titus, Duke University Medical Center
Joseph S. Wolenski, Yale University

Teaching Assistants
Ken Belanger, Duke University
Mary Lynn Benka, Oregon State University
Linda Ferrans, Johns Hopkins University
Margaret Kenna, Duke University
Koen Visscher, Princeton University

Course Assistants
Caroline Day, Yale University
Raymond Murray, County College of Morris

Students
ShaAvhree Buckman, Washington University School Medicine
Smaranda Burlacu, Howard Hughes Medical Institute
Laura Cole, Ohio University
Ana DePina, Dartmouth College
Prabha Dias, Scripps Research Institute
Suzanne Gaudet, Harvard University
Aaron Granger, Yale School of Medicine
Robert Grant, University of California, San Francisco
Amanda Hayward-Lester, Texas Tech University
Sher Karki, University of Pennsylvania

Matthew Lee, University of Southern California
Christi Magrath, Tulane University Medical Center
Suzanne (Stovall) Mann, Bowman Gray School of Medicine
Oana Marcu, University of Western Ontario
Sandra Marques, George Washington University
André Nussenzweig, Memorial Sloan-Kettering Cancer Center
Adam Pack, SUNY Health Science Center, Syracuse
Peter Piepenhagen, Stanford University
Manisha Raje, University of Kansas
Samara Reck-Peterson, University of Pennsylvania
Wendy Reed, Johns Hopkins University
Frederick Reitz, University of Washington
Fabrice Roegiers, Station Zoologique, France
Sheree Rybak, Carnegie Mellon University
Adrian Salic, Harvard University
Eric Scarfone, University of Montpellier
Galen Schneider, University of North Carolina
Erik Schultes, University of California, Los Angeles
Jennifer Smith-Hall, Indiana University School of Medicine
Viktor Stolc, Yale University
Luis Vidali, University of Massachusetts, Amherst
James Walker, University of Cambridge, UK
Jennifer Waters, University of North Carolina
Naoyuki Yamamoto, Nippon Medical School, Japan
Judith Yanowitz, Princeton University
Karen Yeow, University of Manitoba, Canada

Short Courses

Analytical & Quantitative Light Microscopy (May 12–20)

Directors

Greenfield Sluder, Worcester Foundation for Experimental Biology
David Wolf, Worcester Foundation for Experimental Biology

Course Faculty and Lecturers

William B. Amos, Medical Research Council, UK
Richard Cardullo, University of California, Riverside
Frederick Fay, University of Massachusetts Medical School
Shinya Inoué, Marine Biological Laboratory
Edward Salmon, University of North Carolina, Chapel Hill
Randi Silver, Cornell University Medical College
Kenneth Spring, National Institutes of Health
D. Lansing Taylor, Carnegie Mellon University

Teaching Assistants

Christine McKinnon, Worcester Foundation for Experimental Biology
Frederick Miller, Worcester Foundation for Experimental Biology
Elizabeth Thompson, Worcester Foundation for Experimental Biology

Students

Eiki Adachi, Medical Research Council, UK
Paul Bianco, University of California, Riverside
Daniel Cordova, Marine Biological Laboratory
Robert Davis, Worcester Foundation for Experimental Biology
Ed Devlin, Hampden-Sydney College
Joseph Di Salvo, University of North Carolina, Chapel Hill
Seth Fraden, Cornell University Medical College
Yue Hu, Worcester Foundation for Experimental Biology
Marty Jacobson, National Institutes of Health
Maria Jure-Kunkel, Worcester Foundation for Experimental Biology
Linda McMeekin, Worcester Foundation for Experimental Biology
Robert Monette, UMass Medical School
Adam Myerov, Carnegie Mellon University
Thomas Pitta, Rowland Institute for Science
Karl Richter, Marine Biological Laboratory
Angeliki Rigos, Marine Biological Laboratory
Lauren Robertson, Marine Biological Laboratory
Laura Romberg, University of California, San Francisco
Clifford Slayman, Yale School of Medicine
Robert Specian, Louisiana State University Medical Center
Sandra Spence, Noran Instruments
Jennifer Waters, University of North Carolina
Simon Watkins, University of Pittsburgh
James Wilhelm, University of California, San Francisco
Ping Xia, National Institutes of Health
Yang Zeng, Worcester Foundation for Experimental Biology

Fundamental Issues in Vision Research (August 14–27)

Director

David S. Papermaster, University of Texas Health Science Center, San Antonio

Course Faculty

Bob Barlow, Syracuse University
Robert Baughman, Harvard Medical School
David Beebe, Uniformed Services University of the Health Sciences
George Benedek, Massachusetts Institute of Technology
Eliot Berson, Massachusetts Eye and Ear Infirmary
Richard Brubaker, Mayo Clinic
Connie Cepko, Harvard Medical School
John Dowling, Harvard University
Judah Folkman, Harvard Medical School
Daniel Goodenough, Harvard Medical School
Robert Grainger, University of Virginia
Paul Hargrave, University of Florida
John Hassel, Eye & Ear Institute of Pittsburgh
Fielding Hejtmancik, National Eye Institute, NIH
Jonathan Horton, University of California
Joseph Horwitz, Jules Stein Eye Institute
Douglas Johnson, Mayo Clinic
Ehud Kaplan, Rockefeller University
Carl Kupfer, National Eye Institute, NIH
Wen-Hwa Lee, University of Texas Health Science Center
Robert Malchow, University of Illinois
Richard Masland, Harvard Medical School
Anthony Movshon, New York University
Jeremy Nathans, Johns Hopkins University School of Medicine
James Nathanson, Massachusetts General Hospital
Eric Newman, University of Minnesota
Krzysztof Palczewski, University of Washington
Joram Piatigorsky, National Eye Institute, NIH
Haohua Qian, Harvard University
Robert Rando, Harvard Medical School
Elio Raviola, Harvard Medical School
Julia Richards, University of Michigan
Barry Rouse, University of Tennessee

Dwight Stambolian, University of Pennsylvania
Henry Sun, New York University Medical Center
Charles Zucker, University of California, San Diego

Lab Coordinator
Nancy Ransom, University of Texas Health Science Center, San Antonio

Course Administrator
Carol Masch, University of Texas Health Science Center, San Antonio

Course Assistant
Zera Herskovits, Yale University

Students
Kent Anderson, Baylor College of Medicine
Brian Brooks, University of Pennsylvania
Jinghua Tsai Chang, Johns Hopkins University
Victoria Connaughton, University of Texas, Houston
Dorette Ellis-Ibidapo, University of South Florida
Anna Francesconi, Dyson Vision Research Institute
Lin Gan, MD Anderson Cancer Center
Kim Gottshall, University of California, San Diego
Abigail Jensen, University College London, UK
Simon John, University of North Carolina
Brian Link, Oregon Health Sciences University
Andrew Magnet, University of California, San Diego
James Marrs, Stanford University
Judith Mays, MGH/Harvard Medical School
Scott McPherson, University of Minnesota
Linda Musil, Harvard Medical School
Sandra Ryeom, Cornell University Medical College
Katherine Strissel, Massachusetts General Hospital
Daniel Sullivan, National Eye Institute, NIH
John Torseth, University of Minnesota
Robert Wordinger, University of North Texas

Medical Informatics (May 31–June 7)

Director
Homer Warner, University of Utah School of Medicine

Course Faculty
Paul Clayton, Columbia Presbyterian Medical Center
Peter Haug, University of Utah School of Medicine
Donald D.A.B. Lindberg, National Library of Medicine
David Lipman, National Library of Medicine
Daniel Masys, Listerhill Center for Biomedical Communications
Carol Newton, University of California School of Medicine, Los Angeles
Catherine Norton, Marine Biological Laboratory
David Remsen, Marine Biological Laboratory
Rick Rodgers, National Library of Medicine
Robert Sideli, Columbia Presbyterian Medical Center

Lab Coordinator
Sylvia Jessen, University of Utah School of Medicine

Students
Elizabeth Alger, UMDNJ-New Jersey Medical School
Jeroan Allison, University of Alabama, Birmingham
Michael Altman, Northwestern University Medical School
Ralph Arcari, University of Connecticut
Donald Boudreau, Louisiana State University
Lavonda Broadnax, DC General Hospital
Holly Buchanan, Medical College of Georgia
William Casey, Nassau County Medical Center
Christine Chastain-Warheit, Medical Center of Delaware
William Cordell, Methodist Hospital
Stanley Freedman, Scripps Clinic
Sarah Garrison, Lincoln Hospital, Bronx, NY
Stephen Grund, Massachusetts General Hospital
Beverly Hill, Indiana University
Frank Keary, U.S. Department of State
Emmet Kenney, Yale Primary Care Research Program
Michele Klein, Children's Hospital of Michigan
Anthony Kwak, University of California, Los Angeles
James Legler, University Texas Health Science Center
Maria Lenaz, St. Margaret's Center for Women/Infants
Elizabeth Like, Countway Library/Harvard Medical School
Catherine MacLeod, Rush Medical College
Ellen Marks, Wayne State University
Paul McKinney, Dallas VAMC
Leon Moore, University of Maryland, Baltimore
Kathleen Oliver, NIH Library
Miranda Pao, University of Michigan
Gail Persily, University of California, San Francisco
Valerie Summers, University of Kentucky
Kenneth Williams, University of Massachusetts

Methods in Computational Neuroscience (July 31–August 27)

Directors
David Kleinfeld, AT&T Bell Laboratories
David W. Tank, AT&T Bell Laboratories

Course Faculty
Lawrence Abbott, Brandeis University
Joseph Atick, Rockefeller University
Mark Bear, Brown University
William Bialek, NEC Research Institute,
Ronald Calabrese, Emory University
Carmen Canavier, Baylor College of Medicine
Kerry Delaney, Simon Fraser University
Rodney Douglas, MRC, UK
Bard Ermentrout, University of Pittsburgh
Apostolos Georgopoulos, Veterans Administration Medical Center
Charles Gray, University of California, Davis
John Hopfield, California Institute of Technology
Christof Koch, California Institute of Technology
Nancy Kopell, Boston University
Stephen Kosslyn, Harvard University
Terry Kovacs, AT&T Bell Laboratories
John Lisman, Brandeis University
Rodolfo Llinás, New York University Medical Center
Kevin Martin, University of North Carolina
John Maunsell, Baylor College of Medicine
David McCormick, Yale University School of Medicine
Alan Peters, Boston University School of Medicine
John Rinzel, National Institutes of Health
Terrance Sejnowski, Salk Institute
H. Sebastian Seung, AT&T Bell Laboratories

Shihab Shamma, University of Maryland
Arthur Sherman, National Institutes of Health
Boris Shraiman, AT&T Bell Laboratories
Karen Sigvardt, University of California, Davis
Frederick Sigworth, Yale School of Medicine
Haim Sompolinsky, Hebrew University, Israel
Ben Stowbridge, AT&T Bell Laboratories
Roger Traub, IBM Corporation
Michael Vanier, California Institute of Technology
John White, University of Iowa
Matthew Wilson, University of Arizona

Lab Instructors
Michael Hines, Duke University Medical Center
Roderick Jensen, Wesleyan University

Course Assistant
Joy Langford

Students
John Anderson, University of Cambridge
Joshua Berke, Harvard University
Dana Cohen, Hebrew University, Jerusalem
Gennady Cymbalyuk, Institute of Mathematical Problems of Biology, Russia
Akira Date, Tokyo University of Agriculture & Technology
Christopher deCharms, University of California, San Francisco
Opher Donchin, Hebrew University, Israel
Stacia Friedman-Hill, University of California, Davis
Christopher Hickie, Yale University School of Medicine
John Kebabian, Research Biochemicals International
InSong Koh, Boston University
Jürgen Kupper, Ecole Normale Superieure, France
Peter Latham, University of Maryland
Heather Lennox, Carleton University, Canada
Anita Luethi, Brain Research Institute, University of Zürich,
Nicholas Poolos, Harvard Medical School
Ramnarayan Ramachandran, Johns Hopkins University
Lawrence Saul, Massachusetts Institute of Technology
Eric Schwartz, University of Chicago
Akaysha Tang, Harvard University
Toby Velte, University of Minnesota
Jun Zhu, University of Wisconsin Medical School

Microinjection Techniques (May 24–31)

Director
Robert B. Silver, Cornell University

Course Faculty
Suzanne Chandler, Cornell University
Karen Kindle, Cornell University
Douglas Kline, Kent State University
Paul McNeil, The Medical College of Georgia
Jeb Oblek, Cornell University
Eric Shelden, University of Connecticut

Course Assistants
Gwendolyn Jeun, Cornell University
Lisa Mehlmann, Kent State University

Students
Sandra Baksi, Environmental Protection Agency
Peter Bannerman, Children's Hospital of Philadelphia
David Cole, Utah State University
Robert Donahue, National Institutes of Health
Carol Gregorio, Scripps Research Institute
David Hessinger, Loma Linda University School of Medicine
David Leaf, Western Washington University
Terry McCann, Babraham Institute
Lesley Mills, University of Rhode Island
Alexander Minin, Protein Research Institute, Russia
Stephen Pasquale, Washington University
Ulrich Schaible, Washington University
William Schuyler, Atlanta Veterans Affairs Medical Center
Ching-hwa Sung, Johns Hopkins University School of Medicine

Rapid Measurement of Neurotransmitter Signals in the Central Nervous System (Session I: August 19–22; Session II: August 24–28)

Director
Greg Gerhardt, University of Colorado Health Science Center

Course Faculty
Kate Bowenkamp, University of Colorado Health Sciences Center
Michael Doherty, Douglas Hospital Research Center
Marilyn Friedemann, University of Colorado Health Sciences Center
Don Gash, Lexington, KY
Alain Gratton, Douglas Hospital Research Center
Harold Haut, Medical Systems Corporation
Alex Hoffman, University of Colorado Health Sciences Center
Michael Palmer, University of Colorado Health Sciences Center
Michael Parrish, University of Colorado Health Sciences Center
William Proctor, University of Colorado Health Sciences Center
Scott Robinson, University of Colorado Health Sciences Center
Steve Robinson, University of Colorado Health Sciences Center
Craig Van Horn, Brigham & Women's Hospital

Course Coordinator
Laura Lee Lamothe, University of Colorado Health Sciences Center

Students, Session I
Rodrigo Andrade, St. Louis University School of Medicine
Karen Bach, University of Wisconsin, Madison
Tilmann Brotz, Friedrich-Miescher-Laboratory, Germany
Dipanjan Chakravarty, Southern Illinois University School of Medicine
Deborah Cory-Slechta, University of Rochester
Subimal Datta, Harvard Medical School
Lyn Daws, University of Texas Health Science Center
Bromfield Hine, University of Puerto Rico
Susan Hochstenbach, University of Western Ontario, Canada
Rodrigo Iturriaga, Catholic University of Chile, Chile
Sathasiva Kandasamy, Armed Forces Radiobiology Research Institute
Prakash Kara, University of Alabama, Birmingham
Sergei Kirov, National Institutes of Health Gerontology Research Center
Gordon Mitchell, University of Wisconsin
David Mogul, Northwestern University

Shoji Nagatani, Nagoya University, Japan
Vladimir Parpura, Iowa State University
Patricia Rosas-Arellano, University of Western Ontario, Canada
Philip Shea, Geo Centers
Dennison Smith, Oberlin College
Philip Starr, Children's Hospital, Boston
Vishnu Suppiramaniam, Tuskegee University
Lidia Szczupak, University of California, San Diego
Fletcher Wason, Cambridge Neuroscience, Inc.
Christina Zuch, University of Rochester

Students, Session II
Sonia Connaughton, Cambridge Neuroscience
Carlos Cream, Dartmouth Medical School
Adrian Dunn, Louisiana State University Medical Center, Shreveport
Daniel Feller, VA Medical Center, Portland
Dwayne Godwin, State University of New York, Stony Brook
Laszlo Harsing, Institute for Drug Research, Budapest, Hungary
Bettye Hollins, Medical College of Georgia
Michael Kramer, Pennsylvania Hospital
Lauren Liets, University of California, Davis
Anthony Lombardino, Rockefeller University
Janea Mack, Meharry Medical College
Yong-Gou Park, Yonsei University College of Medicine, Seoul, Korea
David Smith, University of Pennsylvania
Andrew Spielman, New York University
Robert Stingele, Johns Hopkins University
Anthony Stretton, University of Wisconsin, Madison
Artur Swiergiel, LSU Medical Center
Chuanyao Tong, Bowman Gray School of Medicine
Timothy Turner, Tufts University
Kaido Viik, Burroughs Wellcome
Carol Watkins, Massachusetts Institute of Technology
Yuri Zagvazdin, University of Tennessee

Optical Microscopy and Imaging in the Biomedical Sciences (October 15–22)

Director
Colin S. Izzard, State University of New York, Albany

Course Faculty and Lecturers
Steven M. Block, Rowland Institute for Science
Gary R. Bright, Case Western Reserve University
Fredric S. Fay, University of Massachusetts Medical School
Robert Hard, State University of New York, Buffalo
Shinya Inoué, Marine Biological Laboratory
Ernst Keller, Carl Zeiss, Inc.
Greta M. Lee, University of North Carolina
John M. Murray, University of Pennsylvania
Kenneth R. Spring, National Institutes of Health, NHLBI

Teaching Assistants
Joseph A. DePasquale, New York State Department of Health
Loretta M. Memmo, State University of New York, Albany
Gerald Rupp, State University of New York, Buffalo

Students
Reiko Arimoto, Nikon Corporation
Gary Bassell, Harvard Medical School
Hilary Beggs, University of North Carolina, Chapel Hill
Judith Berman, University of Minnesota
Solange Brown, Harvard Medical School
Kirk Czymmek, DuPont Company
Fiona Doetsch, Rockefeller University
Daniel Erb, Miami Project, University of Miami
Michael Esterman, Lilly Research Labs
James Gordon, Poloroid Corporation
Joseph Italiano, Florida State University
Marie-Helene Jouvin, National Institutes of Health
Li Ma, Columbia University
Fraser McDonald, University of London, UK
Gero Miesenboeck, Sloan-Kettering Institute
Luiz Monteiro-Leal, Federal University of Rio de Janeiro
Andrew Nechkin, The Johns Hopkins University
Robert Scott, Georgia Institute of Technology
Daniella Steel, McGill University, Canada
Edith Suss-Toby, National Institutes of Health
Keisuke Suzuki, Olympus Optical Co., Ltd.
Douglas Taatjes, University of Vermont
Tomomi Tani, University of Tokyo, Japan
Barry Ticho, Children's Hospital, Boston

Workshop on Molecular Evolution (August 7–19)

Director
Mitchell L. Sogin, Marine Biological Laboratory

Course Faculty
Dan Davison, University of Houston
Joseph Felsenstein, University of Washington
Walter Fitch, University of California, Irvine
George Fox, University of Houston
Robin Guttell, University of Colorado
David Hillis, University of Texas
Rick Hudson, University of California, Irvine
Laura Landweber, Harvard University
David Maddison, University of Arizona
Roger Milkman, University of Iowa
Catherine Norton, Marine Biological Laboratory
Stephen O'Brien, National Cancer Institute
Gary Olsen, University of Illinois
Norman Pace, Indiana University
Margaret Riley, Yale University
Monica Riley, Marine Biological Laboratory
Terry Speed, University of California, Berkeley
David Swofford, Smithsonian Institution
Peter Waddell, Massey University
Bruce Walsh, University of Arizona

Teaching Assistant
Saira Mian, University of California, Santa Cruz

Course Consultant
Brendan Reilly, Software Editing Corporation

Students
Joe Bernardo, University of Texas, Austin
Robert Browne, Wake Forest University

John Burke, University of Houston
Dana Campbell, Harvard University
Carol Casavant, University of Idaho
Joby Chesnick, Lafayette College
Mary Crabtree, Centers for Disease Control, Colorado
Richard Davis, San Francisco State University
Alison Davis, University of Southern California
Art Edison, University of Wisconsin, Madison
Jonathan Eisen, Stanford University
Anjay Elzanowski, National Center for Biotechnology Information
Melinda Fagan, Stanford University
Marcia Fisher, Cornell University
Paul Flook, Basel University, Switzerland
James Fogleman, University of Denver
Silvana Gaudieri, University of Western Australia, Australia
Angela Gawthrop, University of Glasgow, UK
Yvonne Gräser, Institute of Microbiology, Berlin, Germany
Bill Hahn, Smithsonian Institution
Aaron Halpern, Los Alamos National Laboratory
Healy Hamilton, University of California, Berkeley
Phillip Harris, Oregon State University
Daniel Haydon, University of Oxford, UK
Catherine Jones, Oxford University, UK
Brian Kinkle, University of Cincinnati
Anne-Mette Krabbe-Pedersen, University of Aarhus, Germany
Armand Leroi, Albert Einstein College of Medicine
Marc Lipsitch, University of Oxford, UK
Stephen Lougheed, Queen's University, Canada
Russell Malmberg, University of Georgia
Magdalena Martinez-Canamero, University of Granada, Spain
Lynn Messinger, University of Wisconsin
Weiland Meyer, Duke University Medical Center
Andrew Mitchell, University of Maryland
Jon Norenburg, Smithsonian Institution
Jane Norman, University of Illinois, Chicago
Diana Northup, University of New Mexico
Fred Opperdoes, ICP-Brussels, Belgium
Tom Quinn, University of Denver
Allen Rogerson, St. Lawrence University
Shane Sarver, University of Miami/RSMAS
Christian Schlötterer, Zoologisches Institut, Germany
Karl Schmid, University of Munich, Germany
Barathi Sethuraman, University of California, Berkeley
Andrew Shedlock, University of Washington
Gerald Shields, University of Alaska, Fairbanks
Janet Siefert, University of Houston
Joana Silva, University of Arizona
Pedro Silva, University of Lisbon, Uppsala, Sweden
Felipe Soto-Adames, University of Illinois, Urbana-Champaign
Birgit Staehe, University of California, Santa Cruz
Eleanor Steinberg, University of Washington
Randall Terry, University of Wyoming
Miranda von Dornum, Harvard University
Mary White, Southeastern Louisiana University
Birgitta Winnepenninckx, University of Antwerp, Belgium
Grace Wyngaard, James Madison University
Anne Yoder, Harvard University
Sarah Zehr, Harvard University
Giuseppe Zuccarello, University of California, Santa Cruz

Summer Research

Principal Investigators

Alkon, Daniel L., National Institutes of Health
Allen, Nina S., Wake Forest University
Armstrong, Clay, University of Pennsylvania
Armstrong, Peter B., University of California, Davis
Augustine, George J., Duke University Medical Center

Barlow, Jr., Robert B., Syracuse University Institute for Sensory Research
Bearer, Elaine, Brown University
Beauge, Luis, Instituto M. y M. Ferreyra, Argentina
Bennett, Michael V. L., Albert Einstein College of Medicine
Berberian, Graciela Elso de, Instituto M. y M. Ferreyra, Argentina
Berlin, Joshua, Graduate Hospital
Bloom, George S., The University of Texas Southwestern Medical Center, Dallas
Bodznick, David, Wesleyan University
Borgese, Thomas A., Lehman College, CUNY
Boron, Walter F., Yale University Medical School
Brady, Scott T., The University of Texas Southwestern Medical Center, Dallas
Burdick, Carolyn J., Brooklyn College, CUNY
Burger, Max M., Friedrich Miescher Institut, Switzerland

Cardell, Robert R., University of Cincinnati
Chaet, A. B., University of West Florida
Chang, Donald C., Hong Kong University of Science & Technology, Hong Kong
Chappel, Richard L., Hunter College, CUNY
Charlton, Milton, University of Toronto, Canada
Clay, John, National Institutes of Health
Cohen, Lawrence B., Yale University School of Medicine
Cohen, William D., Hunter College, CUNY
Crutcher, Keith A., University of Cincinnati

D'Avanzo, Charlene, Hampshire College
Dan, Yang, Columbia University
Davis, Graeme W., University of Massachusetts
De Weer, Paul, University of Pennsylvania School of Medicine
Di Polo, Reinaldo, IVIC, Venezuela

Ehrlich, Barbara, University of Connecticut

Fay, Richard, Parmly Hearing Institute
Feng, Guoping, State University of New York, Buffalo
Finch, Elizabeth Ann, Duke University Medical Center
Fishman, Harvey M., The University of Texas Medical Branch, Galveston

Gadsby, David, The Rockefeller University
Gainer, Harold, National Institutes of Health
Garcia-Blanco, Mariano A., Duke University Medical Center
Garrick, Rita Anne, Fordham University College, Lincoln Center
Giuditta, Antonio, University of Naples, Italy
Goldman, Robert D., Northwestern University Medical School
Gould, Robert, New York State Institute of Basic Research in Developmental Disabilities
Gyoeva, Fatima, Russian Academy of Sciences, Institute of Protein Research

Haimo, Leah, University of California, Riverside
Hall, Zach W., University of California School of Medicine, San Francisco
Halvorson, Harlyn O., University of Massachusetts, Dartmouth
Hardin, John, Medical College of Georgia
Henry, Jonathan, University of Illinois
Highstein, Steven M., Washington University School of Medicine
Holmgren, Miguel, The Chicago Medical School
Holz, IV, George G., Harvard Medical School, Massachusetts General Hospital
Hoskin, Francis C. G., Illinois Institute of Technology
Humphreys, Tom, University of Hawaii

Jaffe, Laurinda, University of Connecticut Health Center
Johnston, Daniel, Baylor College of Medicine
Johnston, Rebecca, University of Arizona

Kaneshiro, Edna, University of Cincinnati
Kaplan, Barry, Western Psychiatric Institute & Clinic
Kuhns, William, The Hospital for Sick Children, Canada
Kumar, Ajit, George Washington University School of Medicine
Kuznetsov, Sergei, University of Rostock, Germany

Landowne, David, University of Miami
Lane, Mary C., University of California, Berkeley
Langford, George, Dartmouth College
Laskin, Jeffrey, University of Medicine and Dentistry of New Jersey
Laufer, Hans, University of Connecticut
Lemon, William C., University of Arizona
Lester, Roger, University of Arkansas Medical Sciences
Lipicky, Raymond J., Food and Drug Administration
Llinás, Rodolfo R., New York University Medical Center

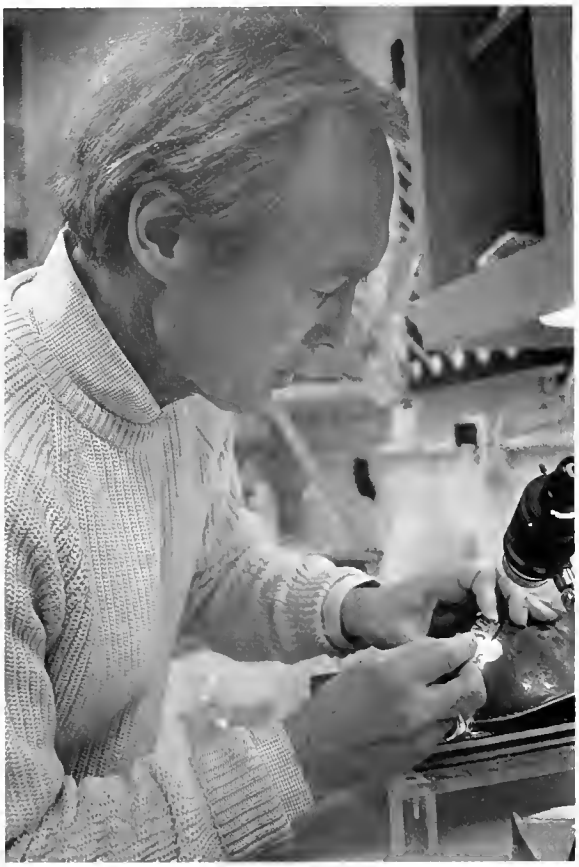

Principal Investigator Robert Barlow, Jr. (Syracuse University).

Makarenko, Vladimir, Russian Academy of Sciences, Russia
Malchow, Robert Paul, University of Illinois College of Medicine
Maranto, Anthony, St. Elizabeth's Hospital
Martindale, Mark, University of Chicago
Metuzals, Janis, University of Ottawa, Canada
Miyakawa, Hiroyoshi, Tokyo College of Pharmacy
Moore, Lisa, Albert Einstein College of Medicine
Moorman, Stephen, UNT Health Science Center, Fort Worth
Moreno, Alonso P., State University of New York, Buffalo
Murray, Andrew, University of California, San Francisco

Nasi, Enrico, Boston University School of Medicine
Nierhaus, Knud, Max Planck Institute for Molecular Genetics, Germany

Palazzo, Robert E., University of Kansas
Pant, Harish, National Institutes of Health
Pozzo-Miller, Lucas D., Roche Institute of Molecular Biology

Qian, Haohua, Harvard University
Quigley, James P., State University of New York, Stony Brook

Rakowski, Robert F., University of Health Sciences/The Chicago Medical School
Rasmussen, Howard, College of Georgia
Ratner, Nancy, University of Cincinnati
Reese, Thomas S., National Institutes of Health
Rieder, Conly L., Wadsworth Center for Labs & Research
Ripps, Harris, University of Illinois College of Medicine
Rome, Lawrence, University of Pennsylvania
Ross, William, New York Medical College
Ruderman, Joan V., Harvard Medical School
Russell, John M., Medical College of Pennsylvania

Saitoh, Setsuo, Hokkaido Central Fisheries Experimental Station
Salmon, Edward, University of North Carolina, Chapel Hill
Sarda, Rafael, Consejo Superior Investigaciones Cientificas, Spain
Schweizer, Felix E., Duke University
Sharp, Andrew A., Brandeis University
Silver, Robert B., Cornell University
Sloboda, Roger D., Dartmouth College
Sluder, Greenfield, Worcester Foundation for Experimental Biology
Sobel, Erik C., AT&T Bell Laboratories, Inc.
Steinacker, Antoinette, University of Puerto Rico Medical Sciences
Sugimori, Mutuysuki, New York University Medical Center
Swenson, Katherine I., Duke University Medical Center

Telzer, Bruce, Pomona College
Trinkaus, John P., Yale University
Troll, Walter, New York University Medical Center
Tytell, Michael, Bowman Gray School of Medicine of Wake Forest University

Weiss, Dieter, University of Rostock, Germany
Wylie, Douglas R., New York University Medical Center

Yamoah, Ebenezer, University of Texas Medical School
Yoshioka, Tohru, Waseda University, Japan

Zago, Cristina, National Research Council
Zigman, Seymour, University of Rochester School of Medicine and Dentistry
Zottoli, Steven J., Williams College
Zuazago de Ortiz, Conchita, University of Puerto Rico

Other Research Personnel

Altamirano, Anibal A., Medical College of Pennsylvania
Alvarez, Guillermo, University of Seville, Spain
Andreu-Sanchez, Maria E., University of Alicante, Spain
Andrews, S. Brian, National Institutes of Health
Araneda, Ricardo, Albert Einstein College of Medicine
Armstrong, Clara, University of Pennsylvania

Backskai, Brian, University of California, La Jolla
Bau, Mu-Yeh, University of Texas Southwestern Medical Center
Benech, Juan Claudio, Instituto de Investigaciones Biologicas, Uruguay
Bittner, George D., University of Texas, Austin
Boakye, Maxwell, National Institutes of Health
Boyle, Richard, Oregon Health Science University
Breitwieser, Gerda E., Johns Hopkins School of Medicine
Brown, Joel E., Albert Einstein College of Medicine
Burns, Marie, Duke University
Busch, Karina, Miami University, Ohio

Calhoun, Benjamin, Medical College of Georgia
Callaway, Joseph, New York Medical College
Cameron, Mark, Harvey Mudd College
Carroll, David J., University of Connecticut Health Center
Chen, Barry, National Institutes of Health

Chludzinski, John, National Institutes of Health
Christofi, Geri, University College London
Chun, Jong Tai, University of Pittsburgh
Cohen, Avrum, Yale University
Cohen, Darien, Dartmouth College
Collin, Carlos, National Institutes of Health
Coughlin, David, University of Pennsylvania
Crispino, Marianna, University of Naples

Dadacay, Alma Villa, Hunter College
Dawson, Timothy Charles, University of Kansas
DeBello, William, Duke University
Dehnbostel, Denise, UNT Health Science Center, Fort Worth
Dodge, Frederick, Syracuse University
Dodge, Susan, University of North Carolina, Chapel Hill
Donaghy, Brenda, University of Iowa
Dopp, Elke, University of Rostock, Germany
Drazba, Judy, National Institutes of Health
Dresbach, Thomas, Max Planck Institute for Brain Research, Germany

Eddleman, Chris, University of Texas, Austin
Eilers, Jems, Universitat des Saarlandes, Germany
Ellis-Thipado, Doretta, University of South Florida
Escalona de Motta, Gladys, University of Puerto Rico

Favit, Antonella, National Institutes of Health
Fernandez-Busquets, Xavier, Fredrich Miescher Institut, Switzerland
Flucher, Bernhard, National Institutes of Health

Galbraith, James, University of California, San Diego
Gallant, Paul E., National Institutes of Health
Gerosa, Daniela, Friedrich Miescher Institut, Switzerland
Giraud, Lisette, University of Puerto Rico
Godell, Chris, University of Texas, Galveston
Goldman, Anne E., Northwestern University Medical School
Gomez, Maria, Boston University School of Medicine
Grant, Philip, National Institutes of Health
Greenfield, Benjamin, Brown University
Guerra, Ernesto, American Psychological Association
Guillfoyle, Kerry Jo., Hampshire College

Hammes, Michelle, Hampshire College
Harris-Collazo, Raul, University of California, San Diego
Heck, Diane, University of Medicine and Dentistry of New Jersey
Hershko, Avram, Israel Institute of Technology, Israel
Hershko, Judith, Israel Institute of Technology, Israel
Hogan, Emilia M., Yale University Medical School
Horoyan, Marianne, National Institutes of Health
Huerta, Julio, Hunter College, CUNY
Hunt, James, Duke University

Jarchow, Janina, Friedrich Miescher Institut, Switzerland
Johnson, Donald, Lehman College, CUNY
Jones, James, American Psychological Association
Jones, Kevin, Duke University
Jue, Renata, Dartmouth College

Kaech, Stefanie, National Institutes of Health
Kaftan, Edward, University of Connecticut Health Center
Kamino, Kohtaro, Tokyo Medical and Dental University School of Medicine, Japan
Kaplan, Ehud, Rockefeller University
Kaplan, Ilene M., Union College

Principal Investigator Sergei Kuznetsov (University of Rostock).

Kawahara, Shigenori, University of Tokyo, Japan
Kelly, Mary, State University of New York Health Science Center
Kelman, Elise S., Montefiore Medical Center
Keynan, Alex, Hebrew University, Israel
Khan, Sohaib, University of Cincinnati
Khodakah, Kamran, University of Pennsylvania
Khuon, Satya, Northwestern University Medical School
Kirino, Yutaka, University of Tokyo, Japan
Knudsen, Knud D., Food and Drug Administration
Konnerth, Arthur, Universitat des Saarlandes, Germany
Kudo, Yoshihisa, Mitsubishi Kasei Life Science Institute, Japan

Lahav, Shirley, Israel Institute of Technology, Israel
Landau, Matthew, Stockton State College
Lang, Eric, New York University Medical Center
Lasser-Ross, Nechama, New York Medical College
Liu, Lei, University of Connecticut
Lopez, Veronica, University of California, Berkeley
Lu, Jin, University of Texas Medical Branch
Lyddone, Clay, University of Kansas

Martinez, Jr., Joe L., University of California, Berkeley
Master, Viraj, University of Chicago
Matheisz, Katherine, Syracuse University
McNeil, Paul, Georgia Medical College
Melchior, Ralph, University of California, Davis
Meng, Chunling, Hong Kong University of Science and Technology, Hong Kong
Mensinger, Allen F., Washington University
Minkoff, Charles, Duke University Medical Center
Miyaguchi, Katsuyuki, National Institutes of Health
Montgomery, John C., University of Auckland, New Zealand
Moreira, Jorge E., National Institutes of Health

Necela, Brian, University of West Florida

Ogielski, Andrew, Bell Communications Research
Olds, James L., National Institutes of Health

Palos, Teresa, University of California, Los Angeles
Parker, Libbie Lynn, Duke University
Passaglia, Christopher, Syracuse University
Perez, Reynaldo, University of Puerto Rico
Pfister, K. Kevin, University of Virginia School of Medicine

Poenie, Martin, University of Texas, Austin
Porcello, Darrell M., Bowdoin College
Powell, Angela, Spelman College
Powell, Angella M., Spelman College
Powers, Maureen, Vanderbilt University
Pumplin, David W., University of Maryland School of Medicine

Qu, Xiangdong, New York University Medical Center
Quinn, Kerry, University of Connecticut Health Center

Rabbitt, Richard, University of Utah
Radominska, Anna, University of Arkansas for Medical Sciences
Rayos, Nancy, Hunter College
Reed, Robyn, Wake Forest University
Reyes, Rosario, University of Oregon
Romero, Michael, University of Washington
Rotllant, Guiomar, Instituto de Ciencias del Mar, Spain
Rule, Randall, University of California, Berkeley
Russell, Joshua C., Medical College of Pennsylvania

Sakakibara, Manabu, Tokai University, Japan
Saver, Michelle, University of Calgary, Canada
Schauer, Stephen, Franklin and Marshall College
Schiffmann, Dietmar, University of Rostock, Germany
Shih, John, California Institute of Technology
Shrier, Alvin, McGill University
Sparks, Christopher, University of North Texas
Spencer, C. Ian, Graduate Hospital
Srimal, Subita, Indian Institute of Science, India
Sterkenburg, Cynthia, University of Texas, Austin
Stockbridge, Norman, Food and Drug Administration
Sudakin, Valery, Israel Institute of Technology, Israel
Swank, Douglas, University of Pennsylvania School of Medicine
Syme, Doug, University of Pennsylvania

Tabares, Lucia, University of Seville School of Medicine, Spain
Takac, Peter, Institute of Zoology & Ecozoology, Slovak Republic
Takahashi, Megumi, Yokohama City University School of Medicine, Japan
Terasaki, Mark, National Institutes of Health
Todora, Michael, University of Texas, Austin
Treat, Susan, University of Arkansas for Medical Sciences

Umbach, Joy, University of California, Los Angeles

Valdes, Lexia, Barry University
Vargas, Fernando, Food and Drug Administration
Vogel, Jackie, University of Kansas
Vojta, Beth, University of Pittsburgh

Walton, Peggy L., Washington University School of Medicine
Warner, Anne, Dartmouth College

Xie, Ping, Hong Kong University of Science and Technology, Hong Kong

Yang, Tsau, Yale University School of Medicine
Ye, Jane, Dartmouth College
Yeh, Jennifer, Medical College of Georgia

Zakevicius, Jane M., University of Illinois at Chicago College of Medicine
Zavilowitz, Joseph, Albert Einstein College of Medicine
Zecevic, Dejan, Yale University School of Medicine
Zecevic, Nada, University of Connecticut Health Center
Zigman, Bunnie R., University of Rochester Medical Center
Zukin, R. Suzanne, Albert Einstein College of Medicine

Library Readers

Alkon, Daniel, National Institutes of Health
Allen, Garland, Washington University
Alliegro, Mark C., Louisiana State University Medical Center
Anderson, Everett, Harvard Medical School

Baccetti, Baccio, Siena, Italy
Benjamin, Thomas, Harvard Medical School
Bernhard, Jeffrey, University of Massachusetts Medical Center
Bernheimer, Alan, NYU Medical Center
Breinin, Goodwin, NYU Medical Center

Candelas, Graciela, University of Puerto Rico
Cariello, Lucio, Stazione Zoologica, Italy
Clark, Arnold, Woods Hole, MA
Clarkson, Kenneth, AT&T Bell Labs
Cohen, Leonard, American Health Foundation
Cohen, Seymour, Woods Hole, MA
Collier, Marjorie, St. Peters' College
Copeland, D. Eugene, Woods Hole, MA
Corliss, Bruce, Duke University
Corwin, Jeffrey, University of Virginia
Cowling, Vincent, SUNY, Albany

D'Alessio, Guiseppe, Stazione Zoologica, Italy
Dixon, Keith, Flinders University
Duncan, Thomas, Nichols College

Eisen, Herman N., Massachusetts Institute of Technology
Epstein, Herman, Woods Hole, MA

Federici, Celine, Woods Hole, MA
Feldman, Susan, New Jersey Medical School
Fitzpatrick, Thomas, Woods Hole, MA
Frenkel, Krystyna, NYU Medical Center
Friedler, Gladys, Boston University School of Medicine

Galatzer-Levy, R., University of Illinois
Goldfarb, Ronald, University of Pittsburgh Medical School
Goldstein, Moise, Johns Hopkins University
Grossman, Albert, NYU Medical Center
Gruner, John, Cephalon Inc.
Guttenplan, Joseph, NYU Dental Center

Hall, Valerie, Nantucket High School
Hepler, Peter, University of Massachusetts
Herskovits, Theodore, Fordham University
Hill, Richard, Michigan State University
Hines, Michael, Duke University Medical Center

Ilans, Joseph, Case Western Reserve University
Inoue, Sadyuki, McGill University, Canada

Jacobson, Allan, University of Massachusetts Medical School
Josephson, Beth, Ocean Arks International

Kaltenbach, Jane, Mount Holyoke College
Kaminer, Benjamin, Boston University School of Medicine

Bryozoan book collection in the MBL Rare Books Room.

Karlin, Arthur, Columbia University
Kelly, Robert, University of Illinois
Kramer, F. R., Public Health Research Institute, NY
Krane, Stephen, Massachusetts General Hospital
King, Kenneth, Falmouth, MA

Laderman, Aimlee, Yale University
Landsberg, Joseph, CSIRO, Australia
Laster, Joseph, University of Massachusetts Medical Center
Lee, John, City College of CUNY
Leighton, Joseph, Aeron Biotechnology, Inc.
Leonard, Chris, New York University
Linck, Richard, University of Minnesota
Lorand, Laszlo, Northwestern University Medical School
Luporini, P., MCA, Camerino, Italy

Martin, Donald C., Woods Hole, MA
Mauzerall, David, The Rockefeller University
Michaelson, James, Massachusetts General Hospital
Mizell, Merle, Tulane University
Moore, John, Duke University Medical Center
Morrell, F., Rush Medical Center
Mounier, Franc, University of Paris, France

Narahashi, Toshio, Northwestern University
Naugle, John, North Falmouth, MA
Nickerson, Peter, SUNY, Buffalo
Nierhaus, Knud, Max Planck Institute, Germany

Ohki, Shinpei, State University
Olds, James, National Institutes of Health

Pappas, George, University of Illinois
Person, Philip, Sloan Kettering Institute
Peirce, Sidney, University of Maryland
Plummer-Cobb, Jewel, California State University
Prusch, Robert D., Gonzaga University

Rabinowitz, Michael, Marine Biological Laboratory
Ravetch, Robert T., Sloan Kettering Institute
Reynolds, George, Princeton University
Rose, Birgit, University of Miami Medical School
Rosenbluth, Jack, NYU Medical Center
Rosenbluth, Raja, Simon Fraser University
Rosenkranz, Herbert, University of Pittsburgh
Roth, Lorraine, Brookline, MA
Ryan, Terrance, Regeneron Pharmaceuticals

Sanger, Jean M., University of Pennsylvania
Sanger, Joseph, University of Pennsylvania
Schifellite, Carmen, Atkinson College
Schippers, Jay, Jacksonville, FL
Sears, James, University of Massachusetts, Dartmouth
Segal, Sheldon, Rockefeller Foundation
Shanklin, Douglas, University of Tennessee
Sheetz, Michael, Duke University Medical Center
Shepard, Frank, Deep Sea Research
Shepro, David, Boston University
Sonnenblick, B. P., Rutgers University
Spector, Abraham, Columbia University
Spiegel, Evelyn, Dartmouth College
Spiegel, Melvin, Dartmouth College
Spotte, Stephen, University of Connecticut
Stephenson, William, Earlham College
Stuart, Ann, University of North Carolina
Sundquist, Eric, US Geological Survey
Sweet, Frederick, Washington University

Trager, William, The Rockefeller University
Troll, Walter, NYU Medical Center
Tweedell, Kenyon, University of Notre Dame
Tykocinski, Judith, Case Western Reserve University

Van Holde, Kensal, Oregon State University

Walton, Alan John, Cavendish Lab
Wangh, Lawrence, Brandeis University
Warren, Leonard, Wistar Institute
Webb, Marguerite, Woods Hole, MA
Weidner, Earl, Louisiana State University
Weir, Gary, US Historical Center
Weissmann, Gerald, NYU Medical Center
Whittaker, J. R., University of New Brunswick, Canada
Wilber, Charles, Colorado State University
Wittenberg, Beatrice, Albert Einstein College
Wittenberg, Jonathan, Albert Einstein College
Wolfteich, Jonathan, Woods Hole Oceanographic Institution

Yevick, George, Stevens Institute of Technology

Domestic Institutions Represented

Alabama, University of, Birmingham
Alaska, University of, Fairbanks
Albert Einstein College of Medicine
American Psychological Association
Arizona, University of
Arkansas, University of, Medical Sciences
ARLDN, Tucson
Armed Forces Radiobiology Research Institute
AT&T Bell Laboratories
Atlanta Veterans Affairs Medical Center

Barnard College
Barry University
Baylor College of Medicine

Bell Communications Research
Boston University
Bowdoin College
Bowman Gray School of Medicine
Brandeis University
Brooklyn College, CUNY
Brown University
Burroughs Wellcome

California Institute of Technology
California Institute of Technology, Beckman Institute
California, University of, Berkeley
California, University of, Davis
California, University of, Irvine
California, University of, La Jolla
California, University of, Los Angeles
California, University of, Riverside
California, University of, San Diego
California, University of, San Francisco
California, University of, Santa Barbara
California, University of, Santa Cruz
California, University of, School of Medicine
Cambridge Neuroscience, Inc.
Carleton University
Carnegie Mellon University
Case Western Reserve University
Center for Great Lakes Studies
Centers for Disease Control, Colorado
Chicago, University of
Children's Hospital of Michigan
Children's Hospital of Philadelphia
Children's Hospital, Boston
Cincinnati, University of
Cold Spring Harbor Laboratory
Colorado, University of
Columbia University
Columbia University College of Physicians & Surgeons
Connecticut, University of, Health Center
Connecticut, University of
Cornell University
Cornell University Medical College

Dallas VAMC
Dartmouth College
Dartmouth Medical School
Denver, University of
DC General Hospital
Duke University
Duke University Medical Center
Duke University School of Medicine
DuPont Company
Dyson Vision Research Institute

Emory University
Environmental Protection Agency

Florida State University
Food and Drug Administration
Fordham University College, Lincoln Center
Franklin and Marshall College

George Washington University
Georgia Institute of Technology
Georgia Medical College
Georgia, College of
Georgia, University of

Hampden-Sydney College
Hampshire College
Harvard Medical School
Harvard University
Harvey Mudd College
Houston, University of
Howard Hughes Medical Institute
Hunter College, CUNY

Idaho, University of
Illinois Institute of Technology
Illinois, University of
Illinois, University of, Chicago College of Medicine
Illinois, University of, Urbana-Champaign
Indiana University
Indiana University School of Medicine
Iowa State University
Iowa, University of

James Madison University
Jefferson Medical College
Johns Hopkins University
Johns Hopkins University School of Medicine

Kansas, University of
Kentucky, University of
Kewalo Laboratory, Pacific Biomedical Research Center

Lafayette College
Lehman College, CUNY
Lilly Research Labs
Lincoln Hospital, Bronx, NY
Loma Linda University School of Medicine
Los Alamos National Laboratory
Louisiana State University
Louisiana State University Medical Center
Loyola University of Chicago

Maryland, University of, Baltimore
Maryland, University of, School of Medicine
Massachusetts General Hospital
Massachusetts Institute of Technology
Massachusetts, University of
Massachusetts, University of, Amherst
Massachusetts, University of, Dartmouth
Massachusetts, University of, Medical School
Mayo Graduate School
MD Anderson Cancer Center
Medical Center of Delaware
Medical College of Georgia
Medical College of Pennsylvania
Meharry Medical College
Memorial Sloan-Kettering Cancer Center
Methodist Hospital
Miami Project, University of Miami

Miami University
Miami, University of, School of Medicine
Miami, University of, RSMAS
Michigan State University
Michigan, University of
Minnesota, University of
Minnesota, University of, School of Medicine
Montefiore Medical Center
Montpellier, University of

Nassau County Medical
National Center for Biotechnology Information
National Institutes of Health
National Institutes of Health Gerontology Research Center
National Institutes of Health, NINDS
National Institutes of Health, NEI
New England Medical Center
New Jersey, University of Medicine and Dentistry of
New Mexico, University of
New York Medical College
New York State Institute of Basic Research in Developmental Disabilities
New York University
New York University Medical Center
Nikon Corporation
Noran Instruments
North Carolina, University of, Chapel Hill
Northern Arizona University
North Texas, University of
North Texas, University of, Health Science Center, Fort Worth
Northwestern University
Northwestern University Medical School

Oberlin College
Ohio University
Oklahoma, University of
Olympus Optical Co., Ltd.
Oregon Health Sciences University
Oregon State University
Oregon, University of

Pennsylvania Hospital
Pennsylvania, University of
Pennsylvania, University of, School of Medicine
Pittsburgh, University of
Pittsburgh, University of, School of Medicine
Poloroid Corporation
Pomona College
Princeton University
Puerto Rico, University of
Puerto Rico, University of, Medical Sciences

Research Biochemicals International
Rhode Island, University of
Roche Institute of Molecular Biology
Rochester, University of, Medical Center
Rochester, University of, School of Medicine & Dentistry
Rockefeller University

Rowland Institute for Science
Rush Medical College
Rutgers University

San Francisco State University
Scripps Clinic
Scripps Research Institute
Seattle Biomedical Research Institute
Skidmore College
Sloan-Kettering Institute
Smithsonian Institution
South Carolina, University of
Southeastern Louisiana University
Southern California, University of
Southern Illinois University School of Medicine
South Florida, University of
Spelman College
St. Elizabeth's Hospital
St. Lawrence University
St. Louis University School of Medicine
St. Margaret's Center for Women/Infants
Stanford University
State University of New York Health Science Center
State University of New York, Buffalo
State University of New York, Stony Brook
Stockton State College
Syracuse University

Syracuse University Institute for Sensory Research

Tennessee, University of
Texas Tech University HSC
Texas, University of, Austin
Texas, University of, Galveston
Texas, University of, Health Science Center, San Antonio
Texas, University of, Medical Branch, Galveston
Texas, University of, Houston
Texas, University of, Southwestern Medical Center, Dallas
The George Washington University
Toledo, University of
Tufts University
Tulane University Medical Center
Tuskegee University

U. S. Department of Agriculture
U. S. Department of State
Uniformed Services University of the Health Sciences
Union College
Utah State University
Utah, University of

VA Medical Center, Portland
Vanderbilt School of Medicine
Vanderbilt University
Vermont, University of
Virginia, University of, School of Medicine

Wadsworth Center for Labs and Research
Wake Forest University
Washington University
Washington, University of
Washington, University of, School of Medicine
Washington University School Medicine
Wayne State University
Wesleyan University
West Florida, University of
West Virginia University
Western Washington University
Williams College
Wisconsin, University of
Wisconsin, University of, Medical School
Worcester Foundation for Experimental Biology
Wyoming, University of

Yale Primary Care Research Program
Yale University
Yale University School of Medicine

Foreign Institutions Represented

Alicante, University, Spain
Auckland, University of, New Zealand

Babraham Institute, UK
Basel University, Switzerland
Bogor Agricultural University, Indonesia
Brain Research Institute University of Zürich, Switzerland
Bristol University, UK

Calgary, University of, Canada
Cambridge, University of, UK
Carol Davila University of Medicine, Romania
Catholic University of Chile, Chile
CNRS, France
Consejo Superior Investigaciones Cientificas, Spain
Copenhagen University, Denmark

Ecole Normale Superieure, France

Federal University of Rio de Janeiro, Brazil
Fredrich Miescher Institut, Switzerland

Guy's Hospital, London

Hebrew University, Israel
Hokkaido Central Fisheries Experimental Station, Japan

Hong Kong University of Science & Technology, Hong Kong

ICP-Brussels, Belgium
I.V.I.C., Venezuela
INSA, France
INSERM, France
Institute for Drug Research, Budapest, Hungary
Institute of Mathematical Problems of Biology, Russia
Institute of Microbiology, Berlin
Instituto di biologia dello Sviluppo, Italy
Indian Institute of Science, India
Institute of Protein Research, Russia
Instituto de Ciencias del Mar, Spain
Instituto de Investigaciones Biologicas, Uruguay
Instituto M. y M. Ferreyra, Argentina
Israel Institute of Technology, Israel

Jiangsu Institute of Parasitic Diseases, China

Kochi University, Japan
Kyoto University, Japan

Laboratoire de Neurobiologie, ENS
London, University College of, England

Max Planck Institute for Biological Cybernetics, Germany
Max Planck Institute for Developmental Biology, Germany
Max Planck Institute of Immunobiology, Germany
Max Planck Institute for Molecular Genetics, Germany
Medical Research Council, UK
McGill University, Canada
Mitsubishi Kasei Life Science Institute, Japan
MRC Laboratory of Molecular Biology

Naples, University of, Italy
Nagoya University, Japan
National Museums of Kenya, Kenya
National Research Council, Italy
Netherlands Cancer Institute, The Netherlands
Nippon Medical School, Japan

Ottawa, University of, Canada
Oxford University, UK

Pasteur Institute, France
Philipps Universität Marburg, Germany
Protein Research Institute, Russia

Queen's University, Canada

RIKEN, Japan
Rostock, University of, Germany
Royal Free Hospital School of Medicine, UK

Russian Academy of Sciences, Russia

Seville, University of, Spain
Slovak Republic, Institute of Zoology & Ecozoology, Slovak Republic
Station Zoologique, France
Stazione Zoologica A. Dohrn, Italy

Tata Institute of Fundamental Research, India
Tel Aviv University, Israel
The Hospital for Sick Children, Canada
Tokai University, Japan
Tokyo College of Pharmacy, Japan
Tokyo Medical and Dental University School of Medicine, Japan
Tokyo, University of, Japan
Tokyo, University of Agriculture & Technology, Japan
Toronto, University, Canada

Universitat des Saarlandes, Germany
Universidad del Valle, Columbia
Universitat Konstanz, Germany
Universitat Oldenburg, Germany
University College London, UK
University of Aarhus, Denmark
University of Antwerp, Belgium
University of Bonn, Germany
University of British Columbia, Canada
University of Cambridge, UK
University of Glasgow, UK
University of Granada, Spain
University of Groningen, Germany
University of Hamburg, Germany
University of Koln, Germany
University of Lethbridge, Canada
University of Lisbon, Portugal
University of London, UK
University of Manitoba, Canada
University of Munich, Germany
University of Pisa, Italy
University of Oxford, UK
University of Paris, France
University of Tokyo, Japan
University of Western Australia, Australia
University of Western Ontario, Canada
Uppsala University, Sweden

Waseda University, Japan
Weizmann Institute of Science, Israel
Wellcome/CRC Institute, UK

Yokohama City University School of Medicine, Japan
Yonsei University College of Medicine Seoul, Korea

Zoologisches Institut, Germany

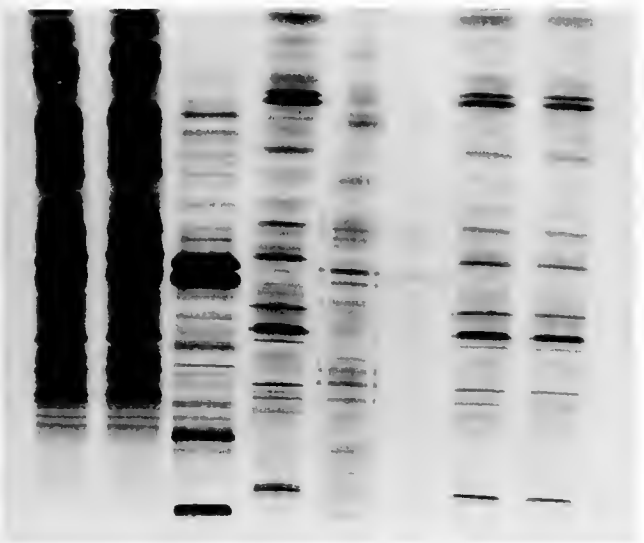

Year-Round Research Programs

Architectural Dynamics in Living Cells Program

Established in 1992, this program focuses on architectural dynamics in living cells—the timely and coordinated assembly and disassembly of macromolecular structures essential for the proper functioning, division, motility, and differentiation of cells; the spatial and temporal organization of these structures; and their physiological and genetic control. The program is also devoted to the development and application of powerful new imaging and manipulation devices that permit such studies directly in living cells and functional cell-free extracts. The Architectural Dynamics in Living Cells Program promotes interdisciplinary research and consists of resident core investigators and a cadre of adjunct members.

Resident Core Investigators

Inoué, Shinya, Distinguished Scientist
Mei, Guang, Research Associate
Oldenbourg, Rudolf, Associate Scientist
Stemmer, Andreas, Visiting Assistant Scientist

Staff

Knudson, Robert, Instrument Development Engineer
Leighton, Jane, Executive Assistant

Visiting Investigators

Rieko Arimoto, Nikon Corporation, Tokyo, Japan
Theodore D. Inoué, Universal Imaging Corporation, West Chester, PA
Andrew Murray, University of California, San Francisco
Fabrice Roegiers, Station Zoologique, Villefranche-sur-Mer, France
Edward D. Salmon, University of North Carolina, Chapel Hill
Keisuke Suzuki, Olympus Corporation, Hachioji, Japan
Phong Tran, University of North Carolina, Chapel Hill

Boston University Marine Program

Faculty

Atema, Jelle, Professor of Biology, Director
Dionne, Vincent, Professor of Biology
Humes, Arthur G., Professor of Biology Emeritus
Kaufman, Les, Associate Professor of Biology
Lobel, Phillip, Associate Professor of Biology
Tamm, Sidney L., Professor of Biology
Valiela, Ivan, Professor of Biology
Voigt, Rainer, Research Associate Professor

Staff

Guilfoyle, Kerry, Course Coordinator
Hahn, Dorothy, Senior Administrative Secretary
O'Brien, Todd, Staff Assistant
Pedersen, Jennifer, Program Assistant
Schillizzi, Cynthia, Program Manager

Visiting Faculty and Investigators

D'Avanzo, Charlene, Hampshire College
Hinkle, Greg, MBL
Kremer, James, USC
Margulis, Lynn, UMass-Amherst
Mulsow, Sandor, Bedford Institute of Oceanography
Rietsma, Carol, SUNY New Paltz
Sardet, Christian, Villefranche Zoological Station
Simmons, William, Visiting Lecturer, Boston University
Wainwright, Norman, MBL
Ward, Nathalie, Center for Coastal Studies

Research Staff

Basil, Jennifer, Postdoctoral Investigator
Breithaupt, Thomas, Postdoctoral Investigator
Collins, Glynnis, Visiting Research Assistant
Delay, Rona, Postdoctoral Investigator
Dennison, William, University of Sydney

Dubin, Adrienne, Postdoctoral Investigator
Eisthen, Heather, Postdoctoral Investigator
Foreman, Kenneth, Postdoctoral Investigator
Gerardo, Hortense, Postdoctoral Investigator
Grasso, Frank, Postdoctoral Investigator
McConnell, Joanne, Postdoctoral Investigator
Nixon, Jennifer, Research Assistant
Soucy, Lori, Research Assistant
Seely, Brad, Visiting Research Assistant
Tamm, Signhild, Senior Research Associate

Graduate Students

PhD students

Balint, Claire
Batjakas, Ioannis
Behr, Peter
Bushmann, Paul
Dale, Jonathan
Farley, Lynda
Gomez, George
Hauxwell, Jennifer
Hersh, Douglas
Karavanich, Christy
LaMontagne, Michael
Lowe, Brian
Loynes, Janet
Ma, Diana
McClelland, James
Oliver, Steven
Portnoy, John
Tamse, Armando
Usup, Gires
Zhou, Qiao

MA students

Ashcraft, Susan
Bayha, Keith
Bocking, Beatrice
Brazik, David
Burkhalter, Brenda
DiNunno, Paul
Economakis, Alistair
Fricke, Julie
Goldstein, Jennifer
Kerr, Lisa
Ludlow, Amanda
Maglic, Boris
Nathan, Miselis
Philibotte, Jason
Pinto-Torres, Sonia
Rader, Lauren
Schreiber, Suzanne
Tomasky, Gabrielle
Wittenberg, Kim

Summer 1994 Undergraduate Interns

Bartholomew, Aaron
Bertrand, Virginie
Boxhill, Jessica
Chalfoun, Anna
de Marles, Axe
Ellis, Melissal
Han, Tina
Harrison, Timothy
Horne, C. Ashton
Hurlburt, Peter
Leonard, Ann
McDonnell, Kristin
Monti, Jill
Rudy, Michelle
Tolly, Krystal
Tyndale, Libby
Vazquez, Lory Sandiago
White, Brad

Undergraduate Students, Fall 1994

Barneby, Sebastian
Beaudette, Britte
Bhatt, Sonal
Bielawski, April
Bota, Dalena
Boyle, Bridget
Canizio, Casey
Cappa, Aimie
Cardinale, Nicole
Carlson, Daphne
Dean, Tony
Downing, Amy
DeGrenier, Jennifer
DeSantis, Krystal
Elsasser, Emily
Ewell, Cara
Gibbons, Lynn
Haeuber, Elaina
Hammel, Scott
Henchar, Teresa
Hoddinott, Jennifer
Hooper, Brian
Horal, Melissa
Horne, C. Ashton
Kelly, Christopher
Kulawiak, Karen
Levin, Ilse
Mastaitis, Jason
Mela, Alexandra
Mendoza, Daniel
Milikow, Davis
Mohammadian, Marton
Mosconi, Christopher
Palmer, Robin
Pollard, Amina
Portante, Gerald
Richards, Kyle
Sadler, Theo
Scarfo, Julie
Schaffhauser, Lori
Schrader, Heather
Sikorski, Kristan
Sleigh, Kimberly
Steinert, Cara
Tauber, Julia
Tschaepe, Nikol
Uhlenhopp, Amy
Vincent, Lara
Wey, Patricia

Williams, Josh
Witkop, Kimberlee
Yung, Angela

Laboratory of Jelle Atema

Many organisms use chemical signals as their main source of information about the environment. These signals are transported in the marine environment by turbulent currents, viscous flow, and molecular diffusion. Receptor organs extract signals through various physical & biological filtering processes. Currently, the lobster with its exquisite sense of taste and smell, is our major model to study the signal filtering capabilities of the whole animal and the tuning properties of its receptor cells. Research focuses on food signals and pheromones used in courtship and dominance, neurophysiology of receptor cells, behavior guided or modulated by chemical signals, computational models of odor plumes and neural filters, and underwater robotics.

Laboratory of Vincent Dionne

Odors are powerful stimuli. They can focus the attention, elicit behaviors (or misbehaviors), and even resurrect forgotten memories. These actions are directed by the central nervous system, but they depend upon the initial transduction of chemical signals by olfactory receptor neurons in the nasal passages. More than just a single process appears to underlie odor transduction, and the intracellular pathways that are used are far more diverse than once thought. Hundreds of putative odor receptor molecules have been identified that work through several different second messengers to modulate the activity of various types of membrane ion channels. Our studies are being conducted with aquatic salamanders using amino acids and other soluble chemical stimuli which these animals perceive as odors. Using electrophysiological and molecular approaches, the research examines how these cellular components produce odor detection, and how odors are identified and discriminated.

Laboratory of Arthur G. Humes

Research interests include systematics, development, host specificity, and geographical distribution of copepods associated with marine invertebrates. Current research is on taxonomic studies of copepods from invertebrates in the tropical Indo-Pacific area, and poecilostomatoid and siphonostomatoid copepods from deep-sea hydrothermal vents and cold seeps.

Laboratory of Philip Lobel

This laboratory is developing a complete model of the interactions of man and nature in the Johnston Atoll lagoon. Johnston Atoll has been occupied continuously by the military since the 1930s and provides a unique opportunity for assessing the biological impacts of pollution. Unlike a city harbor, chemical spills at the atoll are documented as to location, date, and amount.

Laboratory of Sidney Tamm

Marine model systems offer unique experimental advantages for solving basic problems in cell biology and physiology. In particular, comb jellies (ctenophores), important members of the marine zooplankton, possess the largest cilia and smooth muscles in nature, a simple nervous system, and interesting feeding and locomotory behaviors. We use ctenophores to investigate the mechanism of ciliary movement and ciliary coordination, the neural and ionic control of cilia (particularly stimulus-evoked intraciliary calcium transients and distribution of ciliary calcium channels), geotaxis and mechanosensory transduction by motile cilia statocyst, structure and function of smooth muscle, double-modality sensory receptors and the cytoskeleton, and evolution of neurotransmitters, and a new type of reversible cell-cell adhesion that closes the mouth of *Beroë*, a voracious predator of other ctenophores. In addition, we use a termite protozoan with a continuously rotating head to investigate novel types of cell motility, the fluid nature of cell membranes, and remarkable prokaryotic-eukaryotic motility symbioses.

Laboratory of Ivan Valiela

Our major research activity involves the Waquoit Bay Land Margin Ecosystems Research Project. This work examines how human activity in coastal watersheds (including landscape use and urbanization) increases nutrient loading to groundwater and streams. Nutrients in groundwater are transported to the sea, and, after biogeochemical transformation, enter coastal waters. There, increased nutrients bring about a series of changes. The Waquoit Bay LMER is designed to help understand and model the coupling of land use and consequences to receiving waters, to study the processes involved, and to assess consequences and opportunities for coastal management.

A second long-term research topic is the structure and function of salt marsh ecosystems, including the processes of predation, herbivory, decomposition, and nutrient cycles.

Calcium Patterning Program

This laboratory investigates the role played by calcium ions in a wide range of fundamental cell processes; in developing eggs, in differentiated tissues, and in cell extracts. This is possible through the use of aequorin, a bioluminescent protein complex. Aequorin can either be microinjected into cells or transgenically expressed without disturbing function or development. The pattern of luminescence that is emitted by an aequorin-loaded cell reveals changing patterns and levels of free calcium within the cell (or its progeny). Photons are collected and correlated with dynamic cellular events by an imaging system developed in our laboratory. This technique has some substantial advantages over other methods of imaging intracellular calcium and as a result supports an extensive collaborative research effort. The laboratory is currently studying cytokinesis in frog and fish eggs; cell cycle control in sea urchin and surf clam eggs; polarity expression in frog eggs; tip growth in pollen tubes; injury and degeneration in neurons; mechanisms of fertilization in sea urchins; differentiation in slime molds; and calcium release in cell extracts from frog eggs. The laboratory is supported by the NSF to both pursue biological questions and to develop the aequorin-based imaging technique. Great emphasis is being placed on the development of transgenic strains of both animals and plants that express the transfected apo-aequorin gene. We are currently working on slime molds, zebrafish, mice and tobacco seedlings that all express the jellyfish gene.

Staff

Miller, Andrew L., Assistant Scientist
Jaffe, Lionel F., Senior Scientist

Visiting Investigators

Azhar, Mohamed, Indian Institute of Science, Bangalore, India
Bozhkova, Valentina, Russian Academy of Sciences, Russia

Browne, Carole, Wake Forest University
Chauhan, Amrit, Macalester College
Creton, Robert, University of Utrecht, The Netherlands
Cubitt, Andrew, C., UCSD
Denegre, Jim, University of California, Irvine
Eckberg, Bill, Howard University
Fluck, Richard, A., Franklin and Marshal College
Galione, Antony, Oxford University, UK
Huebner, Erwin, University of Manitoba, Canada
Kaminer, Benny, Boston University
Machesky, Laura, MRC, Cambridge, UK
McWilliams, Harry
Miller, Brent, Purdue University
Sardet, Christian, Villefranche-sur-Mer, France
Speksnijder, Johanna, E., Hubrecht Laboratory, The Netherlands

The Ecosystems Center

The Center carries out research and education in ecosystems ecology. Terrestrial and aquatic scientists work in a wide variety of ecosystems ranging from the streams, lakes, and tundra of the Alaskan Arctic (limits on plant primary production) to sediments of Massachusetts Bay (controls of nitrogen cycling), to forests in New England (effects of soil warming on carbon and nitrogen cycling) and South America (effects on greenhouse gas fluxes of conversion of rain forest to pasture) and to large estuaries in the Gulf of Maine (effects on the plankton and benthos of nutrients and organic matter in stream runoff). Many projects, such as those dealing with carbon and nitrogen cycling in forests, streams, and estuaries, use the stable isotopes ^{13}C and ^{15}N to investigate natural processes. A mass spectrometer facility is available at the Center. Data from field and laboratory research are used to construct mathematical models of whole-system responses to change. Some of these models are combined with geographically referenced data to produce estimates of how environmental changes affect key ecosystem indexes such as net primary productivity and carbon storage throughout the world's terrestrial biosphere. The results of the Center's research are applied, wherever possible, to the questions of the successful management of the natural resources of the earth. In addition, the ecological expertise of the staff is made available to public affairs groups and government agencies who deal with problems such as acid rain, coastal eutrophication, and possible carbon dioxide-caused climate change. There are opportunities for postdoctoral fellows and graduate students.

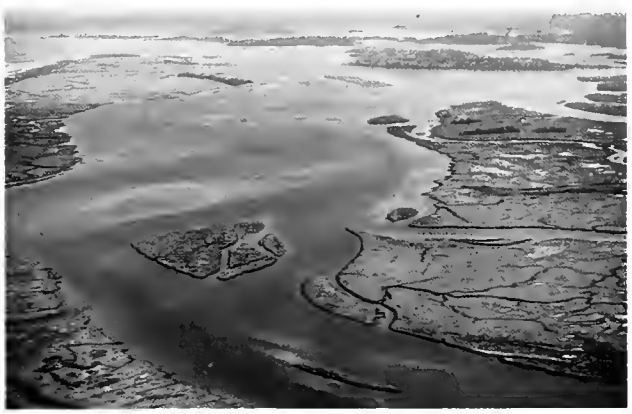

Aerial view of Plum Island Sound Estuary, where the Ecosystems Center is studying carbon and nitrogen dynamics and food web structure.

(Photo by Bruce Peterson)

Staff

Hobbie, John E., Co-Director
Melillo, Jerry M., Co-Director
Bahr, Michele
Buffam, Ishi
Castro, Mark
Castro, Nancy
Catricala, Christina
Deegan, Linda
Donovan, Suzanne
Dornblaser, Mark
Downs, Martha
Drummey, Todd
Dugan, Deirdre
Fry, Brian
Garritt, Robert
Giblin, Anne
Giehtbrock, David
Harvey, Christopher
Helfrich, John
Hopkinson, Charles
Jones, David
Kicklighter, David
Kwiatkowski, Bonnie
Laundre, James
McGuire, A. David
McKane, Robert
Monahan, Jean
Murray, Georgia
Nadelhoffer, Knute
Neill, Christopher
Newkirk, Kathleen
Nolin, Amy
Pennington, Susan
Peterson, Bruce
Rastetter, Edward
Redmond, Leslie
Regan, Kathleen
Ricca, Andrea
Scanlon, Deborah
Seifert, Mary Ann
Shaver, Gaius
Steudler, Paul
Tholke, Kristin
Tucker, Jane
Wollheim, Wilfred

Postdoctorals

Fernandes, David
Johnson, Loretta
Pan, Yude
Vallino, Joseph
Williams, Mathew
Xiao, Xiangming

Consultants

Bowles, Francis
Bowles, Margaret
Schwarzman, Elisabeth
Thomson, Lee

Laboratory for Marine Animal Health

The laboratory provides diagnostic, consultative research, and educational services to the institutions and scientists of the Woods Hole community concerned with marine animal health. Diseases of wild, captive, and cultured animals are investigated.

Staff

Abt, Donald A., Director and The Robert R. Marshak Term Professor of Aquatic Animal Medicine and Pathology, School of Veterinary Medicine, University of Pennsylvania
Bullis, Robert A., Research Assistant Professor of Microbiology, University of Pennsylvania
Leibovitz, Louis, Director Emeritus
McCafferty, Michelle, Histology Technician, University of Pennsylvania
Moniz, Priscilla C., Secretary
Smolowitz, Roxanna M., Research Associate in Pathology, University of Pennsylvania
Wadman, Elizabeth A., Microbiology Technician, University of Pennsylvania

Laboratory of Aquatic Biomedicine

This laboratory investigates leukemias of soft shell clams. Monoclonal antibodies developed by this laboratory and techniques in molecular biology are used to investigate the differences between normal and leukemic cells and their ontogeny. The impact of pollutants on leukemogenesis is currently being studied with an emphasis on regional superfund sites.

Staff

Reinisch, Carol L., Investigator, MBL, and Chairperson, Department of Comparative Medicine, Tufts University School of Veterinary Medicine

Laboratory of Cell Biochemistry

This laboratory uses cell and molecular biological methods to study the regulation of gene expression in marine fish. Current emphasis is on gene products involved in heme metabolism including: (a) aminolevulinate synthase, the first and rate determining enzyme of heme production; (b) cytochrome P450, a heme-requiring catalyst for oxidation of hydrophobic chemicals; and (c) heme oxygenase, a stress-induced, microsomal enzyme that catalyzes the first reaction of heme degradation. The expression of all three enzymes is affected by endogeneous and pharmacological agents as well as xenobiotics and carcinogens. We have cloned and sequenced cDNAs for both the erthyroid and housekeeping forms of aminolevulinate synthase, have developed specific probes for cytochrome P450, and, by RT-PCR, are generating a homologous probe for heme oxygenase. When that is completed, we will have a battery of fish-specific molecular biological reagents that can be used to monitor environmental effects on heme biosynthesis, utilization, and degradation. It is expected that such simultaneous analyses will be much more informative than measurements made on only one aspect. We recently have shown that isolated fish hepatocytes regulate heme biosynthesis in a manner resembling that in terrestrial vertebrates (including humans), and we are using primary cultures of fish hepatocytes to address some long-standing biomedical questions regarding the mechanisms of that regulation. Because preliminary sequence alignments indicate that aminolevulinate synthase has an interesting evolutionary history that bears on the endosymbiont hypothesis for the origin of animal mitochondria, these studies will be extended to include comparative molecular biology of aminolevulinate synthases from invertebrates and lower eukaryotes.

Staff

Cornell, Neal W., Senior Scientist
Faggart, Maura A., Research Assistant
Martin, Holly A., Research Assistant
Macarro, Jackie, Laboratory Assistant

Visiting Scientists

Fox, T. O., Harvard Medical School
Schaffer, Walter T., NIH

Laboratory of Cell Communication

Established in 1994, this laboratory is devoted to the study of intercellular communication. The research focuses on the cell-to-cell channel, a membrane channel built into the junctions between cells. This channel provides one of the most basic forms of intercellular communication in organs and tissues. The work is aimed at the molecular physiology of this channel, in particular, at the mechanisms that regulate the communication. Electrophysiological-, fluorescent-tracer-, and molecular biological techniques are used to this end. As was recently discovered in this laboratory, the channel is the conduit of growth-regulating signals. It is instrumental in a basic feedback loop whereby cells in organs and tissues control their number; in a variety of cancer forms it is crippled. Work is aimed now at the mechanisms of growth control and at correcting cancer growth by transferring the gene for the cell-to-cell channel protein from normal cells into the cancer cells. Molecular genetic techniques are used in this endeavor.

Staff

Werner Loewenstein, Senior Scientist
Birgit Rose, Senior Scientist
Tracy Jillson, Research Assistant

Laboratory of Shinya Inoué

Study of the molecular mechanism and control of mitosis, cell division, cell motility, and cell morphogenesis, with emphasis on biophysical studies made directly on single living cells, especially developing eggs in marine invertebrates. Development of biophysical instrumentation and methodology, such as polarization optical and video microscopy and digital image processing techniques, and exploration of their underlying theory are an integral part of the laboratory's effort.

Staff

Inoué, Shinya, Distinguished Scientist
Knudson, Robert, Instrument Development Engineer
Leighton, Jane, Executive Assistant
Maccaro, Jackie, Laboratory Assistant
Mei, Guang, Research Associate
Stemmer, Andreas, Visiting Assistant Scientist
Woodward, Bertha M., Laboratory Manager

Laboratory of Alan M. Kuzirian

Research in this laboratory explores the functional morphology and ultrastructure of various organ systems present in opisthobranch mollusks. The program includes mariculture of the nudibranch, *Hermissenda crassicornis*, with emphasis on developing reliable culture methods for rearing and maintaining this animal as a research resource. Studies include optimization of adult and larval nutrition, control of facultative pathogens and disease, development of morphologic criteria for staging larvae and juveniles, and metamorphic induction. Morphologic studies stress the ontogeny of neural and sensory structures, and neurochemicals associated with the photic and vestibular systems which have been used as models systems in learning and memory studies.

Concurrent with these studies is the development of a new technique to obtain and reconstruct serial block face images (SBFI) of epoxy-embedded or cryoprepared tissues sectioned or freeze-fractured/freeze-etched inside an SEM by an *in situ* miniature ultramicrotome.

Collaborative research includes histochemical investigations on strontium's role in initiating calcification in molluscan embryos (shell and statoliths), as well as immunocytochemical labelling of cell-surface and secretory product antigens using monoclonal and polyclonal antibodies on *Hermissenda* sensory and neurosecretory neurons *in situ*, and in cell culture. Toxicity studies on heavy metal effects on *Hermissenda* learning and physiology of cultured neurons are also being conducted.

Additional collaborative research includes DNA fingerprinting of *Hermissenda* using RAPD-PCR techniques in preparation for genetic strain development, as well as chemical ecological studies of the roles natural products play in larval metamorphosis and predator-prey recognition and defense mechanisms. Systematic and taxonomic studies of nudibranch mollusks are also of interest.

Staff

Kuzirian, Alan M., Associate Scientist
Tamse, Catherine T., Research Assistant

Visiting Investigators

Avila, Conxita, Postdoctoral Associate, Centre d'Estudis Avançats de Blanes, Blanes, Spain
Chikarmane, Hemant, Assistant Scientist, MBL
Leighton, Stephen B., Biomed. Engineering/Instrumen. Branch, NCRR-NIH

Laboratory of Rudolf Oldenbourg

The laboratory develops advanced instrumentation in light microscopy and investigates physical optics relevant to microscope imaging for high resolution studies of architectural dynamics in living cells and cell components. The current focus of the laboratory is the development of a new polarized light microscope that combines microscope optics with new electro-optical components, video, and digital image processing for fast analysis of specimen birefringence over the entire viewing field at the highest resolution of the light microscope. Biological systems currently investigated with the new pol-scope are microtubule-based structures (mitotic spindles, asters, single microtubules), striated muscles (myofibril), and virus liquid crystals.

Staff

Rudolf Oldenbourg, Associate Scientist
Guang Mei, Research Associate
Robert Knudson, Instrumentation Engineer

Laboratory of Nancy Rafferty

This laboratory investigates the role of the lens cytoskeleton and its associated proteins in the maintenance of lens shape, in lens accommodation and development of cataract when the cytoskeleton is disrupted. Studies include an assessment of the role of cytosolic free calcium on homeostasis of the lens cytoskeleton, the localization of various cytoskeletal proteins in lens epithelium, and determination of the relative amounts of soluble actin to filamentous actin in lens cells during aging. Most of these studies employ an elasmobranch fish and rabbit model using primary cultures of lens epithelium and electron and immunofluorescence microscopy.

Staff

Rafferty, Nancy S., Scientist, Northwestern University
Rafferty, Keen A., Research Associate

Laboratory of Sensory Physiology

Since 1973, the Laboratory has conducted research on various facets of vision. Current investigations focus on structural, functional, and mechanistic aspects of visual pigments. The chemical basis of color vision is investigated principally with light-microscope-based absorption spectroscopy. In addition to fresh preparations from fish and amphibians, *in vitro* model systems are studied with infrared and other spectroscopic techniques. The aim is a thorough understanding of the chemistry that underlies spectral tuning.

Staff

Harosi, Ferenc I., Associate Scientist, MBL, and Boston University School of Medicine

Visiting Investigator

Sándorfy, C., Université de Montréal, Canada

Laboratory of Osamu Shimomura

Biochemical mechanisms involved in the bioluminescence of various luminous organisms are investigated. Based on the results obtained in this laboratory, improved forms of bioluminescent probes are designed and produced for the measurements of intracellular free calcium and superoxide anion.

The toadfish

Staff

Shimomura, Osamu, Senior Scientist, MBL, and Boston University School of Medicine
Shimomura, Akemi, Research Assistant

Laboratory of Raquel Sussman

We investigate the molecular mechanism of DNA damage-inducible functions in *E. coli*. Present studies deal with novel genes that affect radiation-induced mutagenesis and analysis of RecA functions. In addition, we have been developing techniques for genomic mapping and collaborating in the isolation of neuronal genes in squid.

Staff

Sussman, Raquel, Associate Scientist

Visiting Investigators

Gwen Szent-Gyorgyi
Berberian, Graciela, Instituto de Investigacion Medica, Cordoba, Argentina

Molecular Evolution of Genomes

Research in this laboratory focuses on the molecular evolution and gene expression in the bacterium *Escherichia coli*. In a collaborative effort, a database containing information on the intermediary metabolism and biochemical pathways of *E. coli* is being developed. When completed, this database is expected to contain information on each metabolic reaction, the enzyme, the reactants, products, cofactors, activators, inhibitors, kinetics, equilibrium constants, binding constants, etc.

Related research is on the evolution of the *E. coli* DNA and organization of the genes in the chromosome. Comparative nucleotide and amino acid sequence data provide information on the evolutionary relationships of *E. coli* genes to other genes in the *E. coli* genome and to homologous genes in related bacteria.

Staff

Riley, Monica, Senior Scientist
Pellegrino-Toole, Alida, Research Assistant

Molecular Evolution Program

Molecular biology has shifted studies of early evolution and biodiversity from the arena of hypothetical scenario to one of experimental science. The comparison of genetic elements that have been transmitted from generation to generation makes possible the measurement of genetic differences between members of populations, species, and even between kingdoms of organisms. These measurements permit inference of the very same evolutionary framework in which morphological and biochemical differences among organisms arose and provides a practical metric to assess biodiversity.

This laboratory relies upon structural studies of ribosomal RNAs and actin genes to measure genetic differences between divergent taxa. As a result our understanding of the universal tree of life is very different from the plant-animal dichotomy articulated by early systematists or today's text book standard, the "Five Kingdoms" (plants, animals, fungi, protists and bacteria). Instead of being relatively recent biological inventions, eukaryotes appear to represent a discrete lineage that may be as old as the archaebacterial and eubacterial lines of descent. The earliest branching lineages are represented by protists that lack mitochondria and live in the near absence of oxygen. Compared to more derived eukaryotes, these organisms have simple cytoskeletons and membrane networks instead of a well-organized Golgi apparatus. In addition to the early branching patterns, boundaries separating major eukaryotic groups have been redefined. The three "higher" kingdoms (Fungi, Plantae, and Animalia) are now joined by two novel complex evolutionary assemblages, the "Alveolates" (ciliates, apicomplexans, and dinoflagellates) and the "Stramenopiles" (oomycetes, labyrinthulids, xanthophytes, phaeophytes, chrysophytes, and diatoms). Both assemblages include numerous marine organisms of ecological and economical importance; their phenotypic diversity is roughly equivalent to that seen in the other eukaryotic kingdoms. More remarkably, fungi and animals must have shared a recent common ancestry exclusive of any other eukaryotic groups.

Recently we have integrated our studies of rRNA evolution into microbial ecology and biodiversity projects. We have demonstrated a co-evolution between fungal symbionts and leaf-cutting ants that has lasted for more than 80 million years. In collaboration with the Ecosystems Center we are using molecular techniques to catalog prokaryotic populations in Toolik Lake in Alaska. Other efforts are directed towards population and systematic studies of brachiopods and lobsters.

Staff

Sogin, Mitchell L., Director and Senior Scientist
Hinkle, Greg, Postdoctoral Research Associate
Leipe, Detlev, Postdoctoral Research Associate
Morrison, Hilary G., Postdoctoral Research Associate
Silberman, Jeffrey, Postdoctoral Research Associate

Visiting Investigator

Barnhisel, Rae, Postdoctoral Sloan Fellow

National Vibrating Probe Facility

This Facility develops and makes available techniques for the non-invasive measurement of trans-membrane ion flux. Two types of systems are now housed in the Facility for general use; they are the non-invasive voltage probe (NVP_{PD}) and the non-invasive ion-selective probe (NVP_I). In both cases the vibration of the probes results in a highly sensitive self-referencing electrode with vibration-coherent signals being averaged and abstracted from noise. Both techniques are primarily utilized in the study of steady-state currents. The NVP_{PD} is the more sensitive, measuring nanovolt fields relating to net current flow across membranes of tissues and cells. The NVP_I has the added advantage of measuring the net flux of individual ions and, being based on commercially available ionophores, is broadly applicable. Further, it is one of the few methods available for measuring the movements of ions involved in non-electrogenic transport, for example the activity of pumps and porters.

The weak voltages associated with relatively steady-state currents reflect numerous aspects of cell physiology important in normal conditions. Frequently these currents are perturbed by disease or damage. Our current applications reflect the diversity of function. Single cell studies are numerous, and include research on proton and potassium-linked regulation in oxyntic cells of the stomach wall, free-radical-induced perturbation of neuronal calcium homeostasis, 2nd messenger regulation of trans-membrane ion flux, lead toxicity and developmental currents from oocytes and embryos. Ion regulation at the tissue and organismal level are also being studied, particularly with reference to the regulation of the brain microenvironment, hearing, and tissue regeneration.

Two new systems are in development. The first is the vibrating BioKelvin probe which will measure the weak fields around tissue in a gaseous environment. Our specific goal is to use this new machine in the study of skin. Also under development is a vibrating oxygen probe which will be used in the study of cell respiration.

Staff

Jaffe, Lionel F., Director Emeritus
Smith, Peter J. S., Director
Hammar, Katherine, Research Assistant
Land, Stephen C. Lakian Fellow
McLaughlin, Jane A., Research Assistant
Sanger, Richard H., Senior Electronics Technician
Shipley, Alan M., Research Associate

Sabbatical Visitors

Kunkel, Joseph G., University of Massachusetts, Amherst
Ryan, James, Hobart and William Smith College

Visiting Investigators

Allen, Nina, Wake Forest
Aloulou, Amine, Institut National Agronomique, Paris-Griguon
Baikie, Iain, Aberdeen, UK
Brown, Dennis, Harvard Medical School/Mass General Hospital
Demarest, Jeffery, Juniata College
Devlin, Leah, Penn State University
Estee Lauder Co.
Fishman, Harvey, University of Texas, Galveston
Hill, Susan, Michigan State
Hill, Robert B., University of Rhode Island
Huebner, Erwin, University of Manitoba, Winnipeg
Keefe, David, Yale University School of Medicine
Leech, Colin, Harvard Medical School/Mass General Hospital
Rahemtulla, Firoz, University of Alabama
Tytell, Michael, Wake Forest
Wall, Betty, Independent Investigator
Yamoah, Ebenezer, Johns Hopkins University, School of Medicine

Honors

Friday Evening Lectures

Jon Miller, Chicago Academy of Sciences, June 24, *"The Public Understanding of Basic Biomedical Concepts"*
George Langford, Dartmouth College, July 1, *"Actin-Dependent Movement of Organelles in the Squid Giant Axon"*
Walter Freeman, University of California, Berkeley, July 8 (Lang Lecturer), *"Some Thoughts on a Role for Music in the Neurobiology of Learning"*
Thomas Eisner, Cornell University, July 15, *"The Hidden Value of Nature"*
Zach Hall, University of California, San Francisco, July 21, 22 (Forbes Lecturer), *"How Nerves Talk to Muscles During Synapse Function: the Role of Agrin"* and *"The Nicotinic Acetylcholine Receptor: Putting it all Together"*
Carla Shatz, University of California, Berkeley, July 29 (Monsanto Lecturer), *"Order From Disorder in Visual System Development"*
Harold Varmus, National Institutes of Health, August 5 (Glassman Lecturer), *"New Direction at the NIH"*
Stephen O'Brien, National Cancer Institute, August 12, *"Retracing the Natural History of Endangered Species: Lessons From the Big Cats"*
Evelyn Fox Keller, Massachusetts Institute of Technology, August 19, *"Gender, Language, and Science"*

Fellowships and Scholarships

In 1994, the MBL awarded research fellowships amounting to $156,922 to 17 scientists from around the world who investigated topics ranging from the physiological regulation of muscle contraction to the biochemical analysis of ion exchange in nerves to the effect of nutrient loading on fish production in local estuaries. Scholarship support amounting to $357,162 was awarded to 131 students in the MBL's six summer courses.

Donors who made a gift to the Fellowship and Scholarship Programs during 1994 are noted below. Those individuals who received fellowships and scholarships follow.

Robert Day Allen Fellowship

Drs. Jean M. and Joseph W. Sanger

American Society for Cell Biology Scholarships

Dr. Elizabeth Marincola

Frederik B. Bang Fellowship Fund

Mrs. Betsy G. Bang

Charles R. Crane Fellowship Fund

Ms. Judith E. Casey

The Jean and Katsuma Dan Fellowship Fund

Dr. and Mrs. Teru Hayashi
Mrs. Eleanor Steinbach

Bernard Davis Fellowship and Scholarships

Mr. and Mrs. Harold Abrams
Dr. Porter W. Anderson, Jr.
Mrs. Ann S. Butler
Drs. Herman N. Eisen and Natalie A. Aronson
Mr. and Mrs. Robert H. Silsbee
Dr. and Mrs. Edward O. Wilson

Aline D. Gross Scholarship Fund

Mr. and Mrs. Alfred Weisberg

Ann E. Kammer Memorial Fellowship Fund

Mr. Richard M. Eakin
Ms. Jean G. Malamud
Ms. Jane E. Schroeder

Stephen W. Kuffler Fellowship

Drs. Clay M. and Clara F. Armstrong

Lakian Postdoctoral Scholar

Lakian Foundation

Lakian Summer Fellowships

Lakian Foundation

MBL Research Fellowships

Dr. and Mrs. Shinya Inoué
Dr. and Mrs. J. P. Trinkaus

James A. and Faith Miller Fellowship Fund

Dr. Gwynn C. Akin
Drs. Madeline P. and William D. Burbanck
Mr. and Mrs. Hubert W. Burden
Dr. E. Robert Burns
Prof. and Mrs. Donald Eugene Copeland
Mr. and Mrs. James L. Culberson
Dr. and Mrs. Rolland Golden
Dr. and Mrs. Richard G. Hibbs
Mr. and Mrs. Felix Inigo
Dr. Kenneth H. Jones
Mr. and Mrs. Andrew Lees
Mrs. Charles Levie
Ms. Barbara Baker Louden
Dr. and Mrs. John J. Martinek
Mr. and Mrs. Dennis J. McLane
Mr. and Mrs. David A. Miller
Mr. and Mrs. Edward A. Miller
Cdr. and Mrs. James P. Miller
Mr. and Mrs. John Oberpriller
Dr. John E. Pauly
Dr. and Mrs. Dwight E. Phillips
Mr. and Mrs. Richard D. Rink
Dr. and Mrs. S. Meryl Rose
Ms. Helen M. Rosenthal
Ms. Susan L. Rosenthal
Dr. and Mrs. Charles M. Roser, Sr.
Mr. and Mrs. Herbert Shanker
Dr. and Mrs. Philip Sieg
Mr. Robert G. Summers, Jr.
Mr. and Mrs. John Valois
Mr. and Mrs. William P. Wood
Dr. and Mrs. Rizkalla Zakhary

Mountain Memorial Fund

Mr. and Mrs. Dean C. Allard, Jr.
Mr. Scott M. Allard
Dr. Garland E. Allen
Ms. Brenda J. Bodian
Ms. Elinor W. Bodian
Ms. Helen Bodian & Mr. Roger Alcaly
Mr. and Mrs. Donald Carroll
Ms. Mildred S. Carson
Mr. and Mrs. Robert W. Cavenagh
Dr. and Mrs. Gary S. Cohen
Mr. and Mrs. Brewster H. Gere, Jr.
Mr. and Mrs. R. G. Gillette
Ms. Elizabeth J. Goulett
Dr. and Mrs. Harlyn O. Halvorson
Ms. Lois Hoffman
Mr. and Mrs. Alan J. Jacobsen
Mrs. Virginia Stokes Jones
Dr. and Mrs. Benjamin Kaminer
Ms. Anne C. Kimball
Mr. Kenneth H. Lange
Ms. Charlotte Z. LeMay
Ms. Kathryn H. Miller
Mr. and Mrs. James E. Milligan
Dr. Isabel Mountain
Ms. Helen T. North
The Grace Jones Richardson Trust
Mr. and Mrs. Thomas H. Roberts
Mr. and Mrs. Henry J. Rose
Dr. Joel L. Rosenbaum
Dr. and Mrs. Robert G. Savarese
Dr. and Mrs. R. Walter Schlesinger
Mr. and Mrs. Herbert G. Sparrow
Mr. and Mrs. John W. Stewart
Dr. and Mrs. William N. Thomas
Mrs. Roberta Tracy
Mr. and Mrs. George E. Webster
Mr. and Mrs. Andrew Yen

Nikon Fellowship

Nikon, Inc.

Science Writing Fellowships Program

The American Academy of Neurology
The American Association of Immunologists
The American Federation for Clinical Research
The American Society for Biochemistry and Molecular Biology
The American Society for Cell Biology
The American Society for Investigative Pathology
American Society for Microbiology
The American Society for Neurochemistry, Inc.
Association of Anatomy, Cell Biology, and Neurobiology Chairpersons
Association for Research in Vision and Ophthalmology
Burroughs Wellcome Fund
Foundation for Microbiology
Friendship Fund
John S. and James L. Knight Foundation
Merck & Company, Inc.
Society for Neuroscience

We are also grateful to the Charles A Dana Foundation for its continued support of this program.

The Moshe Shilo Memorial Scholarship Fund

Dr. and Mrs. Harlyn O. Halvorson
Dr. and Mrs. J. Woodland Hastings
Dr. and Mrs. Laszlo Lorand

Howard A. Schneiderman Scholarship

Mrs. Howard Schneiderman

The Evelyn and Melvin Spiegel Fellowship Fund

Drs. Jean and Joseph W. Sanger
Drs. Evelyn and Melvin Spiegel

H. B. Steinbach Fellowship

Mrs. H. Burr Steinbach
Mr. and Mrs. Volker Ulbrich

Marjorie W. Stetten Scholarship Fund

Dr. and Mrs. W. Redwood Wright

Horace W. Stunkard Fellowship

Dr. and Mrs. Albert J. Stunkard

The Walter L. Wilson Endowed Scholarship Fund

Mr. and Mrs. Larry McLean
Mr. and Mrs. Raymond Rapaport
Mrs. Marian Rigaumont
Dr. Jean Wilson
Mr. and Mrs. Ross A. Wilson
Mr. and Mrs. Wayne V. Wilson

Young Scholars/Fellows Program

Dr. Frank M. Child, III
Mr. and Mrs. Leonard D. Friedman
Dr. and Mrs. Laszlo Lorand
Dr. and Mrs. Jerry M. Melillo
Mr. and Mrs. John R. Peterson

Philip H. Presley Memorial Scholarships

Carl Zeiss, Inc.

Post-Course Research Support Provided by

Carl Zeiss Inc.
Universal Imaging Corporation

Fellowships Awarded

MBL Summer Research Fellows

• Joshua R. Berlin, a *Lakian Research Fellow*, is a Research Scientist at the Bockus Research Institute in Philadelphia, PA. Berlin looked at local calcium transients during muscle excitation-contraction coupling.

• Graciela Elso de Berberian, a *Frederik B. Bang Fellow*, is a Research Associate at the Instituto M y M. Ferreyra, Argentina. Elso de Berberian studied the biochemical characterization of Na^+/Ca^{++} exchanger in nerve cells.

• Mariano Garcia-Blanco, a *William Townsend Porter Fellow*, is an Assistant Professor at Duke University Medical Center. Garcia-Blanco examined rRNA trafficking.

• Fatima Gyoeva, funded by the *Lucy B. Lemann Fellowship Fund and the MBL Research Fellowship Fund*, is an investigator at the Russian Academy of Sciences Institute of Protein Research. Gyoeva used biochemical and immunochemical methods to identify kinesin receptors in fish melanophores.

• Valerie A. Hall, supported by the *Frank A. Brown Memorial Fund and the John O. Crane Fellowship Fund*, is a high school teacher in Nantucket, MA. Hall spent her summer writing a high school oceanography/marine biology textbook.

• Jonathan J. Henry, an *MBL Associates Fellow*, is an Assistant Professor at the University of Illinois. Henry analyzed cell lineage of the nemertean, *Cerebratulus lacteau*. Specifically, he considered the evolution of spiralian development.

• Mary Constance Lane, supported by *the Evelyn and Melvin Spiegel Fellowship Fund, the H. B. Steinbach Fellowship Fund, the MBL Associates Fellowship Fund, the James A. and Faith Miller Fellowship Fund, and the MBL Research Fellowship Fund*, is a Postdoctoral Fellow from the University of California, Berkeley. Lane looked at the role of microtubules in morphogenesis.

• William Lemon, a *Lakian Research Fellow*, is a Postdoctoral Fellow from the University of Arizona. Lemon optically recorded magnetically induced neural activity in the brain of the honeybee, *Apis mellifera*.

• Vladimir I. Makarenko, a *James S. McDonnell Foundation Fellow*, is a Physicist from the Russian Academy of Sciences Institute of Mathematical Problems of Biology, Laboratory of Neural Networks in Russia. While at the MBL, Makarenko used computers to model neural networks.

• Anthony Maranto, supported by the *Frank R. Lillie and the MBL Fellowship Funds*, is an Assistant Professor at Tufts University Medical School. Maranto examined the characterization and function of biochemical receptors in surf clams and sea urchins.

• Stephen Moorman, funded by the *Stephen W. Kuffler and the Lucy B. Lemann Fellowship Funds*, is an Assistant Professor at the UNT Health Science Center at Fort Worth, TX. Moorman studied oligodendrocyte interactions during development.

• Andrew Murray, a *Nikon Inc. Fellow*, is an Assistant Professor at the University of California, San Francisco. Murray used high resolution microscopy to study mitosis in extracts from frog eggs and yeast.

• Knud Nierhaus, funded by the *MBL Associates and the Herbert W. Rand Fellowship Funds*, is a Professor at the Max Planck Institute for Molecular Genetics in Germany. He worked on his book, *Translation of the Genetic Message*, which deals with protein biosynthesis.

• Haohua Qian, a *Bernard Davis Fellow*, is a Postdoctoral Fellow at Harvard University. Qian, a neurobiologist, looked at the properties of GABA receptors on the glial cells of the skate retina.

• Edward Salmon, a *Herbert W. Rand Fellow*, is a Professor at the University of North Carolina, Chapel Hill. Salmon, a cell biologist, used high resolution microscopy to study mitosis in extracts of frog eggs and yeast.

• Rafael Sardá, an *MBL Associates Fellow*, is a scientist at the Centro de Estudios Avanzados de Blanes, Spain. Sarda, an ecologist, studied nutrient loading in the watersheds of Waquoit Bay. Specifically, he looked at the effect of nutrient loading on benthic invertebrate assemblages.

• Cristina Zago, an *MBL Associates Fellow*, is a researcher at the Instituto per lo Studio della Dinamica delle Grandi Masse in Venice, Italy. Zago analyzed heavy metal distribution in porewaters using various chemical equilibrium computer models.

Grass Fellows

• Yang Dan, Columbia University. Dan engaged in optical studies of electrical activity in a circuit of neurons.

• Graeme W. Davis, University of Massachusetts, Amherst. Davis examined functional synaptic specificity and the activity of the calcium-activated potassium channel at the *Drosophila* neuromuscular junction.

• Guoping Feng, State University of New York, Buffalo. Feng performed a functional analysis of tipE, a mutation affecting sodium channels in *Drosophila*.

• Elizabeth Ann Finch, Harvard Medical School. Finch studied molecular mechanisms of synaptic plasticity.

• Miguel Holmgren, Chicago Medical School. Holmgren examined charge translocation by the NA^+/K^+ pump in internally perfused squid giant axon.

• Rebecca M. Johnston, University of Arizona. Johnston looked at the developmental fate and modulation of rhythmic motor patterns in the hawkmoth, *Manduca sexta*.

• Lucas D. Pozzo Miller, Roche Institute of Molecular Biology. Miller examined integrative properties of the first order giant neurons from the ganglion magnocellularis of the squid, *Loligo pealei*.

• Lisa K. Moore, Albert Einstein College of Medicine. Moore studied horizontal cell gap junctional communication in teleost retina, and, specifically, modulation by retinoic acid.

• Felix E. Schweizer, Stanford University Medical Center. Schweizer examined the role of interactions between a-SNAP and synaptotagmin/p65 for neurotransmitter release at the giant synapse of the squid, *Loligo pealei*.

• Andrew A. Sharp, Brandeis University. Sharp studied the role of synaptic inhibition and I_h in controlling the heartbeat oscillator in the leech, *Hirudo medicinalis*.

• Eric C. Sobel, AT&T Bell Laboratories. Sobel looked at the anatomical and physiological characterization of visual space constancy neurons in the crayfish.

• Ebenezer N. Yamoah, University of Texas HSC at Houston. Yamoah examined calcium fluxes in the photoreceptors and cultured neurons of the sea slug, *Hermissenda crassicornis*.

Science Writing Fellows

Pallava Bagla, Publications & Information Directorate, India
Yvonne Baskin, Freelance
Cara Birrittieri, New England Cable News
Giovanna Breu, *People* magazine
Matthew Crenson, *Dallas Morning News*
Dian Duthie, CBC-TV Newsday, Canada
Alberto Enriquez, *Mail Tribune*
S. Paul Gasek, Stony Brook Films
Scott LaFee, *San Diego Union-Tribune*
Ed Regis, Freelance
Richard Saltus, *The Boston Globe*
Richard Stone, *Science* magazine
Mutsumi Yoshida, *Newton* magazine, Japan
David Zimmerman, *PROBE*

Scholarships Awarded

Bernard Davis Scholarship Fund

Michael Cerio, University of Connecticut
Ilka Faath, University of Bonn, Germany
Ute Muh, Phillipps-Universitat Marburg, Germany

Daniel S. Grosch Scholarship Fund

Paula van Schie, Rutgers University

Frank R. Lillie Scholarship Fund

Smaranda Burlacu, University of Texas
Martin Garcia-Castro, Wellcome/CRC Institute, UK
Akemi Hanamura, Cold Spring Harbor Laboratory
Ole Kjaerulff, Copenhagen University, Denmark

William Townsend Porter Scholarship Fund

Max Boakye, National Institutes of Health
ShaAvhree Buckman, Washington University School of Medicine
Ana DePina, Dartmouth College
Mildred Morales, Albert Einstein College of Medicine
Wendy Reed, Johns Hopkins University
James Scott, Center for Great Lakes Studies
Andrea Torres-Perez, Stanford University
Madeline Vargas, University of Connecticut

Herbert W. Rand Scholarship Fund

Ruth Empson, University of Koln, Germany
Martin Garcia-Castro, Wellcome/CRC Institute, UK
Patricio Huerta, Brandeis University
Boris Kablar, University of Pisa, Italy
Ole Kjaerulff, Copenhagen University, Denmark
Peter Kloppenburg, University of Arizona
Oana Marcu, University of Western Ontario, Canada
Christophe Pouzat, Ecole Normale Superieure, France
Fabrice Roegiers, Station Zoologique, France
Eric Scarfone, University of Montpellier, France
Dinesh Vernool, Rutgers University
Karen Yeow, University of Manitoba, Canada

American Society for Cell Biology Scholarships

ShaAvhree Buckman, Washington University School of Medicine
Ana DePina, Dartmouth College
Mildred Morales, Albert Einstein College of Medicine
Wendy Reed, Johns Hopkins University
James Scott, Center for Great Lakes Studies
Andrea Torres-Perez, Stanford University
Madeline Vargas, University of Connecticut

Biology Club of the City of New York Scholarship Fund

Sowmyalakshmi Rasika, Rockefeller University

Father Arsenius Boyer Scholarship Fund

Akemi Hanamura, Cold Spring Harbor Laboratory
Stefan Schuster, Max Plank Institute, Germany

C. Lalor Burdick Scholarship Fund

Boris Kablar, University of Pisa, Italy

Gary N. Calkins Scholarship Fund

Melchiorre Cervello, Instituto di Biologia dello Sviluppo del Consiglio, Italy

Frances S. Claff Scholarship Fund

Melchioore Cervello, Instituto di Biologia della Sviluppo del Consiglio, Italy

Edwin Grant Conklin Scholarship Fund

Melchiorre Cervello, Instituto di Biologia della Sviluppo del Consiglio, Italy
Daniel Martinez, University of California, Irvine

Lucretia Crocker Scholarship Fund

Peter Kloppenburg, University of Arizona
Adrian Salic, Harvard University

William F. and Irene C. Diller Scholarship Fund

Xiaohua Gong, Scripps Research Institute
Boris Kablar, University of Pisa, Italy

Caswell Grave Scholarship Fund

Frederic Ampe, Laboratoire de Physiologie, INSA, France
Max Boakye, National Institutes of Health
Ruth Empson, University of Koln, Germany
Paula van Schie, Rutgers University

Aline D. Gross Scholarship Fund

Ruth Empson, University of Koln, Germany
Sowmyalakshmi Rasika, Rockefeller University

William Randolph Hearst Educational Endowment Scholarships

John Allison, Vanderbilt Medical School
Catherine Brennan, University of Southern California
Dawn Konrad, University of Washington
Elizabeth Laxson, University of Wisconsin, Madison
Christi Magrath, Tulane University Medical Center
Sarah McHatton, University of California, Davis
Julie Olson, University of North Carolina
Debra Tumbula, University of Georgia

Howard Hughes Medical Institute Educational Program Scholarship Funding

Mark DeSouza, University of Southern California
Patricio Huerta, Brandeis University
Radma Mahmood, Guy's Hospital, UK
Sandra Marques, George Washington University
Annette Neubuser, Max Planck Institute, Germany
Sandra Nicola, Carol Davila University of Medicine
Christophe Pouzat, Ecole Normale Superieure, France
Manisha Raje, University of Kansas
Stefan Schuster, Max Planck Institute, Germany
Shiri Venezia, Tel Aviv University, Israel
James Walker, University of Cambridge, UK

Merkel H. Jacobs Scholarship Fund

James Walker, University of Cambridge, UK

Arthur Klorfein Scholarship Fund

Anna Di Gregorio, Anton Dohrn Stazione Zoologica, Italy
Martin Garcia-Castro, Wellcome/CRC Institute, UK
Xiaohua Gong, Scripps Research Institute
Daniel Martinez, University of California, Irvine
Stefan Schuster, Max Planck Institute, Germany

Jacques Loeb Founders' Scholarship Fund

Luis Vidali, University of Massachusetts, Amherst

John D. and Catherine T. MacArthur Foundation Scholarships

Billy Apola, National Museums of Kenya, Kenya
Hani Atamna, Hebrew University, Israel
Leonard Basco, University of Paris, France
Socrates Herrera Valencia, Universidad del Valle, Columbia
Laura Knoll, Washington University
Susan Little, University of Georgia
Stephen Manale, Louisiana State University
Deborah Schechtman, Weizmann Institute of Science, Israel
Andrea Smith, University of Alabama
Martine Soete, INSERM, France
Andrea Torres-Perez, Stanford University
Henri van der Heyde, University of Wisconsin, Madison
Fred van Leeuwen, Netherlands Cancer Institute
Ulrike Zelck, University of Hamburg, Germany
Xiaonong Zhou, Jiangsu Institute of Parasitic Diseases, China

S. O. Mast Memorial Fund Scholarships

Amanda Hayward-Lester, Texas Tech University
Luis Vidali, University of Massachusetts, Amherst

Allen R. Memhard Memorial Fund Scholarships

Melchiorre Cervello, Institute di Biologia dello Sviluppo del Consiglio, Italy

Michigan State University Center for Microbial Ecology Scholarship

James Scott, Center for Great Lakes Studies

James S. Mountain Memorial Fund, Inc. Scholarships

Robert Grant, University of California, San Francisco
Amanda Hayward-Lester, Texas Tech University

Peter Piepenhagen, Stanford University
Samara Reck-Peterson, University of Pennsylvania
Jennifer Smith-Hall, Indiana University School of Medicine

Planetary Biology Institute Scholarships

Mary Rothermich, University of Massachusetts
Marc van der Maarel, University of Groningen, Germany

Society for Developmental Biology Scholarships

Julie Kuhlman, Cornell Medical College
Elizabeth Laxson, University of Wisconsin, Madison
Ivan Moskowitz, University of Wisconsin, Madison
Kevin Peterson, University of California, Los Angeles
Melissa Shirley, Case Western Reserve University

Society of General Physiologists Scholarships

1993

Joshua Gold, Stanford University
Richard J. Kollman, University of Texas Southwestern Medical Center
Richard Mullins, University of Kentucky
Christopher Rose, Harvard University

1994

Michael S. Fee, AT & T Bell Laboratories
Martin Garcia-Castro, University of Cambridge, U.K.
Frederick B. Reitz, University of Washington
Karel Svoboda, AT & T Bell Laboratories

Moshe Shilo Memorial Scholarship Fund

Shiri Venezia, Tel Aviv University, Israel

Marjorie W. Stetten Scholarship Fund

Michael Cerio, University of Connecticut
Stefan Schuster, Max Planck Institute, Germany

William Morton Wheeler Family Founders' Scholarships

Max Boakye, National Institutes of Health
Christophe Pouzat, Ecole Normale Superieure, France

Philip H. Presley Memorial Scholarships

Maneesha Inamdar, Tata Institute of Fundamental Research, India
Teresa Nick, Yale University
Antonius Suwanto, Bogor Agricultural University

Board of Trustees and Committees

Corporation Officers and Trustees

Chairman of the Board of Trustees, Sheldon J. Segal, The Population Council, New York, NY
Vice Chairman of the Board of Trustees, Robert E. Mainer, The Boston Company, Boston, MA
President of the Corporation, James D. Ebert, Johns Hopkins University, Baltimore, MD
Director and Chief Executive Officer, John E. Burris, Marine Biological Laboratory, Woods Hole, MA*
Chair of the Science Council, George M. Langford, Dartmouth College, Hanover, NH*
Treasurer, Robert D. Manz, Helmer & Associates, Waltham, MA*
Clerk of the Corporation, Neil Jacobs, Hale and Dorr, Boston, MA

Class of 1998

John R. Lakian, The Fort Hill Group, Inc.
Joan V. Ruderman, Harvard Medical School
Sheldon J. Segal, The Population Council
Alfred Zeien, The Gillette Company

Class of 1997

Frederick Bay, Josephine Bay Paul and C. Michael Paul Foundation, Inc.
Martha W. Cox, Hobe Sound, FL
Mary J. Greer, Cambridge, MA
Thomas D. Pollard, John Hopkins Medical School
William C. Steere, Jr., Pfizer Inc.
Gerald Weissmann, New York University School of Medicine

Class of 1996

Norman Bernstein, Norman Bernstein Management, Inc.
Alexander W. Clowes, University of Washington School of Medicine
Eric H. Davidson, California Institute of Technology
Robert D. Goldman, Northwestern University Medical School
Paul A. Marks, Memorial Sloan-Kettering Cancer Center
Irving W. Rabb, Stop & Shop Company—*retired*

* *Ex officio*
† *Deceased*

Class of 1995

Mary-Ellen Cunningham, Grosse Pointe Farms, MI
Neil Jacobs, Hale and Dorr
Edward A. Kravitz, Harvard Medical School
Robert E. Mainer, The Boston Company

Honorary Trustees

William T. Golden, New York, NY
Ellen R. Grass, The Grass Foundation
Homer P. Smith, Woods Hole, MA†

Emeriti

Edward A. Adelberg, Yale University, New Haven, CT
John B. Buck, Sykesville, MD
Seymour S. Cohen, Woods Hole, MA
Arthur L. Colwin, Key Biscayne, FL
Laura Hunter Colwin, Key Biscayne, FL
D. Eugene Copeland, Marine Biological Laboratory, Woods Hole, MA
Sears Crowell, Indiana University, Bloomington, IN
Alexander T. Daignault, Boston, MA
Teru Hayashi, Woods Hole, MA
Ruth Hubbard, Cambridge, MA
Lewis Kleinholz, Reed College, Portland, OR
Maurice E. Krahl, Tucson, AZ
Charles B. Metz, Miami, FL
Keith R. Porter, University of Pennsylvania, Philadelphia, PA
C. Ladd Prosser, University of Illinois, Urbana, IL
S. Meryl Rose, Waquoit, MA†
W. D. Russell-Hunter, Syracuse University, Syracuse, NY
John W. Saunders, Jr., Waquoit, MA
Mary Sears, Woods Hole, MA
David Shepro, Boston University, Boston, MA
D. Thomas Trigg, Wellesley, MA
Walter S. Vincent, Woods Hole, MA
George Wald, Cambridge, MA

Science Council

George M. Langford, Chairman
Donald A. Abt
John E. Burris*

Ronald L. Calabrese
Neal W. Cornell (thru 8/94)
Barbara E. Ehrlich (thru 8/94)
John E. Hobbie (thru 8/94)
Shinya Inoué
Irwin B. Levitan
Knute Nadelhoffer (from 8/94)
Robert E. Palazzo
Robert B. Silver (from 8/94)
Mitchell Sogin (from 8/94)
Ann E. Stuart

Executive Committee of the Board of Trustees

Sheldon J. Segal, Chairman
Frederick Bay
John E. Burris*
Mary-Ellen Cunningham
Robert D. Goldman
George Langford*
Robert E. Mainer, Vice-Chairman
Robert Manz*
Thomas D. Pollard
Gerald Weissmann

Standing Committees of the Board of Trustees

Development

Mary-Ellen Cunningham, Chair
Robert Barlow
Fred Bay
Martha Cox
James Ebert
Neil Jacobs
John Lakian
Franklin Loew
William Speck
William Steere

Finance and Investment

Robert Mainer, Chairman
Norman Bernstein
Alexander Clowes
Eric Davidson
Donald DeHart
Neil Jacobs
John Lakian
Werner Lowenstein
Robert Manz
Irving Rabb

Nominating

Gerald Weissmann, Chairman
Alexander Clowes
Martha Cox
Mary-Ellen Cunningham
Mary Greer
George Langford
Thomas Pollard
Sheldon Segal
William Steere

Facilities and Capital Equipment

Robert Goldman, Chairman
Jelle Atema
Al Chaet
Frank Loew
Jerry Melillo
Joan Ruderman
Robert Silver

Long-Range Planning

Fred Bay, Co-Chair
Thomas Pollard, Co-Chair
Eric Davidson
John Dowling
Gerald Fischbach
Robert Goldman
Mary Greer
George Langford
Robert Manz
Joan Ruderman
Mitchell Sogin

Corporation Standing Committees

Buildings & Grounds

Alfred B. Chaet, Chairman
Barbara Boyer
Lawrence B. Cohen
Richard D. Cutler*
William Eckberg
Barry Fleet*
Ferenc Harosi
Joe Hayes*
Kenyon Tweedel

Fellowships

Thoru Pederson, Chairman
Kathleen Dunlap
John Rummel*

* *Ex officio*

Ann Giblin
José Lemos
Eduardo Macagno
Carol L. Reinisch

Housing, Food Service, and Child Care

Stephen Highstein, Chairman
Elaine Bearer
Donald C. Chang
Milton Charlton
Richard Cutler*
Robert Gould
Stephen Highstein
LouAnn King*
Daryl Stokes

Education

Ronald L. Calabrese, Co-Chair
Irwin Levitan, Co-Chair
Elaine Bearer
Dorianne Chrysler*
Vincent Dionne
Janet Heasman
Holger W. Jannasch
Michael E. Mendelsohn
John D. Rummel*
Steven J. Zottoli

MBL/WHOI Library Joint Advisory

David Shepro, Chair
Judith Ashmore, MBL*
Susan Berteaux, WHOI*

Henry Dick, WHOI
Kevin Friedland, NMFS
Steve Gegg, WHOI*
John Hobbie, MBL
Mark Kurz, WHOI
Catherine Norton, MBL/WHOI*
Monica Riley, MBL
Jim Robb, USGS
Peter J. S. Smith, MBL
Bruce Warren, WHOI

* *Ex officio*

Research Services

Peter Armstrong, Chairman
Neal Cornell
Richard Cutler*
Kenneth Foreman
Louis Kerr
William Kuhns
Andy Mattox*
James Quigley
John Rummel*
Peter J. S. Smith
Paul Steudler
Michael Tytell

Research Space

Hans Laufer, Chairman
Paul DeWeer
David Landowne
Eduardo Macagno
Andy Mattox*
Jerry M. Melillo
Robert Silver
Steven Treistman
Ivan Valiela
Richard Vallee

Laboratory Support Staff*

Biological Bulletin
Clapp, Pamela L., Managing Editor
Gibson, Victoria R.
McCaffrey, Karen

Controller's Office
Speer, John W., Controller

Accounting Services
Afonso, Janis E.
Binda, Ellen F.
Campbell, Ruth B.
Davis, Doris C.
Ghetti, Pamela M.
Gilmore, Mary F.
Hobbs, Roger W., Jr.
Lancaster, Cindy
Poravas, Maria

Chem Room
Schorer, Timothy M.
Shepherd, Denise M.

Purchasing
Hall, Lionel E., Jr.
Shepherd, Denise M.

Director's Office
Burris, John E., Director and CEO
Catania, Didia
Kaufmann, Sandra J.
Nelson, Mary F.
Leighton, Jane L.

External Affairs
Carotenuto, Frank C., Director
Aspinwall, Duncan P.
Berthel, Dorothy
Black, Nancy O.
Faxon, Wendy P.
Lessard, Kelley J.
Nelson, Mary F.

Associates Program
Armstrong, Ellen P., Liaison
Brown, M. Kathryn S., Gift Shop

Communications Office
Clapp, Pamela L., Director
Liles, Beth R.
Moorhouse, Laura A.

Housing
King, LouAnn D., Conference Center and Housing Manager
Barry, Maureen J.
Johnson, Frances N.

Telephone Office
Baker, Ida M.
Geggatt, Agnes L.
Mayne, Pamela
Ridley, Alberta W.

Human Resources
Goux, Susan P., Manager
Donovan, Marcia H.

Journal of Membrane Biology
Loewenstein, Werner R., Editor
Fay, Catherine H
Howard, Linda L.
Lynch, Kathleen F.

MBL/WHOI Library
Stonehill, David L., Director
Norton, Catherine N., Head Librarian
Ashmore, Judith A.
Costa, Marguerite E.
Drury, Eulalie A.
Mirra, Anthony J.
Nelson, Heidi
Pratson, Patricia G.
deVeer, Joseph M.
Zuwallack, Barbara A.
Zuwallack, Raymond J.
Zuwallack, Ronald L.

Copy Service Center
Mountford, Rebecca J., Supervisor
Barry, Maureen J.
Jesse, Martha V.
LaPlante, Robert F.
Mancini, Mary E.
Tebeau, Christopher

Information Systems Division
Norton, Catherine N., Director
Hamre, Lynne
Remsen, David
Renna, Denis J.
Space, David B.
Tollios, Constantine D.

Safety Services
Mattox, Andrew H., Environmental, Health, and Safety Manager

Services, Projects, and Facilities
Cutler, Richard D., Manager
Enos, Joyce B.

* *Including persons who joined or left the staff during 1994*

Apparatus
Barnes, Franklin D.
Haskins, William A.

Building Services and Grounds
Hayes, Joseph N., Superintendent
Allen, Wayne D.
Anderson, Lewis B.
Barnes, Susan M.
Beaudoin, Helen
Boucher, Richard L.
Callahan, John J.
Collins, Paul J.
Dorris, John J.
Dutra, Roger S., Jr.
Gibbons, Roberto G.
Gonsalves, Nelson
Illgen, Robert F.
Krajewski, Viola I.
Luther, Herbert
Lynch, Henry L.
Mancini, Mary E.
McNamara, Noreen M.
Rattacasa, Frank D.
Serrano, Robert A.

Plant Operations and Maintenance
Fleet, Barry M., Superintendent
Barnes, John S.
Blunt, Hugh F.
Bourgoin, Lee E.
Carini, Robert J.
Carroll, James R.
Fish, David L., Jr.
Fuglister, C. Kurt
Gonsalves, Walter W., Jr.
Hathaway, Peter J.
Justason, C. Scott
Lochhead, William M.
Lunn, Alan G.
McAdams, Herbert M. III
McHugh, Michael O.
Mills, Stephen A.
Olive, Charles W., Jr.
Schoepf, Claude
Serrano, Robert A.
Sexton, Andrew

Machine Shop
Sylvia, Frank E.

Marine Resources Center
Enos, Edward G., Jr., Superintendent
Boucher, Richard L.
Cipoletta, Charles D.
Fisher, H. Thomas, Jr.
Grossman, William M.
Moniz, Priscilla C.
Sexton, Andrew W.
Sullivan, Daniel A.
Tassinari, Eugene

MRC Life Support System
Mebane, William N., Systems Operator
Hanley, Janice S.

Photolab
Golder, Linda M.
Golder, Robert J.

Research Administration & Educational Programs

Rummel, John D., Director
Chrysler, Dorianne
Hamel, Carol C.
Huffer, Linda
Hunt, Sharon L.
Kaufmann, Sandra J.
Lynch, Kathleen F.

Central Microscopy Facility
Kerr, Louis M.

Temporary Employees

Michael Baptiste
DeGiorgis, Joseph A.
DiPasqua, Andrew K.
Gilbrook, Maggie M.
Mansfield, Darren P.
O'Connor, Patricia M.
Paris, Susan J.
Stukey, Jetly
Till, Geoffrey A.

Summer Support Staff

Andrews, Ethan
Andrews, Mark
Antonangeli, Donald, Jr.
Atwood, Karl M.
Baldic, David P.
Berrios, Kelly L.
Bolton, Jason D.
Boyer, Paul L.
Cameron, Lawrence M.
Chappell, Carol L.
Crabb, Andrew H.
Cutler, Laura
DeLinks, Elisabeth
DeMenil, Ben
Diachun, Peter J.
Fitton, Robert R.
Greenfield, Benjamin
Halfant, Jennie A.
Higham, Benjamin T.
Horne, Joseph M.
Jearld, Saba A.
Just, Thomas E.
Kagoyire, Diane B.
Kay, Paul A.
Kilpatrick, Andrew J.
Kilpatrick, Brian
Langford, George II
Lewis, Barry
Lovell, Lynne
Luther, Jonathan A.
Melillo, Edward D.
Michael, Samuel A.
Monteiro, Salvatore
Moyer, Lisa A.
Nelson, Beth
O'Connor, John E.
Ordway, Cheryl C.
Pennington, Marc
Price, Elizabeth C.
Rakowski, Cara E.
Regan, John F.
Richmond, Hazel E.
Roache, Kathryn H.
Sacks, Audrey B.
Saintours, Frederick H., Jr.
Shephard, Jillian M.
Smith, Mandy L.
Snow, Jason M.
Sonnabend, Aaron P.
Stephen, Michael J.
Tong, Cherry
Ulbrich, Ciona
Varao, John
Welch, Christine E.
Welenc, Karen P.
Wetzel, Ernest D.
Woitkiewicz, Mark D.

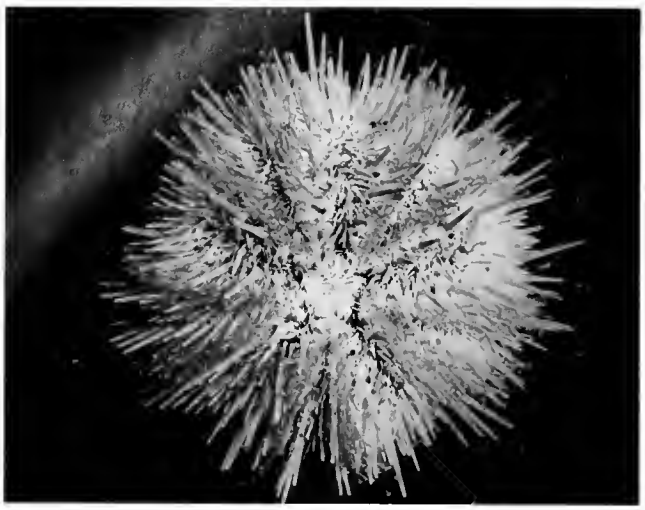

Members of the Corporation*

Life Members

Adelberg, Edward A., Peabody Museum, Yale University, New Haven, CT 06520
Amatniek, Ernest, 4797 Boston Post Road, Pelham Manor, NY 10803

Bang, Betsy G., 76 F.R. Lillie Road, Woods Hole, MA 02543
Bartlett, James H., Department of Physics, University of Alabama, Box 870324, Tuscaloosa, AL 35487-0324
Bernheimer, Alan W., Department of Microbiology, New York University Medical Center, 550 First Ave., New York, NY 10016
Bertholf, Lloyd M., Westminster Village #2114, 2025 E. Lincoln St., Bloomington, IL 61701-5995
Bosch, Herman F., Box 617, Woods Hole, MA 02543
Bridgman, A. Josephine, 913 Wesley Woods Towers, 1825 Clifton Rd., NE, Atlanta, GA 30329
Buck, John B., 7200 Third Ave., #C020, Sykesville, MD 21784
Burbanck, Madeline P., Box 15134, Atlanta, GA 30333
Burbanck, William D., Box 15134, Atlanta, GA 30333

Carlson, Francis D., Johns Hopkins University, Biophysics Department, Jenkins Hall, N. Charles Street, Baltimore, MD 21218
Clark, Arnold M., 53 Wilson Rd., Woods Hole, MA 02543
Cohen, Seymour S., 10 Carrot Hill Rd., Woods Hole, MA 02543-1206
Colwin, Arthur L., 320 Woodcrest Rd., Key Biscayne, FL 33149
Colwin, Laura Hunter, 320 Woodcrest, Key Biscayne, FL 33149
Cooperstein, Sherwin J., Professor Emeritus and Acting Head, Department of Anatomy, MC3405, University of Connecticut Health Center, 263 Farmington Avenue, Farmington, CT 06030-3405
Copeland, D. E., Marine Biological Laboratory, Woods Hole, MA 02543
Corliss, John O., P. O. Box 53008, Albuquerque, NM 87153
Costello, Helen M., Carolina Meadows, Villa 137, Chapel Hill, NC 27514
Crouse, Helen, Rt 3, Box 213, Hayesville, NC 28904

Dudley, Patricia L., 3200 Alki Avenue, SW, #401, Seattle, WA 98116

Edwards, Charles, 2244 Harbour Court Drive, Longboat Key, FL 34228
Erulkar, Solomon D., 318 Kent Road, Bala Cynwyd, PA 19004

Failla, Patricia M., 2149 Loblolly Lane, Johns Island, SC 29455
Ferguson, James K. W., 56 Clarkehaven St., Thornhill, Ontario L4J 2B4 Canada

Glusman, Murray, New York State Psychiatric Institute, 722 West 168th Street, Unit #70, New York, NY 10032
Goldman, David, 63 Loop Rd., Falmouth, MA 02540
Graham, Herbert, 36 Wilson Rd., Woods Hole, MA 02543
Green, James W., 409 Grant Ave., Highland Park, NJ 08904

Hamburger, Viktor, Department of Biology, Washington University, St. Louis, MO 63130
Hamilton, Howard L., Department of Biology, University of Virginia, 238 Gilmer Hall, Charlottesville, VA 22901
Harding, Clifford V., Jr., 54 Two Ponds Road, Falmouth, MA 02540
Haschemeyer, Audrey E. V., 21 Glendon Road, Woods Hole, MA 02543
Hauschka, Theodore S., FD1, Box 781, Damariscotta, ME 04543
Hisaw, F. L., 5925 SW Plymouth Drive, Corvallis, OR 97330
Hoskin, Francis C. G., % Dr. John E. Walker, United States Army Natick RD & E Center, SAT NC-YSM, Kansas Street, Natick, MA 01760-5020
Hubbard, Ruth, Biological Laboratories, Harvard University, Cambridge, MA 02138
Humes, Arthur G., Boston University Marine Program, Marine Biological Laboratory, Woods Hole, MA 02543
Hurwitz, Charles, Veterans Administration Hospital, Basic Science Research Laboratory, Albany, NY 12208

Karush, Fred, Department of Microbiology, University of Pennsylvania School of Medicine, Philadelphia, PA 19104-6076 (deceased)
Kingsbury, John M., Department of Plant Biology, Cornell University, Plant Science Building, Ithaca, NY 14853
Kleinholz, Lewis, Department of Biology, Reed College, 3203 SE Woodstock Blvd., Portland, OR 97202

Laderman, Ezra, Yale University, School of Music, New Haven, CT 06520
Laulfer, Max A., Address unknown
LeFevre, Paul G., 15 Agassiz Road, Woods Hole, MA 02543
Levine, Rachmiel, City of Hope Medical Center, Shapiro Building, Duarte, CA 91010
Lochhead, John H., 49 Woodlawn Rd., London SW6 6PS, England, UK

* Including action of the 1994 Annual Meeting.

Loewus, Frank A., Washington State University, Institute of Biological Chemistry, Pullman, WA 99164
Loftfield, Robert B., Department of Biochemistry, University of New Mexico School of Medicine, Albuquerque, NM 87131

Magruder, Samuel R., 270 Cedar Lane, Paducah, KY 42001
Malkiel, Saul, Allergic Diseases, Inc., 130 Lincoln St., Worcester, MA 01609
Martin, Lowell V., 10 Buzzards Bay Avenue, Woods Hole, MA 02543
Mathews, Rita W., Box 131, Southfield, MA 01259
Moore, John A., Department of Biology, University of California, Riverside, CA 92521
Moscona, Arthur A., University of Chicago, Department of Molecular Genetics and Cell Biology, 920 East 58th Street, Chicago, IL 60637
Mountain, Isabel, Arleigh Burke Pavilion, 1739 Kirby Road, McLean, VA 22101
Musacchia, Xavier J., P.O. Box 5054, Della Vista, AR 72714-0054

Nasatir, Maimon, P. O. Box 379, Ojai, CA 93024-0379

Pollister, A. W., 8 Euclid Ave., Belle Mead, NJ 08502
Porter, Keith R., 74 Pasture Lane, #319 Beaumont, Bryn Mawr, PA 19010
Prosser, C. Ladd, Department of Physiology, Burrill Hall 524, University of Illinois, Urbana, IL 61801
Prytz, Margaret McDonald, Address unknown

Ratner, Sarah, Department of Biochemistry, Public Health Research Institute, 455 First Ave., New York, NY 10016
Renn, Charles E., Address unknown
Reynolds, George, Department of Physics, Princeton University, Jadwin Hall, Princeton, NJ 08544
Rice, Robert V., 30 Burnham Dr., Falmouth, MA 02540
Richards, A. Glenn, 942 Cromwell Ave., St. Paul, MN 55114 (deceased)
Rockstein, Morris, 600 Biltmore Way, Apt. 805, Coral Gables, FL 33134
Ronkin, Raphael R., 3212 McKinley St., NW, Washington, DC 20015-1635
Rose, S. Meryl, 32 Crosby Ln., E. Falmouth, MA 02536 (deceased)

Sanders, Howard, Woods Hole Oceanographic Institution, Woods Hole, MA 02543
Sato, Hidemi, Faculty of Social Science, Nagano University, Shiminogo, Ueda, Nagano 386-12, Japan
Saz, Arthur K., Georgetown University Medical School, Department of Immunology, Washington, DC 20007
Scharrer, Berta, Department of Anatomy, Albert Einstein College of Medicine, 1300 Morris Park Avenue, Bronx, NY 10461
Schlesinger, R. Walter, University of Medicine and Dentistry of New Jersey, Department of Molecular Genetics and Microbiology, Robert Wood Johnson Medical School, Piscataway, NJ 08854-5635
Schmitt, F. O., Room 16-512, Massachusetts Institute of Technology, Cambridge, MA 02139
Scott, Allan C., Colby College, Waterville, ME 04901
Silverstein, Arthur M., The Johns Hopkins Hospital, Johns Hopkins University, Institute of the History of Medicine, 1900 E. Monument Street, Baltimore, MD 21205
Smith, Homer P., 8 Quissett Ave., Woods Hole, MA 02543 (deceased)
Smith, Paul F., P. O. Box 264, Woods Hole, MA 02543
Sonnenblick, B. P., 515A Heritage Hill Village, Southbury, CT 06488
Steinhardt, Jacinto, 1508 Spruce St., Berkeley, CA 94709
Stephens, Grover C., Department of Ecology & Evolutionary Biology, School of Biological Sciences, University of California, Irvine, CA 92717

Taylor, Robert E., 20 Harbor Hill Rd., Woods Hole, MA 02543
Thorndike, W. Nicholas, Wellington Management Company, 200 State Street, Boston, MA 02109
Trager, William, The Rockefeller University, 1230 York Ave., New York, NY 10021-6399

Villee, Claude A., Harvard Medical School, Carol L. Countway Library, 25 Shattuck Street, Boston, MA 02115
Vincent, Walter S., 16 F.R. Lillie Rd., Woods Hole, MA 02543

Wald, George, Harvard University, 16 Divinity Avenue, Cambridge, MA 02138
Waterman, T. H., Yale University, 210 OML Biology Department, Box 6666, New Haven, CT 06511
Wiercinski, Floyd J., 21 Glenview Road, Glenview, IL 60025
Wigley, Roland L., 35 Wilson Rd., Woods Hole, MA 02543
Wilber, Charles G., Department of Biology, Forensic Science Lab, Colorado State University, Fort Collins, CO 80523

Zinn, Donald J., Department of Zoology, University of Rhode Island, Kingston, RI 02881
Zweifach, Benjamin W., 8811 Nottingham Place, La Jolla, CA 92037

Members

Abt, Donald A., Marine Biological Laboratory, Laboratory for Marine Animal Health, Woods Hole, MA 02543
Acheson, George H., 25 Quissett Ave., Woods Hole, MA 02543
Adams, James A., Florida A & M University, Department of Biology, Tallahasee, FL 32307-0077
Adelman, William J., Jr., 160 Locust St., Falmouth, MA 02540
Afzelius, Bjorn, Wenner-Gren Institute, University of Stockholm, Stockholm, Sweden
Alberte, Randall S., Department of Molecular Genetics and Cell Biology, University of Chicago, 1103 E. 57th Street, Chicago, IL 60637
Alkon, Daniel, Laboratory of Adaptive Systems, National Institutes of Health, 36 Convent Drive, 36/4A21, Bethesda, MD 20892-4124
Allen, Garland E., Department of Biology, Washington University, Box 1137, One Brookings Drive, St. Louis, MO 63130-4899
Allen, Nina S., Department of Biology, Wake Forest University, Box 7325, Winston-Salem, NC 27109
Anderson, Everett, Department Cell Biology, Harvard Medical School, 25 Shattuck St., Boston, MA 02115
Anderson, J. M., 110 Roat St., Ithaca, NY 14850
Anderson, Porter W., 6855 East Edgewater Drive, #2A, Coral Gables, FL 33133
Armett-Kibel, Christine, Dean of Science Faculty, University of Massachusetts, Boston, MA 02125
Armstrong, Clay M., Department of Physiology, University of Pennsylvania Medical School, 8701 Richards Bldg., Philadelphia, PA 19104-6085
Armstrong, Ellen P., Marine Biological Laboratory, Woods Hole, MA 02543
Armstrong, Peter B., Section of Molecular/Cellular Biology, University of California, Davis, CA 95616-8755
Arnold, John M., Pacific Biomedical Research Center, 209A Snyder Hall, University of Hawaii, Honolulu, HI 96822-2233
Arnold, William A., Biology Division, Oak Ridge National Laboratory, Oak Ridge, TN 37830
Ashton, Robert W., Esq., Bay Foundation, 18th Floor, 99 Wall St., New York, NY 10005
Atema, Jelle, Boston University Marine Program, Marine Biological Laboratory, Woods Hole, MA 02543

Augustine Jr., George J., Department of Neurobiology, Duke University Medical Center, PO Box 3209, Durham, NC 27710
Ayers, Donald E., 4607 1/2 MacArthur Blvd., NW #B, Washington, DC 20007-2533

Baccetti, Baccio, Institute of Zoology, University of Siena, 53100 Siena, Italy
Baker, Robert G., Department of Physiology and Biophysics, New York University Medical Center, 550 First Ave., New York, NY 10016
Baldwin, Thomas O., Department of Biochemistry and Biophysics, Texas A&M University, College Station, TX 77843
Barlow, Robert B., Jr., Institute for Sensory Research, Syracuse University, Merrill Lane, Syracuse, NY 13244-5290
Barry, Daniel T., 2415 Fairwind Dr., Houston, TX 77062-4756
Barry, Susan R., Mount Holyoke College, Dept. of Biological Sciences, So. Hadley, MA 01075
Bartell, Clelmer K., 2000 Lake Shore Drive, New Orleans, LA 70122 (resigned)
Bass, Andrew H., Seely Mudd Hall, Department of Neurobiology, Cornell University, Ithaca, NY 14853
Battelle, Barbara-Anne, Whitney Laboratory, University of Florida, 9505 Ocean Shore Blvd., St. Augustine, FL 32086
Bay, Frederick, Bay Foundation, 99 Wall St., 18th Fl., New York, NY 10005
Baylor, Martha B., P. O. Box 93, Woods Hole, MA 02543
Bearer, Elaine L., Division of Biology & Medicine, Department of Pathology, Brown University, Box G, Providence, RI 02912
Beauge, Luis Alberto, Department of Biophysics, Instituto M.y.M. Ferreyra, Casilla de Correo 389, 5000 Cordoba, Argentina
Beck, Lyle V., 2455 Tamarack Trail, Apt. 8, Bloomington, IN 47408
Begenisich, Ted, Department of Physiology, University of Rochester, Medical Center, Box 642, 601 Elmwood Ave., Rochester, NY 14642
Begg, David A., Department of Anatomy & Cell Biology, University of Alberta, Edmonton, Alberta T6G 2H7, Canada
Bell, Eugene, 305 Commonwealth Avenue, Boston, MA 02115
Benjamin, Thomas L., Harvard Medical School, Pathology, D2-230, 200 Longwood Avenue, Boston, MA 02115
Bennett, M. V. L., Albert Einstein College of Medicine, Department of Neuroscience, 1410 Pelham Pkwy. S., Bronx, NY 10461
Bennett, Miriam F., Department of Biology, Colby College, Waterville, ME 04901
Berg, Carl J., Jr., P. O. Box 769, Kilauea, Kauai, HI 96754-0769
Berlin, Suzanne T., 5 Highland St., Gloucester, MA 01930
Berne, Robert M., Department of Physiology, University of Virginia, School of Medicine, Box 116, MR4, Charlottesville, VA 22903
Bernstein, Norman, Diane and Norman Bernstein Foundation, Inc., 5301 Wisconsin Ave., #600, Washington, DC 20015-2015
Bezanilla, Francisco, Department of Physiology, University of California, Los Angeles, CA 90024
Biggers, John D., Department of Physiology, Harvard Medical School, Boston, MA 02115
Bishop, Stephen H., Department of Zoology, Iowa State University, Ames, IA 50010
Blaustein, Mordecai P., Department of Physiology, School of Medicine, University of Maryland, 655 W. Baltimore Street, Baltimore, MD 21201
Blennemann, Dieter, 50 Old Stone Bridge Road, Cos Cob, CT 06807
Bloom, George S., Department of Cell Biology and Neuroscience, The University of Texas Southwestern Medical Center, 5223 Harry Hines Blvd., Dallas, TX 75235-9039
Bloom, Kerry S., Department of Biology, University of North Carolina, 623 Fordham Hall, Chapel Hill, NC 27516
Bodznick, David A., Department of Biology, Wesleyan University, Lawn Avenue, Middletown, CT 06457-0170
Boettiger, Edward G., 17 Eastwood Road, Storrs Mansfield, CT 06268-2401
Boolootian, Richard A., Science Software Systems, Inc., 3576 Woodcliff Rd., Sherman Oaks, CA 91403
Borgese, Thomas A., Department of Biology, Lehman College, CUNY, Bedford Park Blvd., West, Bronx, NY 10468
Borisy, Gary G., Laboratory of Molecular Biology, University of Wisconsin, Madison, WI 53706
Borst, David W., Jr., Department of Biological Sciences, Illinois State University, Normal, IL 61790-4120
Bowles, Francis P., Ecosystems Center, Marine Biological Laboratory, Woods Hole, MA 02543
Boyer, Barbara C., Department of Biology, Union College, Schenectady, NY 12308
Brandhorst, Bruce P., Institute of Molecular Biology and Biochemistry, Department of Biological Sciences, Simon Fraser University, Burnaby, BC V5A 156, Canada
Brinley, F. J., Neurological Disorders Program, NINCDS, NIH, 812 Federal Building, Bethesda, MD 20892
Brown, Stephen C., Department of Biological Sciences, SUNY, Albany, NY 12222
Brown, William L., Retired Chairman, Bank of Boston, 100 Federal St. 01-23-11, Boston, MA 02106-2016
Browne, Carole L., Department of Biology, Wake Forest University, Winston-Salem, NC 27109
Browne, Robert A., Department of Biology, Wake Forest University, Box 7325, Winston-Salem, NC 27109
Bryant, Shirley H., Department of Pharmacology and Cell Biophysics, ML 575, University of Cincinnati, Cincinnati, OH 45267
Bucklin, Anne C., University of New Hampshire, Ocean Process Analysis Lab, 142 Morse Hall, Durham, NH 03824
Bullis, Robert A., Marine Biological Laboratory, LMAH, Woods Hole, MA 02543
Burd, Gail Deerin, Department of Molecular and Cell Biology, Life Sciences South, Rm 444, University of Arizona, Tucson, AZ 85721
Burdick, Carolyn J., Department of Biology, Brooklyn College, 2900 Bedford Avenue, Brooklyn, NY 11210
Burger, Max, Freidrich Miesner Institut Bau 1060 Postfach 2543, Basel 4002, Switzerland
Burgos, Mario, IHEM Medical School, UNC Conicet, Casilla de Correo 56, 5500 Mendoza, Argentina
Burky, Albert, Department of Biology, University of Dayton, Dayton, OH 45469
Burris, John E., Marine Biological Laboratory, Woods Hole, MA 02543
Burstyn, Harold L., Morrison Law Firm, The Morrison Building, 145 North Fifth Avenue, Mt. Vernon, NY 10550
Bursztajn, Sherry, Harvard Medical School, Mailman Research Center, 115 Mill St., Belmont, MA 02178
Busa, William, Department of Biology, Johns Hopkins University, 3400 N. Charles St., Baltimore, MD 21218

Calabrese, Ronald L., Department of Biology, Emory University, 1555 Pierce Drive, Atlanta, GA 30322
Callaway, Joseph C., Department of Physiology, New York Medical College, Basic Sciences Bldg., Valhalla, NY 10595
Calvin, Katherine Graubard, University of Washington, Department of Zoology, NJ-15, Seattle, WA 98195
Cameron, Andrew, Department of Biology, California Institute of Technology, Pasadena, CA 91125
Campbell, Richard H., Bang-Campbell Associates, Box 402, Eel Pond Place, Woods Hole, MA 02543

Candelas, Graciela C., Department of Biology, University of Puerto Rico, PO Box 23360, San Juan, PR 00931-3360
Carew, Thomas J., Department of Psychology, Yale University, P. O. Box 11A, Yale Station, New Haven, CT 06520
Cariello, Lucio, Biochemistry Department, Stazione Zoologica, Villa Comunale, 80121 Naples, Italy
Case, James, University of California, Associate Vice Chancellor of Research, Santa Barbara, CA 93106
Cassidy, Rev. J. D., Providence College, Priory of St. Thomas Aquinas, Providence, RI 02918
Cavanaugh, Colleen M., Harvard University, Biological Laboratories, 16 Divinity Ave., Cambridge, MA 02138
Cebra, John J., Department of Biology, Leidy Labs, G-6, University of Pennsylvania, Philadelphia, PA 19174
Chaet, Alfred B., University of West Florida, Department of Cell & Molecular Biology, 11000 University Parkway, Pensacola, FL 32514
Chambers, Edward L., Department of Physiology and Biophysics, University of Miami, School of Medicine, P. O. Box 016430, Miami, FL 33101
Chang, Donald C., Hong Kong University of Science & Technology, Department of Biology, Clear Water Bay, Kowloon, Hong Kong
Chappell, Richard L., Department of Biological Sciences, Hunter College, Box 210, 695 Park Ave., New York, NY 10021
Chen, Thomas T., Center for Marine Biotechnology, University of Maryland, 600 E. Lombard St., Baltimore, MD 21202
Chikarmane, Hemant M., Marine Biological Laboratory, Woods Hole, MA 02543
Child, Frank M., III, 28 Lawrence Farm Road, Woods Hole, MA 02543
Chisholm, Rex L., Department of Cell Biology, Northwestern University Medical School, Chicago, IL 60611
Citkowitz, Elena, Hospital of St. Raphael, Lipid Disorders Clinic, 1450 Chapel Street, New Haven, CT 06511
Clark, Eloise E., Vice President, Bowling Green State University, Bowling Green, OH 43403
Clark, Hays, 26 Deer Park Drive, Greenwich, CT 06830
Clark, James M., 210 Emerald Lane, Palm Beach, FL 33480
Clark, Wallis H., Jr., 7922 NW 71st Street, Gainsville, FL 32606
Claude, Philippa, University of Wisconsin, Primate Center, 1223 Capital Court, Madison, WI 53715
Clay, John R., Laboratory of Biophysics, NIH, 36/2C02, Bethesda, MD 20892
Clowes, Alexander W., Department of Surgery RF-25, University of Washington School of Medicine, Seattle, WA 98195
Clutter, Mary, Office of the Director, Room 518, National Science Foundation, Washington, DC 20550
Cobb, Jewel Plummer, California State University, 5151 State University Drive, Los Angeles, CA 90032-8500
Cohen, Carolyn, Rosenstiel Basic Medical Sciences Research Center, Brandeis University, Waltham, MA 02254
Cohen, Lawrence B., Department of Physiology, Yale University School of Medicine, 333 Cedar Street, New Haven, CT 06510-8026
Cohen, Maynard, Department of Neurological Sciences, Rush Medical College, 600 South Paulina, Chicago, IL 60612
Cohen, Rochelle S., Department of Anatomy, University of Illinois, 808 W. Wood Street, Chicago, IL 60612
Cohen, William D., Department of Biological Sciences, Hunter College, 695 Park Ave., Box 79, New York, NY 10021
Coleman, Annette W., Division of Biology and Medicine, Brown University, Providence, RI 01912
Collier, Jack R., Department of Biology, Brooklyn College, Bedford & Avenue H, Brooklyn, NY 11210
Collier, Marjorie McCann, Biology Department, Saint Peter's College, 2641 Kennedy Boulevard, Jersey City, NJ 07306
Collin, Carlos, National Institutes of Health, Laboratory of Adaptive Systems, Bldg. 36, B308, Bethesda, MD 20892-0226
Cook, Joseph A., The Edna McConnell Clark Foundation, 250 Park Ave., New York, NY 10177-0026
Cornell, Neal W., Marine Biological Laboratory, Woods Hole, MA 02543
Cornwall, Melvin C., Jr., Department of Physiology L714, Boston University School of Medicine, 80 E. Concord St., Boston, MA 02118
Corson, David Wesley, Jr., Storm Eye Institute, Room 537, 171 Ashley Avenue, Charleston, SC 29425
Corwin, Jeffrey T., Department of Otolaryngology, Health Science Center, University of Virginia Medical Center, Box 396, Charlottesville, VA 22908
Costello, Walter J., Department of Zoology Z/BS, College of Medicine, Ohio University, Athens, OH 45701
Couch, Ernest F., Department of Biology, Texas Christian University, Fort Worth, TX 76129
Crane, Sylvia E., 438 Wendover Drive, Princeton, NJ 08540
Cremer-Bartels, Gertrud, Universitats Augenklinik, 44 Munster, Germany
Crow, Terry J., Department of Neurobiology and Anatomy, University of Texas Medical School, Houston, TX 77225
Crowell, Sears, Department of Biology, Indiana University, Bloomington, IN 47405
Crowther, Robert, Department of Biology, University of New Brunswick, BS 45111, Fredericton, NB, Canada E3B 6E1
Cunningham, Mary-Ellen, 62 Cloverly Road, Grosse Pointe Farms, MI 48236
Currier, David L., P. O. Box 2476, Vineyard Haven, MA 02568
Cutler, Richard, Marine Biological Laboratory, Woods Hole, MA 02543

D'Alessio, Giuseppe, Department of Organic & Biological Chemistry, University of Naples, Via Mezzocannone 16, Naples, Italy 80134
D'Avanzo, Charlene, Department of Natural Science, Hampshire College, Amherst, MA 01002
Daignault, Alexander T., 29 Quisset Harbor Rd., Falmouth, MA 02540
Dan, Katsuma, Tokyo Metropolitan Union, 1-1 Minami-Osawa, Hachioji City 192-03, Tokyo, Japan
David, John R., Tropical Public Health, Harvard School of Public Health, 665 Huntington Ave., Boston, MA 02115
Davidson, Eric H., Division of Biology, 156-29, California Institute of Technology, 1201 E. California Blvd., Pasadena, CA 91125
Davis, Joel P., P.O. Box 208, Brooksville, ME 04617
Daw, Nigel W., 5 Old Pawson Rd., Branford, CT 06405
Deegan, Linda A., The Ecosystems Center, Marine Biological Laboratory, Woods Hole, MA 02543
DeGroof, Robert C., 145 Water Crest Dr., Doylestown, PA 18901
DeHaan, Robert L., Department of Anatomy and Cell Biology, Emory University School of Medicine, Atlanta, GA 30322
DeLanney, Louis E., The Parkinson's Institute, 1170 Morse Avenue, Sunnyvale, CA 94089
Denkla, Marth B., Kennedy-Krieger Institute, Johns Hopkins School of Medicine, 707 North Broadway, Baltimore, MD 21205
Dentler, William L., Department of Physiology & Cell Biology, University of Kansas, 4011 Haworth Hall, Lawrence, KS 66044
DePhillips, Henry A., Jr., Department of Chemistry, Trinity College, 300 Summit Street, Hartford, CT 06106
DeSimone, Douglas W., Department of Anatomy and Cell Biology, Box 439, Health Sciences Center, University of Virginia, Charlottesville, VA 22908
DeToledo-Morrell, Leyla, Rush-Presbyterian-St. Lukes Medical Center, 1653 West Congress Parkway, Chicago, IL 60612

Dettbarn, Wolf-Dietrich, Department of Pharmacology, School of Medicine, Vanderbilt University, Nashville, TN 37232
De Weer, Paul J., Department of Physiology, University of Pennsylvania School of Medicine, Philadelphia, PA 19104-6085
Dionne, Vincent E., Boston University Marine Program, Marine Biological Laboratory, Woods Hole, MA 02543
Dixon, Keith E., School of Biological Sciences, Flinders University, Bedford Park, 5042, South Australia, Australia
Dowling, John E., The Biological Laboratories, Harvard University, 16 Divinity St., Cambridge, MA 02138
DuBois, Arthur Brooks, John B. Pierce Foundation Laboratory, 290 Congress Ave., New Haven, CT 06519
Duncan, Thomas K., Department of Environmental Sciences, Nichols College, Dudley, MA 01571
Dunham, Philip B., Department of Biology, Syracuse University, Syracuse, NY 13244
Dunlap, Kathleen, Department of Physiology, Tufts University Medical School, Boston, MA 02111
Dunlap, Paul V., Department of Biology, Woods Hole Oceanographic Institution, Redfield 316, Woods Hole, MA 02543
Dworkin, Martin, Department of Microbiology, University of Minnesota, 1460 Mayo Bldg., Box 196 UMHC, Minneapolis, MN 55455-0312

Ebert, James D., Department of Biology, Homewood, The Johns Hopkins University, 3400 No. Charles St., Baltimore, MD 21218
Eckberg, William R., Howard University, Department of Zoology, P.O. Box 887, Admin. Bldg., Washington, DC 20059
Edds, Kenneth T., R&D Systems, Inc., Hematology Division, 614 McKinley Place, NE, Minneapolis, MN 55413
Eder, Howard A., Albert Einstein College of Medicine, 1300 Morris Park Ave., Bronx, NY 10461
Edstrom, Joan, 2515 Milton Hills Dr., Charlottesville, VA 22901
Egyud, Laszlo G., Cell Research Corporation, 100 Inman Street, Cambridge, MA 02139
Ehrlich, Barbara E., Division of Cardiology, University of Connecticut School of Medicine, 263 Farmington Avenue, Farmington, CT 06030
Eisen, Arthur Z., Division of Dermatology, Washington University, St. Louis, MO 63110
Eisen, Herman N., Massachusetts Institute of Technology, Center for Cancer Research, E17-128, 77 Massachusetts Ave., Cambridge, MA 02139
Elder, Hugh Young, Institute of Physiology, University of Glasgow, Glasgow, Scotland G12 8QQ
Elliott, Gerald F., The Open University Research Unit, Foxcombe Hall, Berkeley Rd., Boars Hill, Oxford, England OX1 5HR
Englund, Paul T., Department of Biological Chemistry, Johns Hopkins University, 725 No. Wolfe St., Baltimore, MD 21205
Epel, David, Hopkins Marine Station, Pacific Grove, CA 93950
Epstein, Herman T., 18 Lawrence Farm Road, Woods Hole, MA 02543
Epstein, Ray L., 1602 West Olympia St., Hernando, FL 34442

Farb, David H., Department of Pharmacology L603, Boston University School of Medicine, 80 E. Concord St., Boston, MA 02118
Farmanfarmaian, A., Department of Biological Sciences, Nelson Biological Laboratory, Rutgers University, POB 1059, Piscataway, NJ 08855
Feinman, Richard D., Box 8, Department of Biochemistry, SUNY Health Science Center, 450 Clarkson Avenue, Brooklyn, NY 11203
Feldman, Susan C., Department of Anatomy, University of Medicine and Dentistry of New Jersey, New Jersey Medical School, 100 Bergen St., Newark, NJ 07103
Fessenden, Jane, 225 Lakeview Ave., Falmouth, MA 02540
Festoff, Barry W., Neurology Service (151), Veterans Administration Medical Center, 4801 Linwood Blvd., Kansas City, MO 64128
Fink, Rachel D., Department of Biological Sciences, Clapp Laboratory, Mount Holyoke College, South Hadley, MA 01075
Finkelstein, Alan, Albert Einstein College of Medicine, 1300 Morris Park Ave., Bronx, NY 10461
Fischbach, Gerald, Department of Neurobiology, Harvard Medical School, 220 Longwood Ave., Boston, MA 02115
Fishman, Harvey M., Department of Physiology and Biophysics, University of Texas Medical Branch, 301 Univ. Blvd., Galveston, TX 77555-0641
Flanagan, Dennis, 12 Gay St., New York, NY 10014
Fluck, Richard Allen, Department of Biology, Franklin & Marshall College, Box 3003, Lancaster, PA 17604-3003
Foreman, K. H., Boston University Marine Program, Marine Biological Laboratory, Woods Hole, MA 02543
Fox, Thomas Oren, Division of Medical Sciences, Harvard Medical School, 260 Longwood Ave., Boston, MA 02115
Franzini-Armstrong, Clara, School of Medicine, University of Pennsylvania, 330 S. 46th Street, Philadelphia, PA 19143
Frazier, Donald T., Department of Physiology and Biophysics, University of Kentucky Medical Center, Lexington, KY 40536
French, Robert J., Health Sciences Center, University of Calgary, Calgary, Alberta, T2N 4N1, Canada
Friedler, Gladys, Boston University School of Medicine, 80 East Concord Street, Boston, MA 02118 (resigned)
Fry, Brian, Department of Biology, Florida International University, OE Building, Room 239, Miami, FL 33199-0001
Fulton, Chandler M., Department of Biology, Brandeis University, Waltham, MA 02254
Furshpan, Edwin J., Department of Neurophysiology, Harvard Medical School, 220 Longwood Ave., Boston, MA 02115
Futrelle, Robert P., College of Computer Science, Northeastern University, 360 Huntington Avenue, Boston, MA 02115

Gabriel, Mordecai, Department of Biology, Brooklyn College, 2900 Bedford Ave., Brooklyn, NY 11210
Gadsby, David C., Laboratory of Cardiac Physiology, The Rockefeller University, 1230 York Avenue, New York, NY 10021-6399
Gainer, Harold, Lab of Functional Neurochemistry, NIH, Bldg. 36, Room 4D-20, Bethesda, MD 20892
Galatzer-Levy, Robert M., 180 N. Michigan Avenue, Chicago, IL 60601
Gall, Joseph G., Carnegie Institution, 115 West University Parkway, Baltimore, MD 21210
Garber, Sarah S., Department of Physiology, Medical College of Pennsylvania, 2900 Queen Ln., Philadelphia, PA 19129
Gascoyne, Peter, Box 85E, University of Texas, M. D. Anderson Hospital and Tumor Institute, 6723 Bertner Avenue, Box 85E, Houston, TX 77030
Gelperin, Alan, Department of Biophysics, AT&T Bell Labs, Room 1C464, 600 Mountain Avenue, Murray Hill, NJ 07974
German, James L., III, Lab of Human Genetics, The New York Blood Center, 310 East 67th St., New York, NY 10021
Gibbs, Martin, Institute for Photobiology of Cells and Organelles, Brandeis University, Waltham, MA 02254
Giblin, Anne E., Ecosystems Center, Marine Biological Laboratory, Woods Hole, MA 02543
Gibson, A. Jane, Department of Biochemistry, Cornell University, Ithaca, NY 14850
Gifford, Prosser, 540 N Street, SW, S-903, Washington, DC 20024
Gilbert, Daniel L., Clinical Neuroscience Branch, NIH/NINDS, Bldg. 36, Room 5A09A, Bethesda, MD 20892

Giudice, Giovanni, Dipartimento di Biologia Cellulare e Dello Sviluppo, I-90123, Via Archirafi 22, Universita di Palermo, Palermo, Italy

Giuditta, Antonio, Department of General Physiology, University of Naples, Via Mezzocannone 8, Naples, Italy 80134

Glynn, Paul, 2770 Beechwood Blvd., Pittsburgh, PA 15217

Golden, William T., American Museum of Natural History, 40 Wall St., Room 4201, New York, NY 10005

Goldman, Robert D., Department of Cell, Molecular and Structural Biology, Northwestern University, 303 E. Chicago Ave., Chicago, IL 60611

Goldsmith, Paul K., NIH, Bldg. 10, Room 9C-101, Bethesda, MD 20892

Goldsmith, Timothy H., Department of Biology, Yale University, New Haven, CT 06510

Goldstein, Moise H., Jr., ECE Department, Barton Hall, Johns Hopkins University, Baltimore, MD 21218

Goodman, Lesley Jean, Department of Biological Sciences, Queen Mary College, Mile End Road, London, E1 4NS, England, UK

Gould, Robert Michael, Institute for Basic Research in Developmental Disabilities, 1050 Forest Hill Rd., Staten Island, NY 10314

Gould, Stephen J., Museum of Comparative Zoology, Agassiz Museum, Harvard University, Cambridge, MA 02138 (resigned)

Govind, C. K., Life Sciences Division, Scarborough College, 1265 Military Trail, West Hill, Ontario, M1C 1A4, Canada

Grace, Dick, Doreen Grace Fund, The Brain Center, Seanest Drive, Promontory Pt., New Seabury, MA 02649

Graf, Werner, Rockefeller University, 1230 York Ave., New York, NY 10021

Grant, Philip, 2939 Van Ness Street, N.W., Apt. 302, Washington, DC 20008

Grass, Ellen R., The Grass Foundation, 77 Reservoir Rd., Quincy, MA 02170

Grassle, Judith, Institute of Marine & Coastal Studies, Rutgers University, Box 231, New Brunswick, NJ 08903

Greenberg, Everett Peter, Department of Microbiology, College of Medicine, University of Iowa, Iowa City, IA 52242

Greenberg, Michael J., Whitney Laboratory, University of Florida, 9505 Ocean Shore Blvd., St. Augustine, FL 32086-8623

Greer, Mary J., 16 Hillside Ave., Cambridge, MA 02140

Griffin, Donald R., Concord Field Station, Harvard University, Old Causeway Road, Bedford, MA 01730

Gross, Paul R., Center for Advanced Studies, University of Virginia, 444 Cabell Hall, Charlottesville, VA 22903

Grossman, Albert, New York University Medical Center, 550 First Ave., New York, NY 10016

Grossman, Lawrence, Department of Biochemistry, Johns Hopkins University, 615 North Wolfe Street, Baltimore, MD 21205

Gruner, John, Cephalon, Inc., 145 Brandywine Parkway, W. Chester, PA 19380-4245

Gunning, A. Robert, P. O. Box 165, Falmouth, MA 02541

Gwilliam, G. P., Department of Biology, Reed College, Portland, OR 97202

Haimo, Leah, Department of Biology, University of California, Riverside, CA 92521

Hall, Linda M., Department of Biochemistry and Pharmacology, SUNY, 317 Hochstetter, Buffalo, NY 14260

Hall, Zack W., Department of Physiology, University of California, P.O. Box 0444, San Francisco, CA 94143

Halvorson, Harlyn O., 26 Fay Road, P.O. Box 81, Woods Hole, MA 02543

Hamlett, Nancy V., Department of Biology, Harvey Mudd College, 301 E. 12th St., Claremont, CA 91711

Haneji, Tatsuji, Kyushu Dental College, Department of Anatomy, 2-6-1, Manazuru, Kokurakita-Ku, Kitakyushu 803, Japan

Hanlon, Roger T., University of Texas Medical Branch, Marine Biomedical Institute, 200 University Boulevard, Galveston, TX 77550-2772

Hanna, Robert B., Department of Environmental Science and Forestry, SUNY, Syracuse, NY 13210

Harosi, Ferenc I., Laboratory of Sensory Physiology, Marine Biological Laboratory, Woods Hole, MA 02543

Harrigan, June F., 7415 Makaa Place, Honolulu, HI 96825

Harrington, Glenn W., Weber State University, Department of Microbiology, Ogden, UT 84408

Hastings, J. W., The Biological Laboratories, Harvard University, 16 Divinity Street, Cambridge, MA 02138-2020

Hayashi, Teru, 7105 SW 112 Place, Miami, FL 33173

Haydon-Baillie, Wensley G., Porton Int., 2 Lowndes Place, London, SW1X 8DD, England, UK

Hayes, Raymond L., Jr., Department of Anatomy, Howard University, College of Medicine, 520 W St., NW, Washington, DC 20059

Hepler, Peter K., Department of Botany, University of Massachusetts, Amherst, MA 01003

Herndon, Walter R., University of Tennessee, Department of Botany, Knoxville, TN 37996-1100

Herskovits, Theodore T., Department of Chemistry, Fordham University, John Mulcahy Hall, Room 638, Bronx, NY 10458

Hiatt, Howard H., Department of Medicine, Brigham and Women's Hospital, 75 Francis Street, Boston, MA 02115

Highstein, Stephen M., Department of Otolaryngology, Box 8115, Washington University School of Medicine, St. Louis, MO 63110

Hildebrand, John G., Arizona Research Laboratories, Division of Neurobiology, 603 Gould-Simpson Science Building, University of Arizona, Tucson, AZ 85721

Hill, Richard W., Department of Zoology, Michigan State University, E. Lansing, MI 48824

Hill, Susan D., Department of Zoology, Michigan State University, E. Lansing, MI 48824

Hillis, Llewellya, Smithsonian Tropical Research Institute, Unit 0948 APO-AA, Miami, FL 34002-0948

Hillman, Peter, Department of Biology, Life Sciences & Neurobiology, Hebrew University, Jerusalem 91904, Israel

Hinegardner, Ralph T., Division of Natural Sciences, University of California, Santa Cruz, CA 95064

Hines, Michael, Department of Computer Science, Yale University, P.O. Box 208205, New Haven, CT 06520-8285

Hinsch, Gertrude, W., Department of Biology, University of South Florida, Tampa, FL 33620

Hobbie, John E., Ecosystems Center, Marine Biological Laboratory, Woods Hole, MA 02543

Hodge, Alan J., 3843 Mt. Blackburn Ave., San Diego, CA 92111

Hoffman, Joseph, Department of Cellular and Molecular Physiology, School of Medicine, Yale University, New Haven, CT 06515

Hollyfield, Joe G., Baylor School of Medicine, Texas Medical Center, Houston, TX 77030

Holz, IV, George G, Massachusetts General Hospital, Laboratory of Molecular Endocrinology, Wellman 320, 50 Blossom St., Boston, MA 02114

Hopkinson, Charles S., Jr., Ecosystems Center, Marine Biological Laboratory, Woods Hole, MA 02543

Hoy, Ronald R., Section of Neurobiology and Behavior, Cornell University, Ithaca, NY 14853

Hufnagel-Zackroff, Linda A., Department of Microbiology, University of Rhode Island, Kingston, RI 02881

Hummon, William D., Department of Biological Sciences, Ohio University, Athens, OH 45701

Humphreys, Susie H., Food and Drug Administration, HFS-156 Switzer, 200 C Street, SW, Washington, DC 20204-0001
Humphreys, Tom D., University of Hawaii, Kewalo Marine Lab, 41 Ahui St., Honolulu, HI 96813
Hunt, Richard T., ICRF, Clare Hall Laboratories, South Mimms Potter's Bar, Herb EN6-3LD, England
Hunter, Robert D., Department of Biological Sciences, Oakland University, Rochester, MI 48309-4401
Huxley, Hugh E., Department of Biology, Rosenstiel Center, Brandeis University, Waltham, MA 02154
Hynes, Thomas J., Jr., Meredith and Grew, Inc., 160 Federal Street, Boston, MA 02110-1701

Ilan, Joseph, Department of Developmental Genetics and Anatomy, Case Western Reserve University School of Medicine, Cleveland, OH 44106
Ingoglia, Nicholas, Department of Physiology, New Jersey Medical School, 100 Bergen St., Newark, NJ 07103
Inoué, Saduyki, Department of Anatomy, McGill University Cancer Centre, 3640 University St., Montreal, PQ H3A 2B2, Canada
Inoué, Shinya, Marine Biological Laboratory, Woods Hole, MA 02543
Isselhacher, Kurt J., Massachusetts General Hospital Cancer Center, Charlestown, MA 02129
Issidorides, Marietta, R., Department of Psychiatry, University of Athens, Monis Petraki 8, Athens, 140 Greece
Izzard, Colin S., Department of Biological Sciences, SUNY, 1400 Washington Ave., Albany, NY 12222

Jacobs, Neil, Hale & Dorr, 60 State St., Boston, MA 02109
Jaffe, Lionel, Marine Biological Laboratory, Woods Hole, MA 02543
Jannasch, Holger W., Department of Biology, Woods Hole Oceanographic Institution, Woods Hole, MA 02543
Jeffery, William R., Bodega Marine Laboratory, University of California, Box 247, Bodega Bay, CA 94923
Johnston, Daniel, Division of Neuroscience, Baylor College of Medicine, 1 Baylor Plaza, Houston, TX 77030
Josephson, Robert K., Department of Psychobiology, University of California, Irvine, CA 92717

Kaczmarek, Leonard K., Department of Pharmacology, Yale University School of Medicine, 333 Cedar St., New Haven, CT 06520
Kaley, Gabor, Department of Physiology, Basic Sciences Building, New York Medical College, Valhalla, NY 10595
Kaltenbach, Jane, Department of Biological Sciences, Mount Holyoke College, South Hadley, MA 01075
Kaminer, Benjamin, Department of Physiology, School of Medicine, Boston University, 80 East Concord St., Boston, MA 02118
Kaneshiro, Edna S., Department of Biological Sciences, University of Cincinnati, JL 006, Cincinnati, OH 45221-0006
Kao, Chien-yuan, Department of Pharmacology, Box 29, SUNY, Downstate Medical Center, 450 Clarkson Avenue, Brooklyn, NY 11203
Kaplan, Ehud, Department of Biophysics, The Rockefeller University, 1230 York Ave., New York, NY 10024
Karakashian, Stephen J., Apt. 16-F, 165 West 91st St., New York, NY 10024
Karlin, Arthur, Department of Biochemistry, Columbia University, 630 West 168th St., New York, NY 10032
Katz, George M., Fundamental and Experimental Research Labs, Merck Sharp and Dohme, P. O. Box 2000, Rahway, NJ 07065
Kelley, Darcy Brisbane, Columbia University, Department of Biological Sciences, 911 Sherman Fairchild Ctr., New York, NY 10032
Kelly, Robert E., Department of Anatomy, University of Illinois, P. O. Box 6998, Chicago, IL 60680
Kemp, Norman E., Department of Biology, University of Michigan, Ann Arbor, MI 48109
Kendall, John P., Faneuil Hall Associates, 176 Federal Street, 2nd Floor, Boston, MA 02110
Kendall, Richard E., 26 Green Harbor Road, East Falmouth, MA 02536
Kerr, Louis M., Marine Biological Laboratory, Woods Hole, MA 02543
Keynan, Alexander, Laboratory for Developmental and Molecular Biology, Department of Biochemistry, Hebrew University of Jerusalem, Givat-Ram, Jerusalem, Israel
Khan, Shahid M. M., Department of Anatomy & Structural Biology, Albert Einstein College of Medicine, 1300 Morris Park Ave., Bronx, NY 10461
Kiehart, Daniel P., Department of Cellular Biology, Duke University Medical Center, Box 3709, 307 Nanaline Duke Bldg., Durham, NC 27710
Kirk, Mark D., Division of Biological Sciences, University of Missouri, Columbia, MO 65211 (resigned)
Klotz, Irving M., Department of Chemistry, Northwestern University, Evanston, IL 60201
Knudson, Robert A., Marine Biological Laboratory, Instrument Development Lab, Woods Hole, MA 02543
Koide, Samuel S., Population Council, The Rockefeller University, 1230 York Avenue, New York, NY 10021
Kornberg, Sir Hans, The Master's Lodge, Christ's College, Cambridge CB2 3BU, England, UK
Kosower, Edward M., Department of Chemistry, Tel Aviv University, Ramat-Aviv, Tel Aviv, Israel 69978
Krahl, M. E., 2783 W. Casas Circle, Tucson, AZ 85741
Krane, Stephen M., Arthritis Unit, Massachusetts General Hospital, Fruit Street, Boston, MA 02114
Krauss, Robert, FASEB, 9650 Rockville Pike, Bethesda, MD 20814
Kravitz, Edward A., Department of Neurobiology, Harvard Medical School, 220 Longwood Ave., Boston, MA 02115
Kriebel, Mahlon E., Department of Physiology, SUNY Health Science Center, Syracuse, NY 13210
Kristan, William B., Jr., Department of Biology B-022, University of California San Diego, La Jolla, CA 92093
Kropinski, Andrew M. B., Department of Microbiology/Immunology, Queen's University, Kingston, Ontario K7L 3N6, Canada
Kuhns, William J., Hospital for Sick Children, Department of Biochemistry Research, Toronto, Ontario M5G 1X8, Canada
Kusano, Kiyoshi, NIH, Bldg. 36, Room 4D-20, Bethesda, MD 20892
Kuzirian, Alan M., Marine Biological Laboratory, Woods Hole, MA 02543

Laderman, Aimlee, Yale University School of Forestry and Environmental Studies, 370 Prospect, New Haven, CT 06511
LaMarche, Paul H., Eastern Maine Medical Center, 489 State St., Bangor, ME 04401
Landis, Dennis M. D., Department of Developmental Genetics and Anatomy, Case Western Reserve University School of Medicine, Cleveland, OH 44106
Landowne, David, Department of Physiology, P. O. Box 016430, University of Miami School of Medicine, Miami, FL 33101
Langford, George M., Department of Biological Sciences, Dartmouth College, 6044 Gilman Laboratory, Hanover, NH 03755
Lasser-Ross, Nechama, Department of Physiology, New York Medical College, Valhalla, NY 10595
Laster, Leonard, University of Massachusetts Medical School, 55 Lake Avenue, North, Worcester, MA 01655

Laufer, Hans, Department of Biological Science, Molecular and Cell Biology, Group U-125, University of Connecticut, Storrs, CT 06269-3125

Lazarow, Paul B., Department of Cell Biology and Anatomy, Mount Sinai Medical School, Box 1007, 5th Avenue & 100th Street, New York, NY 10021

Lazarus, Maurice, Federated Department Stores, Inc., Sears Cresent, City Hall Plaza, Boston, MA 02108

Leadbetter, Edward R., Department of Molecular and Cell Biology, U-131, University of Connecticut, Storrs, CT 06268

Lederberg, Joshua, The Rockefeller University, 1230 York Ave., New York, NY 10021

Lee, John J., Department of Biology, City College of CUNY, Convent Ave. and 138th St., New York, NY 10031

Lehy, Donald B., 35 Willow Field Dr., N. Falmouth, MA 02556

Leibovitz, Louis, 3 Kettle Hole Road, Falmouth, MA 02540

Leighton, Joseph, Aeron Biotechnology, Inc., 1933 Davis Street, #310, San Leandro, CA 94577

Leighton, Stephen, NIH, Bldg. 13 3W13, Bethesda, MD 20892

Leinwand, Leslie Ann, Department of Microbiology and Immunology, Albert Einstein College of Medicine, 1300 Morris Park Ave., Bronx, NY 10461

Lerman, Sidney, Eye Research Lab, Room 41, New York Medical College, 100 Grasslands Ave., Valhalla, NY 10595

Lerner, Aaron B., Department of Dermatology, PO Box 3333, Yale University, School of Medicine, New Haven, CT 06510

Lester, Henry A., Division of Biology, California Institute of Technology, 156-29, Pasadena, CA 91125

Levin, Jack, Veterans Administration Medical Center, 111 H2, 4150 Clement St., San Francisco, CA 94121

Levine, Richard B., ARL, Division of Neurobiology, University of Arizona, 611 Gould-Simpson Bldg., Tucson, AZ 85721

Levinthal, Francoise, Department of Biological Sciences, Columbia University, Broadway & 116th Street, New York, NY 10026

Levitan, Herbert, National Science Foundation, 4201 Wilson Boulevard, Room 835, Arlington, VA 22230

Levitan, Irwin B., Center for Complex Systems, Brandeis University, Waltham, MA 02254

Linck, Richard W., Department of Cell Biology and Neuroanatomy, University of Minnesota, 321 Church Street, S. E., Minneapolis, MN 55455

Lipicky, Raymond J., Food & Drug Administration, 1451 Rockville Pike, Room 5093, Rockville, MD 20852

Lisman, John E., Department of Biology, Brandeis University, Waltham, MA 02254

Liuzzi, Anthony, 320 Beacon St., Boston, MA 02116

Llinás, Rodolfo R., Department of Physiology and Biophysics, New York University Medical Center, 550 First Ave., New York, NY 10016

Loew, Franklin M., Tufts University School of Veterinary Medicine, 200 Westboro Rd., N. Grafton, MA 01536-1895

Loewenstein, Birgit R., Marine Biological Laboratory, Woods Hole, MA 02543

Loewenstein, Werner R., Marine Biological Laboratory, Woods Hole, MA 02543

London, Irving M., Massachusetts Institute of Technology, Harvard-MIT Division, E-25-551, Cambridge, MA 02139

Longo, Frank J., Department of Anatomy, University of Iowa, Iowa City, IA 52442

Lorand, Laszlo, Northwestern University Medical School, CMS Biology, Searle 4-555, 303 East Chicago, Chicago, IL 60611-3008

Luckenbill-Edds, Louise, Department of Biological Sciences, Irvine Hall, Ohio University, Athens, OH 45701

Macagno, Eduardo R., 1003B Fairchild, Department of Biosciences, Columbia University, New York, NY 10027

MacNichol, E. F., Jr., Department of Physiology, Boston University School of Medicine, 80 E. Concord St., Boston, MA 02118

Maglott-Duffield, Donna R., American Type Culture Collection, 12301 Parklawn Drive, Rockville, MD 20852-1776

Maienschein, Jane Ann, Department of Philosophy, Arizona State University, Tempe, AZ 85287-2004

Mainer, Robert, The Boston Company, One Boston Place, OBP-15-D, Boston, MA 02108

Malbon, Craig Curtis, Department of Pharmacology, Health Sciences Center, SUNY, Stony Brook, NY 11794-8651

Manalis, Richard S., Department of Biological Sciences, Indiana University—Purdue University at Fort Wayne, 2101 Coliseum Blvd., E., Fort Wayne, IN 46805

Mangum, Charlotte P., Department of Biology, College of William and Mary, Williamsburg, VA 23187-8795

Manz, Robert D., Helmer and Associates, Suite 1310, 950 Winter St., Walthan, MA 02154

Margulis, Lynn, Botany Department, University of Massachusetts, Morrill Science Center, Amherst, MA 01003

Marinucci, Andrew C., 102 Nancy Drive, Mercerville, NJ 08619

Marsh, Julian B., Department of Biochemistry and Physiology, Medical College of Pennsylvania, 3300 Henry Ave., Philadelphia, PA 19129

Martinez, Jr., Joe L., Division of Life Sciences, University of Texas, 6900 North Loop, 1604 West, San Antonio, TX 78249-0662

Martinez-Palomo, Adolfo, Seccion de Patologia Experimental, Cinvesav-ipn, 07000 Mexico, D.F. A.P., 140740, Mexico

Maser, Morton, Woods Hole Education Assoc., P. O. Box EM, Woods Hole, MA 02543 (deceased)

Mastroianni, Luigi, Jr., Department of Obstetrics and Gynecology, Hospital of the University of Pennsylvania, 106 Dulles, 3400 Spruce Street, Philadelphia, PA 19104-4283

Matteson, Donald R., Department of Biophysics, University of Maryland School of Medicine, 660 West Redwood Street, Baltimore, MD 21201

Mautner, Henry G., Department of Biochemistry, Tufts University School of Medicine, 136 Harrison Ave., Boston, MA 02111

Manzerall, David, The Rockefeller University, 1230 York Ave., New York, NY 10021

McCann, Frances, Department of Physiology, Dartmouth Medical School, Lebanon, NH 03756

McLaughlin, Jane A., Marine Biological Laboratory, Woods Hole, MA 02543

McMahon, Robert F., Department of Biology, Box 19498, University of Texas, Arlington, TX 76019

Meedel, Thomas, Biology Department, Rhode Island College, 600 Mt. Pleasant Ave., Providence, RI 02908

Meinertzhagen, Ian A., Department of Psychology, Life Sciences Center, Dalhousie University, Halifax, Nova Scotia B3H 4J1, Canada

Meiss, Dennis E., Immunodiagnostic Laboratories, 488 McCormick St., San Leandro, CA 94577

Melillo, Jerry M., Ecosystems Center, Marine Biological Laboratory, Woods Hole, MA 02543

Mellon, DeForest, Jr., Department of Biology, Gilmer Hall, University of Virginia, Charlottesville, VA 22903

Mellon, Richard P., P. O. Box 187, Laughlintown, PA 15655

Mendelsohn, Michael E., Cardiovascular Division, Harvard Medical School, 75 Francis Street, Boston, MA 02115

Metuzals, Janis, Department of Pathology, University of Ottawa, 451 Smythe Road, Ottawa, Ontario K1H 8M5, Canada

Metz, Charles B., 7220 SW 124th St., Miami, FL 33156

Miledi, Ricardo, Department of Psychobiology, University of California, 2205 Biological Science II, Irvine, CA 92717
Milkman, Roger, Department of Biology, University of Iowa, Iowa City, IA 52242
Miller, Andrew L., Marine Biological Laboratory, Woods Hole, MA 02543
Mills, Robert, 10315 44th Avenue, W 12 H Street, Bradenton, FL 34210
Misevic, Gradimir, Department of Research, University Hospital of Basel, Mebelstrasse 20, CH-4031, Basel, Switzerland
Mitchell, Ralph, DAS, Harvard University, 29 Oxford Street, Cambridge, MA 02138
Miyakawa, Hiroyoshi, Tokyo College of Pharmacy, Laboratory of Cellular Neurobiology, 1432-1 Horinouchi, Hachiouji, Tokyo 192-03, Japan
Miyamoto, David M., Department of Biology, Drew University, Madison, NJ 07940
Mizell, Merle, Department of Cell & Molecular Biology, Tulane University, New Orleans, LA 70118
Moore, John W., Department of Neurobiology, Box 3209, Duke University Medical Center, Durham, NC 27710
Moore, Lee E., Department of Physiology and Biophysics, University of Texas Medical Branch, Galveston, TX 77550
Morin, James G., Department of Biology, University of California, Los Angeles, CA 90024
Morrell, Frank, Department of Neurological Science, Rush Medical Center, 1653 W. Congress Parkway, Chicago, IL 60612
Morse, Patricia M., University of Washington Marine Labs, 620 University Rd., Friday Harbor, WA 98250
Morse, Stephen Scott, The Rockefeller University, 1230 York Ave., Box 120, New York, NY 10021-6399
Mote, Michael I., Department of Biology, Temple University, Philadelphia, PA 19122
Muller, Kenneth J., Department of Physiology and Biophysics, University of Miami School of Medicine, Miami, FL 33101
Murray, Andrew W., Department of Physiology, University of California, Box 0444, 513 Parnassus Ave., San Francisco, CA 94143-0444
Murray, Sandra Ann, Department of Neurology, Anatomy and Cell Science, University of Pittsburgh School of Medicine, Pittsburgh, PA 15261

Nabrit, S. M., 686 Beckwith St., SW, Atlanta, GA 30314
Nadelhoffer, Knute, Marine Biological Laboratory, Ecosystems Center, Woods Hole, MA 02543
Naka, Ken-ichi, 2-9-2 Tatsumi Higashi, Okazaki, Japan 444
Nakajima, Shigehiro, Department of Pharmacology and Cell Biology, University of Illinois College of Medicine at Chicago, 835 S. Wolcott Ave., Chicago, IL 60612
Nakajima, Yasoko, Department of Anatomy and Cell Biology, University of Illinois College of Medicine at Chicago, M/C 512, Chicago, IL 60612
Narahashi, Toshio, Department of Pharmacology, Northwestern University Medical School, 303 East Chicago Ave., Chicago, IL 60611
Nasi, Enrico, Department of Physiology, Boston University School of Medicine, R-406, 80 E. Concord St., Boston, MA 02118
Nealson, Kenneth H., Great Lakes Research Center, University of Milwaukee, 600 E. Greenfield Ave., Milwaukee, WI 53204
Nelson, Leonard, Department of Physiology, CS10008, Medical College of Ohio, Toledo, OH 43699
Nelson, Margaret C., Section of Neurobiology and Behavior, Cornell University, Ithaca, NY 14850
Nicholls, John G., Biocenter, Klingelbergstrasse 70, Basel 4056, Switzerland
Nickerson, Peter A., Department of Pathology, SUNY, Buffalo, NY 14214
Nicosia, Santo V., Department of Pathology, University of South Florida, College of Medicine, Box 11, 12901 North 30th St., Tampa, FL 33612
Noe, Bryan D., Department of Anatomy and Cell Biology, Emory University School of Medicine, Atlanta, GA 30322
Northcutt, R. Glenn, University of California, San Diego, Neuroscience 0201, 9500 Gilman Drive, La Jolla, CA 92093-0201
Norton, Catherine N., Marine Biological Laboratory, Woods Hole, MA 02543
Nusbaum, Michael P., Department of Neuroscience, University of Pennsylvania School of Medicine, 215 Stemmler Hall, Philadelphia, PA 19104-6074

O'Herron, Jonathan, Jonathan & Shirley O'Herron Foundation, One Rockefeller Plaza, New York, NY 10020
O'Melia, Anne F., 16 Evergreen Lane, Chappaqua, New York 10514
Obaid, Ana Lia, Department of Neuroscience, University of Pennsylvania School of Medicine, 234 Stemmler Hall, Philadelphia, PA 19104-6074
Ohki, Shinpei, Department of Biophysical Sciences, SUNY at Buffalo, 224 Cary Hall, Buffalo, NY 14214
Oldenbourg, Rudolf, Marine Biological Laboratory, Woods Hole, MA 02543
Olds, James L., NIH, 9/1W125, Bldg. 9, Bethesda, MD 20892
Olins, Ada L., University of Tennessee-Oak Ridge, Graduate School of Biomedical Sciences, Biology Division ORNL, P. O. Box 2009, Oak Ridge, TN 37831-8077
Olins, Donald E., University of Tennessee-Oak Ridge, Graduate School of Biomedical Sciences, Biology Division ORNL, P. O. Box 2009, Oak Ridge, TN 37831-8077
Oschman, James L., 31 Whittier Street, Dover, NH 03820

Palazzo, Robert E., Department of Physiology & Cell Biology, Haworth Hall, University of Kansas, Lawrence, KS 66045
Palmer, John D., Department of Zoology, University of Massachusetts, 221 Morrill Science Center, Amherst, MA 01003
Palti, Yoram, Rappaport Institution, Technion, POB 9697, Haifa, 31096 Israel (resigned)
Pant, Harish C., NINCDS/NIH, Laboratory of Neurochemistry, Bldg. 36, Room 4D-20, Bethesda, MD 20892
Pappas, George D., Department of Anatomy, College of Medicine, University of Illinois, 808 South Wolcott St., Chicago, IL 60612
Pardee, Arthur B., Dana-Farber Cancer Institute, D810, 44 Binney Street, Boston, MA 02115
Pardy, Roosevelt L., School of Life Sciences, University of Nebraska, Lincoln, NE 68588
Parmentier, James L., 175 S. Great Road, Lincoln, MA 01773-4112
Passano, Leonard M., Department of Zoology, Birge Hall, University of Wisconsin, Madison, WI 53706
Pearlman, Alan L., Cell Biology, Box 8228, School of Medicine, Washington University, St. Louis, MO 63110
Pederson, Thoru, Worcester Foundation for Experimental Biology, Shrewsbury, MA 01545
Perkins, C. D., 400 Hilltop Terrace, Alexandria, VA 22301
Person, Philip, 137-87 75th Road, Flushing, NY 11367
Peterson, Bruce J., Marine Biological Laboratory, Ecosystems Center, Woods Hole, MA 02543
Pethig, Ronald, School of Electronic Engineering Science, University College of N. Wales, Dean St., Bangor, Gwynedd, LL57 IUT, UK
Pfohl, Ronald J., Department of Zoology, Miami University, Oxford, OH 45056
Pierce, Sidney K., Jr., Department of Zoology, University of Maryland, College Park, MD 20742

Poindexter, Jeanne S., Barnard College, Columbia University, 3009 Broadway, New York, NY 10027-6598
Pollard, Harvey B., NIH, NIDDKD, Lab of Cell Biology & Genetics, Bldg. 8, Rm. 401, Bethesda, MD 20892
Pollard, Thomas D., Department of Cell Biology and Anatomy, Johns Hopkins University, 725 North Wolfe St., Baltimore, MD 21205
Porter, Beverly H., 5542 Windysun Ct., Columbia, MD 21045
Porter, Mary E., Department of Cell Biology and Neurology, University of Minnesota, 4-147 Jackson Hall, Minneapolis, MN 55455
Potter, David, Department of Neurobiology, Harvard Medical School, 25 Shattuck St., Boston, MA 02115
Potts, William T., Department of Biology, University of Lancaster, Lancaster, England, UK
Powers, Dennis A., Hopkins Marine Station, Stanford University, Pacific Grove, CA 93950
Powers, Maureen K., Department of Psychology, 301 Arts & Science Psych Building, Vanderbilt University, Nashville, TN 37240
Pratt, Melanie M., VITAS Healthcare Corporation, 100 S. Biscayne Boulevard, Miami, FL 33101
Prendergast, Robert A., Wilmer Institute, Johns Hopkins Hospital, 601 N. Broadway, Baltimore, MD 21287-9142
Presley, Phillip H., Carl Zeiss, Inc., 1 Zeiss Drive, Thornwood, NY 10594 (deceased)
Price, Carl A., Waksman Institute of Microbiology, Rutgers University, P. O. Box 759, Piscataway, NJ 08854
Prior, David J., Department of Biological Sciences, NAU Box 5640, Northern Arizona University, Flagstaff, AZ 86011
Prusch, Robert D., Department of Life Sciences, Gonzaga University, Spokane, WA 99258
Purves, Dale, Department of Neurobiology, Duke University Medical Center, Box 3209, 1011 Bryan Research Building, Durham, NC 27710

Quigley, James, Department of Pathology, SUNY Health Science Center, BHS Tower 9, Rm. 140, Stony Brook, NY 11794-8691

Rabb, Irving W., 1010 Memorial Drive, Cambridge, MA 02138
Rabin, Harvey, DuPont Merck Pharmaceutical, R&D Division, Exp. Station 328/358, Wilmington, DE 19880
Rabinowitz, Michael B., Marine Biological Laboratory, Woods Hole, MA 02543
Rafferty, Nancy S., Marine Biological Laboratory, Woods Hole, MA 02543
Rakowski, Robert F., Department of Physiology and Biophysics, UHS/The Chicago Medical School, 3333 Greenbay Rd., N. Chicago, IL 60064
Ramon, Fidel, Division of Post Graduate Studies and Investigation, Faculty of Medicine, Universidad Nacional Autonoma de Mexico, CU, Mexico, D. F. 04510
Ranzi, Silvio, Sez Zoologia Scienze Naturali, Dip di Biologia, Via Coloria 26, 20133, Milano, Italy
Rastetter, Edward B., Ecosystems Center, Marine Biological Laboratory, Woods Hole, MA 02543
Rebhun, Lionel I., Department of Biology, Gilmer Hall 43, University of Virginia, Charlottesville, VA 22901
Reddan, John R., Department of Biological Sciences, Oakland University, Rochester, MI 48309-4401
Reese, Barbara F., NINCDS/NIH, Bldg. 36, Room 3B26, 9000 Rockville Pike, Bethesda, MD 20892 (resigned)
Reese, Thomas S., NINCDS/NIH, Bldg. 36, Room 2A21, 9000 Rockville Pike, Bethesda, MD 20892
Reinisch, Carol L., Department of Comparative Medicine, Tufts University School of Veterinary Medicine, 200 Westboro Rd., Bldg. 20, North Grafton, MA 01536
Rich, Alexander, Department of Biology 16-735, Massachusetts Institute of Technology, Cambridge, MA 02139
Rickles, Frederick R., Center for Disease Control, MS-D02, 1600 Clifton Road, NE, Atlanta, GA 30333
Riley, Monica, Marine Biological Laboratory, Woods Hole, MA 02543
Ripps, Harris, Department of Ophthalmology, University of Illinois, 1855 W. Taylor Street, Chicago, IL 60611
Ritchie, Murdoch, Department of Pharmacology, Yale University School of Medicine, 333 Cedar St., New Haven, CT 06510
Robinson, Denis M., 200 Ocean Lane Drive #908, Key Biscayne, FL 33149 (deceased)
Rome, Lawrence C., Department of Biology, University of Pennsylvania, Philadelphia, PA 19104
Rosenbaum, Joel L., Department of Biology, 310 Kline Biology Tower, Yale University, New Haven, CT 06520
Rosenbluth, Jack, Department of Physiology, New York University School of Medicine, 550 First Ave., New York, NY 10016
Rosenbluth, Raja, Simon Fraser University, Institute of Molecular Biology and Biochemistry, Burnaby, BC, Canada, V5A 1S6
Rosenfield, Allan, Columbia University School of Public Health, 600 West 168th Street, New York, NY 10032-3702
Roslansky, John, Box 208, 26 Bar Neck Road, Woods Hole, MA 02543
Roslansky, Priscilla F., 57 Buzzards Bay Ave., Woods Hole, MA 02543
Ross, William N., Department of Physiology, New York Medical College, Valhalla, NY 10595
Roth, Jay S., P. O. Box 692, Woods Hole, MA 02543
Rowland, Lewis P., Neurological Institute, 710 West 168th St., New York, NY 10032
Ruderman, Joan V., Department of Anatomy and Cell Biology, Harvard University School of Medicine, 220 Longwood Ave., Boston, MA 02115
Rushforth, Norman B., Department of Biology, Case Western Reserve University, Cleveland, OH 44106
Russell-Hunter, W. D., 711 Howard Street, Easton, MD 21601-3934

Saffo, Mary Beth, Life Sciences Department, Arizona State University, West, P. O. Box 37100, Phoenix, AZ 85069-7100
Sager, Ruth, Dana Farber Cancer Institute, 44 Binney St., Boston, MA 02115
Sagi, Amir, Department of Life Sciences, Ben-Gurion University of the Negev, P.O. Box 653, Bee-Sheva, Israel, 84105
Salama, Guy, Department of Physiology, University of Pittsburgh, Pittsburgh, PA 15261
Salmon, Edward D., Department of Biology, Wilson Hall, CB3280, University of North Carolina, Chapel Hill, NC 27599
Salzberg, Brian M., Department of Neuroscience, University of Pennsylvania, School of Medicine, 234 Stemmler Hall, Philadelphia, PA 19104-6074
Sanger, Jean M., Department of Anatomy, University of Pennsylvania, School of Medicine, 36th and Hamilton Walk, Philadelphia, PA 19104-6058
Sanger, Joseph, Department of Anatomy, University of Pennsylvania, School of Medicine, 36th and Hamilton Walk, B-13, Philadelphia, PA 19104-6058
Saunders, John W., Jr., P. O. Box 3381, Waquoit Station, Waquoit, MA 02536
Schachman, Howard K., Department of Molecular Biology, University of California, 229 Stanley Hall #3206, Berkeley, CA 94720-3206
Schatten, Gerald P., Integrated Microscopy Facility for Biomedical Research, University of Wisconsin, 1117 W. Johnson St., Madison, WI 53706

Schatten, Heide, Department of Zoology, University of Wisconsin, Madison, WI 53706

Schiff, Jerome A., Institute for Photobiology of Cells and Organelles, Brandeis University, Waltham, MA 02254

Schmeer, Arlene C., Mercenene Cancer Research Institute, 790 Prospect Street, New Haven, CT 06511

Schmidek, Henry H., Department of Neurosurgery, St. Luke's Hospital, 102 Page St., New Bedford, MA 02740

Schnapp, Bruce J., Department of Cellular & Molecular Physiology, Harvard Medical School, 25 Shattuck St., Boston, MA 02115

Schuel, Herbert, Department of Anatomy and Cell Biology, SUNY, Buffalo, Buffalo, NY 14214

Schwartz, James H., Center for Neurobiology and Behavior, New York State Psychiatric Institute—Research Annex, 722 W. 168th St., 7th Floor, New York, NY 10032

Schweitzer, A. Nicola, Department of Pathology, Brigham & Women's Hospital, 221 Longwood Ave., LMRC 521, Boston, MA 02115

Scofield, Virginia Lee, Department of Microbiology and Immunology, University of California School of Medicine, Los Angeles, CA 90024

Sears, Mary, Woods Hole Oceanographic Institution, Woods Hole, MA 02543

Segal, Sheldon J., The Population Council, One Dag Hammarskjold Plaza, New York, NY 10036

Selman, Kelly, Department of Anatomy and Cell Biology, Box 100235, College of Medicine, University of Florida College of Medicine, Gainesville, FL 32601

Shanklin, Douglas R., Department of Pathology, Room 576, University of Tennessee College of Medicine, 800 Madison Avenue, Memphis, TN 38117

Shashoua, Victor E., Ralph Lowell Labs, Harvard Medical School, McLean Hospital, 115 Mill St., Belmont, MA 02178

Shaver, Gaius R., Ecosystems Center, Marine Biological Laboratory, Woods Hole, MA 02543

Shaver, John R., Department of Zoology, Michigan State University, East Lansing, MI 48824

Sheetz, Michael P., Department of Cell Biology, Duke University Medical Center, Box 3709, 385 Nanaline Duke Bldg., Durham, NC 27710

Shepard, David C., P. O. Box 44, Woods Hole, MA 02543

Shepro, David, Department of Microvascular Research, Boston University, 5 Cummington St., Boston, MA 02215

Sheridan, William F., Biology Department, University of North Dakota, Box 8238, University Station, Grand Forks, ND 58202-8238

Sherman, I. W., Department of Biology, University of California, Riverside, CA 92521

Shimomura, Osamu, Marine Biological Laboratory, Woods Hole, MA 02543

Shipley, Alan M., Marine Biological Laboratory, Woods Hole, MA 02543

Siegel, Irwin M., Department of Ophthalmology, New York University Medical Center, 550 First Avenue, New York, NY 10016

Silver, Robert B., Marine Biological Laboratory, Woods Hole, MA 02543

Siwicki, Kathleen K., Biology Department, Swarthmore College, 500 College Ave., Swarthmore, PA 19081

Sjodin, Raymond A., Department of Biophysics, University of Maryland, Baltimore, MD 21201

Skinner, Dorothy M., Biology Division, Oak Ridge National Laboratory, P. O. Box 2009, Oak Ridge, TN 37831

Sloboda, Roger D., Department of Biological Sciences, 306 Gilman, Dartmouth College, Hanover, NH 03755

Sluder, Greenfield, Worcester Foundation for Experimental Biology, 222 Maple Ave., Shrewsbury, MA 01545

Smith, Peter J. S., Marine Biological Laboratory, National Vibrating Probe Facility, Woods Hole, MA 02543

Smith, Stephen J., Department of Molecular & Cellular Physiology, Beckman Center, Stanford University School of Medicine, Stanford, CA 94305-5426

Smolowitz, Roxanna M., Laboratory of Marine Animal Health, Marine Biological Laboratory, Woods Hole, MA 02543

Sogin, Mitchell, Marine Biological Laboratory, Woods Hole, MA 02543

Sorenson, Martha M., Cidade Universitaria-RFRJ, Department de Bioquimica-ICB/CCS, Rio de Janeiro, RJ 21910, Brasil

Speck, William T., Columbia Presbyterian Medical Center, 161 Ft. Washington Avenue, New York, NY 10032

Spector, Abraham, Department of Ophthalmology, Columbia University, 630 West 168th Street, New York, NY 10032

Speer, John W., Marine Biological Laboratory, Woods Hole, MA 02543

Speksnijder, Johanna E., University of Groningen, Department of Genetics, Kerklaan 30, 9751 NN Haren, The Netherlands

Sperelakis, Nicholas, Department of Physiology & Biophysics, University of Cincinnati, 231 Bethesda Ave., Cincinnati, OH 45267-0576

Spiegel, Evelyn, Department of Biological Sciences, Dartmouth College, 204 Gilman, Hanover, NH 03755

Spiegel, Melvin, Department of Biological Sciences, Dartmouth College, 204 Gilman, Hanover, NH 03755

Spray, David C., Albert Einstein College of Medicine, Department of Neurosciences, 1300 Morris Park Avenue, Bronx, NY 10461

Steele, John Hyslop, Woods Hole Oceanographic Institution, Woods Hole, MA 02543

Steinacker, Antoinette, Dept. of Otolaryngology, Washington University, School of Medicine, Box 8115, 4566 Scott Avenue, St. Louis, MO 63110

Steinberg, Malcolm, Princeton University, Department of Molecular Biology, M-18 Moffett Laboratory, Princeton, NJ 08544-1014

Stemmer, Andreas C., Marine Biological Laboratory, Woods Hole, MA 02543

Stetten, Jane Lazarow, 4701 Willard Ave., Apt. 1413, Chevy Chase, MD 20815-4635

Steudler, Paul A., Ecosystems Center, Marine Biological Laboratory, Woods Hole, MA 02543

Stokes, Darrell R., Emory University, Department of Biology, 1510 Clifton Rd., NE, Atlanta, GA 30322-1100

Stommel, Elijah W., P.O. Box 31, E. Thetford, VT 05043

Stracher, Alfred, Department of Biochemistry, SUNY Health Science Center, 450 Clarkson Ave., Brooklyn, NY 11203

Strehler, Bernard L., 2310 North Laguna Circle Dr., Agoura, CA 91301-2884

Strumwasser, Felix, USUHS, Department of Psychiatry, F. E. Herbert School of Medicine, 4301 Jones Bridge Rd., Bethesda, MD 20814-4799

Stuart, Ann E., Department of Physiology, Medical Sciences Research Bldg. 206H, University of North Carolina, Chapel Hill, NC 27599-7545

Sugden, Donata O., University of Wisconsin, Department of Neurophysiology, 281 Medical Science Building, Madison, WI 53706

Sugimori, Mutsuyuki, Department of Physiology and Neuroscience, Room 442, New York University Medical Center, 550 First Avenue, New York, NY 10016

Summers, William C., Huxley College of Environmental Studies, Western Washington University, Bellingham, WA 98225

Suprenant, Kathy A., Department of Physiology and Cell Biology, 4010 Haworth Hall, University of Kansas, Lawrence, KS 66045
Sussman, Maurice, 72 Carey Lane, Falmouth, MA 02540
Sussman, Raquel B., Marine Biological Laboratory, Woods Hole, MA 02543
Sweet, Frederick, Department of Obstetrics and Gynecology, Box 8064, Washington University School of Medicine, 499 South Euclid, St. Louis, MO 63110
Swenson, Katherine I., Duke University Medical Center, Department of Molecular Cancer, P.O. Box 3686, Durham, NC 27710
Sydlik, Mary Anne, Department of Biology, Westfield State College, Westfield, MA 01086
Szent-Györgyi, Andrew, Department of Biology, Brandeis University, Bassine 244, 415 South Street, Waltham, MA 02254
Szent-Gyorgyi, Gwen P., 45 Nobska Road, Woods Hole, MA 02543
Szuts, Ete Z., 1 Elm Street, Byfield, MA 01922-2728

Tabares, Lucia, Department of Physiology, University of Seville School of Medicine, Avda. Sanchez Pizjuan, 4, Seville 41009, Spain
Tamm, Sidney L., Boston University Marine Program, Marine Biological Laboratory, Woods Hole, MA 02543
Tanzer, Marvin L., University of Connecticut School of Dental Medicine, Department of Biostructure and Function, Farmington, CT 06030-3705
Tasaki, Ichiji, Laboratory of Neurobiology, NIMH/NIH, Bldg. 36, Rm. 2B-16, Bethesda, MD 20892
Taylor, Douglass L., Center for Fluorescence Research, Carnegie Mellon University, 4400 Fifth Avenue, Pittsburgh, PA 15213
Teal, John M., Department of Biology, Woods Hole Oceanographic Institution, Woods Hole, MA 02543
Telfer, William H., Department of Biology, University of Pennsylvania, Philadelphia, PA 19104
Telzer, Bruce, Pomona College, Department of Biology, Thille Building, 175 W. 6th Street, Claremont, CA 91711
Thorndike, W. Nicholas, Wellington Management Company, 200 State St., Boston, MA 02109
Townsel, James G., Department of Physiology, Meharry Medical College, Nashville, TN 37208
Travis, David M., 300 River Road, #311, Manchester, NH 03104-2483
Treistman, Steven N., University of Massachusetts Medical Center, Department of Pharmacology, 55 Lake Avenue North, Worcester, MA 01655
Trigg, D. Thomas, One Federal Street, 9th Floor, Boston, MA 02211
Trinkaus, J. P., Department of Biology, Yale University, New Haven, CT 06511
Troll, Walter, Department of Environmental Medicine, College of Medicine, New York University, New York, NY 10016
Troxler, Robert F., Department of Biochemistry, School of Medicine, Boston University, 80 East Concord St., Boston, MA 02118
Tucker, Edward B., Department of Natural Sciences, Baruch College, CUNY, 17 Lexington Ave., New York, NY 10010
Turner, Ruth D., Mollusk Department, Museum of Comparative Zoology, Harvard University, Cambridge, MA 02138
Tweedell, Kenyon S., Department of Biological Sciences, University of Notre Dame, Notre Dame, IN 46656
Tykocinski, Mark L., Institute of Pathology, Case Western Reserve University, 2085 Adelbert Rd., Cleveland, OH 44106
Tytell, Michael, Department of Anatomy & Neurobiology, Bowman Gray School of Medicine, Wake Forest University, Winston-Salem, NC 27103

Ueno, Hiroshi, Kyoto University, Faculty of Agriculture, Department of Agricultural Chemistry, Sakyo, Kyoto 606, Japan

Valiela, Ivan, Boston University Marine Program, Marine Biological Laboratory, Woods Hole, MA 02543
Vallee, Richard, Cell Biology Group, Worcester Foundation for Experimental Biology, Shrewsbury, MA 01545
Valois, John, 420 Woods Hole Road, Woods Hole, MA 02543
Van Holde, Kensal, Department of Biochemistry and Biophysics, Oregon State University, Corvallis, OR 97331-7503
Vogel, Steven S., LTPB/NICHD, Bldg. 10, Rm. 6C205, Bethesda, MD 20892

Waksman, Byron, Foundation for Microbiology, 300 East 54th St., #5K, New York, NY 10022
Wall, Betty, 9 George St., Woods Hole, MA 02543
Wallace, Robin A., Whitney Laboratory, 9505 Ocean Shore Blvd., St. Augustine, FL 32086 (resigned)
Wang, Ching Chung, Department of Pharmaceutical Chemistry, University of California, San Francisco, CA 94143
Wang, Hsien-yu, Department of Physiology & Biophysics, HSC, University Medical Center, SUNY-Stony Brook, Stony Brook, NY 11794-8633
Wangh, Lawrence J., Department of Biology, Brandeis University, 415 South St., Waltham, MA 02254
Warner, Robert C., Department of Molecular Biology and Biochemistry, University of California, Irvine, CA 92717
Warren, Kenneth S., The Picower Institute for Medical Research, 350 Community Drive, Manhasset, NY
Warren, Leonard, Wistar Institute, 36th and Spruce Streets, Philadelphia, PA 19104
Waterbury, John B., Department of Biology, Woods Hole Oceanographic Institution, Woods Hole, MA 02543
Watson, Stanley, Associates of Cape Cod, Inc., P. O. Box 224, Woods Hole, MA 02543 (deceased)
Waxman, Stephen G., Department of Neurology, P.O. Box 208018, Yale School of Medicine, 333 Cedar Street, New Haven, CT 06510
Webb, H. Marguerite, Marine Biological Laboratory, Woods Hole, MA 02543
Weber, Annemarie, Department of Biochemistry and Biophysics, School of Medicine, University of Pennsylvania, Philadelphia, PA 19066
Weidner, Earl, Department of Zoology and Physiology, Louisiana State University, Baton Rouge, LA 70803
Weiss, Dieter G., Fachbereich Biologie, Institute Tierphysiologie, University of Rostock, D-18051 Rostock Germany
Weiss, Leon P., Department of Animal Biology, School of Veterinary Medicine, University of Pennsylvania, Philadelphia, PA 19104
Weissmann, Gerald, New York University School of Medicine, 550 First Avenue, New York, NY 10016
Werman, Robert, Neurobiology Unit, The Hebrew University, Jerusalem, Israel
Westerfield, R. Monte, The Institute of Neuroscience, University of Oregon, Eugene, OR 97403
Whittaker, J. Richard, Department of Biology, Bag Service #45111, University of New Brunswick, Fredericton, NB E3B 6E1, Canada
Wichterman, Ralph, 31 Buzzards Bay Avenue, Woods Hole, MA 02543
Wilson, Darcy B., San Diego Regional Cancer Center, 3099 Science Park Road, San Diego, CA 92121
Wilson, T. Hastings, Department of Physiology, Harvard Medical School, 25 Shattuck Street, Boston, MA 02115
Witkovsky, Paul, Department of Ophthalmology, New York University Medical Center, 550 First Ave., New York, NY 10016

Wittenberg, Beatrice, Department of Physiology & Biophysics, Albert Einstein College of Medicine, 1300 Morris Park Ave., Bronx, NY 10461

Wittenberg, Jonathan B., Department of Physiology and Biophysics, Albert Einstein College, 1300 Morris Park Ave., Bronx, NY 01461

Wolken, Jerome J., Department of Biological Sciences, Carnegie Mellon University, 440 Fifth Ave., Pittsburgh, PA 15213

Wonderlin, William F., Department of Pharmacology & Toxicology, West Virginia University, Morgantown, WV 26506

Worden, Mary Kate, Department of Neurobiology, Harvard Medical School, 220 Longwood Ave., Boston, MA 02115

Worgul, Basil V., Department of Ophthalmology, Columbia University, 630 West 168th St., New York, NY 10032

Wu, Chau Hsiung, Department of Pharmacology, S215, Northwestern University Medical School, Chicago, IL 60611

Wyttenbach, Charles R., Department of Physiology and Cell Biology, University of Kansas, Lawrence, KS 66045

Yeh, Jay Z., Department of Pharmacology, Northwestern University Medical School, Chicago, IL 60611

Zigman, Seymour, Ophthalmology Research, University of Rochester Medical School, Box 314, 601 Elmwood Avenue, Rochester, NY 14642

Zigmond, Michael J., University of Pittsburgh, 570 Crawford Hall, Pittsburgh, PA 15260

Zimmerberg, Joshua J., NIH, Bldg. 12A, Room 2007, Bethesda, MD 20892

Zottoli, Steven J., Department of Biology, Williams College, Williamstown, MA 01267

Zucker, Robert S., Neurobiology Division, Department of Molecular and Cellular Biology, University of California, Berkeley, CA 94720

Zukin, Ruth Suzanne, Department of Neuroscience, Albert Einstein College of Medicine, 1410 Pelham Parkway South, Bronx, NY 10461

MBL Associates

Executive Board

Megan Jones, President
Mary Ulbrich, Vice President
Deborah G. Senft, Treasurer
Priscilla Roslansky, Secretary
Alfred F. Borg
Jennie P. Brown
Julia S. Child
Elaine Pear Cohen, Arts Chair *(deceased)*
Hanna Hastings
Doris B. Hiatt
Ruth Ann Laster, Membership Chair
Evelyn Laufer
Barbara Little
Robert Livingstone, Jr.
Luigi Mastroianni, Jr.
Jack Pearce
Robert M. Reynolds
Ted Rowan
John Valois
Barbara Wheeler

Sustaining Associate

Dr. and Mrs. Neal W. Cornell
Mr. and Mrs. Jonathan O'Herron
Plymouth Savings Bank

Supporting Associate

Dr. and Mrs. Richard Armstrong
Benthos
Mr. James M. Clark
Mr. and Mrs. LeRoy Clark, Jr.
Dr. and Mrs. Alexander W. Clowes
Mrs. Margaret Clowes
Mr. and Mrs. Ian D. W. Cramer
Dr. and Mrs. James D. Ebert
Mr. and Mrs. David Fausch
Drs. Gerald and Ruth Fischbach
Mr. and Mrs. David Gaiser
Dr. and Mrs. Prosser Gifford
Dr. and Mrs. Howard H. Hiatt
Dr. and Mrs. Leonard Laster
Mr. and Mrs. William K. Mackey
Drs. Luigi and Elaine Mastroianni
Dr. and Mrs. J. Wister Meigs
Mr. and Mrs. David Palmer
Ms. Linda Sallop and Mr. Michael Fenlon
Mr. and Mrs. John E. Sawyer
Drs. Christina and John Tochko

Dual Membership

Mr. and Mrs. David C. Ahearn
Mr. and Mrs. Douglas F. Allison
Dr. and Mrs. Samuel C. Armstrong
Mr. and Mrs. Henry Ashworth
Mr. and Mrs. Duncan P. Aspinwall
Mr. and Mrs. Donald R. Aukamp
Dr. and Mrs. H. Thomas Ballantine, Jr.
Mr. and Mrs. William L. Banks
Mr. and Mrs. R. Channing Barlow
Dr. and Mrs. Robert B. Barlow, Jr.
Mr. and Mrs. John E. Barnes
Mr. and Mrs. Richard T. Baum
Dr. and Mrs. Robert M. Berne
Drs. Alan and Harriet Bernheimer
Mr. and Mrs. Robert O. Bigelow
Dr. and Mrs. Edward G. Boettiger
Dr. and Mrs. Alfred F. Borg
Dr. and Mrs. Thomas A. Borgese
Dr. and Mrs. Francis P. Bowles
Dr. and Mrs. Thornton Brown
Dr. and Mrs. John B. Buck
Dr. and Mrs. John E. Burris
Dr. and Mrs. Francis D. Carlson
Mr. and Mrs. Winslow G. Carlton
Dr. and Mrs. Frank M. Child, III
Dr. and Mrs. Arnold M. Clark
Mr. and Mrs. David L. Crabb
Mr. and Mrs. Melvin C. Crain
Mr. and Mrs. Thomas S. Crane
Dr. and Mrs. John M. Cummings
Mr. and Mrs. Bruce G. Daniels
Dr. and Mrs. Clyde J. Dawe
Drs. Charles and Molly DiCecca
Mr. and Mrs. William P. Dugan
Dr. and Mrs. James J. Ferguson, Jr.
Mr. and Mrs. Frederick S. Fisher, III
Mr. and Mrs. Howard G. Freeman
Mr. and Mrs. Leonard D. Friedman
Dr. and Mrs. Robert A. Frosch
Mr. and Mrs. Robert S. Gilette
Mr. and Mrs. Charles Goodwin
Dr. and Mrs. Harlyn O. Halvorson
Drs. Alexander and Carol Hannenberg
Mrs. Janet M. Harvey
Dr. and Mrs. Richard B. Harvey
Dr. and Mrs. J. Woodland Hastings
Mr. and Mrs. Gray G. Hayward
Dr. and Mrs. John E. Hobbie
Dr. and Mrs. Stuart Hodge
Drs. Francis C. G. Hoskin and Elizabeth M. Farnham
Dr. and Mrs. Robert J. Huettner
Mrs. Mary D. Janney
Mr. and Mrs. DeWitt C. Jones, III
Dr. and Mrs. Benjamin Kaminer
Dr. Peter N. Kivy
Dr. and Mrs. S. Andrew Kulin
Dr. and Mrs. Hans Laufer
Mr. William Lawrence
Dr. and Mrs. Berton J. Leach
Dr. and Mrs. Rachmiel Levine
Mr. and Mrs. James E. Lloyd
Mrs. Ermine W. Lovell
Mrs. Anne Camille Maher
Mr. and Mrs. Bernard Manuel
Mr. and Mrs. Joseph C. Martyna
Mr. and Mrs. Frank J. Mather, III
Mr. and Mrs. James W. Mavor, Jr.
Mr. John J. McMahon
Mr. and Mrs. Arthur V. Meigs
Dr. and Mrs. Jerry M. Melillo
Dr. and Mrs. Charles B. Metz
Mr. and Mrs. Richard Meyers
Mr. and Mrs. Charles A. Mitchell
Dr. and Mrs. Charles H. Montgomery
Mr. and Mrs. Bassett K. Morse

Mr. and Mrs. Frank L. Nickerson
Mr. and Mrs. Clifford T. O'Connell
Dr. and Mrs. George D. Pappas
Mr. and Mrs. Robert Parkinson
Dr. and Mrs. John B. Pearce
Mr. and Mrs. John B. Peri
Dr. and Mrs. Philip Person
Mr. and Mrs. Frederick S. Peters
Mr. and Mrs. E. Joel Peterson
Dr. and Mrs. Anthony Pires
Mr. and Mrs. George H. Plough
Dr. and Mrs. Aubrey Pothier, Jr.
Dr. and Mrs. C. Ladd Prosser
Mr. Allan Ray Putnam
Mr. and Mrs. Robert M. Reynolds
Dr. and Mrs. Renato A. Ricca
Mr. and Mrs. Harold Righter
Mr. and Mrs. John Ripple
Ms. Jean Roberts
Drs. John and Priscilla F. Roslansky
Dr. and Mrs. John D. Rummel
Dr. and Mrs. John W. Saunders, Jr.
Dr. and Mrs. R. Walter Schlesinger
Mr. John Seder and Ms. Frances Plough
Dr. and Mrs. Sheldon J. Segal
Drs. Cecily C. Selby and James S. Coles
Dr. and Mrs. Douglas R. Shanklin
Dr. and Mrs. David Shepro
Mr. and Mrs. Bertram R. Silver
Mr. and Mrs. Jonathan O. Simonds
Mr. and Mrs. Daniel M. Singer
Drs. Frederick and Marguerite Smith
Mr. and Mrs. Homer P. Smith
Mr. and Mrs. Heinz Specht
Dr. and Mrs. William K. Stephenson
Mr. and Mrs. Gerard L. Swope
Mr. and Mrs. Gordon F. Todd
Mr. and Mrs. D. Thomas Trigg
Dr. and Mrs. Walter Troll, Ph.D.
Mr. and Mrs. Volker Ulbrich
Mr. and Mrs. John Valois
Mr. and Mrs. Ronald Veeder
Ms. Susan Veeder
Mr. and Mrs. Samuel Vincent
Mr. and Mrs. Henry Walter
Dr. and Mrs. Henry B. Warren
Mr. and Mrs. John T. Weeks
Mr. and Mrs. Alfred Weisberg
Dr. and Mrs. Gerald Weissman
Dr. and Mrs. Paul S. Wheeler
Mr. and Mrs. Leslie J. Wilson
Mr. and Mrs. Bruce Zimmerli
Dr. and Mrs. Donald J. Zinn

Individual Associates

Dr. Frederick W. Ackroyd
Mrs. Marion S. Adelberg
Mr. Henry Albers
Dr. Nina S. Allen
Drs. James and Helene Anderson
Mrs. Kimball C. Atwood, III
Mr. Everett E. Bagley
Mr. and Mrs. C. John Berg
Ms. Carol L. Bissonnette
Dr. Thomas P. Bleck
Mr. Robert D. Boche
Mrs. Julie Boettiger
Mr. Theodore A. Bonn
Mrs. Frank A. Brown, Jr.
Mrs. Thomas A. Brown
Dr. Robert H. Broyles
Dr. Alan H. Burghauser
Mrs. Beatrice F. Buxton
Mr. Bruce E. Buxton
Mrs. David Campbell
Mr. Frank C. Carotenuto
Dr. Robert H. Carrier
Mrs. Patricia A. Case
Mrs. Shirley R. Chaet
Mrs. Christie L. Chapman
Dr. Sallie Chisholm
Dr. Peter L. Clark
Ms. Ann P. Cleary
Dr. Laurence P. Cloud
Mr. Allen W. Clowes
Dr. Jewel Plummer Cobb
Mrs. Elaine Pear Cohen (deceased)
Prof. Donald Eugene Copeland
Dr. Helen M. Costello
Dr. Vincent Cowling
Dr. Sylvia E. Crane
Ms. Charlotte E. Cross
Ms. Dorothy Crossley
Miss Helen Crossley
Mrs. Villa B. Crowell
Dr. Morton Davidson
Mr. David L. Donovan
Ms. Suzanne Droban
Mr. and Mrs. Charles E. Eastman
Mr. Raymond Eliott
Mr. Gordon C. Estabrooks
Mr. William M. Ferry
Mr. John W. Folino, Jr.
Mr. Paul J. Freyheit
Dr. John J. Funkhouser
Mrs. Paul M. Fye
Miss Eleanor Garfield
Dr. James L. German, III
Mr. Charles Gifford
Mrs. Rebeckah D. Glazebrook
Mr. Michael P. Goldring
Mrs. Phyllis Goldstein
Mr. and Mrs. John Grassle
Mrs. Edith T. Grosch
Mrs. Mona Gross
Mrs. Barbara Grossman
Dr. Harry O. Haakonsen
Mrs. Valerie A. Hall
Ms. Mary Elizabeth Hamstrom
Dr. Robert R. Haubrich
Dr. David S. Hays
Mrs. H. D. Hibbitt
Mrs. Bertha V. Hill
Mrs. Eleanor M. Hirschfield
Mrs. Helen Hodosh (deceased)
Mrs. Mary Jean Howard
Ms. Susan A. Huettner
Miss Elizabeth B. Jackson
Mrs. Margaret Jenkins
Mrs. Barbara W. Jones
Mr. Fred Karush
Mrs. Jessie Keosian
Mrs. Patricia E. Keoughan
Dr. Ben Korgen
Mr. Ezra Laderman
Mrs. Rodney C. Larcom
Ms. Rebecca Lash
Mr. and Mrs. F. Arthur Le Blond
Dr. Marian E. LeFevre
Dr. Mortimer Levitz
Mr. Lennart Lindberg
Mr. Timothy Lindner
Mrs. Barbara C. Little
Mr. Robert Livingstone, Jr.
Mrs. Sarah Loessel
Mr. Richard C. Lovering
Miss Doris L. Low
Dr. and Mrs. Philip B. Maples
Dr. Julian B. Marsh
Mrs. Jane C. McCormack
Mrs. Nella W. McElroy
Mr. Paul McGonigle
Ms. Mary W. McKoan
Ms. Cornelia McMurtrie
Mr. Mentor Metaxas
Dr. Daniel G. Miller
Mrs. Florence E. Mixer
Mrs. Anna Monroy
Mrs. Mary E. Montgomery
Dr. Isabel Mountain
Mrs. Eleanor M. Nace
Mr. Paul F. Nace, Jr.
Mr. John E. Naugle
Dr. Pamela Nelson
Ms. Catherine N. Norton
Mr. Thomas O'Neil
Dr. Renee Bennett O'Sullivan
Dr. Janice S. Olszowka
Mrs. Malcolm S. Park
Ms. Joan Pearlman
Dr. Judith Pederson
Mr. Raymond W. Peterson
Mrs. F. Carol Price
Mr. John S. Price
Mrs. Cynthia Rankin
Mrs. Julia S. Rankin
Dr. Samuel O. Raymond
Ms. A. Kathy Regis
Mr. John Riina
Dr. Monica Riley
Mr. Alexander Meigs Rives
Mrs. Lola E. Robertson
Ms. Hilde Rosenthal
Mrs. Atholie K. Rosett
Ms. Virginia F. Ross
Mr. Edward Rowan
Mr. Francis C. Ryder
Mrs. Ruth L. Saz
Dr. Edward K. Scheer

Mr. Peter J. Schwamb
Mrs. Elsie M. Scott
Mrs. Deborah G. Senft
Mrs. Harriet S. Shapiro
Dr. Charlotte Shemin
Dr. James Sidie
Mrs. Virginia B. Sinnott
Mrs. Diana M. Smith
Mrs. Perle Sonnenblick
Dr. William T. Speck
Dr. Evelyn Spiegel
Mrs. H. Burr Steinbach
Ms. Gail Stetten
Mrs. Jane Lazarow Stetten
Mr. Robert Stump
Mr. Albert H. Swain
Mr. James K. Taylor
Mrs. Linda L. Timmins
Mrs. Ida Trager
Miss Natalie Trousof
Ms. Ciona Ulbrich
Mrs. Barbara Van Holde
Dr. Claude A. Villee, Jr.
Mrs. Dorothy Villee
Mrs. Eve Warren
Dr. Gary Wessel
Dr. William M. Wheeler
Mrs. Barbara Whitehead
Mr. Geoffrey G. Whitney, Jr.
Mrs. A.A.T. Wickersham
Mrs. Clare M. Wilber
Dr. William M. Winn
Ms. Nancy Woitkoski
Dr. Sumner Zacks

MBL Associates Gift Shop Volunteers

Margaret Armstrong
Barbara Atwood
Harriet Bernheimer
Gloria Borgese
Jennie Brown
Kitty Brown
Elizabeth Buck
Julia Child
Vera Clark
Peggy Clowes
Jewel Cobb
Janet Daniels
Fran Eastman
Alma Ebert
Margaret German
Violet Gifford
Rose Grant
Edie Grosch
Barbara Grossman
Jean Halvorson
Pat Hancock
Hanna Hastings
Helen Hodosh
Sally Karush
Barbara Little
Sally Loessel
Winnie Mackey
Miriam Mauzerall
Mary Mavor
Polly Miles
Florence Mixer
Lorraine Mizell
Eleanor Nace
Bertha Person
Liz Price
Linda Rakowski
Julie Rankin
Jean Ripps
Lilyan Sauders
Marilyn Shepro
Cynthia Smith
Peggy Smith
Louise Specht
Susie Steinbach
Jane Stetton
Peg Talcot
Eleanor Troll
Natalie Trousof
Mary Ulbrich
Barbara Van Holde
Alice Veeder
Joan Wheeler
Clare Wilber

MBL Summer Tour Guides

Betsy Bang
John Buck
Sears Crowell
Barbara Little
Julie Rankin
Lola Robertson
Priscilla Roslansky
Mary Ulbrich
Donald Zinn
Margery Zinn

Certificate of Organization
Articles of Amendment
Bylaws

Certificate of Organization

(On File in the Office of the Secretary of the Commonwealth)

No. 3170

We, Alpheus Hyatt, President, William Stanford Stevens, Treasurer, and William T. Sedgwick, Edward G. Gardiner, Susan Mims and Charles Sedgwick Minot being a majority of the Trustees of the Marine Biological Laboratory in compliance with the requirements of the fourth section of chapter one hundred and fifteen of the Public Statutes do hereby certify that the following is a true copy of the agreement of association to constitute said Corporation, with the names of the subscribers thereto:

We, whose names are hereto subscribed, do, by this agreement, associate ourselves with the intention to constitute a Corporation according to the provisions of the one hundred and fifteenth chapter of the Public Statutes of the Commonwealth of Massachusetts, and the Acts in amendment thereof and in addition thereto.

The name by which the Corporation shall be known is
THE MARINE BIOLOGICAL LABORATORY.

The purpose for which the Corporation is constituted is to establish and maintain a laboratory or station for scientific study and investigations, and a school for instruction in biology and natural history.
The place within which the Corporation is established or located is the city of Boston within said Commonwealth.
The amount of its capital stock is none.
In Witness Whereof, we have hereunto set our hands, this twenty seventh day of February in the year eighteen hundred and eighty-eight, Alpheus Hyatt, Samuel Mills, William T. Sedgwick, Edward G. Gardiner, Charles Sedgwick Minot, William G. Farlow, William Stanford Stevens, Anna D. Phillips, Susan Mims, B. H. Van Vleck.
That the first meeting of the subscribers to said agreement was held on the thirteenth day of March in the year eighteen hundred and eighty-eight.
In Witness Whereof, we have hereunto signed our names, this thirteenth day of March in the year eighteen hundred and eighty-eight, Alpheus Hyatt, President, William Stanford Stevens, Treasurer, Edward G. Gardiner, William T. Sedgwick, Susan Mims, Charles Sedgwick Minot.
(Approved on March 20, 1988 as follows:
I hereby certify that it appears upon an examination of the within written certificate and the records of the corporation duly submitted to my inspection, that the requirements of sections one, two and three of chapter one hundred and fifteen, and sections eighteen, twenty and twenty-one of chapter one hundred and six, of the Public Statutes, have been complied with and I hereby approve said certificate this twentieth day of March A.D. eighteen hundred and eighty-eight.

Charles Endicott
Commissioner of Corporations)

Articles of Amendment

(On File in the Office of the Secretary of the Commonwealth)

We, James D. Ebert, President, and David Shepro, Clerk of the Marine Biological Laboratory, located at Woods Hole, Massachusetts 02543, do hereby certify that the following amendment to the Articles of Organization of the Corporation was duly adopted at a meeting held on August 15, 1975, as adjourned to August 29, 1975, by vote of 444 members, being at least two-thirds of its members legally qualified to vote in the meeting of the corporation:

Voted: That the Certificate of Organization of this corporation be and it hereby is amended by the addition of the following provisions:
"No Officer, Trustee or Corporate Member of the corporation shall be personally liable for the payment or satisfaction of any obligation or liabilities incurred as a result of, or otherwise in connection with, any commitments, agreements, activities or affairs of the corporation.
"Except as otherwise specifically provided by the Bylaws of the corporation, meetings of the Corporate Members of the corporation may be held anywhere in the United States.
"The Trustees of the corporation may make, amend or repeal the Bylaws of the corporation in whole or in part, except with respect to any provisions thereof which shall by law, this Certificate or the bylaws of the corporation, require action by the Corporate Members."

The foregoing amendment will become effective when these articles of amendment are filed in accordance with Chapter 180, Section 7 of the General Laws unless these articles specify, in accordance with the vote adopting the amendment, a later effective date not more than thirty days after such filing, in which event the amendment will become effective on such later date.

In Witness whereof and Under the Penalties of Perjury, we have hereto signed our names this 2nd day of September, in the year 1975, James D. Ebert, President; David Shepro, Clerk.
(Approved on October 24, 1975, as follows:
I hereby approve the within articles of amendment and, the filing fee in the amount of $10 having been paid, said articles are deemed to have been filed with me this 24th day of October, 1975.

Paul Guzzi
Secretary of the Commonwealth)

Bylaws

(Revised August 7, 1992 and December 10, 1992)

ARTICLE I—THE CORPORATION

A. *Name and Purpose* The name of the Corporation shall be The Marine Biological Laboratory. The Corporation's purpose shall be to establish and maintain

a laboratory or station for scientific study and investigation and a school for instruction in biology and natural history.

B *Nondiscrimination* The Corporation shall not discriminate on the basis of age, religion, color, race, national or ethnic origin, sex or sexual preference in its policies on employment and administration or in its educational and other programs.

ARTICLE II—MEMBERSHIP

A *Members.* The Members of the Corporation ("Members") shall consist of persons elected by the Board of Trustees (the "Board"), upon such terms and conditions and in accordance with such procedures, not inconsistent with law or these Bylaws, as may be determined by the Board. At any regular or special meeting of the Board, the Board may elect new Members. Members shall have no voting or other rights with respect to the Corporation or its activities except as specified in these Bylaws, and any Member may vote at any meeting of the Members in person only and not by proxy. Members shall serve until their death or resignation unless earlier removed with or without cause by the affirmative vote of two-thirds of the Trustees then in office. Any Member who has retired from his or her home institution may, upon written request to the Corporation, be designated a Life Member. Life Members shall not have the right to vote and shall not be assessed for dues.

B. *Meetings.* The annual meeting of the Members shall be held on the Friday following the first Tuesday in August of each year, at the Laboratory of the Corporation in Woods Hole, Massachusetts, at 9:30 a.m. The Chairperson of the Board shall preside at meetings of the Corporation. If no annual meeting is held in accordance with the foregoing provision, a special meeting may be held in lieu thereof with the same effect as the annual meeting, and in such case all references in these Bylaws, except in this Article II.B., to the annual meeting of the Members shall be deemed to refer to such special meeting. Members shall transact business as may properly come before the meeting. Special meetings of the Members may be called by the Chairperson or the Trustees, and shall be called by the Clerk, or in the case of the death, absence, incapacity or refusal by the Clerk, by any other officer, upon written application of Members representing at least ten percent of the smallest quorum of Members required for a vote upon any matter at the annual meeting of the Members, to be held at such time and place as may be designated.

C. *Quorum* One hundred (100) Members shall constitute a quorum at any meeting. Except as otherwise required by law or these Bylaws, the affirmative vote of a majority of the Members voting in person at a meeting attended by a quorum shall constitute action on behalf of the Members.

D. *Notice of Meetings* Notice of any annual meeting or special meeting of Members, if necessary, shall be given by the Clerk by mailing notice of the time and place and purpose of such meeting at least 15 days before such meeting to each Member at his or her address as shown on the records of the Corporation.

E. *Waiver of Notice* Whenever notice of a meeting is required to be given a Member, under any provision of the Articles or Organization or Bylaws of the Corporation, a written waiver thereof, executed before or after the Meeting by such Member, or his or her duly authorized attorney, shall be deemed equivalent to such notice.

F. *Adjournments.* Any meeting of the Members may be adjourned to any other time and place by the vote of a majority of those Members present at the meeting, whether or not such Members constitute a quorum, or by any officer entitled to preside at or to act as Clerk of such meeting, if no Member is present or represented. It shall not be necessary to notify any Members of any adjournment unless no Member is present or represented at the meeting which is adjourned, in which case, notice of the adjournment shall be given in accordance with Article II.D. Any business which could have been transacted at any meeting of the Members as originally called may be transacted at an adjournment thereof.

ARTICLE III—ASSOCIATES OF THE CORPORATION

Associates of the Corporation The Associates of the Marine Biological Laboratory shall be an unincorporated group of persons (including associations and corporations) interested in the Laboratory and shall be organized and operated under the general supervision and authority of the Trustees. The Associates of the Marine Biological Laboratory shall have no voting rights.

ARTICLE IV—BOARD OF TRUSTEES

A *Powers* The Board of Trustees shall have the control and management of the affairs of the Corporation. The Trustees shall elect a Chairperson of the Board who shall serve until his or her successor is elected and qualified. They shall annually elect a President of the Corporation. They shall annually elect a Vice Chairperson of the Board who shall be Vice Chairperson of the meetings of the Corporation. They shall annually elect a Treasurer. They shall annually elect a Clerk, who shall be a resident of Massachusetts. They shall elect Trustees-at-Large as specified in this Article IV. They shall appoint a Director of the Laboratory for a term not to exceed five years, provided the term shall not exceed one year if the candidate has attained the age of 65 years prior to the date of the appointment. They shall choose such other officers and agents as they shall think best. They may fix the compensation of all officers and agents of the Corporation and may remove them at any time. They may fill vacancies occurring in any of the offices. The Board shall have the power to choose an Executive Committee from their own number as provided in Article V, and to delegate to such Committee such of their own powers as they may deem expedient in addition to those powers conferred by Article V. They shall, from time to time, elect Members to the Corporation upon such terms and conditions as they shall have determined, not inconsistent with law or these Bylaws.

B *Composition and Election*

(1) The Board shall include 24 Trustees elected by the Board as provided below:

(a) At least six Trustees ("Corporate Trustees") shall be Members who are scientists, and the other Trustees ("Trustees-at-Large") shall be individuals who need not be Members or otherwise affiliated with the Corporation.

(b) The 24 elected Trustees shall be divided into four classes of six Trustees each, with one class to be elected each year to serve for a term of four years, and with each such class to include at least one Corporate Trustee. Such classes of Trustees shall be designated by the year of expiration of their respective terms.

(2) The Board shall also include the Chief Executive Officer, Treasurer and the Chairperson of the Science Council, who shall be *ex officio* voting members of the Board.

(3) Although Members or Trustees may recommend individuals for nomination as Trustees, nominations for Trustee elections shall be made by the Nominating Committee in its sole discretion. The Board may also elect Trustees who have not been nominated by the Nominating Committee.

C. *Eligibility* A Corporate Trustee or a Trustee-at-Large who has been elected to an initial four-year term or remaining portion thereof, of which he/she has served at least two years, shall be eligible for re-election to a second four-year term, but shall be ineligible for re-election to any subsequent term until one year has elapsed after he/she has last served as a Trustee.

D. *Removal* Any Trustee may be removed from office at any time with or without cause, by vote of a majority of the Members entitled to vote in the election of Trustees; or for cause, by vote of two-thirds of the Trustees then in office. A Trustee may be removed for cause only if notice of such action shall have been given to all of the Trustees or Members entitled to vote, as the case may be, prior to the meeting at which such action is to be taken and if the Trustee to be so removed shall have been given reasonable notice and opportunity to be heard before the body proposing to remove him or her.

E. *Vacancies* Any vacancy in the Board may be filled by vote of a majority of the remaining Trustees present at a meeting of Trustees at which a quorum is present. Any vacancy in the Board resulting from the resignation or removal of a Corporate Trustee shall be filled by a Member who is a scientist.

F. *Meetings* Meetings of the Board shall be held from time to time, not less frequently than twice annually, as determined by the Board. Special meetings of Trustees may be called by the Chairperson, or by any seven Trustees, to be held at such time and place as may be designated. The Chairperson of the Board, when present, shall preside over all meetings of the Trustees. Written notice shall be sent to a Trustee's usual or last known place of residence at least two weeks before the meeting. Notice of a meeting need not be given to any Trustee if a written waiver of notice executed by such Trustee before or after the meeting is filed with the records of the meeting, or if such Trustee shall attend the meeting without protesting prior thereto or at its commencement the lack of notice given to him or her.

G. *Quorum and Action by Trustees* A majority of all Trustees then in office shall constitute a quorum. Any meeting of Trustees may be adjourned by vote of a majority of Trustees present, whether or not a quorum is present, and the meeting may be held as adjourned without further notice. When a quorum is present at any meeting of the Trustees, a majority of the Trustees present and voting (excluding abstentions) shall decide any question, including the election of officers, unless otherwise required by law, the Articles of Organization or these Bylaws.

H *Transfers of Interests in Land* There shall be no transfer of title nor long-term lease of real property held by the Corporation without prior approval of not less than two-thirds of the Trustees. Such real property transactions shall be finally acted upon at a meeting of the Board only if presented and discussed at a prior meeting of the Board. Either meeting may be a special meeting and no less than four weeks shall elapse between the two meetings. Any property acquired by the Corporation after December 1, 1989 may be sold, any mortgage or pledge of real

property (regardless of when acquired) to secure borrowings by the Corporation may be granted, and any transfer of title or interest in real property pursuant to the foreclosure or endorsement of any such mortgage or pledge of real property may be effected by any holder of a mortgage or pledge of real property of the Corporation, with the prior approval of not less than two-thirds of the Trustees (other than any Trustee or Trustees with a direct or indirect financial interest in the transaction being considered for approval) who are present at a regular or special meeting of the Board at which there is a quorum.

ARTICLE V—COMMITTEES

A. *Executive Committee.* There shall be an Executive Committee of the Board of Trustees which shall consist of not more than eleven (11) Trustees, including *ex officio* Trustees, elected by the Board.

The Chairperson of the Board shall act as Chairperson of the Executive Committee and the Vice Chairperson as Vice Chairperson. The Executive Committee shall meet at such times and places and upon such notice and appoint such subcommittees as the Committee shall determine.

The Executive Committee shall have and may exercise all the powers of the Board during the intervals between meetings of the Board except those powers specifically withheld, from time to time, by vote of the Board or by law. The Executive Committee may also appoint such committees, including persons who are not Trustees, as it may, from time to time, approve to make recommendations with respect to matters to be acted upon by the Executive Committee or the Board.

The Executive Committee shall keep appropriate minutes of its meetings, which shall be reported to the Board. Any actions taken by the Executive Committee shall also be reported to the Board.

B. *Nominating Committee.* There shall be a Nominating Committee which shall consist of not fewer than four nor more than six Trustees appointed by the Board in a manner which shall reflect the balance between Corporate Trustees and Trustees-at-Large on the Board. The Nominating Committee shall nominate persons for election as Corporate Trustees and Trustees-at-Large, Chairperson of the Board, Vice Chairperson of the Board, President, Treasurer, Clerk, Director of the Laboratory and such other officers, if any, as needed, in accordance with the requirements of these Bylaws. The Nominating Committee shall also be responsible for overseeing the training of new Trustees. The Chairperson of the Board of Trustees shall appoint the Chairperson of the Nominating Committee. The Chairperson of the Science Council shall be an *ex officio* voting member of the Nominating Committee.

C. *Science Council.* There shall be a Science Council (the "Council") which shall consist of Members of the Corporation elected to the Council by vote of the Members of the Corporation, and which shall advise the Board with respect to matters concerning the Corporation's mission, its scientific and instructional endeavors, and the appointment and promotions of persons or committees with responsibility for matters requiring scientific expertise. Unless otherwise approved by a majority of the members of the Council, the Chairperson of the Council shall be elected annually by the Council. The chief executive officer of the Corporation shall be an *ex officio* voting member of the Council.

D. *Board of Overseers.* There shall be a Board of Overseers which shall consist of not fewer than five nor more than eight scientists who have expertise concerning matters with which the Corporation is involved. Members of the Board of Overseers may or may not be Members of the Corporation and may be appointed by the Board of Trustees on the basis of recommendations submitted from scientists and scientific organizations or societies. The Board of Overseers shall be available to review and offer recommendations to the officers, Trustees and Science Council regarding scientific activities conducted or proposed by the Corporation and shall meet from time to time, not less frequently than annually, as determined by the Board of Trustees.

E. *Board Committees Generally.* The Trustees may elect or appoint one or more other committees (including, but not limited to, an Investment Committee, a Development Committee, an Audit Committee, a Facilities and Capital Equipment Committee and a Long-Range Planning Committee) and may delegate to any such committee or committees any or all of their powers, except those which by law, the Articles of Organization or these Bylaws the Trustees are prohibited from delegating; provided that any committee to which the powers of the Trustees are delegated shall consist solely of Trustees. The members of any such committee shall have such tenure and duties as the Trustees shall determine. The Investment Committee, which shall oversee the management of the Corporation's endowment funds and marketable securities shall include as *ex officio* members, the Chairperson of the Board, the Treasurer and the Chairperson of the Audit Committee, together with such Trustees as may be required for not less than two-thirds of the Investment Committee to consist of Trustees. Except as otherwise provided by these Bylaws or determined by the Trustees, any such committee may make rules for the conduct of its business, but, unless otherwise provided by the Trustees or in such rules, its business shall be conducted as nearly as possible in the same manner as is provided by these Bylaws for the Trustees.

F. *Actions Without a Meeting.* Any action required or permitted to be taken at any meeting of the Executive Committee or any other committee elected by the Trustees may be taken without a meeting if all members of such committees consent to the action in writing and such written consents are filed with the records of meetings. Members of the Executive Committee or any other committee elected by the Trustees may also participate in any meeting by means of a telephone conference call, or otherwise take action in such a manner as may, from time to time, be permitted by law.

G. *Manual of Procedures.* The Board of Trustees, on the recommendation of the Executive Committee, shall establish guidelines and modifications thereof to be recorded in a Manual of Procedures. Guidelines shall establish procedures for: (1) Nomination and election of members of the Corporation, Board of Trustees and Executive Committee; (2) Election of Officers; (3) Formation and Function of Standing Committees.

ARTICLE VI—OFFICERS

A. *Enumeration.* The officers of the Corporation shall consist of a President, a Treasurer and a Clerk, and such other officers having the powers of President, Treasurer and Clerk as the Board may determine, and a Director of the Laboratory. The Corporation may have such other officers and assistant officers as the Board may determine, including (without limitation) a Chairperson of the Board, Vice Chairperson and one or more Vice Presidents, Assistant Treasurers or Assistant Clerks. Any two or more offices may be held by the same person. The Chairperson and Vice Chairperson of the Board shall be elected by and from the Trustees, but other officers of the Corporation need not be Trustees or Members. If required by the Trustees, any officer shall give the Corporation a bond for the faithful performance of his or her duties in such amount and with such surety or sureties as shall be satisfactory to the Trustees.

B. *Tenure.* Except as otherwise provided by law, by the Articles of Organization or by these Bylaws, the President, Treasurer, and all other officers shall hold office until the first meeting of the Board following the annual meeting of Members and thereafter, until his or her successor is chosen and qualified.

C. *Resignation.* Any officer may resign by delivering his or her written resignation to the Corporation at its principal office or to the President or Clerk and such resignation shall be effective upon receipt unless it is specified to be effective at some other time or upon the happening of some other event.

D. *Removal.* The Board may remove any officer with or without cause by a vote of a majority of the entire number of Trustees then in office, at a meeting of the Board called for that purpose and for which notice of the purpose thereof has been given, provided that an officer may be removed for cause only after having an opportunity to be heard by the Board at a meeting of the Board at which a quorum is personally present and voting.

E. *Vacancy.* A vacancy in any office may be filled for the unexpired balance of the term by vote of a majority of the Trustees present at any meeting of Trustees at which a quorum is present or by written consent of all of the Trustees, if less than a quorum of Trustees shall remain in office.

F. *Chairperson.* The Chairperson shall have such powers and duties as may be determined by the Board and, unless otherwise determined by the Board, shall serve in that capacity for a term coterminous with his or her term as Trustee.

G. *Vice Chairperson.* The Vice Chairperson shall perform the duties and exercise the powers of the Chairperson in the absence or disability of the Chairperson, and shall perform such other duties and possess such other powers as may be determined by the Board. Unless otherwise determined by the Board, the Vice Chairperson shall serve for a one-year term.

H. *Director.* The Director shall be the chief operating officer and, unless otherwise voted by the Trustees, the chief executive officer of the Corporation. The Director shall, subject to the direction of the Trustees, have general supervision of the Laboratory and control of the business of the Corporation. At the annual meeting, the Director shall submit a report of the operations of the Corporation for such year and a statement of its affairs, and shall, from time to time, report to the Board all matters within his or her knowledge which the interests of the Corporation may require to be brought to its notice.

I. *Deputy Director.* The Deputy Director, if any, or if there shall be more than one, the Deputy Directors in the order determined by the Trustees, shall, in the absence or disability of the Director, perform the duties and exercise the powers of the Director and shall perform such other duties and shall have such other powers as the Trustees may, from time to time, prescribe.

J. *President* The President shall have the powers and duties as may be vested in him or her by the Board.

K. *Treasurer and Assistant Treasurer* The Treasurer shall, subject to the direction of the Trustees, have general charge of the financial affairs of the Corporation, including its long-range financial planning, and shall cause to be kept accurate books of account. The Treasurer shall prepare a yearly report on the financial status of the Corporation to be delivered at the annual meeting. The Treasurer shall also prepare or oversee all filings required by the Commonwealth of Massachusetts, the Internal Revenue Service, or other Federal and State Agencies. The account of the Treasurer shall be audited annually by a certified public accountant.

The Assistant Treasurer, if any, or if there shall be more than one, the Assistant Treasurers in the order determined by the Trustees, shall, in the absence or disability of the Treasurer, perform the duties and exercise the powers of the Treasurer, shall perform such other duties and shall have such other powers as the Trustees may, from time to time, prescribe.

L. *Clerk and Assistant Clerk* The Clerk shall be a resident of the Commonwealth of Massachusetts, unless the Corporation has designated a resident agent in the manner provided by law. The minutes or records of all meetings of the Trustees and Members shall be kept by the Clerk who shall record, upon the record books of the Corporation, minutes of the proceedings at such meetings. He or she shall have custody of the record books of the Corporation and shall have such other powers and shall perform such other duties as the Trustees may, from time to time, prescribe.

The Assistant Clerk, if any, or if there shall be more than one, the Assistant Clerks in the order determined by the Trustees, shall, in the absence or disability of the Clerk, perform the duties and exercise the powers of the Clerk and shall perform such other duties and shall have such other powers as the Trustees may, from time to time, prescribe.

In the absence of the Clerk and an Assistant Clerk from any meeting, a temporary Clerk shall be appointed at the meeting.

M. *Other Powers and Duties* Each officer shall have in addition to the duties and powers specifically set forth in these Bylaws, such duties and powers as are customarily incident to his or her office, and such duties and powers as the Trustees may, from time to time, designate.

ARTICLE VII—AMENDMENTS

These Bylaws may be amended by the affirmative vote of the Members at any meeting, provided that notice of the substance of the proposed amendment is stated in the notice of such meeting. As authorized by the Articles of Organization, the Trustees, by a majority of their number then in office, may also make, amend or repeal these Bylaws, in whole or in part, except with respect to (a) the provisions of these Bylaws governing (i) the removal of Trustees and (ii) the amendment of these Bylaws and (b) any provisions of these Bylaws which by law, the Articles of Organization or these Bylaws, requires action by the Members.

No later than the time of giving notice of meeting of Members next following the making, amending or repealing by the Trustees of any Bylaw, notice thereof stating the substance of such change shall be given to all Members entitled to vote on amending the Bylaws.

Any Bylaw adopted by the Trustees may be amended or repealed by the Members entitled to vote on amending the Bylaws.

ARTICLE VIII—INDEMNITY

Except as otherwise provided below, the Corporation shall, to the extent legally permissible, indemnify each person who is, or shall have been, a Trustee, director or officer of the Corporation or who is serving, or shall have served at the request of the Corporation as a Trustee, director or officer of another organization in which the Corporation directly or indirectly has any interest as a shareholder, creditor or otherwise, against all liabilities and expenses (including judgments, fines, penalties, and reasonable attorneys' fees and all amounts paid, other than to the Corporation or such other organization, in compromise or settlement) imposed upon or incurred by any such person in connection with, or arising out of, the defense or disposition of any action, suit or other proceeding, whether civil or criminal, in which he or she may be a defendant or with which he or she may be threatened or otherwise involved, directly or indirectly, by reason of his or her being or having been such a Trustee, director or officer.

The Corporation shall provide no indemnification with respect to any matter as to which any such Trustee, director or officer shall be finally adjudicated in such action, suit or proceeding not to have acted in good faith in the reasonable belief that his or her action was in the best interests of the Corporation. The Corporation shall provide no indemnification with respect to any matter settled or comprised unless such matter shall have been approved as in the best interests of the Corporation, after notice that indemnification is involved, by (i) a disinterested majority of the Board of the Executive Committee, or (ii) a majority of the Members.

Indemnification may include payment by the Corporation of expenses in defending a civil or criminal action or proceeding in advance of the final disposition of such action or proceeding upon receipt of an undertaking by the person indemnified to repay such payment if it is ultimately determined that such person is not entitled to indemnification under the provisions of this Article VIII, or under any applicable law.

As used in the Article VIII, the terms "Trustee," "director," and "officer" include their respective heirs, executors, administrators and legal representatives, and an "interested" Trustee, director or officer is one against whom in such capacity the proceeding in question or another proceeding on the same or similar grounds is then pending.

To assure indemnification under this Article VIII of all persons who are determined by the Corporation or otherwise to be or to have been "fiduciaries" of any employee benefits plan of the Corporation which may exist, from time to time, this Article VIII shall be interpreted as follows: (i) "another organization" shall be deemed to include such an employee benefit plan, including without limitation, any plan of the Corporation which is governed by the Act of Congress entitled "Employee Retirement Income Security Act of 1974," as amended, from time to time, ("ERISA"); (ii) "Trustee" shall be deemed to include any person requested by the Corporation to serve as such for an employee benefit plan where the performance by such person of his or her duties to the Corporation also imposes duties on, or otherwise involves services by, such person to the plan or participants or beneficiaries of the plan; (iii) "fines" shall be deemed to include any excise tax plan pursuant to ERISA, and (iv) actions taken or omitted by a person with respect to an employee benefit plan in the performance of such person's duties for a purpose reasonably believed by such person to be in the interest of the participants and beneficiaries of the plan shall be deemed to be for a purpose which is in the best interests of the Corporation.

The right of indemnification provided in this Article VIII shall not be exclusive of or affect any other rights to which any Trustee, director or officer may be entitled under any agreement, statute, vote of Members or otherwise. The Corporation's obligation to provide indemnification under this Article VIII shall be offset to the extent of any other source of indemnification of any otherwise applicable insurance coverage under a policy maintained by the Corporation or any other person. Nothing contained in the Article shall affect any rights to which employees and corporate personnel other than Trustees, directors or officers may be entitled by contract, by vote of the Board or of the Executive Committee or otherwise.

ARTICLE IX—DISSOLUTION

The consent of every Trustee shall be necessary to effect a dissolution of the Marine Biological Laboratory. In case of dissolution, the property shall be disposed of in such a manner and upon such terms as shall be determined by the affirmative vote of two-thirds of the Trustees then in office in accordance with the laws of the Commonwealth of Massachusetts.

ARTICLE X—MISCELLANEOUS PROVISIONS

A. *Fiscal Year* Except as otherwise determined by the Trustees, the fiscal year of the Corporation shall end on December 31st of each year.

B. *Seal* Unless otherwise determined by the Trustees, the Corporation may have a seal in such form as the Trustees may determine, from time to time.

C. *Execution of Instruments* All checks, deeds, leases, transfers, contracts, bonds, notes and other obligations authorized to be executed by an officer of the Corporation in its behalf shall be signed by the Director or the Treasurer except as the Trustees may generally or in particular cases otherwise determine. A certificate by the Clerk or an Assistant Clerk, or a temporary Clerk, as to any action taken by the Members, Board of Trustees or any officer or representative of the Corporation shall as to all persons who rely thereon in good faith be conclusive evidence of such action.

D. *Corporate Records* The original, or attested copies, of the Articles of Organization, Bylaws and records of all meetings of the Members shall be kept in Massachusetts at the principal office of the Corporation, or at an office of the Corporation's Clerk or resident agent. Said copies and records need not all be kept in the same office. They shall be available at all reasonable times for inspection by any Member for any proper purpose, but not to secure a list of Members for a purpose other than in the interest of the applicant, as a Member, relative to the affairs of the Corporation.

E. *Articles of Organization* All references in these Bylaws to the Articles of Organization shall be deemed to refer to the Articles of Organization of the Corporation, as amended and in effect, from time to time.

F. *Transactions with Interested Parties* In the absence of fraud, no contract or other transaction between this Corporation and any other corporation or any firm, association, partnership or person shall be affected or invalidated by the fact that any Trustee or officer of this Corporation is pecuniarily or otherwise interested in or is a director, member or officer of such other corporation or of such firm, association or partnership or in a party to or is pecuniarily or otherwise interested in such contract or other transaction or is in any way connected with any person or person, firm, association, partnership, or corporation pecuniarily or otherwise interested therein; provided that the fact that he or she individually or as a director, member or officer of such corporation, firm, association or partnership in such a party or is so interested shall be disclosed to or shall have been known by the Board of Trustees or a majority of such Members thereof as shall be present at a meeting of the Board of Trustees at which action upon any such contract or transaction shall be taken; any Trustee may be counted in determining the existence of a quorum and may vote at any meeting of the Board of Trustees for the purpose of authorizing any such contract or transaction with like force and effect as if he/she were not so interested, or were not a director, member or officer of such other corporation, firm, association or partnership, provided that any vote with respect to such contract or transaction must be adopted by a majority of the Trustees then in office who have no interest in such contract or transaction.

CONTENTS

Volume 189 Number 2

THE BIOLOGICAL BULLETIN

OCTOBER/NOVEMBER, 1995

Published by the Marine Biological Laboratory

THE BIOLOGICAL BULLETIN

PUBLISHED BY
THE MARINE BIOLOGICAL LABORATORY

OCTOBER/NOVEMBER, 1995

Printed and Issued by
LANCASTER PRESS, Inc.
3575 HEMPLAND ROAD
LANCASTER, PA

THE BIOLOGICAL BULLETIN

THE BIOLOGICAL BULLETIN is published six times a year by the Marine Biological Laboratory, MBL Street, Woods Hole, Massachusetts 02543.

Subscriptions and similar matter should be addressed to Subscription Manager, THE BIOLOGICAL BULLETIN, Marine Biological Laboratory, Woods Hole, Massachusetts 02543. Single numbers, $37.50. Subscription per volume (three issues), $92.50 ($185.00 per year for six issues).

Communications relative to manuscripts should be sent to Michael J. Greenberg, Editor-in-Chief, or Pamela L. Clapp, Managing Editor, at the Marine Biological Laboratory, Woods Hole, Massachusetts 02543. Telephone: (508) 548-3705, ext. 428. FAX: 508-540-6902. E-mail: pelapp@hoh.mbl.edu.

THE BIOLOGICAL BULLETIN is indexed in bibliographic services including *Index Medicus* and MEDLINE, *Chemical Abstracts, Current Contents*, and *CABS (Current Awareness in Biological Sciences)*.

Printed on acid free paper,
effective with Volume 180, Issue 1, 1991.

POSTMASTER: Send address changes to THE BIOLOGICAL BULLETIN, Marine Biological Laboratory, Woods Hole, MA 02543.

Second-class postage paid at Woods Hole, MA, and additional mailing offices.
ISSN 0006-3185

INSTRUCTIONS TO AUTHORS

The Biological Bulletin accepts outstanding original research reports of general interest to biologists throughout the world. Papers are usually of intermediate length (10–40 manuscript pages). A limited number of solicited review papers may be accepted after formal review. A paper will usually appear within four months after its acceptance.

Very short, especially topical papers (less than 9 manuscript pages including tables, figures, and bibliography) will be published in a separate section entitled "Research Notes." A Research Note in *The Biological Bulletin* follows the format of similar notes in *Nature*. It should open with a summary paragraph of 150 to 200 words comprising the introduction and the conclusions. The rest of the text should continue on without subheadings, and there should be no more than 30 references. References should be referred to in the text by number, and listed in the Literature Cited section in the order that they appear in the text. Unlike references in *Nature*, references in the Research Notes section should conform in punctuation and arrangement to the style of recent issues of *The Biological Bulletin*. Materials and Methods should be incorporated into appropriate figure legends. See the article by Lohmann *et al.* (October 1990, Vol. **179**: 214–218) for sample style. A Research Note will usually appear within two months after its acceptance.

The Editorial Board requests that regular manuscripts conform to the requirements set below; those manuscripts that do not conform will be returned to authors for correction before review.

1. ***Manuscripts.*** Manuscripts, including figures, should be submitted in triplicate. (Xerox copies of photographs are not acceptable for review purposes.) The submission letter accompanying the manuscript should include a telephone number, a FAX number, and (if possible) an E-mail address for the corresponding author. The original manuscript must be typed in no smaller than 12 pitch or 10 point, using double spacing (*including* figure legends, footnotes, bibliography, etc.) on one side of 16- or 20-lb. bond paper, 8½ by 11 inches. Please, no right justification. Manuscripts should be proofread carefully and errors corrected legibly in black ink. Pages should be numbered consecutively. Margins on all sides should be at least 1 inch (2.5 cm). Manuscripts should conform to the *Council of Biology Editors Style Manual*, 5th Edition (Council of Biology Editors, 1983) and to American spelling. Unusual abbreviations should be kept to a minimum and should be spelled out on first reference as well as defined in a footnote on the title page. Manuscripts should be divided into the following components: Title page, Abstract (of no more than 200 words), Introduction, Materials and Methods, Results, Discussion, Acknowledgments, Literature Cited, Tables, and Figure Legends. In addition, authors should supply a list of words and phrases under which the article should be indexed.

2. ***Title page.*** The title page consists of a condensed title or running head of no more than 35 letters and spaces, the manuscript title, authors' names and appropriate addresses, and footnotes listing present addresses, acknowledgments or contribution numbers, and explanation of unusual abbreviations.

3. ***Figures.*** The dimensions of the printed page, 7 by 9 inches, should be kept in mind in preparing figures for publication. We recommend that figures be about 1½ times the linear dimensions of the final printing desired, and that the ratio of the largest to the smallest letter or number and of the thickest to the thinnest line not exceed 1:1.5. Explanatory matter generally should be included in legends, although axes should always be identified on the illustration itself. Figures should be prepared for reproduction as either line cuts or halftones. Figures to be reproduced as line cuts should be unmounted glossy photographic reproductions or drawn in black ink on white paper, good-quality tracing cloth or plastic, or blue-lined coordinate paper. Those to be reproduced as halftones should be mounted on board, with both designating numbers or letters and scale

bars affixed directly to the figures. All figures should be numbered in consecutive order, with no distinction between text and plate figures. The author's name and an arrow indicating orientation should appear on the reverse side of all figures.

4. ***Tables, footnotes, figure legends, etc.*** Authors should follow the style in a recent issue of *The Biological Bulletin* in preparing table headings, figure legends, and the like. Because of the high cost of setting tabular material in type, authors are asked to limit such material as much as possible. Tables, with their headings and footnotes, should be typed on separate sheets, numbered with consecutive Roman numerals, and placed after the Literature Cited. Figure legends should contain enough information to make the figure intelligible separate from the text. Legends should be typed double spaced, with consecutive Arabic numbers, on a separate sheet at the end of the paper. Footnotes should be limited to authors' current addresses, acknowledgments or contribution numbers, and explanation of unusual abbreviations. All such footnotes should appear on the title page. Footnotes are not normally permitted in the body of the text.

5. ***Literature cited.*** In the text, literature should be cited by the Harvard system, with papers by more than two authors cited as Jones *et al.*, 1980. Personal communications and material in preparation or in press should be cited in the text only, with author's initials and institutions, unless the material has been formally accepted and a volume number can be supplied. The list of references following the text should be headed Literature Cited, and must be typed double spaced on separate pages, conforming in punctuation and arrangement to the style of recent issues of *The Biological Bulletin*. Citations should include complete titles and inclusive pagination. Journal abbreviations should normally follow those of the U. S. A. Standards Institute (USASI), as adopted by BIOLOGICAL ABSTRACTS and CHEMICAL ABSTRACTS, with the minor differences set out below. The most generally useful list of biological journal titles is that published each year by BIOLOGICAL ABSTRACTS (BIOSIS List of Serials; the most recent issue). Foreign authors, and others who are accustomed to using THE WORLD LIST OF SCIENTIFIC PERIODICALS, may find a booklet published by the Biological Council of the U.K. (obtainable from the Institute of Biology, 41 Queen's Gate, London, S.W.7, England, U.K.) useful, since it sets out the WORLD LIST abbreviations for most biological journals with notes of the USASI abbreviations where these differ. CHEMICAL ABSTRACTS publishes quarterly supplements of additional abbreviations. The following points of reference style for THE BIOLOGICAL BULLETIN differ from USASI (or modified WORLD LIST) usage:

A. Journal abbreviations, and book titles, all underlined (for *italics*)

B. All components of abbreviations with initial capitals (not as European usage in WORLD LIST *e.g., J. Cell. Comp. Physiol.* NOT *J. cell. comp. Physiol.*)

C. *All* abbreviated components must be followed by a period, whole word components *must not* (*i.e., J. Cancer Res.*)

D. Space between all components (*e.g., J. Cell. Comp. Physiol.*, not *J.Cell.Comp.Physiol.*)

E. Unusual words in journal titles should be spelled out in full, rather than employing new abbreviations invented by the author. For example, use *Rit Vísindafjélags Islendinga* without abbreviation.

F. All single word journal titles in full (*e.g., Veliger, Ecology, Brain*).

G. The order of abbreviated components should be the same as the word order of the complete title (*i.e., Proc.* and *Trans.* placed where they appear, not transposed as in some BIOLOGICAL ABSTRACTS listings).

H. A few well-known international journals in their preferred forms rather than WORLD LIST or USASI usage (*e.g., Nature, Science, Evolution* NOT *Nature, Lond., Science, N.Y., Evolution, Lancaster, Pa.*)

6. ***Reprints, page proofs, and charges.*** Authors receive their first 100 reprints (without covers) free of charge. Additional reprints may be ordered at time of publication and normally will be delivered about two to three months after the issue date. Authors (or delegates for foreign authors) will receive page proofs of articles shortly before publication. They will be charged the current cost of printers' time for corrections to these (other than corrections of printers' or editors' errors). Other than these charges for authors' alterations, *The Biological Bulletin* does not have page charges.

GRASS.
First and Still the Best!

Grass Instrument Company has been the world leader in EEG and research instrumentation since 1935. Now Grass is a division of Astro-Med, Inc. For 25 years, Astro-Med has been the technology leader in high performance specialty printing systems for aerospace, industrial and medical applications. And now, Grass products, acclaimed for accuracy and reliability, are available directly from Astro-Med's Sales and Service Centers nation-wide.

For Physiological Research — The Model K2G Polygraph

K2G polygraph combines the advanced data acquisition and recording technology of Astro-Med with the wide variety of Grass physiological amplifiers. Now you can acquire, display, store, and analyze data — up to 32 channels. Ideal for demanding physiological and pharmacological research in industry and universities.

For EEG/Polysomnography — The Model 9

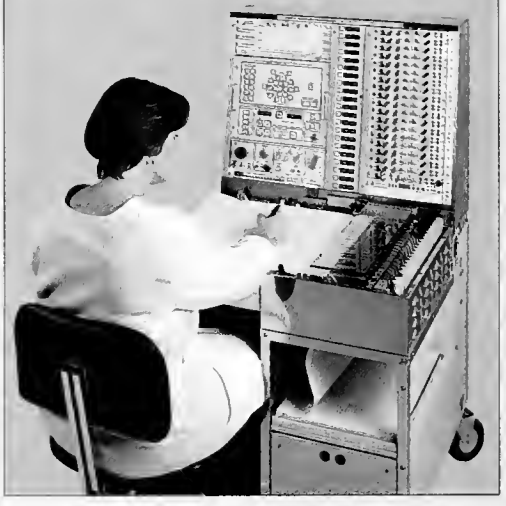

Model 9 Electroencephalograph features instant access to user-programmable montages (there is memory for up to 64) for pediatric, sleep, OR, as well as basic EEG applications. Unique electrode selection system utilizes soft keys, and large LEDs display the electrode derivation for each channel. Available in sizes up to 25 channels.

And to complement these systems...

Transducers **Stimulators** **Electrodes**

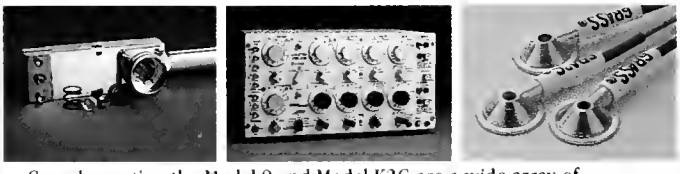

Complementing the Model 9 and Model K2G are a wide array of stimulators, transducers and electrodes, plus genuine Grass chart paper, pens, inks, cream and more.

Astro-Med, Inc GRASS INSTRUMENT DIVISION™

Grass Instrument Division
Astro-Med, Inc.

World Headquarters
Astro-Med Industrial Park, West Warwick,
Rhode Island 02893 U.S.A.
Phone: (401) 828-4000, Fax: (401) 822-2430
Toll-Free Phone (U.S.A.only): (800) 343-4039

Representatives and distributors located throughout the world

CANADA • Tel.(514) 449-2727 • Fax (514) 449-2755
Toll-Free 1-800-565-2216 (Canada Only)
UNITED KINGDOM • Tel.(01628) 668836
Fax (01628) 664994
FRANCE • Tél.(1) 34.82.09.00 • Fax (1) 34.82.05.71
GERMANY • Tel.(49) 06106/75033 • Fax (49) 06106/771121
ITALY • Tel.(02) 26411909 • Fax (02) 26412828

Reference: *Biol. Bull.* **189**: 69–76. (October/November, 1995)

Sulfide as a Chemical Stimulus for Deep-Sea Hydrothermal Vent Shrimp

G. H. RENNINGER[1,*], L. KASS[2], R. A. GLEESON[3], C. L. VAN DOVER[4,†], B.-A. BATTELLE[3], R. N. JINKS[5], E. D. HERZOG[6], AND S. C. CHAMBERLAIN[5]

[1]*Biophysics Group, Department of Physics, University of Guelph, Guelph, Ontario N1G 2W1, Canada;* [2]*Department of Zoology, University of Maine, Orono, Maine 04469;* [3]*C. V. Whitney Laboratory, University of Florida, St. Augustine, Florida 32086;* [4]*Duke University Marine Laboratory, Beaufort, NC 28516;* [5]*Institute for Sensory Research and Department of Bioengineering & Neuroscience, Syracuse University, Syracuse, New York 13244-5290; and* [6]*Department of Biology, University of Virginia, Charlottesville, Virginia 22903*

Organisms dependent on deep-sea hydrothermal vents for their existence face extinction when their vents expire, unless they can establish populations on neighboring vents or on new vent sites. Propagules, including larvae and motile adults, are readily dispersed broadly by seafloor currents, but how they recognize active hydrothermal sites is problematical. Compelling evidence that vent organisms can find and colonize hydrothermal sites has been provided by a series of observations on the East Pacific Rise (1). New hydrothermal vents created there following a volcanic eruption on the seafloor in March 1991 were colonized by sessile invertebrates in less than one year. On the Mid-Atlantic Ridge, shrimp that normally cluster on sulfide surfaces have been observed to swim directly back to the surfaces when displaced from them. How do vent animals locate new or existing vents? Passive transport by currents (2) or active swimming without guidance by some physical cue is not likely to result in success (3). Chemicals present in hydrothermal fluids have been proposed as attractants. We provide the first evidence of a chemosensory response in a vent invertebrate to sulfides, which are prevalent in vent fluids and provide the energy for chemosynthetic primary production at vents.

During recent field work at hydrothermal vents on the Mid-Atlantic Ridge where extremely motile shrimp (*Rimicaris exoculata* and a smaller, possibly new, *Rimicaris* sp.) dominate the surfaces of sulfide chimneys, we documented a strong orientation behavior of shrimp, perhaps guided by chemical cues, to a piece of sulfide removed from a chimney (Fig. 1). Specimens of *Rimicaris* sp. and *R. exoculata* collected by the deep submergence vehicle (DSV) *Alvin* survived sufficiently long aboard ship to allow us to examine physiological responses of antennal nerves to various chemical stimulants, as well as to preserve antennal filaments for later electron microscopic examination. The shrimp possess first and second antennae (Fig. 2A) similar to those of other decapod crustaceans whose antennae are known to respond to chemical as well as to tactile stimuli (4). The first and second antennae both bear sensilla (Fig. 2B; 1 sensillum/66 μm of filament circumference on average for *Rimicaris* sp. and 1/48 μm for *R. exoculata*) with an open pore at their tips (Fig. 2C, D). Transmission electron microscopy (TEM) reveals that each sensillum is innervated by 10 to 14 sensory dendrites (Fig. 2E, F). Light microscopic and TEM studies indicate that the channel containing the sensory dendritic segments extends to the pore at the tip of the sensillum, and that at least some of the dendritic processes in the channel reach the pore.

Nerves in excised filaments of both antennae frequently showed spontaneous activity and responded to tactile stimuli. Antennal filaments also responded to a variety of chemical stimuli, including an homogenate of bacterial cells isolated from the vents and mixtures of amino acids. We tested 7 filaments of the second antenna, and 4 medial filaments and 5 lateral filaments of the first antenna. The largest and most robust response was evoked in filaments

Received 3 May 1995; accepted 28 July 1995.

* To whom correspondence should be addressed.

† Present address: West Coast National Undersea Research Center, PO Box 757220, University of Alaska, Fairbanks, AK 99775.

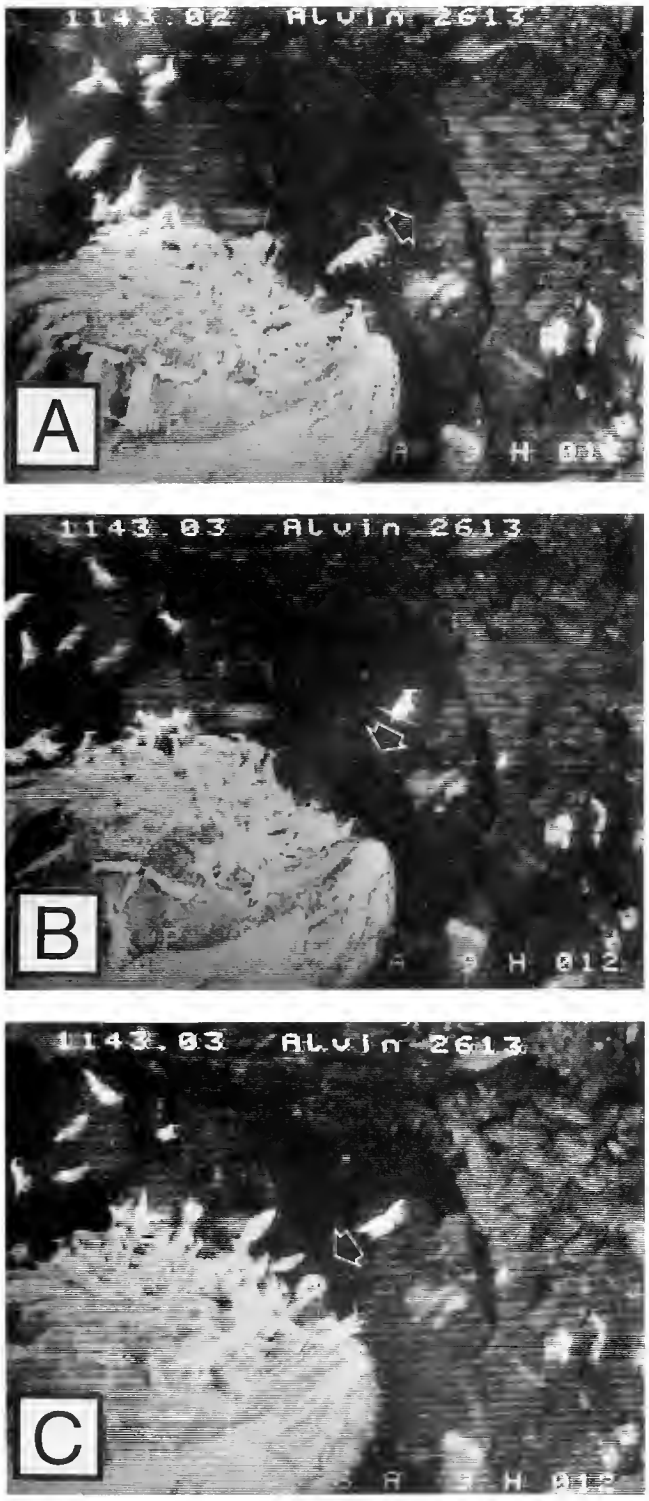

Figure 1. (A) A startled hydrothermal vent shrimp swims off a sulfide-bearing rock sample taken from a vent chimney, (B) reorients itself towards the rock, and then (C) swims back to the rock. Similar behavior by other shrimp occurred several times during collection of the rock sample by DSV *Alvin*. From videotape of DSV *Alvin* dive number 2613 on 14 June 1993 at the Snake Pit site on the Mid-Atlantic Ridge.

of the second antenna on exposure to solutions of Na_2S (Fig. 3A). All seven filaments tested responded to Na_2S; the response could be eliminated by removing the stimulant and could be evoked repeatedly. The steady-state response increased with the concentration of Na_2S. In the four filaments of the second antenna used to study the response to Na_2S at different concentrations, the relative responses (Fig. 3B) were (mean ± standard error of the mean): 0.113 ± 0.054 (n = 3) at [Na_2S] = 1.3 mM; 0.567 ± 0.137 (n = 4) at 13 mM; 0.654 ± 0.148 (n = 4) at 130 mM; and 1.014 ± 0.140 (n = 4) at 1300 mM. Two control solutions were used on two of these four filaments. The first was artificial seawater (ASW) with pH = 8, matching the pH of the lowest Na_2S concentration used, which gave a relative response of −0.078 ± 0.010. The second control solution (pH 13) was ASW with pH adjusted to 13, equal to that of the 1300 mM Na_2S solution, which gave a relative response of −0.030 ± 0.050. Three each of the medial and lateral filaments of the first antenna were tested for sensitivity to Na_2S. The medial filament of the first antenna responded less consistently than filaments of the second antenna in what appeared to be a transient manner. The lateral filament responded little, if at all, to Na_2S.

Of the three antennal filaments, only the responses of the second antenna showed a significant concentration dependence. A linear regression analysis of the mean values of the second antenna's responses as a function of log[Na_2S] gave a slope significantly different from zero ($P < 0.05$). Based on general experience with chemical senses, we expect that the actual dependence of the second antenna's response on sulfide concentration is not this linear one, but rather a sigmoidal dependence (10). The trend of the responses suggests that the threshold concentration for the sensory cells in the second antenna lies in the micromolar range of sulfide concentrations.

The responses of excised filaments of the second antenna of *Rimicaris* sp. and *R. exoculata* to stimulation by dissolved sulfide suggest that vent shrimp may be able

Figure 2. (A) Lateral view of *Rimicaris* sp., a small orange-colored hydrothermal vent shrimp collected at the Snake Pit site, together with dorsal view of cephalothorax, showing the two first antennae (each with a short medial and lateral filament close to the midline) and the two second antennae (each having one long filament shown deployed laterally); scale bar = 5 mm. (B) The second antenna of *Rimicaris* sp. showing the distribution of sensilla near the distal border of each segment. Bacterial populations encrust the surface, giving it a mottled appearance (scale = 25 μm). The second antenna of *Rimicaris exoculata* is similar in structure. For SEM examination, antennae were removed from animals which had been fixed in 5% paraformaldehyde in 0.1 M Sorensen's phosphate buffer (pH 7.2) immediately after arrival at the ocean's surface. The tissue was dehydrated in a graded ethanol series, immersed in hexamethyldisilazane for 5–10 min and air dried (5). Pieces of dried antennae were mounted on stubs, coated with gold, and examined using an

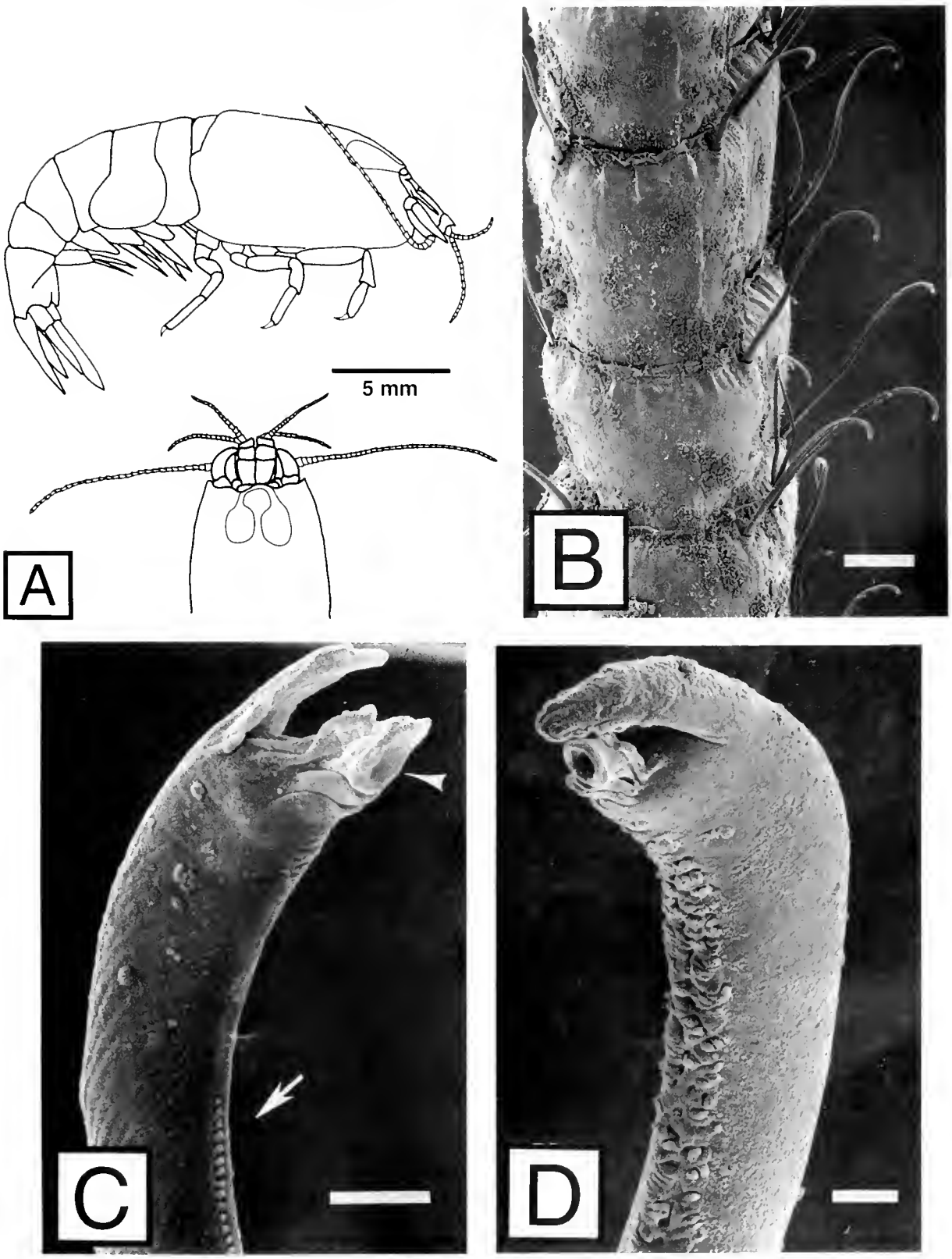

Hitachi 4000 scanning electron microscope at 6.0 kV. (C) A sensillum on the second antenna of *Rimicaris* sp. At the tip of the sensillum, fingerlike projections extend above the laterally facing terminal pore (arrowhead). Proximal to the pore are regularly arranged button-like microstructures (arrow) which are associated with the distal third of the sensillum (scale = 1 μm). (D) The sensilla on the second antenna of *R. exoculata* are similar in structure, with irregular crenulations replacing the button-like microstructures (scale = 1 μm).

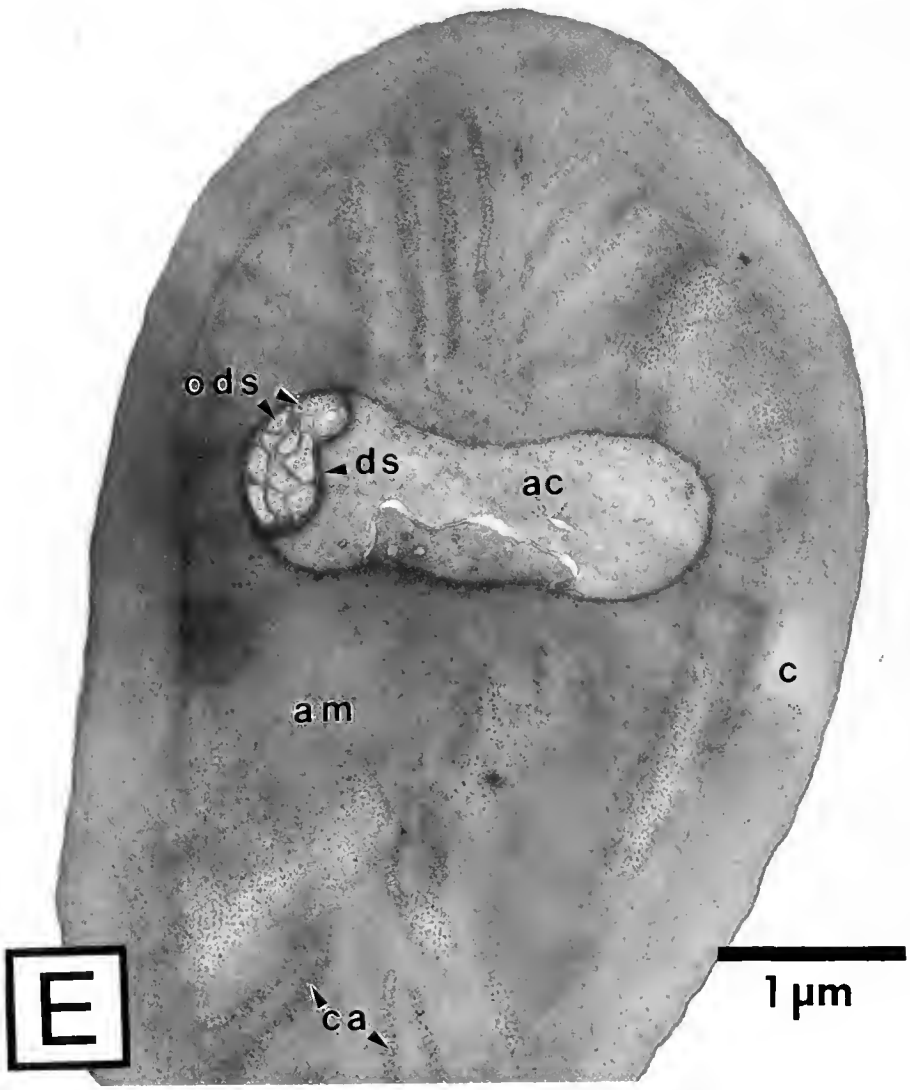

Figure 2. (E) Cross section in the proximal region of a sensillum from the second antenna of *R. exoculata*. The sensillum is composed of three major layers: a cuticle (*c*); an inner core of amorphous material (*am*) penetrated by canals (*ca*); and a central channel containing the processes of auxiliary cells (*ac*), together with the outer dendritic segments (*ods*) of sensory neurons. In this region the outer dendritic segments are surrounded by a well-developed dendritic sheath (*ds*). For TEM examination, antennae were removed from animals immediately after they were brought to the ocean's surface. The antennae were fixed overnight in 0.1 *M* Sorensen's phosphate buffer (PB; pH 7.2) containing 5% paraformaldehyde, 0.8% glutaraldehyde, 3% NaCl and 4.5% sucrose. Subsequently, antennae were (1) washed in PB containing 8% sucrose, 3 times for 5 min each; (2) post-fixed in PB containing 8% sucrose and 1% osmium tetroxide for 1 h; (3) washed in distilled water, 3 times for 5 min each; (4) dehydrated in a graded ethanol series followed by transfer to propylene oxide; and (5) embedded in Epon-araldite. Thin cross sections of the antennular sensilla were cut on an RMC MT-6000 XL ultramicrotome, stained with 5% aqueous uranyl acetate and lead citrate, and viewed on a Zeiss 10C transmission electron microscope.

to sense sulfides at concentrations occurring naturally in their environment, *e.g.*, 2–15 m*M* in vent fluids from the Menez Gwen and Lucky Strike segments, 0.01–1.0 μM in the vicinity of known venting sites 2–5 m above the bottom (7), 1–300 μM at diffuse, low temperature vents (8), and 6 m*M* at the orifice of a black smoker at the Snake Pit site (9). Sulfide may be useful principally as a short-range stimulus over distances of tens of meters from its source. Sulfide emitted from vents is oxidized in the seawater surrounding the vents, with a half-life of 380 h (11, 12). This half-life, however, is significantly shortened by the presence of sulfide-utilizing bacteria associated with

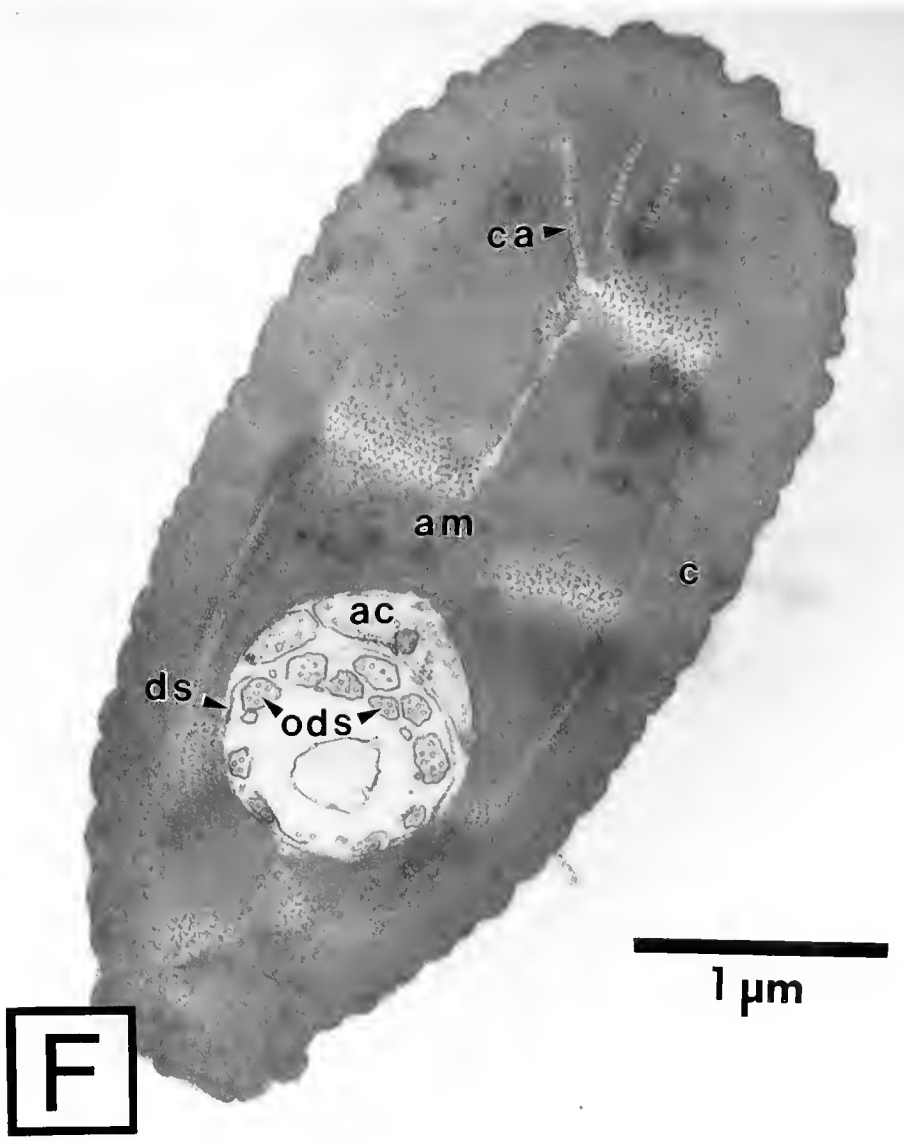

Figure 2. (F) Cross section in the distal portion of a sensillum from the second antenna of *R. exoculata*. In this region the outer dendritic segments are more dispersed and the dendritic sheath is fragmented.

the vents (13). Other compounds associated with hydrothermal plumes, such as methane which can be detected analytically tens of kilometers from the plume source (14), should be investigated for their ability to stimulate vent invertebrate chemoreceptors and thus possibly serve as long-distance cues.

Our observations that the antennae of vent shrimp are sensitive to sulfides led us to ask whether the antennae of other shrimp are sensitive to sulfides. The suction electrodes used on hydrothermal vent shrimp axons failed to reveal any response to sulfides or other chemical stimuli from excised antennal filaments of two species of shallow-water shrimp, *Penaeus aztecus* and *Palaemonetes pugio*, although the filaments responded to tactile stimuli and were spontaneously active. We then used suction electrodes with finer tips especially developed to study chemosensory responses from antennal filaments of decapod crustaceans (15, 16) which allowed better discrimination between axon bundles in the second antenna of *P. azteeus*. We found that chemosensory axons which responded to broad-spectrum odorants also responded to sulfide stimulation in a concentration-dependent way (Fig. 4). The relative responses were 0.010 ± 0.012 (n = 3) for [Na_2S] = 1.3 mM; 0.083 ± 0.009 (n = 3) for 13 mM; 0.138 ± 0.019 (n = 4) for 130 mM; and 0.52 (n = 1) for 1300 mM. We used three control solutions in these experiments: ASW [−0.030 ± 0.020 (n = 2)]; pH 13 [0.26 (n = 1)]; and ASW with the pH adjusted to 10 to match

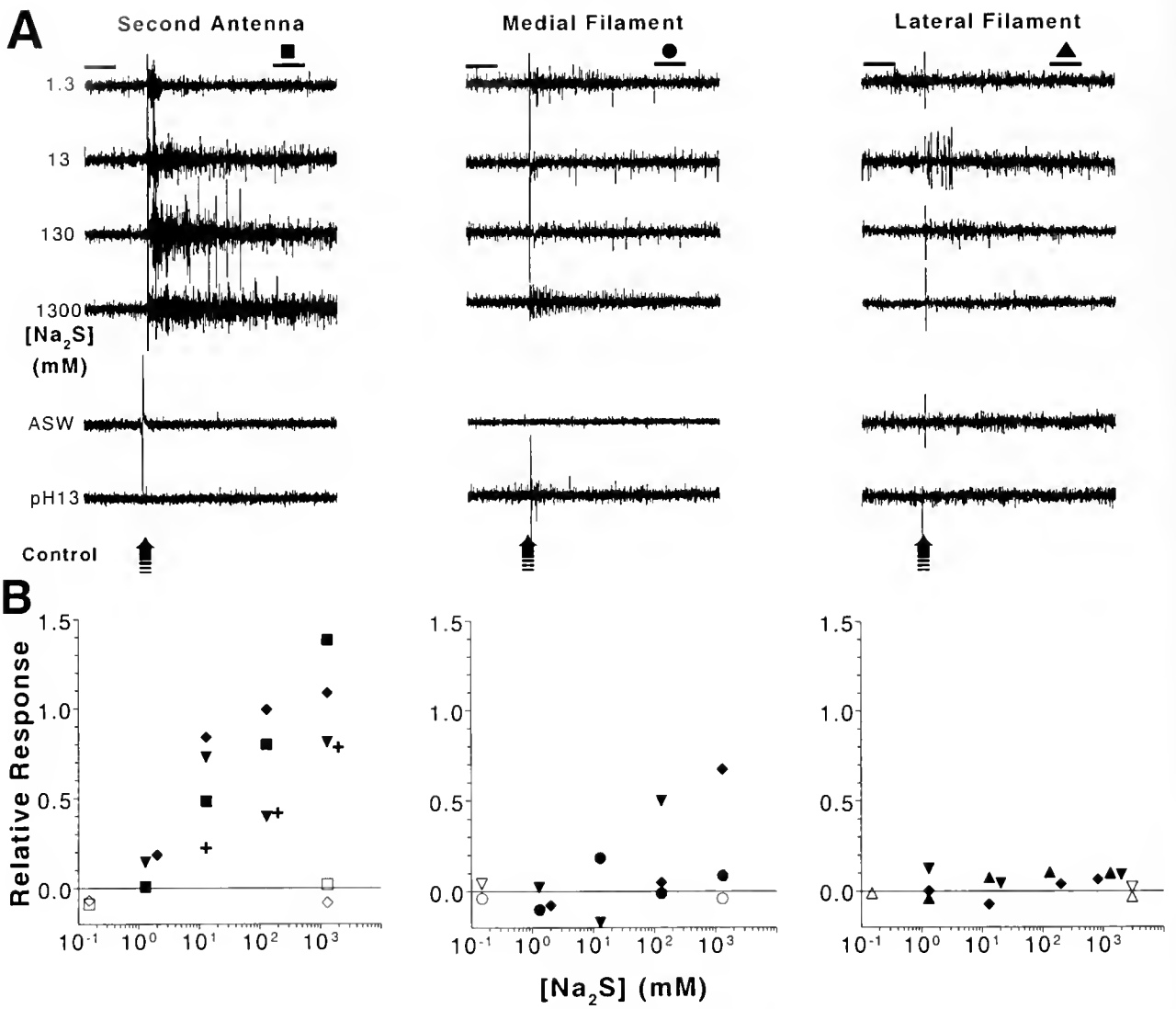

Figure 3. (A) Examples of multiunit nerve responses to solutions of Na_2S in the second antenna, and in the medial and lateral filaments of the first antenna excised from *Rimicaris* sp. The bold vertical arrow 0.5 s after the beginning of each 2 s record indicates when the stimulus, whether one of the Na_2S or control solutions, was applied. Transient responses following the exposure may have been due to tactile receptors activated by fluid motion. The activity following the transient response increased significantly with $[Na_2S]$ in the second antenna. Exposure of filaments of either antenna to control solutions, either artificial seawater (ASW) or pH 13, evoked little or no response. These electrophysiological recordings from antennal filaments of hydrothermal vent shrimp collected from the Snake Pit site on the Mid-Atlantic Ridge (depth *ca* 3600 m) were made aboard R/V *Atlantis II* Filaments were excised from active shrimp and maintained in *Limulus* physiological solution (6). Several segments of the exoskeleton were removed to expose a short length of antennal nerve, which was either wholly or partially drawn into a suction electrode filled with the same solution. Filaments with spontaneous nerve activity and sensitivity to tactile stimuli were judged to be in good physiological condition and were chosen for further experimentation. A single drop of the test solution was gently merged with the fluid surface next to the antenna away from the tip of the suction electrode. Because of the differential behavior of the axonal responses from the various filaments, it is unlikely that the responses of the second antenna are due to some general injury response of the exposed ends of the axons to sulfide. Test solutions were as follows: Na_2S was dissolved in distilled water at a concentration of 1.3 *M* (pH 13), which was then diluted with ASW to produce lower concentrations (130 m*M*, pH 10.5; 13 m*M*, pH 9.5; 1.3 m*M*, pH 8). The stimulating solutions contained several chemical species of sulfide, namely, HS^-, H_2S, S_2^-, and NaHS, with concentrations dependent on the pH of the solution. In the pH range of the experiments, sulfide was present predominantly (> 90%) in the form HS^-. (B) Steady-state relative responses to concentrations of Na_2S and controls. Individual responses have been occasionally offset in the plot for the sake of clarity. The relative responses to Na_2S calculated for the sample recordings shown in (A) are represented here by the symbols shown in (A): ■ represents the second antennal responses in (A); ●, the medial filament of the first antenna; and ▲, the lateral filament. The other solid symbols represent responses to sulfides of the other filaments tested, whose responses are not shown in (A). Open symbols represent responses to the ASW control (shown near 0.1 on the abscissa) or to the pH 13 control (shown at or near 1300) for the filaments whose responses to sulfide are indicated by the corresponding solid symbols. Because individual nerve impulses could not be distinguished in these recordings, we determined the relative response for each filament in the following way: we calculated the root-mean-square (rms) deviation of the signal about its mean over an interval of duration 0.25 s beginning 0.5 s before exposure (B), together with the rms deviation over a similar 0.25 s interval beginning 1 s after exposure (R); then we took the relative response r to equal (R/B) − 1. These intervals are indicated by heavy horizontal bars in (A).

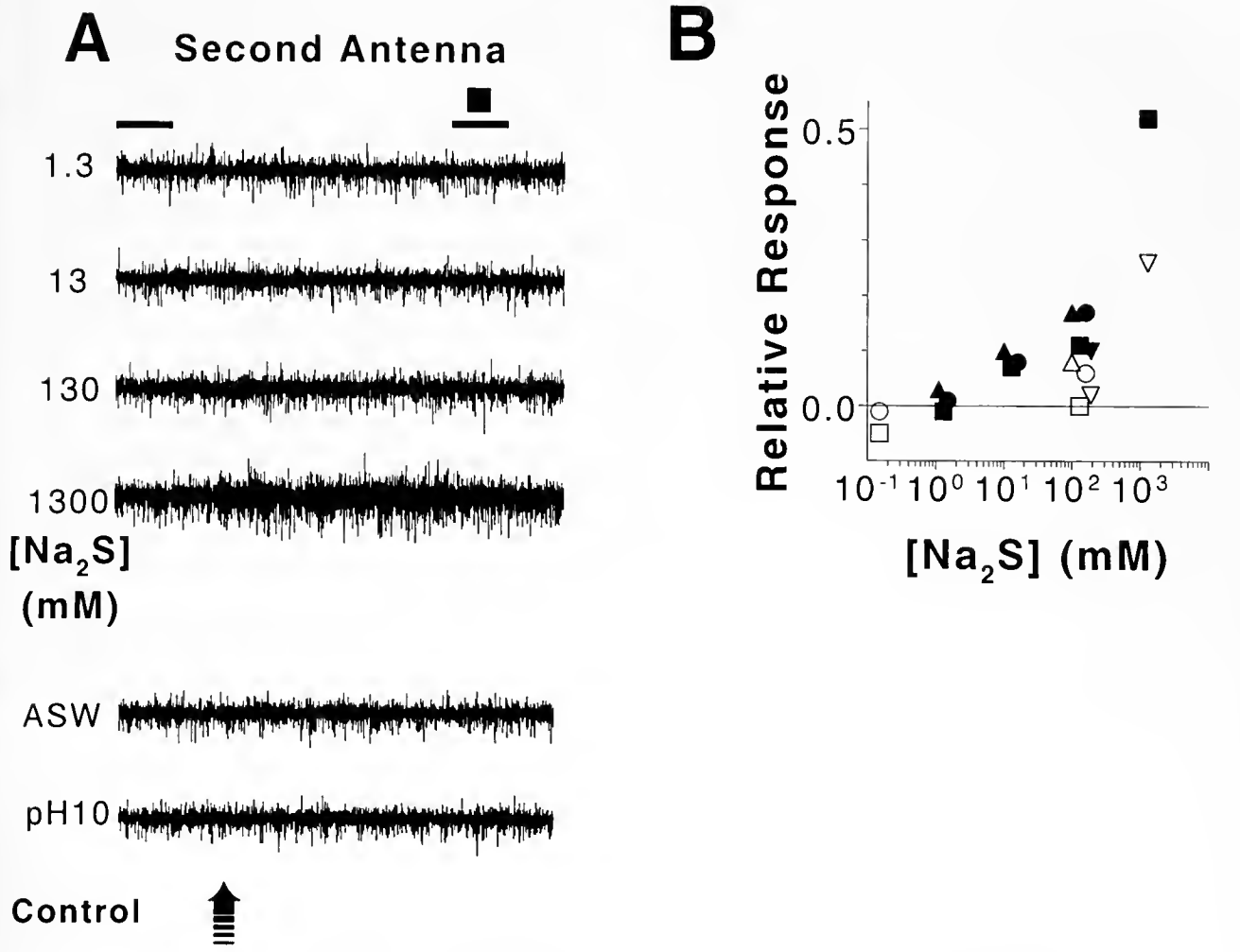

Figure 4. (A) Examples of multiunit nerve response from the second antenna of the shallow-water shrimp *Panaeus aztecus* to solutions of Na_2S and to control solutions. The experimental procedures used for *P. aztecus* are described in (15, 16). See Figure 3A for other details. (B) Steady-state relative responses to concentrations of Na_2S and controls. Note the expanded response scale in comparison with Figure 3B. The solid symbol ■ represents the relative responses to Na_2S shown in (A); the other solid symbols represent sulfide responses of the other second antennae tested. The open symbols represent responses to the three control solutions used on the antennal filaments whose sulfide responses are indicated by the corresponding solid symbols, namely, ASW (shown near 0.1), pH 10 (shown at or near 130), and pH 13 (shown at or near 1300). See Figure 3B for other details.

the pH of the 130 mM Na_2S solution [pH 10, giving a response = 0.040 ± 0.018 ($n = 4$)].

While the second antennae of both vent and shallow water shrimp responded to Na_2S, there are major differences between them. First, the axons of *P. aztecus* responded vigorously to the pH 13 control solution, unlike those of *Rimicaris* sp. or *R. exoculata*. Thus, the response to Na_2S in *P. aztecus* was confounded by a sensitivity to high pH. Second, the axons of *P. aztecus* responded only for about 40 min after excision, while axons of *Rimicaris* sp. and *R. exoculata* responded repeatedly to sulfide stimulation for several hours, and, in one experiment on *R. exoculata*, for 24 h. Furthermore, sensilla on the second antenna of *Rimicaris* sp. and *R. exoculata* are more numerous than those in *P. aztecus* (1 sensillum/231 μm of filament circumference) and *P. pugio* (1 sensillum/110 μm). Although we do not know how many chemosensory neurons there are in each sensillum or what their individual sensitivities are, the larger density of sensilla in the vent species suggests that they may have an enhaneed chemosensory capacity.

To our knowledge, this is the first physiological demonstration of a sensory response to a geochemical stimulus in a vent invertebrate. Sulfides have been reported to serve as physical cues for other invertebrates: a shallow-water polychaete may use sulfides as a settlement cue (17), but

this is controversial (18); and a tropical tick is attracted to sulfides in mammalian breath (19). In behavioral experiments on the shrimp *Palaemonetes vulgaris*, concentrations of $H_2S < 0.08$ m*M* evoked an avoidance response (N. Sofranko and C. L. Van Dover, unpub. data). The sulfide response which we have found in hydrothermal vent shrimp may thus be an adaptation of a widespread sulfide sensitivity in shrimp to the particular environment created by the hydrothermal vents. Behavioral studies on sulfide sensitivity of vent shrimp will be required to determine whether the responses we have observed are in fact used by the shrimp in orientation or other behaviors. If the antennal responses initiate behavior in vent shrimp, the behavioral threshold may well lie below the neural threshold. Such differences between thresholds for sensory cells and for behavior, which have been attributed to the convergence of the sensory afferents onto a relatively smaller population of cells in the central nervous system, have been discussed for the spiny lobster, *Panulirus interruptus*, in which the behavioral sensitivity to ATP is 30 times greater than the sensory cellular sensitivity (20), and for the American cockroach (21) and moths (22, 23).

Acknowledgments

We thank the scientists aboard R/V *Atlantis II* on cruise 129-7 for helpful advice and discussions. We are indebted to the *Alvin* Group and the crew of R/V *Atlantis II* for the success of the cruise. We thank Lorraine McDowell and Richard Mitchell for technical assistance. This work was supported in part by NSF USA and NSERC Canada.

Literature Cited

1. **Lutz, R. A., T. M. Shank, D. J. Fornari, R. M. Haymon, M. D. Lilley, K. L. Von Damme, and D. Desbruyeres. 1994.** Rapid growth at deep-sea vents. *Nature* **371:** 663–664.
2. **Lupton, J. E., J. R. Delaney, H. P. Johnson, and M. K. Tivey. 1985.** Entrainment and vertical transport of deep-ocean water by buoyant hydrothermal plumes. *Nature* **316:** 621–623.
3. **Lutz, R. A., D. Jablonski, D. C. Rhoads, and R. D. Turner. 1980.** Larval dispersal of a deep-sea hydrothermal vent bivalve from the Galapagos Rift. *Mar. Biol.* **57:** 127–133.
4. **Ache, B. W. 1982.** Chemoreception and thermoreception. Pp. 369–398 in *Biology of Crustacea*, vol. 3, Atwood, H. L. and Sandeman, D. C., eds., Academic Press, New York.
5. **Nation, J. L. 1983.** Specialization in the alimentary canal of some mole crickets (Orthoptera: Gryllotalpidae). *Int. J. Insect Morphol. Embryol.* **12:** 201–210.
6. **Zhang, H-J., R. N. Jinks, A. C. Wishart, B.-A. Battelle, S. C. Chamberlain, W. H. Fahrenbach, and L. Kass. 1994.** An enzymatically enhanced recording technique for *Limulus* ventral photoreceptors: physiology, biochemistry, and morphology. *Visual Neurosci.* **11:** 41–52.
7. **Radford-Knoery, J., J.-L. Charlou, J.-P. Donval, Y. Fouquet, H. Pellé, H. Ondréas, I. Costa, N. L. Lourenço, M. K. Tivey, and M. Ségonzac. 1994.** Sulfide as a hydrothermal plume tracer. *EOS, Transactions of the Am. Geophys. Union* **75,** No. 44 (Supplement): 313.
8. **Johnson, K. S., J. J. Childress, R. R. Hessler, C. N. Sakamoto-Arnold, and C. L. Beehler. 1988.** Chemical and biological interactions in the Rose Garden hydrothermal vent field, Galapagos spreading center. *Deep-Sea Res.* **35:** 1723–1744.
9. **Campbell, A. C., M. R. Palmer, G. P. Klinkhammer, T. S. Bowers, J. M. Edmond, J. R. Lawrence, J. F. Casus, G. Thompson, S. Humphris, P. Rona, and J. A. Karson. 1988.** Chemistry of hot springs on the Mid-Atlantic Ridge. *Nature* **335:** 514–519.
10. **Kaissling, K.-E. 1986.** Chemo-electrical transduction in insect olfactory receptors. *Ann. Rev. Neurosci.* **9:** 121–145.
11. **Millero, F. J., S. Hubinger, M. Fernandez, and S. Garnett. 1987.** Oxidation of H_2S in seawater as a function of temperature, pH and ionic strength. *Environ. Sci. Technol.* **21:** 439–443.
12. **Johnson, K. S., J. J. Childress, C. L. Beehler, and C. N. Sakamoto. 1994.** Biogeochemistry of hydrothermal vent mussel communities: the deep-sea analogue to the intertidal zone. *Deep-Sea Res.* **41:** 993–1011.
13. **Jannasch, H. W., C. O. Wirsen, and S. Molyneaux. 1991.** Chemoautotrophic sulfur-oxidizing bacteria from the Black Sea. *Deep-Sea Res.* **38** (Suppl. 2): 1105–1120.
14. **de Angelis, M. A., M. D. Lilley, E. J. Olson, and J. A. Baross. 1993.** Methane oxidation in deep-sea hydrothermal plumes of the Endeavour Segment of the Juan de Fuca Ridge. *Deep-Sea Res.* **40:** 1169–1186.
15. **Gleeson, R. A., W. E. S. Carr, and H. G. Trapido-Rosenthal. 1989.** ATP-sensitive chemoreceptors: antagonism by other nucleotides and the potential implications of ectonucleotidase activity. *Brain Res.* **497:** 12–20.
16. **Trapido-Rosenthal, H. G., W. E. S. Carr, and R. A. Gleeson. 1989.** Biochemistry of purinergic olfaction: the importance of nucleotide dephosphorylation. Pp. 243–287 in *Chemical Senses*, vol. 1, Brand, J. G., Cagan, R. H., Teeter, J. H., and Kare, M. R., eds. Marcel Dekker, New York.
17. **Cuomo, M. C. 1985.** Sulphide as a larval settlement cue for *Capitella* sp. I. *Biogeochemistry* **1:** 169–181.
18. **Dubilier, N. 1988.** H_2S—A settlement cue or a toxic substance for *Capitella* sp. I larvae? *Biol. Bull.* **174:** 30–38.
19. **Steullet, P., and P. M. Guerin. 1992.** Perception of breath components by the tropical bont tick, *Amblyommavariegatum* Fabricius (Ixodidae). *J. Comp. Physiol. A* **170:** 677–685.
20. **Zimmer-Faust, R. K., R. A. Gleeson, and W. E. S. Carr. 1988.** The behavioral response of spiny lobsters to ATP: Evidence for mediation by P_2-like chemosensory receptors. *Biol. Bull.* **175:** 167–174.
21. **Boeckh, J., and P. Selsam. 1984.** Quantitative investigation of the odour specificity of central olfactory neurones in the American cockroach. *Chem. Senses* **9:** 369–380.
22. **Boeckh, J., and V. Boeckh. 1979.** Threshold and odor specificity of pheromone-sensitive neurons in the deutocerebrum of *Anthera pernyi* and *A. polyphemus* (Saturnidae). *J. Comp. Physiol. A* **132:** 235–242.
23. **Olberg, R. M. 1983.** Interneurons sensitive to female pheromone in the deutocerebrum of the male silkworm moth, *Bombyx mori*. *Physiol. Entomol.* **8:** 187–239.

Reference: *Biol. Bull.* **189:** 77–80. (October/November, 1995)

Cephalopods Occupy the Ecological Niche of Epipelagic Fish in the Antarctic Polar Frontal Zone

PAUL G. RODHOUSE AND MARTIN G. WHITE

British Antarctic Survey, Natural Environment Research Council, High Cross, Madingley Road, Cambridge CB3 OET, UK

Recent data from research cruises and exploratory fishing in the Antarctic Polar Frontal Zone (APFZ) of the Scotia Sea, together with data from dietary studies of Antarctic vertebrate predators, have revealed a large, previously overlooked trophic system in the Southern Ocean (Fig. 1). The upper trophic levels of this open-ocean epipelagic community are exceptional in that they contain no fish species. Fishes are replaced by cephalopods, including the ommastrephid squid, Martialia hyadesi. *This squid preys on mesopelagic myctophids (lanternfish), which feed largely on copepods. We identify here a geographically distinct, Antarctic, open-ocean food chain which is of importance to air breathing predator species but where Antarctic krill,* Euphausia superba, *is absent. This system is probably prevalent in areas of higher primary productivity, especially the Scotia Sea and near the peri-Antarctic islands. Squid stocks in the APFZ may have potential for commercial exploitation, but they, and the predators they support, are likely to be sensitive to overfishing. Squid have a short, semelparous lifecycle, so overfishing in a single year can cause a stock to collapse.*

The presence of this trophic system was already evident among the results of the *Discovery* expeditions. Large quantities of squid remains, especially their indigestible beaks, were found in the gut contents of several albatross and seal species (1). But because *E. superba* is so conspicuous and plays such an important role in the diet of vertebrate predators (especially commercially exploited baleen whales), and as these crustaceans were amenable to marine biological research methods of the day, the cephalopod trophic system in the vast but remote region of the APFZ was largely ignored.

Received 18 May 1995; accepted 27 July 1995.

Abbreviations: APFZ = Antarctic Polar Frontal Zone; BAS = British Antarctic Survey.

Following a review of the resources of the Southern Ocean (2) that noted the possible presence of large cephalopod stocks, studies of the cephalopod prey of vertebrate predators breeding at South Georgia (Fig. 2) in the 1970s (3) revealed that an unidentified ommastrephid, *Todarodes?* sp. dominated the diet of some species. Collections of cephalopod remains in the predator regurgitations at South Georgia (4,5) made in the 1980s by scientists of the British Antarctic Survey (BAS), coincided with a large "by-catch" of the little-known ommastrephid *M. hyadesi* in the new fishery for the squid *Illex argentinus* on the Patagonian Shelf during 1986 (6). A comparison of material from both sources revealed that the species being taken by predators, previously identified as *Todarodes?* sp., was *M. hyadesi*. Exploratory fishing by Japanese squid jiggers in the APFZ west of South Georgia subsequently caught commercial quantities of *M. hyadesi* near the surface (<50 m), confirming the presence of this species in the Scotia Sea (6). Although stock size cannot be assessed at present, annual predator consumption of *M. hyadesi* in the region is estimated at >330,000 tonnes (7). Stomach contents of jigged specimens showed they had fed on a community of myctophid fish dominated by *Kreffichthys anderssoni* (8). Myctophids feed largely on copepods, so this food chain may be partially or fully independent of the *Euphausia superba* trophic system. Elsewhere in the APFZ, myctophids have recently been identified as the major food resource for other higher predators such as the king penguin (9).

During the 1994 research cruise of RRS *James Clark Ross* (BAS) satellite-tagged albatross predators of *M. hyadesi* and other squid were tracked to the APFZ, north of South Georgia; there the pelagic community exploited by the birds was sampled with a commercial trawl. The samples included the squids *M. hyadesi*, *Moroteuthis knipovitchi* (the major prey of southern elephant seals), *Go-*

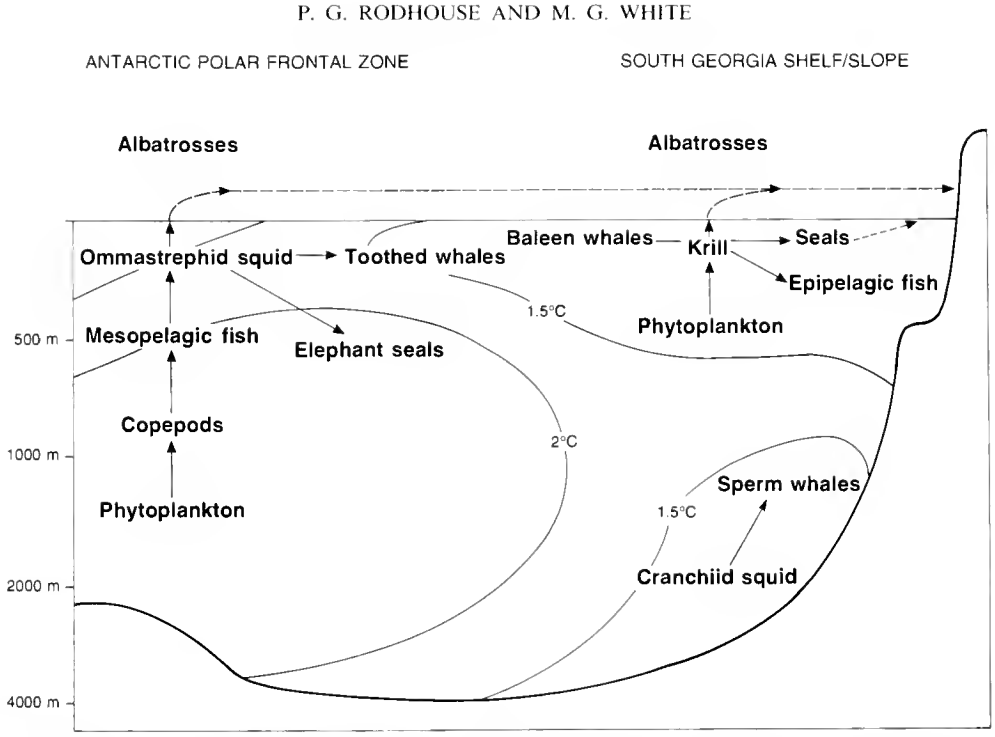

Figure 1. Spatial relationship between the myctophid/cephalopod trophic system at the Antarctic Polar Frontal Zone and the *Euphausia superba* based system on the South Georgia shelf and slope (positions of organisms in the water column do not represent their bathymetric distribution).

natus antarcticus, *Galiteuthis glacialis*, and *Brachioteuthis* sp. (Rodhouse, P. G. *et al.*, BAS, in prep). The data confirmed that, in the Southern Ocean, in the vicinity of the APFZ, *M. hyadesi* occurs near the surface (<100 m). Albatross predators breeding at South Georgia and large male sperm whales feeding in the vicinity of the islands (10) exploit different, geographically separated, cephalopod communities. The whales' diet does not include significant numbers of *M. hyadesi;* rather it is dominated, in terms of biomass, by the gigantic Antarctic cranchiid squid, *Mesonychoteuthis hamiltoni*.

The biological oceanography of the APFZ is poorly understood. Primary productivity in the ice-free zone of the Southern Ocean is generally low (11). Strong westerly winds generally maintain a deep mixed layer, but composite Coastal Zone Color Scanner images reveal regions of high concentrations of phytoplankton pigment, indicating enhanced productivity in the Scotia Sea, in the vicinity of the Scotia Arc, and near the peri-Antarctic islands (12). In the ice-free zone of the Scotia Sea, the pelagic community is dominated by copepods, small euphausiids, gelatinous zooplankton, and myctophids (13,14). Elsewhere in the APFZ, *M. hyadesi* has been recorded from the Kerguelen (15) and Macquarie (16) islands, suggesting that this squid occurs in areas of enhanced productivity in the pelagic community.

The composition of the Antarctic pelagic fish community is unusual by comparison with such communities in other oceans, because epipelagic fish families are absent. Key components of the pelagic food-web in temperate and tropical seas—clupeids, carangids, scombrids and their predators, the oceanic sharks—are absent or rare vagrants on the periphery of the Southern Ocean. At shallow depths around the Antarctic Continent and the peri-Antarctic islands, demersal fish, mostly members of the endemic suborder Notothenioidei, dominate the fish fauna. Most species are demersal as adults, but a small number, notably *Pleuragramma antarcticum* near the continent and *Champsocephalus gunnari* in the vicinity of islands, have become secondarily adapted to inhabit pelagic habitats. Others are temporarily pelagic during early ontogeny. By contrast, the fish fauna of the open ocean is limited to deepwater bathypelagic and mesopelagic species. Of these, the myctophids predominate, and are sufficiently abundant to support a fishery (17). In the north Scotia Sea, mesopelagic fish, mainly myctophids, constitute up to 18% of the total nekton biomass and are the main component of the biomass available to higher predators (13,14). But epipelagic fish are absent, and we now conclude these are replaced by a cephalopod community dominated by ommastrephid squid.

An epipelagic system dominated by cephalopods is possibly the consequence of physiological constraints on fish in cold sub-Antarctic or Antarctic waters, that do not apply to the cephalopods; or may have arisen because the life cycle traits of cephalopods may be better adapted to

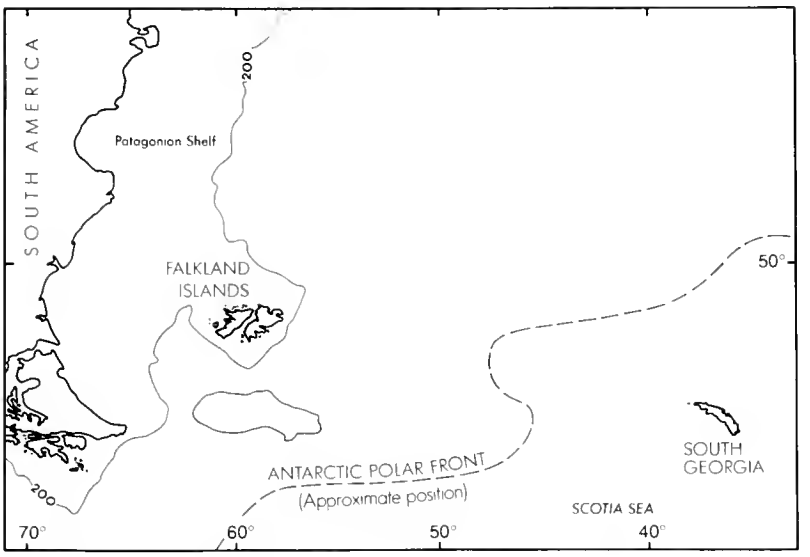

Figure 2. Atlantic sector of the Southern Ocean showing the position of South Georgia and the Antarctic Polar Front.

the physical environment of the APFZ. The relatively short life span of cephalopods might allow them to complete the life cycle, at least from the planktonic to the nektonic phase, before they are flushed out of productive regions by the fast-flowing Antarctic Circumpolar Current. If epipelagic communities in other remote oceanic regions are similarly dominated by cephalopods, then comparative studies may shed light on these questions.

As finfish stocks have declined globally, cephalopod catches have grown and, in terms of dollar value of the catch, are currently rated third in world importance after shrimp and tuna (18). Pressures on fish stocks continue to increase, and conflict at sea between fishing nations is likely to escalate in the absence of political will to reduce fishing effort. Under these circumstances, new cephalopod stocks are likely to be sought as an alternative, high-value resource. Stocks of *M. hyadesi* straddle the region administered by the Commission for the Conservation of Antarctic Marine Living Resources, and the high seas to the north. This will complicate management of any future fishery in the region. Given the important role of cephalopods in the diet of several species of higher predator in the Antarctic (19) and the vulnerability of short-lived, semelparous species to overexploitation, the ecological consequences of an unmanaged fishery for cephalopods in the Southern Ocean are potentially severe.

Acknowledgments

Cephalopod research at the British Antarctic Survey (BAS) owes much to collaboration with John Croxall and Peter Prince in the Higher Predators Programme.

Literature Cited

1. **Harrison-Matthews, M. A. 1929.** The natural history of the elephant seal with notes on other seals found at South Georgia. *Discovery Rep.* **1:** 235–256.
2. **Everson, I. 1977.** *The Living Resources of the Southern Ocean.* FAO Southern Ocean Fisheries Programme GLO/SO/77/1: 156 pp.
3. **Clarke, M. R., and P. A. Prince. 1981.** Cephalopod remains in the regurgitations of the black-browed and grey-headed albatrosses at South Georgia. *Br. Antarct. Surv. Bull.* **54:** 1–7.
4. **Rodhouse, P. G., M. R. Clarke, and A. W. A. Murray. 1989.** Cephalopod prey of the wandering albatross *Diomedea exulans*. *Mar. Biol.* **96:** 1–10.
5. **Rodhouse, P. G., P. A. Prince, M. R. Clarke, and A. W. A. Murray. 1990.** Cephalopod prey of the grey-headed albatross *Diomedea chrysostoma*. *Mar. Biol.* **104:** 353–362.
6. **Rodhouse, P. G. 1991.** Population studies of *Martialia hyadesi* (Cephalopoda: Ommastrephidae) at the Antarctic Polar Front and Patagonian Shelf, South Atlantic. *Bull. Mar. Sci.* **49:** 404–418.
7. **Rodhouse, P. G., J. P. Croxall, and P. A. Prince. 1993.** Towards an assessment of the stock of the ommastrephid squid *Martialia hyadesi* in the Scotia Sea: data from predators. Pp. 433–440 in *Recent Advances in Cephalopod Fisheries Biology*, T. Okutani, R. K. O'Dor, and T. Kubodera, eds. Tokai University Press, Tokyo.
8. **Rodhouse, P. G., M. G. White, and M. R. R. Jones. 1992.** Trophic relations of the cephalopod *Martialia hyadesi* (Teuthoidea: Ommastrephidae) at the Antarctic Polar Front. *Mar. Biol.* **114:** 415–421.
9. **Adams, N. J., and N. T. Klages. 1987.** Seasonal variations in the diet of the king penguin (*Aptenodytes patagonicus*) at sub-Antarctic Marion Island. *J. Zool. Lond.* **212:** 303–324.
10. **Clarke, M. R. 1980.** Cephalopoda in the diet of sperm whales of the Southern Hemisphere and their bearing on sperm whale biology. *Discovery Rep.* **37:** 1–324.
11. **Hempel, G. 1985.** On the biology of the polar seas especially the Southern Ocean. Pp. 3–34 in *Marine Biology of Polar Regions and Effects of Stress on Marine Organisms*, J. S. Gray and M. E. Christiansen, eds. John Wiley, Chichester.

12. **Comiso, J. C., C. R. McClain, C. W. Sullivan, J. P. Ryan, and C. L. Leonard. 1993.** Coastal zone color scanner pigment concentrations in the Southern Ocean and relationships to geophysical surface features. *J Geophys. Res* **98:** 2419–2451.

13. **Piatkowski, U., P. G. Rodhouse, M. G. White, D. G. Bone, and C. Symon. 1994.** Nekton community of the Scotia Sea as sampled by the RMT25 during austral summer. *Mar Ecol Prog. Ser* **11:** 13–28.

14. **Rodhouse, P. G., U. Piatkowski, E. J. Murphy, M. G. White, and D. G. Bone. 1994.** Utility and limits of biomass spectra: the nekton community sampled with the RMT25 in the Scotia Sea during austral summer. *Mar Ecol. Prog. Ser* **112:** 29–39.

15. **Piatkowski, U., P. G. Rodhouse, and G. Duhamel. 1991.** Occurrence of the cephalopod *Martialia hyadesi* (Teuthoidea: Ommastrephidae) at the Kerguelen Islands in the Indian Ocean sector of the Southern Ocean. *Polar Biol.* **11:** 273–275.

16. **O'Sullivan, D. B., G. W. Johnstone, K. R. Kerry, and M. J. Imber. 1983.** A mass stranding of squid *Martialia hyadesi* Rochebrune and Mabille (Teuthoidea; Ommastrephidae) at Macquarie Island. *Pap Proc R Soc. Tasmania* **117:** 161–163.

17. **Sabourenkov, E. N. 1991.** Mesopelagic fish of the Southern Ocean—Summary results of recent Soviet studies. *Commission for the Conservation of Antarctic Marine Living Resources, Hobart, Australia* SC-CAMLR-SSP/7: 433–457.

18. **FAO Fisheries Department. 1993.** Fisheries and the law of the sea: a decade of change. *FAO Fisheries Circular*, No. **853:** 66 pp, Rome.

19. **Laws, R. M. 1985.** Ecology of the Southern Ocean. *Am. Sci.* **73:** 26–40.

Reference: *Biol. Bull.* **189**: 81–90. (October/November, 1995)

Phylogenetic Position of the Dicyemid Mesozoa Inferred from 18S rDNA Sequences

TOMOE KATAYAMA[1], HIROSHI WADA[2], HIDETAKA FURUYA[3], NORIYUKI SATOH[2], AND MASAMICHI YAMAMOTO[1]

[1]*Ushimado Marine Laboratory, Okayama University, Okayama 701-43,* [2]*Department of Zoology, Kyoto University, Kyoto 606-01, and* [3]*Department of Biology, Osaka University, Toyonaka 560, Japan*

Abstract. The dicyemid mesozoa, obligate symbionts in the cephalopod kidney, are simply organized multicellular animals. They have long been the subject of phylogenetic debates. Some authors have suggested that dicyemids represent an offshoot from an early metazoan ancestor. Other workers considered them to be degenerated progeny of higher metazoa, possibly parasitic trematodes. We determined the almost complete nucleotide sequences of 18S rDNA in two species of dicyemid, *Dicyema orientale* and *Dicyema acuticephalum*, isolated purely from cephalopod urine. We compared these sequences with sequences determined in the present study from three flatworm species, as well as with a variety of eukaryote sequences obtained from databases. The phylogenetic trees reconstructed with the use of the neighbor-joining, maximum-parsimony, and maximum-likelihood methods indicated that the dicyemids belong among the triploblastic animals (Bilateria). However, we cannot firmly establish the position of the dicyemids within the Bilateria because we cannot ignore the problem of long branch attraction between the myxozoans, dicyemids, nematodes, and acoel flatworms. The present results favor the hypothesis that the dicyemids do not represent an early divergent metazoan group, but rather a group degenerated from a triploblastic ancestor.

Introduction

The dicyemids are simply organized multicellular animals consisting of an outer layer of 20–40 ciliated somatic cells and an inner core of one long axial cell. They are obligate symbionts in the kidney of cephalopods. Their life cycle is complex; the asexually produced vermiform embryos increase the population in the host, while the infusoriform embryos arising from fertilized eggs pass out of the host body with the urine and are thought to infect another cephalopod host (Brusca and Brusca, 1990).

The dicyemid mesozoans have long been the subject of a phylogenetic controversy (Brusca and Brusca, 1990; Willmer, 1990). They were at first considered to be an extant link between the Protozoa and the Metazoa (Hyman, 1959). However, the resemblance of their complex life cycles to those of parasitic trematodes has led some authors to propose that the dicyemids are descended from an established metazoan group and that their simple body organization results from degeneration attributable to parasitism (Nouvel, 1948; McConnaughey, 1951; Stunkard, 1954; Ginetsinskaya, 1988). Others still view the simple body construction of dicyemids as truly primitive and hold that the group represents an offshoot from early divergent metazoa (Dodson, 1956; Hyman, 1959; Lapan and Morowitz, 1974).

The phylogenetic relationships of eukaryotes have recently come under intense scrutiny in the light of new molecular data. Phylogenetic analyses using nucleotide sequences of 5S rRNA suggested that a dicyemid (*Dicyema misakiense*) diverged early among such lower metazoa as sponges, cnidarians, and flatworms (Ohama *et al.*, 1984; Hori and Osawa, 1987). But phylogenetic trees based upon comparisons of about 120 sites in the nucleotide sequences of 5S rRNA were different from those inferred from longer nucleotide sequences of 18S or 28S ribosomal RNA (Field *et al.*, 1988; Christen *et al.*, 1991; Katayama *et al.*, 1993; Wainright *et al.*, 1993; Kobayashi *et al.*, 1993). We have sequenced 18S ribosomal RNA

Received 7 July 1994; accepted 5 July 1995.

Correspondence: Dr. Masamichi Yamamoto, Ushimado Marine Laboratory, Okayama University, Ushimado, Okayama, 701-43 Japan.

genes (18S rDNA) in two species of the dicyemid mesozoa. Our comparison of the nucleotide sequences of small-subunit rDNA for a variety of organisms indicates that the dicyemids belong among the triploblastic animals.

Materials and Methods

Biological materials

We determined almost the entire sequence of 18S rDNA in two species of dicyemid mesozoans and three species of turbellarians (Platyhelminthes). Pure samples of the dicyemids *Dicyema acuticephalum* and *Dicyema orientale* were collected from the urine of *Octopus vulgaris* and *Sepioteuthis lessoniana*, respectively (Furuya *et al.*, 1992a). Specimens of *Convoluta naikaiensis* (Acoela) and *Planocera multitentaculata* (Polycladida) were collected on the shore near the Ushimado Marine Laboratory. Specimens of *Dugesia japonica* (Tricladida) were obtained from the brook near the Ushimado Marine Laboratory. All were frozen quickly and kept at −80°C until use.

In addition to the sequences of the above five species, we used the sequences of 23 eukaryotes—including animals, protists, plants, and fungi—for which almost complete 18S rDNA sequences were available in databases. The species used and their accession numbers are as follows: *Paramecium tetraurelia* (Ciliophora), X03772; *Oxytricha nova* (Ciliophora), X03948; *Crypthecodinium cohnii* (Dinozoa), M64245; *Theileria annulata* (Apicomplexa), M64243; *Sarcocystis muris* (Apicomplexa), M64244; *Hartmanella vermiformis* (Rhizopoda), M95168; *Saccharomyces cerevisiae* (Fungi), J01353; *Filobasidiella neoformans* (Fungi), X60183; *Arabidopsis thaliana* (Plantae), X16077; *Volvox carteri* (Plantae), X53904; *Beroe cucumis* (Ctenophora), D15068; *Trichoplax adhaerens* (Placozoa), L10828; *Anemonia sulcata* (Cnidaria), X53498; *Scypha ciliata* (Porifera), L10827; *Henneguya* sp. (Myxozoa), U13826; *Caenorhabditis elegans* (Nematoda), X03680; *Moliniformis moliniformis* (Acanthocephala), Z19562; *Schistosoma mansoni* (Trematoda), X53047; *Crassostrea gigas* (Bivalvia), X60315; *Artemia salina* (Crustacea), X01723; *Sagitta crassa* (Chaetognatha), D14363; *Asterias amurensis* (Asteroidea), D14358; and *Xenopus laevis* (Vertebrata), X04025.

DNA isolation

Genomic DNA was extracted by the method described previously (Wada *et al.*, 1992). In brief, the frozen samples were lysed in TE buffer (10 m*M* Tris-HCl, 0.1 *M* EDTA, pH 8.0) containing 0.5% sodium dodecyl sulfate. After digestion with proteinase K (100 μg/ml) at 50°C for 3 h, DNA was extracted with phenol and precipitated in ethanol and an equal volume of 5.0 *M* ammonium acetate. Samples resuspended in TE buffer were further purified by RNase A digestion (20 μg/ml) at 37°C for 1 h followed by ethanol precipitation.

Amplification of 18S rDNA

The 18S rDNA was amplified by the polymerase chain reaction (PCR; Saiki *et al.*, 1988) in an Air Thermo-cycler 1645 (Idaho Technology). Almost the entire length of 18S rDNA was amplified using synthetic oligonucleotides, 5′-CTGGTTGATCCTGCCAG-3′ (primer 0) and 5′-CCTTGTTACGACTT-3′ (primer 10) as the terminal primers. Amplifications were performed in 50 μl of 50 m*M* Tris-HCl (pH 8.5), 250 μg/ml BSA, 2 m*M* Mg^{2+}, with 0.2 m*M* each dNTP, 50 p*M* primers, template DNA (5–10 ng), and 2 U Taq DNA polymerase (TOYOBO). The temperature regimen for 35 cycles was 20 s at 94°C, 30 s at 50°C, and 90 s at 74°C.

Determination of DNA sequences

After purification of the amplified DNA by electrophoresis in a 0.8% agarose gel, the nucleotide sequence was directly determined by dideoxy chain-termination (Sanger *et al.*, 1977) using Sequenase ver 2.0 (USB) and [^{35}S]-dATP (Amersham). All DNA samples were sequenced in both directions and from several separate amplifications with terminal primers (0 and 10) and internal primers. The internal primers used were primer-1 (5′-CCGGAGAGGGAGCCTGA-3′), primer-2 (antisense of primer-1), primer-3 (5′-CAGCAGCCGCGGTAATT-3′), primer-4 (antisense of primer-3), primer-5 (5′-GCGAA-AGCATTTGCCAA-3′), primer-6 (antisense of primer 5), primer-7 (5′-GAAACT(TC)AAAGGAAT-3′), primer-8 (antisense of primer-7), and primer-9 (5′-ACGGGC-GGTGTGT(AG)C-3′). The positions corresponding to these primers in 18S rDNA sequences are shown in Figure 1. The continuity of the DNA fragments was confirmed by overlapping of the sequences.

Phylogenetic analyses

Sequences were aligned manually on the basis of maximum nucleotide similarity (Fig. 1). Alignment gaps were inserted to account for putative length differences between sequences. Some regions could be confidently aligned and were presumed to be homologous. However, we could not unequivocally determine the optimal alignment for the regions containing deletions, insertions, or highly variable sequences. We excluded positions from the analysis according to the following rule: Positions where a gap was present for any taxon were not used in analyses. In the present study, we found this simple rule alone adequate for excluding the regions of ambiguous homology (the regions where two or more equally optimal alignments were present) from the analysis because in those

regions alignment gaps were always serially inserted in many sequences. The phylogenetic trees were reconstructed using the PHYLIP package version 3.5c (Felsenstein, 1989) and fastDNAML (Olsen *et al.*, 1993). Tree-building procedures used were the neighbor-joining (Saitou and Nei, 1987), the maximum-parsimony (Fitch, 1971), and the maximum-likelihood (Felsenstein, 1981). For the neighbor-joining analysis, evolutionary distance values were calculated by the formula of Jukes and Cantor (1969). The degree of support for internal branches of the trees in the neighbor-joining and the maximum-parsimony trees was assessed by bootstrap levels of support (Felsenstein, 1985) determined by 500 bootstrap repetitions.

Results

In *D. acuticephalum, D. orientale, Convoluta naikaiensis, Dugesia japonica,* and *Planocera multitentaculata,* almost the entire length of 18S rDNA was amplified by PCR from the genomic DNA. The sequence (1500–1700 bp) was determined directly from PCR products. The sequences have been deposited in databases (GSDB, DDBJ, EMBL, and NCBI) under the following accession numbers: D26529 for *D. acuticephalum;* D26530, *D. orientale;* D17558, *Convoluta naikaiensis;* D17560, *Dugesia japonica;* D17562, *Planocera multitentaculata.* To infer the phylogenetic position of the dicyemids within the eukaryotes, we aligned the almost complete nucleotide sequences of 18S rDNA of the above five species with the 23 eukaryote sequences we obtained from databases. Metazoan taxa were chosen to represent phyla broadly; protozoan taxa were chosen to represent the more recently derived groups. Figure 1 shows a sample of the alignment for 9 out of 28 species included in the present analysis. This alignment reveals that throughout the eukaryotes the sequences are highly conserved in some regions and highly variable in others. After exclusion of the regions of ambiguous homology, 1070 sites (Fig. 1) remained for phylogenetic inference. Phylogenetic trees shown were reconstructed by the neighbor-joining (Fig. 2), the maximum-parsimony (Fig. 3), and the maximum-likelihood (Fig. 4) analyses.

Among the phylogenetic trees reconstructed by the three methods, the topologies were largely congruent with one another, though branching with low bootstrap support within the metazoan lineage showed somewhat conflicting arrangements. The metazoans—including triploblasts (Bilateria), diploblasts, dicyemids, and a myxozoan—formed a monophyletic assemblage in the three trees. Within the metazoan assemblage, triploblasts formed a discrete monophyletic unit together with the mesozoa and the Myxozoa. The branches of triploblasts were in general longer than those of other taxa.

The grouping of the dicyemids with the triploblastic animals was supported by a bootstrap value of 100% in both the neighbor-joining (Fig. 2) and the maximum-parsimony (Fig. 3) analyses (because of the enormous computation time required, bootstrapping was not performed in the maximum-likelihood analysis). In the trees reconstructed by the three methods, dicyemids were grouped with *Caenorhabditis elegans* (a nematode), *Henneguya* sp. (a myxozoan), and *Convoluta naikaiensis* (an acoel flatworm), though bootstrap confidence level for this grouping was low.

To corroborate the inclusion of the dicyemids in the triploblastic lineage, we analyzed subsets of taxa shown in the present paper as well as several different sets of taxa including some of the following species (the accession numbers for 18S rDNA data are shown in parentheses): *Cryptomonas phi* (X57162), *Babesia bovis* (M87566), *Tetilla japonica* (D15067), *Sycon calcaravis* (D15066), *Mnemiopsis leidyi* (L10826), *Tripedalia cystophora* (L10829), *Paraspadella gotoi* (D14362), *Antedon serrata* (D14357), *Strongylocentrotus intermedius* (D14365), *Balanoglossus carnosus* (D14359), *Oikopleura* sp. (D14360), *Branchiostoma floridae* (M19571), *Homo sapiens* (X03205). In all sets of taxa analyzed, triploblasts formed a monophyletic unit and the dicyemids were placed within the triploblastic clade with high bootstrap confidence level. Grouping of *Caenorhabditis, Convoluta, Henneguya,* and *Dicyema* were consistently observed. *Trichoplax,* another enigmatic animal whose phylogenetic position is controversial (Brusca and Brusca, 1990; Willmer, 1990), was always positioned outside the triploblastic assemblage, confirming analyses by Wainwright *et al.* (1993).

Discussion

The present molecular phylogenetic study based upon comparisons of nucleotide sequences of 18S rDNA shows that triploblastic animals form a monophyletic assemblage within the metazoan subtree and that the dicyemid mesozoa are an ingroup of the monophyletic unit of triploblastic animals. Monophyly of triploblastic animals has repeatedly been shown in previous molecular phylogenetic analyses with 18S or 28S rDNA sequences (Field *et al.*, 1988; Christen *et al.*, 1991; Wainright *et al.*, 1993; Kobayashi *et al.*, 1993; Smother *et al.*, 1994). The present analysis confirms the recent claim by Smother *et al.* (1994) based upon 18S rDNA sequences that the Myxozoa are closely related to the triploblastic animals.

As in phylogenetic trees previously constructed on the basis of rDNA sequences (Christen *et al.*, 1991; Wainright *et al.*, 1993; Smother *et al.*, 1994), *Trichoplax,* which had once tentatively been grouped in the phylum Mesozoa (see Brusca and Brusca, 1990), was positioned within the

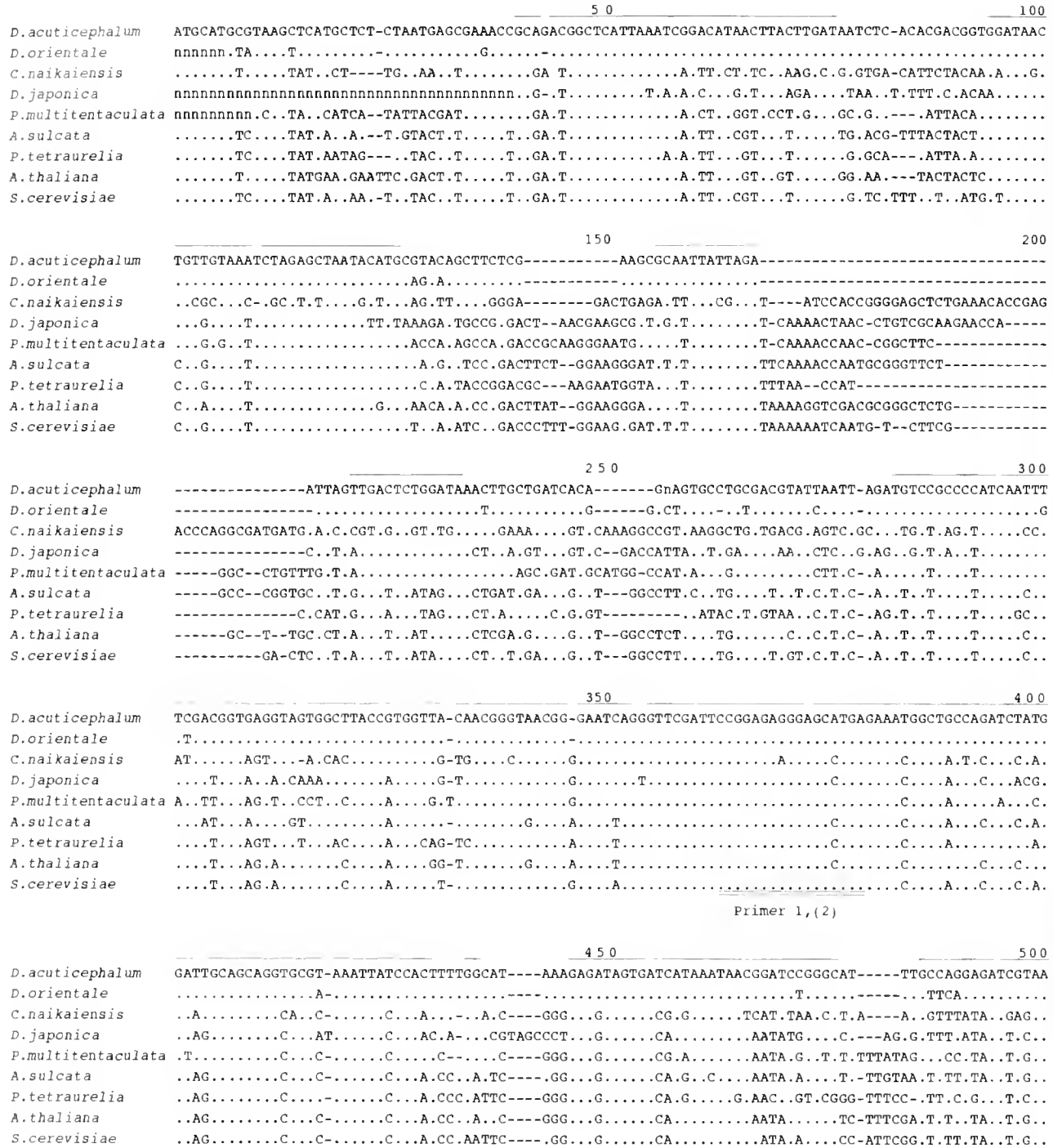

Figure 1. Nucleotide base sequences of 18S rDNA from two dicyemids, *Dicyema acuticephalum* and *Dicyema orientale*, and three flatworms, *Convoluta naikaiensis*, *Dugesia japonica*, and *Planocera multitentaculata*. The sequences are aligned to that of small-subunit rDNA of a diploblast, *Anemonia sulcata*; a protist, *Paramecium tetraurelia*; a plant, *Arabidopsis thaliana*, and a fungus, *Saccharomyces cerevisiae*. A period indicates that the base at that position is identical to that in *D. acuticephalum*, a hyphen indicates a gap, and an "n" indicates an undetermined site. The 1070 positions used for phylogenetic inference are shown by single lines above the alignment. The positions corresponding to the internal primers are shown by double lines below the alignment. The primers whose numbers are in parentheses are antisense to the sequence shown here.

```
                                                                         550                                          600
D.acuticephalum      TGAAATAACT-GTAAAAGCTTTAATGAATG-CAATTGGAGGGCAAGTCTGGTGCCAG-CAGCCGCG-CAATTCCAGT-TCCAATAGTGTATACTAAAGTT
D.orientale          ........TC-.................C.-..........................-........-.........-......................
C.naikaiensis        ......GGA.-CG.......CC.....TGAC.G.G.A....................-..C..---T..A....CC..T.CA..C....CGATG....
D.japonica           ...G.ACTA.TT....TA.....TCA.G.AT..........................-........-T.......C-........C.....T.......
P.multitentaculata   ...GT.C..C-T....CC.A....C..G.AC..........................G........-T.......C-........C.....T.......
A.sulcata            ...GT.C.AC-T....TC......C..GGAT.C........................-........GT.......C-........C.....T.......
P.tetraurelia        ...G....G.-CC...TC.G.A..C..T.AA..........................-........GT.......C-........C.......T.....
A.thaliana           ...GT.C.A.-C....TC.C....C..GGAT.C........................-........GT.......C-........C.....T.T.....
S.cerevisiae         ...GT.C.A.-.....TA.C....C..GGAA..........................-........GT.......C-........C.....T.......
                                                                                  Primer 3,(4)

                                                                         650                                          700
D.acuticephalum      GCTGCAGTTGAAAAGCTCGTAGTTGGATCTCGGTGTGCTAGTACGTAATCGCG-TGCTAGTAGGCCTTTG--CTATAGTTAG--ACTATG----------
D.orientale          ..................................CT......CG..C..A-..--..AA............--CTGTAGT.G..T---------------
C.naikaiensis        .....GT..A...................G--.T..G..T.TGA..CATC..C.AT--AC.CATTGCGCGTA..G..GCCTCG..GCCCATCCTT--CG
D.japonica           .T.CG....A...............A.AT.GA.GAAATG.T.TATAT.A--A.T.TA.GACT.ATTA.C.AGA.CCT--.CCTTCTCCGTCGTGATATTC
P.multitentaculata   .T.......A...................GA.GA.TAG..CCA-C.GGTTG.CC..AT.GCTA-.AC.TGTGGC.CAGCCTGC.TAG.CGGTGAT--TG
A.sulcata            .T.......A.................CT....G...G--CACG.CCGGTC..CC..A...GT.T.AC..G---CCG.GCC.CTCT.C.TCGCAAAGAC-
P.tetraurelia        .T.......A...............A.AT...AGTCAG.TACTA..TGG.T.TTC.TC...TA.TTAA.TGAT.C.CCG.CTAC.A.CCCTTTTGCGCT-
A.thaliana           .T.......A...............A.C..T..GA..G--..CG.CCGGTC..CCTT.G..GT.-.A...G---TCG.C.T.TCC..TC.GTCGGCGATA
S.cerevisiae         .T.......A...............A.CT.T..GCCCG--..TG.CCGGTC..A.TT.TTCGT.T-AC..GAT.TCCAACG.GGC..T.CCTTCTGGCTA

                                                                         750                                          800
D.acuticephalum      ---------------------------------------------GC--TTTACCTTGAACAAA-ATAGAGTGCTTAAGGC-AAGCATTCTGCTTG-A
D.orientale          ---------------------------------------GCTACG..--...............-...............-....-A........A.
C.naikaiensis        CATCGATGATATTAGTTGCACTTTGTTGTGACGACTAGTGGAAACGGTGTT..C..T....GT...-T.......T.C..A..-..C.T..GG.A...C.
D.japonica           GTTAAGTGCACTTTATTGGGATCTTTTACAA--TAACCGACAA-------G.....T.....A...-T...........A..G.G..T.ATGCT.GCAT
P.multitentaculata   TTTTGGTGCTCTTAATTGAGTGCCTTAATTGCCCG---GCCA-------CG.....T.....A...AT.G.......C..AT.-.G..CCAA...C..A.
A.sulcata            CGCGTGTGCTCTTGACTGAGTGTGCGCGGGAGTTGCGA-----------CG.....T.....A...-T.......T.C..A..-.G..-CAGC.....A.
P.tetraurelia        ---TTAGGGTTGCAGCTGGGCGAGTAG------------ACAA--------..........A...-T.......T.CC....-.G.T-C.TC..CG.A.
A.thaliana           CGCTCCTGGTCTTAATTGGCCGGGT-CGTGCCTCCGGCG----------CTG....T.....G...-T.........C..A..-....C.A.GCTC..G.
S.cerevisiae         ACCTTGAGTCCTTG--TGGCTCT-TG-GCGAACCAGGA-----------CT.....T.....A...-T.......T.C..A..-.G..G.AT....C.A.

                                                                         850                                          900
D.acuticephalum      TATCTAAGCATGGAATAATAGAATAAGAC-TTTTCTA--------TTGGTT-ACG-A-TAGTAAAAGTAATG-TTAACAGAGACAGCCGGGGGCATCCGT
D.orientale          .....C................A.....-......G---------.....T..C-.G..............A.............A.........T...
C.naikaiensis        ..ATAA.............G..GA.T...-C.GAG.CAACGTTTTGAACGCGGT.GCTGTTGCTCG..G...A..G.A..GA....G.........TT..
D.japonica           AT..GTT............GA.........-..CGG.TTTATTTTG......TT..-.AAC--TG........A....A.........-.........AT..
P.multitentaculata   C.GA.CTCG..CC......CA..A--....-..CnG.TCTATTTTG..-...TT..G.AC.--TG........A....G..G.....A.........T...
A.sulcata            ..CA...............G.....G...-..GGG.TCTATTTTG......TCT.G.ACC--TG........A....G..G.....TT........T...
P.tetraurelia        ..CA.T.............G.....G...-..GGG.C---TTTTG......TTA.G.C.----TG.......A....T..G.....AT........TA..
A.thaliana           ..CA.T.......G....C.TC...G..T-..CGA.CCTATTGTG....C.TCG.G.TC----GG.......A.......G.....T.........T...
S.cerevisiae         ...A.T..................G...G...GG.TCTATTTTG......TCTAGGACC---.TC.......A....T..G...G.T..........G..

                                                                         950                                         1000
D.acuticephalum      ATTGCTCCGTTATAGGTGAAATTCGTAGATCGGTGCAGGACGTA-CTACAGCGAA-GCATTTGCCAAC-ATGTTTTCATTAATCAAGAACGACAGTTGGA
D.orientale          .....A...C..G...........................A.-..........-..........G-..............................
C.naikaiensis        ......A.....G..........T.G.....TG...A...AA.-....T.....A...........GA..............................A..
D.japonica           ..GCTGGT.C..G..........TG...C.ATCAGCA....A.A....T.....A...........GA.............................CA..
P.multitentaculata   .....GGT.GG.G..........T.G....ATC...A..GCC--..........A...........GA.............................CA..
A.sulcata            ...-.GTT..C.G..........T.G...TTAC.A.A....A.-....T.....A...........GA..............................A..
P.tetraurelia        ...TAATT..C.G..........T.G...TTA.TA.A...TA.-..TAT.....A...........GG..............................A.G
A.thaliana           ...T.ATA..C.G..........T.G...TTA..A.A....A.-.A..T.....A...........GG................................G
S.cerevisiae         ...CAATT..C-C..........T.G...TTA.TG.A...TA.-....T.....A...........GG.C............................A.G
                                                                                 Primer 5,(6)
                                                                        1050                                         1100
D.acuticephalum      GTATCGAAGTCGATTAGATCTCGTCGTAGTTCCAACTATAAACGATGCCAACTAGCACTCCGCTGATAATATTTGGATACATTAGCGGGTGGCTTCCGGG
D.orientale          ................................................................A....G..--TTTG...........T.........
C.naikaiensis        ....TA...AG.......AC.C.....A...T...C......TT.A......TA.GA.TT.TCCC.GTCCC-.CTCG..TGGGCAA.AATTTAA.....
D.japonica           .G.......A....C....AC....C......TG..C......T......T..GA.GAGTTAGC..AGGATA..TA..CATC.T..TA.AA.TCA.....
P.multitentaculata   .GT......A....C....AC....C......TG..C................G...A....T..CG.T.GCGA.TTCGATCC.A....CA..C......
A.sulcata            .GC......A....C....AC....C.....AT...C............G.....GGA..A.AGAG.GT...-......GACC.CTTT..CAC...AG...
P.tetraurelia        .G...A...A....C....AC.........CTT..........T..A..G.....AG...G.AA.GGT.ATA-.ATTAGTCCCTTTC..CAT.G.AA.A.
A.thaliana           .GC......A....C....AC....C....CT....C............G..C..GGA..A..G...GT.GC..AT.GGAC.CC..T..CAC...AT.A.
S.cerevisiae         .G.......AT...C....AC.........CTT...C......T.....G....--GA..G.G..G.GT.T...TA..GACCC.CTC...AC...A..A.
```

```
                                                                1150                                                                1200
D.acuticephalum     AAACCAAAGTCTTTGGGTTCCGGGGGAAGT-ATGGTTGCAAAGCTGAAACTTAAAGGAATTGAC-GGAAGGGCACCACCAGGAGTGGAGCTTGCG-CTCA
D.orientale         ...............................-.......-.....................-.....-.............-......-....C....-..-.
C.naikaiensis       ..........T.A.T.................-..........ATC.....................-.....................C....-..T.
D.japonica          ............A.................G.....................................-.....................-...-C....--..T.
P.multitentaculata  ..............................-.....................................T....A....-...A...........C....G..T.
A.sulcata           ..........T........T......G...-.....................................-.....................C....-..T.
P.tetraurelia       ...T...............T.....G...-.....C....G.....................................-.....C....G..T.
A.thaliana          ...T......T..............G...-.....C....G.....................................-.....C....G..T.
S.cerevisiae        ...T................T.....G...-.....C....G.....................-.....................C....G..-.
                                                                                    Primer 7(8)

                                                                1250                                                                1300
D.acuticephalum     ATTTGACTCAACGCAGAAAAACTCACCCGGGCCGAACACAGTGAGGATTGACAGACTGATAGCTTTTTCTTGATACTGTGGGTAGTGGTGCATGGCCGTT
D.orientale         ............A.....................................................................................
C.naikaiensis       ............A.G.GG.........A..T..AG...TCT.A............TA.TATA.-C.C..A.A..CAGA....CG..............
D.japonica          ............A.G.G...TT..C.....T...G....T..............T........C.........T.G......G..............
P.multitentaculata  ............A.G.G.............C...G....T..............T...A....C.........T.G......G..............
A.sulcata           ............A.G.GG.........A..T..AG...T..GA............T...G....C.........T..A.....G..............
P.tetraurelia       ............A.G.GG.....T...A..T.AA....TG.ATG...........T...A....C.........T..A.....G..............
A.thaliana          ............A.G.GG.....T...A..T..AG...T...A..............G....C.........T..A.....G..............
S.cerevisiae        ............A.G.GG.........A..T..AG.....A.A............T...G....C.........TT.......G..............

                                                                1350                                                                1400
D.acuticephalum     -GTTGGTTGGTTGGAGTGATTTGTCTGGTTTATTCCGATAACGAACGAGACTCAGACTTACTTACTAGTCGTACGATTCTAGTTGT---------ACGAC
D.orientale         -.........-.........C.........A.......................AG.C...........T..TT....G.T.G.CG-------AT-.A..
C.naikaiensis       -C..A...A.-.........C.........A...................TCTT.G.CA.T.A.A...GAAAG.AG.A.CGAGGTA---TTGCAA.-AG.
D.japonica          -C..A.....-.....C.........A....A.....................TA....G..A.A....GTATTT...T..AC.CGTCAAATAAT-.AC.
P.multitentaculata  -C..A.....-.....C.............A.....................TAG.C....A.A....ACACTC..C.ATT.GTG--TGAGTGC-....
A.sulcata           -C..A.....-...................A......T.............CTTA..C.G..A.A....TACG.CCA..GC.A..G----GCAAC-TA..
P.tetraurelia       -C..A.....-...................A.....................CTTA..C.G..A......TTGCTTG.GAACAACAG------GTA-TA..
A.thaliana          -C..A.....-.....C.............A......T.............CTCAG.C.G..A.....CTACGT.GAGGC.TCCC.--TCACGGC-..G.
S.cerevisiae        TC.CA.....-................C..A...G...............CTTA..C....A.A....G..G.T.GCA.TTGCTG----GTTAT-.C..

                                                                1450                                                                1500
D.acuticephalum     TACTAAGAAGGATCAGTG---------TGAAAACACTTGAAAATGAGCAATAACAGGTCTGTGATTGCCCTTAGA-CGTTCGGGGC-GCACGCGTGCTAC
D.orientale         ...-T...G-.........----------.TT...ACAC.T.....................................-.....-.........T.A.....C.....
C.naikaiensis       .T..T...G.C.CTGT.CCGAATTTAAAT.CGGA.AGC...GTGAG.....................-..........-T....T..A.T.......C.....
D.japonica          .T..T.....A..A.A.A------GCG.CT.CGT.AA......A.....................-.....A....-T..C.....GC.......C.....
P.multitentaculata  .T..T..GG...CA....-----GCAT.C..GC..TAC.....................-..........-T..C......C.......C.....
A.sulcata           .T..T...G...CTGT..------GTG.TT..C..AAGTC.GGAAG.....................-..........-T....T....C.......C.....
P.tetraurelia       .T..T...G...CT.TGT-----ATGTAAGTGCATGGAAGTTTAAG.....................-.....C....-...C.T....C.......C.....
A.thaliana          .T..T...G...CT.TG.----CCGTT.AGGCCA.GGAAGTTTGAG.....................-..........-T....T....C.......C.....
S.cerevisiae        .T..T...G...CT.TC.----GTTTCAAGCCGATGGAAGTTTGAG.....................-..........A.....T....C.......C.....

                                                                1550                                                                1600
D.acuticephalum     AATGAAGAAAGCAGAGGG-------GGTTTTGCTTGGAAAAGCGAACTAAGCCT-TAAAATTTCTTCGTGGCAGGAATCGAGGCTTGTAATTATTCCTCG
D.orientale         ....G.........T...-------T..C.........C.....A.G..G.....-.....................A.....................
C.naikaiensis       .C..T.CTCTA.....T.-TGAAAAACC.AAT..A.AG.GGATTGGGA..T.ACAG..CGGAGAAATT.T.AG..G....T.CA.....C.T..G.A..
D.japonica          ....GCAGTTC..AC.A.--TAATACC..AAC..A.A..T..TTGGGC..T.T.G.G...CACTG....AA....G..T.T.AA..........T.A.A
P.multitentaculata  .C....T.GC.T.AC.A.--TTATTCTCC.GATCC.A..GG.TCGGGC..C.TGT.G...CC.A......A....G....G.............C..
A.sulcata           .C...C..TGT..AC.A.----TCTCTCC...GCC.A..GGT.TGGG...T.T.C.C...CA..G.....CTG..G..A..TCA...C....T..GA..T
P.tetraurelia       .C...CACGTT...C.A.CTTATTTACC.G.C.CGAA.GGGCACGGGA..T.T.G.T.GGACGTG.....CTG..G..A..TCT...C......AGA..T
A.thaliana          .C...T.T.TT..AC.A.----TTCACACC.TGCC.AC.GGC.CGGG...T.T.-.G.......A.....ATG..G..A..TCA...C....G..GG..T
S.cerevisiae        .C...C.G.GC...C.A.----TCTAACC...GCC.AG.GGT.TTGG...T.T.G.G...C.C.G.....CTG..G..A...CA..........G...T

                                                                1650                                                    1684
D.acuticephalum     TGCACAAGGAATTCCTAGTAATCGC-AGGTCATTAGCCTGCAATGATTACGTCCCTGCCCTTTGTACACACCGCCCGTCGCTAC
D.orientale         ......................-.....................................................................
C.naikaiensis       ..A..CC.........C....AT.G-.A....AC.A.T.CT.T.....................-.....................
D.japonica          ..A..G..............G...A.A...nnnnn.nnT..T.nnnnnnnnnnnnn.....................................
P.multitentaculata  ..A..G..............G...-.A.....A.A.T...GT.....................................................
A.sulcata           ..A..G..............G...-GA.....C...TC..GT.....................................................
P.tetraurelia       ..A..G..........T....G.A.-.......C......TGC...A.....................................C.
A.thaliana          .CA..G..............G...-GA.....C...TC..GT...C.....................................C.
S.cerevisiae        .CA..G..............G...-.A.....C...T...GT.....................................G
                                                                                    Primer(9)
```

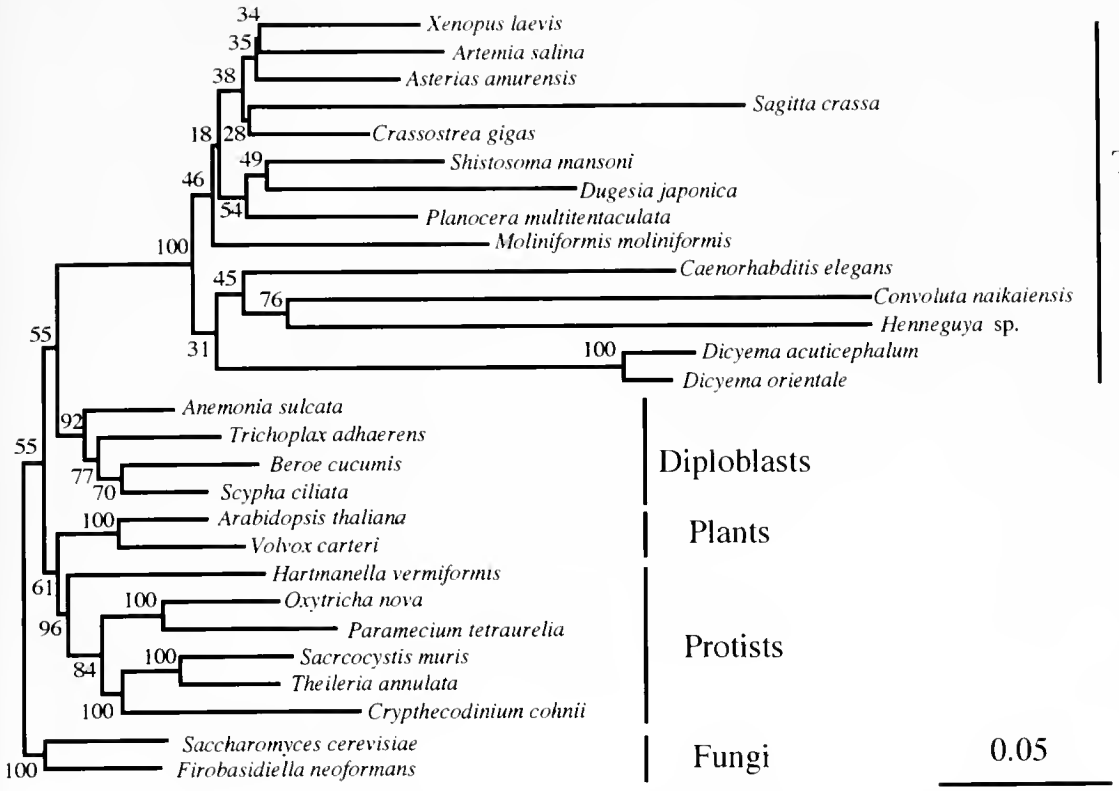

Figure 2. Neighbor-joining trees showing the phylogenetic position of the dicyemids among 28 representative eukaryotic taxa. The tree was reconstructed on the basis of the pairwise distances of Jukes and Cantor (1969) using DNADIST and NEIGHBOR programs (PHYLIP package, version 3.5c). The tree was rooted by using *Saccharomyces cerevisiae* as an outgroup. Branch lengths are proportional to the scale given in substitutions per sequence position. The percentage of 500 neighbor-joining bootstrap replicates is shown at the node the value is supporting.

diploblastic assemblage. This study does not support a close relationship between *Trichoplax* and mesozoans.

These sequence data do not firmly establish the position of the dicyemids within the triploblastic assemblage. In the phylogenetic trees obtained by three different methods, the dicyemids formed a monophyletic unit with the myxozoans, nematodes, and acoel flatworms. They are all considered to be early divergent groups in one widely accepted phylogeny. The early divergence of acoel flatworms in triploblastic evolution has been suggested by Katayama *et al.* (1993) from comparisons of partial 18S rDNA sequences. However, the myxozoans, dicyemids, nematodes, and acoel flatworms were all represented by a long branch in the phylogenetic trees (a high nucleotide substitution rate). Hence we cannot ignore the possibility that these long branches produce artifactual groupings within the triploblastic assemblage (Van de Peer *et al.*, 1993).

With regard to the topology of triploblast phyla, the present phylogenetic trees contradict those of some previous analyses of 18S rDNA sequences in some points. The Platyhelminthes did not form a monophyletic unit as previously shown by Katayama *et al.* (1993). Monophyly of the deuterostomes and the protostomes has repeatedly been shown in the molecular phylogeny of 18S rDNA (Wada and Satoh, 1994; Raff *et al.*, 1994; Halanych *et al.*, 1995), but neither group was monophyletic in all trees of the present analysis. Triploblastic phyla are poorly resolved in the molecular phylogenetic trees of 18S rDNA; *i.e.*, nodes defining phyla are not supported by high bootstrap values. Therefore, the topology of the trees depends largely on the choice of taxa. Philippe *et al.* (1994) have showed that by eliminating rapidly evolving species from the analysis, discrepancies between molecular and traditional phylogeny partly disappear and bootstrap values rise at some nodes. Since we only intended to show the placement of the dicyemids firmly within the triploblasts, we chose taxa representing a broad spectrum of eukaryote phyla without regard to consistency with the traditional view of triploblast phylogeny.

There have been opposing views on the role of the dicyemid mesozoa in the story of metazoan evolution. Some

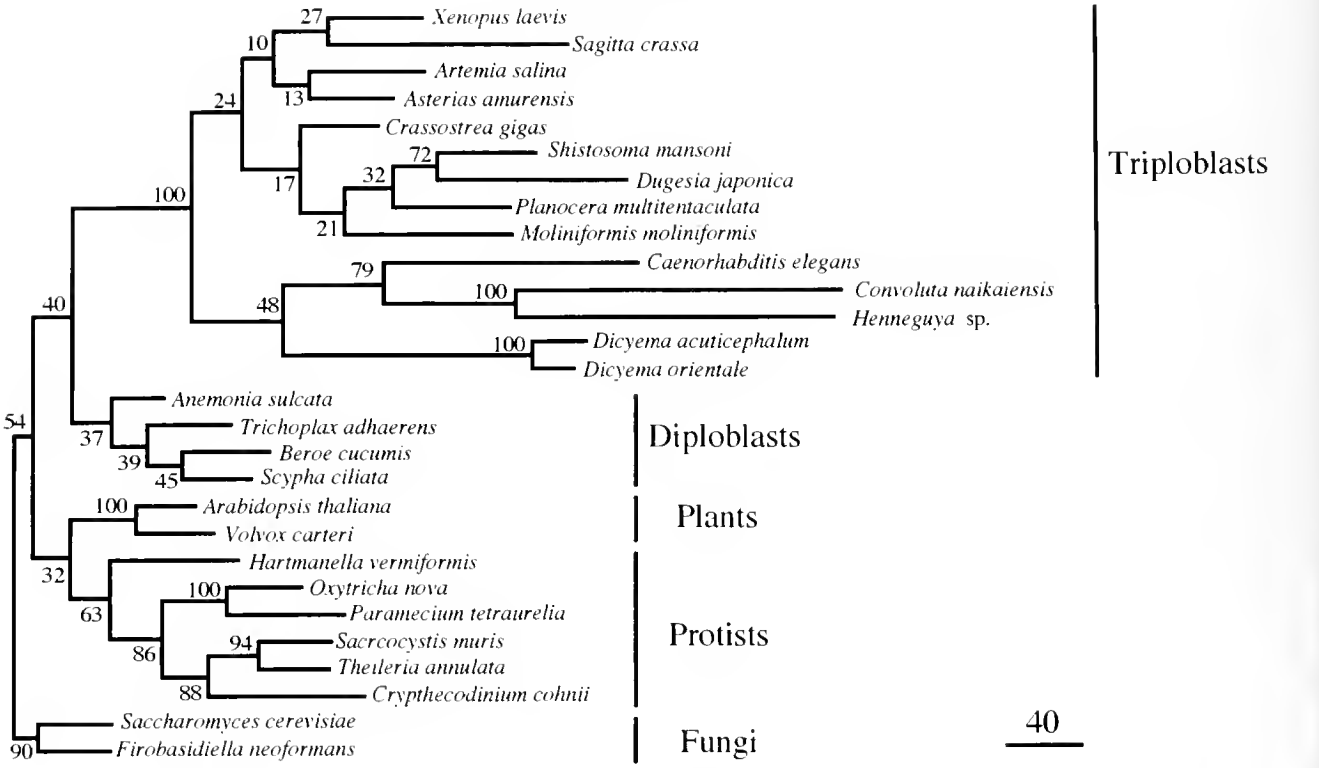

Figure 3. The consensus tree obtained using the maximum-parsimony algorithm with bootstrap resampling (DNAPARS, SEQBOOT, and CONSENSE programs of PHYLIP package, version 3.5c), showing the phylogenetic position of the dicyemids among 28 representative eukaryotic taxa. The percentage of 500 parsimony replicates is shown at the node the value is supporting. The tree was rooted by using *Saccharomyces cerevisiae* as an outgroup. Branch lengths are proportional to the scale given in number of substitutions (a total of 2807). This tree is different from the three most parsimonious trees in the positions of *Crassostrea gigas* and *Moliniformis moliniformis* within the assemblage of the coelomate triploblasts.

authors have proposed that the dicyemids are a missing link between unicellular organisms and multicellular animals (Dodson, 1956; Hyman, 1959; Lapan and Morowitz, 1974; Ohama *et al.*, 1984), while others have claimed that they are an animal group degenerated as a result of parasitism (Nouvel, 1948; McConnaughey, 1951; Stunkard, 1954; Ginetsinskaya, 1988). The phylogenetic trees inferred from comparisons of nucleotide sequences of 5S rRNA suggested that the dicyemids emerged first among the metazoa examined and that triclad flatworms, nematodes, enidarians, and sponges followed, in that order (Ohama *et al.*, 1984, Hori and Osawa, 1987). This suggestion does not, however, accord with the present result and the previous inferences about metazoan phylogeny based upon 18S and 28S rDNA sequences (Field *et al.*, 1988; Christen *et al.*, 1991; Wainright *et al.*, 1993; Kobayashi *et al.*, 1993). Discrepancies are partly ascribable to differences in the methods used to infer phylogenetic relationships. In contrast to the 18S and 28S rDNA trees reconstructed by the neighbor-joining, maximum-parsimony, and maximum-likelihood methods, the above 5S rRNA trees have been reconstructed by unweighted and weighted pair group methods using arithmetic averages (UPGMA and WPGMA, respectively), which are valid under the assumption that rates of nucleotide substitution are constant among taxa analyzed (Sokal and Mitchener, 1958). However, the essential point is that the 5S rRNA is too small to contain signal sufficient to allow precise inference of phylogenetic relationships. Because of large standard errors, sequential orders of branching of the dicyemids, flatworms, nematodes, enidarians, and sponges shown in the above 5S rRNA trees appear to be statistically insignificant. Recently Halanych (1991) analyzed the sequence data of 5S rRNA with the maximum-parsimony method. The phylogenetic tree obtained was inconsistent with phylogenies based on 18S and 28S rDNA data, and few nodes in the tree were supported by bootstrap value at a significant level.

The present results do not appear to support the proposition that the dicyemids are a truly primitive group linking unicellular organisms with multicellular metazoa. Instead, our results favor the view that the dicyemids are

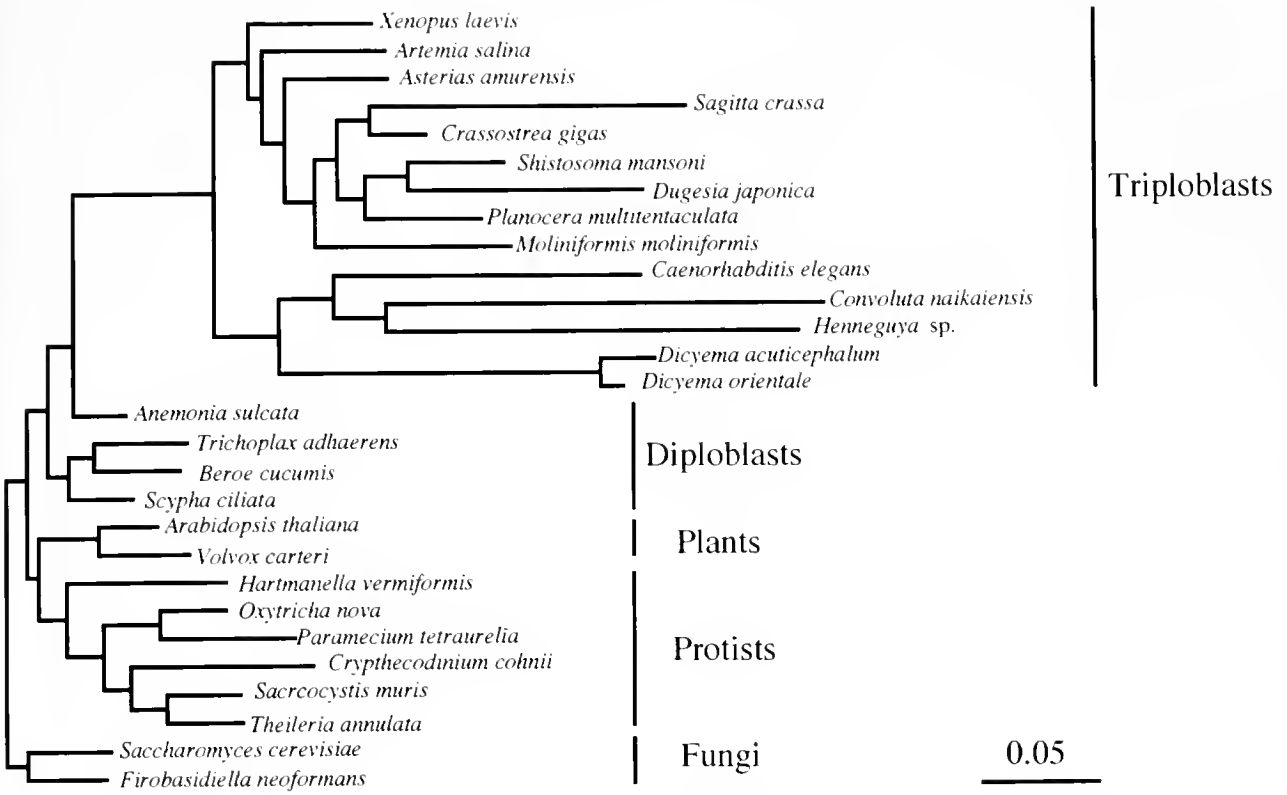

Figure 4. Maximum-likelihood tree showing the phylogenetic position of the dicyemids among 28 representative eukaryotic groups. The tree was obtained using the fastDNAML algorithm with a transition/transversion ratio of 1.48, which gave the best maximum-likelihood score (ln likelihood = −11909.45548). Branch lengths are proportional to the scale given in substitutions per sequence position. Because of the long computation time (more than 12 h per replication), bootstrapping was not performed.

degeneratively simple animals descended from a more complex triploblastic ancestor. Recent close observations of dicyemid development (Furuya *et al.*, 1992b, 1994) do not contradict the present inference; spiral cleavage, a determinative mode of cell division, and the formation of stereoblastula-like structure through epiboly, as seen in the development of vermiform and infusoriform embryos, are reminiscent of flatworms. Myxozoans are also regarded as an extreme example of the degeneration characteristic of parasitic evolution (Smother *et al.*, 1994). At present we can say little about the ancestor from which the dicyemids were derived. Molecular analyses that include other lower turbellarian groups (for example, the Catenulida and the Nemertodermatida) and the Orthonectida, a group tentatively included in the Mesozoa, will provide further information for understanding the phylogenetic position of the dicyemids.

Acknowledgments

We thank Dr. T. Miyata and Mr. N. Nikoh of Kyoto University for their kind help in reconstructing the phylogenetic trees. We also thank Dr. K. Tsuneki and Dr. Y. Koshida of Osaka University for their valuable suggestions. T. Katayama and H. Wada are supported by a JSPS (Japan Society for the Promotion of Science) Predoctoral Fellowship for Japanese Junior Scientists with Research Grant 0360 and 2447, respectively. H. Furuya is partly supported by a grant from Fujiwara Natural History Foundation.

Literature Cited

Brusca, R. C., and G. J. Brusca. 1990. *Invertebrates* Sinauer Assoc., Sunderland, Massachusetts. Pp. 171–178.

Christen, R., A. Ratto, A. Baroin, R. Perasso, K. G. Grell, and A. Adoutte. 1991. An analysis of the origin of metazoans, using comparisons of partial sequences of the 28S RNA, reveals an early emergence of triploblasts. *EMBO J* **10:** 499–503.

Dodson, E. O. 1956. A note on the systematic position of the Mesozoa. *Syst. Zool.* **5:** 37–40.

Felsenstein, J. 1981. Evolutionary trees from DNA sequences: a maximum likelihood approach. *J. Mol. Evol.* **17:** 368–376.

Felsenstein, J. 1985. Confidence limits on phylogenies; an approach using the bootstrap. *Evolution* **39:** 783–791.

Felsenstein, J. 1989. PHYLIP—phylogeny inference package (version 3.2). *Cladistics* **5:** 164–166.

Field, K. G., G. J. Olsen, D. J. Lane, S. T. Giovannoni, M. T. Ghieselin, E. C. Raff, N. R. Pace, and R. A. Raff. 1988. Molecular phylogeny of the animal kingdom. *Science* **239:** 748–753.

Fitch, W. M. 1971. Toward defining the course of evolution: minimum change for a specified tree topology. *Syst. Zool.* **20:** 406–416.

Furuya, H., K. Tsuneki, and Y. Koshida. 1992a. Two new species of the genus *Dicyema* (Mesozoa) from octopuses of Japan with notes on *D. misakiense* and *D. acuticephalum*. *Zool. Sci.* **9:** 423–437.

Furuya, H., K. Tsuneki, and Y. Koshida. 1992b. Development of the infusoriform embryo of *Dicyema japonicum* (Mesozoa: Dicyemidae). *Biol. Bull.* **183:** 248–257.

Furuya, H., K. Tsuneki, and Y. Koshida. 1994. The development of the vermiform embryos of two mesozoans, *Dicyema acuticephalum* and *Dicyema japonica*. *Zool. Sci.* **11:** 235–246.

Ginetsinskaya, T. A. 1988. *Trematodes, Their Life Cycles, Biology and Evolution.* Amerind Publishing Co. Pvt. Ltd., New Dehli. (Translation of the original Russian edition, 1968.)

Halanych, K. M. 1991. 5S ribosomal RNA sequences inappropriate for phylogenetic reconstruction. *Mol. Biol. Evol.* **8:** 249–253.

Halanych, K. M., J. D. Bacheller, A. M. A. Aguinaldo, S. M. Liva, D. M. Hills, and J. A. Lake. 1995. Evidence from 18S ribosomal DNA that the lophophorates are protostome animals. *Science* **267:** 1641–1643.

Hori, H., and S. Osawa. 1987. Origin and evolution of organisms as deduced from 5S ribosomal RNA sequences. *Mol. Biol. Evol.* **4:** 445–472.

Hyman, L. H. 1959. *The Invertebrates, Vol. V.* McGraw-Hill, New York. Pp. 323–365.

Jukes, T. H., and R. C. Cantor. 1969. Evolution of protein molecules. Pp. 21–132 in *Mammalian Protein Metabolism*, H. N. Munro, ed. Academic Press, New York.

Katayama, T., M. Yamamoto, H. Wada, and N. Satoh. 1993. Phylogenetic position of acoel turbellarians inferred from partial 18S rDNA sequences. *Zool. Sci.* **10:** 529–536.

Kobayashi, M., M. Takahashi, H. Wada, and N. Satoh. 1993. Molecular phylogeny inferred from sequences of small subunit ribosomal DNA, supports the monophyly of the metazoa. *Zool. Sci.* **10:** 827–833.

Lapan, E. A., and H. J. Morowitz. 1974. Characterization of mesozoan dispersal larva. *Exp. Cell Res.* **94:** 277–282.

McConnaughey, B. H. 1951. The life cycle of the dicyemid Mesozoa. *Univ. Calif. Publ. Zool.* **55:** 295–336.

Nouvel, H. 1948. Les Dicyémides. 2e partie: infusoriforme, teratologie, spécificité du parasitisme, affinités. *Arch. Biol.* **59:** 147–223.

Ohama T., T. Kumazaki, H. Hori, and S. Osawa. 1984. Evolution of multicellular animals as deduced from 5S rRNA sequences: a possible early emergence of the Mesozoa. *Nuc. Acid Res.* **12:** 5101–5108.

Olsen, G. J., H. Matsuda, H. Hagstrom, and R. Overbeek. 1993. FastDNAml: A tool for construction of phylogenetic trees of DNA sequences using maximum likelihood. *Comput. Appl. Biosci.* **10:** 41–48.

Philippe, H., A. Chenuli, and A. Adoutte. 1994. Can the Cambrian explosion be inferred through molecular phylogeny? *Development* **1994 (suppl.):** 15–25.

Raff, R. A., C. R. Marshall, and J. M. Tubereville. 1994. Using DNA sequences to unravel the Cambrian radiation of the animal phyla. *Annu. Rev. Ecol. Syst.* **25:** 351–375.

Saiki, R. K., D. H. Gelfand, S. Stoffel, S. J. Scharf, R. Higuchi, G. T. Horn, K. B. Mullis, and A. H. Erlich. 1988. Primer-directed enzymatic amplification of DNA with a thermostable DNA polymerase. *Science* **239:** 487–491.

Saitou, N., and M. Nei. 1987. The neighbor-joining method; a new method for reconstructing phylogenetic trees. *Mol. Biol. Evol.* **4:** 406–425.

Sanger, F., S. Nicklen, and A. R. Coulson. 1977. DNA sequencing with chain-terminating inhibitors. *Proc. Natl. Acad. Sci. USA* **74:** 5463–5467.

Smother, J. F., C. D. von Dohlen, L. H. Smith Jr., and R. D. Spal. 1994. Molecular evidence that the myxozoan protists are metazoans. *Science* **265:** 1719–1721.

Sokal, R. R., and C. D. Mitchener. 1958. A statistical method for evaluating systematic relationships. *Univ. Kans. Sci. Bull.* **28:** 1490–1438.

Stunkard, H. W. 1954. The life history and systematic relations of the mesozoa. *Q. Rev. Biol.* **29:** 230–244.

Van de Peer, Y., J-M. Neefs, P. De Rijk, and R. De Wachter. 1993. Reconstructing evolution from eukaryotic small-ribosomal-subunit RNA sequences: Calibration of the molecular clock. *J. Mol. Evol.* **37:** 221–232.

Wada, H., K. W. Makabe, M. Nakauchi, and N. Satoh. 1992. Phylogenetic relationships between solitary and colonial ascidians, as inferred from the sequence of the central region of their respective 18S rDNAs. *Biol. Bull.* **183:** 448–455.

Wada, H., and N. Satoh. 1994. Details of the evolutionary history from invertebrates to vertebrates, as deduced from the sequences of 18S rDNA. *Proc. Natl. Acad. Sci. USA* **91:** 1801–1804.

Wainright, P. O., G. Hinkle, M. L. Sogin, and S. K. Stickel. 1993. Monophyletic origins of the metazoa: an evolutionary link with fungi. *Science* **260:** 340–342.

Willmer, P. 1990. *Invertebrate Relationships.* Cambridge Univ. Press, Cambridge.

Reference: *Biol. Bull.* **189**: 91–105. (October/November, 1995)

The Incidence and Morphology of Subcuticular Bacteria in the Echinoderm Fauna of New Zealand

MAEVE S. KELLY[1], M. F. BARKER[2], J. DOUGLAS McKENZIE[1,*], AND JAN POWELL[3,‡]

[1]*The Scottish Association for Marine Science, PO Box 3, Oban, Argyll, Scotland,*
[2]*Departments of Marine Science and Zoology and* [3]*Department of Microbiology, University of Otago, Dunedin, New Zealand*

Abstract. New Zealand echinoderms (33 species drawn from all five extant classes) were examined for the presence of symbiotic bacteria by fluorescence and electron microscopy. Gram-negative, subcuticular bacteria (SCB) were found in 17 species from four classes. The SCB could be classified into two major morphological types. Some species had both types of SCB. The distribution of SCB was not obviously linked to host ecology but did appear to be related to host phylogeny. Related species usually all have SCB or all lack them. The number of SCB in five species was estimated to be between 8.41×10^8 and 4.96×10^9 g^{-1} ash-free dry weight of host tissue. Significant differences in bacterial load and relative proportions of the different types of bacteria were found among three congeneric echinoids (*Pseudechinus huttoni, P. albocinctus* and *P. novaezealandia*). *Ophiocoma bollonsi* was peculiar in having groups of bacteria enclosed in host cells (bacteriocytes) within the connective tissue of the tube feet.

Introduction

Symbiotic associations are increasingly seen as pathways for evolutionary innovation, allowing organisms to transcend the biochemical limitations of their own genome by harnessing the different biochemical capabilities of a symbiont (Margulis, 1981; Douglas, 1994). Examples of marine organisms utilizing symbionts to exploit otherwise closed energy sources include corals that use dinoflagellates to provide them with carbon fixed *via* photosynthesis (Muscatine *et al.*, 1984) and a variety of marine invertebrates that exploit the energy potential of free sulfide through the activities of sulfide-oxidizing bacteria (*e.g.*, Cavanaugh *et al.*, 1981). Symbioses between invertebrates and bacteria occur in protozoans (Fenchel *et al.*, 1977; Saffo, 1990); sponges (Vacelet and Donadey, 1977); cnidarians (Palincsar *et al.*, 1989); nematodes and turbellarians (Ott *et al.*, 1982); annelids (Giere, 1981; Hausmann, 1982); pogonophorans (Cavanaugh *et al.*, 1981); echiurans (Bosch, 1976); bivalve molluscs (Southward, 1986); cephalopods (McFall-Ngai, 1994); bryozoans (Lutaud, 1969); echinoderms (Holland and Nealson, 1978); tunicates (Mackie and Bone, 1978); and pterobranchs (Welsch, 1984). New symbioses are frequently reported (*e.g.*, Menon and Arp, 1993; Haszprunar *et al.*, in press). In some cases the biological role of the symbionts is obvious (*e.g.*, chemoautotrophic associations where the host lacks a gut), but in most it is enigmatic.

Echinoderms from all five extant classes are known to harbor symbiotic bacteria between the epidermal cells and the overlying layers of the cuticle (Holland and Nealson, 1978; Féral, 1980; McKenzie, 1987). These so-called subcuticular bacteria, or SCB (Holland and Nealson, 1978), have been recorded from Atlantic species of echinoderms (Holland and Nealson, 1978; Féral, 1980; McKenzie, 1987; Walker and Lesser, 1989; McKenzie and Kelly, 1994), from Australian crinoids (McKenzie, 1992), and from northeast Pacific ophiuroids (McKenzie and Kelly, 1994). The symbiosis is, therefore, geographically and phylogenetically widespread. Information on the exact distribution of SCB amongst echinoderms is, however, very vague. Some species are known to lack SCB (McKenzie and Kelly, 1994), and it may be possible to correlate the presence or absence of SCB with some common aspect of their hosts' biology if there is a large enough data set upon which to make such a comparison. The morphology of bacteria can also be useful in determining the probable trophic role of the symbionts. Likewise, a

Received 15 August 1994; accepted 25 July 1995.

* Author to whom correspondence should be addressed.

‡ Current address: Division of Infectious Diseases, University of Maryland School of Medicine, Baltimore, Maryland 21201.

high ratio of symbiont-to-host biomass may help identify particularly important associations. To this end we have been surveying a large number of echinoderm species from around the world for the presence, abundance, and morphology of SCB. This paper details the results of a study of 33 species of echinoderms that are found around New Zealand. Some preliminary results of this study were reported in Kelly *et al.* (in press).

Materials and Methods

Echinoderms were collected between October 1992 and January 1993, by beam trawl on the mid-shelf region off Otago harbor at a depth of 64 m (45°46.632′ 170°52.881′) and at a deeper water site of 120 m (45°44.539′ 171°01.197′), and by shore collections from the intertidal zone adjacent to Portobello Marine Laboratory. Some species were also collected from the intertidal zone at Matheson Rocks, north of Auckland, North Island. Animals were examined with epifluorescence light microscopy and tissues promptly fixed for transmission electron microscopy (TEM).

The epifluorescent microscopy was according to Hobbie *et al.* (1977) as adapted by Kelly and McKenzie (1992). A tube foot was removed, placed on a glass slide, stained with acridine orange at a concentration of 0.003% and gently squashed with the coverslip. This action frees many of the SCB from the tissue. Usually, 3–10 individuals of each species were examined for the presence of SCB. The bacterial load was quantified in three species of *Pseudechinus;* in *Asterodon miliaris, Ophiocoma bollonsi,* and *Amphipholis squamata;* and in juvenile *Pseudechinus huttoni* (diameters of 14–18 mm). Rods and spirals were counted separately for the three species of *Pseudechinus* and for the juvenile *P. huttoni.*

For direct counts of bacterial numbers, larger pieces of tissue were removed from the seven species mentioned above and homogenized with either a hand-held glass tissue grinder or an Ultraturrex mechanical tissue homogenizer. For ophiuroids, a piece of arm was used; for echinoids, a portion of test was taken from the ambulacral groove area. Care was taken not to rupture the gut as the test was removed. The tissue was homogenized at a ratio of 1 g tissue: 2 ml of filtered (0.1 μm) seawater and then mixed with an equal volume of acridine orange. An exact volume of the homogenate (5 μl) was slide-mounted using No. 1 22 × 22 mm coverslips. In each homogenate, all the bacteria observed within an eyepiece-mounted Whipple grid (at 1000× magnification) were counted from 20 randomly selected areas. The whole process was repeated twice for each of 10 animals. Because individual *Amphipholis squamata* are small, homogenates were made from pooled individuals (one of 8 and one of 11 individuals). To check the accuracy of the counting technique, 10 counts were made from one homogenate of *P. huttoni* test. External or contaminant bacteria, which were only rarely seen, differed obviously in size and appearance from the SCB. The number of SCB was expressed per gram of tissue wet weight and per gram of ash-free dry weight, to allow a comparison between species with different ratios of soft tissue to skeletal calcite. For wet weights, tissue samples were rinsed in filtered (0.1 μm) seawater, shaken to remove excess surface water, and then weighed. For dry weights, tissues were dried at 40°C until they reached a constant weight. Ash weights were obtained after tissues were incinerated in a muffle furnace at 400°C. Ash-free dry weights were obtained by subtracting the ash weight from the dry weight for each sample. Microscopical observations and counts of the bacteria were made with an Olympus Vanox epifluorescence microscope.

In preparation for TEM, tissues from three individuals of each species (where available) were fixed in 4% glutaraldehyde in 0.1 *M* cacodylate buffer, rinsed in fresh buffer and decalcified, if necessary, in saturated EDTA. Postfixation was with 1% osmium tetroxide in filtered seawater, followed by dehydration in ethanol and embedding in Agar 100 resin. Silver sections were cut on an LKB III microtome, stained with ethanoic uranyl acetate and aqueous Reynold's lead citrate, and examined on a JEOL 100S at 60 Kv.

Attempts were made to culture symbionts from the ophiuroids *A. squamata* and *Ophiocoma bollonsi* and the echinoid *Pseudechinus huttoni.* The experimental procedures for *A. squamata* were (a) that of Walker and Lesser (1989)—surface sterilization of whole animals in 70% isopropyl alcohol for 30 s followed by two rinses in 75% sterile artificial seawater (ASW) prior to homogenization in sterile glassware and plating on agar; (b) a modified procedure (Lesser, pers. comm) as above but with surface sterilization time reduced to 5 s; and (c) an alternative method using protocol *b* but separating the arms from the disk of the animals before homogenization. For *O. bollonsi,* only tissue from the arm was used; a portion of the arm was surface sterilized and then the tube feet were removed and homogenized. The homogenate was then spread on plates or used to inoculate liquid culture medium. For *P. huttoni,* small squares of test from the ambulacral groove were surface sterilized and treated as above. Animals that had not been subjected to the surface sterilization procedures were used as controls. The brittlestar *Ophionereis fasciata,* which does not have SCB, was used as a further control. The tube feet or portions of tissue were placed in a watch glass and ground with a glass grinder. The glassware was surface sterilized with 70% ethanol. Marine broth (Difco, 300 μl) was used as a diluent.

Ultraviolet (UV) exposure and repeated washing in autoclaved filtered seawater were investigated as alternative methods for surface sterilization. Tube feet from *O. bollonsi* and arms from *A. squamata* were exposed to UV

for 2, 5, 10, and 15 min prior to homogenization in 300 μl diluent. Whole *A. squamata* and squares of the test of *P. huttoni* were washed up to five times in autoclaved filtered seawater. Homogenates were made of the *A. squamata* arms and of the squares of urchin test. The homogenates were prepared in 300 l diluent, then plated on agar and inoculated in broth as outlined below. Equivalent untreated tissues were used for controls.

The medium used was Zobell's modified 2216E prepared with 75% (w/v) ASW. Salt solutions (1 *M*) for the ASW were prepared and autoclaved. The agar was then prepared, the yeast and peptone were added, and the agar was autoclaved and held at 56°C. To prevent precipitation of the sterile salt solutions, they were warmed and added to the agar before the plates were poured. To determine the number of colony-forming units (CFU) per animal, logarithmic dilutions were prepared in marine broth and spread plated. The dilution broths were also cultured as enrichment for slow-growing or stressed organisms unable to grow initially on solid medium. The plates were incubated at room temperature (18–21°C) and examined daily for bacterial growth. After 48 h, the resulting bacterial colonies were counted and CFU per sample were determined. The plates were then maintained for up to 21 days to observe the appearance of any slower growing colonies.

Results

General observations

Table I shows the number of species within each class that were examined and the number and percentage that were found to harbor SCB. Of the 33 species of New Zealand echinoderms examined, 17 had SCB (Table II). When the SCB load was substantial, the bacteria were easy to find with epifluorescence. However, in some cases, TEM examination demonstrated SCB that had escaped detection by epifluorescence.

Table I

Number of species examined and number and percentage with SCB

Class	Number of species	Number (%) with SCB
Echinoidea	7	5 (71)
Ophiuroidea	9	5 (56)
Asteroidea	14	5 (36)
Holothuroidea	2	2 (100)
Crinoidea	1	0 (0)
Total	33	17 (51.5)

Bacterial morphology

In all of the echinoderms examined, the SCB appeared to be gram-negative as they had two membranes (Figs. 4, 11) surrounding the cytosol (Neidhart *et al.*, 1990). The periplasmic layer between the two membranes was usually thin and homogeneous. None of the bacteria appeared flagellated, nor were pili observed. The cytosol usually evenly surrounded the nucleoid area and was usually rather homogeneous, with no evidence of either internal membranes (other than membrane-bound vacuoles) or granular inclusions. Round spaces in the cytosol, indicating where material had been lost during processing, were not infrequent and may be poly-β-hydroxybutyrate storage areas (Berkeley, 1979). The DNA in the nucleoid was often condensed into an electron-dense lobulated structure (Fig. 3), but in some SCB it was much more diffuse (Fig. 5).

The SCB from the New Zealand species of echinoderms were more variable in their morphology than those previously encountered. McKenzie and Kelly (1994) described three morphological types of bacteria from ophiuroids (Types 1–3). Type 1 SCB are short rods that characteristically occur as paired bacteria within a single, complex capsule. This type has been found only in species of *Ophiothrix*, although another brittlestar, *Ophiopholis aculeata*, has SCB that are intermediate between Type 1 and Type 3 SCB. SCB of Type 2 were the most common. They are long, thin (0.1–0.2 μm), often electron-dense rods with little evident ultrastructure. They lack capsules and rarely have vacuoles. They are usually spirals, but vary from perfectly straight rods through spirals with long wave-lengths (Figs. 5, 7A) to tightly kinked spirals with short wave-lengths (Fig. 9). Type 3 SCB are straight, broad (0.2–0.5 μm) rods, often with capsules and characteristically with vacuoles, though these are not always present. The New Zealand species could be further categorized into three subdivisions of Type 3 SCB. The first subtype is the "classic" Type 3 as described by McKenzie and Kelly (1994). The second subtype differs in having far more vacuoles than normally encountered in Type 3 SCB. This subtype was found in *Ophiomyxa brevimira* (Fig. 10) and *Stichopus mollis* (Fig. 2). The third subtype was found in the three species of *Pseudechinus*. It was a straight, baton-shaped rod with a well-defined, granular periplasmic layer and no obvious vacuoles (Fig. 3).

In some species, more than one type of SCB was found within a single host. Fixation artifact or pathology can, however, result in Type 2 SCB resembling Type 3 SCB, and care has to be taken not to confuse such artifacts with genuine Type 3 SCB. Bacteria appear to swell in fixation, causing the membranes to become more distinct and space to appear around the chromatin (Fig. 7B). The shape of the bacterium can become more rounded and eventually irregular. In severe cases, the chromatin is isolated in the center of the bacterium and the cell membranes are greatly disrupted. Such bacteria can be mistaken for poorly fixed host microvilli or blebbed pieces of epidermal tissue.

Table II

Observation and description of SCB as seen under epifluorescent (EF) and transmission electron microscopy (TEM)

CLASS Order Family	Species and authority*	SCB EF/TEM†	SCB Description‡
CRINOIDEA			
Comatulida			
Comasteridae	*Comanthus novazealandiae*[2] Clark	n/n	Some bacteria found on surface not SCB, TEM only.
HOLOTHUROIDEA			
Aspidochirotida			
Stichopodidae	*Stichopus mollis* (Hutton)	n/y	Short rods, T3.
Apodida			
Chiridotidae	*Trochodota dunedinensis* (Parker)	n/y	Short, electron dense rods, T?
ECHINOIDEA			
Cidaroida			
Cidaroidae	*Gonocidaris umbraculum*[3] (Hutton)	y/y	Short rods, 1–2 μm, T3
Echinacea			
Temnopleuridae	*Pseudechinus huttoni* Benham	y/y	Rods 2–3 μm and spirals, spirals can be >10 μm, T2 & T3.
	Pseudechinus novaezealandiae (Mortensen)	y/y	Rods and spirals, spirals can be >10 μm, T2 & T3.
	Pseudechinus albocinctus (Hutton)	y/y	Rods and spirals, spirals can be >10 μm, T2 & T3.
Echinometridae	*Evechinus chloroticus* (Valenciennes)	n/n	
Clypeasteroida			
Arachnoidae	*Fellaster zelandiae*[3N] (Gray)	y/y	Spirals, difficult to find T2.
Spatangoida			
Lovenidae	*Echinocardium cordatum*[N] (Pennant)	n/–	TEM specimens poorly fixed.
ASTEROIDEA			
Paxillosida			
Asteropectinidae	*Astropecten prinugenus* (Mortensen)	y/y	Short rods, 2–3 μm and spirals, T2.
	Astropecten polyacanthus[1] Muller & Troschel	n/n	Cuticle not preserved.
Valvatida			
Asterinidae	*Patiriella regularis* Verrill	y/y	Spirals 5–8 μm, T2.
Goniasteridae	*Pentagonaster pulchellus* Gray	n/–	
Odontasteridae	*Asterodon miliaris* (Gray)	y/y	Rods 3 μm, sometimes in short chains of 2–3. Spirals seen only with TEM, T2 & T3.
	Odontaster benhami (Mortensen)	y/y	Straight rods, 10 μm and spirals 10 μm, T2 & T3.
Ophidiasteridae	*Ophidiaster kermadecensis*[1N]	n/y	Rods with vacuoles and coats, T3?
Spinulosida			
Echinasteridae	*Henricia ralphae* Fell	n/n	
Forcipulatida			
Asteriidae	*Sclerasterias mollis* (Hutton)	n/n	
	Coscinasterias calamaria (Gray)	n/n	
	Allostichaster insignis (Farquhar)	n/n	
	Allostichaster polyplax (Muller & Troschel)	n/n	
	Astrostole scabra[1] (Hutton)	n/n	
	Calvasterias suteri (de Loriol)	n/–	
OPHIUROIDEA			
Phrynophiurida			
Asteroschematidae	*Astrobrachion constrictum*[2] (Farquhar)	n/y	Spirals, T2.
Ophiomyxidae	*Ophiomyxa brevirima* Clark	y/y	Short rods, occasional spirals. Only T3 with TEM.
Ophiurida			
Amphiuridae	*Amphipholis squamata* Delle Chiaje	y/y	Long rods 3–4 μm, shorter fat rods (2 μm) often in chains of 2, T3
	Amphiura abernethyi[1] Fell	y/–	Rods 4–5 μm EF only
	Amphiura amokurae Mortensen	y/y	Spirals 6–8 μm, T2. Unusually broad, 0.25–0.30 μm.
Ophiocomidae	*Ophiocoma bolloni* Farquhar	y/B	5 μm thin rods seen with EF, sometimes faint, bacteriocytes with TEM.
	Ophiopteris antipodum Smith	y/n	5 μm rods seen with EF, sometimes faint
Ophiodermatidae	*Pectinura maculata* (Verill)	n/n	
Ophionereidae	*Ophionereis fasciata* (Hutton)	n/n	

* 1, 2, or 3 = number of specimens available if 3 or less; N = collected from North Island

† y = seen; n = not seen, – = no sample; B = bacteriocyte.

‡ T2 = Type 2 SCB; T3 = Type 3 SCB. Lengths are from epifluorescence measurements.

Occurrence within class

Crinoidea: Examination of the pinnules of *Comanthus novaezealandiae* by epifluorescent microscopy revealed no evidence of SCB. A few large bacteria were found in TEM sections, but these were outside the cuticle and were not considered to be invasive or to be any type of SCB. The same type of bacteria were found in both specimens examined, collected at the same time and location.

Holothuroidea: The apodous holothurian *Trochodota dunedinensis* appeared to have an unusual form of SCB

that could not be easily classified as belonging to any of the major types of SCB (Fig. 1). These were uncommon and had an electron-dense, filamentous appearance. SCB of a similar morphology have been found in *Labidoplax digitata*, another apodous holothurian (Kelly and McKenzie, 1995). SCB were commonly present in TEM sections of the aspidochirote holothurian *Stichopus mollis*, although none had been found previously with epifluorescence. These short rods had numerous vacuoles (Fig. 2).

Echinoidea: SCB, in the form of short rods, were found in *Goniocidaris umbraculum*, a representative of the primitive subclass Perischoechinoidea. SCB were easily found by epifluorescence in all the specimens that were examined. TEM fixation of both the host cytoplasm and bacteria was poor, but the symbionts appeared to be Type 3 SCB, with internal vacuoles. The material in these vacuoles was often lost, forming a hole in the section.

SCB were found in all three species of the genus *Pseudechinus*. Each had two distinct morphological types of bacteria: straight, baton-shaped rods (Fig. 3) and a typical Type 2 spiral form (Fig. 4). Both forms could be seen with epifluorescence and TEM. The SCB were found lying both below and within the fibrous layer of the cuticle. In both types of SCB the chromatin was usually condensed into thick, electron-dense fibers running up the center of the bacteria. The baton-shaped rods had the appearance of being rigid and had rounded caps at either end of the baton (Fig. 3), rather than tapering at their ends. The most striking feature of this type of SCB was the well-defined, granular periplasmic space. The three species of *Pseudechinus* were collected throughout the austral summer months, and SCB were always present regardless of the reproductive condition or size of the host. The smallest *P. huttoni* collected had a diameter of 14 mm and was probably less than 2 years old.

Detection of SCB by epifluorescence microscopy of tube feet from the sand dollar *Fellaster zelandiae* was difficult. A few irregular rods were seen, but the fluorescence faded unusually quickly. The same dampening effect has been noted when examining some other echinoids (for example, *Evechinus chloroticus*) and some darkly pigmented ophiuroids. TEM showed that the symbionts in *F. zelandiae* were spiral Type 2 SCB, though few were seen.

No SCB were found in specimens of *Echinocardium cordatum* with either technique. None of the specimens of *E. cordatum* fixed for TEM had retained their cuticles, and their morphology was also poorly preserved.

Asteroidea: With epifluorescence, SCB were difficult to find in *Astropecten primigenius*. In only one specimen were a few rods and spirals observed. In contrast, TEM of this species revealed that typical Type 2 SCB were common in the fibrous part of the cuticle (Fig. 5), where they sometimes appeared to be aligned parallel to the fibers of the lower cuticle. Larger, misshapen bacteria, which were probably distorted Type 2 SCB, were also seen. No SCB were found in the single specimen of *A. polyacanthus* from Auckland. The cuticle was not intact in this specimen.

In the cushion star *Patiriella regularis*, abundant spiral-shaped SCB with little internal specialization were found with epifluorescence, and TEM revealed Type 2 SCB in the lower, fibrous part of the cuticle. *Asterodon miliaris* and *Odontaster benhami* are biscuit stars that are extremely difficult to tell apart, being identifiable by the number of projections on the oral plates (Fell, 1962). Even so, the two species were readily distinguished on the basis of their SCB. With epifluorescent microscopy (Fig. 6A), *A. miliaris* had mostly straight, brightly fluorescing rods, forming short chains of 2–3 cells; whereas *O. benhami* had a mixture of two morphological types. TEM showed, however, that *A. miliaris* did have both Type 3 and Type 2 SCB, though the latter were much less common than they were in *O. benhami*. The Type 3 SCB in *O. benhami* were often dumb-bell shaped (Fig. 6B). In the one specimen of *Ophidiaster kermadecensis* that was examined, no SCB were found with epifluorescence microscopy. A few Type 3 rods with vacuoles and well-developed capsules were found amongst the microvilli in TEM sections. These were probably SCB but, as the specimen lacked its cuticle, this requires confirmation. The remaining seastar of the Order Valvatida, *Pentagonaster pulchellus*, was examined only by epifluorescent microscopy and no SCB were noted.

No SCB were found in *Henricia* or in any of the seastars belonging to the order Forcipulatida with either epifluorescence or TEM. Rod-shaped bacteria were commonly found in TEM sections of a single specimen of *Calvasterias suteri;* however, the tissues were considerably disrupted and bacteria were found throughout the sections, including in connective tissue. These bacteria are probably not SCB and may be pathogenic, but further study will be necessary to confirm this. A single bacterium was found embedded in an indentation of the outermost layer of the cuticle of a specimen of *Sclerasterias mollis*. This was not thought to be an SCB.

Ophiuroidea: Many SCB were found in TEM examination of decalcified arm tips from *Astrobrachion constrictum* (Fig. 7A). They were spirals but were occasionally seen to vary in cross-sectional area (Fig. 7B). The larger types are probably an artifact resulting from the swelling of the more commonly seen form. However, no bacteria were found when the tube feet were examined with epifluorescence. The small amount of soft tissue on the arms and the small tube feet make epifluorescent examination of tissue squashes difficult, whereas the SCB are found more easily with TEM after decalcification.

Numerous thin, rod-shaped bacteria were found in tube-foot squash preparations from *Ophiocoma bollonsi* and *Ophiopteris antipodum*. The fluorescence faded very rapidly in homogenates of the tissue of these species,

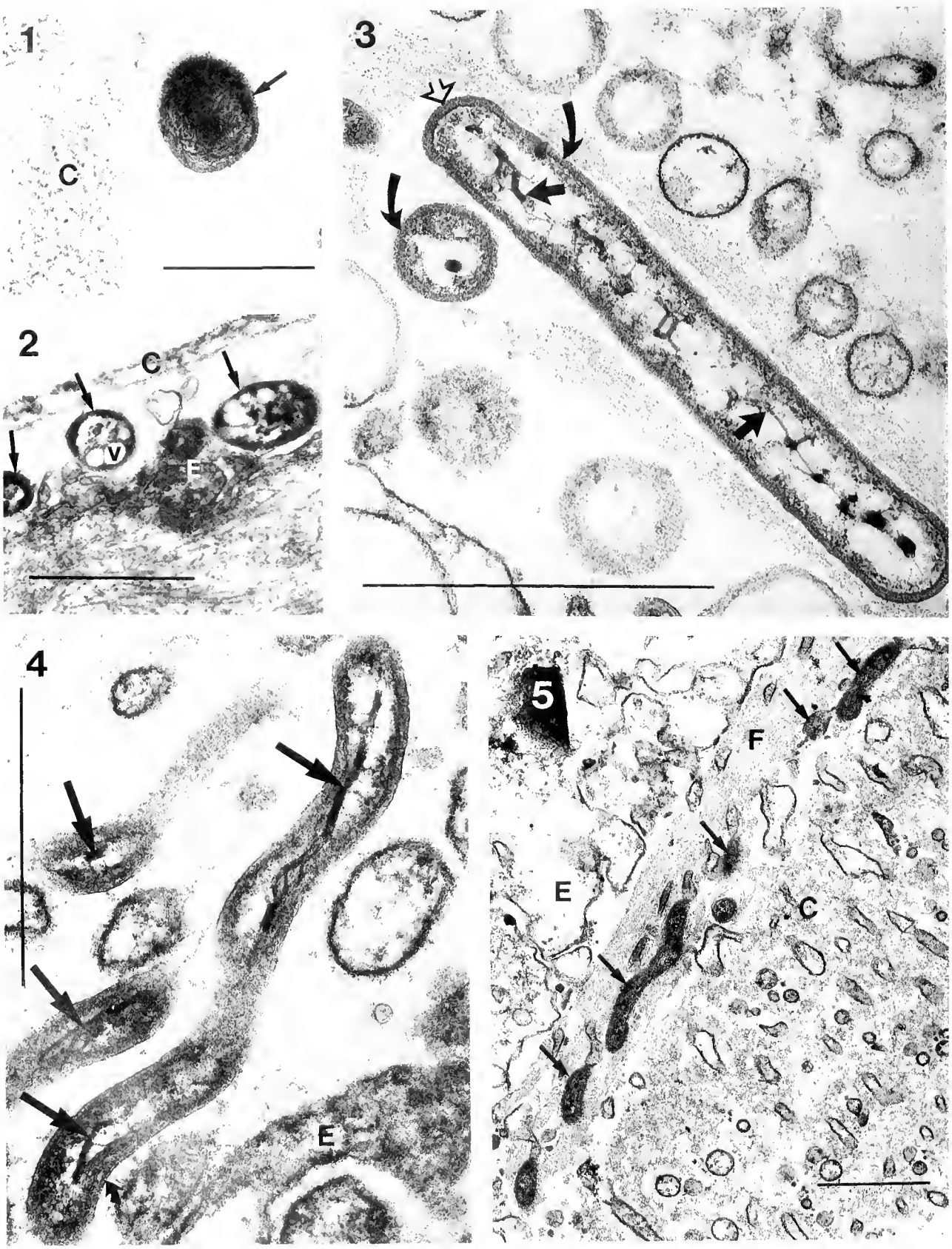

Figures 1–5. Scale bars represent 1 μm

making counting difficult. Despite intensive searching with TEM, no SCB were ever found lying in the subcuticular space of either species, although the bacteria were always found in tube foot squash preparations with epifluorescent microscopy. This initially led to the assumption that the bacteria were in discrete areas of the subcuticular space and might have been missed during TEM examination. However, large bacteriocytes packed with long, spiral-shaped bacteria were later found in the connective tissue of *O. bollonsi* (Fig. 8). The bacteriocytes were about 10 μm diameter in TEM micrographs. Occasionally the spiral bacteria were seen free in the tissue. *Ophiomyxa brevirnira* had a mixture of morphological types of SCB: short rods, often forming chains of two; longer rods; and a few spiral forms were seen with epifluorescence. With TEM, short, heavily vacuolated Type 3 rods were found to be the predominant type. Holes often formed in the sections where there were vacuoles (Fig. 10).

Two species of *Amphiura* were examined. *A. amokurae* was very common under stones along the beach adjacent to the Portobello laboratory. One specimen of *A. abernethyi* was obtained by trawl from a depth of 120 m outside Otago Harbor. *A. amokurae* had long, tightly bound, spiral SCB that were obvious in both epifluorescence and electron microscopy (Fig. 9). These had an unusually large diameter for Type 2 SCB. In *A. abernethyi*, straight rods, 4–5 μm long, were seen with epifluorescence, but the only available specimen was in poor condition when fixed for TEM, and no cuticle or bacteria could be found around the surface. *Amphipholis squamata* had long, vacuolated, rod-shaped bacteria (Fig. 11). These were very common and were easily seen with both electron and light microscopy.

Quantification

The results of the quantification of bacterial load for all three species of *Pseudechinus*, *Asterodon miliaris*, *Ophiocoma bollonsi*, *Amphipholis squamata*, and juvenile *Pseudechinus huttoni* (test diameters of 14–18 mm) are given in Table III. No significant differences were found between arms or ambulacral areas from the same individual animal for any of the species (Student's *t* and Wilcoxon signed rank test). To measure the variability of the counting technique, 10 counts were made from one homogenate of *P. huttoni* test. The mean count per 20 fields of view was 17.9, with a standard deviation of 4.63. Rods and spirals were also counted separately for the three species of *Pseudechinus* and for juvenile *P. huttoni*. A one-way analysis of variance (ANOVA) and a Fisher's least significant difference test (LSD) was then applied to the data (Table IV). *P. huttoni* adults and juveniles both had greater numbers of rods than spirals ($P < 0.05$). The other two species had more spirals than rods, though these differences were not significant. As can be seen from Table IV, there are numerous significant differences between the species in their relative numbers of rods and spirals.

Culturing

The methods described in Walker and Lesser (1989) and Lesser and Blakemore (1990) (*i.e.*, plating the homogenates of *A. squamata* following a surface sterilization in 70% isopropyl alcohol for 30 s), failed to produce bacterial colonies on agar plates. However, when whole animals were treated for only 5 s, prior to separate homogenization of arms and disks, bacterial colonies grew on plates inoculated from homogenates of the disks (1.5×10^2 mixed CFU/disk) but not from the arms. This compares with 2.6×10^4 and 2.6×10^3 CFU for control (not surface sterilized) arms and disks respectively. Although the plates were examined daily, no fresh colonies appeared in a 10–14 day period as described by Lesser and Blakemore (1990) or after 14–21 days as described by Lesser (pers. comm. to MSK).

The other species produced results similar to those obtained from *A. squamata*. The surface sterilization for 5 s usually resulted in no colony formation on plates, but nonsterilized animals produced colonies regardless of whether they contained SCB (*P. huttoni*) or not (*Ophiocoma bollonsi* and *Ophionereis fasciata*). In the few cases

Figure 1. Transverse section of SCB (arrow) from *Trochodota dunedinensis* body wall, lying beneath the cuticle (C) of the body wall. SCB coat has fibrous appearance.

Figure 2. Transverse sections through Type 3 SCB (arrows) beneath the cuticle (C) of *Stichopus mollis* tube foot. SCB have numerous vacuoles (v). E, epidermal support cell.

Figure 3. Baton-shaped SCB from *Pseudechinus huttoni* tube foot, longitudinal section and transverse section. The chromatin is condensed into electron-dense fibers running along the center of the bacterium (arrow). Note granular appearance of periplasmic space (curved arrow) and rounded cap-like ends (open arrow).

Figure 4. Type 2 spiral form SCB from *Pseudechinus huttoni* tube foot, showing condensed chromatin fibers (arrows) and double membranes characteristic of Gram negative bacterium (curved arrow). E, epidermal support cell.

Figure 5. Typical Type 2 SCB (arrows) situated in the lower fibrous part of the cuticle (F) in *Astropecten primigenus* tube foot. SCB sometimes appear aligned with the fibers of the lower cuticle. C, outer layer of cuticle; E, epidermal support cells.

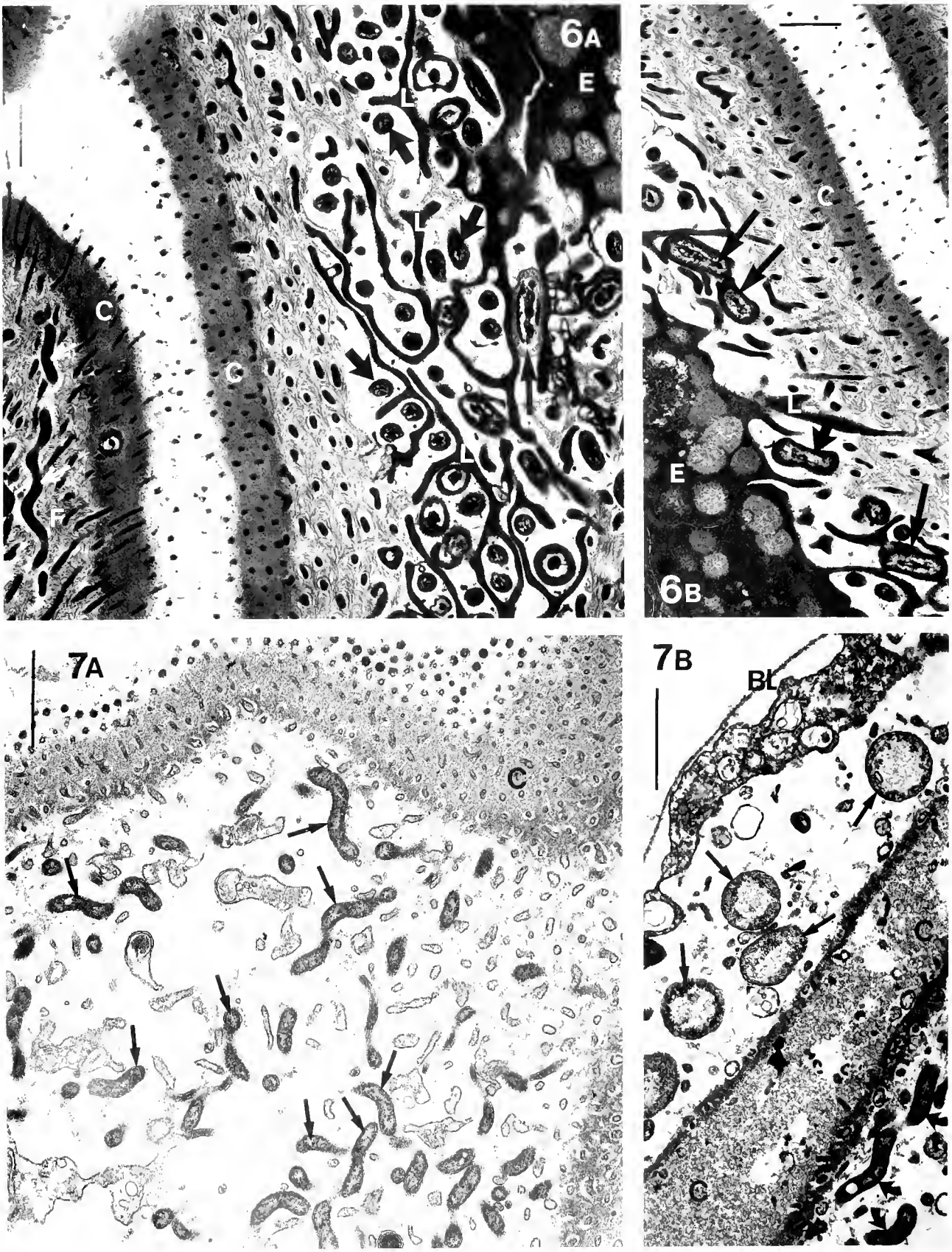

Figures 6–7. Scale bars represent 1 μm

in which colonies did form, these were always of more than one type and of similar morphology to the colonies growing on control plates.

The UV treatments reduced the number of bacterial colonies from the *A. squamata* arms but did not totally eliminate the bacteria, even at longer exposure times. The resulting bacterial colonies were of a variety of morphological types and were similar to those on the control agar plates. Few colonies were isolated from the nonsterilized tube-foot homogenates of *O. bollonsi* or from those given a short UV exposure; no bacteria were cultured from tube feet exposed to UV for longer time periods. Repeated washing with sterile ASW had no apparent effect in reducing the number of colony-forming bacteria associated with the echinoderms tested. Whenever bacteria were cultured, the variety of colony morphologies was similar to that of control animals.

Discussion

About half of the echinoderm species we examined from New Zealand contained SCB. In a survey of 63 species of echinoderms from the shelf seas around the British Isles, more than 60% had SCB (Kelly and McKenzie, in press). These surveys and most of the other information on SCB distribution have been from temperate, shallow-water echinoderm faunas. The distribution of SCB in tropical and polar echinoderms is unknown, though McKenzie (1992) described SCB in crinoids from the Great Barrier Reef, Australia. SCB have also been found in deep-sea holothurians (Roberts *et al.*, 1991) and deep-sea ophiuroids (unpub. obs.). There is no obvious correlation between the occurrence of SCB and the habitat, feeding strategy, or other ecological aspects of the host. The New Zealand echinoderms were collected from a range of habitats, including sandy beaches, rocky shores, and depths of 60 m and 120 m. SCB were found in animals of different reproductive condition and size or age. Again, the number of SCB within a species was apparently not linked to host ecology. Similar conclusions were reached in other studies (McKenzie and Kelly, 1994; Kelly and McKenzie, in press). SCB are thus a general, though not universal, phenomenon of echinoderms rather than being found only in particular ecological groupings of species.

One factor that does relate to SCB distribution is host phylogeny. The following generalities are supported by the present observations and those of earlier studies. (1) When SCB are recorded from a species, then all individuals of that species will have symbionts; (2) species congeneric with a symbiont-containing species will all have SCB; and (3) co-familial species will probably all have or all lack SCB (McKenzie and Kelly, 1994; Kelly and McKenzie, in press). Every individual of well-studied species, such as the three *Pseudechinus* species, had SCB. *Amphipholis squamata* from New Zealand (this study), North America (Walker and Lesser, 1989) and North Europe (McKenzie and Kelly, 1994) all appear to have morphologically identical SCB. It would be interesting to check the molecular similarities between the hosts and between the symbionts from these separate regions. The presence of SCB in all three species of *Pseudechinus* supports the second generality; this is also true for the brittlestar genus *Amphiura*. SCB were present in both New Zealand species and have also been found in three European species of *Amphiura* (Kelly and McKenzie, in press). SCB have been recorded from *Astropecten irregularis* and three species of *Echinocardium* (Holland and Nealson, 1978; Kelly and McKenzie in press). The failure to demonstrate SCB in the New Zealand species *Astropecten polyacanthus* and *Echinocardium cordatum* was probably due to the poor cuticular fixation in all the specimens examined; further investigations of these species may reveal their presence. Three Australian species of the feather star genus *Comanthus* (*C. timorensis*, *C. parvicirrus*, and *C. alternans*) were examined by McKenzie (1992). None had SCB, as was the case for the New Zealand *C. novozealandiae*. Examples of co-familial species either having or lacking SCB are best seen in the asteroids. *Asterodon* and *Odontaster* both have SCB. *Patiriella* belongs to the Asterinidae and SCB have also been reported from other species in this family (Cameron and Holland, 1983; Souza Santos and Sasso, 1970; Kelly and McKenzie, in press). None of the species belonging to the family Asteriidae (*Sclerasterias*, *Coscinasterias*, *Allostichaster*, *Astrostole* and *Calvasterias*) had SCB. The earlier report of *Calvasterias* having SCB (Kelly *et al.*, 1994) was erroneous.

McKenzie and Kelly (1994) noted a correlation between SCB morphology and host phylogeny in ophiuroids. Species within a genus usually all have similar SCB, and this is sometimes also true of co-familial species. This correlation is partially supported by the results from the New Zealand species, but there are exceptions. In specimens

Figure 6. (A) Mixed morphological types of SCB in *Odontaster benhami* tube foot. Type 2 SCB (white arrows) in the lower fibrous layer (F) of the cuticle (C) and Type 3 SCB mostly in transverse section (arrows). L, lamellae of support cells; E, epidermal support cell. (B) Dumbbell-shaped Type 3 SCB (arrows) lying below the cuticle (C). L, lamellae of support cells; E, epidermal support cell.

Figure 7. (A) Numerous Type 2 SCB (arrows) lying beneath the cuticle (C) of *Astrobrachion constrictum* tube foot. BL, basal lamima. (B) Two opposing surfaces of tube foot from *Astrobrachion constrictum* (C). On the upper left the SCB in transverse section appear enlarged and distorted (arrows). On the lower right the SCB appear as typical Type 2 SCB (curved arrows). E, epidermal support cell.

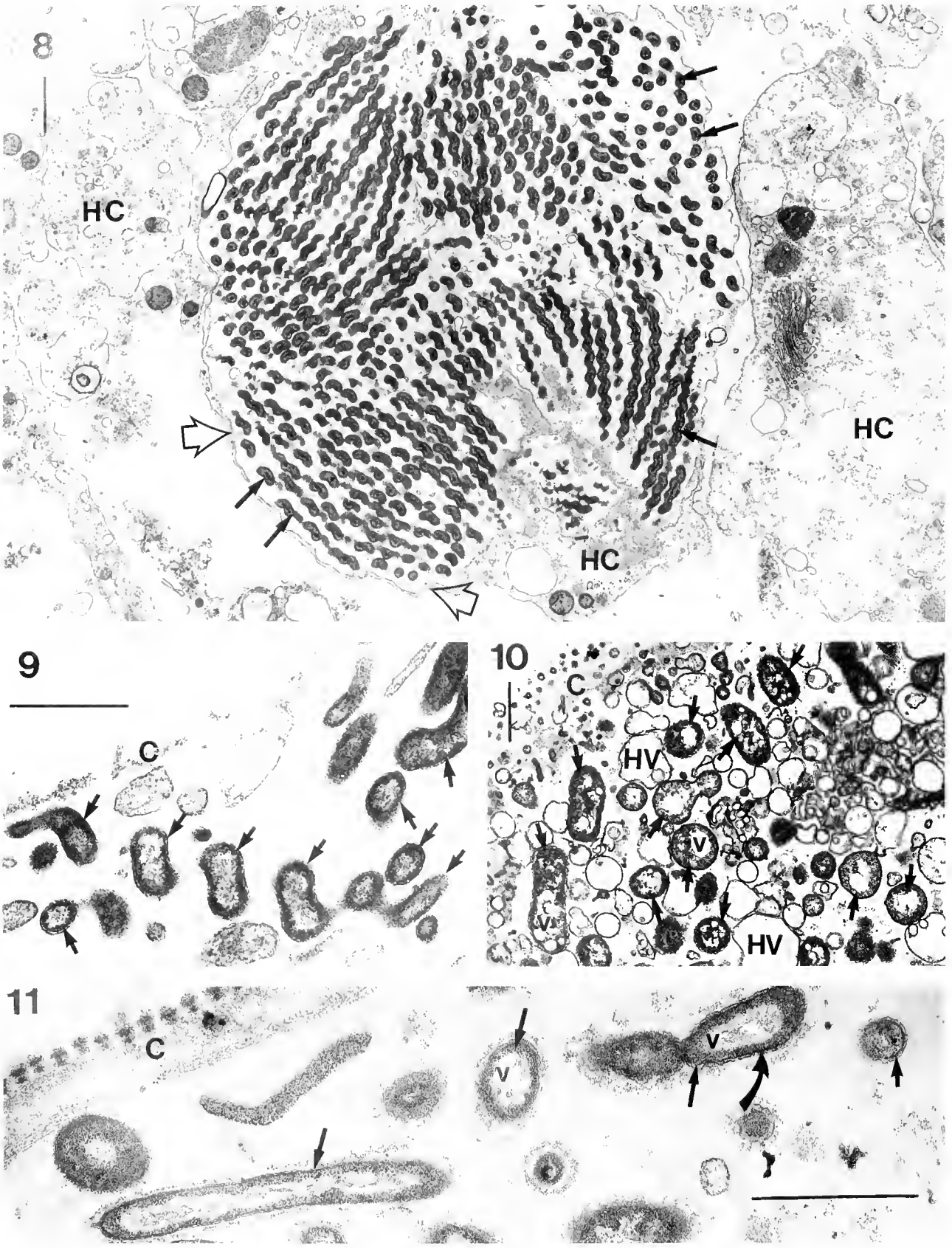

Figures 8–11. Scale bars represent 1 μm.

of *Amphiura filiformis* and *A. chiajei* collected from the British Isles (McKenzie and Kelly, 1994), the SCB are Type 3 rods, classically with membrane-bound vacuoles tearing to form holes in the sections. Spiral forms have occasionally been seen with the epifluorescent microscope but not so far with TEM, the straight rods being much more numerous. McKenzie and Kelly (1994) found a single Type 2 SCB in another amphiurid (*Microphiopholis atra*). *A. amokurae* is apparently unusual amongst amphiurids in having a predominance of Type 2 SCB instead of the Type 3 that might have been predicted. The fact that some species have two types of SCB, combined with the low overall level of variation in SCB morphology, limits the usefulness of bacterial morphology as a character in investigating possible co-evolution between the symbionts and their hosts.

It is not known if the different morphological types of SCB represent separate genotypes. Other symbioses show evidence that bacteria with different morphologies have different genetic identities. Among homopteran insects, 55% of the species are thought to contain more than one type of symbiont (Buchner, 1966), and both sulfide-oxidizing and methylotrophic symbionts have been found within the same bivalve host (Fisher *et al.*, 1993). The fact that the three *Pseudechinus* species (Table IV) and *Asterodon miliaris* and *Odontaster benhami* consistently differ in the ratio of the SCB types within them may indicate that the morphotypes reflect different bacterial genotypes. Alternatively, this difference could result from a single SCB genotype having morphological plasticity within its echinoderm host. The ability of a single genotype to exhibit considerable pleomorphism in response to subtle environmental variations is known in many bacteria (Berkeley, 1979) and has been recorded in symbioses such as some mycetocyte-insect associations (Houk and Griffiths, 1980; Smith and Douglas, 1987). The presence of both major types of SCB is phylogenetically widespread, and it may be that they are both potentially present in all species. This would strengthen the argument that the types are phenotypic variants rather than different genotypes. Molecular investigations of 16S rRNA variation within the symbionts of single species could be the best way of resolving question.

The estimates of bacterial loading in New Zealand's echinoderms were similar to those recorded for ophiuroids from the British Isles. McKenzie and Kelly (1994) estimated a bacterial load of 4.60×10^9 g^{-1} AFDW for *Amphipholis squamata* collected from the west coast of Scotland. This compares to 4.96×10^9 g^{-1} AFDW for *A. squamata* from New Zealand. The figure for *A. squamata* given by Lesser and Blakemore (1990) is not directly comparable; it relates to bacterial colonies per animal rather than to SCB g^{-1} AFDW. *Pseudechinus huttoni* had a high bacterial loading, only slightly lower than that recorded from *A. squamata* and considerably higher than that of the other two species of *Pseudechinus*. The three species of *Pseudechinus* are broadly sympatric subtidally on the Otago coast and maintain genetic isolation from each other, although they can be readily hybridized in the laboratory. Color is the most obvious character distinguishing the species, although there are other morphological differences such as test thickness and length of spines. The differences in overall bacterial load and in the ratios of the types of SCB present therefore warrant further investigation.

Few comparative figures are available from other symbioses. The density of SCB in all the species is similar to the bacterial loading in the trophosome of vestimentiferans (up to 10^9 bacteria g^{-1} wwt—Cavanaugh *et al.*, 1981; Powell and Somero, 1983). The echinoderm symbionts clearly have the potential to be metabolically important to their hosts. However, the trophosome is a much higher proportion of the total body mass of pogonophorans than the integumental tissues are in echinoderms, so any contribution of SCB to their hosts' holistic energy budget is likely to be proportionately lower.

Walker and Lesser (1989) claimed to have cultured SCB from *Amphipholis squamata*, which they identified as an undescribed species of *Vibrio*. Attempts to reproduce this result from New Zealand *A. squamata* and from other symbiont-containing echinoderms (this study and unpublished observations from Scottish echinoderms) did not produce any evidence of a symbiont in culture. It is difficult to see how any SCB could have survived the sterilization described in Lesser and Blakemore (1990). Even a 5-s exposure to isopropyl alcohol killed the host, so 30 s of exposure would have penetrated the cuticle and presumably killed the SCB. In our experiments, bacteria never grew when the animals had more than a 5-s exposure to isopropyl alcohol. Even those that occasionally grew at an exposure of 5 s were probably associated with the surface or gut rather than being symbionts, because they always formed mixed colonies morphologically identical

Figure 8. Spiral-shaped bacteria (arrows) in a bacteriocyte from the connective tissue of an *Ophiocoma bollonsi* tube foot. HC, host cell; open arrows, host cell membrane.

Figure 9. Tightly kinked spiral form Type 2 SCB (arrow) from a tube foot of *Amphiura amokurae*. C, cuticle.

Figure 10. Type 3 SCB (arrows) from a tube foot of *Ophiomyxa brevimira*. SCB have numerous vacuoles (v). C, cuticle; HV vacuoles of host origin in sub-cuticular space.

Figure 11. Vacuolated Type 2 rods from a tube foot of *Amphipholis squamata*. Curved arrow indicates double membranes around SCB. C, cuticle; v, vacuoles.

to those from controls. No bacterial colonies of the type reported by Walker and Lesser (1989) were observed, even after 21 days. These results do not necessarily mean that the bacterium isolated by Walker and Lesser (1989) was not the symbiont. The SCB of *A. squamata* from the east coast of the United States could be different from the New Zealand or European symbionts and could either be resistant to isopropyl alcohol or have simpler culturing requirements. Successful isolation into culture of a bacterial symbiont from marine organisms is, however, very rare. Only the luminescent symbionts of some fish and squid (Hastings and Nealson, 1981; McFall-Ngai, 1994) have definitely been cultured, and these bacteria are commonly occurring, free-living forms. The problems of symbiont isolation are illustrated by a meticulous attempt by Wood and Kelly (1989) to culture chemoautotrophic bacteria from the bivalve *Thyasira flexuosa.* They isolated a sulfide-oxidizer of the genus *Thiobacillus* and proposed it as the symbiont of *T. flexuosa;* however, when genetic sequences of the cultured bacterium were compared to the symbionts, it was found that they were not the same (Marine Biological Association of the United Kingdom Annual Report 1991–1992).

As evidence that the bacteria they cultured were indeed SCB, Walker and Lesser (1989) produced polyclonal antibodies to whole bacterial cells, then used these antibodies to label sections of the host material. The SCB reacted with the polyclonal antibodies. Unfortunately, these authors did not try to determine the specificity of their antibodies to the cultured bacterial isolate by testing them against either a range of bacteria isolated from the gut and outer surfaces of *A. squamata,* or against other marine bacteria. It is therefore possible that these antibodies were not *Vibrio*-specific. Nor did these authors cross-react the antibodies with other *Vibrio* strains. It would not be surprising if SCB were related to the genus *Vibrio,* because unculturable symbionts from flashlight and angler fishes (Haygood and Distel, 1993) were shown to be related to vibrios. The polyclonal antibody results do show that the cultured bacterium shares an antigen with the SCB, but further investigations—preferably with monoclonal antibodies and *in situ* hybridization with species-specific rRNA probes (Distel *et al.,* 1991)—are needed to show that the cultured bacteria are genuinely the same as the SCB.

Table IV

Fisher's least-square difference table for comparisons of rods (Type 3 SCB) and spirals (Type 2 SCB) between Pseudechinus huttoni *(PH);* P. huttoni *juveniles (PHJ),* P. novaezealandiae *(PN), and* P. albocinctus *(PA); significance is at* $P < 0.05$

Comparison	Significance
PA rods > PN rods	0.0260
PH rods > PA rods	<0.0001
PHJ rods > PA rods	0.0017
PA spirals > PA rods	NS
PA rods > PN spirals	NS
PA rods > PH spirals	NS
PA rods > PHJ spirals	NS
PH rods > PN rods	<0.0001
PHJ rods > PN rods	<0.0001
PA spirals > PN rods	0.002
PN spirals > PN rods	NS
PH spirals > PN rods	NS
PHJ spirals > PN rods	NS
PH rods > PHJ rods	<0.0001
PH rods > PA spirals	<0.0001
PH rods > PN spirals	<0.0001
PH rods > PH spirals	<0.0001
PH rods > PHJ spirals	<0.0001
PHJ rods > PA spirals	NS
PHJ rods > PN spirals	0.0005
PHJ rods > PH spirals	<0.0001
PHJ rods > PHJ spirals	<0.0001
PA spirals > PN spirals	0.0486
PA spirals > PH spirals	0.0015
PA spirals > PHJ spirals	0.0066
PN spirals > PH spirals	NS
PN spirals > PHJ spirals	NS
PHJ spirals > PH spirals	NS

Table III

Bacterial counts per gram of tissue wet weight (WWT) and ash-free dry weight (AFDW)

Species	Weight of tissue (g)	Count from homogenate (standard deviation)	SCB g^{-1} WWT	SCB g^{-1} AFDW
Pseudechinus huttoni	0.958	37.0 (13.0)	2.19×10^8	4.48×10^9
P. albocinctus	0.986	16.8 (10.5)	9.96×10^7	2.17×10^9
P. novaezealandiae	0.608	6.37 (5.2)	3.77×10^7	8.41×10^8
P. huttoni juveniles	0.314	22.1 (12.4)	1.31×10^8	2.67×10^9
Asterodon miliaris	0.577	34.3 (19.6)	2.03×10^8	1.99×10^9
*Amphipholis squamata**	0.030	83.8 (14.0)	4.96×10^8	4.96×10^9
Ophiocoma bollonsi	0.849	6.9 (6.0)	4.09×10^7	4.41×10^8

The wet weight is an average per homogenate; the counts are an average of 20 fields of view and a total count of rods and spirals.

* AFDW conversion factor taken from Scottish west coast specimens (McKenzie and Kelly, 1994).

If SCB are unculturable, identifying the nature of their interaction with their hosts is more difficult. There has been a great deal of interest in associations between chemoautotrophic bacteria and various marine invertebrates. There is, however, no positive evidence suggesting that SCB are chemoautotrophs. Bacterial morphology sometimes provides clues to trophic biology (Berkeley, 1979), but the morphology of the SCB from the New Zealand echinoderms was not particularly informative. Type 2 SCB showed little internal specialization; even vacuoles were rare. The Type 3 SCB from the New Zealand species were more diverse. The profusion of vacuoles seen in the brittlestar *Ophiomyxa* and the holothurian *Stichopus mollis* may indicate that these bacteria are more unusual than other SCB so far observed. There was, however, no evidence of the specialized membrane stacks known from symbiotic methylotrophs (Fisher *et al.*, 1993) and nitrifiers (Stanier *et al.*, 1977). Nor was there any evidence of the sulfur storage observed in some sulfide-oxidizing symbionts (Southward, 1986). The lack of obvious morphological clues need not exclude chemoautotrophy. Some other sulfide-oxidizers, for example, do not store sulfur and they resemble SCB (Southward, 1986). Given the large number and diversity of host species, some SCB may yet prove to be chemoautotrophic.

Many investigators favor the suggestion that SCB metabolize dissolved organic material (DOM) (Holland and Nealson, 1978; Walker and Lesser, 1989), and some evidence supports this hypothesis. In *Amphipholis squamata,* SCB can take up dissolved amino acids, and this uptake precedes any translocation of synthesized proteins to the host (Walker and Lesser, 1989; Lesser and Walker, 1992). Host epidermal cells frequently phagocytose SCB (Walker and Lesser, 1989; Roberts *et al.*, 1991; McKenzie and Kelly, 1994). SCB could have a nutritive role if they used DOM as an energy source, then were "cropped" by the host through phagocytosis. It is more usual, however, for a host to benefit from the products of its symbionts than to ingest the bacteria themselves (Douglas, 1994), and it may be that only moribund SCB are phagocytosed. The division rate of the SCB is unknown—there are only estimates for standing crop—but given the frequency of observations of phagocytosis, it may be high. Lesser and Walker (1992) concluded, however, that the rate of DOM uptake was too low to provide a significant energy source to the host. They based this conclusion on a comparison between a symbiont-containing ophiuroid, *Amphipholis squamata,* and a species that lacked SCB. Unfortunately, the latter was *Ophiopholis aculeata,* a species that definitely possesses SCB, albeit in lower numbers than are found in *A. squamata* (McKenzie and Kelly, 1994). The role of SCB in DOM uptake has, therefore, still to be defined. Because of the density of symbionts observed in some species, the possible contribution of SCB to DOM uptake in echinoderms must be considered in investigations of growth and regeneration.

Although the bacteria seen in the bacteriocytes of *O. bollonsi* had a regular, "crimped" appearance when viewed with TEM, they are probably the same as the faintly fluorescing rods seen in the tube-foot squash preparations, the "crimped" shape being too small to be resolved with epifluorescence microscopy. These bacteria are not SCB, and both this species and *Ophiopteris antipodum* have been discounted from previous estimates of the numbers of species that, on the basis of epifluorescent evidence, are thought to harbor SCB (Kelly *et al.*, 1994). The bacteria counted in the homogenate of arm tissue from *Ophiocoma bollonsi* were probably also released from the bacteriocytes. The counts made from homogenates of *Ophiocoma bollonsi* (Table III) suggest that these bacteria are almost as abundant as SCB in other species. *Ophiopteris papillosa* from the northwestern coast of America is similar to *Ophiopteris antipodum* in that the rod-shaped bacteria seen with epifluorescence could not be found under the cuticle with TEM (McKenzie and Kelly, 1994). Further investigations may reveal bacteriocytes in these species also. Nothing is known of the biology of the bacteriocytes, but the host animals appear healthy. Large cells, filled with rod-shaped bacteria, have also been found in the crinoid *Calamocrinus diomedae* (Holland *et al.*, 1991). Similar structures have been found in other stalked crinoids (U. Welsh, pers. comm.) and in the comatulids *Antedon bifida* (Kelly and McKenzie, in press) and *A. petasus* (Heinzeller and Welsch, 1994). These bacteria may be a second type of symbiont, but they are also reminiscent of rickettsial infections of marine invertebrates (Sparks, 1985), which often have no obvious pathological effects on their hosts.

The SCB in New Zealand echinoderms are very similar to those in echinoderms from Europe and North America. Although some of the SCB have interesting morphologies that have not previously been encountered, almost all of the SCB from New Zealand species can be classified within two major types. The overall pattern of SCB distribution is similar to that in other echinoderm faunas (Kelly and McKenzie, in press) and no ecological trends in their distribution are obvious. The New Zealand study highlights both the restricted degree of variation in SCB morphology and the possibility that more than one type of SCB can occur within a single host species. It also strengthens the observation that closely related species are all likely to either have SCB or lack them (McKenzie and Kelly, 1994). The recorded densities of SCB indicate that they are potentially important to their hosts, although their exact functions are as yet unknown. None appear to be chemoautotrophs. Molecular techniques will be the best way to investigate the links between host phylogeny and SCB distribution. In the absence of isolated symbionts, experiments comparing nonsymbiotic species with ones con-

taining SCB may be the most productive means to explore trophic interactions between SCB and their hosts.

Acknowledgments

This work was partly funded by the Waitangi Fellowship to MSK from The Bank of Scotland and by Mobil North Sea Ltd. We thank the Directors of the Portobello and Dunstaffnage Marine Laboratories for the use of the facilities; and Mr. Alan Mitchell and the staff at the South Campus EM Unit, University of Otago; the crew of the R. V. *Munida;* and Dr. Mark James for their technical support.

Literature Cited

Berkeley, R. C. W. 1979. Structure and classification of prokaryotic micro-organisms. Pp. 135–175 in L. E. Hawker and A. H. Linton, eds. *Micro-organisms: Function, Form and Environment.* (2nd Edition). Arnold, London.

Bosch, C. 1976. Sur un noveau type de symbiose chez la Bonellie (*Bonellha viridis,* Echiurien). *C. R. Acad. Sci. Paris* **282:** 2179–2182.

Bosch, I. 1992. Widespread symbiosis between bacteria and sea star larvae in epipelagic regions of the North Atlantic. *Mar. Biol.* **114:** 495–502.

Buchner, P. 1966. *Endosymbiosis of Animals with Plant Microorganisms.* Wiley, New York. 909 pp.

Cameron, R. A., and N. D. Holland. 1983. Electron microscopy of extracellular materials during the development of a seastar, *Patiria miniata* (Echinodermata; Asteroidea). *Cell Tissue Res.* **234:** 193–200.

Cavanaugh, C. M., S. L. Gardiner, M. L. S. Jones, H. W. Jannasch, and J. B. Waterbury. 1981. Prokaryotic cells in the hydrothermal vent tube worm *Riftia pachyptila;* possible chemoautotrophic symbionts. *Science* **213:** 340–342.

Distel, D. L., E. F. DeLong, and J. B. Waterbury. 1991. Phylogenetic characterisation and in situ localization of the bacterial symbiont of shipworms (Teredinidae: Bivalvia) by using 16S rRNA sequence analysis and oligodeoxynucleotide probe hybridization. *Appl. Environ. Microbiol.* **57:** 2376–2382.

Douglas, A. E. 1994. *Symbiotic Interactions.* Oxford University Press, Oxford. 148 pp.

Féral, J. P. 1980. Cuticule et bacteries associées aux épidermes digestif et tégumentaire de *Leptosynapta galliennei* (Herapath) (Holothuroidea: Apoda)—premières donnécs. Pp. 285–290 in *Echinoderms Present and Past.* M. Jangoux., ed. Balkema, Rotterdam.

Fell, H. B. 1962. *Native Sea Stars.* A. H. and A. W. Reed, Wellington.

Fenchel, T., T. Perry, and A. Thane. 1977. Anaerobiosis and symbiosis with bacteria in free-living ciliates. *J. Protozool.* **24:** 154–163.

Fisher, C. R., J. M. Brooks, J. S. Vodenichar, J. M. Zande, J. J. Childress, and R. A. Burke, Jr. 1993. The co-occurrence of methanotrophic and chemoautotrophic sulfur-oxidising bacterial symbionts in a deep-sea mussel. *Mar. Ecol.* **14:** 277–289.

Giere, O. 1981. The gutless marine oligochaete *Phallodrilus leukodermatus.* Structural studies on an aberrant tubificid associated with bacteria. *Mar. Ecol. Prog. Ser.* **5:** 353–357.

Hastings, J. W., and K. H. Nealson. 1981. The symbiotic luminous bacteria. Pp. 1332–1345 in *The Prokaryotes—A Handbook of Habitats, Isolation and Identification of Bacteria.* M. P. Starr *et al.*, eds. Springer-Verlag, Berlin.

Haszprunar, G., K. Schaefer, A. Waren, and S. Hain. 1995. Bacterial symbionts in the epidermis of an Antarctic neopilinid limpet (Mollusca, Monoplacophora). *Proc. Roy. Soc. Lond.*, in press.

Hausmann, K. 1982. Elektronenmikroskopische Untersuchungen an *Anaitides mucosa* (Annelida Polychaeta). Cuticula and Cilien, Schleimzellen und Schleimextrusion. *Helgol. wiss. Meeresunters* **35:** 79–96.

Haygood, M. G., and D. L. Distel. 1993. Bioluminescent symbionts of flashlight fishes and deep-sea anglerfishes from unique lineages related to the genus *Vibrio. Nature* **363:** 154–156.

Heinzeller, T., and U. Welsch. 1994. Crinoidea. Pp. 9–148 in *Microscopic Anatomy of Invertebrates, Volume 14: Echinodermata.* Wiley-Liss, New York.

Hobbie, R. J., R. J. Daley, and S. Jasper. 1977. Use of nucleopore filters for counting bacteria by fluorescence microscopy. *Appl. Environ. Microbiol.* **33:** 1225–1228.

Holland, N. D., and K. H. Nealson. 1978. The fine structure of the echinoderm cuticle and subcuticular bacteria of echinoderms. *Acta Zool. (Stockh.)* **59:** 169–185.

Holland, N. D., J. C. Grimmer, and K. Wiegmann. 1991. The structure of the sea lily *Calamocrinus diomedae* with special reference to the articulations, skeletal microstructure, axial organs and stalk tissues (Crinoida, Millericrinida). *Zoomorphology* **110:** 115–132.

Houk, E. J., and G. W. Griffiths. 1980. Intracellular symbiotes of the Homoptera. *Ann. Rev. Entomol.* **25:** 161–187.

Kelly, M. S., and J. D. McKenzie. 1992. The quantification of subcuticular bacteria in echinoderms. Pp. 225–228 in *Echinoderm Research 1991,* L. Scalera-Liaci and C. Canicattì, eds. Balkema, Rotterdam.

Kelly, M. S., J. D. McKenzie, and M. F. Barker. 1994. Sub-cuticular bacteria: their incidence in the echinoderms of the British Isles and New Zealand. Pp. 33–38 in *Echinoderms. Dijon,* B. David *et al.*, eds. Balkema, Rotterdam.

Kelly, M. S., and J. D. McKenzie. 1995. A survey of the occurrence and morphology of sub-cuticular bacteria in shelf echinoderms from the north-east Atlantic. *Mar. Biol.* in press.

Lesser, M. P., and R. P. Blakemore. 1990. Description of a novel symbiotic bacterium from the brittlestar *Amphipholis squamata. Appl. Environ. Microbiol.* **56:** 2436–2440.

Lesser, M. P., and C. W. Walker. 1992. Comparative study of the uptake of dissolved amino acids in sympatric brittlestars with and without endosymbiotic bacteria. *Comp. Biochem. Physiol.* **101B:** 217–223.

Lutaud, G. 1969. La nature des corps funiculaires des cellularines bryozoaires chilostomes. *Arch. Zool. Exp. Gen.* **110:** 2–30.

McFall-Ngai, M. J. 1994. Animal-bacterial interactions in the early life-history of marine invertebrates: the *Euprymna scolopes/Vibrio fischeria* symbiosis. *Am. Zool.* **34:** 554–561.

McKenzie, J. D. 1987. The ultrastructure of the tentacles of eleven species of dendrochirote holothurians studied with special reference to the surface coats and papillae. *Cell Tissue Res.* **248:** 187–199.

McKenzie, J. D. 1992. Comparative morphology of crinoid tube feet. Pp. 73–79 in *Echinoderm Research 1991,* L. Scalera-Liaci and C. Cancattì, eds. Balkema, Rotterdam.

McKenzie, J. D., and M. S. Kelly. 1994. A comparative study of subcuticular bacteria in brittlestars (Echinodermata: Ophiuroidea). *Mar. Biol.* **120:** 65–80.

Mackie, G. O., and Q. Bone. 1978. Luminescence and associated effector activity in *Pyrosoma* (Tunicata: Pyrosomida). *Proc. Roy. Soc. Lond. B* **202:** 483–495.

Margulis, L. 1981. *Symbiosis in Cell Evolution.* Freeman, San Francisco. P. 418.

Menon, J. G., and A. J. Arp. 1993. The integument of the marine echiuran worm *Urechis caupo. Biol. Bull.* **185:** 440–454.

Muscatine, L., P. Falkowski, J. Porter, and Z. Dubinsky. 1984. Fate of photosynthetically-fixed carbon in light and shade-adapted colonies of the symbiotic coral *Stylophora pistillata. Proc. Roy. Soc. Lond. B* **222:** 181–202.

Neidhardt, F. C., J. L. Ingraham, and M. Schaechter. 1990. *Physiology of the Bacterial Cell: A Molecular Approach.* Sinauer, Sunderland, MA.

Ott, J., G. Rieger, R. Rieger, and F. Enderes. 1982. New mouthless interstitial worms from the sulphide system: symbiosis with prokaryotes. *Mar. Ecol.* 3: 313–333.

Palinesar, E. E., W. R. Jones, J. S. Palinesar, M. A. Glogowski, and J. L. Mastro. 1989. Bacterial aggregates within the epidermis of the sea anemone *Aiptasia pallida*. *Biol. Bull.* **177:** 130–140.

Powell, M. A., and G. N. Somero. 1983. Blood components prevent blood poisoning of respiration of the hydrothermal vent tube worm *Riftia pachyptila*. *Science* **219:** 297–299.

Roberts, D., D. S. M. Billet, G. McCartney, and G. E. Hayes. 1991. Procaryotes on the tentacles of deep-sea holothurians: a novel form of dietary supplementation. *Limnol. Oceanogr.* **36:** 1447–1452.

Saffo, M. B. 1990. Symbiosis within a symbiosis: intracellular bacteria within the endosymbiotic protist *Nephromyces*. *Mar. Biol.* **107:** 291–296.

Smith, D. C., and A. E. Douglas. 1987. *The Biology of Symbiosis.* Arnold, London.

Sparks, A. K. 1985. *Synopsis of Invertebrate Pathology.* Elsevier, Amsterdam. P. 423.

Southward, E. C. 1986. Gill symbionts in thyasirids and other bivalve molluscs. *J. Mar. Biol. Ass. U. K.* **66:** 889–914.

Souza Santos, H., and W. S. Sasso. 1970. Ultrastructural and histochemical studies on the epithelium revestment layer in the tube feet of the starfish *Asterina stellifera*. *J. Morphol.* **130:** 287–296.

Stanier, R. Y., E. A. Adelberg, and J. L. Ingraham. 1977. *General Microbiology.* MacMillan, London.

Vacelet, J., and C. Donadey. 1977. Electron microscopy study of the association between some sponges and bacteria. *J. Exp. Mar. Biol. Ecol.* **30:** 301–314.

Walker, C. W., and M. P. Lesser. 1989. Nutrition and development of brooded embryos in the brittlestar *Amphipholis squamata*: do endosymbiotic bacteria play a role. *Mar. Biol.* **103:** 519–530.

Welsch, U. 1984. Hemichordata. Pp. 791–799 in J. Bereiter-Hann, A. G. Matoltsy, and K. S. Richards, eds. *Biology of the Integument, Vol 1.* Springer Verlag, Berlin.

Wood, A. P., and D. P. Kelly. 1989. Isolation and physiological characterisation of *Thiobacillus thyasiris* sp. nov., a novel marine facultative autotroph and the putative symbiont of *Thyasira flexuosa*. *Arch. Microbiol.* **152:** 160–166.

Reference: *Biol. Bull.* 189: 106–112. (October/November, 1995)

Coexistence and Possible Parasitism of Somatic and Germ Cell Lines in Chimeras of the Colonial Urochordate *Botryllus schlosseri*

ZEEV PANCER[1,2], HARRIET GERSHON[2], AND BARUCH RINKEVICH[1,*]

[1]*Israel Oceanographic & Limnological Research, National Institute of Oceanography, Tel-Shikmona, P.O.B. 8030, Haifa 31080, Israel, and* [2]*Department of Immunology, The Bruce Rappaport Faculty of Medicine, Technion-Israel Institute of Technology, P.O.B. 9649, Haifa 31096, Israel*

Abstract. Fusion between conspecifics (chimerism) is a well-documented phenomenon in a variety of taxa. Chimerism and the subsequent mixing of genetically different stem cell lines may lead to competition between cell lineages for positions in the germ line and to somatic and germ cell parasitism. It is suggested that somatic compatibility systems evolved to alleviate the costs and the threat of such cell lineage competition. Allogeneic colonies of the ascidian *Botryllus schlosseri* form vascular chimeras based on matching in one or both alleles on one highly polymorphic fusibility haplotype. Thereafter, one of the partners is completely or partially resorbed. Here we used a polymorphic molecular marker (PCR typing at a microsatellite locus) to follow somatic and gametic consequences of chimera formation. Twenty-two chimeras and subclone samples were established from 12 different genotype combinations, in which blood cells, zooids, and gonads were typed 45–130 days thereafter. Somatic coexistence of both partners was recorded in 73% of the subcloned chimeras (83% of chimeric entities) up to 100 days after disconnection between genotypes and in all chimeras where colony-resorption was completed. Both genotypes were present in 23% of the sampled gonads (in 33% of the chimeras), and in 22% of the cases, germ cells of the second partner only were detected. Injection of allogeneic but compatible blood cells into three recipient colonies revealed proliferation of the donor cells in one case, 100 days after injection. To further evaluate somatic and germ cell parasitism in chimeric organisms, we propose four key features that characterize cell lineage competition processes. These include the somatic embryogenesis mode of development, the capability for independent existence of stem cells, the disproportionate share of gametic output within chimeras, and the existence of hierarchial responses.

Received 16 March 1995; accepted 27 July 1995.

* To whom correspondence should be addressed.

Introduction

Genetically non-homogeneous organisms may be established through somatic mutations or via chimerism, the fusion between genetically distinct conspecifics. While most somatic mutation variants are evolutionarily irrelevant (Van Valen, 1988), chimeric entities have been documented in nature from a variety of protists, plants, and animals, belonging to at least nine phyla (Buss, 1982). Several studies (Buss, 1982; Grosberg and Quinn, 1986; Rinkevich and Weissman, 1987a, 1992a) have discussed the evolutionary significance of these natural chimeras by evaluating the fitness costs and benefits of chimerism as compared to the state of genetically homogeneous entities. While several sets of benefits were attributed to natural chimerism (Buss, 1982; Grosberg and Quinn, 1986), particular attention has been paid to the potential costs resulting from the mixing of genetically distinct cell lines within chimeras. This is relevant especially in those cases where germ line sequestration remains undetermined until late in ontogeny, or is never accomplished during the lifespan of an organism (Buss, 1982, 1983; Grosberg and Quinn, 1986; Rinkevich and Weissman, 1987a, 1992a). Within the shared morphological and physiological environments of chimeric entities, one genotype could gain a disproportionate share of germ cells at the expense of the other partner (germ cell parasitism), or one genotype may use the tissues and energy reservoirs of the other

member in the chimera for general maintenance (somatic cell parasitism). Examples on the morphological, cellular, and biochemical levels of the displacement of one cell lineage in the chimera at the expense of another were documented in several groups of organisms (reviewed in Rinkevich and Weissman, 1987a; Grosberg, 1988). However, there is still no direct documentation for such a process in which molecular markers were used.

A typical colony of the urochordate *Botryllus schlosseri*, a subtidal species that can be found worldwide, is composed of a few to several hundreds of modular units called zooids, which are arranged in star-shaped structures (systems) and are connected to each other via a ramified blood system. In this group of organisms, a line of stem cells retains the ability to differentiate into either germ cells or somatic tissue throughout the lifespan of the colony (Berrill and Liu, 1948), continuously replacing aging differentiated cells. Consequently, all zooids within a single colony are genetically identical, having been derived by blastogenesis from a single founder zooid, by a complex but highly synchronized weekly developmental cycle. Zooids and blood vessels are embedded within the tunic, a translucent organic matrix, which bears sausage-like termini of blood vessels, called ampullae, in the colony's periphery. When a colony is split in nature or experimentally into two or more fragments, each subclone usually continues to grow independently to form a larger colony.

Recent interest in botryllid ascidians has centered on allogeneic recognition and its consequences. Pairs of colonies that meet naturally in the wild or are placed in contact under laboratory conditions either fuse their contacting peripheral ampullae to form a vascular parabiont (cytomictical chimera; Rinkevich and Weissman, 1987a), or develop cytotoxic lesions in the contact zone (reviewed in Taneda *et al.*, 1985; Weissman *et al.*, 1990; Rinkevich, 1992). This allorecognition is genetically controlled by a single, highly polymorphic, fusibility/histocompatibility (Fu/HC; Weissman *et al.*, 1990) haplotype with multiple codominantly expressed alleles. Fusion may be established between genotypes which match in one or both Fu/HC alleles. Rejecting colonies share no Fu/HC alleles (Scofield *et al.*, 1982). Controlled laboratory experiments on *Botryllus* chimeras revealed that the zooids from one genotype in each specific chimera are all morphologically eliminated within a few days to several months by massive phagocytosis, leaving the zooids of the other partner intact (Rinkevich and Weissman, 1987a, b, 1992a, b; Weissman *et al.*, 1990; Rinkevich *et al.*, 1993). This phenomenon, called "colony resorption" (Rinkevich and Weissman, 1987b), typically occurs at the end of a blastogenic cycle and appears to be controlled genetically by a multilevel hierarchial organization of histocompatibility alleles (Rinkevich, 1993; Rinkevich *et al.*, 1993). In addition to this resorption phenomenon, a few studies have documented, within chimeras, germ cell transfer and establishment between different partners (Sabbadin and Zaniolo, 1979; Rinkevich and Weissman, 1987a). These preliminary results further indicate that chimerism may present substantial fitness costs over the long term through cell lineage competition, parasitism, or a combination of both processes (Buss, 1982; Grosberg and Quinn, 1986; Rinkevich and Weissman, 1987a, 1992a; Sabbadin and Astorri, 1988).

Materials and Methods

Animals

Botryllus schlosseri colonies were cultured in the laboratory as previously described (Boyd *et al.*, 1986; Rinkevich and Weissman, 1987b, 1992a; Rinkevich *et al.*, 1993). Experimental colonies were isolated from among the progeny of our laboratory stock, which originated about a year earlier from Monterey marina, CA, USA. Newly metamorphosed colonies were raised individually, each attached to glass slides (50 × 75 mm).

Colony allorecognition assays

The technique of colony allorecognition assay (CAA) is the most common assay used for revealing self-nonself discrimination potential in botryllid ascidians (Rinkevich, 1992, 1995; Saito *et al.*, 1994). In this assay, small or large groups of zooids at the growing edges of the colonies are isolated by dissecting them from each colony without injuring their surrounding ampullae. Subclones from two colonies are put on glass slides in pairs and placed so that they contact one another with their extending ampullae. They are usually allowed to fasten themselves to the slides by placing them in a moisture chamber for 30–45 min before transferring to the tanks or to the sea. The CAA was performed on all botryllid ascidians where specificity was analyzed. Observations on the contact sites and colonies were made under the dissecting microscope at least once a week to confirm the location of "each partner" in the chimera in accordance with the developing buds during successive blastogenic cycles. A complete mixture of blood-borne pigment cells was recorded <14 days after fusion (Rinkevich and Weissman, 1987b).

Experimental procedures

Polymorphic molecular markers, such as microsatellite loci, may be most suitable for individual identification of genotypes within *B. schlosseri* chimeras. Microsatellites are tandem repeats (usually >100 bp long) of very short nucleotide motifs (1–6 bp long) that are dispersed abundantly and randomly through eukaryotic genomes. Since each of the microsatellites is flanked within the DNA ma-

terial by unique sequences, they can be amplified *in vitro* using the polymerase chain reaction (PCR; Queller *et al.*, 1983). We used the protocol developed for PCR typing at *B. schlosseri* microsatellite locus 811, which has been found to be highly polymorphic in two *Botryllus* populations (Pancer, 1994; Pancer *et al.*, 1994). Twenty-three laboratory-raised colonies were typed at microsatellite 811 and were assigned to their fusibility status by employing colony allorecognition assays (Rinkevich, 1992, 1995; Saito *et al.*, 1994) on different pair combinations.

Samples for typing were either a small tissue fragment (T); or hemolymph (H); or a single zooid (Z), and the gonad (G), if present in that zooid. Gonads are situated on both sides of the zooids, composed of lobulated testes and ovaries. In this study the sperm and the small oocytes from each gonad were sampled as a whole in the PCR reaction. Whenever the state of the chimeras allowed, simultaneous sampling of several zooids was performed. Tissue samples were transferred into 1.5-ml test tubes, rinsed with 0.5 ml filtered (0.2 μM, Schleichter & Schuell) seawater, and were then boiled for 5 min in 100 μl TE, dispersed by pipetting through an aerosol-free tip (EL-KAY, Labsystems) and centrifuged at 12000 $\times$ *g* for 5 min. The supernatant was discarded, the pellet resuspended in 10–20 μl of PCR-lysis buffer (20 m*M* DTT, 10^{-3}% SDS and 0.5 mg/ml Proteinase K) and incubated for 1 h at 55°C with occasional vortexing. At the end the sample was boiled again for 5 min. Amplifications were performed on a PTC-100 thermal cycler (MJ Research) in 10 μl reaction mixtures containing 1 μl of the sample, 4 pmoles each of the forward and reverse primers, 200 μ*M* of each dNTP, 0.1 μCi [α-^{32}P]dCTP, 5% DMSO, 0.5 U *Taq* DNA polymerase and buffer (Boehringer, Mannheim). The cycling parameters were 3 min at 96°C followed by 30 cycles of 45 s at 95°C, 75 s at 60°C, and 15 s at 74°C. The reactions were stopped by the addition of 5 μl Sequenase stop solution (USB), denatured for 5 min at 95°C, then 2 μl of each sample were electrophoresed on a 6% denaturing polyacrylamide gel. Detection threshold was determined experimentally in cell mixtures of 1000 cells total, containing different proportions of two homozygous colonies. Cells of a genotype mixed 1:10–1:20 with cells of a second genotype could be detected following three exposure days of the film (Pancer, 1994).

For microinjections, a siliconized micropipette mounted on a micromanipulator was inserted into a large blood vessel. Five to seven microliters of hemolymph were drawn. The micropipette's contents were then injected into the recipient colony's blood vessels. Several cell counts revealed approximately 2.5–5 $\times$ 10^4 blood cells in that volume.

Results

We studied 22 whole chimeras and chimeric subclones that were established from 12 different genotype combinations (Table I, Fig. 1a–c). Different parts of the colony's body, including blood cells, individual zooids, pieces of tissue, and gonads were sampled 45–130 days after establishment of the chimeras or 15–100 days after disconnections between the partners in the chimera as a result of subcloning, spontaneous disconnection, or after immunological resorption (Table I).

In four genotype combinations (chimeras A, B, C, G, Table I, Fig. 1a–c), we sampled 2–5 subclones from each original chimera at different times following chimera formation or disconnection (experimentally or spontaneously). In one of these chimeras (G) a hierarchial response was documented. Seventy days following chimera formation, genotype BE was recorded in all DD regions sampled (cases 13, 15, 16), while genotype DD was not detected in the BE regions (cases 12, 14). In pair combination C (cases 8, 9) the two subclones varied, since one contained both genotypes in the zooid soma 55 days following fusion, while the second was not detected in the other partner's soma 70 days after chimera formation. Although subclones of pair combinations A and B were not assigned to their pretyped genotypes, it is clear that six out of the seven subclones possessed soma of both genotypes up to 125 days after chimera formation (Table I, Fig. 1a–c). In six (75%) of the remaining eight chimeras, the other partner's soma was detected, together with the resident partner's soma, up to 60 days after fusion. Most interestingly, in all four chimeras where colony resorption was completed (cases 17, 19–21, Table I, Fig. 1c), the resorbed genotype was clearly detected together with the "winner's" genotype, even 35 days after resorption. In summary, both genotypes were recorded in 16 (73%) of the subclones and 10 (83%) of the chimeras (Table I).

In 13 of the cases (9 chimeras) studied, gonads (excluding mature oocytes) were sampled from the same zooids where the soma was typed. In three cases (33% of chimeras, nos. H, J, L, Table I, Fig. 1c) both genotypes were present simultaneously in the gonads. These chimeras were sampled 20–30 days after a complete immunological resorption of one partner in the chimera was recorded (75% of the studied resorptions). In all the nine cases (five chimeras) where the partners were disconnected experimentally or spontaneously, we did not record any chimeric situation in the gonads up to 100 days after separation. However, in two of these cases (nos. 3, 12; Table I, Fig. 1a,c), the gonads were typed as belonging to the other genotype in the chimera while the corresponding zooid's soma was only of the original genotype.

In an additional set of experiments, blood cells were injected from pretyped Fu/HC-compatible allogeneic donors into the blood system of three different recipient colonies (colonies C1–C3, Fig. 1d). The recipient colonies were sampled 20 days after injection and then 30–80 days thereafter (50–100 days after injection). In one case (C3,

Table 1

Typing at locus 811 of soma and gonads within B. schlosseri *chimeras, 45–130 days following fusion*

Case no.	Microsatellite typing of chimera partners I:II	Chimera and subclone code[a]	Typing chimeras, following disconnections or resorptions: Typing times (days): Following chimera formation	Typing chimeras, following disconnections or resorptions: Typing times (days): Following disconnection or resorption[b]	Type of[c]: Soma I:II	Type of[c]: Gonads I:II
1	BE:DD	A1	125	95, E	+++:−++	nd
2		A2	45	15, E	+++:−++	nd*
3		A3	130	100, E	−−−:+++	+++:−−−
4	AA:DD	B1	45	15, E	+++:−++	nd*
5		B2	45	15, E	+++:−−+	nd*
6		B3	125	95, E	+++:+++	+++:−−−
7		B4	125	95, E	+++:−−+	+++:−−−
8	AA:DD	C1 [AA]	55	20, E; 40, S	+++:+++	nd*
9		C2 [AA]	70	35, E; 55, S	+++:−−−	nd*
10	AA:BE	D [AA]	45	30, S	+++:+++	nd*
11	AD:DD	E [DD]	45	35, S	−−−:+++	nd*
12	BE:DD	G1 [BE]	70	20, S	+++:−−−	−−−:+++
13		G1 [DD]	70	20, S	+++:+++	nd
14		G2 [BE]	70	50, E	+++:−−−	+++:−−−
15		G3 [DD]	70	50, E	+++:+++	−−−:+++
16		G4 [DD]	70	50, E	+++:+++	−−−:+++
17	AD:BE	H [BE]	60	30, R	+++:+++	+++:+++
18	BE:DD	I [BE]	65	40, S	+++:−−−	+++:−−−
19	AA:CC	J [CC]	55	25, R	+++:+++	−−+:+++
20	AA:BE	K [BE]	55	35, R	+++:+++	−−−:+++
21	AA:CC	L [AA]	50	20, R	+++:+++	+++:+++
22	CC:DD	N [DD]	40	30, S	+++:+++	−−−:+++
Both genotypes recorded in:		subclones			16 (73%)	3 (23%)
		chimeric entities			10 (83%)	3 (33%)
A single genotype recorded in:		subclones			6 (27%)	10 (77%)
		chimeric entities			2 (17%)	6 (67%)
Only the other partner recorded in:		subclones			0 (0%)	2 (15%)
		chimeric entities			0 (0%)	2 (22%)

[a] Twelve chimeras are designated by capital letters (A–N). When applicable, their corresponding subclones are marked with numbers. In brackets: The original resident's typed alleles at locus 811 (not recorded for chimeras A and B). Chimeras A, B refer to Figure 1a, chimera G to Figure 1b, c and chimeras H, J, K, L to Figure 1c.

[b] Time elapsed since disconnections in the chimeras due to subcloning, an experimental manipulating (E); spontaneous disconnection (Rinkevich and Weissman, 1989) between the partners in the chimera (S), or resorption (R) of one partner (Rinkevich and Weissman, 1987b, 1992a, b; Weissman *et al.*, 1990; Rinkevich *et al.*, 1993).

[c] Soma typing was performed from either a tissue fragment or a single zooid. The gonad was from the same zooid sampled for soma. nd = not determined due to non-reproductive state. *Asterisks designate dying colonies, sampled from the last remains. Autoradiographic patterns were digitized into one of four categories: a strong signal on the film after an overnight exposure (+++) or a weak signal (−++); detection only after three exposure days (−−+) or below the detection threshold (−−−).

Fig. 1d), the hemolymph of the recipient unequivocally showed also the injected partner's genotype, which may indicate a proliferative process for the injected blood cells. However, in the sampled zooid and gonads of this recipient, the injected genotype was below the detection threshold.

Discussion

In five of the nine ovigerous chimeras (56%) we documented situations where vascular fusion between allogenic *B. schlosseri* colonies led to free exchange of stem cells (that eventually become germ cells) across the former boundary between the two genotypes and to incubation of foreign germ lines within the gonads. In two of the cases only the other partner's germ cells were detected. The immunological resorption phenomenon (Rinkevich and Weissman, 1987b, 1992a, b; Weissman *et al.*, 1990; Rinkevich *et al.*, 1993), in which one partner in a *Botryllus* chimera is morphologically eliminated by phagocytosis, does not exclude the possibility that the "resorbed genome" will be reestablished and coexist within the "win-

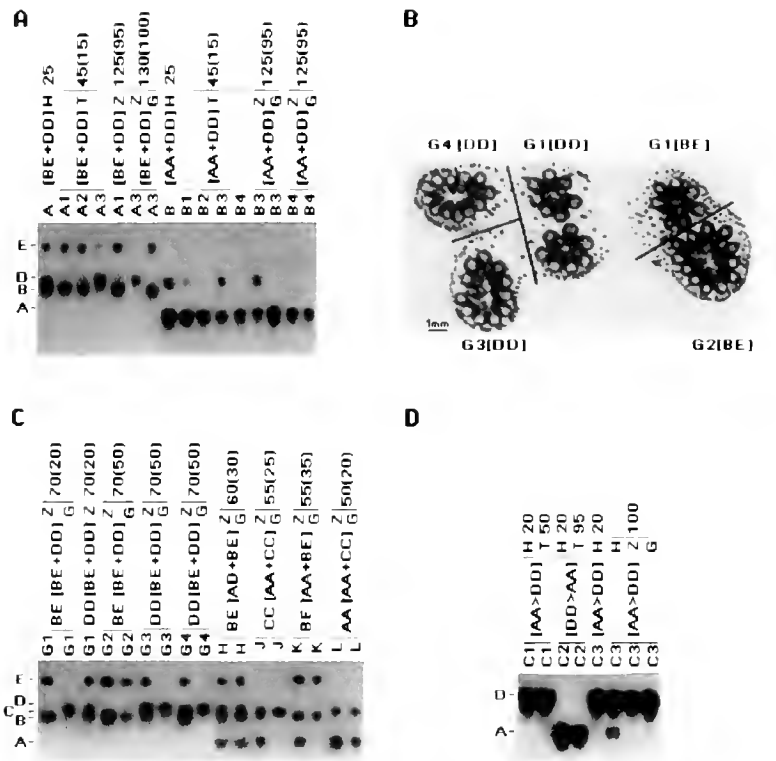

Figure 1. (A) Typing at microsatellite locus 811 of genotype combinations A and B (divided into subclones A1–A3 and B1–B4). Allelic typing (21) of the partners is shown in brackets. Compartments sampled are the hemolymph (H); a tissue fragment (T); a single zooid (Z) and if present, from the gonads (G) of the same zooid. Chimeras were first sampled 25 days after vascular anastomosis, after subcloning (numbers in parentheses denote days after subcloning), and upon sexual maturation. Predetermined alleles in the population (A = 216 bp, B = 232, C = 236, D = 240, E = 268) are depicted at the left side. Horizontal bar-lines group simultaneous sampling of subclones, or samples from several compartments of a single subclone. An overnight exposure of the film is shown. (B) A pictorial outline of genotype combination G depicting the corresponding subclones. The chimera was cut into 4 subclones, 20 days after fusion (marked lines in the figure): G1, the original chimera with three systems; G2, a single system, an outgrowth from genotype BE; G3 and G4, each a single system originating from genotype DD. Thirty days later (50 days after chimera formation) subclone G1 disconnected naturally along the region of fusion, into subclone G1 [BE] and subclone G1 [DD]. The bar line represents 1 mm. (C) Typing at microsatellite locus 811 of genotype combinations G, H, J, K, L. Allelic typing of the partners in each chimera is shown in brackets. Sampling days and compartments as in Figure 1a. Subclone sampling from genotype combination G is as depicted in Figure 1b. Genotype combinations H, J, K, L were sampled after the resorption of one partner in each (numbers are for day after fusion; numbers in parentheses denote days after resorption). An overnight exposure of the film is shown. (D) Typing of three recipient colonies which were microinjected with allogeneic-compatible hemolymph (C1–C3). Only C3 was in good condition, which allowed full screening of: hemolymph (H), a zooid (Z) and the gonad it contained. Sampling of C1 and C2 was from the last remaining tissue fragment (T). Horizontal bars group chronological sampling, or from various sources (C3). A three-day exposure of the film is shown.

ner" partner's body in both the soma (100%) and the gonads (75%). Under these conditions, one genotype in the chimera could parasitize the other (Buss, 1982, 1983; Grosberg and Quinn, 1986; Rinkevich and Weissman, 1987a, 1992a; Grosberg, 1988) by somatic or germ cell parasitism through competitive processes among the genotypes over somatic and gametic positions. The potential for cell lineage competition and parasitism in botryllid ascidians stems from the documentation that these animals maintain self-perpetuating stem cell lineages throughout their lifespan (Berrill and Liu, 1948) as do many other organisms (Buss, 1982, 1983). The displacement of one cell lineage by another in some other groups has been suggested to occur in chimeras of cellular slime molds (Buss, 1982), myxomycetes (Clark and Collins, 1973), fungi (Davis, 1959), sponges (Van de Vyver, 1988; Mukai, 1992), and hydractiniid hydroids (Hauenschild, 1956; Muller, 1964).

The results of the present study do not unequivocally prove somatic and germ cell parasitism. Parasites by def-

inition live at the expense of a host organism (Michalakis *et al.*, 1992). However, parasite/host relationships may reflect a continuum flanked by two extremes. At the one, the parasite may cause the host's death. At the other, the parasite may evolve as "benign." This occurs when parasite and host have a relatively large "shared desiderata list" (Dawkins, 1990). Unfortunately, the literature deals primarily with parasitism by species of distant taxa from the hosts, and there is almost no theoretical treatment to intraspecific parasitism on the cellular level. Therefore, we define germ/somatic cell parasitism in the *Botryllus* chimeric system as follows: 1. Incubation of any number of alien male/female germ cells within gonads. This is especially marked where one genotype's oocytes acquire nutrients from follicle cells (Manni *et al.*, 1994) of another genotype, or compete for space and nutrition (Sabbadin and Zaniolo, 1979) with other developed germ cells. 2. Penetration and establishment of alien somatic cells as an integral part of the resident's soma (zooids), where they can support the development of germ cells. However, in the absence of cell lineage competition, chimeras should show stable sexual expression, with the original germ cells in the appropriate region of the chimera (Sabbadin and Astorri, 1988; Shenk, 1991). When cell lineage competition occurs, four key features may be assigned to characterize the processes involved within chimeric organisms: 1. Cell lineage competition is evolutionarily relevant to taxa developing through the somatic embryogenesis or epigenetic developmental types, where totipotent stem cells are competent to produce germ cells at any point in ontogeny or during most of the lifespan of the organism, respectively (Buss, 1982, 1983; Tuomi and Vuorisalo, 1989). 2. These cell lineages should be capable of increasing in frequency, eventually establishing an independent existence (Buss, 1982). 3. Competing cell lineages in chimeric entities should gain a disproportionate share of gametic output by, for example, restricting the differentiation of the totipotent cells to gametic descendants, while using the somatic constituents of the other partner for maintenance and space provisions for gametes (Buss, 1982, 1983; Buss and Green, 1985; Grosberg, 1988; Sabbadin and Astorri, 1988). 4. Either transitive or nontransitive hierarchial responses for somatic/germ cell parasitism should be established in chimeric combinations from each studied group of compatible genotypes. This also provides further insights into the genetic rules operating for the cell lineage competition processes. Somatic embryogenesis (Berrill and Liu, 1948; Buss, 1982, 1983; Rinkevich and Weissman, 1987a, 1992a; Grosberg, 1988), proliferation of foreign cells in the blood (Fig. 1d; Sabbadin and Zaniolo, 1979), and foreign gametic output (Sabbadin and Zaniolo, 1979; Sabbadin and Astorri, 1988; Fig. 1a–c, Table 1) have already been attributed to *B. schlosseri* chimeras. There is also evidence for a hierarchial relationship for somatic positions in *Botryllus* chimeras (cases 12–16, Table 1, Fig. 1b,c).

In the vast majority of the chimeras (83%) including all chimeras where colony resorption was recorded, and in 73% of all subclones studied, both genotypes were recorded in the soma (Table 1, Fig. 1a–c). One may therefore postulate for the opposite conclusion that these outcomes are characteristic to synergistic relationships between the genotypes within the chimeras in which, for example, each partner in the chimera expresses proportionally its capacities for somatic growth or gametic-product differentiation. In such a case, the chimeric growth/reproductive output should be greater than that of each genotype alone. Previous results, however, showed that neither growth rates nor reproductive activities were improved in *Botryllus* chimeras as compared to single colonies or rejecting partners (Rinkevich and Weissman, 1992a). It should also be taken into consideration that the above results may be the outcome of a chaotic situation within the chimeras in which free circulating germ cell primordia are positioned haphazardly within the developing gonads. This possibility may be critically evaluated by establishing possible hierarchial relationships for gametic positions in *Botryllus* chimeras. The surprising result that even after a complete resorption of one partner in the chimera, the resorbed genotype may continue to thrive, not only in the form of germ cells but also as an integral part of the "winner's" soma, may further suggest that the Fu/HC (Weissman *et al.*, 1990) and the resorption-histocompatibility (Re/HC; Rinkevich, 1993) loci that are very effective in self-nonself discrimination of many already determined cell lineages do not distinguish (or do not activate the effector arm against) the most important group of the stem cells. In such a scenario, the freely circulating stem cells may uninterruptedly differentiate into both gametes and somatic tissues throughout the life span of the original chimera and its corresponding subclones, which are created by splitting the chimera into fragments. Different subclones probably possess unlike proportions of the mixed genotype's stem cells, which may result in the variations observed for the chimeric constituents of both soma and gametes. Therefore, more attention should be paid to possible interactions between different lines of stem cells (such as the displacement of one at the expense of another) rather than to the idea of somatic germ cell parasitism in the context of the evolution of somatic tissue compatibility (Buss, 1982; Buss and Green, 1985; Rinkevich and Weissman, 1987a; Grosberg, 1988).

Within *B. schlosseri* chimeras, transferred cells between genotypes may persist for many blastogeneic generations as circulating elements before maturing as sperm or eggs (Sabbadin and Zaniolo, 1979; Sabbadin and Astorri, 1988). In *B. schlosseri*, therefore, stem cells are probably the level at which natural selection could act, rather than,

as believed, at the colony level (Tuomi and Vuorisalo, 1989). By using molecular markers, such as microsatellites, new discoveries can shed more light on the evolutionary processes that shaped chimerism and the detailed consequences of fusion between compatible allogeneic organisms.

Acknowledgments

We are grateful to R. K. Grosberg and D. Stoner for critically reading the manuscript, to R. Pancer for editing a first draft of the manuscript, and to Elul productions for graphic assistance. This study was supported by a Career Development Award to B.R. from the Israel Cancer Research Foundation—U.S., a grant from the U.S.–Israel Binational Science Foundation, and a grant from S. Price, NAF/IOLR.

Literature Cited

Berrill, N. J., and C. K. Liu. 1948. Germ plasm, Weissmann, and Hydrozoa. *Q. Rev. Biol.* **23:** 124–132.

Boyd, H. C., S. K. Brown, J. A. Harp, and I. L. Weissman. 1986. Growth and sexual maturation of laboratory-cultured Monterey *Botryllus schlosseri*. *Biol. Bull.* **170:** 91–109.

Buss, L. W. 1982. Somatic cell parasitism and the evolution of somatic tissue compatibility. *Proc. Natl. Acad. Sci. USA* **79:** 5337–5341.

Buss, L. W. 1983. Somatic variation and evolution. *Paleobiology* **9:** 12–16.

Buss, L. W., and D. R. Green. 1985. Histoincompatibility in vertebrates: the relict hypothesis. *Dev. Comp. Immunol.* **9:** 191–201.

Clark, J., and O. R. Collins. 1973. Directional cytotoxic reactions between incompatible plasmodia of *Didymium iridis*. *Genetics* **73:** 247–257.

Davis, R. 1959. Asexual selection in *Neurospora crassa*. *Genetics* **44:** 1291–1308.

Dawkins, R. 1990. Parasites, desiderata lists and the paradox of the organism. *Parasitology* **100:** S63–S73.

Grosberg, R. K. 1988. The evolution of allorecognition specificity in clonal invertebrates. *Q. Rev. Biol.* **63:** 377–412.

Grosberg, R. K., and J. F. Quinn. 1986. The genetic control and consequences of kin recognition by the larvae of a colonial marine invertebrate. *Nature* **322:** 456–459.

Hauenschild, C. von. 1956. Uber die Vererbung einer Gewebevertraglichkeits-Eigenschaft bei dem Hydroidpolypen *Hydractinia echinata*. *Z. Naturforsch.* **11b:** 132–138.

Manni, L., G. Zaniolo, and P. Burighel. 1994. Ultrastructural study of oogenesis in the compound ascidian *Botryllus schlosseri* (Tunicata). *Acta Zool.* **75:** 101–113.

Michalakis, Y., I. Olivieri, F. Renaud, and M. Raymond. 1992. Pleiotropic action of parasites: How to be good for the host. *TREE* **7:** 59–62.

Mukai, H. 1992. Allogeneic recognition and sex differentiation in chimeras of the freshwater sponge *Ephydatia muelleri*. *J. Exp. Zool.* **237:** 241–255.

Muller, W. 1964. Experimentelle Untersuchungen uber Stockentwicklung, Polypendifferenzierung und Sexualchimaren bei *Hydractinia echinata*. *Wilhelm Roux Archiv* **155:** 181–268.

Pancer, Z. 1994. Somatic and gametic consequences of chimerism in the colonial protochordate *Botryllus schlosseri*. Ph.D. Dissertation, Technion—Israel Inst. Technol.

Pancer, Z., H. Gershon, and B. Rinkevich. 1994. Direct typing of polymorphic microsatellites in the colonial tunicate *Botryllus schlosseri* (Ascidiacea). *Biochem. Biophys. Res. Commun.* **203:** 646–651.

Queller, D. C., J. E. Strassmann, and C. R. Hughes. 1983. Microsatellites and kinship. *TREE* **8:** 285–288.

Rinkevich, B. 1992. Aspects of the incompatibility nature in botryllid ascidians. *Anim. Biol.* **1:** 17–28.

Rinkevich, B. 1993. Immunological resorption in *Botryllus schlosseri* (Tunicata) chimeras is characterized by multilevel hierarchial organization of histocompatibility alleles. A speculative endeavor. *Biol. Bull.* **184:** 342–345.

Rinkevich, B. 1995. Morphologically related allorecognition assays in botryllid ascidians. Pp. 17–21 in *Techniques in Fish Immunology, 4. Immunology and Pathology of Aquatic Invertebrates*, J. S. Stolen, T. C. Fletcher, S. A. Smith, T. J. Zelikoff, S. L. Kaattari, R. S. Anderson, K. Söderhäll, and B. A. Weaks-Perkins, eds. SOS Publications, Fair Haven, NJ.

Rinkevich, B., and I. L. Weissman. 1987a. Chimeras in colonial invertebrates: a synergistic symbiosis or somatic and germ parasitism? *Symbiosis* **4:** 117–134.

Rinkevich, B., and I. L. Weissman. 1987b. A long-term study of fused subclones of a compound ascidian. The resorption phenomenon. *J. Zool. (Lond.)* **213:** 717–733.

Rinkevich, B., and I. L. Weissman. 1989. Variation in the outcomes following chimera formation in the colonial tunicate *Botryllus schlosseri*. *Bull. Mar. Sci.* **45:** 213–227.

Rinkevich, B., and I. L. Weissman. 1992a. Chimeras vs genetically homogeneous individuals: potential fitness costs and benefits. *Oikos* **63:** 119–124.

Rinkevich, B., and I. L. Weissman. 1992b. Allogeneic resorption in colonial proto-chordates—consequences of nonself recognition. *Devel. Comp. Immun.* **16:** 275–286.

Rinkevich, B., Y. Saito, and I. L. Weissman. 1993. A colonial invertebrate species that displays a hierarchy of allorecognition responses. *Biol. Bull.* **184:** 79–86.

Sabbadin, A., and C. Astorri. 1988. Chimeras and histocompatibility in the colonial ascidian *Botryllus schlosseri*. *Dev. Comp. Immunol.* **12:** 737–747.

Sabbadin, A., and G. Zaniolo. 1979. Sexual differentiation and germ cell transfer in the colonial ascidian *Botryllus schlosseri*. *J. Exp. Zool.* **207:** 289–304.

Saito, Y., E. Hirose, and H. Watanabe. 1994. Allorecognition in compound ascidians. *Int. J. Dev. Biol.* **38:** 237–247.

Scofield, V. L., J. M. Schlumpberger, L. A. West, and I. L. Weissman. 1982. Protochordate allorecognition is controlled by an MHC-like gene system. *Nature* **295:** 499–502.

Shenk, M. A. 1991. Allorecognition in the colonial marine hydroid *Hydractinia* (Cnidaria/Hydrozoa). *Am. Zool.* **31:** 549–557.

Taneda, Y., Y. Saito, and H. Watanabe. 1985. Self or nonself discrimination in ascidians. *Zool. Sci.* **2:** 433–442.

Tuomi, J., and T. Vuorisalo. 1989. Hierarchial selection in modular organisms. *TREE* **4:** 209–213.

Van de Vyver, G. 1988. Histocompatibility responses in freshwater sponges: A model for studies of cell-cell interactions in natural populations and experimental systems. Pp. 1–14 in *Invertebrate Historecognition*, R. K. Grosberg, D. Hedgecock, and R. K. Nelson, eds. Plenum, New York.

Van Valen, L. M. 1988. Is somatic selection an evolutionary force? *Evolut. Theory* **8:** 163–167.

Weissman, I. L., Y. Saito, and B. Rinkevich. 1990. Allorecognition histocompatibility in a protochordate species: Is the relationship to MHC semantic or structural? *Immun. Rev.* **113:** 227–241.

Reference: *Biol. Bull.* **189:** 113–119. (October/November, 1995)

Sexual Dimorphism and Niche Divergence in a Mid-Water Octopod (Cephalopoda: Bolitaenidae)

JANET R. VOIGHT

Department of Zoology, The Field Museum of Natural History, Roosevelt Rd. at Lake Shore Drive, Chicago, Illinois 60605

Abstract. In the translucent mid-water octopod *Eledonella pygmaea*, the posterior salivary glands that release proteolytic enzymes into the esophageal crop grow five times faster in males than in females. I suggest that the sexes vertically partition the water column and that large glands have evolved in males as a result of their deep-water habitat. Members of the species undergo ontogenetic vertical descent and are suggested to mate at the lower end of the adult depth range where receptive females signal males with light organs. Selection for increased fitness is inferred to result in females increasing their fecundity by feeding at the upper limit of the adult range and in mature males increasing their encounters with mates by living at depths where mating occurs. To further increase their fitness, mature males—despite occurring in a prey-limited habitat—must expend energy to visually detect potential mates, to travel over wide areas, and to attempt to copulate. To increase the energy available to them, males at depth may exploit bioluminescent prey. The large glands protect the translucent males from increased predation by physically blocking light emitted by bioluminescent prey in their crops, and by speeding digestion.

Introduction

Because it acts directly on sexually dimorphic traits, sexual selection, produced by interaction between the sexes, has been assigned a primary role in the evolution and maintenance of sexual dimorphism. Ecological factors contribute to, and theoretically drive, the evolution of sexual dimorphism but are rarely considered to be major factors in its evolution (Slatkin, 1984; Shine, 1989). Slatkin (1984) noted three ways in which ecological factors, produced by the interaction of members of each sex with the environment, could result in sexual dimorphism. Sexual dimorphism could evolve when a species has a dimorphic niche, due to sex-linked differences in ecological or social roles, when two or more optima exist for both sexes, or when very high competitive pressure results in divergence of the niches the sexes occupy, allowing resource partitioning. Selander (1972) argued that ecological factors are most likely to result in sexual dimorphism of the trophic organs, although this need not always be the case.

This paper describes sexual dimorphism in posterior salivary gland size in the mid-water octopod *Eledonella pygmaea* Verrill. Selection on males to find mates and on females to increase their fecundity is hypothesized to have led to sexually dimorphic niches. Dimorphism in the glands, which are thought to produce and release proteolytic enzymes (Boucaud-Camou and Boucher-Rodoni, 1983), is hypothesized to be due to the divergence of posterior salivary gland growth in males, as an ecological adaptation to their deep-water distribution.

Biology of Eledonella pygmaea *Verrill*

Members of the species *Eledonella pygmaea*, typical of the little-known bolitaenid octopods, occur at depths greater than 100 m in mid-latitudes (Thore, 1949). Members of the family Bolitaenidae descend in the water column as they mature. Although juveniles occur near the upper limits of the species range, larger individuals occur variably between depths of 500 and 3250 m (Thore, 1949; Young, 1978). Gravid and nearly gravid females are collected only from the deepest part of the species range, although brooding females are collected from shallow depths of the adult range. This distributional pattern led Young (1978) to conclude that mating occurs at the lower limit of the species depth range and that hatchlings are released near the upper limit of the adult distribution.

Received 2 September 1994; accepted 7 July 1995.

Fully mature males, defined as those carrying spermatophores (Mangold, 1987), have not to my knowledge been reported in the literature. Low-density salts contained in fluid-filled vacuoles in the arm and mantle musculature may allow the animals to approach neutral buoyancy (Denton and Shaw, 1961). The fluid in the muscles may also increase the translucence of the animals and their susceptibility to severe damage during trawl collection, a feature which precludes direct behavioral observations of the animals.

The general anatomy of the anterior digestive system is typical of incirrate octopods (Thore, 1949), all of which are predators. The esophagus and its diverticulum, the crop, lie on the dorsal surface of the digestive gland within the mantle cavity (Fig. 1). A pair of posterior salivary glands straddle the esophagus at the level of the crop diverticulum (Fig. 1); the anterior salivary glands are attached to the buccal mass. Two ducts, one from each posterior salivary gland, merge to follow the esophagus anteriorly to the buccal mass at the center of the arms. A second duct from each gland enters the crop diverticulum directly. The opening of the crop is muscular, but its saccular portion, in preserved specimens, is nearly transparent. As in all incirrate octopods, the dorsal viscera are covered by a sheath that carries chromatophore organs. The distribution of these organs is distinctive in bolitaenids; few chromatophore organs are broadly scattered over the dorsal crop, but chromatophore organs are densely packed over the stomach, just dorsal to the tip of the mantle.

Females of *E. pygmaea* and other bolitaenids develop a circumoral light organ at sexual maturity, apparently to attract potential mates (Robison and Young, 1981). The light organ is probably not used in feeding, first because the octopod could not see prey attracted to it, and second because the green color of the emitted light is thought to be ineffective in luring prey (Robison and Young, 1981). Females are not thought to feed after the circumoral light organ develops.

Mature females are characterized by the circumoral light organ and increased pigmentation on the web and arm crown (Rancurel, 1970, Plate II; Robison and Young, 1981). Females brooding eggs are characterized by a sealed buccal mass, a deep web, and deterioration of the digestive system (Young, 1972a; 1978). As females become senescent, their consistency becomes very gelatinous, parasites

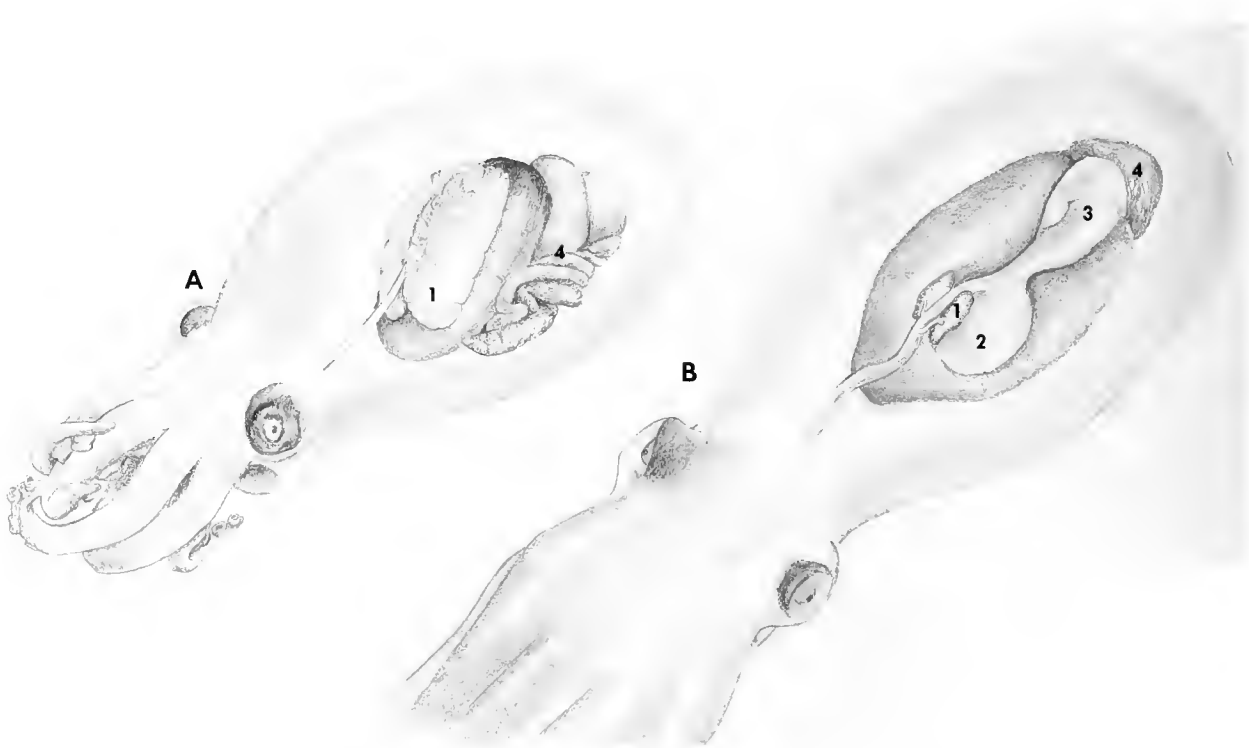

Figure 1. An oblique view of a male (A) and a dorsal view of a female (B) specimen of *Eledonella pygmaea*. The dorsal mantle has been removed in both specimens to show the esophagus entering the mantle cavity and the posterior salivary glands (1) on the dorsal surface of the digestive gland which, in the female (B), straddles the esophageal crop (2). (1) the posterior salivary glands; (2) esophageal crop, visible only in the female (B); (3) stomach, visible only in (B) after removal of the overlying membrane with its chromatophore organs; and (4) the gonad and (in A) the accessory male ducts.

become more prominent, and the digestive gland is reduced and becomes nearly transparent (Young, 1978; Voight, pers. obs.). Deterioration of the digestive organs supports the hypothesis that bolitaenids produce a single clutch of eggs, as is typical of octopods (Mangold, 1987). In addition, females probably brood their eggs in their arm crown until the eggs hatch (Young, 1972a). As the mouth is at the center of the arm crown, brooding eggs would be inconsistent with feeding.

In laboratory experiments, bioluminescence has been elicited from the digestive glands of 10 bolitaenid specimens, collected near Oahu, Hawaii, and identified as *E. pygmaea* and *Japetella diaphana* (Young *et al.*, 1979). The digestive glands of "most specimens of both species" (Young *et al.*, 1979: p. 74) examined were reported to emit detectable light, but neither the gills ($n = 3$) nor the stomach ($n = 1$) did so. Unfortunately, neither the sex nor the feeding status of the bioluminescent bolitaenids was reported.

Materials and Methods

Sixty specimens of *Eledonella pygmaea* (Table I) that share meristic characters of the gill lamellae and suckers are the basis of this study. The sex of each specimen was determined by internal examination: males were identified by the presence of a single genital duct and females by the presence of paired genital ducts; the sex of one individual could not be determined. *G*-tests were used to determine whether the sex composition of the sample differed from unity and whether the presence of senescent females and of juveniles significantly differed with the month of the year. A Wilcoxon two-sample test was used to look for significant size differences between the sexes.

Because accurate measurement required that the specimens be dissected, only 40 of the comparatively rare specimens were measured for this analysis. The 11 measurements recorded included dorsal mantle length, from the midpoint between the eyes to the posterior tip of the mantle; mantle width, measured with the calipers touching the digestive gland through the mantle wall; head width, the maximum width of the head including the eyes; digestive gland length, the maximum length of the organ; posterior salivary gland length, tip to tip on the dorsal surface on the left gland; pupil length, along its longest axis; eye length, along its greatest axis; and arm length, from the first sucker to the arm tip on the oral surface. Arm lengths were averaged within each of the four arm pairs. Additional characters, such as esophageal crop diameter, were not measured because preservation bias caused by the presence or absence of food in the crop at fixation violated assumptions implicit in the application of morphometric analyses to soft-bodied organisms (Voight, 1991) and because clearly defined endpoints on which to base the measurements are absent. In this analysis, preserved specimens of a wide range of sizes are included.

Data were transformed to natural logarithms (ln), a technique that preserves allometries, standardizes variances, and produces a scale-invariant covariance matrix (Jolicoeur, 1963). The ln-transformed data were entered into a principal components analysis (hereafter referred to as PCA) using PROC FACTOR in SAS (SAS Inst., 1987); and principal components (hereafter termed PC)

Table I

Summary of information for the lots of specimens examined: museum catalog number, collection locality, number of specimens, and collection date and depth

Museum number[1]	Latitude (°N)	Longitude (°W)	*N*	Collection month, year	Depth (m)
FMNH 78332**	32°13.3′	64°37′	2	August 1948	730–820
FMNH 278057	32°13′	64°40.5′	1	July 1948	1953
USNM 792006**	32°04′	63°58′	29	August 1971	0–1025
FMNH 78333	32°	64°51.7′	1	July 1948	1000–1100
UMML 31.2564	29°4′	87°37′	1	April 1961	186
UMML 31.171	28°58′	88°00′	1	October 1953	1544–1730
UMML 31.2030*	26°30′	90°42′	1	July 1959	2790
UMML 31.2031*	23°35.25–36.3′	76°54.25–55.1′	1	April 1975	1000
UMML 31.2032	23°59.7–24°1.2′	75°46.75–47.5′	1	November 1974	1900
UMML 31.2033*	23°38.0–40.5′	76°52.4–55.25′	1	August 1975	1000
UMML 31.1701*	23°12.6	90°44.1′	3	November 1975	2000
UMML 31.2207	21°56.3–51′	65°4.0–64°57.5′	1	July 1971	1000
UMML 31.2565	19°16′	65°51′	2	July 1971	7282–7363

[1] FMNH = The Field Museum of Natural History; UMML = The University of Miami Marine Laboratory; USNM = The United States Museum of Natural History.

* Lots with one senescent female; ** lots with two senescent females.

were computed from the covariance matrix (*e.g.* Strauss, 1985). The algorithm requires that individuals without complete data be deleted; due to trawl damage, the number of specimens contributing to the multivariate analysis was limited to 35: 11 males, 23 females, and one unknown.

PCA is a powerful multivariate technique that examines patterns of morphological variation regardless of *a priori* group definitions. Because culturing individuals through the life cycle and analyzing their growth at regular intervals is impossible in this species, this analysis uses each preserved specimen as a proxy for the species at that size. In this manner, analysis of museum specimens quantifies allometric patterns. Analysis of specimens of a wide size range, as in this case, is predicted to reveal that size contributes most morphological variation observed. All measurement data from each specimen entered in the analysis are predicted to reflect, to a greater or lesser extent, the specimen's size, as the parts are expected to increase with increasing size. PCA identifies this unique pattern of strong positive covariance among the characters it analyzes as overall size. This size variation is assigned to a component, usually PC1, that can be recognized by the uniformly large positive loadings of each character. Partitioning size to a single component allows the analysis to consider shape variation without the confounding effects of size. The absolute value of the loading of each character on each component identifies how that character contributes to size (on PC1) and shape variation (on subsequent components). Each specimen is assigned a score on each component; the score signifies its position on that component relative to the others in the analysis.

When PCA revealed that a single measurement—posterior salivary gland length—contributed most size-free shape variation, the natural logarithm of that measurement was plotted against ln mantle length to express the shape variation of the gland in two dimensions. This procedure also increased the number of specimens (12 males and 28 females) contributing to the calculation of the equation of the line describing the growth of the character in members of each sex relative to mantle length.

The distribution of chromatophore organs on the sheath superficial to the crop was compared between males and females, as was the transparency of the sheath. The esophageal crops of nine individuals were opened and their contents examined. To test whether the olfactory papillae (the paired, fan-shaped papillae projecting from the lateral edges of the mantle opening) are sexually dimorphic, as olfactory organs frequently are in fishes from depths of 1000–4000 m (Marshall, 1967), the maximum dimension of the right olfactory papilla was plotted against mantle length for 7 male and 10 female specimens. The papillae detect water-borne chemicals in squids (Gilly and Lucero, 1992); whether the organs function in this manner in octopods is yet to be demonstrated.

Results

As predicted, size contributed most (82.0%) of the morphological variation revealed by PCA (Table II). One measurement, posterior salivary gland length, contributed most of the size-free shape variation (8.48% of the total morphological variation). This variation is due to differences between males and females, as is evident when individual scores on PC2 (size-free shape variation) are plotted against PC1 (overall size variation) (Fig. 2). Digestive gland length contributed most to shape variation on PC3, due largely to data from a single senescent female.

The dimorphism is evident in individuals with mantle lengths greater than 18 mm (Fig. 3). The growth rates of the posterior salivary glands relative to mantle length differed strongly between the sexes. The positively allometric growth of male posterior salivary gland length (PSG) relative to mantle length (ML), with both expressed as natural logs (ln), is described by the equation:

$$\ln \text{PSG} = 2.3\ (\ln \text{ML}) - 4.97.$$

The allometric coefficient of posterior salivary gland length in females is one-fifth of the gland's coefficient in males; its negatively allometric growth is described by the equation:

$$\ln \text{PSG} = 0.46\ (\ln \text{ML}).$$

The dimorphism of posterior salivary gland size appears to correlate with qualitative characters. Although the dis-

Table II

Loadings of each of the 11 characters on the first three principal components (PC) from the analysis of 35 specimens of Eledonella pygmaea

Character	PC1	PC2	PC3
Mantle length	0.941	−0.007	0.178
Mantle width	0.903	−0.135	0.151
Head width	0.950	−0.064	0.106
Digestive gland length	0.787	0.194	0.533
Posterior salivary gland length	0.531	0.834	−0.146
Pupil length	0.716	0.154	0.273
Eye length	0.890	0.015	0.255
Arm length I	0.975	−0.120	−0.092
Arm length II	0.968	−0.120	−0.132
Arm length III	0.984	−0.001	−0.116
Arm length IV	0.966	−0.138	−0.020
Total proportion of variation explained by each component:	82.00	8.48	3.74

PC1 represents overall size variation, as is indicated by the strongly positive loadings for each character. PC2 represents size-free variation in posterior salivary gland length, as is indicated by the character's singularly large loading on PC2. PC3 represents size-free variation in digestive gland length, as is indicated by its high loading.

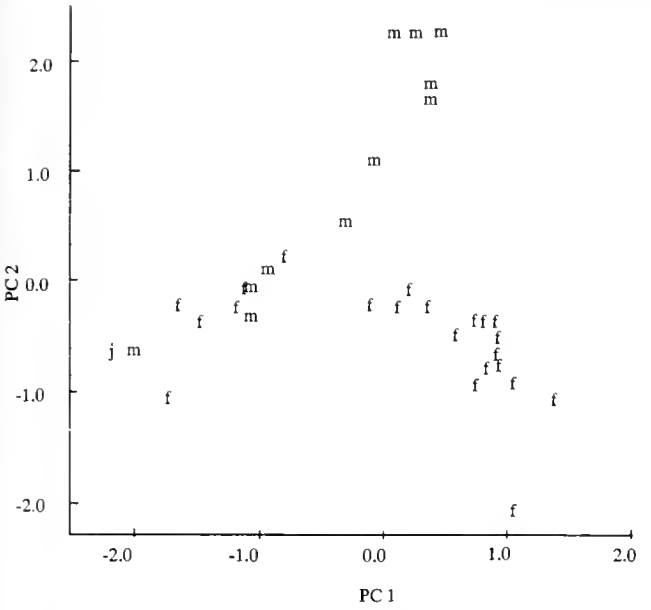

Figure 2. Specimen scores on principal component 2 (PC2) (representing size-free shape variation in posterior salivary gland length) are plotted against scores on principal component 1 (PC1) (representing overall size). m, male specimens; f, female specimens; j, specimen of unknown sex.

tribution of chromatophore organs on the sheath over the dorsal viscera appears to be very nearly the same in both sexes, the transparency of the sheath differs with sex. In preserved males, the silvery iridescence of the sheath effectively obscures the underlying organs; the sheath had to be removed to see the underlying posterior salivary glands that effectively cover the small crop (Fig. 1a). In females, the crop and its contents are readily visible through the sheath; the posterior salivary glands cover only the medial portion of the large crop (Fig. 1b).

The crops of three of the six males examined were empty; the crops of the three other males and all three females contained fish scales, parts of crustacean exoskeletons, and an apparently parasitic worm. The only prey item that was identifiable to species was a conspecific, identified by an arm, in the crop of a female.

The olfactory papillae of males and females were similar in size. Damage to the skin overlying the eye appeared to be associated with distortion of the papillae, regardless of the sex of the specimen.

The sex ratio was significantly female-biased (38 females to 21 males, $G = 4.97$; $p < 0.05$). Among the specimens examined, the incidence of individuals smaller than 10 mm mantle length did not significantly differ among the months for which samples were available ($G = 1.39$; $p > 0.05$). Of the specimens analyzed, those with the longest mantles, the traditional estimator of cephalopod size (Fig. 3), and with the highest PC1 scores (Fig. 2) were female. The PC1 scores of males and females did not, however, significantly differ (Wilcoxon two-sample test, $t = 1.49$; $p > 0.40$).

Eight of the 38 females examined appeared to be reproductively mature or nearing senescence. The largest ovarian eggs found in a female were 1.85 mm long, only 0.15 mm less than the longest egg definitively reported as being from a specimen of *Eledonella* (Young, 1978); no hatchlings were present. The incidence of senescent females did not significantly differ among the months for which samples were available ($G = 1.16$; $p > 0.05$). The collection depths of the post-brooding, senescent females are uninformative about the depth at which mating occurs. Among the male specimens examined, none were reproductively mature, *i.e.*, none contained spermatophores; but males with enlarged reproductive organs were found, and these were probably nearing sexual maturity.

Discussion

The growth rate, relative to the mantle length, of the posterior salivary glands is five times faster in males of *Eledonella pygmaea* than it is in females, and as a result, the glands of males are up to two-and-a-half times larger than those of conspecific females of similar size (Fig. 1). Relying on distributional data from Young (1978) and our limited biological knowledge of the species, I argue

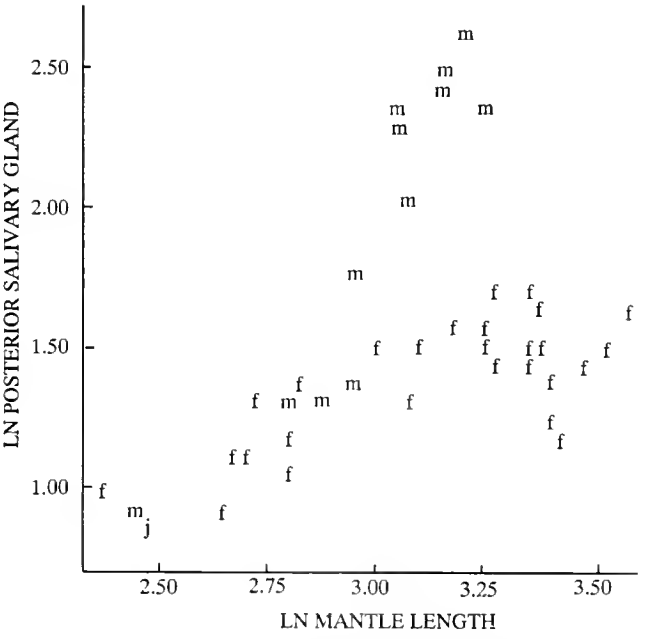

Figure 3. The natural logarithm (ln) of posterior salivary gland length is plotted against ln mantle length for 40 individuals of *Eledonella pygmaea*. m, male specimens; f, female specimens; j, specimen of unknown sex. For the equations of the lines describing the glands growth in males and females, see text.

that this sexual dimorphism results from the adaptation of males to their deep-water habitat. Further, I posit that inferred sex-specific selective forces are responsible for sexually dimorphic depth distributions.

To discuss the evolution of a character, its primitive condition must be established, and in this case, I consider small posterior salivary glands to be the ancestral condition. The Bolitaenidae appears to be the basal lineage of the suborder Incirrata (Voight, unpub. data). Members of the sister taxon, the suborder Cirrata, lack posterior salivary glands in the mantle cavity; the glands of the outgroup, the order Vampyromorpha, are very small (Young, 1964). Sexual dimorphism of the glands and the particularly large size they reach in males appear to be uniquely shared among bolitaenid species (Voight, unpub. data).

Given the difficulties in observing bolitaenids in nature, we must infer how selective pressures on males and females differ, as differences are required for sexual dimorphism to evolve. Selection acts to increase the depth distribution of males. A corollary to Young's (1978) hypothesis that bolitaenids mate at great depths predicts that mature males occur at those depths to increase the number of receptive females they encounter. Selection also acts to intensify the sensitivity of males to light cues and to increase male mobility. Because responding to a female's light cue increases a male's chances of mating (Robison and Young, 1981), males that are better able to detect bioluminescence will have higher fitness. To further increase the number of receptive females that they detect, males should be highly mobile. Males that move across broad areas are likely to see more mates than are males who search only locally. The absence of mature males from trawl collections (this study, $n = 60$; Young, 1978, $n = 80$), if due to net avoidance, supports the hypothesis of increased male mobility.

In females, selection acts to increase fecundity, a feature tightly linked to body size in cephalopods (Mangold, 1987). To grow large rapidly, females may remain in comparatively shallow depths where the crustaceans and fishes that females and juvenile males exploit as prey are more abundant. Females descend to greater depths only when ready to mate. Selection will not heighten sensitivity to bioluminescence or increase mobility in females, except to the extent that the traits are under selection in conspecific males.

The sex-specific selective forces outlined above suggest that the variability in size at which bolitaenids descend to adult depths documented by Young (1978) is sex-linked. Reproductively mature males occur at the lower end of the species' depth range; females occur at these depths only when ready to mate. If this hypothesis of habitat-partitioning between the sexes is supported, the evolution of large posterior salivary glands in males can be argued to relate to ecological factors.

As mature males descend in the water column, the abundance of familiar prey declines, and their energy costs may increase. Males must pay the metabolic costs thought to be associated with high visual acuity (Childress, 1995) if they are to detect mates. To meet these metabolic demands, maintain their capacity for high mobility, and prolong their survival in this habitat, I suggest that males use their visual acuity to exploit bioluminescent prey, which increases in abundance with depth.

The shift, with depth, to the selection of bioluminescent prey carries with it a major liability. A translucent bolitaenid risks predation if prey in its crop emits light. Enlarged posterior salivary glands, however, reduce the risk of predation in two ways. First, the large glands, and the iridescence of the sheath overlying the dorsal viscera, effectively cover the crop of males and would physically block light emitted from within it. Second, assuming that large glands release greater volumes of proteolytic enzymes than do small glands, large glands would speed the catabolism of bioluminescent chemicals.

One could argue that, if gland size correlates with the potency or volume of the proteolytic enzymes released, males with large glands would digest prey more quickly, lowering their energetic cost of swimming, but the digestive gland is a primary site of food absorption in cephalopods (Boucaud-Camou and Boucher-Rodoni, 1983). Therefore, if males were under selection to maintain constant body weight by speeding the digestion and absorption of prey, the digestive gland should also be dimorphic. PCA falsifies this prediction (Table II).

Alternatively, one could argue that females face a similar liability. Among octopuses, however, gravid females are rarely active predators. As their eggs enlarge, females typically reduce their feeding rates (Mangold, 1987). If this generalization holds true for bolitaenids, gravid females are not likely to ingest prey while near the lower limits of the species range. This physiological pattern also argues against sexual cannibalism as a routine strategy in the species. Although sexual cannibalism explains the presence of a conspecific in the crop of a female, so does the animal having fed in the trawl. Sexual cannibalism also explains the rarity of mature males, as does the hypothesis of increased male mobility.

The presence of sexually dimorphic posterior salivary glands was unsuspected in this taxon. This striking difference in the digestive system had been attributed to dissimilar nutritional states of the specimens (Thore, 1949) and to the existence of cryptic species (Young, 1972b). Indeed, sex-linked differences have not been noted in any of the taxonomically diverse deep-sea predators in which dark peritoneums or digestive organs have been suggested to camouflage bioluminescent prey (*e.g.*, vampyromorph

cephalopods, Pickford, 1949; fishes, McAllister, 1961). The rarity with which deep-sea animals such as these are seen in nature may limit our ability to document a sex-linked difference, especially if the sexes partition habitats, as suggested here.

If the posterior salivary glands camouflage ingested luminescent prey as effectively as this study indicates, direct observation of living animals may not detect their presence. Museum specimens collected incidentally in the previous half century through a variety of research efforts do, however, provide the anatomical and allometric data that are critical not only to documenting the patterns, but to generating this hypothesis of its evolution, including polarity assessment. Although the hypotheses could not have been generated using observations of live animals, the critical tests of the hypotheses—determining prey preferences and energetic costs experienced by males at depth—cannot be conducted on preserved specimens. Expanding the techniques we apply to the study of these rare deep-sea animals will increase our knowledge of one of the least-known habitats of the world, the mid-water depths, and provide evolutionary insight into questions of broad importance and biological complexity.

Acknowledgments

I thank David R. Pensgard for providing the illustrations, and N. A. Voss, the University of Miami Marine Laboratory, C. F. E. Roper, the United States National Museum, and F. Naggs, the Natural History Museum (London), for allowing me to study specimens in their care. R. E. Young, M. J. Brooks, and R. E. Strauss made helpful comments in the course of this research. Anonymous reviewers made very helpful comments to improve this paper. The research was supported by NSF DEB-9306925.

Literature Cited

Boucaud-Camou, E., and R. Boucher-Rodoni. 1983. Feeding and digestion in cephalopods. Pp. 149–187 in *The Mollusca* Vol. 5, A. S. M. Saleuddin and K. M. Wilbur, eds. Academic Press, New York.

Childress, J. J. 1995. Are there physiological and biochemical adaptations of metabolism in deep-sea animals? *Trends Ecol. Evol.* **10:** 30–36.

Denton, E. J., and T. I. Shaw. 1961. The buoyancy of gelatinous marine animals. *J. Physiol. (Lond.)* **161:** 14–15.

Gilly, W. F., and M. T. Lucero. 1992. Behavioral responses to chemical stimulation of the olfactory organ in the squid *Loligo opalescens*. *J. Exp. Biol.* **162:** 209–229.

Jolicoeur, P. 1963. The multivariate generalization of the allometry equation. *Biometrics* **19:** 497–499.

McAllister, D. E. 1961. A collection of oceanic fishes from off British Columbia with a discussion of the evolution of black peritoneum. *Nat. Mus. Can. Bull.* **172:** 39–43.

Mangold, K. 1987. Reproduction. Pp. 157–200 in *Cephalopod Life Cycles Vol. 2*, P. R. Boyle, ed. Academic Press, London.

Marshall, N. B. 1967. The olfactory organs of bathypelagic fishes. *Symp. Zool. Soc. Lond.* **19:** 57–70.

Pickford, G. E. 1949. *Vampyroteuthis infernalis* Chun. An archaic dibranchiate cephalopod. II External anatomy. *Dana Rep.* **32:** 1–132.

Rancurel, P. 1970. Les contenus stomacaux d'*Alepisaurus ferox* dans le sud-ouest Pacifique (Céphalopodes). *Cah. O.R.S.T.O.M. Sér. Océanogr.* **8(4):** 3–87.

Robison, B. H., and R. E. Young. 1981. Bioluminescence in pelagic octopods. *Pac. Sci.* **35:** 39–44.

SAS Institute, 1987. Cary, N. Carolina.

Selander, R. K. 1972. Sexual selection and dimorphism in birds. Pp. 180–230 in *Sexual Selection and the Descent of Man 1871–1971*, B. Campbell, ed. Aldine Publ. Co., Chicago.

Shine, R. 1989. Ecological causes for the evolution of sexual dimorphism: A review of the evidence. *Quart. Rev. Biol.* **64:** 419–461.

Slatkin, M. 1984. Ecological causes of sexual dimorphism. *Evolution* **38:** 622–630.

Strauss, R. E. 1985. Evolutionary allometry and variation in body form in the South American catfish genus *Corydoras* (Callichthyidae). *Syst. Zool.* **34:** 381–396.

Thore, S. 1949. Investigations of the 'Dana' octopoda: Bolitaenidae, Amphitretidae, Vitreledonellidae, and Alloposidae. *Dana Rep.* **33:** 1–85.

Voight, J. R. 1991. Morphological variation in octopod specimens: Reassessing the assumption of preservation-induced deformation. *Malacologia* **33:** 241–253.

Young, R. E. 1964. The anatomy of the vampire squid. M. S. thesis, University of Southern California, Los Angeles. 234 pp.

Young, R. E. 1972a. Brooding in a bathypelagic octopus. *Pac. Sci.* **26:** 400–404.

Young, R. E. 1972b. The systematics and areal distribution of pelagic cephalopods from the seas off southern California. *Smithson. Contrib. Zool.* **97:** 1–159.

Young, R. E. 1978. Vertical distribution and photosensitive vesicles of pelagic cephalopods from Hawaiian waters. *Fish. Bull.* **76:** 583–615.

Young, R. E., C. F. E. Roper, K. Mangold, G. Leisman, and F. G. Hochberg, 1979. Luminescence from non-bioluminescent tissues in oceanic cephalopods. *Mar. Biol.* **53:** 69–77.

Reference: *Biol. Bull.* 189: 120–127. (October/November, 1995)

Behavioral Control of Swash-Riding in the Clam *Donax variabilis*

OLAF ELLERS*

Department of Zoology, Duke University, Durham, North Carolina 27706

Abstract. Clams of the species *Donax variabilis* migrate shoreward during rising tides and seaward during falling tides. These clams spend most of the time in the sand, emerging several times per tidal cycle to ride waves. Migration is not merely a passive result of waves eroding clams out of the sand; rather clams actively jump out of the sand and ride specific waves. Such active migration is experimentally demonstrated during a falling tide by comparing the motion of dead and live clams: live clams emerge from the sand and move seaward even when dead ones do not. As low tide approaches, live clams become progressively less active. They cease migrating for 2 hours around low tide and resume jumping to migrate shoreward after the tide has turned. During the rising tide, far from being passive, the clams jump out to ride only the largest 20% of waves. Specifically, they choose swash that have the largest excursion, *i.e.*, those swash that move furthest on the beach.

Introduction

The coquina clam, *Donax variabilis*, lives on southeastern North American shores on coarse-grained, sandy beaches with moderate to high waves. *D. variabilis* migrates shoreward with the rising tide and seaward with the falling tide, as do many other animals that live on wave-exposed beaches (*e.g.*, other *Donax spp.*, mole crabs, mysids, gastropods, amphipods, and isopods: McLachlan *et al.*, 1979).

Migration by *D. variabilis* is accomplished in a series of steps. Most of the time, these clams stay in the sand. Several times per tidal cycle, each clam emerges from the sand and flow from waves drags it to a new position where it again digs in. I have named this method of locomotion "swash-riding" (Ellers, 1987, 1988), where swash-riding is the process of emerging from the sand, riding flow from a wave, and digging in again. Swash-riding does not necessarily lead to migration. For instance, *D. faba* swash-rides without migrating (McLachlan and Hesp, 1984), and a gastropod, *Bullia digitalis*, swash-rides and uses positive chemotaxis to locate moving prey in the surf and swash zones (Odendaal *et al.*, 1992). But in *D. variabilis*, a series of swash-rides usually becomes a migration. By migrating, a clam maintains its position at the sea's edge, *i.e.*, in the region of the beach that is alternately underwater and exposed to air every few seconds as waves arrive on the shore.

In the tumultuous milieu of breaking waves, eroding sand, and rip currents at the edge of such a beach, how much control do these clams have over their migrations? One reasonable hypothesis is that the clams are eroded forcibly out of the sand by waves during a falling tide and that they then must swash-ride shoreward during the incoming tide to maintain their intertidal location on the beach.

That hypothesis has some support. Jacobson (1955) suggested that *D. fossor* was migrating as the passive result of wave action. Wade (1967a) suggested that emergence of *D. denticulatus* into the backwash was usually a passive result of clams being washed out of the sand. Mikkelsen (1981) described two populations of *D. variabilis:* one population lived on a high-slope beach with relatively large waves and migrated; the other population lived on a low-slope beach with smaller waves and did not migrate. Beaches with lower slopes and smaller waves have been associated with non-migratory or partially migratory populations (*e.g.*, in *D. striatus:* Wade, 1967b; in *D. gouldii:* Irwin, 1973). Edgren (1959) described a population of *D. variabilis* that migrated only after a storm. Those

Received 9 September 1994; accepted 27 July 1995.

* Current address: Section of Evolution and Ecology, Division of Biological Sciences, University of California, Davis, CA 95616.

observations suggest that migration might be a passive, wave-driven process.

An alternative hypothesis is that the clams choose to migrate, behaviorally maintaining their position at the sea's edge. In this alternative view, clams are not usually washed out of the sand; rather they actively push themselves out using their feet. In this view, physical disturbance is neither the proximal nor the ultimate cause of migration. Instead, other ultimate causes are imaginable. Perhaps more filterable food is available in water stirred up by waves, and the clams are merely following the food. Many aspects of migration could be beneficial: avoiding predators, or avoiding the overheating that might occur if they remained behind in the intertidal during the falling tide. No specific ultimate cause for migration is advocated in the present paper; the main point is to distinguish between clams being forcibly dislodged by waves and clams actively emerging to ride waves.

In marine invertebrates there are many other migratory behaviors in which the relative contributions of active and passive determinants of net motion are important. For instance, the diurnal vertical migrations of brachyuran larvae may determine the direction of transport by currents: early larval stages spend nights in the neuston when land breezes tend to transport them offshore; later larval stages migrate down during the night hours, and surface currents from sea breezes thus tend to transport them onshore (Shanks, 1986). The net movement of hypothetical invertebrate larvae has been modeled in computer simulations that evaluated the relative influence and interaction of light- and tide-cued vertical migrations, swimming speed, turbulent mixing, and tidal and nontidal flows (Smith and Stoner, 1993); in specific tidal channels modeled, nontidal flows dominated the effect of vertical migration. For lobster larvae, a combination of directed swimming of fourth stage larvae and ocean currents was necessary to account for onshore recruitment (Katz *et al.*, 1994). Interactions of behavior and passive movement by flow are thus important to the biology of marine invertebrate larvae.

Passive movement by flows is not only important in the larval phase, but can also be significant in the juvenile or adult phases. The adults of a botryllid ascidian dispersed 200 times further by rafting in currents than did swimming larvae of the same species (Worcester, 1994). Further, adults of 17 mollusc species (with or without a planktonic larval phase) and an asteroid have been observed dispersing by rafting (Martel and Chia, 1991). In a tellinid bivalve, *Macoma balthica*, postlarval juveniles migrated to new tidal flat habitats by secreting long hyaline threads and being dragged by currents (Beukema and de Vlas, 1989), or by becoming positively buoyant and floating in currents (Sörlin, 1988). The latter is an inducible response to a combined stimulus of temperature change and water movement. In all these examples, animals achieve movement to new locations by a combination of behavioral and passive phenomena. In this and following papers (Ellers, 1995a, b) I investigate the relative contributions of passive and active factors to migratory movements of another tellinacean clam.

That *D. variabilis* clams choose to migrate in the shoreward direction is easily observed because, during rising tides, clams emerge from sand before an incoming wave reaches the location where they are buried. However, during the falling tide, clams emerge directly into the backwash; the question of whether this emergence is active or passive thus cannot be answered by direct observation, but can be addressed in a field experiment.

During the rising tide, when clams clearly choose to migrate, they might choose specific waves to ride, or they might merely jump in advance of random shorewardly moving waves. I present three field experiments: the first assesses whether clams actively jump out into the backwash during falling tides or are passively eroded by receding waves; the second observes clam behavior at low tide; the third demonstrates the degree to which these clams choose waves during the rising tide.

Materials and Methods

Location

All observations were made on sandy beaches near Pine Knoll Shores and Atlantic Beach, North Carolina. These beaches are on the outer coast of a barrier island, experience moderate to large waves, and have relatively coarse-grained sand. *D. variabilis* is densely but patchily distributed along the length of this island.

Behavior during the falling tide

To determine whether clams are eroded from the sand or actively push themselves out, paired dead and live clams were planted in the sand during a falling tide. Two hundred and thirty-four clams, killed by exposure to 30% alcohol, were marked with pink nail polish and planted in the beach, each one about 2 to 3 cm away from a live clam marked with red nail polish and similarly planted.

Locations of all the pink- and red-marked clams were designated with thin poles inserted into the beach. Poles were inserted sufficiently far from the planted clams that wave-caused erosion of sand around the poles did not excavate any experimental clams.

These clams were planted in four groups during a falling tide—4.0, 3.5, 2.5, and 1.5 h before low tide. They were planted in the wetted portion of the beach, *i.e.*, in the swash zone, amidst other, actively migrating, *D. variabilis*. At low tide, when the poles were high and dry, the sand adjacent to the poles was dug up and clams of each color

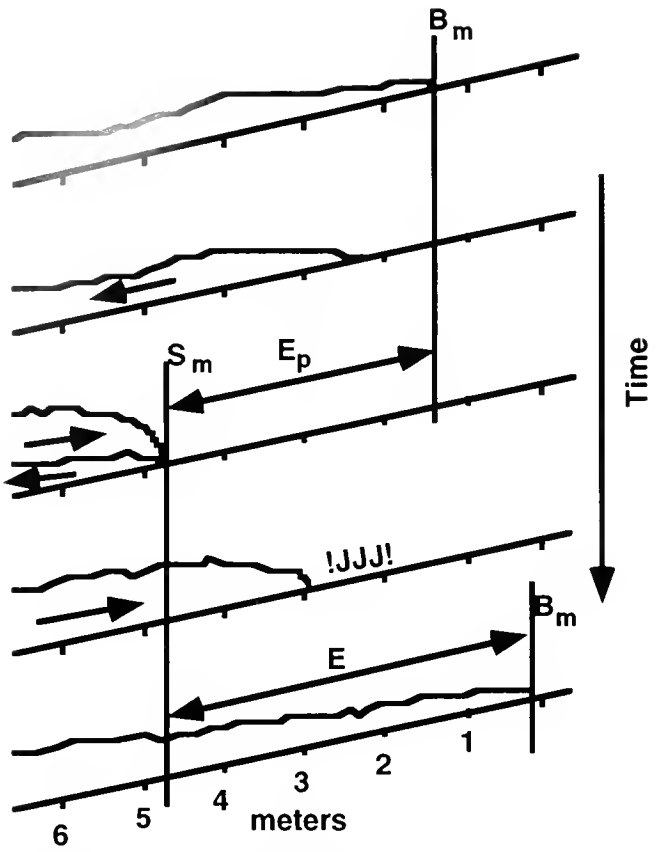

Figure 1. A smaller and then a larger wave on a beach, viewed in vertical section. Water directions are indicated with unidirectional arrows. !JJJ! indicates the place and time that clams might jump. The variables are (1) $\mathbf{B_m}$, the "beachward maximum," the position on the beach where the swash becomes backwash; (2) $\mathbf{S_m}$, the "seaward minimum," the position on the beach where the previous backwash meets the swash; (3) **E**, the "excursion of the swash," the distance that the swash moves in the shoreward direction after passing the previous backwash; and (4) $\mathbf{E_p}$, the "excursion of the previous backwash," the distance that the previous backwash moved in the seaward direction before passing the swash.

were counted. At the time they were planted, each group of clams had been divided topographically into subgroups of 4, 5, or 10 pairs of clams to facilitate subsequent statistical analysis (35 subgroups were created).

To test whether the erosion rates of dead clams in the above experiment were specific to the day on which that experiment was done, an additional 450 dead clams were planted during 6 different days over 3 summer months and the proportion remaining in their original locations was surveyed at low tide. This replication was done only with the dead clams because seaward movement of live clams during falling tides had been observed on hundreds of summer days during 3 years and was also documented in observations described in the next section.

One question that arises is whether marking live clams with nail polish itself influences the behavior of clams. Live clams handled and painted with nail polish, however, appeared to behave quite naturally after marking. A laboratory comparison of painted and unpainted clams showed similar burrowing speeds, similar emergence responses to knocking sound stimuli (see Ellers, 1995a, for an explanation of the stimulus), and similar siphon retraction responses to sudden light increases. Furthermore, field observations showed that marked clams released on the sand surface on the beach swash-rode and burrowed in a manner indistinguishable from naturally swash-riding clams. Finally, live marked clams were observed swash-riding on the beach up to 2 months after marking. Thus, the marking procedure itself did not appear to adversely affect the behavior of clams.

Behavior at low tide

On 6 summer days during 1985, transects were dug at low tide, perpendicular to the long axis of the beach. The number of clams found in a 30-cm by 30-cm area was recorded every meter along the transect. The average position of the water's edge at low tide was also recorded. Behavior of clams was observed during the period from 1.5 h before to 1.5 h after low tide.

Behavior during the rising tide

Flags, painted with numbers 1 through 35, were planted in a row perpendicular to the beach, in numerical sequence at 1-m intervals. Flags bracketed the area of the beach wetted by swash and backwash—the base of the most shoreward flag was always dry; the most seaward flag was always wet.

The sea's edge moves seaward and shoreward alternately as waves reach the shore, wash up on the beach, and run off the beach again. The location of the edge of the water was monitored by recording each beachward-maximum, $\mathbf{B_m}$, and seaward-minumum, $\mathbf{S_m}$, position (Fig. 1). Simultaneously, the activity of the clams was monitored. If clams jump, they do so after the water's edge has reached a seaward-minimum position and before the edge of the water reaches a new beachward-maximum position. Their behavior can thus be associated with a particular incoming swash.

Whether clams jumped for a particular swash was recorded during rising tides on 4 days in June and July. The excursion of the swash, **E**, and the excursion of the previous backwash, $\mathbf{E_p}$, were calculated by the appropriate subtractions of the relevant values of $\mathbf{B_m}$ and $\mathbf{S_m}$ (Fig. 1). Observations were started not less than 1 h after low tide and were halted no more than $2\frac{1}{2}$ h before high tide. Observations on any particular day were made continuously for 1 to 2 h (Table I).

Table 1

Numbers of observations, frequency of swashes, and frequency of jumping on each of the 4 days of observations

Day	# of Swashes	# of Jumps	Swashes/ Min.	Jumps/ Swash
1	294	69	4.2	0.24
2	379	85	4.9	0.22
3	602	74	5.2	0.12
4	481	149	5.3	0.31

Results

Behavior during the falling tide

In trials involving live and dead clams, 50%–80% of dead clams were not eroded from the sand by waves (Fig. 2). In experiments involving only dead clams, an average of 49% (range of 43%–100%) of the dead clams planted were not eroded from the sand; thus the trials with dead and live clams had typical erosion rates.

When dead and live clams were planted in pairs, a significantly larger proportion of live than dead clams left the sand in each of the four groups (Fig. 2). Only a tiny fraction, 4.7%, of live clams that were planted 4 and 3 h before low tide stayed in the sand in their original positions and were recovered at low tide. Significantly more, 30% to 50%, of live clams planted at 2 h before low tide stayed in the sand in their original positions and were recovered at low tide. Thus, as low tide approaches, more live clams stay in the sand. In contrast, dead clams planted close to the time of low tide washed out only slightly less often than clams planted closer to the time of high tide ($P = 0.05$, Mann-Whitney U-test).

Behavior at low tide

At low tide, the population was found at or just shoreward of the average position of the water's edge (Fig. 3). A large fraction of the population was often found in sand that was no longer being wetted by even the most shorewardly reaching swash. The location of the center of the population varied relative to the average position of the waves at low tide. On 14 May, for instance, most of the population was at the average position of the water's edge at low tide. In contrast, on 5 June, the population was 22 m shoreward of the water's edge.

Many clams had stopped migrating and were essentially stranded during the 1–2 h around the time when the tide turns. From 0.5 h before low tide until 0.5 h after low tide, no clams were seen jumping out of the sand. During the time from 0.5 to 1.5 h on either side of low tide, the numbers of clams seen jumping were relatively low compared to the numbers of clams seen jumping during the middle of the rising tides. Although quantitative results are given for just 6 days, I observed the same pattern of cessation of migration around low tide during the three summers, May through August, I watched clam behavior on North Carolina beaches.

Behavior during the rising tide

D. variabilis clams evidently chose specific waves. Swash arrived on shore at an average rate of 5.0 swashes per minute during 1755 observed swashes. Clams jumped for 20% of these waves (Table 1). On all 4 days, clams jumped for swash with relatively large excursion, **E** (Fig. 4A). Specifically, the clams jumped for a larger fraction of large than of small waves. The ratio C/T (where C is the number of swash chosen in a swash size-class and T is the total number of swash in that size class) is the proportion of the swash of a given size that the clams ride. C/T increases for increasing **E** on all 4 days.

The largest excursions of the swash are **E** = 14 to 18 m; the smallest are **E** = 1 to 4 m. Choosing waves could make a large difference in the net motion of clams. Clams can move much further shoreward for each swash-ride by jumping into the largest swash instead of the smallest swash. For comparison, the intertidal width that clams traverse is 40 to 50 m.

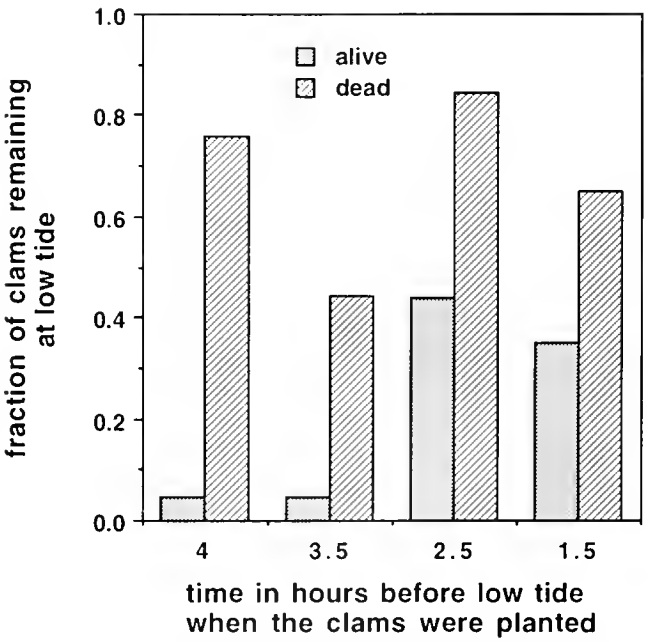

Figure 2. Fraction of dead and live *D. variabilis* remaining in the sand after being planted a certain number of hours before low tide. More live than dead clams leave the sand ($P < 0.01$), suggesting that live clams choose to jump out. Fewer live clams leave the sand close to the time of low tide than leave at mid-tide ($P < 0.01$), suggesting that clams reduce or halt migration just before the time of low tide. (Probabilities were calculated using Mann-Whitney U-tests.)

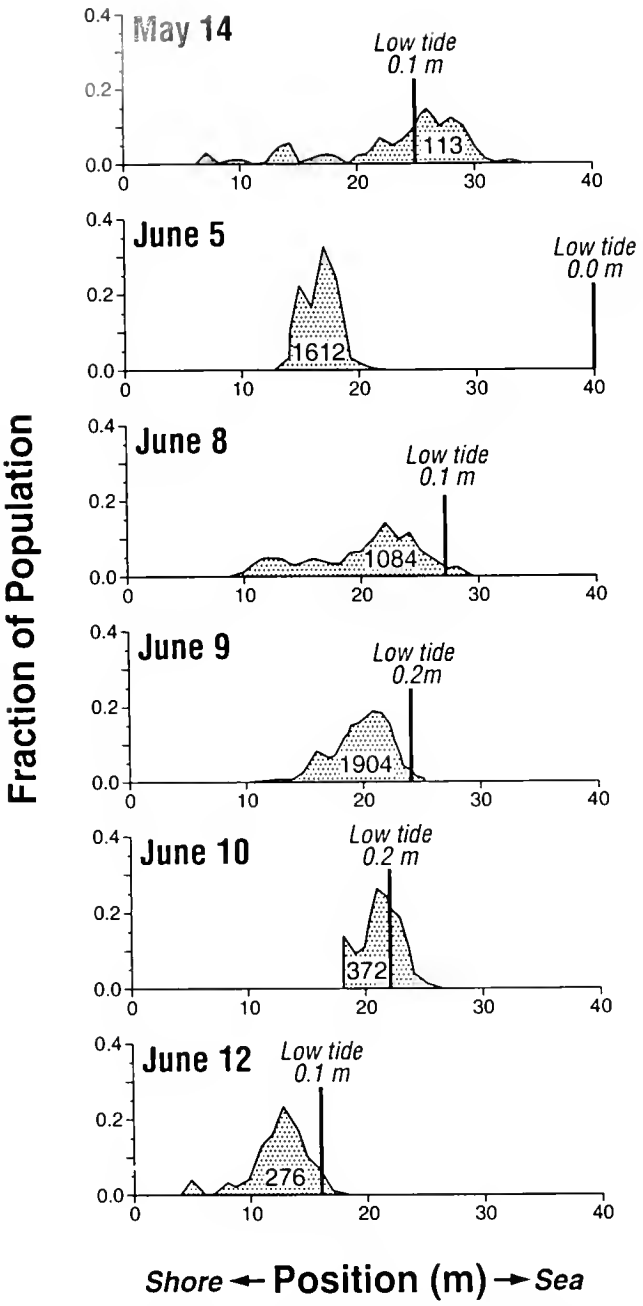

Figure 3. The fraction of the population found at each position along transects perpendicular to the shoreline, on a beach at low tide on several days. The vertical black bar marks the average position of the sea's edge at low tide. (The meter markers were not in the same location each day; the profile of the beach changes daily.) The vertical height of each low tide is given beside the vertical line. The total number of clams counted is given in the shaded area. Most days, the population is found shoreward of the sea's edge at low tide, out of reach of any swash. Usually, the clams do not migrate at all within 1 h of low tide.

Clams chose waves that moved relatively large distances in the shoreward direction. They jumped for such large swash before the swash reached them. How do they predict the size of incoming swash? One testable hypothesis is that there are patterns to the waves. For instance, if the size of incoming swash is correlated with the excursion of the previous backwash, then the excursion of the preceding backwash, $\mathbf{E_p}$, could be a cue. I found that $\mathbf{E_p}$ is not correlated with the next excursion of the swash, **E**, (R^2 = 0.07, 0.04, 0.28, 0.4, on the 4 days), so it would be a poor predictor of **E**. Indeed the clams are not using $\mathbf{E_p}$ since C/T does not increase with increasing $\mathbf{E_p}$ (Fig. 4B).

Two variables determine the excursion of the swash, **E**, the variables $\mathbf{B_m}$ and $\mathbf{S_m}$ (Fig. 1). On some days clams rode swash that moved significantly farther shoreward ($\mathbf{B_m}$) than swash they did not ride ($P < 0.0001$, F-test, multiple regression with dummy variables, Weisberg,

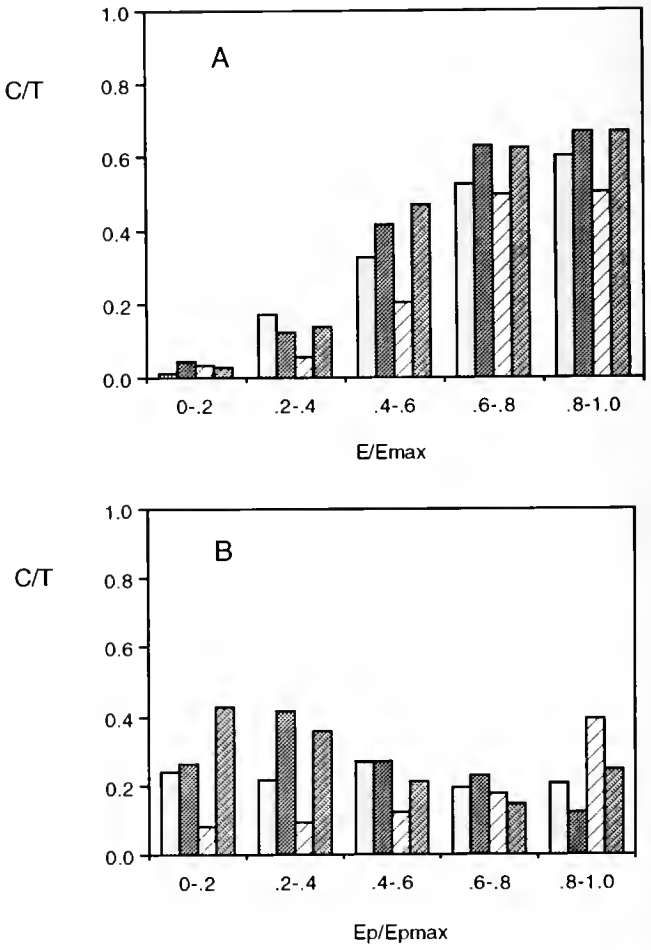

Figure 4. The proportion of swashes in size classes chosen for riding by clams. C/T is chosen waves divided by total waves in a wave size category. Different shading denotes 4 separate days of observations. (A) Half of the largest swashes (high $\mathbf{E/E_{max}}$) are ridden, whereas small swashes are almost never chosen. $\mathbf{E/E_{max}}$ is excursion divided by maximum excursion observed on a given day. (B) The proportion of chosen swashes having relatively large excursions of the previous backwashes (large $\mathbf{E_p/E_{pmax}}$). Swashes with large $\mathbf{E_p}$ are not chosen systematically. *D. variabilis* choose to ride swashes that have a large excursion, **E**, not swashes that have a large excursion of the previous backwash, $\mathbf{E_p}$.

1980). On other days, clams rode waves that started significantly farther seaward ($\mathbf{S_m}$) than swash they did not ride ($P < 0.0001$, same kind of test). Although on some days clams appear to be riding swash according to extreme values of $\mathbf{B_m}$ or $\mathbf{S_m}$ relative to the average $\mathbf{B_m}$ or $\mathbf{S_m}$ at that time, this pattern is inconsistent among days. In contrast, riding swash with large excursion ($\mathbf{B_m} - \mathbf{S_m}$ is applicable to all days.

Discussion

Comparison of the movements of dead and live clams planted in the sand shows that, during a falling tide, *Donax variabilis* clams actively emerge into the backwash, which then moves them seaward. Such active emergence contradicts the alternative hypothesis of a more passive role for *Donax spp.* during migration (see Introduction). For instance, it was suggested that *D. denticulatus* emerges from the sand passively to move seaward during the falling tide (Wade, 1967a). Wade suggested that a *D. denticulatus* clam would detect the increased drying of the sand as the tide receded and respond by retracting its foot and siphons, thus decreasing its purchase in the sand and enabling backwash to scour it from the sand and wash it seaward. In contrast, the current experiment shows that, for *D. variabilis* in the studied beach, mere retraction of the foot would not usually be sufficient to cause dislodgment by erosion (dead clams were dislodged only 50% of the time). In fact, live clams moved seaward much more often than dead clams, which suggests that live clams actively emerged from, or jumped out of, the sand. Indeed, I have observed jumping responses during times corresponding to falling tides in laboratory experiments on endogenous rhythms (Ellers, 1995a). Thus, I conclude that live clams of this species often actively push themselves out of the sand and into the backwash to be moved seaward by flow.

A series of such rides in the backwash becomes a seaward migration. If live clams relied on erosion to initiate their seaward rides in the backwash, only 20% to 50% of the population at a given location on the beach could move seaward (as did the dead clams, Fig. 2). Considering that a minimum of three swash-rides is required to complete a migration (minimum beach width divided by maximum excursion), the fraction of the population completing a seaward migration passively would be 0.008 to 0.125. Therefore, passive erosion could not be used to migrate seaward on these beaches. As a result of active seaward migration, almost the entire population has moved to the lower end of the intertidal at low tide (Figs. 2 and 3).

Erosion undoubtedly sometimes forces clams out of the sand. Erosive forces on a clam under the sand are occasionally larger than the force that a clam can exert with its foot (Ellers, 1988). Although erosion necessitates the ability to cope with (ride in) flow and to dig in again, it does not necessitate migration. *D. variabilis* use a systematic series of rides in the swash and the backwash to migrate.

This systematic series of seaward swash-rides in *D. variabilis* ends about 0.5 to 1 h before low tide. At that time the clams cease migrating and are left at or just shoreward of the edge of the sea at low tide (Fig. 3). Migration resumes about 0.5 to 1 h after low tide, with clams then moving in the shoreward direction. Others have also reported populations of *Donax spp.* that do not necessarily follow the water's edge to the low-water limit (see Introduction). In some populations, the location of the population on the beach at low tide follows a regular pattern. For instance, *D. serra* migrates following the position of the low-tide water table (Donn *et al.*, 1986). The water table is further seaward on the beach during spring tides than during neap tides. In laboratory experiments with *D. variabilis*, an endogenous rhythm has been observed in which a quiescent period occurs around the time of low tide (Ellers, 1995a). During that period, clams do not show jumping responses. The rhythm is thus a proximal cause of the systematic cessation of migration close to low tide in *D. variabilis*.

When migration resumes in the shoreward direction, many clams in the population can be seen simultaneously jumping out of the sand just shoreward of incoming waves. This behavior has been reported for *D. semigranosus* (Mori, 1938, 1950) and for *D. variabilis* (Turner and Belding, 1957). Not only do the clams jump in front of incoming waves, they jump only for the biggest waves. Several measures of wave size might be appropriate: wave height, breaker height, bore height, distance traveled, and maximum shoreward position that a swash wets.

My quantitative data show that, during the rising tide, these clams ride waves shoreward, using primarily the 20% of waves that move the largest distance in the shoreward direction. Those are not necessarily the swash that end their travels furthest shoreward; neither are they necessarily the swash that start the furthest seaward. The consequence of riding these largest swash is thus to be at neither the shorewardmost nor the seawardmost extent of the swash-zone. Rather, riding the biggest swash maximizes shoreward distance traveled and minimizes number of swash-rides per migration. In terms of absolute distance, the effect is remarkable—the clams can choose a swash that moves 18 m shoreward rather than the 1-m excursion of the smallest waves. By timing their active emergence from the sand, *D. variabilis* clams control their swash-riding.

The clams choose swash with large excursion, $\mathbf{E}$. But they jump before a shoreward swash reaches them. What cues the clams to jump for these swash? Swashes with large $\mathbf{E}$ are created on dissipative beaches by collapsing

bores of large height. The initial velocity, U_0, of the swash immediately following bore collapse is given by

$$U_0 = U' + 2\sqrt{g\,h'} \quad (1)$$

where U' is the speed of the bore front, h' is bore height, and g is gravitational acceleration. The excursion of the swash is

$$E = \frac{U_0}{g \tan \beta} \quad (2)$$

where β is the slope of the beach. Both the velocity and swash excursion on real beaches were within 10% of these theoretical predictions (Bradshaw, 1982). Thus if clams could detect the height of the bore, they could predict the swash excursion. Larger bores presumably make louder sounds as they collapse. If the clams listened to the sound of the bore, they could predict the excursion of the swash formed from it.

Anecdotal reports for *D. semigranosus* (Mori, 1938, 1950) and *D. variabilis* (Turner and Belding, 1957) suggest that during rising tides, sounds created by incoming waves cue the clams to emerge in front of swash. The present study demonstrates that clams emerge in front of swash with large excursion, and eqns (1) and (2) give a mechanism for linking sound production by an incoming wave to the production of a large swash excursion. I have demonstrated appropriate responses by *D. variabilis* to wave-like sounds in the laboratory in the absence of waves or other possible cues (Ellers, 1995a).

Behavior thus controls swash-riding and migration by *D. variabilis* on these beaches by controlling the timing of emergence of the clams from the sand. Morphology further controls a clam's motion while it is pushed by flow from waves (Ellers, 1995b).

Rather than being at the mercy of the tumultuous milieu of breaking waves, eroding sand, and rip currents at the edge of a beach, these clams make use of flows. Other animals such as mole crabs, some gastropods, and amphipods presumably use similar strategies on exposed beaches. Unlike the familiar paradigm for sessile organisms on rocky shores, in which organisms avoid dislodgment primarily by avoiding flow forces such as streamlining, etc. (Vogel, 1981; Denny, 1988), the parallel paradigm for organisms that live on shifting substrata is that they use flow forces for locomotion.

Acknowledgments

This research is part of the author's Ph.D. dissertation completed at Duke University. NSERC postgraduate scholarships, Duke University teaching assistantships, and a Cocos Foundation Training Grant in Morphology supported the author. The Lerner-Gray Fund for Marine Research (American Museum of Natural History) and a Grant-in-Aid of Research from Sigma Xi supported this project. I acknowledge the Duke University Marine Laboratory for use of its facilities. I am grateful to the many friends who selflessly volunteered to assist with field work on the beach. I also thank my thesis supervisor, S. Vogel, and committee members, V. L. Roth, E. J. Shaughnessy, V. A. Tucker, and S. A. Wainwright.

Literature Cited

Beukema, J. J., and J. de Vlas. 1989. Tidal-current transport of thread-drifting postlarval juveniles of the bivalve *Macoma balthica* from the Wadden Sea to the North Sea. *Mar. Ecol. Prog. Ser.* **52:** 193–200.

Bradshaw, M. 1982. Bores and swash on natural beaches. *Coastal Studies Unit Technical Report No. 82/4.* Coastal Studies Unit, Department of Geography, The University of Sydney, Sydney, NSW, Australia.

Denny, M. W. 1988. *Biology and the Mechanics of the Wave-Swept Environment.* Princeton University Press, Princeton, NJ.

Donn, T. E., Jr., D. J. Clarke, A. McLachlan, and P. du Toit. 1986. Distribution and abundance of *Donax serra* Röding (Bivalvia: Donacidae) as related to beach morphology. I. Semilunar migrations. *J. Exp. Mar. Biol. Ecol.* **102:** 121–131.

Edgren, R. A. 1959. Coquinas (*Donax variabilis*) on a Florida beach. *Ecology* **40:** 498–502.

Ellers, O. 1987. Passive orientation of benthic animals in flow. Pp. 45–68 in *Signposts in the Sea. Proceedings of a Multidisciplinary Workshop on Marine Animal Orientation and Migration,* W. F. Herrnkind and A. B. Thistle, eds. Dept. of Biological Science, Florida State University, Tallahassee.

Ellers, O. 1988. Locomotion via swash-riding in the clam *Donax variabilis.* Ph.D. Dissertation, Duke University, Durham, NC.

Ellers, O. 1995a. Discrimination among wave-generated sounds by a swash-riding clam. *Biol. Bull.* **189:** 128–137.

Ellers, O. 1995b. Form and motion of *Donax variabilis* in flow. *Biol. Bull.* **189:** 138–147.

Irwin, T. H. 1973. The intertidal behavior of the bean clam, *Donax gouldii* Dall, 1921. *Veliger* **15:** 206–212.

Jacobson, M. K. 1955. Observations on *Donax fossor* Say at Rockaway Beach, New York. *Nautilus* **68:** 73–77.

Katz, C. H., J. S. Cobb, and M. Spaulding. 1994. Larval behavior, hydrodynamic transport, and potential offshore-to-inshore recruitment in the American lobster *Homarus americanus. Mar. Ecol. Prog. Ser.* **103:** 265–273.

Martel, A., and F. Chia. 1991. Drifting and dispersal of small bivalves and gastropods with direct development. *J. Exp. Mar. Biol. Ecol.* **150:** 131–147.

McLachlan, A., and P. Hesp. 1984. Faunal response to morphology and water circulation of a sandy beach with cusps. *Mar. Ecol. Prog. Ser.* **19:** 133–144.

McLachlan, A., T. Wooldridge, and G. van der Horst. 1979. Tidal movements of the macrofauna on an exposed sandy beach in South Africa. *J. Zool., Lond.* **187:** 433–442.

Mikkelsen, P. S. 1981. A comparison of two Florida populations of the coquina clam, *Donax variabilis* Say, 1822 (Bivalvia: Donacidae). I. Intertidal density, distribution and migration. *Veliger* **3:** 230–239.

Mori, S. 1938. Characteristic tidal rhythmic migration of a mussel, *Donax semigranosus* Dunker, and the experimental analysis of its behaviour at the flood tide. *Dobutsugaku Zasshi,* [=*Zool. Mag. (Japan)*] **50:** 1–12.

Mori, S. 1950. Characteristic tidal rhythmic migration of a mussel, *Donax semigranosus* Dunker, and the experimental analysis of its

behaviour (II). *Dobutsugaku Zasshi* [= *Zool. Mag. (Japan)*] **59**: 87–89.

Odendaal, F. J., P. Turchin, G. Hoy, P. Wickens, J. Wells, and G. Schroeder. 1992. *Bullia digitalis* (Gastropoda) actively pursues moving prey by swash-riding. *J. Zool.* **228**: 103–113.

Shanks, A. L. 1986. Vertical migration and cross-shelf dispersal of larval *Cancer* spp. and *Randalia ornata* (Crustacea: Brachyura) off the coast of southern California. *Mar. Biol.* **92**: 189–199.

Smith, N. P., and A. W. Stoner. 1993. Computer simulation of larval transport through tidal channels: Role of vertical migration. *Estuarine Coastal Shelf Sci.* **37**: 43–58.

Sörlin, T. 1988. Floating behaviour in the tellinid bivalve *Macoma balthica* (L.) *Oecologia* **77**: 273–277.

Turner, H. J., Jr., and D. L. Belding. 1957. The tidal migrations of *Donax variabilis* Say. *Limnol. Oceanogr.* **2**: 120–124.

Vogel, S. 1981. *Life in Moving Fluids.* Princeton University Press, Princeton, NJ.

Wade, B. 1967a. Studies on the biology of the West Indian Beach clam, *Donax denticulatus* Linné. I. Ecology. *Bull. Mar. Sci.* **17**: 149–174.

Wade, B. 1967b. On the taxonomy, morphology, and ecology of the beach clam, *Donax striatus* Linné. *Bull. Mar. Sci.* **17**: 723–740.

Weisberg, S. 1980. *Applied Linear Regression.* John Wiley and Sons, New York.

Worcester, S. E. 1994. Adult rafting versus larval swimming: dispersal and recruitment of a botryllid ascidian on eelgrass. *Mar. Biol.* **121**: 309–317.

Reference: *Biol Bull* 189: 128–137. (October/November, 1995)

Discrimination Among Wave-Generated Sounds by a Swash-Riding Clam

OLAF ELLERS*

Department of Zoology, Duke University, Durham, North Carolina 27706

Abstract. Clams, *Donax variabilis*, responded to sound stimuli presented to them in a laboratory aquarium by jumping out of the sand, lying on the sand for several seconds, and digging in again. On a beach, clams jump out of the sand and ride waves, migrating shoreward with the rising tide and seaward with the falling tide. Parallels between clam behavior on a beach and that elicited in the laboratory suggest that clams cue on wave sounds to jump out of the sand. Three aspects of the response to sound were parallel. (i) Clams were most responsive to low-frequency sounds similar to those produced on a beach by waves rolling onto shore. (ii) Clams were also more responsive to louder sounds; on a beach, clams jump preferentially for the largest (loudest) 20% of waves. (iii) Responsiveness in the laboratory had an endogenous tidal rhythm, with highest activity occurring at high tide and no activity occurring at low tide; this rhythm corresponds to the activity of clams on the beach from which they were collected. By using sounds to identify large waves, clams can ride selected waves and continuously maintain position at the sea's edge as the tide floods and ebbs.

Introduction

Large populations of the coquina clam, *Donax variabilis*, migrate on sandy beaches, shoreward with the rising tide and seaward with the falling tide (as do many other clams in this genus). An individual *D. variabilis*, which can be up to 3 cm long, normally resides with the posterior edge of its shell about 2 to 7 mm under the surface of the sand. To migrate, several times each tidal cycle, it jumps out of the sand (pushing its shell upward by thrusting two to five times downward with its foot) and rides flow from waves. This method of locomotion has been named "swash-riding" (Ellers, 1987, 1988).

Individual *D. variabilis* control where waves move them, in part, by choosing to ride specific waves (Ellers, 1995a). On a rising tide, clams jump out of the sand preferentially for the biggest waves; *i.e.*, the ones that drag them the largest distance in the shoreward direction. Astonishingly, the clams jump out of the sand before the arrival of such waves, thus effectively predicting which waves will carry them the furthest. The cues that enable this behavior have not been previously investigated.

One explanation for this discriminatory and anticipatory feat is that clams might detect sounds from waves and use differences in the character of these sounds to select waves. Sound is a reasonable candidate as a cue that enables clams to discriminate among waves because a physical mechanism linking louder sounds to larger waves is plausible. On dissipative beaches where the clams live, a breaking wave becomes a bore (a traveling cliff-like structure of tumbling water) and the bore becomes swash, which the clams ride. The higher the bore, the larger the excursion of the swash (Bradshaw, 1982). Since a higher bore has more potential energy—it has farther to fall—it tends to create more intense vibrations as water falls off its leading edge, thus emitting a louder sound. Sound is also a reasonable cue that enables clams to anticipate waves since sound travels faster than, and in front of, the bore, thus announcing its arrival. Species of *Donax* respond to sound or vibration by either jumping out of the sand or burrowing more deeply (Mori, 1938, 1950; Loesch, 1957; Turner and Belding, 1957; Tiffany, 1971; Trueman, 1971), but no quantitative data describing either wave sounds or sounds that elicited responses from clams are available.

Reports of animals using flow-induced sounds as behavioral cues are very rare. Flow-induced low-frequency sounds and infrasounds emanate from weather patterns,

Received 9 September 1994; accepted 27 July 1995.

* Current address: Section of Evolution and Ecology, Division of Biological Sciences, University of California, Davis, CA 95616.

topographic features, and ocean waves; such sounds can travel thousands of kilometers. Birds are able to detect infrasounds and may be able to orient relative to such features because birds can detect Doppler shifts associated with flying away from or towards infrasound sources (Kreithen and Quine, 1979). Detection of low-frequency sound and infrasound has also been shown in fish (Karlsen, 1992a, b) and cephalopods (Packard *et al.*, 1990). The function of infrasound detection in these cases is unclear, but may be related to orientation, detection of surface waves, short-term inertial guidance, or detection of low-frequency flows (Bleckmann *et al.*, 1991) from swimming motions of other fish. Avoidance of continuously vibrating sound sources in darkness has been demonstrated in herring (Blaxter and Batty, 1985).

Sound is mechanical energy (created by a vibration) that propagates through a medium as a result of kinetic and potential energy being alternately stored and released elastically by the medium. Sound propagates either through the air or through the wet beach sand at the speeds of sound in those media. As the sound vibrations travel past a point, they are detectable as temporal changes in velocity, displacement, or pressure; the latter can be measured using a hydrophone.

To determine whether listening for and distinguishing among waves is possible under the sand, I recorded wave sounds by using a hydrophone planted under the sand amidst a population of burrowed *D. variabilis*. Then, in a laboratory, I tested whether clams would respond by jumping out of the sand when wave-like sounds were presented in the absence of waves. I also used recorded wave sounds and several artificial sounds of varying loudness and frequency to test the frequency and loudness specificity of clams' responses.

The above experiments must be considered in the light of suggestions of a tidal rhythm of responsiveness to sound. Behavior of *D. variabilis* on a beach changes with time of tide (Ellers, 1995a), and jumping responses to vibration were observed during rising tides only (Turner and Belding, 1957) or during all tidal phases (Tiffany, 1971). An endogenous rhythm was suggested for *D. semigranosus* (Mori, 1938, 1950). Tidal rhythms are often found in coastal marine invertebrates, particularly in crustaceans, molluscs, and polychaetes (for a review, see Naylor, 1985). An endogenous tidal rhythm of shell gaping has been documented in a venerid clam (Williams *et al.*, 1993). Therefore, I also tested for an endogenous tidal rhythm of responsiveness to sound.

Materials and Methods

Specimens

Immediately preceding each laboratory experiment, fresh *Donax variabilis* were collected from a beach (subsequently "the" beach) near Pine Knoll Shores on the seaward side of Bogue Bank, a barrier island off North Carolina. The clams were transported with sand and seawater in a thermally insulated container to the Duke University Marine Laboratory, a half-hour drive from the beach. (An insulated container is crucial; if clams heat up even slightly in transit, they subsequently show no behavioral responses.) Clams were placed in an aquarium, where they dug into sand.

General acoustic tests and analyses

Acoustic tests in the laboratory were done in a glass aquarium (50 cm long by 26 cm wide by 30 cm high) placed on a plywood table. The bottom 8 cm of the aquarium was covered with sand from the beach, and seawater was added to a depth of 28 cm.

Sounds were produced in several ways. Knocking with knuckles on the plywood table produced a low-frequency sound. In addition, sounds were produced using an underwater loudspeaker (20 cm diameter) made of polystyrene foam. The loudspeaker, located 10 cm from one end of the aquarium and partially buried in the sand, was driven by a tape recorder. Sounds played were either recorded from waves on the beach or synthesized by a sine wave generator circuit.

To determine the sound pattern reaching the clams, sounds were recorded by hydrophones buried in the sand at various locations in the aquarium. The signal from the hydrophone was amplified and digitized (8-bit resolution) at a sampling rate of 8192 Hz. This sampling rate allows detection of sounds below 4096 Hz. Higher sampling rates were unnecessary because very little sound was detected at higher frequencies when higher sampling rates were tried.

To analyze the data, several standard methods were used. Sound pressure was plotted as a function of time. The pressure functions were transformed into frequency spectra in which sound amplitude is plotted as a function of frequency. This transformation was performed using a Fast Fourier Transform (FFT) computer algorithm (Burrus and Parks, 1985, p. 107). The FFT algorithm produces a complex number for each frequency; the amplitude at each frequency interval is twice the absolute value of that complex number divided by the square root of the number of samples. Frequency resolution is the reciprocal of the time interval sampled (a 0.5-s sample of sound resolves into 2-Hz intervals).

I represented loudness of sound as either the root-mean-square (RMS) of the pressure trace over an interval of interest or as the logarithm of that value. Loudness is a subjective concept; because humans judge the relative loudness of two sounds as the ratio of their intensities, loudness is often represented using a logarithmic (decibel)

scale (Kinsler *et al.*, 1982). One conventional measure of sound levels is the intensity level (*IL*):

$$IL = 10 \log_{10}\left(\frac{I}{I_{\text{ref}}}\right) \quad (1)$$

where I is the measured intensity and I_{ref} is a reference intensity. Intensity is the rate at which sound energy flows through a unit area. But for both plane and spherical waves,

$$I = \frac{P_e^2}{\rho c} \quad (2)$$

where P_e = RMS sound pressure, ρ = density, and c = the speed of sound in the medium in which the sound is traveling. Although an approximate speed of sound in wet sand is obtainable from the literature, the exact speed of sound in the wet sand in the present experiment is unknown. Therefore, I present P_e rather than the derived quantity, I.

Furthermore, it is not clear, *a priori*, that clams should respond logarithmically to sound. Therefore, I present all data numerically as either pressure or P_e, but relative loudness is assumed to be represented by the ratios of the P_e values (reflected in a logarithmically transformed P_e axis in graphs that include several sounds). I also give the following conversions to a common measure called the sound pressure level, SPL:

$$\text{SPL} = 20 \log_{10}\left(\frac{P_e}{P_{\text{ref}}}\right) \quad (3)$$

where P_{ref} = a reference pressure. For instance, a P_e of 200 Pa has an SPL of 200 dB re 1 μ Pa, whereas a P_e of 1 Pa has an SPL of 120 dB re 1 μ Pa.

Wave sounds recorded under the sand on a beach

Sounds of waves approaching the shore were recorded on the beach during several summer days. A hydrophone was buried amidst the clam population at the same depth (2–7 mm) to which these clams burrow.

The hydrophone was attached to a tape recorder that had two input-channels: one channel recorded wave sounds; the other channel simultaneously recorded an observer's verbal description of the waves. Wave sounds were thus matched with particular events in the waves. Wave sounds were plotted as pressure *versus* time or as frequency spectra calculated from 0.5-s intervals starting between 0.5 and 1 s before the arrival of swash at the hydrophone.

Tidal variation in responsiveness of clams to sounds

Clams were collected from the beach, transported to the laboratory, and placed in the aquarium. There they were exposed to natural light and dark cycles through a large window on one side of the room, but the fluorescent room lights were kept on constantly day and night to allow observation of clam behavior. About once each hour for several days, sounds were produced by knuckle knocking that was continued until no new clams emerged for 30 s. The number of clams emerging in response to each knocking stimulus was counted. A hydrophone planted in the sand in the middle of the aquarium recorded the sounds for subsequent spectral analysis. This protocol was repeated for several collections of between 100 and 170 clams each.

Collections were made on two types of days. During the first type, high tide was between noon and midnight and between midnight and noon; during the second type, high tide coincided with midnight and noon. Thus the two types of days have noon and midnight falling either in or out of phase with high tide. Comparison of temporal patterns of responsiveness on the two types of days indicates whether there is a tidal or a daily rhythm of responsiveness.

A second experiment was performed according to the same protocol except that the window was blocked off, excluding sunlight and moonlight, and the room lights were turned off except for a few seconds during sampling periods.

Clams' responsiveness to sounds from waves

Clams were collected from the beach and placed in the aquarium in front of the speaker, where they dug into the sand. Recorded sounds of waves approaching the beach (about 200 successive swash) were presented to these clams during a 45-min period starting around the time of high tide. Clam responses were observed. A hydrophone in the sand 5 cm in front of the speaker monitored the loudness of the stimuli reaching the clams. This protocol was repeated on three summer days in an experiment involving a total of 210 clams.

Frequency and amplitude specificity of responses

To test specificity of responses to sounds, I subjected clams buried in the sand in the aquarium to specific synthesized sound stimuli of different frequencies and loudnesses. Sounds were presented using the underwater loudspeaker. Sounds were (i) broadband low-frequency sound, (ii) a pure low-frequency tone (with quieter, higher frequency harmonics), and (iii) a pure high-frequency tone (with quieter, higher frequency harmonics). Each presented sound was recorded by a hydrophone buried in the sand 5 cm in front of the speaker. The RMS sound pressures (P_e) and frequency spectra were calculated.

Eighty clams were collected on the beach 30 min before high tide, transported to the laboratory, and placed hap-

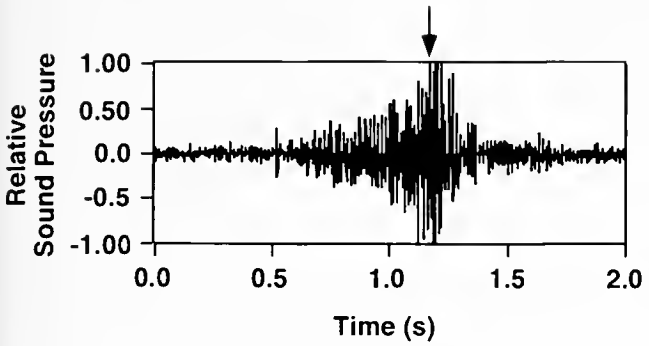

Figure 1. The sound of a wave approaching a beach as recorded from a hydrophone buried in the sand amidst the clams. Sound is represented as pressure *versus* time, with larger excursions of the pressure trace representing louder sounds. Relative sound pressure is relative to the highest pressure occurring in this trace. During the time preceding a wave's arrival at the hydrophone, a low-frequency rumble of increasing loudness is heard, culminating in a sudden increase in loudness when the wave reaches the hydrophone (arrow). Between waves there is relative silence.

hazardly in the aquarium, between the front of the speaker and the far end of the aquarium. Sounds were played to the clams during a 35-min period starting 10 min after high tide.

The sounds were presented to the clams at regular intervals (1 min silence between presentations); the signal was always of 22 ± 1 s duration. Each sound was played at a variety of intensities seven times in a row. The high-frequency signal was played first, then the broadband low-frequency signal, then the pure tone low-frequency signal. The number of clams jumping out of the sand for each stimulus was recorded. Significances of differences in responses were analyzed by regression analysis with dummy variables (Weisberg, 1980). (Statistical significance, throughout this paper, is considered to occur when the probability that the null hypothesis is true is less than 0.05.)

On two other days, additional experiments were performed according to a protocol that was identical except for the following. Instead of the three stimuli described above, a variety of synthesized low-frequency stimuli in the range of 20–100 Hz were presented. The stimuli were presented at irregular, more widely spaced intervals in random order and over a longer period of time (starting 40 min after and ending 3 h and 15 min after high tide). The number of clams responding was analyzed as a function of loudness, log (P_e), and time after high tide.

Attenuation of sound and frequency responsiveness

The results of the experiments on frequency and amplitude specificity must be interpreted relative to the frequency-specific attenuation of sound. Attenuation in the aquarium was measured by placing a hydrophone in the sand at 4, 10, 20, 30, and 40 cm in front of the speaker. Four pure tones, covering the range of frequencies used as stimuli, were individually played by the speaker. Attenuation of sound was calculated for each as the ratio of P_e at each distance divided by P_e at 4 cm from the speaker.

Results

Wave sounds recorded under the sand on a beach

Recorded wave sounds had characteristic patterns of loudness and frequency. A bore approaching the shore made a low rumbling sound that became louder as the bore approached the hydrophone (Fig. 1). Bigger bores made louder sounds than smaller ones as they approached the hydrophone. The rumbling noise of an approaching bore consists predominantly of low frequencies ranging from 40 to 300 Hz, with the largest amplitudes being in the range of 60 to 100 Hz (Fig. 2A).

When a bore or swash reached the hydrophone, there was an additional sudden increase in loudness (arrow in Fig. 1). After a bore reached the hydrophone, the frequency content shifted toward more high-frequency components. As a bore or swash continued beachward, the sound loudness diminished.

The backwash also produced a distinct sound. It was softer than the upwash, sounded gurgly and uneven in loudness, and had more high-frequency components than swash.

Responses of clams to knocking sounds

Knocking on the plywood table under the aquarium produced a low-frequency sound with frequencies similar

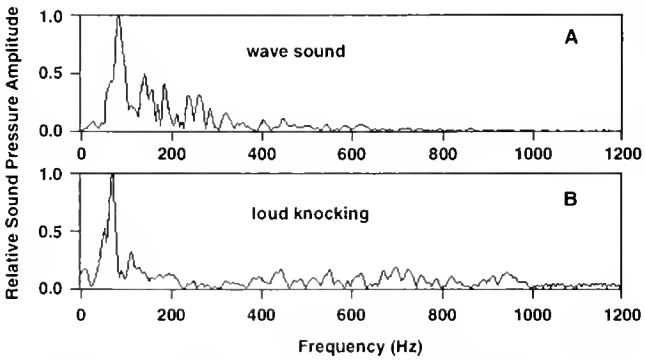

Figure 2. Comparison of frequency spectra of wave and knocking sounds that stimulate clams to jump. (A) A typical spectrum of a wave sound during a 0.5-s interval that starts between 0.5 and 1 s before swash reaches the hydrophone. The rumbling sound that precedes the arrival of swash at the hydrophone consists mainly of low-frequency components. (B) The frequency spectrum of knocking sounds presented to clams. Knocking contains low-frequency sounds similar to those which precede the arrival of swash at a spot on the beach.

to those of a bore approaching the beach (Fig. 2). *Donax variabilis* clams often responded to knocking by jumping out of the sand (Fig. 3). After a clam emerged from the sand, it fell on one valve or the other, often with siphon and foot extended. This behavior mimicked that of clams jumping out in front of swash on the beach. Clams lay on the sand for 3 to 30 s before digging in again. Occasionally, individual clams only partially emerged from the sand. Such hesitant clams could be induced to emerge completely by increasing either the loudness or the duration of knocking (suggesting that clams sum sound stimuli over time).

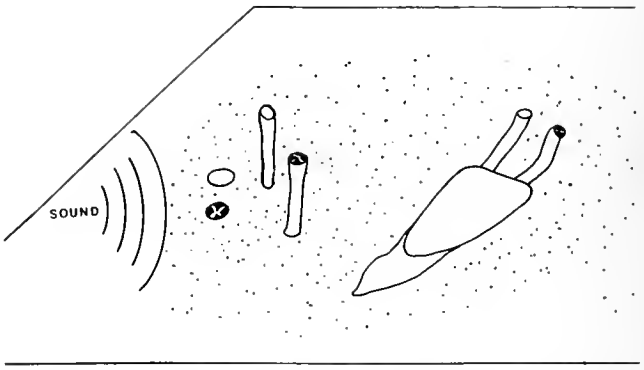

Figure 3. Observed responses of clams to sound stimuli. In a clam that did not visibly respond, only the clam's exhalant and inhalant (frilled) siphon were visible at the surface of the sand (at left). Clams responded either by elongating their siphons (middle), usually in response to a high-frequency (832-Hz) tone, or they jumped out of the sand and lay with siphons and foot waving (at right). After 10–30 s, a clam that had jumped would again burrow into the sand.

Tidal variation in responsiveness of clams to knocking sounds

The number of clams that jumped out of the sand depended on the time of tide, not on the time of day (Fig. 4a). Similar results were obtained when room lights were off and natural light cues were unavailable (Fig. 4b). The clams never jumped within 1 to 2 h of low tide; the number jumping increased as high tide approached, reached a maximum at high tide, and decreased after high tide. This tidal rhythm persisted in the absence of direct tidal cues (*e.g.*, the aquarium's water level did not change), and independent of the light regime provided. The tidal rhythm persisted for three to five tidal cycles; subsequently no responses to sound could be elicited.

The maximum percentage of clams jumping at a given time was only 20%. Jumping clams were not always the same individuals (individuals are recognizable by distinctive shell markings). Therefore, the 20% maximal response rate was not due merely to complete non-responsiveness in the other 80% of clams. Thus, individual clams become responsive and unresponsive several times per tidal cycle. At high tide, a larger fraction of the clams are in a responsive phase than at other times of tide.

Clams' responsiveness to sounds from waves

On all 3 days, some of the clams (maximally 20% at any given time) within a 15-cm radius of the speaker sometimes jumped out of the sand while wave sounds were being presented. In contrast, during an entire summer of observations, I never observed clams jumping in the absence of sound stimuli.

Wave sounds presented to clams consisted of naturally occurring, quiet periods several seconds long, interspersed with the rumble of incoming waves. Whereas some wave sounds elicited responses, others not obviously different elicited no responses. Because of the complex nature of wave sounds, specific features to which clams responded could not be identified unambiguously. Nevertheless, jumps often coincided with the pre-arrival rumble. The loudness, P_e, of 0.5-s samples of sound during pre-arrival rumbles was typically 30 Pa, which is similar to the loudness of artificial sound stimuli that elicited the responses reported below.

Frequency and amplitude specificity of responses

Two separate behavioral responses to sound were observed—siphon elongation and jumping out of the sand (Fig. 3). Siphon elongation was qualitatively noted to occur primarily in response to higher frequencies (*e.g.*, 500 and 832 Hz tones). Such elongation of the siphons was never seen in the absence of sound stimuli. This is the first report in the literature of siphon elongation as a response to sound, and its potential function is unknown.

The jumping responses were quantitatively analyzed. The frequency spectra of the sound stimuli are shown in Figure 5. At all frequencies, more clams jumped in response to louder sounds (Fig. 6). The number of clams jumping was linearly related to loudness as represented by log (P_e). For both the pure tone and the broadband low-frequency sounds, this linear relationship was tight (correlation = 0.98) and the slope was significantly nonzero ($P < 0.001$), whereas for the pure high-frequency tone, the relationship was less tight (correlation = 0.6), and the slope was not significantly different from zero ($P = 0.1$). The frequency composition did not affect responsiveness; both pure tone and broadband low-frequency sounds elicited similar numbers of clams that jumped at a given loudness (low-frequency slopes not significantly different from each other). At a given loudness, more clams jumped in response to low- than to high-frequency sounds (slopes of the low-frequency sounds were significantly higher than the slope of the high-frequency tone). No clam was ever observed jumping in the absence of a sound stimulus.

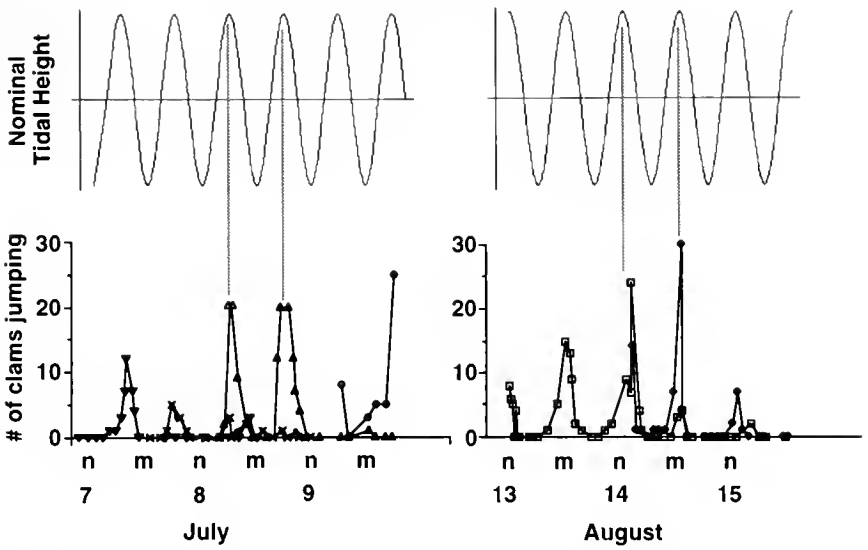

Figure 4a. Number of *D. variabilis* clams in the laboratory jumping in response to knocking sounds relative to time of day and tide. Noon is n; midnight is m. Clams were most responsive around the time of high tide and showed no response around the time of low tide. Clams responded for only three to five tidal cycles after they had been taken from the beach. The pattern shown is a compilation of several collections (represented by different symbols) taken on different days from the same beach. Room lights were continuously on in this experiment.

In the 2 additional days of experiments, performed during falling tides with several other synthesized low-frequency stimuli, jumping responses were consistent with those already described. Specifically, the number of clams responding increased with loudness, log (P_e), and decreased with increasing time after high tide (multiple regression, $P < 0.001$; loudness variable: $P < 0.01$, time variable: $P < 0.01$, $n = 35$). A cumulative total of 147 responses were observed in 35 trials during those 2 days.

On these 3 days of experiments, clams responding to sounds jumped only if they were less than 14 cm from the speaker, and most responding clams were less than 5 cm from the speaker face. The proximity of responding clams to the sound source raises the possibility of near-field effects (complicated wave interference patterns), which would complicate interpretation of the responses. A near field exists (close to a vibrating piston in an infinite baffle, an approximation to the geometry of the speaker: Kinsler *et al.*, 1982, *inter alia*) only if the diameter (0.2 m) of the speaker is greater than the sound's wavelength. For an 832-Hz sound the wavelength is 1.8 m (wavelength = speed of sound divided by frequency; speed of sound in coarse silt sea bottoms assumed = 1540 m/s; Kinsler *et al.*, 1982). The speaker is even smaller compared to the longer wavelengths of lower frequency sounds. Therefore, near-field effects are negligible in the present experiment. The spatial response pattern of clams must, however, also be considered with respect to frequency-dependent attenuation of sound.

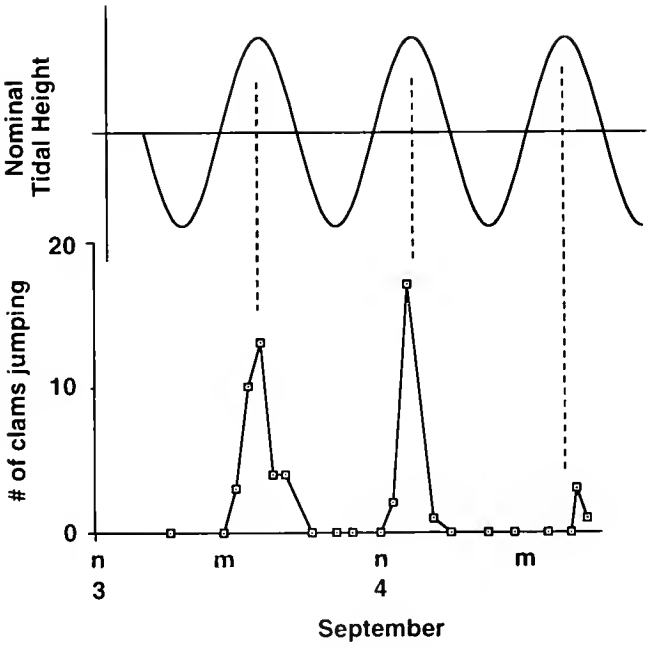

Figure 4b. Number of *D. variabilis* clams in the laboratory jumping in response to knocking sounds relative to time of day and tide. The results are similar to those shown in Figure 4a, but in this experiment room lights were off except for a few seconds during sampling.

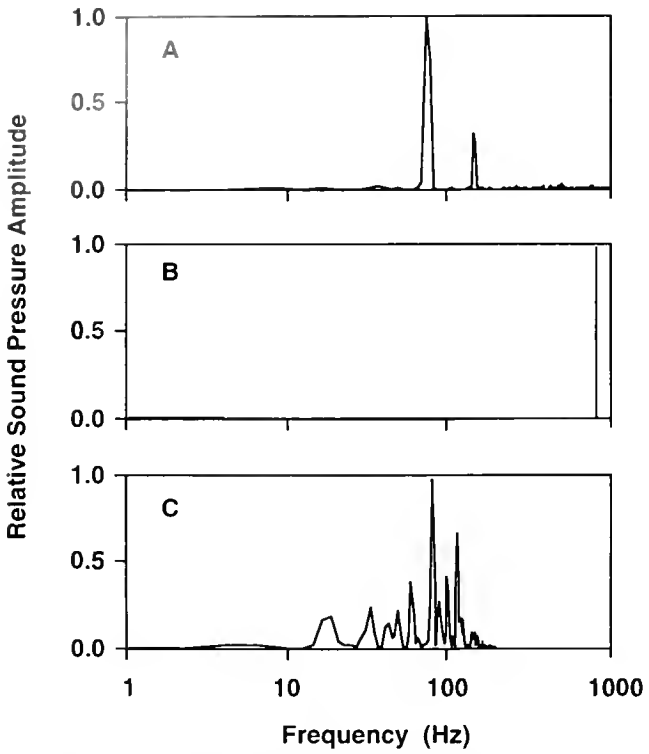

Figure 5. Frequency spectra of three artificially produced sounds presented to clams to test their responses to different sounds. The pure tone, low-frequency stimulus consisted of a 72-Hz tone with a harmonic at 144 Hz (A); the pure tone, high-frequency stimulus consisted of a 832-Hz tone (B) and a small harmonic at 1664 Hz (not shown); and the broadband, low-frequency noise had major frequency components ranging from 20 to 140 Hz (C). These frequency spectra were recorded with a hydrophone planted in the sand amidst the clams and thus represent stimuli to which the clams were exposed. Responses of clams to these sounds are shown in Figure 6.

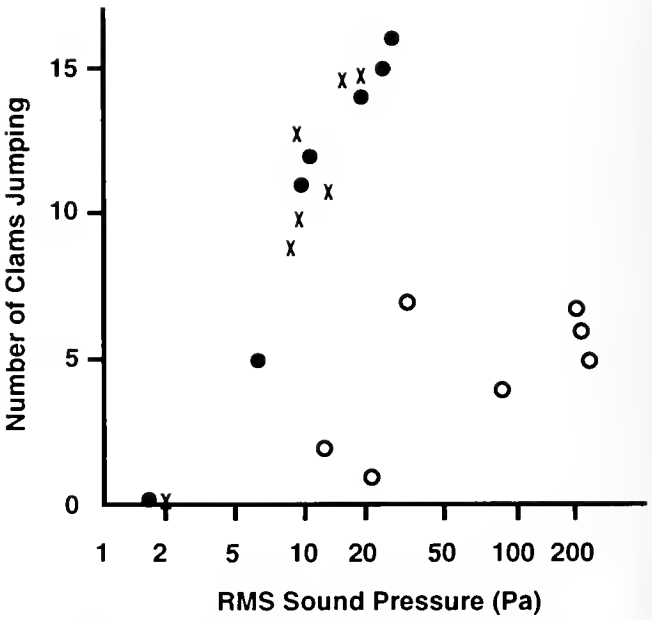

Figure 6. Number of clams jumping in response to sounds of different loudness and frequency. Louder sounds have higher root-mean-square (RMS) pressures. Three distinct frequency spectra (Fig. 5) were presented. More clams jump at a given loudness for both broadband (20 to 140 Hz, ×) and pure tone (72-Hz, ●) low-frequency sound than for a high-frequency (832-Hz, ○) sound.

Attenuation of sound and frequency responsiveness

High frequencies attenuated more rapidly with distance from the source than did low frequencies (Fig. 7), which raises the possibility that clam responses that appeared to be frequency dependent (Fig. 6) might actually have been attenuation artifacts. The degree to which attenuation of frequency-dependent responses is contributing to the observed differential responses can be determined by considering the measured extent of attenuation in the aquarium in this experiment. Two sounds (832 and 72 Hz) of equal P_e at 4 cm from the speaker attenuated differentially; consequently, at 30 cm, the 832-Hz sound was only 10% as loud as the 72-Hz sound (Fig. 7). At 4 cm, the loudest 832-Hz stimuli were 10 times louder than the loudest 72-Hz stimuli (Fig. 6); conservatively assuming a 10% relative attenuation, at distances greater than 4 cm, the loudest 832-Hz sounds were at least as loud as the loudest 72-Hz sounds. Yet only half to a third as many clams responded to the loudest high-frequency sounds as responded to the

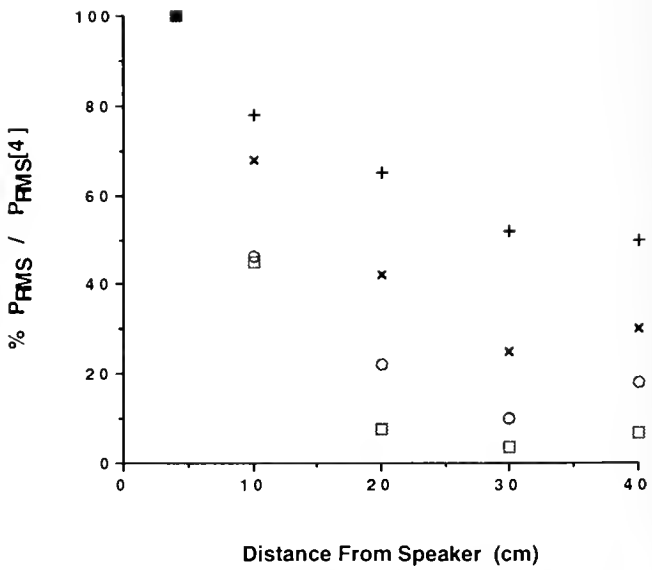

Figure 7. Frequency-specific attenuation of sound in the sand in the aquarium in which acoustic tests were performed (□ 832 Hz; ○ 500 Hz; > 250 Hz; + 72 Hz). The hydrophone was planted in the sand along the midline of the tank at several distances in front of the speaker. Attenuation is expressed as % RMS sound pressure at the given distance from the loudspeaker divided by RMS sound pressure 4 cm from the face of the speaker. (The slight increase in sound at the point farthest from the speaker is probably due to sound patterns caused by partial reflection of sound waves off the aquarium wall.)

loudest low-frequency sounds. Therefore, although differential sound attenuation must have contributed to the observed difference in responsiveness to different frequencies, it cannot explain the entire difference. *D. variabilis* clams are more responsive to low-frequency sounds in their jumping response.

Discussion

Wave sounds as cues for swash-riding

The proposition that *Donax variabilis* clams use sounds from waves as cues for swash-riding is supported by direct findings of responsiveness of clams to appropriate sounds and by parallels between behaviors elicited in the laboratory and observed on the beach. On the beach, these clams jump in response to waves; in a laboratory, in the absence of waves, these clams jumped in response to wave sounds and to artificially produced sounds that contained frequencies similar to those of wave sounds. Wave sounds recorded in the beach amidst coquina clams show distinct patterns of sound that allow the clams to predict the size and timing of incoming swash. For example, the loudness of a wave's sound predicts the excursion of that wave's swash. On the beach, clams preferentially jump for swash of large excursion (Ellers, 1995a); in the laboratory, clams were more responsive to louder sounds. Further correspondence between beach and laboratory is found in the observed endogenous tidal rhythm. Clams in the laboratory, which were isolated from direct tidal cues, were most responsive to sounds at high tide, and did not respond at all to sounds within 1 to 2 h of low tide. On the beach, clams did not jump out of the sand to ride waves within 1 to 2 h of low tide (Ellers, 1995a).

Taken together, these results indicate that sound is a major cue in determining whether these clams jump out of the sand to swash-ride. Loud sounds from large waves stimulate the clams to jump, and an endogenous rhythm of responsiveness modulates the jumping behavior and is thus a proximate cause of the characteristic tidal migration of these clams. This is the first report demonstrating use of flow-induced sounds by an invertebrate.

Detection of pressure or velocity signals by clams

An acoustic effect, associated with how close a responding clam is to the speaker, gives insight into possible mechanisms by which these clams may detect sounds. Sound can be detected as temporal changes in either pressure or velocity of the vibrating medium at a point. The hydrophone used in this experiment detects pressure. In contrast, organisms may use mechanisms (tiny hairs or cilia) that detect motion (velocity) rather than pressure. For a sound wave far from its source, pressure amplitude is directly proportional to velocity amplitude (Kinsler *et al.*, 1982). For sound close to its source, however, velocity and pressure are not directly proportional, and velocity attenuates more rapidly than pressure. By convention, this effect is considered important (Bobber, 1970) if the distance from the source to the receiver (hydrophone or clam) is less than half a wavelength (0.9 and 11 m for 832- and 72-Hz sounds, respectively). Therefore, in the area where the clams responded to sound, the velocity signal attenuated more rapidly than the pressure signal.

If clams had been detecting pressure, then louder sounds should have caused responses throughout the aquarium. For instance, 72-Hz sound attenuated P_e by a maximum of 50% in the aquarium (Fig. 7); therefore, a signal with twice the threshold P_e at 4 cm should have caused responses throughout the aquarium. But clams more than 15 cm from the speaker never jumped; thus, they did not jump appropriately further away when the pressure signal was increased. Since the velocity signal attenuates more with distance than the pressure signal, the locations of responding clams suggest that the animals detected velocity rather than pressure. Other more complex possibilities exist, however, regarding the transmitting medium and the sensor used. For instance, scorpions have detectors both for compressional (sound) waves under the sand and for waves traveling on the interface between air and sand (Brownell, 1984).

Population versus individual responses

Loudness and frequency were not the only factors determining whether clams jumped in response to a sound. In fact, although clams jumped in connection with specific recorded wave sounds, they ignored many waves of equal loudness. Similar indifference to otherwise suitable stimuli was also observed in the rhythm experiments; a maximum of 20% of clams responded, even at the maximally responsive times. Perhaps the responsiveness of individual clams shifts several times per tidal cycle. The relative length or frequency of the responsive periods may change with time of tide, so that a larger fraction of clams is responsive at high tide than at low tide.

Endogenous tidal rhythm

An endogenous rhythm should persist for some time in the absence of cues. In the current experiment, the tidal rhythm in responsiveness persisted without tidal cues and irrespective of potential light cues, thus supporting the endogenous nature of the tidal rhythm. But the rhythm persisted only for three to five tidal cycles under laboratory conditions, suggesting either that the rhythm is a damped oscillator or that a clock is still running but its expression is blocked. For instance, lack of food may force cessation of jumping. Such small numbers of persisting cycles are sometimes observed for tidal rhythms; *e.g.*, a tidal rhythm

for phototaxis in larval grass shrimp persisted for only two to three cycles without cues (Douglass *et al.*, 1992).

It was suggested that *D. variabilis* has no endogenous tidal rhythm (Tiffany, 1971) when clams transplanted to a beach with a different tidal cycle were observed following the new tidal cycle within 24 h. Given the endogenous rhythm I observed (Fig. 4), an alternative interpretation is that the clock or damped oscillator was rapidly reset by the new conditions.

Additional stimuli on the beach may further modify responses in nature relative to those observed in the laboratory. For instance, the rhythm I observed was symmetrical during rising and falling tides. Clam responses were identical with respect to sound occurring any given time before and after high tide, at least within the limited ability of the present experiment to detect asymmetries. In contrast, observations on the beach show that some asymmetries in behavior exist. On the beach, clams jumped in advance of beachward-moving swash during the rising tide, but jumped into the backwash during the falling tide.

Asymmetries may be difficult to detect: behavior in the laboratory may not exactly mimic behavior on the beach because only partial cues are available. For instance, the relative amount of time that clams are covered by water may serve as a cue in nature. On a beach, the water level above the clams is constantly changing; in the aquarium, the water level remained unchanged.

Another natural cue that may be missing in the laboratory is the stimulus of being moved by a wave. In the aquarium, after a clam jumped out of the sand it lay on the sand and dug in again after 10–30 s. If immediately re-exposed to the same stimulus, a responsive clam often jumped out again (pers. obs.). Perhaps, on a beach, after a clam has been moved by a wave, its responsiveness to sound stimuli is reduced for some time.

Usefulness of sound cues to marine animals

Endogenous tidal rhythms are common in intertidal animals. Another swash-rider, the amphipod *Synchelidium sp.* (Enright, 1961a, 1963; Forward, 1980, 1986), has endogenous tidal rhythms in response to light (Forward, 1980) and pressure (Enright, 1961b). Endogenous tidal rhythms probably occur in other swash-riders: *e.g.*, mole crabs, *Emerita analoga* (Cubit, 1969) and *Remipes truncatifrons* (Mori, 1938); and gastropods, *Terebra salleana* (Kornicker, 1961), *Hastula inconstans* (Miller, 1979), *Bullia sp.* (Ansell and Trevallion, 1969; McLachlan and Young, 1982), and *Olivella biplicata* (Johnson, 1966). Other *Donax spp.* that swash-ride (*e.g., D. incarnatus* and *D. denticulatus:* Ansell and Trueman, 1973; *D. serra:* Donn, 1987; and many others), may also respond to wave sounds on endogenous rhythms.

Whereas many populations of *D. variabilis* have been reported as migratory, at least during summer months, some populations either do not migrate or migrate only occasionally. There are many possible explanations for a cessation of migration, although none have been experimentally investigated. The role that sound plays in migration should be considered in that context. For example, one population of migratory *D. variabilis* that lived on steep-sloped beaches has been contrasted with another non-migratory population that lived on a more gently sloping beach (Mikkelsen, 1981). Perhaps waves on the gently sloping beach do not generate sounds that are sufficiently loud or sufficiently distinctive to produce selective jumping responses.

Finally, since sound and vibrational cues from waves are so obvious, and so obviously useful, even non-swash-riding marine animals might use them. For instance, an urchin might tighten its grip on rocks in preparation for a particularly large wave, or an anemone might adjust its stiffness in preparation for a wave impact. I have observed both an anemone, *Anthopleura elegantissima*, and a sea urchin, *Strongylocentrotus purpuratus*, to respond to vibrations in the frequency range generated by waves.

In any case, the clams I studied are literally in tune with their environment.

Acknowledgments

This research is part of the author's Ph.D. dissertation completed at Duke University. I thank my thesis supervisor, S. Vogel, and committee members, V. L. Roth, E. J. Shaughnessy, V. A. Tucker, and S. A. Wainwright. NSERC postgraduate scholarships, Duke University teaching assistantships and a Cocos Foundation Training Grant in Morphology supported the author. Duke University Marine Laboratory provided facilities. I also thank S. A. Wainwright, who generously funded acoustic equipment; B. Hunnings, electronics technician, who built the sine-wave generator; and A. Johnson who critically read the manuscript.

Literature Cited

Ansell, A. D., and A. Trevallion. 1969. Behavioural adaptations of intertidal mollusks from a tropical sandy beach. *J. Exp. Mar. Biol. Ecol.* **4:** 9–35.

Ansell, A. D., and E. R. Trueman. 1973. The energy cost of migration of the bivalve *Donax* on tropical sandy beaches. *Mar. Behav. Physiol.* **2:** 21–32.

Blaxter, J. H. S., and R. S. Batty. 1985. Herring behaviour in the dark: Responses to stationary and continuously vibrating obstacles. *J. Mar. Biol. Assoc. U.K.* **65:** 1031–1049.

Bleckmann, H., T. Breithaupt, R. Blickhan, and J. Tautz. 1991. The time course and frequency content of hydrodynamic events caused by moving fish, frogs, and crustaceans. *J. Comp. Physiol. A* **168:** 749–757.

Bobber, R. J. 1970. *Underwater Electroacoustic Measurements.* Naval Research Laboratory, Washington, DC.

Bradshaw, M. 1982. Bores and swash on natural beaches. *Coastal Studies Unit Technical Report No. 82/4.* Coastal Studies Unit, Department of Geography, The University of Sydney, Sydney, NSW, Australia.

Brownell, P. H. 1984. Prey detection by the sand scorpion. *Sci. Am.* **251:** 86–97.

Burrus, C. S., and T. W. Parks. 1985. *DFT/FFT and Convolution Algorithms—Theory and Implementation.* John Wiley and Sons, New York.

Cubit, J. 1969. Behaviour and physical forces causing migration and aggregation of the sand crab *Emerita analoga* (Stimpson). *Ecology* **50:** 118–123.

Donn, T. E., Jr. 1987. Longshore distribution of *Donax serra* in two log-spiral bays in the eastern Cape, South Africa. *Mar. Ecol. Prog. Ser.* **35:** 217–222.

Douglass, J. K., J. H. Wilson, and R. B. Forward. 1992. A tidal rhythm in phototaxis of larval grass shrimp (*Palaemonetes pugio*). *Mar. Behav. Physiol.* **19:** 159–173.

Ellers, O. 1987. Passive orientation of benthic animals in flow. Pp. 45–68 in *Signposts in the Sea, Proceedings of a Multidisciplinary Workshop on Marine Animal Orientation and Migration,* W. F. Herrnkind and A. B. Thistle, eds. Dept. of Biological Science, Florida State University, Tallahassee.

Ellers, O. 1988. Locomotion via swash-riding in the clam *Donax variabilis.* Ph.D. Dissertation, Duke University, Durham, NC.

Ellers, O. 1995a. Behavioral control of swash-riding in the clam *Donax variabilis. Biol. Bull.* **189:** 120–127.

Enright, J. T. 1961a. Distribution, population dynamics and behavior of a sand beach crustacean *Synchelidium sp.* Ph.D. Dissertation, University of California at Los Angeles.

Enright, J. T. 1961b. Pressure sensitivity of an amphipod. *Science* **133:** 758–760.

Enright, J. T. 1963. Responses of an amphipod to pressure changes. *Comp. Biochem. Physiol.* **7:** 131–145.

Forward, R. B. 1980. Phototaxis of a sand-beach amphipod: physiology and tidal rhythms. *J. Comp. Physiol.* **135:** 243–250.

Forward, R. B. 1986. Behavioral responses of a sand-beach amphipod to light and pressure. *J. Exp. Mar. Biol. Ecol.* **102:** 55–74.

Johnsnn, P. T. 1966. On *Donax* and other sandy beach inhabitants. *Veliger* **9:** 29–30.

Karlsen, H. E. 1992a. The inner ear is responsible for detection of infrasound in the perch (*Perca fluviatilis*). *J. Exp. Biol.* **171:** 163–172.

Karlsen, H. E. 1992b. Infrasound sensitivity in the plaice (*Pleuronectes platessa*). *J. Exp. Biol.* **171:** 173–187.

Kinsler, L. E., A. R. Frey, A. B. Coppens, and J. V. Sanders. 1982. *Fundamentals of Acoustics,* 3rd ed. John Wiley and Sons, New York.

Kornicker, L. S. 1961. Observations on the behaviour of the littoral gastropod *Terebra salleana. Ecology* **42:** 207.

Kreithen, M. L., and D. B. Quine, 1979. Infrasound detection by the homing pigeon: A behavioral audiogram. *J. Comp. Physiol.* **129:** 1–4.

Loesch, H. C. 1957. Studies on the ecology of two species of *Donax* on Mustang Island, Texas. *Inst. Mar. Sci.* **4:** 201–227.

McLachlan, A., and N. Young. 1982. Effects of low temperature on the burrowing rates of four sandy beach mollusks. *J. Exp. Mar. Biol. Ecol.* **65:** 275–284.

Mikkelsen, P. S. 1981. A comparison of two Florida populations of the coquina clam, *Donax variabilis* Say, 1822 (Bivalvia: Donacidae). 1. Intertidal density, distribution and migration. *Veliger* **3:** 230–239.

Miller, W. 1979. The biology of *Hastula inconstans* (Hinds, 1984) and a discussion of life history similarities among other Hastulas of similar proboscis type. *Pac. Sci.* **33:** 289–306.

Mori, S. 1938. Characteristic tidal rhythmic migration of a mussel, *Donax semigranosus* Dunker, and the experimental analysis of its behaviour at the flood tide. *Dobutsugaku Zasski.* [=*Zool. Mag. (Japan)*] **50:** 1–12.

Mori, S. 1950. Characteristic tidal rhythmic migration of a mussel, *Donax semigranosus* Dunker, and the experimental analysis of its behaviour (II). *Dobutsugaku Zasski* [=*Zool. Mag. (Japan)*] **59:** 87–89.

Naylor, E. 1985. Tidally rhythmic behaviour of marine animals. *Symp. the Soc. Exp. Biol.* **39:** 63–93.

Packard, A., H. E. Karlsen, and O. Sand. 1990. Low frequency hearing in cephalopods. *J. Comp. Physiol. A* **166:** 501–505.

Tiffany, W. J. III. 1971. The tidal migration of *Donax variabilis* Say (Mollusca: Bivalvia). *Veliger* **14:** 82–85.

Trueman, E. R. 1971. The control of burrowing and the migratory behaviour of *Donax denticulatus* (Bivalvia: Tellinacea). *J. Zool., Lond.* **165:** 453–469.

Turner, H. J., Jr., and D. L. Belding. 1957. The tidal migrations of *Donax variabilis* Say. *Limnol. Oceanogr.* **2:** 120–124.

Weisberg, S. 1980. *Applied Linear Regression.* John Wiley and Sons, New York.

Williams, B. G., J. D. Palmer, and D. N. Hutchinson. 1993. Comparative studies of tidal rhythms XIII. Is a clam clock similar to those of other intertidal animals? *Mar. Behav. Physiol.* **24:** 1–14.

Reference: *Biol. Bull.* 189: 138–147. (October/November, 1995)

Form and Motion of *Donax variabilis* in Flow

OLAF ELLERS*

Department of Zoology, Duke University, Durham, North Carolina 27706

Abstract. The coquina clam, *Donax variabilis*, rides flow from waves, migrating shoreward during rising tides and seaward during falling tides. This method of locomotion, swash-riding, is controlled not only behaviorally but also morphologically. The shape of this clam causes it to orient passively; a clam rotates in flow, usually in backwash, until its anterior end is upstream. Rotation is about a vertical axis through a pivotal point where the shell touches the sand. The density, weight distribution, and wedge-like shape are all important in effecting orientation. Such orientation is significant because it contributes to stability of motion. On an unoriented clam, upward lift can be higher than its underwater weight—a circumstance that results in uncontrollable tumbling. In contrast, once oriented with its anterior end upstream, a clam experiences downward lift that contributes to its stability while sliding in backwash. Furthermore, when the anterior end is upstream, drag is reduced relative to when the ventral, dorsal, or posterior ends are upstream. Since orientation occurs only above a minimum velocity, it has the effect of slowing a clam's motion over the substratum in rapid flows. Stability, drag, and speed reduction enhance a clam's ability to gain a foothold and dig in after a swash-ride, before wave flows can wash it off the beach and out to sea.

Introduction

The coquina clam, *Donax variabilis*, migrates seaward with the falling tide and shoreward with the rising tide by using a method of locomotion called swash-riding (Ellers, 1987, 1988). Swash-riding involves jumping out of the sand, being pushed by a wave to a new location, and digging in again. For an individual clam, the net movement per swash-ride depends in part on behavior. For instance, by using sound to sense the size and timing of incoming waves (Ellers, 1995b), these clams emerge to ride only the largest waves (Ellers, 1995a). The net movement per swash-ride may also depend on a clam's shape, just as shape has consequences for performance in other forms of locomotion such as running or flying.

Consider events during a shoreward migration consisting of several swash-rides. During each swash-ride, a clam is pushed shoreward, but does not stop moving at the most shoreward point of its travel because backwash pulls it seaward. To make net shoreward progress, it must gain a foothold while moving and dig in before backwash carries it seaward of its original position. How far flow moves a clam and whether it gains a foothold depend on forces the clam experiences in flow, which in turn depend on the clam's shape. The present study seeks to identify shape, or form, that influences the motion of a swash-riding clam.

The motion of an object in flow can be of two dramatically different types. An object can orient to a stable position like a weather vane or it can tumble chaotically like a hat. A *D. variabilis* clam moves like a weather vane. If the water flowing past an individual *D. variabilis* changes direction, the clam rotates to maintain a certain orientation with respect to flow (Fig. 1). The clam rotates about a vertical axis through a pivotal point where the shell touches the sand. In the oriented position, the clam's anterior end is upstream and the posterior end is downstream. Once oriented, a clam slides stably before gaining a foothold and digging into the sand (Fig. 2).

This orientation was suggested to be caused by activity of the siphons in *D. fossor* (Jacobson, 1955) and in *D. semigranosus* (Mori, 1938). However, dead *D. denticulatus* (Wade, 1967) and dead *D. variabilis* (Tiffany, 1971; Ellers, 1987, 1988) orient the same way as live ones, thus demonstrating the passive nature of orientation.

Not every shape orients and slides stably in backwash. For example, a bivalve, the cross-hatched lucine *Divari-*

Received 9 September 1994; accepted 27 July 1995.

* Current address: Section of Evolution and Ecology, Division of Biological Sciences, University of California, Davis, CA 95616.

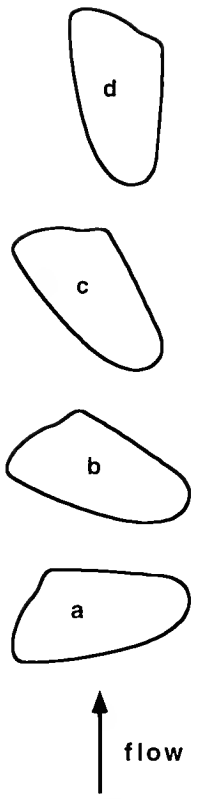

Figure 1. A coquina clam, *D. variabilis*, orienting passively in flow. A clam starts out in an arbitrary position, *e.g.*, ventral edge upstream (a). In flow it rotates, passing through positions (b) and (c) until it reaches the stable orientation with the anterior end upstream (d). Orientation is rapid and can occur during <0.1 s. The clam may slide downstream during orientation, as shown, or remain stationary while rotating.

cella quadrisculata, stands on edge and rolls like a wheel (pers. obs.). Another bivalve, the sunray Venus *Macrocallista nimbosa*, slides in a variety of orientations and tumbles occasionally. A very light bivalve, the tellin *Tellina iris* tumbles chaotically. A sand dollar, *Mellita quinquiesperforata*, flips end over end in surf. Similar characteristic motions of these objects occur in a flow tank. Therefore, orientation by *D. variabilis* is a special consequence of the shape of *D. variabilis*, not a general characteristic of bivalves or other invertebrates that live exposed to flow.

Furthermore, orientation is common among swash-riding species. Among the swash-riding gastropods and mole crabs for which information is available, all orient (Ellers, 1987). Other swash-riders include a variety of amphipods, but observations of orientation are unavailable for those species.

Orientation in *D. variabilis* usually occurs in the backwash rather than the swash, presumably because flow in the swash is too turbulent. Swash forms from a collapsing bore that itself originates from a breaking wave. The speeds of resulting flows are relevant to the fluid dynamics of a swash-riding clam. The speed of the leading edge of swash initially increases, then decreases as it moves shoreward. Maximum speeds (Bradshaw, 1982) ranged from 4.5 to 6 m s^{-1} from waves with breaker heights of 0.9 to 1.4 m on a steeply sloped beach (slope expressed as rise-to-run ratio was 0.16); and the maximum speed recorded on a shallow beach (slope of 0.03), where bore collapse takes longer, was 3 m s^{-1}. Backwash speed is typically less than swash speed. Maximum backwash speed, just shoreward of the next incoming bore, was 1.2 m s^{-1} on a beach with slope of 0.03 (Bradshaw, 1982). The average speed was 0.70 m s^{-1} among 21 backwashes. Backwash generally increases in speed as it flows seaward. I observed *D. variabilis* riding flows on beaches typically having a slope of 0.1, but varying from 0.05 at low tide to 0.13 at high tide.

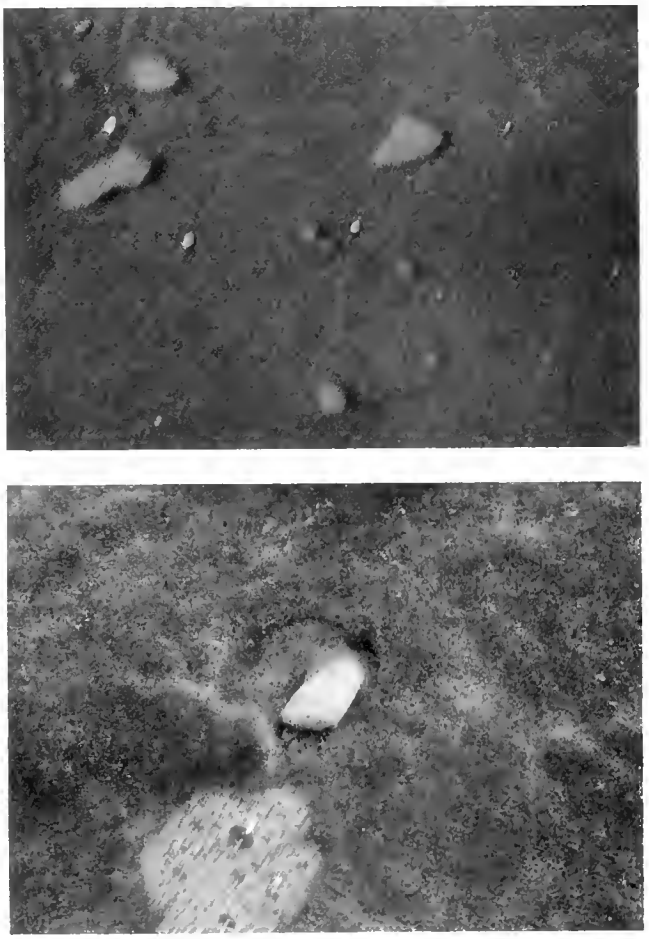

Figure 2. Coquina clams, *D. variabilis*, in flow on a beach. Flow is from upper right to lower left and is indicated by the streaks from the moving bubbles on the surface of the water. The upper photo shows clams swash-riding and oriented with the anterior end upstream. The lower photo shows a clam on a beach, having just achieved a foothold, shortly before it burrows into the sand. The foot is visible at the pointy, anterior end, and the siphons are visible at the blunt, posterior end.

This study seeks to determine morphological features of *D. variabilis* that are important in causing orientation; and to determine the functional consequences of orientation for movement of *D. variabilis* during swash-riding. Relevant are forces and moments of forces due to friction between clam and sand; gravity; buoyancy; drag; vertical and horizontal lifts (lift is defined as a force normal to flow, and there are always two mutually perpendicular lift vectors normal to the flow direction). By combining measurements and assumptions about forces and their distribution, I identify morphological features that cause orientation and contribute to stability once oriented. By comparing the forces on an oriented and unoriented clam, I infer the function of orientation. In addition to measuring velocities, forces, and pressures, I experimentally manipulated the weight distribution of a *D. variabilis* clam and observed the resulting changes of the clam's motion in flow.

Materials and Methods

Backwash speed

On a North Carolina beach with a slope of 0.1, where *Donax variabilis* occurs, buoyant plastic beads (1 cm diameter) were dropped into the backwash and photographed at an exposure of 1/4 s. On the photographs, beads appear as streaks, and streak length was calibrated using a series of stakes planted in the beach at 1-m intervals along a transect perpendicular to the beach at the same location. It was assumed that the plastic beads moved at the same speed as the backwash. Error in the velocity calculated was determined by a propagation or errors analysis using estimated errors in the shutter speed and distance measures (Ellers, 1988).

Force distribution, due to flow, on an oriented and unoriented clam

To investigate the influence of shape and orientation on flow forces experienced by *D. variabilis* clams, the distribution of forces acting normal to the surface of a clam, and their associated moments, were determined. Local force normal to a surface equals local pressure multiplied by local surface area perpendicular to the force. Moment of a local force about the pivotal point equals the vector cross-product of location and force (location is a distance vector from the pivotal point to the force). Thus pressures, areas, and locations must be measured.

The pressure distribution was estimated by measuring pressure at many points on the surface of a scaled model clam that was 5 times larger than a real *D. variabilis* clam. A model was used because direct measurement of the distribution of pressures on such small clams (maximum length of real clams = 3 cm) is not feasible. Pressure measurements on the scale model were made in a wind tunnel. Flows relevant to clams on the beach were mimicked in the wind tunnel by maintaining dynamic similarity (constant Reynolds number, Re). Due to equivalence of Euler number in dynamically similar flows (Shames, 1982), forces on an object determined in air were translated to forces on that object in seawater using

$$F_c = F_m \frac{\mu_w^2 \rho_a}{\mu_a^2 \rho_w}$$

where F_c and F_m are the forces on the template clam and model, μ_w and μ_a are the dynamic viscosities of seawater and air, and ρ_w and ρ_a are the densities of seawater and air. Assuming 20°C for both air and seawater, the conversion was

$$F_c = 4.14\ F_m$$

The model was carved according to measurements of the shape of the outside of the left valve of a 2.2-cm-long *D. variabilis* clam. The valve was attached to a horizontal plane above which the valve protruded. A spring-loaded displacement gage measured vertical distance, and calibrated drives were used to determine horizontal coordinates. This apparatus gave a grid of 3-dimensional coordinates outlining the valve's shape. The grid had a vertical measurement every millimeter in both horizontal directions with more closely spaced measurements taken in regions where vertical measurements changed too rapidly with horizontal distance.

A model 5 times larger than the measured valve and a mirror-image right valve were fabricated to within ±0.5 mm (maximum error) of the scaled measurements of shape. When the two valves were attached to each other, a hollow space existed inside. Eighty holes were drilled in the model and a hollow steel pipe, 0.26 mm in external diameter, was attached to the middle of the posterior end such that the interior of the pipe led to the hollow inside the model. The holes were covered with tape; during pressure measurements, one hole at a time was uncovered till pressure at all holes had been measured.

The model was placed on the floor of a large wind tunnel (Tucker and Parrott, 1970). The pipe that protruded from the posterior end of the model was attached to a pressure sensor *via* rubber tubing. On the other side of the pressure sensor was another rubber tube that connected to a reference hole in a horizontal flat plate located in and parallel to mainstream flow (40 cm above the tunnel floor). The reference hole was 1 mm in diameter and 0.1 m downstream of the leading edge of the plate. Measurement is made of the difference between the reference pressure at the hole in the plate and the pressure at the open hole on the model clam. The same apparatus was previously used to measure pressures on model squids (Vogel, 1985). The pressure signal was digitized (12-bit)

into a computer for data analysis. For each hole, 30 replicate pressure measurements were taken.

In the wind tunnel, the model was positioned on its left side at a tilt that was within ±3° of the angle at which a live clam lies in seawater. In seawater, a live clam lies with the plane of symmetry (between the right and left valves) at an angle of 11 ± 2° to the horizontal in both the anterior-posterior direction and the dorsal-ventral direction. These angles were measured using a protractor, from a photograph of a live clam lying on the bottom of a transparent aquarium filled with seawater. The photograph was taken from 10 m away to minimize distortion due to perspective.

Six sets of pressure measurements were made. Two were made at a mainstream air speed of 2.6 m s^{-1}, the equivalent of 0.91 m s^{-1} in 20°C seawater. The other four sets were made at a wind speed of 4.6 m s^{-1}, the equivalent of 1.6 m s^{-1} in 20°C seawater. Orientations of the model in the faster flows were (1) anterior end upstream, (2) posterior end upstream, (3) ventral edge upstream, and (4) dorsal edge upstream. In the slower flows, only orientations (1) and (3) were tested.

When the anterior end was upstream, the dorsal edge was at 3.6° (< ±3° error) counter-clockwise (when looking from above) relative to mainstream flow. The other orientations were rotated 90°, 180°, and 270° with respect to that position.

Three perpendicular components of force are obtained by multiplying pressures by projected areas perpendicular to each component (with appropriate sign conventions). Projected areas were obtained from six photographs, parallel to all sides of a cube, of the model taken from a distance of 15–20 m with a 200-mm lens (the large distance minimizes systematic distortion of area resulting from perspective). Area was measured by weighing areas cut out of the photographs and also, for comparison and estimation of errors, by digitizing the areas with a digitizing tablet and a computer. Error in the area measurement, including bias from area distortion (the difference between the area of calibration square centimeters in front of and behind the clam model) and imprecision (estimated as the standard deviation of repeated measurements), was always less than ±10%. For the moment calculations, the 3-dimensional location coordinates of all holes were also measured from these photographs. Location was measured with an error less than ±7%. The (0,0,0) coordinate was placed at the pivotal point (the point at which the shell touches the ground).

A propagation of errors analysis was performed according to standard formulas (see p. 28 in Schulz, 1945; Ku, 1969). Errors propagated through the moment, and force calculations were the measured standard deviation of pressure at each hole, and an assumed ±10% of the area and ±7% of the distance at each hole.

Another source of error, not expressed in the propagation analysis, is the contribution of tangential forces acting on the surface of the clam. Total force is the sum of forces normal and tangential to the surface, but only the normal forces are measured here. Tangential forces can reasonably be ignored because, for non-streamlined objects at the relevant Re values, tangential forces are relatively small. For instance, friction drag (due to components of tangential forces) is much smaller than pressure drag (due to components of normal forces). For a cylinder perpendicular to flow, pressure drag is 87% and 97% of total drag at Re = 10^3 and 10^4, respectively (Vogel, 1981). Also, for ellipsoidal shapes, with length-to-diameter ratios ranging from 2:1 (long axis parallel to flow) through 1:1 (sphere) to 1:2 (long axis perpendicular to flow), pressure drag ranges from >80% up to >95% of total drag, respectively, at Re = 7×10^4 (Hoerner, 1965). These results apply at subcritical Re values; *i.e.*, in flows in which there is separation of flow on the object. Flow around clams is comparable since (i) flow separates on these clams (observed using dyes and inferred from pressure measurements: see results), and (ii) clams have length-to-diameter ratio of 2:1 or 1:2 depending on orientation, and (iii) measurements were made at Re = 1.9 and 3.4×10^4. Thus, components of normal forces measured here will tend to underestimate drag forces, perhaps by as much as 5%–20%.

The relative size of the clam and the boundary layer also affects pressure measurements; thus the velocity distribution existing in the wind tunnel under experimental conditions is given for comparison. It was measured at a mainstream wind of 2.6 m s^{-1} using a Pitot tube and the same pressure sensor as was used for the clam. Velocity was calculated from

$$\Delta p = \frac{\rho U^2}{2}$$

where Δp is the pressure difference between the static and dynamic openings of the Pitot tube, ρ is the density of the medium, and U is the velocity of the flow at that point (Vogel, 1981).

Density, weight and size of D. variabilis *and density of other Bivalvia*

Live *D. variabilis* specimens of a range of sizes were weighed while they were immersed in water and in air. A formula based on Archimedes Principle was used to calculate the density, ρ_D, of *D. variabilis*.

$$\rho_D = \frac{\rho_s W_A}{(W_A - W_W)}$$

where ρ_s is the density of seawater, W_A is the weight of the clam in air, and W_W is the weight of the clam in sea-

water. The general shape of these clams is also relevant. Using calipers, basic dimension measurements were made of the anterior–posterior, ventral–dorsal, and left–right distances on the same clams.

The densities of other bivalve species, chosen haphazardly on North Carolina beaches, were determined in the same way (three specimens each of seven species were measured). Specimens of the same size as a large individual of *D. variabilis* (2–3 cm long) were used to minimize potential allometric effects on the comparison.

Density, weight distribution, and size effects on orientation

Motions of *D. variabilis* shells of various sizes with experimentally altered density and weight distribution were qualitatively observed in steady flows up to 60 cm s^{-1} in a recirculating flow tank. Tendency to orient and the flow speed at which orientation occurred were noted.

Weight distribution was altered by placing Plasticene in the posterior end and an air bubble in the anterior end (and *vice versa*), of empty *D. variabilis* shells. (Altering weight distribution also unavoidably altered density.) Density was altered by completely filling empty *D. variabilis* shells with candle wax, Silicone rubber or Plasticene; the resulting densities of filled shells were 1.5, 1.7 and 2.0 ($\times 10^3$ kg m^{-3}), respectively. (Altering density unavoidably alters weight distribution slightly.) Shells were placed in flow with four initial orientations: ventral, dorsal, posterior, or anterior edges upstream.

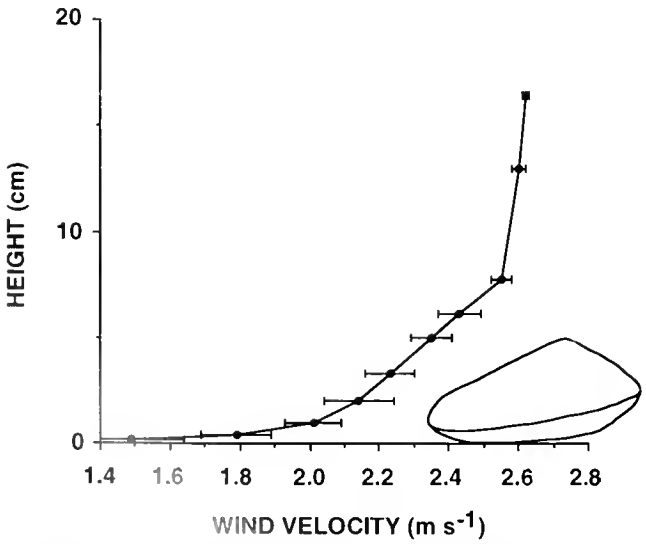

Figure 3. The wind-speed distribution in the tunnel in which pressure measurements on the clam model were made. The mainstream velocity was equivalent to 0.91 m s^{-1} in seawater. The clam was well inside the boundary layer, and is shown for scale (it was not in the tunnel while the speed distribution was measured). Error bars show 1 SD.

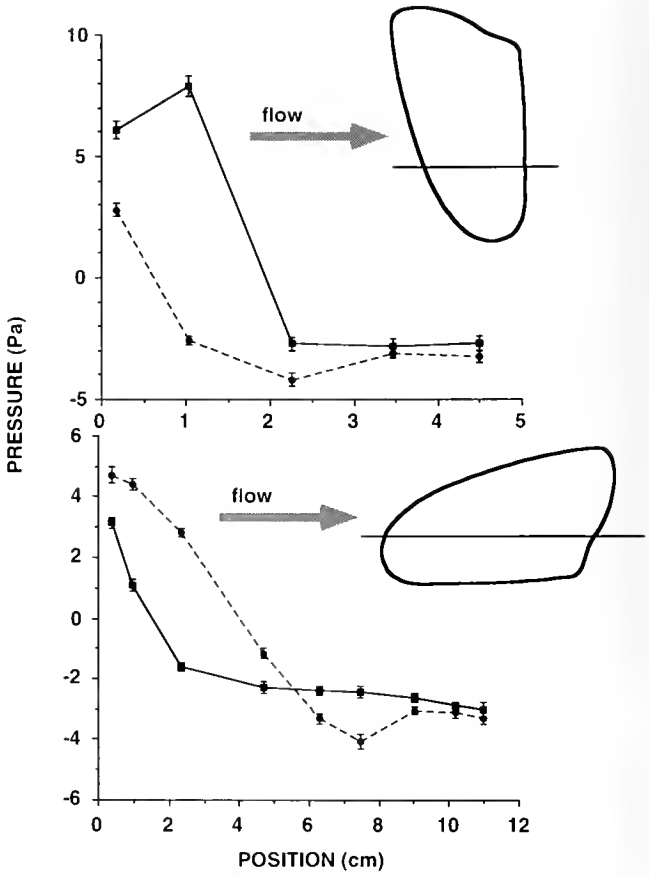

Figure 4. Pressure measurements taken along transects with the clam oriented with the ventral edge upstream and the anterior end upstream. Positive pressures indicate forces acting inward normal to the surface; negative ones indicate outward forces. Dashed line joins upper (right) valve measurements; solid line joins lower (left) valve measurements. Error bars are 1 SD. (For comparison, mainstream wind velocity was 4.6 m s^{-1}, which corresponds to a dynamic pressure of 13 Pa.)

Results

Backwash speed

The average speed of 33 beads was 0.76 ± 0.20 m s^{-1} standard deviation. Speed ranged from 1.1 to 0.38 m s^{-1}. Inaccuracy bounds (>95% confidence intervals) from a propagation of errors estimate are ±11% for the higher speeds, and ±26% for the lower speeds.

Force distribution due to flow on an oriented and unoriented clam

In the wind tunnel, a clam model was located within the gradient of speeds of the boundary layer (Fig. 3). The model's shape altered the velocity distribution around it, which caused pressures on the model. Observed pressure distributions (Fig. 4) are similar to those typical of a bluff body such as a cylinder perpendicular to flow in that, first,

on the upstream side, pressures were high (causing forces pushing downstream); second, partway downstream, pressures became negative (causing outward forces) as flow sped up around the clam; and third, at the downstream end, pressures did not recover (did not become positive as they would have done in an ideal fluid or on a streamlined shape), thus giving rise to pressure drag and signaling separation of flow on the model.

Unlike the pressure distribution on a cylinder, however, time-averaged pressures on the upper and lower surfaces were unequal and resulted in lift. Different characteristic pressure distributions were observed when the anterior end was upstream, as in other orientations. When the ventral edge was upstream, the upper valve always experienced lesser pressures than the lower valve, thus giving rise to upward lift. In contrast, when the anterior end was upstream, the pressure was alternately lesser on the lower and then on the upper surface as flow proceeded downstream; forces from these pressures summed to downward lift.

The overall effects of the pressure distributions in oriented and unoriented clam models are summarized by the resulting forces and moments (Table I). Lift was downward when the anterior end was upstream and upward when the model was in any other orientation. Drag when oriented with the anterior end upstream was less than drag in any other orientation.

When oriented with the anterior end upstream, the model clam experienced a moment tending to force rotation of the anterior end into the sand (Table I; Fig. 5). In other orientations there was also an analogous moment tending to push the anterior end into the sand. Orientation towards the stable position with the anterior upstream may be enhanced by such a moment because it tends to cause tilting; tilting moves the pivotal point anteriorly, thus increasing rotational moments about the vertical, pivotal z-axis.

Even without such tilting, when oriented with the ventral, dorsal, or posterior ends upstream, there were large moments tending to rotate the clam model about the vertical axis and towards an orientation with the anterior end upstream (Fig. 6). In contrast, when the anterior end was upstream, the clam model experienced much smaller moments about the vertical, z-axis. The anterior upstream orientation is rotationally stable.

Density, weight, and size of D. variabilis *and density of other Bivalvia*

D. variabilis is one of the densest bivalves measured (Table II). Size and weight are described for 20 specimens. The (ventral–dorsal distance) = 0.51 (anterior–posterior distance) + 0.081, $r^2 = 0.995$; and the (left–right distance) = 0.36 (anterior–posterior distance) + 0.028, $r^2 = 0.98$, with all distances in centimeters. The anterior–posterior distances ranged from 0.51 to 2.3 cm, and corresponding weights ranged between $7.6\ 10^{-5}$ and $6.8\ 10^{-3}$ N. The (weight in seawater) = $6.2\ 10^{-4}$ (anterior–posterior distance)$^{2.9}$, $r^2 = 0.99$, with weight in N and distance in centimeters.

Density, weight distribution, and size effects on orientation

The tendency to orient with the anterior end upstream in flow is affected by a combination of density, weight distribution, and size (Table III). When shells oriented, they rotated around a vertical axis through the pivotal point and did so while either sliding downstream or remaining at their original location. Weight distribution affected the location of the pivotal axis: the more relatively

Table I

Forces and moments due to flow-induced normal forces at two speeds in seawater (converted from wind tunnel measurements using dynamic similarity)

End Upstream	Speed m s^{-1}	Drag $\times 10^{-4}$ N	$Lift_H \times 10^{-4}$ N	$Lift_V \times 10^{-4}$ N	$M_x \times 10^{-6}$ Nm	$M_y \times 10^{-6}$ Nm	$M_z \times 10^{-6}$ Nm
Anterior	0.91	72 ± 2.8	−39 ± 2.9	−22 ± 4.6	16 ± 2.6	−3.0 ± 3.3	14 ± 2.6
Anterior	1.6	310 ± 10	−130 ± 11	−94 ± 17	17 ± 11	−31 ± 14	49 ± 10
Posterior	1.6	600 ± 15	−330 ± 17	470 ± 26	160 ± 22	570 ± 27	340 ± 17
Dorsal	1.6	960 ± 24	340 ± 19	810 ± 41	−220 ± 26	530 ± 24	140 ± 13
Ventral	0.91	200 ± 6.6	66 ± 6.2	54 ± 12	11 ± 7.8	65 ± 7.3	−88 ± 4.6
Ventral	1.6	560 ± 17	120 ± 14	500 ± 29	67 ± 17	270 ± 15	−240 ± 10

These measurements apply to a *D. variabilis* clam with an anterior–posterior distance of 2.2 cm. For comparison, this clam weighs 61×10^{-4} N in seawater. The coordinate system used for the moments is right-handed* and the positive x-axis is downstream, the positive z-axis is up. Errors, determined by propagation of errors analysis, that approximate 1 SD are shown. $Lift_H$ is horizontal lift; $Lift_V$ is vertical lift; M_x is the moment about the x-axis; M_y is the moment about the y-axis; M_z is the moment about the z-axis.

* Sign convention for moments: if you point your right-hand thumb in the positive direction along the axis about which a moment is tending to cause rotation, then a positive moment tends to cause rotation in the direction that your fingers are pointing. A negative moment tends to cause rotation in the opposite direction.

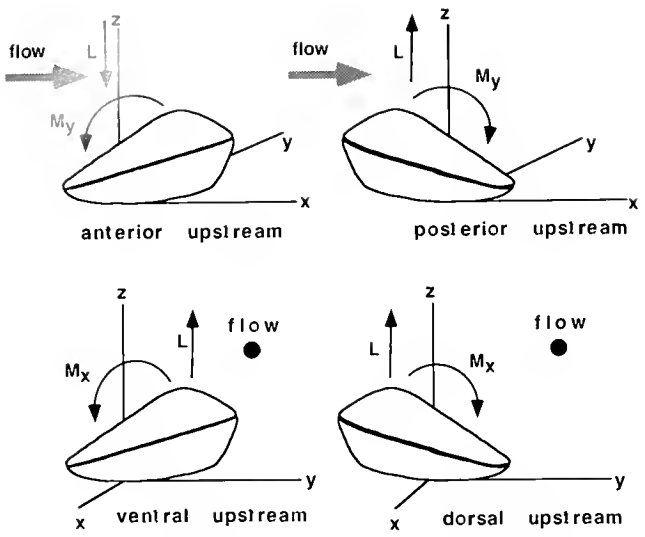

Figure 5. Vertical lift forces and moments tending to tilt a clam's anterior end downward in flow in four different orientations. (Magnitudes not to scale.) The dot indicates flow out of the page: the x-axis is positive downstream. For other symbol and axis definitions see Table I.

heavy the anterior end, the closer the pivotal axis was to the anterior end and the more likely the clam was to orient with the anterior end upstream. If the posterior end was sufficiently heavy, then the pivotal axis lay closer to the middle and no orientation was stable. Denser or larger clams oriented with the anterior end upstream at higher flow speeds. The densest filled shells tested did not orient with the anterior upstream at any of the tested speeds.

Discussion

Morphological causes of passive orientation to a rotationally stable position

A clam orients with the anterior end upstream because moments about a vertical axis through the pivotal point tend to rotate the anterior end upstream (Table I; Fig. 6). Once the anterior end is upstream, the moment about that vertical axis is smaller. Further, rotational moments reverse direction if a clam rotates past that position; thus, once the anterior end is upstream, it tends to stay there.

Larger moments that occur when posterior, ventral, or dorsal edges are upstream are a combined result of the wedge-like shape of *D. variabilis* and the location of the pivotal point. The wedge-like shape creates larger moments by having unequal projected areas, subject to pressure drag, on either side of the vertical axis through the pivotal point. Likewise, if the pivotal point is located close to one end of the clam, then unequal projected areas exist on either side of the vertical axis.

The location of the pivotal point is determined both by a clam's weight distribution and by forces from flow. Forces from flow tilt a clam such that the anterior end is pushed into the sand (Table I; Fig. 5), which moves the pivotal point anteriorly. Tilting thus further increases the projected area on one side of the pivotal axis and increases the moment, tending to cause orientation with the anterior end upstream. Experimentally changing the tilt by changing the weight distribution (using an air bubble and Plasticene in opposite ends) either enhanced or prevented orientation. When the posterior end was heavier and tilted down, the pivotal point moved posteriorly and orientation was prevented because the projected area that gives rise to orienting moments was nearly equal on either side of the vertical axis. Conversely, when the anterior end was heavier and tilted downward, orientation occurred in the flow tank even in relatively slow flow.

In general, orientation depends on flow speed. A minimum flow speed is required because static friction between clam and sand prevents rotation below critical forces and speeds. Equations modeling force balances just prior to rotation show that larger or denser clams require higher flow speeds to start rotating (Ellers, 1987, 1988). Similarly, experiments showed that higher minimum flow speeds are required for orientation of larger and denser shells (Table III).

Density is also crucial in keeping the pivotal point on the ground. If a shell is too light, upward lift can temporarily raise the shell, which results in tumbling rather than orientation. For example, less dense bivalves, such

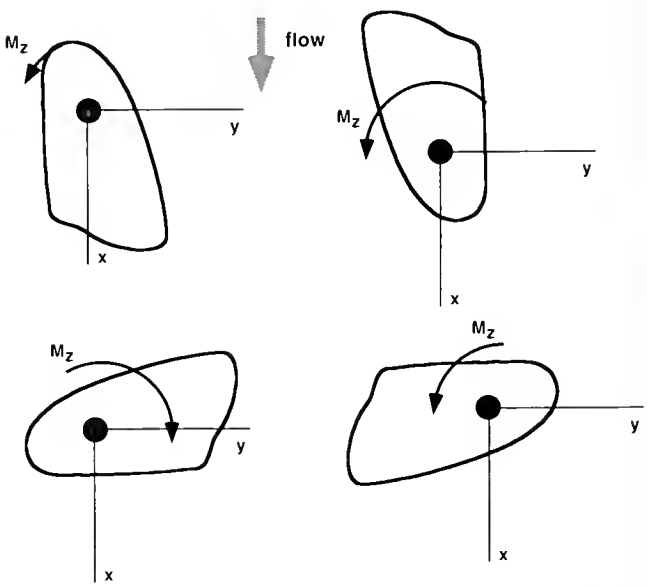

Figure 6. Moments tending to rotate a clam about the vertical, z-axis through the pivotal point. Four initial orientations are shown. Moments tend to rotate a clam towards a position with the anterior end upstream (upper left). That orientation is stable because rotational moments are nearly zero and rotational moments change sign (and direction) if a clam rotates past that orientation. (Magnitudes not to scale.)

Table II

Densities of several species of clams found on North Carolina beaches; most bivalve species are less dense than D. variabilis, *which has a density of 1.65 ± 0.5 SD,* n = *20*

Species	Density × 10^3 kg m^{-3}
Chione cancellata	1.66
Mercenaria mercenaria	1.54
Spisula raveneli	1.47
Macrocallista nimbosa	1.53
Divaricella quadrisculata	1.40
Tellina iris	1.26
Tagellus plebeius	1.17

as *Tellina iris* or *Tagellus plebeius*, tumbled when placed in backwash. Thus, the high density of *D. variabilis* among bivalves (Table II), may be crucial for orientation during swash-riding. A *D. variabilis* clam is in danger of being lifted off the sand in flows from waves: the underwater weight of a clam, 2.2 cm long, is less than its upward lift when it is oriented with the posterior, ventral, or dorsal edge upstream (Table I) in a flow of 1.6 m s^{-1}. In contrast, at 0.91 m s^{-1}, this clam is slightly heavier than the lift it experiences; orientation to a stable position could occur.

Forces exerted on a *D. variabilis* clam at flow speeds encountered in backwash can be expected to cause orientation: observed speeds in the backwash averaged 0.76 m s^{-1}, and 60% of the observed speeds were between 0.56 and 0.96 m s^{-1}. Indeed, these clams often orient in backwash (Fig. 2). Flow speeds of swash are usually higher, reaching a maximum of 3 m s^{-1} even on shallow-sloped beaches (Bradshaw, 1982); thus forces exerted on *D. variabilis* at flow speeds encountered in swash can cause tumbling. Indeed, on a beach, clams often tumble in swash, usually orienting with the anterior end upstream when the swash slows as it reaches its maximum beachward position, or in slower flow in the backwash.

These measurements and observations suggest that the shape and density of *D. variabilis* clams are a complex of morphological characters that act in concert and that are crucial in creating orientation in flow. Further, there is a range of flow speeds in which *D. variabilis* clams can rotate to a stable orientation, and speeds in that range are common on beaches on which these clams live.

Consequences of orientation: a stable, slower ride

When a *D. variabilis* clam is oriented with the anterior end upstream, it experiences less drag than in any other orientation (Table I). Furthermore, it experiences downward lift. Lower drag is primarily attributable to the lower projected surface area exposed to pressure drag when a clam's long axis is parallel to flow. Downward lift is primarily due to the downward tilt of the anterior end of the clam relative to the posterior end, which effectively creates a negative angle of attack relative to flow. Lower drag and downward lift result in a stable, slower ride.

Lower drag resulting in slower speed relative to the substratum may seem initially counterintuitive because drag is most commonly encountered as a force that impedes motion. During swash-riding, however, drag is a force that propels a clam. A higher drag results in a sliding speed more nearly water speed, and therefore a greater ground speed. Conversely, lower drag and downward lift (higher friction with the ground) cause slower speeds of swash-riding relative to the substratum.

During slower, stable sliding with the anterior end upstream, the foot, which protrudes from the anterior end, has a better chance of achieving a foothold than if the clam were tumbling, rotating, or oriented any other way. After gaining a foothold, the sand upstream of a clam tends to get scoured out (Fig. 2), which assists a clam in digging into the sand. On a beach, dead shells oriented with the anterior end upstream were sometimes observed to sink passively into the scoured sand just upstream of their shells. Thus, orientation with the anterior end upstream enhances a clam's ability to stop moving and to burrow into the sand after a swash-ride.

A clam's ability to maintain position on the beach or to make net shoreward progress during shoreward migration depends on its being able to establish a foothold before being washed out to sea. Gaining a foothold while the backwash is flowing is therefore crucial. Orientation with the anterior end upstream, with its concomitant reduced drag and downward lift, may be the decisive factor in making migration by swash-riding possible.

Table III

Qualitative observations of the effects of weight distribution, density, and size on the tendency of D. variabilis *shells to orient passively with the anterior end upstream*

Variable	Level	Final Orientation in Flow
Weight distribution	Light anterior	No orientation
	Light posterior	Anterior upstream always
Density	1.5 × 10^3 kg m^{-3}	Anterior upstream usually
	1.7 × 10^3 kg m^{-3}	Anterior upstream occasionally
	2.0 × 10^3 kg m^{-3}	No orientation
Size*	2.2 cm	Anterior upstream above 40 cm s^{-1}
	1.5 cm	Anterior upstream above 30 cm s^{-1}
	1.2 cm	Anterior upstream above 25 cm s^{-1}

Shells were experimentally altered as indicated and were placed in a flow tank with one of the initial orientations (anterior, posterior, ventral, or dorsal edge upstream). Max. flows tested were 60 cm s^{-1}.

* Numbers shown are for filled shells of density 1.5 × 10^3 kg m^{-3}.

Morphological and behavioral control of swash-riding

That shape can affect movement of clam-like objects in waves has been demonstrated previously (Lever, 1958; Lever *et al.*, 1961, 1964, 1968). Wave-induced, passive, net movement of many thousands of manufactured model *Donax vittatus* valves were observed over one tidal cycle. Right valves were swept seaward, whereas left valves remained on the beach; less dense valves moved further than more dense ones; larger shells remained on the beach longer than smaller ones. Thus, net passive movement of valves by waves depends on density, size, and shape. Likewise, the movements of whole, live clams also depend on these variables. *D. variabilis* clams control where waves move them by using a combination of behavior and a complex of morphological characters: the wedge-like shape, high density, and anteriorly located pivotal point.

A *D. variabilis* clam can modulate its speed on the beach relative to the speeds of the swash and backwash occurring under a range of wave conditions. On days with only small waves and slow swash and backwash speeds, clams protract foot and siphons (pers. obs.), thus increasing drag and clam speed by exposing more area to flow. On days with higher waves, clams keep foot and siphons retracted, decreasing their speed relative to flow. If flow speeds are sufficiently high to cause orientation, a clam orients with the anterior end upstream, which reduces drag and thus again reduces clam speed relative to flow speed. If flow speeds are so high that the clam tends to tumble before it can orient, then the clam tumbles in flow and moves nearly at flow speeds until the flow slows down, as it usually does in the backwash. Once the flow is sufficiently slow for orientation, a clam can regain a foothold.

Ecological and evolutionary consequences

Net movement in waves, the number of swash-rides required for migration, and hence the energy cost of migration (Ansell and Trueman, 1973), depend on both the prevailing wave conditions and the shape and behavior of a swash-riding clam. Flow speeds from waves typically depend on beach structure and wave conditions. Whether *D. variabilis* clams can live on a given beach will depend on the prevalence of suitable flow speeds on the beach. Flow speeds must typically be fast enough to overcome friction between clam and sand, but slow enough that lift-off does not occur in the backwash.

The functional morphology of swash-riding thus suggests that the swash-riding performance of a *Donax* species should be related to typical flows on the beaches on which it lives. An intriguing comparison species is the largest (7 cm long) *Donax* species, *Donax serra*, which swash-rides but migrates on a semilunar cycle (Donn *et al.*, 1986) rather than a tidal cycle. Zonation patterns of different populations of *D. serra* were found to be statistically explained by the morphological characters weight, surface area, and elongation; populations found higher in the intertidal had thicker valves and higher density than those found lower in the intertidal (Donn, 1990).

Similarly, the ecology of sandy beaches may depend on the flow regime of swash and backwash. The physical environment, described by wave-regime parameters, was found to control species richness of sandy beach fauna (McLachlan *et al.*, 1993). Body size and means of locomotion (such as swash-riding) were suggested as important parameters in determining the extent to which organisms were able to live on beaches as the swash "climate" became harsher.

The functional morphology of swash-riding clams also suggests characters that may have been important in the evolution of swash-riding in donacid bivalves. Since swash-riding is enabled by high density, a wedge-like shape, and an anteriorly located pivotal point, evolution of these characters is predicted to be correlated with swash-riding. A large range of donacid species inhabiting a range of beach types exists in the world. Independent contrasts methods (Harvey and Pagel, 1991) and morphological comparisons using functional morphospaces (Ellers and Telford, 1991; Moore and Ellers, 1993) could be applied to test whether these characters are evolutionarily correlated with swash-riding.

Acknowledgments

This research is part of the author's Ph.D. dissertation completed at Duke University. I thank my thesis supervisor, S. Vogel, and committee members, V. L. Roth, E. J. Shaughnessy, V. A. Tucker, and S. A. Wainwright. NSERC postgraduate scholarships, Duke University teaching assistantships, and a Cocos Foundation Training Grant in Morphology supported the author. I thank A. S. Johnson for reading the manuscript and S. Vogel for writing the digitizer communication code.

Literature Cited

Ansell, A. D., and E. R. Trueman. 1973. The energy cost of migration of the bivalve *Donax* on tropical sandy beaches. *Mar. Behav. Physiol.* **2**: 21–32.

Bradshaw, M. 1982. Bores and swash on natural beaches. *Coastal Studies Unit Technical Report No. 82/4* Coastal Studies Unit, Department of Geography, The University of Sydney, Sydney, NSW, Australia.

Donn, T. E., Jr. 1990. Morphometrics of *Donax serra* Röding (Bivalvia: Donacidae) populations with contrasting zonation patterns. *J Coastal Res.* **6**: 893–901.

Donn, T. E., Jr., D. J. Clarke, A. McLachlan, and P. du Toit. 1986. Distribution and abundance of *Donax serra* Röding (Bivalvia: Donacidae) as related to beach morphology. I. Semilunar migrations. *J. Exp. Mar. Biol. Ecol.* **102**: 121–131.

Ellers, O. 1987. Passive orientation of benthic animals in flow. Pp. 45–68 in *Signposts in the Sea. Proceedings of a Multidisciplinary*

Workshop on Marine Animal Orientation and Migration, W. F. Herrnkind and A. B. Thistle, eds. Dept. of Biological Science, Florida State University, Tallahassee.

Ellers, O. 1988. Locomotion via swash-riding in the clam *Donax variabilis* Ph.D. Dissertation, Duke University, Durham, NC.

Ellers, O. 1995a. Behavioral control of swash-riding in the clam *Donax variabilis*. *Biol. Bull.* **189:** 120–127.

Ellers, O. 1995b. Discrimination among wave-generated sounds by a swash-riding clam. *Biol. Bull.* **189:** 128–137.

Ellers, O., and M. Telford. 1991. Forces generated by the jaws of clypeasteroids (Echinodermata: Echinoidea). *J. Exp. Biol* **155:** 585–603.

Harvey, P. H., and M. D. Pagel. 1991. *The Comparative Method in Evolutionary Biology*. Oxford University Press, Oxford. 239 pp.

Hoerner, S. F. 1965. *Fluid-Dynamic Drag*. S. F. Hoerner, 2 King Lane, Greenbriar, Brick Town, NJ 08723.

Jacobson, M. K. 1955. Observations on *Donax fossor* Say at Rockaway Beach, New York. *Nautilus* **68:** 73–77.

Ku, H. H. 1969. Notes on the use of propagation of error formulas. Pp. 331–263 to 341–273 in Chapter 5, Section 2 of *Precision Measurements and Calibration, Statistical Concepts and Procedures*, Special Publication 300, Vol. 1, H. H. Ku., ed. U.S. Dept. of Commerce, National Bureau of Standards.

Lever, J. 1958. Quantitative beach research I. The "left-right phenomenon": sorting of lamellibranch valves on sandy beaches. *Basteria* **22:** 21–51.

Lever, J., M. van den Bosch, H. Cook, T. van Dijk, A. J. H. Thiadens, and R. Thijssen. 1964. Quantitative beach research III. An experiment with artificial valves of *Donax vittatus*. *Neth. J. Sea Res.* **2:** 458–492.

Lever, J., A. Kessler, A. P. van Overbeeke, and R. Thijssen. 1961. Quantitative beach research II: The "hole effect": a second mode of sorting of lamellibranch valves on sandy beaches. *Neth. J. Sea Res.* **1:** 339–358.

Lever, J., and R. Thijssen. 1968. Sorting phenomena during transport of shell valves on sandy beaches studied with the use of artificial valves. *Symp. Zool. Soc. Lond* **22:** 259–271.

McLachlan, A., E. Jaramillo, T. E. Donn, and F. Wessels. 1993. Sandy beach macrofauna communities and their control by the physical environment: a geographical comparison. *J. Coastal Res.* Special Issue **15:** 27–38.

Moore, A. M. F., and O. Ellers. 1993. A functional morphospace, based on dimensionless numbers, for a circumferential calcite stabilizing structure in sand dollars. *J. Theor. Biol.* **162:** 253–266.

Mori, S. 1938. Characteristic tidal rhythmic migration of a mussel, *Donax semigranosus* Dunker, and the experimental analysis of its behaviour at the flood tide. *Dobutsugaku Zasshi*, [=*Zool. Mag. (Japan)*] **50:** 1–12.

Schulz, G. 1945. *Formelsammlung zur praktischen Mathematik*, Göschen Band 1110. W. de Gruyter, Berlin.

Shames, I. H. 1982. *Mechanics of Fluids* McGraw Hill Book Co., New York.

Tiffany, W. J. III. 1971. The tidal migration of *Donax variabilis* Say (Mollusca: Bivalvia). *Veliger* **14:** 82–85.

Tucker, V. A., and G. C. Parrott. 1970. Aerodynamics of gliding flight in a falcon and other birds. *J. Exp. Biol* **52:** 345–367.

Vogel, S. 1981. *Life in Moving Fluids*. Princeton University Press, Princeton, NJ.

Vogel, S. 1985. Flow-assisted shell reopening in swimming scallops. *Biol. Bull.* **169:** 624–630.

Wade, B. 1967. Studies on the biology of the West Indian Beach clam, *Donax denticulatus* Linné. 1. Ecology. *Bull. Mar. Sci* **17:** 149–174.

Reference: *Biol. Bull.* 189: 148–158. (October/November, 1995)

Morphology and Physiology of the Thoracic and Abdominal Stretch Receptors of the Isopod Crustacean *Ligia exotica*

AKIYOSHI NIIDA, YOSHIKO TAKATSUKI*, AND TSUNEO YAMAGUCHI

Department of Biology, Faculty of Science, Okayama University, Tsushima, Okayama 700, Japan

Abstract. In the terrestrial isopod *Ligia exotica*, paired stretch receptors, each comprising a separate rapidly and slowly adapting receptor cell, were found in the third to eighth thoracic segments and first five abdominal segments. The dendritic endings of the two sensory cells in each receptor terminate on a common receptor muscle; the cross-striation of this fiber is homogeneous throughout the segments. But the dendritic endings of the receptor cells differ: the rapidly adapting cell has a club-shaped ending restricted to the middle of the receptor muscle, whereas the slowly adapting receptor cell has a bifurcating ending that extends along the entire length of the muscle. Stretch applied to the receptor muscle evokes characteristically different responses in the two sensory cells. The slowly adapting receptor cell has a lower firing threshold and fires continuously for the duration of the stretch, while the rapidly adapting receptor cell has a higher threshold and fires a brief burst at the beginning of the stimulus. However, application of an intense stimulus will evoke continuous firing of the rapidly adapting receptor, which then changes to intermittent bursts. The adaptive significance of such a response is not known, nor is it likely to occur in nature. However, this unusual response is intrinsic to the rapidly adapting cell, as it can be evoked by current injection. In the second thoracic segment, instead of rapidly and slowly adapting cells, we found a single slowly adapting cell with a long robust dendrite attached to the extensor muscle.

Introduction

Phylogenetically, *Ligia* and the pill bug *Armadillidum vulgare* belong to the same suborder (Oniscoidea) of Isopoda. Both show a similar segmental pattern: a mobile thorax occupying a large part of the body and a reduced abdomen. The two animals also show distinct segmental movements of the body. The pill bug sluggishly rolls up in a spherical shape in response to noxious stimuli to its body or to the removal of its substratum. *Ligia*, in contrast, cannot roll up in this manner in response to such stimuli; rather, as in its swimming behavior, it shows the rapid upward and downward movements of the thoracico-abdominal segments. Niida *et al.* (1990) studied the stretch receptors that might correlate with the pill bug's sluggish conglobating behavior, and demonstrated that all the stretch receptors throughout thoracic and abdominal segments were of the slowly adapting type. Alexander (1971) recorded rapidly adapting discharges from the thoracic stretch receptors of *Ligia oceanica;* but slowly adapting stretch receptors, such as those in the abdomen of the crayfish *Procambarus clarkii* (Wiersma *et al.*, 1953), have not been reported in *Ligia*.

The existence of slowly adapting stretch receptors in *Ligia* is strongly suggested by the behavior described above, which surely requires postural controls. In addition, two types of stretch receptors—slowly and rapidly adapting—occur commonly in the abdomens of the decapod (Wiersma *et al.*, 1953) and stomatopod (Pilgrim, 1964). Even the N-cells, which are located in the most anterior segment of the thorax and have been considered as remnants of retrograde stretch receptors in the abdomen (Wiersma and Pilgrim, 1961), show slowly adapting impulse discharges in response to imposed stimuli. We thus assume that the slowly adapting stretch receptor should also predominate in *Ligia*.

The goal of this research is to understand the functional roles of the thoracic stretch receptor, especially anteriorly located ones, which would be closely related to segmental

Received 26 July 1994; accepted 26 July 1995.

* Present address: Department of Oral Science, Kyushu Dental College, Manazuru 2-61-1, Kokura, Kita-Kyushu 803, Japan.

movements. The present study thus characterized the stretch receptors of *Ligia exotica* both morphologically and physiologically. Some of the results presented here were reported in an earlier abstract (Takatsuki *et al.*, 1992).

Materials and Methods

Animals

Specimens of *Ligia exotica*, 30–35 mm in total length, were collected at the coast of the Seto Inland Sea near Ushimado Marine Laboratory, Faculty of Science, Okayama University, Japan. They were kept under a photoperiodic regime of 12 h light:12 h dark at 20°C. Both males and females were used in the experiments.

Identification of stretch receptors

Conventional vital staining with methylene blue was used, as well as axonal filling with nickel chloride. In the latter staining technique, the cut distal stump of the dorsal nerve of the third nerve root in the thoracic ganglion was introduced into a glass capillary filled with 0.2 *M* $NiCl_2$. The preparation was stored at 4°C for 12–24 h to allow diffusion of the $NiCl_2$, which was precipitated by the addition of rubeanic acid. Stretch receptors identified by both staining methods were isolated and mounted in gelatin on glass slides.

Preparation for recording

The responses of the stretch receptors to imposed stimuli were recorded *in situ* and *in vitro*. The following three types of preparations were used.

1. A semi-intact preparation was used when flexion was imposed *in situ*. After animals were anesthetized in cold seawater and decapitated, the legs and the 6th abdominal segment were cut off. The viscera were then dissected away from the cut end of the 6th abdominal segment, and the nerve cord was left intact. Such preparations were immediately flushed with seawater to prevent the deterioration of stretch receptors and nervous tissue by endogenous digestive enzymes.
2. A consecutive tergite preparation was used for imposed stretch experiments. The semi-intact preparation described above was cut with scissors along the midline of the sternite so that the trunk was bisected into two stripes of hemisegments from which the nerve cord was removed. These hemisegment preparations were then further cut into pieces of two consecutive tergites each.
3. A preparation of isolated stretch receptor was used for *in vitro* experiments. The dorsal nerve containing the axons of the stretch receptors was cut at its proximal end. The stretch receptor was then isolated by cutting the receptor muscle near its insertion.

Each of these three preparations, when complete, was then transferred to an experimental chamber filled with seawater. Most experiments were carried out in seawater cooled to 15–18°C. But at times a physiological saline for *Ligia*, prepared by Yamagishi (1985) based on the composition of *Ligia* serum (Parrey, 1953), was also used. We found no remarkable difference in impulse discharges for at least 5 h between seawater and physiological saline.

Stimulation and recording

Flexion experiments. For extracellular recording from the stretch receptors in the 7th thoracic segment, all the anterior tergites up to the 6th thoracic segment were fixed ventral side up on a silver plate with instantaneous adhesive, while the free movable tergite of the 6th abdominal segment was pierced with a hook-shaped needle connected to the vertically moving central pin of a vibrator device (Fig. 1A). The vibrator device, with a frequency response from DC to 200 Hz, was driven by applying a ramp-and-hold pulse by which flexion size of the abdomen to the horizontal was varied from 0° to 60°. The flexion-induced responses were recorded from the dorsal nerve of the 3rd

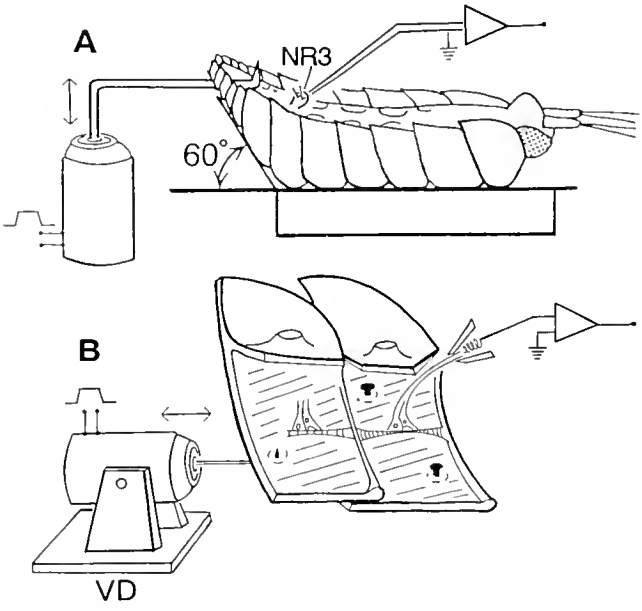

Figure 1. Experimental setup for recording responses from stretch receptors. (A) *In vivo* preparation. A flexion stimulus was delivered by a vibration device with an L-shaped arm that moves upward. In the experiments reported here, the flexion was produced by flexing the abdomen to 60° to the horizontal. Resultant responses were recorded with a tungsten hook electrode attached to the 3rd nerve root. (B) *In situ* preparation. One end of a pair of the bisected tergites was fixed with insect pins, and the other was connected to a vibration device that delivered the stretch stimulus. Stretch-induced activities of the receptor cells were recorded through a suction electrode attached to the distal cut end of the dorsal nerve of NR3. NR3, 3rd nerve root; VD, vibration device.

nerve root of the 6th thoracic ganglion with a tungsten hook electrode insulated by addition of mineral oil.

Imposed stretch experiments. The tergite just anterior to the segment containing the stretch receptors to be studied was fixed with an insect pin ventral side up. The free end posterior to the segment to be studied was connected to the horizontally moving pin of the vibrator device through the hook-shaped needle in the same manner as described above (Fig. 1B). A controlled stretch stimulus was thus delivered to the receptor muscle in the relevant segment, and the resulting responses were obtained from the dorsal nerve of the 3rd nerve root; the dorsal nerve was cut distally and introduced into a suction electrode made of a glass capillary.

In vitro experiments. Intracellular recordings were made for two purposes. The first was to determine which of the two receptor cells was responsible for a given response: *i.e.*, the slowly or rapidly adapting response to stretch stimuli. Each of the receptor cells was impaled with a glass microelectrode filled with 3 *M* KCl. Subsequently, imposed stimuli were delivered; each end of the receptor muscle of an isolated stretch receptor was gripped with a clamp mounted on a micromanipulator with which the receptor muscle was manually stretched. The second purpose was to analyze the characteristics of the intermittent discharges (described later) specific to the rapidly adapting stretch receptors of *L. exotica*. A bridge circuit was used in the analysis of the intermittent bursts, so current was injected into the receptor cell and the concomitant responses were recorded through a single microelectrode that was filled with 3 *M* KCl and had an impedance of 20–30 MΩ.

Results

As described below, segmental stretch receptors occur bilaterally in the thoracic and the abdominal segments of *L. exotica*. For simplicity, the results will be described from one side only, and we refer to the thoracic and the abdominal stretch receptors as TSR and ASR, respectively. This study demonstrated the existence of slowly and rapidly adapting stretch receptors differing both physiologically and morphologically. A few animals did not respond to the stretch stimuli, where current injection into the stretch receptor cells produced a response comparable to that obtained by stretching. In *Ligia*, therefore, mechanical transduction might be greatly influenced by the mechanical deformation that occurs during the dissection of stretch receptors.

Spatial organization of stretch receptors

The segmental trunk of *L. exotica* is composed of eight thoracic and six abdominal segments; because the first thoracic segment is fused with the head, the main part of the thorax forms seven segments, *i.e.*, the 2nd to 8th segments. Figure 2A shows the spatial organization of stretch receptors in the thoracic and abdominal segments, where each stretch receptor, except for TSR-1 (Fig. 2A), comprises a set of paired receptor cells and a single specialized receptor muscle. The TSR-1 possesses no specialized receptor muscle; instead, the musculature associated with the TSR-1 is an ordinary dorsal extensor muscle. The dendrite of the TSR-1, in its course, is partially attached to the articular membrane of the anterior ridge of the 3rd thoracic segment and runs toward its insertion in the anterior edge of the extensor muscle of the 2nd thoracic segment.

The characteristic organization of stretch receptors appears in TSR-2, which is located between the 3rd and 4th thoracic segments. A long receptor muscle (*ca.* 5 mm in 3.5 cm body length) has its posterior insertion on the anterior ridge of the 5th segment and runs through the 4th segment to the articular membrane of the anterior ridge of the 3rd segment. A pair of functionally differentiated receptor cells terminates on this receptor muscle within the 4th thoracic segment.

In the 5th thoracic segment, the anterior and posterior insertions of the receptor muscle lie on the individual anterior ridge of the 5th and 6th thoracic segments (Fig. 2A). This arrangement of the anterior and posterior insertions also occurs in the receptor muscle of the 6th thoracic segment. The arrangement in the most posterior of the thoracic segments is different again: anterior insertions of the receptor muscles of the 7th and 8th thoracic segments are in the connective tissue of each leg muscle of the 7th and 8th thoracic segments, whereas their posterior insertions occurred on the anterior ridges of the 8th thoracic and 1st abdominal segments, respectively (Fig. 2A).

TSR-1, as can be seen in Figure 2A, lies medially in association with the extensor muscle, but TSR-2 and subsequent stretch receptors lie somewhat dorsolaterally, and much more laterally than abdominal stretch receptors in the crayfish. The thoracic receptor muscles are shorter in successively more posterior segments, whereas abdominal receptor muscles become longer posteriorly (Fig. 2A).

Axonal pathway of stretch receptors

The 3rd nerve root of each thoracic ganglion branches complexly: the dorsal nerve in this 3rd root provides a common pathway both for the central projection of the axons of stretch receptor cells and for efferents to the extensor muscle (Fig. 3A). A pair of the axons of the thoracic stretch receptor cells (rapidly and slowly adapting cells) bifurcate at the 3rd nerve root and course in two directions in pairs; one runs towards the subesophageal ganglion and the other towards the 6th abdominal ganglion (unpub. obs.). In the abdomen, the axons of the stretch receptor

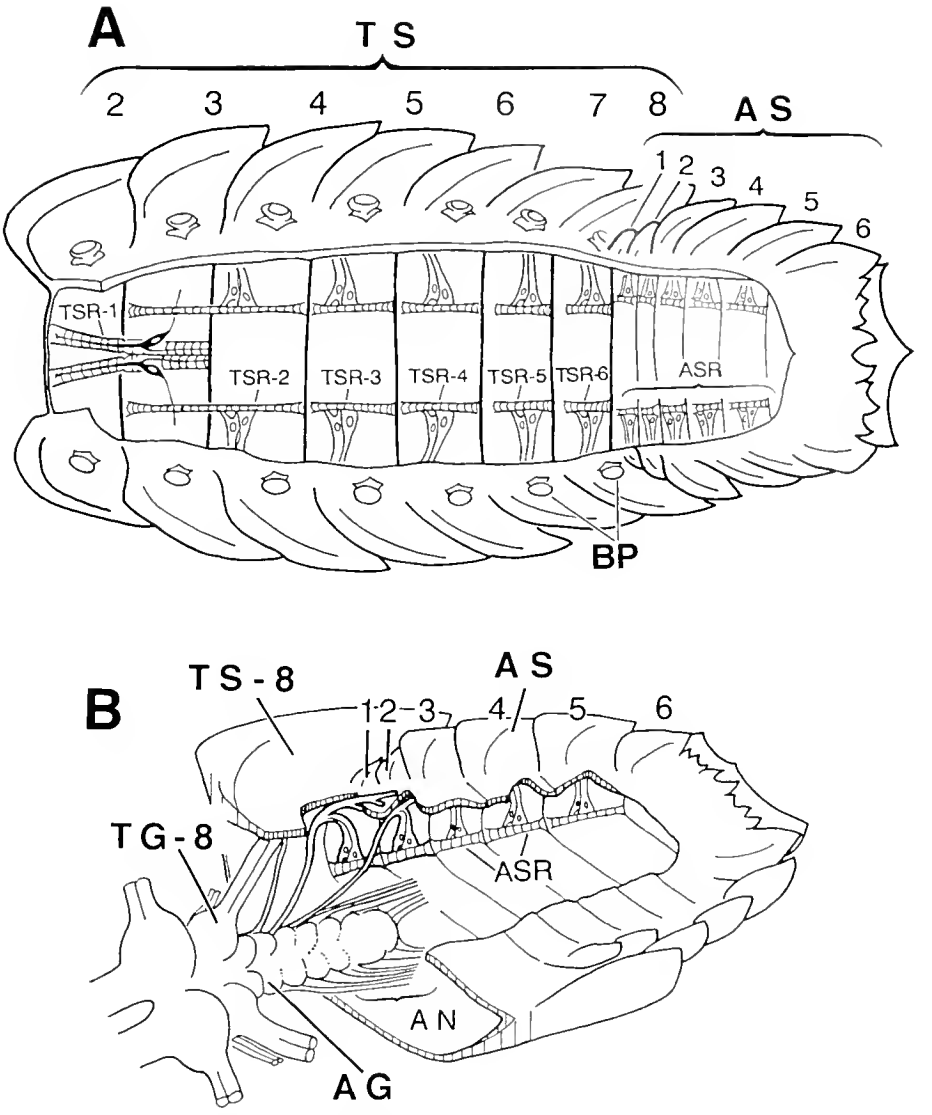

Figure 2. Organization of thoracic and abdominal stretch receptors (A) and the central connection of abdominal stretch receptors (B). (A) and (B) are viewed from the ventral side, and the viscera were removed as well as all muscles, except for those with which the stretch receptors are associated. In (A), head and legs are removed, and the first thoracic segment is not depicted because it is fused with the head. AG, abdominal ganglion; AN, abdominal nerve; AS, abdominal segment; ASR, abdominal stretch receptor; BP, basal propodite; TG-8, 8th thoracic ganglion; TS-8, 8th thoracic segment; TSR, thoracic stretch receptor. Numerals after TSR and ASR indicate position in the sequence of the segmental stretch receptors.

cells run through the abdominal nerve (Fig. 2B) and enter the several fused abdominal ganglia.

Morphological characteristics

Thoracic stretch receptors. TSR-1 has an extremely long dendritic process extending from a bipolar receptor cell located in the ventral surface of the medial extensor muscle of the 3rd thoracic segment (Fig. 2A). The dendritic process is quite stout in the anterior ridge of the 3rd thoracic segment, but as it extends forward, it gradually thins, running in close contact with the extensor muscle. The dendrite is attached to the muscle at its anterior extremity in the 2nd thoracic segment. Thus, although the length of the dendritic process depends on the total body length, in animals 3 to 4 cm long, it measures 2 to 3 mm from the receptor cell soma. Running posteriorly, a thin strand originates from the initial part of the stout dendrite, but its insertion could not be traced precisely.

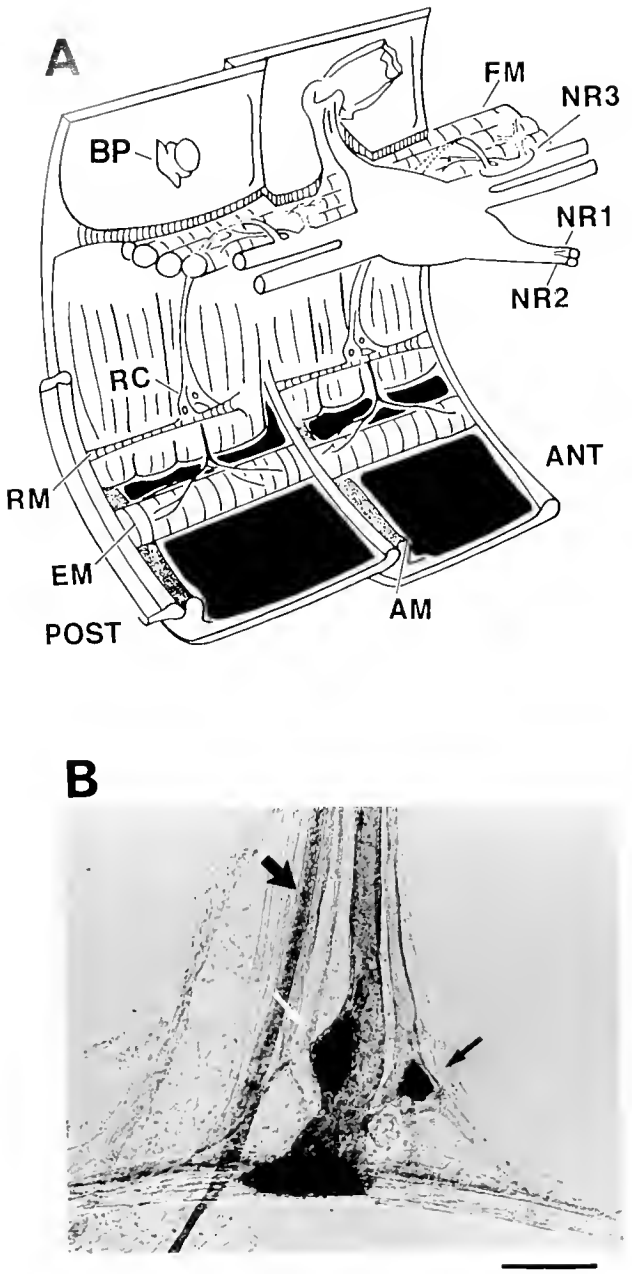

Figure 3. (A) Spatial arrangement of stretch receptors in the 6th and 7th thoracic segments and the central connections of stretch receptors. The figure, viewed from the ventral side, shows hemisegments with part of the lateral side of the tergites not depicted. NR1 and 2 run towards the pereopod, whereas the dorsal nerve of NR3 provides a common pathway for the central projection of the axon of the stretch receptors and for the efferent fiber to the extensor muscle (EM). Note that the anterior insertion of receptor muscle of the 7th thoracic segment occurs in the leg muscle of the same thoracic segment. (B) Photomicrograph of a thoracic stretch receptor (TSR-3) stained by axonal filling with nickel chloride. Thick arrowhead indicates an efferent to the extensor muscle. Thin white and black arrowheads indicate C-type (rapidly adapting) and B-type (slowly adapting) stretch receptors, respectively. Scale bar, 200 μm. ANT, anterior; AM, articular membrane; BP, basal protopodite; EM, extensor muscle; FM, flexor muscle; NR1, 1st nerve root; NR2, 2nd nerve root; RC, receptor cells; RM, receptor muscle; POST, posterior.

With the exception of TSR-1, the receptor cells of the stretch receptors in both thoracic and abdominal segments were classified morphologically into two different types on the basis of their dendrites: club-shaped cells (C-type) and bifurcating cells (B-type) (Fig. 3B). The characteristics of these cell types emerge from schematic illustrations of the stretch receptors in the 2nd to 8th thoracic segments (Fig. 4). Each C-type cell shows a stout dendrite attached to the central part of the receptor muscle. In contrast, the branching dendrites of B-type cells run in both directions along the total length of the receptor muscles. The dendritic processes of both C- and B-type cells are much longer in TSR-2 than those of the stretch receptors in other thoracic segments. Another characteristic of the stretch receptors is the homogeneous striation of the receptor muscles throughout thoracic and abdominal segments. Although systematic measurements were not made, the sarcomere length of the receptor muscle in the 7th thoracic segment was 3.6 ± 0.18 (mean ± SD) μm. Of course, this muscle—in every segment—is shared by slowly and rapidly adapting stretch receptor cells. In the crayfish, however, the sarcomeres are short (3.3 μm) in the receptor muscle of the rapidly adapting stretch receptor, and long (6.5 μm) in that of the slowly adapting stretch receptor (Komuro, 1981).

Abdominal stretch receptors. The morphology of the abdominal stretch receptors (Fig. 5) is similar in general to that of the thoracic receptors: *i.e.*, there are C-type and B-type receptor cells, and they are attached to the single receptor muscles with homogeneous striations. But the B-type receptor cells of the 2nd and 3rd abdominal segments show morphological variations in the manner of the bifurcation of their dendrites. Generally, the dendrites of the B-type receptor cells in the 2nd and 3rd abdominal segments bifurcated in close contact with the receptor muscle, as in ASR-1 (Fig. 5), but some receptor cells show a dendritic branching pattern; *e.g.*, in ASR-4 the dendrite branches distally to the receptor muscle. Another difference from the TSR is that the dorsal extensor muscle closely parallels the abdominal receptor muscle. This anatomical arrangement closely resembles that of the crayfish, *Procambarus clarkii* (Wiersma *et al.*, 1953).

In situ *response of stretch receptors to imposed flexion*

Figure 6 shows a representative *in situ* recording from TSR-5 of the 7th thoracic segment in response to abdominal flexion in the ventral direction (upward imposed flexion). The flexion was imposed with a vibrator device driven by a ramp-and-hold pulse of 0.05 Hz; the animal was ventral side up, and the abdominal flexion was 60° from the horizontal axis (Fig. 1A). The evoked responses showed slowly and rapidly adapting impulse discharges or phasic and tonic responses, as shown in

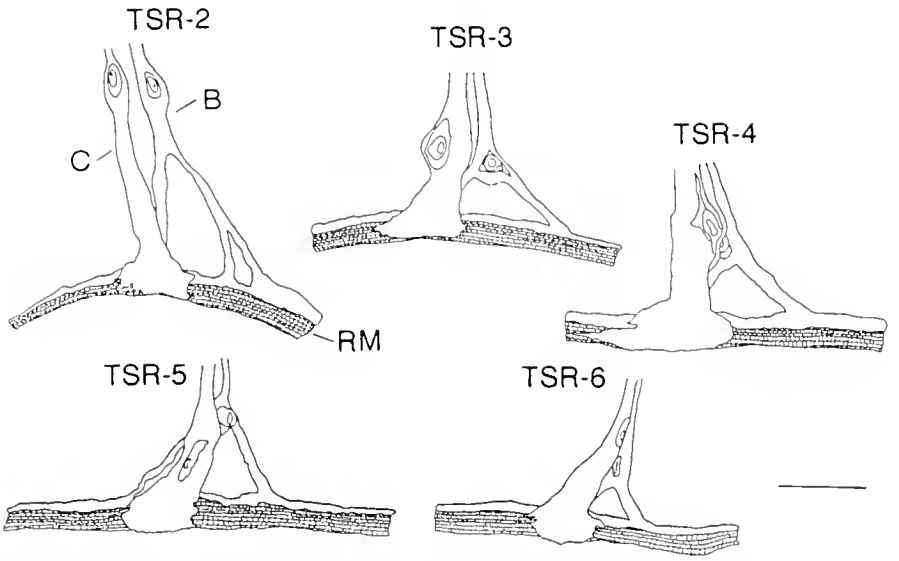

Figure 4. Schematic drawings of thoracic stretch receptors. The drawings in this and the next figures were based on specimens stained with methylene blue. B, B-type cell; C, C-type cell. Note that the cross-striation within every receptor muscle, from TSR-2 to TSR-6, is homogeneous. Scale bar, 100 μm.

the inset of Figure 6. The adaptive time courses of impulse discharges from rapidly and slowly adapting stretch receptors are also shown in Figure 6a and b. The phasic response has longer latency due to the slow rise of the stimulus delivered at 0.05 Hz; the phasic quality indicates dependence on the velocity; *i.e.*, the rate of displacement (angle/s) of the thoracic segment by the flexion stimulus (Fig. 7). Similar responses accompanied by tonic impulse discharges were recorded from the TSR-5 upon abdominal extension (downward imposed flexion) (data not shown). Extension produced much lower impulse frequencies than flexion, even when the degree of the applied stimulus was the same. In the presence of motor activities of the extensor neuron,

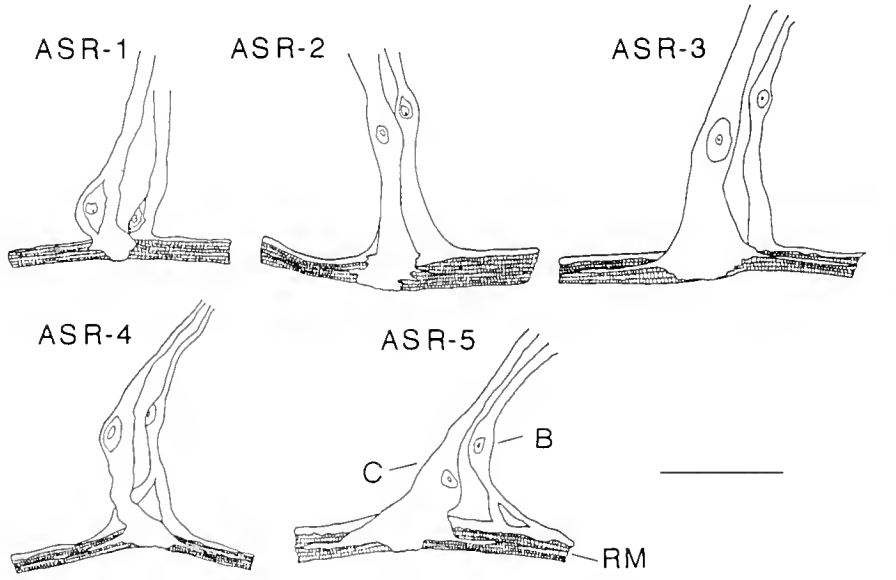

Figure 5. Schematic drawings of abdominal stretch receptors. Homogeneous cross-striation is similarly noted in the abdominal receptor muscles. B, B-type cell; C, C-type cell. Scale bar, 100 μm.

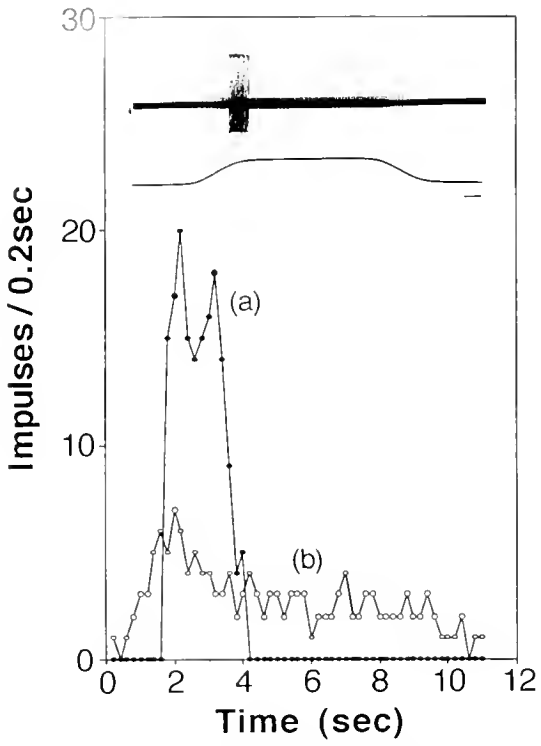

Figure 6. Response of TSR-5 (*in situ* preparation) to imposed flexion. (a) and (b): the time courses of impulse discharges in the rapidly and slowly adapting stretch receptors, respectively. Inset: responses from the two types of stretch receptors. Lower trace, flexion amplitude (60° from horizontal). Time scale, 1 s.

however, impulse frequencies of the TSR-5 were somewhat increased (data not shown).

Response of thoracic stretch receptors to stretch stimuli

Both slowly and rapidly adapting impulse discharges were evoked from each stretch receptor in the 3rd to 8th thoracic segments by an imposed stretch stimulus. In contrast, TSR-1 in the most anterior segment is a simple stretch receptor and its response is only slowly adapting (not shown). To represent activities of the stretch receptors with both slowly and rapidly adapting cells, the records from TSR-2 are shown in Figure 8, and two kinds of impulse discharges differing in their frequency and amplitude can be seen (Fig. 8A). One was derived from a slowly adapting receptor cell and showed a tonic impulse discharge that gradually adapted as long as the receptor muscle was stretched. In this particular receptor, the ongoing tonic impulse discharges appeared before the stretch stimulus because we extended the receptor muscle slightly while securing the thoracic segment with insect pins to the cork platform in the experimental chamber. In this experiment, therefore, we took the initial length of the receptor muscle with the slight extension as its apparent zero length.

When the receptor muscle was stretched in increments of 0.03 mm (Fig. 8B), a notable phasic response occurred at an increment of 0.25 mm from the relative zero length of the receptor muscle (Fig. 8B). This indicates that the cells showing a phasic response possess a higher threshold for a given length of stretch than cells showing a tonic response, and they might be more sensitive to transient segmental movement. On the other hand, tonic cells might serve as positional detectors: thus, when the receptor muscle was stretched in steps of 0.05 mm, up to 0.9 mm, a linear relationship was observed between impulse frequency and the length of stretch in the range of 0.45 to 0.9 mm (Fig. 8C). This relationship holds good only in the dynamic range of the stretch receptor; *i.e.*, the impulse discharge saturates when the stretch stimulus is much larger (see Fig. 10b).

Identification of particular response characteristics to either B-type or to C-type cells was demonstrated by intracellular recording. A microelectrode was used to penetrate either B-type or C-type cells that had been identified under a binocular microscope. When stretch stimuli or current injections were applied, a slowly adapting response was recorded from the B-type (not shown), and the rapidly adapting response was recorded from the C-type receptor cells (Fig. 9B).

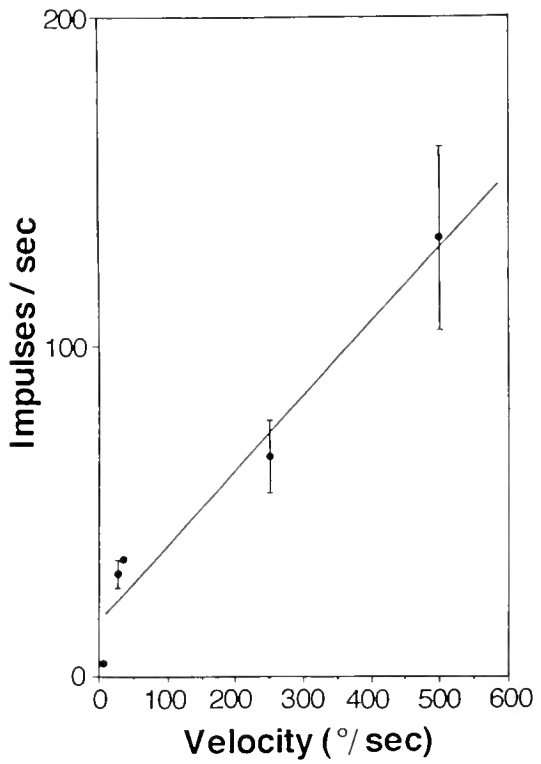

Figure 7. Effect of the velocity of imposed flexion on the response of stretch receptors. These data were obtained by varying the ramp slopes in the experiment shown in Figure 6. Points with vertical bars represent mean ± SD.

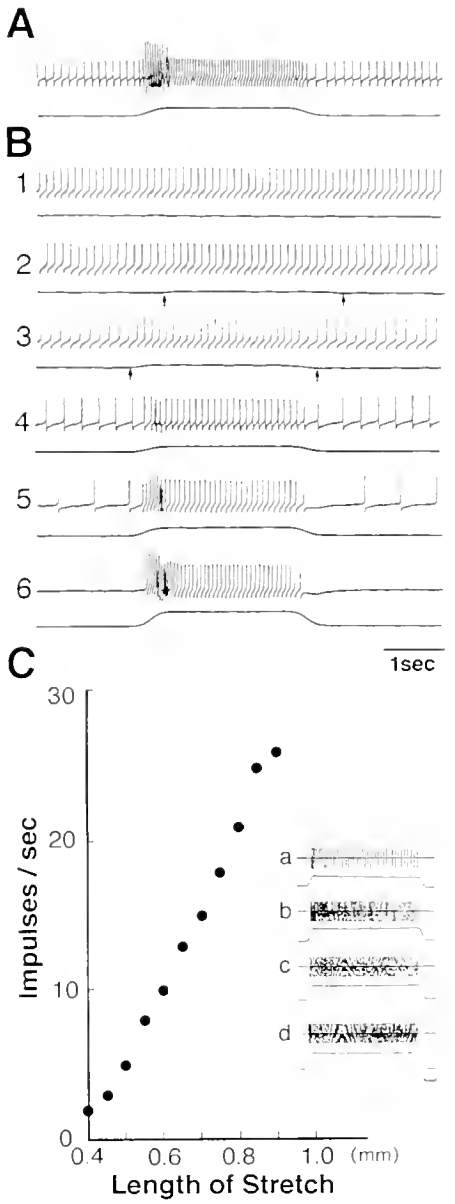

Figure 8. (A) Typical stretch-induced response of the *in situ* thoracic stretch receptor, TSR-2, showing both rapidly and slowly adapting responses. Stretch amplitude, 0.3 mm. (B) Responses of TSR-2 in the same specimen as in (A) to various lengths of stretching. In (A) and (B), the lower record in each pair represents the relative amplitude of the applied flexion. B_1, 0 mm; B_2, 0.03 mm; B_3, 0.06 mm; B_4, 0.09 mm; B_5, 0.12 mm; B_6, 0.25. Arrows indicates beginning and cessation of stretch stimulus. (C) Relationship between length of stretch and frequency of impulses. These data were taken from an *in situ* preparation of TSR-5 obtained from a specimen different from that in (A). Inset shows some of the responses and stimulus amplitude (lower traces) that were plotted. (a) to (d) correspond to stretch of 0.5, 0.6, 0.7, and 0.8 mm, respectively. Time scale (inset), 2 s. In (A), (B), and (C), recordings were made extracellularly through a suction electrode.

A closer examination of the phasic response led to unexpected results. When the receptor muscle was stretched beyond a certain length, the usual pattern of the phasic response changed to maintained discharge of intermittent bursts (Fig. 9A). In this case, the receptor (TSR-5) was stimulated with a 0.6-mm stretch. Within 8.4 s after the onset of stimulus, a stretch-induced response with the usual impulse discharge pattern of a rapidly adapting stretch receptor occurred. But by 8.6 s after the onset of the stimulus, intermittent bursting began and lasted for the duration of the stretch stimulation. In Figure 9A, two groups of impulse bursts appear at the rising phase of stimulation (arrowheads). This was caused by the unevenness of manually imposed stretch stimulus. Intermittent bursts equivalent to those evoked by stretch stimulus were also produced by intracellular injection of electrical current (Fig. 9B, 5nA in this case). The occurrence of this phenomenon is illustrated graphically in Figure 9C and D. No intermittent bursts occurred after a current injection of 3nA (Fig. 9C) and the evoked responses ceased in about 4 s. But at 8nA (bottom line in Fig. 9D), and about 18 s after current injection, intermittent bursts appeared and lasted for 40 s. The outcome of this experiment is shown in the inset of Figure 9D, with intermittent bursts still occurring in the penultimate 10 s of a 5-min stimulus.

However, the question remained: Could this phenomenon be produced by a much stronger imposed stimulus beyond the functional range of the receptor? This possibility might be excluded by the observation that the frequency of intermittent bursts increased linearly until 0.8 mm (Fig. 10a). Because we adopted the stretch stimulus of 0.6 mm, we could exclude the above possibility. This stretch amplitude was also within physiological range of the tonic response cell. The tonic response cell, which was simultaneously activated (since both type of receptor cells have a common single receptor muscle), responded with an increase of impulse discharges, even up to 1.0 mm (Fig. 10b), corresponding to a 30% increase in the total length of the receptor muscle.

Response of the abdominal stretch receptor

As can be seen in Figure 11, slowly adapting and rapidly adapting responses also appeared in the abdominal stretch receptors (inset of Fig. 11). These responses are similar to those in the thorax, but the rapidly adapting receptor cells of the abdomen never showed the intermittent bursts observed in those of the thorax. As in the thorax, instead of the stretch, a certain amount of current injection could cause an equivalent response in the stretch receptors. Injection of 4nA (Fig. 11a), or even the much larger current of 8nA (Fig. 11b), induced no intermittent bursts in the abdomen. Although a current of 8nA was sufficient to evoke intermittent bursts in thoracic receptors, injection even beyond 8nA generated no intermittent bursts in the abdominal stretch receptors.

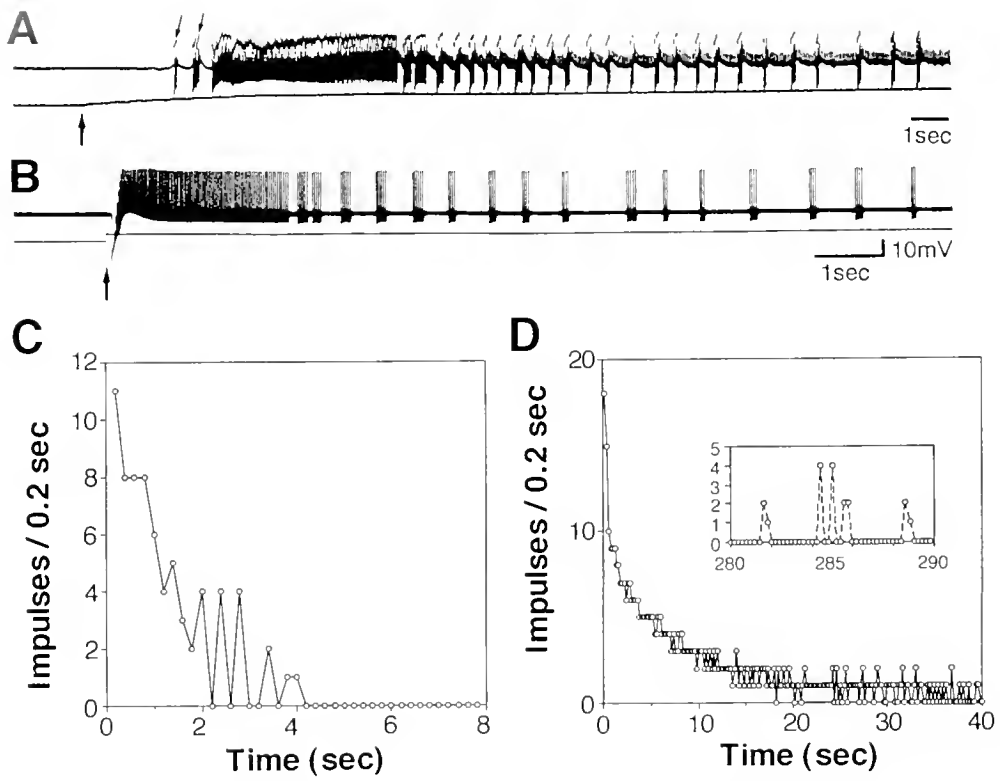

Figure 9. (A) Intermittent bursts in response to an imposed stretch, recorded extracellularly from the rapidly adapting receptor cell in an *in situ* preparation of TSR-5 to an imposed stretch. Stretch amplitude (lower trace), 0.6 mm. Thin arrows indicate impulse bursts caused by an uneven stretch stimulus imposed manually. The small impulse discharges indicate the activities of the slowly adapting stretch receptor. (B) Similar intermittent impulse discharges produced by current injection applied intracellularly; recordings were made intracellularly from a C-type cell. Thick arrows in (A) and (B) indicate the onset of stretch stimulus and current injection, respectively. (C) A current of 3 nA caused no intermittent bursts. (D) At 8 nA, intermittent bursts occurred about 20 s after beginning current injection; they were maintained throughout a 5-min stimulus (inset).

Discussion

Intrinsic response property of the rapidly adapting stretch receptor

The intermittent bursts of the rapidly adapting receptor cell that were observed during imposed stretch experiments were dependent on the extent of a stretch stimulus. As can be seen in Figure 10a, stretching within the range of 0.6 to 0.8 mm would not be unusual, because concomitant impulse discharges increased with the increment of stretch. This type of response is clearly specific to the thoracic rapidly adapting stretch receptor cells, because application of electrical current to the rapidly adapting stretch receptors of the abdomen did not alter their response pattern and evoked no intermittent bursts (a, b in Fig. 11). Such a stable response pattern as that in the abdomen of *L. exotica* occurs also in the rapidly adapting abdominal stretch receptors of crayfish (Nakajima and Onodera, 1969), which showed a phasic response with any intensity of applied electrical current.

On the other hand, segmental *in situ* flexion induced no intermittent bursts (Fig. 6). One reason for this inconsistency might be the absence or presence of inhibitory inputs from central neurons to the stretch receptor cells; specimens for stretch-imposed experiments are isolated from the central connection. An unequal stimulus amplitude between imposed flexion and stretch experiments might also account for the difference in response.

Segmental mobility and response type of stretch receptor

Unlike the segments in large crustaceans such as crayfish, all isopod segments are mobile, suggesting that all of the stretch receptors should be equipped with a specialized receptor muscle on which the dendrite of the receptor cell terminates. This assumption is derived from a concept by Bush and Laverack (1982): in the Crustacea, evolution progresses with increasing sclerotization, and thoracic segments are consequently immobilized; anterior rapidly adapting stretch receptors are lost first, followed by slowly

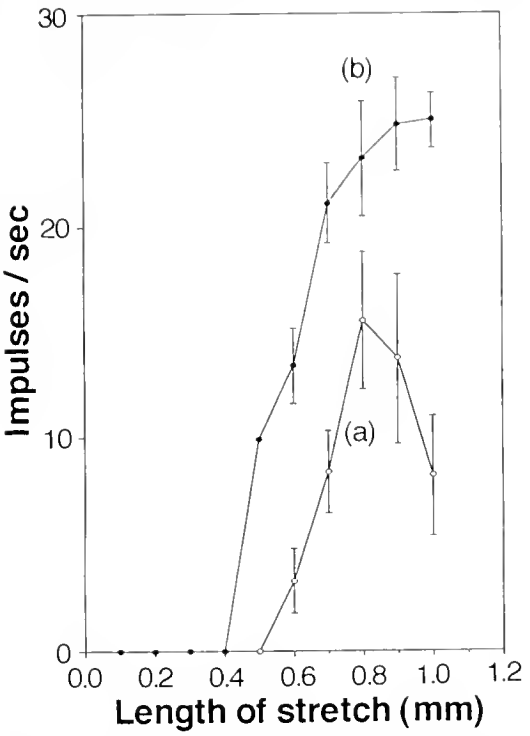

Figure 10. Frequency plots based on recording from two receptor cells (TSR-5) to various lengths of stretch. (a) and (b): rapidly and slowly adapting receptor cells, respectively. Paired slowly and rapidly adapting receptor cells were simultaneously activated, because they have a single common receptor muscle. Points with vertical bars represent mean ± SD.

adapting stretch receptors; these are finally replaced by N-cells, which have no specialized receptor muscles. The stretch receptor of the 2nd thoracic segment of *Ligia* has no specialized receptor muscles, a lack also reported in pill bugs (Niida *et al.*, 1990). This type of stretch receptor may be equivalent to the N-cells of large decapods (Alexandrowicz, 1952; Wiersma and Pilgrim, 1961) and of *Squilla mantis* (Crustacea, Stomatopoda) (Pilgrim, 1964). *S. mantis* has "free" thoracic segments that are mobile; thus, in contrast to the Decapoda, this species contains a complete set of stretch receptors, each with a specialized receptor muscle and a receptor cell, from the abdominal segment up to the 5th thoracic segment.

In *Squilla*, the N-cell, termed SR-α (Wiersma and Pilgrim, 1961), lies only in the 2nd thoracic segment. This segmental organization is the same as that in *Ligia*, but the responses of the stretch receptors of the 3rd thoracic segment differ in these two animals. The response in *Squilla* is only of the slowly adapting type, whereas the receptors in *Ligia* show both slowly and rapidly adapting responses. Therefore, the 3rd thoracic segment may be more mobile in *Ligia* than in *Squilla*. The appearance, within the Isopoda, of a segmentally arranged series of stretch receptors comprising sensory cells of two types thus further supports the hypothesis by Alexandrowicz (1967): the organization of the thoracic stretch receptors is closely related to the mobility of the thorax.

Comparison of the structure of receptor muscle in other Crustacea

As already stated, the receptor muscle of *Ligia* is a single structure throughout each segment. In large Crustacea, such a single receptor muscle appears in the anterior thoracic segments; *e.g.*, *Astacus* has it in the 7th thoracic segment, *Homalus* in the 7th thoracic segment, and *Squilla* in the 3rd and 4th thoracic segments (for review, see Bush and Laverack, 1982). The more posterior thoracic segments and successive abdominal segments of each animal have two separate receptor muscles. In the pill bug (Niida *et al.*, 1990; Niida *et al.*, 1991), unlike *Ligia*, the receptor muscle that spans the 3rd and 4th thoracic segments separates completely, and from the 5th to 8th thoracic segments each pair of receptor muscle runs closely together—but Moser's observation (1976) is somewhat different from ours. In the abdomen, parallel receptor muscles connect tightly with each other in the anterior ridge of a targum and run toward the adjacent segment, separating into two muscle components. Thus the variation in the organization of the receptor muscle might be difficult to account for on the basis of evolutionary sequence alone in a limited number of animals; adaptive behaviors specific to the relevant animal should be also considered.

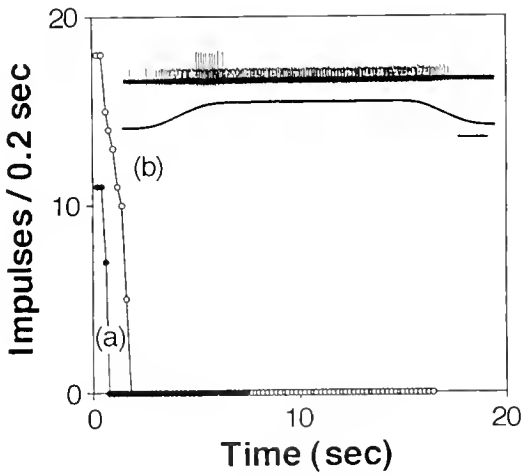

Figure 11. Inset: Extracellularly recorded responses from rapidly and slowly adapting abdominal stretch receptors (ASR-2). Lower trace, stretch amplitude (0.22 mm). Time scale, 2 s. Graph: Time courses of impulse discharges by the rapidly adapting receptor cell of ASR-2. Impulse discharges recorded intracellularly were evoked by intracellular current injection. (a), 4 nA; (b), 8 nA.

The sarcomere length, as one of the characteristics of the differentiated receptor muscle, may be noted; because in crayfish, a slowly adapting receptor cell and a rapidly adapting receptor cell have receptor muscles with a long sarcomere and a short one, respectively (Komuro, 1981). The same is the case with *Squilla* (Alexandrowicz, 1967). In contrast, in *Ligia*, microscopic observation of the cross-striation of the receptor muscles (not measured except in the 6th thoracic segment) did not reveal any difference in sarcomere length in each segment. Accordingly, the differentiated function of stretch receptors in *Ligia* should be attributable to the specific morphology of receptor cells (B-type, C-type cells) coupled with their response properties, rather than to sarcomere length.

When this receptor muscle is passively stretched, both of the receptor cells associated with it (B-type and C-type) should be synchronously stimulated, but the behavioral significance is difficult to evaluate.

Adaptive behavior and thoracic stretch receptor

The slowly adapting stretch receptor of the crayfish has been regarded as a positional detector of abdominal flexion, whereas the rapidly adapting stretch receptor is believed to function when the fast muscular system is activated, such as during swimming and escape (Wiersma and Pilgrim, 1961). In *L. exotica*, the abdominal and posterior thoracic segments, as well as the uropod styles, flex in the dorsal and ventral directions. This segmental movement is related to swimming, but is also sequentially elicited by another key stimulus: When pereopods of *L. exotica* are dipped in a large quantity of water, the animal attempts to stand, elevating its body and beginning to raise and lower its styles to the substrate. This behavior might be coupled with the water-conducting system that has been extensively studied (for review, see Warburg, 1993; Hoese, 1984). In this system, water is taken up from water droplets by the capillary action of the pereopods and enters the marsupium; the extra water is released by the touch of the styles to the ground. In performing this behavior, the animals must obtain continuous, momentary information about the position of their styles with respect to the ground and about the velocity of flexion. In the anterior thoracic segments, although the functional roles of the rapidly and slowly adapting stretch receptors are unclear, both types of stretch receptors would be required for sophisticated segmental movements. For instance, when opening the breeding pouch, which occurs in the 2nd to posterior thoracic segments of females, the animal presses its anterior thoracic segments against the substrate and simultaneously lifts its posterior segment by supporting the abdominal segments with the styles.

Acknowledgments

This work was supported by Ryoubi Teien Foundation and in part by a Grant in Aid from the Ministry of Education, Science and Culture of Japan to TY for scientific research.

Literature Cited

Alexander, C. G. 1971. Observations on receptor mechanisms in *Ligia oceanica* (Linn.) *Comp. Biochem. Physiol.* **40A:** 339–347.

Alexandrowicz, J. S. 1952. Receptor elements in the thoracic muscles of *Homarus vulgaris* and *Palinurus vulgaris*. *Quart. J. Microsc. Sci.* **93:** 315–346.

Alexandrowicz, J. S. 1956. Receptor elements in the muscles of *Leander serratus*. *J. Mar. Biol. Ass. UK* **35:** 129–144.

Alexandrowicz, J. S. 1967. Receptor organs in thoracic and abdominal muscles of Crustacea. *Biol. Rev.* **42:** 288–326.

Bush, B. M. H., and M. S. Laverack. 1982. Mechanoreception. Pp. 399–468 in *The Biology of Crustacea*, Vol. 3, H. L. Atwood and D. C. Sandeman, eds. Academic Press, New York.

Hoese, B. 1984. The marsupium in terrestrial isopods. Pp. 65–76 in *Biology of Terrestrial Isopods*, S. L. Sutton and D. M. Holdich, eds. Oxford University Press, New York.

Komuro, T. 1981. Fine structural study of the abdominal muscle receptor organs of the crayfish (*Procambarus clarkii*). Fast and slow receptor muscles. *Tissue & Cell* **13:** 79–92.

Moser, H. 1976. Muscle receptor organs (MRO) in Isopoda (Crustacea)—histological observations. *Mikroskopie* **31:** 350–362.

Nakajima, S., and K. Onodera. 1969. Membrane properties of the mechanism of sensory adaptation. *J. Physiol.* **200:** 161–185.

Niida, A., K. Sadakane, and T. Yamaguchi. 1990a. Stretch receptor organs in the thorax of a terrestrial isopod (*Armadillidium vulgare*). *J. Exp. Biol.* **149:** 515–519.

Niida, A., K. Sadakane, and T. Yamaguchi. 1991. Abdominal stretch receptor organs of *Armadillidium vulgare* (Crustacea, Isopoda) *Zool. Sci.* **8:** 187–191.

Parrey, G. 1953. Osmotic and ionic regulation in the isopod crustacean *Ligia oceanica*. *J. Exp. Biol.* **30:** 567–574.

Pilgrim, R. L. C. 1964. Stretch receptor organs in *Squilla mantis* Latr. (Crustacea: Stomatopoda). *J. Exp. Biol.* **41:** 793–804.

Takatsuki, Y., A. Niida, and T. Yamaguchi. 1992. Stretch receptor organs in the thorax and abdomen of *Ligia exotica* (Crustacea, Isopoda). *Zool. Sci.* **9:** 1243.

Warburg, M. R. 1993. *Evolutionary Biology of Land Isopods*. Springer Verlag, Berlin.

Wiersma, C. A. G., E. Furshpan, and E. Florey. 1953. Physiological and pharmacological observations on muscle receptor organs of the crayfish, *Cambrus clarku* Girard. *J. Exp. Biol.* **30:** 136–150.

Wiersma, C. A. G., and R. L. C. Pilgrim. 1961. Thoracic stretch receptors in crayfish and rock lobster. *Comp. Biochem. Physiol.* **2:** 51–64.

Yamagishi, H. 1985. Spontaneous activity and pacemaker property of neurons in the cardiac ganglion of an isopod, *Ligia exotica*. *Comp. Biochem. Physiol.* **81A:** 55–62.

Reference: *Biol. Bull.* **189:** 159–167. (October/November, 1995)

Transport and Metabolism of Alanine and Palmitic Acid by Field-Collected Larvae of *Tedania ignis* (Porifera, Demospongiae): Estimated Consequences of Limited Label Translocation

WILLIAM B. JAECKLE

Smithsonian Marine Station at Link Port, 5612 Old Dixie Highway, Fort Pierce, Florida 34946

Abstract. The epidermis of larvae of *Tedania ignis* (Porifera, Demospongiae) is uniformly ciliated except for the posterior pole. The epidermal cells are long, columnar, and monociliate; each cilium arises from an epidermal crypt; symbiotic bacteria were not observed in larval cells. These lecithotrophic ("nonfeeding") larvae can feed by assimilating dissolved organic materials (DOM) from seawater. Larvae transported both the amino acid alanine (mean = 2.73 pmol larva^{-1} h^{-1}; [S] = 1 μM) and the fatty acid palmitic acid (mean = 16.27 pmol larva^{-1} h^{-1}; [S] = 1 μM) from seawater. Following assimilation, the label from alanine was recovered primarily in small molecular weight compounds; the label from palmitic acid was localized chiefly in the lipid fraction. Estimates of the contribution of transport to metabolism (mean respiration rate = 940.7 pmol O_2 larva^{-1} h^{-1}) reveal that alanine transport is energetically insignificant. Palmitic acid transport, in contrast, could account for 21%–55% of larval metabolism. Autoradiographic analysis of the distribution of the label in larvae suggests that epidermal cells are the chief recipients of the assimilated materials. Thus, the contribution of transport to whole-larva metabolism may underestimate the tissue-specific value. At palmitic acid concentrations of 1 and 0.25 μM, the contribution of transport to the estimated metabolism of the epidermis would be 131% and 33% of energy requirements. Thus, the potential benefits of DOM to larvae are dependent not only on the nature of the epidermal transporters and the solute concentration, but also the degree to which materials are distributed among tissues.

Received 1 July 1993; accepted 11 July 1995.

Current address: Friday Harbor Laboratories, 620 University Road, Friday Harbor, WA 98250.

Contribution #384 to the Smithsonian Marine Station at Link Port.

Introduction

The energy requirements for development of "nonfeeding" (lecithotrophic) larvae of marine invertebrates have historically been thought to be solely derived from the catabolism of maternally provided stores (Chia, 1974; Crisp, 1974; Day and McEdward, 1984). In recent years, however, it has been shown that nonfeeding embryos and larvae can obtain energy from the environment through the transport of dissolved organic materials (DOM) from seawater (Reish and Stephens, 1969; Jaeckle and Manahan, 1989a; Manahan *et al.*, 1989; Welborn and Manahan, 1990; Jaeckle, 1994). Prefeeding embryos of planktotrophic (feeding) larvae can also assimilate organic materials from seawater (*e.g.*, Monroy and Tolis, 1961; Tyler *et al.*, 1966; Epel, 1972; Karp and Weems, 1975; Manahan, 1983a; Schneider and Whitten, 1987).

Analyses of the energetics of larval development indicate that DOM transport by nonfeeding larvae and embryos may be important. The contribution of organic solute transport to metabolic processes can be estimated by comparing joules supplied (through transport) with joules expended (metabolic rate) (Stephens, 1963; Wright, 1981; Manahan *et al.*, 1983; Jaeckle and Manahan, 1989a). These comparisons reveal that the potential energetic benefits of DOM transport vary among both transported compounds and larval forms. In general, for compounds at a concentration of 1 μM, the estimated contribution of transport to the metabolism of nonfeeding larvae and prefeeding embryos ranges from <1% to *ca.* 35% for free amino acids and sugars (Jaeckle and Manahan, 1989a,

1992; Jaeckle, 1994) and from *ca.* 20% to 70% for the fatty acid palmitic acid (Jaeckle, 1994). Thus the potential nutritional and energetic value of DOM in seawater to nonfeeding life history stages of invertebrates is a function of both the quantity and the quality of the organic compounds present and the physiological capacities of the larva.

Most published studies on DOM transport report the capabilities of embryos and larvae of temperate-water species to exploit this potential source of nutriment and energy (see Manahan, 1990, for a recent review). Of these studies, few (Karp and Weems, 1975; DeBurgh and Burke, 1983; Manahan and Crisp, 1983) have examined the spatial distribution of a label (initially associated with the assimilated molecules) within the larval body and how the distribution pattern of the label changes over time. Further, where translocation of materials has been suggested, the larvae used were planktotrophic and the appearance of label in interior cells, *i.e.*, the digestive system, cannot be attributed solely to the assimilatory activity of the ectoderm and subsequent translocation to interior cells *via* a blood-vascular system (*e.g.*, Ruppert and Carle, 1983).

The objectives of this study were to measure transport and metabolism of an amino acid and a fatty acid from seawater, to determine the rates of oxygen consumption, and to follow the distribution of a ^3H label within the larval body (using light-microscopic autoradiography) in field-collected parenchymula larvae of the demosponge *Tedania ignis*. The results of these experiments reveal that for larvae of *T. ignis* the calculated contribution of DOM to whole-larva metabolism is highly dependent on the available solute in solution. Transport and metabolism of palmitic acid ([S] = 1 μM) could account for an average of 37% of the metabolic demand, while <1% of the metabolic rate could be supplied through alanine transport. Following transport, the distribution of the label in larval tissue is not uniform; most of the label was detected in the epidermis after a 2-h continuous exposure to the label. Comparison of the rates of DOM transport to estimates of the metabolic rate of the epidermis reveals that the energetic significance of DOM transport to the epithelium apparently responsible for material assimilation can be very high (>90% compensation of the estimated metabolic rate of the epidermis).

Materials and Methods

Collection and handling of larvae

Larvae of *Tedania ignis* were collected from general plankton samples taken from the Fort Pierce Inlet (*ca.* 27° 28′ N; 80° 18′ W) during April–June of 1991. All samples were collected during flooding tides by deploying a 0.5-m plankton net with 202-μm (mesh size) netting in the tidal flow for 10–15 minutes. Samples were sorted at the Smithsonian Marine Station at Link Port as soon as possible (<1 h) after collection. Larvae of *T. ignis* were placed in 0.2-μm (pore size) filtered seawater (hereafter termed seawater) and held at a temperature of 22.5°C.

Measurement of morphological and physical characteristics

Before the linear dimensions of *Tedania* larvae were measured, individuals were fixed by immersion in 1% OsO_4 in seawater for 1 h, washed in seawater, and then measured (±0.5 μm) using a compound microscope equipped with an ocular micrometer.

For morphological inspection, larvae of *Tedania ignis* were processed in a number of ways. For examination of surface structures, larvae were fixed in 1% OsO_4 in seawater for 1 h, washed with seawater, dehydrated with an ascending ethanol series, and critical-point dried using CO_2 as the transition fluid. The specimens were mounted on stubs, coated with a gold-palladium mixture, and examined using a Novascan 30 scanning electron microscope. For light microscopic histology and autoradiography and transmission electron microscopy, specimens were initially fixed in 2.5% glutaraldehyde in seawater and then post-fixed in 2% OsO_4 in a 1.25% solution of $NaHCO_3$. This material was dehydrated using ethanol, transferred into propylene oxide, and embedded in an epoxy resin (Epon 812). Thick sections (*ca.* 1 μm) were cut with a glass knife, stained with "Richardson's stain" (Richardson *et al.*, 1960) and examined with a compound microscope. Thin sections (*ca.* 60 nm) were cut with a diamond knife, stained with saturated aqueous solutions of lead citrate and of uranyl acetate, and examined with a Zeiss EM-9S transmission electron microscope.

For determinations of larval organic weight (biomass), larvae were processed using the procedures described in Jaeckle and Manahan (1989b).

Measurement of oxygen consumption

The respiration rate of *Tedania ignis* larvae was measured following the procedures outlined in Jaeckle (1994) at a temperature of 22.5 ± 0.05°C. All measured respiration values were corrected for the self-consumption rate of the electrode (<9% of the larval respiration rate). The rate of oxygen consumption (mol O_2 larva^{-1} h^{-1}) was calculated as the slope of a regression line of the collected data, divided by the number of larvae, and multiplied by 60 min/h. The measured rates of oxygen consumption were converted to the energy units by using an oxyenthalpic equivalent of 480 kJ mol O_2^{-1} (the average oxyenthalpic equivalent for protein [527 kJ mol O_2^{-1}], lipid [441 kJ mol O_2^{-1}], and carbohydrate [473 kJ mol O_2^{-1}], all from Gnaiger [1983]).

Alanine and palmitic acid transport

Larvae were transferred to 10 ml of seawater in an autoclave-sterilized 20-ml scintillation vial (for experiments with palmitic acid, the vial was previously silanized with Silvue [SDS Coatings, Inc.]). All transport was measured at larval concentration of ≤4 larvae/ml and an added solute concentration of 1 μM. After the addition of the label (^{3}H-alanine or ^{3}H-palmitic acid, New England Nuclear, specific activities 70 or 84 Ci/mmol and 60 Ci/mmol, respectively) and cold carrier, the vial was mixed by inversion and the first sample removed. Each sample of larvae (≤5 larvae per sample) was treated following the methods described in Jaeckle and Manahan (1989a). For one experiment, the rate of alanine transport was measured as the accumulation of radioactivity in larvae after 1 h of continuous exposure to the label. For all other experiments, the measured amount of radioactivity per larva (corrected for signal quenching) was converted to moles of material per individual, and the rate of transport was calculated as the slope of a regression line describing the relationship between moles of material per larva and time.

Alanine and palmitic acid metabolism

Larvae remaining after the 1-h incubation in the solution of either ^{3}H-alanine or palmitic acid (see above) were removed and pipetted onto a glass-fiber filter. The sample of larvae was gently washed twice with 20 ml each of cold (5°C) seawater, and the number of individuals on the filter was counted. After washing, the filters were then placed into a −70°C freezer to stop all metabolic activity of the larvae. The sample of larvae was then lyophilized for 8 h (<10 μm Hg), 5 ml of distilled water was added, and the larval tissue was homogenized using an ultrasonic tissue disrupter (Fisher model #300). Samples of the tissue homogenate were separated into general biochemical fractions (protein, lipid, and small molecular weight compounds) using the methods described in Jaeckle and Manahan (1989b). Each resulting fraction and a sample of the intact homogenate were dissolved in tissue solubilizer, and the radioactivity in each sample was measured 48 h after the addition of scintillation cocktail. The measured amount of radioactivity per fraction (corrected for signal quenching) was converted to a percentage of the total by dividing the radioactivity in each fraction by the amount of radioactivity in the sample of tissue homogenate.

Localization of the label following assimilation within larvae

Light-microscopic autoradiography was used to determine the location of the ^{3}H-label in larvae. Larvae were continuously exposed to radiolabeled alanine and palmitic acid (each at 1 μM added concentration) for 10, 60, or 120 min. At the end of each exposure, the larvae were washed twice with seawater (10 ml each time) and fixed and processed as described above. Serial thick sections were cut, then secured onto acid-cleaned microscope slides. The slides were immersed into a liquid photographic emulsion (Ilford #Kd.5), air dried for 24 h, and stored in a light-tight box at 5°C. The slides were developed according to manufacturer specifications, and the autoradiograms were examined and photographed with a compound microscope.

Results

Physical characteristics

Field-collected parenchymula larvae of *Tedania ignis* are orange-red in coloration and averaged 818.5 ± 17.5 μm in length and 576.3 ± 17.7 μm in width (both mean ± 1 standard error (SE); n = 16 larvae). The average length:width ratio for these larvae was 1.4 ± 0.1 (mean ± 1 SE, n = 16 larvae). With the sole exception of the posterior pole (assigned as the trailing pole during swimming), the larvae were uniformly ciliated (Fig. 1). The epidermis is composed primarily of long, thin, monociliate cells (Figs. 2, 3); each cilium emerges from the cell body through an epidermal crypt or pit (Fig. 3). This morphological examination of the epidermis did not reveal either intra- or extracellular bacteria (not shown); hence the measured rates of solute transport (below) represent the physiological activity of larval cells alone.

The average weight of a *Tedania* parenchymula larva was 16.99 ± 0.72 μg/larva (mean ± 1 SE, n = 14 groups of larvae @ <7 larvae/group).

Alanine and palmitic acid transport

Both alanine and palmitic acid were transported from seawater by larvae of *Tedania ignis*, but the rates of transport differed between the two compounds. Alanine was transported at rates that averaged 2.73 ± 0.6 pmol alanine larva^{-1} h^{-1} (mean ± 1 SE, n = 3 experiments). The rates of palmitic acid transport were nearly 6× higher and averaged 16.27 ± 2.3 pmol palmitic acid larva^{-1} h^{-1} (mean ± 1 SE, n = 4 experiments). The fate of the radioactive label in larval tissue also differed between the two compounds. For larvae exposed to ^{3}H-alanine, most of the label (64%) was recovered in the small molecular weight compound fraction, *e.g.*, soluble in cold 5% trichloroacetic acid (TCA). The remaining label was found in the TCA-insoluble (macromolecular) fraction (23%) and in lipoic materials (14%) localized in the $CHCl_3$-soluble fraction. For larvae exposed to ^{3}H-palmitic acid, most of the material was recovered in the $CHCl_3$-soluble fraction (79%), and the remaining radioactivity was divided between the

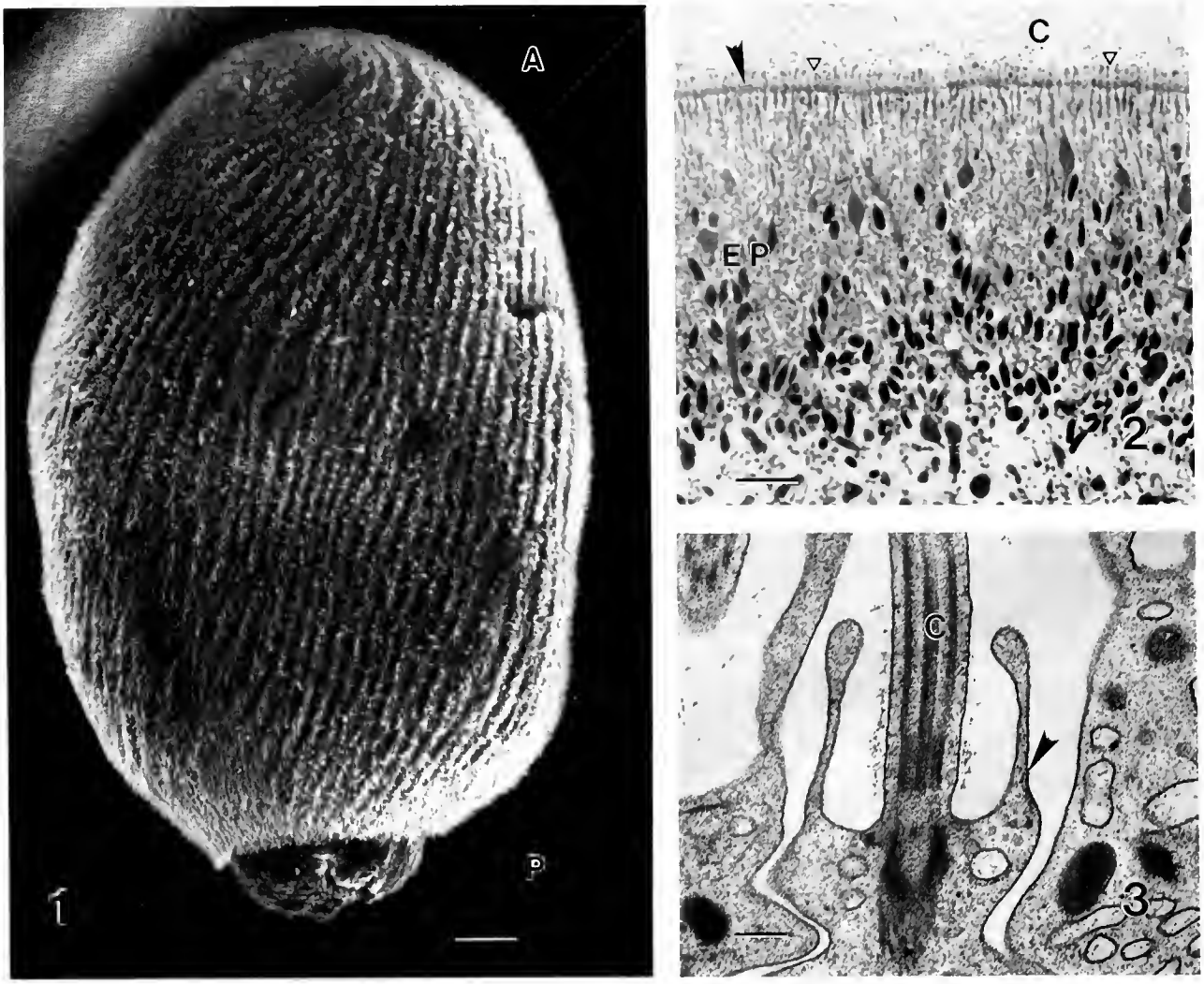

Figure 1. Scanning electron micrograph of a lateral view of a field-collected larva of *Tedania ignis*. The anterior (A) and posterior (P) regions of the larvae were designated as the leading and trailing poles during swimming. Scale bar = 50 μm.

Figures 2 and 3. Light and transmission electron micrographs of the epidermis of parenchymulae of *Tedania ignis*.

Figure 2. Light micrograph of a larva of *Tedania ignis*. The epidermis (EP) is composed primarily of thin, columnar, ciliated cells. Subapically a continuous line (large arrowhead) is present and is suggestive of intercellular junctional complexes. The presence of epidermal crypts from which the cilia (C) arise at the apices of the ciliated cells is denoted by the small arrowheads. Scale bar = 10 μm.

Figure 3. Transmission electron micrograph of the apical region of a ciliated epidermal cell of a larva of *Tedania ignis*. A single cilium (C) can be seen emerging from the epidermal crypt of the epidermal cell. Scale bar = 0.25 μm.

TCA-soluble fraction (14%) and the TCA-insoluble fraction (8%).

Larval respiration

The respiration rate (O_2 consumption) of larvae of *Tedania ignis* was variable among the groups of larvae examined. Values ranged from 846.8 to 1113.9 pmol O_2 $larva^{-1}$ h^{-1}, with an average of 940.7 ± 70.0 pmol O_2 $larva^{-1}$ h^{-1} (mean ± 1 SE, n = 5 independent collections of larvae).

Autoradiographic analysis of the distribution of the ^3H-label

The biochemical nature (macromolecular or small molecular weight) of the molecules containing the label

cannot be ascertained by light-microscopic autoradiography of glutaraldehyde-fixed material. Glutaraldehyde is a good preservative of cellular details, in part because it acts by cross-linking primary amines. This activity may result in a false intracellular localization of the label, if the label-bearing molecule resides in the extracellular space (*e.g.*, Peters and Ashley, 1967). However, the autoradiographic analysis presented here was designed to ascertain whether the label, after transport, was distributed throughout the entire larval body, not to determine the pathway of material movement (paracellular or transcellular).

After 10 min of exposure to either ^{3}H-alanine or palmitic acid, the label is found in or around the cells of the epidermis (Fig. 4A), as evidenced in the autoradiograms by the appearance of silver granules overlying these cells. Even though larvae were continuously exposed to the label for up to 2 h, examination of the autoradiograms (Fig. 4A–C) indicates that most of the label remained associated with the cells of the epidermis.

Discussion

Most research on the larvae of demosponges has focused on their morphological or behavioral characters (*e.g.*, Berquist *et al.*, 1970; Woollacott, 1990, 1993; Kaye and Reiswig, 1991). The morphology of the epidermis of larvae of *Tedania ignis* (subclass Poecilosclerida) closely approximates that described for larvae of the haplosclerid demosponge *Haliclona tubifera* (Woollacott, 1993). For both species, the epidermis is composed chiefly of elongate columnar cells (each with a single cilium arising from an epidermal crypt). The posterior pole is aciliate in both, but the enlarged ciliary band that exists at the intersection of the lateral and posterior surfaces in *H. tubifera* larvae is wanting in larvae of *T. ignis*. The physiological significance of the epidermal crypts remains unknown, but these depressions in the larval epidermis do increase the apical surface area of the cells and represent a potential morphological correlate to solute transport (Oschman, 1978).

Although parenchymula larvae of *Tedania ignis* lack a functional digestive system, these larvae have the physiological capacity to acquire nutrients and energy from their environment through the transport of DOM from seawater. A comparison of the energy acquired through transport with the metabolic rate indicates that the potential energetic importance of alanine and palmitic acid transport differs (Table I). The energy supplied through

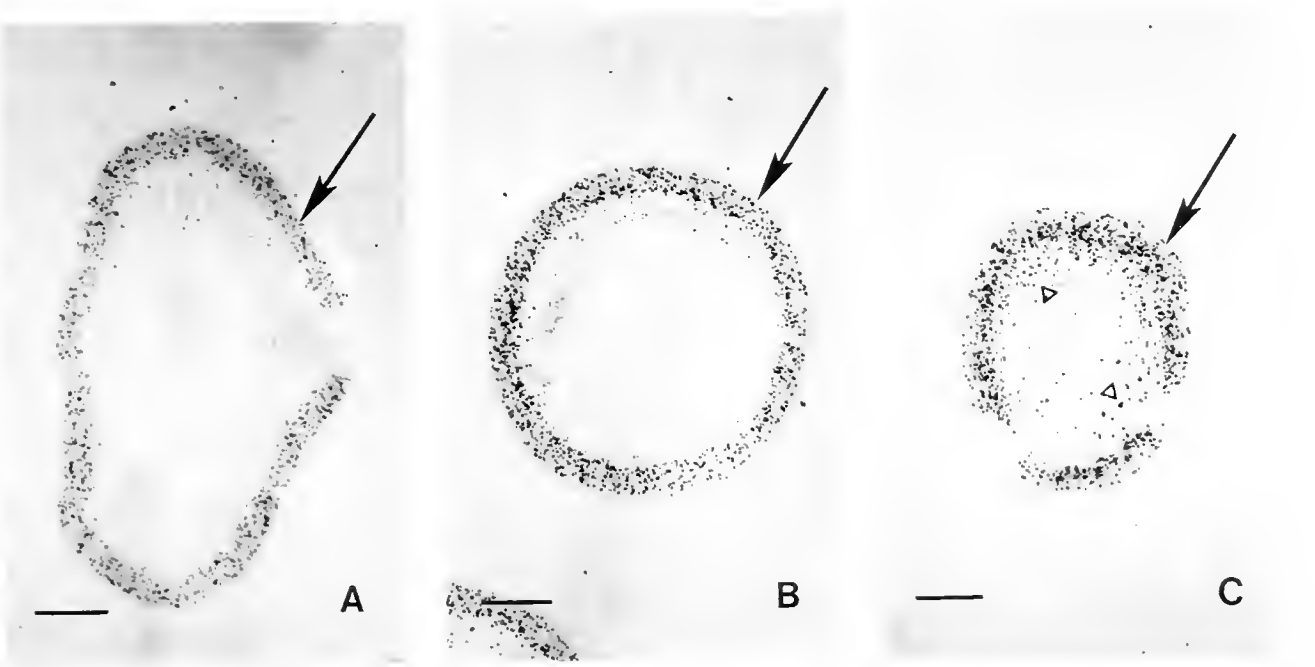

Figure 4. Light microscopic audioradiograms depicting the distribution of the radioactive label in transverse sections of larvae of *Tedania ignis* that were exposed to ^{3}H-palmitic acid for different periods of time. (A) After 10 min of exposure to ^{3}H-palmitic acid, the presence of latent images (reduced silver grains) overlies only the cells of the epidermis (arrow). Scale bar = 303 μm. (B) After a 1-h exposure, the number of latent images over the epidermis has increased, but no label is detectable over other regions of the section. Scale bar = 303 μm. (C) After 2 h of continuous exposure to ^{3}H-palmitic acid, the latent images are more intense and the label primarily overlies the epidermis, but there is evidence for the presence of radioactive materials in interior regions of the larva. Scale bar = 303 μm.

Table I

Comparison of the potential contribution of palmitic acid and alanine transport ([S] = 1 μM) to the energy metabolism of Tedania ignis *larvae*

Solute	Transport[1]	O_2 demand[2]	Metabolism[3]	% Compensation[4]	[S] for 100% compensation[5]
Palmitic acid	13.19	317.17	940.66	33.7	3.0
	22.54	518.42	940.66	55.1	1.8
	11.86	272.78	940.66	20.9	3.4
	16.27	374.30	940.66	39.8	2.5
avg.	16.27	370.67		37.4	2.7
s.d.	4.66	106.91		14.2	0.7
Alanine	1.77	5.31	940.66	0.6	166.7
	3.87	11.61	940.66	1.2	83.3
	2.53	7.59	940.66	0.8	125.0
avg.	2.72	8.17		0.6	166.7
s.d.	1.06	3.19		0.3	41.7

[1] Transport rate = pmol × $larva^{-1}$ h^{-1}.

[2] O_2 demand = the transport rate × the mol O_2 required for complete catabolism of palmitic acid (23 mol O_2/mol Pal) and alanine (3 mol O_2/mol Ala).

[3] Metabolism = the average respiration rate per larva (pmol O_2 × $larva^{-1}$ h^{-1}).

[4] % Compensation = the oxygen demand ÷ the metabolic rate × 100.

[5] [S] for complete compensation = 100 ÷ % compensation of the metabolic rate.

alanine transport ([S] = 1 μM) could supply <1% of metabolic demands, and complete compensation of the metabolic rate from alanine transport would require ecologically unrealistic alanine concentrations for seawater samples (range: 83–167 μM). In contrast, the energy contribution supplied through palmitic acid transport ([S] = 1 μM) may be quantitatively important. The average transport rate of palmitic acid is nearly 6× that found for alanine transport and, owing to the difference in energy content of the two compounds, the energy acquired through palmitic acid transport could supply between 21% and 55% (mean ± 1 SE = 37.4% ± 7.1; Table I) of the metabolic demand. A palmitic acid concentration ranging from 2 to 3 μM would be necessary if all of the energy requirements of *Tedania* larvae were supplied solely through the transport and catabolism of this compound.

Following transport of both alanine and palmitic acid, the ^{3}H-label was recovered in each of the measured biochemical fractions (protein, lipids, and small molecular weight compounds). Because a ^{3}H-label was used in the experiments, the pathways that place the label in each of the three fractions remain unresolved. Yet a comparison of results of experiments using either ^{3}H-alanine or palmitic acid revealed a differential distribution of the label among the biochemical fractions. After alanine transport, most of the label was recovered in the small molecular weight fraction followed, in sequence, by the macromolecular and lipid fractions. This pattern of label distribution following alanine transport is consistent with previously published accounts in which ^{14}C served as the radioactive label (Manahan, 1983b; Jaeckle and Manahan, 1989a,c). The distribution of label recovered in larvae exposed to ^{3}H-palmitic acid was different; most of the label was found in the lipid fraction, with the remainder being localized in the small molecular weight compounds and macromolecule fractions. This pattern of label distribution compares well with that described for adult *Stauronereis rudolphi* (Annelida: Polychaeta) after exposure to ^{14}C-1-palmitic acid (Testerman, 1972).

The concentrations of both free amino acids and free fatty acids in seawater vary from below detection (< fM) to low μM levels (Testerman, 1972; Bunde and Fried, 1978; Mopper and Lindroth, 1982; Carlucci *et al.*, 1984; Fuhrman and Bell, 1985; Laanbroek *et al.*, 1985). Thus the estimates of energetic contribution presented above are dependent upon the physiological state of the larvae and the concentration of the organic materials in seawater. For larvae of *Tedania ignis*, even when exposed to high concentrations of amino acids in surface waters (μM), the net energetic benefit is likely to be small. The concentration of free fatty acids in subtropical Floridian waters was reported to be 50–80 $\mu g\ l^{-1}$, a range that is equivalent to about 0.25 μM palmitic acid (Bunde and Fried, 1978). At this concentration, assuming that the K_+ of the palmitic acid transporter is greater than 1.0 μM, the energetic contribution of transport to the larva would be, on average, 9.4% of the metabolic demand.

Attempts to quantify the energetic importance of the transport of organic solutes from seawater usually involve a comparison of the energy gained (through transport) to the metabolic rate. Material assimilation, however, is a regional process restricted to the outer epithelium of lecithotrophic larvae and, in contrast, metabolic rate sums over the metabolic activities of all cells. Comparison of

energy supply (transport) and demand (O_2 consumption) for lecithotrophic larvae is based on the assumption that the transported organic solutes are distributed throughout the entire larval body. For larvae of *Tedania ignis*, the assumption of translocation to parenchymal tissues after assimilation by the outer epithelium does not seem to be true. Examinations of autoradiograms of larvae exposed to radiolabeled alanine and palmitic acid for up to 2 h reveals that nearly all the label remains with the cells putatively responsible for transport.

The suggestion that DOM transport may be a regionally important source of nutrition and energy is not new. Earlier researchers (*e.g.*, Pequignat, 1966; Ferguson, 1967, 1970) working on DOM transport in adult invertebrates suggested that the epidermis may be the sole recipient of the assimilated materials and that there is little translocation of materials from the adult endoderm to the ectoderm. Later studies (*e.g.*, Pearse and Pearse, 1973; Pequignat, 1973; Ferguson, 1980; Chien and Rice, 1985; Rice and Stephens, 1987) indicated that there could be translocation of material to interior cells and that the viability of the epidermis was not dependent upon exogenously supplied nutrients. In his review of integumentary transport by invertebrates, Wright (1988) reported that "the nutritional impact of DOM uptake may vary with the specific integumental site of transport: over much of the surface of the integument, accumulated substrates will support the nutritional needs of those cells; uptake into other integumental regions may result in a rapid transcellular movement of accumulated materials to the hemolymph for transport to deeper tissues. To the extent that this type of specialized 'partitioning' of accumulated DOM occurs in the integument, the calculation of the nutritional potential that have been described here will, of course, under- or overestimate the nutritional potential of uptake for a given organism or tissue."

Table II

The contribution of palmitic acid and alanine transport to the metabolism of the larval epidermis at substrate concentrations of 1 μM and 0.25 μM

Solute	O_2 demand (1 μM, 0.25 μM)[1]	% Compensation (1 μM, 0.25 μM)[2]
Palmitic acid	370.7, 92.7	131%, 33%
Alanine	8.2, 2.0	3%, <1%

The estimated metabolic rate of the epidermis (282.2 pmol O_2 × epidermis^{-1} h^{-1}) is calculated as the estimated weight fraction of the epidermis (0.3) times the average metabolic rate of the intact larvae (940.7 pmol O_2 × larva^{-1} h^{-1}).

[1] O_2 demand ([S] = 1 μM) = the transport rate × the mol O_2 required for complete catabolism of palmitic acid (23 mol O_2/mol Pal) and alanine (3 mol O_2/mol Ala). O_2 demand ([S] = 0.25 μM) is calculated by dividing the O_2 demand (1 μM) by 4 (Pal and Ala transport is assumed to be first-order at substrate concentrations of 1 μM or lower).

[2] % Compensation of the metabolic rate of the epidermis is calculated by dividing the O_2 demand$_{(epidermis)}$ by the estimated metabolic rate$_{(epidermis)}$ and multiplying by 100.

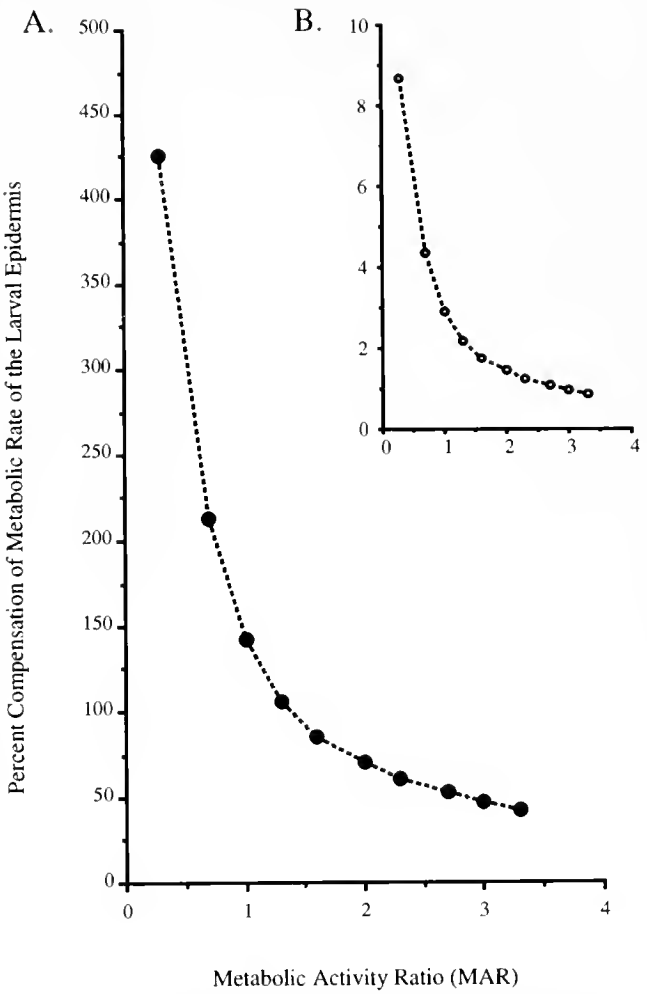

Figure 5. The change in the estimated contribution of palmitic acid (A) and alanine (B) transport ([S] = 1 μM each) from seawater to the metabolism of the epidermis of larvae of *Tedania ignis*. The range in metabolic activity ratios (MARs) represents the relative difference in the metabolic activities of epidermal cells and internal cells.

The estimated contributions of DOM transport to the metabolism of *Tedania ignis* larvae are detailed in Table I. If, however, most of the assimilated DOM from seawater is metabolized solely by the cells responsible for transport, then evaluations of the energetic importance of this form of nutrient acquisition underestimate the potential *epidermis*-specific value. In larvae of *T. ignis*, assimilated materials apparently remain within the epidermis; to estimate the importance of transport to the metabolism of the epidermis of *Tedania* larvae, the following analysis was done. Cross-sections (1 μm thick) of *Tedania* larvae were photographed and the negatives printed. From the

photographs, the cross-sections of three larvae were cut out and weighed on an analytical balance. The area of the section representing the epidermis was then cut out and the remaining photographic images of the internal cells were reweighed. If it is assumed that larvae of *T. ignis* are cylindrical and that all cells have the same weight density, then the areal proportion of the epidermis in the photograph is equal to the proportion of a larva's organic weight that is represented by the cells. On the basis of this analysis, the epidermis of *T. ignis* larvae represents, on average, 30% of the total larval biomass (*ca.* 5 μg). If all cells of a larva have the same respiration rate, then the metabolic rate of the epidermis is 282.2 pmol O_2 $larva^{-1}$ h^{-1} (0.3 · 940.7 O_2 $larva^{-1}$ h^{-1}). The energetic contribution of palmitic acid transport ([S] = 1 μM and 0.25 μM) to the metabolism of the larval epidermis is potentially important (Table II). It seems unlikely, however, that the metabolic rate is constant among all cells, given the morphological differences among cell types in sponge larvae (Woollacott, 1990, 1993). The theoretical contribution from transport to metabolism can be adjusted to account for the differences in cellular metabolism. Changes in the potential contribution of alanine and palmitic acid transport to metabolism as a function of the relative activities of the external and internal cells are shown in Figure 5. In this figure, a metabolic activity ratio (MAR) of 1 represents the condition in which the metabolic rate of the epidermal cells is directly proportional to their weight-fraction of larval tissue; *i.e.*, all cells respire at the same weight-specific rate. A metabolic activity ratio of 2 equals the condition in which the metabolic rate of the epidermal cells is twice that of their interior counterparts. Complete compensation of the estimated metabolic demand of the epidermis would be provided through palmitic acid transport ([S] = 1 μM) at a MAR < 1.3. For alanine transport alone, 100% compensation of the metabolic rate could not be accomplished.

Sponge parenchymula larvae can live in plankton for periods of time lasting from hours to days (*e.g.*, Berquist *et al.*, 1970; Woollacott, 1990, 1993; Kaye and Reiswig, 1991). During their planktonic existence they are functionally incapable of ingesting particulate forms of food. Despite this inadequacy, these lecithotrophic larvae are physiologically capable of assimilating DOM from seawater across their epidermis; hence they are not nutritionally independent of their environment. The potential benefits obtained through DOM transport and metabolism are not, however, dependent only on the substrate concentration and the class and species of the organic materials present in seawater, but also on whether the assimilated materials are distributed among all larval cells.

Acknowledgments

I thank Dr. Shirley Pomponi (Harbor Branch Oceanographic Institution) for identifying juveniles of the larvae used in this study, Ms. Julie Piriano for assisting with the scanning electron microscopy, and Dr. Mary Rice (Smithsonian Marine Station at Link Port) for providing the equipment necessary to complete this project. This manuscript was significantly improved by the comments of Dr. E. J. Balser and two anonymous reviewers. This research was supported by a fellowship from the Smithsonian Institution to W. B. Jaeckle.

Literature Cited

Berquist, P. R., M. E. Sinclair, and J. Hogg. 1970. Adaptation to intertidal existence: Reproductive cycles and larval behavior in Demospongiae. *Symp. Zool. Soc. Lond.* **25:** 247–271.

Bunde, T. A., and M. Fried. 1978. The uptake of dissolved free fatty acids from seawater by a marine filter feeder *Crassostrea virginica*. *Comp. Biochem. Physiol.* **60A:** 139–144.

Carlucci, A. F., D. B. Craven, and S. M. Hendrichs. 1984. Diel production of dissolved free amino acids in waters off southern California. *Appl. Environ. Microbiol.* **48:** 165–170.

Chia, F. S. 1974. Classification and adaptive significance of developmental patterns in marine invertebrates. *Thalassia Jugosl.* **10:** 121–130.

Chien, P. K., and M. A. Rice. 1985. Autoradiographic localization of exogenously supplied amino acids after uptake by the polychaete *Glycera dibranchiata* Ehlers. *Wasmann. J. Biol.* **43:** 60–71.

Crisp, D. J. 1974. Energy relations of marine invertebrate larvae. *Thalassia Jugosl.* **10:** 103–120.

Day, R., and L. McEdward. 1984. Aspects of the physiology and ecology of pelagic larvae of marine benthic invertebrates. Pp. 93–120 in *Marine Plankton Life Cycle Strategies*, K. A. Steidinger and L. A. Walker, eds. CRC Press, Inc., Boca Raton, Florida.

DeBurgh, M. E., and R. D. Burke. 1983. Uptake of dissolved amino acids by embryos and larvae of *Dendraster excentricus* Eschscholtz (Echinodermata: Echinoidea). *Can. J. Zool.* **61:** 349–354.

Epel, D. 1972. Activation of an Na^+-dependent amino acid transport system upon fertilization of sea urchin eggs. *Exp. Cell Res.* **72:** 74–89.

Ferguson, J. C. 1967. An autoradiographic study of the utilization of free amino acids by starfishes. *Biol. Bull.* **133:** 317–329.

Ferguson, J. C. 1970. An autoradiographic study of the translocation and utilization of amino acids by starfishes. *Biol. Bull* **141:** 122–129.

Ferguson, J. C. 1980. The non-dependency of a starfish on epidermal uptake of dissolved organic matter. *Comp. Biochem. Physiol.* **66A:** 461–465.

Fuhrman, J. A., and T. M. Bell. 1985. Biological considerations in the measurement of dissolved free amino acids in seawater and implications for chemical and biological studies. *Mar. Ecol. Prog. Ser.* **25:** 13–21.

Gnaiger, E. 1983. Calculations and energetic and biochemical equivalents of respiratory oxygen consumption. Pp. 337–345 in *Polarographic Oxygen Sensors*, E. Gnaiger and H. Forstner, ed. Springer-Verlag, Berlin.

Jaeckle, W. B. 1994. Rates of energy consumption and acquisition by lecithotrophic larvae of *Bugula neritina* (Bryozoa: Cheilostomata). *Mar. Biol.* **119:** 517–523.

Jaeckle, W. B., and D. T. Manahan. 1989a. Feeding by a "nonfeeding" larva: uptake of dissolved amino acids from seawater by lecithotrophic larvae of the gastropod *Haliotis rufescens*. *Mar. Biol.* **103:** 87–94.

Jaeckle, W. B., and D. T. Manahan. 1989b. Growth and energy imbalance during the development of a lecithotrophic molluscan larva *Haliotis rufescens*. *Biol. Bull.* **177:** 237–246.

Jaeckle, W. B., and D. T. Manahan. 1989c. Amino acid uptake and metabolism by larvae of the marine worm *Urechis caupo* (Echiura), a new species in axenic culture. *Biol. Bull.* **176:** 317–326.

Jaeckle, W. B., and D. T. Manahan. 1992. Experimental manipulations of the organic chemistry of seawater: implications for studies of energy budgets in marine invertebrate larvae (Mollusca, Echinodermata). *J. Exp. Mar. Biol. Ecol.* **156:** 273–284.

Karp, G. C., and M. D. Weems. 1975. ^{3}H-amino acid uptake and incorporation in sea urchin gastrulae and exogastrulae: an autoradiographic study. *J. Exp. Zool.* **194:** 535–546.

Kaye, H. R., and H. M. Reiswig. 1991. Sexual reproduction in four Caribbean commercial sponges. III. Larval behavior, settlement, and metamorphosis. *Invertebr. Reprod. Dev.* **19:** 25–35.

Laanbroek, H. J., J. C. Verplanke, K de Visscher, and R. De Vuyst. 1985. Distribution of phyto- and bacterioplankton growth and biomass parameters, dissolved inorganic nutrients and free amino acids during a spring bloom in Oosterschelde basin, the Netherlands. *Mar. Ecol. Prog. Ser.* **25:** 1–11.

Manahan, D. T. 1983a. The uptake of dissolved glycine following fertilization of oyster eggs, *Crassostrea gigas* (Thunderg). *J. Exp. Mar. Biol. Ecol.* **68:** 53–58.

Manahan, D. T. 1983b. The uptake and metabolism of dissolved amino acids by bivalve larvae. *Biol. Bull.* **164:** 236–250.

Manahan, D. T. 1990. Adaptations by invertebrate larvae for nutrient acquisition from seawater. *Am. Zool.* **30:** 147–160.

Manahan, D. T., and D. J. Crisp. 1983. Autoradiographic studies on the uptake of dissolved amino acids from seawater by bivalve larvae. *J. Mar. Biol. Ass. U.K.* **63:** 673–682.

Manahan, D. T., J. P. Davis, and G. C. Stephens. 1983. Bacteria-free sea urchin larvae: selective uptake of neutral amino acids from seawater. *Science* **220:** 204–206.

Manahan, D. T., W. B. Jaeckle, and S. D. Nourizadeh. 1989. Ontogenic changes in the rates of amino acid transport from seawater by marine invertebrate larvae (Echinodermata, Echiura, Mollusca). *Biol. Bull.* **176:** 161–168.

Monroy, A., and H. Tolis. 1961. Uptake of radioactive glucose and amino acids and their utilization for incorporation into proteins during maturation and fertilization of the eggs of *Asterias forbesii* and *Spisula solidissima*. *Biol. Bull.* **147:** 456–460.

Mopper, K., and P. Lindroth. 1982. Diel and depth variations in dissolved free amino acids and ammonium in the Baltic Sea determined by shipboard HPLC analysis. *Limnol. Oceanogr.* **27:** 336–347.

Oschman, J. L. 1978. Morphological correlates of transport. Pp. 55–92 in *Membrane Transport in Biology*, vol. 3, G. Giebisch, D. C. Tosteson, and H. H. Ussing, eds. Springer-Verlag, Berlin.

Pearse, J. S., and V. B. Pearse. 1973. Removal of glycine from solution by the sea urchin *Strongylocentrotus purpuratus*. *Mar. Biol.* **19:** 281–284.

Pequignat, E. 1966. 'Skin digestion' and epidermal absorption in irregular and regular urchins and their probable relation to the outflow of spherule-coelomocytes. *Nature* **210:** 397–399.

Pequignat, E. 1973. A kinetic and autoradiographic study of the direct assimilation of amino acids and glucose by organs of the mussel *Mytilus edulis*. *Mar. Biol.* **19:** 227–244.

Peters, T., and C. A. Ashley. 1967. An artefact in radioautography due to binding of free amino acids to tissues by fixatives. *J. Cell Biol.* **33:** 53–60.

Reish, D. J., and G. C. Stephens. 1969. Uptake of organic materials by aquatic invertebrates. V. The influence of age on the uptake of glycine-C14 by the polychaete *Neanthes arenaceodentata*. *Mar. Biol.* **3:** 352–355.

Rice, M. A., and G. C. Stephens. 1987. Uptake and internal distribution of exogenously supplied amino acids in the Pacific oyster, *Crassostrea gigas* (Thunberg). *Aquaculture* **66:** 19–31.

Richardson, K. C., L. Jarret, and H. E. Finke. 1960. Embedding in epoxy resins for ultrathin sectioning in electron microscopy. *Stain Tech.* **35:** 313–323.

Ruppert, E. E., and K. J. Carle. 1983. Morphology of metazoan circulatory systems. *Zoomorphology* **103:** 193–208.

Schneider, E. G., and D. J. Whitten. 1987. Uptake and metabolism of nucleosides by embryos of the sea urchin *Strongylocentrotus purpuratus*. *Exp. Cell. Res.* **168:** 1–14.

Stephens, G. C. 1963. Uptake of organic materials by aquatic invertebrates. II. Accumulation of amino acids by the bamboo worm, *Clymenella torquata*. *Comp. Biochem. Physiol.* **10:** 191–202.

Testerman, J. K. 1972. Accumulation of free fatty acids from seawater by marine invertebrates. *Biol. Bull.* **142:** 160–177.

Tyler, A., J. Piatigorsky, and H. Ozaki. 1966. Influence of individual amino acids on uptake and incorporation of valine, glutamic acid, and arginine by unfertilized and fertilized sea urchin eggs. *Biol. Bull.* **131:** 204–217.

Welborn, J. R., and D. T. Manahan. 1990. Direct measurement of sugar uptake from seawater into molluscan larvae. *Mar. Ecol. Prog. Ser.* **65:** 233–239.

Woollacott, R. M. 1990. Structure and swimming behavior of the larva of *Halichondria melanodocia*. (Porifera: Demospongiae). *J. Morph.* **205:** 135–145.

Woollacott, R. M. 1993. Structure and swimming behavior of the larva of *Haliclona tubifera* (Porifera: Demospongiae). *J. Morph.* **218:** 301–321.

Wright, S. H. 1981. A nutritional role for amino acid transport in filter-feeding marine invertebrates. *Am. Zool.* **22:** 621–634.

Wright, S. H. 1988. Nutrient transport across the integument of marine invertebrates. Pp. 173–218 in *Advances in Environmental and Comparative Physiology*, Vol. 2, R. Gilles, ed. Springer-Verlag, Berlin.

Reference: *Biol. Bull.* 189: 168–174. (October/November, 1995)

Role of Digestive Gland in the Energetic Metabolism of *Penaeus setiferus*

CARLOS ROSAS[1], ANDREA BOLONGARO-CREVENNA[2], ADOLFO SÁNCHEZ[1], GABRIELA GAXIOLA[1], LUIS SOTO[2], AND ELVA ESCOBAR[2]

[1]*Laboratorio de Ecofisiología, Depto. de Biología, Fac. de Ciencias UNAM, México 04510, D.F. México, and* [2]*Laboratorio de Ecología del Bentos, Instituto de Ciencias del Mar y Limnología, UNAM, México 04510, D.F. México*

Abstract. We determined the role of the digestive gland in the respiratory metabolism of *Penaeus setiferus* adult males as a step toward proposing a feeding schedule based on the cycle of activity in the digestive gland. We measured pre- and postprandial values for oxygen consumption rate and hemolymph glucose concentrations in live animals, and oxygen consumption rate and glycogen concentration in excised digestive gland. After the animals were fed, which enhanced general metabolic activity, these indices changed. There was a high correlation between the oxygen consumption rate of the animal and the glucose concentration in the hemolymph, and between the oxygen consumption rate by the digestive gland and the glycogen concentration in the digestive gland, all in relation to time after feeding. Correlations support the hypothesis that the energy demand depends upon the metabolic substrate concentration. In this theory, glucose sustains muscle activity (during ingestion of food) and glycogen is the product of the digestive gland during food assimilation. Our observations of metabolic dynamics during the feeding period allowed us to examine the feeding process. The metabolic activity of the digestive gland was highest 6 h after feeding. This could mean that assimilation, having started 2 h after food intake, peaked 6 h after feeding. Eight hours after feeding, the oxygen consumption rate of the digestive gland decreased and fell to values similar to those recorded for animals subjected to 72 h of fasting.

Received 23 September 1994; accepted 29 June 1995.

Abbreviations AHI, apparent heat increment; afdw, ash-free dry weight; dw, dry weight.

Introduction

The digestive gland (also known as the midgut gland or hepatopancreas) of decapod crustaceans serves the dual role of secreting enzymes and absorbing digested food. This gland is composed of embryonic (E) cells, which give rise to two basic cell types: R cells (Restzellen), which store nutrients, and F cells (Fibrillenzellen), which secrete enzymes (Hirsch and Jacobs, 1930). The F cells develop into B cells (Blasenzellen), a more mature secretory stage with a large vacuole containing digestive enzymes (Gibson and Barker, 1979). The overall functions of the digestive gland, including the temporal relationship of secretion and absorption to food intake, have been assessed in several species. Because many of those studies used histochemical methods, the results are difficult to interpret.

Gibson and Barker (1979) reported that in the digestive gland of *Homarus americanus*, B cells were replaced 12 h after food ingestion, and in *Penaeus semisulcatus* the highest activity of proteolytic enzymes was evident within 7 to 10 h. Al-Mohanna and Nott (1987) detected in the latter species a cycle of maximum enzymatic activity 6 h after food intake, with production of feces containing B cells, membranous remains, and particulate matter after 24 h. Hopkin and Nott (1980) found that in *Carcinus maenas*, digestion and absorption took about 12 h after feeding and were followed by an excretory phase lasting from about 12 to 48 h after feeding.

Despite the amount of information published on the activity and characteristics of the crustacean digestive gland, little is known about its role in respiratory activity during feeding. Several authors (*e.g.*, Beamish and Trippel, 1990) recognized that the apparent heat increment (AHI;

previously referred to as specific dynamic action, SDA) is an indicator of the mechanical and biochemical processes associated with the ingestion and assimilation of food. Although muscular tissue is responsible for the mechanical activity, the digestive gland is the site of metabolic functions that break the stomach contents down biochemically. Hence, the AHI may result from addition of the energy used in the above two processes; this constitutes a considerable percentage of the daily energy budget in aquatic organisms (Du-Preez *et al.*, 1992; Chakraborty *et al.*, 1993).

In aquaculture, AHI has been used in the selection of diets for raising shrimp; thus it is imperative to determine the magnitude of energy costs associated with feeding activity. No previous studies have correlated this energy cost to digestive gland metabolism during food ingestion. Therefore, no approximations have been made that allow the differentiation of components of the AHI and the role of the digestive gland in these processes. Our study was aimed at determining the role of the digestive gland in the respiratory metabolism of *Penaeus setiferus*. At various stages while the shrimp were ingesting and assimilating food, we measured the rate of oxygen consumption in live animals and in the digestive gland; the content of glucose in hemolymph; and the content of glycogen in the digestive gland.

Materials and Methods

Animals

Thirty-nine sexually mature male shrimp (*P. setiferus;* 37.57 ± 0.54 g wet weight) were caught on the continental shelf off Laguna de Términos, Campeche, México. In the laboratory, the shrimp were placed in 1000-l flow-through tanks, with aerated seawater, under a light/dark cycle of 14/10 h. After 24 h of conditioning, shrimp were left without food for 72 h to provide fasting conditions. During the experiment, salinity was kept at 32‰ and temperature at 28 ± 1°C.

Oxygen consumption rate in whole live shrimp

After the fasting period, 6 shrimp were placed in a 1-l chamber connected to a flow-through respirometer (0.1 l/min) (Martinez-Otero and Díaz-Iglesia, 1975), in which they were acclimated for 8 h before the experiments were conducted. Oxygen consumption rate was estimated by the difference in oxygen concentration in the input and output of the chamber. The difference was multiplied by the flow rate and corrected for a control chamber without organisms. Metabolic rate was recorded at time 0 (animals fasting 72 h) and at 1, 2, 4, 6, and 24 h after a meal of 1 g squid meat (*Loligo brevis*) was given and totally ingested. These times were selected on the basis of the finding that the major activity of the digestive gland in *P. semisulcatus* occurs between 1 and 6 h after feeding (Al-Mohanna and Nott, 1987).

At the end of the experimental phase, all animals were sacrified and fresh weight, dry weight (dw), and ash-free dry weight (afdw) determined. Results of oxygen consumption measurements were expressed in milligrams of oxygen per gram per hour afdw (Sanchez *et al.*, 1991). AHI was estimated as the difference between feeding and fasting rates of oxygen consumption (Du Preez *et al.*, 1992). This difference was transformed using the exocaloric coefficient of 3.53 cal/mg O_2 consumed (Elliot and Davison, 1975), and expressed in relation to a mean afdw of 11.4 g/(animal · 24 h).

Digestive gland oxygen consumption rate

A total of 15 shrimp were used for this experiment. Fasted (72 h) animals were placed in a 600-l tank with filtered seawater. The digestive glands of animals chosen at random were dissected and placed in physiological solution for crustaceans (Prosser, 1973). This solution was made with NaCl (26.42 g/l), KCl (1.12 g/l), $CaCl_2$ (2.78 g/l), $MgCl_2$ (0.32 g/l), $MgSO_4$ (0.49 g/l), H_3BO_3 (0.53 g/l), and NaOH (0.192 g/l) with a pH of 7.6. Each digestive gland was cut in two, and each half was considered a duplicate of the other. Rate of oxygen consumption was measured in fasting shrimp (72 h) and at 1, 2, 6, and 8 h after feeding. Each piece of digestive gland was placed in a microrespirometer chamber with 2 ml of previously aerated physiological solution. The oxygen concentration in the chambers was measured, under gentle agitation, with a Strathkelvin Model 781 oxygen meter equipped with a high-sensitivity membrane (12.5 μm) electrode. This system was connected to a thermostat that kept temperature at 28 ± 0.01°C during the experiment. Measurements lasted for 3 to 5 min, recording oxygen variations every 10 s. Due to the uniformity of readings, only the results obtained 30 s after sectioning the digestive gland were used.

Glycogen concentrations in digestive gland and glucose in hemolymph

Glycogen was measured in digestive gland sections from 18 shrimp at time 0 (after 72 h fasting), and at 1, 2, 4, 6, and 24 h after feeding. Glycogen was extracted with anthrone reagent. This reagent consisted of a solution of 0.05% anthrone, 1% thiourea, and 72% H_2SO_4 (Carroll *et al.*, 1956). The digestive gland was first homogenized in trichloroacetic acid (TCA; 5%) for 3 min. After centrifugation (3000 rpm) the supernatant was filtered (acid-free paper) and quantified. This procedure was performed

Table I

Oxygen consumation rate (VO_2), blood glucose concentration, and digestive gland glycogen concentration of Penaeus setiferus *in relation to time after feeding*

	Intact animals		Digestive gland		
Time H	VO_2 mg O_2/(g afdw · h)	Glucose mmol/l	Wet weight g	VO_2 mg O_2/(g afdw · h)	Glycogen mg/100 g dw
0	1.01	1.66	0.62	1300	1.70
	(0.22)	(0.01)	(0.01)	(130)	(0.14)
1	1.56	5.46	1.28	1310	2.08
	(0.09)	(0.40)	(0.17)	(107)	(0.43)
2	1.25	5.71	1.02	1507	4.10
	(0.75)	(0.01)	(0.07)	(204)	(0.43)
4	1.45	5.67	0.80	—	12.06
	(0.19)	(0.19)	(0.01)		(0.84)
6	1.12	5.45	0.92	2027	17.41
	(0.10)	(0.02)	(0.05)	(112)	(0.14)
8	—	—	—	1250	—
				112	
24	0.93	1.28	0.59	—	0.74
	(0.07)	(0.01)	(0.06)		(0.06)
N by measurement	6	3	3	3	3
Total	6	18		15	

Values as mean. SEM in parentheses.

three times. One ml of TCA filtrate was pipetted into a Pyrex centrifuge tube and mixed with 5 volumes of 95% ethanol. The tubes were placed in a water bath at 37°C for 3 h. After precipitation occurred, the tubes were centrifuged at 3000 rpm for 15 min. The packed glycogen was dissolved by addition of 2 ml of distilled water. Ten ml of anthrone reagent was delivered into each tube with vigorous blowing, and the tubes were placed in a cold (4°C) tap water bath. Later all tubes were placed in a boiling water bath for 15 min. The contents of the tubes were transferred to a colorimeter tube and read at 620 nm after the instrument was adjusted with the reagent blank (distilled water plus anthrone reagent). A standard was prepared by adding 2 ml of standard glucose solution containing 0.1 mg of glucose to anthrone reagent.

Glucose concentration in the hemolymph

Glucose was measured in hemolymph from the same shrimp used for the glycogen determination. Before the digestive gland was excised, 200 μl of hemolymph was extracted from the pericardium of each shrimp. A 12.5% solution of sodium citrate was used to prevent clotting (Martin *et al.*, 1991). The glucose concentration in the hemolymph was measured with a commercial kit for medical diagnosis (Merckotest 3306, Rosas *et al.*, 1992a).

Statistical analysis

Analysis of variance (ANOVA) was used to test the significance of the results obtained. Duncan's multiple range test (Zar, 1974) was used to determine differences in the means of oxygen consumption of whole animals, oxygen consumption of digestive gland, glycogen concentration in digestive gland, and glucose concentration in hemolymph. For all groups, an analysis of covariance was performed between the rate of oxygen consumption by the animal and the concentration of glucose in hemolymph and between the rate of oxygen consumption by the digestive gland and the concentration of glycogen in the hemolymph.

Results

Respiratory metabolism and levels of glucose and glycogen changed with time after feeding (Table I). The oxygen consumption rate of live organisms was higher between 1 and 4 h after feeding ($p < 0.05$) than at time zero. A respiratory rate increase of 54% and an AHI of 1.95 cal/(g afdw · h), equivalent to 533.3 cal/(11.4 g afdw · day), were obtained (Table II). Daily AHI was 8.5% of the energy of the ingested food (Table II). Subsequently there was a reduction of about 28% in oxygen consumption rate (as observed at 6 h after feeding), and the oxygen consumption rate returned to the initial level by 24 h after feeding (Table I).

Digestive gland weight increased after 1 h, from 0.62 to 1.28 g dw/animal, then diminishing gradually in the 2 and 6 h observations. The lowest value was obtained 24 h after feeding (Table I). Digestive gland oxygen consump-

Table II

Apparent heat increment (AHI) calculated for Penaeus setiferus

	mg O_2/ (g afdw · h)	cal/ (g afdw · h)	cal/ (11.4 g afdw · h)
AHI	0.55 ± 0.03	1.95 ± 0.09	533.5 ± 26.7
AHI % of the energy of the ingested food	—	—	8.5

Values as mean ± SEM. Shrimp wet weight: 37.57 ± 0.51 g; shrimp ash-free dry weight: 11.4 ± 0.16 g; energy content of *Loligo brevis*: 6300 cal/g afdw.

tion rate remained constant between time zero and 1 h, with an average of 1305 mg O_2/(g dw · h) (Table I). A gradual increase was detected until it reached its highest level, 6 h after feeding, which was 56% higher than for fasting animals (Table I) ($p < 0.05$). The oxygen consumption rate of the digestive gland was returned to fasting levels 8 h after feeding.

Hemolymph glucose concentration showed a significant increase by 1 h after feeding (Table I). Recorded values were 1.66 mmol/l in starved animals and 5.46 mmol/l in fed shrimp. The hemolymph glucose level of fed shrimp remained stable between 1 and 6 h, the average value being 5.5 mmol/l. Twenty-four hours after feeding, glucose concentration had fallen to 1.28 mmol/l, observed in starved animals ($p < 0.05$).

Glycogen in digestive gland showed a gradual increase after 2 h of feeding, reaching a maximum 10.2 times larger than fasting animals at 6 h (Table I). Twenty-four hours after feeding, glycogen levels were significantly lower than those observed before feeding.

The oxygen consumption rate of the animal was correlated with hemolymph glucose ($r = 0.78$), and the oxygen consumption rate of the digestive gland was correlated with glycogen concentration ($r = 0.99$; Table III). In both cases, values of r and p confirm a positive relationship between responses, which are positive and linear ($p < 0.05$).

Discussion

The use of mature male shrimp in this study excludes the effect of biochemical processes related to gonadal maturation, thus assuring that the results were due solely to the activity of the digestive gland. In previous studies, Rosas *et al.* (1992a, b) showed that in a 24-h cycle, the oxygen consumption rate and the hemolymph glucose concentration of *P. setiferus* were highest between 9 and 16 h after feeding, which assures an 8-h interval of general metabolic stability. In the present study we used previous results to select a time period for observation of metabolic changes due to feeding, thus eliminating possible effects of circadian rhythm upon metabolic activity.

Apparent heat increment (AHI) is related to an increase in oxygen consumption rate induced by locomotory activity, capture, ingestion and digestion of food, and biochemical activity related to absorption of material (Beamish and Trippel, 1990). These expenditures of energy can constitute a high percentage of the energy used by shrimp. If we consider organisms with an average weight of 40 g dw (11.4 g afdw), a squid diet with a caloric value of 1890 cal/g afdw (Del Barco, 1975), and an AHI of 533.5 cal/(11.4 g afdw · day), it is possible to infer that the AHI corresponds to 8.5% of the daily metabolized energy (Table II). Although the AHI levels might change depending on the quality and quantity of food, our results can be applied to squid (*Loligo brevis*) diets normally given to reproductive shrimp. Du Preez *et al.* (1992) reported an AHI of 2.4% to 19.5% of ingested energy for juveniles of *Penaeus monodon* fed shrimp muscle, and 2% to 17% for shrimp fed with commercial balanced feed. In another study, Nelson *et al.* (1977) reported that in juvenile *Macrobrachium rosenbergii*, the AHI fluctuates from 7.4% to 27.5% of available energy, depending on the type of feed, with the highest level found in those fed on tubifid worms.

From the results of this study it is possible to isolate some components of the energy costs associated with AHI, and shed some light on utilization and assimilation (Table IV). Because of the difficulty in estimating each AHI component directly, we attempted to differentiate them on the basis of their respective times. Once food was provided, the animals displayed intensive muscular activity (pleopod motion), which contrasted with the no-motion behavior observed within the respirometer chamber during the 8-h acclimatization period. As the first three pairs of pereiopods secure the food, it is fragmented and passed onto the mouth parts for ingestion. Contact digestion then begins (Gibson and Barker, 1979; Al-Mohanna and Nott, 1987) (Table IV). This behavior occurred during the first hour after feeding and coincided with the elevation of hemolymph glucose concentration and oxygen consump-

Table III

Oxygen consumption rate (mg O_2/(g afdw · h)) and concentrations of hemolymph glucose (mmol/l) correlation (A) and digestive gland oxygen consumption rate (mg O_2/(g dw · h)) and digestive gland glycogen (mg/g) correlation (B) of Penaeus setiferus

	a	*b*	*r*	*p*<
A	0.83	0.09	0.78	0.05
B	1185.30	0.70	0.99	0.002

$Y = a + bX$. Values from all groups.

Table IV

Feeding schedule of Penaeus setiferus

Stage	Activity	Source	Associated time	Metabolic substrate
I	Excitation, Ingestion, and Contact digestion (Stomach)	Maximum VO_2 (AHI)	1	Glucose (5.5 mmol/l)
II	Absorption of small particles and Chyme digestion (Lumen)	Weight increment of DG VO_2 DG VO_2 AHI	1–2	Glucose (5.5 mmol/l) Proteins (?) Lipids (?)
III	Assimilation and Synthesis	Maximum VO_2 DG Glycogen (17.41 mg/100 g dw)	6	Glucose (5.5 mmol/l) Proteins (?) Lipids (?)
IV	Feces production and Digestive gland metabolic rate reduction		8	
V	General metabolic reduction		24	Less glucose than T_0 57% less glycogen than in T_0

VO_2 (AHI) is the oxygen consumption rate of whole animals; VO_2 DG is the digestive gland oxygen consumption rate; DG is the digestive gland. This schedule integrated all results obtained.

tion noted 1 h after feeding (Table I). Taking into account that the oxygen consumption of the digestive gland remained constant, we attribute the increase in oxygen consumption to the mechanical aspects of feeding (muscle excitement, ingestion, and contact digestion). During this time glycogen reserves in muscular tissue and digestive gland provide glucose in hemolymph as fuel for these activities. The correlation between oxygen consumption rate and glucose level in hemolymph reported for crustaceans in this and other works can be used as an indicator of this process (Table III) (Ramos and Fernandez, 1981; Brito and Diaz-Iglesia, 1987; Diaz-Iglesia *et al.*, 1987; Rosas *et al.*, 1992a).

Digestive gland weight increased as a function of time after feeding. A maximum weight of 1.28 g was reached 1 h after feeding; this value was twice as high as that recorded for fasting animals. If we attribute this difference in weight to the amount of food in the digestive gland (Al-Mohanna and Nott, 1987), we can evaluate the efficiency of incorporation of ingested squid. Considering that 1 g of food was available per shrimp and using initial weight of the digestive gland, we estimate an efficiency of 66% of ingested food. In view of this result and those reported by Al-Mohanna and Nott (1987), for aquaculture purposes it is the activity of the digestive gland rather than the ingestion of the food that should be considered in establishing a feeding schedule for *P. setiferus*.

Once the food is digested in the gut, the chyme and fine particles are digested in the lumen and absorbed by diffusion to the inner portions of the digestive gland tubules, thus initiating the accumulation of glycogen (Al-Mohanna and Nott, 1987; Hopkin and Nott, 1980). The 140% increase in the glycogen concentration in the digestive glands that took place 2 h after feeding could indicate the onset of glucogen synthesis (Tables I and IV). Because these processes require energy, we would expect the oxygen consumption of the digestive gland to increase. In fact, a 56% increase in oxygen consumption was recorded in the digestive gland of *P. setiferus* after 6 h (Table I). This increase can be correlated to the calorigenic effect induced by the food in the digestive gland. In this study, the oxygen consumption rate of the digestive gland was 1287% higher than that of intact animals. Although we have no explanation for such a high consumption rate, these results are similar to those obtained by other authors. Conceiçao (1993) and Diaz-Iglesia *et al.* (1995) recently found that in feeding *Panulirus argus*, the oxygen consumption rate of the digestive gland was 312% higher than that observed in living lobsters. The lack of endogenous controls during *in vitro* experiments could account for the high metabolic rate found for *Penaeus setiferus* and *Panulirus argus*. Schmidt-Nielsen (1984) stated that "the metabolic rate in homologous tissues (liver, for example) is relatively constant, irrespective of body size, but this rate is restricted or depressed in the large animals by some 'central' control or other 'organismic' factor resident in the intact organism." Although this observation was based on data for mammals, it might apply equally well to shrimp and explain metabolism-depressing factors in the digestive gland. Hormones from the eyestalks could also be responsible for the metabolic control of the digestive gland in living animals (Silverthorn, 1975a, b; Kleinholz, 1976; Madyastha and Rangneker, 1976; Mauviot and Castell, 1976; Radakrishnan and Vijakumaran, 1984; Rosas *et al.*, 1991). The presence of elevated glycogen levels concomitant with an increase in the oxygen consumption rate by the digestive gland may point to the synthesis of reserves during this period mirroring the as-

similation of ingested food (Table IV). This hypothesis is supported by the correlation between metabolic activity and glycogen concentrations (Table III).

Major activity of the digestive gland has been reported 6 h after feeding activity in *P. semisulcatus* (Al-Mohanna and Nott, 1987). This elapsed time could mirror the highest respiratory activity in the digestive gland of *P. setiferus* (Table I) and indicate that assimilation, having started 2 h after food intake, would peak 6 h after feeding. Eight hours later, the oxygen consumption of the digestive gland could decrease and fall to values similar to those recorded for digestive gland tissue from animals subjected to 72 h of fasting (Table I). Although the amount of energy lost as heat cannot be precisely accounted for in all the processes in this study, the largest amount of energy consumed was associated with the mechanical processes of feeding, as evidenced by the oxygen consumption of living animals 1–2 h after feeding (Table I).

The accumulation of glycogen as storage material can also be used as an indicator of the energetic potential of the diet, because glycogen is the source of glucose for metabolic use and for the synthesis of chitin (Gwing and Stevenson, 1979; Chan *et al.*, 1988). Considering that molting is an important factor in shrimp growth, the dynamics of glucose could be useful in determining the diet for shrimp species.

Acknowledgments

The experimental work was done at the Centro de Investigaciones Pesqueras (CRIP) of Campeche, of the Instituto Nacional de la Pesca, under a collaborative program with the Faculty of Science, UNAM. The project was partially financed by DGAPA project IN-201292 given to Dr. Luis A. Soto and Dr. Carlos Rosas. Our recognition for their support in laboratory work goes to M. Eugenia Chimal and Mauricia Borja.

Literature Cited

Al-Mohanna, S. Y., and J. A. Nott. 1987. R cells and the digestive cycle in *Penaeus semisulcatus* (Crustacea: Decapoda). *Mar. Biol.* **95:** 129–137.

Beamish, F. W. H., and E. A. Trippel. 1990. Heat increment: a static or dynamic dimension in bioenergetic models? *Trans. Am. Fish. Soc.* **119:** 649–661.

Brito, R. P., and E. Diaz-Iglesia. 1987. Efecto de la extirpación de los pedúnculos oculares sobre el consumo de oxígeno de juveniles de langosta *Panulirus argus*. *Rev. Invest. Mar.* **8:** 71–81.

Carroll, N. V., R. W. Longley, and J. H. Roe. 1956. The determination of glycogen in liver and muscle by use of anthrone reagent. *J. Biol. Chem.* **215:** 583–593.

Chakraborty, S. C., L. G. Ross, and B. Ross. 1992. Specific dynamic action and feeding metabolism in common carp, *Cyprinus carpio* L. *Comp. Biochem. Physiol.* **103A:** 809–815.

Chan, S. M., S. M. Ranking, and L. L. Keley. 1988. Characterization of the molt stages in *Penaeus vannamei*: setogenesis and hemolymph levels of total protein, ecdysteroids and glucose. *Biol. Bull.* **175:** 185–192.

Conceiçao, R. N. 1993. Biometria, genética-bioquímica y ecofisiologia de postlarvas y juveniles de la langosta *Panulirus argus* (Latreille, 1804) (Crustacea, Decapoda). Master's thesis, Universidad de la Habana. 93 pp.

Del Barco, G. F. 1975. Contenido calórico de algunos organismos costeros. *Res. Invest.* **2:** 255–260.

Diaz-Iglesia, E., R. P. Brito, and I. Hernandez. 1987. Efecto de la ablación del complejo neurosecretor peduncular en juveniles de langosta *Panulirus argus* II. Algunos aspectos metabólicos. *Rev. Investig. Mar.* **8:** 81–93.

Diaz-Iglesia, E., R. N. de Lima Conceiçao, R. Brito Pérez, y M. Báez Hidalgo. 1995. Flujos bioenergéticos en juveniles de langosta *Panulirus argus* (Latreille, 1804) en ayuno y alimentados con dieta natural. *Rev. Investig. Mar.* **16**(2): in press.

Du Preez, H. H., H-Y. Chen, and C-S. Hsieh. 1992. Apparent specific dynamic action of food in the grass shrimp, *Penaeus monodon* Fabricius. *Comp. Biochem. Physiol.* **103A:** 173–178.

Elliot, J. M., and W. Davison. 1975. Equivalents of oxygen consumption in animal energetics. *Oecologia* **19:** 195–201.

Gibson, R., and P. L. Barker. 1979. The decapod hepatopancreas. *Oceanogr. Mar. Biol. Ann. Rev.* **17:** 285–346.

Gwing, J. F., and J. R. Stevenson. 1979. Role of acetylglucosamine in chitin synthesis in crayfish. I correlation of C-acetylglucosamine incorporation with stages of the moult cycle. *Comp. Biochem. Physiol.* **45B:** 769–776.

Hirsch G. C., and W. Jacobs. 1930. Der Arbeitsrhythmus der mitteldarmdrtse von *Aztacus leptodactylus* 2. Teil: Wachstum als primarer faktor des rhythmus eines polyphasischen organigen skretionssystems. *Z. Vergl. Physiol.* **12:** 524–558.

Hopkin, S. P., and J. A. Nott. 1980. Studies on the digestive cycle of the shore crab *Carcinus maenas* (L) with special reference to the B cells in the hepatopancreas. *J. Mar. Biol. Assoc. UK* **60:** 891–907.

Kleinholz, L. H. 1976. Crustacean neurosecretory hormones on physiological specificity. *Am. Zool.* **16:** 151–166.

Madyastha, M. M., and P. V. Rangneker. 1976. Metabolic effects of eyestalk removal in the crab *Varuna litterata* (Fabricius). *Hydrobiol.* **48:** 25–31.

Martin, G. G., J. E. Hose, S. Omori, C. Chong, T. Hoodnhoy, and N. McKrell. 1991. Localization and roles of coagulogen and transglutaminase in hemolymph coagulation in decapod crustaceans. *Comp. Biochem. Physiol.* **100B:** 517–522.

Martinez-Otero, A., and E. Díaz-Iglesia. 1975. Instalación respirométrica para el estudio de la acción de los agentes la acción de los agentes en el agua de mar. *Revista de Investigaciones Marinas* **8:** 1–6.

Mauviot, J. C., and J. D. Castell. 1976. Molt and growth enhancing effects of bilateral eyestalk ablation on juvenile and adult American lobster (*Homarus americanus*). *J. Fish. Res. Board Can.* **33:** 1922–1929.

Nelson, S. G., H. W. Li, and A. W. Knight. 1977. Calorie, carbon and nitrogen metabolism of juvenile *Macrobrachium rosembergii* (De Man) (Crustacea, Palaemonidae) with regard to trophic position. *Comp. Biochem. Physiol.* **59A:** 319–327.

Prosser, C. L., ed. 1973. *Comparative Animal Physiology.* Saunders Co., Philadelphia.

Radakrishnan, E. V., and M. Vijakumaran. 1984. Effects of eyestalk ablation in spiny lobster *Panulirus homarus* (Linnaeus). I: On moulting and growth. *Indian J. Fish.* **31:** 130–147.

Ramos L., and I. Fernandez. 1981. Variacion del metabolismo glucidico durante el ciclo reproductor en la especie *Penaeus notialis* (Perez Farfante, 1967). *Rev. Invest. Mar.* **2:** 141–156.

Rosas, C., C. Vanegas, G. Alcaraz, and F. Diaz. 1991. Effect of eyestalk ablation on oxygen consumption of *Callinectes similis* exposed to salinity changes. *Comp. Biochem. Physiol.* **100A:** 75–80.

Rosas, C., A. Sanchez, E. Escovar, L. A. Soto, and A. Bolongaro-Crevenna. 1992a. Daily variations of oxygen consumption and glucose hemolymph level related to morphophysiological and ecological adaptations of crustacea. *Comp. Biochem. Physiol.* **101A:** 323–328.

Rosas, C., A. Sanchez, L. A. Soto, E. Escovar, and A. Bolongaro-Crevenna. 1992b. Oxygen consumption and metabolic amplitude of decapod crustaceans from the northwest continental shelf of the Gulf of Mexico. *Comp. Biochem. Physiol.* **101A:** 491–496.

Sanchez, A., C. Rosas, E. Escobar, and L. A. Soto. 1991. Skeleton weight free oxygen consumption related to adaptations to environment and habits of six crustacean species. *Comp. Biochem. Physiol.* **100A:** 69–73.

Schmidt-Nielsen, K. 1984. *Scaling: Why Is Size So Important?* Cambridge University Press, New York. 242 pp.

Silverthorn, S. V. 1975a. Hormonal involvement in thermal acclimation in the fiddler crab *Uca pugilator* (Bosch). I: Effect of eyestalk extracts on whole animal respiration. *Comp. Biochem. Physiol.* **50A:** 281–283.

Silverthorn, S. V. 1975b. Hormonal involvement in thermal acclimation in the fiddler crab *Uca pugilator* (Bosch). II: Effects of extracts on whole animal respiration. *Comp. Biochem. Physiol.* **50A:** 285–290.

Zar, J. H. 1974. *Biostatistical Analysis.* Prentice Hall, Englewood Cliffs, NJ.

Reference: *Biol. Bull.* **189**: 175–184. (October/November, 1995)

Bioassay and Preliminary Characterization of Ovigerous-Hair Stripping Substance (OHSS) in Hatch Water of Crab Larvae

MASAYUKI SAIGUSA

Okayama University, Faculty of Science, Department of Biology, Tsushima 2-1-1, Okayama 700, Japan

Abstract. Hatch water (the filtrated medium into which zoea larvae have been released) of the estuarine terrestrial crab *Sesarma haematocheir* (akate-gani) contains a substance that causes premature detachment of embryos from ovigerous females. Detachment occurs when the ovigerous hairs along the female's ovigerous setae slip out of the investment coat that binds them to the embryos through stalks, or funiculi. The active factor, which I call ovigerous-hair stripping substance (OHSS), is released outside of the egg capsule at the time of hatching, and is not secreted by the female. This study describes the results of a quantitative assay for measuring the activity of OHSS. Activity is measured as the percentage of hairs on a seta that can be induced to slip out of the coat without damage. Experiments with an extract of crushed embryos indicated that OHSS is present up to 2 days before hatching. Its activity was destroyed by heat and trypsin, suggesting that it is a protein. Its molecular size was estimated by gel filtration to be 15–20 kDa in *S. haematocheir* and 30 kDa in *S. pictum*. Reciprocal tests among different species indicated that OHSS occurs widely in intertidal and estuarine crabs.

Introduction

After oviposition, the embryos of decapod crustaceans are wrapped in a thick membrane and clustered on the ovigerous setae beneath the abdomen of the female. Many fine hairs (*i.e.*, ovigerous hairs) are arranged along the seta, and the embryos are attached to these hairs by a stalk: the funiculus. The mechanism by which the fertilized egg is attached to the ovigerous hairs and the source of the material that makes up the funiculus and the egg capsule have been subjects of controversy for many years (*e.g.*, Andrews, 1906; Yonge, 1937, 1946; Mawson and Yonge, 1938; Linder, 1960; Suko, 1961; Cheung, 1966; Fisher and Clark, 1983; Goudeau and Lachaise, 1980, 1983; Goudeau *et al.*, 1987; Talbot and Demers, 1993).

In addition to the funiculus, the embryo attachment system involves a clear coat that wraps around (invests) the ovigerous hairs (Saigusa, 1994). The funiculus is therefore not connected to the ovigerous hairs directly, but indirectly through the coat—a fact not previously reported. The investing coat may be composed of the same materials that make up the funiculus and the outer layer of the egg capsule, but this notion has not been tested adequately.

While attached to the ovigerous hairs, the embryos are ventilated by the movement of pleopod setae. When development is completed, the egg capsule breaks, and the zoeas hatch and are released into the water by a special fanning movement of the female's abdomen (larval release is described in Saigusa, 1982). After the larvae have been released, the empty egg cases, funiculi, and investing coats remain attached to the ovigerous hairs. Soon, however, a substance released at the time of hatching causes the ovigerous hairs to slip out of the investment coat, detaching the funiculi and empty egg cases; the active factor is called 'ovigerous-hair stripping substance' (OHSS) (Saigusa, 1994). Within a few hours, the ovigerous hairs are cleaned without damage, and in a few days a new clutch of fertilized eggs is attached to the hairs. Because OHSS is released at the time of hatching, one might suppose it to be directly involved in hatching. But there is no evidence that this factor is a hatching enzyme of the sort known in many groups of animals (Saigusa, 1994).

Received 21 December 1992; accepted 25 July 1995.

If the medium in which hatching and larval release has occurred is filtered, the resulting solution—called hatch water—can affect other ovigerous females, causing all of their embryos to slip off the ovigerous hairs and out of the brooding space without hatching. This effect on whole crabs was used in the preceding experiments (Saigusa, 1994) to assay the activity of the OHSS contained in hatch water. To investigate the properties of this substance further, however, an assay that would require only small amounts of active material was essential.

In this study, therefore, I have used only segments of ovigerous setae with their attached embryos in a quantitative assay of the effect of OHSS. This substance is a protein released into the medium at the time that the egg capsule breaks. The molecular weight of OHSS was estimated by gel filtration. Reciprocal tests with several species suggest that OHSS occurs widely in intertidal and estuarine crabs.

Materials and Methods

Handling of ovigerous females for assays

Individuals of the terrestrial red-handed crab, *Sesarma haematocheir,* were collected from the thicket along a small estuary at Kasaoka, Okayama Prefecture, Japan, in 1992 and 1993. After collection, the crabs were quickly brought into the experimental rooms, where they were kept in several plastic containers (70 cm long, 40 cm wide, and 25 cm high) containing shallow water (about 1 cm deep) and hiding spaces. The light and temperature were controlled, respectively, at LD 15:9 and 24 ± 1°C. The assay is sensitive and seemed to be influenced by even very small quantities of OHSS mixed into the water. So when one or more females released their larvae into a container, *all* the females kept in that container were returned to the field. To avoid this problem, females were usually used for assay within a few days after collection.

Preparation of hatch water

As reported elsewhere (Saigusa, 1994), OHSS is contained in hatch water, *i.e.,* the filtered medium in which zoea larvae have hatched. The color of the embryos carried by females changes from dark brown to brownish green according to the stage of development, which can, therefore, be estimated by visual inspection. To obtain hatch water, females with mature embryos (brownish green) that were due to hatch within a few days were collected in the field (*i.e.,* in Kasaoka) (Saigusa, 1982).

As shown earlier (*e.g.,* Saigusa, 1988), hatching and larval release by estuarine crabs are under the control of a circatidal rhythm the phase of which can be shifted in the laboratory by the 24-h light cycle. When these females were kept under a day-night cycle in phase with that in the field (*i.e.,* light-on at 0500 and light-off at 2000), the larvae hatched at night at about the time of high tide. The ovigerous females were placed individually in glass or plastic beakers (8.5 cm in diameter, 12 cm in height) containing 30 ml of diluted seawater (10 ppt) or the same quantity of distilled water. The solution was aerated for 1 day before use. The medium was changed every day if larval were not released.

Hatching of estuarine crabs is highly synchronized; all of the embryos may hatch within about 5–30 min in the laboratory (see Saigusa, 1992, 1993). As soon as hatching was complete and the female had released all of her zoeas into the medium, she was removed, and the medium was filtered through nylon mesh to remove the zoeas. This filtered medium was immediately transferred to a small bottle, and was stored at −15°C until used; at this temperature, the activity of OHSS is maintained for at least half a year. But almost all of the experiments were done with hatch water that had been collected within the month.

Assay of OHSS activity

I have not yet found an artificial substrate that is acted upon by OHSS, so an efficient biological assay was developed, as follows. Female crabs have four pairs of abdominal appendages, each of which consists of plumose and ovigerous seta. Embryos are attached to the ovigerous hairs arranged along the ovigerous seta, by the funiculi (for details, see Saigusa, 1994). Several ovigerous setae with their clusters of embryos still attached were cut off from many females and subdivided, usually into six segments, under the stereomicroscope (Fig. 1a, b). Each segment with its cluster of embryos—hereinafter called an egg cluster—(Fig. 1a) was immersed in 0.5 ml of 10 ppt seawater (SW), or the same quantity of hatch water. The medium and egg clusters were incubated for various times in a plastic culture dish with 24 wells, each 1.6 cm in diameter and 1.7 cm in height. This dish was shaken back and forth (3–4 cm) at 100–120 times per min in the experimental rooms.

After the incubation, each egg cluster was again placed in a glass dish with 10 ppt SW or distilled water. The dish was put under a stereomicroscope, and fine forceps were used to pull the embryos gently away from their seta. When an egg cluster incubated in 10 ppt SW was pulled, about 90% of the ovigerous hairs were broken away from the seta (Fig. 1c). But of the clusters incubated with hatch water, about 80% slipped off easily and without damage (Fig. 1d). The activity of OHSS was therefore taken as the percentage of the hairs stripped clean and undamaged to the total number of hairs along the segment of seta.

Time course of the effect of OHSS with diluted hatch water

Hatch water collected from a single female was diluted 3, 9, and 27 times, and the time course of OHSS activity

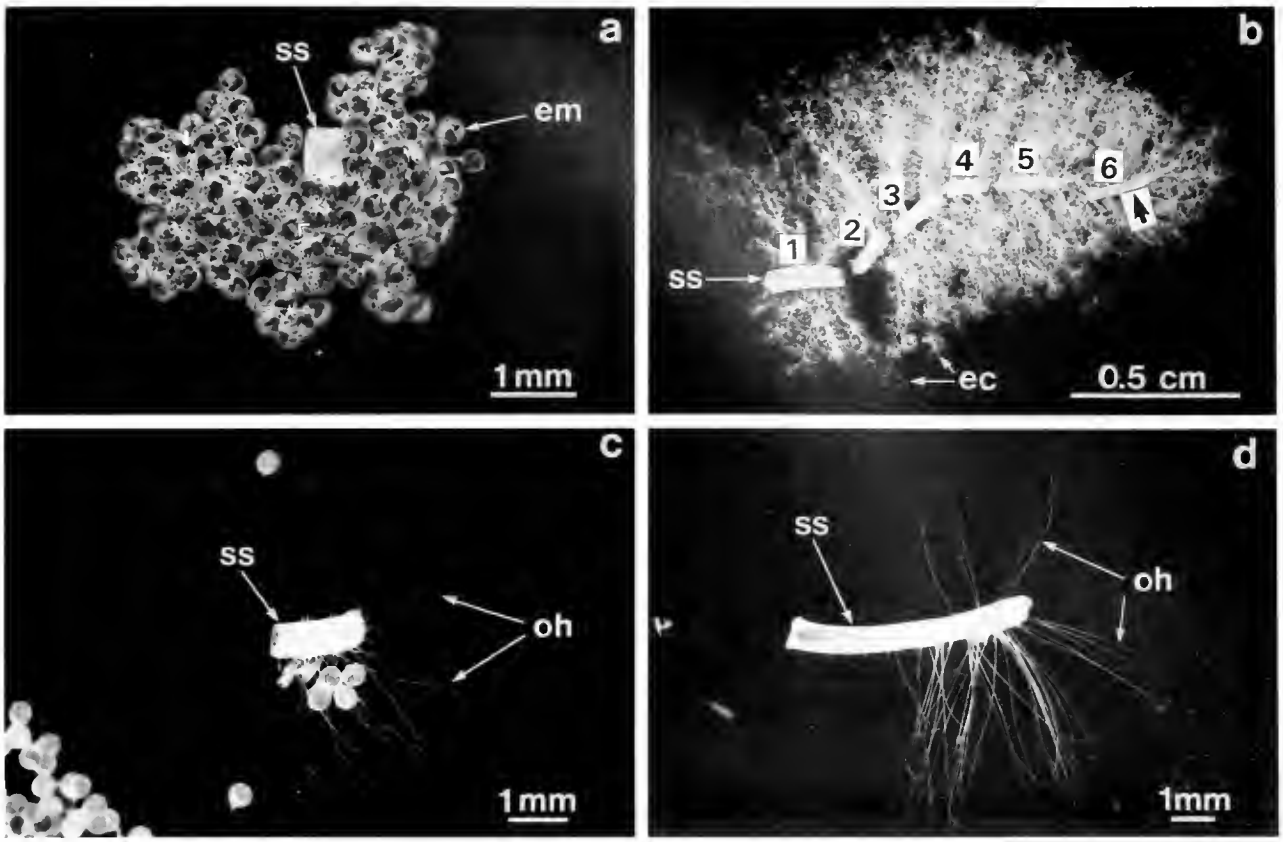

Figure 1. A method for assessing the activity of OHSS. (a) One of the setal segments (*ss*) subdivided before hatching, with its developing embryos (*em*) still attached. (b) An ovigerous seta is cut into six pieces (1–6). The arrow shows where the tip of the seta is removed (see text for details). This figure shows a seta just after the zoeas have hatched, leaving the empty egg cases (*ec*) still attached to ovigerous hairs which, however, are visible. (c) Ovigerous hairs (*oh*) incubated in 10 ppt SW, and the attached embryos then pulled gently away with forceps. (d) The same, but the ovigerous hairs (*oh*) incubated in hatch water. Note that many of the hairs incubated in seawater are broken off (compare c and d).

was compared with that of undiluted samples. This experiment was carried out with hatch water of *S. haematocheir* and *S. pictum*.

Appearance of OHSS activity in living females

To determine when OHSS is released, either by the larvae or by the female, one or two ovigerous setae were detached from the female before and after hatching. Before hatching, unhatched embryos were attached to the setae, but after the release of larvae, only the remnants (*i.e.*, broken egg capsules, funiculi, and the investment coat) remained on the setae. These setae were subdivided, and the embryos or the remnants were pulled with forceps. Time of hatching and larval release was determined and recorded by the photoelectric switch method described earlier (Saigusa, 1992, 1993).

Presence of OHSS activity before hatching

Embryonic development of *S. haematocheir* can be divided into four stages by visual inspection: the early stage (10 days), from the start of cleavage to just before the formation of eye pigments; the intermediate stage (10 days), from eye pigment formation to completion of the compound eyes; the late stage (1 week), in which the egg color changes from brown to brownish green; and the final stage (*i.e.*, mature embryos), in which hatching should occur within a few days.

To examine whether active OHSS is present before hatching, egg clusters of various developmental stages were examined: *i.e.*, two or three ovigerous setae with their attached embryos were detached from the females and crushed by hand for a few minutes, with 3 ml of 10 ppt SW per one seta. Aliquots (0.5 ml) of this embryo extract, uncentrifuged, were immediately pipetted into the wells of a culture dish. Freshly detached egg clusters were placed into this solution, and OHSS activity was monitored 4 h later. Time of hatching and larval release by the females that had yielded the experimental egg clusters was also monitored by the photoelectric switch method.

Susceptibility of OHSS to trypsin

Two milligrams of trypsin (porcine pancreatic "trypsin 1:250," Difco Laboratories) was dissolved in 20 ml of hatch water. The solution was divided into aliquots and incubated at 35°C for either 75 min or 3 h. These solutions were then transferred to room temperature (about 25°C). Egg clusters were placed into this solution, and OHSS activity was examined for the next 4 h. Furthermore, to test whether trypsin itself causes the wrapping coat to slip off the ovigerous hair, egg clusters were incubated for 4 h at 25°C, with 0.5 ml of 10 ppt SW containing only trypsin, and at the same concentration.

Gel filtration

Hatch water collected from several females was centrifuged at 15,000 rpm for 30 min at 5°C to remove the solid materials. The supernatant was freeze-dried and was then reconstituted in 1 ml of 10 m*M* Tris-HCl buffer (pH 7.5). This test sample, containing Blue Dextran (Pharmacia) and 1 M NaCl for calibration, was applied to a Sephacryl S-200 (Pharmacia) column (45 cm × 1.3 cm i.d.), and fractions (0.8 ml) were collected at 10-min intervals. The column was eluted with the Tris-HCl buffer, and the protein in each fraction was monitored with a Beckman DU-65 spectrophotometer at O.D. 280 nm.

The activity of OHSS in the fractions from gel filtration was determined by the method of Shirai (1986), as follows. A series of threefold dilutions of each active fraction was prepared, and an egg cluster was immersed in each dilution and tested by gentle pulling with forceps. The response—the percentage of stripped, undamaged hairs in each solution—was then plotted against the log of the dilution (Fig. 2). The potency of a fraction was expressed as the dilution producing a half-maximal effect (ED_{50}). But because the maximal response in this assay is about 80% and the minimum is about 10% (dashed lines in Fig. 2), the ED_{50} was taken as the dilution producing 45% stripped ovigerous hairs (shown as –· · –· · – in Fig. 2).

OHSS in other species. Females of *S. erythrodactylum*, *S. pictum*, and *S. dehaani* bearing embryos that appeared likely to hatch within a few days were collected from the field at Kasaoka and brought into the laboratory. Hatch water from these crabs was obtained in the same way as from *S. haematocheir*, although the quantity and salinity of the medium varied with the body size of each species and the ambient water into which larvae would normally be released (*i.e.*, 20 ml of 20 ppt SW for *S. pictum;* 15 ml of 20 ppt SW for *S. erythrodactylum;* and 40 ml of 10 ppt SW for *S. dehaani*). The filtered medium was frozen at −15°C until it was used.

Hatch waters of these additional three species and *S. haematocheir* were applied to the unhatched embryos of six species (listed in Table II). Females carrying unhatched embryos were collected from each habitat, and the ovigerous setae with their attached egg clusters were cut into 2–6 pieces according to the size of the crab. Experimental procedures were the same as for *S. haematocheir*. Time of incubation was 4–6 h, depending upon the species that provided the egg clusters.

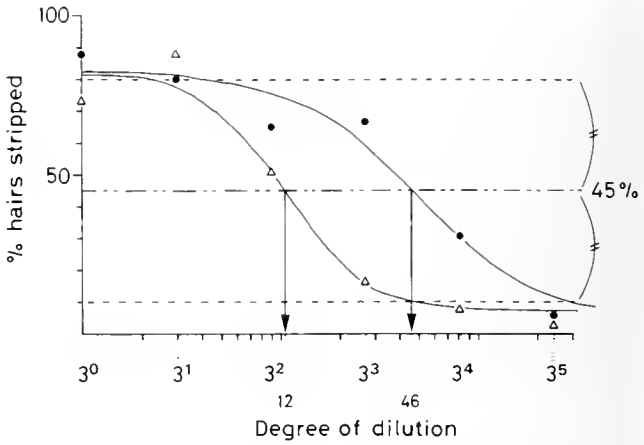

Figure 2. Dilution-response curves of crude and concentrated hatch water; the degree of dilution is scaled logarithmically (base 3). Broken lines show the maximum and minimum percentages of ovigerous hairs that were stripped off the investing coat without damage. The dilution-response curves for crude hatch water (open triangles) and concentrated hatch water (black circles) were drawn by hand without statistical treatment. Activity units are taken as the values of the dilution at which each dose-response curve intersects the 45% level (downward arrows): *i.e.*, 12 (crude) and 46 (concentrated) units in these preparations.

To examine further whether the effect of OHSS is different among species, the hatch water collected from several females of *S. pictum* was pooled, and assayed with egg clusters of *S. haematocheir*, *S. erythrodactylum*, and *Hemigrapsus sanguineus*. The time course of the effect of OHSS was monitored every 15 min or 1 h.

Results

Development of the assay

The following preliminary experiments were aimed at understanding the variables in the assay and thus improving its reliability. The ovigerous setae with their egg clusters were cut off and subdivided, usually into six segments (Fig. 1a). As shown earlier (Saigusa, 1994), most ovigerous hairs are arranged in whorls along the ovigerous seta. The length of these hairs depends upon their position along the seta (Fig. 1b): *i.e.*, the hairs along positions 2–5 are longest; those at the tip of the seta (position 6) are shortest; and those at the base (position 1) are of intermediate length (see also Fig. 6B in Saigusa, 1994).

The first question was whether the length of the hairs would affect the ease with which they slip out of the investing coat. When incubated with 10 ppt SW, the shortest

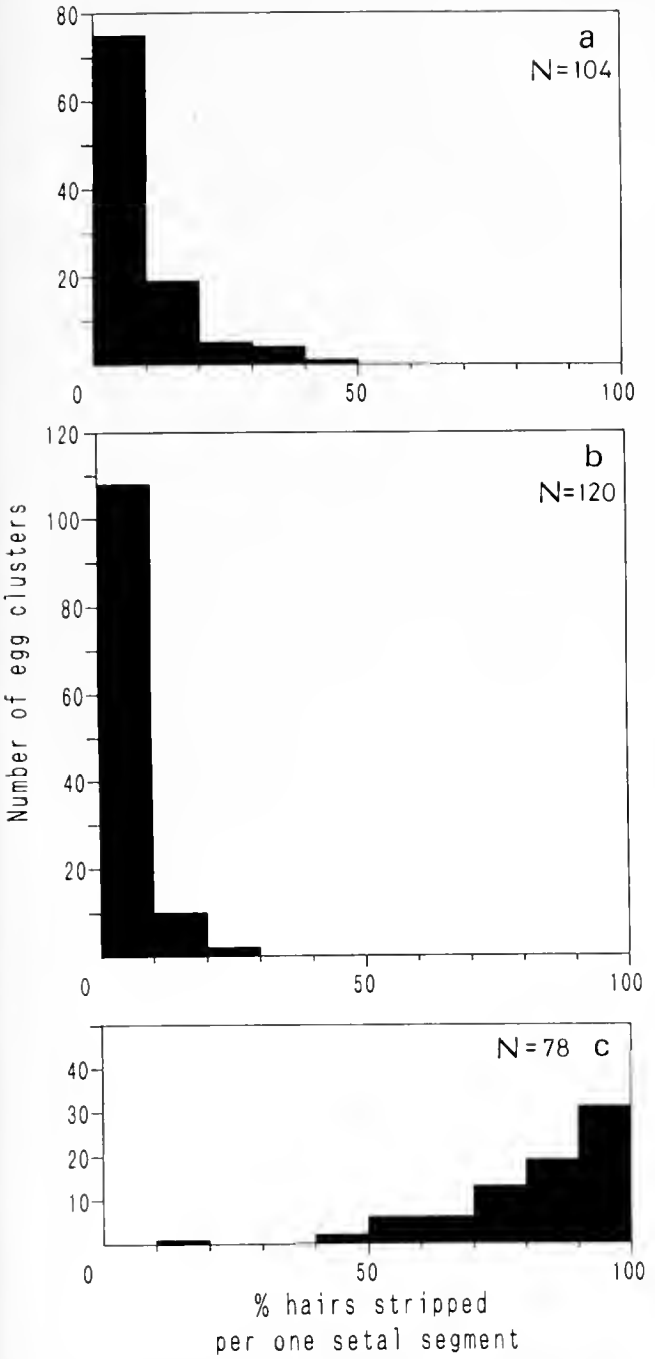

Figure 3. Distribution of the number of segments in which the percentage of the ovigerous hairs that slipped out of the coat without damage was estimated. (a) Data from experiments in which the tip of the seta remained (incubation in 10 ppt SW). (b) Data from experiments in which the seta was cut at its tip as shown in Figure 1a (incubation with 10 ppt SW). (c) Embryo clusters treated with hatch water. N = Total number of subdivided setal segments with their attached egg clusters. The percentage for each setal segment is shown at intervals of 10%.

hairs certainly tended to slip out most easily. This tendency was especially marked at the tip of the seta (Fig. 3a). So in most of the experiments, the tip of the ovigerous seta was cut away before use (arrow in Fig. 1b). On average, only 10% of the hairs were stripped clean without damage (Fig. 3b). In contrast, about 80% of the egg clusters slipped off when the preparation was placed into hatch water (Fig. 3c).

A further difficulty is that the response to a given concentration of OHSS is considerably different even among the egg clusters produced by the same female. Figure 4 shows the response of two groups of the egg clusters that were separated from one female and both immersed in hatch water with the same concentration of OHSS. Although the percentage of stripped hairs fluctuated considerably, it clearly increased with time, reaching a maximum in 1–3 h (*e.g.*, Fig. 4). In contrast, control egg clusters immersed in 10% seawater showed no such increase in the percentage of stripping. The fluctuation in the responses suggests that the adhesion between the investing coat and the ovigerous hairs is also variable, even in the same female.

Concentration-dependence of OHSS activity

Unhatched embryos detached from two females of *S. haematocheir* were incubated with a series of threefold dilutions of hatch water collected from one female, and the time course of the effect of OHSS was monitored (Fig.

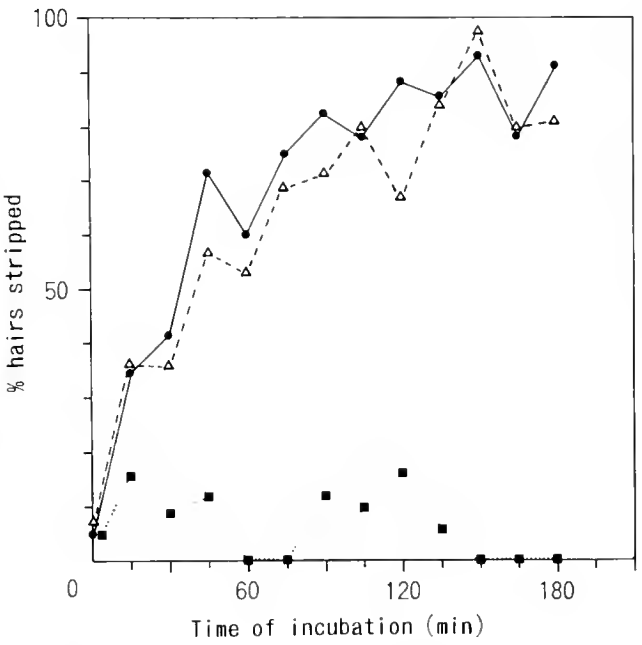

Figure 4. A typical time course of the effect of *S. haematocheir* hatch water on the stripping of unhatched embryos of the same specimen. Two egg clusters were incubated in hatch water from one female (●—● and △- - -△), and one incubated in 10 ppt SW (■· · ·■). These egg clusters were all separated from a single female. The broken line shows the response curve of the mean value between the two preparations immersed in hatch water.

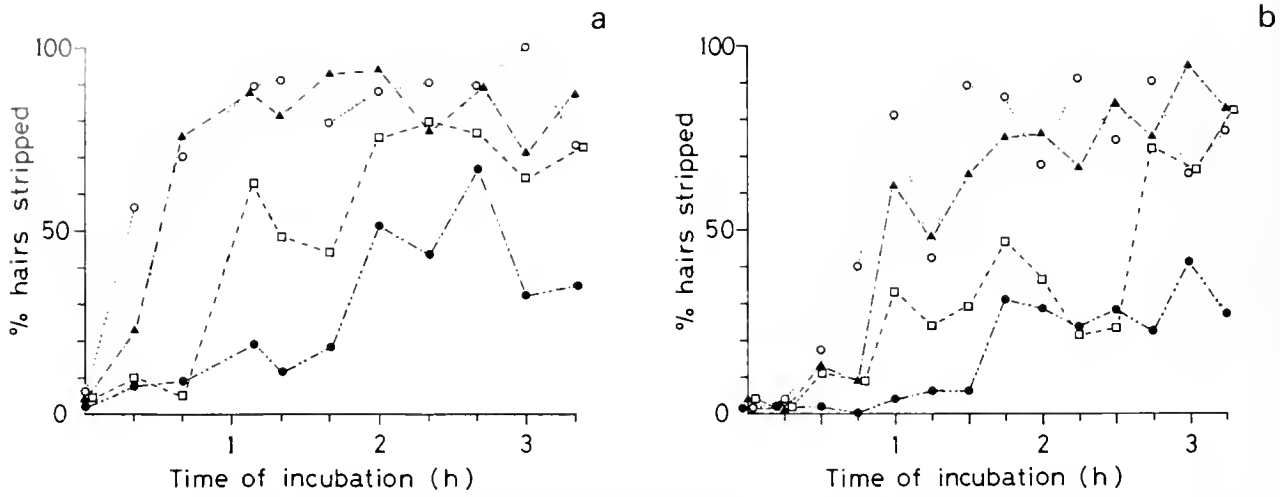

Figure 5. Time course showing the effect of diluting of hatch water with 10 ppt SW. (a) *S. haematocheir* embryos incubated with *S. haematocheir* hatch water. (b) *S. pictum* embryos incubated with *S. pictum* hatch water. No dilution (○· · ·○); 3-fold dilution (▲–·–·–▲); 9-fold dilution (□- -□); 27-fold dilution (●–· · –●).

5a). In the groups of embryos placed into undiluted and threefold-dilute hatch water, half-maximal activity of OHSS was reached in 20–30 min and was largely completed (about 85%) after 60–80 min of treatment. A ninefold dilution of hatch water became equiactive to the undiluted solution in an hour, and the maximum response was decreased to 60%–70%. Finally, the maximum activity of a 27-fold dilute solution was reduced about 30%.

The effect of dilution of hatch water was also tested in *S. pictum* (Fig. 5b). In this experiment, embryos detached from two females of *S. pictum* were placed into a series of threefold dilutions of *S. pictum* hatch water. Although the percentage of slipped hairs also fluctuated in this species, the trends in Figure 5b were very similar to those of Figure 5a.

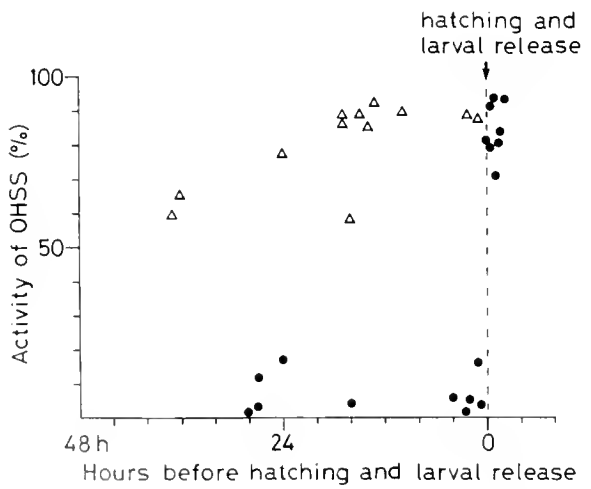

Figure 6. OHSS activity within the embryos before, and just after, hatching and larval release. Solid circles (●): percentage of stripped hairs on setae detached from the females. These setae were taken from females with unhatched embryos (before hatching and larval release), as well as those with remnants (after the release of larvae). They are not treated with hatch water. Open triangles (△): hairs on setae that were incubated in a solution of crushed embryos for 4 h, and then pulled with forceps.

Appearance of the activity in the embryo and the timing of release outside the egg membrane

To determine the time that OHSS has an effect on living females, the activity of the substance before the time of hatching and larval release was compared with the activity afterward. Until just before hatching, most ovigerous hairs were broken when the egg cluster was detached and pulled with a forceps; but just after larval release, the hairs easily slipped out of the coat (solid circles in Fig. 6). This indicates that OHSS is released at the time of hatching, either by the zoeas or by the female.

Furthermore, to determine whether the OHSS activity appears in the embryos before hatching, freshly detached embryos were incubated with the material containing crushed embryos. No activity was detected in the embryos, even at late stages of development (data not shown). But activity was clearly detected in embryos that should have hatched within 48 h (triangles in Fig. 6). Thus, OHSS seems to accumulate in the embryos before hatching. Because the activity is not detected outside of the egg case just before hatching, we can suppose that its release is associated with breakage of the egg capsule.

Gel filtration

Lyophilized hatch water collected from four specimens of *S. haematocheir* was redissolved and subjected to gel

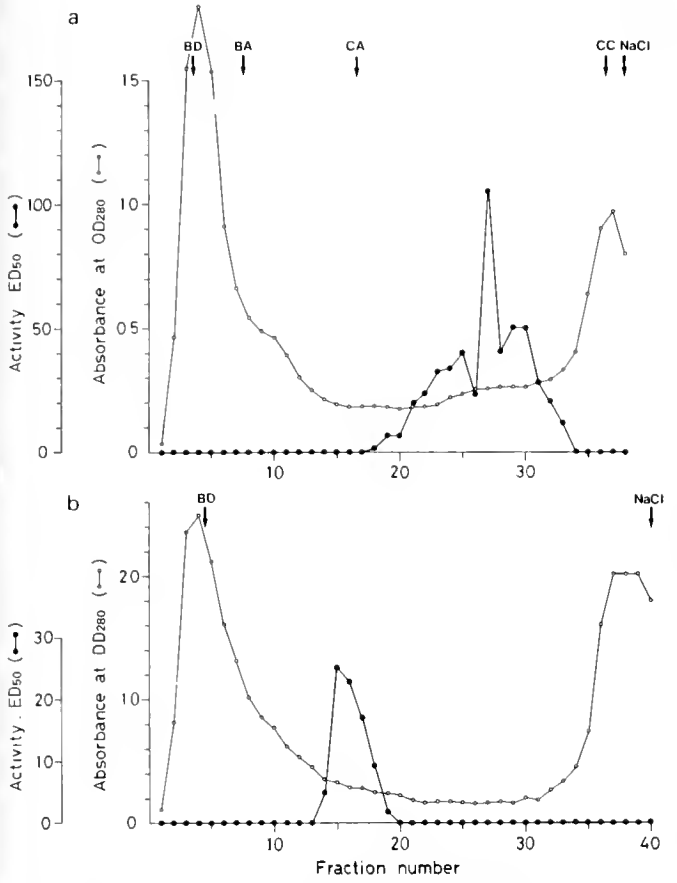

Figure 7. Gel filtration of hatch water. (a) *S. haematocheir.* Lyophilized hatch water collected from four specimens was reconstituted and passed through a Sephacryl S-200 column equilibrated with 10 m*M* Tris-HCl buffer (pH 7.5). Egg clusters of *S. haematocheir* were incubated with each fraction for 1.5 h, and the OHSS activity was assayed (protocol in text). Downward arrows show elution peaks of blue dextran (BD), bovine serum albumin (BA), carbonic anhydrase (CA), cytochrome c (CC), and NaCl. These markers were passed through the column without hatch water. (b) *S. pictum.* Test sample was obtained from three females of *S. pictum*, and passed through the same column after reconstitution with the same buffer. Embryos of *S. haematocheir* were incubated for 5 h, and the OHSS activity was then assayed. Note species differences.

filtration on a column of Sephacryl S-200. The activity of each fraction was assayed with unhatched embryos of the same species. As shown elsewhere (*e.g.*, Fig. 5), activity is variable, so the experiments were repeated 12 times, always with similar results. Figure 7a shows one of these experiments. The activity of OHSS extends over a wide range of fractions. The molecular size of OHSS was estimated to be 15–20 kDa by a comparison of its elution volume with those of standard proteins: *i.e.*, bovine serum albumin (66 kDa), carbonic anhydrase (29 kDa), and cytochrome *c* (12.4 kDa).

Hatch water collected from three females of *S. pictum* was subjected to the same gel filtration protocol that was used with *S. haematocheir*, and the activity was also assayed with embryos of *S. haematocheir*. This separation was repeated four times with similar results. As shown in Figure 7b, OHSS of *S. pictum* eluted as a single peak, and the molecular size was estimated by comparison with standards to be about 30 kDa.

Table I

The effect of boiling and trypsin treatment on the OHSS activity of hatch water from Sesarma haematocheir

Experiments	Percentage of stripped hairs ($\bar{X} \pm SD$)*
Dilute SW (10 ppt)	0 (±0)
Trypsin solution	2.6 (±4.7)
Hatch water	82.2 (±9.8)
Boiling of hatch water	3.6 (±2.5)
Trypsin treatment of hatch water (75 min)	69.1 (±11.8)
Trypsin treatment of hatch water (4 h)	8.3 (±6.8)

* In all cases, the number of setal segments tested was 12.

Effect of trypsin

A few tests were conducted to examine the nature of OHSS. As indicated in Table I, its activity was eliminated when hatch water was heated for 5 min. The activity was also somewhat decreased when the hatch water was treated with trypsin for 75 min, and was completely lost with 3 h of treatment. On the other hand, trypsin itself did not affect the coat, although this enzyme often decomposed the basement of the ovigerous hairs. These experiments suggest that OHSS is a protein.

Species distribution of OHSS activity

Table II summarizes the reciprocal tests in which hatch waters from four species of *Sesarma* were applied to the

Table II

Reciprocal tests on the effect of OHSS

Source of hatch water	Source of cluster of embryos	Percentage of stripped hairs ($\bar{X} \pm SD$)* Hatch water	10 ppt SW
Sesarma dehaani	*S. haematocheir*	81.9 ± 9.2 (12)	3.8 ± 4.1 (12)
S. erythrodactylum	*S. erythrodactylum*	84.5 ± 13.1 (6)	5.2 ± 5.7 (6)
	S. pictum	89.3 ± 6.3 (4)	2.2 ± 3.8 (4)
	S. haematocheir	61.7 ± 18.6 (6)	3.7 ± 5.1 (6)
S. haematocheir	*S. bidens*	99.2 ± 1.3 (4)	8.4 ± 5.5 (4)
	Gaetice depressus	49.7 ± 8.9 (6)	1.9 ± 2.1 (6)
S. pictum	*Hemigrapsus sanguineus*	41.7 ± 22.5 (6)	1.6 ± 1.0 (6)
	S. erythrodactylum	94.1 ± 3.7 (6)	3.7 ± 3.5 (6)
	S. haematocheir	60.8 ± 12.1 (4)	2.6 ± 2.6 (4)
	S. pictum	64.1 ± 11.5 (6)	5.0 ± 6.3 (6)

* Number of setal segments tested is in parentheses.

embryos of six species of crab. All species were affected by all types of hatch water, suggesting that OHSS occurs widely in intertidal and estuarine crabs.

But there was a clear difference in the time course of activity among species. Figure 8a, b summarizes the results of experiments in which *S. pictum* hatch water with the same OHSS concentration was applied to the embryos of *S. erythrodactylum*, *S. haematocheir*, and *Hemigrapsus sanguineus*. In *S. erythrodactylum*, the maximal activity was reached after 1 h of incubation (Fig. 8a), but more than 5 h was needed for *H. sanguineus* (Fig. 8b).

Discussion

Hatch water of the estuarine terrestrial crab *Sesarma haematocheir* contains a substance that causes premature detachment of embryos from ovigerous females. The active factor—ovigerous-hair stripping substance (OHSS)—is released outside of the egg case at the time of hatching, and is not released by the female. Its molecular size was estimated by gel filtration to be 15–20 kDa in *S. haematocheir* and 30 kDa in *S. pictum*. These results raise the following five issues in relation to the OHSS activity and its function: species specificity, timing of synthesis and secretion, mode of action, characterization, and composition of the investment.

Species specificity of OHSS activity

As shown in Figure 7b, OHSS activity of *S. haematocheir* can be assayed with egg clusters of *S. pictum*. Reciprocal tests among different species indicate that OHSS occurs widely in intertidal and estuarine crabs (Table II). Thus, the hatch water from one species of crab has an effect on the embryos of other species. On the other hand, a given concentration of hatch water from one species can, in its action on crabs of other species, have very different time courses (Fig. 8). This disparity suggests that the response to OHSS differs among species. For example, the length of the ovigerous hairs differs among species, so the strength of the bond between the coat and the ovigerous hairs might also differ, causing the variation in time course. Moreover, the molecular size of OHSS is different in *S. haematocheir* and *S. pictum* (Fig. 7). This suggests that the molecular structure of OHSS might also vary, and it might have a different effect when applied to the embryos of other species.

Timing of OHSS synthesis and secretion

As shown elsewhere (Saigusa, 1992), clusters of *S. haematocheir* embryos that are detached from the female within 48–49.5 h of larval release all hatch successfully; but embryos that have been detached from the female for longer periods do not hatch at all, though they are obviously alive and have the potential of hatching (see also Saigusa, 1993). These results suggests that the hatching process is a distinct program initiated near the end of embryonic development (Saigusa, 1992).

No activity appeared outside of the egg case until hatching occurred. But a homogenate of embryos clearly showed that the activity was present in embryos that should have been in the process of hatching (Fig. 6). Because no activity was detected in earlier developmental

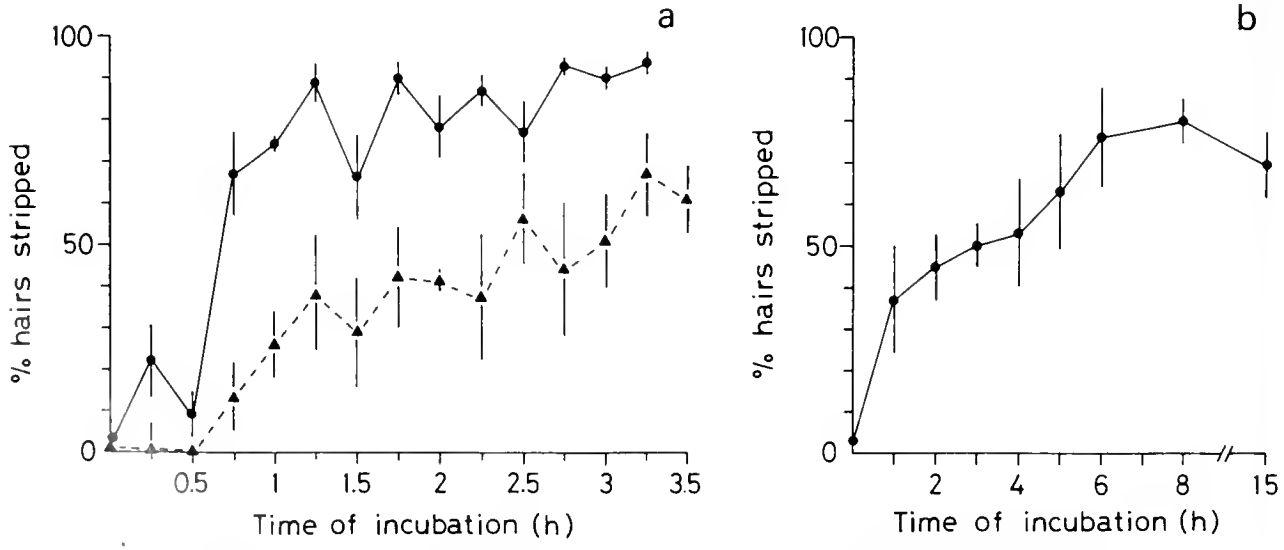

Figure 8. Time course of the effect of OHSS when hatch water from *S. pictum* was applied to the embryos of other species. (a) Embryos of *S. erythrodactylum* (solid circles) and *S. haematocheir* (solid triangles); (b) Embryos of *Hemigrapsus sanguineus* (solid circles).

stages, we can speculate that OHSS begins to be produced only immediately before the start of hatching. Further studies are required to determine the exact timing of OHSS synthesis and secretion in the unhatched embryos.

Mode of action of OHSS

The embryos that slip off the ovigerous hairs are always associated with the funiculus and the wrapping coat, and scanning electron microscopy revealed no morphological changes, either on the coat or the hair (Saigusa, 1994). Goudeau and Lachaise (1983) showed a cross section of the wrapping coat in the shore crab *Carcinus maenas*. Their figure suggests that the material of the funiculus is coiled around the ovigerous hair without any additional substance. If this is the case in *S. haematocheir*, it is not plausible that OHSS invades the space between the coat and the ovigerous hair. So I suppose that OHSS works directly on the coat, perhaps softening it, so that the hairs can separate from the investment coat. But what is the mechanism by which this substance softens the coat?

Identity of OHSS

One possibility is that OHSS is a protease that partially digests the layers of the investment coat. Embryos of many groups of animals (*e.g.*, fishes, sea urchins, and amphibians) release a protease that digests egg membrane or egg capsule to cause hatching (for a review, see Saigusa, 1994). DeVries and Forward (1991) also reported a proteolytic enzyme released near the time of hatching in three species of estuarine crabs. It is not known whether OHSS is a proteolytic enzyme, nor whether it acts as a hatching enzyme. But if so, then OHSS may partially degrade, not only the egg capsule, but also the investment coat, causing them to slip off the ovigerous hairs.

Another possibility is that OHSS is a type of chitinase such as is known in many kinds of animals and plants. Chitin is a stable sugar complex constituting the exocuticle, endocuticle, and membraneous layer in crustaceans. It is hydrolyzed by two enzymes in sequence: chitinase, which converts the long chitin polymers into small oligosaccharides; and chitobiase (β-*N*-acetylglucosaminidase), which hydrolyzes these chito-oligomers into *N*-acetyl-D-glucosamine (Lunt and Kent, 1960; Jeuniaux, 1966; O'Brien *et al.*, 1993). These enzymes might be degrading the coat wrapping the ovigerous hairs until it is able to slip off the hairs. The problem with this notion is that such enzymes might also degrade the skin of the zocas.

Composition of the investment coat, funiculus, and egg envelope

In crabs, the funiculus extends to the coat investing the ovigerous hair, which suggests that the same material forms both the funiculus and the investment coat (Saigusa, 1994). As shown in Goudeau and Lachaise (1980), the structure and formation of the egg envelope of the shore crab *Carcinus maenas* are complex. Cheung (1966) showed that the egg envelope and funiculus of this species are not affected by pepsin or trypsin, though the yolk of the embryos is easily digested. Cheung concluded that at least the outer layer (*i.e.*, trichromatic membranes in her paper) consists largely of non-proteinous substances. Furthermore, our pictures by the transmission electron microscopy indicate that this material makes up the surface layer of the egg envelope of crabs (unpub. data). If OHSS softens the tissue of the investment coat, it would also work on the outer layer of the egg envelope, softening the envelope. This might contribute to the case of hatching and might enhance hatching synchrony. In any event, morphological and experimental studies on this coat might help in identifying OHSS.

Acknowledgments

Gel filtration chromatography was done at Ushimado Marine Laboratory, Okayama University. I thank Dr. Tadashi Akiyama for technical assistance. I am also indebted to Dr. Hiroko Shirai for her frequent advice on experimental procedures.

Literature Cited

Andrews, E. A. 1906. Egg-laying of crayfish. *Am. Nat.* **40:** 343–356.

Cheung, T. S. 1966. The development of egg-membranes and egg attachment in the shore crab, *Carcinus maenas*, and some related decapods. *J. Mar. Biol. Assoc. UK* **46:** 373–400.

De Vries, M. C., and R. B. Forward, Jr. 1991. Mechanisms of crustacean egg hatching: evidence for enzyme release by crab embryos. *Mar. Biol.* **110:** 281–291.

Fisher, W. S., and W. H. Clark, Jr. 1983. Eggs of *Palaemon macrodactylus*: I. Attachment to the pleopods and formation of the outer investment coat. *Biol. Bull.* **164:** 189–200.

Goudeau, M., and F. Lachaise. 1980. Fine structure and secretion of the capsule enclosing the embryo in a crab (*Carcinus maenas* (L.)). *Tissue & Cell* **12:** 287–308.

Goudeau, M., and F. Lachaise. 1983. Structure of the egg funiculus and deposition of embryonic envelopes in a crab. *Tissue & Cell* **15:** 47–62.

Goudeau, M., P. Talbot, and R. Harper. 1987. Mechanism of egg attachment stalk formation in the lobster, *Homarus*. *Gamete Res.* **18:** 279–289.

Jeuniaux, C. 1966. Chitinases. *Methods Enzymol.* **8:** 644–650.

Linder, H. J. 1960. Studies on the fresh water fairy shrimp *Chirocephalopsis bundyi* (Forbes). II. Histochemistry of egg-shell formation. *J. Morph.* **107:** 259–284.

Lunt, M. R., and P. W. Kent. 1960. A chitinase system from *Carcinus maenas*. *Biochim. Biophys. Acta* **44:** 371–373.

Mawson, M. L., and C. M. Yonge. 1938. The origin and nature of the egg membranes in *Chirocephalus diaphanus*. *Quart. J. Micr. Sci.* **80:** 553–565.

O'Brien, J. J., S. S. Kumari, and D. M. Skinner. 1993. Differential localization of specific proteins in the exoskeleton of the Bermuda

land crab. Pp. 79–111 in *The Crustacean Integument*, M. N. Horst and J. A. Freeman, eds. CRC Press, Boca Raton, FL.

Saigusa, M. 1982. Larval release rhythm coinciding with solar day and tidal cycles in the terrestrial crab *Sesarma*. *Biol. Bull.* **162:** 371–386.

Saigusa, M. 1988. Entrainment of tidal and semilunar rhythms by artificial moonlight cycles. *Biol. Bull.* **174:** 126–138.

Saigusa, M. 1992. Control of hatching in an estuarine terrestrial crab. I. Hatching of embryos detached from the female and emergence of mature larvae. *Biol. Bull.* **183:** 401–408.

Saigusa, M. 1993. Control of hatching in an estuarine terrestrial crab. II. Exchange of a cluster of embryos between two females. *Biol. Bull.* **184:** 186–202.

Saigusa, M. 1994. A substance inducing the loss of premature embryos from ovigerous crabs. *Biol. Bull.* **186:** 81–89.

Shirai, H. 1986. Gonad-stimulating and maturation-inducing substance. Pp. 73–88 in *Methods in Cell Biology*, Vol. 27. Academic Press, Washington.

Suko, T. 1961. Studies on the development of the crayfish. VII. The hatching and the hatched young. *Sci. Rep. Saitama Univ. (Ser. B)* **4:** 37–42.

Talbot, P., and D. Demers. 1993. Tegumental glands of Crustacea. Pp. 151–191 in *The Crustacean Integument*, M. N. Horst and J. A. Freeman, eds. CRC Press, Boca Raton, FL.

Yonge, C. M. 1937. The nature and significance of the membranes surrounding the developing eggs of *Homarus vulgaris* and other Decapoda. *Proc. Zool. Soc. Lond. (Ser. A)* **107:** 499–517 (plus 1 plate).

Yonge, C. M. 1946. Permeability and properties of the membranes surrounding the developing egg of *Homarus vulgaris*. *J. Mar. Biol. Assoc. U.K.* **26:** 432–438.

Reference: *Biol. Bull.* **189**: 185–262. (October/November, 1995)

Reports of Papers Presented at the General Scientific Meetings of the Marine Biological Laboratory

August 14 to 16, 1995

Program Chairs:
Robert Paul Malchow, University of Illinois at Chicago
Anne Giblin, Ecosystems Center, MBL
Kathleen Siwicki, Swarthmore College

Roxanna Smolowitz, Laboratory for Marine Animal Health, MBL
Antoinnette Steinacker, Washington University
Joel Tabb, Dartmouth College
Sidney Tamm, Boston University Marine Program, MBL
Mark Terasaki, University of Connecticut Health Center
Jane Tucker, Ecosystems Center, MBL
Ivan Valiela, Boston University Marine Program, MBL
Joseph Vallino, Ecosystems Center, MBL
Matt Wachowiak, The Whitney Laboratory
James Walker, University of Cambridge
Jerome Wolken, Carnegie Mellon University
Seymour Zigman, University of Rochester Medical School
Steve Zottoli, Williams College

Contents

Biophysics

Comparative Physiology and Biochemistry

Behavior

Physiological Ecology and Behavior

Ecology: Fish and Invertebrates

ABSTRACTS

In addition to the work described here in Short Reports, the following papers were also presented. The abstracts of these papers are available from the Marine Biological Laboratory Archives, Woods Hole, MA 02543.

Reference: *Biol. Bull.* **189**: 190–195. (October/November, 1995)

Introduction to Featured Articles: A Resurgence of Experimental Embryology

Around the last turn of the century, outstanding biologists, such as E. B. Wilson, E. G. Conklin, F. R. Lillie, T. H. Morgan, and J. Loeb, came to the Marine Biological Laboratory to study the details of embryonic development of a rich diversity of marine organisms. These workers were searching for homologies in the pattern of cleavage and development and in the origin of the organ-forming regions of these embryos. The information that was compiled then has had a powerful and persistent influence on our thinking about the evolution of development, and about the role of development in the evolution of metazoan body plans.

Although the successes of the early experimental embryologists were far-reaching, decades were to pass before the mechanisms underlying the events they had observed were discovered. Indeed, our understanding of cellular and molecular processes has increased rapidly in recent years, and many of the central questions asked a century ago—and never answered—have now become tractable. In particular, the evolution of development—long the subject of speculation—is now becoming one of the most exciting areas of experimental *biology.*

This year's featured reports illustrate how new disciplines and methods can be applied with great effectiveness to tough, old, but still very attractive biological problems. The authors of these reports—Jonathan Q. Henry, Mark Q. Martindale, and Barbara C. Boyer—use modern techniques to analyze cell lineage in diverse marine animals. Their experiments are aimed at the mechanisms that generate form and pattern during embryogenesis and the modification of those mechanisms in organisms that have evolved from a common ancestor. These reports provide, in brief, new information about "the ways in which embryos are put together and how they work."

—Michael J. Greenberg
Editor-in-Chief

Reference: *Biol. Bull.* **189**: 190–192. (October/November, 1995)

Diagonal Development: Establishment of the Anal Axis in the Ctenophore *Mnemiopsis leidyi*

Mark Q. Martindale (University of Chicago, Department of Organismal Biology and Anatomy, Chicago, Illinois 60637) and Jonathan Q. Henry

The Ctenophora is a phylum of biradially symmetrical marine carnivores, the comb jellies. These animals possess an outer epidermis that is separated from an inner gastrodermis by a largely acellular mesoglea. Although ctenophores have been thought to be diploblastic, definitive muscle cells reside in the mesoglea and in association with both epithelial layers. The major body axis—the oral-aboral axis (Fig. 1a)—is the intersection of two orthogonally situated planes of mirror symmetry: the sagittal plane passes through the plane of the flattened stomadeum; and the tentacular plane passes through the two tentacle pouches. These planes of symmetry define four quadrants, each containing two of the eight ctene rows, half of a tentacular apparatus, and one quarter of the apical sensory organ. The biradial symmetry of these animals is reflected in their embryonic development in which the first cleavage plane corresponds to the sagittal plane and the second to the tentacular plane (1, 2). Thus, each of the first four blastomeres generates one of the four body quadrants.

At the aboral end of all ctenophores, two anal canals open at the anal pores in two diametrically opposed quadrants (Fig. 1b). The location of these pores appears to be conserved in all ctenophore species and provides another axis of rotational (but not mirror) symmetry, which we refer to as the anal axis. The oblique orientation of the anal axis suggests that it might arise asymmetrically during the development of the four cell quadrants. We have investigated the ontogeny of the anal axis by performing cell lineage studies in the ctenophore *Mnemiopsis leidyi*. One or more identified blastomeres up through the 32-cell stage were impaled with glass microelectrodes and injected with the fluorescent lipophilic dye, DiI (Molecular Probes Inc., Eugene, OR) dissolved in vegetable oil (3). A 100 mg/ml DiI stock was made

in ethanol and diluted 20-fold in soybean oil. Injected cells continued to divide normally and the injections had no observable effect on development. Embryos were reared at 19°C; and after 24 to 48 h, the cydippid larvae were examined by fluorescence microscopy for the presence of labeled anal canals.

Four-cell stage embryos divide to give rise to four middle (M) cells and four end (E) cells. Our injections of blastomeres at the 32-cell stage show that the anal canals are derived from the endodermal derivatives of the second order macromeres of the M lineage, the 2M blastomeres (Fig. 1c, d). Injections of 2M blas-

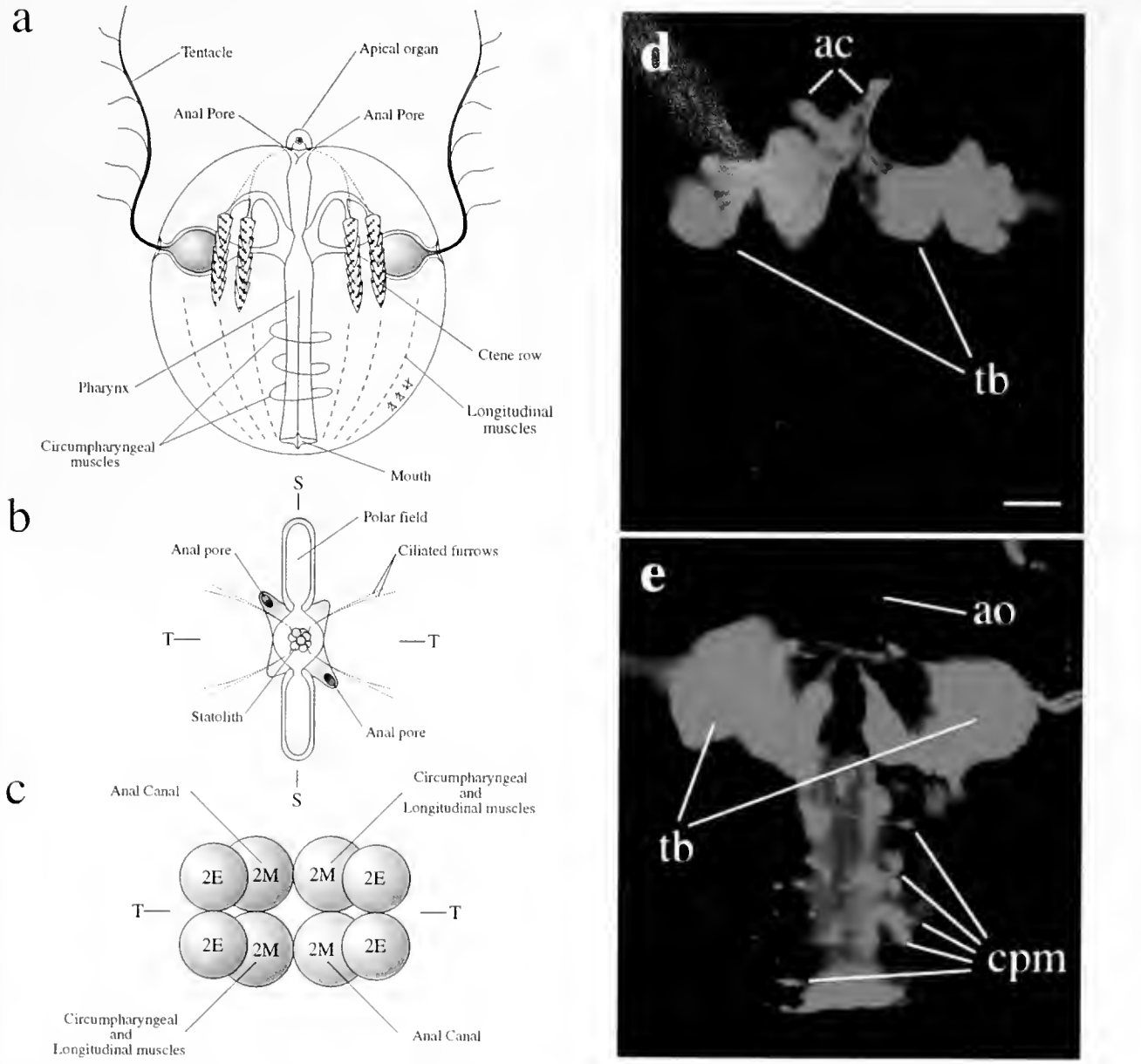

Figure 1. *Development of the anal axis in the ctenophore* Mnemiopsis leidyi. *(a) Side view of a cydippid larva. The two tentacles define the tentacular plane of mirror symmetry (*i.e., *in the plane of the paper); an apical sensory organ is situated at the aboral pole. (b) Aboral view of the apical organ showing the location of the two anal pores. (c) Aboral view, showing the four 2M and 2E macromeres, of a 32-cell stage* Mnemiopsis *embryo. The 24 aboral micromeres are not shown for the sake of clarity. Two diagonally opposed pairs of 2M macromeres, one situated top left and bottom right, and the other top right and bottom left, can be identified. Each pair gives rise to distinct structures in the cydippid larva. The diagonal fates of these macromeres are indicated. (d) and (e) Color fluorescence micrographs of cydippid larvae, oriented the same way as in Figure 1a (aboral pole up), in which two different diagonal pairs of 2M macromeres were injected with lineage tracer. Note that there is staining associated with the tentacle bulbs (tb) and endoderm under the ctene rows in both photos. (d) The unlabeled apical organ sits in the crotch of the two diagonally labeled anal canals (ac), but there is no staining associated with the pharynx at the oral end of the larva. (e) In contrast, there is no staining of the anal canals in the vicinity of the apical organ (ao) in this larva, but the circumpharyngeal muscles (cpm) are labeled. See Fig. 1c for the positions of the two pairs of 2M cells injected. T = the tentacular plane; S = the sagittal plane. Scale bar = 50 μm.*

tomeres show that only two of the four 2M macromeres generate anal canals. These cells are located diagonal to one another (Fig. 1c) and do not generate any other cell types present in the mesoglea. The remaining two 2M macromeres produce longitudinal and circumpharyngeal muscle cells (Fig. 1c, e). Thus, the four quadrants of the ctenophore embryo are not identical. Two cells at the four-cell stage are capable of forming circumpharyngeal muscle cells but not anal canals, whereas the other two cells are capable of forming anal canals but not circumpharyngeal muscles. Cell deletion experiments confirm this precocious specification (Henry and Martindale, unpub. data), indicating that developmental potential is being segregated asymmetrically as early as the second division in these embryos. No bilaterian embryos we know display features of diagonal development. The presence of the two developmental axes specifying anal canals and circumpharyngeal muscles, in addition to the anatomically defined sagittal and tentacular axes, warrants a reassessment of the "biradial" condition in these animals, and the alignment of the Ctenophora with their probable sister taxon, the Cnidaria, as a group of radially symmetrical animals, the Coelenterata (4, 5).

This paper is dedicated to the memory of Dr. Sebastian Beroë on the 20th anniversary of his tragic death from cholera. The authors appreciate the generosity of the Marine Biological Laboratory community in facilitating these studies, and S. Q. Irvine for help with the collection of animals. J.Q.H. (J.J.H.) was supported as an MBL Associates Fellow and a Lemann Fellow. M.Q.M. was supported by the NSF and the Illinois chapter of the American Cancer Society.

Literature Cited

1. **Reverberi, G., and G. Ortolani. 1963.** *Acta Embryol. Morphol. Exper* **6**: 175–190.
2. **Freeman, G. 1976.** *Develop. Biol.* **49**: 143–177.
3. **Terasaki, M., and L. Jaffe. 1991.** *J. Cell Biol.* **114**: 929–940.
4. **Christen, R., A. Ratto, A. Baroin, R. Perasso, K. G. Grell, and A. Adoutte. 1991.** *EMBO J* **10**: 499–503.
5. **Morris, S. C. 1993.** *Nature* **361**: 219–225.

Reference: *Biol. Bull.* **189**: 192–193. (October/November, 1995)

The Experimental Alteration of Cell Lineages in the Nemertean *Cerebratulus lacteus:* Implications for the Precocious Establishment of Embryonic Axial Properties

Jonathan Q. Henry (University of Illinois, Department of Cell and Structural Biology, Urbana, Illinois 61801) and Mark Q. Martindale

Spiralians, including the molluscs, annelids, and nemerteans, are characterized by a highly stereotypic pattern of embryonic cell divisions, which is based on the establishment of four discrete cell quadrants. In molluscan and annelid embryos, these are the dorsal, ventral, left- and right-lateral quadrants, and they generate respective portions of the larval and adult body plan. In some species the first and second cleavage divisions are equal, and the blastomeres of the four-celled embryo are identical in size. Experiments with equally cleaving molluscan embryos reveal that any one of the first four blastomeres can assume the fate of the dorsal quadrant, which in turn directs the development of the other quadrants. Quadrant identities, and the dorsoventral axis, are established relatively late through cell-cell interactions following the fifth cleavage division. In other spiralian embryos, the first two cleavages are unequal, so the dorsoventral axis is established precociously, at the four-cell stage, through the differential segregation of developmental determinants within the dorsal cell quadrant (1).

Nemertean embryos typically display equal cleavage; but the identity of the four cell quadrants differs from those described above. The first and second cleavage divisions normally correspond to the frontal plane and the plane of bilateral symmetry, generating left- and right-ventral and left- and right-dorsal quadrants. In some embryos the first cleavage plane corresponds to the frontal plane, and the second to the plane of bilateral symmetry. In other embryos the order is reversed. In either case, the end result is the same (2).

Are quadrant identities and the dorsoventral axis in nemerteans established late by virtue of cell-cell interaction, as in other equal-cleavers, or are they set up precociously as a consequence of the early cleavage divisions, perhaps relative to some underlying axial properties? We have examined this question by shifting the orientation of the spindle, thus altering the plane of the first cleavage. Fertilized eggs of *Cerebratulus lacteus* were compressed to about 170% of their normal diameter, from just after first polar body formation but before the formation of the first cleavage spindle, until first cleavage was completed (Fig. 1a). The cleavage spindle is forced to align parallel to the plane of compression. As cytokinesis always occurs perpendicular to the cleavage spindle (3), the first cleavage plane was altered in some embryos relative to the animal-vegetal axis. Compression was released after first cleavage and one cell was microinjected with Fluoro-Ruby (10,000 MW rhodamine-conjugated dextran, Molecular Probes, Eugene, OR). Because the boundary between labeled and unlabeled ectodermal domains corresponded to the first cleavage plan, the fluorescent label made it possible to analyze the relationship between the first cleavage plane and the dorsoventral axis in the resulting pilidium larva. Cell divisions occurred equally, and successive cleavages appeared to proceed normally. In the majority of treated embryos (64 cases) cleavage

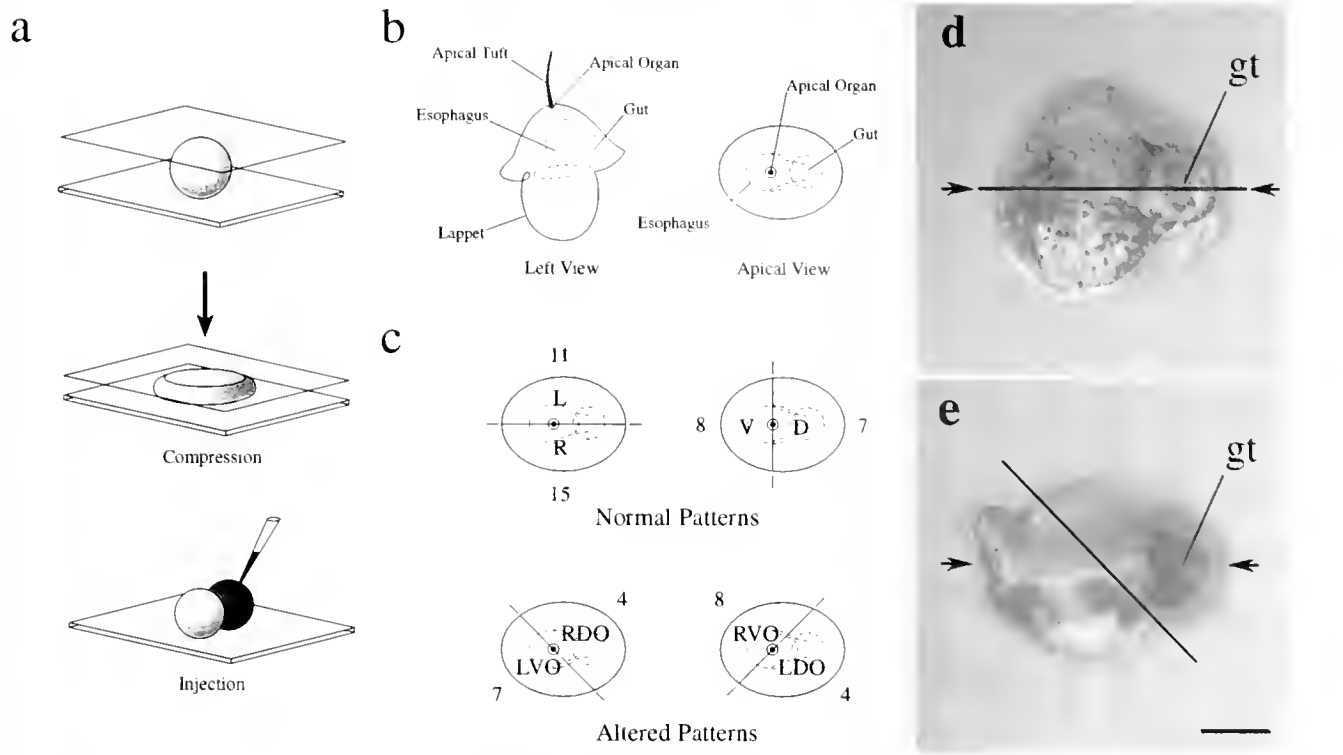

Figure 1. *Experimental alteration of cell lineages in the nemertean* Cerebratulus lacteus. *(a) Procedure employed to shift the plane of the first cleavage division. Fertilized eggs were compressed to orient the spindle parallel to the plane of compression. After first cleavage, the coverslip was removed and one blastomere was injected with a fluorescent lineage tracer at the two-cell stage. (b) Diagrams showing left lateral and apical views of the pilidium larva. The dorsal side is to the right, and the ventral side to the left. (c) Normal and altered labeling patterns observed in this study (apical views shown). The line dividing the larvae in half corresponds to the boundary between labeled and unlabeled ectodermal domains, and thus to the first cleavage plane. Numbers indicate the number of cases displaying each of the indicated labeling patterns. L, left; R, right; D, dorsal; V, ventral; LVO, left ventral oblique; RDO, right dorsal oblique; RVO, right ventral oblique; LDO, left dorsal oblique, labeling patterns. A wide range of oblique labeling patterns was actually observed, but they are lumped into four general categories here for the sake of simplicity. (d) Combined DIC and fluorescence micrographs showing one of the four normal labeling patterns (R, right), in which the first cleavage plane corresponds to the plane of bilateral symmetry. View is from the oral pole, opposite the apical organ. Line demarcates the labeled and unlabeled ectodermal domains. Arrows mark the plane of bilateral symmetry. Dorsal side is to the right. gt, gut. (e) An altered labeling pattern (RVO, right ventral oblique), in which the first cleavage plane passed obliquely relative to the plane of bilateral symmetry and the frontal plane. Scale bar equals 50 μm.*

and subsequent development to the pilidium larva (Fig. 1b) were normal. Forty-one of these cases displayed one of the four normal patterns (Fig. 1c, d), indicating that there was no dissociation between the early cleavage planes and the dorsoventral axis in these cases. On the other hand, 23 larvae displayed altered relationships in which the first cleavage plane was oriented obliquely to the larval dorsoventral axis (Fig. 1c, e).

The altered relationships observed in these experiments indicate that the plane of first cleavage does not play a causal role in establishing the dorsoventral axis in the nemertean *C. lacteus*. Thus, quadrant identity is established precociously relative to an underlying system of axial properties present in the fertilized egg before first cleavage. Normally, to generate the four typical nemertean cell quadrants, some mechanism must link the early cleavage divisions to this scaffold of axial information. It is remarkable that alternate cell lineages were produced without disturbing larval development, and in some cases quadrant relationships similar to those found in annelids and molluscs were generated. These results support the argument proposed by Martindale and Henry (4) that cleavage geometry may have been uncoupled from an underlying scaffold of axial information, leading to the generation of different cell lineages during the course of spiralian evolution.

The authors thank the generous community of the Marine Biological Laboratory. J.Q.H. was supported as an MBL Associates Fellow and a Lemann Fellow. M.Q.M. was supported by NSF and the Illinois chapter of the A.C.S.

Literature Cited

1. **van den Biggelaar, J. A. M., and P. Guerrier. 1983.** Pp 179–213 in *The Mollusca* N. H. Verdonk, J. A. M. van den Biggelaar, and A. S. Tompa, eds. Academic Press, New York.
2. **Henry, J. Q. and M. Q. Martindale. 1994.** *Dev. Genetics* **15**: 64–78.
3. **Rappaport, R. 1986.** *Int. Rev. Cytol.* **105**: 245–281.
4. **Martindale, M. Q., and J. Q. Henry. 1995.** *Development* 121:3175–3185.

Reference: *Biol. Bull.* **189:** 194–195. (October/November, 1995)

Axial Specification in a Basal Member of the Spiralian Clade: Lineage Relationships of the First Four Cells to the Larval Body Plan in the Polyclad Turbellarian *Hoploplana inquilina*

Jonathan Q. Henry, Mark Q. Martindale, and Barbara C. Boyer (Department of Biology, Union College, Schenectady, New York 12308)

The Spiralia comprises several invertebrate phyla including the molluscs, annelids, nemerteans, sipunculids, echiurans, and some turbellarian platyhelminths. These animals share many common features of embryonic development including a stereotypic pattern of cell divisions referred to as spiral cleavage. In most molluscs and annelids, first cleavage occurs oblique to the future plane of bilateral symmetry and generates two blastomeres, designated AB and CD. At second cleavage, these cells divide to produce the four primary embryonic cells, or quadrants, called A, B, C, and D, which give rise respectively to the left,

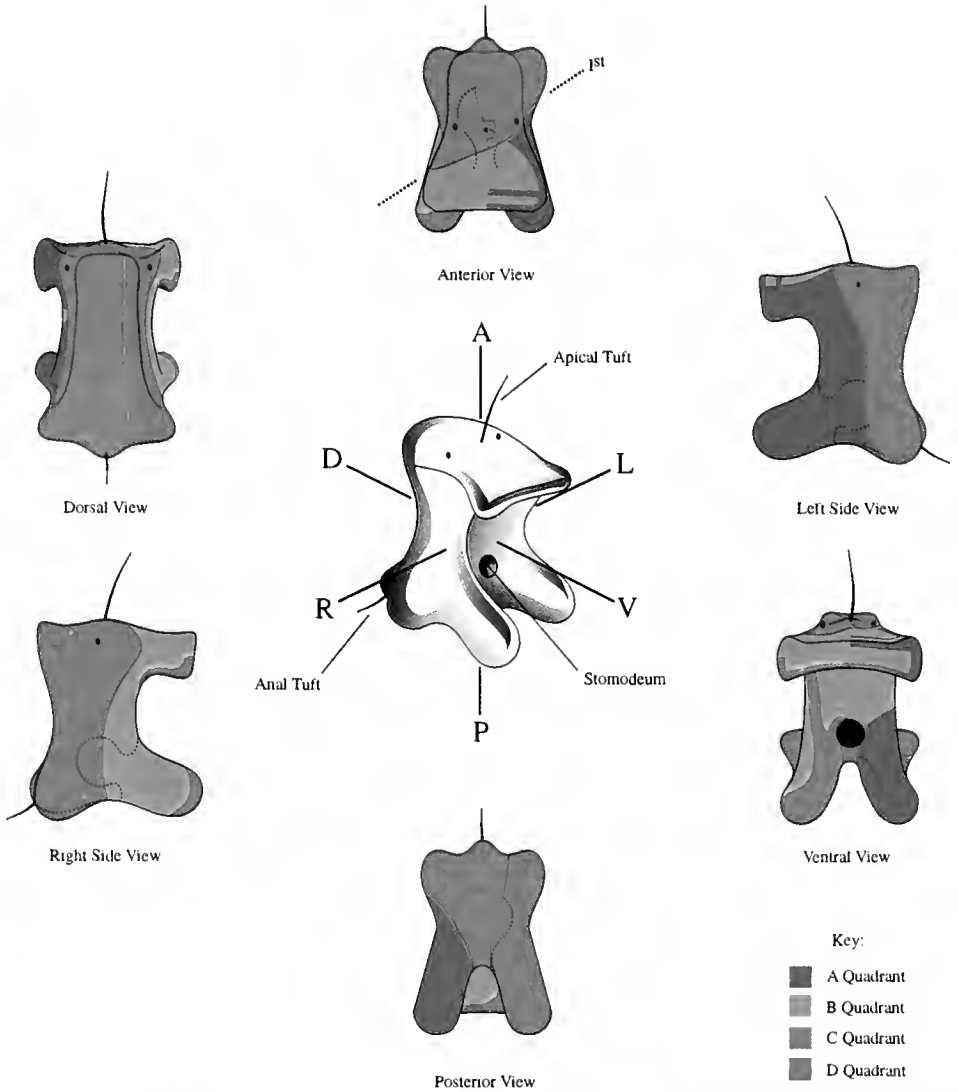

Figure 1. *Ectodermal territories of the A, B, C, and D cell quadrants in the Müller's larva of* Hoploplana inquilina. *The central illustration portrays the 5-day Müller's larva in an oblique, right-frontal 3-D perspective. Lines indicate the anterior-posterior (A-P), dorsal-ventral (D-V) and right-left (R-L) axes. The apical tuft, anal tuft, and stomodeum are also labeled. Flanking colored illustrations portray the six different surfaces of the larva as indicated. Each of the four ectodermal territories derived from the four cell quadrants is colored as shown in the key. The apical organ corresponds to the embryonic animal pole, and the stomodeum corresponds to the embryonic vegetal pole. The A and C quadrants contribute to the formation of the apical tuft, whereas all four quadrants contribute to the formation of the stomodeum. During development, the various ectodermal territories become somewhat distorted through the formation of the oral hood and the various larval lobes. The oblique orientation of the first cleavage plane relative to the larval dorsoventral axis is shown for the apical view. Thus, the locations of the four cell quadrants (A, B, C, and D) are similar to those found in polychaete annelids and molluscs. Anterior and posterior views are oriented with the dorsal surface upward and the ventral surface downward. Dorsal, ventral, right, and left views are oriented with the anterior surface upward and the posterior surface downward.*

ventral, right, and dorsal regions of the larval and adult body plan. Cell lineage studies have revealed such homology in the fates of the four embryonic quadrants in representatives of several of the spiralian phyla (1–3); but recent evidence in both molluscan and nemertean embryos indicates significant differences in the fates of the embryonic quadrants in certain members of the Spiralia (4, 5).

Polyclad turbellarians are thought to represent basal members of the spiralian clade. An early study indicated that their development is based on a quadrant system similar to that of annelids and molluscs (6), but more recent experimental analyses have suggested that assignment of cell fate may not be strictly correlated with specific quadrants (7, 8, 9). To resolve this controversy, we have examined the fates of the first four blastomeres—and hence the relationship of the first two cleavage planes—to the larval body of the polyclad *Hoploplana inquilina*. The first cell division generates two equally sized blastomeres, but the second division in both cells is unequal, producing a four-cell stage in which the two larger cells meet at the vegetal pole (vegetal cross-furrow). We labeled the outside surface of individual blastomeres at the two- and four-cell stages with a tiny drop of soybean oil containing 5.0 mg/ml DiI (Molecular Probes, Inc., Eugene, OR) delivered with a pressurized glass micropipet (Chris Q. Doe, pers. comm.). The embryos were raised at 22°C, and the labeling patterns were examined 5–6 days later.

Figure 1 is a summary of ectodermal labeling patterns from 38 cases labeled at the two-cell stage and 60 cases at the four-cell stage. That the first two cleavage planes are oblique to the plane of bilateral symmetry is clearly seen. The orientation of the first cleavage plane is indicated on the anterior view shown in Figure 1. Although a relatively complex pattern of morphogenesis takes place during the development of the Müller's larva, driven in part by the dorsolateral expansion of the dorsolateral ectodermal domains and the formation of the oral hood and various larval lobes, we have clearly identified A, B, C, and D quadrants similar in relationship to those of annelids and molluscs.

One of the vegetal cross-furrow blastomeres was labeled in 22 four-cell stage embryos; of these only one did not generate a ventral (B) or dorsal (D) quadrant. Similarly, of the 38 embryos in which a non-cross-furrow cell was marked, all but one produced a labeled left (A) or right (C) quadrant. These results indicate that the vegetal cross-furrow cells are reliable indicators of the dorsoventral axis, and the non-cross-furrow blastomeres of the left-right axis. This is similar to the situation found in annelids and molluscs (3).

These results confirm and extend the classical work of Surface on *Hoploplana* (6), though he did not map the fates of the four quadrants as far as the Müller's larva stage. The identification of the A, B, C, and D cell quadrants with a consistent relationship to the axes of bilateral symmetry in this basal member of the spiralian clade suggests that this association may represent the ancestral condition for this large group of protostome invertebrates.

J.Q.H. (J.J.H.) was supported as an MBL Associates' Fellow and a Lemann Fellow. M.Q.M. was supported by NSF and the Illinois Chapter of the American Cancer Society. B.C.B. was supported by the Union College Faculty Research Fund.

Literature Cited

1. **Wilson, E. B. 1898.** Pp. 21–42 in *Biological Lectures of the Marine Biological Laboratory*, Woods Hole, MA, Ginn and Co., Boston.
2. **Wilmer, P. 1990.** Pp. 199–222 in *Invertebrate Relationships, Patterns in Animal Evolution*. Cambridge University Press, Cambridge.
3. **Verdonk, N. H., and J. A. M. van den Biggelaar. 1983.** Pp. 91–122 in *The Mollusca* N. H. Verdonk, J. A. M. van den Biggelaar, and A. S. Tompa, eds. Academic Press, New York.
4. **Damen, P. 1994.** Cell lineage, and specification of developmental fate and dorsoventral organisation in the mollusc *Patella vulgata*. Thesis Universiteit Utrecht. CIP-DATA KONINKLIJKE BIBLIOTHEEK, DEN HAAG.
5. **Henry, J. Q., and M. Q. Martindale. 1994.** *Dev. Genetics* **15**: 64–78.
6. **Surface, F. M. 1907.** *Proc. Acad Nat. Sci. Phil.* **59**: 514–559.
7. **Boyer, B. C. 1986.** *Int. J. Invert. Repro. Dev.* **9**: 243–251.
8. **Boyer, B. C. 1987.** *Roux's Arch. Dev. Biol.* **196**: 158–164.
9. **Boyer, B. C. 1989.** *Biol. Bull.* **177**: 338–343.

Reference: *Biol. Bull.* 189: 196–197. (October/November, 1995)

Sex on the Brain but the Heart Is Not Really In It: Developmental Heart Defects Associated with Aquatic Pollution and Microinjection of Hexachlorobenzene into the Japanese Medaka Embryo

Merle Mizell (Center for Bioenvironmental Research, [1]Department of Cell and Molecular Biology, Tulane University, New Orleans, Louisiana, 70118), Eric Romig, William Hartley, and Arumthavarani Thiyagarajah

Hexachlorobenzene (HCB) was found in high concentration [280 mg/Kg (ppm)] in the sediment of the Mississippi River Basin (MRB) near Baton Rouge, Louisiana, in an area known as Devil's Swamp. Such pollution has created the need for an effective biomarker or sentinel species for ecological and health risk assessment (1). Embryos of the Japanese medaka (*Oryzias latipes*) are transparent, and this feature together with a new method of microinjection provides an efficient and sensitive means of delivering chemicals and observing the systemic and genotoxic effects during embryonic differentiation. Recently fertilized medaka embryos were collected from our breeding colony at the Tulane University Center for Bioenvironmental Research. The embryos were cleaned, staged, and then placed in a plastic injection slide specially machined at the Marine Biological Laboratory for this project. HCB was dissolved in vegetable oil and made up in several concentrations. The range of injected concentrations was 100 mg/l (ppm) to 0.1 μg/l (ppm) of HCB. Vegetable oil lacking HCB was injected as a negative control. The volume of the injected droplet was always 40 nl. Embryonic growth and differentiation was monitored daily in these transparent embryos, and deviations from normal development were videorecorded. The fish were grown out for either 6 months or one year, and then sacrificed for histopathological examination.

Although our histopathology study is still in progress, we have encountered a curious finding. One of the embryos injected with 0.1 μg/l HCB possessed ectopic gonads in its cranial cavity. This female's ectopic gonad contained well-developed testicular tissue; although not arranged in tubules, it consisted of primordial germ cells, including well-differentiated spermatocytes and spermatids. None of the other animals examined in this experimental series, exhibited such structures.

However careful routine monitoring of our breeding colony revealed that 2 out of 86 fish sacrificed due to disease or injury contained similar ectopic hermaphroditic gonads in the cranial cavity (2). Therefore, the ectopic cranial gonads observed in the current study cannot be attributed to the HCB microinjection. Our breeding colony was maintained in dechlorinated New Orleans municipal water that was further treated by five separate filtering units and met the standards of the American Public Health Association for culture and toxicity testing of aquatic organisms. All of our animals are now housed, bred, and maintained in recirculating spring water.

Ectopia is an anomaly due to errors of morphogenesis that position an organ or tissue outside its normal anatomical locus. Ectopic tissues have been reported in all classes of vertebrates. Indeed, ectopic thyroid tissue often undergoes proliferation in response to organochlorines (3). Nevertheless, prior to these three cases, discussed above, ectopic gonads in the cranial cavity had never been reported in vertebrates. Moreover, all three cases of ectopic consisted of *hermaphrodidic* gonads. The events (or lack of events) leading to these anomalous animals undoubtedly are of fundamental importance and environmental pollution may be involved in its occurrence. We are currently attempting to uncover the cause of the ectopic gonads in our microinjection studies. We are also monitoring the Devil's Swamp resident fish for similar gonadal anomalies.

HCB was microinjected into the perivitelline space of embryos either 24 h or 128 h post fertilization. Embryos exposed to HCB at 24 h after fertilization exhibited profound circulatory defects. Fifty embryos were exposed to each concentration of HCB. At 0.1 ppm HCB there was a 2% incidence of circulatory defects. And at 1.0 ppm there was a 6% incidence; at 10 ppm the incidence increased to 8%. At 100 ppm the incidence of circulatory defects plateaued at 12.5%. Control embryos that were injected with oil or were uninjected lacked circulatory defects. The affected embryos invariably had reduced, or even were devoid of, extra- or intraembryonic circulation. The heart, in a typical case, was little more than a thin tube stretching between the yolk sac and the embryo, so this defect was easily visualized upon examination (4). Embryos with severe circulatory defects also exhibited pericardial edema which displaced the yolk sac to one side (Fig. 1). Heart rate was markedly decreased. Histopathological examination revealed that the cardiac musculature was often reduced to sparce, abnormal trabeculae and other gross heart malformations which were frequently accompanied by dilated kidney tubules and cystic kidneys.

The HCB concentration in the Devil's Swamp sediment was three times greater than the highest dose of HCB injected into

Figure 1. *Typical hexachlorobenzene (HCB) cardiovascular malformation in a medaka embryo which was microinjected 24 h after fertilization. The single dose of HCB administered was 0.1 μg/l (ppm). The embryo was unable to hatch and thus was manually removed from its chorion and photographed 216 h after injection. The heart consists of a thin tube (arrow) surrounded by an enlarged, edematous pericardial cavity.*

the embryos. HCB has been shown to cause circulatory defects common to several other aromatic compounds: toluene, carbaryl, parathion, tolbutamide, dinitrophenol, and 2,4,5-trichlorophenoxyacetic acid (4, 5, 6, 7). The abnormalities observed in the developing medaka heart are similar in several respects to those seen in zebrafish embryos treated with retinoic acid (8). The anterior-posterior axis of the heart is truncated, especially affecting the anterior region, as in zebrafish (and *Xenopus*) heart development (8). These effects seem both dose-dependent as well as stage-dependent. Because the circulatory defects uncovered in our studies are lethal, resident aquatic species of Devil's Swamp that are exposed to HCB during embryonic development may experience appreciable early mortality. These aquatic populations are currently being followed.

Supported by grants from the Department of Energy and the Department of Defense.

Literature Cited

1. **Abel, P. D. 1989.** *Reviews on Environmental Health* **8:** 119–155.
2. **Hartley, W., A. Thiyagarajah, and M. Mizell. 1995.** *J. Aquatic Animal Health* **7:** 172–177.
3. **Hoover, K. L. 1984.** *Natl. Cancer Inst. Monograph* **65:** 275–289.
4. **Weis, P., and J. Weis. 1974.** *Teratology* **10:** 263–268.
5. **Schreiweis, D. O., and G. J. Murray. 1976.** **Teratology 14:** 287–268.
6. **Smithberg, M. 1962.** *Am. J. Anat.* **111:** 205–213.
7. **Wilde, C. E. Jr., and R. B. Crawford. 1966.** *Exp. Cell Res.* **44:** 471–488.
8. **Stanier, D. Y., and M. C. Fishman. 1992.** *Dev. Biol.* **153:** 91–101.

Reference: *Biol. Bull.* **189:** 197–198. (October/November, 1995)

Pattern of Potassium Ion and Proton Currents in the Ovariole of the Cockroach, *Periplaneta americana*, Indicates Future Embryonic Polarity

Joseph G. Kunkel and Ellen Faszewski (National Vibrating Probe Facility, Marine Biological Laboratory)

Ionic currents are associated with developing patterns in various organisms (1) and are ascribed to the movement of various ions. The function of these currents in each system is still unclear. We previously reported a pattern of ionic current about the vitellogenic follicles of cockroaches and termites (2). This group of insects is particularly interesting because of the simplicity of their ovarian follicles: a large oocyte surrounded by a single cell layered follicle epithelium. The observed pattern of currents, which we investigated with the older wire probe technology, indicates the location of the future embryonic germ band. We now report the identity of the ions involved, which we investigated using the recently developed non-invasive ion selective electrode technology at the National Vibrating Probe Facility, MBL, Woods Hole (3). Microelectrodes with tips of 2 μm were filled with 15 μm columns of liquid ion exchanger (LIX) cocktails. Potassium-sensitive LIX (Fluka Potassium Ionophore I-cocktail A) and proton-sensitive LIX (Fluka Hydrogen Ionophore I-cocktail A) were used. The microelectrodes, oscillated 10 μm in the X-, Y-, and Z-directions to measure μV gradients in those dimensions, were propelled by stepper motors controlled by computer software, 3DVIS, designed to measure 3-D patterns. Total flux was calculated by vector addition of the measured X-, Y- and Z-μV difference components. The efficiency of the K^+ electrode to measure K^+ flux was 80%: that of the proton electrode is also assumed to be high, but the effects of buffering in physiological salines are unclear. We therefore report our proton flux in terms of μV drop over a measured distance which can be interpreted as pH difference. Ovaries of the cockroach were dissected into cockroach Ringer, and the individual ovarioles were separated from connective tissue. Single ovarioles were transferred to a measurement chamber bathed in an appropriate saline. For measuring potassium, the *Periplaneta* Ringer of Smith was used (157 m*M* Na^+, 3 m*M* K^+, 2 m*M* Ca^{++}, 2 m*M* Mg^{++}, 165 m*M* Cl and 8.6 m*M* Hepes, pH 7.2). For protons, the same Ringer, but with a weaker buffer (Hepes, 0.96 m*M*) was used to prevent the dampening of proton fluxes.

We measured substantial outward K^+ and proton gradients at the anterior end of each vitellogenic follicle within an ovariole, Figure 1A. The pattern of both the proton and K^+ gradients were largely identical, outward about an anterior polar cap, with the exception that a generalized lower level outward proton current was observed about the entire follicle. This low level outward current may reflect a generalized respiratory secretion of CO_2 from the tissue in general. No ion gradients were detected around previtellogenic follicles or around follicles close to, or after, chorion formation (Fig. 1B). The major gradients of ions exit the follicle through a tight epithelium of follicle cells that form a cap over the anterior pole of the follicle. The follicle anterior pole can be thought of as the vegetal pole of the *Periplaneta* oocyte; this is because the embryonic germ band will develop at the posterior pole. The location of the germ band can be considered the animal pole. Aside from the vegetal polar cap of 'tight' epithelium, the remainder of the follicle cell epithelium around the vitellogenic follicle is 'patent' (4), allowing the bathing medium to reach the oocyte surface. The extent to which the observed currents are electrically coupled between the follicle cells and oocyte is unknown; but TEM sections show that all follicle cells are morphologically coupled to the oocyte via gap junctions. We suggest that the tight cap of follicle cells at the anterior pole act as a polarized epithelium, responsible for the pumping of ions, which we see (Fig. 1). In many insects the V-type ATPase is responsible for pumping of protons. This pump is sensitive to the inhibitor Bafilomycin A1 from *Streptomyces griseus*. In several oocytes, which we treated with 1 μ*M* Bafilomycin, the peak proton flux seen at the anterior cap of the follicle was inhibited by up to 60% over a period of 15 min. This finding

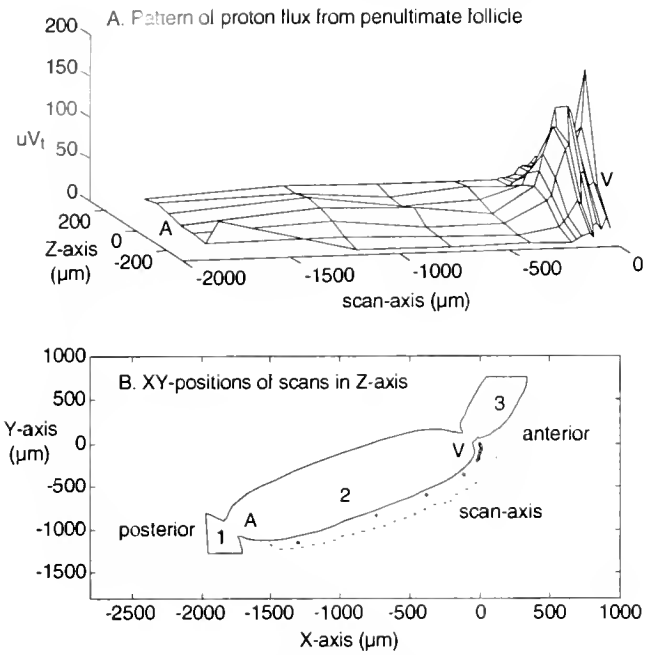

Figure 1. *Pattern of proton movement about a vitellogenic ovarian follicle of* Periplaneta americana. *The animal (A) and vegetal (V) pole positions of the penultimate follicle are indicated in both 1A and 1B. A. Total-μV drop (μV_t) over the oscillation distance (10 μm) in three-dimensions. The scan-axis represents the linear additive distance from the (0,0) XY-location at the anterior end of the penultimate follicle to other locations along the scan route as depicted in Figure 1B (58 mV represents 1 pH unit of proton concentration difference with a measured background pH of 7.1). B. Outline of a section of ovariole including the anterior tip of the terminal follicle (labeled 1, chorionated and scheduled to ovulate in 1 day), the entire penultimate follicle (labeled 2, vitellogenic and to be ovulated in 4 days), and a portion of the pen-penultimate follicle (labeled 3, as yet non-vitellogenic and to be ovulated in 7 days). The 14 XY-positions of 7 3-D scans in the Z-axis are indicated. These positions were transformed into scan axis locations corresponding to the 14 × 7 mesh of points plotted versus measured μV-difference in Figure 1A. The anterior and posterior polarity of the ovariole is labeled.*

suggests that a portion of the observed gradients are generated by the V-type proton pump and the established proton gradient might be further utilized by a K^+/H^+ exchange pump to produce the outward K^+ flux at the anterior pole. If a gradient of ions is being created through or around the enclosed oocyte by electrical coupling with the follicle cell layer, a force to influence the polarity of the future embryo may be at play.

The hospitality and advice of Peter J. S. Smith at the National Vibrating Probe Facility was a deciding factor in our progress on this project. We also thank Jeffery R. Demerest for sharing his experience with proton LIXs. This research was supported by grants to the National Vibrating Probe Facility and from the Biotechnology Program of the University of Massachusetts at Amherst.

Literature Cited

1. **Jaffe, L. F. 1991.** *Phil. Trans. R. Soc. London* **295:** 553–556.
2. **Kunkel, J. G. 1991.** *In Vivo* **5:** 443–456.
3. **Smith, P. J. S., R. H. Sanger, and L. F. Jaffe. 1994.** *Meth. Cell Biol.* **40:** 115–134.
4. **Zhang, Y. and J. G. Kunkel. 1992.** *Tissue & Cell* **24:** 905–917.

Reference: *Biol. Bull.* **189:** 198–199. (October/November, 1995)

Chemotaxis, Aggregation Behavior, and Foot Formation in *Dictyostelium discoideum* Amoeba Controlled by Microbeam Uncaging of Cyclic-AMP

Yoshio Fukui and Shinya Inoué (Marine Biological Laboratory)

At a certain stage of development, amoebae of the cellular slime mold *Dictyostelium discoideum* signal to each other by secreting c-AMP [cyclic-3′,5′ adenosine monophosphate (1, 2, 3)]—and then aggregate. We analyzed the responses of aggregation-competent amoebae to brief applied pulses of c-AMP under high-resolution video DIC (differential interference or Nomarski contrast) microscopy.

Miniature sources of c-AMP pulses were generated by illuminating caged c-AMP (4) with a 366-nm-wavelength UV (ultraviolet) microbeam delivered as 3-ms flashes repeated every 0.65 s; we had added the caged c-AMP to the buffer and agar layer overlying the amoebae (5). A Zeiss Ultrafluar (UV- and visible light-transmitting, 100×/1.25 NA, glycerol immersion objective) lens equipped with a DIC prism replaced a conventional condenser to focus a highly reduced image of a first-surface micromirror, placed in front of the field diaphragm, superimposed with the DIC image of the specimen. The UV-reflecting micromirror was located at the focus of the UV source, an auxiliary 100-Watt Hg-arc lamp with quartz collector, 366-nm bandpass filter, and electrically activated shutter. The $2.2 \times 3.0\ \mu m^2$/UV image can be seen as a bright rectangle at the tip of the dark shadow of the mirror support in Figure 1A and B, slightly off center from the visible (546 nm) light image of the specimen in DIC. Moving the micromirror or specimen carrier placed the source of c-AMP in different locations relative to one or more amoebae.

Migrating aggregation-stage amoebae responded to the c-AMP pulses by turning towards the source (Fig. 1A) and migrating it. The first amoeba to reach the source engulfed it, and the others spiraled and aggregated around this first amoeba, which remained at the source (Fig. 1B). When the artificial source of c-AMP was removed by shutting off the UV flashes, all the amoebae dispersed

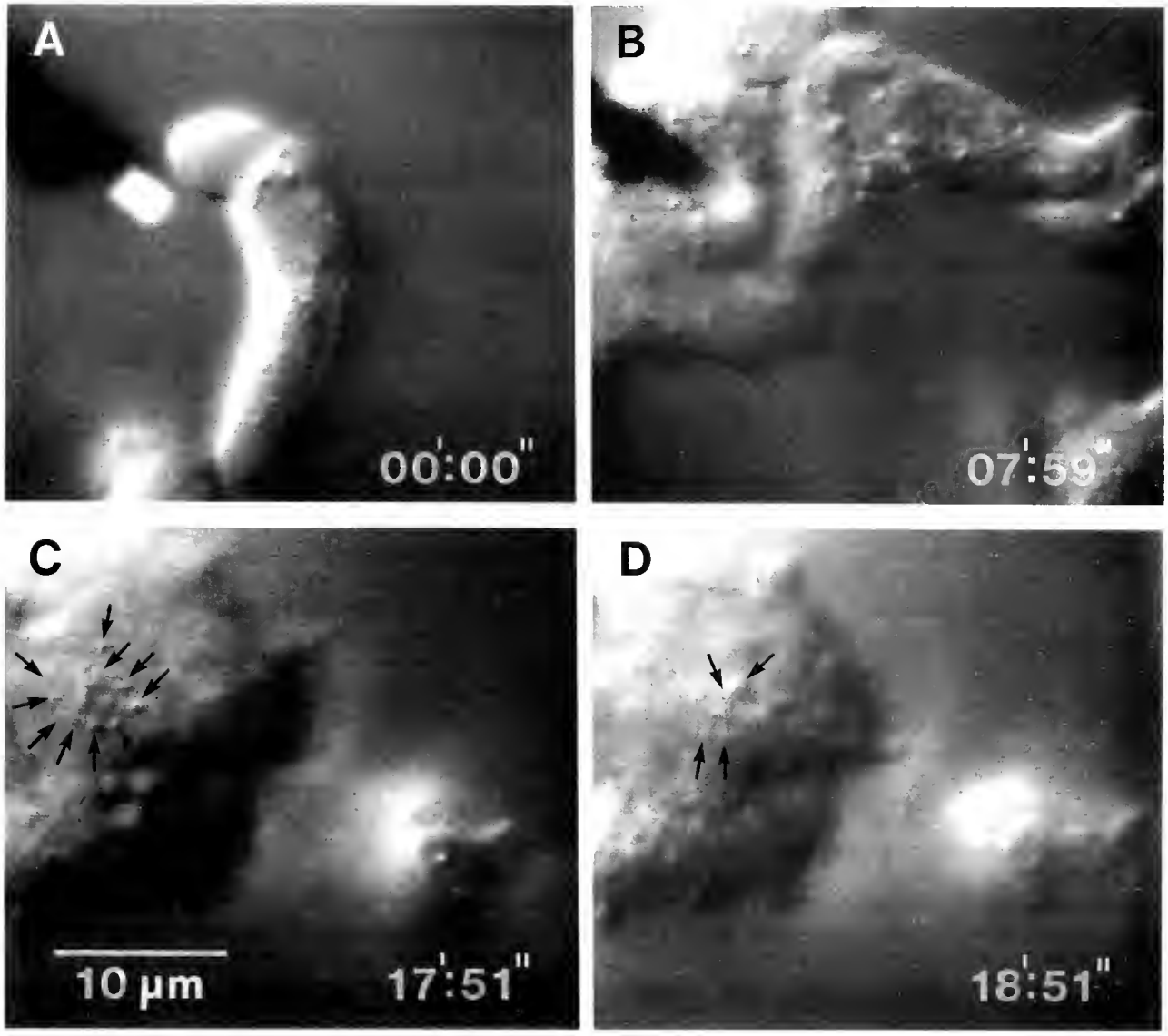

Figure 1. *Response of aggregation-competent slime mold amoebae to 366-nm microbeam uncaging of caged c-AMP. The microbeam was positioned near the side of this amoeba, and the UV flashes were started 1 minute 27 seconds before the frame A. See text. Time in minutes.seconds after A.*

and headed towards their natural source, an aggregate formed by many amoebae located outside the induced territory.

Early during aggregation, most amoebae remained in loose contact with each other and slowly spiralled around the center of the aggregate. Whether in a naturally formed aggregate made up of many scores of cells or in an artificially induced aggregate made up of only a few cells, the amoeba located in the center became stationary relative to the substratum. Through-focus observations indicated that such an amoeba anchored itself to the soft substrate by protruding knobby "feet" into the agar surface. In the artificially induced aggregate, the central amoeba generated and maintained its feet (small arrows in Fig. 1C; the UV micromirror is retracted and focus is now on the agar surface) so long as the c-AMP pulses (UV flashes) were continued. Once the UV flashes were turned off, the feet were gradually retracted (Fig. 1D). If the UV flashes were restarted within a minute or so, the feet reformed, and the departing outer amoebae rejoined the aggregate. The process was completely reversible and could be repeated many times. Thus we have established a tool for investigating localized and reversible c-AMP-mediated modulation of chemotaxis and cell response.

Supported by NIH grants R01 GM 39548 to YF and R37 GM 31617 to SI.

Literature Cited

1. **Bonner, J. T. 1971.** *Ann. Rev. Microbiol.* **25:** 75–92.
2. **Gerisch, G. 1987.** *Annu. Rev. Biochem.* **56:** 853–879.
3. **Devreotes, P. 1989.** *Science* **245:** 1054–1058.
4. **Nerbonne, J. M., S. Richard, J. Nargeot and H. A. Lester. 1984.** *Nature* **310:** 74–76.
5. **Fukui, Y. and S. Inoué. 1991.** *Cell Motil. Cytoskel.* **18:** 41–54.

Reference: *Biol. Bull.* **189**: 200. (October/November, 1995)

Identification of Calcium Flux in Single Preimplantation Mouse Embryos with the Calcium-Sensitive Vibrating Probe

David Keefe (Yale University School of Medicine, Department of Obstetrics and Gynecology), John Pepperell, Paulo Rinaudo, Joseph Kunkel, and Peter Smith

Although aging affects nearly every aspect of female reproduction, oocytes are believed to be major targets. Oocytes are long-lived, post-mitotic cells and donation of these cells by young females to older ones clearly ameliorates the effects of aging on reproductive success (1). Elucidation of the mechanisms underlying reproductive aging is of basic importance because the senescence of oocytes provides a model of aging of other long-lived, post-mitotic cells. Moreover, many women now delay marriage and childbearing until their late thirties, when the effects of aging on fertility can become clinically significant (2). A non-invasive technique that could be used to assay the developmental potential of an embryo before implantation would both facilitate the diagnosis of reproductive senescence and help middle-aged women decide whether to depend on their own oocytes and pursue costly reproductive therapies, or to pursue alternatives such as adoption or oocyte donation.

Disruption of intracellular calcium [Ca]$_i$ regulation is an important mechanism underlying senescence in many long-lived cells (3). Normally, the plasma membrane has at least two systems that contribute to maintaining low [Ca]$_i$: a Na/Ca exchanger powered by the Na-K ATPase, and a Ca-ATPase (4). Both of these systems have been implicated in cell injury and senescence (3, 4). Inhibition of the Na-K ATPase by ouabain alters *in vitro* development of mouse preimplantation embryos (7).

In this study we employed the calcium-selective vibrating probe to test directly the hypothesis that mouse preimplantation embryos exhibit steady-state calcium currents. Moreover, to develop the vibrating probe as a non-invasive assay of the developmental potential of such embryos, we have begun to map steady state calcium flux in mouse embryos with differing developmental potential.

After hybrid matings (B6C3F1 × B6D2F1), mouse embryos were removed surgically at the two cell stage and either studied at this stage or cultured to the four- or eight-cell stages in M2 medium supplemented with 0.4% BSA at 37°C in 5% CO_2. The two-cell stage embryos were washed at least twice in a modified M2 medium containing only 50 μM calcium and then transferred in the same medium to petri dishes coated with high-molecular weight polylysine to which the embryos adhered. Embryos were then examined for a calcium flux at room temperature ($\approx$22°C). Measurement of the voltages associated with steady-state transmembrane calcium flux were done as previously described (8). The calcium-sensitive electrodes, after calibration to determine their Nernstian characteristics, were positioned within about 1 μm of an embryo's zona pellucida. The distribution of the efflux was mapped by moving the probe to at least four quadrants of the embryo's circumference. Images of the embryos were recorded with a video printer so that morphology could be correlated with steady-state calcium flux. After experimentation embryos were routinely returned to normal M2 medium and kept at 37°C in 5% CO_2, where cell division was monitored.

Morphology combined with growth allowed us to divide the two cell stage embryos into two classes:

1. Morphologically normal or capable of further cleavage.
2. Morphologically fragmented or incapable of further cleavage.

In the case of the first class of embryos, there was a strong calcium efflux signal measured in all cases. In 10 preparations this signal had an amplitude of $-21.22\ \mu V \pm 5.7$ (mean $\pm$ standard deviation). Initial observations from the four quadrants did not exhibit any differences in the microvolts recorded. In class 2 embryos there was no measurable calcium efflux signal. Of 5 embryos examined, the signal at the plasma membrane was $-1.75\ \mu V \pm 5.28$. Background was $2.07\ \mu V \pm 2.24$.

We conclude that mouse preimplantation embryos, which retain their developmental potential (Class 1), exhibit a steady state transmembrane calcium efflux as measured by the non-invasive, vibrating calcium selective electrode. The efflux mapped in a symmetrical pattern about the embryo, with no polarity observed. Embryos with impaired developmental potential, as measured either by a fragmented morphology or subsequent failure to divide (Class 2), failed to exhibit a steady state calcium efflux equivalent to that observed in Class 1 embryos. The absence of an equivalent efflux in those embryos, which subsequently failed to grow further, suggests that the steady state calcium efflux may be a viable assay of the health of the embryo.

Supported by NIH K08HD01099, the American Society for Reproductive Medicine (D.K.) and NIH National Center for Research Resources, P41RR01395 (P.J.S.S.).

Literature Cited

1. **vom Saal, F. S., C. E. Finch, and J. S. Nelson. 1994.** Pp 1213–1314 in *The Physiology of Reproduction,* E. Knobil, J. Neil, eds. Raven Press New York.
2. **Keefe, D., T. Niven-Fairchild, S. Powell, and S. Buradagunta. 1995.** *Fertil. Steril* **64**: 577–583.
3. **Rasmussen, H. 1986.** *New Engl. J. Med* **314**: 1094–1164.
4. **Eckert, A., H. Hartmann, H. Forstl, and W. E. Muller. 1994.** *Life Sci.* **25**: 2019–2029.
5. **Robinson, D. H., and D. J. Benos. 1991.** *Current Topics in Membranes* **39**: 121–150.
6. **Overstrom, E. W., D. J. Benos, and J. D. Biggers. 1989.** *J. Reprod. Fert* **85**: 283–295.
7. **Dumoulin, J. C. M., A. H. J. Michiels, M. Bras, M. H. Pieter, J. P. Geraedts, and J. L. H. Evers. 1993.** *Human Reprod.* **8**: 1469–1476.
8. **Smith, P. J. S., R. H. Sanger, L. F. Jaffe. 1994.** Pp. 115–134 in *Methods in Cell Biology* **40**: R. Nuccitelli, ed. Academic Press, San Diego.

Reference: *Biol. Bull.* **189:** 201. (October/November, 1995)

Inhibitors of Protein Phosphatases (Okadaic Acid and Tautomycin) Block Sea Urchin Development

Walter Troll (New York University Medical Center), Naoko Sueoka, Eisaboro Sueoka, Jeffrey D. Laskin, and Diane E. Heck

Protein phosphorylation, regulated by protein kinases and phosphatases, is critical for cell growth, regulation, and development (1–3). Phosphatase inhibitors, which prolong the phosphorylated state of proteins, can often perturb cell development. Our laboratory has been interested in utilizing two of these compounds, okadaic acid, isolated from the marine sponge *Halichondria okadai*, and tautomycin, isolated from *Streptomyces spirover ticillatus*, to examine the role of phosphatases in sea urchin development. Previous work demonstrated that these compounds are effective inhibitors of serine and threonine phosphatases, in particular, phosphatases 1 (PP-1) and 2A (PP-2A) (4). Okadaic acid is more selective, preferentially inhibiting PP-2A, whereas tautomycin inhibits PP-1 and 2A with equal effectiveness (4). Recent studies indicate that PP-1 may be important in the initial responses of sea urchin eggs to fertilization (5). In the present studies we sought to determine whether okadaic acid and tautomycin could differentially modify fertilization and early development in the sea urchin *Arbacia punctulata*.

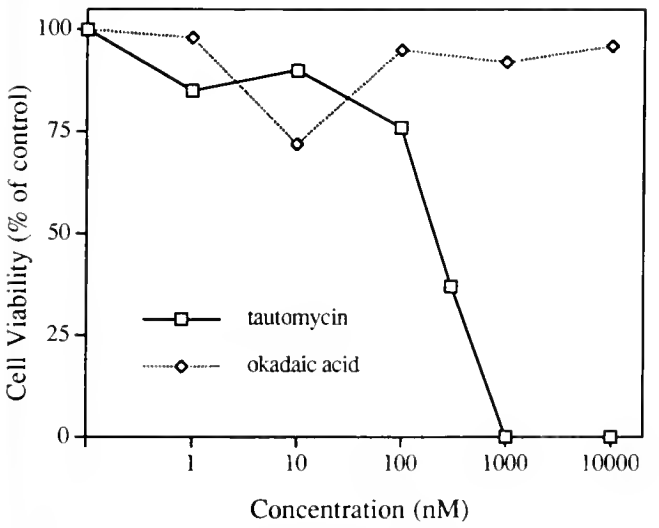

Figure 1. *Effects of phosphatase inhibitors on the viability of sea urchin embryos. Eggs obtained from* Arbacia punctulata *were fertilized* in vitro *in the presence of increasing concentrations of okadaic acid (broken line) or tautomycin (solid line). The percentage of viable embryos was calculated from the number of embryos that were freely rotating 24 h after fertilization.*

In initial experiments, sea urchin sperm and eggs were incubated with increasing concentrations of okadaic acid and tautomycin (1–1000 n*M*). We found that these compounds had no effect on sperm activation or on early events of fertilization (not shown). Thus, in all cases, >95% of the eggs raised fertilization membranes and formed embryos. We also found that blastula rotation, representing a later stage of differentiation, was selectively inhibited by tautomycin but not okadaic acid. Tautomycin was a potent inhibitor of the transition into the rotating blastula stage and was dose dependent at concentrations of 100–1000 n*M* (Fig. 1). Embryos treated with okadaic acid, however, did not exhibit this effect (Fig. 1). No embryos treated with tautomycin (100 n*M*–10 μM) developed into plutei (data not shown). Only very high concentrations of okadaic acid (1–10 μM) inhibited the hatching of plutei, consistent with the small effect of this compound on the initial development of motility.

In conclusion, tautomycin, but not okadaic acid, is an effective inhibitor of sea urchin development, acting on the maturation into rotating blastula. We speculate that the preferential inhibition of PP-1 by tautomycin may reflect differential roles of PP-1 and PP-2A in this process.

Literature Cited

1. **Racker, E. 1992.** *Curr. Top. Cell Regul.* **33:** 127–143.
2. **Kreimer, D. I., and Y. S. Khotimchenko. 1995.** *Comp. Biochem. Physiol. A Comp. Physiol.* **110:** 95–105.
3. **Ribot, H. D., E. A. Eisenmann, and W. H. Kinsey. 1984.** *J. Biol. Chem.* **259:** 5333–5338.
4. **Suganuma, M., H. Fujiki, S. Okabe, S. Nishiwaki, D. Brautigan, T. S. Ingebritsen, and M. R. Rosner. 1992.** *Toxicon* **30:** 873–878.
5. **Tosuji, H., I. Mabuchi, N. Fusetani, and T. Nakazawa. 1992.** *Proc. Natl. Acad. Sci. USA* **89:** 10613–10617.

Reference: *Biol. Bull.* **189:** 201–202. (October/November, 1995)

Reversible Regression of Cytokinesis Induced by Ca^{2+} Ionophore

Keisuke Suzuki, Fabrice Roegiers, Phong Tran, and Shinya Inoué (Marine Biological Laboratory)

Transient changes in intracellular free Ca^{2+} concentration are spatially and temporally coupled to specific cell cycle events such as mitosis and cytokinesis (*e.g.*, 1, 2). In the sea urchin embryo, an endogenous rise in Ca^{2+} precedes cytokinesis (3); and in the medaka embryo, this transient Ca^{2+} increase is localized to the cleavage furrow (4). Injection of Ca^{2+} chelators into the sand dollar embryo prior to cytokinesis arrests development and inhibits furrow formation (5). We have examined

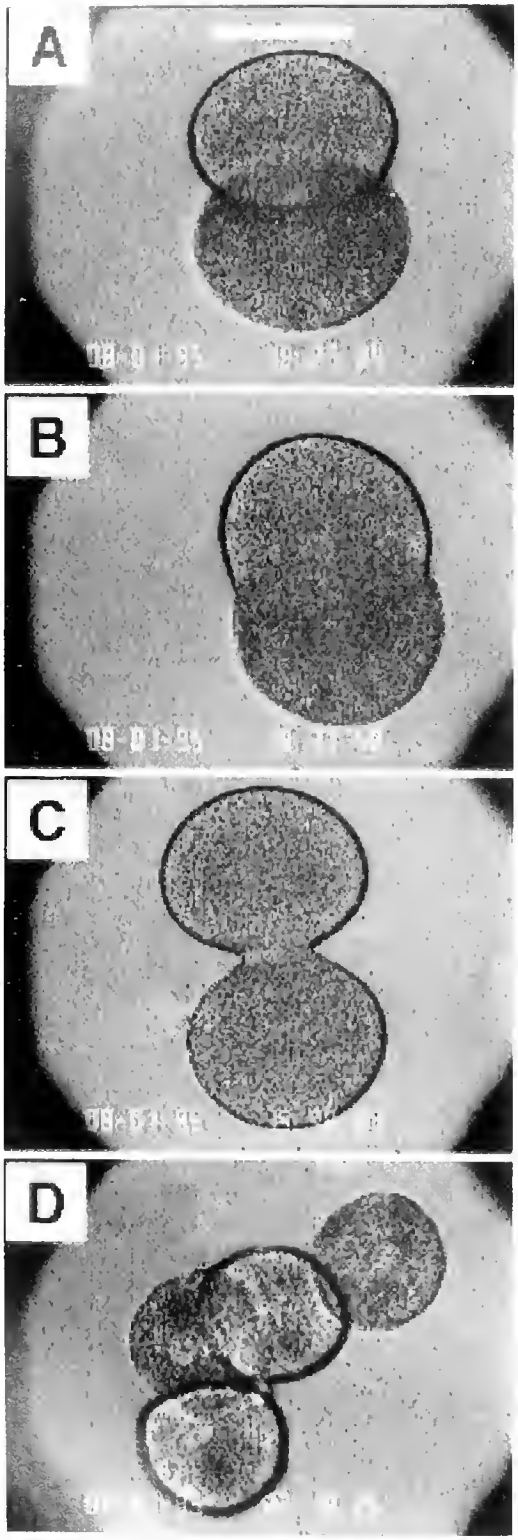

Figure 1. Lytechinus variegatus *embryo at early stages of development imaged with polarized light microscopy. (A) Embryo at first cell division cycle, with cleavage furrow at the time of A23187 perfusion. (B) Cleavage furrow regression induced by A23187. (C) Cytokinesis resumed at the same site when the A23187 was washed out with ASW. (D) The same embryo continued through cell division and development at the next cycle after a single A23187 treatment and ASW washing. Bar = 50 μm.*

further the roles that Ca^{2+} plays in cytokinesis, specifically downstream of cleavage furrow formation; our approach was to induce a global Ca^{2+} increase within the sea urchin embryo.

Lytechinus variegatus eggs and sperm were collected by electrically stimulating the sea urchins. The eggs were fertilized and the embryos developed in artificial seawater (ASW) containing about 10 m*M* Ca^{2+}. The fertilization envelope was removed from the fertilized eggs by washing with a digestion mix containing 1 m*M* DTT and 15 μg/ml pronase at pH 8.9. The eggs were then place in a wedge-profiled perfusion chamber and observed with polarized light microscopy.

At 18°C, the fertilized sea urchin eggs completed the first cell division in ~2 h, with the cleavage furrow appearing at ~1:45 h. After the first few minutes of furrow formation, we perfused the eggs with ASW containing 5 μg/ml A23187, a Ca^{2+} ionophore and an effective transporter that presumably causes a global influx of extracellular Ca^{2+} into the dividing egg.

Figure 1A shows a sea urchin egg with cleavage furrow just before A23187 perfusion. Furrow progression in the egg immediately stopped and the furrow regressed outwardly (Fig. 1B) until the egg returned to its original spherical shape. This furrow regression was reversible, and cytokinesis resumed *at the same site* when the A23187 was washed out with ASW within 10–20 min of the initial A23187 perfusion (Fig. 1C). The cycle of cleavage furrow regression in A23187 followed by the resumption of cytokinesis after washing could be repeated two to three times with the same cell. After two cycles of A23187 application and ASW washing, the embryo continued to divide and develop. Cells exposed to 5 μg/ml of A23187 for more than 15–20 min did not survive the treatment.

To our knowledge, this is the first example of a reversible regression of cytokinesis induced by Ca^{2+} ionophore A23187. A previous study by Arnold (6) showed that A23187 enhances furrowing in the squid embryo, but the concentration of ionophore used in those experiments was not stated. In our study, the reversible regression of cytokinesis was dependent on temperature, extracellular Ca^{2+} concentration, ionophore concentration, stage of the cell cycle, and ionophore exposure time. We have not yet determined the exact mechanism underlying the reversible regression of cytokinesis induced by A23187. However, we propose that A23187 causes a global increase in free Ca^{2+} that may activate actin severing proteins or deactivate actin cross-linking proteins; or alternatively, Ca^{2+} modulates binding of myosin to actin filaments directly or via a Ca^{2+} sensitive kinase such as myosin light chain kinase or protein kinase C.

We gratefully acknowledge the support of members of the MBL Architectural Dynamics in the Living Cell Program; support from Olympus Corporation to K.S.; support from CNRS/NSF to C. Sardet for F.R.; and support from MBL Eric F. Fries Fellowship to P.T. and NIH grant GM-31617 to S.I.

Literature Cited

1. **Silver, R. B. 1990.** *Ann New York Acad. Sci* **582:** 207–221.
2. **Hepler, P. K. 1992.** *Int. Rev. Cyto.* **138:** 239–268.
3. **Ciapa, B., D. Pesando, M. Wilding, and M. Whitaker. 1994.** *Nature* **368:** 875–878.
4. **Fluck, R. A., A. L. Miller, and L. F. Jaffe. 1991.** *J. Cell Biol.* **115:** 1259–1265.
5. **Silver, R. B. 1989.** *Dev. Biol.* **131:** 11–26.
6. **Arnold, J. M. 1975.** *Cytobiologie* **11:** 1–9.

Reference: *Biol. Bull.* **189**: 203–204. (October/November, 1995)

Leukotriene B_4 Induces Release of Calcium From Endomembrane Stores *In Vivo* in Eggs and Second Cell Cycle Blastomeres of the Sand Dollar *Echinaracnius parma*

Robert B. Silver (Marine Biological Laboratory)

Nuclear envelope breakdown (NEB) is preceded by a large signal of intracellular free calcium (Ca_i^{2+}) composed of several thousand individual events of elevation of Ca_i^{2+} concentration. Each event represents a release of Ca_i^{2+} from endomembrane stores to the cytoplasm, and we have described them as quantum emission domains (Ca_i^{2+}-QEDs) (1, 2, 5–7; Silver *et al.*, unpublished). Individual calcium release events were visualized as bright observable blobs in aequorin labeled cells (6, 7), and they occur within restricted regions of space called microdomains (6, 7). I reasoned that an agonist capable of evoking such events should be generated locally, should be present for a very brief period of time, and should thus trigger NEB or other processes that are signaled, initiated, coordinated, or controlled by elevations of intracellularly derived Ca_i^{2+} concentration. And, in fact, this laboratory has shown that the reduced form of leukotriene B_4 (LTB_4) could induce release of Ca^{2+} from endomembranes isolated from unfertilized eggs and from second cell cycle blastomeres of the sand dollar (*Echinaracnius parma*) (8). The release of Ca^{2+} from isolated endomembranes by LTB_4 *in vitro* was similar to that observed with 1,4,5-inositol trisphosphate (8); but oxidized LTB_4 was ineffective. Arachidonic acid (AA) derivatives play a role in a wide variety of cellular processes (9–13), including: vascular contraction cycles, neutrophil activation, activation of DNA synthesis, aggregation of marine sponge cells, and activation of tumor necrosis factor.

In the current study, the potential role of AA or major AA-derived metabolites as putative agonists for release of Ca^{2+} from endomembrane stores was tested *in vivo*. AA metabolites were microinjected into aequorin-loaded (6, 7, 15) sand dollar (*Echinaracnius parma*) eggs or mitotic second cell cycle blastomeres, and the emission of Ca^{2+}-dependent photon signals was followed as previously described (6–7; Silver *et al.*, unpublished).

Candidate agonists were tested at pipette concentrations ranging between 10^{-9} *M* and 10^{-3} *M*; the final equilibrium dilution factor was estimated at about 10^4 (1, 14), so the estimated intracellular equilibrium concentrations were between 10^{-13} to 10^{-7} *M*. I used the microinjection method (1, 2) originally developed by Hiramoto (16): the aqueous sample and an oil droplet of equal volumes were co-injected into the cell. The candidate agonists tested were partially dried from ethanol stock solutions, diluted into dimethyl sulfoxide (DMSO), reconcentrated under dry N_2 gas, and then diluted in injection buffer (Ca^{2+}-free phosphate buffered saline; 1, 14). To reduce the possibility that the samples would oxidize before being injected, they were kept in the dark and under dry N_2 gas until just before the pipette was loaded. Given the high degree of solubility in aqueous media of the AA metabolites and the rapidity of the microinjection procedure, I assumed that the majority of the sample remained in the aqueous phase before injection. Control injections of injection buffer, DMSO diluted 10-fold in injection buffer, deionized H_2O, and vegetable oil evoked no increase in detectable Ca^{2+}-dependent aequorin luminescence. Each condition was tested at least four times, in separate cells, to assure reproducability of the detected response (*e.g.*, 1, 2).

Ca^{2+} release from endomembranes was elicited *in vivo* by LTB_4 injection. No release of Ca^{2+} was evoked from isolated endomembrane stores *in vivo* by: AA, prostaglandins (G_2, H_2, E_2, $F_{2\alpha}$), thromboxane A_2, leukotriene A_4 (LTA_4), leukotriene C_4, leukotriene A_5, leukotriene C_5, leukotriene B_5, and oxidized LTB_4. Ca^{2+} (as calcium chloride solution) and Ca^{2+} released from endomembrane stores by divalent ionophore A23187 also evoked luminescence in the aequorin labeled cells. The conserved PSTAIR peptide of the cell cycle related kinase p34 cdc^2 was also injected to test an earlier report of its ability to serve as an agonist of endomembrane Ca^{2+} channels (17). PSTAIR did not evoke the release of Ca^{2+} from endomembrane stores; the positive effects seen earlier could have been due to impurities attributable to differences in preparation of the synthetic peptide.

In summary, only LTB_4, of all the AA-derived candidate agonists, evoked a release of Ca^{2+} from endomembrane stores—seen as a substantial increase in the number and density of calcium release events emitted from the injected cell upon injection of the candidate agonist. The total amount of Ca^{2+} released was proportional to the amount of LTB_4, 1,4,5-IP_3, or Ca^{2+} ($CaCl_2$ at a pipette concentration of 10^{-3} *M*) injected. Observations showed that, at these relatively high concentrations of LTB_4, the Ca^{2+} events spread radially from the point of injection at a rate of about 5 micrometers s^{-1}, ending at the inner surface of the plasma membrane; Jaffe has reviewed similar native Ca^{2+} waves associated with fertilization (18). The pattern spread of calcium release events evoked by injection of unbuffered Ca^{2+} was highly limited, indicating a high native Ca^{2+}-buffering capacity within the intracellular compartment; as such, the diffusional spread of Ca^{2+} injected into the cell would be highly restricted in space.

Injection of LTB_4 or 1,4,5-IP_3 also elevated the fertilization envelopes of sand dollar eggs regardless of the recipe of Ca^{2+}-free artificial seawater (MBL or Jamarin) used; each seawater preparation fully supported normal embryonic development at least to the pluteus stage. Eggs injected with LTB_4 typically showed a more complete and native fertilization envelope elevation than those injected with 1,4,5-IP_3; eggs injected with $CaCl_2$ solutions did not often elevate their fertilization envelopes, most likely due to the high intrinsic intracellular Ca^{2+} buffering capacity preventing local Ca_i^{2+} concentration from reaching sufficiently elevated levels to induce the secretory processes necessary for elevation of the fertilization envelope.

LTB_4 has the features of a putative agonist, evoking the release of Ca^{2+} from endomembrane stores *in vivo* to control Ca_i^{2+}-dependent processes within microdomains in eggs and mitotic second cell cycle blastomeres. Such a pulsed release of Ca^{2+} is consistent with the calcium-dependent luminescence patterns observed in aequorin-loaded eggs and mitotic cells (*e.g.*, 1, 5, 8).

Grant support by NSF is gratefully acknowledged. Aequorin preparations (15) were generously provided by Dr. Shimomura (Marine Biological Laboratory) and his colleagues Drs. Inouye, Musicki, and Kishi. The author is grateful to the reviewers for their many helpful and well considered suggestions made in the final preparation of this manuscript.

Literature Cited

1. **Silver, R. B. 1989.** *Dev. Biol.* **131:** 11–26.
2. **Silver, R. B. 1990.** *Ann. N. Y. Acad. Sci.* **582:** 207–221.
3. **Llinás, R., M. Sugimori, and R. B. Silver. 1992.** *Science* **256:** 677–679.
4. **Berridge, M. J., and R. F. Irvine. 1989.** *Nature* **341:** 197–205.
5. **Silver, R. B. 1986.** *J. Cell Biol.* **103:** 140a.
6. **Silver, R. B. 1994.** *Biol. Bull.* **187:** 235–237.
7. **Silver, R. B., A. P. Reeves, M. Whitman, and B. Kelley. 1994.** *Biol. Bull.* **187:** 237–238.
8. **Silver, R. B., J. B. Oblak, G. S. Jeun, J. Sung, and T. Dutta. 1994.** *Biol. Bull.* **187:** 242–244.
9. **Samuelsson, B. 1983.** *Science* **220:** 568–575.
10. **Samuelsson, B., S.-E. Dahlén, J. Å. Lindgren, C. A. Rouzer, and C. N. Serhan. 1987.** *Science* **237:** 1171–1176.
11. **Buttner, N., S. A. Siegelbaum, and A. Volterra. 1989.** *Nature* **342:** 553–555.
12. **Rich, A. M., G. Weissmann, C. Anderson, L. Vosshall, K. A. Haines, T. Humphreys, and P. Dunham. 1984.** *Biochem. Biophys. Res. Comm.* **121:** 863–870.
13. **Hayakawa, M., N. Ishida, K. Takeuchi, S. Shibamoto, T. Hori, N. Oku, F. Ito, and M. Tsujimoto. 1993.** *J. Biol. Chem.* **268:** 11290–11295.
14. **Silver, R. B. 1986.** *Proc. Nat. Acad. Sci. U.S.A.* **83:** 4302–4306.
15. **Shimomura, O., S. Inouye, B. Musicki, and Y. Kishi. 1990.** *Biochem J* **270:** 309–322.
16. **Hiramoto, Y. 1974.** *Exp. Cell Res.* **87:** 403–406.
17. **Picard, A., J. C. Cavadore, P. Lory, J. C. Bernengo, C. Ojeda, and M. Doree. 1990.** *Science* **247:** 327–329.
18. **Jaffe, L. 1993.** *Cell Calcium* **14:** 736–745.

Reference: *Biol. Bull* **189:** 204–205. (October/November, 1995)

Anaphase Spindle Dynamics Under D_2O-enhanced Microtubule Polymerization

Mira Krendel and Shinya Inoué (Marine Biological Laboratory)

Heavy water (D_2O) promotes microtubule polymerization both *in vitro* and *in vivo* (1, 2, 3). Possible mechanism for the enhancement of microtubule polymerization by D_2O is stabilization of hydrophobic interactions between tubulin dimers (2). Microtubules are the primary fibrous components of the mitotic and meiotic spindles, and treatment of dividing cells with heavy water increases spindle birefringence which reflects enhanced microtubule assembly. Polymerization and depolymerization of microtubules are thought to be important for the spindle functions in chromosome separation and they should therefore be precisely regulated during cell division. High concentrations of D_2O (more than 70%) have been shown to block mitosis (4). We have investigated the effects of increased polymerization of microtubules in the presence of D_2O on the first meiotic division in *Chaetopterus pergamentaceous* oocytes.

Birefringent yolk granules present in oocytes interfere with the observation of spindle birefringence under polarized light microscope. Therefore, clear oocyte fragments were prepared by a modification of the centrifugation method described in (5). Oocytes were layered onto a "cushion" consisting of 10 parts of 1.1 *M* sucrose, and 1 part ASW (Artificial Sea Water) and were centrifuged in a microcentrifuge at 7,000 rpm for 8 min and at 14,000 rpm for 4 min. Oocyte fragments were collected from the sucrose-seawater interface, washed with seawater, and mounted for observation in a wedge-profiled perfusion chamber. After preparation, the fragments remained arrested in the metaphase of the first meiotic division unless they were induced to proceed through the cell-division cycle by the addition of sperm. Spindle birefringence was observed using either polarized light microscopy with video and digital contrast enhancement or the new pol-scope (6).

Addition of ASW containing 40–50% D_2O to oocytes in metaphase or anaphase significantly increased spindle birefringence (Fig. 1A, C). The area occupied by the spindle in the plane of focus also increased, on average, by one-third upon addition of D_2O. The increased spindle birefringence persisted until anaphase, when the spindle was rapidly disassembled (Fig. 1B, D). Meiotic division and first polar body formation in the presence of D_2O proceeded without significant delay. No decrease in birefringence with time was observed in oocyte fragments that were incubated in D_2O without fertilization, indicating that the rapid fading of birefringence in cells completing meiosis was a function of the cell cycle and did not reflect a transient effect of D_2O. These results indicate that the promotion of microtubule polymerization by up to 50% D_2O does not significantly interfere with the mechanisms responsible for shortening and disassembly

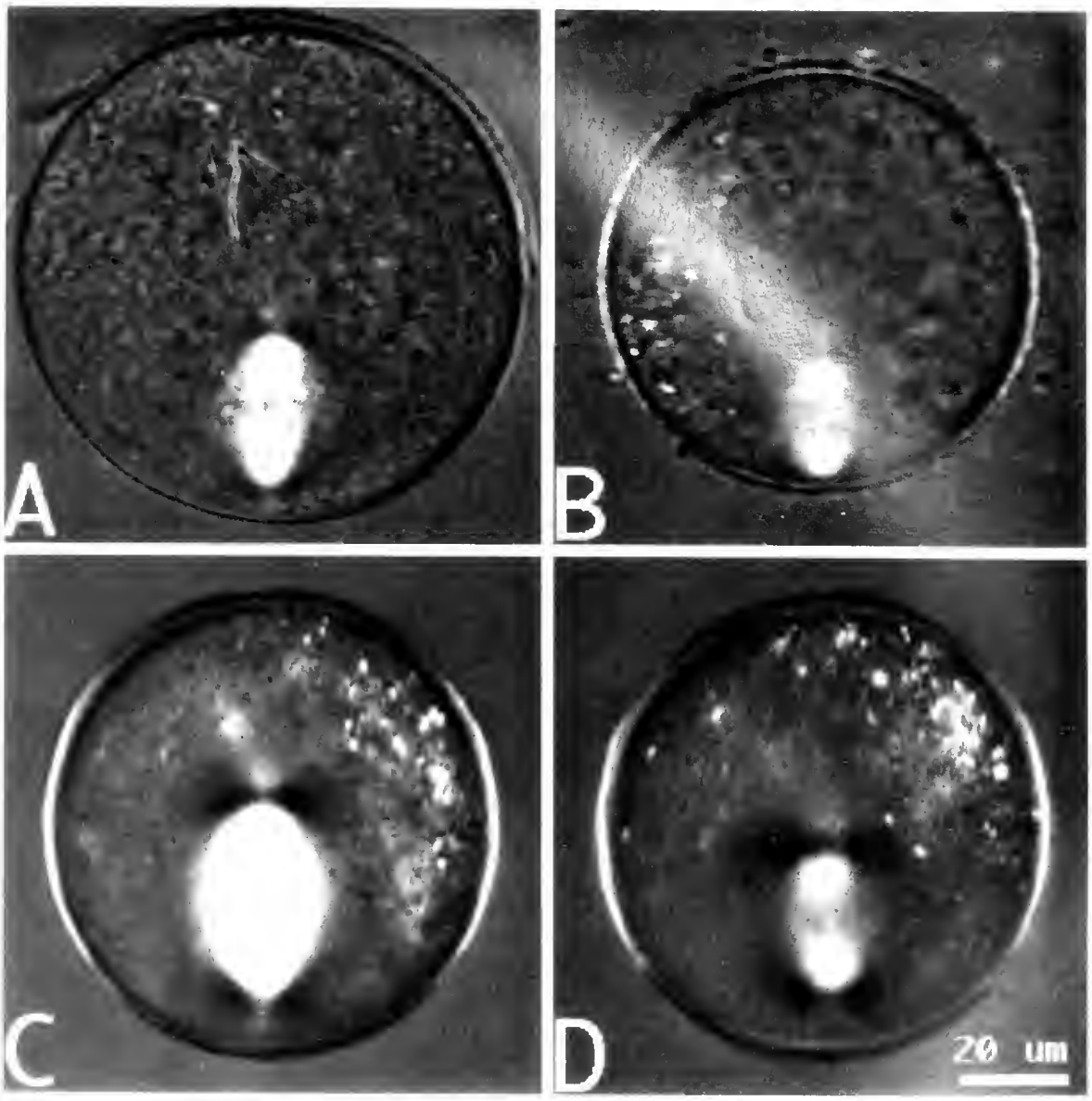

Figure 1. *Effect of D_2O on the first meiotic division in* Chaetopterus pergamentaceous *oocytes. (A), (B) Metaphase and anaphase, respectively, of the first meiotic division in control oocytes. (C), (D) First meiotic division in the oocyte treated with 40% D_2O prior to fertilization. Note the increase in spindle size and birefringence in metaphase (C) in comparison to control oocytes. As the D_2O-treated oocyte goes through anaphase, the spindle fibers shorten and spindle birefringence decreases (D).*

of spindle fibers during anaphase chromosome movement. The inability of D_2O to prevent disassembly of anaphase spindle microtubules may indicate that the concentration of assembly-competent tubulin is reduced in cells completing anaphase.

We thank Rudolf Oldenbourg for his help with the use of the pol-scope. We also thank Universal Imaging Corporation for the Physiology post-course fellowship to M. K. This work was supported by the NIH grant R37 GM31617 awarded to S. I.

Literature Cited

1. **Olmsted, J. B., and G. G. Borisy. 1973.** *Biochemistry* **12:** 4282–4289.
2. **Ho, T. J., and H. Sato. 1984.** *Biochim. Biophys. Acta* **800:** 21–27.
3. **Inoué, S., and H. Sato. 1967.** *J. Gen. Physiol. Suppl.* **50:** 259–288.
4. **Gross, P. R., and W. Spindel. 1960.** *Science* **131:** 37–39.
5. **Inoué, S. 1952.** *Exp. Cell Res. Suppl.* **2:** 305–318.
6. **Oldenbourg, R., and G. Mei. 1995.** *J. Microsc.*, in press.

Reference: *Biol. Bull.* **189**: 206. (October/November, 1995)

Quantifying Single and Bundled Microtubules with the Polarized Light Microscope

Phong Tran, E. D. Salmon, and Rudolf Oldenbourg (Marine Biological Laboratory)

Polarized light microscopy has been an important tool for noninvasive imaging of fine structures directly in living cells (1). One of us (R.O.) has improved the polarizing microscope by developing a precision universal compensator made of electronically controlled liquid crystal devices and circular polarizers. Combined with special processing software, the new "pol-scope" can image cellular fine structures with high sensitivity and resolution, irrespective of specimen orientation (2).

We have used the pol-scope to image and quantify the inherent optical properties of single and bundled microtubules. The ability to image the dynamics of a single microtubule in real time has been demonstrated with light microscopy techniques such as darkfield, differential interference contrast (DIC), and fluorescence. However, each of these techniques has limitations that make them non-ideal for quantitative measurements of microtubule density and distribution. For instance, darkfield and DIC microscopy, while noninvasive, cannot image and quantify the number of microtubules in a dense region of microtubules found in the mitotic spindle; and fluorescence microscopy, while quantitative, is invasive and suffers from photobleaching. The pol-scope is noninvasive, does not suffer from photobleaching, and is quantitative because it measures the inherent optical properties of microtubules.

Phosphocellulose-purified bovine brain tubulin was allowed to spontaneously assemble into microtubules, and was then stabilized with 10 μM taxol. The stabilized single microtubules were induced to form bundles of various numbers by the addition of inactive KAR3, a kinesin-like microtubule motor that bundles microtubules. The microtubules were then allowed to adhere to the coverslip surface of a slide chamber precoated with KAR3. Using a Nikon PlanApo 60×/1.4NA low-strain objective and a matching Nikon Universal 1.4NA condenser on the pol-scope, we imaged single microtubules with polarized light.

Figure 1A shows a microtubule bundle imaged with DIC microscopy, which cannot easily be used to determine the exact number of microtubules making up the bundle. For comparison, Figure 1B shows the retardance image of the same bundle of microtubules consisting of clearly distinct regions of one, two, and three microtubules observed with the pol-scope. The retardance of a single microtubule was measured to be 0.07 ± 0.02 nm [n = 30]. The retardance slow axis is parallel to the long axis of the microtubule. In addition, the retardance values were found to be quantized and increased linearly with the number of microtubules in the bundle (Fig. 1C).

We will use the new pol-scope to noninvasively quantify the distribution and dynamics of spindle microtubules in dividing cells.

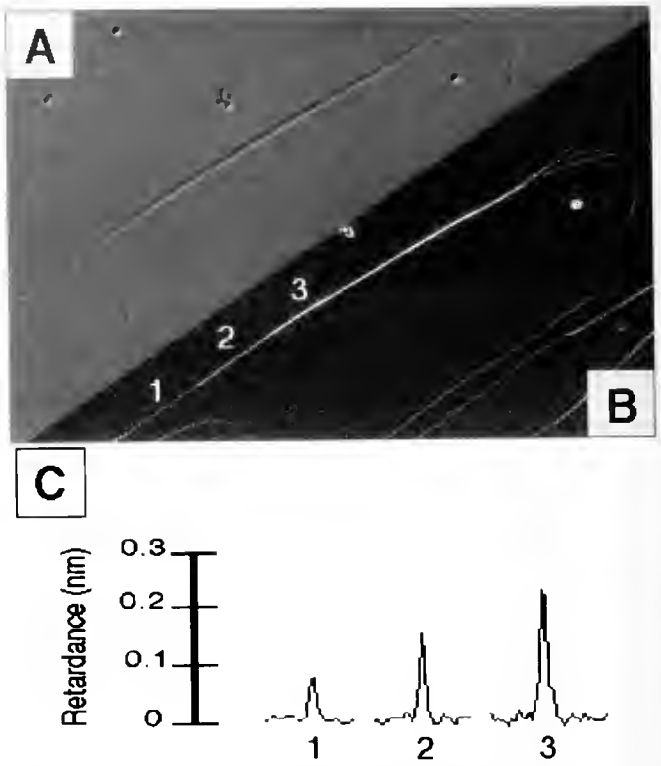

Figure 1. *Spontaneously assembled microtubules stabilized with taxol and imaged with differential-interference-contrast (DIC) microscopy and the new pol-scope using a Nikon Microphot-SA microscope equipped with a 100-watt Hg arc lamp illuminator, Nikon PlanApo 60×/1.4NA objective, and Nikon Universal 1.4NA condenser. (A) A small bundle of microtubules observed under DIC, and with digital background subtraction. (B) The same microtubule bundle observed with the pol-scope, and with background subtraction (horizontal image dimension 35 μm); (C) The measured retardance of one, two, and three microtubules*

We gratefully acknowledge the support of members of the MBL Architectural Dynamics in the Living Cell Program, as well as NIH grants GM-49210 to R.O., GM-24364 to E.D.S., and MBL Eric F. Fries Fellowship to P.T.

Literature Cited

1. **Inoué, S. 1953.** *Chromosoma* 5: 199–208.
2. **Oldenbourg, R. and G. Mei. 1995.** *J. Microsc.* in press.

Reference: *Biol. Bull.* **189**: 207. (October/November, 1995)

Acetylcholine-Induced Ca^{2+} Flux across the Sarcolemma of an Echinoderm Smooth Muscle

C. Leah Devlin (Department of Biology, Penn State University Ogontz Campus, Abington, PA 19001) and Peter J. S. Smith

Acetylcholine (ACh) causes slow contractions of the longitudinal muscle of the body wall (LMBW) of a sea cucumber, *Sclerodactyla briareus*. These contractions are inhibited by Ca^{2+} channel blockers diltiazem and verapamil (1). We therefore chose the LMBW as a model system and the vibrating Ca^{2+}-selective electrode as our method to test the hypothesis that ACh may be stimulating Ca^{2+} influx across the sarcolemma of smooth muscle, thus providing a source of Ca^{2+} during excitation-contraction (E-C) coupling.

Technical aspects and applications of the vibrating Ca^{2+}-selective electrode technique have been described (2). To record Ca^{2+} flux across the sarcolemma, the electrode (placed 15 μm from the tissue) was used to measure voltage differences at the two extremes of vibration 10 μm apart. Therefore, measurements at the LMBW were recorded at a distance 5 microns or less from the muscle surface. All background (control) recordings were conducted at an electrode distance of greater than 450 microns from the muscle surface. PC-based software controlled the vibration of the electrode and calculated the voltage (μV) difference between vibration extremes (2). The electrode vibrated at a frequency of 0.3 Hz at a right angle to the long axis of the strap-like LMBW. This low vibration frequency minimized mixing of the media and reduced noise in the system. The data measured in μV was converted to Ca^{2+} ion flux in pmol cm^{-2} s^{-1} using a modification of the Fick equation (2).

A wide range of concentrations of ACh (10^{-9} *M* to 10^{-3} *M*) stimulated a Ca^{2+} efflux that was both dose- and time-dependent. This efflux was probably the result of recovery from a preceding, rapid Ca^{2+} influx that could not be detected by the relatively slow time constant of the ionophore in the electrode tip. Because 10^{-6} *M* ACh lies in the mid-range of effective doses and was the dose used in an earlier mechanical study (1), it was chosen as the concentration to be challenged by the Ca^{2+} channel blocking agents. Treatment with 10^{-6} *M* ACh caused a Ca^{2+} efflux on the order of 3.39 pmol cm^{-2} s^{-1} (S.D. = 0.91 pmol cm^{-2} s^{-1}, N = 6).

We then tested two L-type Ca^{2+} channel blockers, diltiazem and verapamil, and two non-specific Ca^{2+} blockers, cobalt chloride and lanthanum chloride, on Ca^{2+} efflux induced by 10^{-6} *M* ACh. 10^{-5} *M* diltiazem or verapamil inhibited efflux caused by 10^{-6} *M* ACh by 52% (N = 6) and 88% (N = 6), respectively. 10^{-4} *M* cobalt chloride or lanthanum chloride inhibited ACh-induced Ca^{2+} efflux by 62% (N = 6) and 92% (N = 6), respectively. These data suggest that the entry of extracellular Ca^{2+} through voltage-gated Ca^{2+} channels is source of the ion mobilized during E-C coupling.

Alternative sources for Ca^{2+} release and sequestration in the LMBW may be a series of elongated subsarcolemmal sacs running in parallel to the sarcolemma in the LMBW of *Sclerodactyla briareus* (3). Chen (3) suggests that excitation of the membrane could cause a release of Ca^{2+} from these internal sacs in a system similar to that in vertebrate skeletal muscle. Suzuki (4) suggests that calcium-containing pyroantimonate precipitates found along the inner membrane surface could be a Ca^{2+} source during E-C coupling as well.

To elucidate possible mechanisms of Ca^{2+} extrusion we chose agents that would alter the normal activity of the Na-Ca exchanger or the Ca^{2+}-ATPase. In the first series of experiments, Na^+ ions were removed from the bathing saline and replaced with the same concentration (423 m*M*) of lithium (Li^+); the aim was to test the hypothesis that Na^+ may enter through an ACh receptor-complex in the LMBW similar to that of the mammalian nicotinic ACh receptor. Li^+ is an ion that can pass through Na^+ channels but cannot be substituted for Na^+ in the Na-Ca exchanger (5). When we replaced Na^+ in the bathing saline with Li^+ and then applied ACh, Ca^{2+} efflux was inhibited by about 50% (N = 6). This result indicates that Na^+ ions are necessary, first, as a stimulus for Ca^{2+} mobilization through voltage-gate channels or from an intracellular source, or perhaps during Na^+-induced Ca^{2+}-release (5). A preliminary experiment (N = 1) showed that treatment of the LMBW with a Ca^{2+}-ATPase inhibitor, cyclopiazonic acid (10^{-5} *M*) blocked ACh-induced Ca^{2+} efflux by only 22%. The experiments above suggest that the probable mechanism of Ca^{2+} extrusion in the LMBW is the Na-Ca exchanger, a more energy efficient mechanism than the Ca^{2+}-ATPase.

We propose that the ACh-induced Ca^{2+} efflux is an indirect measure of Ca^{2+} influx through voltage-gated Ca^{2+} channels. Because Ca^{2+} influx (and the reciprocal efflux) was inhibited by the L-type channel blockers diltiazem and verapamil, we suggest that L-type Ca^{2+} channels are present in echinoderm smooth muscle. The opening of these voltage-gated Ca^{2+} channels was regulated by Na^+ influx as revealed by Li^+ substitution experiments. The process of Ca^{2+} extrusion is probably the result of the Na-Ca exchanger that expels excess intracellular Ca^{2+} while Na^+ flows in across the membrane, rather than the activity of a sarcolemmal Ca^{2+}-ATPase. Further tests with pharmacological probes and metabolic blockers are planned to distinguish between these alternatives.

This research was supported by an MBL Fellowship and Penn State University Research Development Grant awarded to C. L. Devlin as well as by P41RR01395. Thanks are extended to Professor C. Ladd Prosser for his suggestions on lithium-substitution experiments.

Literature Cited

1. **Devlin, C. L. 1993.** *Comp. Biochem. Physiol.* **160C**: 573–577.
2. **Smith, P. J. S., Sanger, R., and L. F. Jaffe. 1994.** Pp. 115–134 in *Methods of Cell Biology: A Practical Guide to the Study of Calcium in the Living Cell, Vol 40,* R. Nuccitelli, ed. Academic Press, San Diego.
3. **Chen, C. 1983.** Ph.D. Thesis, University of Rhode Island.
4. **Suzuki, S. 1982.** *Cell Tissue Res* **222**: 11–24.
5. **Lipp, P., and E. Niggli. 1994.** *J Physiol.* **474**: 439–446.

Reference: *Biol. Bull.* **189**: 208–209. (October/November, 1995)

Retardation of the Spread of Extracellular Ca^{2+} into Transected, Unsealed Squid Giant Axons

Harvey M. Fishman (University of Texas Medical Branch), Todd L. Krause, Andrew L. Miller, and George D. Bittner

Survival of an axon after injury (*e.g.*, transection) requires a mechanism that prevents internal accumulation of extracellular Ca^{2+}, which causes degeneration (1). Repair of a transected axon by the rapid formation (<1 h) of a seal (2) is one such mechanism; but, some axons lack the ability to seal rapidly, yet remain functional for hours (2). We now describe the spread of Ca^{2+}-induced aequorin luminescence and the decay of injury current density (I_i) carried by Ca^{2+} (I_{iCa}) in transected, unsealed giant axons (GAs) excised from squid (*Loligo pealei*).

We assessed Ca^{2+} movement at the cut end of unsealed GAs (Fig. 1A), beginning 5 min after axonal transection, by analyzing accumulated photon (luminous) images (Fig. 1B, C) emitted by

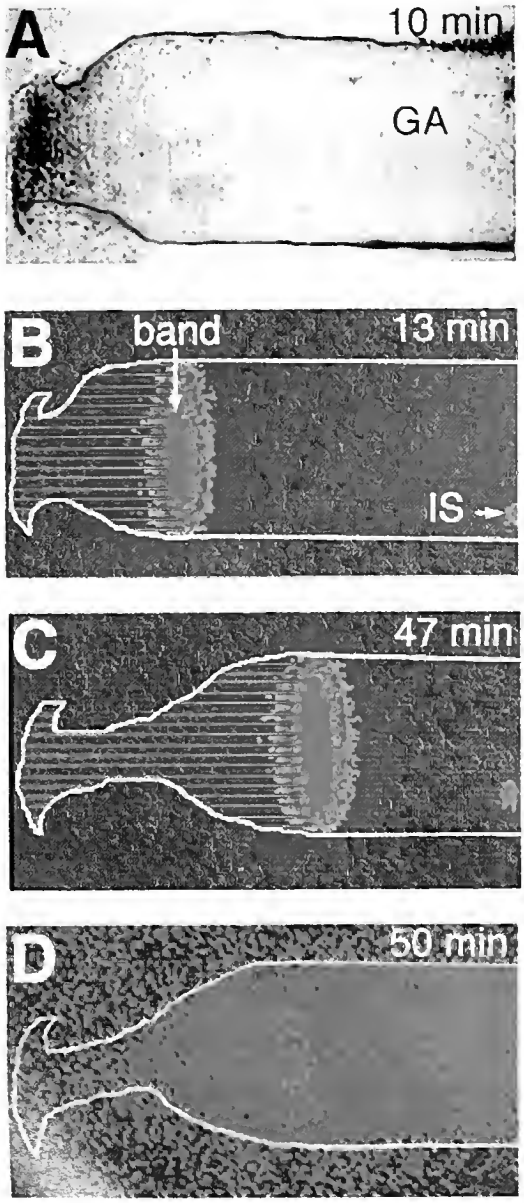

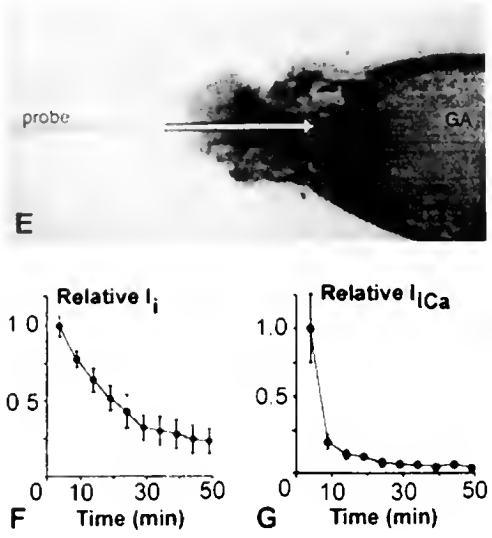

Figure 1. *(A) Severed end of a squid giant axon 10 min after transection in artificial seawater (ASW: 430 mM NaCl, 10 mM KCl, 10 mM $CaCl_2$, 50 mM $MgCl_2$, 5 mM TrisCl). (B) and (C) Luminous images (reflecting Ca^{2+} distribution) from photons emitted by recombinant aequorin inside the transected axon in (A) during 2-min collection intervals at 13 and 47 min post-severence. A mixture of 85% aequorin (recombinant) and 15% fluorescein-conjugated aequorin was pressure-injected with a microelectrode into the axon [injected volume (30 nl) was <0.5% of the entire axoplasmic volume]. The injection procedure and the detection system for luminescence and fluorescence were as described previously (3). Outlines of the axon shown in (A), obtained within minutes of each accumulated photon image, were drawn in white on luminous images (B)–(D). Horizontal red lines mark the region of "spent" aequorin. (D). Fluorescence of fluorescein-conjugated aequorin at 50 min post severance showing that aequorin was distributed uniformly in the GA. IS = aequorin injection site. Scale and color bar = 1 mm and Ca^{2+} concentration from background (black) to saturation (red). (E, F, G) Ca^{2+} movement into the cut end of a squid GA measured with an extracellular Ca^{2+}-selective vibrating probe. (E) Current-density vector (arrow) determined at the tip of a Ca^{2+}-selective vibrating probe at the cut end of a GA in ASW, 15 min after transection. The one-dimensional Ca^{2+}-selective vibrating probe, filled with a calcium ionophore (Fluka Chemika #21048), was as described previously (7). Arrow length = 32 μA/cm²; 300 μm. (F) and (G) Temporal decline of injury current density, I_i, relative to the initial value 5 min after transection (closed circles, n = 5) and of the portion of injury current density carried by Ca^{2+}, I_{iCa}, relative to the initial value 5 min after transection (closed circles; n = 5) determined in the 50-min interval following transection of GAs. Paired axonal segments, obtained from the transection of a GA, were measured simultaneously, one with a nonselective probe (I_i) and the other with a Ca^{2+}-selective probe (I_{iCa}). All determinations were made parallel to the longitudinal axis of axons and with the tip of the probe placed 216 μm from the cut end.*

aequorin-loaded axons (3). Intact GAs in artificial seawater (ASW) emitted light only where aequorin had been injected into an axon (IS, Fig. 1B). In Ca^{2+}-free ASW, the GA displayed no luminescence (n = 4). These data suggest that Mg^{2+} did not contribute to luminescence (4), and that the light emitted from GAs severed in ASW resulted from the movement of Ca^{2+} into the GAs rather than from an injury-induced release of intra-axonal stores of Ca^{2+}.

After transection of aequorin-loaded GAs, a luminous band moved slowly into the cut end (n = 19). At 13 min after transection of a representative axon, the center of the band was 364 μm from the cut end (Fig. 1B); at 47 min after transection (Fig. 1C), the band was 424 μm from the cut end (60 μm from its location at 13 min). When the rate of movement of the luminous band was analyzed at 2-min intervals, the band velocity was 0.35 μm/s at 10 min after transection and 0.25 μm/s at 35 min after transection. After axonal shortening (0.20 μm/s) in the region of the luminous-band movement (within 1 mm of the cut end) was taken into account (5), the actual rate of movement of the luminous band (reflecting the spread of extracellular Ca^{2+} into the transected axon) with time was significantly retarded (from 0.15 μm/s to 0.05 μm/s) at 10 and 35 min, respectively, following transection.

As a second measure of retardation of the spread of Ca^{2+} into the cut end of a GA, we used, extracellularly (Fig. 1E), either a nonselective vibrating probe that measured the density of injury current produced by all ions (I_i), or an ion-selective probe that measured the density of injury current produced by Ca^{2+} (I_{iCa}) (6, 7). To compare temporal changes in I_i with I_{iCa}, paired segments of the *same* GA (*i.e.*, the two axonal segments resulting from a transection) were always measured simultaneously, one with the nonselective probe and the other with the Ca^{2+}-selective probe.

In the 50-min interval following axonal transection in four GAs, inwardly directed I_i declined 75% (Fig. 1F: 1504.4 ± 108.2 (SE) $\mu A/cm^2$ at 4 min, to 341.4 ± 123.7 $\mu A/cm^2$ at 50 min). In the first 10 min following transection, I_i declined 22%. The large, persistent I_i (341.4 $\mu A/cm^2$) at 50 min is consistent with previous findings (2) that GAs do not seal within 2.5 h. Other preliminary experiments (data not shown), with an Na^+-selective probe, demonstrated that most of I_i was carried by Na^+.

In the 50-min interval following axonal transection, inwardly directed I_{iCa} declined 97% (Fig. 1G: 99.4 ± 23.6 $\mu A/cm^2$ at 4 min, to 3.5 ± 0.8 $\mu A/cm^2$ at 50 min). In the first 10 min following axonal transection, I_{iCa} declined 80%. These data suggest that Ca^{2+} movement contributes only a small amount (~1%) to I_i at post-severance times >20 min. Furthermore, in separate experiments (n = 3), when the ASW was replaced with Ca^{2+}-free ASW, at post-severance times >20 min, I_i was not significantly different from the curve in Fig. 1F.

In summary, two independent measures—*i.e.*, the decreased velocity with time of the luminous band of aequorin and the more rapid decay of I_{iCa} relative to the decay of I_i—both suggest that giant axons from squid possess a Ca^{2+}-specific mechanism capable of retarding the spread of Ca^{2+}, driven by the high extracellular concentration (10 mM), into a severed, unsealed cut end minutes after transection.

We thank Dr. L. F. Jaffe and The National Vibrating Probe Facility for discussions and the use of facilities, A. Shipley and E. Karplus for technical assistance, and Drs. O. Shimomura, S. Inouye, and Prof. Y. Kishi for the supply of aequorins. Supported by NIH grant NS31256 and ATP grant 003658-296.

Literature Cited

1. **Schlaepfer, W. W., and R. P. Bunge. 1973.** *J. Cell Biol* **59:** 456–470.
2. **Krause, T. L., H. M. Fishman, M. L. Ballinger, and G. D. Bittner. 1994.** *J. Neurosci.* **14(11)** part I:6638–6651.
3. **Miller, A. L., E. Karplus, and L. F. Jaffe. 1994.** *Methods in Cell Biology,* R. Nuccitelli, ed., vol **40:** 306–335, Academic Press, NY.
4. **Blinks, J. R. 1982.** Pp 1–38 *Techniques in Cellular Physiology-Part II.* Elsevier/North Holland Scientific Publishers, Amsterdam.
5. **Todora, M. A., H. M. Fishman, T. L. Krause, and G. D. Bittner. 1994.** *Neurosci. Ltrs.* **179:** 57–59.
6. **Jaffe, L. F., and R. Nuccitelli. 1974.** *J. Cell Biol.* **63:** 614–628.
7. **Smith, P. J. S., R. H. Sanger, and L. F. Jaffe. 1994.** *Methods in Cell Biology,* R. Nuccitelli, ed., vol. **40:** 115–134, Academic Press, NY.

Reference: *Biol. Bull.* **189:** 209–210. (October/November, 1995)

Effects of Exogenous Heat Shock Protein (hsp70) on Neuronal Calcium Flux

Peter J. S. Smith (Marine Biological Laboratory), Katherine Hammar, and Michael Tytell

Understanding the molecular and cellular responses of neural tissue to injury has been a driving force behind a large body of neuroscience research. Such information can provide the bases for strategies designed to facilitate repair and recovery of function. One promising approach involves research into the class of proteins known as heat shock proteins (hsp). This study uses an hsp belonging to a family of characteristic size: 70 kDaltons (hsp70). These molecules appear to be linked to cell survival after acute metabolic stress, being first described in the brain after traumatic injury (1). By the late 1980s it was clear that many different types of trauma to the nervous system increase the production of the inducible form of hsp70 (hsp_i; 2). Further evidence suggested that elevated hsp_i is correlated with an increased survival of neurons; for example, transfection mediated expression of human hsp70, protects rat dorsal root ganglion neurons and glia from severe heat stress (3).

Although heat shock proteins are normally intracellular constituents, with trauma up-regulating their expression, this study

has taken an unconventional approach—delivering the protein exogenously. The rationale is twofold. First, hsp need not always be synthesized by the host cell. Glia, for example, can transfer hsp across the axolemma (4); spermatozoa are provided with hsp70 from the seminal fluid that remains associated with the outer membrane (5); and exogenous application of hsp70 can have such profound effects as protecting the retina from light damage (6) and influencing neuronal survival after axotomy (7). Secondly, hsp appears to insert into membranes, inducing channels in planar bilayers and promoting the insertion of other protein molecules by altering their conformation during, as well as before or after membrane insertion (8). The possibility that exogenously applied heat shock protein 70 might alter cellular ion homeostasis is the focus of this study.

We have used two methods to investigate the effect that exogenous application of hsp70, at a concentration of 2.5 $\mu g \cdot ml^{-1}$, might have on cellular ion transport: non-invasive vibrating ion-selective probes and real-time confocal imaging. The emphasis has been on calcium ion homeostasis. Our model has been the aplysiid bag cell neuron cultured by methods already described (9). Cells were grown in artificial seawater on clean glass coverslips (No. 2). All cells were examined after 1 or 2 days in culture. Measurement of the trans-membrane calcium flux was done as previously described (10).

Two reporter probes for studying intracellular free calcium were used, Fluo-3-AM or Indo-1-AM (Molecular Probes, Eugene, Oregon); their performance was indistinguishable, and Fluo-3-AM results will be discussed here. Cells were loaded in the dark with 2 $\mu mol \cdot l^{-1}$ Fluo-3-AM dissolved in DMSO for 30 min at room temperature. Imaging was done with a Nikon RCM-8000 confocal microscope. Laser light levels were minimized to avoid cellular damage.

All experiments were conducted in artificial seawater (ASW) with reduced calcium (50–100 $\mu mol \cdot l^{-1}$) and elevated magnesium (67 $mmol \cdot l^{-1}$).

Resting neurons, cultured in ASW, show a steady state measurable calcium efflux across the plasma membrane of the soma, as measured by the non-invasive vibrating calcium selective probe. This flux is modulated by pharmacological compounds, such as thapsigargin (R. J. Knox, unpub.) as well as phorbol esters and cGMP (11). The range of efflux values recorded is remarkably uniform, normally being between 30–40 μV, equivalent to a flux of 2–3 $pmol \cdot cm^{-2} \cdot s^{-1}$. The variation in microvolts for 8 neurons from this study is 38 $\mu V \pm 7$ (mean ± standard deviation). Preincubation of the neurons in hsp70 (StressGen) for 2 h prior to measurement causes a dramatic elevation of the measured efflux ($n = 7$: 110 $\mu V \pm 43$). This elevated level of activity remains even 24 h after the hsp has been removed from the bathing medium. Shorter incubation times of 30–60 min, followed by washout, also show an elevated transmembrane efflux. In all the above experiments hsp70 was removed from the medium prior to the measurement of transmembrane calcium flux.

Attempts to measure the onset of this elevated efflux during the initial application of hsp70 were frustrated by the interaction of hsp70 with the calcium-selective liquid membrane tipping the ion probe. The electrode is tipped with a 30 μm column of calcium ionophore cocktail A (FLUKA) and the hsp70 must either insert into the lipophilic carrier or interfere with the ionophore itself.

Imaging carried out during hsp exposure revealed little change in free cytosolic calcium levels even over periods of 30 min to 1 h. The implication of this surprising observation is quite profound, in that the marked increase in transmembrane soma efflux is not a response to a pronounced increase in the free cytosolic calcium level. Some other explanation must be sought.

As yet we can only speculate about the mechanism by which hsp70 modulates the transmembrane calcium efflux. The lack of any noticeable increase in the free-calcium level within the cell implies a direct action on transmembrane calcium regulation. Heat shock proteins and calcium are clearly related in that a rise in intracellular calcium or an increase in transmembrane calcium current causes hsp induction, as with Epstein-Barr virus infection (12). We seem to be observing a quite different series of events. Because elevated cellular hsp correlates with cellular protection, our results suggest that one feature of the protection mechanism of hsp involves altered calcium ion homeostasis.

This research was supported by NIH grant No. P41 RR01395 funding the National Vibrating Probe Facility—National Center for Research Resources (PJSS). The authors are indebted to John Dow of Nikon Instruments for technical assistance.

Literature Cited

1. **Currie, R. W. and F. P. White. 1981.** *Science* **214:** 72–73.
2. **Mayer, J. and I. Brown, eds. 1994.** *Heat Shock Proteins in the Nervous System* Academic Press NY.
3. **Uney, J. B., J. N. C. Kew, K. Staley, P. Tyers, and M. V. Sofroniew. 1993.** *FEBS Letts.* **334:** 313–316.
4. **Sheller, R. A., M. Tytell, M. Smyers, and G. D. Bittner. 1995.** *J. Neurosci. Res* **41:** 324–334.
5. **Miller, D., S. Brough, and O. al-Harbi. 1992.** *Hum Reprod* **7:** 637–645.
6. **Tytell, M., M. F. Barbe, and I. R. Brown. 1994.** *J Neurosci. Res.* **38:** 19–31.
7. **Tytell, M., L. Li, and L. J. Houenou. 1994.** *Trans. Amer. Soc. Neurochem* **25:** 187.
8. **Alder, G. M., B. M. Austen, C. L. Bashford, A. Mehlert, and C. A. Pasternak. 1990.** *Bioscience Rep.* **10:** 509–518.
9. **Knox, R. J., E. A. Quattrocki, J. A. Connor, and L. K. Kaczmarek. 1992.** *Neuron* **8:** 883–889.
10. **Smith, P. J. S., R. H. Sanger, and L. F. Jaffe. 1994.** *Methods Cell Biol.* **40:** 115–134.
11. **Yamoah, E., and P. J. S. Smith. 1994.** *Biol Bull* **187:** 1043.
12. **Cheung, R. K., and H. M. Dosch. 1993.** *Virology* **193:** 700–708.

Reference: *Biol. Bull.* **189**: 211–212. (October/November, 1995)

Regional Differences in Directional Response Properties of Afferents Along the Saccule of the Toadfish, *Opsanus tau*

Peggy L. Edds-Walton and Richard R. Fay (Marine Biological Laboratory)

The inner ears of fishes consist of three otolithic endorgans: the saccule, lagena, and utricle. In most fishes the saccule is believed to be the primary auditory endorgan, responding to acoustic particle motion, sound pressure, or both, depending on species (1). Previously, we investigated the frequency and directional response characteristics of afferents from the rostral saccule to determine whether the direction of a sound source could be encoded. We found that most afferents are highly directional, with widely ranging "best directions" (2). We have extended our study to determine whether variation in three-dimensional directional response characteristics can be related to the morphological orientation of the sensory hair cells along the saccule.

The toadfish saccule lies along the longitudinal axis of the fish and is slanted and tilted slightly away from a parasagittal plane. The orientations of the hair cells shift gradually along the rostrocaudal axis of the saccule (Fig. 1A). The saccular nerve has divisions that vary in size and location, but distinct rostral and caudal bundles are always present, and a distinct middle bundle is often present. We recorded extracellularly from afferents near their point of exit from the saccule, in the most rostral location of the saccular nerve, the middle bundle, or the most caudal location of the saccular nerve. For each afferent, we measured sensitivity and directionality in three-dimensional space.

After surgery to reveal the saccular nerve, the lightly anesthetized (aminobenzoic acid, methanesulfonate salt, Sigma) and paralyzed (pancuronium bromide, Sigma) toadfish was placed in a specially designed head-holder in a saltwater-filled cylinder. We made extracellular recordings of the activity of saccular afferents while oscillating the toadfish (= particle motion stimulation). Linear oscillations were produced by paired orthogonal shakers in the horizontal plane and a vertical shaker. Inputs to the three shaker channels were computer-controlled to produce sinusoidal motion along six axes (0°, 30°, 60°, 90°, 120°, 150°) in both horizontal and mid-sagittal planes.

Afferents in the rostral bundle (Fig. 1B) tended to have best elevations below 45° (mean = 23°), with a large variety of best azimuths. These cells probably innervated hair cells found in the most rostral saccule, based on the locations of our electrodes and their directional characteristics. Afferents in the middle bundle (Fig. 1C) tended to have the highest best elevations (mean = 49°) and the least variable best azimuths, which is consistent with the less variable, dorsal-ventral hair cell orientations in the middle saccule. The lowest elevations in these data (0–15°) may represent afferents that were innervating hair cells in the more rostral region of the middle saccule (large arrow, Fig. 1A). Lastly, the responses of caudal afferents (Fig. 1D) resembled those in the rostral bundle (mean = 35°), which is consistent with the similarity in hair cell orientations in the two areas.

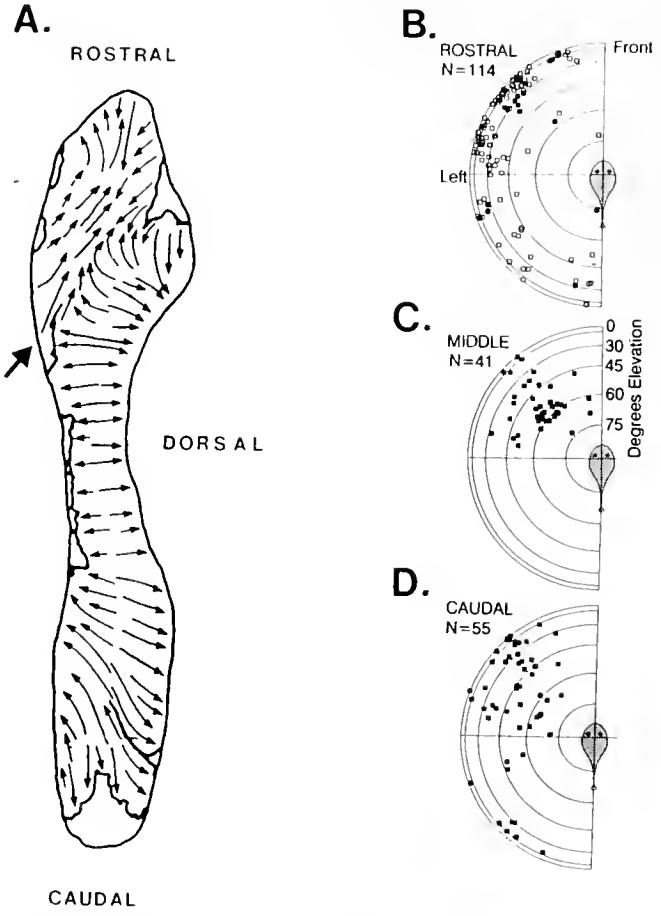

Figure 1. *(A) The saccule of the toadfish (modified from 5). The arrows represent the hair cell orientation and the presumed best direction for that region of the saccule, based on what is known about the electrophysiology of hair cells. The large arrow indicates the edge of the "middle" region of the saccule (the open areas were lost during preparation for electron microscopy.) (B–D) Polar plots of best azimuths and elevations for individual saccular afferents from the rostral (B), middle (C), and caudal (D) bundles of the saccular nerve. The fish cartoon is in the center of the flattened "globe"; the "North Pole" is at the center of the smallest circle, and the perimeter is the "equator." All responses were arbitrarily plotted in the "northern hemisphere" and to the left of the fish. Open boxes in (A) are 1994 data; filled boxes are current data*

The most sensitive afferents of each bundle responded to displacements of less than 1 nm. This displacement is approximately equal to that of the mammalian basilar membrane at

the threshold of hearing (3). The neurally coded output of the toadfish saccule appears sufficient to account for sound detection thresholds (4) and could be used to compute the axis of particle motion.

Our protocol was approved by the Institutional Animal Care and Use Committee. This project has been supported by Program Project Grant #1PO1DC018737 from NIH, NIDCD. Thanks to Philip Ording for help with trigonometry.

Literature Cited

1. **Fay, R. R., and A. N. Popper. 1975.** *J. Exp. Biol.* **62:** 379–388.
2. **Fay, R. R., P. L. Edds-Walton, and S. M. Highstein. 1994.** *Biol. Bull.* **187:** 259–260.
3. **Sellick, P. M., R. B. Patuzzi, and B. M. Johnstone. 1982.** *J. Acoust. Soc. Am.* **72:** 131–141.
4. **Fish, J., and G. Offutt. 1971.** *J. Acoust. Soc. Am.* **51:** 1318–1321.
5. **Edds-Walton, P. L., and A. N. Popper. 1995.** *Acta Zool.* **76:** 257–265.

Reference: *Biol. Bull.* **189:** 212–213. (October/November, 1995)

Optical Imaging of Intrinsic Signals from the *Limulus* Optic Nerve

Estela V. O'Brien (The Rockefeller University) and Robert B. Barlow

We report here visually evoked changes in the reflectance properties of the optic nerve of the horseshoe crab (*Limulus polyphemus*). Because this signal results from small changes in the optical properties of neural tissue and can be imaged optically without the application of exogenous dyes, it is called an intrinsic signal. Such signals provide a minimally invasive means of sampling the activity of many neurons simultaneously (1). First measured by Hill and Keynes (2), intrinsic signals are small (fractional changes of ~1/10,000 of reflected light) and have multiple sources that are thought to include light-scattering changes in response to stimulation, metabolism-linked changes associated with changes in the transition states of intrinsic chromophores, and changes in blood volume. Past studies by Hill and Keynes (2) and Cohen *et al.* (3) revealed that light-scattering changes occur during and after electrical stimulation in excised crab and squid axons. The time course of these changes in invertebrate nerve preparations during continuous stimulation is slow. Their initial rise above baseline lags behind the stimulus by 300–500 ms and is similar to the time course of the visually evoked signal measured in mammalian cortex *in vivo*, which presumably contains multiple components (1). After the offset of electrical stimulation, however, the light-scattering signals of excised invertebrate preparations decay much slower than those recorded in response to visual stimuli in mammalian cortex *in vivo*.

We have studied the spatial extent and the time course of both electrically and visually evoked activity in the excised *Limulus* optic nerve. Figure 1 illustrates the optical imaging of intrinsic signals in the optic nerve of the lateral eye of the horseshoe crab. The excised nerve was bathed in a *Limulus* Ringers solution (430 m*M* NaCl, 10 m*M* KCl, 10 m*M* $CaCl_2$, 10 m*M* $MgCl_2$, 20 m*M* $MgSO_4$, 100 m*M* HEPES, 100 m*M* TES) and stimulated with a Grass stimulator and stimulus isolation unit via a suction electrode attached to one end of the nerve. A stabilized DC tungsten light source illuminated the nerve with 600-nm light, and a cooled charge-coupled device (CCD) camera (Photometrics) acquired images of the nerve that were synchronized to the stimulation (10-Hz train of 1-ms pulses). In most cases, a recording suction electrode monitored the compound action potential at the other end of the excised nerve. Once we detected the compound action potential, we crushed the nerve midway between the two electrodes and measured the spatial extent of optical signals generated by the nerve.

In a second experiment, we excised the retina together with a 2-cm length of nerve and placed the preparation in a bath with a light-impermeable shroud that optically isolated the nerve from the retina. Visual stimulation consisted of a bright white light (10 ms flash duration, 1-Hz flash repetition) aimed at the retina through a light pipe and diffuser. As in the first experiment, we synchronized the collection of optical data to the stimulation and analyzed the optical data with extensions of Karhunen-Loeve principal components analysis to extract spatial maps of the intrinsic signals and their normalized time course (4).

Figure 1A is an image of the *Limulus* optic nerve with a crush in the center as captured by the CCD camera. Figure 1B is the activity map of the same nerve in response to electrical stimulation. Note that the activity is localized to the region proximal to the crush, and the mean intensity per pixel proximal to the crush is a factor of 2 greater than that distal to the crush. We found that visual stimulation also evokes intrinsic signals in the optic nerve, and we measured the time course for both the electrically and visually evoked activity. The normalized time course of the signals evoked in the nerve by 10 s of electrical stimulation (Fig. 1C) is similar to that of the electrically evoked light-scattering changes measured by Cohen and Keynes (5). Figure 1D shows the normalized time course of intrinsic signals in response to visual stimulation. These signals can be fully accounted for by light-scattering changes. The time course of the return to baseline after stimulus offset (Fig. 1C) is slower than that measured in mammalian cortex.

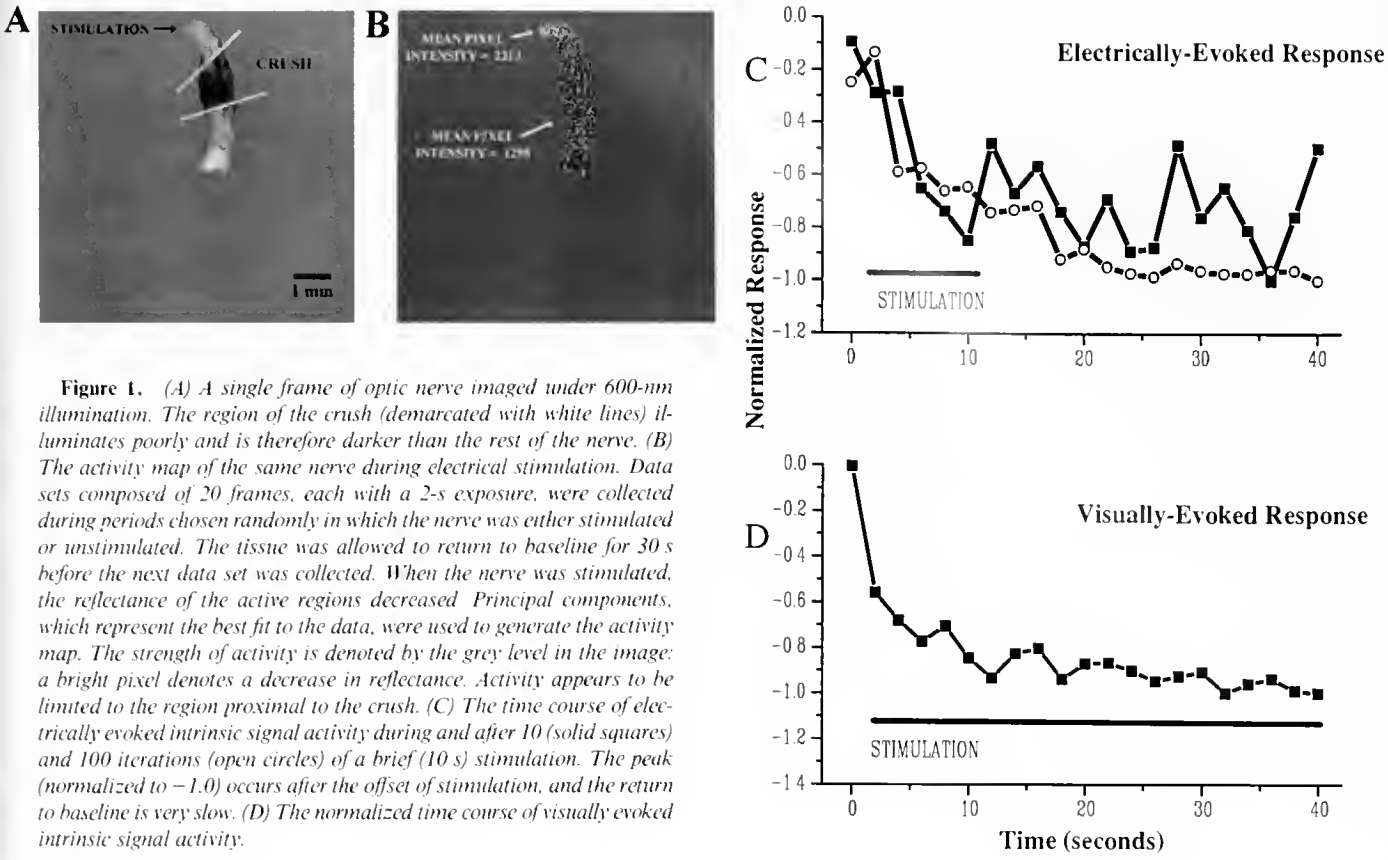

Figure 1. *(A) A single frame of optic nerve imaged under 600-nm illumination. The region of the crush (demarcated with white lines) illuminates poorly and is therefore darker than the rest of the nerve. (B) The activity map of the same nerve during electrical stimulation. Data sets composed of 20 frames, each with a 2-s exposure, were collected during periods chosen randomly in which the nerve was either stimulated or unstimulated. The tissue was allowed to return to baseline for 30 s before the next data set was collected. When the nerve was stimulated, the reflectance of the active regions decreased. Principal components, which represent the best fit to the data, were used to generate the activity map. The strength of activity is denoted by the grey level in the image: a bright pixel denotes a decrease in reflectance. Activity appears to be limited to the region proximal to the crush. (C) The time course of electrically evoked intrinsic signal activity during and after 10 (solid squares) and 100 iterations (open circles) of a brief (10 s) stimulation. The peak (normalized to −1.0) occurs after the offset of stimulation, and the return to baseline is very slow. (D) The normalized time course of visually evoked intrinsic signal activity.*

Our results indicate that optical intrinsic signals can be recorded from visual pathways in the invertebrate nervous system. These intrinsic signals should be fruitful for studying spatially localized regions of activity and for differentiating the variables which contribute to the intrinsic signal.

This work is supported by NSF grant BNS9309539 and NIH grants EY06476, EY00667, and MH49741. E. V. O'Brien is a Grass Fellow at the Marine Biological Laboratory, Woods Hole.

Literature Cited

1. **Grinvald, A., R. D. Frostig, E. Lieke, and R. Hildesheim. 1988.** *Physiol. Rev.* **68:** 1285–1366.
2. **Hill, D. K., and R. D. Keynes. 1949.** *J. Physiol.* **108:** 278–281.
3. **Cohen, L. B., R. D. Keynes, and B. Hille. 1968.** *Nature* **218:** 438–441.
4. **Sirovich, L., and R. M. Everson. 1992.** *Int. J. Supercomp. App.* **6(1):** 50–68.
5. **Cohen, L. B., and R. D. Keynes. 1971.** *J. Physiol.* **212:** 259–275.

Reference: *Biol. Bull.* **189:** 213–215. (October/November, 1995)

Limulus Is Tuned into Its Visual Environment

C. L. Passaglia, F. A. Dodge, and R. B. Barlow (Syracuse University, Syracuse, New York 13244)

Every spring millions of horseshoe crabs invade the shallow waters along the eastern coast of North America in search of mates. Behavioral studies show that male crabs use vision to find mates, whereas female crabs use vision to avoid other nesting crabs (1, 2, 3). Horseshoe crabs reliably detect one another under a variety of environmental lighting conditions despite differences in the contrast of their carapaces. They must also cope with visual interference from water turbidity, seaweed, fish, sandbars, etc. Under these conditions, it is remarkable that male crabs can detect black and grey cylindrical targets of similar size and contrast as females equally well day and night (3). *Limulus* appears to achieve such visual performance by tuning into the natural fluctuations of light in its environment.

How do males detect low-contrast objects such as a grey target or a female crab of light carapace (Fig. 1A)? We approach this question by recording the spike discharges of single optic nerve

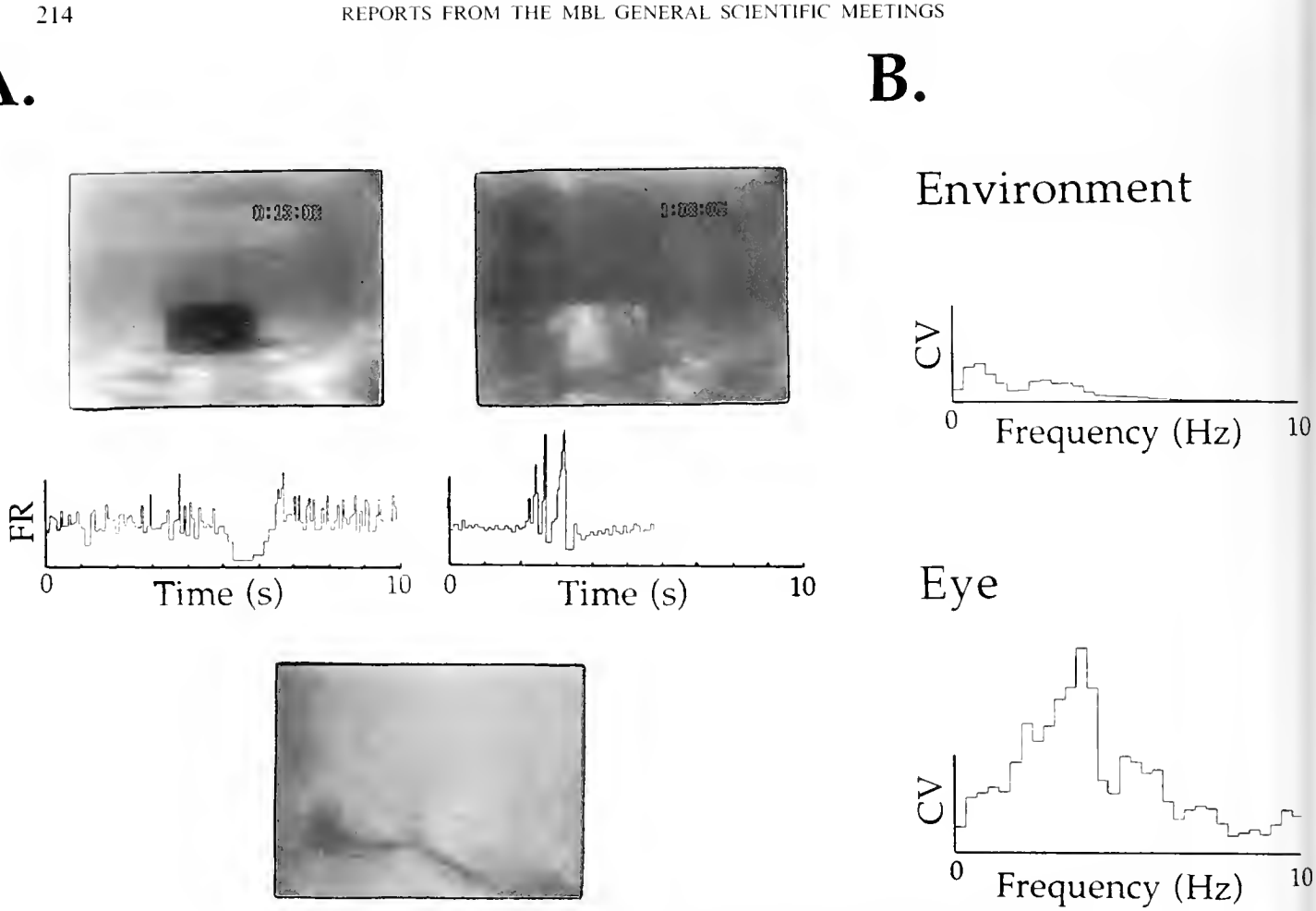

Figure 1. *(A) Top. Images of a black target, grey target, and female horseshoe crab taken with an underwater videocamera mounted on a crab and aligned in the direction of view of the recorded ommatidium. Notice the bands of light reflected from the grey target and female. Bottom: The optic nerve responses recorded from single ommatidia as the crab moved past the above targets. The average instantaneous firing rates (FR) when the ommatidium was not viewing the target were ~14 and ~11 impulses per second for the left and right experiments respectively. (B) Top. Power spectrum of the light signal reflected from the grey target. Bottom. Power spectrum of the train of optic nerve impulses recorded from a single ommatidium viewing the grey target. Notice that the eye amplifies the environmental light signals in the 2–4 Hz range while attenuating those at lower frequencies. For the purpose of comparison, the power spectra of the light signal and spike train were plotted (bin width of 0.3 Hz) on a common ordinate scale after normalization by the square of their respective means.*

fibers while a crab is moving freely in the ocean or is pulled along a track (4). We mount a small underwater camera above the eye, align it with the optic axis of the recorded unit, and record what the crab sees as it passes by an object of known contrast. We store the images and spikes on vidcotape for subsequent analysis with NIH-Image and other software installed in a 660AV Macintosh computer.

Black and grey targets modulate the firing rate of optic nerve fibers as they move past the eye (Fig. 1A). Despite their difference in contrast, both targets evoke sizeable responses consistent with the male's ability to find them (2). High-contrast black targets decrease the firing rate of optic nerve fibers, whereas low-contrast grey targets generally increase the firing rate in a quasi-periodic manner. Such peculiar responses to grey targets in the ocean are unlike those evoked by uniform large-field stimuli in the laboratory.

The source of the large periodic responses to low-contrast grey targets appears to be the natural fluctuations of light in the animal's underwater environment. As waves move overhead, they focus light onto the sandy bottom that sweep across the scene at a rate of 2–4 Hz. The flickering light highlights reflective surfaces against the murky background that scatters light and degrades the appearance of objects. As a result, grey targets and horseshoe crabs generate bright, quasi-periodic signals that stimulate units in synchrony with the traveling overhead waves (Fig. 1A). Because the periodic signals also move through space, the

activity of nearby receptors in the eye that see an object becomes correlated (5).

The lateral eye is highly sensitive to the flickering light from the overhead waves. A large component of the light reflected from grey targets centers at ~2–4 Hz which is the peak of the temporal transfer function of the eye (Fig. 1B; 6, 7, 8). Phototransduction mechanisms set the underlying shape of the transfer function, which two inhibitory processes then sharpen and amplify (6, 7). As a result, the power spectrum of the spike train recorded from receptors viewing the grey target grows considerably in the range of 2–4 Hz (Fig. 1B).

In this paper we show that a consideration of the natural environment of an animal can lead to a better understanding of its visual system. The *Limulus* eye appears to be adapted to a particular feature of its environment—the flickering light reflected off the carapace of a potential mate. These light signals help males detect a female irrespective of the contrast of her carapace. Frequency tuning of vision is not unique to horseshoe crabs and has been observed in many animals, such as cats (9) and humans (10). Perhaps their lighting environment also deserves a closer look.

Supported by NSF grant BNS9309539 and NIH grants MH49741 and EY00667.

Literature Cited

1. **Barlow, R. B., L. C. Ireland, and L. Kass. 1982.** *Nature* **296:** 65–66.
2. **Powers, M. K., R. B. Barlow, and L. Kass. 1991.** *Vis. Neurosci.* **7:** 179–186.
3. **Herzog, E. H., M. K. Powers, and R. B. Barlow. 1996.** *Vis. Neurosci.* in press.
4. **Herzog, E. H., C. L. Passaglia, S. A. Dodge, N. D. Levine, and R. B. Barlow. 1993.** *Biol. Bull.* **185:** 307–308.
5. **Dodge, F. A., D. M. Porcello, S. A. Dodge, E. Kaplan, and R. B. Barlow. 1994.** *Biol. Bull.* **187:** 261–262.
6. **Ratliff, F., B. W. Knight, J. Toyoda, and H. K. Hartline. 1967.** *Science* **158:** 392–393.
7. **Knight, B. W., J. Toyoda, and F. A. Dodge. 1970.** *J. Gen. Physiol.* **56:** 421–437.
8. **Batra, R. and R. B. Barlow. 1990.** *J. Gen. Physiol* **95:** 229–244.
9. **Frishman, L. J., A. W. Freeman, J. B. Troy, D. E. Schweitzer-Tong, and C. Enroth-Cugell. 1987.** *J. Gen. Physiol.* **89:** 599–628.
10. **Robson, J. G. 1966.** *J. Opt. Soc. Am.* **56:** 1141–1142.

Reference: *Biol. Bull.* **189:** 215–216. (October/November, 1995)

Flutter-Like Response in Visual Cortex of the Semi-Isolated Turtle Brain

James C. Prechtl (Marine Biology Research Div., Scripps Institution of Oceanography, University of California San Diego, La Jolla, California 92093-0202)

There is increasing evidence that high-frequency synchronization of specific, distributed neuron populations is a reliable correlate of some forms of sensory processing (1, 2) and of some attentive sensori-motor behaviors (3, 4, 5). The function and fine structure of such responses is, however, still unclear. In the turtle, every salient change in retinal input, whether due to a stimulus or self-induced by visual orienting, is correlated with widely distributed 20-Hz field potentials in its visual cortex (6). The oscillation has a spindle form and its amplitude and frequency modulates with a slow potential of <4 Hz. Although this response represents increased coherence in the 15- to 25-Hz band between spatially separated loci, recent analyses with linear electrode arrays show that, along the rostro-caudal axis, systematic phase lags are observed between most waves (7). The phase lags change from cycle to cycle and represent velocities between 0.05 and 0.3 m/s. Synchronous cycles also occur in each response. Although this response has been called an oscillation, its complex temporal and spatial features suggest that a better descriptor would be the term "flutter" (*i.e.*, a rapid, nonstationary undulation). Here I report that a flutter-like response is also observed with visual stimulation in a semi-isolated brain preparation (epipial 11-electrode linear array, 250 μm spacing). The flutter-like response is contrasted with a more regular and synchronous type of oscillation that was induced in three of the preparations with DC electrical stimulation.

The semi-isolated brain is prepared by sectioning cranial nerves V–XII and the spinal cord under anesthesia (NIH guidelines), followed by intravascular perfusion with oxygenated artificial cerebrospinal fluid (8). Although this preparation lacks the tonic somatic and visceral afference of an intact animal, moving stimuli (black bar, 20-cm distant, 8.5 cm/s) still induce a flutter response.

Figure 1 (upper traces) shows a high-amplitude segment of visually induced responses recorded, 2 mm apart, from the rostral (solid line) and caudal (dotted) poles of the visual cortex. Annotated time intervals indicate wave lags; intermediate lags are also recorded from the middle seven electrodes (data not shown). The lower superimposed oscillatory responses in Figure 1, recorded with the same electrodes, were induced after 9 s of anodal DC stimulation with a blunt surface electrode placed on the

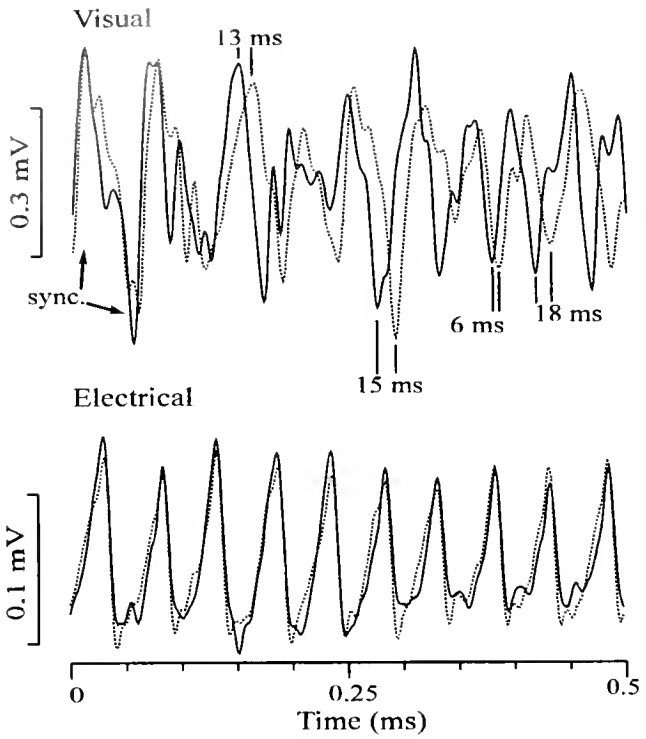

Figure 1. *Visually (upper traces) and electrically (lower) induced local field potential oscillations recorded from rostral (solid trace) and caudal (dotted, 2-mm span) electrodes in turtle visual cortex. Annotation on upper traces indicates synchronous and lagged cycles. Lower traces show the highly regular oscillation recorded from the same loci during DC electrical stimulation (digital band pass-5–100 Hz; 1024 pts/s).*

lateral margin of the visual cortex. The responses to electrical stimulation in the three animals studied were complex and varied over time, but they all included 1–2-s intervals in which more than 95% of the waves in the 15–25 Hz band appeared synchronous (*i.e.*, <3 ms lag/mm; Fig. 1 lower traces). In contrast, 1-s samples from visually induced responses in the same animals never included more than 4 waves of near synchrony (*i.e.*, <25%) (Fig. 1, top traces). These results indicate that although the turtle's visual cortex is capable of spatially synchronizing along the rostro-caudal axis in the 20-Hz band, visual stimulation in both the intact and semi-isolated brain induces a flutter-like response that is dominated by systematic phase differences. In the awake and attentive animal, flutter occurs during changes in visual processing. The possible role of this response in cognitive processing remains to be discovered.

This work was inspired by discussions with M. Hofmann and T. H. Bullock, and supported by NINDS grants to THB.

Literature Cited

1. **Freeman, W. J. 1959.** *J. Neurophysiol.* **22:** 644–666.
2. **Gray, C. M. 1994.** *J Comput Neurosci* **1:** 11–38.
3. **Bouyer, J. J., C. Tilquin, and A. Rougeul. 1983.** *EEG Clin. Neurophysiol.* **55:** 180–187.
4. **Murthy, V. N., and E. E. Fetz. 1992.** *Proc. Natl. Acad. Sci. U.S.A* **89:** 5670–5674.
5. **Nicolelis, M. A. L., L. A. Baccala, R. C. S. Lin, and J. K. Chapin. 1995.** *Science* **268:** 1353–1358.
6. **Prechtl, J. C. 1994.** *Proc. Natl. Acad. Sci. U.S.A.* **91:** 12467–12471.
7. **Prechtl, J. C., and T. H. Bullock. 1995.** Proc. 2nd Joint Symp. Neural Comp, CalTech-UCSD Institute for Neural Computation, UC San Diego (in press).
8. **Mori, K., M. C. Nowycky, and G. M. Shepherd. 1981.** *J. Physiol. (Lond.)* **314:** 281–294.

Reference: *Biol Bull* **189:** 216–218. (October/November, 1995)

The Neurofilamentous Network–Smooth Endoplasmic Reticulum Complex in Transected Squid Giant Axon

J. Metuzals (University of Ottawa), H. M. Fishman, and I. A. Robb

At the cytoskeleton-membrane interface, Ca^{2+}-activated proteases (calpain system) influence important signal pathways that control the diverse behavior of intracellular proteins and organelles (1). Characteristic changes of membranes in association with cytoskeletal assemblies occur in nervous tissue after injury and in neurodegenerative diseases (2). The squid giant nerve fiber provides a simple, easily utilized model with which to explore the basic mechanisms of cytoskeletal interactions with membranes. We have used transmission electron microscopy of squid (*Loligo pealei*) giant nerve fibers to identify the factors that initiate the degenerative events that follow transection in Ca^{2+}-containing seawater.

The fibers were fixed in a standard glutaraldehyde-formaldehyde mixture (Figs. 1A–C), and some were also treated with osmium tetroxide-potassium ferrocyanide (Fig. 1D) which enabled the observation of Ca^{2+}-containing structures (3). Electron micrographs of transected fibers were compared with many series of electron micrographs of normal fibers prepared under different conditions of fixation and embedding. The dynamic behavior of the neurofilamentous network (NFN) associated with the axolemma and with the subaxolemmal cisternae of the smooth endoplasmic reticulum (SER) in the squid giant axon has been suggested, and Ca^{2+} has been localized in the subaxolemmal cisternae (4). The NFN is altered by Ca^{2+}-activated proteases, and the cleaved products reassemble into characteristic aggregates (5). The sinuous form of the tubules constituting the SER and their association with neurofilaments have been observed (6); the authors concluded that the tubules were primarily regulating the concentration of Ca^{2+} in the axoplasm.

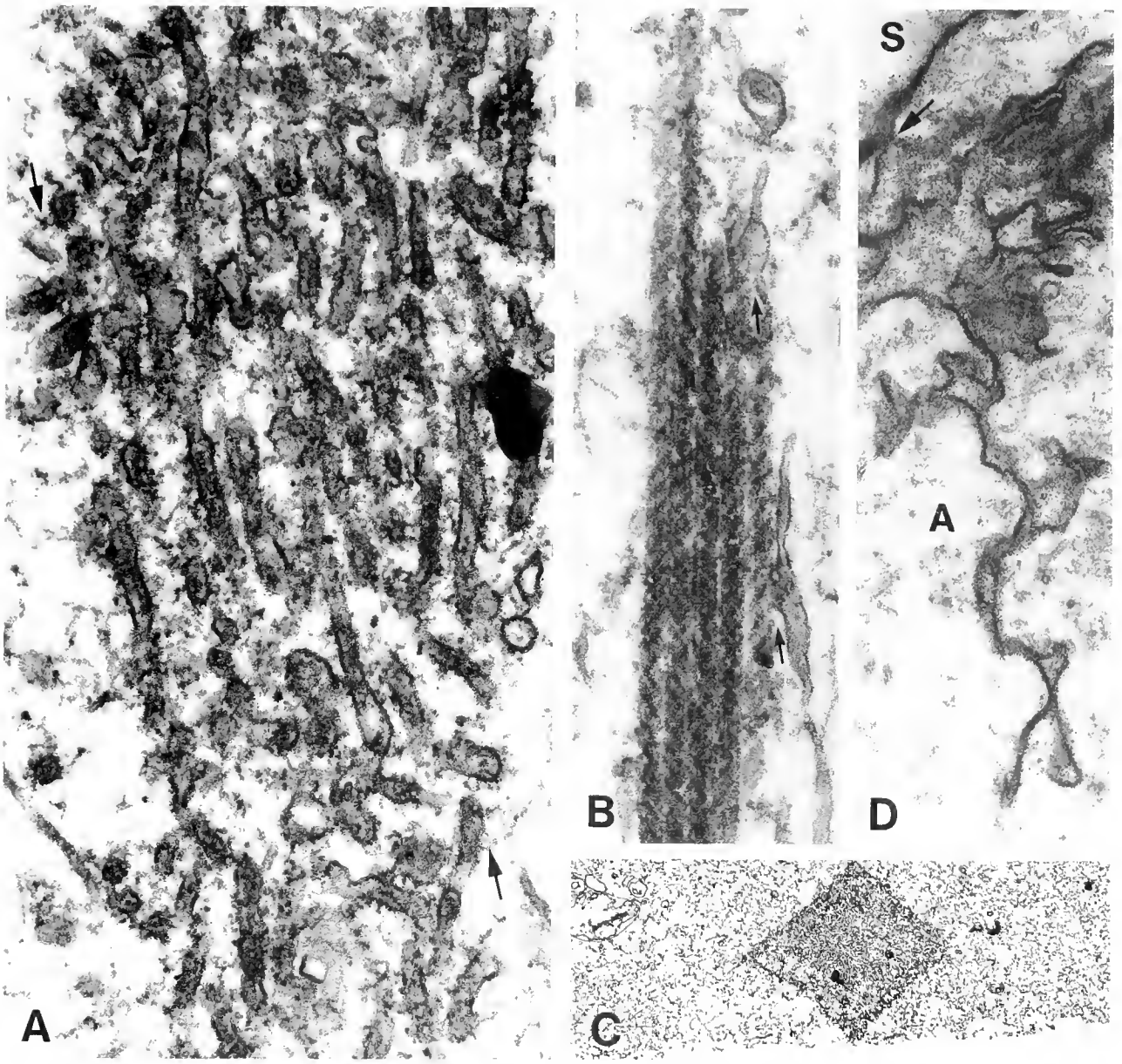

Figure 1. *(A) NFN-SER complex localized in the axoplasm close to the cortex. The NFN surrounds the profiles of the SER and extends to the tubes (arrows). × 104,000. (B) Paracrystalline helical braids consisting of intercoiled strands, fibers and filaments. Associations with SER (arrows). × 75,000. (C) Rectangular densities of debris of filaments and SER surrounded by modified neurofilaments. × 15,000. (D) Twisted, osmiophilic protrusions of NFN-SER complex deep into the axoplasm, contact of the complex with the axolemma (arrow). axon (A), Schwann cell (S). Osmium tetroxide-potassium ferrocyanide. × 100,000. All fibers were transected 10 min before fixation.*

Five hallmarks of pathologically modified NFN-SER complex were identified in the transected axons: (a) Characteristic *aggregates* of SER tubes, surrounded by NFN can be identified close to the cortex of the axoplasm (Fig. 1A). The tubes are not parallel to each other and often show a sinuous form. The NFN also appears to be attached to the tubes (Fig. 1A, arrows). (b) *Braided* structures composed of filaments, in association with NFN and SER, can be seen (Fig. 1B). (c) *Paracrystalline domains* (not shown) of modified NFN surrounded by modified SER were observed close to the transection site. (d) *Rectangular dense bodies* (Fig. 1C) of modified NFN and SER are also found close to the cut axonal end. Finally (e), osmium tetroxide-ferrocyanide stained *finger-like protrusions* of the NFN-SER complex (Fig. 1D) extend from the axoplasmic cortex deep into the axoplasm. The staining of these structures indicates the presence of Ca^{2+}. A gradual transition from normal NFNs to modified ones can be observed in micrographs, indicating that the modified filaments originate from the NFN.

Our observations of the structural modifications induced by injury (transection) support our hypothesis that

the NFN-SER complex is highly dynamic. The origin of the different structures of the NFN-SER complex in transected axons (Fig. 1A–D) can be explained by the activation of different calpains which are dependent on intracellular pH and Ca^{2+} concentration (1). The formation of braided paracrystalline assemblies and dense bodies may reflect similar basic mechanisms operating in neurodegenerative diseases (7).

In summary, transection induces segregation, modification, and reassembly of the components of the NFN-SER complex. Consequently, we conclude that the NFN and the SER are complex and interactive structures that are likely to have an important role both in response to injury and in the pathogenesis of neurodegenerative diseases.

Supported by NIH grant NS31256.

Literature Cited

1. **Nixon, R. A., K. I. Saito, F. Grynspan, W. R. Griffin, S. Katayama, T. Honda, P. S. Mohan, P. S. Shea, and M. Beermann. 1994.** Pp. 77–91 in *Calcium Hypothesis of Aging and Dementia* J. F. Disterhoft, W. H. Gispen, J. Traber, and J. Khachaturian, eds. Ann. NY Acad. Sci. vol 747, Plenum, NY.
2. **Fishman, H. M., and J. Metuzals. 1993.** *Biol. Bull.* **185:** 292–293.
3. **Hayat, M. A. 1989.** *Principles and Techniques of Electron Microscopy.* CRC Press, Inc., Boca Raton, Florida.
4. **Metuzals, J., I. Tasaki, S. Terakawa, and D. F. Clapin. 1981.** *Cell Tissue Res.* **221:** 1–15.
5. **Metuzals, J., H. Pant, H. Gainer, P. A. M. Eagles, N. S. White, and S. Houghton. 1988.** *Cell Tissue Res.* **252:** 249–262.
6. **Burton, P. R., and L. A. Laveri. 1985.** *J. Neurosci.* **5:** 3047–3060.
7. **Hill, W. D., V. M.-Y. Lee, H. I. Hurtig, J. M. Murray, and J. Q. Trojanowski. 1991.** *J. Comp. Neurol.* **309:** 150–160.

Reference: *Biol. Bull.* **189:** 218–219. (October/November, 1995)

Fluorescent Labeling of the Glial Sheath of Giant Nerve Fibers

C. S. Eddleman (University of Texas Medical Branch), C. M. Godell, H. M. Fishman, M. Tytell, and G. D. Bittner

Glial-axonal interactions are essential for the maintenance and regulation of vital axonal processes, including the response to injury and heat shock (1, 2). Interactions between adaxonal glia and axons have been reported for intact and severed axons from squid (3) and crayfish (4). But many putative glial functions have not been documented in living tissue because the adaxonal glial layer is only 2–6 μm thick and is not easily localized with certainty in conventional light microscopy. We now report that the cell membrane permeable fluorogenic substrate calcein acetoxymethyl (AM) ester, which is converted to an impermeable and fluorescent derivative by esterases, differentially labels the adaxonal glial cells and other structures in the glial sheath surrounding the squid giant axon (GA) and the crayfish medial giant axon (MGA).

Giant axons from squid (*Loligo pealei*) and crayfish (*Procambaris clarkii*) were excised and isolated as described previously (3, 5). Isolated GAs were placed in 0.5 ml of artificial seawater (ASW: 430 m*M* NaCl, 5 m*M* KCl, 10 m*M* $CaCl_2$, 50 m*M* $MgCl_2$, Tris-Cl buffered to pH 7.4 at room temperature); and isolated MGAs were placed in van Harreveld's solution (vanH: 205 m*M* NaCl, 5.4 m*M* KCl, 13.5 m*M* $CaCl_2$, 2.6 m*M* $MgCl_2$, 10 m*M* HEPES buffered at pH 7.35 at room temperature) contained in a chamber constructed of wax or petroleum jelly on a glass slide. GAs and MGAs were pulse-loaded with calcein AM, which is pH- and temperature-insensitive under physiological conditions, by incubation for 10 min in ASW or vanH containing 1 μ*M* calcein AM, followed by replacement with ASW or vanH without calcein AM. A glass coverslip was placed over the preparation to minimize evaporation and changes of osmolality. Axons were viewed with a laser-scanning confocal microscope (Zeiss, LSM-410) at wavelengths of 488 and 568 nm. After calcein AM was removed from the external bath, observations were made for up to 2 h without significant change in the distribution of fluorescence intensity. The intensity of the stored digital image was scanned with Zeiss LSM software (version 3.8).

Within 5 min after the removal of calcein AM from the bath, both differential image contrast (DIC, Fig. 1A, B) and confocal fluorescent images (Fig. 1C, D) were obtained. Fluorescence intensity scans of axonal cross sections showed a pronounced difference in fluorescence intensity (Fig. 1C, D) between the axoplasm and sheath. In separate experiments (not shown), the axoplasm was loaded with hydrophilic fluorescent dye (Texas Red) before exposing the giant axons to calcein AM for 10 min. Calcein fluorescence was observed as a thin (6–12 μm) band surrounding a central core of Texas Red fluorescence, indicating that the sheath surrounding the axons was predominantly labeled by calcein, and the axoplasm by Texas Red. When calcein AM remained in the bath for up to 1 h, the fluorescence intensity of the axoplasm uniformly increased with time. Nevertheless, even after 1 h, calcein fluorescence was always significantly lower in the axon than in the sheath. One interpretation of these data is that the esterase level in the axoplasm is much lower than that in the adaxonal glia and other sheath structures. Images of the sheath at higher magnification (Fig. 1E, F) showed that the thickness of the calcein fluorescence band (glial layer of the sheath) was about 2.5 μm in the GA and about 5 μm in the MGA, in agreement with previous values obtained by electron microscopy from fixed GAs (3, 6) and MGAs (7). To ensure that calcein AM filled the adaxonal glial cells, acridine orange, a fluorescent nucleic acid dye, was also used to localize the nuclei in the glial cytoplasm. The resulting fluorescence band (data not shown) corresponded well to the glial localization made with calcein AM (Fig. 1E, F).

In summary, our data from GAs and MGAs indicate that adaxonal glia and other structures in the glial sheath may have a greater esterase activity than does axoplasm, thereby producing a more intense fluorescence band of calcein in the sheath compared to the axoplasm. Furthermore, these observations provide evidence that calcein AM can be used to preferentially label the sheath, in particular the glial cell cytosol, in contrast to previous

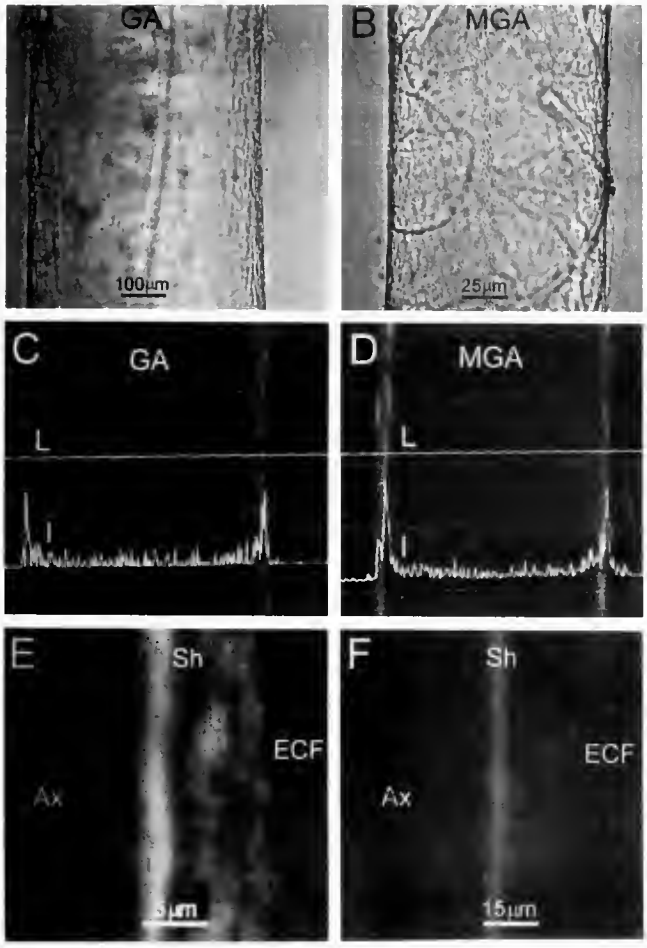

Figure 1. *(A, B) DIC images of a squid giant axon (GA) and a crayfish medial giant axon (MGA) in artificial seawater (ASW) and van Harreveld's solution (van H), respectively. (C, D) Confocal, fluorescence (at 488 nm) images of the corresponding axon segments in (A) and (B). Five minutes after calcein AM removal from the bath, intensity (I) along scan line (L) across the fluorescence images shows deviations above background (baseline) in the axon and suggests the presence of axoplasmic esterases, albeit at a lower concentration than that of the sheath (marked by the fluorescence band and the two peaks in I). Thin, horizontal lines constitute the intensity scale: 0, 20, 40, 60, and 80% maximum intensity, with 0 corresponding to the lowest line. (E, F) Higher magnification confocal, fluorescence (at 488 nm) images of GA and MGA segments. The glial thickness is ~2.5 μm in the GA and ~5 μm in the MGA. The presence of calcein in other sheath structures surrounding the GA (E) can be seen. Notice that 5 min after pulse-labeling these axons with calcein AM, fluorescence in the axon (Ax) and extracellular fluid (ECF) is undetectable, but the sheath (Sh) fluoresces intensely. All confocal images are optical sections (<5 μm thick) through the longitudinal axis of an axon.*

markers of glial cell nuclei, providing a significant new method for evaluating glial-axonal interactions in the living preparation.

We thank Louis Kerr and Carl Zeiss Inc. for use of equipment and facilities. Supported by NIH (NS31256) and ATP (003658-296).

Literature Cited

1. **Lieberman, E. M., P. T. Hargittai, and R. M. Grossfeld. 1994.** *PIN* **44:** 333–376.
2. **Bittner, G. D. 1991.** *TINS* **14(5):** 188–93.
3. **Krause, T. L., H. M. Fishman, M. Ballinger, and G. D. Bittner. 1994.** *J. Neurosci.* **14:** 6638–6651.
4. **Eddleman, C. S., C. M. Godell, H. M. Fishman, and G. D. Bittner. 1995.** *J. Neurochem.* **64:** S25D.
5. **Sheller, R., and G. D. Bittner. 1992.** *Brain Res.* **580:** 68–80.
6. **Villegas, G. M., and R. Villegas. 1968.** *J. Gen. Physiol.* **51:** 44s–60s.
7. **Ballinger, M., and G. D. Bittner. 1980.** *Cell Tiss. Res.* **208:** 123–133.

Reference: *Biol. Bull.* **189:** 219–220. (October/November, 1995)

Effect of pH Buffers on Proton Secretion from Gastric Oxyntic Cells Measured with Vibrating Ion-Selective Microelectrodes

Jeffery R. Demarest (Department of Biology, Juniata College, Huntingdon, PA 16652) and James L. M. Morgan

Assessing proton pump (H^+/K^+-ATPase) activity in isolated mammalian gastric oxyntic cells has been possible only with indirect methods, such as the measurement of oxygen consumption, or the accumulation of weak bases (*e.g.*, ^{14}C-aminopyrine) in acid-containing compartments formed within the cells by the sealing off of the cannalicular-secretory membrane (1). In contrast, non-mammalian gastric oxyntic cells do not form an intracellular cannaliculus or other acid-accumulating compartment. Oxyntic cells enzymatically isolated from *Necturus* gastric mucosa retain apical to basolateral membrane polarity and exhibit the pronounced increase in apical membrane area and the activation of Cl channels that characterizes their stimulation in the intact mucosa (2). But the absence of any acid-accumulating compartment prevented us from determining whether these cells were actually secreting protons in response to stimulation. We have, therefore, turned to vibrating ion-selective electrodes to measure proton secretion by discrete regions of the membranes of individual isolated *Necturus* oxyntic cells. Proton selective liquid ion-exchange (Fluka Hydrogen Ionophore Cocktail B) microelectrodes with tip diameters of 1–2 μm and 90% response times of ≤300 mS were vibrated at 0.3–0.5 Hz over a distance of 10–15 μm at a distance of ~1 μm from the apical or basolateral surface of isolated oxyntic cells. Proton fluxes were calculated from the difference in $[H^+]$ measured at the extremes of the electrode excursion and the rate of diffusion of H^+ in the bathing media. In order to maintain the bulk so-

lution at a stable pH near normal for these animals (7.9 at 22°C) and a bicarbonate level sufficient to support acid secretion, proton fluxes were measured in lightly buffered ([HEPES] = 1 m*M*) bicarbonate-containing media ($[HCO_3^-]$ = 5 m*M*). However, the inclusion of buffers in the media attenuates the extracellular proton gradient by dramatically increasing the already high mobility of protons in aqueous solution.

Proton secretion from a cell produces a gradient of concentration that decreases from the cell surface outward into the bathing medium. In an unbuffered medium the concentration profile of this gradient, as a function of distance from the cell surface, constantly changes with time as protons accumulate in the media adjacent to the cell. By facilitating the diffusion of protons, inclusion of pH buffers in the solution tends to dissipate the gradient more rapidly than simple diffusion alone. In addition to providing a stable pH in the bulk solution for reference, buffers also stabilize the concentration profile, thus producing a standing gradient. To calculate the total flux of protons (^TJ_H) from vibrating electrode measurements in the presence of buffers, the diffusional (^DJ_H) and facilitated (^FJ_H) movement of protons down the gradient must be taken into account.

$$^TJ_H = {}^DJ_H + {}^FJ_H \quad (1)$$

The diffusional flux of protons (^DJ_H) is equal to the product of the diffusion coefficient for protons (D_H) and the proton gradient ($d[H^+]/dx$),

$$^DJ_H = D_H \cdot (d[H^+]/dx) \quad (2)$$

and the facilitated flux can be shown to be (3),

$$^FJ_H = D_{B1} \cdot (d[B1]/dx) + D_{B2} \cdot (d[B2]/dx) + \cdots + D_{Bn} \cdot (d[Bn]/dx) \quad (3)$$

where D_{B1} is the diffusion coefficient of a buffer species and (d[B1]/dx) is the gradient of concentration of the proton acceptor form of the buffer. Dividing equation (3) by (2) yields:

$$^FJ_H/{}^DJ_H = (D_{B1}/D_H) \cdot (d[B1]/d[H^+]) + (D_{B2}/D_H) \cdot (d[B2]/d[H^+]) + \cdots + (D_{Bn}/D_H) \cdot (d[Bn]/d[H^+]). \quad (4)$$

The terms ($d[B1]/d[H^+]$), ($d[B2]/d[H^+]$), etc., are the buffering capacities (β_{B1}, β_{B2}, etc.) of the buffer species, which can be calculated from their respective concentrations and dissociation constants (4):

$$\beta_{Bn} = d(Bn)/d[H] = B/[H^+]\{f/(1 + f)^2\} \quad (4a)$$

where $f = K_d/[H^+]$ and K_d is the dissociation constant.

Substituting the buffering capacities into equation (4), solving for ^FJ_H and substituting into equation (1) yields:

$$^TJ_H = (D_H + D_{B1} \cdot \beta_{B1} + D_{B2} \cdot \beta_{B2} + \cdots + D_{Bn} \cdot \beta_{Bn}) \cdot (d[H^+]/dx). \quad (5)$$

The buffers used in the present experiments effectively enhanced the diffusion of protons by a factor of 2249 (*i.e.*, 1374 by 1 m*M* HEPES and 875 by 5 m*M* HCO_3^-).

We calculated $d[H^+]/dx$ from the probe output as described previously (5). Using literature values for the constants (6) and an estimate for D_{HEPES} of 0.62×10^{-5} cm^2/s, flux density in p*M*/$cm^2 \cdot s$ at the midpoint of the probe excursion (*i.e.*, ~5 μm from the cell surface) was calculated from equation (5).

In resting cells, before activating the H^+/K^+-ATPase, a metabolically dependent, basal level of proton flux was measured uniformly from all surfaces of the cells. After 20–40 min of stimulation of acid secretion with dibutyryl cyclic adenosine monophosphate (1 m*M*), the apical proton flux alone had increased by 270 ± 47% from 8.6 ± 1.8 p*M*/$cm^2 \cdot s$ (mean ± SEM; n = 6). Stimulated, but not basal, apical flux was inhibited by SCH-28080 (10^{-7} *M*), a specific inhibitor of the gastric H^+/K^+-ATPase.

These results indicate that isolated *Necturus* oxyntic cells retain functional secretory polarity as well as morphological polarity. This technique enables the determination of the activity and distribution of an electroneutral ion pump, thereby characterizing net transcellular transport in single isolated secretory epithelial cells.

Supported by the Howard Hughes Medical Institute Undergraduate Biological Sciences Education Program and the National Vibrating Probe Facility. The authors thank Kelley A. Gebhardt and Stephen J. Eikenberry for technical assistance.

Literature Cited

1. **Soll, A. H. 1980.** *Am J Physiol.* **238:** G366–G375.
2. **Demarest, J. R., D. D. F. Loo, and G. Sachs. 1989.** *Science* **245:** 402–404.
3. **Speksnijder, J. E., D. W. Corson, C. Sardet, and L. F. Jaffe. 1989.** *Dev. Biol.* **135:** 182–190.
4. **Edsall, J. T., and J. Wyman. 1958.** *Biophysical Chemistry,* Vol. 1. Academic Press, New York.
5. **Kühtreiber, W. M., and L. F. Jaffe. 1990.** *J. Cell Biol.* **110:** 1565–1573.
6. **Robinson, R. A., and R. H. Stokes. 1959.** *Electrolyte Solutions,* 2nd Ed. Butterworths, London.

Reference: *Biol. Bull.* **189:** 220–222. (October/November, 1995)

Transmission of Polarized Light through Sunfish Double Cones Reveals Minute Optical Anisotropies

Iñigo Novales Flamarique (University of Victoria), Rudolf Oldenbourg, and Ferenc I. Hárosi

Many fish retinas possess paired photoreceptors termed double cones. At the level of the inner segment, tangential cross sections show double cones to be approximately elliptical, with a partitioning membrane along the minor axis of the ellipse (Fig. 1A). Furthermore, the cones are arranged in square or row mosaic patterns.

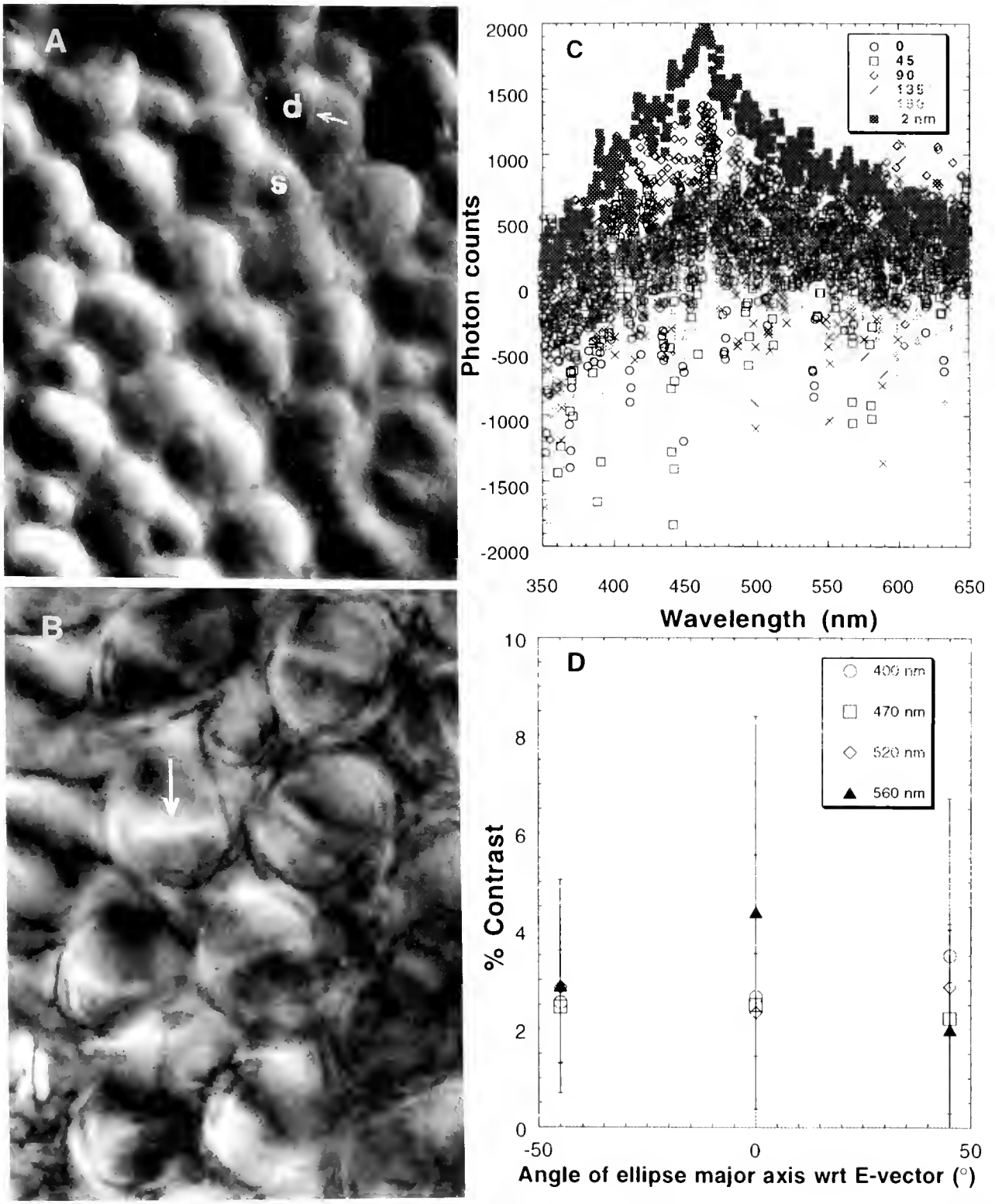

Figure 1. *(A) Differential interference contrast image of sunfish retinal mosaic. d, double cone; s, single cone; arrow points to a partitioning membrane. (B) NPS birefringence image: arrow indicates slow axis of propagation near the partitioning membrane; retardance scale from 0 nm (black) to 2 nm (white). (C) Retardance counts for a double cone at various cone orientations using MSP; top trace was obtained with a 2-nm quartz standard. (D) % contrast for double cone transmission at various cone orientations (n = 5) for 4 wavelengths; % contrast = 2 $(I_{min} - I_x)/(I_{min} + I_x)$, where I_{min} denotes the incident E-vector aligned with the minor axis of the ellipse, and I_x is a variable cone orientation. In (C) and (D), 0° corresponds to the incident E-vector parallel to the major axis of the ellipse.*

The retina of the green sunfish (*Lepomis cyanellus*) is primarily arranged in a square mosaic, with double cones forming the sides of the square (1, 2). Behavioral studies show that this fish can detect the electric field vector of linearly polarized light, exhibiting sensitivity maxima to horizontal and vertical E-vectors (2). These observations led to the hypothesis that polarization detection in this fish relies on the "geometric birefringence" waveguide properties of double cone ellipsoids (3). According to this hypothesis, photons with E-vectors along the major axis of the ellipse would be guided more effectively than those along the minor axis, thus constituting a mechanism for the detection of polarized light.

The experiments presented here were designed to measure the transmission of polarized light through double cones in the retinas of green sunfish and pumpkinseed (*Lepomis gibbosus*). Ventro-temporal retinal quadrants were placed in slide wells filled with Ringer solution, and the preparations were sealed with cover slips. Rod-free areas comprising end-on oriented cones were examined using microspectrophotometry (MSP) and the New Polarized Light Microscope (NPS) (4). We used condensors with 0.45–0.5 NA to approximate physiological illumination. Two types of experiments were conducted. In one type, birefringence was measured as retinal retardance between crossed polarizers for various cone orientations. In the second type, transmission of linearly polarized light fluxes was measured through double cones for various cone orientations.

Results from both instruments show that the retardance for double cone ellipsoids never exceeded 2 nm (Fig. 1B, C), with the highest values found along the partitioning membranes. NPS analysis further showed that the orientation of the slow axis in the elliptical cross section was variable for different locations. In addition, polarization contrast (3), determined from transmitted light fluxes polarized along the minor and major axes, was in the order of 1–3% and showed independence of wavelength (Fig. 1D).

A retardance of 2 nm corresponds to a difference in refractive index of 0.0002 between the slow- and fast-propagating axes of double cones. This difference is about 100 times smaller than the value that can be calculated from the previous waveguide model (3).

We conclude from these studies that the optical anisotropies at the inner segment of cones are very small, and that birefringence-based waveguiding is an unlikely mechanism to explain polarization sensitivity in sunfish. We noticed, however, the possibility that the partitioning membrane of the double cones, which appears to be planar, might act as a dielectric mirror. The polarization anisotropy caused by reflection from such a mirror is consistent with these results.

This work was sponsored by a Grass Fellowship in Neurophysiology to JNF.

Literature Cited

1. **Cameron, D. A., and S. S. Easter, Jr. 1993.** *Vis. Neurosci.* **10:** 375–384.
2. **Cameron, D. A., and E. N. Pugh, Jr. 1991.** *Nature* **353:** 161–164.
3. **Rowe, M. P., N. Engheta, S. S. Easter, Jr., and E. N. Pugh, Jr. 1994.** *J. Opt. Soc. Am. A* **11:** 55–70.
4. **Oldenbourg, R., and G. Mei. 1995.** *J. Microscopy*, in press.

Reference: *Biol. Bull.* **189:** 222–223. (October/November, 1995)

Dogfish (*Mustelus canis*) Lens Catalase Reduces H_2O_2-Induced Opacification

Seymour Zigman, Nancy S. Rafferty, and Mark Schultz (University of Rochester School of Medicine & Dentistry, Rochester, New York, NY 14642, and Marine Biological Laboratory)

Previous studies showed that UV_A radiation *in vitro* causes opalescence in dogfish lenses (1, 2). Protection against this change is afforded by α-tocopherol, which also protects cytoskeletal actin and catalase from damage (2–5). We thus hypothesize that UV_A causes lens opalescence by reducing the activity of the major antioxidative enzyme (6) so that even normal levels of H_2O_2 can oxidize lens constituents and lead to cataracts.

Our purpose was (a) to determine if inhibition of catalase anti-oxidative activity by photooxidation *in vitro* causes opalescence in dogfish lens and (b) to observe the damage produced by UV radiation and the protection afforded by deferoxamine to catalase activity and cytoskeletal proteins.

Dogfish lenses were incubated in elasmobranch Ringer's medium under 95% air and 5% CO_2. Lens clarity was assessed by viewing a pattern of computer-generated fish scales through the lens and by slit-lamp photography. Catalase activity, measured as O_2 production, was determined with an O_2 meter and electrode (Microelectrodes, Inc.). Catalase inhibition and cytoskeletal protein degradation were measured on lenses that received ~9 J/cm^2/h of UV_A (99.9% UV-A, 0.1% UV-B) radiation. Cytoskeletal immunocytochemistry was done on fixed lens epithelia double-labeled with rabbit antibodies *vs* α-tubulin-FITC and rhodamine-phalloidin. Samples were photographed with a Zeiss Axiophot fluorescence microscope.

Our results showed that lenses pre-exposed to 90 J/cm^2 of UV_A and challenged with 0.1 to 1.0 m*M* [H_2O_2] developed dense cortical opalescence (Table Ia). Deferoxamine (10 m*M*) partially protected lens clarity and catalase activity (Table Ib). In irradiated cells, the filamentous nature of microtubules had degraded nearly completely. Fluorescence appeared to be associated with the plasma membranes and microtubule organizing centers. In unirradiated cells, brightly displayed microtubules extended from the nuclei to the periphery of the cell. Deferoxamine partially protected microtubules against the effects described above.

The results lead us to two conclusions. (1) Catalase activity in lens epithelium is inhibited by UV_A so that near-normal levels

Table 1

a. Dogfish lens opacification by H_2O_2 after UV_A Irradiation

Lens treatment	$[H_2O_2]$ m*M*	Results: Verbal	Results: Photograph
Unexposed	0.1	clear	
	1.0	clear	
UV_A-exposed	0.1	opal	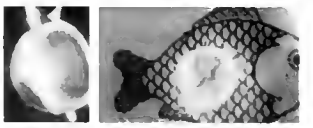
	1.0	opal	

Opal = opalescent; UV_A-exposure 11 h, H_2O_2 exposure 11 h.

b. Deferoxamine protection of lens catalase activity

Lens treatment	% O_2 increase per min	Catalase activity units
Unexposed	4.25 ± 0.86	0.49
Unexposed plus (10 m*M*) deferoxamine	3.05 ± 0.87	0.40
UV_A-exposed	0.75 ± 0.37	0.11
UV_A-exposed plus (10 m*M*) deferoxamine	1.78 ± 0.50	0.24

± = Standard deviation.
UV_A-exposure = 2 mW/cm^2; 18 h; 20°C; Lens weight = 400 ± 50 mg.

of H_2O_2 in the fluid medium (*i.e.*, aqueous humor) can cause lens opalescence. (2) Microtubules are damaged by UV_A radiation and are partially protected by deferoxamine.

This research was supported by the National Eye Institute Ey-00459 and Research to Prevent Blindness Senior Scientific Investigator Award. Thanks to B. R. Zigman for preparation of the manuscript.

Literature Cited

1. **Zigman, S., N. S. Rafferty, and R. B. Wheeler, Jr. 1991.** *Biol. Bull.* **181:** 341–342.
2. **Zigman, S., N. S. Rafferty, D. L. Scholz, and K. Lowe. 1992.** *Exp. Eye Res* **55:** 193–201.
3. **Zigman, S., and N. S. Rafferty. 1994.** *Comp. Biochem. Physiol.* **109A:** 463–467.
4. **Zigman, S., T. McDaniel, J. B. Schultz, J. Reddan, and M. Meydani. 1995.** *Mol Cell Biochem* **143:** 35–46.
5. **Zigman, S., T. Yulo, and G. A. Greiss. 1976.** *Mol Cell. Biochem.* **11:** 131–135.
6. **Fuchs, J., T. Hufelet, L. M. Rothfuss, D. S. Wilson, G. Carcamo, and L. Packer. 1989.** *Photochem Photobiol.* **50:** 739–744.

Reference: *Biol. Bull.* **189:** 223–225. (October/November, 1995)

Sulfotransferase Activities in the Marine Sponge *Microciona prolifera:* Correlation with Sulfated Glycan Adhesive Structures

William J. Kuhns, Max M. Burger, and Gradimir Misevic (Marine Biological Laboratory)

Sulfated glycans in matrix and on cell membranes mediate a variety of cell functions (1, 2). Their highly charged nature is known to influence cell-cell adhesion and cell communication (3, 4). Sulfated structures have been demonstrated in the adhesive proteoglycan (AP) of *Microciona* with a specific aggregation-blocking monoclonal antibody termed Block 2 that reacted with purified proteoglycan oligosaccharides. One epitope was identified as a sulfated disaccharide, 3-SO_3-*N*-acetylglucosamine-β1-

3-fucose. A second nonreactive compound was identified as a sulfated galactose-linked tetrasaccharide (5). On the basis of these structures, we predict that sponge tissue contains specific sulfotransferases (sulfo-T) as the biosynthetic enzymes involved in the sulfation process.

To explore this possibility, we performed assays for sulfo-T using Triton-extracted sponge microsomes (7.5–12.5 mg/ml) in the presence of chemically defined monosaccharide acceptor substrates at concentrations of 20–320 n*M*. The co-substrate and active sulfate donor was radiolabeled 3′-phosphoadenosine 5′-phosphosulfate ((^{35}S)PAPS) 7 μM (2145 dpm/pmol) in the presence of pyrophosphatase and sulfatase inhibitors and 10 m*M* Mg^{2+} buffered at pH 6.3. The total volume of the reaction mixture was 40 μl (6). After incubation for 1 h at 37°, the reaction was terminated by adding 10 μl of 2% sodium borate/20 m*M* EDTA. Separation of unreacted PAPS from sulfated product was accomplished by thin-layer chromatography using a solvent system containing acetonitrile, water and methanol (4:1:0.2), or high-voltage electrophoresis using 1% sodium borate buffer at pH 9.1. The figures for product yield, expressed as picomoles, were the average of duplicate values from which had been subtracted picomoles present in endogenous assays in which acceptor had been omitted. The biosynthesized product was expressed as picomoles per hour per milligram of protein (pmol/h/mg).

Acceptor substrates were monosaccharides or derivatized monosaccharides representing sugars known to occur in *Microciona* AP. They included β-D-fucose, α-L-fucose, β-D-glucuronide phenyl, β-phenyl-*N*-acetyl-D-glucosamine(GlcNAc), phenyl-*N* acetyl-α-D-galactosamine(GalNAc), phenyl-α-D-mannoside and phenyl-β-D-galactoside(Gal). Of these, phenyl-GlcNAc and phenyl-Gal gave measurable product yields, but assays using 5 m*M* phenyl (phenol) alone were negative. In the case of phenyl-GlcNAc, substrate-product curves generated from assays with graded quantities of acceptor (20 to 320 nmol) demonstrated V_{max} and K_m values of 50 pmol/h/mg and 1 m*M*, respectively. The proposed reaction is visualized as follows:

GlcNAc-0-phenyl

$$+ (^{35}\text{S})\text{PAPS} \xrightarrow{\text{sulfo-T}} {}^{35}\text{SO}_3\text{-0-GlcNAc-0-phenyl} + \text{PAP}.$$

Final confirmation of the position of the sulfate linkage will require additional detailed analyses of scaled-up quantities of product (6).

The cellular localization of sulfated glycan was determined by immunohistochemical techniques on fixed sections of washed *Microciona* cell pellets stained with Block 2 primary antibody and horseradish peroxidase-labeled secondary antibody. A mixed pattern of stained and nonstained cells was found, with the most intense staining present intracellularly and on surface membranes of the larger cell population, including cells interpreted as archeocytes (Fig. 1). This finding suggests that immunoseparation of a selected cell cohort may be a useful preparative technique when preparing purified enzyme.

In summary, the enzyme activities defined in this study are consistent with earlier findings of sulfated glycan structures (5) and suggest that quantitative recoveries of pure enzymes will be of importance in studying their regulatory role in sponge cell

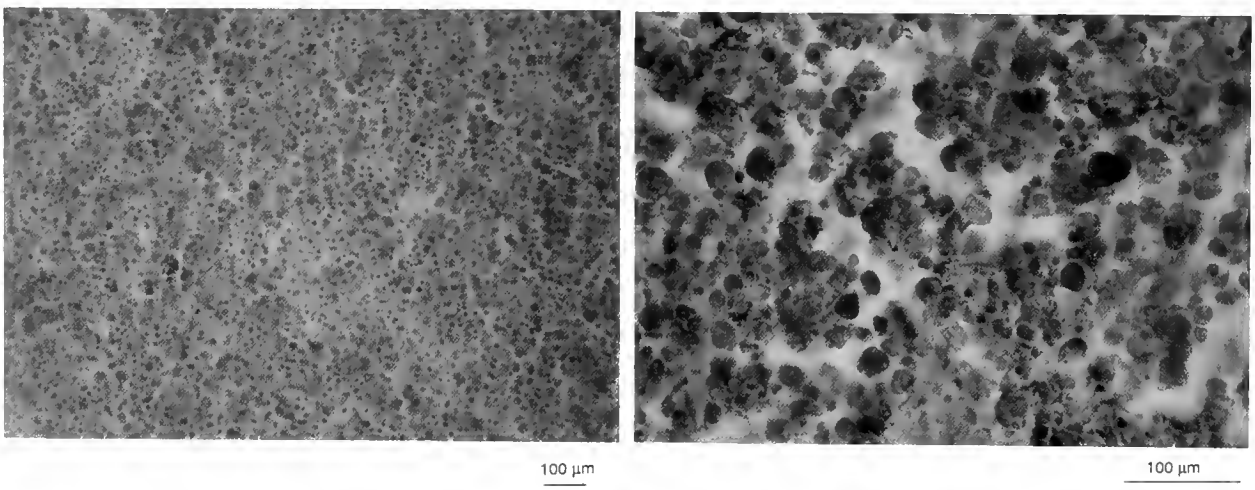

Figure 1. *Comparison of control (left) and treated (right) sections of washed cell pellets from* Microciona prolifera. *The cell pellets had been fixed in formalin–artificial seawater, sectioned (5 µm), deparaffinized, and stained with Block 2 monoclonal primary antibody (1–200) followed by anti-mouse horseradish peroxidase secondary antibody (1–2500) and color development with diaminobenzidine (hematoxylin was the counterstain). A section from which primary antibody had been omitted shows only counterstained cells (left). In contrast to the control, a test slide shows a mixed population of peroxidase stained and unstained cells (right). The relative magnifications are indicated by scale bars (bottom left). Many of the large stained cells resemble archeocytes and exhibit internal as well as peripheral membrane reactivity. This surface reactivity is visualized particularly well as a fine dark brown line that encircles three large cells in triangular configuration near the middle of the section toward the bottom. Other large cells in this section are similarly encircled. Smaller faintly stained cells may be choanocytes.*

adhesion. The circumstances under which sponge cell adhesion might be influenced by these enzyme activities or their products are unclear, but may be clarified by experiments using sulfo-T inhibitors or sulfatases, or calibrations of enzyme product responses by sponge cells after the manipulation of environmental sulfate (7).

The authors thank Dr. Roxanna Smolowitz for her help in the preparation of the photographs.

Literature Cited

1. **Green, E., *et al.* 1986.** *Mol. Cell Biochem.* **71:** 81–100.
2. **Cheng, P., *et al.* 1989.** *J. Clin. Invest.* **84:** 68–72.
3. **Imai, Y., *et al.* 1992.** *Nature* **361:** 555–557.
4. **Brandley, B., *et al.* 1993.** *Glycobiology* **3:** 633–639.
5. **Spillmann, D., *et al.* 1995.** *J. Biol. Chem.* **270:** 5089–5097.
6. **Kuhns, W., *et al.*** *Glycobiology.* In press.
7. **Kuhns, W., *et al.* 1995.** *J. Cell. Biochem.* **57:** 71–89.

Reference: *Biol. Bull.* **189:** 225–226. (October/November, 1995)

Preliminary Investigations on the Scavenger Receptors of the Amebocyte of the American Horseshoe Crab, *Limulus polyphemus*

Ronald T. Aimes, James P. Quigley, Snehasikta Swarnakar, Dudley K. Strickland, and Peter B. Armstrong (Department of Molecular and Cellular Biology, University of California, Davis, California 95616-8755)

The clearance of a variety of ligands from the tissue fluids of mammals is mediated by a group of cell-surface proteins known as the scavenger receptors. These receptors bind and mediate the endocytosis of target molecules including low-density lipoprotein (LDL), urokinase-type plasminogen-activator–plasminogen activator inhibitor-1 complexes, and protease-reacted α_2-macroglobulin (α_2M) (1). The LDL-receptor-related protein/α_2M-receptor (LRP/α_2M-R) is a member of the LDL receptor gene family consisting of at least six cell-surface receptors. Three of these receptors—LRP, the LDL receptor, and the Heymann nephritis antigen (gp330)—are known to bind a 39 kDa intracellular receptor-associated protein (RAP) (2). RAP binds with high affinity in a calcium-dependent manner and copurifies with these receptors during ligand affinity chromatography.

Previous work from our laboratory (3) demonstrated that fluorescently labeled protease-reacted *Limulus polyphemus* α_2M is cleared from the blood of *Limulus* with a concomitant association of fluorescent label with the amebocytes suggesting the presence of a specific α_2M receptor on the amebocyte. We have used RAP-affinity chromatography (4) to search for this and other scavenger receptors in the blood cells (amebocytes) of *Limulus polyphemus*. Amebocytes were collected from adult animals (5); washed twice with sterile, lipopolysaccharide-free 3% NaCl; resuspended in the same buffer; and lysed by the addition of an equal volume of 2× lysis buffer [0.1 *M* HEPES, 0.3 *M* NaCl, 0.02 *M* $CaCl_2$, 2.0% Triton X-100 (TX-100), 0.1% Tween-20, 10 μM 1,10-phenanthroline, 50 μM 3,4-dichloroisocoumarin, 2 μM trans-epoxysuccinyl-L-leucylamino(4-guanidino)-butane, 2 μM pepstatin A, and 1 m*M* phenylmethylsulfonyl fluoride, pH 7.4]. The samples were vortexed, and the insoluble material was removed by centrifugation at 14,000 rpm in a microcentrifuge. Nonspecific Sepharose-binding proteins were removed (following addition of calcium to make a con-

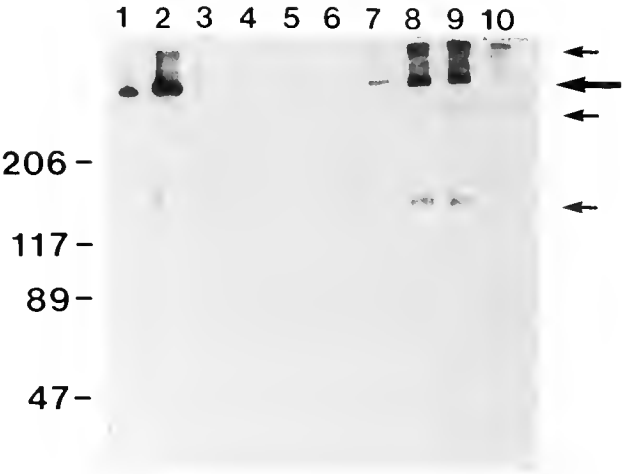

Figure 1. *RAP-ligand blot of a representative* Limulus *amebocyte lysate and RAP-Sepharose purified material. The same pattern of RAP-binding proteins has been found in eight purifications of the RAP-binding proteins from five different amebocyte lysates. Samples were electrophoresed on a standard 6% polyacrylamide-SDS gel and electrophoretically transferred to nitrocellulose membranes. The membranes were processed as previously described (4), using recombinant human RAP as a ligand. RAP binding was detected with a polyclonal anti-human RAP antibody followed by goat anti-rabbit-peroxidase conjugated second antibody and development with SuperSignal CL-HRP Substrate System (Pierce, Rockford, IL). Lane 1, 100 ng purified human LRP; lane 2, 5 μl Sepharose 4B-cleared* Limulus *amebocyte lysate; lane 3, 7.5 μl RAP-Sepharose unbound material; lanes 4–5, 35 μl aliquots of column wash; lanes 6–10, 30 μl aliquots of RAP-Sepharose pH 2.0 eluted material. Arrows indicate positions of RAP-binding proteins found in* Limulus *amebocyte extracts; large arrow indicates the* Limulus *RAP-binding protein with the same electrophoretic position as human LRP. Positions of molecular mass standards are indicated on the left in kilodaltons.*

centration of 10 m*M*) by chromatography on a Sepahrose 4B column equilibrated in 50 m*M* Tris (pH 8.0), 0.15 *M* NaCl, 0.01 *M* $CaCl_2$, 0.5% TX-100, 0.05% Tween-20. The unbound material (4 ml) was collected, applied to a recombinant human RAP-Sepharose column (3-ml bed volume), and washed with 30 ml of buffer. The bound material was eluted with glycine (pH 2.0), 0.15 *M* NaCl, 0.05% TX-100, 0.05% Tween-20; 1.5-ml fractions were collected and immediately neutralized with 1 *M* Tris pH 8.0; and aliquots were analyzed by RAP ligand blotting (4). Figure 1 shows that the *Limulus* amebocyte contains proteins capable of binding to human recombinant RAP, and that these proteins can be specifically removed from the cell lysates (lane 3) by RAP-affinity. At least one protein in the lysate (lane 2) and the RAP-affinity purified material (lane 6–10; large arrow) has electrophoretic mobility similar to that of purified human placental LRP (lane 1).

We have shown that *Limulus* amebocytes contain a RAP-binding protein with similar characteristics to human LRP. The fact that the horseshoe crab contains a cell-associated protein with an electrophoretic mobility similar to that of human LRP and that is capable of binding human RAP suggests a high degree of conservation in scavenger receptor evolution. This potential receptor for molecules targeted for clearance from the circulation (*e.g.*, protease-reacted α_2M) may help explain the rapid clearance of trypsin from the circulation in experimental animals (3). The ability of the RAP-binding proteins from *Limulus* to bind protease-reacted α_2M and other potential ligands has not been demonstrated and is being pursued.

Supported by Grant No. MCB-9218460 from the National Science Foundation. R. Aimes is a 1995 Marine Biological Laboratory Bang Fellow.

Literature Cited

1. **Krieger, M., and J. Herz. 1994.** *Ann. Rev. Biochem.* **63:** 601–637.
2. **Ashcom, J. D., S. E. Tiller, K. Dickerson, J. L. Cravens, W. S. Argraves, and D. K. Strickland. 1990.** *J. Cell. Biol.* **110:** 1041–1048.
3. **Melchior, R., J. P. Quigley, and P. B. Armstrong. 1995.** *J. Biol. Chem.* **270:** 13496–13502.
4. **Battey, F. D., M. E. Gåfvels, D. J. FitzGerald, W. S. Argraves, D. A. Chappell, J. F. Strauss, III, and D. K. Strickland. 1994.** *J. Biol. Chem.* **269:** 23268–23273.
5. **Armstrong, P. B. 1985.** Pp. 253–258 in *Blood Cells of Marine Invertebrates*, W. D. Cohen, ed. A. R. Liss, New York.

Reference: *Biol. Bull.* **189:** 226–227. (October/November, 1995)

Regulation of the Plasma Cytolytic Pathway of *Limulus polyphemus* by α_2-Macroglobulin

Snehasikta Swarnakar, Ralph Melchior, James P. Quigley, and Peter B. Armstrong (Department of Molecular and Cellular Biology, University of California, Davis, California 95616-8755)

An important immune defense strategy of higher animals is to kill invading pathogens with soluble agents in the plasma, usually proteins, that provoke the cytolysis of foreign cells. These cytolytic systems are typically under precise regulation to prevent unintended damage to the cells and extracellular matrix of the tissues of the host. The plasma cytolytic system of the horseshoe crab, *Limulus*, which is mediated by a single effector protein—the sialic acid-binding lectin known as limulin (1)—is regulated specifically by the protease-reacted form of the plasma protease inhibitor α_2-macroglobulin (LAM for Limulus Alpha-2-Macroglobulin) (Table 1, line 4). Limulin is a member of the pentraxin family of proteins and is organized as a homoduodecamer of 25 kDa subunits (1, 2), and LAM is a soluble protease-binding protein organized as a homodimer of 185 kDa subunits (3). Reaction of LAM with the small primary amine methylamine (MA) induces an activation similar to that produced by proteases (3, 4) and yields a conformation that is similarly inhibitory to limulin (Table 1, line 3).

Cytolysis of foreign cells was detected by the hemolysis of sheep erythrocytes (5). Protease- and MA-reacted LAM, but not native LAM, depressed the hemolytic action of purified limulin at a ratio of 30–80 moles of LAM per mole of limulin (Table 1). The addition of trypsin or MA reduced the hemolytic activity of whole plasma (5); presumably they react with endogenous LAM in the plasma, and the product then reduces the hemolytic

Table 1

Regulation of the hemolytic activity of purified limulin by trypsin- and methylamine (MA)-reacted Limulus *α_2-macroglobulin (LAM)*

Hemolysis condition: 10 n*M* Limulin[2] + native or reacted LAM	Hemolysis[1] (Mean ± standard error)
No addition	51.5 ± 5.2%
860 n*M* LAM[3]	51.1 ± 1.4%
780 n*M* MA-LAM[4]	11.1 ± 1.4%
780 n*M* trypsin-LAM[5]	19.0 ± 9.8%
420 n*M* trypsin/STI	46.3 ± 6.2%
420 n*M* trypsin/PMSF	53.8 ± 5.8%

[1] Fraction of erythrocytes hemolyzed. Hemolysis was conducted as previously described (5) (3×10^7 erythrocytes per sample, final sample volume 0.8 ml, 0.19 *M* NaCl, 0.15 m*M* $CaCl_2$, 0.5 m*M* $MgCl_2$, 2.5% glucose, 0.1% gelatin, 2.5 m*M* barbital, pH 7.3, 4 h incubation at room T—after which the intact cells were removed by centrifugation and the released hemoglobin was measured spectrophotometrically at 412 nm and was compared with full hemolysis produced by hypotonic lysis of an aliquoit of erythrocytes).

[2] Limulin was purified as in (1).

[3] LAM was purified as in (3).

[4] LAM was treated overnight with 200 m*M* MA, pH 8.0.

[5] LAM was treated with 2-fold excess trypsin, then the trypsin was inactivated with phenylmethylsulfonylfluoride (PMSF) and a 2-fold excess soybean trypsin inhibitor (STI).

activity of limulin. The inhibitory activity of protease- or MA-reacted LAM was seldom complete and was actually absent at molar ratios of LAM:limulin below 20–30 or at high concentrations of limulin. *Limulus* plasma contains 1–5 μM LAM (6) and about 30–50 nM limulin (as estimated from the hemolytic activity of plasma). Trypsin inactivated by treatment with soybean trypsin inhibitor (STI) or phenylmethylsulfonylfluoride (PMSF) failed to inhibit hemolysis by purified limulin (Table I, lines 5, 6) or whole plasma. Although native LAM did not influence the lytic activity of limulin, it did reverse the inhibitory effects of protease- or MA-reacted LAM in a dose-dependent manner (data not shown). At present we have no explanation for this effect.

In parallel with an inhibition of hemolysis, protease- and MA-reacted LAM inhibited the hemagglutinating activity of limulin. One hemagglutination unit of limulin for sheep erythrocytes was 2.5 nM. Inhibition was produced by 300–400 nM MA- or trypsin-LAM. Inhibition by native LAM was detected at 700 nM.

The apparent target of protease-reacted LAM is limulin, rather than the erythrocytes. Pretreatment of erythrocytes with MA-LAM did not prevent their subsequent hemolysis by limulin. MA- and protease-reacted LAM both bound limulin more avidly than did unreacted LAM. Immunoprecipitation with anti-limulin antiserum co-precipitated MA- and trypsin-LAM, but not native LAM; substrate-immobilized limulin bound MA- and trypsin-activated LAM with a Kd of about 10 nM, but failed to bind native, unactivated LAM.

This work was supported by Grant No. MCB-9218460 from the National Science Foundation.

Literature Cited

1. **Armstrong, P. B., S. Misquith, S. Srimal, R. Melchior, and J. P. Quigley. 1994.** *Biol Bull.* **187:** 227–228.
2. **Tennent, G. A., P. J. G. Butler, T. Hutton, A. R. Woolfitt, D. J. Harvey, T. W. Rademacher, and M. B. Pepys. 1993.** *Eur J Biochem.* **214:** 91–97.
3. **Armstrong, P. B., W. F. Mangle, J. S. Wall, J. F. Hainfield, K. E. Van Holde, A. Ikai, and J. P. Quigley. 1991.** *J Biol. Chem* **266:** 2526–2530.
4. **Quigley, J. P., A. Ikai, H. Arakawa, T. Osada, and P. B. Armstrong. 1991.** *J Biol. Chem* **266:** 19426–19431.
5. **Armstrong, P. B., M. T. Armstrong, and J. P. Quigley. 1993.** *Mol. Immunol* **30:** 929–934.
6. **Enghild, J. J., I. B. Thogersen, G. Salvesen, G. H. Fey, N. L. Figler, S. L. Gonias, and S. V. Pizzo. 1990.** *Biochemistry* **29:** 10070–10080.

Reference: *Biol. Bull.* **189:** 227–228. (October/November, 1995)

Characterization and Use of Isolated Toadfish Hepatocytes for Studies of Heme Synthesis and Utilization

Neal W. Cornell (Marine Biological Laboratory), Mark E. Hahn, and Holly A. Martin

The steady-state level of hepatic heme is the net result of biosynthesis, degradation, and incorporation of heme into hemoproteins within the liver. The rate of synthesis is controlled by 5-aminolevulinate synthase (ALS), the first enzyme of the pathway; likewise, heme oxygenase (HO), the first enzyme of the degradative pathway, sets the rate of heme catabolism. Liver contains many different hemoproteins, but the turnover of cytochrome P_{450} (P_{450}) quantitatively accounts for the major fraction of heme utilization. All three of these enzymes are known to be inducible by xenobiotics and toxicological agents (1–3), and the long-range aim of our studies is to determine the effects of environmental contaminants on ALS, HO, and P_{450} in the marine fish *Opsanus tau* (toadfish).

The lack of inbred, regimen-raised stocks of marine fish can present serious difficulties in studies of complex hepatic processes. To minimize such difficulties, we are conducting our studies with isolated liver cells prepared by the collagenase perfusion method (4). Some characteristics of toadfish hepatocytes have been determined both to allow results obtained with the isolated cells to be referred to the intact liver and also to have criteria for evaluating the quality of each cell preparation. From one toadfish, we obtain 5–5.5 $\times$ 10^8 cells—enough to establish 20–50 primary cultures, thus allowing many tests to be run with cells from the same fish. Toadfish hepatocytes have a median diameter of 15 μm, and there are 3.4 $\times$ 10^8 cells per gram wet wt. Comparative values for rat hepatocytes are 20–25 μm and 1.2 $\times$ 10^8 cells/g wet wt. ATP content has been shown to be an indicator of cell integrity and viability for rat hepatocytes (5), and the same is assumed to be true for toadfish hepatocytes. ATP in freeze-clamped toadfish liver (*i.e., in vivo*) was determined to be 1.84 μmol/g wet wt, and freshly isolated hepatocytes had a similar content (1.79 μmol/g wet wt). After 3 days in culture, however, the cellular ATP content had risen to 2.15 μmol/g wet wt. The latter approaches the value (2.5 μmol/g wet wt) characteristic of rat liver *in vivo* and of isolated rat liver cells. Protein contents were also measured for the two types of cells and found to be 120–150 mg/g wet wt (toadfish cells) and 180–200 mg/g wet wt (rat cells). Finally, consistent with fish liver being the principal site of both lipid biosynthesis and lipid storage, initial isolates of toadfish cells are laden with lipid droplets. Those extracellular lipid droplets can be eliminated by centrifuging toadfish hepatocytes through a layer of 25% sucrose; this minor modification of the standard procedure for preparing hepatocytes permits cells of good quality and useful quantity to be obtained from toadfish liver.

With regard to heme metabolism, we previously reported (6) that toadfish hepatic ALS is inducible by several agents, most strongly by succinyl acetone (SA), an inactivator of aminolev-

ulinate dehydratase, the second enzyme of the heme biosynthetic pathway. In land vertebrates, the induction of ALS by SA has been suggested to result from a decrease in hepatic free heme, a feedback regulator of ALS. This also seems to be the case with toadfish liver, since the 15- to 20-fold induction of ALS by 0.5 m*M* SA is completely blocked by 10 μM heme added to the culture medium. We now have shown that ALS is induced by a polychlorinated biphenyl (PCB) that also causes a strong induction of P_{450} in toadfish hepatocytes. The specific PCB congener chosen for initial testing, 3,3′,4,4′,5-pentachlorobiphenyl (IUPAC No. 126), was added to hepatocyte culture medium at 1, 10, 100, and 1000 n*M*. Induction of P_{450} was maximal at 100 n*M*; at that dose, ethoxyresorufin *O*-deethylase (enzyme activity of P_{450}1A1 (2, 7)) was increased by about 200-fold relative to untreated cells. The simultaneous presence of 0.5 m*M* SA had no significant effect on the induction of P_{450}. Induction of ALS was also maximal at 100 n*M* PCB and, both in the absence and in the presence of 0.5 m*M* SA, ALS activity was increased by about 50% relative to the appropriate control (*i.e.*, either untreated cultures or those with SA but no PCB). These results indicate that the intracellular pool of free heme is large enough to support enhanced production of P_{450}, even when additional heme synthesis is blocked by SA. At the same time, the diminution in free heme caused by SA is sufficient to permit a smaller but significant increase in ALS. Because HO activity is very low and, consequently, difficult to measure in fish liver, we are currently developing a cDNA probe for HO mRNA to permit assessment of xenobiotic effects on heme degradation.

This work was supported by Endeavour Foundation (N.W.C.) and, for M. E. H. of the Woods Hole Oceanographic Institution, by Sea Grant Project No. R/P-49 and the Penzance Endowed Fund in Support of Scientific Staff.

Literature Cited

1. **Marks, G. S., S. A. McCluskey, J. E. Mackie, D. S. Riddick, and C. A. James. 1988.** *FASEB J.* **2:** 2772–2783.
2. **Hahn, M. E., and J. J. Stegeman. 1994.** *Toxicol. Appl. Pharmacol.* **127:** 187–198.
3. **Maines, M. D. 1988.** *FASEB J.* **2:** 2557–2568.
4. **Berry, M. N., and D. S. Friend. 1969.** *J. Cell Biol.* **43:** 506–520.
5. **Cornell, N. W. 1983.** Pp. 11–20 in *Isolation, Characterization and Use of Hepatocytes*, R. A. Harris and N. W. Cornell, eds. Elsevier, New York.
6. **Bruning, G., M. Ferkowicz, and N. Cornell. 1993.** *Biol. Bull.* **185:** 327.
7. **Klotz, A. V., J. J. Stegeman, and C. Walsh. 1983.** *Arch. Biochem. Biophys.* **226:** 578–592.

Reference: *Biol. Bull.* **189:** 228–229. (October/November, 1995)

Suppression of Ca^{2+} Flux During the Transition to Anoxia in Turtle Hepatocytes Revealed by a Non-Invasive Ca^{2+}-Selective Vibrating Probe

S. C. Land and P. J. S. Smith (National Vibrating Probe Facility, Marine Biological Laboratory)

The coordination of cellular events during anoxic metabolic suppression has been studied with a hepatocyte preparation isolated from a vertebrate facultative anaerobe, the western painted turtle [(*Chrysemys picta bellii*) (1, 2)]. A significant fraction of the fall in total ATP demand during anoxic metabolic suppression is due to a 70% reduction in rates of Na^+/K^+ ATPase activity. Despite these changes, the cell membrane potential remains at −30 mV throughout anoxia (3). This implies that anoxia-induced metabolic suppression involves a cessation of flux through ion channels that is coordinated with a decrease in ion-pump ATPase activities (4).

The present study examines the suppression of extracellular Ca^{2+} flux (the net measure of Ca^{2+} ATPase, transporter and channel activity) during the transition to anoxia in turtle hepatocytes. Cells were prepared as described (1) and cultured on laminin-coated glass coverslips ($<10^3$ cells · cm^{-2}). Extracellular Ca^{2+} flux was measured with a Ca^{2+}-selective vibrating probe (5) from cells maintained in BSA-free, Ca^{2+}-depleted medium ($[Ca^{2+}]_e$ was 10–50 μM) containing 10 m*M* Mg^{2+}. Under these conditions, cells demonstrated a steady-state Ca^{2+} efflux of −25.2 ± 8.6 μV/cell (mean ± SD) over 1 week of culture at 18°C. In each experiment, anoxia was achieved by the infusion of a nitrogen/CO_2 atmosphere into a chamber surrounding the culture, and dissolved O_2 concentrations ($[O_2]$) were monitored simultaneously with a polarographic O_2 microelectrode.

A representative experiment is shown in Figure 1A, and compiled steady-state data are shown in Figure 1B. The Ca^{2+} efflux was diminished by 75% during anoxia, and it recovered towards control values on re-oxygenation. Notably, this suppression of the Ca^{2+} flux began early in the transition to anoxia and had reached a new steady-state while $[O_2]$ was above 10 μM, and therefore still theoretically saturating at the mitochondria (6). In previous experiments we noted that aerobic administration of KCN (inhibits mitochondrial oxidative phosphorylation) does not diminish net Ca^{2+} efflux, but when O_2 is depleted, Ca^{2+} efflux is reversibly suppressed (data not shown). Clearly, the reduction in Ca^{2+} efflux in the transition to anoxia is an O_2-dependent effect, but it occurs early in the transition to anoxia, and is independent of the role of O_2 in aerobic metabolism. Therefore we tentatively suggest that O_2-receptive mechanisms may be operative in the modulation of Ca^{2+} efflux in anoxia [as demonstrated in the control of hypoxia-associated protein expression in these cells (7)].

The observed hypoxia-induced suppression of Ca^{2+} efflux to a new steady state lends support to the concept that the preservation of the cell membrane potential during metabolic suppression is coordinated among multiple processes. We are now investigating the role of O_2 in the control of membrane and metabolic events during the transition to anoxia.

This work was conducted with the generous support of a Lak-

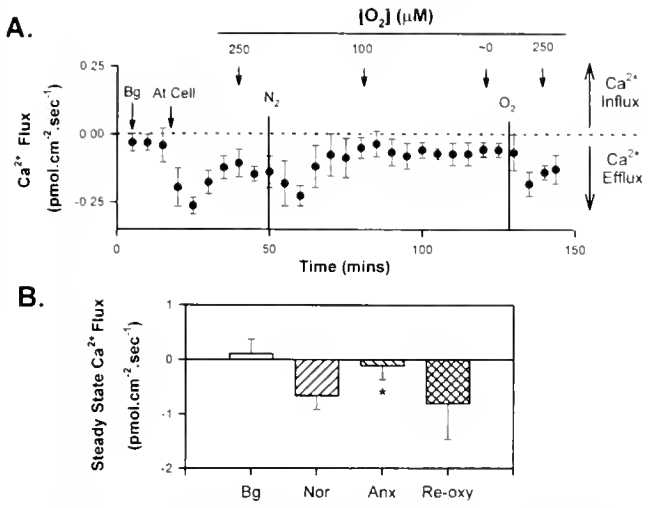

Figure 1. *(A) Representative experiment demonstrating the suppression of net Ca^{2+} efflux during the transition to anoxia. A Ca^{2+}-selective electrode was vibrated at 0.3 Hz over a distance of 10 μm adjacent to the cell membrane (At Cell). Background measures were taken 80 μm from the cell over the same plane of vibration. Measured O_2-concentrations are in* μM. *Each plotted value represents the mean ± SD of 10 independent data points within each 100 collected. (B) Compiled steady-state Ca^{2+} flux data. Values are means ± SD,* n = 6 *measurements taken on cells from independent cultures.* *P = 0.01 *(paired Student's* t*-test relative to control). All experiments were conducted at 23–25°C. Abbreviations: Bg, background; Nor, normoxia; Ax, anoxia; Re-oxy, re-oxygenation.*

ian Postdoctoral Fellowship to SCL. The National Vibrating Probe Facility is supported by NCRR.

Literature Cited

1. **Buck, L. T., S. C. Land, and P. W. Hochachka. 1993.** *Am. J Physiol.* **265(R34):** R49–R56.
2. **Land, S. C., and N. J. Bernier. 1995.** Pp. 379–410 in *Biochemistry and Molecular Biology of Fishes, Vol. 5.* P. W. Hochachka and T. P. Mommsen, eds. Elsevier, Amsterdam.
3. **Buck, L. T., and P. W. Hochachka. 1993.** *Am. J Physiol.* **265(R34):** R1014–R1019.
4. **Hochachka, P. W. 1986.** *Science* **231:** 234–241.
5. **Smith, P. J. S., R. H. Sanger, and L. F. Jaffe. 1994.** *Meth. Cell F. Biol.* **40:** 115–134.
6. **Jones, D. P., T. Y. Aw, and A. H. Sillau. 1990.** *Experientia* **46:** 1180–1185.
7. **Land, S. C., and P. W. Hochachka. 1995.** *Proc. Natl. Acad. Sci. USA* **92:** 7505–7509.

Reference: *Biol. Bull.* **189:** 229–230. (October/November, 1995)

Immunohistochemical Localization of Saxitoxin in the Siphon Epithelium of the Butter Clam, *Saxidomus giganteus*

Roxanna Smolowitz (Laboratory for Marine Animal Health, School of Veterinary Medicine, University of Pennsylvania, Marine Biological Laboratory) and Greg Doucette

Saxitoxin (STX) and its derivatives, the causes of a lethal mammalian neurotoxic disease called paralytic shellfish poisoning (PSP), are produced by several dinoflagellate genera including *Alexandrium, Gymnodinium,* and *Pyrodinium* (1). Butter clams preferentially accumulate saxitoxin in their siphon tips where the toxin can remain active for years: this is a defense mechanism that significantly reduces predation of the clams (2). However, the siphon cell type in which toxin accumulates has not been identified. A recent study determined that nontoxic butter clams fed *Alexandrium* containing gonyautoxin (GTX) and neosaxitoxin (NEO), but no STX, accumulated STX in the siphon and became toxic. The authors suggested that some mechanism other than metabolic conversion of GTX and NEO to STX was occurring since GTX and NEO were depurated from the clams before STX began to accumulate in the siphon (3).

Kodama (4) suggested that, in some cases, the interaction of bacteria with dinoflagellates could be responsible for the production of PSP toxin by the dinoflagellates. Indeed, *Alteromonas,* a bacterium, was recently cultured from PSP-producing dinoflagellates (G. Doucette, unpub. data). Kodama (4) further suggested that toxin-producing bacteria associated with the dinoflagellates could be important in the production and accumulation of toxin in bivalves.

Toxic butter clams were collected from a restricted area in Washington State containing toxic clams. Nontoxic butter clams were collected from a nearby clean area. Sections of siphon and other organs from four toxic and two nontoxic clams were fixed in 10% buffered formalin in seawater and processed in paraffin according to standard methods. Paraffin sections were stained with an avidin-biotin immunochemical stain and a peroxidase tag.

A specific antibody (USA rabbit polyclonal antibody [USA PAB]; donated by Dr. D. Anderson, Woods Hole Oceanographic Institution) was used at 1/250 dilution in PBS. Staining controls consisted of either normal rabbit serum (NRS) at dilutions of 1/1000 and 1/2000 or nondirected rabbit antibody isotype control (control AB) (Zymed 08-6199) substituted for the specific antibody. Sections were evaluated with an Olympus BH-2 photomicroscope.

Evaluation of immunohistochemically stained sections of toxic butter clam siphon showed multifocal specific staining in the columnar epithelium of the outer (periostracial) surface of the

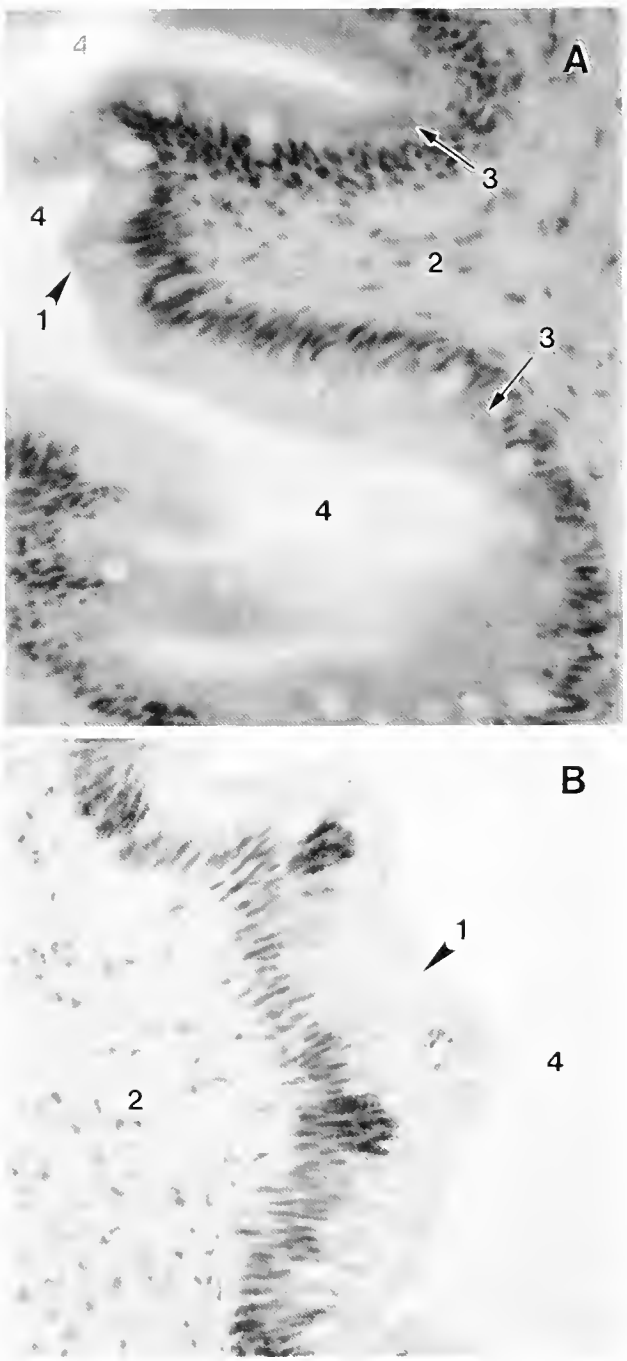

siphon. Staining was predominately present in the epithelium covering the tip and midportion of the siphon. Specific staining was intracellular and granular, and it was located within the apical 2/3 of the cells (Fig. 1A). No other organs or cell types in the animals showed specific staining.

Staining was not present in control sections in which NRS or control AB was substituted for USA PAB, or in sections of siphon from nontoxic butter clams when stained with USA PAB (Fig. 1B) or control solutions.

Histologic staining of siphon sections for bacteria adjacent to or within epithelial cells was negative. Thus, bacteria seem not to be responsible for the occurrence of STX in these cells. Alternately, individual or small groups of bacteria could be in residence in or between the epithelial cells; such small accumulations of bacteria are not easily detected with a histologic stain.

Now that we have identified STX in the columnar epithelial cells of the siphon's outer surface, we will use TEM coupled with immunocytochemical staining to identify the organelles that store STX, and possibly, associated bacteria.

This work was supported by University of Pennsylvania Formula Funds.

Literature Cited

1. **Anderson, D. M. 1990.** Pp. 41–51 in *Toxic Marine Phytoplankton*, E. Graneli, B. Sundsrom, L. Edler, and D. M. Anderson, eds. Elsevier, New York.
2. **Kvitek, R. G. 1993.** Pp. 407–411 in *Toxic Phytoplankton Blooms in the Sea*, T. J. Smayda and Y. Shimizu, eds. Elsevier, New York.
3. **Beitler, M. K., and J. Liston. 1990.** Pp. 257–262 in *Toxic Marine Phytoplankton*, E. Graneli, B. Sundstrom, L. Edler, and D. M. Anderson, eds. Elsevier, New York.
4. **Kodama, M. 1990.** Pp. 52–61 in *Toxic Marine Phytoplankton*, E. Graneli, B. Sundsrom, L. Edler, and D. M. Anderson, eds. Elsevier, New York.

Figure 1. *Photomicrographs of sections of contracted siphon immunohistochemically stained with a 1/250 dilution of anti-STX USA rabbit polyclonal antibody and counterstained with Mayers hematoxylin. The periostracum was removed from the outer surface of the siphon before processing. (A) Granular specific staining is present in the apical 2/3 of the columnar epithelial cells of the outer surface of a toxic clam's siphon (100×). (B) No specific staining is present in the columnar epithelium of the outer surface of this nontoxic clam's siphon (100×). 1, columnar epithelium of the outer (periostracial) surface of the siphon; 2, subepithelial connective tissue of the siphon; 3, specific granular staining; 4, space representing the area outside of the animal's body (external to the contracted siphon).*

Reference: *Biol. Bull.* **189**: 231–232. (October/November, 1995)

Explorations of Turbulent Odor Plumes with an Autonomous Underwater Robot

T. R. Consi (MIT Sea Grant Program), F. Grasso, D. Mountain, and J. Atema

Lobsters extract information from complex signals in turbulent odor plumes and it guides them to mates or food sources. To test hypotheses about this guidance information, we have developed a robot as a physical model of a lobster. Here we present the results of experiments designed to test the efficacy of amplitude information—a single component of a complex signal—in guidance. The robot used a bilateral pair of conductivity sensors (sensor surface spacing = 5–7 cm, 5 cm separating two 1-cm wide sensors) to sense a salt plume simulating an odor plume.

The experiments were performed in a fresh-water flume with a mean flow rate of 0.6 cm/s. A 0.76 *M* NaCl solution (containing crystal violet for visualization and ethanol to adjust buoyancy) was injected parallel to the flow from a 2 mm diameter nozzle into the flume at a rate of 250 ml/min. The resulting plume had two distinct regions: a proximal cone originating at the source, and a distal patch field downstream from the jet. The proximal jet is the region where the velocity of the jet exceeds the mean flow in the flume. The distal patch field corresponds to plume positions downstream from the proximal cone where the mean flow is the major source of plume velocity (relative to the floor).

Two robot control algorithms were tested:

1. The robot turns toward the side with the higher salt conductance signal or goes forward if the difference between the right and left sensor signals drop below 9 μS.
2. As in #1, with the added feature that the robot goes backward if the conductances of both sensors drop below a threshold of 7 μS.

The robot was placed in the center of the flume, 90 cm downstream from the plume source, and was started in two orientations for each algorithm: pointed upstream directly into the oncoming plume, and pointed 45 degrees to the right of the plume axis. Each of the four conditions (2 orientations and 2 algorithms) was replicated 10 times. The robot's trajectory was recorded by a video camera. Data from a single run using algorithm #1 are presented in Figure 1.

As the robot moved through the patch field, its behavior was characterized by sequences of abrupt, brief turns that occurred at irregular intervals. When it entered the proximal jet, the robot moved with more regular side-to-side oscillations: a characteristic series of alternating smooth left and right turns (often of greater magnitude than those seen in the distal patch field). Once inside the proximal jet the robot often found its way to the source (50% algorithm #1 and 72% algorithm #2).

The starting orientation had a substantial effect on the success of the algorithms. Algorithm #2 with the robot pointing into the plume had a higher rate of direct "hits" onto the source than algorithm #1 with the same orientation (66% *vs* 33%). We attribute the greater failure rate of algorithm #1 to the fact that when both sensors happen to exit the plume, algorithm #1 moves the robot in a straight line away from the point of exit. The

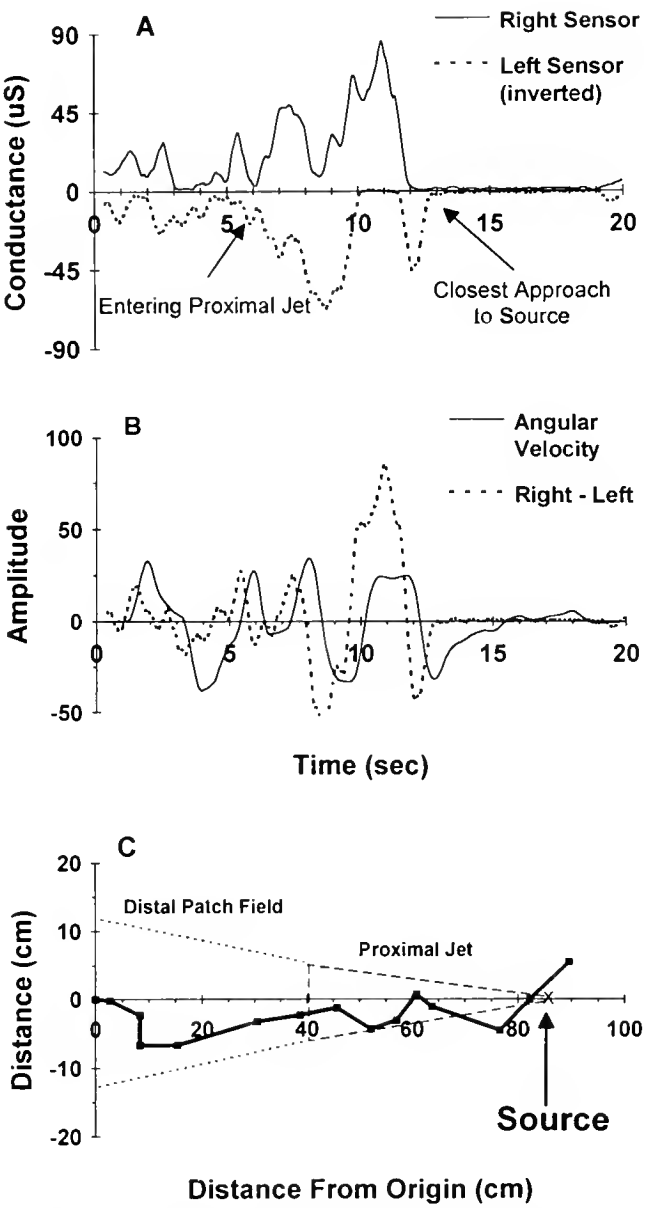

Figure 1. *(A) Right and left conductance measurements during an experimental run (algorithm #1, robot start pointed up the central plume axis). Left sensor data were inverted for visualization purposes. (B) Conductance difference (right–left) and turning rate. Vertical scale is in μs for conductance difference and in deg/s for turning rate. Turning events follow sensor signal differences by 0.6 s. (C) Robot trajectory during the same run as Figure 1a, b. Points are robot positions at 1-s intervals. The dotted lines denote the plume at the end of the experiment and show the region where the proximal cone makes the transition into the distal patch field*

back-up behavior of algorithm #2 corrects for plume exit. Orienting the robot at 45 degrees reduced the probability of the robot finding the cone and thus reduced the probability of the robot finding the source (algorithm #1: 33% *vs* 0%, algorithm #2: 66% *vs* 10%).

These experiments show that simple bilateral amplitude comparisons generally suffice to guide a robot within the proximal jet of a chemical plume. Lobsters may use such an algorithm for guidance in the proximal cone. This simplest algorithm fails in the distal patch field where the structure of the chemical signal is less regular. Lobsters show different behavioral strategies at different distances from the source of an odor. Consequently, additional algorithms will be required for successful guidance of the robot from greater distances toward the proximal cone. This gradual build-up of algorithm complexity, coupled with lobster behavior analysis, is expected to lead to a general understanding of guidance principles in odor plumes.

Supported by NSF Grant BES-9315791 to J.A.

Reference: *Biol. Bull.* **189:** 232–233. (October/November, 1995)

Effects of Varying Plume Turbulence on Temporal Concentration Signals Available to Orienting Lobsters

Kevin Dittmer, Frank Grasso, and Jelle Atema (Boston University Marine Program, Marine Biological Laboratory)

Lobsters locate odor sources in turbulent plumes (1, 2). Based on the speed and accuracy with which lobsters orient to such odor sources, Moore, Scholz, and Atema (2) argued that these animals are guided by temporal features of the odor concentration profile arriving at their chemoreceptors as a series of concentration peaks. Physical investigations (3, 4, 5) of the temporal odor signal identified a number of peak parameters as candidate guidance cues. These physical studies and the behavioral ones were both conducted using axisymmetrical jet plumes generated in a single turbulent regime (defined by mean flow through the flume and jet injection rate). Here we extend the physical investigations to include multiple turbulent regimes. Specifically we aim to address the question: Do the candidate peak parameter gradients identified by Moore and Atema (5) retain their guidance potential for the lobster in plumes generated with different source injection rates?

To facilitate these initial measurements, we created saline plumes (source 0.76 *M* NaCl) containing dye and ethanol for neutral buoyancy in a fresh-water flume (366 × 90 × 36 cm, mean flow 0.7 cm/s). Conductivity measurements enabled us to estimate salt concentration at 40 Hz or about 10 times the signal frequency resolution of lobster chemoreceptor cells (6). The electrochemical methods used in the previous studies (5) were limited to 10 Hz. This allowed us to record the signal amplitude while minimizing temporal distortions due to signal masquerading in the bandwidth of lobster chemoreceptor cells (6). Our interest here is in turbulent (inertial) dispersal where flow dominates molecular transport. Ethanol is not measured and salt, as well as dopamine which was used in some of our earlier studies, are useful tracers for turbulent mixing processes. The use of salt plumes also complements our studies with a robot that orients with conductivity sensors. Although salt and ethanol diffuse differently than food odors at the molecular scale, we observed no visual differences in plume structure between odor plumes and ethanol-salt plumes. Thus, this study provides a reasonable physical model of a food odor plume in a way that informs future behavioral and robot orientation studies.

We estimated the salt plume concentration time-course (from measured conductivity) at five distances along the flume midline from the source (0, 25, 50, 75, and 100 cm). To produce different plumes we varied the rate of source injection [(3 ml/min), (40 ml/min), (80 ml/min), (120 ml/min) and (160 ml/min)]. Each injection was delivered continuously through a 2.2-mm inner diameter glass tube located at the flume midline 9 cm from the flume floor. Conductivity measurements were taken with a pair of silver-tipped electrodes placed 9 cm from the flume floor (approximate lobster antennule height). The electrodes had a 1-mm spatial separation (scale of a lobster sensillum). Thus, we sampled a horizontal line through each plume at an elevation and spatial scale that matched that of the lobster lateral antennule receptors.

We converted the conductivity profiles to concentration (moles/liter). In agreement with earlier studies, the temporal profiles that we examined were so patchy that accurate estimates of the concentration gradient would require greater than 30 s of sampling. We therefore turned to an analysis of the temporal parameters of the patches themselves. Patches in the spatial domain are seen as peaks in the concentration profile. Peaks were defined (5) as the profile region between the time the concentration exceeded the background by 0.75 m*M* and the time the concentration fell below 30% of the maximum concentration of the peak. We examined five peak parameters: peak height (PH, maximum concentration), rise-time (PR, time from the beginning of a peak to its maximum), peak slope (PS, ratio of peak height to rise-time), peak duration (PD time from peak start to end), and interpeak interval (IPI, time between consecutive peak maxima).

We used a two-way ANOVA to analyze the effects of distance and injection rate on each of the five peak parameters. These analyses indicated significant effects of injection rate and distance on all five peak parameters ($P < 0.001$ all analyses). These results are consistent with earlier studies (5). They also revealed significant interactions of distance and injection rate on all five peak parameters. ($P < 0.001$ all analyses.)

However, *post hoc* analyses (GT2 test for unequal sample sizes) indicated that only a few of the parameters form gradients that could be used as cues to the source. The effects of most injection rates were only distinguishable nearest the source ($P < 0.05$, all distance by injection comparisons at 25 cm). Only the slowest injection rate was significantly different from all other injection rates at all distances ($P < 0.05$, for all distance by injection comparisons with the injection rate of 3 ml/min). Not all comparisons between adjacent distances at a given injection rate were significantly different. To cite one example, the primary effect of distance on rise time could be traced to the comparison between 25 and 100 cm ($P < 0.001$). Comparisons of PR at intervening distances indicated nonsignificant differences. Only PH and PS showed significant differences between all distances for any given injection rate ($P < 0.05$ for all comparisons) except the slowest injection rate (3 ml/min). In PH there was a significant distance by injection interaction at an injection rate of 120 ml/min ($P < 0.01$). Otherwise PS and PH decreased monotonically with distance from the source.

The results allow us to draw four conclusions (that pertain to the orientation of lobsters and robots): 1. A strategy of climbing PH or PS gradients within a single plume will eventually lead to the source, except for plumes generated by our slowest injection rate. 2. The parameters IPI, PR, and PD are not reliable cues to the source when the plume is sampled at 25-cm intervals along the midline regardless of injection rate. 3. The slowest injection rate (a single ribbon-like filament) does not afford a significant gradient of any of the five peak parameters. 4. PH and PS not only provide good spatial gradients over 100 cm, they also allow us to differentiate between source injection rates at a distance of 25 cm from the source. We infer that lobsters or robots could use spatial gradients of PH and PS to locate odor sources up to 100 cm away. Information about the strength of the jet source gradually improves until it becomes clear at 25 cm from the source.

We thank Dr. Jennifer Basil, Dr. Rainer Voigt, and Dr. Richard Hill for help and practical advice. This work was supported by NSF grant BES-9315791 to J. A. and awards from the Woods Hole Marine Science Consortium Fund, Michigan State University Honors College, and the Jeffrey Boetcher Travel Fund to K. D.

Literature Cited

1. **Basil, J., and J. Atema. 1994.** *Biol. Bull.* **187:** 272–273.
2. **Moore, P., N. Scholz and J. Atema. 1991.** *J. Chem. Ecol.* **17:** 1293–1307.
3. **Moore, P., N. Scholz, L. Lacomis and J. Atema. 1991.** *Biol. Bull.* **177:** 329.
4. **Moore, P., G. Gerhardt, and J. Atema. 1989.** *Chem. Senses* **14:** 829–845.
5. **Moore, P., and J. Atema. 1991.** *Biol. Bull.* **181:** 408–418.
6. **Gomez, G., R. Voigt, and J. Atema. 1994.** *J. Comp. Physiol.* **174:** 803–811.

Reference: *Biol. Bull.* **189:** 233–234. (October/November, 1995)

Accumulation and Retention of Dimethylsulfoniopropionate by Bivalve Molluscs: High and Nonnormal Variation

Richard W. Hill (Department of Zoology, Michigan State University, East Lansing, MI 48824), John W. H. Dacey, David K. D. Hill, Judith E. McDowell, and Dale F. Leavitt

Dimethylsulfoniopropionate (DMSP) is a principal sulfur compound of many bivalve molluscs (1, 2, 3). Many phytoplankters synthesize DMSP (4), and bivalves are assumed to accumulate DMSP from phytoplankton in their diet.

DMSP is of current interest in bivalve biology for two major reasons, both linked to the production of volatile dimethyl sulfide (DMS) from breakdown of DMSP (nonvolatile). First, DMS is evidently a critical component of the normal taste and odor of many bivalves (2, 5). Second, DMS that enters the atmosphere can affect climate (6, 7). Estimates of the biomass of *Mytilus edulis* in the Baltic Sea (8), together with known filtering rates, suggest that water equivalent to half the Baltic is filtered by *M. edulis* each year. Much faster filtration of bodies of water by communities of bivalves can occur (9). Thus, on local—albeit not global—scales, major fractions of phytoplanktonically produced DMSP may be processed by bivalves, and the molluscs might thereby significantly affect transfer of biogenic sulfur to the atmosphere.

Prior reports on DMSP in bivalves (1, 2, 3, 5) typically rest on small sample sizes and stress average results. Our purpose is to bring to light remarkable features of individual variation in the extent of accumulation of DMSP. We illustrate using data from two ongoing studies of DSMP in *M. edulis*, one on field levels, the second on retention.

Tissues were prepared for analysis by incubation in cold 1–2 N KOH within sealed serum bottles, converting DMSP to DMS (10). Headspace gas from the bottles was analyzed by gas chromatography (Chromosil 330 column, Sievers 350B chemiluminescence detector).

The July data in Figure 1 depict whole-body DMSP/g for 15 mussels collected at Sandwich, Massachusetts, in July 1992. Even though all animals were from a single clump and were within a restricted size range (6.2–8.1 cm shell length), their accumulations of DMSP/g varied enormously (standard deviation = 54% of mean). This cannot be attributed merely to differences in feeding history just before collection because we know (see below)

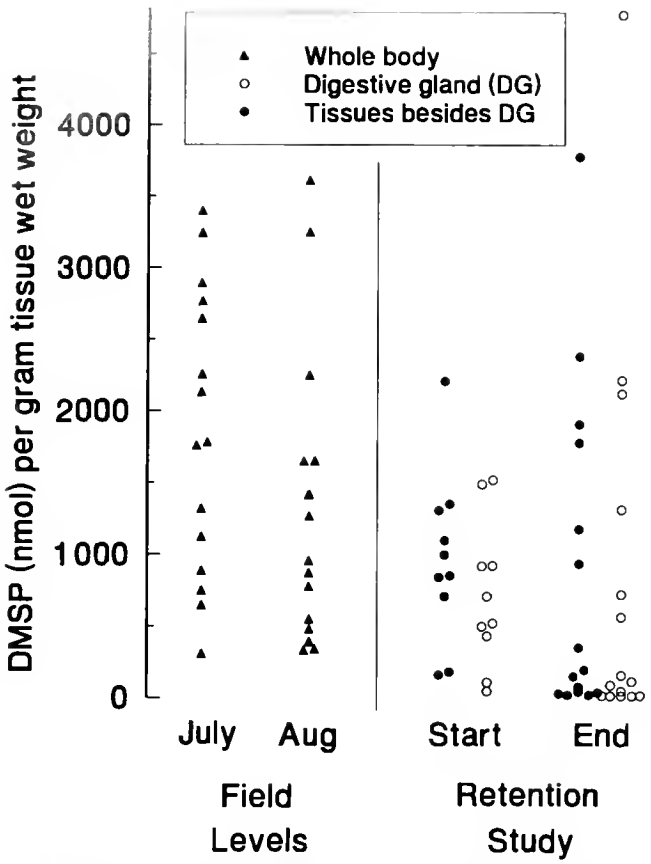

Figure 1. *Distribution of DMSP/g in four groups of* Mytilus edulis. *Each point represents one mussel. Lateral displacement of points is for clarity. Field levels are for whole animals freshly collected during 2 months. Mussels in the retention study were deprived of DMSP in food for 5 weeks. They were divided into digestive glands and other tissues for analysis.*

that variation in tissues outside the digestive gland is as great as that in the digestive gland, and tissue burdens do not change rapidly in bivalves (1). The August data (Fig. 1) represent 15 mussels from a single clump collected at Sandwich in August 1992. These results show nonnormality of distribution (skewed, $P < 0.03$; 11) as well as high variation. We find that, among *M. edulis* living as neighbors, high variation in DMSP/g is the rule, and nonnormality is common. High variation is seen in published data for *Mya arenaria* (2).

Each *M. edulis* was subdivided into two parts—the digestive gland and the rest of the body—for the retention study in Figure 1. The mussels (6.0–7.5 cm length) were collected from 1 m^2 at Sandwich. The start sample shows 10 animals soon after collection. The end sample depicts 15 mussels after 5 weeks of living in filtered water and being given only DMSP-free food. The distributions in the latter sample are the most strongly nonnormal we have encountered (skewed, $P < 0.002$ for digestive gland, $P < 0.01$ for other tissues). Evidently, some individuals voided DMSP during the 5 weeks of nonexposure, but others retained it tightly. Slow turnover has been reported previously (1).

The features of the statistical distribution of DMSP accumulation in *M. edulis* emphasized here raise both biological questions and practical concerns. Biologically, we can now only wonder why neighbors often differ so strongly in accumulation; DMSP/g is not correlated with shell length or other parameters we have examined. The tight retention of DMSP by some individuals is remarkable and raises the possibility that DMSP may have a functional role in bivalves. At a practical level, the contribution of high variation in DMSP/g to variation in taste needs investigation. Further, the distributional features we report often create havoc in experimental designs. When mussels are fed DMSP-containing food, we believe the short-term fate of most DMSP is accumulation in tissues, but testing this hypothesis is challenging because the high intrinsic variation in DMSP/g makes statistical discrimination of fed and control groups difficult (12).

S. Hill, D. Franks, B. Lancaster, F. Nichy, D. Radosh, and E. Enos made necessary contributions. Supported in part by NSF OCE91-02532.

Literature Cited

1. **Ackman, R. G., and H. J. Hingley. 1968.** *J. Fish. Res. Board Can.* **25:** 267–284.
2. **Brooke, R. O., J. M. Mendelsohn, and F. J. King. 1968.** *J. Fish. Res. Board Can.* **25:** 2453–2460.
3. **Iida, H., and T. Tokunaga. 1986.** *Bull. Jap. Soc. Sci. Fish.* **52:** 557–563.
4. **Keller, M. D., W. K. Bellows, and R. R. L. Guillard. 1989.** Pp. 167–182 in *Biogenic Sulfur in the Environment*, E. S. Saltzman and W. J. Cooper, eds. Amer. Chem. Soc., Washington, DC.
5. **Ronald, A. P., and W. A. B. Thomson. 1964.** *J. Fish. Res. Board Can.* **21:** 1481–1487.
6. **Shaw, G. 1983.** *Clim. Change* **5:** 297–303.
7. **Charlson, R. J., J. E. Lovelock, M. O. Andreae, and S. G. Warren. 1987.** *Nature* **326:** 655–661.
8. **Kautsky, N., and I. Wallentinus. 1980.** *Ophelia*, **Suppl. 1:** 17–30.
9. **Smaal, A. C., and T. C. Prins. 1993.** Pp. 271–298 in *Bivalve Filter Feeders in Estuarine and Coastal Ecosystem Processes*, R. F. Dame, ed. Springer-Verlag, New York.
10. **Dacey, J. W. H., and N. V. Blough. 1987.** *Geophys. Res. Lett.* **14:** 1246–1249.
11. **D'Agostino, R. B., and G. L. Tietjen. 1973.** *Biometrika* **60:** 169–173.
12. **Hill, R. W., J. W. H. Dacey, J. E. McDowell, and D. F. Leavitt. 1993.** *Biol. Bull.* **185:** 322–323.

Reference: *Biol. Bull.* **189:** 235–236. (October/November, 1995)

Accumulation of Dimethylsulfoniopropionate in *Geukensia demissa* Depends on Trophic Interactions

Bradley A. White (Department of Zoology, Michigan State University, East Lansing, MI 48824), Richard W. Hill, and John W. H. Dacey

Dimethyl sulfide (DMS) constitutes up to half of the atmospheric sulfur produced biogenically (1, 2) and may affect global climate (3). A major source of atmospheric DMS is the enzymatic cleavage of dimethylsulfoniopropionate (DMSP), which is synthesized by many phytoplankters (4, 5) and a few vascular plants, including *Spartina alterniflora* (5). Most DMSP is released following rupture of cell walls (6, 7) and is then subject to microbial degradation to DMS (8, 9). Little attention has been given to salt marsh DMSP fluxes outside the autotrophic and microbial components of the food web.

The purpose of this study was to explore DMSP pathways within the Great Sippewissett Marsh (Falmouth, Massachusetts), determining in particular whether tissue concentrations of DMSP in *Geukensia demissa* vary with food resources. *G. demissa*, the ribbed mussel, is the dominant animal in salt marshes in the eastern United States (10). Ribbed mussels in the Great Sippewissett Marsh filter most of the marsh water during each tidal cycle (11) and thus are likely to play a key role in marsh DMSP fluxes. *G. demissa* can directly consume *S. alterniflora* detritus in addition to plankton and bacteria (12). Peterson *et al.* showed that the isotopic composition of *G. demissa* in the Great Sippewissett Marsh follows a horizontal gradient reflecting a shift in available food resources, from a diet high in phytoplankton (up to 70%) near the bay, to mostly *Spartina* detritus (80%) in the marsh interior (13). Delta values for ^{34}S isotope indicate that much of this shift occurs in a relatively short region along the tidal channel between sites 3 and 4 (Fig. 1).

We hypothesized that mussels near the bay would have relatively high levels of DMSP due to a diet rich in live phytoplankton. Conversely, mussels in the interior of the marsh were expected to have lower levels of DMSP. Their diet is dominated by *Spartina* detritus, which, if directly consumed, would probably be depleted of DMSP by leaching, and if indirectly consumed *via* bacteria and nanozooplankton filtration, would likely be depleted of DMSP by microbial decomposition. We expected this shift in DMSP concentration to be most dramatic between site 4 and all others, following the shift in ^{34}S delta values (Fig. 1).

The mussel collection sites in Figure 1 were chosen to correspond to isotope study sites (13). Five mussels (5–7.5 cm long) were collected from each site in August 1994, and the digestive glands were analyzed separately from the rest of the body. The samples were incubated in 2*N* KOH in sealed vials at 25°C for 24 h, allowing DMS from hydroxide decomposition of DMSP to partition to equilibrium. Mussel DMSP content was calculated from determinations of DMS in headspace samples by gas chromatography (Chromosil 330 column, Sievers 350B Sulfur Chemiluminescence Detector).

To test for differences among collection sites, the Kruskal-Wallis nonparametric procedure was used (SPSS/PC+). Variances for DMSP/g in mussels are often high and nonnormal (14). In our study, they were also nonhomogeneous. The Kruskal-Wallis test eliminates dependency on normal distributions, homogeneity of variances, and other parametric test assumptions. In spite of small sample sizes and high variation within sites—both decreasing the likelihood of detecting differences—the DMSP concentration in digestive glands ($P = 0.011$) and

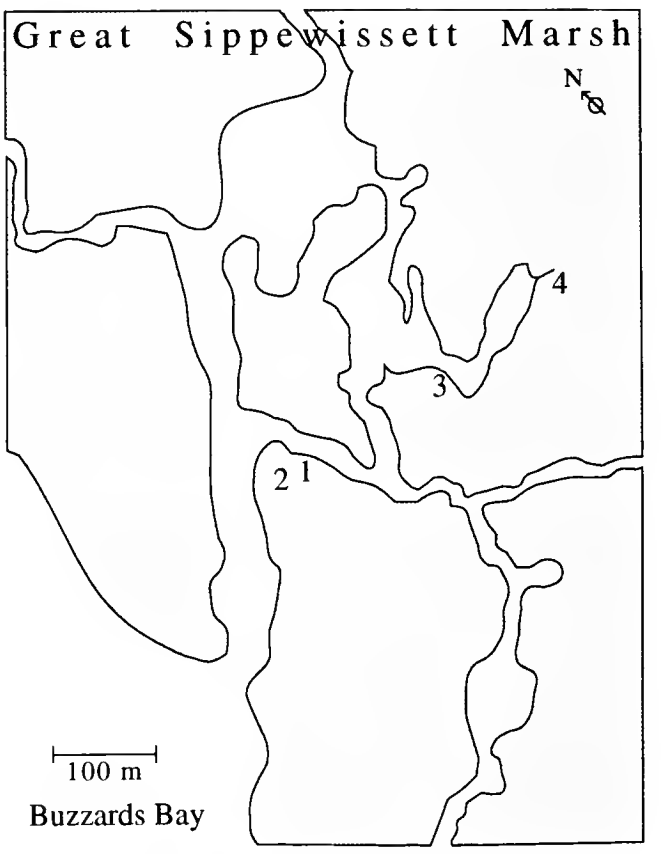

Site	DMSP concentration (nmol/g) Digestive gland $\bar{Y}$	Digestive gland S.D.	Rest of body $\bar{Y}$	Rest of body S.D.	Delta ^{34}S isotope ratio
1	449.9	128.4	99.4	36.7	+12.14 [a]
2	569.0	421.2	154.7	126.0	— [b]
3	590.6	319.0	98.1	46.1	+ 8.55
4	121.7	33.1	41.2	17.7	+ 0.54 [c]

Figure 1. *Aerial view of* Geukensia demissa *sampling sites in Great Sippewissett Marsh adapted from Peterson* et al. *(13). The table reports means and standard deviations for DMSP concentration (nmol/g) in digestive gland and the rest of the body tissue, and delta values for ^{34}S isotope at each of the four sites on the map. Only larger tidal channels are shown. At site 2, mussels were collected from a panne on the marsh surface. Mussels at other sites were collected from the creek bank. Site 4 is a mosquito ditch. a = adjacent creek bank, b = no value reported, c = neighboring mosquito ditch*

the rest of the body tissue ($P = 0.051$) proved to be lower at site 4 than for other sites.

As hypothesized, from the main tidal channel to the marsh interior, DMSP concentration undergoes a shift that reflects the isotopic gradient. This evidence suggests spatial heterogeneity in DMSP fluxes through *G. demissa* concordant with trophic differences in the marsh. The shift is greatest for the digestive gland tissue, which contained relatively high levels of DMSP.

The dynamics and functional significance of DMSP in individual mussels, the extent of direct *versus* indirect consumption of *Spartina* detritus, and the rate of detrital DMSP loss remain undetermined. Measurement of DMSP in the water column at various sites in the marsh will further elucidate these relationships. We are in the process of expanding the data set reported here to clarify *Geukensia* DMSP gradients in the marsh.

This study was conducted as part of a Woods Hole Marine Science Consortium internship to B. A. W., and was supported in part by NSF OCE 9102532. We thank Ivan Valiela for his assistance.

Literature Cited

1. **Andreae, M. O., and H. Raemdonck. 1983.** *Science* **221:** 744–747.
2. **Bates, T. S., J. D. Cline, R. H. Gammon, and S. R. Kelly-Hansen. 1987.** *J Geophys. Res.* **92:** 2930–2938.
3. **Charleston, R. J., J. E. Lovelock, M. O. Andreae, and S. G. Warren. 1987.** *Nature* **326:** 655–661.
4. **Andreae, M. O. 1986.** Pp. 331–362 in *The Role of Air-Sea Exchange in Geochemical Cycling*, P. Buat-Menard, ed. D. Reidel, Dordrecht, The Netherlands.
5. **Charlston, R. J. 1995.** Pp. 251–262 in *Biotic Feedbacks in the Global Climatic System*, G. M. Woodwell and F. T. Mackenzie, eds. Oxford University Press, New York.
6. **Dacey, J. W. H., G. M. King, and S. G. Wakeham. 1987.** *Nature* **330:** 643–645.
7. **Kiene, R. P. 1988.** *FEMS Microbiol. Ecol.* **53:** 71–78.
8. **Krouse, H. R., and R. G. L. McCready. 1979.** Pp. 401–431 in *Biogeochemical Cycling of Mineral Forming Elements*, P. A. Trudinger and D. J. Swaine, eds. Elsevier, Amsterdam.
9. **Ledyard, K. M., E. F. DeLong, and J. W. H. Dacey. 1993.** *Arch. Microbiol.* **160:** 312–318.
10. **Bertness, M. D. 1984.** *Ecology* **65:** 1794–1807.
11. **Jordan, T. E., and I. Valiela. 1982.** *Limnol. Oceanogr.* **27:** 75–90.
12. **Langdon, C. J., and R. I. E. Newell. 1990.** *Mar. Ecol. Prog. Ser.* **58:** 299–310.
13. **Peterson, B. J., R. W. Howarth, and R. H. Garritt. 1985.** *Science* **227:** 1361–1363.
14. **Hill, R. W., J. W. H. Dacey, D. K. D. Hill, J. E. McDowell, and D. F. Leavitt. 1995.** *Bio. Bull.* **189:** 000–000.

Reference: *Biol. Bull.* **189:** 236–237. (October/November, 1995)

Localization of Digestion Activities in the Sea Anemone *Haliplanella luciae*

Dirk Bumann (Marine Biological Laboratory)

Among Cnidaria, the Anthozoa have many radial septa called mesenteries, which project from the body wall into the gastric cavity. Anthozoa are typically larger than other cnidarians and therefore might have needed to increase their inner surface/body weight ratios. Therefore, a generally proposed function of the mesenteries is to enhance the gastrodermal surface, and thereby the digestive capacity (1). Cells that secrete enzymes for extracellular digestion are highly localized in small areas at the edges of the mesenteries called filaments (2). Hence, any enhancement of the digestive capabilities would be only due to an increase in the number of cells absorbing food fragments. Indeed, the whole gastrodermis is capable of endocytosis in sea anemones (2, 3).

In the studies discussed above, however, artificial food was used, and the results contradict those obtained many decades ago, also with artificial food, indicating that the septa were mainly active in absorption (4, 5). It is possible that only parts of the gastrodermis are active when little food is available, whereas major fractions become active when food is abundant (as observed for the scyphozoan *Aurelia aurita*, D. B. and G. Jarms, unpub. obs.). In the early experiments, the digestive capacity of the sea anemones may not have been saturated. Moreover, the relevance of experiments with artificial food for the functional significance of the mesenteries is doubtful. Hence experiments with natural food and feeding to satiation are needed to critically test the hypothesis.

The anthozoan *Haliplanella luciae*, obtained from Mill Pond, Woods Hole, Massachusetts, was fed to satiation with protists and crustaceans, which are major constituents of their natural diet (2, 6). To trace ingestion, digestion, and absorption, the food was labeled with fluorescent dyes. Digestion in living anemones (10 per food type) was observed with fluorescence microscopy for 2–4 h after feeding. Additionally, some anemones were anesthetized and fixed at given time intervals up to 6 h after feeding. After bisection, they were examined with a dissecting scope. For intracellular localization of dyes, dissected pieces of the anemones were examined with a fluorescence microscope.

For microphagous feeding (2), yeast cells were labeled with the dye Evans blue. *Haliplanella* ingested yeast cells and mixed them with mucus in the basal part of the pharynx. The yeast-containing mucus was transported to the edges of the mesenteries where, in all anemones tested, absorption almost exclusively occurred. Little absorption could be detected in the tentacle gastrodermis and none at all was seen in the rest of the mesenteries or in the column wall, even after 6 h in the presence of 5×10^6 yeast cells ml^{-1}. However, isolated column wall fragments can

Figure 1. *Longitudinal section of the sea anemone* Haliplanella luciae *fixed 4 h after feeding to satiation with* Artemia salina *nauplii labeled with Evans blue. The arrowheads indicate the mesenterial regions adjacent to the filaments where endocytosis almost exclusively occurred. The scale bar represents 1 mm.*

absorb yeast cells or other particles in *Haliplanella*. Apparently in intact *Haliplanella*, all yeast cells ingested are trapped in the pharyngal mucus and therefore might not be available to the column wall cells. On the other hand, a small fraction of the artificial food India ink passed the pharynx without being trapped and was then absorbed in the whole gastrodermis as previously observed in other species (2). The differential affinities of yeast and India ink for mucus are currently under investigation.

For macrophagous feeding, *Artemia salina* nauplii were covalently labeled with the dyes Texas red sulfonyl chloride and fluorescein isothiocyanate, or non-covalently labeled with Evans blue (7). The flexible mesenteries formed tight sacs around all ingested nauplii as observed previously (8, 9). These food sacs were further wrapped with mucus as shown by mucicarmine staining. During extracellular digestion of the wrapped food, very little of the three dyes could be detected in the gastric cavity in all ten tested anemones, which indicated that particulate food fragments as well as soluble constituents (*e.g.*, the water-soluble dye Evans blue) were almost completely trapped in the mesenterial sacs. Hence, no mixing of the digestive juices occurred within the gastric cavity. This explains why very little digestive enzymes were previously detected in the gastric cavity during digestion (9, 10). Endocytosis took place almost exclusively in the mesenterial regions directly adjacent to the filaments, even when the animals were fed to satiation (Fig. 1). No endocytosis was detected in the rest of the mesenteries or column walls.

In summary, the results show that in *Haliplanella* only a very small part of the gastrodermal surface area is used for digestion of natural food. This is not due to a general lack of uptake capabilities in the other areas, but is due to a highly localized digestion during which even soluble food constituents remain trapped in the sacks formed by the mesenteries. Only small fractions of artificial food were absorbed in the column walls. Enhancement of the gastrodermal surface area as the main function of the mesenteries (1) is not likely, at least in this species. Instead, mesenteries serve mainly biomechanical functions (11).

I thank the Deutsche Forschungsgemeinschaft for financial support in the form of a postdoctoral fellowship (Bu 971/-1) and Alan Kuzirian, Eugene Tassinari, Hemant Chikarmane, and Gerhard Jarms for helpful discussions and support.

Literature Cited

1. **Schuchert, P. 1993.** *Z. Zool. Syst. Evol.-forsch.* **31:** 161–173.
2. **Van Praet, M. 1985.** *Adv. Mar. Biol.* **22:** 65–99.
3. **Van Praet, M. 1980.** *Reprod. Nutr. Dev.* **20:** 1393–1399.
4. **Metschnikoff, E. 1880.** *Zool. Anz.* **3:** 261–263.
5. **Mesnil, F. 1901.** *Ann. Inst. Past.* **15:** 352–397.
6. **Chintiroglou, C. 1992.** *Helgol. Meeresunters.* **46:** 53–62.
7. **Dunne, J. F., and Littlefield, C. L. 1983.** Pp. 131–140 in *Hydra: Research Methods*, H. M. Lenhoff, ed. Plenum Press, New York.
8. **MacGinitie, G. E., and MacGinitie, N. 1949.** *Natural History of Marine Animals*, p. 126. McGraw-Hill, New York.
9. **Nicol, J. A. C. 1959.** *J. Mar. Biol. Assoc. U.K.* **38:** 469–476.
10. **Krijgsam, B. J., and Talbot, F. H. 1953.** *Arch. Int. Physiol.* **61:** 277–291.
11. **Batham, E. J., and Pantin, C. F. A. 1950.** *J. Exp. Biol.* **27:** 264–289.

Reference: *Biol. Bull.* **189:** 237–238. (October/November, 1995)

Natural Diets for *Hermissenda crassicornis* Mariculture

Conxita Avila and Alan M. Kuzirian (Marine Biological Laboratory)

A main goal at the *Hermissenda* Resource Facility is to maximize maintenance conditions for survival, fecundity, and development rates on a steady, year-round basis (1). At times, the main laboratory food, the hydroid *Tubularia crocea*, is difficult to obtain. For that reason, some alternative artificial diets, such as crab meat and fish food pellets, have been used to feed *Hermissenda* juveniles (2, 3). Of the diets tested, soft fish food pellets gave optimal results, although water fouling could not be com-

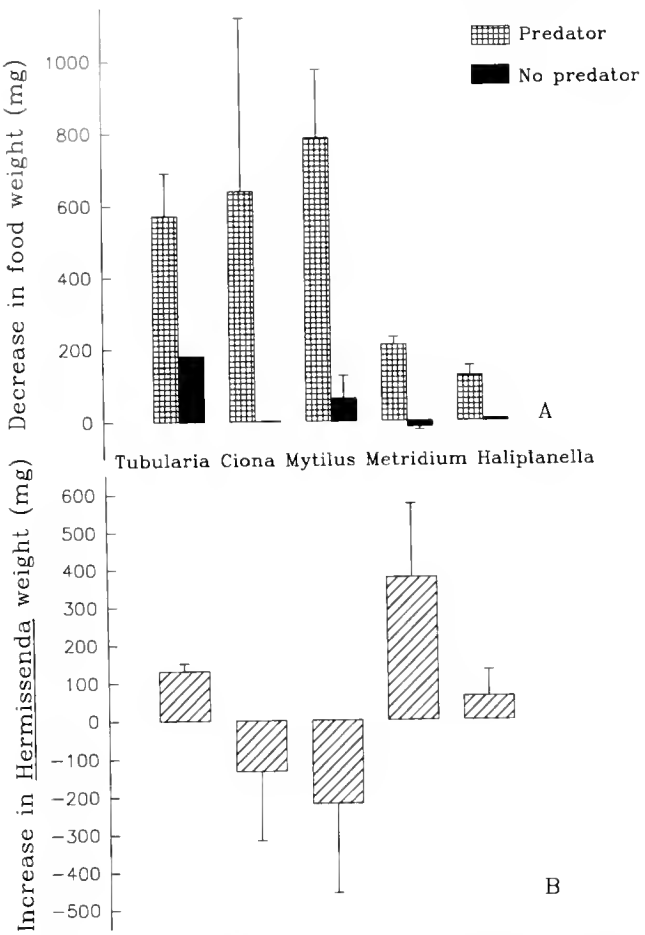

Figure 1. Hermissenda crassicornis *feeding experiment with five different diets, the hydroid* Tubularia crocea, *the tunicate* Ciona intestinalis, *the mussel* Mytilus edulis, *and the anemones* Metridium senile *and* Haliplanella luciae. *(A) Decrease in the food weight (mg) in the presence and absence of* H. crassicornis. *(B) Increase in weight (mg) in* H. crassicornis *with different diets. Values are means of three replicates ±SE.*

pletely avoided (2). Therefore, we found it useful to try additional natural diets that could not only provide a temporary food source, but also allow adult *Hermissenda* to grow and produce egg masses.

We tested the tunicate *Ciona intestinalis*, the mussel *Mytilus edulis*, the anemones *Metridium senile* and *Haliplanella luciae*, with the hydroid *T. crocea* as a control. Adult *Hermissenda* (three replicates/treatment) were maintained in individual 200-ml containers at 12°C and fed *ad libitum*, except those on the *Haliplanella* diet. The cnidarians were offered live, while the tunicates (cut) and mussels (opened) were offered fresh. The seawater was changed every other day, and food was added as necessary. Food items and the *Hermissenda* specimens were weighed before and after the experiment, which lasted 1 week. Eggs laid were also weighed. In addition, food items were kept in containers without predators to evaluate changes in weight other than those accounted for by consumption. Data were statistically analyzed by using ANOVA and the Student-Newman-Keuls test.

Our data indicate that all the food items were eaten by *Hermissenda* (Fig. 1A), although the amounts consumed yielded different growth rates. Changes in food weight from causes other than predation were minimal (Fig. 1A). Most specimens laid at least one egg mass, with the exception of those on the tunicate diet and two animals on the mussel diet. As in other studies with opisthobranch molluscs (4), egg mass and adult weight were considered together as the cumulative increase in weight (Fig. 1B). Statistical analysis indicated that the treatments produced significantly different weight gains (ANOVA, $p = 0.03$, d.f. = 4). The results of the Student-Newman-Keuls test indicated significant differences between the following pairs of diets: *Tubularia/Ciona* ($p = 0.04$), *Tubularia/Mytilus* ($p = 0.04$), *Ciona/Metridium* ($p = 0.019$), *Mytilus/Metridium* ($p = 0.017$), and *Metridium/Haliplanella* ($p = 0.039$). Therefore, for the growth of *Hermissenda* in the laboratory, the *Tubularia* diet is better than the *Ciona* or *Mytilus* diets. Furthermore, the *Metridium* diet is better than the *Ciona*, *Mytilus*, or *Haliplanella* diets. The *Ciona* and *Mytilus* diets, although eaten by *Hermissenda*, resulted in significant weight loss and a rapid increase in water fouling. All the cnidarian foods produced a weight increase in *Hermissenda*, with no effects on water quality. The weight gain was most significant for animals fed with *M. senile*, followed by *T. crocea*, and then *H. luciae* (Fig. 1B). *H. luciae*, which was confirmed as a suitable prey in two earlier experiments (not reported here), was rapidly eaten by *Hermissenda*, but could not be used *ad libitum* due to limited availability. Further experiments should analyze the long-term effects of these different diets, particularly *Metridium* and *Haliplanella*, both on adult growth and on reproductive effort.

A Spanish Government postdoctoral fellowship to C.A. is gratefully acknowledged. This research was supported by an NCRR-NIH grant (P40-RR03820) to A.M.K. *H. luciae* was kindly provided by C. M. Chester of the University of New Hampshire.

Literature Cited

1. **Kuzirian, A. M., C. T. Tamse, and E. Yamoah. 1989.** *Am. Zool.* **29**: 333.
2. **Yamoah, E., A. M. Kuzirian, D. Phie, and L. Matzel. 1988.** *Biol. Bull.* **175**: 309.
3. **Harrigan, J. F., and D. L. Aikon. 1978.** *Biol. Bull.* **154**: 430–439.
4. **Havenhand, J. N., and C. D. Todd. 1988.** *J. Exp. Mar. Biol. Ecol.* **118**: 173–189.

Reference: *Biol. Bull.* **189**: 239. (October/November, 1995)

The Effect of Temperature on the Relationship Between a Ciliated Protozoan, *Trichodina cottidarum*, and the Longhorn Sculpin, *Myoxocephalus octodecemspinosus*

David C. Brazik and Robert A. Bullis (School of Veterinary Medicine, University of Pennsylvania, Marine Biological Laboratory)

The longhorn sculpin (*Myoxocephalus octodecemspinosus*) is the host of *Trichodina cottidarum*, a frequent inhabitant of the gills. Natural repellents in the mucus of the fish's surface help limit the number of *Trichodina* present (1). The antimicrobial properties of this protective layer either diminish or change when an animal becomes stressed, allowing *Trichodina* to increase in numbers, which causes damage to the gills. Sculpins captured and held at colder temperatures exhibited little mortality, but as the ambient temperature rose in the spring, sculpin mortality associated with protozoal branchitis increased (Bullis, unpub. data). Thus, increased water temperature may play a deleterious role in the relationship between these organisms.

Forty sculpin were obtained from the Marine Resources Center of the Marine Biological Laboratory. Four 20-gallon tanks were set up with running ambient seawater and each had an undergravel filter of native sand. Ten fish were placed in each aquarium. Heaters were placed in three tanks to slowly raise the temperature of the water by 2°C per day for 5 days. One tank was heated and held at 10°C, two at 15°C, and the fourth tank remained at ambient (~5°C) for the remainder of the experiment (4 weeks). One of the 15° tanks was used as a treatment tank. After ~50% of this group had died and been confirmed as being *Trichodina* positive, the temperature was allowed to return to ambient in an attempt to retard protozoal growth. Water quality was tested weekly to ensure that there was no build-up of ammonia or nitrite that could damage the gills of the animals. The fish were not fed during the experiment.

Tanks were observed daily for mortality. When a fish died, its gills were examined for signs of petechiation, and the second gill arch was removed and examined microscopically for the presence of *Trichodina*. Infections were rated as mild (<1 parasite/100× field), moderate (1–10/field), or severe (>10/field).

Survival patterns indicate that fish lived longer at the lower temperatures (Fig. 1). The fish population decreased fastest in the 15°C tank and slowest in the ambient-water tank. Lowering the water temperature only prolonged the time until mortality.

Because *Trichodina* is normally found in wild populations of sculpins, these fish must enter the captive environment already harboring this protozoan (2). In the wild, only mild (80%) and moderate (20%) infections were seen. After only 10 days in captivity, a relatively even distribution of infection (36% mild, 21% mod., 43% severe) was noted in captive fish. Clearly, the captive environment is playing a role in the development of this disease.

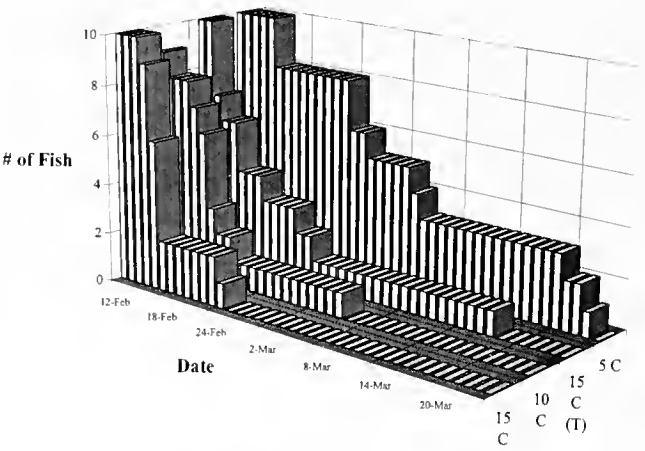

Figure 1. *Shows the survival in the captive environment of longhorn sculpins held at different temperatures. Survival was greatest in animals that were held at ambient temperature (5°C). The onset of mortality was faster in fish held at higher temperatures. Allowing the temperature to return to ambient in the 15°C (T) prolonged the survival of fish as compared to the group that remained at 15°C.*

Fluctuation in temperature and high stocking density were environmental stresses that should have been avoided. Better temperature control and an understanding of the role that anemia plays are essential to further elucidating the problem. But currently, low temperatures and short holding times are the most effective means of maintaining the health of sculpins in captivity.

David Brazik is a student in the Marine Program at Bowling Green State University. The authors thank the Boston University Marine Program for supplying us with laboratory space and supplies, Dr. Rainer Voigt for assisting with the experimental setup, and Mr. Ed Enos of the MBL Marine Resources Department for generously donating the fish used in this project.

Literature Cited

1. **Lom, J., and I. Dykova. 1992.** Pp. 269–279 in *Protozoan Parasites of Fishes.* Elsevier, Amsterdam.
2. **Lom, J., and M. Laird. 1969.** *Can. J. Zool.* **47**: 1367–1380.

Reference: *Biol. Bull.* 189: 240–241. (October/November, 1995)

A Settlement Bioassay Assessing the Response of Soft Shell Clam Larvae to Sediments from Various Sites in Massachusetts Bay

M. Wintermyer, D. Leavitt, and J. McDowell (Woods Hole Oceanographic Institution, Woods Hole, Massachusetts 02543)

Many environmental influences including pollution, predation, water currents, and food availability can impact the survival and settlement of bivalve larvae (1). Larval survival and settlement are key factors in structuring populations of the soft shell clam (*Mya arenaria*) (2). If larval survival and settlement are impacted by environmental contaminants, one could expect to observe changes in population structure of soft shell clams at the experimental sites. A settlement bioassay was performed using soft shell clam larvae to determine the impacts on survival and settlement of the larvae on various levels of contaminated sediments collected from Massachusetts.

Hatchery-reared larvae of the soft shell clam were exposed to sediment collected from five sites within Massachusetts Bay: Wellfleet Harbor, Barnstable Harbor, Saugus River, Quincy/Neponset River, and Fort Point Channel. The five test sediments are known to represent a range of polycyclic aromatic hydrocarbon levels based on analyses by Moore *et al.* (3). Several of the sites (Fort Point Channel, Saugus, and Quincy/Neponset) are within the city limits of areas highly industrialized and whose marine ecosystems are influenced by many nonpoint sources of pollution. The contaminant status of the five sites is as follows: Wellfleet Harbor and Barnstable Harbor are minimally impacted, Quincy/Neponset River and Saugus River are moderately contaminated, and Fort Point Channel is highly contaminated. Two controls, filtered seawater (no sediment) and an artificial sediment composed of microbeads, were also used. The sediments were wet-sieved through a 96-μm-mesh screen and centrifuged to remove all sediment from the water column. The 96-h assay was performed using 24-well tissue culture plates. Each of the sediment treatments consisted of 10 replicates. Each well received 2 ml of filtered (0.45 μm) seawater; controls had either seawater alone or seawater plus 1 ml of microbeads. Competent larvae were added at a density of 30 larvae per 1 ml of the test sediment as described by Phelps *et al.* (4). Survival and settlement were assessed visually after the 96 h. Larvae were considered to be in the veliger stage if they were swimming in the water column; settled larvae were identified by the appearance of a foot and a dorsoventrally flattened shell. Dead larvae were opaque and often infected with protozoans. Although neutral red dye is sometimes used to aid in distinguishing settled larvae from dead larvae, this was not necessary with *M. arenaria*.

The results of this bioassay are depicted in Figure 1. The filtered seawater control had significantly less settlement than any other treatment: 33.0% of the living larvae settled in the filtered seawater compared to 98.2% in the control microbead sediment, indicating that the larvae required a sediment substrate for settlement. Survival was 20%–30% higher for larvae exposed to control treatments than for larvae exposed to test sediments. The difference between the controls and test treatments was significant for sediment from Wellfleet Harbor (a site with low contamination), possibly because it was anoxic. The control microbead sediment had the highest number of settled larvae (225), but percent settlement was not significantly different among all six test sediments (range of 89%–100% of living larvae settled).

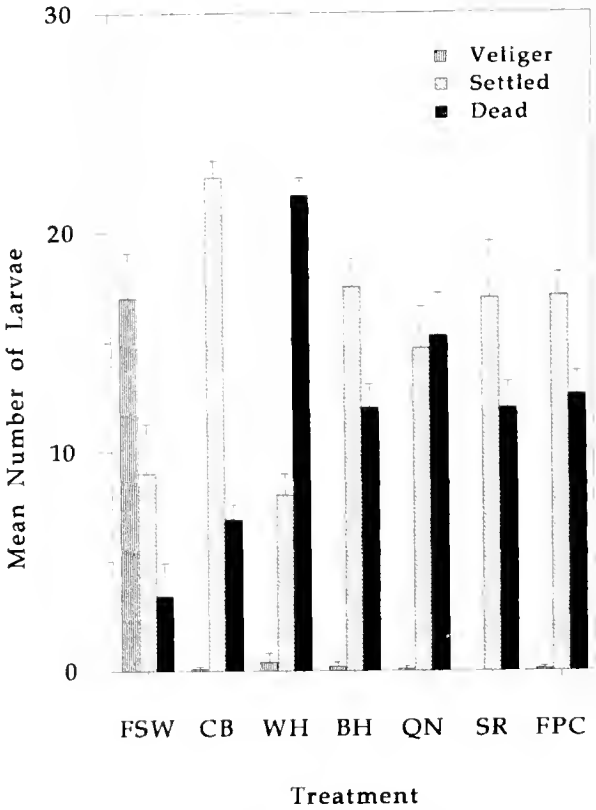

Figure 1. *Mean number of swimming veligers, settled larvae, and dead larvae from the settlement bioassay assessed after 96 h. Filtered seawater (FWS) and control microbead sediment (CB) are control treatments. Wellfleet Harbor (WH) and Barnstable Harbor (BH) are minimally impacted sites, Saugus River (SR) and Quincy/Neponset (QN) are moderately contaminated, and Fort Point Channel (FPC) is highly contaminated*

This work demonstrates that each of the six sediments, regardless of contaminant loading, was able to induce settlement of the soft shell clam larvae. Larval mortality was not different between sites, with the exception of an apparent anoxic condition in Wellfleet sediment. It is unlikely, on the basis of these experimental results, that the mortality and settlement of soft shell

clam larvae could affect the structure of the population. Differences in population structure are more likely to be caused by other factors, including the availability of larvae and post-settlement mortality.

Literature Cited

1. **Wilbur, K. 1983.** Pp. 299–336 in *The Mollusca*, vol. 3, N. H. Verdonk, J. A. M. Van Den Biggelaar, and A. S. Tompa, eds. Academic Press, New York.
2. **Broussean, D. J. 1976.** P. 151. Ph.D. Dissertation. Univ. of Massachusetts, Amherst, MA.
3. **Moore, M., R. Smolowitz, D. Leavitt, B. Jensen, B. Woodin, and J. Stegeman. 1995.** *National Estuarine Program Coastal Technology Transfer Conference*, New Orleans, Feb. 13–16.
4. **Phelps, H., and K. Warner. 1990.** *Bull. Environ. Contam. Toxicol.* **44:** 197–204.

Reference: *Biol. Bull.* **189:** 241–242. (October/November, 1995)

Invertebrate Response to Nutrient-Induced Changes in Macrophyte Assemblages in Waquoit Bay

Jenny Ahern, Julie Lyons, James McClelland, and Ivan Valiela (Boston University Marine Program, Marine Biological Laboratory)

Coastal marine systems such as Waquoit Bay, Massachusetts, have experienced a major increase in nutrient loads through groundwater in recent decades (1). Five estuaries of Waquoit Bay (Childs River, Hamblin Pond, Jehu Pond, Quashnet River, and Sage Lot Pond) are subject to different nutrient loads due to different land uses in their watersheds (1). Nutrient loading prompts replacement of eelgrass (*Zostera marina*) by macroalgae-dominated communities (2). In this paper we address whether the vegetation changes caused by nutrient loading result in parallel changes in the benthic fauna of the affected areas.

In each of the five estuaries, the macrophyte and invertebrate communities were sampled at 10 sites (randomly selected within representative depth strata) with an Eckman dredge (0.15 m^2), June–August 1995. Samples were rinsed through a 1-mm sieve. Macrophytes were sorted by species, dried, and weighed (aboveground biomass only for eelgrass). Macroinvertebrates were categorized into taxonomic groupings and counted.

The estuaries varied widely in eelgrass and macroalgal biomass (Fig. 1). Benthic invertebrate density did not change markedly with the decrease in eelgrass biomass from Sage Lot Pond and Jehu Pond to the other estuaries (Fig. 1, top). In contrast, invertebrate density showed a clear inverse relationship with macroalgal biomass ($r^2 = 0.5$, $P = 0.003$) (Fig. 1, bottom). Childs River, the most nutrient-loaded site, had a consistently higher macroalgal biomass and a lower invertebrate density (Fig. 1, bottom). The other sites (shown without initials in Fig. 1) had much lower macroalgal biomass than Childs River, but still show a strong negative relationship between invertebrate density and macroalgal biomass ($r^2 = 0.3$, $P = 0.07$) when Childs River points are excluded. The other estuaries did not, however, have consistently different macroalgal biomass from each other.

Although the decrease in eelgrass biomass did not alter invertebrate density, it did change faunal composition. In eelgrass-dominated communities (Jehu Pond, Sage Lot Pond), polychaetes composed 26% of the invertebrate abundance, whereas in macroalgae-dominated communities polychaetes increased to 41% of benthic invertebrates. Changes in the abundance of a single species in response to eelgrass loss have been documented for shellfish species of Waquoit Bay (1).

Many factors may influence invertebrate abundance in estuaries. Low-oxygen conditions associated with accumulations of macroalgae (3) may be responsible for the decrease in invertebrate density with increasing macroalgae biomass; this oxygen

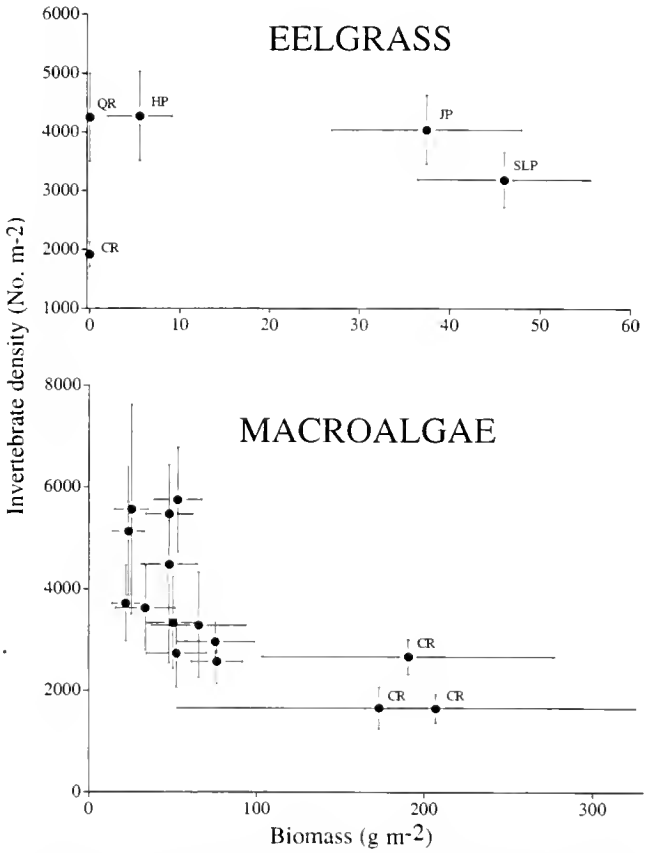

Figure 1. *Invertebrate density versus biomass of eelgrass (top) and macroalgae (bottom) in five estuaries of Waquoit Bay. Samples were taken June–August 1995. Points are summer average ± SE (n = 30) (top) and monthly average ± SE (n = 10) (bottom).*

depletion is caused by an imbalance between respiration and photosynthesis during periods of low irradiance. Childs River, in particular, has more frequent anoxic events than other Waquoit Bay estuaries (4), possibly accounting for the lower densities of invertebrates in this estuary. Salinity was 25–30‰ near the bottom at all sites, suggesting that this variable was not a significant factor. Differential predation, sediment composition, and depth may also influence invertebrate density and taxonomic composition, thus contributing to the variability of the data.

Nutrient loading from watersheds has induced replacement of eelgrass by macroalgae-dominated communities in many shallow estuaries (2, 5). Our study demonstrates that these shifts in macrophyte assemblages may play a key role in macrobenthic invertebrate community changes. Both eelgrass-dominated and macroalgae-dominated sites can support comparable invertebrate densities; however, as macroalgae increase, benthic invertebrate numbers decrease. The switch in dominance from eelgrass to macroalgae is also accompanied by changes in taxonomic composition.

This work was supported by REU-NSF (OCE 9300490), NOAA (NA170R21101), and the Waquoit Bay Fellowship.

Literature Cited

1. **Valiela, I., *et al.* 1992.** *Estuaries* **15:** 443–457.
2. **Duarte, C. M. 1995.** *Ophelia* **41:** 87–112.
3. **Ileip, C. 1995.** *Ophelia* **41:** 113–136.
4. **D'Avanzo, C., and J. N. Kremer. 1994.** *Estuaries* **17:** 131–139.
5. **Lyons, J. A., J. Ahern, J. McClelland, and I. Valiela. 1995.** *Biol. Bull.* **189:** 255–256.

Reference: *Biol. Bull* **189**: 242–243. (October/November, 1995)

Effect of Changing Plant Morphology on Invertebrate Susceptibility to Predation in Eelgrass Beds

Matthew C. Preisser and Linda A. Deegan (Marine Biological Laboratory)

Long-term coastal eutrophication leads to changes in the macrophyte community in eelgrass beds by allowing macroalgae to outcompete the eelgrass (1). Changes in plant species may affect predation on the invertebrate community by altering habitat morphology. This study analyzed predation rates, in habitats of contrasting plant morphology, on two invertebrate species that exhibit different strategies for avoiding predation.

Rates of predation by *Fundulus heteroclitus* on the isopod *Erichsonella filiformis* and the amphipod *Lysianopsis alba* were measured in the laboratory under conditions simulating three habitats: no vegetation, eelgrass (*Zostera marina*), and the macroalga *Cladophora* spp. Twelve trials of each experimental treatment were run, each with 80 g (wet biomass) of vegetation in a 20-l aquarium flushed with running ambient seawater. The same aquaria and vegetation were used for the 12 replications of each treatment; new prey and predators were introduced at the beginning of each of these trials. Macrophyte densities were comparable to those encountered in the field.

Twenty individuals of a single prey species were placed in each tank and allowed to acclimate for 45 min. One *Fundulus* (starved for 24 h) was then introduced. This prey density, higher than the natural field density, was used to allow the predator to forage for the full experiment. The fish was removed after 1 h and the remaining prey were counted. Missing prey were assumed to have been eaten; no invertebrates were found partially eaten or dead. Predation rate was calculated as the percentage of prey eaten during the 1-h interval.

Predation on *Erichsonella* was lowest (30.4%) in eelgrass (Fig. 1, top). With its long thin body and green coloration, this isopod resembles a blade of eelgrass. The strategy of "background matching" may make detection by visual predators difficult in eelgrass habitats. Predation was moderate (47.1%) in the aquaria with *Cladophora*, possibly because the algae provided some structure and a green background. Predation was highest (94.2%) in the 'no vegetation' treatment because the isopod is not a strong swimmer and had no refuge.

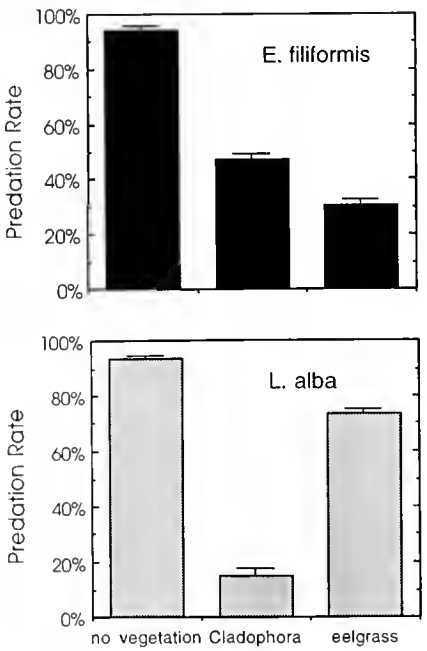

Figure 1. *Predation rate (mean % ± standard error) of* Fundulus heteroclitus *on* Erichsonella filiformis *(top) and* Lysianopsis alba *(bottom) in habitats of differing morphology.*

Predation on *Lysianopsis* was lowest (15.4%) in *Cladophora* (Fig. 1, bottom), which forms a thick intertwining mat. The amphipod's strategy for avoiding predation was to burrow deep into the algae, putting itself out of the reach of the predator. In the field, however, such behavior might be hindered by the anoxic conditions often found in the mat. The experimental methodology of this study allowed for a fairly complete exchange of the interstitial mat water, which resulted in aerobic conditions throughout the mat. Predation was high (73.8%) in the eelgrass, probably because crawling and burrowing amphipods cannot take advantage of the vertical structure of the plant. Predation was highest (93.3%) in the 'no vegetation' treatment because there was no substrate available to provide protection.

Predation rate was analyzed in a one-factor ANOVA ($P = 0.05$). Differences among treatment means were evaluated using Fisher's PLSD ($P = 0.05$). There were strong differences in predation rates between prey in different vegetation types ($F = 227.615$). All predation rates were different from each other except in the 'no vegetation' treatment.

Many invertebrate species are highly dependent upon macrophyte structure and color for protection against predation (2). Alteration of the primary producer community due to eutrophication may change the structure of the habitat and may potentially have second-order effects on the invertebrate community.

This study was supported by the Boston University Marine Program and the Cox Foundation.

Literature Cited

1. **Valiela, I., *et al.* 1992.** *Estuaries* **15:** 443–457.
2. **Nelson, W. G. 1979.** *J. Exp. Mar. Biol. Ecol.* **38:** 225–245.

Reference: *Biol. Bull.* **189:** 243–244. (October/November, 1995)

Effect of Algal Cover on Size-Selective Predation of *Gammarus mucronatus* by the Striped Killifish, *Fundulus majalis*

Chaka Drake, Peter J. Behr, and Ivan Valiela (Boston University Marine Program, Marine Biological Laboratory)

The relative sizes of predators and prey influence top-down control of prey as well as success of predation (1). The striped killifish, *Fundulus majalis*, is an abundant predator (2) in estuaries of Waquoit Bay and often feeds on the amphipod *Gammarus mucronatus*, one of the most common benthic species in the Bay.

Predation by fish is also affected by the physical structure of the habitat in which predation takes place (3, 4). In Waquoit Bay, one major aspect of habitat structure is the presence or absence of macroalgae. To determine the effects of macroalgal cover and its possible interactions with size-selective predation, we tested predation by different sizes of *F. majalis* on different sizes of *G. mucronatus* in the presence and absence of the green alga *Cladophora vagabunda*. *C. vagabunda* is the dominant macroalgal species in the Bay.

Fish, amphipods, and algae were collected from estuaries of Waquoit Bay, Massachusetts. The specimens were held in flow-through seawater tanks for 2–5 days before use in experiments. *C. vagabunda* was cleaned of all debris and organisms before use in experiments. Individuals of *G. mucronatus* were separated into three size categories, small (0.3–0.8 mm), medium (0.8–1.3 mm), and large (1.4–2.0 mm), by measuring from eye to

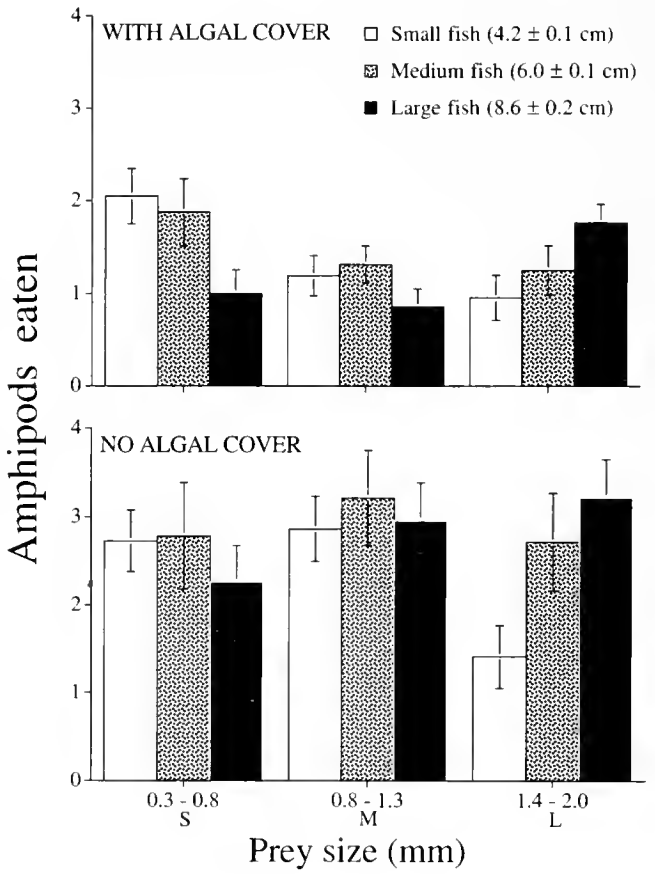

Figure 1. *Consumption (amphipods eaten ± SE) of* Gammarus mucronatus *of different size by* Fundulus majalis *of different size with (top), and without (bottom) cover of the alga* Cladophora vagabunda. *Consumption was over a 2-h period*

second abdominal segment. *F. majalis* specimens were also placed into three total-length size categories: small (2.9–4.9 cm), medium (5.0–6.9 cm), and large (7.0–12.4 cm).

Five small, medium, and large *G. mucronatus* were placed in 3-l-capacity jars with a 1.7-l volume of loosely packed *C. vagabunda*. The amphipods were allowed to acclimate to the jars for 1 h before addition of *F. majalis*. Fish were fed 2 h prior to experimentation and then placed individually within the 3-l jars to feed for 2 h. After the feeding period, the fish were removed and measured. The amphipods remaining in the jars were categorized by size class and counted. The trial runs were made with algae (58 replicates) and without algae (60 replicates). A three-way ANOVA was used for comparison of cover, prey size, and predator size.

Consumption was affected by algal cover ($F = 62.4$; $P < 0.001$) and an interaction between sizes of prey and predators ($F = 4.8$; $P < 0.001$). Prey consumption was about twice as high in the absence of algae (Fig. 1). In jars containing algae, the large fish consumed fewer small prey than smaller fish (Fig. 1, top left). Additionally, small fish consumed fewer large prey than larger fish (Fig. 1, right top and bottom). Intermediate-sized prey were fed upon at about the same amount, regardless of size of fish (Fig. 1, middle top and bottom). The presence or absence of macroalgal cover did not affect size-selective feeding (the F value for the 3-way interaction was 0.2; $P = 0.960$).

The data suggest that as fish grow, their food preferences change from small to large prey, so that predation is exerted on different parts of benthic invertebrate populations. Macroalgal cover reduced predation success, but did not change size selectivity.

This work was supported by a Waquoit Bay Land Margin Ecosystems Research REU internship.

Literature Cited

1. **Ryer, C. 1988.** *Mar. Ecol. Prog. Ser.* **48**: 37–45.
2. **Werme, C. E. 1981.** Ph.D. Dissertation. Boston University. 126 pp.
3. **Vince, S., *et al.* 1976.** *J. Exp. Mar. Biol. Ecol.* **23**: 255–266.
4. **Jones, G., *et al.* 1991.** Pp. 171–172 in *The Ecology of Fishes on Coral Reefs*, P. Sale, ed. Academic Press, San Diego.

Reference: *Biol. Bull.* **189**: 244–245. (October/November, 1995)

Effect of Macroalgal Species and Nitrogen-Loading Rates on Colonization of Macroalgae by Herbivorous Amphipods

Nicole Martinez, Jennifer Hauxwell, and Ivan Valiela (Boston University Marine Program, Marine Biological Laboratory)

The macroalgae *Cladophora vagabunda* (green, filamentous) and *Gracilaria tikvahiae* (red, branching) are common in estuaries of Waquoit Bay subject to different nitrogen-loading rates (1). The total biomass and relative abundances of the two macroalgal species may depend not only on nitrogen-loading rates (1, 2) but also on significant consumption by herbivorous amphipods (Hauxwell *et al.*, unpub.). Because food preference of an abundant grazer can significantly decrease the abundance of targeted macroalgae and alter competitive interactions among producers (3), we conducted a colonization experiment to determine (1) whether grazers prefer *C. vagabunda* or *G. tikvahiae* and (2) whether preferences for the two macroalgal species differ in estuaries subject to different nitrogen-loading rates.

Because relatively small amphipod herbivores hide within the macroalgae they consume, preference may be linked not only to food quality (nitrogen content, digestibility) but also to the amount of shelter an alga affords from predation. To assess grazer macroalgal substrate preference, we deployed three (30 × 16 × 10 cm) cages containing equal volumes of either *C. vagabunda* (34 g ww) or *G. tikvahiae* (60 g ww) in estuaries with high (Childs River) and low (Sage Lot Pond) nitrogen loadings (1) and measured colonization by amphipods. To assess whether shelter was important as a cue in selection by grazers, we eliminated food cues from a third treatment by replacing the macroalgae with an equivalent volume of plastic mesh.

C. vagabunda and *G. tikvahiae* were collected and cleaned of grazers before being placed in cages, and were indigenous to the estuary in which they were used. The cages, constructed with 2-mm mesh to allow entry of grazers while retaining algae, were secured to the algal mat by attaching both ends to reinforcing rods driven into the sediment. Swivels were used to connect each end to a string loop around the reinforcing rod, which enabled a snorkeler to detach the cage without disturbing its contents. Cages were retrieved after 1 week; while one snorkeler detached an end, another placed a bag around the entire cage to retain all grazers. Grazer density and species composition were recorded for each cage. Three replicates of each of the algal species were installed in each estuary. Six one-week trials were run during midsummer.

There were seasonal patterns in the data (ANOVA, $P < 0.05$ in all cases), showing peak abundances in midsummer. This trend parallels survey data obtained from our these estuaries (J. McClelland, unpub.). However, where preferences were found, the proportion of grazers found in *C. vagabunda* relative to *G. tikvahiae* was similar across trials. We therefore present averages pooled across trials.

Provision of cover alone did not seem to influence grazer substrate preference, because amphipods preferred algae over artificial cover in all cases (Table I). The preference of amphipods between the two algal species differed between estuaries (Table

Table 1

Number (mean ± standard error) of amphipods of different species found in experimental cages containing either Cladophora vagabunda, Gracilaria tikvahiae, *or artificial cover at estuaries with high (Childs River) and low (Sage Lot Pond) nitrogen-loading rates. Because these species are not readily distinguishable, data for* Ampithoe longimana *and* Cymadusa compta *were combined*

	Childs River			Sage Lot Pond		
Grazers	*Cladophora vagabunda*	*Gracilaria tikvahiae*	Cover Treatment	*Cladophora vagabunda*	*Gracilaria tikvahiae*	Cover Treatment
Microdeutopus gryllotalpa	147 ± 33	28 ± 5	18 ± 6	128 ± 32	184 ± 65	44 ± 10
Ampithoe longimana/ Cymadusa compta	149 ± 54	156 ± 34	66 ± 13	15 ± 8	29 ± 11	9 ± 3
Total Grazers	304 ± 66	188 ± 38	85 ± 17	157 ± 40	244 ± 63	59 ± 9

I). In Childs River, *Microdeutopus gryllotalpa* clearly preferred *C. vagabunda*, while the other amphipods (*Ampithoe longimana* and *Cymadusa compta*) showed no preference. Total grazers (also including *Lysianopsis alba, Gammarus mucronatus,* and *Corophium* sp.) were found in higher densities in *C. vagabunda* cages than in *G. tikvahiae* cages. In Sage Lot Pond, no significant preferences were apparent.

Our results show (1) that grazers select algae principally on the basis of food value, rather than cover, (2) that *C. vagabunda* is preferred over *G. tikvahiae* by *M. gryllotalpa* and total grazers in estuaries subject to high nutrient loading, and (3) that grazers showed no significant preference at the site with low nitrogen loading. These shifts in preference between sites may be attributed to differences in food quality [as, for example, by increased nitrogen content in more loaded estuaries (2)] as perceived by two amphiod populations. The potential impact of herbivores in controlling macroalgal biomass is therefore directed toward different macroalgal species in different estuaries, and the role of nitrogen loading mediates the colonization by grazers of different macroalgal species.

This work was supported by NSF-Research Experiences for Undergraduates.

Literature Cited

1. **Valiela, I., *et al.* 1992.** *Estuaries* **15:** 443–57.
2. **Peckol, P., *et al.* 1994.** *Mar. Biol.* **121:** 175–185.
3. **Lubchenco, J. 1978.** *Am. Nat.* **112:** 23–39.

Reference: *Biol. Bull.* **189:** 245–246. (October/November, 1995)

Differences in Benthic Invertebrate Assemblages in Two Estuaries of Waquoit Bay Receiving Disparate Nutrient Loads

Rafael Sardá (Centro de Estudios Avanzados de Blanes, CSIC, 17300-Blanes [Girona], Spain), Kenneth Foreman, and Ivan Valiela

We evaluated the effects of nutrient loading on benthic communities by measuring the abundance and composition of macroinfaunal assemblages inhabiting similar habitats within two Waquoit Bay estuaries subject to different rates of nutrient loading. On the basis of water recharge rates and dissolved inorganic nitrogen concentrations in groundwater at the shore, we estimated that each year about 8500 kg of nitrogen enter the Childs River estuary (4.6 moles m^{-2} $year^{-1}$) and roughly 3500 kg (1.5 moles m^{-2} $year^{-1}$) enter the Quashnet River. The intensity of nutrient loading to these estuaries differs primarily because of differences in the density of houses and septic systems within their surrounding watersheds (2).

In both estuaries, the benthic assemblages differed depending on location within the gradient of fresh to saltwater. The polychaete *Amphicteis gunneri* and the amphipod *Leptocheirus plumulosus* dominated faunal abundance and biomass in low-salinity areas of the Quashnet River. In the Childs River, low-salinity areas were dominated by insect larvae. Abundance and diversity were highest in the medium-salinity areas in both rivers. In the Quashnet River, the polychaetes *Streblospio benedicti* and *Amphicteis gunneri*, a tubificid oligochaete that we believe to be a species of *Limnodrillus*, and the anemone *Nematostella vectensis* were the most abundant benthic organisms, and the polychaete *Heteromastus filiformis* was the main contributor to biomass. In the Childs River, the oligochaete was by far the most abundant species, accounting for 70% of the total abundance, and the carnivorous polychaete *Neanthes virens* was the main contributor to biomass. In high-salinity areas, the polychaete

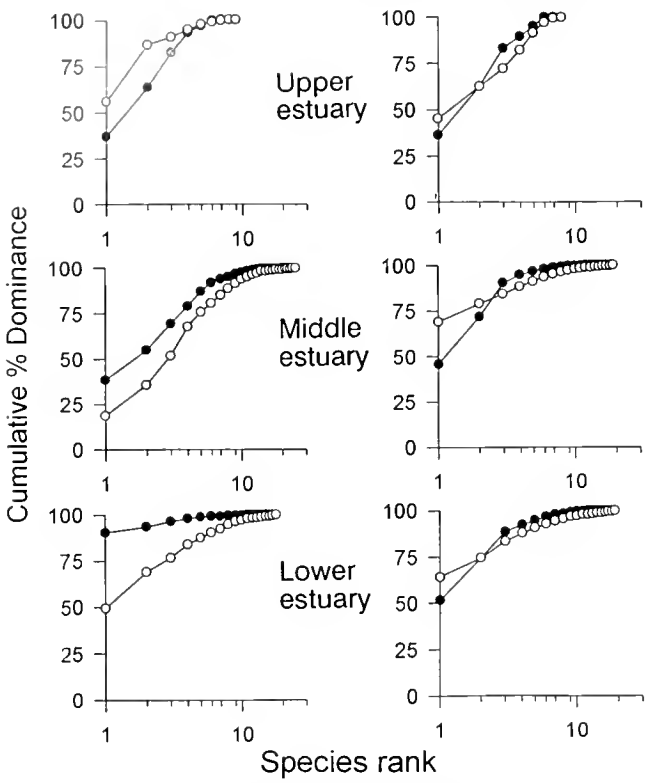

Figure 1. *K-dominance curves for abundance (open circles) and biomass (black circles) of macrofauna in the upper, middle, and lower parts of the Quashnet River (left) and Childs River (right).*

Marenzelleria viridis dominated the benthos of the Quashnet River in both abundance and biomass. In the Childs River, *Lumbricillus* spp. and *Neanthes virens* were again the main contributors.

Salinity appeared to be the primary factor controlling the distribution of the macroinfaunal species; but within any single salinity range, eutrophication seemed to be responsible for differences in the composition and abundance of macrofauna between estuaries. The abundance of oligochaetes and insect larvae and the occurrence of a large carnivore increased with nutrient loading, whereas the number and biomass of other typically resident species decreased. Most significantly, the ratio of polychaetes to oligochaetes was clearly lower in the Childs River (0.36) than in the Quashnet River (3.58).

We contrasted the benthic assemblages within the heavily nutrient-loaded Childs River estuary to those of the more moderately loaded Quashnet River estuary by constructing plots of ranked species dominance (3). The biomass and abundance of each species were ranked from highest to lowest and plotted against the cumulative percent biomass or percent abundance (Fig. 1). Plots in which the k-dominance curve for biomass falls above the curve for abundance are indicative of communities in which the most abundant fauna are large, slower growing species. These communities are indicative of relatively unstressed conditions. Plots in which the curve for abundance falls above the curve for biomass represent communities in which the most abundant species are small and rapidly growing. These are more typical of disturbed or eutrophied communities (1). No large differences were apparent between the k-dominance curves of abundance and biomass in the upper portion of either estuary. In both the middle and lower portions of the estuaries, the evaluation suggests that Childs River, with its more urbanized watershed, is more impacted by nutrient loading than the Quashnet River.

We acknowledge the MBL Associates Fellowship that supported Rafael Sardá during this work.

Literature Cited

1. **Valiela, I., *et al.*, 1992.** *Estuaries* **15(4:)** 443–457.
2. **Warwick, R. M. 1986.** *Mar Biol* **92:** 557–562.
3. **Pearson, T. H., and R. Rosenberg. 1978.** *Oceanogr Mar. Biol. Ann. Rev* **16:** 229–311.

Reference: *Biol Bull.* **189:** 246–247. (October/November, 1995)

Impact on Marine Species of New England Recreational Fishing Policies

Jonathan S. O'Neil (University of Rhode Island) and Ilene M. Kaplan

This study examines the status of the Massachusetts Atlantic cod (*Gadus morhua*) recreational fishery and the potential impact of proposed governmental marine regulations. Data from the 1993 National Marine Fisheries Service's catch and fish surveys along the eastern coastal United States (1) and the 1994 Add-on Marine Recreational Economics Survey of the Marine Recreational Fishing Statistical Survey were examined. Data collection methodology consisted of interviews with fishermen at on-site fishing locations and follow-up telephone interviews. Survey sampling sites were randomly selected from lists of fishing access sites weighted by expected fishing activity.

Reported commercial and recreational landings of Atlantic

cod strongly indicate a decline in this fishery, with the recreational fishery experiencing a greater decline proportionally (see Table 1). The potential decline in recreational stocks is even greater, because statistics on catch and release mortality from recreational fishing are not available.

Fishery managers seeking to reduce the harvest of cod are now targeting the recreational fishing industry. The data collected from the recreational fishermen indicate that they favor the conservation measures that fishery managers are proposing, although a sizeable minority are fearful of restrictions in certain geographic areas and during vacation or leisure time periods (see Table 1).

The data strongly suggest that the economic hardships predicted by operators and owners of businesses related to recreational fishing, particularly in the charter, party, and rental boat sectors, will not be sustained, because recreational fishermen will still pursue this activity. Additional data from this survey, indicating that the motivation to fish stems from experiential variables that are independent of policy limitations (other than a complete moratorium), also support this conclusion. This is a particularly important finding, for it shows how contact with fishermen can actually be used to support ecological measures without impeding economic pursuits. We suggest, however, that interviews be conducted within the business sector.

The data collected in the Add-on Marine Recreational Economics Survey are significant, illustrating that fishermen must be incorporated into policy decisions. We also suggest that, in addition to overfishing, other sources of stock depletion, such as pollution of the habitat, be investigated. A better understanding of the conflicts between ecological and economic interest groups, as well as among different types of fishermen, is essential if fisheries management is to be effective (2, 3, 4, 5).

The authors gratefully acknowledge the assistance of the National Marine Fisheries Service, the Woods Hole Oceanographic Institution, and the Marine Biological Laboratory in Woods Hole, Massachusetts.

Table 1

Decline in cod stocks and Massachusetts recreational fishermen's reactions to proposed regulations

US. Commercial and Recreational Landings (in metric tons)*	1990	1992
U.S. Recreational Landings**	5,200	1,300
U.S. Commercial Landings**	43,400	27,700
Party and Charter Boat Fishermen (n = 60)* **	**Support**	**Oppose**
Limits on the minimum size of fish that can be kept	95%	3%
Limits on the number of fish that can be kept	93%	7%
Limits on the time of year when fish can be kept	83%	17%
Limits on area where fishing can occur	88%	12%
Private and Rental Boat Fishermen (n = 414)* **	**Support**	**Oppose**
Limits on the minimum size of fish that can be kept	95%	5%
Limits on the number of fish that can be kept	92%	8%
Limits on the time of year when fish can be kept	79%	21%
Limits on area where fishing can occur	67%	33%

* NOAA Tech. Mem NMFS-F/NEC-101. 1993.
** Landings for Gulf of Maine, Georges Bank and areas south.
*** Compiled from NMFS Add-On Marine Economics Survey 1994.

Literature Cited

1. **NOAA 1993.** *Tech. Mem.* NMFS-F/NEC-101: 45.
2. **Kaplan, I. M., and B. C. Boyer. 1992.** *Biol. Bull.* **183:** 379–380.
3. **Kaplan, I. M., B. C. Boyer, and D. E. Hoffman. 1990** *Biol. Bull.* **179:** 227.
4. **Kaplan, I. M., B. C. Boyer, and D. E. Hoffman. 1989.** *Biol. Bull.* **177:** 327.
5. **Kaplan, I. M., B. C. Boyer, and K. A. Santos. 1988.** *Biol. Bull.* **175:** 312.

Reference: *Biol. Bull.* **189:** 247–248. (October/November, 1995)

The Effect of Residential and Forested Watershed Land Cover on Nutrient Loading to Hamblin and Jehu Ponds, Waquoit Bay, Massachusetts

Sue Ann Chaplin, Catherine Hunter MacGregor, Ivan Valiela, Kenneth Foreman, and Lori Soucy
(Boston University Marine Program, Marine Biological Laboratory)

Atmospheric deposition, fertilizer use, and wastewater are major sources of nitrogen to watersheds of Waquoit Bay estuaries. Groundwater transports nitrogen from all land covers within Waquoit Bay because precipitation quickly percolates into sands underlying the watershed surface (1). The major land covers in Waquoit Bay watershed are forest and residential. The major external input of nitrogen to forests is atmospheric deposition. The major inputs to residential land parcels are atmospheric deposition as well as fertilizer and wastewater nitrogen. The fate of nitrogen under forested or residential land cover differs (Valiela *et al.*, unpub. data). We asked whether water catchment areas with different proportions of forested and residential land lead to different nitrogen concentrations in groundwater heading to receiving estuaries. To address that question, we measured concentrations of nitrate (NO_3^-), ammonium (NH_4^+), and dissolved organic nitrogen (DON) in groundwater draining from areas with different proportions of forest and residential land cover types.

Jehu and Hamblin Ponds, two estuaries of Waquoit Bay, have both forested and residential areas within their watersheds. We

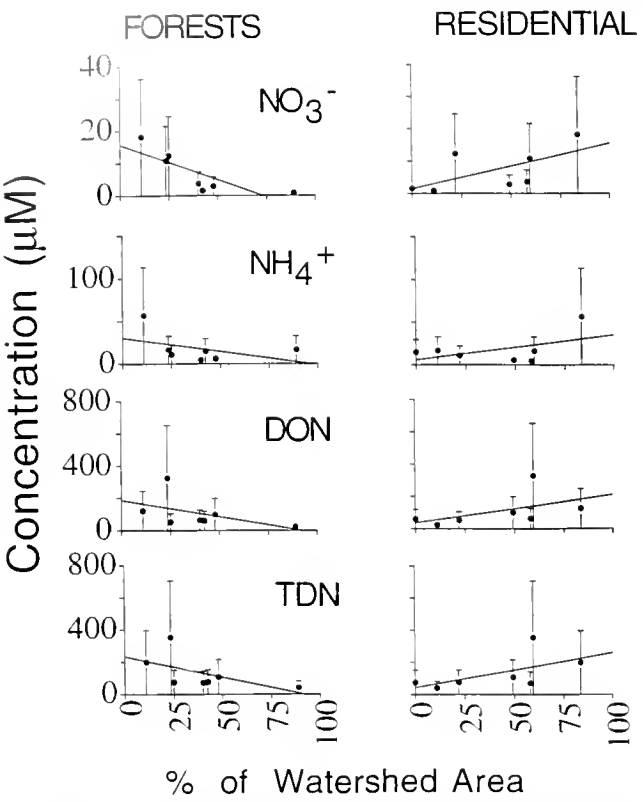

Figure 1. *Concentrations of inorganic and organic nitrogen in groundwater as a function of the percentage of the watershed covered by forests (left panels) and residential areas (right panels) as measured in seven catchment areas of Hamblin and Jehu Ponds. Values are means (±standard error) of samples for DON (dissolved organic nitrogen), nitrate, ammonium, and TDN (total dissolved nitrogen). All regression lines are significant at the 0.05 level.*

divided the watersheds into seven catchment areas, four on Jehu and three on Hamblin. Samples of groundwater were taken at 100-m intervals around each estuary by placing a drive-point piezometer into the soil above the high-water mark. Groundwater was vacuum filtered and acidified with 1 μl of 5 *N* HCl for every 1 ml of sample, and concentrations of NO_3^-, NH_4^+, and dissolved organic nitrogen (DON) were determined using a LACHAT autoanalyzer.

We obtained estimates of forest and residential areas from a geographical information systems map of the Waquoit Bay area. We subdivided the samples of groundwater according to the seven catchment basins, and could therefore plot average nitrogen concentration in groundwater in relation to land use in catchment basins.

The increased proportion of forested and residential areas within a catchment basin was related to the concentration of nitrogen in groundwater about to leave the aquifer (Fig. 1). The more forested the catchment basin, the lower the concentration of nitrogen (Fig. 1, left panel). This observation is consistent with Keeney's conclusion that forests intercept (by storing in the soil and tree biomass and converting nitrate to nitrogen gas) atmospherically derived nitrogen (2).

In contrast, the more residential a catchment basin, the higher the concentration of nitrogen (Fig. 1, right panels). This is probably the result of lower interception of atmospheric nitrogen, combined with the addition of nitrogen from wastewater and lawn fertilizer. This suggests that nitrogen loading in Waquoit Bay depends largely on nitrogen release associated with residential land cover (Valiela *et al.*, unpub. data). As a landscape becomes more urbanized, there will be a progressive increase in nitrogen loads to receiving estuaries, both because of reduction of forest interception and because of increased delivery of wastewater and lawn fertilizer.

The major type of nitrogen delivered to estuaries from urbanized watersheds is dissolved organic nitrogen (DON), with considerable NH_4^+ and smaller concentrations of NO_3^-. These relative concentrations suggest that it is the nitrogen from dwellings near the shore that are making the larger contribution to the load. For example, if wastewater were to travel for any distance in the aquifer, we would expect more nitrification and thus a higher concentration of nitrate (3) than we observed.

Work supported by the WBLMER Research Experience for Undergraduates grant.

Literature Cited

1. **Valiela, I., *et al.* 1992.** *Estuaries* **15:** 443–457.
2. **Lajitha, K., *et al.* 1995.** *Biogeochemistry* **28:** 33–54.
3. **Keeney, D., 1986.** *Critical Reviews in Environmental Control* **16:** 257–304.

Reference: *Biol. Bull.* **189:** 248–249. (October/November, 1995)

Land Cover Effects on Inorganic Nutrients in Groundwater and the Role of Salt Marshes in Interception of Land-Derived Nutrients Entering Estuaries of Waquoit Bay, Massachusetts

Catherine Hunter MacGregor, Sue Ann Chaplin, and Ivan Valiela (Boston University Marine Program, Marine Biological Laboratory)

Nutrients from atmospheric deposition, fertilizer use, and wastewater are delivered to coastal watersheds and have different fates as they are transported through different land covers (1). In an unconsolidated sandy watershed such as that of Waquoit Bay, Massachusetts, hydraulic conductivity is high, and groundwater is the estuary's primary source of fresh water and inorganic

nutrients (1). We assessed the effect of forest area and number of houses on inorganic nutrient concentrations in groundwater leaving Waquoit Bay watersheds with different proportions of these land covers.

Salt marshes grow between land and estuaries, and groundwater-borne nutrients usually have to pass through salt marshes to reach estuaries. Salt marshes are known to support substantial rates of denitrification (2). We hypothesized that only a fraction of the nutrients passing from land through salt marshes make it into estuaries.

To measure the nutrient content of groundwater delivered to Waquoit Bay, samples were collected at the back of the salt marsh fringe all along the periphery of Sage Lot Pond (3, 4), Quashnet River (3, 4), Hamblin Pond, Jehu Pond, and Childs River (3, 4). To find the nutrient content of water that passed through salt marsh, samples of water were taken from outflowing tidal creeks and springs in the salt marsh of Sage Lot Pond (Martin, unpub. data), Hamblin Pond, and Jehu Pond. The Quashnet and Childs Rivers have very little fringing marsh. In all samples, nitrate (NO_3^-) and ammonium (NH_4^+) were measured with a Lachat Autoanalyzer, and phosphate (PO_4^{3+}) was measured by a method adapted from Strickland and Parsons (5).

We first focused on the effect of the two principal land covers, forest and residential land (6), on groundwater nutrient content. To do this, we plotted (Fig. 1, top) mean DIN ($NO_3 + NH_4^+$) and PO_4^{3+} concentrations in groundwater about to leave the aquifer against the percentage of forested area, and against the number of houses per watershed (unpub. data).

We found that the greater the proportion of forested land in a watershed, the lower the concentration of DIN and PO_4^{3+} in groundwater entering the salt marsh (Fig. 1, upper and lower left, black circles). This may be the result of uptake and use of atmospherically delivered DIN and PO_4^{3+} by forests (7).

Houses contribute lawn fertilizer and nutrient-rich septic system wastewater to the watershed (8), so it was not surprising to find that DIN in groundwater entering the salt marsh was positively related to the number of houses in the watersheds (Fig. 1, upper right). There was no significant relationship between the number of houses in the watersheds and PO_4^{3+} concentrations in groundwater entering the marsh (Fig. 1, lower right).

Second, to examine possible interception of nutrients during passage through the salt marsh (Fig. 1, white circles), we looked at concentrations in the samples from tidal creeks and springs in each of the three estuaries that had a marsh fringe. The DIN concentrations in groundwater leaving the salt marsh were lower than in groundwater entering the salt marsh (compare black to white circles, Fig. 1, upper left and right) by 47% at Jehu, 61% at Hamblin, and 43% at Sage Lot (mean = 50%) (Fig. 1, lower left and right). PO_4^{3+} concentrations in groundwater leaving the salt marsh were lower than in groundwater entering the salt marsh by 98% at Jehu and 40% at Hamblin (mean = 69%) (Fig. 1, bottom panels). This suggests that plants and sediments of the salt marsh remove, use, and transform half the inorganic nitrogen and 69% of the phosphorus brought by groundwater as it passes from watershed to estuary.

Forests intercept atmospherically delivered inorganic nitrogen and phosphorus, and houses increase nitrogen and phosphorus loads from land to estuary. Salt marshes growing between land and estuary intercept considerable amounts of land-derived inorganic nitrogen and phosphorus. These results argue the importance of conservation of green land cover and coastal wetlands to maintain estuarine water quality.

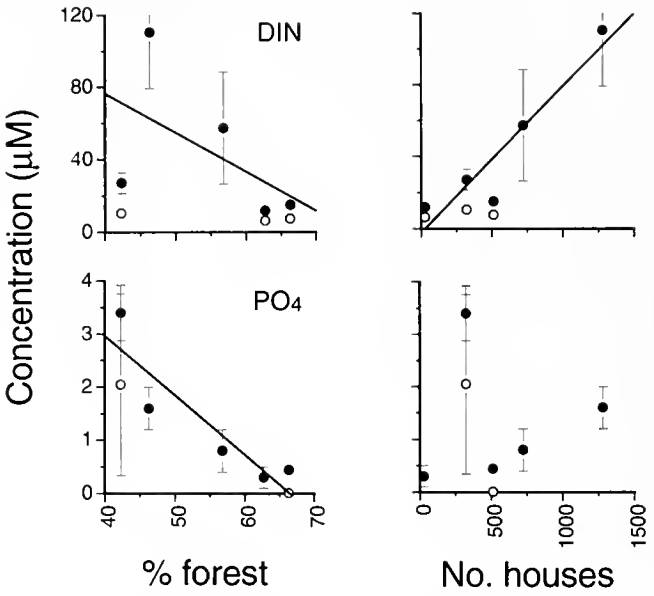

Figure 1. *Mean concentrations of dissolved inorganic nitrogen and phosphate in groundwater (black circles) from watersheds of Waquoit Bay, both plotted in relation to the percentage of forest area in the watersheds (left panels) and to the number of houses on the watersheds (right panels). Concentrations of nutrients in groundwater leaving salt marsh growing along the border of the watersheds and estuaries are shown as unfilled circles. Statistically significant relationships between % forest or No. houses and nutrient concentrations are indicated by the regression line; where the regression was not significant, no line was included. Regression lines and correlations were* $y = -2.15x + 162.27$, $r = 0.54$ *for upper left,* $y = 0.08x - 2.38$, $r = 0.94$ *for upper right;* $y = -0.11 + 7.42$, $r = 0.90$ *for lower right.*

We thank Lori Soucy for her assistance in the laboratory. This research was supported by internships from the Woods Hole Marine Sciences Consortium and Research Experience for Undergraduates through Waquoit Bay Land Margin Ecosystems Research, and by a grant from NOAA Coastal Oceans Program.

Literature Cited

1. **Valiela, I., *et al.* 1990.** *Biogeochemistry* **10:** 177–197.
2. **Johnson, R., *et al.* 1994.** *Biol. Bull.* **187:** 289–290.
3. **McDonnell, K., *et al.* 1994.** *Biol. Bull.* **187:** 276–277.
4. **Rudy, M., *et al.* 1990.** *Biol. Bull.* **187:** 278–279.
5. **Strickland, J., and T. Parsons. 1960.** *Bull. Fish. Res. Board Can* **125:** 1–185.
6. **Valiela, I., *et al.* 1995.** *Ecol. Appl.* In Press.
7. **Lajtha, K., *et al.* 1995.** *Biogeochemistry* **28:** 33–54.
8. **Valiela, I., *et al.* 1992.** *Estuaries* **15:** 443–457.

Reference: *Biol. Bull.* **189:** 250–251. (October/November, 1995)

Pelagic Metabolism in the Parker River/Plum Island Sound Estuarine System

Derrick W. M. Alderman (Bowdoin College), Brian R. Balsis, Ishi D. Buffam, Robert H. Garritt, Charles S. Hopkinson Jr., and Joseph J. Vallino

In this experiment we quantified pelagic metabolism in the Plum Island Sound estuary, Massachusetts. Pelagic metabolism is an important process in estuarine ecosystems, with *in situ* primary production usually being the primary source of organic carbon supporting the trophic web.

Production and respiration were determined by incubating water in bottles for 14 and 24 h every other day for three consecutive weeks in June and July 1995. Water was collected at three stations along the estuary at sunrise and incubated *in situ* at light levels corresponding to 0%, 54%, 90%, and 100% light extinction. Net daytime production (NDP), dark respiration (NR), gross production (GP), and net community production (NCP) were calculated from changes in dissolved oxygen (1) measured by automated Winkler titration. Chlorophyll-*a* concentrations were measured concurrently.

Spatial patterns were evident throughout the estuary. NDP and NCP are highest in the upper water column and decrease with depth. Surface productivity decreases from greater than 100 mmol O_2 m^{-3} d^{-1} in the upper estuary to less than 20 mmol O_2 m^{-3} d^{-1} in the lower Sound (Fig. 1A). Turbidity, as measured by light extinction (Fig. 1B), and chlorophyll levels are highest in the upper estuary (Fig. 1C). Respiration remains relatively constant (averaging −55 mmol O_2 m^{-2} d^{-1}) through much of the estuary, but rises to an average −83 mmol O_2 m^{-2} d^{-1} in the Sound portion of the estuary (conductivities greater than 45 mS cm^{-1}). NCP levels indicate that the water column is net autotrophic until conductivities exceed 46.5 mS cm^{-1} in the Sound, at which point it becomes net heterotrophic (Fig. 1D). This spatial pattern of autotrophy and heterotrophy may reflect the utilization of watershed inputs of inorganic nutrients in the upper estuary and the remineralization of autochthonous organic matter transported downstream to the lower estuary.

Patterns of turbidity and production per unit chlorophyll provide some insight into the controls of primary production in the estuary. The pattern of increasing production per unit chlorophyll down the estuary suggests that production is light-limited. Although the upper estuary contains a larger amount of phytoplankton, as indicated by chlorophyll concentrations, turbidity of the water reduces light availability and hence production per unit chlorophyll. In the Sound, clarity of the water column allows light penetration to all levels, increasing the specific production rate.

Bottle methods for studying metabolism often underestimate total system metabolism because they fail to measure the substantial metabolic contributions by benthic and nektonic communities (1). Estimated benthic respiration in the estuary is −46 mmol m^{-2} d^{-1} (Hopkinson, unpub.). In comparison, pelagic metabolism (−55 and −83 mmol O_2 m^{-2} d^{-1}) contributes 54% to 64% of total system respiration (*i.e.*, sum of benthic and pelagic metabolism). This proportion is similar to what has been observed in comparable estuaries (2). However, in contrast to measurements of whole system respiration (3), respiration estimated from the sum of the benthic and pelagic components is much lower. This difference may be due to the resuspension and mixing of labile organic matter between benthos and water column; this mixing does not occur in bottles or in core tube measures of benthic respiration.

This research was supported by an LMER grant (#OCE-9214461).

Literature Cited

1. **Odum, H. T. 1956.** *Limnol. Oceanogr.* **1:** 102–117.
2. **Hopkinson, C. S. 1985.** *Mar. Biol.* **87:** 19–32.
3. **Balsis, B. R., *et al.* 1995.** *Biol. Bull.* **189:** 252–254.

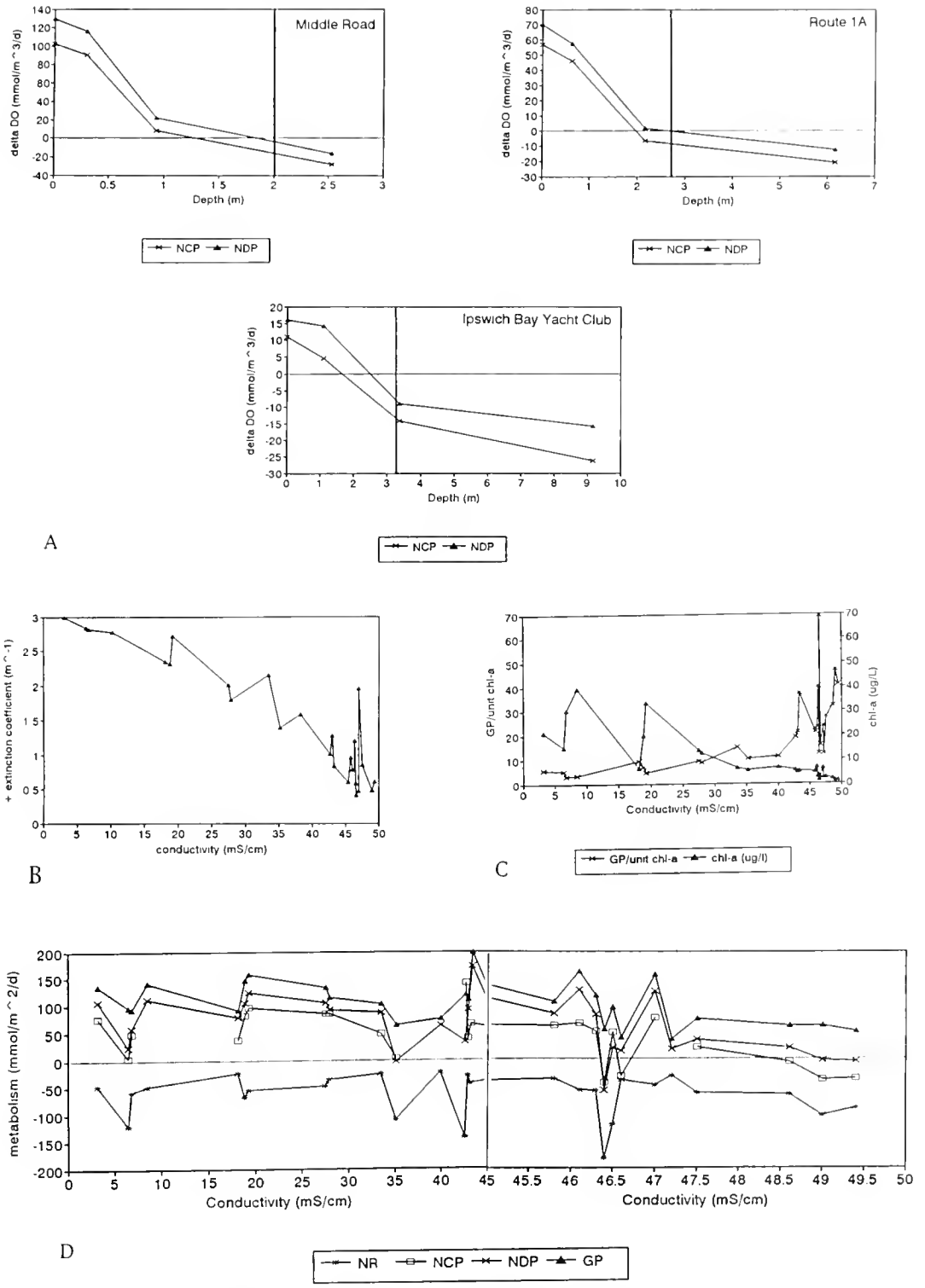

Figure 1. (A) *Depth profiles for sampling sites, averaged over the three-week study period. Points represent depths in water column for 0%, 54%, 90%, and 99.8% (dark) light extinction, the vertical lines are the average depths at each site. For daily profiles, the integrated area under the NCP curve represents net community production (mmol* m^{-2} d^{-1}*); the area under the NDP curve represents net daytime production (mmol* m^{-2} d^{-1}*). (B) Extinction coefficients (given as positive values) along the length of the estuary. (C) Spatial pattern of chl-a (*$\mu g\ l^{-1}$*) and production per unit chl-a (mmol* O_2 m^{-2} d^{-1} *per unit chl-a. (D) Metabolism calculated through changes in BOD bottle oxygen, across a range of conductivities in the estuary (note change in scale on x-axis).*

Reference: *Biol. Bull.* 189: 252–254. (October/November, 1995)

Total System Metabolism of the Plum Island Sound Estuarine System

Brian R. Balsis (Dartmouth College), Derrick W. M. Alderman, Ishi D. Buffam, Robert H. Garritt, Charles S. Hopkinson Jr., and Joseph J. Vallino

In early summer 1995, we surveyed total system metabolism in the Plum Island estuary. Objectives included (1) estimation of ecosystem metabolism via open-water oxygen measurements, (2) determination of the autotrophic and heterotrophic regions of the estuary, and (3) comparison of the loading of organic carbon from the watershed to measurements of autochthonous production.

Metabolism was calculated using two techniques: (1) 24-h Lagrangian surveys at three points in the riverine portion of the estuary at conductivities 2.7 mS/cm, 20.1 mS/cm, and 38.1 mS/cm, and (2) eight dissolved oxygen (DO) transects along the entire length of the estuary, including Plum Island Sound, from 27 June through 29 June. Respiration, gross daytime production (GDP), net daytime production (NDP), and net community production (NCP) were measured according to the procedure of Odum (1).

Lagrangian surveys demonstrated a dynamic pattern of DO change over the day. For example, in the mid-estuary at 20.1 mS/cm, the mass of DO varied over the day from 360 to 450 mmol/m^2 (Fig. 1a). Rates of DO change corrected for flux across the air-sea interface (2) indicated that primary production was highest in late morning and respiration was nearly constant throughout the night (Fig. 1b). Rates of metabolism were comparable at the three conductivities surveyed (Fig. 1c). Gross production

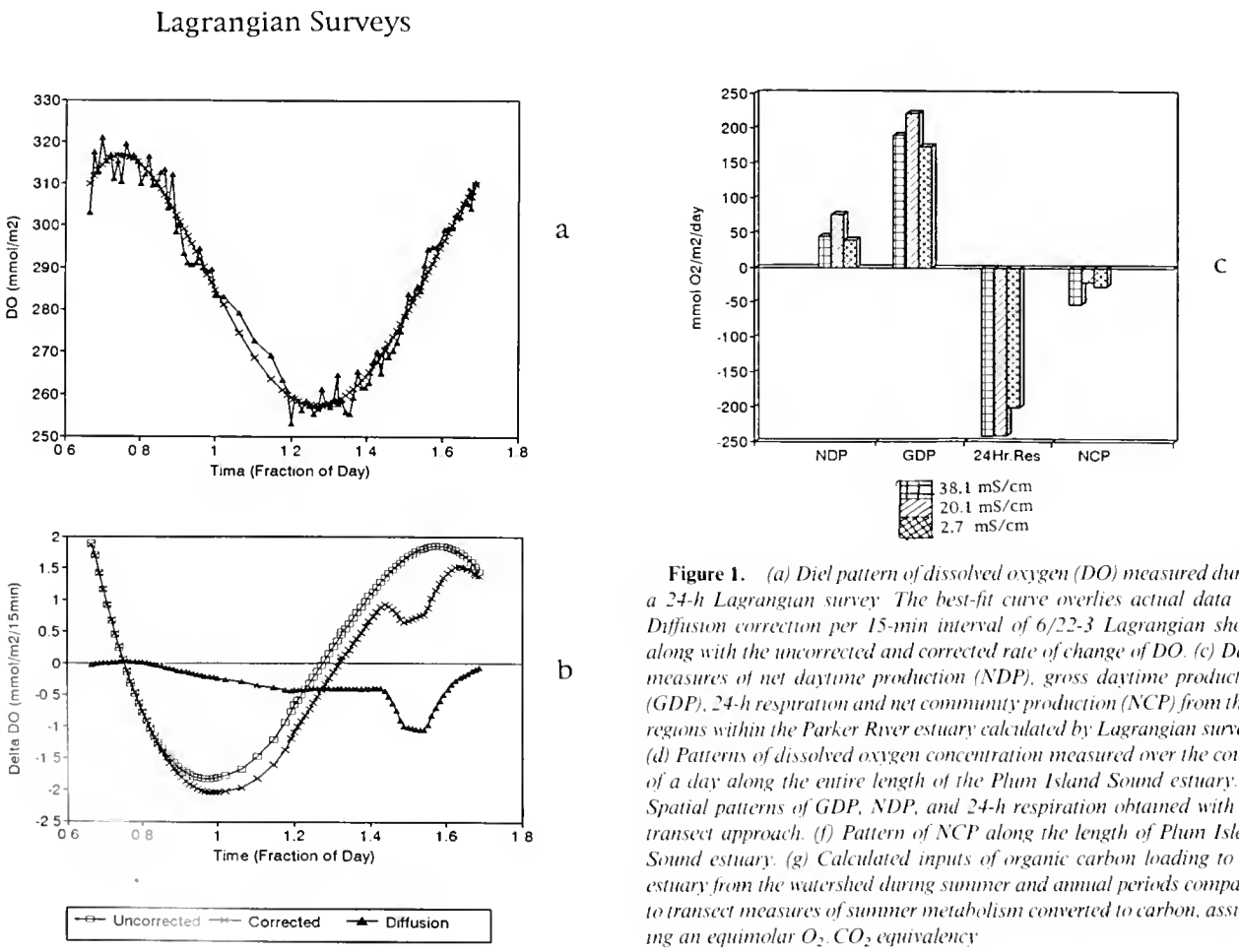

Figure 1. *(a) Diel pattern of dissolved oxygen (DO) measured during a 24-h Lagrangian survey. The best-fit curve overlies actual data. (b) Diffusion correction per 15-min interval of 6/22-3 Lagrangian shown along with the uncorrected and corrected rate of change of DO. (c) Daily measures of net daytime production (NDP), gross daytime production (GDP), 24-h respiration and net community production (NCP) from three regions within the Parker River estuary calculated by Lagrangian surveys. (d) Patterns of dissolved oxygen concentration measured over the course of a day along the entire length of the Plum Island Sound estuary. (e) Spatial patterns of GDP, NDP, and 24-h respiration obtained with the transect approach. (f) Pattern of NCP along the length of Plum Island Sound estuary. (g) Calculated inputs of organic carbon loading to the estuary from the watershed during summer and annual periods compared to transect measures of summer metabolism converted to carbon, assuming an equimolar O_2:CO_2 equivalency*

ranged from 170 to 210 and respiration from 200 to 250 mmol O_2/m^2/day. Overall, NCP was less than zero at all sites and indicated that the system was net heterotrophic and dependent on allochthonous inputs of organic matter.

The transect surveys covered the entire length of the estuary and showed the clearest spatial patterns of metabolism (Fig. 1f–g). Daily DO levels along the length of the estuary ranged from 5.2 to 10.9 mg/l (Fig. 1d). Almost all waters were undersaturated with oxygen throughout the day. GDP ranged from 180 to 300 mmol O_2/m^2/day and NDP ranged from 20 to 150 mmol O_2/m^2/day (Fig. 1e). Spatial patterns of GDP and NDP were similar, being highest in the mid-riverine portion of the estuary (20 mS/cm) and lowest in the lower riverine portion (35 mS/cm). Daily respiration ranged from 200 to 310 mmol O_2/m^2/day. It was lowest in the upper estuary and highest in the mid-estuary (15–20 mS/cm) (Fig. 1e). Patterns of NCP indicated that only the extreme upper estuary was net autotrophic (60 mmol O_2/m^2 per day) (Fig. 1f). Although the patterns illustrated with the two techniques were similar, the transect approach provided much greater spatial information at lower cost and is the recommended method for future studies.

Spatial patterns of metabolism provide clues about the importance of allochthonous inputs of organic matter and inorganic nutrients to the estuary. This system is clearly dependent on allochthonous inputs of organic matter as almost the entire estuary is net heterotrophic (Fig. 1f,g). The regions of highest GDP may reflect the importance of inorganic nutrient inputs from the watershed (in the upper estuary) and the utilization of nutrients remineralized from organic matter that has been transported downstream to the mid-estuary (Fig. 1e). Average daily watershed inputs of organic matter during the summer are insufficient to sustain estuarine metabolism. NCP and 24-h respiration exceed watershed inputs by more than an order of magnitude (Fig. 1g). Two possible explanations could account for

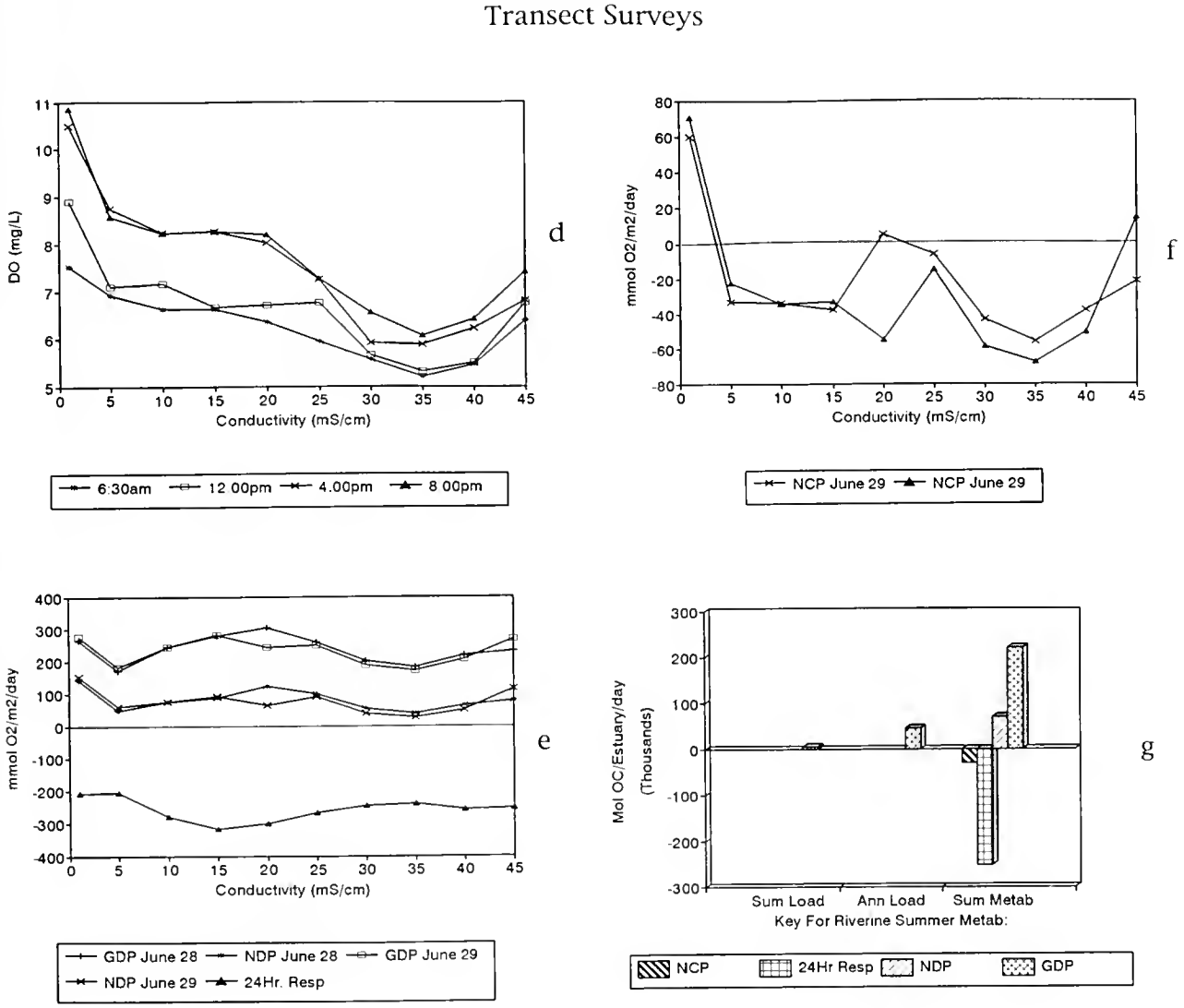

this seasonal pattern: (1) metabolic needs during the summer are met by watershed inputs during the rest of the year, or (2) summer needs are met by inputs from adjacent intertidal marshes.

Literature Cited

1. **Odum, H. T. 1956.** *Limnol. Oceanogr.* **1:** 102–117.
2. **Marino, R., and R. W. Howarth. 1993.** *Estuaries* **16:** 433–445.

Reference: *Biol. Bull.* **189:** 254–255. (October/November, 1995)

Effects of Nitrogen Loading and Salt Marsh Habitat on Gross Primary Production and Chlorophyll *a* in Estuaries of Waquoit Bay

David W. Callaway, Ivan Valiela, Kenneth Foreman, and Lori A. Soucy
(Boston University Marine Program, Marine Biological Laboratory)

Nixon (1) showed, using comparative data from different systems, that increased nitrogen load to shallow coastal estuaries increased production of phytoplankton. Furthermore, it has been well established that the growth of coastal producers is nitrogen limited (2). In Waquoit Bay, we have a complex of separate estuaries that are subject to different nitrogen loading rates (3). This variation in loading rate provides the opportunity to test, in one system, whether increased nitrogen loads result in increased production.

The range of nitrogen loading to the estuaries extended from a high rate of 8.1×10^3 kg N y^{-1} in Childs River to approximately 0.051 kg N y^{-1} in Sage Lot Pond. Because phytoplankton growth in shallow estuaries is nitrogen limited (2), increased loading rates are likely to affect activity and abundance of these primary producers.

Salt marsh habitats are active sites of denitrification and nutrient uptake (2). A strip of salt marsh located between the watershed and the estuary could, therefore, intercept incoming nitrogen and significantly reduce estuarine nitrogen loading. The estuaries of Waquoit Bay are surrounded by different areas of salt marsh. We could, consequently, also evaluate the effects of salt marsh on interception of nitrogen by comparing phytoplankton abundance and activity in estuaries with different extents of fringing salt marsh.

In this paper we ask, first, whether there is a relationship between nitrogen loading rate and phytoplankton abundance and productivity; and second, whether the presence of a salt marsh fringe decreases the nitrogen loading rate and, accordingly, lowers phytoplankton abundance and productivity.

We measured gross primary production (GPP) and chlorophyll *a* concentration at two stations in each of five estuaries of Waquoit Bay (Childs River, Quashnet River, Jehu Pond, Hamblin Pond, and Sage Lot Pond). We used standard light/dark bottle technique with 5-h *in situ* incubation period, and the Winkler titration method to determine primary production of the estuaries. Chlorophyll *a* concentration was measured by the Lorenzen method (4). The nitrogen loading rate was calibrated based on total dissolved nitrogen (DIN) at shore edge, rate of water recharge, and total area of the estuary.

GPP and chlorophyll *a* increased significantly with higher nitrogen loads (Fig. 1, top panels). For the regression of phytoplankton and loading, $P < 0.003$ for both GPP and Chl *a*. In Childs River, for example, the average chlorophyll *a* concentration and GPP levels were about three times as high as those in Sage Lot Pond.

Both GPP rates and chlorophyll *a* concentration decreased in estuaries with larger areas of fringing salt marsh (Fig. 1, middle panels). The cause of this decrease is not well established. The salt marshes could be physically removing phytoplankton from the flooding estuarine water during high tide and, thus, lowering

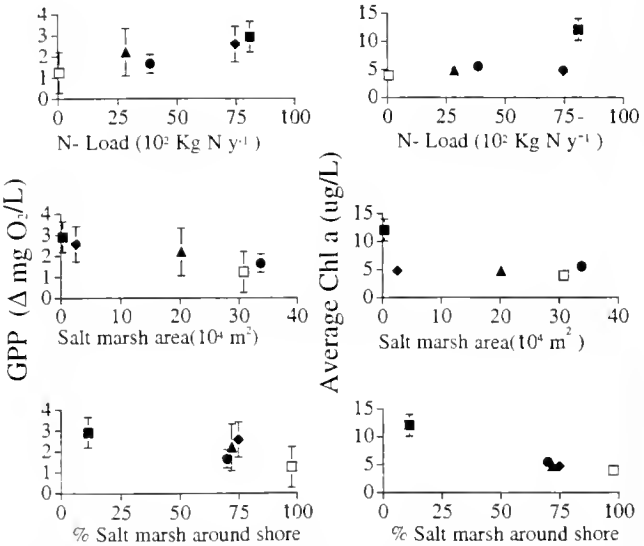

Figure 1. *Gross primary production (left panels) and chlorophyll concentration (right panels) plotted versus nitrogen load (upper panels), salt marsh area (middle panels), and percentage of the periphery of each estuary that is made up of salt marsh. Data from estuaries of Waquoit Bay, including Childs River (black squares), Quashnet River (black diamonds), Jehu Pond (black circles), Hamblin Pond (black triangles), and Sage Lot Pond (open squares).*

GPP and chlorophyll *a*. Because tidal ranges reach, at most, 0.5 m in Waquoit Bay, and coverage of vegetation occurs only during a few days of spring tides each month, this mechanism does not seem convincing. More likely, denitrification and storage of watershed-derived nitrogen in salt marshes could be responsible for a sufficient reduction of nitrogen supplies to lower phytoplankton production. Similar results were obtained when we compared GPP or chlorophyll *a* in relation to the percent of the periphery of each estuary that is composed of salt marsh fringes (Fig. 1, bottom panels).

We therefore conclude that the increase in producer activity due to nitrogen loading from watersheds may be mediated by the extent of salt marsh interposed between land and estuary. Further, salt marshes can decrease the nutrient supply to the estuaries and limit phytoplankton production and chlorophyll *a* levels.

This work was supported by the WBMLER Research Experience for Undergraduates Grant and by a grant from NOAA Coastal Ocean Studies Program.

Literature Cited

1. **Nixon, S. 1988.** *Limnol. Oceanog.* **33:** 1005–1025.
2. **Howarth, R. W. 1992.** *Ann. Rev. Ecol. Syst.* **19:** 89–110.
3. **Valiela, I., *et al.* 1992.** *Estuaries* **15:** 443–457.
4. **Lorenzen, C. J. 1979.** *Limnol. Oceanog.* **24:** 1117–1120.

Reference: *Biol. Bull.* **189:** 255–256. (October/November, 1995)

Macrophyte Abundances in Waquoit Bay Estuaries Subject to Different Nutrient Loads and the Potential Role of Fringing Salt Marsh in Groundwater Nitrogen Interception

Julie Lyons, Jenny Ahern, James McClelland, and Ivan Valiela (Boston University Marine Program, Marine Biological Laboratory)

Increased nutrient loading has shifted seagrass-dominated habitats to macroalgae-dominated habitats in many coastal regions (1). In Waquoit Bay, Massachusetts, eelgrass (*Zostera marina*) has diminished markedly in abundance over the last four decades and been replaced by macroalgae (2). In most estuaries, nitrogen loads are furnished by the adjoining watershed (3, 4, 5), and the major form of nitrogen is nitrate. Many of these estuaries have fringes of salt marsh interposed between land and water. Salt marshes have high rates of denitrification (6), and may therefore act as a buffer against eutrophication, uncoupling the link between the load of nutrients from land and the estuarine benthic vegetation. In this study we investigate the relationship between nutrient loading and macrophyte abundance in estuaries of Waquoit Bay and address the potential role of fringing salt marsh in reducing loadings to estuaries.

Macrophyte abundance was measured from June to August 1995 in five estuaries of Waquoit Bay (Childs River, Quashnet River, Jehu Pond, Hamblin Pond, and Sage Lot Pond). These estuaries receive different nutrient loadings from their watersheds

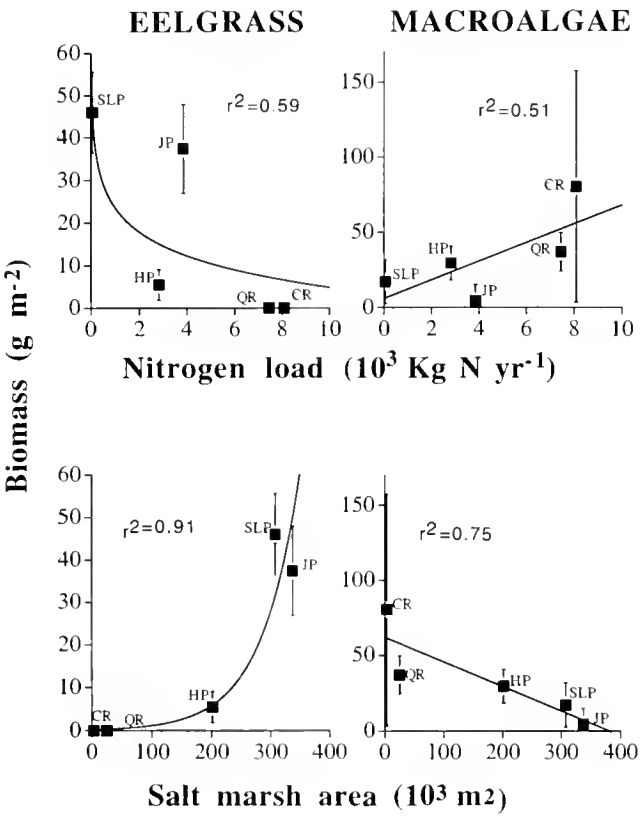

Figure 1. *Macrophyte biomass versus nitrogen loading (top) and salt marsh area (bottom) at Childs River (CR), Quashnet River (QR), Jehu Pond (JP), Hamblin Pond (HP), and Sage Lot Pond (SLP), estuaries of Waquoit Bay sampled June–August 1995. Eelgrass points are mean ± SE, and macroalgae points are medians ± SE_{med} (*n *= 30 for SLP, QR, and CR, and* n *= 50 for HP and JP).*

(Valiela *et al.*, unpub. data) and possess different amounts of surrounding salt marsh. Ten sites at each estuary were sampled with an Eckman dredge (0.15 m^2) at the beginning of each month in all estuaries and at intervening 2-week intervals in Jehu and Hamblin Ponds. Samples were sorted by species, dried, and weighed. Nitrogen loading and salt marsh area showed no relationship (P for regression >0.05). We therefore regressed nutrient loading versus biomass, and salt marsh area versus biomass.

Eelgrass biomass was inversely related to nitrogen loading (Fig. 1, top left; $P = 0.0001$), in contrast to macroalgal biomass, which increased with nutrient loading (top right; $P = 0.0041$). The shapes of the best-fit curves suggest that eelgrass is particularly sensitive to even low rates of additional nutrient loading (Fig. 1, top left), but macroalgae respond linearly over a broader range of nutrient loadings. The correlations (Fig. 1, top), however, have considerable variation; for instance, Jehu Pond has substantially more eelgrass and less algae than would be expected based on nutrient loadings alone. Part of this variability may be associated with the amount of salt marsh in the estuaries. As salt marsh area increases, eelgrass biomass increases (Fig. 1, bottom left; $P = 0.0001$) and macroalgal biomass decreases (Fig. 1, bottom right; $P = 0.0011$). Correlation coefficients for best-fit lines improved for both eelgrass and macroalgal biomass when plotted against salt marsh area (compare r^2 values in top and bottom panels, Fig. 1). This result could be caused by lowered nitrogen loading owing to denitrification in salt marshes.

Seagrass growth is inhibited under increased nitrogen loading and macroalgal growth is enhanced. Eelgrass apparently undergoes rapid, near-exponential reduction in biomass over a narrow range of nutrient loadings, whereas macroalgae respond in a linear fashion over a broader range. The relationship between nutrient loading to coastal watersheds and estuarine macrophytes may, however, be strongly influenced by salt marsh fringing the estuaries. Fringing salt marsh might act as a buffer against nutrient loading, and thus might allow eelgrass beds to be maintained even when they are surrounded by relatively urbanized watersheds.

This work was supported by REU-NSF (OCE 9300490), NOAA (NA170R21101), and The Waquoit Bay Fellowship awarded to J. McClelland.

Literature Cited

1. **Duarte, C. M. 1995.** *Ophelia* **41:** 87–112.
2. **Valiela, I., *et al.* 1992.** *Estuaries* **15:** 443–457.
3. **Giblin, A. E., and A. Gaines. 1990.** *Biogeochemistry* **10:** 309–328.
4. **Simmons, G. M., Jr. 1992.** *Mar. Ecol. Prog. Ser.* **84:** 173–184.
5. **Millham, N. P., and B. L. Howes. 1994.** *Limnol. Oceanogr.* **19:** 1928–1944.
6. **Johnson, R., *et al.* 1994.** *Biol. Bull.* **187:** 289–290.

Reference: *Biol. Bull.* **189:** 256–257. (October/November, 1995)

Effects of Land Use on the Degradability of Dissolved Organic Matter in Three Watersheds of the Plum Island Sound Estuary

Amy G. Uhlenhopp, John E. Hobbie, and Joseph J. Vallino
(The Ecosystems Center, Marine Biological Laboratory)

Different types of land use influence many of the fundamental processes of terrestrial ecosystems and affect the materials moving from land to estuaries and coastal marine systems. One input to estuaries is dissolved organic carbon (DOC); changes in watershed land use have increased the levels of total organic carbon transported to the ocean by 3–5 times those of natural levels (1). Yet it is not clear how much of the DOC entering estuaries is actually used by microbes and contributes to the food web and how much is resistant to degradation and moves out to the oceans. In our experiment, we determined the concentration and degradability of the DOC entering a northern Massachusetts estuary from three areas with different land uses: agriculture, forest, and urban.

Stream water collected 9 August 1994 from agricultural, urbanized, and forested watersheds was filtered (0.2 μm) to remove most of the bacteria and reinoculated with estuarine bacteria (20:1 dilution) from the oligohaline portion of the Parker River in the Plum Island Sound estuary. Inoculated water samples were incubated in 15-l Mylar bags, and changes in bacterial numbers, dissolved organic and inorganic carbon (DOC, DIC), and dissolved oxygen (DO) were analyzed at several time points over a 2-week period.

Bacteria in the agricultural samples consumed a greater amount of oxygen, and did so at a faster rate, than bacteria growing in the urban or forest samples (Fig. 1). The greatest total change of oxygen occurred in the agricultural water samples, a 90.8 μM ($\pm$0.8 μM) decrease. Total changes in the urban and forest bags were, respectively, 41.2 μM ($\pm$1.5 μM) and 34.5 μM ($\pm$6.8 μM). The DOC in the agricultural samples showed a 90.3 μM ($\pm$6.3 μM) decrease; the largest decrease of the three samples (Fig. 1). There was a 48.2 μM ($\pm$5.1 μM) decrease of DOC in the forest samples, and a 33.5 μM ($\pm$4.3 μM) decrease in the urban samples. Most of the DOC consumed was completely oxidized, as DIC concentrations increased by 104 μM, 49 μM, and 33 μM in the agricultural, forest, and urban samples, respectively (Fig. 1).

The actual concentrations of DOC were more than twice as high in the agricultural samples as in either the forest or urban

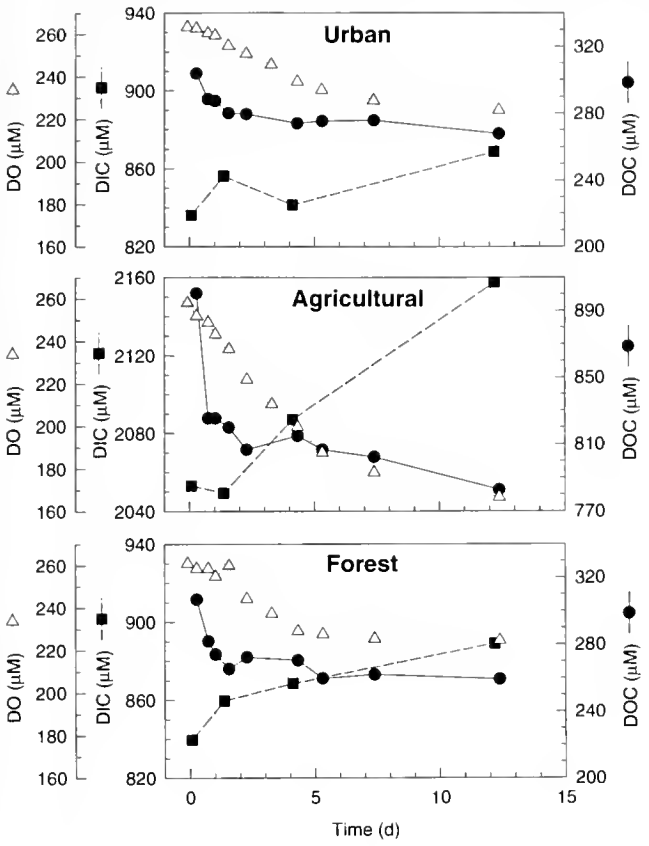

samples. The percentage of the total DOC pool utilized was similar among all three water samples: 15.7% in the forest, 10.3% in the agricultural, and 11.0% in the urban samples.

The organic matter from the agricultural watershed clearly had the greatest potential impact on the estuary. The unexpected conclusion from the experiment, however, is that the total quantity of organic matter is most important; the usable DOC made up a similar percentage of the total in water from all three watersheds.

The research was supported by an LMER grant (NSF-OCE-9214461). We thank Ishi Buffam, David Giehtbrock, Charles Hopkinson, and Eileen Monaghan for advice and assistance with sample analysis.

Literature Cited

1. **Maybeck, M. 1982.** *Am. J. Sci* **282:** 401–450.

Figure 1. *The average concentrations (μM) of dissolved organic carbon (DOC), dissolved inorganic carbon (DIC), and dissolved oxygen (DO) in replicate 15-l Mylar bags during a 13-day incubation. DIC was measured by high-temperature catalytic oxidation, DO by automated Winkler titration, and DIC by precision coulometric CO_2 analyzer.*

Reference: *Biol. Bull.* **189:** 257–258. (October/November, 1995)

Nutrient Limitation of Phytoplankton Growth in Waquoit Bay, Massachusetts

Gabrielle Tomasky and Ivan Valiela (Boston University Marine Program, Marine Biological Laboratory)

Studies of nutrient limitation in fresh water and seawater (1, 2, 3, 4, 5, 6) show that phosphorus limits phytoplankton growth in fresh water and nitrogen does in saline water. Estuaries are situated between a fresh-water source and the sea and are characterized by a gradient of salinities; hence, each estuary must have a point at which the limiting nutrient switches from phosphorus to nitrogen. In this study we asked whether the effect of N or P varies along a fresh to salty gradient within the Childs River estuary of Waquoit Bay, Massachusetts, and whether the limiting roles of N and P vary seasonally.

Bottle enrichment experiments were carried out using water from sites of low (0–9‰), intermediate (10–19‰), and high (20–28‰) salinities. Water was filtered through a 253-μm-mesh net to remove large zooplankton. Enrichment treatments consisted of additions that furnished 100 μM of NO_3 or PO_4; controls received no additions. The treatments were applied to two replicate bottles. All bottles were incubated near the surface in the Bay, and then collected at 1- or 2-day intervals to furnish a time sequence of phytoplankton growth, as measured by chlorophyll concentration. The shallow incubation reduced the probability of light limitation. The containers were incubated in the Bay by attaching them to a floating rack that was anchored to the bottom of the estuary.

Phytoplankton grew in virtually all of the containers over the incubation periods. We calculated chlorophyll-specific growth rates for each month by normalizing growth rates, relative to controls, to compensate for the marked seasonal change in chlorophyll standing crop in Childs River. We calculated the normalized growth rate as $G = (P_e - I_e)/d - (P_c - I_c)/d$, where P_e and I_e are the peak and initial concentrations in the enriched treatments, P_c and I_c are the peak and initial chlorophyll concentrations in the control treatment, and d is the number of days of the incubation.

The normalized phytoplankton growth rates peaked in July–August in all treatments (Fig. 1). The magnitude of the peak depended on the supply of nitrogen or phosphorus and the provenance of the water. In water from the upper reaches of the river, with salinity <10‰, phosphate enrichment prompted a modest increase in phytoplankton growth during summer (Fig. 1, top); note that the standard error of means do not overlap

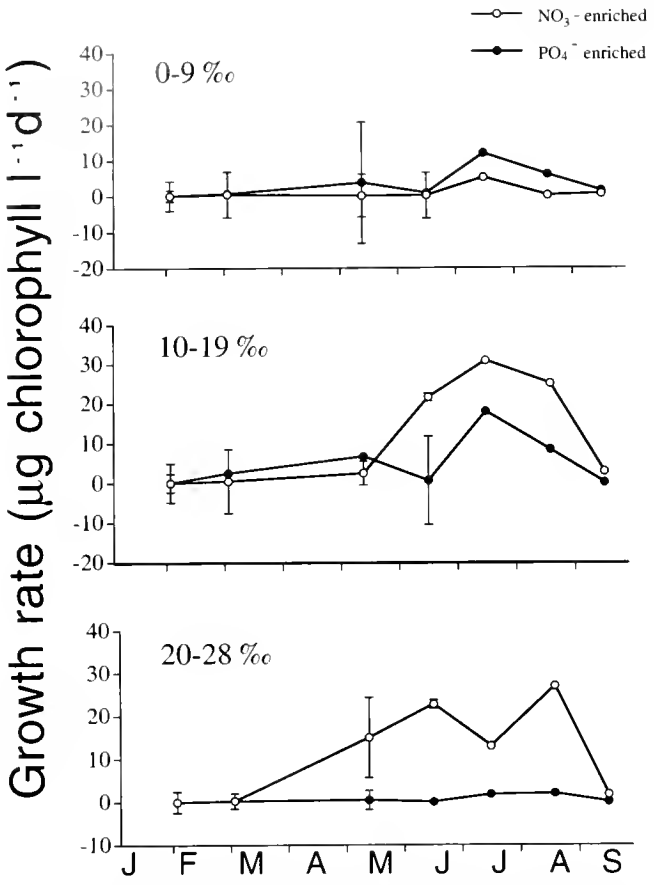

Figure 1. *Normalized phytoplankton growth rates (mean ± propagated SE), relative to controls in each enrichment treatment, shown over the year for the three reaches of Childs River, identified as different ranges of salinity.*

during summer. In water from the lower reaches of Childs River, with salinity >10‰, nitrate stimulated growth during the three summer months. Phosphate stimulated growth for 1 summer month (July) (Fig. 1, middle and bottom); this experiment was run with water of 10‰, it was, therefore, the fresher end of the 10–19‰ range. Nutrient additions stimulated phytoplankton growth during 2 months in water from the upper reaches, 3 months in water from the middle reaches, and 4 months in water from the lower reaches (Fig. 1, top, middle, and bottom). This suggests that phytoplankton found near the mouth of Childs River were more nutrient-limited for more of the year than were cells at the upper reach of the estuary.

Our results show that phytoplankton growth can be nutrient-limited, even in an estuary that receives reasonably high nitrate loads, 2.4 moles N $m^{-2}y^{-1}$ (Valiela *et al.*, unpub.), from its watershed, and where ambient concentrations are reasonably high compared to other seawaters. The range of ambient nitrate concentration was 18–42 μM in the upper reaches of the estuary and 1–16 μM in the intermediate to lower reaches of the estuary, and the range of ambient phosphate concentrations was 0.7–1.9 μM in the upper reaches of the estuary and 0.1–1.5 in the intermediate to lower reaches of the estuary (7). In the fresher end of the estuary there is a suggestion of modest limitation of phytoplankton growth, but because nutrient concentrations are relatively high (7), the growth response, even to P, is modest.

Nitrogen supply controls phytoplankton growth over the warm months in saltier water. There was an apparent switch from P to N limitation within the estuary in water of around 10‰, and there were no evident seasonal shifts in N or P limitation.

The work of the Waquoit Bay Land-Margin Ecosystem Research (LMER) project was supported by grants from NSF (OCE 891479), REU (OCE 9300490), NOAA (NA 170R21101), and NSF/EPA (OCE 8914729).

Literature Cited

1. **Caraco, N., A. Tamse, O. Boutros, and I. Valiela. 1987.** *Can. J. Fish. Aquat. Sci.* **44:** 473–476.
2. **Fisher, T. R., E. R. Peele, J. W. Ammerman, and L. W. Harding. 1992.** *Mar. Ecol. Prog. Ser.* **82:** 51–63.
3. **Howarth, R. W. 1988.** *Ann. Rev. Ecol. Syst.* **19:** 89–110.
4. **Howarth, R. W., and J. J. Cole. 1985.** *Science* **229:** 653–655.
5. **Nixon, S. W., C. A. Oviatt, J. Frithsen, and B. Sullivan. 1986.** *J. Limnol. Soc. South Afr.* **12:** 43–71.
6. **Vince, S., and I. Valiela. 1973.** *Mar. Biol.* **19:** 69–73.
7. **Valiela, I., K. Foreman, M. LaMontagne, D. Hersh, J. Costa, P. Peckol, B. DeMeo-Anderson, C. D'Avanzo, M. Babione, C. H. Sham, J. Brawley, and K. Lajtha. 1992.** *Estuaries* **15:** 443–457.

Reference: *Biol. Bull.* **189:** 258–259. (October/November, 1995)

Effect of Nutrient Enrichment on Phytoplankton Growth in Waquoit Bay, Massachusetts

Cecelia C. Sheridan, Ivan Valiela, Kenneth Foreman, and Lori A. Soucy
(Boston University Marine Program, Marine Biological Laboratory)

The relative importance of nitrogen and phosphorus limitation on growth of coastal phytoplankton has been much discussed (1, 2, 3, 4, 5). In addition, there may be an interaction between nitrogen and phosphorus limitation and the overall rate of nutrient loading in the estuaries. To investigate this interaction, we conduced a set of enrichment experiments in which NO_3^- + PO_4^{3-}, NO_3^-, or PO_4^{3-} was added to water from estuaries of Waquoit Bay that are exposed to different rates of nutrient loading (6).

Experiments were conducted during June, July, and August, 1995. Filtered water samples from 22–31 ppt salinity sites in Childs River, Quashnet River, and Sage Lot Pond were collected

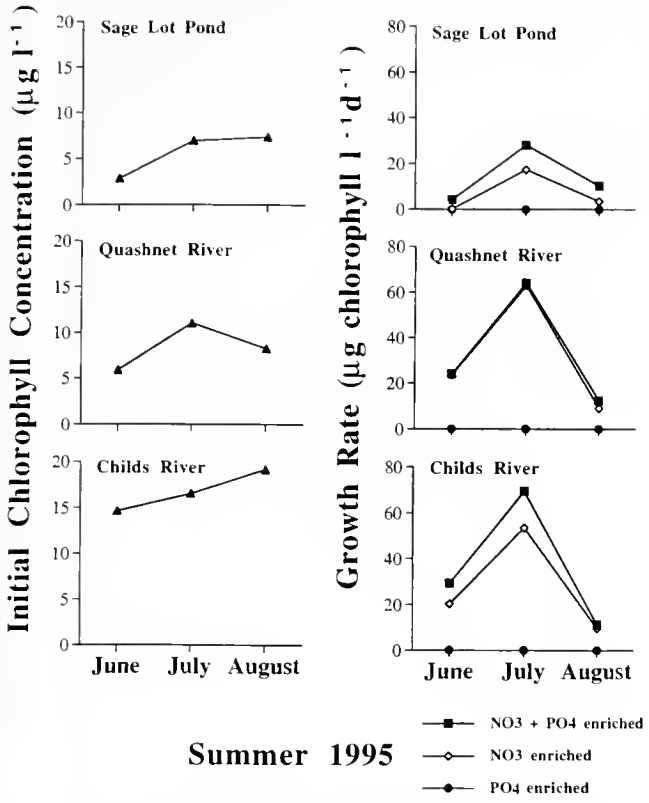

Figure 1. *Left panels: Initial ambient chlorophyll concentrations for Sage Lot Pond, Quashnet River, and Childs River, three estuaries of Waquoit Bay, Massachusetts. Right panels: Phytoplankton growth rates with nitrate + phosphate, nitrate, and phosphate enrichment in water samples from Sage Lot Pond, Quashnet River, and Childs River. Nutrient enrichment experiments were completed in June, July, and August, 1995.*

in 2-l polyethylene bottles. After the addition of 100 μM NO_3^-, 100 μM PO_4^{3-}, or 50 μM NO_3^-/50 μM PO_4^{3-}, control and enriched samples were incubated on site in Waquoit Bay. Water samples harvested between days 0 and 4 of each experiment were analyzed to determine nutrient (ammonium, nitrate, and phosphate) concentrations and phytoplankton biomass (7). Water samples preserved with Lugol's solution were allowed to settle, and then observed by inverted microscopy (8). Growth of phytoplankton was calculated by the equation $G = [(P_e - I_e)/d] - [(P_c - I_c)/d]$ (where P_c and I_c are the peak and initial chlorophyll concentrations in the control treatment, P_e and I_e are the peak and initial concentrations in the enriched treatments, and d is the number of days of incubation). The calculation normalizes growth, compensating for the difference in chlorophyll that occurs over time in the estuary (Fig. 1, left panel).

Phytoplankton growth rates for water samples enriched with NO_3^- and NO_3^- + PO_4^{3-} peaked during mid-July in the three estuaries (Fig. 1, right panel). The phytoplankton was primarily nitrogen-limited: nitrogen addition stimulated growth (in both NO_3^- and NO_3^- + PO_4^{3-} enrichments), but PO_4^{3-} addition alone did not (Fig. 1, right panel). There was some degree of secondary limitation by PO_4^{3-} when NO_3^- was available, as suggested by the moderate increase of chlorophyll growth in NO_3^- + PO_4^{3-} treatment compared to NO_3^- treatment (Fig. 1, right panel).

Surprisingly, the growth response (largely due to nitrogen supply) was most pronounced where the algal cells were chronically exposed to greater nitrogen loading. Compare, for example, the response in Childs River (Fig. 1, bottom right) to that in Sage Lot Pond (Fig. 1, top right). The differences in growth response may be attributed to the threefold higher initial ambient concentration of chlorophyll in Childs River than in Sage Lot Pond (Fig. 1, top and bottom, left panel).

The enriched samples from different estuaries differ in phytoplankton species composition. A bloom of the chain-forming diatom *Rhizosolenia delicatula* comprised 35.7% of the cells in the NO_3^--enriched treatments, and 42.5% of the cells in NO_3^- + PO_4^{3-} enriched samples from Childs River in July. The same diatom made up only 25.5% of the cells in the NO_3^- + PO_4^{3-} enriched samples from Sage Lot Pond in July.

Nitrogen is the primary limiting nutrient in Waquoit Bay. Phosphate plays a secondary role. The different growth responses in estuaries of Waquoit Bay can be attributed to differences in the composition and initial biomass of the phytoplankton.

Work supported by the Waquoit Bay Land Margin Ecosystems Research project and a NSF–REU grant.

Literature Cited

1. **Ryther, J. H., and W. M. Dunstan. 1971.** *Science* **171:** 1008–1013.
2. **Vince, S., and I. Valiela. 1973.** *Mar. Biol.* **19:** 69–73.
3. **Caraco, N., *et al.* 1987.** *Can. J. Fish. Aquat. Sci.* **44:** 473–476.
4. **D'Elia, C. F., *et al.* 1986.** *Can. J. Fish. Aquat. Sci.* **43:** 401–403.
5. **Fisher, T. R., *et al.* 1992.** *Mar. Ecol. Prog. Ser.* **82:** 51–63.
6. **Valiela, I., *et al.* 1992.** *Estuaries* **15:** 443–457.
7. **Wetzel, R. G., and G. E. Likens. 1991.** Pp. 81–165 in *Limnological Analyses*, Springer-Verlag, New York.
8. **Utermohl, H. 1958.** *Mitt. Int. Ver. Theor. Angew. Limnol.* **9:** 1–38.

Reference: *Biol. Bull.* **189:** 260. (October/November, 1995)

Effect of Epiphyte Biomass on Growth Rate of *Zostera marina* in Estuaries Subject to Different Nutrient Loading

Travis Bohrer, Amos Wright, Jennifer Hauxwell, and Ivan Valiela
(Boston University Marine Program, Marine Biological Laboratory)

Nutrient enrichment has been claimed to increase epiphyte biomass growing on eelgrass (*Zostera marina*) leaves (1), and growth of epiphytes on eelgrass leaves can restrict light enough to eventually decrease productivity of eelgrass (2). We examined the effect of nutrient loading to estuaries on growth of eelgrass in three estuaries of Waquoit Bay, Massachusetts, subject to different nutrient-loading rates (3). The estuaries and their nutrient-loading rates are Sage Lot Pond (0.16 g N $m^{-2}y^{-1}$), Hamblin Pond (5.3 g N $m^{-2}y^{-1}$), and Jehu Pond (6.4 g N $m^{-2}y^{-1}$). We also assessed the possible inhibition of eelgrass growth due to the presence of epiphytes by comparing growth rates of cleaned and uncleaned leaves at each site.

To measure growth rates of eelgrass leaves, 20 plants from natural populations were marked in each estuary in July and August 1995. Marking was accomplished by making a needle hole in the sheath. Because the hole moves with the growing leaf, the distance between the hole and sheath scar is a measure of growth rate. Ten of the marked plants were entirely cleaned of epiphytes *in situ* to determine whether epiphytes impaired growth of eelgrass. Plants were harvested 4–6 days after marking. Because leaves of different ages grow at different rates (4), comparisons among estuaries were confined to first (youngest) or second leaves.

In July, growth rates of both the first and second cleaned and uncleaned leaves increased with nutrient load (regression, $P < 0.05$ in each case) (Fig. 1, top and middle) but were largely unaffected by epiphyte removal (2-factor ANOVA: first leaf, $P = 0.49$; second leaf, $P = 0.07$) (Fig. 1, top and middle). These results suggest that, under these nutrient-loading rates, growth of eelgrass is nutrient-limited, rather than light-limited. In August, average growth rates of the first leaves were significantly slower than in July, indicating seasonal decreases in eelgrass growth (Student's *t*-test, $P < 0.05$ in all cases) (Fig. 1, bottom vs. top), and cleaned and uncleaned leaves grew slower as nutrient loading increased (negative slopes in regression) (Fig. 1, bottom). Growth rate did not vary between cleaned and uncleaned leaves (ANOVA: first leaf, $P = 0.23$).

Despite an increase in epiphyte biomass with nutrient load (5), growth rate of eelgrass was unaffected by epiphytes in this experiment. Contrary to what we expected, the July results suggest that nutrient loading increased growth. Other studies have shown eelgrass production increases with nitrogen availability (6, 7). Eelgrass, however, was found only in the three estuaries studied and was absent from other Waquoit Bay estuaries that have higher nutrient loads (Quashnet River, 39.3 g N $m^{-2}y^{-1}$ and Childs River, 45.5 g N $m^{-2}y^{-1}$), and whose benthic primary production has shifted from eelgrass- to macroalgal-dominated habitats. This suggests that nutrient loading may not negatively affect eelgrass production within the range of loading rates of Sage Lot Pond, Hamblin Pond, or Jehu Pond, but does at the higher nutrient-loading rates.

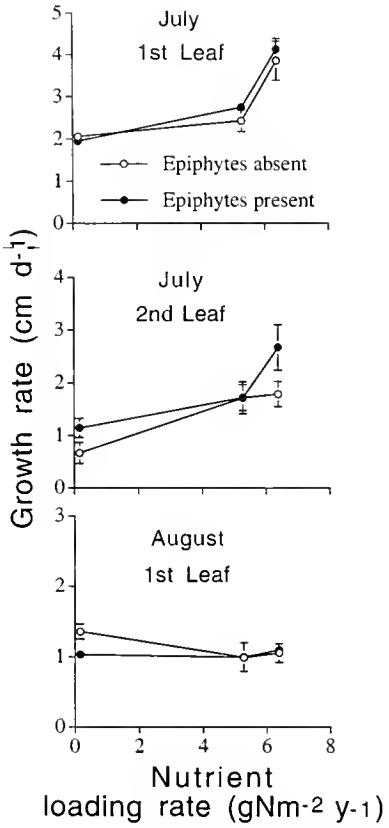

Figure 1. *Eelgrass (*Zostera marina*) growth rate (mean ± SE, cm d^{-1}) vs. nutrient-loading rates (g N m^{-2} y^{-1}) of Sage Lot Pond, Hamblin Pond, and Jehu Pond for leaves with epiphytes absent and present. Leaves were collected in July (1st leaf: top, 2nd leaf: middle) and August (1st leaf: bottom).*

Nutrient loading seems most important for eelgrass growth during the peak growth season (July). Later in the growing season (August) growth rates may be determined by internal physiological controls, changes in light or temperature, and competition for nutrients with phytoplankton or macroalgae.

This work was made possible by WBLMER Research Experience for Undergraduates program and a grant from the NOAA Coastal Oceans Program.

Literature Cited

1. **Borum, J. 1985.** *Mar. Biol.* **87:** 211–218.
2. **Orth, R. J., and K. J. Moore. 1983.** *Science* **222:** 51–53.
3. **Valiela, I., *et al.* 1992.** *Estuaries* **15:** 443–457.
4. **Costa, J. 1988.** Ph.D. Dissertation, Boston University Marine Program.
5. **Wright, A., *et al.* 1995.** *Biol. Bull.* **189:** 261.
6. **Murray, L., *et al.* 1992.** *Aquat. Bot.* **44:** 83–100.
7. **Short, F. T. 1987.** *Aquat. Bot.* **27:** 41–57.

Reference: *Biol. Bull.* **189:** 261. (October/November, 1995)

Growth of Epiphytes on *Zostera marina* in Estuaries Subject to Different Nutrient Loading

Amos Wright, Travis Bohrer, Jennifer Hauxwell, and Ivan Valiela (Boston University Marine Program, Marine Biological Laboratory)

Epiphytes may limit distribution and productivity of seagrasses by reducing the light available to eelgrass blades (1). Primary production of eelgrass (*Zostera marina*) epiphytes increases with nutrients in the water column (2). In Waquoit Bay different estuaries are subject to different N loading rates from their watersheds. This offers the possibility of testing whether the accumulation of epiphytes increases as N supply increases. We investigated the growth of epiphytes on *Z. marina* in Sage Lot Pond (N load = 0.16 g $m^{-2}y^{-1}$), Hamblin Pond (N load = 5.3 g $m^{-2}y^{-1}$), and Jehu Pond (N load = 6.4 g $m^{-2}y^{-1}$).

Epiphyte biomass, including primary producers, animals, and detritus, was quantified by measurement of chlorophyll *a* and epiphyte dry weight. Twenty leaves were collected from each estuary in June and again in July, 1995. To collect leaves of about the same age, the third oldest leaf was always sampled (3). Each leaf was cut into 10-cm sections starting at the youngest end, and the epiphytes were gently scraped off and filtered onto either Whatman glass fiber filters (chl. *a* measurements) or a 200-μm-mesh screen (biomass measurements). Chlorophyll *a* was measured spectrophotometrically after extraction with 90% acetone for 2 days (4).

Epiphyte biomass was much greater on the tops of older leaves than on the bottom of older leaves or on newer leaves (data not shown). This accumulation of epiphytes on older leaf segments suggests that epiphyte biomass depends on the duration of undisturbed colonization and growth. Therefore, to assess the rates of accumulation of epiphyte biomass on eelgrass growing in different estuaries, the age of different leaf segments had to be determined. We calculated the age of each 10-cm segment from measured rates of blade elongation from each estuary (3). These calculated ages allowed us to define the interval of time over which epiphytic biomass had accumulated.

The accumulation of epiphyte biomass and of chlorophyll was highest in the estuary with the largest N load (JP) and lowest in the estuary with the lowest load (SLP) (Fig. 1 top). Thus, the algae that make up part of the epiphytic biomass, as well as the animals and detrital material, all increased faster in the estuary with the highest N load. We know that nutrient concentrations in the water in the three estuaries were in proportion to N loads (unpub. data).

When we plotted the slopes of the regression lines from Figure 1 (top panels) against N loading rates (unpub. data), we found that the accumulation rate of both epiphyte biomass and chlorophyll increased as nitrogen loads to the estuaries increased (Fig. 1, bottom panels).

These results suggest that external N loading controls the growth of epiphytic matter on eelgrass leaves. The more epiphyte biomass, the more light is intercepted before it reaches the leaves. We suggest that nitrogen loading acts through this indirect mechanism to decrease the growth of eelgrass.

Our results clearly show an effect of N load on epiphyte biomass. The further supposed effect on eelgrass growth, however, may be an oversimplification for at least two reasons. First, the

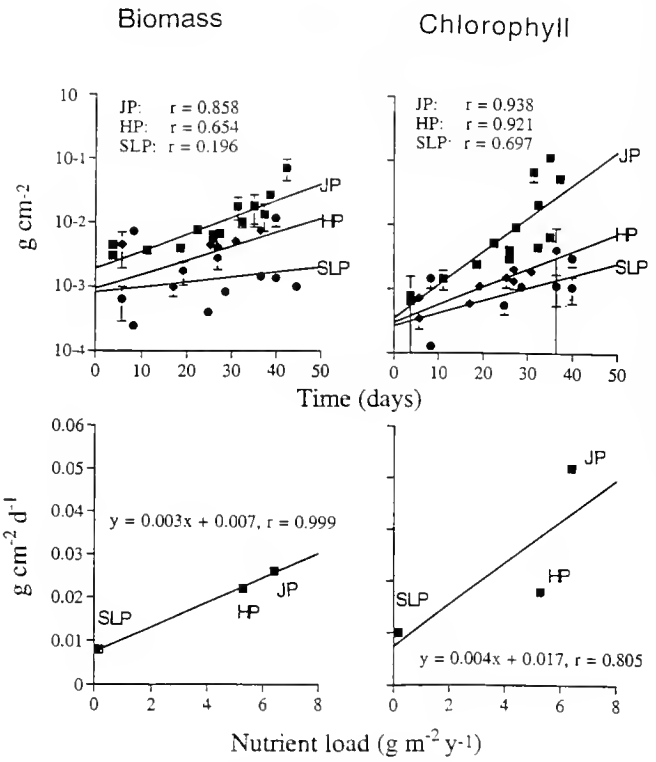

Figure 1. *Biomass (top left) and chlorophyll* a *(top right) in relation to the duration of growth on eelgrass leaves in each of the three estuaries (JP = Jehu Pond, HP = Hamblin Pond, SLP = Sage Lot Pond). Rate of biomass and chlorophyll* a *increases (obtained from slopes of the regressions of the upper two panels) in relation to nitrogen loading rates for the watershed (bottom left and right, respectively).*

effect of loading on growth rate of eelgrass depends on dose, and inhibition of growth is likely only at the highest loading rates within Waquoit Bay estuaries (5). Second, since eelgrass leaves grow basally, and more epiphytic biomass occurs on the older, apical portions of leaves, epiphytes may have less of an effect on total leaf growth than we might suppose. Accumulation of unattached macroalgae around the bases of eelgrass plants may have shading effects on the leaves as important as the effects of does epiphytic biomass.

This work was supported by an internship from the Woods Hole Marine Sciences Consortium and a grant from NOAA Coastal Oceans Program.

Literature Cited

1. **Orth, R. J., and J. V. Montfrans, 1984.** *Aquat Bot* **18:** 43–69.
2. **Borum, J. 1985.** *Mar. Biol.* **87:** 211–218.
3. **Costa, J. 1988.** Ph.D. Dissertation, Boston University Marine Program.
4. **Lorenzen, C. J. 1967.** *Limnol Oceanogr* **12:** 343–346.
5. **Bohrer, T., *et al.* 1995.** *Biol Bull* **189:** 260.

Reference: *Biol. Bull* **189**: 262. (October/November, 1995)

Foliar Release of Ammonium and Dissolved Organic Nitrogen by *Spartina alterniflora*

Cheryl Ann Wolfe, Carol Rietsma, and Ivan Valiela (Boston University Marine Program, Marine Biological Laboratory)

To cope with osmotic stress associated with saline environments, salt marsh plants secrete salt and use amino compounds to balance osmotic pressure (1,2,3). It seems likely that some nitrogen compounds are excreted along with salts (3), but little is known about the magnitude of ammonium (NH_4) and dissolved organic nitrogen (DON) release from salt marsh plants, and even less about this release to the water relative to nitrogen loads received from adjoining watersheds. To investigate rate of release and rate of release per square meter by salt marsh plants, we measured foliar release rate of NH_4 and DON by *Spartina alterniflora,* and compared these rates to nitrogen entering estuaries from watersheds.

We hypothesized that high nitrogen loading to an estuary leads to higher rates of foliar nitrogen release. We tested this by measuring NH_4 and DON foliar exudates from *S. alterniflora* in three estuaries of Waquoit Bay that receive different nitrogen loads (Table I). To measure foliar release, the uppermost, fully extended leaves of *S. alterniflora* were placed, during low tide, in 25-ml test tubes of filtered seawater and incubated for 3 h. The NH_4 released was measured using a LACHAT autoanalyzer and DON was measured using a modified dissolved nitrogen protocol (4).

Rain, dew, and tidal submergence affect leaching from leaves (3). Results of a timecourse experiment suggest that the nitrogen collected in the tubes is that which had accumulated on the leaves since the last time water removed exuded nitrogen. Tidal height measurements showed that plants were not submerged, even during spring high tides. We also concluded from preliminary experiments that dew was not as effective as rain in removing accumulated NH_4 and DON from leaves. Thus we calculated rates of leaching as the amount of NH_4 and DON received in the tubes divided by the number of hours since the last rainfall. Assuming all leached nitrogen reached estuarine waters, we calculated the amount of nitrogen released by *S. alterniflora* leaves into each estuary during the growing season.

The weight-specific release rates of both NH_4 and DON were not significantly different at each location (Table I, cols. 1 and 2). Nitrogen loading from watersheds therefore does not seem to affect rates of foliar release. Increased loading does, however, increase biomass of *S. alterniflora* (Table I, col. 4). Multiplying release rates by standing crop yields the area-specific release of nitrogen. Because of the differences in biomass, area-specific release does seem related to nitrogen load (Table I).

In estuaries subject to larger nitrogen load, the amounts of N released by salt marsh plants per square meter are greater, but the overall release per square meter of marsh is small compared to the external nitrogen load. Sage Lot Pond, the estuary exposed to the lowest nitrogen load, released about 75% of the external inputs. This suggests that in pristine systems, in which atmospheric nitrogen is the largest nitrogen influence, foliar release by salt marsh vegetation can lead to significant release of nitrogen. This is a previously unsuspected mechanism that appears to convey considerable nitrogen to estuaries.

This research was supported by LMER Research Experience for Undergraduates program, and by a grant from NOAA Coastal Ocean Program.

Literature Cited

1. **Pakulski, J. D. 1986.** *Est Coast Shelf Sci* **22:** 385–394.
2. **Jefferies, R. L. 1981.** *BioScience* **31:** 42–46.
3. **Turner, R. E. 1978.** *Limnol. Oceanogr.* **23:** 442–451.
4. **D'Elia, C., *et al.* 1977.** *Limnol Oceanogr* **22:** 760–764.

Table I

Weight-specific nitrogen release rates, area of marsh surrounding the estuary, nitrogen-loading rate to estuary (WBLMER unpub. data), and area-specific nitrogen release; last two columns compare foliar release to loading rates from watershed

Estuary	NH_4 mean release ± SE (μmoles/g · h)	DON mean release ± SE (μmoles/g · h)	Area of marsh (m^2)	N loading rate (kg N/ha/y) from watersheds	*S. alterniflora* biomass (g/m^2)	NH_4 released (kg)[a]	DON released (kg)[a]	% of N load released to estuary	
								NH_4	DON
Jehu Pond	0.03 ± 0.018	0.02 ± 0.010	1.2×10^5	2606	892	231	154	9	6
Hamblin Pond	0.01 ± 0.003	0.03 ± 0.004	9.5×10^4	1615	445	30	91	2	6
Sage Lot Pond	0.03 ± 0.009	0.03 ± 0.012	1.4×10^5	259	307	93	93	36	36

[a] During the entire growing season, while there was significant biomass of grass present.

CONTENTS

Volume 189 Number 3

THE BIOLOGICAL BULLETIN

DECEMBER, 1995

Published by the Marine Biological Laboratory

THE
BIOLOGICAL BULLETIN

PUBLISHED BY

THE MARINE BIOLOGICAL LABORATORY

DECEMBER, 1995

Printed and Issued by
LANCASTER PRESS, Inc.
3575 HEMPLAND ROAD
LANCASTER, PA

THE BIOLOGICAL BULLETIN

THE BIOLOGICAL BULLETIN is published six times a year by the Marine Biological Laboratory, MBL Street, Woods Hole, Massachusetts 02543.

Subscriptions and similar matter should be addressed to Subscription Manager, THE BIOLOGICAL BULLETIN, Marine Biological Laboratory, Woods Hole, Massachusetts 02543. Single numbers, $37.50. Subscription per volume (three issues), $92.50 ($185.00 per year for six issues).

Communications relative to manuscripts should be sent to Michael J. Greenberg, Editor-in-Chief, or Pamela L. Clapp, Managing Editor, at the Marine Biological Laboratory, Woods Hole, Massachusetts 02543. Telephone: (508) 548-3705, ext. 428. FAX: 508-540-6902. E-mail: pclapp@hoh.mbl.edu.

THE BIOLOGICAL BULLETIN is indexed in bibliographic services including *Index Medicus* and MEDLINE, *Chemical Abstracts, Current Contents*, and *CABS (Current Awareness in Biological Sciences)*.

Printed on acid free paper,
effective with Volume 180, Issue 1, 1991.

POSTMASTER: Send address changes to THE BIOLOGICAL BULLETIN, Marine Biological Laboratory, Woods Hole, MA 02543.

Second-class postage paid at Woods Hole, MA, and additional mailing offices.
ISSN 0006-3185

INSTRUCTIONS TO AUTHORS

The Biological Bulletin accepts outstanding original research reports of general interest to biologists throughout the world. Papers are usually of intermediate length (10–40 manuscript pages). A limited number of solicited review papers may be accepted after formal review. A paper will usually appear within four months after its acceptance.

Very short, especially topical papers (less than 9 manuscript pages including tables, figures, and bibliography) will be published in a separate section entitled "Research Notes." A Research Note in *The Biological Bulletin* follows the format of similar notes in *Nature*. It should open with a summary paragraph of 150 to 200 words comprising the introduction and the conclusions. The rest of the text should continue on without subheadings, and there should be no more than 30 references. References should be referred to in the text by number, and listed in the Literature Cited section in the order that they appear in the text. Unlike references in *Nature*, references in the Research Notes section should conform in punctuation and arrangement to the style of recent issues of *The Biological Bulletin*. Materials and Methods should be incorporated into appropriate figure legends. See the article by Lohmann *et al.* (October 1990, Vol. **179:** 214–218) for sample style. A Research Note will usually appear within two months after its acceptance.

The Editorial Board requests that regular manuscripts conform to the requirements set below; those manuscripts that do not conform will be returned to authors for correction before review.

1. ***Manuscripts.*** Manuscripts, including figures, should be submitted in triplicate. (Xerox copies of photographs are not acceptable for review purposes.) The submission letter accompanying the manuscript should include a telephone number, a FAX number, and (if possible) an E-mail address for the corresponding author. The original manuscript must be typed in no smaller than 12 pitch or 10 point, using double spacing (*including* figure legends, footnotes, bibliography, etc.) on one side of 16- or 20-lb. bond paper, 8½ by 11 inches. Please, no right justification. Manuscripts should be proofread carefully and errors corrected legibly in black ink. Pages should be numbered consecutively. Margins on all sides should be at least 1 inch (2.5 cm). Manuscripts should conform to the *Council of Biology Editors Style Manual*, 5th Edition (Council of Biology Editors, 1983) and to American spelling. Unusual abbreviations should be kept to a minimum and should be spelled out on first reference as well as defined in a footnote on the title page. Manuscripts should be divided into the following components: Title page, Abstract (of no more than 200 words), Introduction, Materials and Methods, Results, Discussion, Acknowledgments, Literature Cited, Tables, and Figure Legends. In addition, authors should supply a list of words and phrases under which the article should be indexed.

2. ***Title page.*** The title page consists of a condensed title or running head of no more than 35 letters and spaces, the manuscript title, authors' names and appropriate addresses, and footnotes listing present addresses, acknowledgments or contribution numbers, and explanation of unusual abbreviations.

3. ***Figures.*** The dimensions of the printed page, 7 by 9 inches, should be kept in mind in preparing figures for publication. We recommend that figures be about 1½ times the linear dimensions of the final printing desired, and that the ratio of the largest to the smallest letter or number and of the thickest to the thinnest line not exceed 1:1.5. Explanatory matter generally should be included in legends, although axes should always be identified on the illustration itself. Figures should be prepared for reproduction as either line cuts or halftones. Figures to be reproduced as line cuts should be unmounted glossy photographic reproductions or drawn in black ink on white paper, good-quality tracing cloth or plastic, or blue-lined coordinate paper. Those to be reproduced as halftones should be mounted on board, with both designating numbers or letters and scale

bars affixed directly to the figures. All figures should be numbered in consecutive order, with no distinction between text and plate figures. The author's name and an arrow indicating orientation should appear on the reverse side of all figures.

4. ***Tables, footnotes, figure legends, etc.*** Authors should follow the style in a recent issue of *The Biological Bulletin* in preparing table headings, figure legends, and the like. Because of the high cost of setting tabular material in type, authors are asked to limit such material as much as possible. Tables, with their headings and footnotes, should be typed on separate sheets, numbered with consecutive Roman numerals, and placed after the Literature Cited. Figure legends should contain enough information to make the figure intelligible separate from the text. Legends should be typed double spaced, with consecutive Arabic numbers, on a separate sheet at the end of the paper. Footnotes should be limited to authors' current addresses, acknowledgments or contribution numbers, and explanation of unusual abbreviations. All such footnotes should appear on the title page. Footnotes are not normally permitted in the body of the text.

5. ***Literature cited.*** In the text, literature should be cited by the Harvard system, with papers by more than two authors cited as Jones *et al.*, 1980. Personal communications and material in preparation or in press should be cited in the text only, with author's initials and institutions, unless the material has been formally accepted and a volume number can be supplied. The list of references following the text should be headed Literature Cited, and must be typed double spaced on separate pages, conforming in punctuation and arrangement to the style of recent issues of *The Biological Bulletin*. Citations should include complete titles and inclusive pagination. Journal abbreviations should normally follow those of the U. S. A. Standards Institute (USASI), as adopted by BIOLOGICAL ABSTRACTS and CHEMICAL ABSTRACTS, with the minor differences set out below. The most generally useful list of biological journal titles is that published each year by BIOLOGICAL ABSTRACTS (BIOSIS List of Serials; the most recent issue). Foreign authors, and others who are accustomed to using THE WORLD LIST OF SCIENTIFIC PERIODICALS, may find a booklet published by the Biological Council of the U.K. (obtainable from the Institute of Biology, 41 Queen's Gate, London, S.W.7, England, U.K.) useful, since it sets out the WORLD LIST abbreviations for most biological journals with notes of the USASI abbreviations where these differ. CHEMICAL ABSTRACTS publishes quarterly supplements of additional abbreviations. The following points of reference style for THE BIOLOGICAL BULLETIN differ from USASI (or modified WORLD LIST) usage:

A. Journal abbreviations, and book titles, all underlined (for *italics*)

B. All components of abbreviations with initial capitals (not as European usage in WORLD LIST *e.g., J. Cell. Comp. Physiol.* NOT *J. cell. comp. Physiol.*)

C. *All* abbreviated components must be followed by a period, whole word components *must not* (*i.e., J. Cancer Res.*)

D. Space between all components (*e.g., J. Cell. Comp. Physiol.*, not *J.Cell.Comp.Physiol.*)

E. Unusual words in journal titles should be spelled out in full, rather than employing new abbreviations invented by the author. For example, use *Rit Vísindafjélags Islendinga* without abbreviation.

F. All single word journal titles in full (*e.g., Veliger, Ecology, Brain*).

G. The order of abbreviated components should be the same as the word order of the complete title (*i.e., Proc.* and *Trans.* placed where they appear, not transposed as in some BIOLOGICAL ABSTRACTS listings).

H. A few well-known international journals in their preferred forms rather than WORLD LIST or USASI usage (*e.g., Nature, Science, Evolution* NOT *Nature, Lond., Science, N.Y., Evolution, Lancaster, Pa.*)

6. ***Reprints, page proofs, and charges.*** Authors receive their first 100 reprints (without covers) free of charge. Additional reprints may be ordered at time of publication and normally will be delivered about two to three months after the issue date. Authors (or delegates for foreign authors) will receive page proofs of articles shortly before publication. They will be charged the current cost of printers' time for corrections to these (other than corrections of printers' or editors' errors). Other than these charges for authors' alterations, *The Biological Bulletin* does not have page charges.

CONTENTS

No. 1, August 1995

No. 2, October/November 1995

NEUROBIOLOGY

PHYSIOLOGY

No. 3, December 1995

NEUROBIOLOGY AND BEHAVIOR

PHYSIOLOGY

DEVELOPMENT AND REPRODUCTION

SYMBIOSIS

ECOLOGY AND EVOLUTION

CELL BIOLOGY

Reference: *Biol. Bull.* **189**: 263–271. (December, 1995)

Cephalopod Predation Facilitated by Dinoflagellate Luminescence

KELLIE J. FLEISHER AND JAMES F. CASE*

Marine Science Institute, University of California at Santa Barbara, Santa Barbara, California 93106

Abstract. Predation by nocturnal cephalopods on nonluminous prey was examined in the presence of dinoflagellate bioluminescence. *Sepia officinalis* Linnaeus and *Euprymna scolopes* Berry were tested for predation efficiency in darkness illuminated by the luminescent dinoflagellate *Pyrocystis fusiformis* Murry. Prey were mysids, *Holmesimysis sculpta* (Tattersall); grass shrimp, *Palaemonetes pugio* Holthuis; and mosquito fish, *Gambusia affinis* Baird and Girard. Tests were conducted in aquaria containing 0–20 cells ml^{-1} of *P. fusiformis*. Predation increased as numbers of luminescent dinoflagellates increased. Controls were predation tests in the presence of *P. fusiformis* during nonluminescent photophase or in the absence of dinoflagellates. Movements of squid and prey readily stimulated luminescence. Behavior and correlated luminescence in infrared-illuminated aquaria were recorded by image-intensified and infrared video cameras. *Sepia* strikes on prey were common under luminescent conditions—85% occurred in less than 10 min; but strikes in darkness were rare. *E. scolopes* attacked more frequently than *Sepia*, and almost 90% obtained prey under luminescent conditions. This study demonstrates the ability of squid to use dinoflagellate bioluminescence to locate and capture nonluminous prey. The burglar alarm theory of the adaptive significance of dinoflagellate bioluminescence is supported.

Introduction

At least 20 functions of bioluminescence have been advanced (Tett and Kelly, 1973; Buck, 1978). One of these, the burglar alarm theory, holds that light produced by luminescent prey upon attack by a predator might attract its own predators, thereby reducing predation pressure on the bioluminescent organism. The result would be of little use to the prey unless it survived the attack, for which there is some experimental evidence in dinoflagellates (Buskey *et al.*, 1985). However, even with prey mortality, benefit could accrue to the species as a whole by such a process. This is particularly true in dinoflagellates, which tend to exist in localized clones, so that the sacrifice of some members of the clone would directly favor survival of the luminescent genotype (Burkenroad, 1943). The theory is supported by demonstration that organisms apt to graze on luminescent dinoflagellates are induced by luminescence to undertake evasive behavior that would tend to reduce grazing (Esaias and Curl, 1972; White, 1979; Buskey and Swift, 1983). Until recently, however, there has been little evidence for the second critical element of the theory, namely that higher level predators are able to hunt animals efficiently by the light these latter trigger from bioluminescent organisms, either by feeding on or by moving among them.

Mensinger and Case (1992) showed that juvenile midshipman fish, *Porichthys notatus* Girard, midwater ambush predators, feed efficiently on nonluminescent prey by dinoflagellate light. Here we extend these observations to the Cephalopoda, predators with superb vision (Young, 1991) and remarkably developed hunting behavior. Demonstration that these invertebrate predators are able to hunt effectively with the aid of bioluminescence strongly reinforces the burglar alarm theory. The work also has implications for interpretation of the role of luminescence in the population dynamics of marine organisms.

As predators we used *Euprymna scolopes* Berry, a shallow benthic squid indigenous to the Hawaiian archipelago (Singley, 1983), and *Sepia officinalis* Linnaeus, a benthic-to-midwater cuttlefish found in the Eastern Atlantic Ocean

Received 27 April 1995; accepted 21 September 1995.
*Author to whom correspondence should be addressed.

and the Mediterranean Sea (Boletzky, 1983). *E. scolopes* tends to approximate the ambush attack of the midshipman fish, but from a position on the bottom. *S. officinalis* differs markedly from the midshipman fish in hunting behavior by roving actively in the midwaters.

E. scolopes adults eat primarily mysid shrimp; in aquaria, the young also take *Artemia* (Singley, 1983). Members of this species are active only at night, when they are able to produce bioluminescence from a light organ populated by luminescent bacteria (Singley, 1983; McFall-Ngai and Montgomery, 1990). They camouflage themselves in the sand during daylight. A feeding strategy consisting of approach, tracking, and capture phases, similar to that of *Sepia*, has been reported in other squid (Foyle and O'Dor, 1988). However, our laboratory observations show that *E. scolopes* actually tends to wait for the approach of prey.

S. officinalis adults are roving nocturnal predators that feed on a variety of prey including small crustaceans, fish, or even smaller *Sepia* (Boletzky, 1983). The young eat mainly small crustaceans. The day is spent in the sand and they rise into the water column at night to hunt, aided by a diurnal cycle of buoyancy change (Denton and Gilpin-Brown, 1961). Their vision is excellent and they use both binocular and monocular fixation to locate prey (Messenger, 1968). Attack is by one of two strategies, depending on prey size and potential risk to the attacker: (1) rapid extension of the two prehensile tentacles, or (2) envelopment of the prey (Duval *et al.*, 1984). The tentacle extension process has three phases—attention, positioning, and seizure. The first two are visually controlled, whereas the last is so rapid that there is no time for visual feedback. Accuracy consequently depends on reducing the visual error to near zero (Messenger, 1968).

Materials and Methods

Collection and maintenance of experimental animals

Juvenile and adult *Euprymna scolopes* were generously provided by Professor M. McFall-Ngai, who periodically collected specimens from Kaneohe and Niu Bays on the coast of Oahu, Hawaii. Animals were kept in a 40-gallon aquarium with single-pass, heated seawater (20° −24°C) and a 1.0-cm-deep sand bottom. Experimental animals were kept on a 12:12 light-dark (LD) cycle, the same LD cycle as the rest of the animals in this study. Food consisted of brackish-water grass shrimp (*Palaemonetes pugio* Holthuis). All experiments reported here were done with adults.

Juvenile cuttlefish, *Sepia officinalis*, were purchased from the University of Texas Marine Biomedical Institute, Galveston, Texas (Boletzky and Hanlon, 1983; DeRusha *et al.*, 1989). They were kept in 60-gallon aquaria with single-pass seawater (14° −18°C) and 2.5-to-3.8-cm-deep sand bottoms. All animals in this study were maintained on the same 12:12 LD cycle. Mortality was low, with good survival to reproductive age. Animals used in these experiments were about 2 months old and averaged 25 mm in length. Food consisted of kelp-canopy mysids (*Holmesimysis sculpta* [Tattersall]); top smelt (*Atharinops affinis* Aries), both live and frozen); striped shore crabs (*Pachygrapsus crassipes* Randall); and mosquito fish (*Gambusia affinis* Baird and Girard). Prey varied according to cuttlefish size and food requirements.

The various food and prey animals were obtained and handled as follows. Mysids were collected weekly by dip netting from kelp canopies along the Santa Barbara coast; maintained in aerated, free-flowing aquaria; and used within 10 days of capture. Mosquito fish were obtained every 2 weeks from a local aquarium store; fed daily; and maintained in a 50-gallon aerated, fresh-water tank. Grass shrimp were obtained periodically from a local supplier; maintained in brackish water at room temperature; fed weekly; and used within 15 days. All prey animals appeared to remain in excellent condition during the specified holding periods.

Dinoflagellate culture and luminescence cycle

Unialgal cultures of the dinoflagellate *Pyrocystis fusiformis* Murry were originally supplied by the late B. M. Sweeney and maintained using the techniques of Widder and Case (1982). Cells were maintained on the same 12:12 LD cycle as the squid at between 18° and 20°C, in sterilized filtered seawater enriched with f/2 formula (Guillard and Ryther, 1962) and soil extract, omitting silicate. During the day-phase, cells were illuminated from above with cool-white fluorescent bulbs at 500 μW cm^{-2} as measured by a United Detector Technology Model 40× photometer. Two populations were maintained on opposite LD cycles for simultaneous use of day- and night-phase cells. On experimental days, cell concentrations were determined with a cell-counting chamber (Hausser). Under these conditions, maximum scotophase bioluminescence intensity was 10^{10} photons · cell^{-1} s^{-1}.

Optimal controls for this study would involve use of completely nonluminescent photophase dinoflagellates. However, although the cells used in control experiments were at least 3 h into photophase, as soon as they were placed in darkness at the beginning of the experiment they rapidly recovered enough luminescent capacity to aid vision of the squid. To assess the magnitude of recovery as a function of time in the dark, tests were conducted to quantify mechanically excitable bioluminescence. Cells used for this test were at least 5 h into scotophase. Quantum emission was measured in a 10-in-diameter integrating sphere collector (Labsphere, Inc.), with an RCA model 8850 photon-counting photomultiplier operating

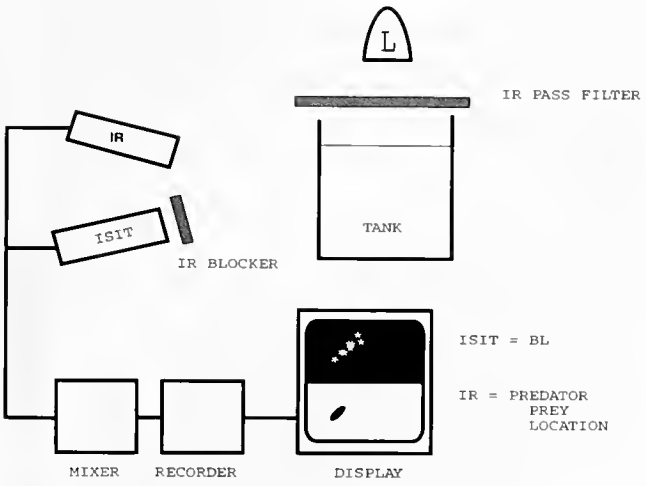

Figure 1. Split-screen video camera arrangement for monitoring predator/prey interactions.

at −1680 V (Latz *et al.*, 1987). Cell samples were stimulated to exhaustion with a stirring rod consisting of a stainless steel shaft with three cross tines, coupled to a DC motor (Latz *et al.*, 1990) operating at a standard speed. Motor speed was measured with a magnetic pick-up mounted on the motor shaft and displayed on a Visi-tach digital ratemeter. Light emission was monitored for 250 ms by ACE-MCS software operating with a channel dwell time of 5 ms. Previously unstimulated cells were run every 15 min for 3 h.

Quantitative predation experiments with Sepia officinalis

Twelve tests with single animals in 12-liter glass tanks were run concurrently in a darkroom. Six were controls, either with dinoflagellates absent or in photophase; and six were experimental tanks with dinoflagellates in scotophase. Tanks were separated by opaque dividers. Water temperature was maintained at 15°C. *S. officinalis* (average mantle length = 23.3 mm ± 0.39; n = 50) were placed in individual tanks no later than 1 h before onset of the dark cycle to allow recovery after transfer. Dinoflagellates in final concentrations of 1, 2, 5, 10, 15, and 20 cells/ml were added 2 h after onset of scotophase. Because cells tend to settle over time, concentrations indicated are for initial conditions. With care taken to minimize bioluminescence, 10 mysids (carapace length: 1.9 mm to 3.6 mm) were added simultaneously to all tanks. Preliminary experiments of up to 6 h were conducted to determine optimal time span and prey density. Results showed that *Sepia* of the ages used (2 to 4 months) were satiated after 3 h and never consumed more than 10 mysids during that time. To minimize disturbance and maintain dark adaptation, the *Sepia* were handled with the aid of an IR-light and IR-image converter. At the end of an experiment, the surviving mysids were counted after the cephalopods had been returned to their home tanks. Experimental tanks were emptied and the sand was washed free of dinoflagellates every night and refilled with filtered seawater the next morning. The laboratory filtering system ensured that the seawater was free of other visibly bioluminescent organisms.

Predator/prey interactions

Behavior of *S. officinalis* and *E. scolopes* was monitored with DAGE MTI image-intensified (ISIT-66LX) and infrared (IR) (SC-66LX) video cameras during predator/prey interactions. The aquarium was illuminated from above by a 25-W incandescent lamp screened by a Kodak IR filter (Wratten No. 87), eliminating wavelengths shorter than 700 nm. A Panasonic special-effects generator (WJ-4600A) produced a horizontal split-screen image of the aquarium. Half of the screen displayed the animals as viewed under IR light, and the other half displayed dinoflagellate luminescence as viewed by the ISIT. The ISIT was fitted with a red-absorbing blue-green glass filter (Melles-Griot BG 18) to block wavelengths longer than 650 nm. Data were stored on a Sony Hi-8 EV C100 video recorder and transferred to a Power Macintosh 8100/80 AV computer for detailed analysis. The experimental arrangements are shown in Figure 1.

In work with *S. officinalis*, 2 h after onset of the dinoflagellate scotophase a single cuttlefish was placed in a 10-l aquarium containing 40 cells ml^{-1} of dinoflagellates. Tank size was determined by limitations of camera resolution. A single mosquito fish (length = 23–36.4 mm)

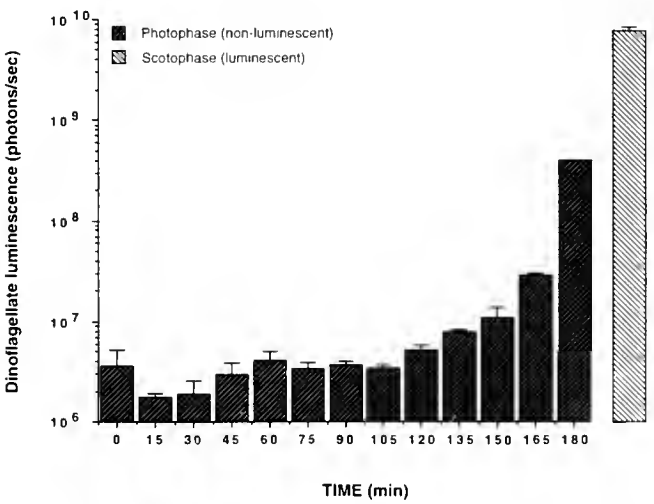

Figure 2. Luminescence produced by photophase dinoflagellates (*Pyrocystis fusiformis*) over a 3-h period after transfer to darkness as compared with cells in scotophase. Error bars represent standard errors.

was added 15 min later. Optimal prey size was determined by the aggressiveness of *Sepia*, which ignored small targets. Events were monitored for a subsequent 30 min with the ISIT/IR video recording system. Four trials were conducted on a given day, for a total number of 20 runs over a 2-month period.

With *E. scolopes*, procedures differed slightly owing to its smaller size. An hour prior to the night cycle, each test animal (average mantle length = 14.15 ± .34 mm; $n = 10$) was moved to an individual 3.5-l experimental aquarium and allowed to acclimate for 3 h. Tank size was small to ensure that strikes could be recorded with high resolution. Each tank was aerated and kept at the same temperature as the holding aquarium (~23°C). Dinoflagellates in final concentrations of 0, 5, 10, 20, and 40 cells/ml were added slowly from a wide-mouth container into each tank to minimize premature stimulation. A single grass shrimp (carapace length = 8.2—11.7 mm) was added 15 min after the dinoflagellates to allow calming time for the squid. *E. scolopes* are significantly harder to feed in captivity than *Sepia*. The prey chosen for this experiment was both familiar to them and large enough to attract their attention. Monitoring continued for a subsequent 30 min. Trials ($n = 5$) were conducted daily, for a total of 90 runs over a 3-month period. Interactions of predators and prey were monitored and analyzed with the same split-screen apparatus used for *Sepia* (Fig. 1).

Results

Dinoflagellate luminescence recovery upon light to dark transfer

P. fusiformis in photophase proved difficult to use as a control because cells became luminescent relatively quickly after being placed in the dark. A similar phenomenon has been observed in *Pyrodinium bahamense* (Biggley *et al.*, 1969) and *Pyrocystis lunula* (Colepicolo, 1992). Our results showed increasing luminescence with passage of time in darkness (Fig. 2). After 3 h in darkness the light produced by 20 cells/ml of photophase *P fusiformis* is comparable to that produced by 1 cell/ml in full scotophase (Fig. 2). This intensity is sufficient to improve the feeding accuracy of *Sepia*. Therefore, to ensure complete darkness, subsequent controls in our experiments contained no dinoflagellates. This would appear reasonable because no adverse effects on the squid or prey were ever seen for the concentrations used; mortality was quite low for both species of cephalopods over the 19-month experimental period.

Predation experiments

These experiments were conducted exclusively on *S. officinalis*. After an acclimation time of 3 h, all animals were behaving normally, hovering above the sand and feeding. Tanks containing *P. fusiformis*, both scotophase (test) and photophase (control), had fewer mysids present at the end of the experiment than did tanks without dinoflagellates. In control tanks containing photophase dinoflagellates, the average number of mysids consumed was from 0.88 to 4.75, increasing with dinoflagellate concentration (Student's *t*-test; no significant difference at any concentration, $P > 0.078 - 0.662$; Fig. 3). This effect is attributed to recovery of luminescent capacity in the course of the experiment. Confirmation comes from the fact that the average number of mysids consumed in tanks containing no dinoflagellates was 0.2 (Fig. 4). By contrast, in the tanks containing scotophase, fully luminescent dinoflagellates, the number eaten varied from 4.2 to 8.0, increasing with dinoflagellate concentration (ANOVA and Dunnett one-sided test; $P < 0.015$; Fig. 4). Thus predation of cuttlefish on mysids was correlated with the presence of scotophase dinoflagellates (*Pyrocystis fusiformis*). Unlike the situation reported for the midshipman fish, *Porichthys notatus* (Mensinger and Case, 1992), no significant inhibition of predation was observed at high dinoflagellate concentrations.

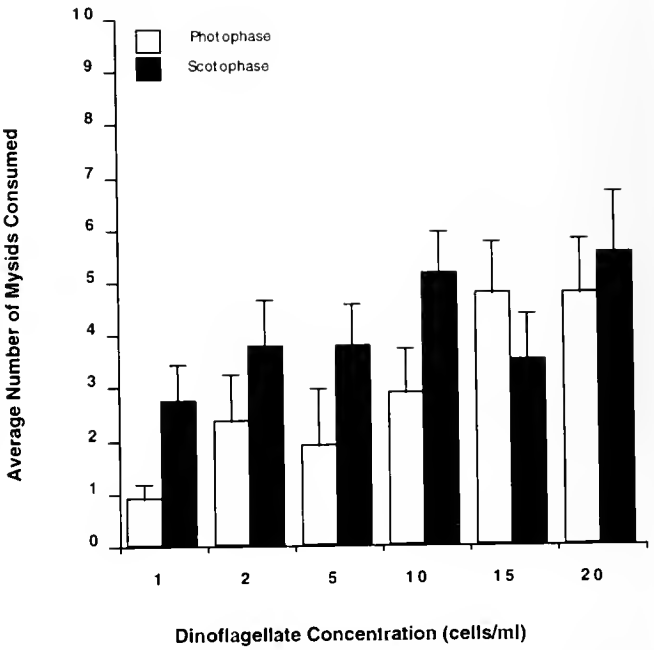

Figure 3. Average number of mysids (*Holmesimysis costata*) consumed by cuttlefish (*Sepia officinalis*) as a function of concentration of scotophase and photophase dinoflagellates (*Pyrocystis fusiformis*). Photophase cells become luminescent as time in darkness progresses (see text). Error bars represent standard errors.

Observations of predator-prey interactions

The dual camera system allowed simultaneous viewing of predator-prey interactions and the resultant lumines-

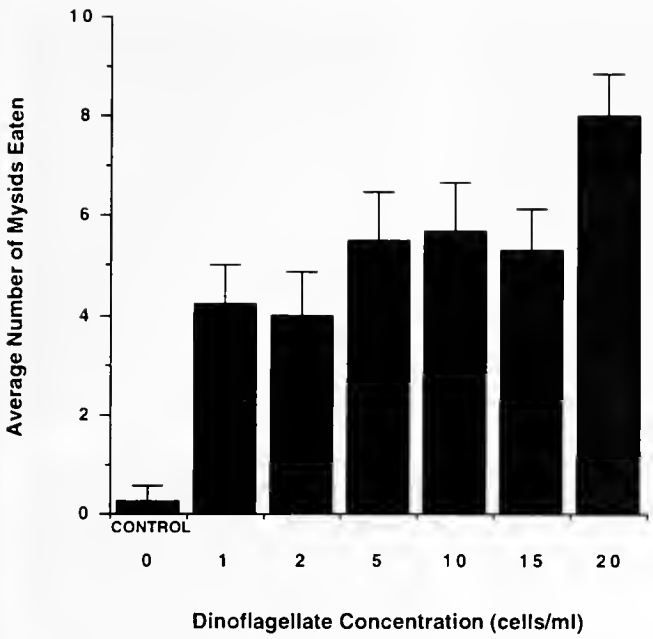

Figure 4. Average number of mysids (*Holmesimysis costata*) consumed by cuttlefish (*Sepia officinalis*) as a function of concentration of luminescent dinoflagellates (*Pyrocystis fusiformis*). Error bars represent standard errors.

cence. No behavioral change was noted between organisms in holding or experimental tanks; thus it was assumed that any direct effect of dinoflagellates (exclusive of bioluminescence) at all concentrations was insufficient to bias the experiments. In experimental runs the dinoflagellate concentration was 40 cells ml^{-1}. Controls for this experiment were conducted without dinoflagellates.

Strikes by *Sepia* and *E. scolopes* were easily discernible using both the IR and ISIT camera (Figs. 5 and 6). Details as fine as eye movements tracking the luminescence were visible with the IR camera. Mosquito fish were observed to trigger luminescence with each tail stroke, which *Sepia* monitored closely. Grass shrimp appendages triggered ample luminescence to attract the attention of *E. scolopes*.

Cuttlefish strikes were all or none, and misses were never observed in a total of 20 attacks. A strike or other rapid movement elicited a large cloud of luminescence that was easily observed with the ISIT camera, but the normal rise and hover movements of *Sepia* triggered no luminescence. Due to acclimation time (15 min), *Sepia* feeding behavior was not affected by the confines of the aquaria, and strikes were primarily away from aquarium walls. Mosquito fish appeared to swim normally under the experimental conditions. Sixty-five percent of the *Sepia* in the presence of scotophase dinoflagellates were successful in prey capture, whereas only 5% of the animals in the control tank (no luminescence) obtained prey (Chi-square test; $P < 0.0001$). Eleven individuals in the presence of luminescence took less than 10 min to capture prey, and all strikes occurred in under 20 min. In the control tanks, only one strike occurred out of 20 tests, and this occurred after almost 30 min (Fig. 7).

Messenger (1968) defined the attack of *S. officinalis* as including three components: attention, positioning, and seizure. Attention, the interval between the time when the prey enters the field of view and when the cuttlefish and prey are on the same axis, can take less than 1 s or it may last for up to 10 s (Messenger, 1968). In this study, the average duration of attention was 10.9 s (SE = ±2; n = 10). Positioning, which begins when the cuttlefish faces the prey and ends with the strike, can last from less than 1 to more than 10 s (Messenger, 1968). During our experiments, *Sepia* averaged 7.3 s (SE = ±1.1; n = 10) for this component of the attack sequence. The final act, seizure, is marked by the extension of the tentacles and ends with the prey held by all arms, taking about 2 s (Messenger, 1968). Our specimens accomplished this in an average of 0.83 s (SE = ±0.05; n = 10).

E. scolopes has a different attack mode. Instead of the hover and strike method of the cuttlefish, *E. scolopes* remains poised on the bottom, frequently in a depression deliberately made by blowing sand with the siphon, where it waits for prey to move within its strike zone. The size of the strike zone varies with each animal but is typically a circle, with the squid at its center, whose radius is about twice the body length of the animal. Once a target is in that strike zone, the squid rapidly turns, points all arms in the direction of the prey, and strikes by launching its two tentacles, as with *Sepia*. Our video analysis shows no evidence, by body movement or other sign, of the attention component noted in the cuttlefish. The actions of *E. scolopes* are similar to those of an ambush predator, going from sedentary directly and rapidly to positioning and seizure. Unlike *Sepia*, *E. scolopes* does not adjust its distance to the prey during positioning. Were it not for the launching of the tentacles, positioning and seizure by this squid would be considered one step. The average time taken by *E. scolopes* for positioning was 1.1 s (SE = ±0.09; n = 10) and for seizure, 0.63 s (SE = ±0.03; n = 10). When a miss occurred, the squid did not pursue the prey and continue the attack immediately, even though the prey's luminescent track was distinct. All movement was easily discernible on the monitor with the ISIT camera, including luminescence induced by siphon exhaust as the squid excavated a resting place in the sand. Motion by the grass shrimp prey, both "walking" along the bottom and swimming, stimulated dinoflagellate luminescence. No noticeable attention was given to prey outside the strike zone.

There was a significant increase in frequency of predation in aquaria containing luminescent dinoflagellates (Fig. 8). In the absence of luminescence, *E. scolopes* struck

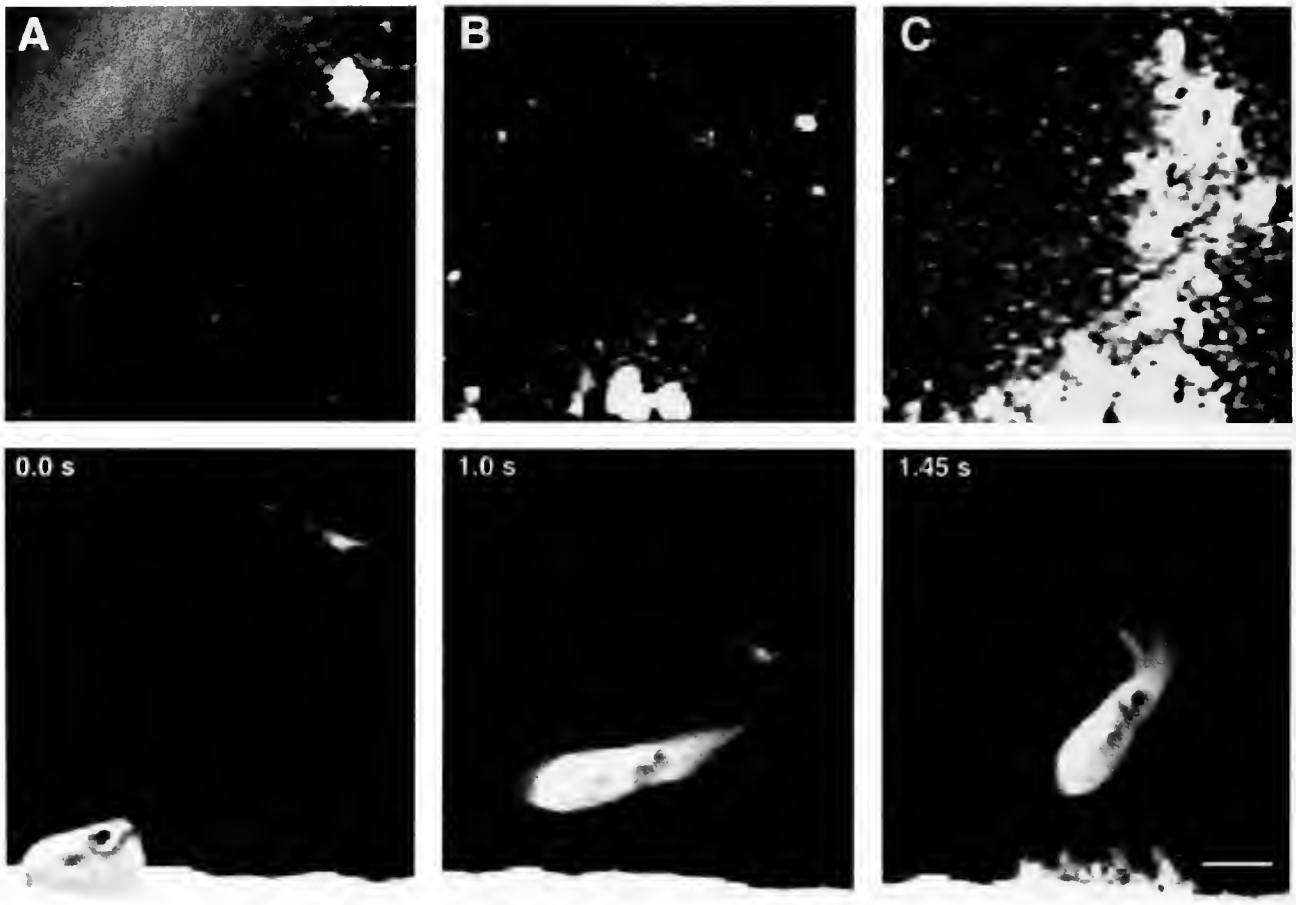

Figure 5. Split-screen video image of *Sepia officinalis* feeding on ghost shrimp (*Palaemonetes pugio*). Image-intensifying camera, top view. Infrared camera, bottom view. (A) Attention; (B) Positioning; (C) Seizure. Luminescence is produced by *Pyrocystis fusiformis* upon being stimulated by ghost shrimp movements. Bar scale = 2 cm.

in only 37% of the total tests (Chi-square test; $P < 0.008$). Under luminescent conditions the frequency was higher: 79% with 20 cells/ml and 63% at a concentration of 40 cells/ml. Comparisons made between concentrations showed no significant differences (Chi-square test; $P = 0.76$), nor did a comparison of strike *rate* among all concentrations (ANOVA and Dunnett one-sided test: $P = 0.46$).

Discussion

Cephalopods employ many sophisticated sensory organs during prey capture, namely eyes, statocysts (Budelmann, 1979), and lateral line analog (Budelmann *et al.*, 1991). Stimuli that induce attacks appear to be primarily visual since prey in an adjacent aquarium are just as likely to be attacked as those swimming in the same aquarium with the cephalopods (Wells, 1958). Both *S. officinalis* and *E. scolopes* are nocturnal predators living in waters where bioluminescent dinoflagellates are present in notable quantities: 11 dinoflagellate cells l^{-1} in the Northeastern Atlantic and >1 cell l^{-1} for tropical waters, to a depth up to 150 m or more depending on clarity and mixing (D. Lapota, pers. comm.). Dinoflagellate concentrations used in these experiments exceed those that occur naturally but are lower than concentrations used in previous burglar alarm studies (Esaias and Curl, 1972; White, 1979; Buskey *et al.*, 1983). Some of the lower concentrations used in our study are not unusual in dinoflagellate bloom conditions.

Locomotion of mysid (*Holmesimysis sculpta*), mosquito fish (*Gambusia affinis*), and grass shrimp (*Palaemonetes pugio*) readily stimulated dinoflagellate (*Pyrocystis fusiformis*) luminescence at all concentrations, illuminating the prey and thereby increasing their susceptibility to squid predation. Their swimming hydrodynamic forces approximate the 1.0 dyne cm^{-2} required to excite luminescence by couette flow (Latz *et al.*, 1994). Luminescence appeared to be the primary factor in inducing predation, as the absence of dinoflagellates resulted

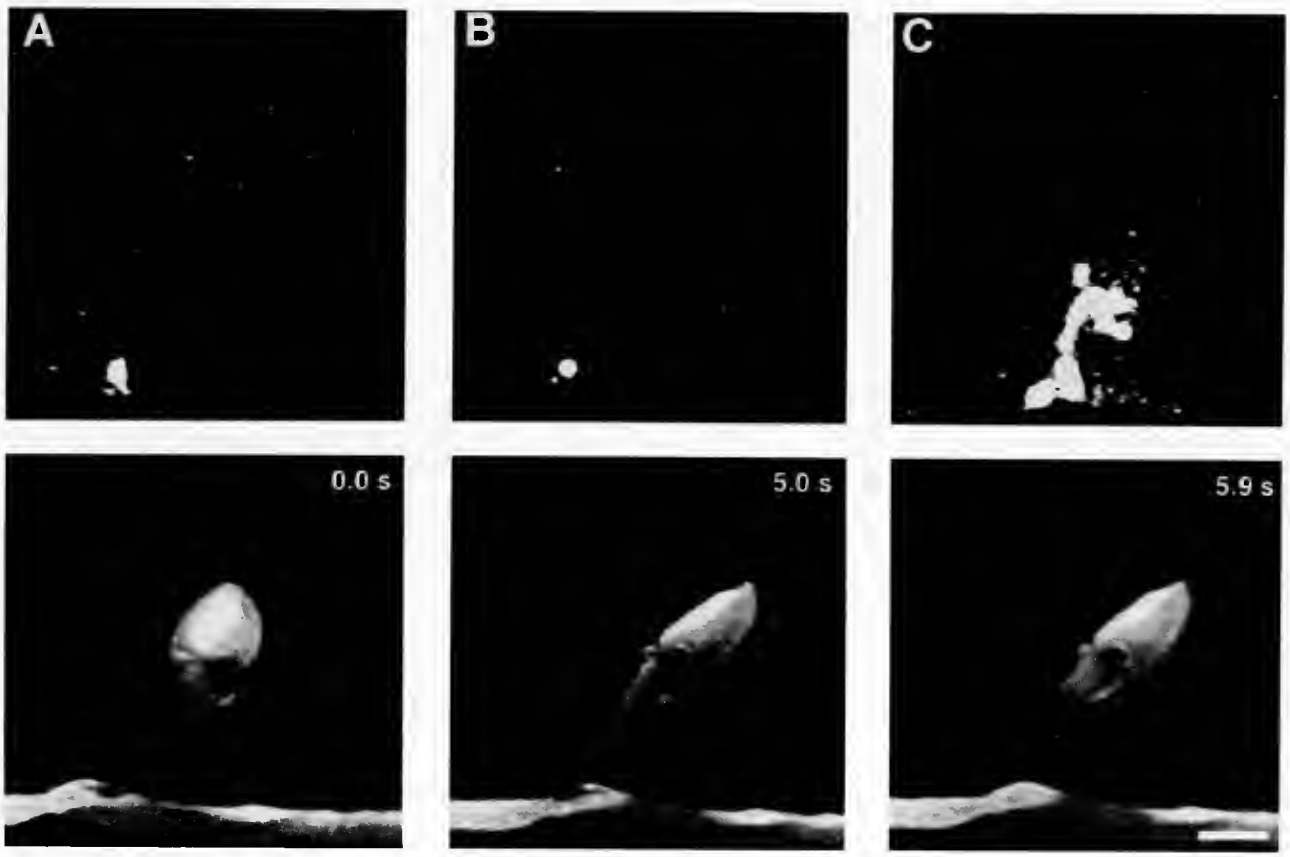

Figure 6. Split-screen video image of *Euprymna scolopes* feeding on ghost shrimp (*Palaemonetes pugio*). Image-intensifying camera, top view. Infrared camera, bottom view. (A) Pre-attack position; (B) Positioning; (C) Seizure. Luminescence is produced by *Pyrocystis fusiformis* stimulated by ghost shrimp movements. Bar scale = 1 cm.

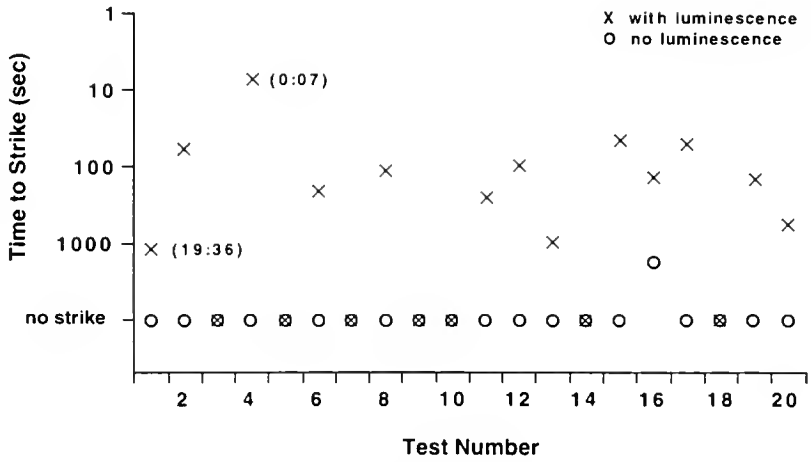

Figure 7. Time required by *Sepia officinalis* to strike mosquito fish (*Gambusia affinis*) in the presence of luminous and nonluminous dinoflagellates (*Pyrocystis fusiformis*).

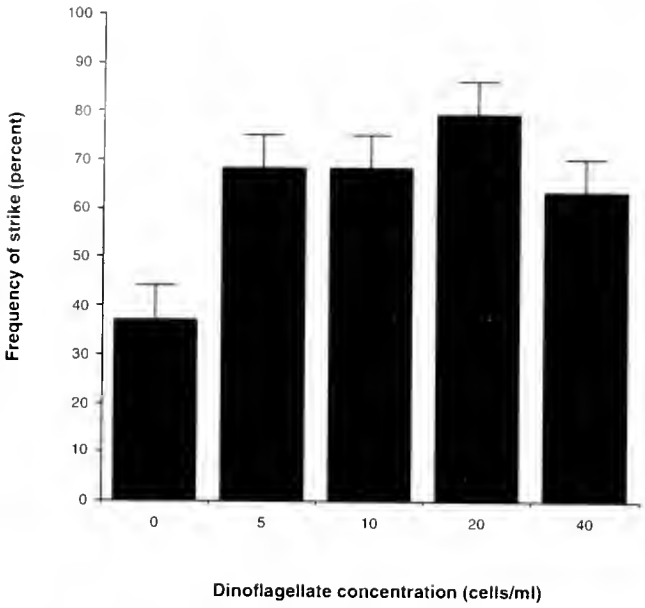

Figure 8. The frequency with which *Euprymna scolopes* attack ghost shrimp (*Palaemonetes pugio*) as a function of concentration of luminescent dinoflagellates (*Pyrocystis fusiformis*). Error bars represent standard errors.

in markedly lower predation. At the same time, the presence of dinoflagellates had no obvious direct detrimental or behavioral effects on prey within the time scale of the experiments.

S. officinalis enters the water column at night to feed. Hovering just off the sand bottom, the cuttlefish either wait for or swim in search of prey. Luminescent dinoflagellates occur naturally in waters off the British coast of France, the Mediterranean, and Great Britain where *S. officinalis* are found. Predation experiments showed that cuttlefish have the ability to use light provided by dinoflagellates to locate prey. Without this light there is little predation success. The higher the dinoflagellate concentration the more prey *S. officinalis* obtained (Fig. 4). We suspect that the ability to regulate bouyancy improves concealment of the cuttlefish from its prey or possible predators by reducing the necessity for locomotor activity.

A difficulty with these experiments was the recovery of luminescence by photophase dinoflagellates in the control tanks (Fig. 2). As bioluminescence competence increased over the 3-hour test, *Sepia* hunted more effectively. Also unexpected was the fact that in total darkness, few prey were attacked. This is contrary to the observations of Budelmann *et al.* (1991), who found that *S. officinalis* uses a lateral line system similar to the mechanoreceptive lateral lines of fish and aquatic amphibians to find about 50% of available prey. In complete darkness, *Sepia* in this experiment consumed significantly less than 50% of available prey (Fig. 4).

Observation of predator/prey interactions with mosquito fish and ISIT/IR video showed that luminescence from dinoflagellates aids *Sepia* to visually locate and strike prey. Prey size and type in these tanks were such that *Sepia* always attacked by discharging its two prehensile tentacles. Video analysis of the predator-prey interactions and correlated bioluminescence clearly showed the eye movements, body orientation, and subsequent strike of individual *S. officinalis* as they followed mosquito fish through luminescent water (Fig. 5). In water populated with scotophase dinoflagellates, 13 out of the 20 *Sepia* successfully struck the prey, and 11 strikes took place in less than 10 min. Without luminescent cells only one strike took place, and this at greater than 29 min. (Fig. 7).

E. scolopes emerges from the sand at night to await prey. Once prey is in an individual's strike zone, the squid orients and strikes—remaining off the bottom for a brief period and then returning to the sand to complete feeding. *E. scolopes* has a slightly different attack mode than *Sepia*. This cephalopod will only strike prey within a defined strike zone and spends little or no time adjusting distance to the prey along the prey axis to ensure seizure (Fig. 6). This, coupled with the highly variable movements of the grass shrimp, may serve to explain the high variance of strike rates. Nonetheless, the frequency with which *E. scolopes* struck was much greater in luminescent water (79%) than in dinoflagellate-free control tanks (37%; Fig. 8). Successful strikes in darkness are unexplainable, but may well involve mechanoreception or near-field acoustic sensitivity. Comparing strikes alone, the rates show no significant differences, indicating no increase or decrease in predation success, due to specific concentration of dinoflagellates. One possible explanation is that the luminescence assisted the squid in locating prey but not necessarily in attack success. Luminescent dinoflagellates occur in measurable quantities on the coast of Hawaii where *E. scolopes* is found.

These experiments, along with those of Mensinger and Case (1992), clearly establish on an experimental basis that predators as widely disparate as fish and cephalopods are able to use the light of dinoflagellates as an effective aid in hunting nonluminescent prey. The work also supports the concept of a more general role for bioluminescence in which detection of bioluminescence, by increasing the sensory domain of nocturnal and deep-sea animals, contributes to their estimation of the carrying capacity of the local environment (Case *et al.*, 1994). Bioluminescent events, typically representing predator/prey interactions, can be seen at several meters distance in clear oceanic waters, and thereby allow animals with good vision to census local populations in a way well beyond the range of sensory modalities other than acoustic.

Acknowledgments

This work was supported by the Office of Naval Research (N0014-94-1-0751) and the FBN fund. We would particularly like to thank M. McFall-Ngai for assistance in obtaining and maintaining *E. scolopes* and J. Forsythe for the same with *S. officinalis*. We are indebted to S. Haddock, J. Moeller, D. Cook, D. Neilson, and Mark Ussini for discussions and assistance in the laboratory. S. Anderson and J. McCullagh, as usual, provided invaluable support in animal maintenance.

Literature Cited

Biggley, W. H., E. Swift, R. J. Buchanan, and H. H. Seliger. 1969. Stimulable and spontaneous bioluminescence in the marine dinoflagellates, *Pyrodinium bahamense, Gonyaulax polyedra,* and *Pyrocystis lunula*. *J. Gen. Physiol.* **54:** 96–122.

Boletzky, S. V. 1983. *Sepia officinalis*. Pp. 31–52 in *Cephalopod Life Cycles,* Vol. 1, P. R. Boyle, ed. Academic Press, London.

Boletzky, S. V., and R. T. Hanlon. 1983. A review of the laboratory maintenance, rearing and culture of cephalopod molluscs. *Mem. Natl. Mus. Victoria.* **44:** 147–187.

Buck, J. B. 1978. Functions and evolutions of bioluminescence. Pp. 419–460 in *Bioluminescence in Action,* P. J. Herring, ed. Academic Press, London.

Burkenroad, M. D. 1943. A possible function of bioluminescence. *J. Mar. Res.* **5:** 161–164.

Budelmann, B. U. 1979. Haircell polarization in the gravity receptor systems of the statocysts of the cephalopods *Sepia officinalis* and *Loligo vulgaris*. *Brain Res.* **160:** 261–270.

Budelmann, B. U., U. Riese, H. Bleckmann. 1991. Structure, function, biological significance of the cuttlefish "Lateral lines." Pp. 201–209 in *The Cuttlefish,* E. Boucard-Camou, ed. Centre de Publications de l'Universite de Caen.

Buskey, E. J., and E. Swift. 1983. Behavioral responses of the coastal copepod *Acartia hudsonica* (Pinhey) to simulated dinoflagellate bioluminescence. *J. Exp. Mar. Biol. Ecol.* **72:** 43–58.

Buskey, E., L. Mills, and E. Swift. 1983. The effects of dinoflagellate bioluminescence on the swimming behavior of a marine copepod. *Limnol. Oceanogr.* **28:** 575–579.

Buskey, E. J., G. T. Reynolds, E. Swift, and A. J. Walton. 1985. Interactions between copepods and bioluminescent dinoflagellates: direct observations using image intensification. *Biol. Bull.* **169:** 530.

Case, J. F., S. H. D. Haddock, and R. Harper. 1994. The ecology of bioluminescence. Pp. 115–122 in *Bioluminescence and Chemiluminescence, Fundamentals and Applied Aspects,* A. K. Campbell, L. J. Kricka and P. E. Stanley, eds. John Wiley and Sons, New York.

Colepicolo, P., T. Roenneberg, D. Morse, W. R. Taylor, and J. W. Hastings. 1993. Circadian regulation of bioluminescence in the dinoflagellate *Pyrocystis lunula*. *J. Phycol.* **29:** 173–179.

Denton, E. J., and J. B. Gilpin-Brown. 1961. The buoyancy of the cuttlefish. *J. Mar. Biol.* **41:** 319–342.

DeRusha, R. H., J. W. Forsythe, F. P. DiMarco, and R. T. Hanlon. 1989. Alternative diets for maintaining and rearing cephalopods in captivity. *Lab. Animal Sci.* **39:** 306–312.

Duval, P., M. Chichery, and R. Chichery. 1984. Prey capture by the cuttlefish (*Sepia officinalis* L): An experimental study of two strategies. *Behav. Proc.* **9:** 13–21.

Esaias, W. E., and H. C. Curl. 1972. Effect of dinoflagellate bioluminescence on copepod ingestion rates. *Limnol. Oceanogr.* **17:** 901–906.

Foyle, T. P., and R. K. O'Dor. 1988. Predatory strategies of squid (*Illex illecebrosus*) attacking small and large fish. *Mar. Behav. Physiol.* **13:** 155–168.

Guillard, R. R. L., and J. H. Ryther. 1962. Studies of marine planktonic diatoms. 1. *Cyclotella nana* (Hustedt) and *Detonula confervacea* (Cleve). *Fran. Can. J. Microbiol.* **8:** 229–239.

Latz, M. I., T. M. Frank, M. R. Bowlby, E. A. Widder, and J. F. Case. 1987. Variability in flash characteristics of a bioluminescent copepod. *Biol. Bull.* **173:** 498–503.

Latz, M. I., M. R. Bowlby, and J. F. Case. 1990. Recovery and stimulation of copepod bioluminescence. *J. Exp. Mar. Biol.* **136:** 1–22.

Latz, M. I., J. F. Case, and R. L. Gran. 1994. Excitation of bioluminescence by laminar fluid shear associated with simple Couette flow. *Limnol. Oceanogr.* **39:** 1424–1439.

McFall-Ngai, M., and M. K. Montgomery. 1990. The anatomy and morphology of the adult bacterial light organ of *Euprymna scolopes* Berry (Cephalopoda:Sepiolidae). *Biol. Bull.* **179:** 332–339.

Mensinger, A. F., and J. F. Case. 1992. Dinoflagellate luminescence increases susceptibility of zooplankton to teleost predation. *Mar. Biol.* **112:** 207–210.

Messenger, J. B. 1968. The visual attack of the cuttlefish, *Sepia officinalis*. *Anim. Behav.* **16:** 342–357.

Singley, C. T. 1983. *Euprymna scolopes*. Pp. 69–74 in *Cephalopod Life Cycles,* Vol. 1, P. R. Boyle, ed. Academic Press, London.

Tett, P. B., and M. G. Kelly. 1973. Marine bioluminescence. *Oceanogr. Mar. Biol.* **11:** 89–173.

Wells, M. J. 1958. Factors affecting reactions to *Mysis* by newly hatched *Sepia*. *Behaviour* **13:** 96–111.

White, H. H. 1979. Effects of dinoflagellate bioluminescence on the ingestion rates of herbivorous zooplankton. *J. Exp. Mar. Biol. Ecol.* **36:** 217–224.

Widder, E. A., and J. F. Case. 1982. Luminescent microsource activity in bioluminescence of the dinoflagellate, *Pyrocystis fusiformis*. *J. Comp. Physiol.* **145:** 517–527.

Young, J. Z. 1991. Light has many meanings for cephalopods. *Vis. Neurosci.* **7:** 1–12.

Reference: *Biol. Bull.* 189: 272–279. (December, 1995)

Behavioral Responses of *Concholepas concholepas* (Bruguière, 1789) Larvae to Natural and Artificial Settlement Cues and Microbial Films

SEBASTIAN R. RODRIGUEZ[1], CARLOS RIQUELME[2], ELISEO O. CAMPOS[1], PAMELA CHAVEZ[2], ENRIQUE BRANDAN[1], AND NIBALDO C. INESTROSA[1]

[1]*Departamento de Biología Celular y Molecular, Facultad de Ciencias Biológicas, Pontificia Universidad Católica de Chile, and* [2]*Departamento de Acuicultura, Facultad de Recursos del Mar, Universidad de Antofagasta*

Abstract. The behavioral responses of veliger larvae of the gastropod *Concholepas concholepas* were studied in the presence of different natural and artificial settlement cues and microbial films. Early pre-competent larvae stopped swimming, sank (due to ciliary arrests, retraction of the velum into the shell, or both), and remained inactive on the substratum when exposed to conspecific mucus and hemolymph. In both cases the effect was time-dependent and the number of larvae showing these behaviors decreased over time. Larvae exposed to NH_4Cl (ammonium ion) showed a similar time- and dose-dependent response. A positive and time-dependent response was also observed when larvae were exposed to different extracellular matrix (ECM) components (*i.e.*, collagen, gelatin, and fibronectin) and sulfated polysaccharides (*i.e.*, carrageenan, heparin, and chondroitin sulfate). In this case the larvae remained attached to the substratum. However, the effect of sulfated polysaccharides on *C. concholepas* larval behavior was faster than that observed with other ECM molecules. We also studied the responses of pre-metamorphic *C. concholepas* larvae exposed to different microbial films. In chemotaxis experiments with different films, with glass as the substratum, larvae showed a significant preference for multispecific and diatoms films. When shells of *C. concholepas* were used as the substratum, the preference for multispecific films was clear and significant. Likewise, larvae showed velar contractions in the presence of all the films tested. Larvae exposed to multispecific films and to the microalga *Prasinocladus marinus* showed an increased ciliar movement. The finding that mucus and hemolymph of conspecific adults and ECM molecules (mainly sulfated polysaccharides) induce the cessation of swimming of *C. concholepas* larvae suggests a possible role for cell-surface receptors in mediating the larval response of marine organisms. Likewise, the positive chemotaxis responses of *C. concholepas* larvae to different microbial films suggest that microorganisms may have a role in bringing larvae close to settlement inducers on the marine benthos.

Received 11 November 1994; accepted 28 July 1995.

Correspondence: Dr. N. C. Inestrosa, Molecular Neurobiology Unit, Catholic University of Chile, Casilla 114-D, Santiago, Chile.

Introduction

Settlement and metamorphosis are key steps during the life cycle of benthic marine invertebrates. A number of artificial and natural settlement-inducing substances have been described (Pawlik, 1992; Rodríguez *et al.*, 1993). Most of the artificial inducers are neuroactive molecules such as neurotransmitters, neurotransmitter precursors, and ions (Morse *et al.*, 1979; Hirata and Hadfield, 1986; Yool *et al.*, 1986; Bonar *et al.*, 1990). Natural inducers are associated with three main sources: conspecific individuals (*e.g.*, Pawlik, 1986), microbial films (Maki *et al.*, 1989), and prey species (Hadfield and Pennington, 1990). Concerning the first source, conspecific mucus is known to induce larval settlement in the gastropod *Haliotis rufescens* (Slattery, 1992). Moreover, it has been proposed that growth factors associated with the mucus could trigger the settlement response in at least some molluscan species (Cantillana and Inestrosa, 1993; Rodríguez *et al.*, 1993). Bacterial films have been reported to induce larval settlement in a number of marine invertebrates (*e.g.*,

Kirchman *et al.*, 1982). In some cases, exopolymers are the stimulus. These are produced by bacteria, possibly as adhesive factors during attachment to the substratum (Maki *et al.*, 1989). In other cases, the active inductive factor from bacterial supernatants could be ammonium ion (NH_4^+) (Bonar *et al.*, 1990). For example, oyster larvae exposed to solutions of NH_4Cl exhibit stereotypical settlement behavior similar to that which normally precedes metamorphosis (Coon *et al.*, 1990).

Morse and Morse (1991) reported that the morphogenetic molecule for a scleractinian coral larvae is a sulfated glycosaminoglycan. In spite of this finding, the possibility that extracellular matrix (ECM) macromolecules play a role in the settlement of marine invertebrate larvae has not been widely explored. Several studies have examined the behavioral response of gastropod pre-competent larvae to different settlement-inducing cues. Results indicate that pre-competent larvae are able to show some of the typical settlement behaviors observed during the metamorphosis of competent ones, such as ciliary arrests and contractions of the velar lobes, when exposed to settlement-inducing substances (Arkett *et al.*, 1987; Barlow, 1990). The pre-competent larvae sometimes retract the velum into the shell, probably due to overstimulation (Barlow, 1990). As a consequence of the settlement behaviors described above, larvae sink and remain transiently inactive on the substratum.

The prosobranch mollusc *Concholepas concholepas* ("loco"), an economically important benthic marine resource along the Chilean coast, is in danger of extinction resulting from overexploitation (Castilla, 1988). We have been studying this species to generate basic information that will eventually allow us to culture it (Urrea *et al.*, 1992; Cantillana and Inestrosa, 1993; Inestrosa *et al.*, 1993a,b; Campos *et al.*, 1994). We previously showed that an excess of K^+ induces metamorphosis in planktonic as well as in laboratory-reared larvae of *C. concholepas* (Inestrosa *et al.*, 1993a; Campos *et al.*, 1994).

Here we report the effect of conspecific mucus and hemolymph, ECM macromolecules, sulfated polysaccharides, and ammonium ion on the behavior of early pre-competent *C. concholepas* larvae. Likewise, we report on the behavioral response of pre-metamorphic larvae to different microbial films isolated from a native area of recruitment of *C. concholepas*.

Materials and Methods

Experimental animals

Adult specimens and egg capsules of *Concholepas concholepas* were collected from the subtidal zone off the central Chilean coast (Las Cruces; 33° 30′ S, 71° 30′ W) and immediately transported to our laboratory in fresh seawater. Capsules were maintained in aerated, membrane-filtered (0.45 μm) seawater at 20–22°C until hatching. For the experiments with natural and artificial cues, early pre-competent veliger larvae just hatched from capsules were acclimated 1–2 days before being used. For experiments with microbial films, pre-metamorphic larvae were obtained from a culture of 75 days as described by Riquelme and Chavez (1995). In brief, veliger larvae were obtained from mature capsules and maintained in 1-l bottles containing membrane-filtered (0.22 μm) seawater at 20°C and with a 14:10 LD photoperiod (60 larvae per liter). The seawater was changed every 2 days. The microalga *Isochrysis galbana* was used as food at a density of around 10^3 cells per liter of larval culture. Larvae of about 1650 μm were maintained at a density of 10 larvae per liter and acclimated for 2 days before using in experiments. These larvae showed all the characteristics of the pre-metamorphic stage of *C. concholepas* described by DiSalvo (1988).

Obtaining mucus and hemolymph

Conspecific mucus was obtained by smoothly scraping the muscular foot of living adult *C. concholepas* with a spatula. After that, the individuals were broken into pieces and placed inside a funnel; the drained hemolymph was collected. Both procedures were carried out in a cold room (4°C). The mucus and the hemolymph were used in experiments immediately after collection.

Obtaining microorganisms

The microorganisms used to create microbial films were isolated from the surface of rocks obtained in the natural area of recruitment of *C. concholepas* on the north coast of Chile (Antofagasta Bay; 23° 39′ S, 71° 30′ W). Four types of microbial films were used for larval behavior experiments: (1) multispecific bacteria–microalgal films (MBM), scraped directly from rocks; (2) monospecific bacterial films, constituted by a periphytic bacterium able to develop a strong film on glass and polystyrene plates; (3) *Prasinocladus marinus* films, produced by a periphytic dominant microalga present on the rocks; and (4) multispecific diatom films. To isolate bacteria, different rocks were scraped. The resulting material was inoculated in agar St 10 for marine bacteria (Ishida *et al.*, 1986) and incubated at 20°C for a week. Different bacterial strains growing in St 10 medium were recognized on the basis of some morphological characters (size, shape, color, and height) of their colonies. These bacterial strains were isolated and tested for their ability to develop a strong film on polystyrene plates. Monospecific bacterial suspensions were placed on petri dishes and rinsed with sterile seawater after 24 h. The strain that was able to remain attached to plates after rinsing was considered a strong periphytic bacterium.

In the case of the microalgal isolation, the scraped material was diluted, inoculated in agar (Provasoli *et al.*, 1957), and incubated at 20°C for 2 weeks with a 14:10 LD photoperiod. The dominant microalgal species, *Prasinocladus marinus*, was isolated by hand under a microscope and also inoculated in Provasoli medium. This species and the diatoms were identified by Professor Gerald Boalch (Citadelhill Plymouth Laboratories, U.K.).

Preparing microbial films

Pieces of *C. concholepas* shell and glass coverslips were offered as substrata to microorganisms. Before being used, substrata were washed with acid and rinsed with abundant seawater to remove all tissue residue. After that, they were deposited in bottles containing 150 ml of seawater. This material was autoclaved before being inoculated with the different strains. The substrata were incubated with the microorganisms in suspension until they developed film. The substrata were washed with sterile seawater and immediately used in experiments. Preliminary experiences showed that 48 h of incubation was sufficient to create a film able to adhere after washing.

Behavioral response bioassays

Larval response to different natural and artificial cues. Conspecific mucus was spread over 24-well culture plates in a homogeneous film. Twenty to thirty early pre-competent veliger larvae were assayed per well in a final volume of 1 ml of filtered seawater. The number of *C. concholepas* larvae that sank as a result of a cessation of swimming (due to ciliary arrest, retraction of the velum into the shell, or both) and remained inactive on the bottom of the wells during a 2-h incubation was recorded using a Wild dissecting microscope. The behavior of 20 to 30 control larvae maintained in wells containing nothing but 1 ml of normal filtered seawater was followed simultaneously with each treatment. Each treatment and each control were performed in triplicate. Hemolymph was loaded into 24-well culture plates (100 μl/plate) and dried overnight. The same procedure was followed with 100 μl of solutions containing 2 μg of fibronectin, carrageenan, chondroitin sulfate, or heparin; or 12 μg of collagen; or 200 μg of gelatin. Higher concentrations of collagen and gelatin were used because no larval response was observed at lower concentrations. The wells were filled with filtered seawater (1 ml) before 20 to 30 larvae were placed in each well. The experiments were followed for 30 min in the case of the hemolymph and 24 h for the ECM components and sulfated polysaccharides. The number of larvae that sank and remained attached to the substratum was recorded as described above. A similar experiment was carried out with hemolymph boiled for 3 min. Together with each treatment, the behavior of 20 to 30 control larvae maintained in wells containing nothing but 1 ml of normal filtered seawater was followed. Each treatment and each control were performed in triplicate.

Larvae were exposed to a range of concentrations of NH_4Cl (*i.e.*, 2, 5, 8, and 10 m*M*). A stock solution of 100 m*M* NH_4Cl was made in seawater and adjusted to pH 8.0 with 1 N NaOH. At the beginning of each bioassay, enough stock solution was added to a volume of seawater (pH 8.0) to generate 1 ml of the desired NH_4Cl final concentration in 24-well culture plates containing 20 to 30 larvae per well. The experiments were followed for 30 min and the number of larvae that sank and remained inactive on the bottom of wells was recorded as previously described. Treatments and controls were performed in triplicate, as described for the other bioassays. The ECM molecules and sulfated polysaccharides were obtained from Sigma Chemical Co. (St. Louis, MO).

The concentration of larvae used in all the above experiments (*i.e.*, 20 to 30 larvae/ml) was similar to the concentration at which larvae were acclimated after hatching and before the assays. In many species, repeated encounters with others causes larvae stop swimming and settle to the bottom of the culture vessel; thus the high density used in our experiments could have affected the results. However, the control larvae in our assays were never observed to stop swimming or settle as a result of encounters among them. The time courses followed in the above experiments were different because the assays were carried out until a clear response was observed.

Chemotaxis to microbial films. Individual assays of chemotactic response to microbial films were carried out in sterile petri dishes containing 15 ml of sterile seawater. Pre-metamorphic larvae and substrata containing microorganisms were placed on opposite sides of the dishes. We considered a response to be positive when larvae moved directly to the substrata and remained close to them, and negative when larvae moved to the edge of the dishes or remained close to the starting point (random movement). Ten pre-metamorphic larvae were simultaneously placed for each type of substratum and continuously observed for 1 h with a Wild dissecting microscope. The controls were carried out using sterile substrata. Each treatment was performed in triplicate. A *G* test (Sokal and Rohlf, 1981) was used for statistical analysis.

Larval activity in response to microbial films. The activity of *C. concholepas* larvae exposed to microbial films was observed. The films were prepared on glass coverslips and assayed in petri dishes as described above. An increased ciliar movement and the presence of contractions of the velum were used as criteria for larval activity. Larvae swimming with the velum extended and retracting it briefly but repeatedly were categorized as presenting velar contractions. Likewise, larvae moving their cilia faster

than the rate observed during a normal swim were considered to be showing an increased ciliary beating. Larvae were directly placed on the films and observed with a Wild dissecting microscope; the number showing an activity response was recorded at intervals of 0–2, 2–4, 4–6, 6–8, and 8–10 min (hereafter 2, 4, 6, 8, and 10 min, respectively). A total of 30 individual bioassays were carried out per film. A G test was used for statistical analysis.

Results

Larval response to different natural and artificial cues

Mucus and hemolymph. To learn about the effect of conspecific natural substances on the behavioral response of *C. concholepas*, early pre-competent larvae of this gastropod were exposed to mucus and hemolymph. In the presence of conspecific mucus, the veliger larvae stopped swimming and sank. The effect of mucus was time-dependent and reached a plateau after 5 min of continuous exposure to the film (Fig. 1). At this time, about 50% of the larvae were inactive on the bottom of the wells and remained in this state for 30 min of incubation (Fig. 1). Thereafter, the number of larvae swimming normally increased, leaving only 10% of the total larvae sunk after 2 h (Fig. 1). Larvae exposed to hemolymph showed a pronounced and quick response. After just 2 min of exposure, the sinking rate was 94% (Fig. 2). Thereafter, the number of larvae showing a cessation of swimming slowly decreased, resulting in a 75% sinking rate after 30 min (Fig. 2). Only a few larvae remained inactive on the bottom (16%) after 2 h of incubation (data not shown). Larvae exposed to boiled hemolymph showed a response similar to that observed with normal hemolymph during the first 2 min. However, the effect was transient because only 50% of the larvae remained sunk after 5 min of incubation (Fig. 2). The number of larvae induced to sink with boiled hemolymph was less than that observed with normal hemolymph throughout the experiment (Fig. 2).

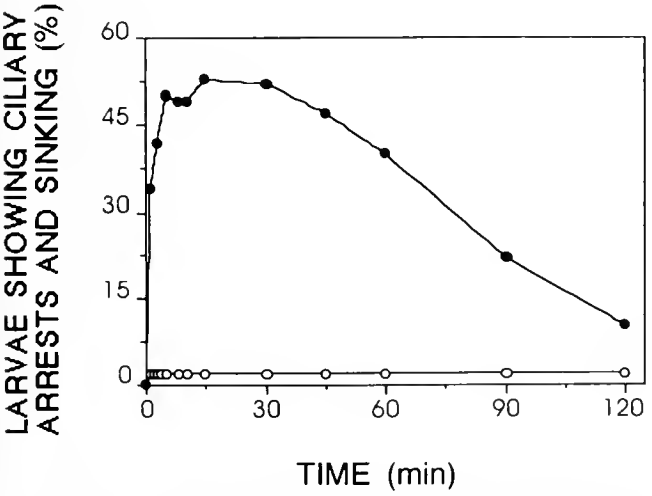

Figure 1. Mean percentage of early pre-competent larvae of *Concholepas concholepas* induced to sink by conspecific mucus after 2 h of incubation. ● = Mucus, and ○ = control.

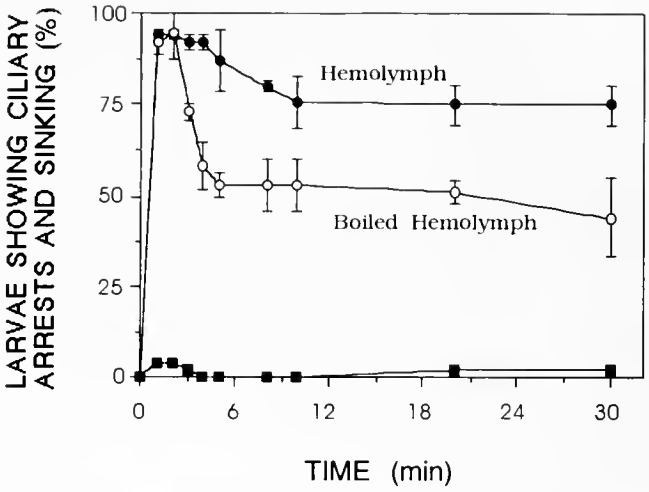

Figure 2. Mean percentage of early pre-competent larvae of *Concholepas concholepas* induced to sink by conspecific hemolymph. ● = Hemolymph, ○ = boiled hemolymph, and ■ = control.

ECM components, sulfated polysaccharides, and NH_4Cl. To study the effect of some artificial cues on the behavioral response of *C. concholepas*, early pre-competent larvae of this mollusc were exposed to different ECM molecules and sulfated polysaccharides. A positive and time-dependent response was observed for all the assayed molecules. After 24 h of incubation, collagen, gelatin, and fibronectin induced sinking rates of 44%, 67%, and 89%, respectively (Fig. 3a). At the same time, rates of 70%, 78%, and 87% were observed when larvae were exposed to carrageenan, heparin, and chondroitin sulfate, respectively (Fig. 3b). The larvae responded to the sulfated polysaccharides more quickly than to the ECM molecules, reaching more than the 50% of the final response after just 2 h of incubation (*i.e.*, sinking rates of 39%, 73%, and 68% with carrageenan, heparin, and chondroitin sulfate, respectively) (see Fig. 3a, b). To test the effect of NH_4Cl on the response of *C. concholepas*, early pre-competent larvae of this gastropod were exposed to different concentrations of ammonium ion. The behavioral response observed was time- and dose-dependent (Fig. 4): it increased rapidly during the first 2 min, reaching sinking rates of 4%, 45%, 48%, and 84% at NH_4Cl final concentrations of 2, 5, 8, and 10 mM, respectively (Fig. 4). Thereafter, the number of larvae that stopped swimming and remained inactive stayed relatively constant, resulting in respective rates of 1%, 39%, 74%, and 98% after 30 min of incubation (Fig. 4). At the end of the experiment, larvae exposed to

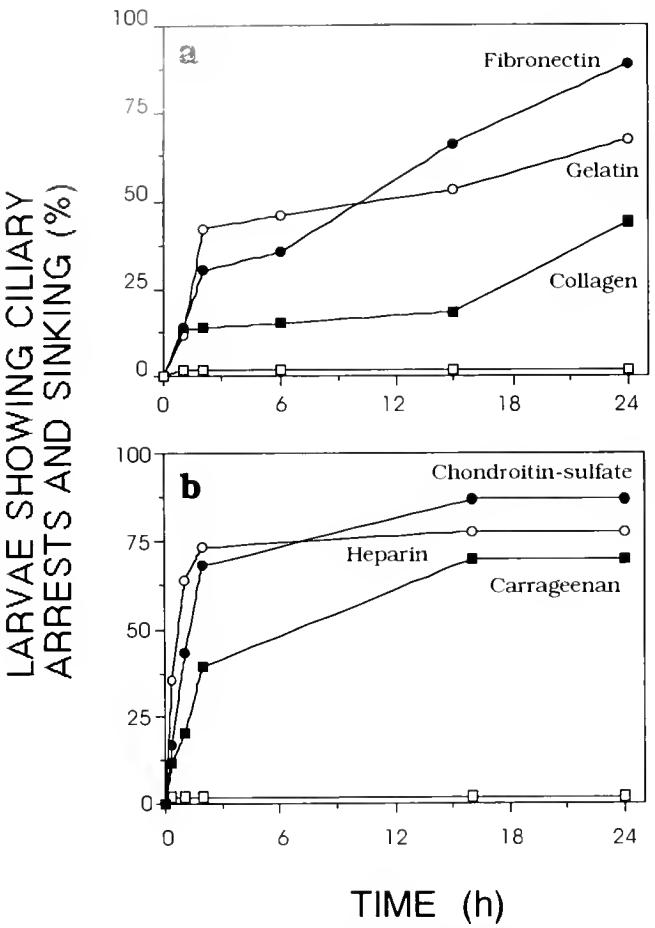

Figure 3. Mean percentage of early pre-competent larvae of *Concholepas concholepas* induced to sink by extracellular matrix (ECM) components and sulfated polysaccharides. (a) Mean percentage of *C. concholepas* larvae induced to sink by ECM constituents. ● = Fibronectin, ○ = gelatin, ■ = collagen, and □ = control. (b) Mean percentage of *C. concholepas* larvae induced to sink by sulfated polysaccharides. ■ = Carrageenan, ● = chondroitin sulfate, ○ = heparin, and □ = control.

10 m*M* NH_4Cl were washed and placed in normal fresh seawater to see if they would recover. Three hours later, all larvae were observed swimming normally (data not shown).

Chemotaxis to microbial films. Microbial films are well known as settlement inducers for a number of benthic marine invertebrates. We studied the attraction responses of pre-metamorphic *C. concholepas* larvae exposed to several such films. In the chemotaxis experiment in which glass plates were coated with different films, the larvae responded positively to *P. marinus*, multispecific, diatom, and bacterial films after 25 min of incubation; rates of attraction were 20%, 30%, 20%, and 20% respectively (Fig. 5a). At that time, no significant difference was observed among the different films (G test with 3 df). However, after 60 min of incubation, the respective rates of larval attraction increased to 40%, 60%, 60%, and 30%, and a significant preference was observed for the multispecific and the diatom films compared to the *P. marinus* and bacterial films ($P < 0.001$, G test with 1 df) (Fig. 5a). When *C. concholepas* shells were used as substrata, a positive response of larvae to *P. marinus*, multispecific, and diatoms films was observed after 25 min of incubation; rates of attraction were 30%, 40%, and 10%, respectively (Fig. 5b). At that time, the attraction to the multispecific and *P. marinus* films was significatively higher than to the diatom films ($P < 0.001$, G test with 1 df). At the end of the experiment, the larvae showed a clear and significant preference for the multispecific films over the other films, with an 80% rate of attraction ($P < 0.001$, G test with 1 df) (Fig. 5b). In the experiments with both glass and shell substrata, the larvae were not attracted to the sterile control at any time.

Larval activity in response to microbial films. The activity of *C. concholepas* larvae exposed to different microbial films was recorded. Larvae showing velar contraction were observed in the presence of all the films after 6 min of incubation (Fig. 6a). The percentage of larvae presenting this behavior was, however, significatively higher for the bacterial films at 4, 6, and 8 min of incubation with 20%, 30%, and 30%, respectively ($P < 0.001$, G test with 1 df). At the end of the experiment, the response to the bacterial film decreased, and no significant difference was observed among the bacterial, multispecific, and diatom treatments (Fig. 6a). On the other hand, the ciliar movement of larvae increased only in the presence of the multispecific and the *P. marinus* films (Fig. 6b). However, the effect of the former was higher after 8 min of incubation. At the end of the ex-

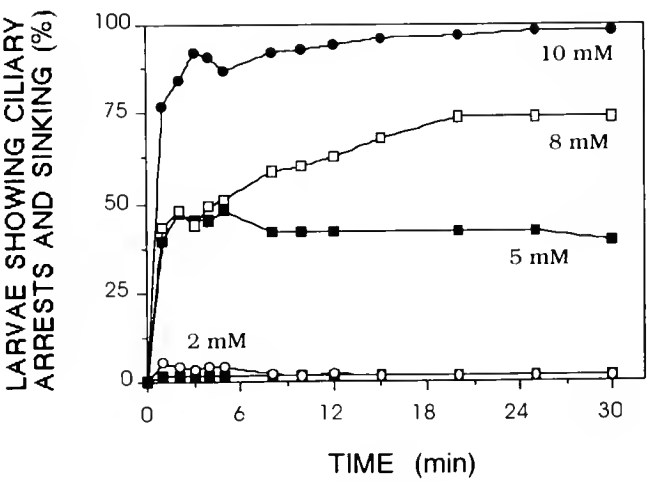

Figure 4. Mean percentage of early pre-competent larvae of *Concholepas concholepas* induced to sink by different concentrations of NH_4Cl. ● = 10 m*M*, □ = 8 m*M*, ■ = 5 m*M*, ○ = 2 m*M*, and □ = control.

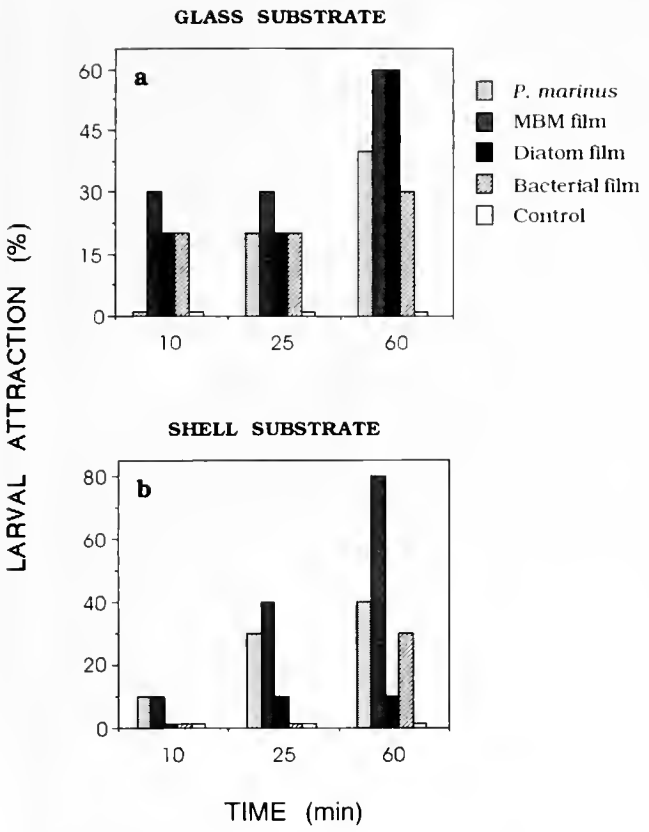

Figure 5. Mean percentage of attraction of pre-metamorphic *Concholepas concholepas* larvae to different microbial films. Microbial films prepared on glass (a) and *C. concholepas* shells (b).

periment, larvae exposed to the bacterial films exhibited an increased ciliar movement, but this response was significantly less than that observed for the other two treatments ($P < 0.001$, G test with 1 df) (Fig. 6b).

Discussion

Mucus and hemolymph

Early pre-competent larvae of *Concholepas concholepas* stopped swimming, sank, and remained inactive on the bottom of the wells when exposed to both mucus and hemolymph of adult individuals. Traces of mobile animals (*e.g.*, mucus) can influence the settlement of sessile animals (*e.g.*, barnacles) (Johnson and Strathmann, 1989), and conspecific mucus induces larval settlement in the abalone *Haliotis rufescens* (Slattery, 1992). Structural factors such as glycoproteins and growth factors as well as bacteria associated with mucus have been suggested as possible morphogens involved in triggering the larval settlement response in gastropods (Slattery, 1992; Cantillana and Inestrosa, 1993). Recently, a heparin-binding growth factor, which shows properties similar to those of fibroblast growth factors (FGF), has been identified in the foot of *C. concholepas* (Cantillana and Inestrosa, 1993). The binding of basic FGF to high-affinity receptors requires the presence of an ECM component (*i.e.*, heparan sulfate proteoglycans) (Yayon *et al.*, 1991). Therefore, it is possible that growth factors in the mucus of mollusc species could be interacting with ECM molecules (mainly sulfated polysaccharides) and then with high-affinity growth factor receptors. On the other hand, it has been hypothesized that lectins (*i.e.*, sugar-binding proteins or glycoproteins of non-immune origin that agglutinate cells or precipitate glycoconjugates) may be involved in the settlement and metamorphosis of marine invertebrate larvae (Maki and Mitchell, 1985). Lectins have been reported in the mucus of different fish species (Kamiya and Shimizu, 1980; Kamiya *et al.*, 1988) as well as in the hemolymph of a number of marine invertebrates such as starfish (Kamiya *et al.*, 1992), barnacles (Kamiya *et al.*, 1987), and isopods (Kaim-Malka, 1993). Therefore, lectins present in the mucus and hemolymph may be another factor mediating the larval settlement of *C. concholepas* and other species. The effect of heated hemolymph was clearly lower than that observed with unheated hemolymph during most of the incubation period. Kamiya *et al.* (1992) found that the hemagglutinating activity of lectins was heat labile in

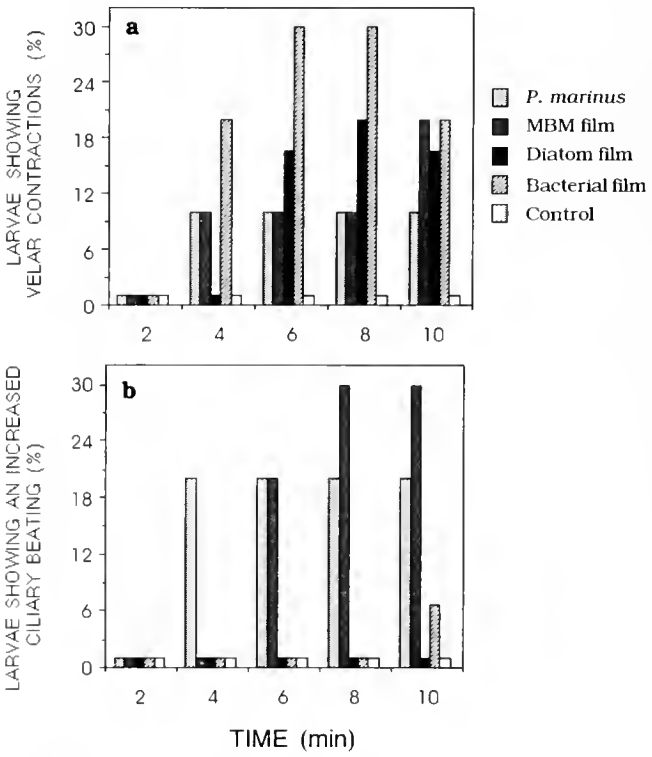

Figure 6. Mean percentage of pre-metamorphic *Concholepas concholepas* larvae showing velar contractions and an increased ciliary beating in response to microbial films. (a) Mean percentage of *C. concholepas* larvae showing velar contractions. (b) Mean percentage of *C. concholepas* larvae showing an increased ciliary beating.

the hemolymph of a starfish, decreasing or disappearing when exposed to high temperatures. A similar effect could have occurred in our case. Why the boiled hemolymph initially affects larvae in the same way that the unheated hemolymph does is not clear—maybe there are two types of cues or responses; in any case further studies are necessary to clarify this matter. The transient effect produced by both natural substances in larvae of *C. concholepas* may be related to some kind of habituation to the cue; alternatively, it may be due to a deficient larval response, given the presence of an immature signal-transduction mechanism.

ECM macromolecules, sulfated polysaccharides, and NH_4Cl

A positive and time-dependent behavioral response was observed in early pre-competent larvae of *C. concholepas* after exposure to ECM molecules and sulfated polysaccharides. In both cases larvae sank and remained attached to the substratum. The effect of sulfated molecules was faster than that of the other ECM components. Morse and Morse (1991) identified the molecule that is biologically active as a morphogen for a scleractinian coral larvae (*i.e., Agaricia humilis*) as a sulfated glycosaminoglycan. Moreover, they showed that some sulfated polysaccharides such as κ- carrageenan, fucoidan, and keratan sulfates induce the metamorphosis of *A. humilis*, but chondroitin sulfates and heparin do not (Morse and Morse, 1991). It was previously demonstrated that larvae of *C. concholepas* incubated in artificial seawater in the absence of sulfate or in presence of a specific sulfation inhibitor show a decrease in their mobility (Urrea *et al.*, 1992; Brandan *et al.*, 1995). The results presented in this work strongly suggest that sulfated polysaccharides play a role in aspects of the settlement of *C. concholepas* larvae. Heparin, which produced one of the most rapid response in larvae of *C. concholepas*, can interact with growth factors (Yayon *et al.*, 1991). In this context, factors associated with the mucus of larvae may be important in this interaction. The results described in this paper suggest that larvae of *C. concholepas* are able to interact with macromolecules found in the ECM, especially those that are sulfated.

A dose- and time-dependent response was observed when early pre-competent larvae of *C. concholepas* were exposed to NH_4^+. Larvae were able to recover their mobility after an extensive washing with fresh seawater. NH_4^+ has been described as an important inducer of settlement behavior in oyster larvae (Coon *et al.*, 1990). Likewise, it has been found that NH_4^+ is the active inductive factor associated with bacterial supernatants (Bonar *et al.*, 1990). Following in this vein, marine zones rich in dissolved organic matter would represent important areas where high settlement of benthic marine invertebrates may occur (Morse, 1990).

Since in many species repeated encounters with others cause the larvae to stop swimming and settle to the bottom of the culture vessel, it is possible that the high larval density used in our experiments affected the results obtained here. However, repeated observations of the behavior of control *C. concholepas* larvae during the assays never showed that larvae stopped swimming or settled as the result of encounters among them. This observation represents a behavioral pattern of remarkable interest, making our results all the more notable.

Chemotaxis and larval activity in response to microbial films

Our results clearly show that microbial films, especially multispecific ones, are able to attract pre-competent larvae of *C. concholepas*. This response is preferentially observed in the presence of multispecific films attached to shell substrata. Moreover, larvae exposed to these films show increased ciliary beating. The role of bacterial films in the settlement of marine invertebrate larvae has been widely studied (*e.g.*, Kirchman *et al.*, 1982; Maki and Mitchell, 1985; Maki *et al.*, 1989; Bonar *et al.*, 1990). However, the effect of microbial films on the attraction of larvae and the eventual role of these films in bringing larvae near to the marine bottom has not received much attention (Pawlik, 1992). Our results suggest a quite important role for microbial films in attracting larvae of *Concholepas concholepas*. This attraction could favor the approach of larvae to the chemical metamorphic inducers on the marine bottom. The higher response of larvae to multispecific films on shell than on glass was perhaps due to a better attachment of the bacteria to an irregular surface. Also it is possible that the films produced on the shell were either more numerous or had a different composition than those on the glass.

In this paper we have provided evidence that pre-competent larvae of *Concholepas concholepas* exposed to different natural and artificial cues exhibit behaviors (*i.e.*, ciliary arrests, contraction of the velar lobes, and retraction of the velum into the shell) similar to those described for competent veliger larvae of other gastropod species during metamorphosis. Likewise, they showed different degrees of attraction to different microbial films isolated from a native recruitment zone of this species. This information on natural and artificial metamorphic inducers of *C. concholepas* larvae may be of paramount importance in developing successful methods for culturing this overexploited species.

Acknowledgments

This work was supported by FONDECYT Grants 3502/89, 0651/91, and 19406/94 to Dr. N. C. Inestrosa and 0997/92 to Dr. C. Riquelme, and by IFS Grant 1407-3F

to Dr. E. Brandan. We thank Prof. Gerald Boalch from Citadelhill Plymouth Labs, U.K., for identifying microalgae and diatoms. During this study S. R. Rodríguez was a Research Fellow from DIUC. He is now a Fellow from Fundación Andes (Dept. of Ecology).

Literature Cited

Arkett, S. A., G. O. Mackie, and C. L. Singla. 1987. Neuronal control of ciliary locomotion in a gastropod veliger (*Calliostoma*). *Biol. Bull.* **173:** 513–526.

Barlow, L. A. 1990. Electrophysiological and behavioral responses of larvae of the red abalone (*Haliotis rufescens*) to settlement-inducing substances. *Bull. Mar. Sci.* **46:** 537–554.

Bonar, D. B., S. L. Coon, M. Walch, R. M. Weiner, and W. Fitt. 1990. Control of oyster settlement and metamorphosis by endogenous and exogenous chemical cues. *Bull. Mar. Sci.* **46:** 484–498.

Brandan, E., S. R. Rodriguez, E. O. Campos, and N. C. Inestrosa. 1995. Extracellular matrix constituents induce larval settlement of *Concholepas concholepas*. Proceedings from the Second Ecuadorian Aquaculture Conference—IFS, Guayaquil, Ecuador (in press).

Campos, E. O., A. Pinto, E. Bustos, S. R. Rodriguez, and N. C. Inestrosa. 1994. Metamorphosis of laboratory-reared larvae of *Concholepas concholepas* (Mollusca; Gastropoda). *Aquaculture* **126:** 299–303.

Cantillana, P., and N. C. Inestrosa. 1993. Presence of a heparin-binding growth factor in *Concholepas concholepas* Bruguière (Mollusca; Gastropoda; Muricidae). *J. Exp. Mar. Biol. Ecol.* **171:** 239–250.

Castilla, J. C. 1988. Una revisión bibliográfica (1980–1988) sobre *Concholepas concholepas* (Gastropoda, Muricidae): problemas pesqueros y experiencias en repoblación. *Biol. Pesq. Chile* **17:** 9–19.

Coon, S. L., M. Walch, W. K. Fitt, R. M. Weiner, and D. B. Bonar. 1990. Ammonia induces settlement behavior in oyster larvae. *Biol. Bull.* **179:** 297–303.

DiSalvo, L. H. 1988. Observations on the larval and post-metamorphic life of *Concholepas concholepas* in laboratory culture. *Veliger* **30:** 358–368.

Hadfield, M. G., and J. T. Pennington. 1990. Nature of the metamorphic signal and its internal transduction in larvae of the nudibranch *Phestilla sibogae*. *Bull. Mar. Sci.* **46:** 455–464.

Hirata, K. Y., and M. G. Hadfield. 1986. The role of choline in metamorphic induction of *Phestilla* (Gastropoda: Nudibranchia). *Comp. Biochem. Physiol.* **84C:** 15–21.

Inestrosa, N. C., M. González, and E. O. Campos. 1993a. Metamorphosis of *Concholepas concholepas* (Bruguière, 1789) induced by excess potassium. *J. Shellfish Res.* **12:** 337–341.

Inestrosa, N. C., M. González, and E. O. Campos. 1993b. Molecular changes induced by metamorphosis in larvae of the prosobranch *Concholepas concholepas* Bruguière (Mollusca; Gastropoda; Muricidae). *J. Exp. Mar. Biol. Ecol.* **168:** 205–215.

Ishida, Y., M. Eguchi, and H. Kadota. 1986. Existence of obligately oligotrophic bacteria as a dominant population in the south China sea and the west Pacific ocean. *Mar. Ecol. Prog. Ser.* **30:** 197–203.

Johnson, L. E., and R. R. Strathmann. 1989. Settling barnacle larvae avoid substrata previously occupied by a mobile predator. *J. Exp. Mar. Biol. Ecol* **128:** 87–103.

Kaim-Malka, R. A. 1993. Electrophoresis study of haemolymph proteins of *Cirolana borealis* (Crustacea, Isopoda). *Comp. Biochem. Physiol.* **106 B:** 131–139.

Kamiya, H., and Y. Shimizu. 1980. Marine biopolymers with cell specificity. II. Purification and characterization of agglutinins from mucus of windowpane flounder *Lophopsetta maculata*. *Biochim. Biophys. Acta* **622:** 171–178.

Kamiya, H., K. Muroto, and R. Goto. 1987. Isolation and characterization of agglutinins from the hemolymph of an acorn barnacle, *Megabalanus volcano*. *Dev. Comp. Immunol.* **11:** 297–307.

Kamiya, H., K. Muroto, and R. Goto. 1988. Purification and properties of agglutinins from conger eel, *Conger myriaster* (Brevoort), skin mucus. *Dev. Comp. Immunol.* **12:** 309–318.

Kamiya, H., K. Muroto, R. Goto, and M. Sakai. 1992. Lectins in the hemolymph of a starfish, *Asterina pectinifera:* purification and characterization. *Dev. Comp. Immunol.* **16:** 243–250.

Kirchman, D., S. Graham, D. Reish, and R. Mitchell. 1982. Bacteria induce settlement and metamorphosis of *Janua (Dexiospira) brasiliensis* Grube (Polychaeta: Spirorbidae). *J. Exp. Mar. Biol. Ecol.* **56:** 153–163.

Maki, J. S., and R. Mitchell. 1985. Involvement of lectins in the settlement and metamorphosis of marine invertebrate larvae. *Biol. Mar. Sci.* **37:** 675–683.

Maki, J. S., D. Rittschof, A. R. Schmidt, A. G. Snyder, and R. Mitchell. 1989. Factors controlling attachment of bryozoan larvae: a comparison of bacterial films and unfilmed surfaces. *Biol. Bull.* **177:** 295–302.

Morse, D. E. 1990. Recent progress in larval settlement and metamorphosis: closing the gaps between molecular biology and ecology. *Bull. Mar. Sci.* **46:** 465–483.

Morse, D. E., and A. N. C. Morse. 1991. Enzymatic characterization of the morphogen recognized by *Agaricia humilis* (Scleractinian coral) larvae. *Biol. Bull.* **181:** 104–122.

Morse, D. E., N. Hooker, H. Duncan, and L. Jensen. 1979. γ-aminobutyric acid, a neurotransmitter, induces planktonic abalone larvae to settle and begin metamorphosis. *Science* **204:** 407–410.

Pawlik, J. R. 1986. Chemical induction of larval settlement and metamorphosis in the reef-building tube worm *Phragmatopoma californica* (Sabellariidae: Polychaeta). *Mar. Biol.* **91:** 59–68.

Pawlik, J. R. 1992. Chemical ecology of settlement of benthic marine invetebrates. *Oceanogr. Mar. Biol. Annu. Rev* **30:** 273–335.

Provasoli, L., J. J. A. McLaughlin, and M. R. Droop. 1957. The development of artificial media for marine algae. *Arch. Mikrobiol.* **25:** 392–428.

Riquelme, C., and P. Chavez. 1995. Colonization of Vibrios on developmental stages of *Concholepas concholepas* (Bruguière, 1789) Mollusca, Muricidae. In: *Ecology in Aquaculture. IFS Workshop*, N. Kaupsky, ed. (in press).

Rodríguez, S. R., F. P. Ojeda, and N. C. Inestrosa. 1993. Settlement of benthic marine invertebrates. *Mar. Ecol. Prog. Ser.* **97:** 193–207.

Slattery, M. 1992. Larval settlement and juvenile survival in the red abalone (*Haliotis rufescens*): an examination of inductive cues and substrate selection. *Aquaculture* **102:** 143–153.

Sokal, R. R., and F. J. Rohlf. 1981. *Biometry*. 2nd ed. Freeman, San Francisco.

Urrea, R., M. González, N. C. Inestrosa, and E. Brandan. 1992. Sulfation is required for mobility of veliger larvae of *Concholepas concholepas* (Mollusca; Gastropoda; Muricidae). *J. Exp. Zool.* **261:** 365–372.

Yayon, A., M. Klagsbrun, J. D. Esko, P. Leder, and D. Ornitz. 1991. Cell surface, heparin-like molecules are required for binding of basic fibroblast growth factors to its high affinity receptor. *Cell* **64:** 841–848.

Yool, A. J., S. M. Grau, M. G. Hadfield, R. A. Jensen, D. A. Markell, and D. E. Morse. 1986. Excess potassium induces larval metamorphosis in four marine invertebrate species. *Biol. Bull.* **170:** 255–266.

Reference: *Biol. Bull.* 189: 280–287. (December, 1995)

Ultrastructural Localization of Antho-RWamides I and II at Neuromuscular Synapses in the Gastrodermis and Oral Sphincter Muscle of the Sea Anemone *Calliactis parasitica*

JANE A. WESTFALL[1], KELLEY L. SAYYAR[1], CAROL F. ELLIOTT[1], AND CORNELIS J. P. GRIMMELIKHUIJZEN[2]

[1]*Department of Anatomy and Physiology, Kansas State University, Manhattan, Kansas 66506 and* [2]*Department of Cell Biology and Anatomy, University of Copenhagen, DK-2100 Copenhagen Ø, Denmark*

Abstract. Light microscopic studies have shown that the sea anemone neuropeptides Antho-RWamides I (<Glu-Ser-Leu-Arg-Trp-NH_2) and II (<Glu-Gly-Leu-Arg-Trp-NH_2) are located in neurons associated with the oral sphincter muscle of the sea anemone *Calliactis parasitica*. In the present ultrastructural study, using the immunogold technique, we found Antho-RWamide-like material in the granular vesicles of neurons that make synaptic contacts with the myonemes of both gastrodermal and oral sphincter muscle cells of *Calliactis*. Gastrodermal nerve cells contained immunoreactive granular vesicles averaging 149.3 ± 4.1 nm in diameter; smaller granular vesicles (47.5 ± 2.5 nm) were present at a labelled synapse. Neurites associated with the sphincter muscle had immunoreactive granular vesicles averaging 78.8 ± 3.3 nm in diameter with smaller granular vesicles (63 ± 4.4 nm) at three labelled neuromuscular synapses. All Antho-RWamide-immunoreactive vesicles were irregularly granular, unlike the typical dense-cored vesicles observed at some other synapses in sea anemones. No evidence was found of storage or release at nonsynaptic sites (paracrine secretion).

The Antho-RWamide immunoreactive neurites innervate the sphincter muscle fibers directly rather than through intermediate neuronal pathways. This is the first ultrastructural evidence of a neuropeptide at a coelenterate neuromuscular synapse.

Received 15 June 1995; accepted 21 September 1995.

Abbreviations BSA, bovine serum albumin; PBS, phosphate-buffered saline.

Introduction

Nervous systems first appeared in cnidarians or in a closely related ancestor group. The basic plan of the cnidarian nervous system is a diffuse network of nerve cells, but in some members of this group, such as medusae, nerve cells also can aggregate in nerve plexuses, nerve rings, or sense organs. Sea anemones have complex neuronal nets and nerve plexuses in both the inner and outer epithelial layers (Grimmelikhuijzen and Westfall, 1995). From sea anemones, a variety of neuropeptides, including the closely related Antho-RWamide I (<Glu-Ser-Leu-Arg-Trp-NH_2) and Antho-RWamide II (<Glu-Gly-Leu-Arg-Trp-NH_2) have been isolated (Graff and Grimmelikhuijzen, 1988a, b; Grimmelikhuijzen *et al.*, 1992). The Antho-RWamides are present in neurons of many body regions of sea anemones, but Antho-RWamide-immunoreactive neurons are especially dense in the upper body column, where they innervate the oral sphincter muscle (Graff and Grimmelikhuijzen, 1988a; Grimmelikhuijzen *et al.*, 1989, 1992). The oral sphincter muscle is a ring of circular muscle fibers embedded in the gelatinous middle layer, the mesoglea, of the upper body wall. During periods of danger and environmental stress, it contracts to close the animal and protect the retracted apical tentacles. The cell bodies of the Antho-RWamide-positive neurons innervating the sphincter appear to be located in the gastrodermis (endoderm) of the upper body wall, whereas their processes project across the mesoglea and ramify into long, fine projections paralleling the circular bundles of sphincter muscle fibers (Graff and Grimmelikhuijzen,

1988a; Grimmelikhuijzen *et al.*, 1989, 1992). No synaptic contacts between neurons and muscle fibers can be seen at the light microscope level.

In physiological experiments, the Antho-RWamides (10^{-8} *M*) induced tonic contractions in isolated oral sphincter muscle rings and cells isolated from the sphincter (McFarlane *et al.*, 1991). Taken together, these data indicate that the Antho-RWamides are transmitters at neuromuscular synapses.

Electron microscopic "immunogold" techniques, using neuropeptide antisera and colloidal gold-conjugated secondary antibodies, have permitted the ultrastructural localization of neuropeptides in dense-cored or granular vesicles of a variety of cnidarian neurons (Koizumi *et al.*, 1989; Singla and Mackie, 1991; Westfall and Grimmelikhuijzen, 1993). Antho-RFamide (<Glu-Gly-Arg-Phe-NH_2), the first sea anemone neuropeptide to be isolated, was demonstrated in dense-cored vesicles of bidirectional, interneuronal synapses of sea anemones (Westfall and Grimmelikhuijzen, 1993). In the present study, using the immunogold technique with an antiserum against the common C terminus of the Antho-RWamides, we were able to label granular synaptic vesicles at neuromuscular junctions of sea anemones. This strongly supports our hypothesis that the Antho-RWamides are transmitters at some cnidarian neuromuscular synapses.

Materials and Methods

Three specimens of the sea anemone *Calliactis parasitica* (sent from Roscoff Station Biologique, France) were anesthetized using 0.3 *M* $MgCl_2$. Once relaxation was sufficient, the animals were cut using Personna Gem super stainless steel blades.

For light microscopy, one animal was placed in 2.5% glutaraldehyde in 0.05 *M* sodium cacodylate, pH 7.4, and cut longitudinally in half. Photographs were taken using an OM-2S Olympus camera attached to a Wild model M75 zoom stereomicroscope to locate the sphincter muscle. Longitudinal slices of the oral sphincter from the other half of the animal were processed, embedded in paraffin, sectioned, mounted on glass slides, and stained with haematoxylin and eosin. Photographs were taken of the sphincter muscle using an Aristoplan image analysis light microscope.

For electron microscopy, two animals were cut longitudinally, and the lower body columns removed. Several longitudinal slices were cut, starting at one edge and proceeding serially. Each slice contained a few tentacles. The slices were placed in one of two fixatives: 4% paraformaldehyde—0.1% glutaraldehyde in 0.1 *M* phosphate buffer, pH 7.4; 4% paraformaldehyde—0.1% glutaraldehyde in 0.1 *M* phosphate buffered saline, pH 6.5 for 30 min, and then pH 11.0 for 3 h (Berod *et al.*, 1981).

All tissues were rinsed in 0.1 *M* phosphate buffer, pH 7.4, dehydrated in ethanol, and then in acetone; infiltrated overnight in a mixture of Epon and Araldite; and cut into small segments for final embedding by taking horizontal slices down the length of the oral sphincter starting at the region near the tentacles.

Thin longitudinal sections of sphincter muscle were cut with a diamond knife and mounted on Formvar-coated, 100-mesh, nickel grids. The sections were rinsed in doubly distilled water (ddH_2O), then exposed to saturated sodium metaperiodate for 30 min to open antigenic sites. After a ddH_2O rinse, the sections were exposed to normal goat serum diluted 1:20 with PBS-Tween-BSA buffer to block nonspecific antigenic sites. They were incubated for 1 h with rabbit antiserum #2061 against Antho-RWamide, diluted 1:50–1:200 with buffer.

After rinsing in buffer, the sections were immunogold stained for 1 h in goat anti-rabbit IgG conjugated to either 5 or 15 nm-gold particles, diluted in buffer 1:10–1:40. After rinsing in buffer with BSA, then in PBS, they were postfixed for 15 min in 2% glutaraldehyde in PBS and rinsed in ddH_2O. The sections were further stained in 7% uranyl acetate in 70% ethanol, then in Reynolds lead citrate and examined in a Philips 400 transmission electron microscope. Because only 2–3 sections covered a grid, and usually 10 grids were used per experiment, the search for synapses was slow and laborious.

Control sections were exposed to Antho-RWamide antiserum (1:200), which had been incubated overnight in 100 μg/ml of Antho-RWamide.

Antiserum #2061 directed against the C terminus (Arg-Trp-NH_2) of both Antho-RWamides I and II was prepared as described by Grimmelikhuijzen (1985). Arg-Trp-NH_2 was a customer synthesis by Bachem (Bubendorf, Switzerland). Only antisera against Arg-Trp-NH_2 and no other antisera against the other sea anemone Arg-X-NH_2 peptides stained neurons in the sphincter muscle (see *e.g.*, Fig. 2 of Grimmelikhuijzen *et al.*, 1992).

To categorize a granule type, measurements were made of 10 randomly selected granules or vesicles per gastrodermal neuron or sphincter muscle neurite, and four to five granules or vesicles per synapse. The reason why only granules were measured in some cases is owing to the fact that the two-pH paraformaldehyde fixation, which worked best for immunogold labeling with antisera to the Antho-RWamides, caused some loss of membrane preservation around many granules.

Results

The oral sphincter muscle of *Calliactis parasitica* was located in a widened region of the upper body column mesoglea (Fig. 1). It was composed of multiple layers of myonemes forming the circular, smooth, muscle fibers

Figure 1. Longitudinal section through whole glutaraldehyde-fixed specimen of *Calliactis parasitica* indicating thickened mesoglea containing oral sphincter muscle (SM) at base of tentacles (T). Note epidermis (E), gastrodermis (G), septa (S), pharynx (P), and basal disk (BD). Bar = 1000 μm.

Figure 2. Light micrograph of a cross section through the oral sphincter muscle (SM). Note longitudinal section of tentacle (T), epidermis (E), diffuse bundles of myonemes (between arrowheads) within the mesoglea, gastrodermis (G), and septa (S). Bar = 100 μm.

encompassing the oral region. In a longitudinal section of the animal, the bundles of oral sphincter myonemes extended one tenth of the length of a 3-cm-long sea anemone and appeared to increase in number near the oral region (Fig. 2). The myonemes extended irregularly towards the epidermis, but stopped abruptly near a band of mesoglea separating them from the gastrodermis.

Using electron microscopy, we observed various-sized granular vesicles in bipolar-like nerve cells of the gastrodermal nerve net. The granules, which averaged 149.3 ± 4.1 nm in diameter, were immunoreactive to Antho-RWamide (Fig. 3). The granules labeled with both 5 nm gold (upper inset Fig. 3) and 15 nm gold (middle inset) and were present at a neuromuscular synapse (lower inset). The synaptic vesicles averaged 47.5 ± 2.5 nm in diameter.

Nerve processes from the gastrodermis crossed the muscle-free border of the mesoglea and entered into the individual oblong bundles of oral sphincter myonemes (Fig. 4). These myonemes were composed of closely packed bundles of myofilaments, aggregated at one side, and of a myofilament-free area at the other side. An

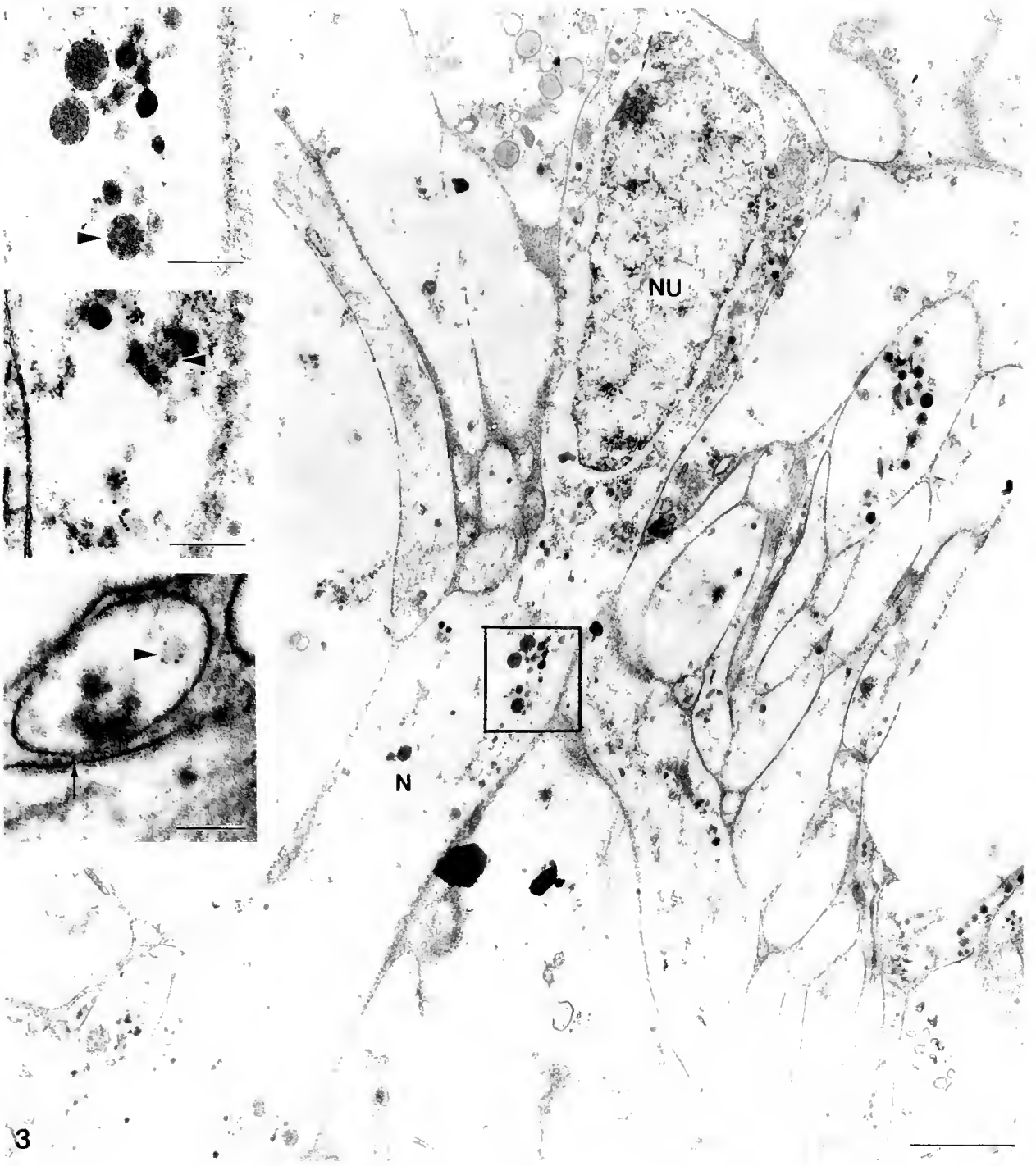

Figure 3. Electron micrograph of neuronal perikaryon and neurite containing granular vesicles immunogold-labeled with antisera to Antho-RWamide in gastrodermal nerve plexus. Note large neurite (N) with various-sized granular vesicles (box) and nucleus (NU) of neuron. Bar = 1 μm. Insets: High magnification of boxed area of neurite with 5 nm gold marker in large granules (arrowhead, upper inset), serial section of neurite with smaller granules labeled with 15 nm gold particles (arrowhead, middle inset), and 5 nm gold particles in granular vesicles (arrowhead, lower inset) at a neuromuscular synapse with transverse filaments in the synaptic cleft (arrow). Bar = 0.25 μm (upper; middle) and 0.1 μm (lower).

Figure 4. Ultrathin section of Antho-RWamide immunoreactive neurite (N) passing into a bundle of oral sphincter myonemes (MY) in the mesoglea (ME). Note small neurites with either clear or granular vesicles (arrowheads). Bar = 1 μm. Inset: High magnification of neurite with immunogold-labeled granular vesicles. Bar = 0.25 μm.

occasional nucleus was observed in these myonemes, suggesting that they are complete muscle cells. The neurites that invaded the sphincter usually were associated with the myofilament-free areas of the myonemes.

Dense, granular vesicles, varying in size and having an average diameter of 78.8 ± 3.3 nm were distributed unequally within the slender, 0.2–0.3 μm-diameter neurites. Groups of these granules were immunoreactive to Antho-RWamide antisera using both 5 and 15 nm gold markers (inset Fig. 4). Most neurites observed within individual bundles of myonemes had densely granular vesicles, although occasional groups of nongranular vesicles were present.

Typical neuromuscular synaptic foci were few in number and difficult to locate in the oral sphincter muscle, but several putative immunoreactive neuromuscular synapses were observed (Fig. 5). The presynaptic vesicles were aligned at the presynaptic membrane opposite a series of cross filaments in the synaptic cleft and a postsynaptic density (Fig. 5b). The synaptic cleft ranged from 9 to 18 nm in width. Sometimes, it took two-to-three serial sections through a synapse to verify the presence of cross filaments in the synaptic cleft at loci where granular vesicles were gold-labeled with antisera to Antho-RWamide. Occasionally, vesicles attached to the presynaptic membrane appeared empty (Fig. 5b), although gold label was present. The synaptic vesicles averaged 63 ± 4.4 nm in diameter.

Experimental serial sections, incubated in Antho-RWamide antisera, had immunoreactive granular vesicles in some neurites (Fig. 6a, b). Control sections, incubated in antisera which had been incubated overnight in 100 μg/ml of Antho-RWamide, did not stain with immunogold (Fig. 6c). A neurite adjacent to those with immunoreactive granular vesicles contained electron-lucent vesicles, which were not immunoreactive to Antho-RWamide antisera (Fig. 6a, b).

Discussion

Both Antho-RWamides I and II stimulate contractions in rings of sphincter muscle and in isolated sphincter muscle cells from *Calliactis parasitica* (McFarlane *et al.*, 1991). In this study, we have found that neurons make

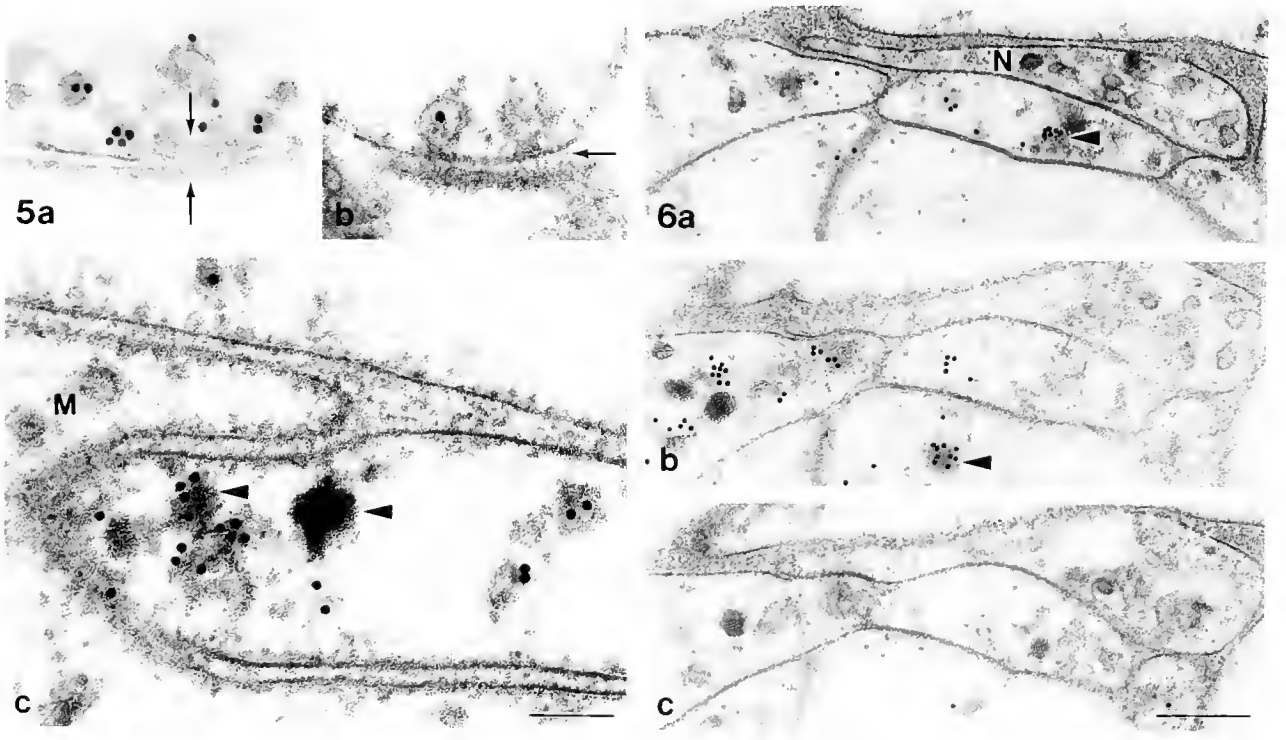

Figure 5. Three examples (a, b, c) of neuromuscular synapses with Antho-RWamide-labelled presynaptic granules and vesicles in oral sphincter muscle. Note parallel pre- and postsynaptic densities (between arrows, a), cross filaments in synaptic cleft (arrow, b), and 15 nm-gold label specific to presynaptic granular vesicles (arrowheads, c). Muscle cell (M). Bar = 0.1 μm.

Figure 6. Three serial thin sections through a cross-sectioned bundle of oral sphincter myonemes revealing immunoreactive granular vesicles in experimental (a,b) and nonimmunoreactive granular vesicles in control section (c). Note clear vesicles without gold label in adjacent upper neurite (N). Bar = 0.25 μm.

morphologically identifiable synapses with the sphincter muscle cells and that these synapses contain Antho-RWamide-immunoreactive granular vesicles. This supports our hypothesis that the Antho-RWamides are transmitters at the neuromuscular junctions of the sphincter.

In a previous study, we located Antho-RFamide immunoreactivity in granular vesicles at two-way interneuronal synapses in the sea anemone *Anthopleura* (Westfall and Grimmelikhuijzen, 1993). Therefore, peptidergic synapses clearly play an important role in primitive nervous systems.

The long slender neurites, which cross the mesoglea to innervate the sphincter muscle, contain Antho-RWamide immunoreactive granules of varying sizes, whereas the granular vesicles at synapses appear to be somewhat smaller. The synthesis of vertebrate neuropeptides follows a stepwise pattern: a prepropeptide is formed in the rough endoplasmic reticulum, then reduced in the Golgi complex to a smaller propeptide and is eventually cleaved into the active peptides in vesicles (Brownstein, 1982). This pattern of synthesis and reduction of the Antho-RWamide precursor may also occur in sea anemone neurons, and it may explain the difference in size between granules in the neurites and in the synapses. Similarly, an immunoreactive nucleated nerve cell in the gastrodermal nerve plexus has both large and small granular vesicles, the latter being denser. Slightly smaller granular vesicles have been observed at an immunoreactive gastrodermal neuromuscular synapse.

Sea anemone muscles undergo spontaneous autonomous movements similar to those of the smooth muscle of the vertebrate intestine, which result in constriction and extension of this tube-like structure (Parker, 1919). Autonomic nerve fibers, which innervate smooth muscle of the vertebrate intestine, do not always terminate with morphologically distinct neuromuscular synapses (Jänig, 1978). A similar situation might exist in the cnidarian smooth muscles. However, some neuromuscular junctions do occur in cnidarians and can be recognized by the presence of dense-cored or clear vesicles (80–100 nm in diameter) aligned on the presynaptic side of a pair of electron-dense synaptic membranes separated by a 15–25 nm-wide cleft (Westfall, 1973).

In this study of gastrodermal and oral sphincter neuromuscular synapses of the sea anemone *Calliactis parasitica*, there are two to four or more granular vesicles aligned at paired, electron-dense, synaptic membranes separated by a 15-nm-wide cleft traversed by a series of cross filaments. The neuromuscular synapses are similar ultrastructurally to the interneuronal synapses in the sea anemone nerve plexus (Westfall, 1970, 1987). Electron-lucent vesicles, which do not label with antisera to Antho-RWamide, are present in a few other neurites. Although nothing is known about the putative neurotransmitter substances at sea anemone neuromuscular synapses with electron-lucent vesicles, this study demonstrates Antho-RWamide immunoreactivity in granular vesicles at neuromuscular synapses.

Ross (1960a,b) has stated that adrenaline causes contraction in sphincter and circular muscle preparations of *Calliactis parasitica* and *Metridium senile;* Wood and Lentz (1964) have claimed that adrenaline is present in the mesenteries of *Metridium*. Other studies have suggested that catecholamines (Dahl *et al.*, 1963; Anctil *et al.*, 1984; DeWaele *et al.*, 1987; Umbriaco *et al.*, 1990) and DOPA (Carlberg, 1983) are present in nerve cells of various anthozoa. Taurine-like immunoreactivity has been reported in the motor nerve net of the scyphozoan jellyfish *Cyanea capillata* (Carlberg *et al.*, 1995). Thus, besides Antho-RWamides, other neuromuscular transmitters also may be present in the anthozoans.

Acknowledgments

Contribution No. 95-570-J of the Kansas Agricultural Experiment Station. We thank Shelly Christenson in the Diagnostic Medicine/Pathobiology Histopathology Laboratory for instruction on the tissue processor and staining apparatus, and Dr. J. W. Sharp for instruction on the Image Analysis System. This study was funded by NSF grant IBN-9120161 to J. A. Westfall and by a grant from the Danish Natural Science Research Council to C. J. P. Grimmelikhuijzen.

Literature Cited

Anctil, M., G. Germain, and L. LaRiviere. 1984. Catecholamines in the coelenterate *Renilla kollikeri*. Uptake and radio autographic localization. *Cell Tiss. Res.* **238**: 69–80.

Berod, A., B. K. Hartman, and J. F. Pujol. 1981. Importance of fixation in immunohistochemistry: use of formaldehyde solutions at variable pH for the localization of tyrosine hydroxylase. *J. Histochem. Cytochem.* **29**: 844–850.

Brownstein, M. J. 1982. Post-translational processing of neuropeptide precursors. *Trends Neurosci.* **5**: 318–320.

Carlberg, M. 1983. Evidence of DOPA in the nerves of sea anemones. *J. Neuronal Transm.* **57**: 75–84.

Carlberg, M., K. Alfredsson, S.-O. Nielsen, and P. A. V. Anderson. 1995. Taurine-like immunoreactivity in the motor nerve net of the jellyfish *Cyanea capillata*. *Biol. Bull.* **188**: 78–82.

Dahl, E., B. Falck, C. von Mecklenburg, and H. Myhrberg. 1963. An adrenergic nervous system in sea anemones. *Q. J. Microsc. Sci.* **104**: 531–534.

DeWaele, J.-P., M. Anctil, and M. Carlberg. 1987. Biogenic catecholamines in the cnidarian *Renilla kollikeri*: radioenzymatic and chromatographic detection. *Can. J. Zool.* **65**: 2458–2465.

Graff, D., and C. J. P. Grimmelikhuijzen. 1988a. Isolation of <Glu-Ser-Leu-Arg-Trp-NH_2, a novel neuropeptide from sea anemones. *Brain Res.* **442**: 354–358.

Graff, D., and C. J. P. Grimmelikhuijzen. 1988b. Isolation of <Glu-Gly-Leu-Arg-Trp-NH_2 (Antho-RWamide II), a novel neuropeptide from sea anemones. *FEBS Lett.* **239**: 137–140.

Grimmelikhuijzen, C. J. P. 1985. Antisera to the sequence Arg-Phe-amide visualize neuronal centralization in hydroid polyps. *Cell Tissue Res.* **241:** 171–182.

Grimmelikhuijzen, C. J. P., and J. A. Westfall. 1995. The nervous systems of cnidarians. Pp. 7–24 in *The Nervous Systems of Invertebrates—An Evolutionary and Comparative Approach*, O. Breidbach and W. Kutsch, eds. Birkhäuser, Basel.

Grimmelikhuijzen, C. J. P., D. Graff, and I. D. McFarlane. 1989. Neurons and neuropeptides in coelenterates. *Arch. Histol. Cytol.* **52:** 265–276.

Grimmelikhuijzen, C. J. P., K. Carstensen, D. Darmer, A. Moosler, H-P Nothaeker, R. K. Reinscheid, C. Schmutzler, H. Vollert, I. McFarlane, and K. L. Rinehart. 1992. Coelenterate neuropeptides: structure, action and biosynthesis. *Am. Zool.* **32:** 1–12.

Jänig, W. 1978. The autonomic nervous system. Pp 220–267 in *Fundamentals of Neurophysiology*, R. F. Schmidt, ed. Springer-Verlag, New York.

Koizumi, O., J. D. Wilson, C. J. P. Grimmelikhuijzen, and J. A. Westfall. 1989. Ultrastructural localization of RFamide-like peptides in neuronal dense-cored vesicles in the peduncle of *Hydra*. *J. Exp Zool.* **249:** 17–22.

McFarlane, I. D., P. A. V. Anderson, and C. J. P. Grimmelikhuijzen. 1991. Effects of three Anthozoan neuropeptides, Antho-RWamide I, Antho-RWamide II and Antho-RFamide, on slow muscles from sea anemones. *J Exp. Biol.* **156:** 419–431.

Parker, G. H. 1919. *The Elementary Nervous System.* J. B. Lippincott, Philadelphia.

Ross, D. M. 1960a. The effects of ions and drugs on neuromuscular preparations of sea anemones. I. On preparations of the column of *Calliactis* and *Metridium*. *J Exp. Biol.* **37:** 732–752.

Ross, D. M. 1960b. The effects of ions and drugs on neuromuscular preparations of sea anemones. II. On sphincter preparations of *Calliactis* and *Metridium*. *J Exp. Biol.* **37:** 753–773.

Singla, C. L., and G. O. Mackie. 1991. Immunogold labelling of FMRFamide-like neuropeptide in neurons of *Aglantha* (Hydromedusae: Trachylina). *Can. J. Zool.* **69:** 800–802.

Umbriaco, D., M. Anctil, and L. Descarries. 1990. Serotonin-immunoreactive neurons in the cnidarian *Renilla koellikeri*. *J. Comp. Neurol.* **291:** 167–178.

Westfall, J. A. 1970. Synapses in a sea anemone, *Metridium* (Anthozoa). Pp. 717–718 in *Microscopie Électronique* 1970, vol. 3, P. Favard, ed. Société Française de Microscopie Électronique, Paris.

Westfall, J. A. 1973. Ultrastructure evidence for neuromuscular systems in coelenterates. *Am. Zool.* **13:** 237–246.

Westfall, J. A., 1987. Ultrastructure of invertebrate synapses. Pp. 3–28 in *Nervous Systems in Invertebrates*, M. A. Ali, ed. Plenum, New York.

Westfall, J. A., and C. J. P. Grimmelikhuijzen. 1993. Antho-RFamide immunoreactivity in neuronal synaptic and nonsynaptic vesicles of sea anemones. *Biol. Bull.* **185:** 109–114.

Wood, J. G., and T. L. Lentz. 1964. Histochemical localization of amines in *Hydra* and in the sea anemone. *Nature* **201:** 88–90.

Reference: *Biol. Bull.* **189**: 288–297. (December, 1995)

Isolation and Partial Characterization of the Pink and Blue Pigments of Pocilloporid and Acroporid Corals

SOPHIE G. DOVE, MISAKI TAKABAYASHI, AND OVE HOEGH-GULDBERG

School of Biological Sciences, Building A08, University of Sydney, 2006 NSW Australia

Abstract. The compounds responsible for the pink and blue colors of two families of hermatypic corals (Pocilloporidae, Acroporidae) from the southern Great Barrier Reef were isolated and biochemically characterized. Isolation of the pink pigment from *Pocillopora damicornis* (named pocilloporin, λ_{max} = 560 nm, 390 nm) revealed that it was a hydrophilic protein dimer with a native molecular weight of approximately 54 kD and subunits of 28 kD. The subunits are not linked by disulfide bonds. Attempts to dissociate the chromophore from the protein proved unsuccessful. Denaturing the protein with heat (60°C) or 5% sodium dodecyl sulfate (SDS) removed the 560-nm absorbance peak without introducing a detectable bathochromic shift. In acetone, ethanol, ether, and chloroform, the pigment precipitates out of solution, leaving a colorless supernatant. These properties suggest that the protein and chromophore are covalently linked. Ion analysis revealed that the pigment does not have metal ions chelated to it. Coral pigments were also isolated from pink morphs of other pocilloporids, *Seriatopora hystrix* (λ_{max} = 560 nm) and *Stylophora pistillata* (λ_{max} = 560 nm); and from bluish regions of the acroporids, *Acropora formosa* (blue; λ_{max} = 590 nm) and *Acropora digitifera* (purple; λ_{max} = 580 nm). With the exception of *A. formosa*, all the corals examined had pigments with the same native (54 kD) and subunit (28 kD) molecular weights as those of *P. damicornis*. *A. formosa* pigment has a native molecular weight of about 82.6 kD and three subunits of 28 kD. The pigments isolated from each of these coral species have properties similar to those described for *P. damicornis*. Isolation and biochemical purification of the pigment enabled the exploration of the function of the pink pigment. Three possibilities were eliminated. The compound does not act as (i) a photoprotectant for shielding the photosynthetic pigments of symbiotic zooxanthellae against excessive irradiances, (ii) a fluorescent coupling agent for amplifying the levels of photosynthetically active radiation available for resident zooxanthellae, or (iii) a UV-screen against the high UV levels of shallow tropical marine environments.

Received 15 November 1994; accepted 5 September 1995.

Introduction

The vivid colors of reef-building corals and other invertebrates are among the most conspicuous elements of a living coral reef. With this in mind, it is perhaps surprising that so little is known about the identity and role of color in reef-associated organisms (Czeczuga, 1983). The pigmentation of reef-building corals occurs in the skeleton of some species and in the ectodermal and endodermal tissues of others (Kawaguti, 1944; Takabayashi and Hoegh-Guldberg, 1995). The chemical identities of compounds responsible for coral color are known only in a few cases. Pigments associated with some hydrocoral and scleractinian coral skeletons have been identified as carotenoprotein complexes (Fox and Wilkie, 1970; Fox, 1972; Ronneberg *et al.*, 1979). Red and green carotenoprotein complexes are also present in askeletal cnidarians such as *Actinia equina* and *Epiactis prolifera* (Czeczuga, 1983). The blue pigment from the skeleton of the hydrocoral *Heliopora caerulea* has been identified as a calcium-bonded biliverdin, which belongs to the tetrapyrrole group of pigments (Tixier, 1945, cited in Fox and Wilkie, 1970). Among the most prominent pigments associated with the tissues of corals are the pinky-mauve pigments that are typical of the Pocilloporidae, Acroporidae, Poritidae, Fungiidae, and Meruliniidae (5 out of the 16 families of reef-building corals, Veron, 1986). Although several skeletal pigments have been purified and identified, the nature of these tissue-associated pigments in corals remains unexplored.

Tissue-based pigments have been extracted from corals in early studies using distilled water or buffer solutions

(Kawaguti, 1944; Shibata, 1969), but further purification and characterization have not been attempted. The Indo-Pacific coral *Pocillopora damicornis* from One Tree Island (southern Great Barrier Reef) shows a range of colony colors from pink to brown. In this case, the color has been identified as due to a hydrophilic compound found in the cells of the coral; the compound is inducible by visible light in the pink morph of *P. damicornis* (Takabayashi and Hoegh-Guldberg, 1995). Interestingly, the presence of this compound in pink morphs is associated with several physiological characteristics such as reduced growth rates (Takabayashi and Hoegh-Guldberg, 1995) and superior competitive abilities relative to the brown morph (Takabayashi, 1994). Despite these correlations, the exact identity and function of this pigment remain elusive.

In this study, the pink pigment from the tissues of *P. damicornis* was isolated and characterized and its function was explored. Pigment complexes were also isolated from the pink morphs of the related pocilloporids *Stylophora pistillata* and *Seriatopora hystrix*, and the blue regions of colonies of the acroporids *Acropora formosa* and *A. digitifera*. The color in all five cases is associated with a similar protein complex, which in the case of *P. damicornis* does not appear to function as a photoprotectant, UV-screening agent, or fluorescent coupling pigment.

Materials and Methods

This is the first study to purify the pigment complex associated with the pink color of *Pocillopora damicornis*. To simplify the description of this compound in the following text, the compound is referred to hereafter as "pocilloporin." Similar compounds from other species (*i.e.*, with the same molecular weight, subunit size, or both) will be referred to as "pocilloporin-like" compounds.

Purification of pocilloporin and pocilloporin-like compounds

Corals (*Pocillopora damicornis, Seriatopora hystrix, Stylophora pistillata, Acropora digitifera*, and *A. formosa*) were collected at a depth of 2 m from One Tree Island lagoon near the One Tree Island Research Station (University of Sydney) at the southern end of the Great Barrier Reef, Australia, in May 1994. Pigments were extracted by immersing coral branches in 0.06 *M* KH_2PO_4, 0.06 *M* K_2HPO_4 pH 6.65 (phosphate buffer = "raw extract"; Takabayashi and Hoegh-Guldberg, 1995) for 24 h at 4°C. Raw extracts were concentrated and partially purified by centrifugation (Centrifuge 17RS, Heraeus Sepatech) through a Centricon 30 (Amicon, molecular weight cutoff = 30 kD, time and speed determined by volume and Centricon specifications). Wavelengths of maximum absorbance (λ_{max}) and protein concentrations were determined spectrophotometrically (Pharmacia Ultrospec III and Autofill III; Whitaker and Granum, 1980).

Gel filtration. Pocilloporin (from *P. damicornis*, λ_{max} = 560 nm) and pocilloporin-like proteins (from *Seriatopora hystrix, Stylophora pistillata*, and the *Acropora* species, λ_{max} = 560–590 nm) were further purified by gel filtration on a Superose FPLC column (Pharmacia, 12 HR 10/30). The sample was eluted from the column with phosphate buffer pH 6.65 at a flow rate of 0.5 ml min^{-1} and the absorbance of the protein was monitored using a multi-wavelength detector (Model 490E; Millipore-Waters, Australia). The major peaks were collected and analyzed by polyacrylamide gel electrophoresis in the presence of sodium dodecyl sulfate (SDS-PAGE) to determine subunit molecular weights. Collected fractions were rerun through the HPLC to determine purity (symmetry and overlay of 280-nm peak and 560-nm peak) and the extinction coefficient for pocilloporin at 560 nm (see below).

SDS-PAGE gel electrophoresis. Polyacrylamide gel electrophoresis (15% running gel) in the presence of sodium dodecyl sulfate (SDS-PAGE) was performed using a modification of the method described by Laemmli (1970). In general, β-mercaptoethanol (5%) was added to all samples and the samples were boiled for 5 min prior to loading on the gel. However, to study the effects of boiling and reducing conditions on the mobility of sample subunits during electrophoresis, boiled and unboiled samples were run in the presence and absence of β-mercaptoethanol, sodium dodecyl sulfate (SDS), or both. In these experiments, and others involving SDS-PAGE, protein subunits were revealed by Coomassie blue staining (Righetti *et al.*, 1990). All gels used Biorad low molecular weight standards.

Properties of isolated compounds

Relationship between pocilloporin and co-eluting protein. To investigate whether pocilloporin was a protein, gel filtration was done on extracts of regions of two colonies of *P. damicornis* that varied in the intensity of pink color. These extracts were used to investigate the relationship between absorbance at 560 nm and co-eluting protein. The relationship between protein abundance (280-nm absorbance, Dawson *et al.*, 1986) and pigment (560-nm absorbance) was measured by relating the area of a defined 280 slice (Fig. 4A) to that of the corresponding 560 slice (Maxima 820 software; Millipore-Waters, Australia). All chromatograms were collected on the same day to minimize the effects of changes in column performance. The same start and end time points were used for delimiting chromatogram slices.

Measurement of extinction coefficient at 560 nm for pocilloporin. The extinction coefficient of pocilloporin, ϵ_{560}, was measured using Beer's law (Nobel, 1983), where the path length of the detector (Model 490E; Millipore-Waters, Australia) was 1 cm, and where the values for A_{560}

and the molar concentration (M) of pocilloporin were derived from 280-nm and 560-nm chromatograms of purified pocilloporin (Fig. 1A). The molar concentration of pocilloporin was calculated in the following manner. The amount of pocilloporin (micrograms) was calculated by converting the area of a very slim "slice" of the 280-nm chromatogram (Area A, Fig. 1A) to protein concentration, using a relationship previously determined between the total area under a 280-nm chromatogram and known amounts of protein from several different colonies of *Pocillopora damicornis* injected through the column (protein in micrograms = 8.89 × area + 0.10, r^2 = 0.95). The volume of each slice was calculated by multiplying the x-axis (time elapsed, Fig. 1A) of the slice by the flow rate (0.5 ml · min^{-1}). The resulting concentration of pocilloporin (grams per liter) was then converted into the molar concentration (M) of pocilloporin by using the native molecular weight of pocilloporin (= 54 kD, see Results). This method was used to determine the extinction coefficient because it required only relatively small amounts of protein and thus could be applied to only the purest of fractions (determined by observation of the symmetrical overlay of the 560-nm and 280-nm chromatograms).

To verify the validity of the above method, the extinction coefficient for pocilloporin at 560 nm was also determined using a more conventional technique employing two methods of measuring protein concentration (Bradford, 1976; Whitaker and Granum, 1980). Five aliquots of raw extract that had been molecular weight filtered (using Centricons) were injected into the gel filtration column, and the pocilloporin fractions collected. The collected fractions were pooled and concentrated, and the absorbances were measured at 235, 280, and 560-nm with a spectrophotometer (Pharmacia Ultraspec III).

Ion content of pocilloporin. Many chromophores include a chelated metal ion (Fox, 1979). To determine whether pocilloporin has a constituent metal ion, the ion content of pure pocilloporin was investigated. Pocilloporin was purified by gel filtration as described above. About 20 μg of protein (10 μl) was placed in 70% nitric acid (AristaR, BHD Chemicals) for 4 h at 95°C, and diluted to 3 ml of 0.7% HNO_3 with Milli-Q distilled water. Ion content was then determined by inductively coupled plasma mass spectroscopy (ICP-MS; Elan 5000, Perkin Elmer) using the total quant peak-hopping option. The blank contained 10 μl of phosphate buffer eluant from HPLC heated in 70% nitric acid (AristaR, BHD Chemicals) and diluted to 3 ml of 0.7% HNO_3 with Milli-Q distilled water.

Thermal lability of pigment compound. The pocilloporin fraction was collected as it eluted from the column. Fractions were concentrated by centrifugation through a Centricon 30. The concentrated sample was aliquoted into 25-μl proportions in 0.6-ml Eppendorf microcentrifuge tubes. Samples were then held in a water bath at temperatures of 40°, 60°, and 100°C for 10 min before being injected onto the column. A control (RT, Fig. 5) sample was injected without incubation in the water bath. Peak area was determined at both 560 nm and 280 nm, and the ratio of 560 nm to 280 nm was determined (Maxima 820 software; Millipore-Waters, Australia). In a separate experiment, pocilloporin was introduced into the (60°C) cell of a spectrophotometer, heated to 60°C, and maintained at this temperature for 10 min, during which it was scanned from 200 nm to 900 nm once every 80 s to determine changes in absorbance profile with heating (Pharmacia Ultraspec III).

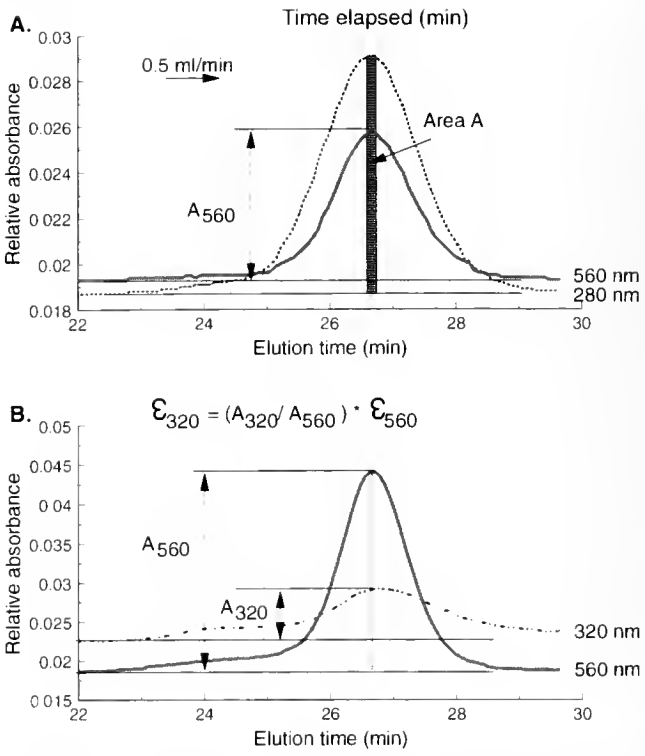

Figure 1. (A) Example of purified pocilloporin showing symmetrical overlay of 560 nm and 280 nm chromatograms and labeled parameters used in the calculation of the extinction coefficient at 560 nm. (B) Calculation of the extinction coefficient for pocilloporin at 320 nm from the extinction coefficient at 560 nm.

Solubility of pocilloporin and pocilloporin-like compounds. Ethanol, acetone, ether, and chloroform were added to separate phosphate buffer extracts (50% v/v each) of the coral tissues. Solubility was checked by looking for a precipitate in samples (1.5 ml) after vortexing and allowing samples to settle.

Effect of denaturing agents on pigment. Five percent SDS was added to phosphate buffer extract of pigment from *P. damicornis*. The raw extract, and the extract after the addition of the denaturing agent, were scanned from 200 nm to 700 nm (Pharmacia Ultraspec III) to measure any bathochromic shifts (λ_{max} shifts). Phosphate buffer extracts from all five coral species were acidified with

H_3PO_4 and neutralized with NaOH. Samples were vortexed and spun for 1 min in an Eppendorf microcentrifuge E, prior to spectrophotometric and visual examination.

The extinction coefficient and the contribution of pocilloporin to the total absorbance of Pocillopora damicornis *at 320 nm.* The extinction coefficient of pocilloporin at 320 nm (ϵ_{320}) was calculated by multiplying the ϵ_{560} for pocilloporin by the ratio of the absorbance at 320 nm to that at 560 nm for four purified samples (Fig. 1B). The greatest possible contribution of pocilloporin to the total UV absorbance (320 nm) was measured in the following manner for five pink colonies of *Pocillopora damicornis.* The total absorbance at 320 nm was measured for raw extracts after they were filtered through glass fiber filters (Millipore) to remove suspended material (no color remained on the filter). The filtered raw extracts contain both mycosporine amino acids (Matthews, 1993) and pocilloporin. The portion of the total 320-nm absorbance due to pocilloporin was calculated from the absorbance at 560 nm of the raw filtered extract multiplied by the ratio of ϵ_{320} to ϵ_{560} (only the pocilloporin fraction of raw extracts absorbs at 560 nm, Fig. 2A). This value was then expressed as a percentage of the total absorbance at 320 nm.

Fluorescent emission measurement. The fluorescent emission (between 390 and 750 nm) of pocilloporin was measured for excitation at 390 and 560 nm (both absorption maxima) with a luminescence spectrometer (LS50B, Perkin Elmer). Phosphate buffer extracts of pink (0.3 mg/ml pocilloporin by Beer's law from ϵ_{560} with A390 = 0.505) and brown (0.1 mg/ml pocilloporin with A390 = 0.519) *P. damicornis* branches, and a partially purified extract of pink branches (retentate after centrifugation through a Centricon 30; 3.7 mg/ml pocilloporin) were used for these measurements. If pocilloporin is to act as an accessory photosynthetic pigment *via* fluorescence, then the concentrations of pocilloporin used in these measurements should yield measurable fluorescence (*cf.* 0.15 μg/ml chlorophyll with A436 = 0.006 provided a detectable fluorescent response for excitement at 436 nm).

Results

Purification of pocilloporin from Pocillopora damicornis

Phosphate buffer extracts of pink and brown morphs of *P. damicornis* had similar complex 280-nm chromatograms (Fig. 2A, D). The key features of these chromatograms were as follows: (i) A peak that also absorbs at 320 nm (data not shown) eluting at 37 min (Fig. 2A, D; MAA), which corresponds to a molecular mass of about 1.3 kD. The 1.3-kD peak contained mycosporine-like amino acids (MAAs) as shown by C18 reverse phase HPLC (data not shown). Previously, MAAs have been shown to elute though gel filtration columns at times that correspond to compounds of about 1.3 kD despite having an actual molecular weight of 0.4 kD (Matthews, 1993). (ii) A void volume peak (v_o) that contains proteins of molecular mass greater than 2000 kD and absorbs slightly at 560 nm (Fig. 2A–F). (iii) A group of overlapping peaks occurring between 20 and 30 min that absorb at 280 nm (Fig. 2A, B, D, E). In this region, the pink morph of *P. damicornis* has a major 560-nm absorbing peak at 26.8 min with a small peak on the front shoulder (Fig. 2C).

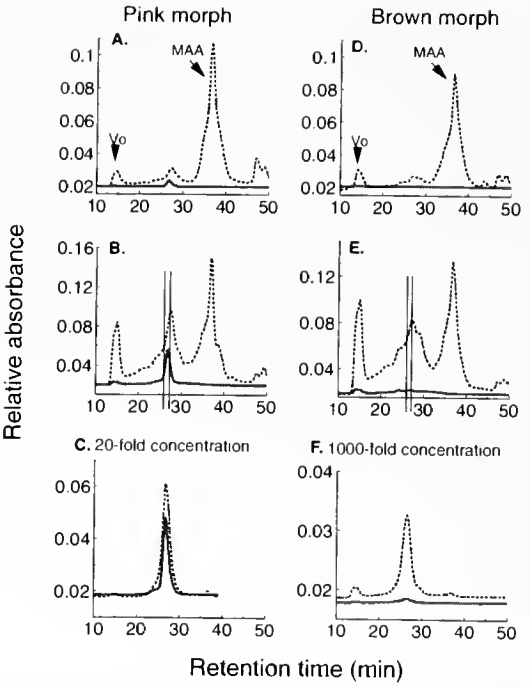

Figure 2. Comparison of the pink and brown morphs of *Pocillopora damicornis,* showing the purification steps for the 560-nm chromatogram peak (pocilloporin). (A and D) Phosphate buffer pigment extracts: V_o indicates void volume; MAA indicates UV-absorbing peak. (B and E) Retentate after centrifugation through a Centricon 30: ‖ indicates 560-nm fraction collected. (C and F) Chromatograms of fractions collected from B and E, respectively. Note concentration difference between C and F.

Centrifugation of the phosphate extract through a Centricon 30 reduced the relative quantity of UV-absorbing compound (*cf.* Fig. 2B, E with Fig. 2A, D). Further purification of the pink fraction revealed that it co-eluted with a 280-nm absorbing fraction, presumably protein with a native molecular weight of about 54 kD (Fig. 2C). Fractions collected at the same elution time (*i.e.,* corresponding to 54 kD proteins) from the brown morphs of *P. damicornis* did not show significant absorbance at 560 nm (Fig. 2F), even when concentrated 1000-fold (as opposed to 20-fold for the pink morph) from the previous step (Fig. 2E, B). Concentrating the purified fractions from the brown morph by 1000-fold resulted in an amplification of contaminating proteins (see end of next paragraph).

SDS-PAGE of pocilloporin fraction (Fig. 2C) from a pink morph of *P. damicornis* showed one major band with a molecular weight of 28 kD (Fig. 3; lanes 4, 5). Other bands that are present were due to contamination inasmuch as their appearance is dependant on the start and end time of fraction collection (*cf.* narrow collection periods shown in Fig. 3; lanes 4, 5, with broader collection period in Fig. 8 *P. damicornis;* lane 5). The presence or absence of β-mercaptoethanol or boiling or SDS did not affect the mobility of this 28-kD band (data not shown), suggesting that disulfide bonds are not involved in the linking of the subunits in the native protein. SDS-PAGE of the same gel filtration fraction taken from a brown *P. damicornis* morph (Fig. 2F) showed a very faint band at 28 kD amongst a smear of other bands with a wide molecular weight range (Fig. 3; lanes 1, 2).

Properties of pocilloporin and related compounds

Relationship between pocilloporin and co-eluting protein. The association between the absorbance at 560 nm and co-eluted protein was investigated to strengthen the conclusion that pocilloporin was a protein present in pigmented coral morphs but absent in unpigmented morphs. The 280-nm chromatograms of brown fragments of *P. damicornis* had a concave shape in the region of the maximal absorbance at 560 nm (26.8 min, Fig. 4A). The 280-nm chromatograms of pink fragments of *P. damicornis* had a convex shape in this region (Fig. 4A). The shape of these curves suggests the absence of a protein in the brown morph that is present in the pink morph of *P. damicornis.* That this protein is bound to or part of the pigmented compound is supported by the strong positive correlation

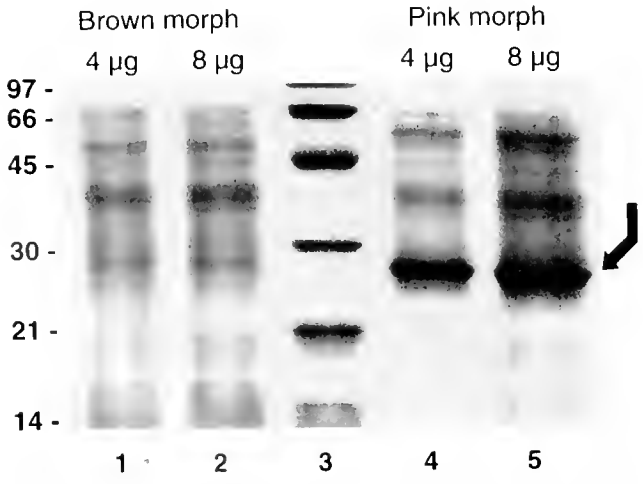

Figure 3. Fifteen percent SDS-PAGE of 560-nm fraction from pink and brown morphs of *Pocillopora damicornis:* Lane 1, 2, brown morph (4 and 8 µg, respectively); lane 3, Biorad low MW standards; lane 4, 5, pink morph (4 and 8 µg, respectively). The band corresponding to a 28-kD subunit is indicated by an arrow.

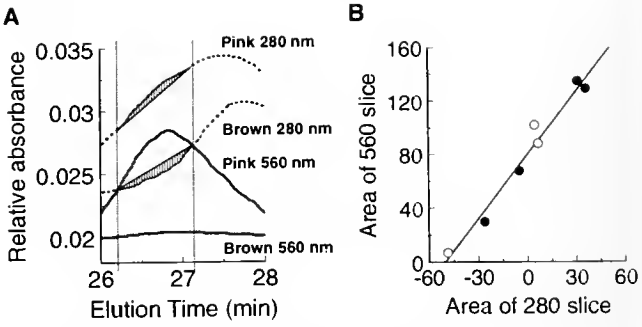

Figure 4. Relationship between absorbance at 560 nm and 280 nm. (A) Chromatograms of phosphate buffer extracts from pink and brown branches of *Pocillopora damicornis;* shaded slices show area used in 280 determination. (B) Linear relationship between area of 560 slice and area of 280 slice: $r^2 = 0.97$; (●) colony 1; (○) colony 2.

between the 560-nm absorption and 280-nm absorption (Fig. 4B; linear relation with $r^2 = 0.97$).

Extinction coefficient. The extinction coefficient (ϵ_{560}) of pocilloporin was determined directly from three independent chromatograms of purified pocilloporin (*e.g.,* Fig. 1A) and was 34059 ± 1635 cm^{-1} M^{-1} (mean ± SEM). The extinction coefficient measured using a spectrophotometer applied to purified protein from five HPLC runs was 31950 cm^{-1} M^{-1} (using the method of Whitaker and Granum, 1980, to measure protein) and 32900 cm^{-1} M^{-1} (using the method of Bradford, 1976, to measure protein). The three methods resulted in extinction coefficients for pocilloporin that were not statistically different ($P > 0.05$), hence verifying the validity of the first method.

Metal ion analysis. The association of metal ions with pocilloporin was investigated using ICP-MS. Total-quant analysis of the ion content of pocilloporin samples revealed no ions occurring at significantly greater levels than background; therefore, pocilloporin does not have an accompanying metal ion in its structure.

Thermal lability of pocilloporin. Chromatograms at 280 nm and 560 nm of pocilloporin from a broad collection around 560 nm are asymmetrical (Fig. 5A), demonstrating that the fraction (in this case) was contaminated with proteins other than pocilloporin. No changes occured to pocilloporin when it was heated to 40°C for 10 min. When heated to 60°C, 280-nm and 560-nm absorbance decreased, as did the relative amount of 560-nm absorbance to 280-nm absorbance. The decrease in the ratio of absorbance at 560 nm to 280 nm may be due to the fact that the contaminants are more thermally stable than pocilloporin. At 100°C, there was a further decrease in both 280- and 560-nm absorbances (Fig. 5A). Spectrophotometric scans of pocilloporin reveal that no bathochromic shifts accompanied the loss of 280-nm and 560-nm absorbance (Fig. 5B; note, baseline shift for sample maintained at 60°C for 10 min). Heating raw extract to 100°C changes the solution to pale yellow. This correlated

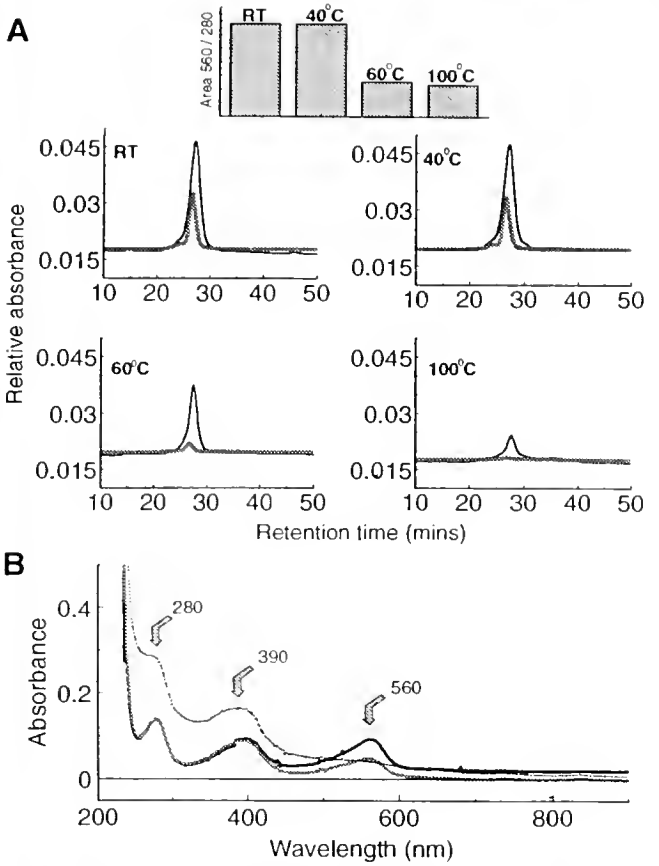

Figure 5. Thermal lability of 560-nm fraction from *Pocillopora damicornis*. RT = control chromatogram; 40°C = chromatogram after heating sample to 40°C for 10 min; 60°C = chromatogram after heating sample to 60°C for 10 min; 100°C = chromatogram after heating sample to 100°C for 10 min. (—) 280-nm, (xxxx) 560-nm chromatograms. Bar chart, showing ratio of 560-nm peak area to 280-nm peak area at each temperature. (B) Wavelength scan of pocilloporin at different temperatures: (—) cell at 25°C, (xxxx) cell at 60°C, (- - -) cell at 60°C after 10 min. Arrows indicate approximate position of λ_{max} in each case.

well with the observation that the 390-nm peak was relatively unaffected by temperature.

Solubility in solvents and the effects of denaturing agents on pigment compounds. For pink *P. damicornis*, 5% SDS gave a white pellet and a colorless supernatant with no absorbance between 360 and 700 nm. Ethanol and acetone gave a pinky-purple precipitate and a colorless supernatant. The supernatant had no peak absorbance between 360 and 700 nm, the precipitate redissolved in phosphate buffer, and the solution had peak absorbances (λ_{max}) at 560 and approximately 385 nm. Colored extracts from all coral species examined were insoluble in ethanol, acetone, ether, and chloroform. In all coral species examined, acidification (pH 4.8) or alkalization (pH 11.2) of phosphate buffer extract altered the color of solutions of pocilloporin to pale orange, with further acidification or alkalization turning solutions yellow and giving rise to a yellow precipitate.

The importance of UV-absorbance by pocilloporin. The ϵ_{320} for pocilloporin was calculated to be 14889 $\pm$ 64 cm^{-1} M^{-1} (mean $\pm$ SEM; n = 4 chromatograms). The proportion (percent) of the total absorbance at 320 nm in raw extracts that was due to pocilloporin was 1.60 $\pm$ 0.49% (mean $\pm$ SEM; n = 5).

Fluorescent emission measurement. Fluorescence (390–750 nm) was not emitted for excitation at 560 nm, from either unpurified extracts of brown and pink *P. damicornis* colonies or partially purified extracts of pocilloporin. Some fluorescence was observed for samples excited at 390 nm. Brown fragments of *P. damicornis* fluoresced at 450 nm and 480 nm. Pink fragments fluoresced only at 450 mm. The intensity of the fluorescence was, however, unrelated to the concentration of pocilloporin in the sample (pink and brown extracts with the same 390-nm absorbance fluoresced with the same intensity at 450 nm). Fluorescence, as a result of 390-nm excitation, was therefore due to compounds other than pocilloporin in raw and partially purified extracts of *P. damicornis*.

Comparison of pocilloporin-like compounds: native and subunit molecular weights within and between families

Stylophora pistillata, *Seriatopora hystrix*, *Acropora digitifera*, and *A. formosa* have 280-nm chromatograms

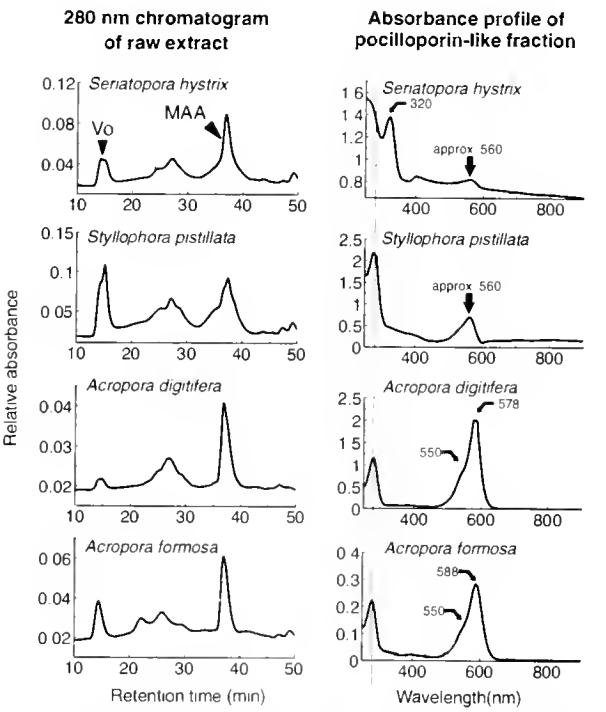

Figure 6. Chromatograms of raw phosphate buffer extracts from four different coral species at 280 nm: V_o, void volume; MAA, mycosporine-like amino acids. λ_{max} determinations of isolated pocilloporin-like compounds. Arrows indicate approximate λ_{max}. Vertical dotted line indicates position of 280-nm absorbance.

similar to those of *Pocillopora damicornis*. All five species have a peak related to the presence of mycosporine-like amino acids that elutes at about 37 min (MAA, Fig. 6), a group of peaks that elute between 20 and 30 min, and a void volume peak that elutes at approximately 14 min (V_o, Fig. 6). *S. hystrix* and *S. pistillata* had λ_{max} about equal to 560 nm (Fig. 6). *A. formosa* had λ_{max} about equal to 578 nm and a shoulder at about 550 nm (Fig. 6). In the blue *Acropora* species, *A. formosa*, there is a shift in the native molecular weight (MW) of the pigment from 54 kD (native MW of *P. damicornis*, *S. hystrix*, *S. pistillata*, and *Acropora digitifera*) to 82.6 kD (*cf.* peak position relative to dotted line, Fig. 7). However, in all coral species examined, SDS-PAGE of corresponding gel filtration fractions showed a single band with a subunit molecular weight of about 28 kD (Fig. 8, data not shown for *A. digitifera*). The front shoulder fractions, which absorb minimally at λ = max (560–590) nm and variably at 400 nm (Fig. 7), show a more complex banding pattern that contains both the 28-kD subunit and a 40-kD subunit amongst a smear of other bands (Fig. 8: *S. pistillata*, lane 1; *P. damicornis*, lane 1; *S. hystrix*, lane 5). Gel filtration chromatograms suggest that compounds absorbing at about 400 nm are more closely associated with a peak whose approximate molecular weight is 112 kD than with the pocilloporin or pocilloporin-like compound peak (Fig. 7).

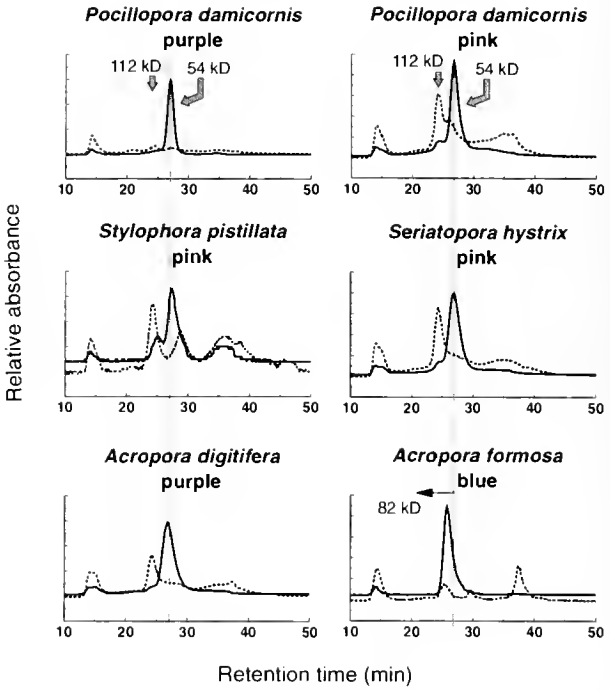

Figure 7. 400-nm (- - -) and 560-nm (—) chromatograms from Centricon 10 (Amicon) centrifuged phosphate buffer extracts from *Pocillopora damicornis*, *Stylophora pistillata*, *Seriatopora hystrix*, *Acropora digitifera*, and *A. formosa*. Dotted line shows approximate position of 54-kD eluting protein.

Discussion

The colors that typify many members of the animal kingdom have a variety of roles that range from crypsis to courtship (McFall-Ngai, 1990; Dawkins and Guilford, 1993). Although the role of color has been explored extensively in some groups (*e.g.*, insects: Endler, 1981; birds: Owen, 1980; fish: Neal, 1993), an understanding of the function of color in others is lacking. Reef-building corals fall into the latter category. This study is the first attempt to isolate and biochemically characterize the compounds responsible for the pink and blue colors of two prominent families of reef-building corals (Pocilloporidae, Acroporidae). Once the protein dimer from *Pocillopora damicornis* (pocilloporin) had been isolated and characterized, its function was explored, and several functions suggested by early studies were solidly rejected.

Biochemical structure of pocilloporin

SDS-polyacrylamide gel electrophoresis and gel filtration of pocilloporin and pocilloporin-like compounds suggest that the pigments from *Pocillopora damicornis*, *Seriatopora hystrix*, *Stylophora pistillata*, and *Acropora digitifera* are protein dimers with native molecular weights of about 54 kD and subunits of 28 kD (Figs. 1–3, 7, 8). The pigment from the blue regions of *A. formosa* is a trimer with a native molecular weight of about 82.6 kD and subunits of 28 kD (Figs. 7, 8). The subunits in the case of *P. damicornis* are not linked by disulfide bonds in the native protein.

All evidence supports the existence of a strong stoichiometric link between the protein and chromophore in pocilloporin. The nature of that link can be explained in several ways. That is, the absorbance at 560 nm could be due to (i) a non-protein compound that is coincidentally eluting with a same-sized protein without any chemical bonding between them; (ii) a chromophore that is non-covalently bonded with a protein to form a chromophore-protein complex, and (iii) a chromophore covalently bonded to the protein.

The first option can be eliminated by the strong correlation between the absorption at 560 nm and the concentration of co-eluting 54-kD protein from colonies differing in the expression of the pink pigment (Fig. 4). In other words, the more of the particular protein there is, the greater the absorbance at 560 nm. Furthermore, a 28-kD subunit existed in significant amounts only in the fractions with a high absorbance at 560 nm and not in fractions that had no absorbance at 560 nm (*e.g.*, extracts of brown colonies, Fig. 3). The second option, that the chromophore is non-covalently linked to the protein, is questionable on the grounds that the chromophore is not easily separated from the protein.

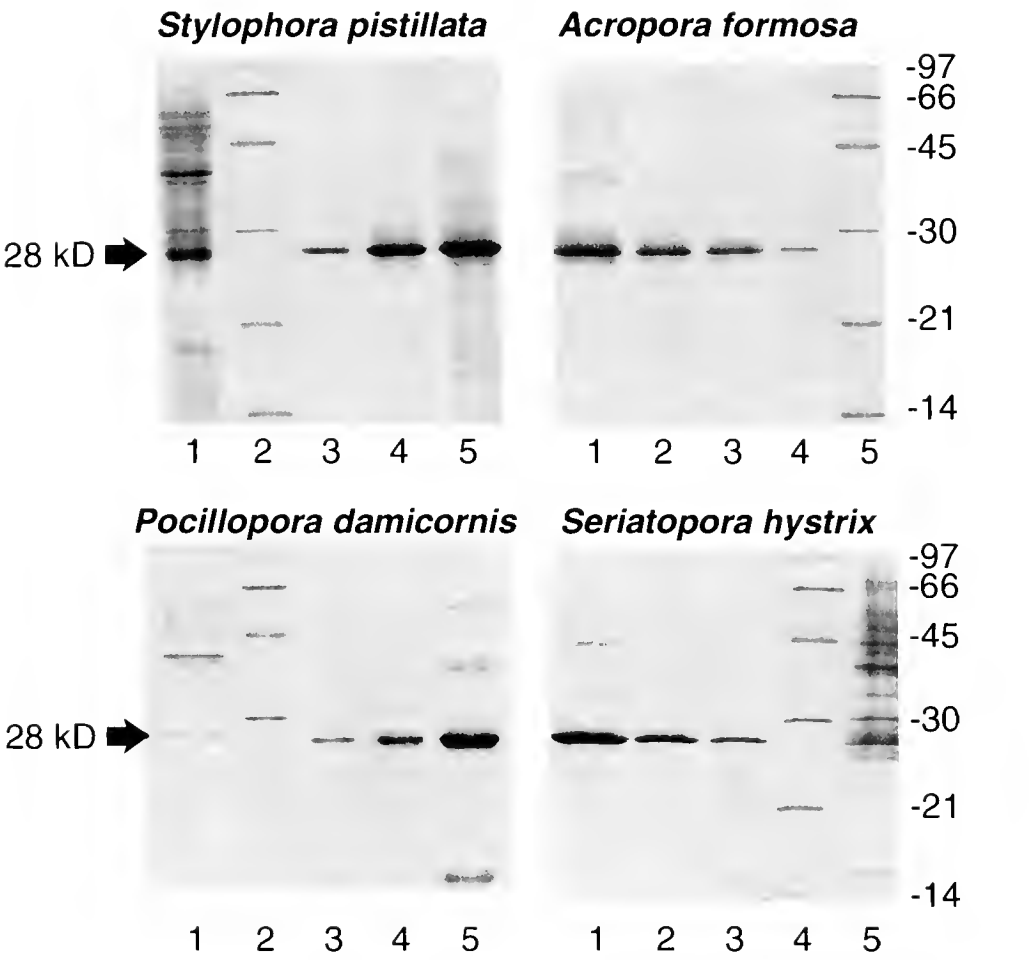

Figure 8. Fifteen percent SDS-PAGE of isolated pigment (pink or blue) fractions from different coral species. *Stylophora pistillata:* lane 1, front shoulder of 560-nm peak (8 μg); lane 2, Standards; lanes 3–5, main 560-nm fraction with 2, 4, 8 μg, respectively. *Acropora formosa:* lanes 1–4 main 580-nm fraction with 8, 6, 4, 2 μg, respectively. *Pocillopora damicornis:* lane 1, front shoulder of 560 peak (4 μg); lane 2, Standards; lanes 3–5, main 560-nm fraction with 2, 4, 6 μg, respectively. *Seriatopora hystrix:* lanes 1–3, main 560-nm fraction with 6, 4, 2 μg, respectively; lane 3, Standards; lane 5, front shoulder of 560-nm peak (8 μg).

Treatments such as 5% SDS, heat, and relatively nonpolar solvents such as acetone liberate carotenoids and other chromophores from their conjugate proteins, resulting in bathochromic shifts in the absorbance of the pigment whilst the protein either denatures (5% SDS, heat) or precipitates out of nonpolar solvents (Cheeseman *et al.*, 1967; Fox, 1979; Milicua *et al.*, 1985; Garate *et al.*, 1986; Zagalsky *et al.*, 1989; Zagalsky *et al.*, 1991). No such reaction was found with pocilloporin or the pocilloporin-like compounds of this study. Treatments with these agents simply resulted in precipitation of the pigment complex from solution.

Pocilloporin-like compounds from the Pocilloporidae and Acroporidae

Several other biochemical properties of pocilloporin and pocilloporin-like compounds were identified in this study. The compounds were hydrophilic, in agreement with the work of Kawaguti (1944) and Shibata (1969), who both extracted similar coral pigments in water. It is curious, however, that Shibata (1969) did not find an absorption peak at 560 nm in the water extracts of *Pocillopora* sp.; the main absorbance peak found in that study was at 480 nm. However, Shibata did not classify the species of *Pocillopora* he used, and his description of the morph as red rather than pink suggests that it may have been a differently pigmented form than the ones used in the present study. Shibata (1969) also described pigments from *Acropora* sp. as having absorbance peaks at 560 nm and 590 nm. Our results for two species of *Acropora* are similar: *A. digitifera* had a λ_{max} at 578 nm and a shoulder at 550 nm. Similarly, *A. formosa* had a λ_{max} at 588 nm and a shoulder at 550 nm (Fig. 6).

The present study did not determine the biochemical pigment group to which the proteins pocilloporin and pocilloporin-like compounds belong; however, some options seem unlikely. No metal ions were found associated with pocilloporin, thus eliminating it from the group of metal-bearing biochromes such as the colored copper proteins and metal-chelated tetrapyrroles (Fox, 1979). The absence of metal ions cannot be attributed to inadequate sample size. Assuming 1 metal ion per protein molecule, we would expect readings in the range of parts per million for the amount of protein introduced into the ICP-MS. This amount is well above the detection capabilities of the ICP-MS, which can measure ion concentrations down to the range of parts per billion (Henshaw *et al.*, 1989). The absorbance of pocilloporin at 560 nm is significantly reduced by short (10-min) exposures to 60°C without any accompanying bathochromic shift (Fig. 5). This extreme thermal sensitivity suggests that this absorbance is not due to more thermally stable compounds such as carotenoids (*e.g.*, those that retain absorbance even when heated at temperatures up to 120°C for 1 h, Lee *et al.*, 1987, 1990). Pocilloporin, therefore, does not appear to involve a carotenoid component and is probably not a carotenoprotein.

Why be pigmented? Possible roles of pocilloporin

Investigation of the biochemical characteristics of pocilloporin did not reveal its function. However, several possible functions are firmly rejected and a narrow range of possibilities remains. The following hypotheses about the function of pocilloporin are rejected.

Pocilloporin as a photoprotectant. In his seminal study of coral color, Kawaguti (1944) proposed that pigments may shade zooxanthellae from excessive sunlight that might otherwise lead to photobleaching of constituent photosynthetic pigments. The results of the present study are counter to this idea. The absorption spectrum of pocilloporin suggested that it did not protect against photobleaching of the major photosynthetic pigments because its absorbance spectrum does not coincide with those of chlorophyll *a* and *c* (Nobel, 1983; Kirk, 1994) and is, if anything, curiously complementary to these compounds. Thus, a role for pocilloporin as a photoprotectant for the photosynthetic pigments of the zooxanthellae is unlikely.

Pocilloporin as an accessory photosynthetic pigment. If pocilloporin were an accessory photosynthetic pigment, the energy absorbed by it would have to be transferred to the photosystems in the zooxanthellae to be used for photosynthesis. This transfer could occur in two ways. The first way is by the direct energy transfer (resonance energy transfer). In this case, light energy absorbed by one molecule is passed to the reaction centers in the photosystems through a chain of energy transfers between closely adjacent molecules (Nobel, 1983). This could happen only if pocilloporin were in proximity to the photosystems. However, most (if not all) of the pocilloporin is associated with the coral tissues (Takabayashi and Hoegh-Guldberg, 1995) and not with the zooxanthellae. Consequently, the direct transfer of excitation energy by resonance transfer from pocilloporin to photosystems is impossible. A second method of energy transfer is through fluorescent coupling. In this case, pocilloporin might absorb light at non-photosynthetic wavelengths and re-fluoresce them at wavelengths suitable for absorption by the primary photosynthetic pigments (Kawaguti, 1944; Schlichter *et al.*, 1988). This type of transfer has been proposed for pigments associated with the animal tissues of the deep-water coral *Leptoseris fragilis*, which transforms short-wavelength, non-photosynthetically active radiation into longer wavelength, photosynthetically active radiation, which is reabsorbed by the photosynthetic pigments of the symbiotic dinoflagellates (Schlichter and Fricke, 1991). This indirect means of energy transfer is, however, unlikely for pocilloporin, which is not fluorescent for excitation at either of its λ_{max}.

Pocilloporin as a UV-screening pigment. The last possibility is that pocilloporin might have UV-absorbing capabilities in addition to its ability to absorb visible light. This is also unlikely because the absorbance of pocilloporin within the UV region of light was minimal (1.6% of the total absorbance of raw extracts at 320 nm). Compounds such as the mycosporine-like amino acids that are abundant in corals are far more potent UV-B-screening agents (Dunlap and Chalker, 1986), a fact that is clear from the comparison of the ϵ_{320} of pocilloporin (14,889 $cm^{-1} M^{-1}$) with the ϵ_{320} of a typical mycosporine-like amino acid (*e.g.*, ϵ_{320} of palythine = 36,200 $cm^{-1} M^{-1}$, Dunlap and Chalker, 1986). These MAAs, especially palythine (λ_{max} = 320 nm), are probably responsible for more than 95% of the absorption by the coral at 320 nm (Dunlap and Chalker, 1986; Dunlap *et al.*, 1988).

The role of pocilloporin remains elusive. Pocilloporin may act as an agent that enhances the abilities of the pigmented morph to resist fouling or predation or to compete successfully (Lang, 1971, 1973; Sheppard, 1979, 1982). It is interesting to note that Rinkevich and Loya (1983) reported the purple morph of *Stylophora pistillata* from the Red Sea to be competitively superior to the yellow morph of the same species, even when they were not touching. Takabayashi (1994) found a similar trend in the competitive abilities of the pink morph of *Pocillopora damicornis*. In this case, the pink morph won significantly more of the contests between pink and brown colonies in grafting experiments, and a distinct pink band was often observed in the tissue of pink colonies at the contact sites between nonsimilar colonies. Pocilloporin, therefore, might function in the coral's immunological and chemical defense systems.

Acknowledgments

The authors thank Dr. Tariq Khan for help with the fluorospectroscopy, and P. Snitch at Royal Prince Alfred Hospital (Sydney) for access to the ICP-MS. This study was supported by an Australian Postgraduate Research Scholarship to SD and a grant from the Great Barrier Reef Marine Park Authority (ENCORE program) and Australian Research Council to OHG. This is publication #6 in the ENCORE series.

Literature Cited

Bradford, M. M. 1976. A rapid and sensitive method for the quantification of microgram quantities of protein utilizing the principle of protein-dye binding. *Anal. Biochem.* **72:** 248–254.

Czeczuga, B. 1983. Investigations of carotenoprotein complexes in animals—VI. *Anemonia sulcata*, the representative of askeletal corals. *Comp. Biochem. Physiol.* **75B:** 181–183.

Cheeseman, D. F., W. L. Lee, and P. F. Zagalsky. 1967. Carotenoproteins in invertebrates. *Biol. Review* **42:** 131–160.

Dawkins, M. S., and J. Guilford. 1993. Color and pattern in relation to sexual and agressive behaviour in the bluehead wrasse—*Thalassoma bifasciatum*. *Behav. Processes* **30(3):** 245–252.

Dawson, R. M., D. C. Elliott, W. H. Elliott, and K. M. Jones. 1986. *Data for Biochemical Research.* Oxford Science Publications, Oxford, 544 pp.

Dunlap, W. C., and B. E. Chalker. 1986. Identification and quantitation of near-uv absorbing compounds (S-320) in a hermatypic scleractinian. *Coral Reefs* **5:** 155–159.

Dunlap, W. C., B. E. Chalker, and J. K. Oliver. 1988. Bathymetric adaptation of reef-building corals at Davies Reef, Great Barrier Reef, Australia. III. UV-B absorbing agents derived from tropical marine organisms of the Great Barrier Reef, Australia. *Proc. 6th Int Coral Reef Symp.* **3:** 89–93.

Endler, J. A. 1981. Progressive background matching in morphs, and a quantitative measure of crypsis. *Biol. J. Linn. Soc.* **22:** 187–231.

Fox, D. L. 1972. Pigmented calcareous skeletons of some corals. *Comp. Biochem. Physiol.* **43B:** 919–927.

Fox, D. L. 1979. *Biochromy.* University of California Press, Berkeley.

Fox, D. L., and D. W. Wilkie. 1970. Somatic and skeletally fixed carotenoids of the purple hydrocoral, *Allopora californica*. *Comp. Biochem. Physiol* **36:** 49–60.

Garate, A. M., J. C. G. Milicua, R. Gomez, and J. M. Macarulla. 1986. Purification and characterization of the blue carotenoprotein from the carapace of the crayfish *Procambarus clarkii* (Girard). *Biochim. Biophys. Acta* **881:** 446–455.

Henshaw, J. M., E. M. Heithmar, and T. A. Hinners. 1989. Inductively coupled plasma mass spectrometric determination of trace metals in surface waters subject to acidic deposition. *Anal. Chem.* **61:** 335–342.

Kawaguti, S. 1944. On the physiology of reef corals VI. Study on the pigments. *Palao Trop. Biol. Stn. Stud.* **2:** 617–673.

Kirk, J. T. O. 1994. *Light and Photosynthesis in Aquatic Ecosystems.* 2nd Ed. Cambridge University Press, Cambridge.

Laemmli, U. K. 1970. Cleavage of structural proteins during the assembly of the head of bacteriophage T4. *Nature* **227:** 680–685.

Lang, J. 1971. Interspecific aggression by scleractinian corals. 1. The rediscovery of *Scolymia cubensis* (Milne Edwards and Haime). *Bull. Mar. Sci.* **21:** 952–959.

Lang, J. 1973. Interspecific aggression by scleractinian corals. 2. Why the race is not only to the swift. *Bull. Mar. Sci.* **23:** 260–279.

Lee, K. H., S. H. Song, and I. H. Jeong. 1987. Quality changes of dried lavers during processing and storage. 2. Quality stability of roasted lavers during processing and storage. *Bull. Korean Fish. Soc.* **20:** 520–528.

Lee, K. H., J. H. Ryuk, I. H. Jeong, and W. J. Jung. 1990. Quality changes of dried lavers during processing and storage. 3. Changes in pigments, trypsin indigestible substrates (TIS) and dietary fiber content during roasting and storage. *Bull. Korean Fish. Soc.* **23:** 280–288.

Matthews, S. 1993. *The Dynamics of Metabolite Transfer from Symbionts of the Coral* Pocillopora damicornis. Honours Thesis, University of Sydney.

McFall-Ngai, M. J. 1990. Crypsis in the pelagic environment. *Am. Zool.* **30:** 175–188.

Milicua, J. C. G., R. Gomez, A. M. Garate, and J. M. Macarulla. 1985. A red carotenoprotein from the carapace of the crayfish, *Procambarus clarkii*. *Comp. Biochem. Physiol.* **81B:** 1023–1025.

Neal, T. J. 1993. A test of the function of juvenile color patterns in the pomacentrid fish *Hypsypops rubicundus* (Teleostei: Pomacentridae) *Pac. Sci.* **47**(3): 240–247.

Nobel, P. S. 1983. *Biophysical Plant Physiology and Ecology.* W. H. Freeman and Co., San Francisco.

Owen, D. 1980. *Camouflage and Mimicry.* The University of Chicago Press, Chicago.

Rønneberg, H., D. L. Fox, and S. Liaaen-Jensen. 1979. Animal carotenoids—carotenoproteins from hydrocorals. *Comp. Biochem. Physiol.* **64B:** 407–408.

Righetti, P. G., E. Gianazza, C. Gelphi, and M. Chiari. 1990. Isoelectric focusing. Pp. 141–405 in *Gel Electrophoresis of Proteins—a Practical Approach* B. D. Hames and D. Rickwood, eds. Oxford University Press, Oxford.

Rinkevich, B., and Y. Loya. 1983. Short term fate of photosynthetic products in a hermatypic coral. *J. Exp. Mar. Biol. Ecol.* **73:** 175–184.

Schlichter, D., H. W. Fricke, and W. Weber. 1988. Evidence for PAR-enhancement by reflection, scattering and fluorescence in the symbiotic deep water coral *Leptoseris fragilis* (PAR = Photosynthetically Active Radiation). *Endocytol. C. Res.* **5:** 83–94.

Schlichter, D., and H. W. Fricke. 1991. Mechanisms of amplification of photosynthetically active radiation in the symbiotic deep-water coral *Leptoseris fragilis*. *Hydrobiologia* **216/217:** 389–394.

Sheppard, C. R. C. 1979. Interspecific aggression between reef corals with reference to their distribution. *Mar. Ecol. Prog. Ser.* **1:** 237–247.

Sheppard, C. R. C. 1982. Coral populations on reef slopes and their major controls. *Mar. Ecol. Prog. Ser.* **7:** 83–115.

Shibata, K. 1969. Pigment and a uv-absorbing substance in corals and a blue-green alga living in the Great Barrier Reef. *Plant Cell Physiol.* **10:** 325–335.

Takabayashi, M. 1994. *Intraspecific Variability in the Reef-Building Coral,* Pocillopora damicornis. Honours Thesis, University of Sydney.

Takabayashi, M., and O. Hoegh-Guldberg. 1995. The ecological and physiological differences between two color morphs of the coral *Pocillopora damicornis*. (*Mar. Biol.*, in press).

Whitaker, J. R., and P. E. Granum. 1980. An absolute method for protein determination based on difference in absorbance at 235 and 280 nm. *Anal. Biochem.* **109:** 156–159.

Veron, J. E. N. 1986. *Corals of Australia and The Indo-Pacific.* Angus and Robertson Publishers, Sydney.

Zagalsky, P. F., F. Haxo, S. Hertzberg, and S. Liaaen-Jensen. 1989. Studies on a blue carotenoprotein, linckiacyanin, isolated from the starfish *Linckia laevigata* (*Echinodermata: Asteroidea*). *Comp. Biochem. Physiol.* **93B:** 339–353.

Zagalsky, P. F., E. E. Eliopoulos, and J. B. C. Findlay. 1991. The lobster carapace carotenoprotein, alpha-crustacyanin. A possible role for tryptophan in the bathochromic spectral shift of protein-bound astaxantin. *Biochem. J.* **274:** 79–83.

Reference: *Biol. Bull.* 189: 298–307. (December, 1995)

Bleaching Patterns of Four Species of Caribbean Reef Corals

W. K. FITT AND M. E. WARNER

Institute of Ecology, University of Georgia, Athens, Georgia 30602

Abstract. Bleaching of reef corals, involving loss of symbiotic algae (= zooxanthellae), loss of algal pigments, or both, has been linked to temperature stress. In this study the effects of high temperature and light on zooxanthellae living in the Caribbean reef corals *Montastrea annularis, M. cavernosa, Agaricia agaricites,* and *A. lamarcki* were studied. Pieces of coral colonies were incubated at ambient seawater temperature (26° ± 1°C), and at 30°, 32°, and 34°C. Symbiotic algae from *M. annularis,* a species of coral from the forereef that commonly bleaches, showed the following sequence of events when exposed to natural light at 32°C: loss of photosynthetic potential measured as fluorescence yield, corresponding reduction of both oxygen production per zooxanthella and P:R (photosynthesis:respiration) ratio, and subsequent reduction in density of algae in relation to surface area of the coral. These parameters were not significantly reduced and no deaths occurred for *M. annularis* or any other coral species maintained at 26° or 30°C. However, the sequence of events was condensed to less than 24 h when *M. annularis* was subjected to 34°C seawater, except that there was little if any reduction in algal density before tissue-sloughing and death occurred between 10 and 24 h. Loss of significant amounts of chlorophyll *a* per alga was not evident for any corals except those maintained at 34°C longer than 10 h. In contrast, symbiotic algae in *M. cavernosa,* a species that rarely bleaches in nature, showed only slight reductions in photosynthesis and fluorescence yield, and no significant loss of algal cells or chlorophyll *a*, when maintained in seawater at 32°C for 2 days. Thus zooxanthellae in *M. cavernosa* appeared to be less affected by sublethal high-temperature stress. Similar contrasting patterns of bleaching were seen in zooxanthellae from the plating coral *Agaricia lamarcki,* which often bleaches during the late summer and fall, compared with zooxanthellae from *A. agaricites,* a coral which bleaches less frequently. In addition, *M. annularis* exposed to sublethal high temperatures and ambient light bleached faster than those kept in dimmer light, supporting past field observations suggesting that light energy is an important component of bleaching in nature. When *M. annularis* was exposed to different wavelengths of natural light at 32°C, the fluorescence yield declined more quickly in the presence of higher energy UV-A and blue light than with other photosynthetically active radiation. Natural levels of UV-B had little effect in this study. These data suggest that the patterns of bleaching seen in nature may be at least partially explained by different tolerances of the symbiotic algae in the corals, and that light plays a significant role in bleaching.

Received 6 December 1994; accepted 14 September 1995.

Introduction

Two major ecological events during the last decade focused the attention of coral reef researchers on the susceptibility of corals and associated reef organisms to the potentially devastating effects of elevated seawater temperatures. The first was the 1982–1983 El Niño Southern Oscillation (ENSO), during which many hard and soft corals from the Great Barrier Reef, the Central Pacific, and eventually the Eastern Pacific bleached as seawater temperatures rose 2°–6°C above normal (Glynn, 1983, 1984; Oliver, 1985; Harriot, 1985; Fisk and Done, 1985; Coffroth *et al.*, 1990; Glynn and D'Croz, 1990). Subsequent coral death was common: up to 97% of the species harboring symbiotic algae were reported dead on some reefs (Glynn and D'Croz, 1990).

The Caribbean-wide "bleaching event" of 1987 again drew attention to warm-water stress in the marine environment, this time coupled with concerns that global warming might be one of the causes (Williams and Williams, 1988). Though bleaching was extensive, total loss

of zooxanthellae from coral tissues was rare, as was death of entire coral colonies (see references in Fitt *et al.*, 1993; Porter and Meier, 1992). Most bleached corals recovered their normal coloration within a year (Szmant and Gassman, 1990; Fitt *et al.*, 1993). The results of both of these events are consistent with the notion that corals and other associated invertebrates are living close to their physiological upper thermal limits during summer months, so that even the smallest increase in seawater temperature may have an effect if the exposure time is long enough (Coles *et al.*, 1976).

Virtually all studies of bleaching support the supposition that summertime bleaching is at least partially linked to the high temperatures (*e.g.*, Yonge and Nichols, 1931a; Jokiel and Coles, 1977; Jaap, 1979; Glynn, 1984; Lasker *et al.*, 1984; Hoegh-Guldberg and Smith, 1989; Glynn and D'Croz, 1991; Gates *et al.*, 1992; Jokiel and Coles, 1990; Fitt *et al.*, 1993). Two of the best examples of the role of temperature involve laboratory experiments, one simulating El Niño conditions in the Eastern Pacific (Glynn and D'Croz, 1990) and the other mimicking the effects of the thermal discharge system of a power generator in Hawaii (Jokiel and Coles, 1977). Both studies clearly showed the immediate, adverse effects on corals of abnormally high temperatures (≥32°C), as well as more subtle bleaching during long-term exposure to temperatures only 1°–2°C above normal ambient (*e.g.*, 30°C).

The relative importance of other environmental factors on bleaching is more contentious. Low salinity and high levels of natural light sometimes show synergistic effects in connection with high temperatures near the limits of tolerance for corals (Coles and Jokiel, 1978; *cf.* Hoegh-Guldberg and Smith, 1989). In addition, high doses of ultraviolet light induce bleaching without increased temperature (Jokiel, 1980; Gleason and Wellington, 1993). Although the role of light in bleaching is interesting, little is currently known about the role of light quantity and quality, especially in relation to photosynthetic action spectra of the symbiotic algae. For instance, UV-B blocking compounds have been described and characterized (Dunlap and Chalker, 1986), and show the expected decrease in concentrations with depth (Dunlap *et al.*, 1988). However, protection by these compounds from UV-A light (*ca.* 320–400 nm) is generally limited at wavelengths greater than 350 nm, where photosynthetic pigments in zooxanthellae begin absorbing light (Jeffrey and Haxo, 1968; Dunlap *et al.*, 1988). This leaves the coral and symbiotic algae exposed to longer UV-A wavelengths and blue light (*ca.* 400–450) (Dunlap *et al.*, 1988), as well as to other photosynthetically active radiation (PAR).

One of the most perplexing aspects of coral bleaching is that some species seem to lose color frequently and quickly during bleaching events, whereas others never seem to bleach. For instance, the Caribbean reef-building coral *Montastrea anularris* is one of the first species to appear discolored during bleaching events, whereas *M. cavernosa* rarely bleaches (Jaap, 1979, 1985). Although differential tolerance of host tissue to environmental stress may explain these patterns, it is also possible that different species or types of zooxanthellae (see Trench, 1993) exhibit different tolerances to temperature and light (*cf.* Fitt, 1985).

One explanation proposed for high-temperature bleaching is that the host digestive cells detach from the mesoglea, carrying zooxanthellae out of the coelenteron, in a fashion seen in cnidarians exposed to cold water stress (Gates *et al.*, 1992). Other investigators have found that cultured zooxanthellae placed in temperatures equal to or higher than 32°C show decreased photosynthetic efficiency (Iglesias-Prieto *et al.*, 1992); this observation suggests that the algae, and not just the host, are responsible for the breakdown of the symbiosis during bleaching. There is still no consensus as to which of the symbiotic partners is more affected by high temperature. In this study we address some of these issues by documenting the sequence of events occurring in zooxanthellae living symbiotically with four species of Caribbean reef corals, and show that both light quantity and quality can be important environmental factors in bleaching.

Materials and Methods

Collection and maintenance of animals

Intact colonies of the reef corals *Agaricia agaricites*, *A. lamarcki*, *Montastrea annularis*, and *M. cavernosa* were collected from a depth of 14–16 m on the forereef off the Discovery Bay Marine Laboratory in Jamaica in the early morning (0700–0800) in February and March of 1993 and 1994. Within 1 h of collection each colony was broken into eight pieces, each with a surface area of 5–10 cm^2, and placed into one of four water-jacketed acrylic incubation chambers containing about 3.5 l of seawater. The clear plastic chambers were exposed to ambient light; their open tops were covered with three layers of screen to reduce the maximum light intensities to slightly less those found at 14–16 m on the reef. Light intensities at noon on a cloudless day on the reef at 15 m were measured on three occasions and ranged between 500–600 $\mu E\ m^{-2}s^{-1}$, maximum intensities measured in the chambers under the screen were 400–475 $\mu E\ m^{-2}s^{-1}$. During the experiments, fresh unfiltered seawater flowed into the chambers at *ca.* 150 m min^{-1} and vigorous aeration from aquarium pumps and air stones kept the water well mixed. Ambient seawater temperatures were 26.0° ± 1.0°C. Coral pieces were allowed to equilibrate in the chambers for 5–15 min at ambient temperature before the start of each experiment. Under ambient temperature and light, control

pieces maintained in chambers showed no adverse or visible effects for at least 4 days.

Experimental protocol

Coral pieces were placed in one of four chambers, each starting out at ambient seawater temperature (26.0°C ± 1.0°C). In three of the chambers, aquarium heaters were used to raise the temperature over a period of about 1 h. Temperatures were kept at 30°, 32°, and 34°C ± 0.5°C. A minimum of four replicate colonies were tested from each species. At least two pieces of each replicate colony were placed into each of the four chambers so that samples could be taken at different times. Coral pieces maintained at 26°, 30°, and 32°C were processed at about 24 and 48 h. Coral pieces exposed to 34°C were sampled 3–5 times during the first 24-h period. Pieces of coral were processed for physiological testing and biomass determinations as detailed below.

Light quality and quantity experiments

Pieces of six replicate heads of *M. annularis* used in experiments testing the effects of light quality and quantity were collected from a patch reef (1–2 m deep) off Key Largo, Florida. Coral pieces were placed in glass petri dishes in a 32°C temperature bath with aeration, where the seawater was changed at least every 4 h throughout the experiment. The quality and quantity of natural ambient light were adjusted with screens and glass cut-off filters (Melles Girot). Corals were exposed to one of the following conditions: natural light with no filters, natural light without UV-B (>320 nm), natural light without UV-A and B (>395 nm), or natural light without UV or blue light (>495 nm). Two layers of window screen covered the entire waterbath to reduce the maximum exposure level to slightly lower than that found *in situ* (<700 μE $m^{-2}s^{-1}$). Some coral pieces (control) were maintained under two layers of window screen without filters, but at 26°C.

Physiological testing and biomass determinations

Coral tissue and zooxanthellae were removed from the coral skeleton with a Water-Pik and subsamples of the homogenate taken for zooxanthellae counts and chlorophyll *a* determinations. The remaining homogenate was filtered through three layers of cheesecloth and centrifuged at 1500 × *g* for 3 min. The pellet was resuspended and washed (recentrifuged) with fresh filtered (0.45 μm) seawater (FSW) at least three times, or until few animal fragments were seen amongst the zooxanthellae in microscopic observations.

Cleaned zooxanthellae were resuspended in FSW at densities between 0.5 and 1.0 × 10^6 zooxanthellae per milliliter. Respiration rates in the dark and photosynthetic rates at 450 μE $m^{-2}s^{-1}$ (above saturation) were determined with a YSI oxygen meter equipped with low-volume (2–10 ml) chambers and magnetic stirrers. Respiration and net photosynthesis rates were added together to give gross photosynthesis rates and standardized to number of zooxanthellae. Gross photosynthesis:respiration (P:R) ratios were calculated from these rates.

Chlorophyll fluorescence of zooxanthellae suspensions was measured with a Turner fluorometer, after a 10-min incubation in darkness. The ratio of fluorescence obtained with additions of DCMU (10^{-5} *M*) in relation to that without DCMU was calculated. Long-term kinetics of chlorophyll fluorescence of zooxanthellae living within the host were recorded with a pulse amplitude modulation fluorometer (model PAM 101, 103; Waltz). The corals were dark-adapted for 10 min under the fiber optic bundle of the fluorometer prior to measurement. The initial fluorescence (Fo) was measured by exposing the coral to a weak pulse of red light (<1 μE m^2s^{-1}). Maximum fluorescence (Fm) was then determined by applying a 1-s pulse of intense white light (>500 μE m^2 s^{-1}). The maximum variable fluorescence was calculated as Fv = Fm − Fo. The value Fv/Fm is used to indicate the photosynthetic efficiency and is proportional to the quantum yield.

Chlorophyll *a* was extracted with acetone by the method of Jeffrey and Humphrey (1975). Total chlorophyll *a* was calculated from absorbance at 663 and 630 nm and standardized per algal cell extracted.

Zooxanthellae densities were calculated from the total number of zooxanthellae and the surface area of the coral. Number of zooxanthellae was determined from replicate (8–10) hemacytometer counts. Surface area was determined by covering the surface of the coral with aluminum foil, weighing the foil, and applying a standard curve relating aluminum weight to area.

Results

High-temperature stress in ambient light

The response of corals and their symbiotic algae to high-temperature stress varied with species of coral, but followed a similar pattern (Figs. 1–4). The pattern is best illustrated with *Montastrea annularis* maintained at 32°C: photosynthetic rates and potential (fluorescence ratio F^{+DCMU}/F^{-DCMU}) as well as P:R (photosynthesis: respiration) ratio all decreased before any significant change in density of zooxanthellae was evident. At 34°C it took less than 24 h for photosynthesis, fluorescence ratios, and the P:R to decrease to 0. The zooxanthellae density and chlorophyll *a* content per zooxanthella changed little at 34°C before coral death was first observed at 19 h. Zooxanthellae from *M. annularis* maintained at 30°C differed little from zooxanthellae isolated from freshly collected

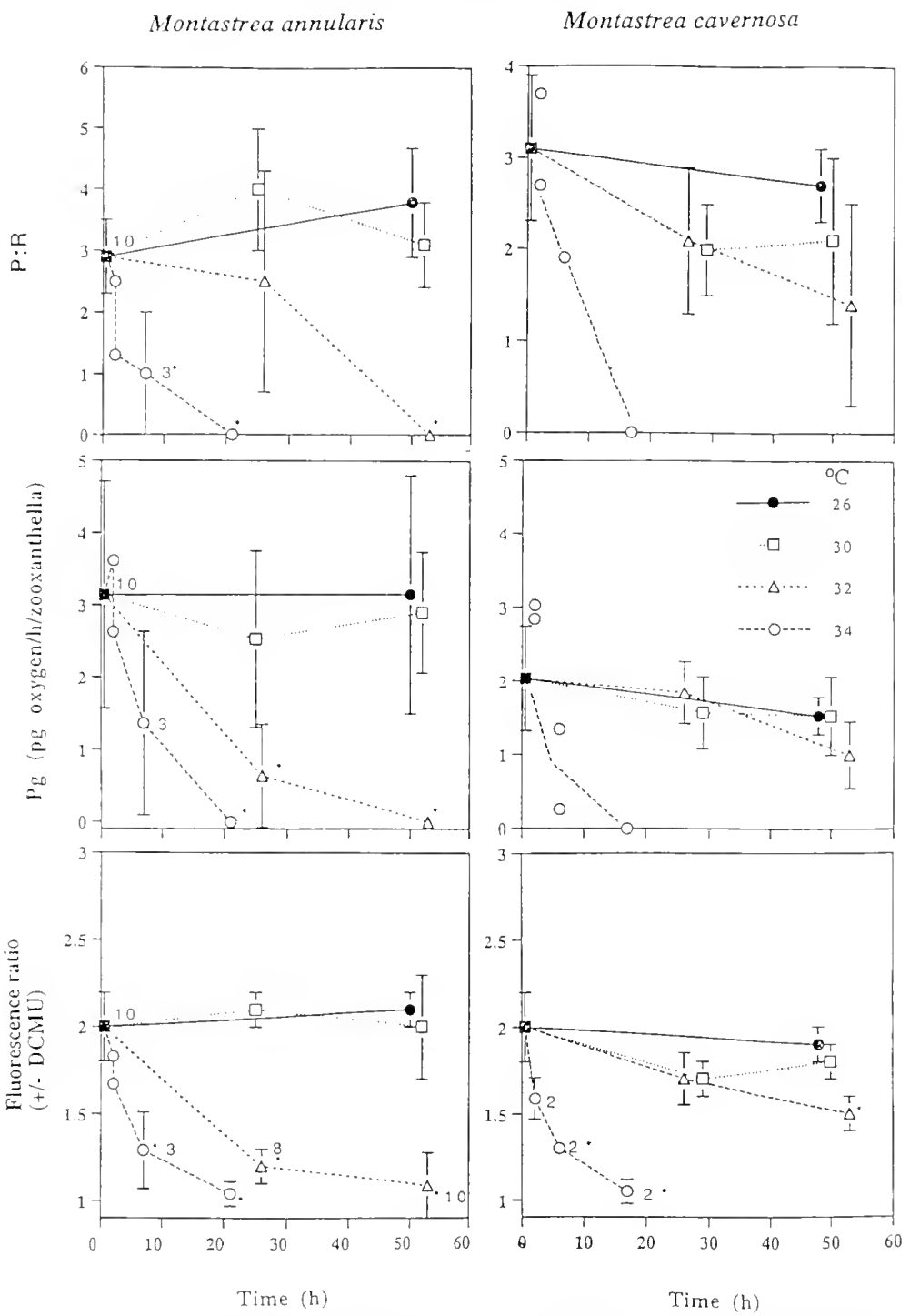

Figure 1. Patterns of bleaching of zooxanthellae in the corals *Montastrea annularis* and *M. cavernosa* exposed to seawater temperatures of 26°C (control), 30°, 32°, and 34°C: gross photosynthesis: respiration ratio (P:R), gross photosynthesis (P_g), and fluorescence ratio (F_{+DCMU}/F_{-DCMU}) in relation to exposure time. All data points are means ± SD, $n = 4$, unless otherwise noted. * = significantly ($P < 0.05$, ANOVA) different from controls.

corals or those maintained at ambient seawater temperature (26° ± 1°C) for 2 days. Chlorophyll *a* per zooxanthella increased slightly over the 2-d experiment, probably due to photoadaptation to the experimental light intensities, which were slightly lower than the light intensities *in situ* (Fig. 2).

M. cavernosa responded somewhat differently to increases of temperature in the light than did *M. annularis*. No significant reductions in the density of zooxanthellae were observed over 53 h at any temperature (Fig. 2). Photosynthesis, fluorescence, and the P:R ratio at 26°, 30°, and 32°C remained relatively stable, except that there was a 25%–50% decrease in these parameters at 53 h at 32°C (Fig. 1). In contrast, photosynthesis, fluorescence, and P:R of the zooxanthellae from *M. cavernosa* declined rapidly at 34°C in a fashion similar to that seen in zooxanthellae from *M. annularis*. Chlorophyll *a* per zooxanthella increased slightly throughout the experiment at all temperatures except 34°C, at which values remained the same or decreased slightly (Fig. 2). Zooxanthellae from *Agaracia lamarcki* appeared to be less tolerant to seawater temperatures of 32° and 34°C than were zooxanthellae from *A. agaricites* (Figs. 3–4). Photosynthesis and the fluorescence ratio of zooxanthellae from *A. lamarcki* declined faster at 34°C than zooxanthellae from *A. agaricites* (Fig. 3). At 32°C, photosynthesis and fluorescence ratios decreased significantly for both species (Fig. 3), and zooxanthellae density was about half of that from corals maintained at 30° or 26°C (Fig. 4). Chlorophyll *a* per zooxanthella did not change significantly ($P > 0.05$, ANOVA) at any temperature for either coral, except for a marked decrease for *A. lamarcki* at 32°C for 48 h (Fig. 4).

High-temperature stress and light

When pieces of *M. annularis* were exposed to different wavelengths of light at 32°C, those experiencing the largest decrease in fluorescence ratio (Fv/Fo) received wavelengths in the UV-A range (320–400 nm) or blue to blue-green light (395–495 nm) (Fig. 5A). Rates of decrease in fluorescence ratio were no different with or without natural levels of UV-B light (<320 nm) in these experiments (ANOVA, $P > 0.05$). Control corals (those maintained at 26°C in natural light with no filters) showed no change in fluorescence ratio throughout the experiment.

Fluorescence ratios (Fv/Fo) of intact *M. annularis* exposed to 32°C declined faster when exposed to higher intensity than lower intensity of natural light (Fig. 5B). Interestingly, a "recovery" trend was observed in the same experiment and in three similar experiments (not included) during periods of cloudy weather.

Discussion

This study shows that symbiotic dinoflagellates living inside of reef corals exhibit a marked decline in their photosynthetic capacity and oxygen evolution when exposed to higher than normal temperatures (32°, 34°C) in natural light for relatively short periods of time. Reductions in photosynthesis and corresponding flow of electrons between photosystems II and I, as indicated by fluorescence ratios, preceded any significant reductions in density of zooxanthellae in the reef-building corals *Montastrea annularis*, *Agaricia lamarcki*, and *A. agaricites*. In addition, zooxanthellae from *M. cavernosa* and *A. agaricites* appeared to be more tolerant to the experimental temperature regimes, showing reduced photosynthetic competence after longer exposure times (>24 h). There was no significant reduction in symbiont density in *M. cavernosa* over the course of the experiment (48–55 h), though probably they too would eventually lose symbiotic algae that were not photosynthetically functional. The data correspond to the bleaching patterns seen in the field; *M. annularis*, and *A. lamarcki* commonly lose color during bleaching events, whereas *M. cavernosa* rarely bleaches and *A. agaricites* sometimes bleaches. The results of this study suggest that the differences seen in nature in bleaching of coral species may be due to the different physiological tolerances of their specific symbiotic algae.

Though it has been clear for some time that the fluorescence patterns and photosynthetic rates of cultured zooxanthellae are altered at moderate increases above control temperatures (e.g., 32° vs. 26°C) (Iglesias-Prieto *et al.*, 1992), there has been debate as to the mechanism of bleaching in relation to mode of release of the zooxanthellae from the coral and the relative health of the symbiont and host (Gates *et al.*, 1992). Hoegh-Guldberg and Smith (1989) clearly showed that bleaching of corals can occur without loss of zooxanthellae, especially when high light intensities "photo-bleach" the algal pigments. However, most bleaching events in nature involve heat stress with full solar radiation, and the loss of both symbiotic dinoflagellates and their photosynthetic pigments has been documented (Kleppel *et al.*, 1989; Porter *et al.*, 1989). In our study, chlorophyll *a* content per zooxanthella varied little, in spite of up to 55 h of exposure to temperatures as high as 34°C. These results are similar to those of Hoegh-Guldberg and Smith (1989), also involving short-term laboratory experiments on corals exposed to elevated temperatures, but in contrast to field observations made during natural bleaching events in the Virgin Islands and southern Florida which showed reductions of chlorophyll *a* ranging from 50% to 80% (Porter *et al.*, 1989; Kleppel *et al.*, 1989). The only reductions seen in chlorophyll content in this study occurred at 34°C at longer exposure times, suggesting that pigment loss during bleaching occurs *after* physiological damage to photosynthesis. During short-term (days) laboratory experiments, zooxanthellae from the more sensitive symbioses appear to leave the host before or during loss of

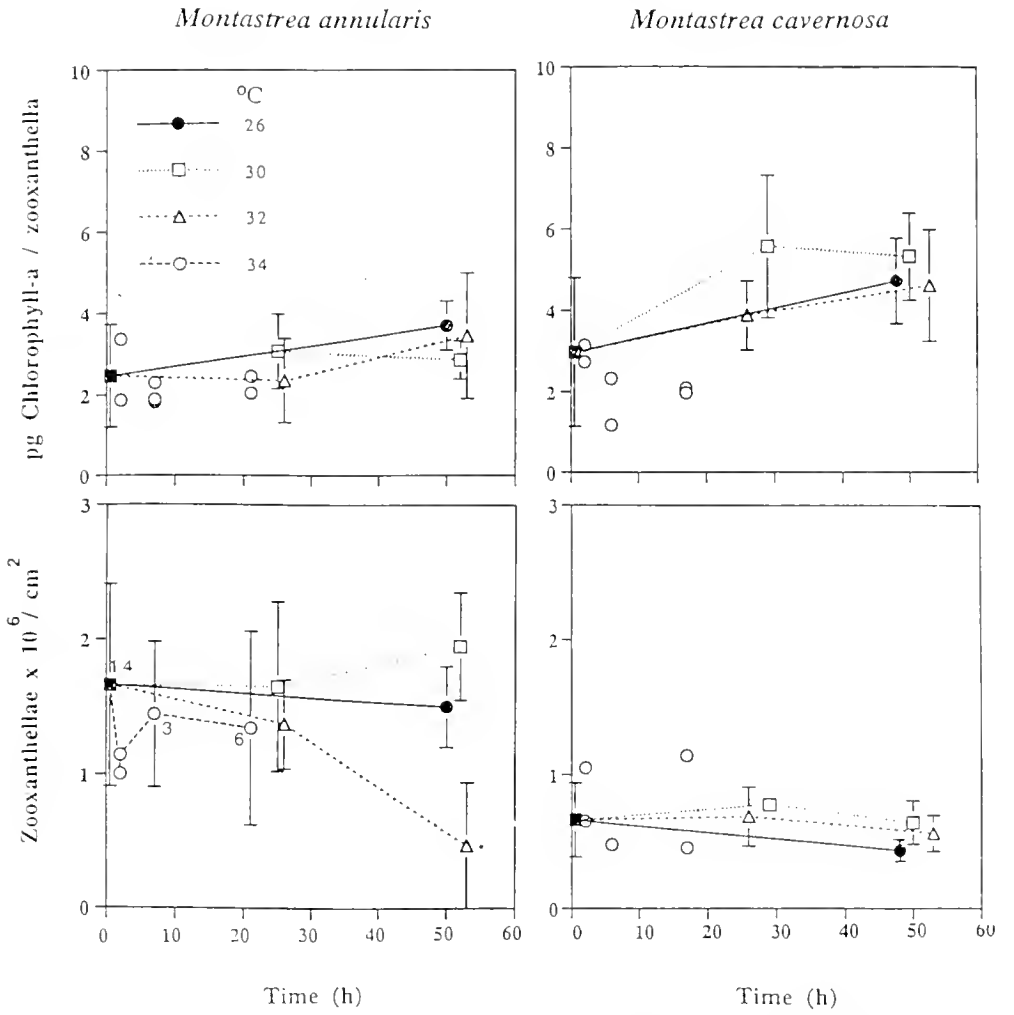

Figure 2. Patterns of bleaching of zooxanthellae in the corals *Montastrea annularis* and *M. cavernosa* exposed to seawater temperatures of 26°C (control), 30°, 32°, and 34°C: chlorophyll *a* per zooxanthella and zooxanthella density in relation to exposure time. All data points are means ± SD, $n = 4$, unless otherwise noted. * = significantly ($P < 0.05$, ANOVA) different from controls.

photosynthetic pigmentation. Longer exposures (weeks) to elevated seawater temperatures (≥30°C) typically involve loss of chlorophyll *a* per zooxanthellae co-occurring with relatively low rates of zooxanthellae expulsion and a decrease in density of zooxanthellae (Glynn and D'Croz, 1990). Thus, loss of photosynthetic pigments appears to be a normal step in warm-water bleaching in nature, and one that indicates algal stress.

When Hoegh-Guldberg and Smith (1989) used chlorophyll data taken from water surrounding the corals to calculate release rates of zooxanthellae from the heat-stressed (30°, 32°C) Pacific corals *Stylophora pistillata* and *Seriatopora hystrix*, expulsion rates increased by a factor of 2 to 10, but only the corals maintained at 32°C showed significant decreases in density of zooxanthellae. In the present study, zooxanthellae density in *Montastrea annularis*, *Agaricia lamarcki*, and *A. agaricites* decreased significantly only *after* photosynthesis and enhanced zooxanthellar fluorescence decreased. Zooxanthellae from *M. cavernosa* were apparently more resistant to the higher temperatures than zooxanthellae in *M. annularis*, in that zooxanthellae density did not change over the 2 days of exposure to 32°C. However, at least some of the zooxanthellae in *M. cavernosa* held 2 days at 32°C showed reduced photosynthetic capacity, and—on the basis of the experiments with *M. annularis*—densities might be expected to decrease after longer exposure times. Similarly, Glynn and D'Croz (1990), who documented steady decreases in density of zooxanthellae from *Pocillopora damicornis* at 30° and 32°C, found that the effects were evident (significantly different from controls) only after 2 weeks or more.

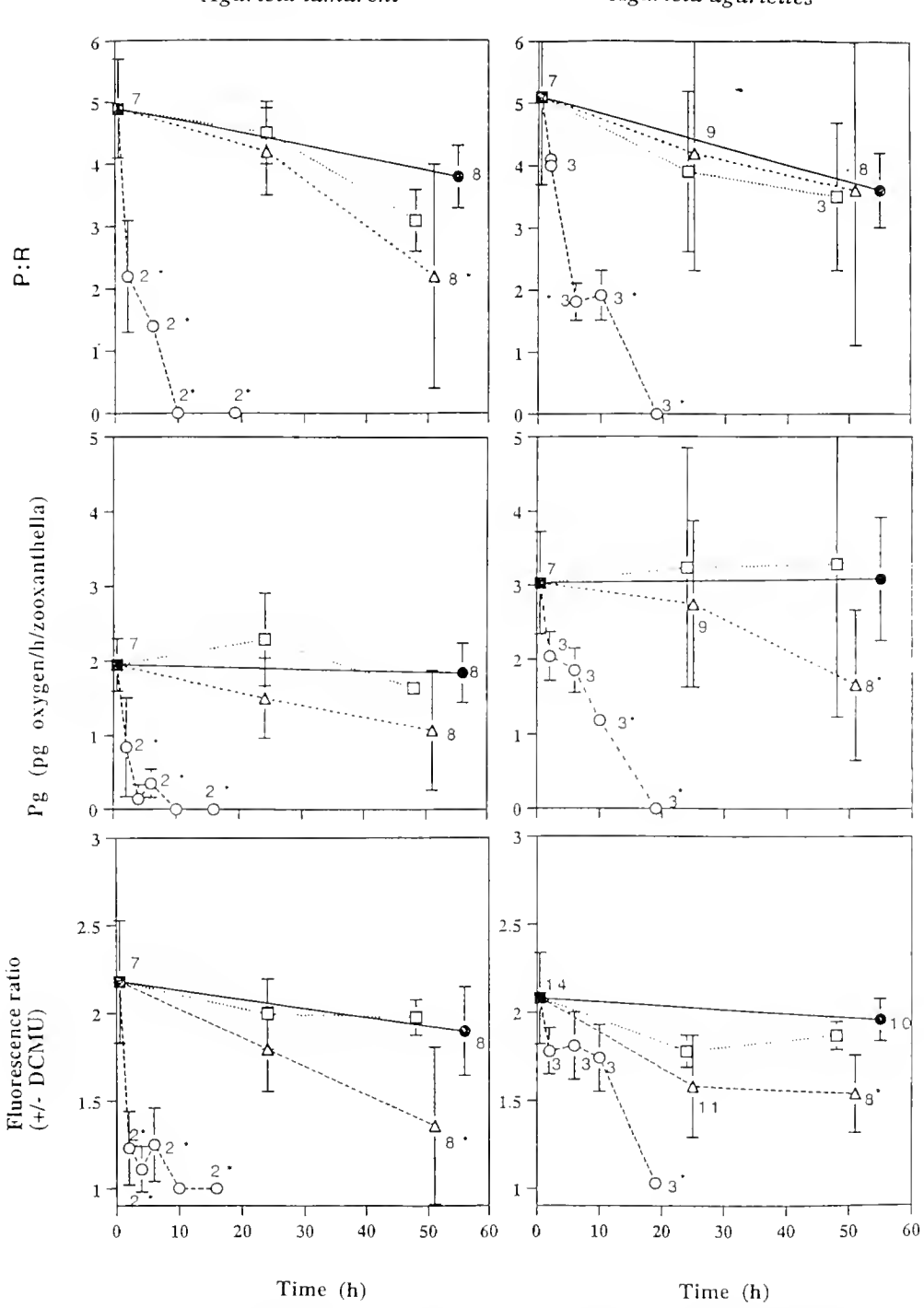

Figure 3. Patterns of bleaching of zooxanthellae in the corals *Agaricia agaricites* and *A. lamarcki* exposed to seawater temperatures of 26°C (control), 30°, 32°, and 34°C: gross photosynthesis: respiration ratio (P:R), gross photosynthesis (P_g), and fluorescence ratio (F_{+DCMU}/F_{-DCMU}) in relation to exposure time. All data points are means ± SD., $n = 4$, unless otherwise noted. * = significantly ($P < 0.05$, ANOVA) different from controls. Symbols as in Figures 1 and 2.

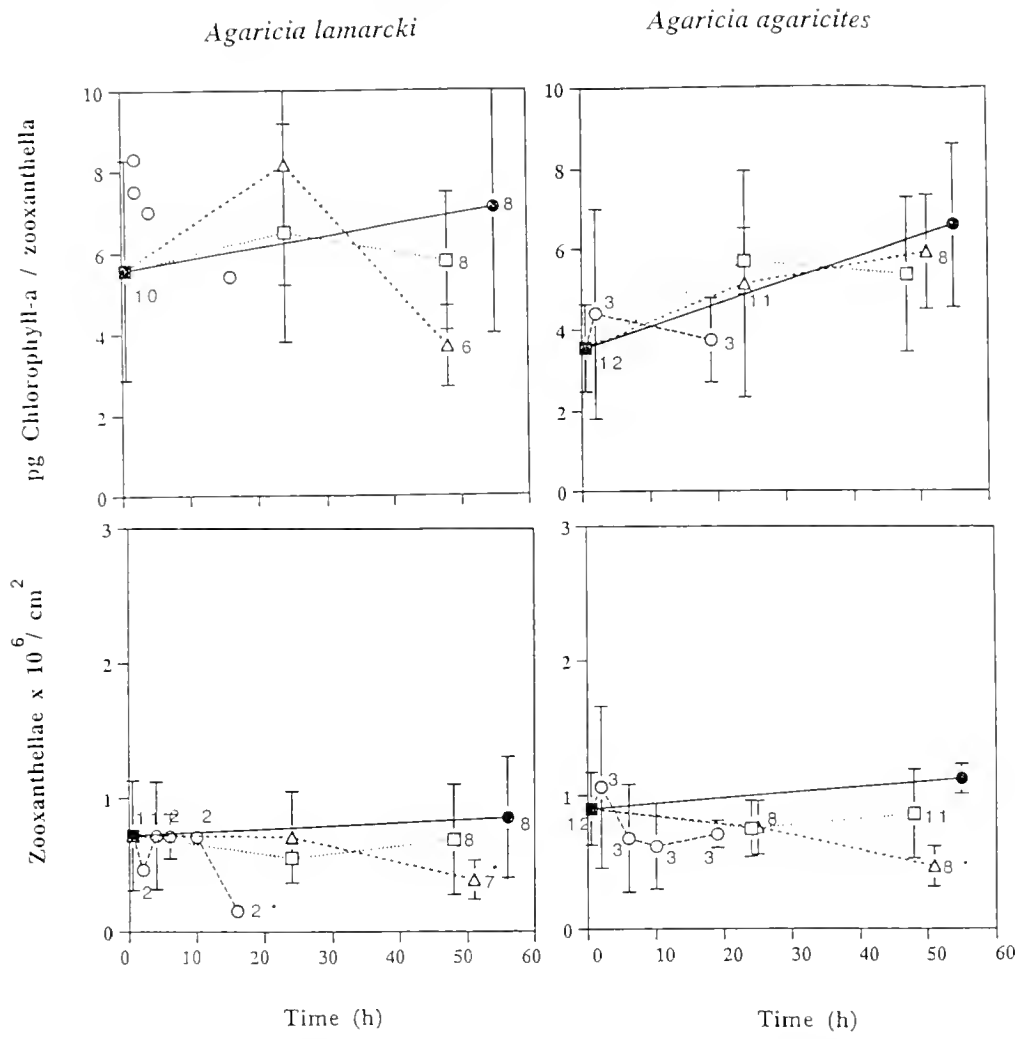

Figure 4. Patterns of bleaching of zooxanthellae in the corals *Agaricia agaricites* and *A. lamarckii* exposed to seawater temperatures of 26°C (control), 30°, 32°, and 34°C: chlorophyll *a* per zooxanthella and zooxanthella density in relation to exposure time. All data points are means ± SD, $n = 4$, unless otherwise noted. * = significantly ($P < 0.05$, ANOVA) different from controls. Symbols as in Figures 1 and 2.

Light and dark rates of zooxanthellar expulsion are identical in *Stylophora pistillata* and *Seriatopora hystrix* maintained at ambient temperature (Hoegh-Guldberg and Smith, 1989). In contrast, corals maintained at high temperatures in the light exhibit higher rates of expulsion (Hoegh-Guldberg and Smith, 1989), resulting in reduced densities of zooxanthellae at 32°C (Hoegh-Guldberg and Smith, 1989; this study). The quantity of light makes a major difference in the kinetics of warm-water-induced bleaching; zooxanthellae kept in dim light take longer, and often require higher temperatures, to achieve the same level of bleaching as seen in brighter light (Fig. 2 this study, Warner and Fitt, unpub.). The quality of light is also a factor in bleaching. Although the effects of large and sudden increases in UV-B can be devastating to zooxanthellae in corals (Lesser *et al.*, 1990; Gleason and Wellington, 1993), most shallow-water corals have UV-protective mycosporine-like amino acids (MAAs) that screen out such dangerous wavelengths. Much more likely sources of synergistic light energy for bleaching are longer wavelength UV-A (wavelengths not screened out by MAAs) and blue light, both important in photosynthesis and therefore not screened out by the coral host (Dunlap *et al.*, 1988). Preliminary experiments show that blue light also promotes bleaching of some types of cultured zooxanthellae much more effectively than the same amount of light at any other part of the visible spectrum (Fitt and Warner, unpub.).

It is not clear at present whether coral death is solely a function of animal tissue death, or if lack or dysfunction of zooxanthellae may trigger or exacerbate events preceding host tissue sloughing and coral death. That the latter

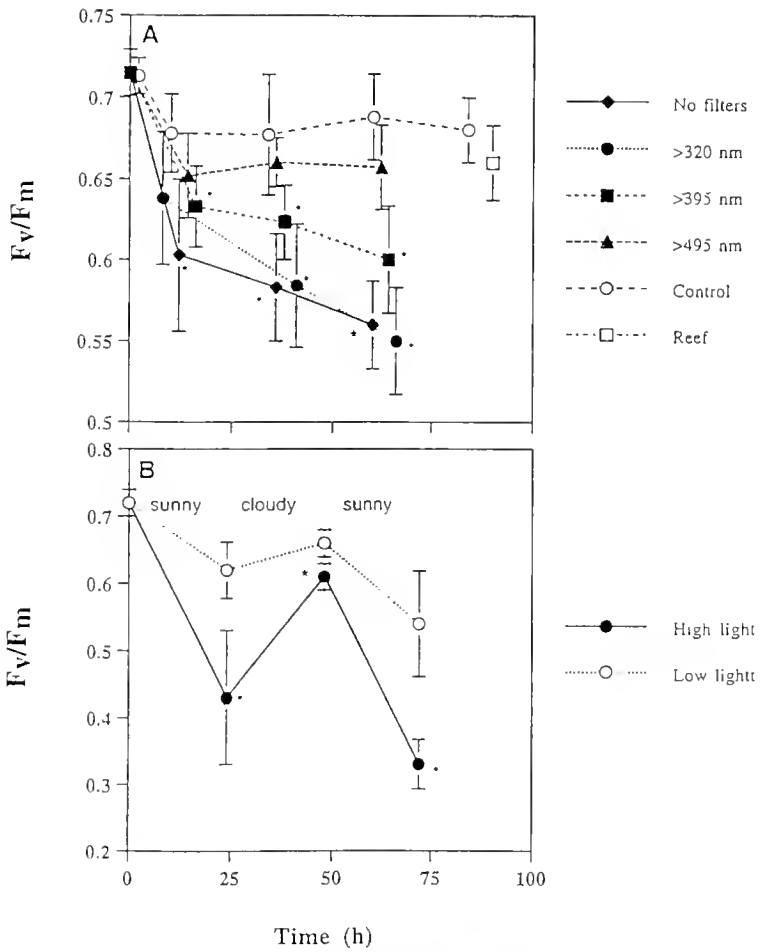

Figure 5. Fluorescence ratios (F_m/F_o) of zooxanthellae in *Montastrea annularis* collected from the reef (28°C) or exposed to seawater temperatures of 26°C (control) and 32°C (all other data) under different wavelengths (A) and intensities (B) of natural light in relation to exposure time. Neutral-density screens were used to adjust maximum intensities to 54% of air ambient (high light) in all experiments. Cut-off filters were used to adjust wavelength (A), and additional neutral-density screens reduced ambient light to 19% of air ambient (low light) in (B). All data points are means ± SD, $n = 6$. * = significantly different from control (A, ANOVA) or low light intensities (B, Student's t test).

can occur in nature was illustrated, on a somewhat longer time scale, in the Eastern Pacific after extensive coral bleaching during the El Niño Southern Oscillation (ENSO) event of 1982–1983 (Glynn, 1983, 1984). Before the widespread local and regional deaths of the corals, no zooxanthellae remained in the tissues of *Pocillopora damicornis* and *Millepora* spp. Temperatures only a few degrees above normal ambient will kill reef corals. Mayer (1914) found that all the reef corals tested in the Dry Tortugas, at the end of the Florida reef tract, died when exposed for an hour to temperatures between 36° and 38°C during the summer. In this early study, the organisms that died at the lowest temperatures tested (*M. annularis*, *A. lamarcki*, and the hydrocoral *Millepora* sp.) are the same species that are the first to react during natural bleaching events (*e.g.*, Williams and Bunkley-Williams, 1988), lending support to the notion that the differential bleaching of zooxanthellate cnidarians exposed to moderately high temperatures in nature reflects the tolerances of their particular zooxanthellae.

Acknowledgments

We thank Drs. R. Smith and G. Schmidt for technical assistance during portions of this study, and W. Wiebe for comments on the manuscript. This research was partially supported by grants from NSF (OCE 9203327, OCE 9349773), ONR (N00014-92-J-1734), and NOAA (CMRC 95-3041). Contribution #2 from the Key Largo Marine Research Laboratory and #575 from the Discovery Bay Marine Laboratory.

Literature Cited

Coffroth, M. A., H. R. Lasker, and K. J. Oliver. 1990. Coral mortality outside of the eastern Pacific during 1982–1983: relationship to El Niño. Pp. 141–182 in *Global Ecological Consequences of the 1982–1983 El Niño-Southern Oscillation*, P. W. Glynn, ed. Elsevier Oceanography Series, Amsterdam.

Coles, S. L., and P. L. Jokiel. 1978. Synergistic effects of temperature, salinity and light on the hermatypic coral *Montipora verrucosa*. *Mar. Biol.* **49:** 187–195.

Coles, S. L., and P. L. Jokiel. 1990. Response of Hawaiian and other Indo-Pacific reef corals to elevated temperature. *Coral Reefs* **8:** 155–162.

Coles, S. L., P. L. Jokiel, and C. R. Lewis. 1976. Thermal tolerance in tropical versus subtropical reef corals. *Pac. Sci.* **30:** 159–166.

Dunlap, W. C., B. E. Chalker, and J. K. Oliver. 1986. Bathymetric adaptations of reef-building corals at Davies Reef, Great Barrier Reef, Australia. III. UV-B absorbing compounds. *J. Exp. Mar. Biol. Ecol.* **104:** 239–248.

Dunlap, W. C., B. E. Chalker, and W. M. Bandaranayake. 1988. Ultraviolet light absorbing agents derived from tropical marine organisms of the Great Barrier Reef, Australia. *Proc. 6th Int. Coral Reef Symp.* **3:** 89–93.

Fisk, D. A., and T. J. Done. 1985. Taxonomic and bathymetric patterns of bleaching in corals, Myrmidon Reef (Queensland). *Proc. 5th Int. Coral Reef Symp.* **6:** 149–154.

Fitt, W. K. 1985. Effect of different strains of the zooxanthella *Symbiodinium microadriaticum* on growth and survival of their coelenterate and molluscan hosts. *Proc. 5th Intl. Coral Reef Symp.* **6:** 131–136.

Fitt, W. K., H. J. Spero, J. Halas, M. W. White, and J. W. Porter. 1993. Recovery of the coral *Montastrea annularis* in the Florida Keys after the 1987 Caribbean "bleaching event." *Coral Reefs* **12:** 57–64.

Gates, R. D., G. Baghdasarian, and L. Muscatine. 1992. Temperature stress causes host cell detachment in symbiotic cnidarians: implications for coral bleaching. *Biol. Bull.* **182:** 324–332.

Gleason, D. F., and G. M. Wellington. 1993. Ultraviolet radiation and coral bleaching. *Nature* **365:** 836–838.

Glynn, P. W. 1983. Extensive "bleaching" and death of reef corals on the Pacific coast of Panama. *Environ. Conserv.* **10:** 149–154.

Glynn, P. W. 1984. Widespread coral mortality and the 1982/83 El Niño warming event. *Environ. Conserv.* **11:** 133–146.

Glynn, P. W., and L. D'Croz. 1990. Experimental evidence for high temperature stress as the cause of El Niño-coincident coral mortality. *Coral Reefs* **8:** 181–191.

Harriott, V. J. 1985. Mortality rates of scleractinian corals before and during a mass bleaching event. *Mar. Ecol.* **21:** 81–88.

Hoegh-Guldberg, O., and G. J. Smith. 1989. The effect of sudden changes in temperature, light and salinity on the population density and export of zooxanthellae from the reef corals *Stylophora pistillata* Esper and *Seriatopora hystrix* Dana. *J. Exp. Mar. Biol. Ecol.* **129:** 279–303.

Iglesias-Prieto, R., J. L. Matta, W. A. Robins, and R. K. Trench. 1992. Photosynthetic response to elevated temperature in the symbiotic dinoflagellate *Symbiodinium microadriaticum* in culture. *Proc. Natl. Acad. Sci.* **89:** 10302–10305.

Jaap, W. C. 1979. Observations on zooxanthellae expulsion at Middle Sambo Reef, Florida Keys. *Bull. Mar. Sci.* **29:** 414–422.

Jaap, W. C. 1985. An epidemic zooxanthellae expulsion during 1983 in the Lower Florida Keys coral reefs: hyperthermic etiology. *Proc. 5th Int. Coral Reef Symp.* **6:** 143–148.

Jeffrey, S. W., and F. T. Haxo. 1968. Photosynthetic pigments of symbiotic dinoflagellates (zooxanthellae) from corals and clams. *Biol. Bull.* **135:** 139–165.

Jeffrey, S. W., and G. F. Humphrey. 1975. New spectrophotometric equations for determining chlorophylls *a*, *b*, c_1 and c_2 in higher plants, algae and natural phytoplankton. *Biochem. Physiol. Planz.* **167:** 191–194.

Jokiel, P. L. 1980. Solar ultraviolet radiation and coral reef epifauna. *Science* **7:** 1069–1071.

Jokiel, P. L., and S. L. Coles. 1977. Effects of temperature on the mortality and growth of Hawaiian reef corals. *Mar. Biol.* **43:** 201–208.

Jokiel, P. L., and S. L. Coles. 1990. Response of Hawaiian and other Indo-Pacific reef corals to elevated temperature. *Coral Reefs* **8:** 155–162.

Kleppel, G. S., R. E. Dodge, and C. J. Reese. 1989. Changes in pigmentation associated with the bleaching of stony corals. *Limnol. Oceanogr.* **34:** 1331–1335.

Lasker, R. L., E. C. Peters, and M. A. Coffroth. 1984. Bleaching of reef coelenterates in the San Blas Islands, Panama. *Coral Reefs* **3:** 183–190.

Lesser, M. P., W. R. Stochaj, D. W. Tapley, and J. M. Shick. 1990. Bleaching in coral reef anthozoans: effects of irradiance, ultraviolet radiation, and temperature on the activities of protective enzymes against active oxygen. *Coral Reefs* **8:** 225–232.

Mayer, A. G. 1914. The effects of temperature upon tropical marine animals. Carnegie Inst. Wash. Publ. Dept. Mar. Biol., *Papers from the Tortugas Lab.* **6**(183): 3–24.

Oliver, J. 1985. Recurrent seasonal bleaching and mortality of corals on the Great Barrier Reef. *Proc. 5th Int. Coral Reef Symp.* **6:** 201–206.

Porter, J. W., and O. Meier. 1992. Quantification of loss and change in Floridean reef coral population. *Am. Zool.* **32:** 625–640.

Porter, J. W., W. K. Fitt, H. J. Spero, C. S. Rogers, and M. W. White. 1989. Bleaching in reef corals: physiological and stable isotopic responses. *Proc. Natl. Acad. Sci.* **86:** 9342–9346.

Szmant, A. M., and N. J. Gassman. 1990. The effects of prolonged "bleaching" on the tissue biomass and reproduction of the reef coral *Montastrea annularis*. *Coral Reefs* **8:** 217–224.

Trench, R. K. 1993. Microalgal-invertebrate symbioses: a review. *Endocytobiosis Cell Res.* **9:** 135–175.

Williams, E. H., and L. Bunkley-Williams. 1988. Circumtropical coral reef bleaching in 1987–1988. *Proc. 6th Coral Reef Symp.* **3:** 313–318.

Yonge, C. M., and A. G. Nichols. 1931. Studies on the physiology of corals. V. The effect of starvation in light and darkness on the relationship between corals and zooxanthellae. *Sci. Rept. Great Barrier Reef Exped. 1928–1929* **1:** 177–211.

Reference: *Biol. Bull.* **189**: 308–319. (December, 1995)

Filtration and Utilization of Laboratory-Cultured Bacteria by *Dreissena polymorpha*, *Corbicula fluminea*, and *Carunculina texasensis*

H. SILVERMAN, E. C. ACHBERGER[1], J. W. LYNN, AND T. H. DIETZ

Department of Zoology and Physiology; [1]Department of Microbiology, Louisiana State University, Baton Rouge, Louisiana 70803

Abstract. *Dreissena polymorpha* consumed about 6 $\times 10^8$ *Escherichia coli* from 20 ml of artificial pondwater (APW) in 30 min under laboratory conditions. The clearance rate per mussel was 143 ± 25 ml g^{-1} dry tissue min^{-1}. The *E. coli* used in these studies ranged from about 1.7 to 2.9 μm in length. ^{35}S-labeled *E. coli* were used to demonstrate that bacteria-derived nutrients were incorporated into mussel tissue. Electrophoretic analysis of mussel and bacterial proteins on 12% polyacrylamide gels allowed the visual determination of incorporation of labeled amino acids into bivalve proteins and demonstrated that intact bacteria were not simply trapped in mussel tissues. The conversion of bacterial-labeled amino acids into mussel protein was about 26%. Similarly, we demonstrated that *D. polymorpha* can use other bacterial species ranging in size from about 1.3 to 4.1 μm, including *Citrobacter freundii*, *Enterobacter aerogenes*, *Serratia marcescens*, *Bacillus megaterium*, and *B. subtilus*. The ability of *D. polymorpha* to take up *E. coli* was compared with that of two other freshwater mussels, *Corbicula fluminea* and *Carunculina texasensis*. On a mussel-dry-weight basis, *D. polymorpha* cleared bacteria 30 to 100 times faster than *Corbicula fluminea* and *Carunculina texasensis*, respectively. The ability to filter *E. coli* appears to be related to the architecture of the cirri on the latero-frontal cells of the gill. Cirri from *Corbicula* and *Dreissena* are similar in size, but *Dreissena* has a larger gill compared to the tissue dry-weight, and has 10^2 times more cirri than found in *Corbicula*. *Carunculina*, the unionid representative, has smaller and fewer cirri, and has relatively limited ability to capture *E. coli*.

Received 5 January 1995; accepted 14 September 1995.

Abbreviations: APW—artificial pondwater; TCA—trichloroacetic acid; PAGE—polyacrylamide gel electrophoresis; SDS—sodium dodecyl sulfate; SEM—scanning electron microscopy

Introduction

Dreissena polymorpha (Pallas) has successfully colonized much of the Great Lakes region of North America. It is currently achieving the same success in the Ohio, Tennessee, and Mississippi river drainages (unpubl. obs.). This organism can filter large amounts of water in a relatively short period, eliminating or greatly reducing the abundance of zooplankton and phytoplankton (Stanczykowska *et al.*, 1976; MacIsaac *et al.*, 1992; Leach, 1993; Bunt *et al.*, 1993). Previous reports indicate that *D. polymorpha* selects food particles in the size range 15–40 μm (Ten Winkel and Davids, 1982), and filters particles >2 μm with almost 100% relative efficiency (Jørgensen *et al.*, 1984). Capture of particles ranging in size from 0.7 μm (Sprung and Rose, 1988) to 750 μm (Ten Winkel and Davids, 1982) has been reported.

Initial capture of particles occurs on the gills of eulamellibranch bivalves and is mediated by the ciliary mechanical systems associated with the gill filaments. While all eulamellibranch gills are organized into filaments, the structure and organization of specialized ciliary appendages associated with the filaments vary from species to species (Atkins, 1938; Morton, 1983). All have lateral ciliated cells that are generally believed to be responsible for moving water through the gill. The latero-frontal cells are positioned between the frontal surface of the filament and the lateral ciliated cells. The ciliary appendages on these cells range from simple cilia in some species, to longer, stiffer cilia in other species, to fused plates of cilia in still others. In bivalves with cirri, the number of cilia per plate varies with species: 11–12 fused cilia in *Carunculina tex-*

asensis, 22–26 in *Mytilus edulis*, and 38–42 fused cilia in *D. polymorpha* (Atkins, 1938; Moore, 1971; Owen, 1974). These structures, together with even more distally located abfrontal and frontal cilia, act in concert to capture and move particles. The ciliated structures, the water currents they produce, and the mucus produced by the gills and palps move food particles toward the mouth (Beninger *et al.*, 1992; 1993; Ward *et al.*, 1993). On the basis of structure alone, some investigators have indicated that cirri or latero-frontal cilia act as a mechanical filtering device that can explain particle trapping in various bivalve species (Owen, 1974; Owen and McCrae, 1976; Silvester and Sleigh, 1984). However, the actual mechanism of particle capture remains a topic of disagreement. Jorgensen (1976, 1982, 1989) has argued that such descriptions fail to account for fluid movements and the complex currents associated with the gill. Recent endoscopic studies directly demonstrated that mucus is involved in transporting particles after their capture by the gill (Beninger *et al.*, 1992; Ward *et al.*, 1993).

In this study, we describe controlled laboratory experiments aimed at assessing how well *D. polymorpha* filters bacteria, and we compare the results to those for other freshwater mussels. The experiments tested the ability of *D. polymorpha*, *Carunculina texasensis* (a unionid representative), and *Corbicula fluminea* to utilize laboratory-cultured *Escherichia coli* as a sole nutrient source. Under laboratory conditions *D. polymorpha* showed rapid filtration and incorporation of ^{35}S-labeled *E. coli*. The clearance of bacteria from artificial pondwater (APW) was faster in *Dreissena* than in either *Corbicula fluminea* or *Carunculina texasensis*. These differences in filtration in laboratory studies suggest that the ability to use natural-sized bacteria in the environment may differ substantially among these freshwater species.

Materials and Methods

Animals

Dreissena polymorpha [range 17–25 mm length; 1.225 ± 0.027 g total live weight (mean ± SE); 0.016 ± 0.000 g dry tissue; n = 160]; was collected from the Mississippi River from screens at the Dow Chemical Plant in Plaquemine, Louisiana. The unionid *Carunculina texasensis* (23–26 mm length; 2.453 ± 0.073 g total live weight; 0.090 ± 0.006 g dry tissue; n = 10) was collected, under permit, from a pond in Baton Rouge, Louisiana; and *Corbicula fluminea* (23–25 mm length; 7.871 ± 0.233 g total live weight; 0.368 ± 0.012 g dry tissue; n = 36) was collected from the Tangipahoa River in southern Mississippi. All species were kept under laboratory conditions in aerated artificial pondwater (APW; 0.5 NaCl, 0.4 $CaCl_2$, 0.2 $NaHCO_3$, 0.05 KCl in mM) with *Dreissena* in APW containing 0.2 mM Mg_2SO_4 (Dietz *et al.*, 1994). Animals were maintained unfed in the laboratory for five days before use.

Labeling of bacteria

Escherichia coli JM83 (Messing, 1979) was used for most of the experiments. For ^{35}S-labeling, *E. coli* were grown in a chemically defined medium containing 5 g glucose, 810 mg NH_4Cl, and 82 mg $MgCl_2 \cdot 7H_2O$ per liter of 0.05 M potassium phosphate buffer, pH 7.2. Added to this was 5 ml of a trace salts solution containing $CaCl_2 \cdot 2H_2O$ (2 g), $MnSO_4 \cdot H_2O$ (1 g), and $FeSO_4 \cdot 7H_2O$ (0.5 g) dissolved in one liter of 0.1 M HCl. For growth of *E. coli* JM83, it was necessary to add 20 μg/ml L-proline and 5 μg/ml thiamine, final concentrations, to the medium. The carbon source, trace salts solution, L-proline, and thiamine were sterilized separately from the rest of the medium. To label the bacteria, *E. coli* were grown at 37°C with shaking aeration for at least four generations in the above medium containing 5 μCi/ml carrier-free $Na_2{}^{35}SO_4$ (Dupont NEN). The final cell density of cultures was approximately 1.3–2 × 10^9 bacteria/ml. Labeled bacteria were collected by centrifugation, washed once in the growth medium without carbon source, and stored in APW at a concentration of 3 × 10^9 bacteria/ml. The cells were stored on ice in pondwater until use. Following this initial transfer, the bacteria did not experience any additional osmotic shock and survived for weeks. *E. coli* grown in this medium were 2.3 ± 0.6 μm long and 0.9 ± 0.1 μm wide (n = 50) and did not clump.

Incorporation of ^{35}S during growth of *E. coli* was measured with a liquid scintillation counter. The bacteria were precipitated in 10% trichloroacetic acid (TCA) and collected on a glass fiber filter. Greater than 70% incorporation of the label was routine.

To determine if filtration of *E. coli* by *D. polymorpha* was novel for freshwater bivalves or whether other bacterial species would be similarly filtered, several other bacteria differing in size (1.3–4.1 μm in length) and shape were tested. A similar ^{35}S-labeling protocol was used to label *Citrobacter freundii*, *Enterobacter aerogenes*, *Serratia marcescens*, *Bacillus subtilus*, and *B. megaterium*. The concentration of bacteria in all suspensions was determined by direct microscopic count using a hemocytometer. Cell dimensions for labeled bacteria were measured from photomicrographs.

Escherichia coli *feeding experiments*

All feeding experiments were carried out in individual containers (test tubes) aerated for the duration of the experiment. Individuals of similar size were selected by weighing, then placed in separate test tubes containing 20 ml of APW. The experiment was started by the addition of bacteria as soon as the bivalves began siphoning.

Siphoning typically began within 10 min of placing animals in the test tube containing pondwater.

Each test tube had 3×10^7 bacteria/ml representing about 1.7×10^5 dpm ^{35}S/ml (200 μl stock bacterial cell suspension). Each day the *E. coli* stock solution (in APW and held on ice) was centrifuged and resuspended in APW. The discarded supernatant was assayed for ^{35}S. Using this assay procedure, we found that *E. coli* did not deteriorate, and that all ^{35}S (>99%) added to an experimental tube was associated with intact bacteria in the APW and not with breakdown products in the supernatant. Control tubes without bivalves received labeled bacteria, were aerated for 20 min, and analyzed. The bath solutions from these tubes were passed through a Millipore filter (0.22 μm) to trap the bacteria. Virtually all of the label in each tube (99.5%) was on the filter, while the supernatant contained 1319 ± 85 dpm/ml (n = 15). Thus, <0.5% of the radioactivity was in the non-particulate material of the assay medium (similar results were obtained by centrifuging the assay medium; less than 1% of the radioactivity remained in the supernatant).

The bivalve filtration studies were initiated by collecting a sample (t_0) of the bath exactly 45 s after inoculation of the pondwater with bacteria. This time interval was required for mixing and was previously determined both visually (methylene blue) and by tracking the distribution of labeled bacteria in test tubes without an animal present. Individual test tubes were usually sampled initially and at the end to avoid disturbing the animals, with final samples collected after 5 to 90 min, depending on the bivalve species. The final sample was taken by mixing the tube and taking a 100-μl sample. For all samples, ^{35}S radioactivity was determined with a liquid scintillation counter (Wiegman *et al.*, 1975). Additional controls for these experiments consisted of dried shells or rinsed, formalin-fixed whole animals placed in individual containers and handled as described above. In none of the controls was radioactivity significantly reduced in the bath. At the conclusion of the experiments, animals were removed from their shells and dried overnight to constant weight at 90°C. Radioactive ^{35}S adsorbed to control (fixed) animal tissue or shell was less than 100 dpm. Incorporation of label was not detectable in the control tissue analyses (see below).

At the end of some experiments, each animal was removed from the tube and rinsed 2–3 times in >500 ml pondwater containing no label, then placed in a separate beaker containing at least 150 ml of APW. The label was allowed to be incorporated into the animal for 48 h, with two additional changes (rinsed 3 × 500 ml) of APW each day. Usually several hundred dpm/ml were released into the APW by an animal during a 12-h period. After 48-h, each animal was removed from the bath and rinsed several times in APW and a blood sample taken by pericardial puncture (Fyhn and Costlow, 1975). Blood sampling location was previously determined by dissection of *D. polymorpha* to identify appropriate landmarks. A syringe needle (15.9 mm, 26 ga) was inserted between the valves between the inhalant and exhalant siphons and into the pericardial cavity located in the vicinity of the posterior margin of the hinge (Dietz *et al.*, 1994). To collect >100 μl of blood, equal to 10–20% of the animal's wet weight, the syringe needle had to be rotated to prevent tissue from occluding the needle orifice. The osmolality of the APW was 4 mOsm and the water contained about 300 dpm/ml radioactivity at the time of collection of blood from the bivalves. Measured osmolarity of the blood ranged between 40 and 42 mOsm, within the normal range previously reported (Dietz *et al.*, 1994), and radioactivity in the blood was 1 to 4 orders of magnitude higher than that found in APW. These data suggest little if any contamination of blood samples by mantle cavity fluid.

Animals were dissected free of the shell and the tissue was dried overnight at 90°C and weighed. The tissue was homogenized in 3% TCA, and the TCA-precipitable pellet was washed twice in TCA and re-pelleted. The final supernatant was discarded and the pellet dissolved in 1 *M* NaOH. A sample of digested tissue was assayed for radioactivity and an aliquot analyzed for protein content using a BioRad protein determination procedure. This allowed us to determine the amount of ^{35}S incorporated following the feeding experiments. The 48-h rinse in large volumes of APW was used to allow passage of any bacteria that might have remained in the gut, and also allowed time for incorporation of radioactive label into clam proteins.

Variations in the basic experimental protocol included experiments designed to compare clearance rates in different volumes of bath (with constant bacterial concentration) and at different bacterial concentrations (while keeping bath volume constant). Volumes tested were 20, 60, and 120 ml. Even with the small 20-ml bath volume, the reduction of bacterial radiolabel followed first-order exponential kinetics. The use of a small volume reduced the amount of radiolabeled waste fluid produced. In addition, we maintained the bath at a constant 20 ml while increasing the number of bacteria present. The latter experiments were designed to assess maximal bacterial clearance under laboratory conditions.

Finally, in an attempt to assess whether repeated exposure to bacteria led to satiation, we exposed some animals to 6×10^8 *E. coli* in 20 ml of bath, assayed bacterial disappearance from the medium over 30 min, waited 30 min and added another 6×10^8 cells; this process was repeated until we determined that the animals were no longer removing bacteria from the bath at the initial rate.

Electrophoretic analysis of ^{35}S-labeled proteins

To demonstrate the assimilation of bacterial sources of sulfur-containing amino acids by *D. polymorpha*, a few animals were dissected directly into liquid nitrogen after 48-h pulse labeling. Each animal, as well as a separate sample of the ^{35}S-labeled *E. coli* (10^9 cells), was placed in 400 μl of ice-cold buffer (10 m*M* Tris-HCl, 1 m*M* EDTA, 10 m*M* NaCl, pH 7.8) with protease inhibitor, 0.7 mg/ml phenylmethylsufonyl fluoride. The samples were partially homogenized by sonic disruption using the microtip probe of an ultrasonic processor (Model W220, Heat Systems-Ultrasonic, Inc.). Samples received four 10-s bursts at a power setting of 2 and were cooled on ice for 3 min between treatments. Following sonication, the samples were centrifuged at 16,000 × *g* for 3 min, and the supernatant fluid was collected on ice. For each cell-free extract, the TCA precipitable radioactivity was determined, and the protein content was assayed. Proteins in the cell-free extracts were separated by electrophoresis on a 12% polyacrylamide gel (PAGE) according to the method of Laemmli (1970). *D. polymorpha* samples contained approximately 100,000 dpm in 60 μg of protein. Following electrophoresis, samples were visualized by staining with Coomassie brilliant blue and by autoradiography with Kodak X-OMAT AR film. Molecular weight standards (Broad range SDS-PAGE Standards, BioRad Laboratories) stained with Coomassie brilliant blue were used to define the banding patterns of the samples.

Cirral structure

Differences in cirral structure and distribution were examined and described using scanning electron microscopy (SEM). Tissue fixation followed modification of previously described procedures (Richard *et al.*, 1991). Animals were fixed for 1 h in 2% glutaraldehyde in phosphate buffer (35-60 mOsm as appropriate to match blood osmolality of the bivalve species). Gills were excised and exposed to glutaraldehyde for an additional hour, rinsed in buffer, and postfixed in 1% osmium tetroxide. Gills were dehydrated in an ethanol series, critical-point dried, mounted on aluminum stubs using carbon tape, and sputter-coated with gold/palladium (20 nm). Gills were examined using a Cambridge 200 scanning electron microscope. For calculations of cirral size and gill surface areas it was necessary to measure the shrinkage associated with tissue processing for SEM examination. For these purposes, several gills from each species were carefully excised and photographed using a dissecting microscope. The tissue was fixed and critical-point dried as described above, then re-photographed to allow determination of tissue shrinkage under our tissue preparation procedures.

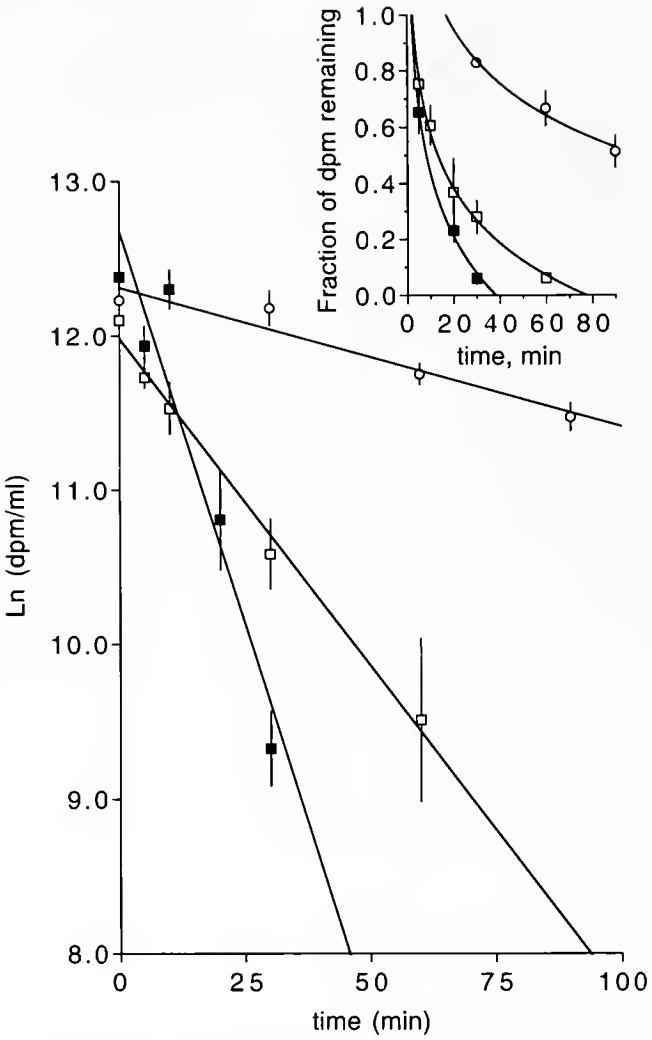

Figure 1. Inset is the time-dependent removal of *Escherichia coli* from pondwater by *Dreissena polymorpha* (filled squares), *Corbicula fluminea* (open squares), or *Caruncula texasensis* (open circles). The vertical lines represent ±1 standard error. The slope of the line of the time-dependent natural logarithmic transformation of radioactive bacteria concentration in the APW is the rate constant (min^{-1}). Each mussel was placed in 20 ml of pondwater containing 6×10^8 bacteria labeled with ^{35}S. Each point represents the mean ± standard error for at least 10 separate animals. The $t_{1/2}$ was 7.1, 16.5, and 77.0 min for *D. polymorpha*, *Corbicula fluminea*, and *Caruncula texasensis*, respectively.

Calculations and statistical analysis

Disappearance of radioactive label from the bath was exponential and followed first-order rate kinetics (rate constant = $\ln(D_0/D_t) \cdot t^{-1}$, D was the dpm/ml at times 0 and t). The half time was calculated from the expression $t_{1/2} = \ln(2)/(\text{rate constant})$. Bacterial clearance rate (C, ml min^{-1}) for each mussel was calculated using the equation $C = V/t \cdot \ln(D_0/D_t)$, where V is volume in ml, D_0 and D_t are bacteria radiolabel concentrations defined above (Riisgård, 1988). Weight-specific clearance (dry soft-

Table I

Rate of ^{35}S-labeled E. coli *uptake by three species of freshwater bivalves*

Bivalve species	*n*	Dry tissue, mg	Rate constant, min^{-1}	Clearance, ml g^{-1} dry tissue min^{-1}
Dreissena polymorpha	20	16 ± 1^c	-0.098 ± 0.011^a	143.1 ± 24.6^a
Corbicula fluminea	32	368 ± 12^a	-0.043 ± 0.002^b	4.4 ± 0.6^b
*Carunculina texasensis**	10	90 ± 6^b	-0.009 ± 0.002^c	1.3 ± 0.2^c

Data expressed as mean ± standard error. Values within a column having different letters were significantly different ($P < 0.01$) using an unpaired Student's *t*-test.

* The same animals were sampled repeatedly at 30-min intervals for 90 min.

tissue mass) data were expressed as ml g^{-1} dry tissue min^{-1}. In some cases we determined the rate constants and calculated clearance from a linear regression of ln(dpm/ml) as a function of time to compare rate constants or to calculate clearance between species or experimental treatments. Differences between species or treatments were determined by ANOVA and were considered significant if $P < 0.05$. Fisher's protected least significant difference (PLSD) was used to determine differences between average values within a group having a significant ANOVA. Differences between regression slopes were determined using Student's *t*-test.

Results

Filtration of E. coli *by freshwater bivalves*

Freshwater bivalves removed *E. coli* from pondwater with first-order exponential kinetics (Fig. 1). The size of the cultured *E. coli* was 2.3 ± 0.6 μm long and 0.9 ± 0.1 μm wide. The bacterial concentration used in these experiments was approximately 3×10^7 per ml in 20 ml APW, and 10–36 animals of each species were used to obtain the average values. The slope of the lines represents the rate constants for removal of bacteria by the different bivalve species (Table I). The rate constants differed statistically ($P < 0.01$) for each species, and *D. polymorpha* had the highest rate and the shortest $t_{1/2}$ (Fig. 1). On a dry weight basis, clearance rates also were highest for *D. polymorpha* and lowest for *Carunculina texasensis*. The rate of clearance exhibited by *D. polymorpha* was 30–100 times greater than that of the other two species.

Incorporation of radioactive bacterial nutrients in bivalve proteins

Disappearance of radiolabel from the bath indicated that the mussels were capable of removing the particles from the water column, but did not necessarily indicate that the particles and their associated nutrients were assimilated. Mussels hold food particles in their digestive tube and perhaps in the mantle cavity for days without digesting them. In addition, we have observed living algae escaping into the water column from pseudofeces released by unionids two days after feeding (S. J. Nichols, pers. comm.; unpub. obs.). However, ^{35}S label was accumulated into the body fluids of the animals 48 h after the pulse feeding (Table II). Given the amount of radiolabel observed in the blood of the animals, it was unlikely that the blood samples were contaminated by the APW. The APW bath containing each *D. polymorpha* had only 302 ± 35 dpm/ml ($n = 5$) at the end of the 48-h period. Each of these bivalve species had label in the blood, and this fluid is presumably maintained in a sterile condition by the animal. Thus, label was likely to be attributable to dissolved ^{35}S-containing matter (amino acids, polypeptides, etc.). Further, 48 h after *Dreissena* were exposed to bacteria, a few animals were fed *Chlorella*. After algal feeding (30 min), the gut tubule was visibly green, and was dissected from the animal for measurement of radioactivity. Only bacteria in the gut contents would be radiolabeled and detected by scintillation counting, and in no case were counts above background recorded.

To determine whether the radioactivity in the mussels was in the form of bacterial protein or had been converted into mussel protein, we used PAGE analysis to compare mussel tissue proteins with *E. coli* proteins. The presence of *E. coli* proteins in the PAGE gels of mussel tissue would indicate that intact bacteria were associated with the mussel body. Figure 2, an autoradiograph of a corresponding

Table II

^{35}S accumulated in the blood of freshwater mussels 48 h after they were fed ^{35}S-labeled E. coli *(3×10^7 bacteria/ml) for 60 min*

Bivalve species	Blood, dpm/ml
Dreissena polymorpha	835070 ± 224170^a
Corbicula fluminea	145694 ± 51875^b
Carunculina texasensis	1840 ± 387^c

Mean ± standard error, $n = 5$ for each species. The means with different letters are significantly different using the unpaired Student's *t*-test ($P < 0.05$).

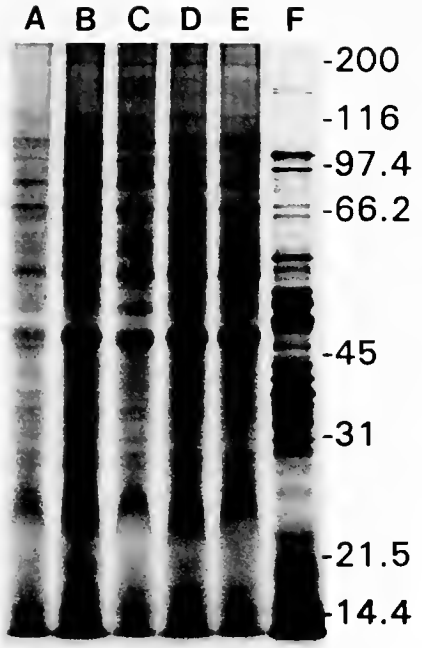

Figure 2. Autoradiograph of a 12% polyacrylamide gel used to electrophoretically separate proteins isolated from the homogenized whole body of *Dreissena polymorpha*. Mussels were allowed 48 h to assimilate ^{35}S-labeled *Escherichia coli* after a 20-min feeding (individual mussels represented in lanes A–E). Lane F represents the solubilized protein fraction of the ^{35}S-labeled *E. coli* used in the feeding experiments. Molecular weight markers were located from the stained gel. Note the similarity between individual *D. polymorpha* (lanes A–E) and the distinctive difference between these lanes and the *E. coli* lane. There was no evidence for the presence of any of the recognized *E. coli* proteins in the *D. polymorpha* lanes (the heavy *E. coli* bands at about 50 kDa and 95–100 kDa were not present in lanes A–E). Conversely, many of the major labeled proteins in the mussel tissue do not appear in the *E. coli* band.

polyacrylamide gel, does not show any overlap between *E. coli* proteins (lane F) and label incorporated into mussel proteins (A–E, each lane representing an individual *D. polymorpha*). The incorporation of ^{35}S into mussel proteins indicated the assimilation of bacterial components; *E. coli* proteins were not present in the bivalve samples.

The lack of bacterial contamination allowed us to determine the incorporation characteristics of nutrients into mussel tissue. Several individuals of each species were allowed to feed on labeled bacteria, removed to pondwater (500 ml, changed twice daily) containing no bacteria or label, and allowed to assimilate label for 48 h following the pulse exposure to radiolabeled bacteria. Whole animals were homogenized, then precipitated in TCA, and the precipitate was dissolved in 1 *M* NaOH. The ^{35}S incorporated into macromolecules/total ^{35}S removed from the bath was 0.29 ± 0.02 (n = 4), 0.23 ± 0.07 (n = 4), and 0.28 ± 0.02 (n = 5) for *D. polymorpha*, *Corbicula fluminea*, and *Carunculina texasensis*, respectively. Thus, regardless of mussel species, about 26% of the label that disappeared from the bath was incorporated into mussel protein 48 h after the pulse feeding experiment. There were no significant differences between animal species in the proportion of ^{35}S assimilated into mussel protein from *E. coli*. Formalin-fixed control tissue had no detectable radioactivity.

Volume of water cleared of bacteria

Increasing the volume of fluid available for clearance by *D. polymorpha* while maintaining a constant concentration of bacteria per milliliter allowed us to determine clearance rates over different volumes, but with differing quantities of total bacteria present in the APW (Fig. 3). The rate constants (slope) for the different volumes were 20 ml, −0.098 ± 0.01 min^{-1}, 60 ml, −0.029 ± 0.001 min^{-1}; 120 ml, −0.009 ± 0.001 min^{-1}. These slopes were significantly different from each other ($P < 0.01$). When expressed as clearance (ml g^{-1} dry tissue min^{-1}), the values were 20 ml, 143 ± 25; 60 ml, 189 ± 26; and 120 ml, 113 ± 11. These weight-specific clearance rates were not significantly different from each other ($P > 0.05$). Because *D. polymorpha* in this data set weighed about 15 ± 1 mg (n = 55), the animals cleared 1.7–2.8 ml animal^{-1} min^{-1} under all experimental conditions, or roughly 2.4–4 liters of water per day for an average animal (about 8.9 l g^{-1} dry tissue day^{-1}).

By varying the concentration of *E. coli* in a constant bath volume and determining the time-dependent (5–60 min) removal of particles from the suspension, we calculated the average clearance rates (Fig. 4). These data

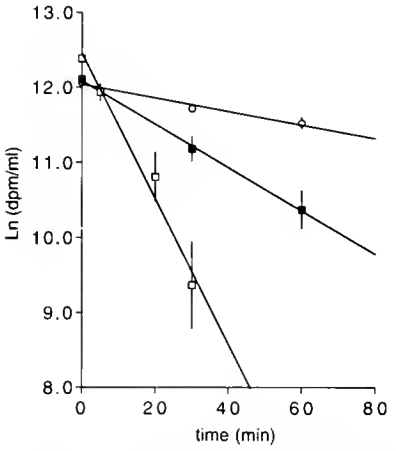

Figure 3. Clearance of ^{35}S-labeled *Escherichia coli* by *Dreissena polymorpha* from different volumes of pondwater containing 3 × 10^7 bacteria/ml. Open squares indicate experiments in 20 ml volume, filled squares in 60 ml, and open circles in 120 ml of pondwater. The vertical line indicates ±1 standard error. The slopes of the lines were significantly different ($P < 0.01$) but when multiplied by the bath volume and normalized to dry tissue weight the clearance values ranged from 113 to 189 ml g^{-1} min^{-1} and were not significantly different ($P > 0.05$).

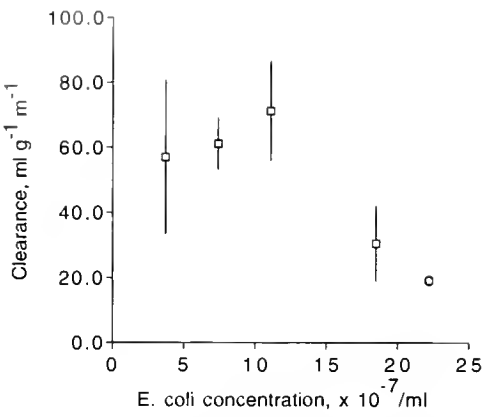

Figure 4. Clearance of *Escherichia coli* from 20 ml of artificial pondwater by *Dreissena polymorpha* as a function of bacterial concentration. Note that bacterial clearance appeared to be approximately constant between 3.7 and 11.1 $\times$ 10^7 bacteria/ml but was reduced at higher bacteria concentrations. The vertical lines represent $\pm$1 standard error.

indicate that *D. polymorpha* had a relatively constant rate of bacterial clearance when exposed to bacterial concentrations ranging from 3.7 to 11 $\times$ 10^7 bacteria/ml, but at concentrations greater than 18 $\times$ 10^7 bacteria/ml the apparent rate of bacterial filtration was significantly reduced ($P < 0.01$).

When bacteria concentration was kept at or below 3 $\times$ 10^7 bacteria/ml, no pseudofeces were observed over 60 min. When higher concentrations of bacteria were used, pseudofeces production was visually observed after roughly 60 min of exposure. Thus at the higher bacteria concentrations, pondwater was cleared of radioactivity but some of the label was deposited in pseudofeces rather than accumulated by the animal.

Maximal uptake of bacteria by D. polymorpha

In a few experiments, we followed the disappearance of *E. coli* from the bath under the standard conditions described in Figure 1, but allowed the mussel to remain in the container and added another aliquot of bacteria to the APW after 30 min. The bath was sampled at t_0 and t_{30} to measure isotope uptake. This procedure was repeated until the animal was no longer removing bacteria at the initial rate. Under these conditions five separate feedings were required before the removal of bacteria by the mussel was reduced (data not shown).

Clearance of other bacterial species

To determine whether bacterial species other than *E. coli* could be filtered, specimens of *D. polymorpha* were exposed to a variety of laboratory strains of several bacterial species of different sizes (0.8–1.1 μm width, 1.3–4.1 μm length), following the protocol used to produce Figure 1. Table III indicates the rates of clearance of the bacterial species by *D. polymorpha*, and the dimensions of each species including *E. coli*. In all cases except one, 55–91% of the bacterial cells were removed from the bath in 30 min and the calculated clearance rates were 50–80 ml g^{-1} dry tissue min^{-1}. The exception was *Bacillus megaterium*, which formed large chains of bacteria. Some of these bacterial chains settled to the bottom of our experimental containers and were not available in the APW for the mussel to filter. In this case, the corresponding clearance rate was significantly lower than for the other bacterial species.

Effects of laboratory storage of mussels on bacterial uptake

Separate experiments were performed on animals acclimated to the laboratory for various periods. Clearance rates of *E. coli* by *D. polymorpha* were not significantly different whether the mussels were tested 18 h after they were collected from the Mississippi River or after they had been stored in the laboratory, unfed, for a week: 105 $\pm$ 17 (n = 10) versus 108 $\pm$ 24 (n = 10) ml g^{-1} dry tissue min^{-1} 18 h after collection and one week later, respectively. Furthermore, these clearance rates were not significantly different from that of *D. polymorpha* maintained in the laboratory, unfed, for several weeks.

Cirral structure

Briefly, the cirrus organelle is composed of two plates of fused cilia and beats from a flexed to an extended position (Moore, 1971; Owen, 1974). In the flexed position the cirri bend up over the frontal surface of the filament. In the extended position, the cirri lie in the interfilament

Table III

Mean cell dimensions (n > 50 for each bacterium) for bacteria used in Dreissena polymorpha *studies measuring the clearance from 20 ml APW*

Bacterium species	Cell dimensions (L $\times$ W) μm	Dry tissue, mg	Clearance, ml g^{-1} dry tissue min^{-1}
Citrobacter freundii	1.3 $\pm$ 0.3 $\times$ 0.8 $\pm$ 0.1	12 $\pm$ 1	64 $\pm$ 12 (9)[a]
Enterobacter aerogenes	1.5 $\pm$ 0.3 $\times$ 0.9 $\pm$ 0.1	17 $\pm$ 2	50 $\pm$ 10 (9)[a]
Serratia marcescens	1.8 $\pm$ 0.5 $\times$ 0.8 $\pm$ 0.1	13 $\pm$ 1	52 $\pm$ 12 (8)[a]
Escherichia coli	2.3 $\pm$ 0.6 $\times$ 0.9 $\pm$ 0.1	18 $\pm$ 4	80 $\pm$ 11 (11)[a]
*Bacillus megaterium**	3.6 $\pm$ 1.0 $\times$ 1.1 $\pm$ 0.2	15 $\pm$ 1	14 $\pm$ 1 (9)[b]
Bacillus subtilus	4.1 $\pm$ 0.8 $\times$ 0.9 $\pm$ 0.2	14 $\pm$ 1	59 $\pm$ 6 (9)[a]

Mean $\pm$ standard error (n). The chains did not remain in suspension during the course of the experiment. Clearance values with different letters are significantly different using Fisher's PLSD test.

* Bacteria in this culture were present in chains with an average length of 14.5 $\pm$ 3.7 μm.

space opposing the cirri from the adjacent filament. When extended, each cirrus, along with its adjacent cirri, forms a filtration trap that does not allow movement of particles down into the ostia of the gill. Trapped particles are passed to the frontal cilia when the cirri bend into their flexed position. Differences in the structure of the cirri of *D. polymorpha, Corbicula fluminea,* and *Carunculina texasensis* are shown in Figure 5. The free tips of the cirral cilia form the filtration traps, and the spaces between ciliary tips are in the 0.5-μm range for *Dreissena.* Note the smaller cirral structure of *C. texasensis* compared with the other two species.

Even with an osmotically balanced fixative, gill shrinkage in *Carunculina texasensis* was 16.6% (dorsal-ventral, long axis of the filament) and 38.9% (anterior-posterior); 14.4% and 33.4% in *Corbicula fluminea;* and 23.0% and 25.2% in *D. polymorpha.* In *Carunculina* and *Corbicula* the differential shrinkage between length and width is due to the relatively rigid connective tissue support. *Carunculina* manifests this support as calcified chitinous rods supporting the filaments. *D. polymorpha* shows less support, and shrinkage was more uniform.

Discussion

Dreissena polymorpha was capable of filtering and ingesting large numbers of laboratory-cultured bacteria from the water column. On an individual animal basis with no standardization for size differences among animals, *Corbicula fluminea* cleared *E. coli* at a significantly lower rate ($P < 0.01$) than did *D. polymorpha,* but at a higher rate than did *Carunculina texasensis.* When standardized on the basis of dry tissue weight, the bacterial clearance rate was 30–100 times higher in *D. polymorpha* than in the other two bivalve species. Standardization on the basis of dry tissue weight provides a convenient normalization for clearance study comparisons. However, surface area of the gill is likely to be physiologically important with regard to the actual mechanism of particle capture. Both *Corbicula fluminea* and *Carunculina texasensis* had gill surface areas that were about 1.5 mm^2/mg dry tissue, whereas *D. polymorpha* had about 14 mm^2/mg dry tissue (Table IV). When gill surface area was used as a normalizing factor, it was apparent that the dreissenid species had a greater ability to capture *E. coli* than did the other two species. A regression analysis comparing *E. coli* clearance from the APW with cirri g^{-1} dry tissue among the bivalve species was highly significant ($r = 0.998$; $P < 0.05$), with 100–200 times more cirri in *D. polymorpha* than in the other bivalves.

In addition to gill surface area, another major difference among these three species was the complexity of the laterofrontal cirri associated with the gill filaments. Gill cirri lie between the lateral ciliated cells and the surface of the filaments. The lateral ciliated cells and perhaps the musculature in eulamellibranch gills provide the force for water movement. Although there is considerable debate on the exact mechanism of particle capture (hydrodynamic vs. direct mechanical contact; see Nielsen *et al.,* 1993), the movement of cirri, frontal and abfrontal cilia are apparently coordinated to intercept, capture, and move particles. Recent endoscopic work indicates that ciliary activity, mucus, and water current are important in transporting particles toward the mouth once they are captured (Beninger *et al.,* 1993; Ward *et al.,* 1993). When the cirri are extended, they are directly in the path of water flow between the filaments. The cirri are positioned to trap particles and direct them toward the filament apex and the frontal cilia when the cirri are flexed (unpub. obs.). In the extended position, cirri form an effective filtration "trap" or "net." Unfortunately, the words *trap* and *net* may seem to exclude the possibility of considering water current generation by the cirri as part of the filtration mechanism or "trap." However, if the term is defined to mean "barrier" or "intercepting unit" then the comments here are compatible with previous endoscopic and microscopic observations of particle transport and particle "bouncing" (Jørgensen, 1976; Ward *et al.,* 1993).

The scanning electron micrographs demonstrate clearly that the cirri of *D. polymorpha* and *Corbicula fluminea* are more complex than those of *Carunculina texasensis.* The cirri in the first two species are composed of two ciliary plates containing as many as 42 cilia per plate (unpub. obs.). The cirri of *Carunculina* are less complex, consisting of 11–13 cirri per plate, and not as long or as rigid as those in the other species (Fig. 5; Table IV). The organization, or number of cirri along the filament (cirri/mm), also was much reduced in *Carunculina* compared to the other species. Although the shorter, less organized cirri were apparently able to intercept some *E. coli, C. texasensis* captured *E. coli* less effectively than did the other two species. The enhanced ability of the species with more complex cirri to filter *E. coli* is consistent with the hypothesis that the cirri are acting as particle-capturing structures (Owen, 1974; Owen and McCrae, 1976). This is likely to be particularly true for small (<2 μm) particles. Indeed, using laser confocal microscopy to study *in vitro* gill strips, we have observed the interaction between 0.75 μm fluorescent particles and individual cirri at a resolution approaching 0.2 μm (unpub. obs.). Morphometric analysis also indicates that when adjusted for animal dry weight, the number of cirri in a standard-sized *Corbicula fluminea* is similar to that in *Carunculina texasensis,* and is about two orders of magnitude less than that of *D. polymorpha* (Table IV). On a dry-weight basis, *D. polymorpha* had a clearance rate two orders of magnitude higher than *Carunculina texasensis* and 30 times greater than *Corbicula fluminea.*

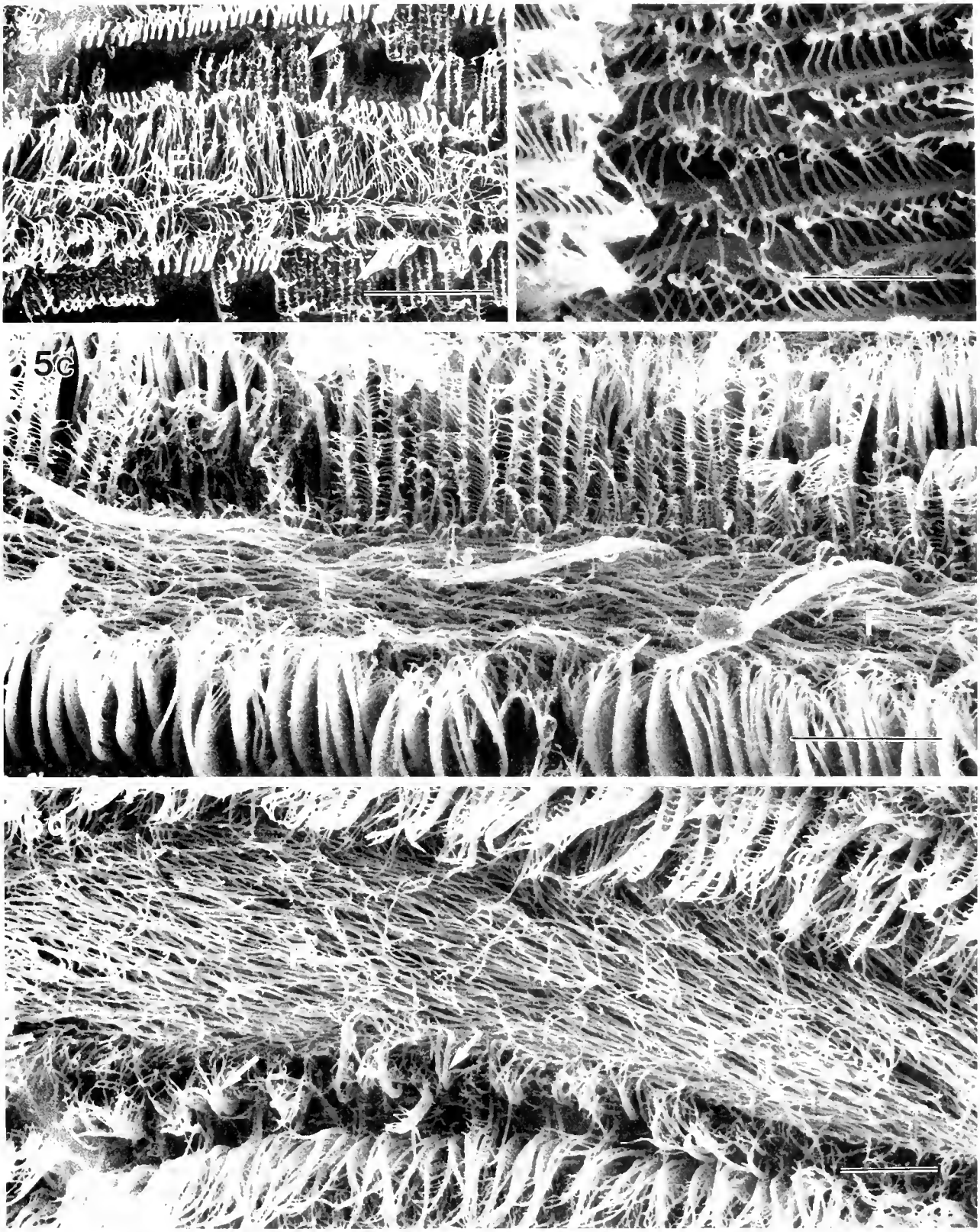

Figure 5. Scanning electron micrographs of gill filaments from *Dreissena polymorpha*, *Corbicula fluminea* and *Carunculina texasensis*. (a) Lower magnification of a *D. polymorpha* gill filament and portions of the

Table IV

Morphometric characteristics of gills from representative bivalves used in bacterial clearance studies

Bivalve species	Animal dry mass, mg	Live gill area, mm^2 per mg dry tissue	Cilia per cirri	Cirri/mm^2 dry gill	Cirri/mm^2 live gill	Cirri/mg dry tissue
Dreissena polymorpha	13.3	13.72	38–42	44,161	16,863	45,556
Corbicula fluminea	392	1.44	32–33	35,802	20,430	330
Carunculina texasensis	100	1.68	11–13	11,263	5,526	189

Many authors have shown that clearance rates of bivalves are dependent on the number of particles in the water column (Morton, 1971; Walz, 1978). Foster-Smith (1975) demonstrated that assimilation efficiency was related to the number of particles taken up by marine bivalves. The same author noted that pseudofeces are produced at particle concentrations associated with high assimilation efficiency. Walz (1978) documented a threshold of clearance below which *Dreissena* does not produce pseudofeces. We observed that no pseudofeces were produced in 30 min at bacterial concentrations that stimulated maximal particle clearance rates. This observation, coupled with our experimental pulse-washout procedures designed to minimize recycling of label, allowed us to estimate the incorporation of ^{35}S directly from bacteria. Despite the differences in filtering ability among the three species, the incorporation of ^{35}S derived from *E. coli* was similar. Even though the absolute quantity of *E. coli* ingested differed among the species, the amount of label incorporated into mussel protein per total label ingested was about 26% and did not differ among the three species.

The present study indicates that, when the results are normalized on a whole-animal basis, *D. polymorpha* and, to a lesser extent, *Corbicula fluminea* were better able to use *E. coli* than was the unionid species studied. However, and perhaps more importantly, on a dry-weight basis *D. polymorpha* was substantially better than either of the other species in clearing *E. coli* from the APW. The differences in ability to use the bacterial food source appear to correlate rather well to the different structures associated with particle capture in these species. The gill of *Dreissena* is large compared to the size of its body, and it has 138 times as many cirri as found in *Corbicula fluminea*. However, *D. polymorpha* cleared bacteria only 32 times faster than did *Corbicula fluminea*. *Corbicula* may move more water per gill surface area to achieve the observed rate of bacterial particle capture (see Way *et al.*, 1990). The differences in clearance rate described here are for a single bacterial species under laboratory conditions, and provide no information on particle selection by these bivalves. The current study also does not address the transport of particles once they are captured.

We recalculated a clearance rate from the data obtained by Reeders *et al.* (1989) for *D. polymorpha* fed a mixed population of algae. Clearance values ranged from 80 to 180 ml g^{-1} dry tissue min^{-1}; the clearance rate we found for laboratory-cultured *E. coli* was within this range. Moreover, in a study in which several marine bivalves were selected on the basis of cirri size, retention efficiencies for particles >5 μm were similar in all species (Riisgård, 1988). However, small (2 μm) particles were poorly retained by bivalves with no cirri, but species with large cirri retained similar-sized particles with 30–70% efficiency (Riisgård, 1988).

adjacent filaments. Note the presence of cirri in both the extended (arrowheads) and flexed (arrows) positions. In the flexed position the cirri tips are located over the frontal cilia (F). The cirri in *D. polymorpha* can extend across the interfilament space. Cirri from opposite sides of the filament in the fully flexed position can cover most of the frontal surface of the filament. (b) Higher magnification of the interfilament space covered by two sets of cirri from adjacent filaments. Note the "net" that is formed by the 38–42 cirri tips. (c) A gill filament from *Corbicula fluminea* showing extended cirri (arrowheads), flexed cirri (arrows), and frontal cilia (F). The filtration net formed by extended cirri is apparent. The length of the cirri indicate that in the extended position the cirri span the interfilament space. There are a large number of cilia tips (32-33) associated with a single cirri. *Corbicula fluminea* also has frontal cirri (C) located among the frontal cilia. (d) A gill filament from *Carunculina texasensis* showing cirri in the extended position (arrowheads) and in the flexed position (arrows) on opposite sides of the frontal cilia (F). Cirri from an adjacent filament at the bottom of the micrograph are in a partially flexed position. Note that individual cirri have only 12–13 free cilia tips per cirri plate (Bars: a = 20 μm; b = 5 μm; c = 10 μm; d = 10 μm).

Determination of the environmental relevance of our observations will require further study. All the bacteria used in these experiments were from laboratory strains. Bacteria in nature tend to be smaller (<1 μm) than those grown in the laboratory (see Table III), and the numbers of bacteria present in the water column will differ from environment to environment as well as from the concentrations studied here (Prieur *et al.*, 1990). However, all of the following have been documented: (1) Food particle density is an important determinant of clearance rate of bacterial-sized particles in *Dreissena*. This is not unusual and has been reported for a number of bivalves feeding on many different particles sizes, including algae, diatoms, bacteria, and detritus (Walz, 1978). (2) *Dreissena* effectively filtered all strains of laboratory-sized bacteria (1–4 μm in length). (3) The 26% efficiency of conversion of *E. coli* proteins into bivalve proteins is well within the limits associated with an energetically feasible food source. (4) The rate at which freshwater bivalves cleared laboratory bacteria was directly related to the size and number of cirri per gill surface area.

The design of this study was purposely simplified to consider only a single component of the bivalve feeding mechanism—that of particle capture or clearance. However, these experiments raise several questions about the biology of freshwater bivalves that require further study. For example, are these species able to derive significant nutrients from natural-sized bacteria in the water column during or between algal blooms? Many studies have demonstrated that bivalves use bacteria present in the water column (*e.g.*, Mikheev and Sorokin, 1966; Lucas *et al.*, 1987; Prieur *et al.*, 1990). In particular, *Mytilus edulis*, a marine species with complex cirri, rapidly clears *E. coli* from the water column in laboratory experiments in which the bacterium was presented as the sole particle source or in the presence of algae (Birbeck and McHenery, 1982; McHenery and Birbeck, 1985). Do pseudofeces deposited on the substrate serve as a nutrient resource to enhance bacterial populations in a microhabitat around freshwater bivalves as has been observed in marine bivalves (Crosby *et al.*, 1990; reviewed by Prieur *et al.*, 1990)? Thus, the potential of freshwater bivalves to use bacteria could be an important factor influencing the distribution of these bivalves and merits continued study.

Acknowledgments

The authors thank Julie Cherry, Ron Bouchard, and Justin Marquez for their outstanding technical assistance. We thank T. R. LeBlanc at the Dow Chemical Company (Plaquemine, LA) for helping us collect zebra mussels. Cory Thompson participated in early experiments on support from a grant to improve undergraduate education from the Howard Hughes Medical Institute to LSU. K. Carman provided useful comment and discussion. We give special tribute to S. J. Nichols for the many hours she has spent sharing her insight on mussel feeding with us. The work was supported by Louisiana Sea Grants R/ZM-1-PD and NA46RG0096 project R/ZMM-1.

Literature Cited

Atkins, D. 1938. On the ciliary mechanisms and interrelationships of lamellibranchs. Part VII. Latero-frontal cilia of the gill filaments and their phylogenetic value. *Q. J. Microsc. Sci.* **80:** 346–430.

Beninger, P. G., J. E. Ward, B. A. MacDonald, and R. J. Thompson. 1992. Gill function and particle transport in *Placopecten magellanicus* (Mollusca: Bivalvia) as revealed using video endoscopy. *Mar. Biol.* **114:** 281–288.

Beninger, P. G., S. St-Jean, Y. Poussart, and J. E. Ward. 1993. Gill function and mucocyte distribution in *Placopecten magellanicus* and *Mytilus edulis* (Mollusca: Bivalvia): the role of mucus in particle transport. *Mar. Ecol. Prog. Ser.* **98:** 275–282.

Birbeck, T. H., and J. G. McHenery. 1982. Degradation of bacteria by *Mytilus edulis*. *Mar. Biol.* **72:** 7–15.

Bunt, C. M., H. J. MacIsaac, and W. G. Sprules. 1993. Pumping rates and projected filtering impacts of juvenile zebra mussels (*Dreissena polymorpha*) in western Lake Erie. *Can. J. Fish. Aquat. Sci.* **50:** 1017–1022.

Crosby, M. P., R. I. E. Newell, and C. J. Langdon. 1990. Bacterial mediation in the utilization of carbon and nitrogen from detrital complexes by *Crassostrea virginica*. *Limnol. Oceanogr.* **35:** 625–639.

Dietz, T. H., D. Lessard, H. Silverman, and J. W. Lynn. 1994. Osmoregulation in *Dreissena polymorpha*: the importance of Na, Cl, K, and particularly Mg. *Biol. Bull.* **187:** 76–83.

Foster-Smith, R. L. 1975. The effect of concentration of suspension on the filtration rates and pseudofaecal production for *Mytilus edulis* L., *Cerastoderma edule* (L.) and *Venerupis pullastra* (Montagu). *J. Exp. Mar. Biol. Ecol.* **17:** 1–22.

Fyhn, H. J., and J. D. Costlow. 1975. Anaerobic sampling of body fluids in bivalve molluscs. *Comp. Biochem. Physiol.* **52A:** 265–268.

Jørgensen, C. B. 1976. Comparative studies on the function of gills in suspension feeding bivalves, with special reference to effects of serotonin. *Biol. Bull.* **151:** 331–343.

Jørgensen, C. B. 1982. Fluid mechanics of the mussel gill: the lateral cilia. *Mar. Biol.* **70:** 275–281.

Jørgensen, C. B. 1989. Water processing in ciliary feeders, with special reference to the bivalve filter pump. *Comp. Biochem. Physiol.* **94A:** 383–394.

Jørgensen, C. B., T. Kiørboe, F. Møhlenberg, and H. U. Riisgård. 1984. Ciliary and mucus-net filter feeding, with special reference to fluid mechanical characteristics. *Mar. Ecol. Prog. Ser.* **15:** 283–292.

Laemmli, U. K. 1970. Cleavage of structural proteins during the assembly of the head of bacteriophage T4. *Nature* **227:** 680–685.

Leach, J. H. 1993. Impacts of the zebra mussel (*Dreissena polymorpha*) on water quality and fish spawning reefs in western Lake Erie. Pp. 381–397 in *Zebra Mussels: Biology, Impacts, and Control*, T. F. Nalepa and D. W. Schloesser, eds. Lewis Publ., Boca Raton, FL.

Lucas, M. I., R. C. Newell, S. E. Shumway, L. J. Seiderer, and R. Bally. 1987. Particle clearance and yield in relation to bacterioplankton and suspended particulate availability in estuarine and open coast populations of the mussel *Mytilus edulis*. *Mar. Ecol. Prog. Ser.* **36:** 215–224.

MacIsaac, H. J., W. G. Sprules, O. E. Johannsson, and J. H. Leach. 1992. Filtering impacts of larval and sessile zebra mussels (*Dreissena polymorpha*) in western Lake Erie. *Oecologia* **92:** 30–39.

McHenery, J. G., and T. H. Birbeck. 1985. Uptake and processing of cultured microorganisms by bivalves. *J. Exp. Mar. Biol. Ecol* **90:** 145–163.

Messing, J. 1979. A multipurpose cloning system based on the single-stranded DNA bacteriophage M13. Pp. 43–49 in *Recombinant DNA Technical Bulletin.* NIH Publication, No. 79–99, 2, Bethesda.

Mikheev, V. P., and Y. L. Sorokin. 1966. Quantitative studies of *Dreissena polymorpha* habits using the radiocarbon method. *Zhurnal Obshchey Biologii* **27:**463–472 (in Russian as cited by Morton, 1971).

Moore, H. J. 1971. The structure of the latero-frontal cirri on the gills of certain lamellibranch molluscs and their role in suspension feeding. *Mar. Biol.* **11:** 23–27.

Morton, B. 1971. Studies on the biology of *Dreissena polymorpha* Pall. V. Some aspects of filter-feeding and the effect of micro-organisms upon the rate of filtration. *Proc. Malacol. Soc. Lond. B* **39:** 289–301.

Morton, B. 1983. Feeding and digestion in bivalvia. Pp. 65–147 in *The Mollusca V. Physiology, Part 2,* A. S. M. Saleuddin and K. M. Wilbur, eds. Academic Press, New York.

Nielsen, N. F., P. S. Larsen, H. U. Riisgård, and C. B. Jørgensen. 1993. Fluid motion and particle retention in the gill of *Mytilus edulis:* video recordings and numerical modelling. *Mar. Biol.* **116:** 61–71.

Owen, G. 1974. Studies on the gill of *Mytilus edulis:* the eu-latero-frontal cirri. *Proc. R. Soc. Lond. B* **187:** 83–91.

Owen, G., and J. M. McCrae. 1976. Further studies on the latero-frontal tracts of bivalves. *Proc. R. Soc. Lond. B* **194:** 527–544.

Prieur, D., G. Mevel, J.-L. Nicolas, A. Plusquellec, and M. Vigneulle. 1990. Interactions between bivalve molluscs and bacteria in the marine environment. *Oceanogr. Mar. Biol. Annu. Rev.* **28:** 277–352.

Reeders, H. H., A. Bij de Vaate, and F. J. Slim. 1989. The filtration rate of *Dreissena polymorpha* (Bivalvia) in three Dutch lakes with reference to biological water quality management. *Freshwater Biol.* **22:** 133–141.

Richard, P. E., T. H. Dietz, and H. Silverman. 1991. Structure of the gill during reproduction in the unionids *Anodonta grandis, Ligumia subrostrata,* and *Carunculina parva texasensis. Can. J. Zool.* **69:** 1744–1754.

Riisgård, H. U. 1988. Efficiency of particle retention and filtration rate in 6 species of Northeast American bivalves. *Mar. Ecol. Prog. Ser.* **45:** 217–233.

Silvester, N. R., and M. A. Sleigh. 1984. Hydrodynamic aspects of particle capture by *Mytilus. J. Mar. Biol. Assoc. U. K.* **64:** 859–879.

Sprung, M., and U. Rose. 1988. Influence of food size and food quantity on the feeding of the mussel *Dreissena polymorpha. Oecologia* **77:** 526–532.

Stanczykowska, A., W. Lawacz, J. Mattice, and K. Lewandowski. 1976. Bivalves as a factor effecting circulation of matter in Lake Mikolajskie (Poland). *Limnologica* **10:** 347–352.

Ten Winkel, E. H., and C. Davids. 1982. Food selection by *Dreissena polymorpha* Pallas (Mollusca: Bivalvia). *Freshwater Biol.* **12:** 553–558.

Walz, N. 1978. The energy balance of the freshwater mussel *Dreissena polymorpha* Pallas in laboratory experiments and in Lake Constance. I. Pattern of activity, feeding, and assimilation efficiency. *Arch. Hydrobiol. Suppl.* **55:** 83–105.

Ward, J. E., B. A. MacDonald, R. J. Thompson, and P. G. Beninger. 1993. Mechanisms of suspension feeding in bivalves: resolution of current controversies by means of endoscopy. *Limnol. Oceanogr.* **38:** 265–272.

Way, C. M., D. J. Hornbach, C. A. Miller-Way, B. S. Payne, and A. C. Miller. 1990. Dynamics of filter-feeding in *Corbicula fluminea* (Bivalvia: Corbiculidae). *Can. J. Zool.* **68:** 115–120.

Wiegman, T., M. G. Woldring, and J. J. Pratt. 1975. A new cocktail for liquid scintillation counting of aqueous radioimmunoassay samples. *Clin. Chim. Acta* **59:** 347–356.

Reference: *Biol. Bull.* 189: 320–329. (December, 1995)

The Effect of Salinity and Temperature on Spawning and Fertilization in the Zebra Mussel *Dreissena polymorpha* (Pallas) from North America

PETER P. FONG[1], KEIICHIRO KYOZUKA[2], JILL DUNCAN, STACY RYNKOWSKI, DANIEL MEKASHA, AND JEFFREY L. RAM*

Department of Physiology, Wayne State University, Detroit, Michigan 48201

Abstract. Zebra mussels have dispersed from their original site of introduction in the Great Lakes into the Mississippi River, Hudson River, and other watersheds in which they will encroach upon brackish water estuaries. To investigate their likelihood of reproductive success in such estuaries, we investigated the conditions of temperature, salinity, and acclimation under which spawning and fertilization could occur. Reproductive function of mussels that were acclimated to salinities up to 7.0 parts per thousand (ppt) at 12°, 20°, and 27°C for 1 to 21 days was tested. Reproductive function of non-acclimated mussels that had been maintained in fresh-water aquaria was also tested in various salinities. Spawning was induced by serotonin, previously demonstrated to elicit spawning of fertile gametes in fresh water. Successful fertilization was indicated by oocyte cleavage after adding sperm. Non-acclimated mussels spawned in salinities of 1.75 and 3.5 ppt at 12°, 20°, and 27°C, but not at 7.0 ppt. Fertilization using gametes from non-acclimated mussels occurred only in fresh water and at 1.75 ppt. Acclimation for as little as 2 days enhanced spawning. Fertilization rate in a salinity of 3.5 ppt improved within 4 days of acclimation and continued at a high level for as long as 21 days of acclimation. Although animals acclimated for 4 days in 3.5 ppt spawned readily when tested in salinities as high as 7.0 ppt, almost no fertilization occurred in 7.0 ppt. The reduction in fertilization at increasing salinities may be due in part to reduced sperm motility. Unfertilized oocytes remain intact for hours in fresh water; however, in salinities as low as 0.7 ppt, unfertilized oocytes tended to rupture within 2 hours. These data show that although sudden increases in salinity produce an immediate decrease in the reproductive capacity of zebra mussels, acclimation to brackish water can occur, and zebra mussels may be able to reproduce in brackish water below 7.0 ppt.

Received 22 August 1994; accepted 14 September 1995.

*To whom all correspondence should be sent.

Present address: [1]Department of Biology, Gettysburg College, Gettysburg, PA 17325, [2]Asamushi Marine Biological Station, Tohoku University, Asmushi, Aomori, 039-34, Japan.

Introduction

Zebra mussels (*Dreissena polymorpha*) have spread rapidly throughout North America since their accidental introduction in the mid-1980s (Hebert *et al.*, 1989). Their geographical distribution and the factors controlling it have been the focus of a number of studies (Mackie *et al.*, 1989; Griffiths *et al.*, 1991; Strayer, 1991; Ramcharan *et al.*, 1992). Strayer and Smith (1993) predicted that the downstream movement of zebra mussels will eventually carry them to estuarine sections of North America. At present, zebra mussels occupy brackish waters in the Hudson River estuary at West Haverstraw, New York (Walton, 1992; D. L. Strayer, pers. comm.), and with populations already well established in the Susquehanna and Mississippi Rivers, areas such as Northern Chesapeake Bay and the Mississippi River delta are at particular risk of invasion.

Unlike most freshwater bivalves, zebra mussels are free-spawners, releasing large numbers of gametes directly into the water, where fertilization occurs (Sprung, 1987). However, environmental tolerance to salinity may not be the same for gametes as for adults. Thus, even though adult zebra mussels may be capable of withstanding a range of salinities, these conditions may be suboptimal or lethal for freshly released gametes and may interfere

with fertilization. Similar situations are common in brackish-water organisms. In the viviparous polychaete *Neanthes limnicola,* higher salinities reduce the number of juveniles born and probably interfere with oogenesis (Fong and Pearse, 1992). In the brackish-water macrophyte *Myriophyllum crispatum,* higher salinities block both sexual and asexual reproduction (James and Hart, 1993). Higher salinities reduce reproductive capacity in brackish-water populations of *Daphnia magna* (Arner and Koivisto, 1993). Eggs of the yellow perch (*Perca flavescens*) suffer higher mortality with increasing salinity (Victoria *et al.,* 1992). In the striped mullet (*Mugil cephalus*), lower salinity reduces fertilization and sperm motility (Lee *et al.,* 1992). Thus salinity may have salient effects on reproductive processes, including spawning and fertilization, in zebra mussels.

Estuarine and brackish-water populations of adult zebra mussels occur throughout Europe in both tidal and nontidal bodies of water (Ludyanskiy *et al.,* 1993); however, no experiments to date have examined the reproductive potential of zebra mussels in different salinities. If reproduction is reduced or inhibited in estuarine areas, then maintenance of adult populations in these areas will depend largely upon larvae derived from upstream sources, and local recruitment will be negligible. Such information is directly relevant for modeling zebra mussel spread (*e.g.,* Neary and Leach, 1992; Ramcharan *et al.,* 1992) in all North American estuaries at risk of invasion, as well as some brackish inland lakes. In the present paper, we report on the effects of salinity and temperature on spawning and fertilization in salinity-acclimated and non-acclimated zebra mussels.

Materials and Methods

Acclimation and spawning experiments

Animals (13–25 mm in length) were collected on several occasions in 1994, from late May to the end of June, from western Lake Erie at Monroe, Michigan, (41° 54'N, 83° 23'W). Mussels were immediately transported to the laboratory and maintained in a thermostatically controlled 70-gallon aquarium at 12°C until use. This main holding tank was originally filled with Detroit tap water, and at intervals the water was partially replaced (up to 20% per week) from the same source. As a result of feeding, sediments associated with animals, the animals themselves, etc., average ion concentrations in the aquarium water are somewhat higher than those in the tap water. This water has been measured to contain 1.0 m*M* sodium, 0.25 m*M* potassium, and 1.4 m*M* calcium (Walker and Ram, 1994).

For acclimation to different conditions of temperature and salinity, clusters of animals were transferred to separate aquaria with the requisite conditions. Before being used in an experiment, animals were individually transferred to vials having the temperature/salinity combination being tested, and except for acute tests, were maintained in individual vials under these conditions for 1 day before testing. A schematic diagram of a typical sequence of holding, acclimating, and testing conditions is illustrated in Figure 1.

Specifically, about five clusters (8 cm diameter) of mussels were placed into 2.5-gallon aquaria equipped with aquarium heaters and cascading water pumps for circulation. Groups of animals were acclimated to 12 different temperature-salinity combinations: aquaria were maintained at 12°, 20°, or 27°C, and at each temperature separate aquaria contained either aquarium water (AW, water from our main holding tank), or water of a higher salinity (1.75, 3.5, or 7.0 ppt). Desired salinities were achieved by diluting Instant Ocean with AW.

Animals were acclimated for up to 21 days without added food, and the water was changed every 3 days. Food was withheld so as not to introduce additional variables in water quality. In histological studies of *Dreissena* starved for 30 days, Bielefeld (1991) reported that gonads were relatively resistant to degeneration compared to digestive gland and that the gonad/body quotient decreased only slightly. Furthermore, as reported in this paper for controls (*e.g.,* AW, 20°C), spawning and fertilization continued to occur at high levels even after animals were maintained without food for up to 21 days.

In our first experimental series, spawning tests (described below) were conducted on days 0 (no acclimation), 1, 2, 6, and 13. Zebra mussels did not survive at 7.0 ppt for more than 2 days. Thus, after 2 days of acclimation, mussels to be tested for spawning in 7.0 ppt were taken from the 3.5-ppt aquaria and transferred to individual vials containing water at 7.0 ppt for 24 h before spawning was tested.

Spawning experiments on acclimated animals were repeated with a second group of animals, but in this case, long-term acclimation to salinities greater than 3.5 ppt was preceded by exposure to intermediate salinities, as described below. Animals tested for spawning on days 0 (no acclimation) and 1 were acclimated in AW, 1.75, 3.5, and 7.0 ppt at 12°, 20°, and 27°C. On day 4, mussels from AW, 1.75, and 3.5 ppt were tested along with mussels tested in 6.0 ppt that had been acclimated for 3 days in 3.5 ppt and then transferred to vials containing 6.0 ppt for the final 24 h preceding testing. On day 7, animals previously acclimated in 1.75 ppt were transferred to 3.5 ppt and those previously in 3.5 ppt were transferred to 5.0 ppt for an additional 7 days. On the 14th day of acclimation, some animals in 5.0 ppt were transferred to vials containing 6.0 and 7.0 ppt and were tested for spawning on the following day.

Spawning was tested by exposing animals to 10^{-3} *M* serotonin (5-hydroxytryptamine; 5-HT), which, as shown

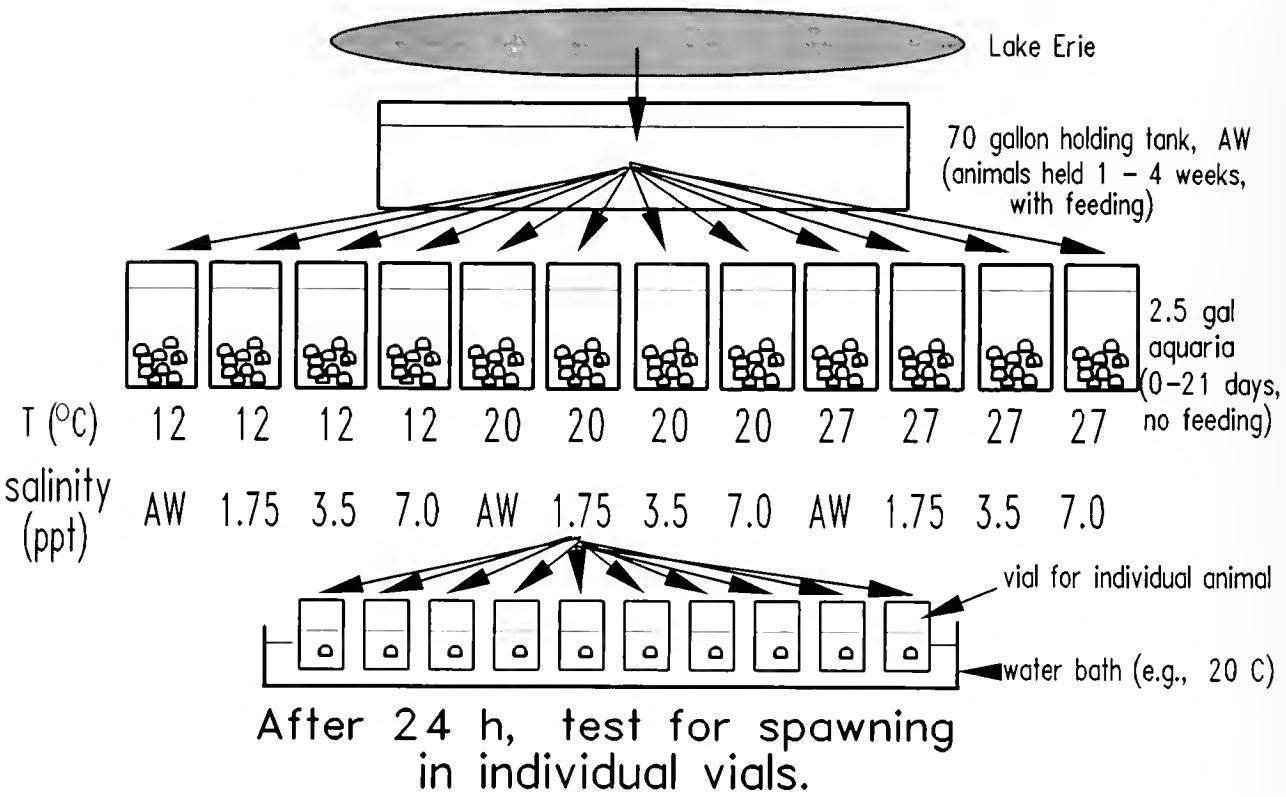

Figure 1. Diagram of the experimental design for testing spawning responsiveness of zebra mussels acclimated to various conditions of salinity and temperature. Testing of spawning responses of individual animals, illustrated here for 10 animals from just one temperature/salinity condition, was similarly performed for all other conditions. Non-acclimated animals (0 days in the 2.5-gal aquaria) went directly from the 70-gal holding tank of aquarium water (AW) into individual vials for testing with serotonin after 1 h in their individual temperature/salinity conditions.

by Ram *et al.* (1993), reliably elicits spawning in fresh water. About 24 h prior to the spawning test, acclimated animals were transferred to vials (1 mussel/vial, 10–15 animals per salinity/temperature condition) containing 9 ml of water at the same salinity and temperature in which they had previously been acclimated. Temperature was maintained by immersing the vials in thermostatically controlled water baths. The test was begun by the addition of 1 ml of 10^{-2} *M* 5-HT to each vial (for a final concentration of 10^{-3} *M*), and spawning was assessed visually and microscopically for up to 4 h after 5-HT addition. After 4 h, the gonads of all nonspawners were dissected and their sex and reproductive maturity determined under compound microscopy to calculate percent spawning in each group. Non-acclimated animals were tested with identical procedures except that they were transferred from the main holding aquarium (AW, 12°C) to vials at the appropriate salinity and temperature and tested for spawning by adding 5-HT 1 h after transfer.

To investigate whether salinity had an effect on the motility of freshly released sperm, we exposed sperm from non-acclimated mussels spawned in AW to salinities of 1.75, 3.5, and 7.0 ppt at room temperature (23°C). Sperm from salinity-acclimated mussels were similarly observed in their respective spawning salinities. Sperm motility was assessed by visual observation with a compound microscope (400×). Sperm were classified as either highly motile (the usual state of sperm in AW), reduced in motility, or immotile.

Fertilization experiments

We tested the effect of salinity on fertilization of oocytes obtained from salinity-acclimated and non-acclimated zebra mussels. Acclimated (for 4 days and 21 days at 20°C) and non-acclimated mussels (n = 30 mussels in each salinity) were placed in individual 20-ml vials in 9 ml of water having salinities of AW, 1.75, 3.5, and 7.0 ppt. All animals tested in 7.0 ppt were initially acclimated in 3.5 ppt and then transferred to 7.0 ppt overnight at 20°C before spawning was induced. To each vial, 1 ml of 10^{-2} *M* 5-HT was added until spawning occurred.

Sperm suspensions were made by mixing equal volumes of sperm from 3 to 5 males at each salinity into a separate vial. These sperm suspensions were then diluted to a density of 10^{10} sperm/ml measured with a hemacytometer. A volume of 10 μl of diluted sperm suspension was added to wells of a 24-well culture plate containing 1.0 ml of oocyte suspension (see below) for a final concentration of 10^8 sperm/ml. At this sperm concentration, high fertilization rates (>75%) can be obtained (data in this paper and unpublished data by K. Kyozuka in this laboratory), although polyspermy may also be occurring (Misamore *et al.*, 1994).

Egg suspensions from single females were prepared by counting the number of spawned oocytes in a 20-μl pipette and adjusting the volume to get a concentration of 1000 oocytes/ml. Oocytes were then diluted by 50% for a final concentration of 500 oocytes per well in 1.01 ml of sperm-egg water, or 1.0 ml of egg suspension alone (no-sperm controls in the 21-day acclimation experiment). All fertilization tests were done at room temperature (23°C). Oocytes were observed at 200× on an inverted microscope up to 3.5 h after the addition of sperm. Between 67 and 124 oocytes from each well were assessed for fertilization, as indicated by cleavage to at least the two-cell stage within 3.5 h. For mussels acclimated for 21 days, we also enumerated the number of oocytes that had ruptured.

Statistical analysis

Effects of acclimation to various salinity and temperature combinations were tested in two similar, albeit not identical, spawning experiments. Similarly, fertilization replicates used oocytes from individual animals independently tested, but the animals had been acclimated together in group tanks in two nonidentical experiments. Since the lack of identical replicates of acclimation conditions prevents us from applying inferential statistics validly, conclusions are drawn on the basis of the consistency of the findings over similar conditions, refraining from using inferential statistics when these cannot be validly applied, as recommended by Hurlbert (1984). Accordingly, some statements regarding whether a response is "higher" or "lower" are made based on consistency or direction of the data, unaccompanied by a statistical analysis. Tests on non-acclimated animals, however, are true replicates of experimental conditions because all animals came from a common holding tank, and each animal was independently exposed in its own vial to a given temperature/salinity condition. For fertilization, the percentage of fertilized oocytes from several females was analyzed by one-way ANOVA. For spawning, analyses for dichotomous data (spawning *vs.* no spawning of individually tested animals; Fisher's exact test) were used to determine if the occurrence of spawning was randomly distributed (null hypothesis). Extensive experience with testing spawning in zebra mussels in this laboratory in a large number of independent experiments over several years (Ram *et al.*, 1993; Fong *et al.*, 1993, 1994) has indicated that under standard conditions (AW, 20–25°C, during June to mid-August) the percentage of animals spawning in response to 10^{-3} *M* 5-HT ranged between 60% and 100%. Furthermore, when 10–15 animals were tested in independent replicates of each experimental condition, percentage differences in spawning of >30% between treatments were usually statistically significant.

Results

Acclimation and spawning experiments

Results of the first acclimation experiment, including data from non-acclimated animals tested in the same series, are illustrated in Figure 2. The percentage of animals spawning was as high as 90% in AW at 20°C. Without acclimation, spawning in 7.0 ppt occurred in <10% of the animals tested, significantly lower than in AW at all temperatures (Fisher's exact test, for 12°C, $P < 0.006$; for 20°C, $P < 0.00007$; for 27°C, $P < 0.04$, Fig. 2A). Intermediate salinity conditions (1.75 ppt, 3.5 ppt) did not differ markedly from spawning tested in AW at all temperatures, although there is a clear tendency, occurring both with and without acclimation, for spawning to occur in a higher percentage of animals at 20°C than at either 12° or 27°C.

With acclimation, spawning rates in the various salinities and temperatures tended to maintain the same relative positions, with the most notable change being a rise to more than 80% in spawning rates tested in 7.0 ppt after 13 days of acclimation. With 1-day acclimation, 7.0 ppt was still inhibitory to spawning (Fig. 2B). After acclimation for 2 days, spawning rates were higher in all conditions except for 7.0 ppt at 27°C. These increases in percent spawning from 1 day to 2 days of acclimation were particularly notable in 7.0 ppt at both 12°C and 20°C (compare 7.0 ppt in Fig. 2B to Fig. 2C). By the 6th day of acclimation, mussels in all conditions spawned at a high percentage, and this continued to the 13th day (Fig. 2D, E).

A repeat of the acclimation experiment yielded similar results. Without acclimation and with a 1-day acclimation, 7.0 ppt was inhibitory to spawning (Figs. 3A, B). As in the first experiment, where differences in spawning as a function of temperature were present, higher spawning rates were observed at 20°C than at either 12°C or 27°C. By the 4th day of acclimation, mussels in all groups spawned at a high percentage (>70%, Fig. 3C) at all temperatures. Mussels tested on the 15th day had been ac-

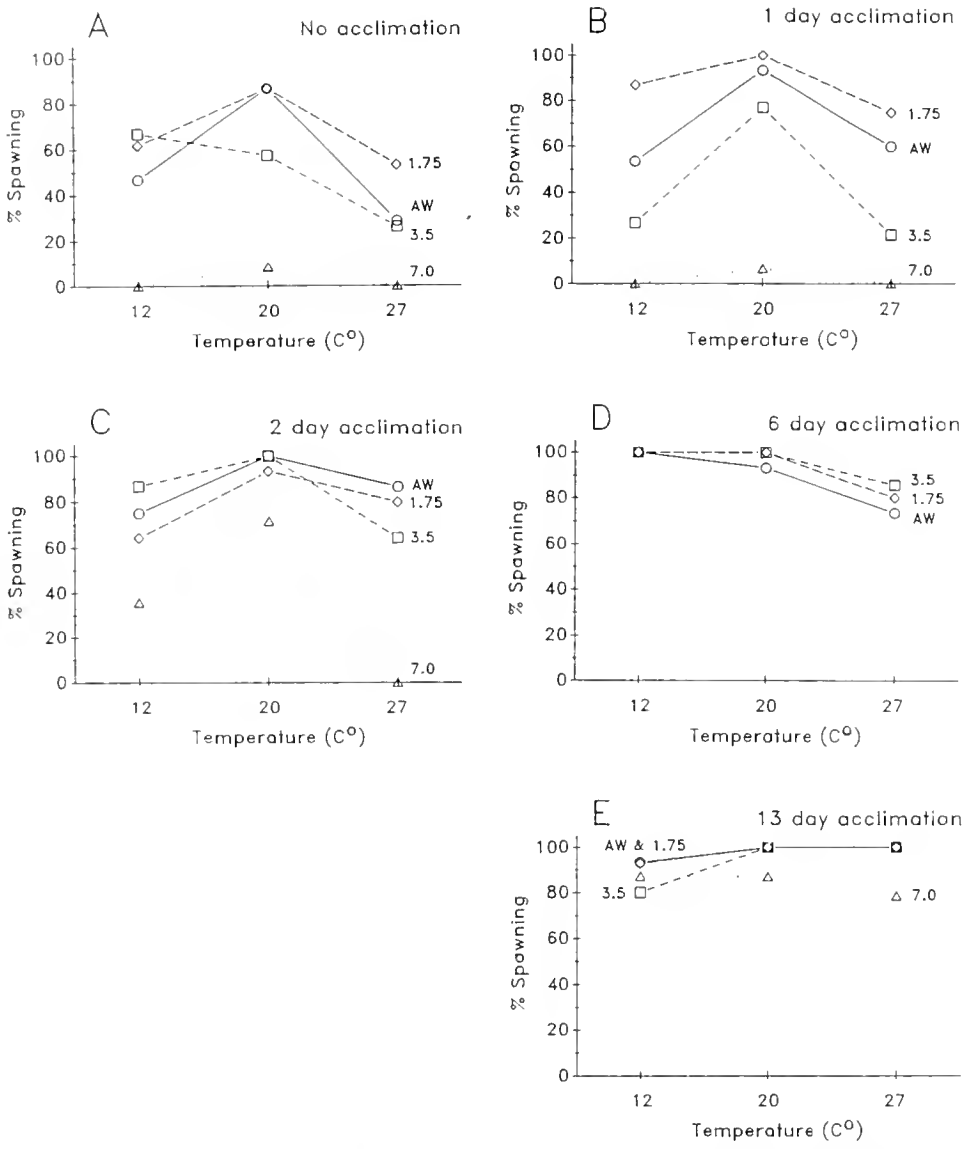

Figure 2. Effect of salinity, temperature, and duration of acclimation on serotonin (10^{-3} *M*)-induced spawning. Zebra mussels were acclimated in aquarium water (AW), 1.75, 3.5, and 7.0 ppt at 12°, 20°, and 27°C and tested for spawning after (A) no acclimation to any salinity/temperature condition (previously maintained in AW, 12°C); (B) 1-day acclimation; (C) 2-day acclimation; (D) 6-day acclimation; and (E) 13-day acclimation. In the 13-day acclimation experiment, mussels tested for spawning in 7.0 ppt were acclimated for 12 days in 3.5 ppt and then transferred to 7.0 ppt for 1 day before testing. Each point represents the percentage of animals spawning out of 12–15 animals tested for each salinity/temperature/duration condition.

climated to a gradual increase in salinity, and all groups spawned at frequencies of 80% or higher (Fig. 3D).

The motility of sperm from non-acclimated mussels was affected by salinity. Sperm taken from aquarium water and transferred directly to either 3.5 or 7.0 ppt exhibited either greatly reduced motility or no movement at all. Sperm transferred to 1.75 ppt had noticeably reduced motility. Sperm spawned from mussels that had been acclimated to higher salinities for 1 to 2 days also showed reduced motility or were completely immotile in all series. By the 6th day of acclimation, however, no obvious reduction in sperm motility was observed at any salinity.

Fertilization experiments

Although 1.75 ppt had no acute or long-term effect on fertilization, higher salinities had inhibitory effects that could be at least partially reversed by acclimation (Fig.

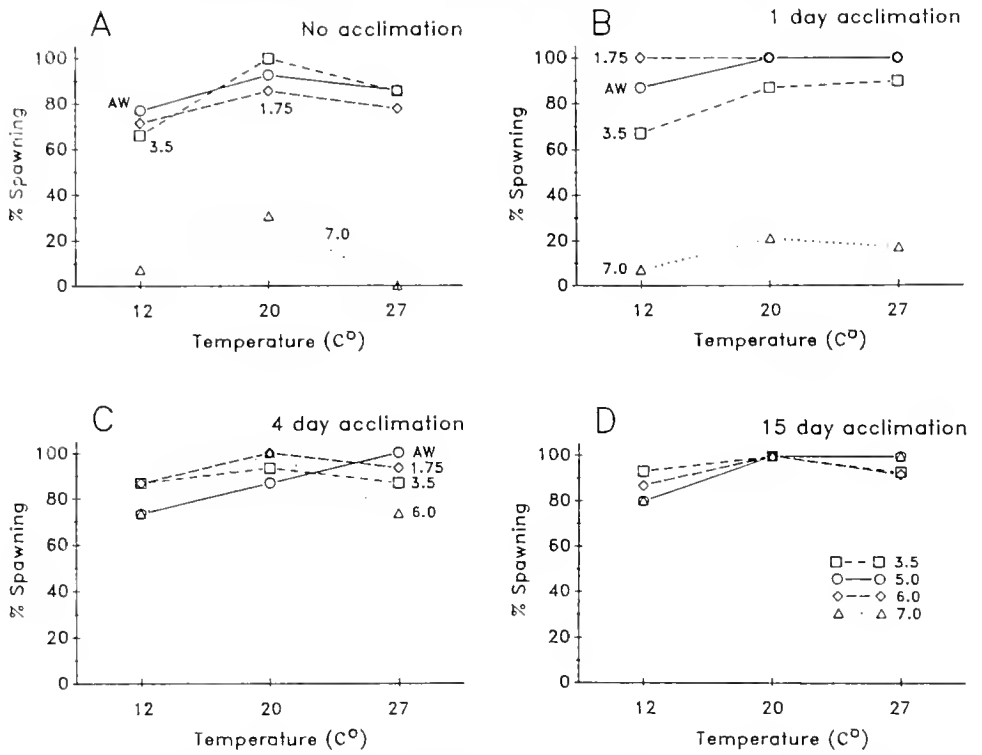

Figure 3. Results of a second experiment on effects of salinity, temperature, and duration of acclimation on serotonin (10^{-3} *M*)-induced spawning. Zebra mussels were acclimated in aquarium water (AW) and various salinities at 12°, 20°, and 27°C and tested for spawning after (A) no acclimation to any salinity/temperature condition (previously maintained in AW, 12°C; (B) 1-day acclimation; (C) 4-day acclimation; and (D) 15-day acclimation. Mussels tested for spawning in 6.0 ppt after 4 days acclimation were acclimated for 3 days in 3.5 ppt and then transferred to 6.0 ppt for 1 day before testing. In the 15-day acclimation tests, all mussels were acclimated gradually to increasing salinities from 1.75 ppt up to their final test salinity as described in the text. All other animals in the experiments were acclimated in their indicated salinities (AW, 1.75, 3.5, and 7.0 ppt) and temperatures (12°, 20°, and 27°C) throughout the acclimation period. Each point represents the percentage of animals spawning out of 10–15 animals tested for each salinity/temperature/duration condition.

4). For non-acclimated mussels, one-way ANOVA of the effect of salinity on log-transformed data of percent fertilization gave $F_{3,12} = 74.2$, $P < 0.0001$ in experiment 1 and $F_{3,8} = 361.8$, $P < 0.0001$ in experiment 2. The percentage of oocytes fertilized in both 3.5 ppt and 7.0 ppt was significantly lower than in both AW and 1.75 ppt (Fisher's LSD, $P < 0.05$ for all four comparisons in both experiments). For acclimated mussels, 7.0 ppt was still inhibitory to fertilization after a 4-day acclimation; however, the point to be noted is that the fertilization rate in 3.5 ppt now overlapped in range with the fertilization rate in AW. The fertilization rate at 3.5 ppt rose from 1.4% ± 0.5% (mean ± SE) in non-acclimated mussels to 37.6% ± 13.6% in 4-day-acclimated mussels. Similarly, after 21 days acclimation, fertilization rates in 3.5 ppt increased to 57% ± 35%, compared to 0% in non-acclimated controls.

During the course of the above fertilization experiments, we noticed that oocytes often ruptured at higher salinities. These observations were quantified in the latter of the two experiments (21-day acclimation and its non-acclimated control, Fig. 5). There was a significant increase in rupturing with elevated salinity in both acclimated and non-acclimated mussels, with and without sperm (one-way ANOVAs: for acclimated mussels without sperm, $F_{2,13} = 61.1$, $P = 0.0001$; with sperm, $F_{2,13} = 5.46$, $P = 0.001$; for non-acclimated mussels without sperm, $F_{3,8} = 6.2$, $P = 0.01$; with sperm, $F_{3,7} = 8.9$, $P = 0.008$). The decrease in oocyte rupturing that occurred in the presence of sperm was apparently due to a protective effect of fertilization. Thus, in 1.75 ppt, in which fertilization occurs at a high rate (Fig. 4), addition of sperm significantly reduced the percentage of oocytes rupturing from >80% to <20% ($P < 0.05$). The effect of sperm addition on the percentage of ruptured oocytes in non-acclimated mussels was not apparent in 3.5 and 7.0 ppt because almost no fertilization occurred at these two salinities. After 21 days of acclimation, in which fertilization occurs at a higher

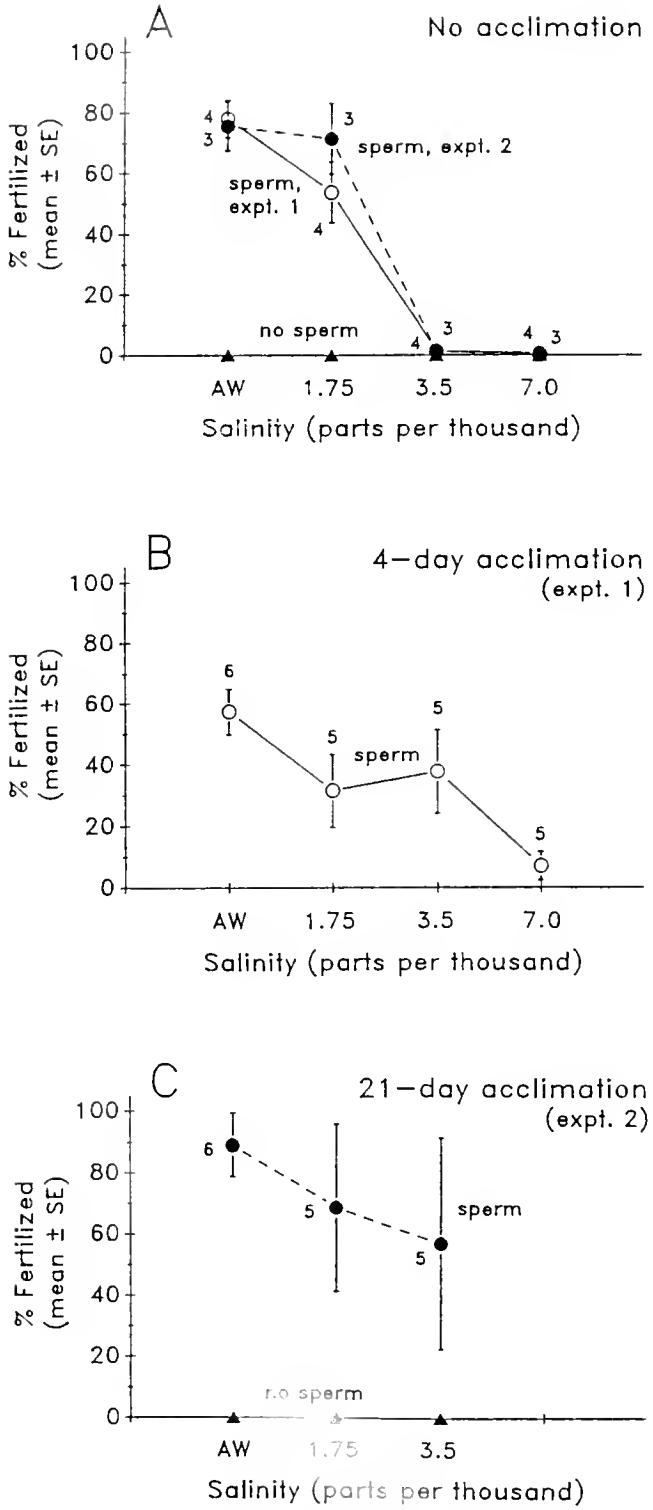

Figure 4. Effect of salinity on fertilization. Percentage of oocytes fertilized when exposed to sperm in aquarium water (AW) and salinities of 1.75, 3.5, or 7.0 ppt after (A) no prior acclimation of source animals (data from two separate experiments); (B) 4-day acclimation of source animals to various salinities at 20°C (experiment 1); and (C) 21-day acclimation of source animals to various salinities (experiment 2). Experiment 2 included "no sperm" controls with each group, none of which resulted in apparent cleavage and development (the end-point for determining that fertilization had occurred). Points and error bars represent the mean ± SE percent of cleaved oocytes observed within 3.5 hours of the addition of sperm. Sample sizes (numbers of females from which oocytes were obtained and tested in separate wells) are given adjacent to error bars.

rate in 3.5 ppt, a significant protective effect of sperm was apparent in both 1.75 ppt and 3.5 ppt ($P < 0.05$).

Because unfertilized oocytes in AW rarely ruptured, and rupturing in 1.75 ppt occurred in >60% of oocytes whether acclimated or not, we wondered what the lower limit of oocyte sensitivity to increased salinity was. To investigate this question, oocytes freshly spawned in AW were exposed to salinities of AW, 0.175, 0.35, 0.7, 1.0, and 1.75 ppt, without sperm, in a 24-well culture plate and observed at intervals of 1 to 2 h. No rupturing occurred after 1 h; however, some oocytes in 1.75 ppt appeared shrivelled. Within 2 h, oocytes began to rupture and, as illustrated in Figure 6, the percentage of ruptured oocytes increased with increasing salinity (linear regression, $r = 0.66$, $P < 0.001$).

Discussion

This is the first study to examine the effects of salinity directly on the reproductive mechanisms of zebra mussels. Previous studies focused on the viability of larvae (Setzler-Hamilton and Wright, 1994) and adults (*e.g.*, Mackie and Kilgour, 1992), and on biogeographic data relating distribution to salt concentrations (Walton, 1992; Strayer and Smith, 1993). The present study has demonstrated that although acute exposure of zebra mussels or their gametes to higher saline conditions is detrimental to spawning, fertilization, sperm motility, and oocyte integrity, acclimation of mussels to elevated saline levels over a period of days results in significant improvement in these indicators of reproductive function.

The improvement in reproductive function with acclimation was particularly striking at 3.5 ppt, the intermediate level of salinity tested. In response to 5-HT, non-acclimated zebra mussels can spawn gametes in salinities from 1.75 to 3.5 ppt, but only rarely in 7.0 ppt (Figs. 2 and 3). Although gametes obtained under these acute conditions can be consistently fertilized at 1.75 ppt, fertilization in 3.5 ppt, without prior acclimation, was practically nil (Fig. 4). Acclimation of animals in 3.5 ppt resulted in increased fertilization rates when tested in 3.5 ppt. Moreover, after acclimation of animals at 3.5 ppt for 4 or more days, spawning could be elicited by 5-HT in salinities as high as 7.0 ppt (Fig. 2 and subsequent experiments). Nevertheless, fertilization rates of oocytes obtained in 7.0 ppt after accli-

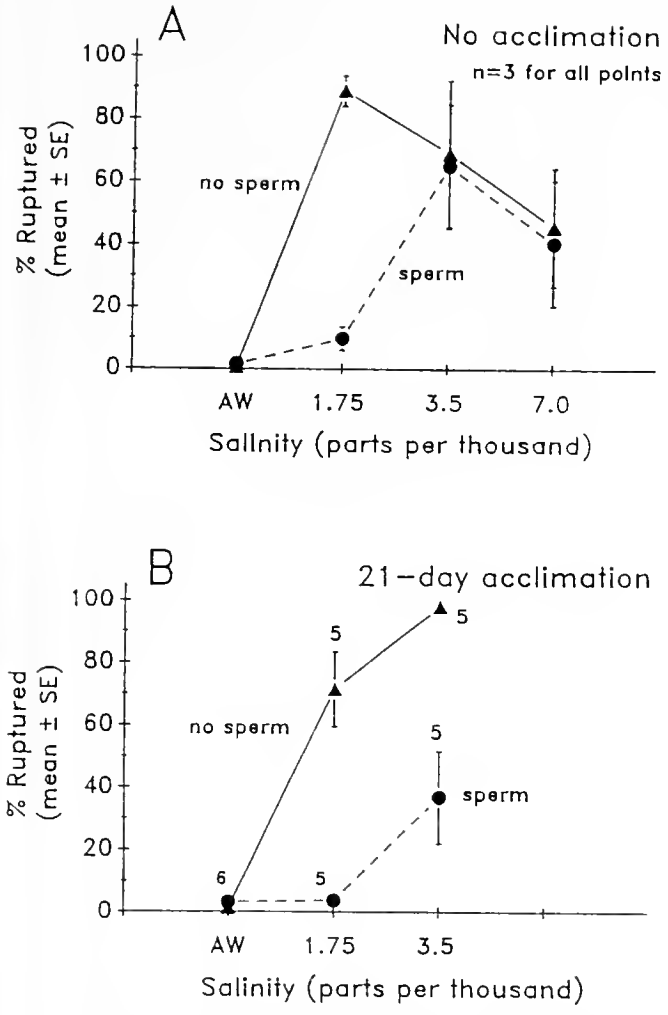

Figure 5. Effect of salinity on oocyte integrity. Percentage of oocytes ruptured was determined within 3.5 h of spawning, for oocytes tested with and without sperm present in aquarium water (AW), and various salinities. (A) Oocytes were from animals not previously acclimated and were tested in AW and salinities of 1.75, 3.5, and 7.0 ppt, $n = 3$ females per group. (B) Oocytes were from animals previously acclimated 21 days at 20°C to AW and salinities of 1.75 and 3.5 ppt and were tested in the same salinities to which they had been acclimated. Sample sizes (number of females from which oocytes were obtained and tested in separate wells) are given adjacent to error bars. Points and error bars represent the mean ± SE percent of oocytes ruptured.

mation remained depressed (Fig. 4). Thus the reproductive function of zebra mussels acclimated for several days to salinities as high as 3.5 ppt recovers to normal levels for several reproductive parameters but, at least within the time-temperature ranges tested, reproductive function at the highest salinity (7.0 ppt) is still significantly below normal.

The acute reduction in fertilization with increasing salinity may be due in part to reduced sperm motility. Sperm from non-acclimated mussels were either immotile or moving slowly in 3.5 and 7.0 ppt, with some reduction in motility at 1.75 ppt. Moreover, mussels acclimated for up to 2 days showed similar immotility in all salinities. Sperm from males acclimated for 6 days showed no reduction in motility, and this may explain the significant increase in fertilization in acclimated animals (albeit tested at 4 and 21 days acclimation) compared to non-acclimated animals tested in the same salinity. It may also explain the trend towards higher fertilization rates between 4-day and 21-day acclimation. In the present study, fertilizations were carried out in about 1 ml of water in 24-well culture plates. This small volume would increase the likelihood of even motility-deficient sperm encountering eggs. In the field, where volumes in which sperm may encounter oocytes are much larger, reduced motility of sperm may reduce fertilization success further than observed here.

Reductions in fertilization success may also be due to osmotic effects on oocytes. Rupture of unfertilized oocytes was evident in salinities as low as 0.175 ppt and increased significantly with salinity even at moderate saline levels. Although oocytes generally took 1 to 2 h to rupture, shrinkage in saline solutions was present (the exact timing and dimensions of such physical changes were not recorded) before rupture. Thus, increased saline levels may reduce the likelihood of fertilization by inducing pathological changes in oocytes between the time that they are exposed to the saline solution and the time that they encounter sperm. Osmotic effects may also explain the reduced motility of non-acclimated sperm. We need to know more about the normal longevity of sperm and egg viability and the normal latency between spawning and fertilization in the field before we can evaluate the importance of salinity-induced oocyte rupture on reproductive success.

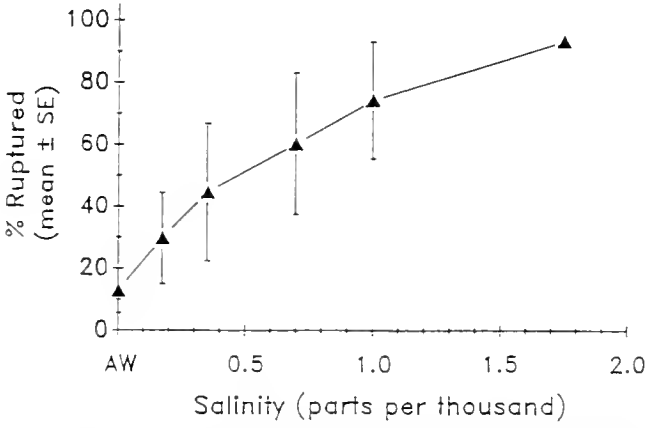

Figure 6. Effect of salinity on integrity of unfertilized oocytes. Female mussels were spawned in aquarium water (AW), and then oocytes were exposed to AW and various salinities up to 1.75 ppt. Oocytes (112 to 144 oocytes from each female under each condition) were observed after 2 h. Points represent the mean ± SE percent of oocytes ruptured for oocytes from 4 females. Linear regression gives $r = 0.66$, with $P < 0.001$.

Fertilization protected oocytes from salinity-induced rupture. Two possible mechanisms for this protection are (1) that secretion of a fertilization envelope provides some ionic/osmotic protection, and (2) that after fertilization, solutes (sugars, proteins, ions) accumulate and provide protection.

Temperature had a modulating effect on spawning in different salinities. Without acclimation, animals were more likely to spawn at 20°C than at either 12°C or 27°C. This was true for three of four salinities in experiment 1 (Fig. 2A) and all four salinities in experiment 2 (Fig. 3A). The higher response at 20°C is in agreement with the results of a previous experiment (Ram *et al.*, 1993), in which the rate of spawning in AW was higher at 20°C that at 12°C or 27°C. These data indicate that sudden rises in temperature into the upper twenties (°C) could inhibit reproductive function in zebra mussels, a suggestion that may explain some of the spawning variations observed in field studies (unpub. data). However, with longer acclimation to higher temperatures, spawning rates under all conditions rose to high levels at all salinities. Thus, despite the somewhat greater inhibitory effects of salinity at high temperatures in non-acclimated mussels, if high temperatures are sustained over long periods, spawning responses can recover to maximal levels within the range of salinity and temperature studied.

Salinity is a limiting factor in the distribution of adult zebra mussels in European brackish waters (Strayer and Smith, 1993). In North America, zebra mussels have spread downstream in the Hudson River estuary as far as West Haverstraw, New York, where salinities reach 4–6 ppt (Walton, 1992). In studies of adult mortality, Mackie and Kilgour (1992) found that the 96-h LC50 for salinity (Instant Ocean) at 19°C was 7.6 ppt for non-acclimated mussels. Acclimated zebra mussels survived longer, but at lower test temperatures. Setzler-Hamilton and Wright (1994) reported that D-hinge larvae of cultured zebra mussels survived at least 48 h at 22°C, but that survival ranged from only 20% at 18°C and 4 ppt to 0.2% at 18°C and 8.0 ppt. The results of our experiments together with these previous observations suggest that the salinity/temperature regime for zebra mussel survival is somewhat less than 7.0 ppt and less than 27°C, and that mussels can reproduce successfully at a salinity of 3.5 ppt. Thus, brackish-water populations of adult zebra mussels could result from both downstream transport of larvae and local recruitment.

This is one of the few investigations into the salinity tolerance of reproductive mechanisms in an invertebrate that abounds in fresh water. Animals living in fresh water must have special adaptations to withstand the osmotic stress of low salinity. Furthermore, if exposure to brackish waters is a possibility, then mechanisms may have evolved for surviving and reproducing in conditions of increasing or varying salinity. In most fresh-water bivalves, fertilization normally occurs within the suprabranchial chamber of the female, from which brooded, parasitic glochidia larvae are released. Zebra mussels represent a rare non-crustacean, freshwater invertebrate with external fertilization and planktotrophic larval development. However, the osmoregulatory mechanisms that allow zebra mussel gametes and larvae to tolerate extremely dilute conditions and to acclimate (as shown here) to brackish-water conditions are unknown. It would be of interest to determine how zebra mussel gametes are protected from osmotic stress in fresh water and what changes take place during acclimation.

Acknowledgments

This research was sponsored in part by grants from the Michigan Sea Grant College Program (NOAA NA16RC0417-01) and from NIH (RR-08167). JD and SR received partial support from the Wayne State University Department of Physiology SURF Program.

Literature Cited

Arner, M., and S. Koivisto. 1993. Effects of salinity on metabolism and life-history characteristics of *Daphnia magna*. *Hydrobiologia* **259:** 69–77.

Bielefeld, U. 1991. Histological observation of gonads and digestive gland in starving *Dreissena polymorpha* (Bivalvia). *Malacologia* **33:** 31–42.

Fong, P. P., and J. S. Pearse. 1992. Photoperiodic regulation of parturition in the self-fertilizing viviparous polychaete *Neanthes limnicola* from central California. *Mar. Biol.* **112:** 81–89.

Fong, P. P., D. M. Wall, and J. L. Ram. 1993. Characterization of serotonin receptors in the regulation of spawning in the zebra mussel *Dreissena polymorpha* (Pallas). *J. Exp. Zool.* **267:** 475–482.

Fong, P. P., K. Kyozuka, H. Abdelghani, J. D. Hardege, and J. L. Ram. 1994. *In vivo* and *in vitro* induction of germinal vesicle breakdown in a freshwater bivalve, the zebra mussel *Dreissena polymorpha* (Pallas). J. Exp. Zool. **269:** 467–474.

Griffiths, R. W., D. W. Schloesser, J. H. Leach, and W. P. Kovalak. 1991. Distribution and dispersal of the zebra mussel (*Dreissena polymorpha*) in the Great Lakes Region. *Can. J. Fish. Aquat. Sci.* **48:** 1381–1388.

Hebert, P. D. N., B. W. Muncaster, and G. L. Mackie. 1989. Ecological and genetic studies on *Dreissena polymorpha* (Pallas): A new mollusc in the Great Lakes. *Can. J. Fish. Aquat. Sci.* **46:** 1587–1591.

Hurlbert, S. H. 1984. Pseudoreplication and the design of ecological field experiments. *Ecol. Monogr.* **54:** 187–211.

James, K. R., and B. T. Hart. 1993. Effect of salinity on four freshwater macrophytes. *Australian J. Mar. Freshwater Res.* **44:** 769–777.

Lee, C. S., C. S. Tamaru, C. D. Kelley, A. Moriwake, and G. T. Miyamoto. 1992. The effect of salinity on the induction of spawning and fertilization in the striped mullet, *Mugil cephalus*. *Aquaculture* **102:** 289–296.

Ludyanskiy, M. L., D. McDonald, and D. MacNeill. 1993. Impact of the zebra mussel, a bivalve invader. *Bioscience* **43:** 533–544.

Mackie, G. L., W. N. Gibbons, B. W. Muncaster, and I. M. Gray. 1989. The zebra mussel, *Dreissena polymorpha*. A synthesis of European experiences and a preview for North America. Report pre-

pared for the Ministry of the Environment, Water Resources Branch, Great Lakes Section, Queen's Printer, Toronto, Ontario.

Mackie, G. L., and B. Kilgour. 1992. Effects of salinity on growth and survival of zebra mussels (*Dreissena polymorpha*). *Abstract, 2nd Int. Zeb. Mus. Res. Conf.*, Rochester, NY.

Misamore, M., T. H. Dietz, H. Silverman, and J. W. Lynn. 1994. Light, fluorescence and laser confocal microscopic analysis of fertilization and polyspermy in serotonin-spawned eggs of *Dreissena polymorpha*. *Am. Zool.* **34:** 65A.

Neary, B. P., and J. H. Leach. 1992. Mapping the potential spread of the zebra mussel *Dreissena polymorpha* in Ontario. *Can J. Fish. Aquat. Sci.* **49:** 406–415.

Ram, J. L., G. W. Crawford, J. U. Walker, J. J. Mojares, N. Patel, P. P. Fong, and K. Kyozuka 1993. Spawning in the zebra mussel *Dreissena polymorpha*: Activation by internal or external application of serotonin. *J. Exp. Zool.* **265:** 587–598.

Ramcharan, C. W., D. K. Padilla, and S. I. Dodson. 1992. Models to predict occurrence and density of the zebra mussel, *Dreissena polymorpha*. *Can. J. Fish. Aquat. Sci.* **49:** 2611–2620.

Setzler-Hamilton, E. M., and D. A. Wright. 1994. Temperature/salinity tolerance in larvae of zebra mussels and its potential impact in northern Chesapeake Bay. *Abstract, Annual Meeting International Association of Great Lakes Research*, Windsor, Ontario.

Sprung, M. 1987. Ecological requirements of developing *Dreissena polymorpha* eggs. *Arch. Hydrobiol. Supp.* **79:** 69–86.

Strayer, D. L. 1991. Projected distribution of the zebra mussel, *Dreissena polymorpha*, in North America. *Can. J. Fish. Aquat. Sci.* **48:** 1389–1395.

Strayer, D. L., and L. C. Smith. 1993. Distribution of the zebra mussel (*Dreissena polymorpha*) in estuaries and brackish waters. Pp. 715–727 in *Zebra Mussels, Biology, Impacts, and Control*, T. F. Nalepa and D. W. Schloesser, eds., Lewis Publishers, CRC Press, Boca Raton, Florida.

Victoria, C. J., B. S. Wilkerson, R. J. Klauda, and E. S. Perry. 1992. Salinity tolerance of yellow perch eggs and larvae from coastal-plain stream populations in Maryland, with comparison to a Pennsylvania Lake population. *Copeia* **1992:** 859–865.

Walker, J. U., and J. L. Ram. 1994. Effects of deionized water on sensitivity of zebra mussels (*Dreissena polymorpha*) to toxic chemicals. *Comp. Biochem. Physiol.* **107C:** 353–358.

Walton, W. C. 1992. The invasion of the Hudson River Estuary by the zebra mussel, *Dreissena polymorpha*, and its subsequent range overlap with the false dark mussel, *Mytilopsis leucophaeta*. *Final Rep. Tibor T. Polgar Fellowship Prog.*, Rutgers Univ, New Brunswick, NJ.

Reference: *Biol. Bull.* 189: 330–339. (December, 1995)

Existence of Three Mechanisms for Blocking Polyspermy in Oocytes of the Mussel *Mytilus edulis*

TATSURU TOGO[1,2,*], KENZI OSANAI[1], AND MASAAKI MORISAWA[2]

[1]*Asamushi Marine Biological Station, Tohoku University, Asamushi, Aomori 039-34, Japan, and*
[2]*Misaki Marine Biological Station, University of Tokyo, Misaki, Miura, Kanagawa 238-02, Japan*

Abstract. We found the existence of a three-step mechanism to block polyspermy in the oocyte of the mussel *Mytilus edulis*. When the oocytes were inseminated within 30 min after spawning, they underwent monospermic fertilization over a wide range of sperm-oocyte ratios up to 5×10^3. A transient depolarization of the oocyte plasma membrane (fertilization potential) was observed immediately after insemination. Low-sodium seawater induced polyspermy and decreased the amplitude of the fertilization potential, suggesting the existence of a fast block to polyspermy that is dependent on depolarization of the plasma membrane. When the fertilized oocytes were inseminated again at a sperm-oocyte ratio that is great enough to give a high rate of polyspermy in initial insemination, many sperm could not undergo the acrosomal reaction and thus could not penetrate fertilized oocytes. The remaining sperm underwent an acrosomal reaction and the acrosomal process protruded through the vitelline coat, but it did not fuse with the oocyte plasma membrane. These findings suggest the existence of two strategies constituting a late polyspermy block: suppression of acrosomal reaction and block of contact or fusion between the plasma membranes of sperm and oocyte.

Introduction

The success of fertilization and the subsequent development of the zygote require the fusion of a single male pronucleus with a female pronucleus. Penetration of the spermatozoon into an oocyte is controlled through several mechanisms (Jaffe and Gould, 1985). Rothschild and Swann (1952) first suggested the existence of a fast polyspermy block at the plasma membrane of the oocyte in the sea urchin. Jaffe (1976) demonstrated that the block was mediated electrically. The fast electrical polyspermy block has been further observed in many animal species, such as starfish (Miyazaki and Hirai, 1979), the echiuroid *Urechis* (Gould-Somero *et al.*, 1979), amphibians (Cross and Elinson, 1980; Grey *et al.*, 1982; Iwao, 1989), the nemertean *Cerebratulus* (Kline *et al.*, 1985), crab (Goudeau and Goudeau, 1989a), lamprey (Kobayashi *et al.*, 1994), and ascidians (Goudeau *et al.*, 1994), as well as in algal protists, among the fucoid seaweeds (Brawley, 1991).

After fusion between the plasma membranes of the gametes, the extracellular coat of the oocyte is altered and forms a fertilization envelope to prevent sperm penetration (zona reaction in mammals). A late polyspermy block mechanism may also operate at the level of the oocyte plasma membrane in *Urechis*. Paul and Gould-Somero (1976) found that the acrosomal process of supernumerary sperm penetrated through the vitelline coat into the perivitelline space of the fertilized oocyte, but sperm could not fuse with the oocyte plasma membrane. The block at the plasma membrane is also found in the nemertean *Cerebratulus* (Kline *et al.*, 1985), in mammals (*e.g.*, Horvath *et al.*, 1993), and in the surf clam *Spisula* (Ziomek and Epel, 1975).

The existence of the electrical block in bivalves was suggested in *Spisula* by Finkel and Wolf (1980), who found that the depolarization of the oocyte plasma membrane occurs soon after insemination and that low-sodium seawater induces polyspermy. A vitelline coat and cortical granules are present in the oocyte cortex in bivalves, but there is no evidence demonstrating the formation of a

Received 10 April 1995; accepted 31 July 1995.

* To whom correspondence should be addressed at Misaki Marine Biological Station, University of Tokyo.

Abbreviations: ASW, artificial seawater; DAPI, 4′,6-diamidino-2-phenylindole; GalNAc, *N*-acetylgalactosamine; NaFSW, sodium-free artificial seawater; NSW, natural seawater; $R_{s/o}$, sperm-oocyte ratio.

fertilization envelope by their structural changes (Longo, 1983; Alliegro and Wright, 1983; Longo *et al.*, 1993); thus the involvement of both structures in the late polyspermy block is uncertain. However, a complete polyspermy block has been demonstrated in oocytes of *Spisula* from which the vitelline coat was removed, suggesting that a complete block to polyspermy occurs at the oocyte plasma membrane in this species (Ziomek and Epel, 1975).

In contrast to *Spisula*, the mussel *Mytilus galloprovincialis* was described as lacking a complete mechanism to block polyspermy (Dufresne-Dubé *et al.*, 1983). Dufresne-Dubé *et al.* (1983) also found induction of polyspermy in *M. galloprovincialis* by lowering the concentration of sodium ions in seawater, but no fertilization potential was observed. We demonstrate here a complete polyspermy block in *Mytilus edulis* and describe its three steps: (1) a fast electrical block, (2) a suppression of the acrosomal reaction, and (3) a block of contact or fusion of the plasma membrane in the gametes.

Materials and Methods

Artificial seawater

Artificial seawater (ASW) consisted of 450 m*M* NaCl, 9.4 m*M* KCl, 10.2 m*M* $CaCl_2$, 48.2 m*M* $MgSO_4$, 5.4 m*M* $NaHCO_3$. When sodium-free artificial seawater (NaFSW) was prepared, NaCl, KCl, and $NaHCO_3$ were replaced with 455.4 m*M* choline chloride (Nacalai Tesque Inc.), 4 m*M* KCl, and 5.4 m*M* $KHCO_3$, respectively. Low-sodium ASWs were prepared by mixing ASW and NaFSW. The pH was adjusted to 8.3 with 1 *N* NaOH for ASW or 1 *N* KOH for NaFSW and low-sodium ASWs just prior to use.

Gametes

Specimens of the mature mussel *Mytilus edulis* were collected from November to April in the vicinity of Asamushi Marine Biological Station (Aomori Prefecture), Tohoku University, and Misaki Marine Biological Station (Kanagawa Prefecture), University of Tokyo. They were kept in aquaria at 10°C. Spawning of oocytes and sperm was induced by transferring the mussels to warm seawater at 25°C. When the mussels started spawning, they were returned to natural seawater (NSW) at 10°C. The oocytes were washed several times with NSW, ASW, or low-sodium ASWs according to the experiments. Concentrations of oocytes were determined by counting the number of oocytes in 5-μl glass capillary tubes. Sperm were collected "dry" and stored at 4°C. Sperm suspensions were prepared by diluting the dry sperm with NSW, ASW, or low-sodium ASWs. Concentrations of sperm in the suspensions were determined by counting the number of sperm, fixed with 1% glutaraldehyde, in a hemacytometer. Sperm-oocyte ratio ($R_{s/o}$) in the medium at insemination was an absolute ratio. All experiments were carried out at room temperature (18°–20°C).

Assay of polyspermy

To remove supernumerary sperm bound to the surface of the oocyte, the inseminated or re-inseminated oocytes were washed with NSW containing 0.001% sodium dodecyl sulfate at 20 min after the first insemination. Oocytes were subsequently fixed with a 3:1 mixture of methanol and acetic acid for 1 h at room temperature. After the oocytes were washed with distilled water, they were stained with 1 μg/ml DAPI (4′,6-diamidino-2-phenylindole) (100 μg/ml in dimethyl sulfoxide as a stock) for 30 min to observe incorporated sperm nuclei. The rate of polyspermy was indicated by the percentage of oocytes that included multiple sperm nuclei. The mean number of sperm nuclei included in an oocyte was determined by counting the number of decondensed sperm nuclei in an oocyte. At least 100 oocytes were observed under a fluorescence microscope (Olympus, BH-2).

Re-insemination experiments

When oocytes were inseminated with a low $R_{s/o}$ (light insemination; $R_{s/o} = 5 \times 10^2 - 1 \times 10^3$), fertilized oocytes were monospermic. At various periods up to 5 min after initial insemination, the monospermic oocytes were inseminated again with a high $R_{s/o}$ (heavy insemination; $R_{s/o} = 8 \times 10^3 - 1 \times 10^4$) sufficient to give a high rate of polyspermy in initial insemination. The length of time during which the sperm remained monospermic upon heavy re-insemination was taken as the completion time for the polyspermy block.

Assay of sperm binding

Fertilized and unfertilized oocytes were fixed with 1% glutaraldehyde in NSW at 30 s after the heavy insemination ($R_{s/o} = 8 \times 10^3 - 1 \times 10^4$), and then the number of bound sperm was counted by scanning the entire oocyte surface under a Nomarski microscope (Nikon, OPTIPHOT). Observations were made on at least 100 oocytes per experiment.

Assay of acrosome reaction

Half of the oocytes from a female were lightly inseminated ($R_{s/o} = 5 \times 10^2 - 1 \times 10^3$). The fertilized oocytes and remaining unfertilized oocytes were washed several times with NSW at 10 min after the initial light insemination. Both unfertilized and fertilized oocytes were inseminated at the $R_{s/o}$ of $3.5 - 4.0 \times 10^3$, and then they

were fixed with 1% glutaraldehyde at 5 min after the insemination. Because the acrosome of *Mytilus* sperm is large (see Fig. 8), acrosome-intact were easily differentiated under a Nomarski microscope from acrosome-reacted sperm and were easily removed after fixation. Thus, an appropriate volume of the suspension was mounted on the glass slide, and the number of acrosome-reacted and acrosome-intact sperm in randomly selected samples of sperm (both bound and unbound on the oocyte surface) was counted under the microscope. As a control, glutaraldehyde-fixed oocytes and sperm were mixed, and the number of acrosome-reacted sperm was counted.

Measurement of membrane potential

To make microelectrodes, glass tubing containing a glass fiber was pulled with a microelectrode puller (Narishige, PN-3), and back-filled with 3 *M* KCl. Resistance of the electrode was 40–60 MΩ. As shown in Figure 1, the chamber was filled with medium such as NSW, ASW, or low-sodium ASWs, which was connected to ground via an Ag-AgCl electrode. An oocyte was held by sucking on the tip of a capillary that was placed in the chamber. Electrode penetration was achieved by lowering the electrode to the oocyte surface perpendicularly and applying an "oscillating" current. Recordings were made with a microelectrode amplifier (Nihon Kohden, MEZ-7200), an oscilloscope (Hitachi, V-212), and a chart recorder (Hitachi, 200). After measurements of the membrane potential, each oocyte was transferred into a hole of a 96-well culture plate, and the first cleavage (about 80 min after insemination at 18°C) was observed. Oocytes were considered to be polyspermic when the first cleavage was abnormal. When cleavage did not occur, or if the microelectrode resistance changed at the end of a measurement compared to the initial value, the data were not used.

Electron microscopy

According to the method of Einsenman and Alfert (1982), gametes were prefixed for 10 min in seawater containing 1% glutaraldehyde (Nacalai Tesque Inc.) and 0.05% osmium tetroxide (TAAB) or in 0.2 *M* sodium cacodylate buffer (pH 7.2) containing 1% glutaraldehyde and 0.05% osmium tetroxide, 0.1 *M* NaCl, and 0.35 *M* sucrose. Then, the samples were fixed for 1 h in 0.2 *M* sodium cacodylate buffer (pH 7.2) containing 4% glutaraldehyde, 0.1 *M* NaCl, and 0.35 *M* sucrose. Postfixation was performed in 0.2 *M* sodium cacodylate buffer (pH 7.2) containing 1% osmium tetroxide and 0.3 *M* NaCl for 1 h. After the fixations, the samples were dehydrated in a graded series of ethanol and embedded in Spurr's resin (Polysciences Inc.). Thin sections were cut with a Porter-Blum MT-1 ultramicrotome, stained with 2% aqueous uranyl acetate and Reynolds' lead citrate (Reynolds, 1963), and observed with a Hitachi H-500 transmission electron microscope.

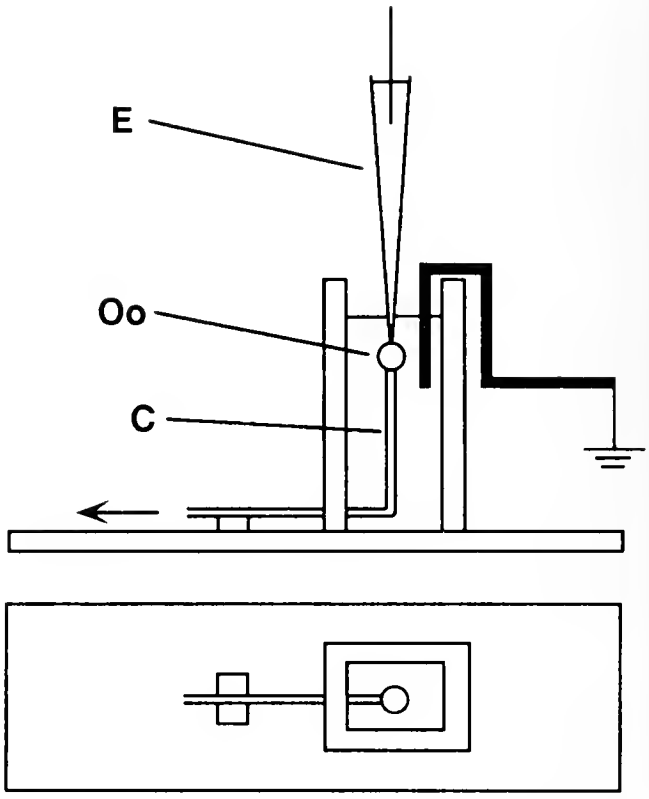

Figure 1. The chamber for the electrophysiological measurements. The oocyte (Oo) was held with a suction capillary tube (C), and the microelectrode (E) was advanced into the oocyte vertically.

Results

Polyspermy block mechanism in the oocyte of Mytilus edulis

When oocytes were collected within 30 min after spawning (fresh oocytes) and inseminated with sperm, 90% of the oocytes were monospermic until $R_{s/o}$ reached 5×10^3; insemination with higher concentration of sperm ($R_{s/o}$ is above 5×10^3) resulted in polyspermy (Fig. 2). The incidence of polyspermy increased when oocytes were aged in seawater before insemination, though the time at which oocytes become polyspermic varied from batch to batch (data not shown). Typical data are shown in Figure 3. When oocytes collected more than 30 min after spawning (old oocytes) were inseminated at a $R_{s/o}$ of 2×10^3, the number of sperm penetrating the oocyte increased with time, reaching a mean of 3.47 when 60-min-old oocytes were inseminated; insemination with a low $R_{s/o}$ (9

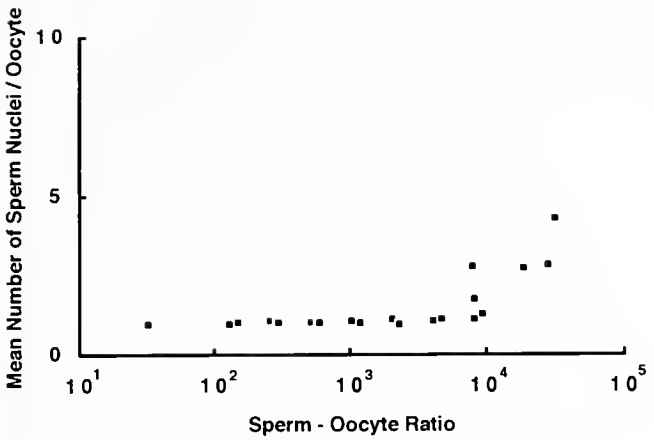

Figure 2. The number of penetrating sperm per fresh oocyte inseminated with various sperm-oocyte ratios. Note that heavy insemination induced polyspermy.

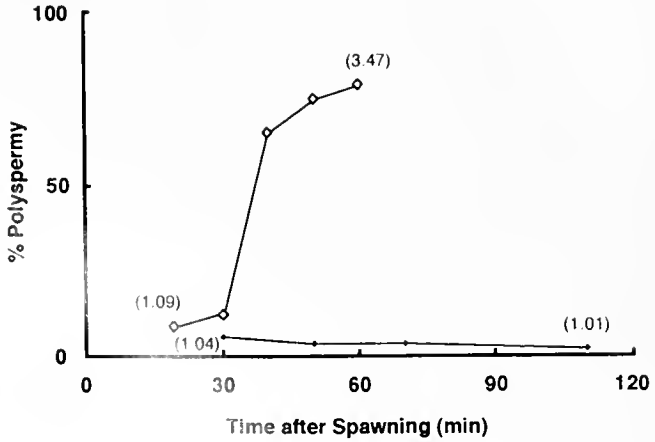

Figure 3. Increase in the rate of polyspermy with passage of time after spawning. The mean number of sperm nuclei per oocyte is in parentheses. $R_{s/o}$ was 9×10^2 (♦) or 2×10^3 (◇).

$\times 10^2$) resulted in monospermic fertilization even in old oocytes (Fig. 3). The number of penetrated sperm in an oocyte increased when $R_{s/o}$ was increased and the time of insemination was delayed; the number of penetrated sperm was 2.68, 3.61, and 4.90 when oocytes of the other batch were inseminated at 50, 90, and 120 min after spawning, whereas the number of sperm was 2.46 when fresh oocytes were inseminated with $R_{s/o}$ of 1×10^4 (data not shown). These data suggest that a mechanism to block polyspermy exists in the oocyte of *Mytilus edulis*, and that it weakens with the passage of time after spawning.

The number of penetrated sperm in a fresh oocyte that was inseminated under heavy insemination conditions was 2.79 (Fig. 4). However, when monospermic oocytes made by fertilization with light insemination of fresh oocytes were re-inseminated at a higher $R_{s/o}$ ($8 \times 10^3 - 1 \times 10^4$; heavy insemination) at 15 and 30 s after the initial light insemination, the number of penetrated sperm per oocyte was 1.38 and 1.18, respectively (Fig. 4). From these results and data from two other batches of oocytes (data not shown), the completion time for polyspermy block was concluded to be 30 s. Thus fresh oocytes acquire a block to polyspermy very rapidly after fertilization.

The fast polyspermy block by fertilization potential

Both the depolarization of the oocyte plasma membrane and the polyspermy block in the marine invertebrates and fucoid seaweeds are known to be suppressed in low-sodium ASW (Gould-Somero *et al.*, 1979; Jaffe, 1980; Kline *et al.*, 1985; Brawley, 1991). When the oocytes of *M. edulis* were lightly inseminated in low-sodium ASW, they became polyspermic (Fig. 5). In ASW, 1.04 sperm penetrated the oocyte, but this number was increased by lowering the sodium ion concentration in ASW, suggesting that a sodium-dependent depolarization causes the fast polyspermy block in *M. edulis*.

It is difficult to insert the microelectrode in *Mytilus* oocytes because the plasma membrane of the oocyte is easily broken by mechanical treatments. In the present study, only eight measurements of the fertilization potential were obtained without damaging the oocytes. The membrane potential of unfertilized *Mytilus* oocytes was -66.0 ± 2.2 mV ($n = 5$) in NSW (Fig. 6A, Table I). Upon insemination, the plasma membrane of the oocyte rapidly

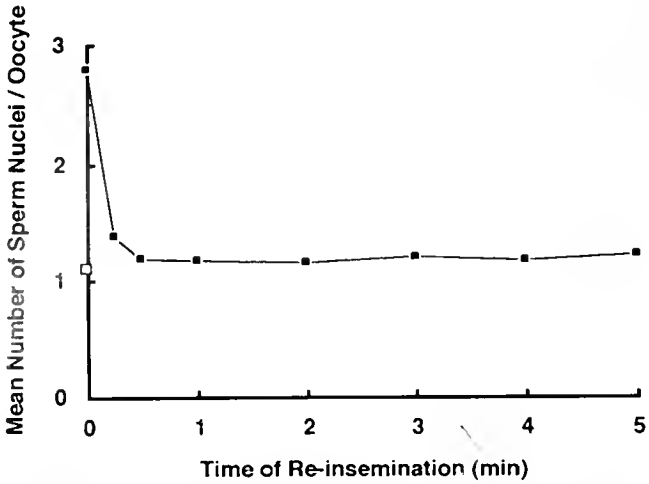

Figure 4. The number of penetrating sperm per oocyte re-inseminated at various times after initial insemination. Values are the mean of 100 oocytes from a single batch. Time zero represents the number of sperm nuclei per oocyte when unfertilized oocytes were heavily (■) or lightly (□) inseminated.

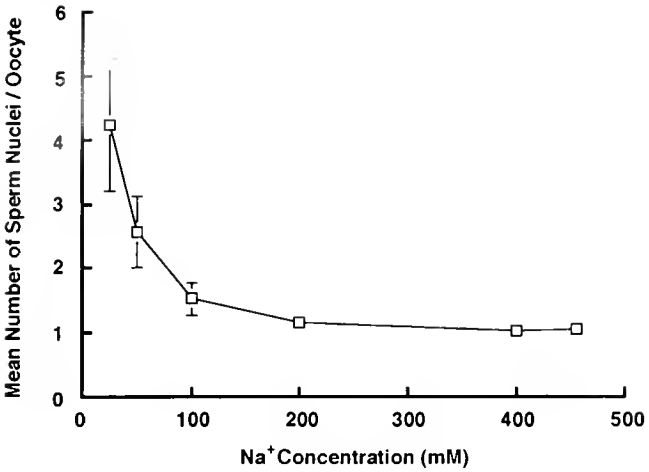

Figure 5. Induction of polyspermy in low-sodium ASW. Oocytes were incubated in low-sodium ASWs for 10 min, and inseminated at $R_{s/o}$ of $5 \times 10^2 - 1 \times 10^3$. Values are the mean ± SEM of five experiments.

depolarized to +59.4 ± 2.2 mV (n = 5) and then repolarized to a steady resting potential of −68.0 ± 3.4 mV (n = 5) at 28.0 ± 5.2 s (n = 5) after the onset of depolarization (Fig. 6A, Table I). After measurement, all the oocytes became normal 2-cell-stage embryos (Table I). A series of oscillating spikes of depolarization (arrows in Fig. 6A) was observed after the membrane potential returned to a resting potential in all oocytes measured in NSW. These spikes may be due to sperm contacts with the oocyte surface, since the frequency of the spikes increased as the concentration of sperm was increased (data not shown).

When the concentration of sodium in ASW was reduced to 50 mM, the resting potential of unfertilized oocytes was −79.3 ± 5.3 mV (n = 3). The membrane of the oocytes depolarized upon insemination, but the peak value in low-sodium ASW was remarkably lower (−56.0 ± 5.0 mV, n = 3) than that in NSW (Fig. 6B, Table I). All the oocytes transferred into normal ASW after the measurement in low-sodium ASW exhibited abnormal cleavage (Table I). Although we attempted to examine fertilization under current-clamp or voltage-clamp conditions, the experiments were unsuccessful because of the difficulty of electrode penetration.

The late polyspermy block

When the fertilized oocytes were heavily re-inseminated ($R_{s/o} = 8 \times 10^3 - 1 \times 10^4$) at 1 min after an initial light insemination ($R_{s/o} = 5 \times 10^2 - 1 \times 10^3$), the number of bound sperm was smaller (0.46) than that in the oocytes initially inseminated at the same $R_{s/o}$ ($R_{s/o} = 8 \times 10^3 - 1 \times 10^4$) (1.0 at time zero in Fig. 7). The number of bound sperm was reduced to 0.32, 0.31, or 0.32 when the oocytes fertilized with a light insemination were heavily re-inseminated at 2, 5, or 10 min after initial insemination in NSW, respectively. When fixative (*e.g.*, glutaraldehyde) was added, almost all the acrosome-intact sperm on the oocyte surface were removed (data not shown). These results suggest that a mechanism to prevent sperm binding through suppression of the acrosomal reaction developed shortly after fertilization.

For investigating the relationship between sperm binding and the acrosomal reaction, the rate of the acrosomal reaction of the re-inseminated sperm was investigated (Fig. 8). When unfertilized oocytes were inseminated at a $R_{s/o}$ of $3.5 - 4 \times 10^3$ and fixed at 5 min after the insemination, the rate of the acrosomal reaction was 77%. However, this rate was reduced to about 27% when fertilized oocytes (10 min after initial insemination) were re-inseminated at $R_{s/o}$ of $3.5 - 4 \times 10^3$ and fixed at 5 min after the re-insemination. Light microscopic observations of living samples also showed that the rate of the acrosome reaction was higher for sperm on the surface of an unfertilized oocyte than for those on a fertilized oocyte (Fig. 8B, C). These results suggest that an acrosomal-reaction-inducing activity is lower on the surface of the fertilized oocytes than on unfertilized oocytes. As a result, sperm hardly undergo the acrosome reaction (Fig. 8) and bind on the surface of the fertilized oocyte (Fig. 7).

When the surfaces of the oocytes that were re-inseminated ($R_{s/o} = 3.5 - 4 \times 10^3$) at 5 min after initial light insemination were observed with a transmission electron microscope, bound sperm had undergone the acrosomal reaction, and the acrosomal process reached the oocyte plasma membrane through the vitelline coat. Typical supernumerary sperm are shown in Figure 9. We examined several serial sections of supernumerary sperm, but we did not find fusion between the supernumerary sperm and the fertilized oocyte. Furthermore, the fertilization cone associated with fertilizing sperm was not observed in these sections or in other single sections. Therefore, we are certain that fertilization of the supernumerary sperm that underwent the acrosomal reaction was prevented at the level of the oocyte plasma membrane.

Discussion

Conflicting results have been reported on the polyspermy block mechanism in bivalves. The oocyte of the surf clam *Spisula* has a complete mechanism to block polyspermy (Ziomek and Epel, 1975; Longo, 1976a). Dufresne-Dubé *et al.* (1983), however, obtained monospermic fertilizations in the mussel *Mytilus galloprovincialis* only when the oocytes were inseminated with a very low concentration of sperm at a range of $R_{s/o}$ between

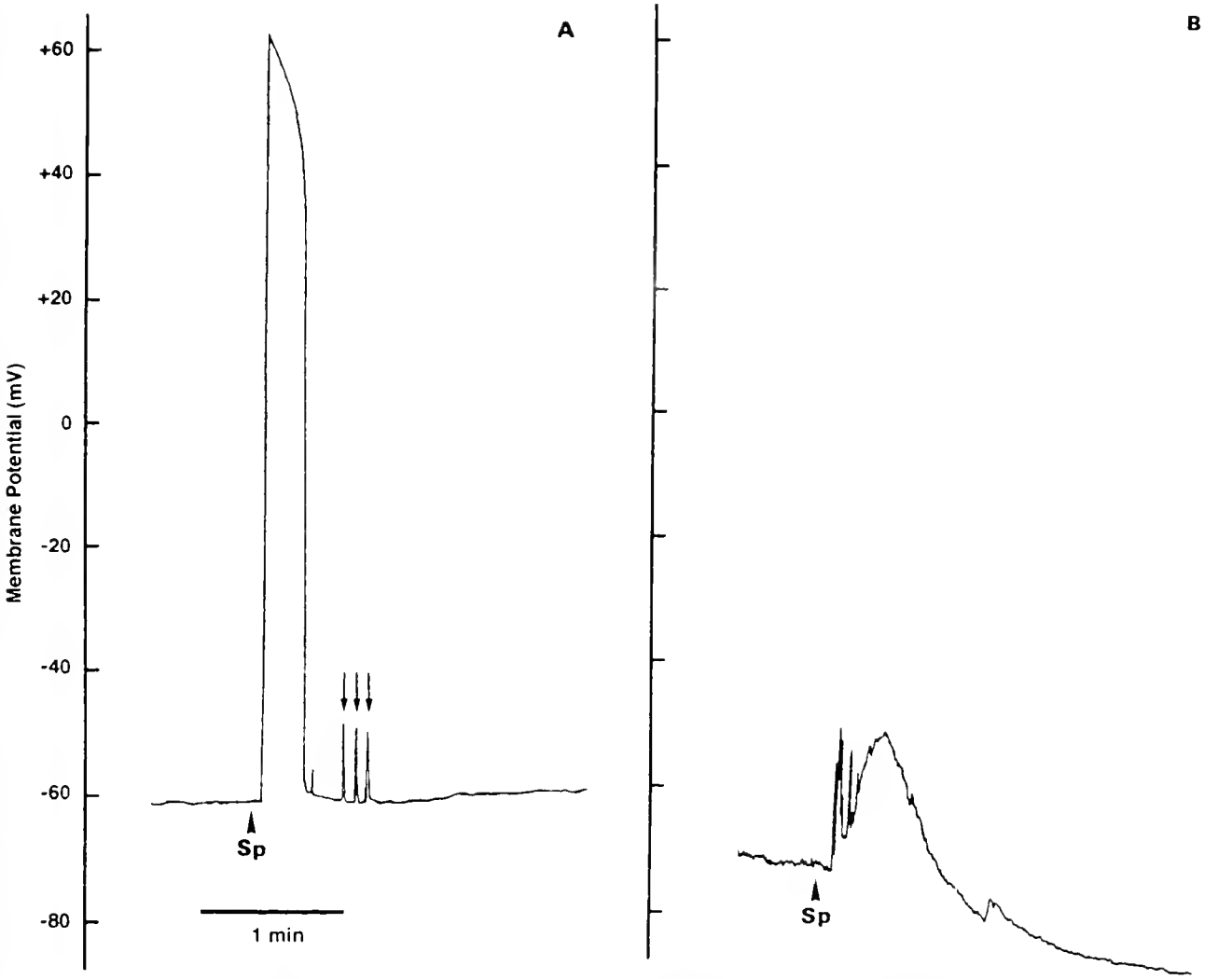

Figure 6. Typical patterns of membrane depolarization of *Mytilus* oocytes at fertilization in NSW (A) or low-sodium ASW (B). Sperm suspension was added to the chamber containing an oocyte at Sp. Sodium concentration in low-sodium ASW was 50 m*M*. Arrows show depolarization spikes.

Table I

Fertilization potential characteristics in Mytilus edulis

Seawater	Resting potential before fertilization (mV)	Resting potential after fertilization (mV)	Peak value (mV)	Duration of fertilization potential[a] (s)	n^b	% polyspermy
NSW	−66.0 ± 2.2	−68.0 ± 2.2	+59.4 ± 2.2	28.0 ± 5.2	5	0 (0/5)
50 m*M*-Na^+	−79.3 ± 5.3	−90.0 ± 2.3	−56.0 ± 5.0	48.7 ± 4.8	3	100 (3/3)

Values are mean ± SE.

[a] Time for which the membrane potential was more positive than resting potential before fertilization.

[b] Number of measurements.

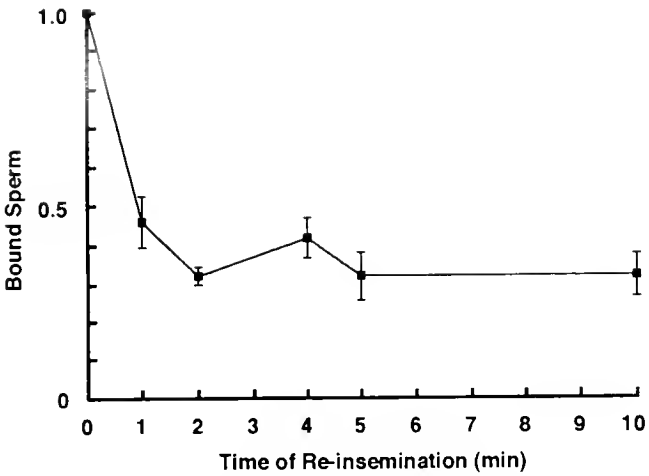

Figure 7. Sperm binding to fertilized oocytes. Fertilized oocytes were heavily re-inseminated at appropriate times and fixed at 30 s after re-insemination. Time zero represents heavily inseminated sperm binding to unfertilized oocytes (control). Values are represented as a ratio of the control value (mean ± SEM of six experiments).

10^1 and 2×10^2, suggesting that no complete block to polyspermy is established in this species. In *Mytilus edulis*, we found here that the oocyte exhibits a complete block to polyspermy after fertilization (Fig. 4), but that the block lasts only 30 min after spawning. Because the incidence of polyspermy increases with time after oocytes are spawned (Fig. 3), use of old oocytes for insemination would lead to the same conclusion for *M. edulis* as Dufresne-Dubé *et al.* (1983) reached for *M. gallo-provincialis*—*i.e.*, that the species lacks a mechanism for complete polyspermy block.

In the brown alga *Fucus* (Brawley, 1991) and in marine invertebrates such as the sea urchin, the starfish, the echiuroid *Urechis*, and the nemertean *Cerebratulus* (Jaffe, 1976, 1980; Miyazaki and Hirai, 1979; Gould-Somero *et al.*, 1979; Kline *et al.*, 1985), the membrane of the oocyte depolarizes at fertilization. In crustaceans, hyperpolarization was observed at fertilization (Goudeau and Goudeau, 1989a, b). All the above reports, except those for crustaceans, also showed that polyspermic fertilization occurs in low-sodium ASW by suppression of the depolarization, and that fertilization is inhibited when the membrane potential is clamped at a positive value. Depolarization of the oocyte plasma membrane also occurred at fertilization in *M. edulis*, and less depolarization and higher polyspermic fertilization were found in low-sodium ASW (Figs. 5 and 6, Table 1), suggesting that an electrical event at the plasma membrane acts as the fast polyspermy block in the oocyte of *Mytilus*.

The fast electrical block is not absolute, and thus high sperm concentrations can sometimes overcome it (see Jaffe and Gould, 1985). An effective late block appears following the fast electrical block (see Fig. 12 in Brawley, 1991). In many species except bivalves, this late block usually accompanies morphological changes in the cortex of the oocyte such as cortical granule breakdown or elevation of the fertilization envelope (Longo, 1983; Jaffe and Gould, 1985). During the formation of the fertilization envelope, sperm-oocyte binding is impaired by enzymes released from the fertilized oocyte, and late polyspermy block is established. For example, during cortical reaction after fertilization, the egg of the sea urchin releases proteases that cause separation of sperm and egg (Vacquier *et al.*, 1972, 1973). Sperm detachment also occurs before

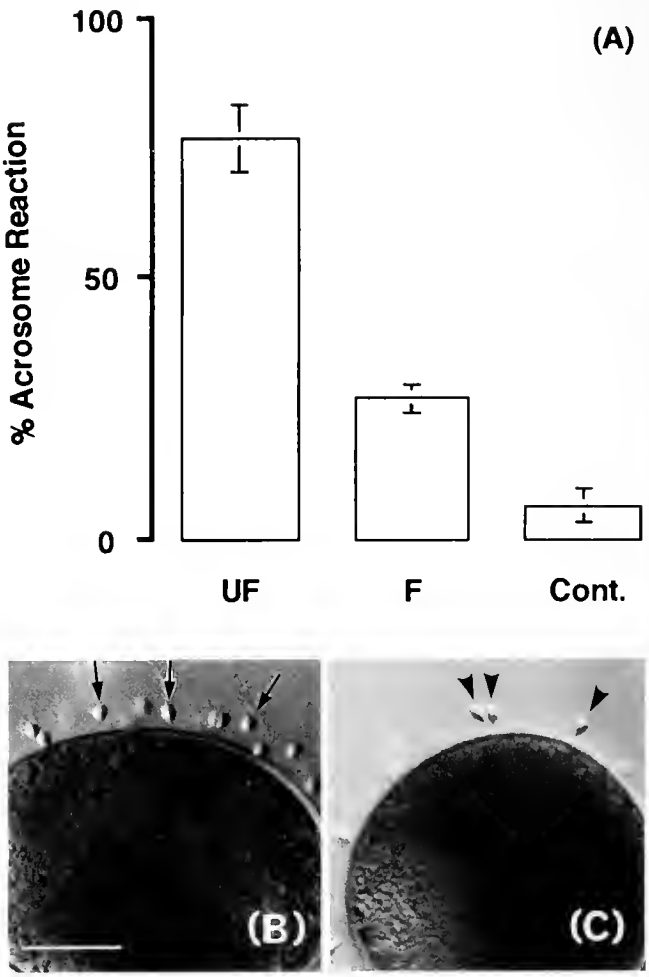

Figure 8. Acrosomal reaction in sperm used to inseminate unfertilized or fertilized oocytes. (A) Control represents the acrosome reaction of fixed sperm inseminating fixed oocytes. Values are the mean ± SEM of four experiments. (B) On the surface of an unfertilized oocyte, many round acrosome-reacted sperm (arrows) are seen. (C) On the surface of a fertilized oocyte, pear-shaped acrosome-intact sperm (arrowheads) are seen. The photographs were taken within 1 min after re-insemination. When fixative was added, almost all acrosome-intact sperm on the oocyte surface were removed (not shown). Bar = 20 μm.

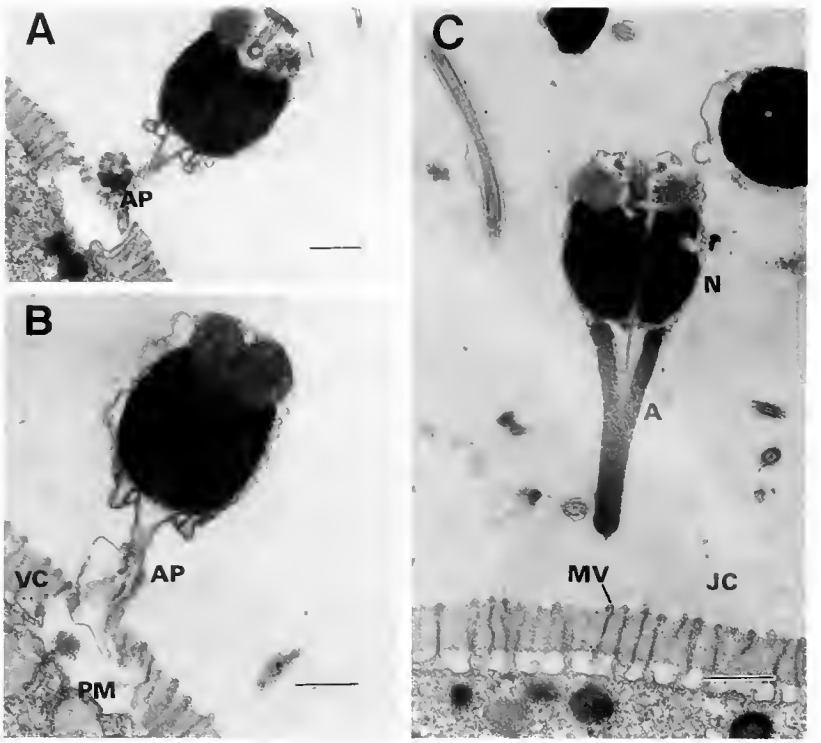

Figure 9. Transmission electron micrographs of supernumerary sperm on the surface of the fertilized oocyte. (A, B) Acrosome-reacted sperm at the oocyte surface. Sperm dissolved the vitelline coat (VC), and protruded the acrosomal process (AP) to the oocyte plasma membrane (PM), but the acrosomal process did not fuse with the oocyte plasma membrane. (C) Some acrosome-intact sperm were observed on the surface of the fertilized oocyte without being removed during fixation. A = acrosome, N = nucleus, JC = jelly coat, MV = microvilli. Bar = 1 μm.

cell-wall formation, and destruction of the sperm "receptor" with the glycosidase released from the egg after fertilization is hypothesized to occur in *Fucus* (Brawley, 1991). In ascidians (*Ascidia, Phallusia, Halocynthia*), sperm recognize *N*-acetylglucosamine residues coming out onto the vitelline coat during fertilization (Lambert, 1986; Honegger, 1982, 1986; Matsuura *et al.*, 1993). Although the type of cortical reaction observed in sea urchins is lacking in ascidian eggs (Rosati *et al.*, 1977), the oocytes rapidly release *N*-acetylglucosaminidase after fertilization, blocking the binding of the sperm to the vitelline coat (Lambert, 1986, 1989; Lambert and Goode, 1992).

Neither ascidians (Rosati *et al.*, 1977) nor many bivalve species, including *M. edulis* (Longo, 1983; Alliegro and Wright, 1983; Longo *et al.*, 1993), display the morphological changes of the oocyte cortex seen during fertilization in sea urchins. Nevertheless, in *M. edulis*, the late polyspermy block that follows the fast electrical mechanism is established by 30 s after fertilization since the duration of the fertilization potential is 30 s (Table 1). One stage of the late polyspermy block in the species seems to be inhibition of sperm-oocyte binding through suppression of the acrosomal reaction (Figs. 7 and 8). The acrosome in sperm on the surface of the oocyte can be in one of two states: unreacted or reacted (Figs. 8 and 9). Therefore, it is possible that the oocyte loses its ability to induce an acrosome reaction after penetration by a fertilizing spermatozoon. In *M. galloprovincialis*, the acrosomal reaction is reportedly triggered when sperm recognize *N*-acetylgalactosamine (GalNAc) residues on the oocyte (Focarelli *et al.*, 1991). Perhaps *Mytilus*, like the ascidians (Lambert and Goode, 1992), release some enzyme from its oocyte so that the "receptor" molecule necessary to induce the acrosomal reaction is destroyed or covered, resulting in an inhibition of sperm-oocyte binding through suppression of the acrosomal reaction. In our preliminary study in *M. edulis*, contrary to the report of Focarelli *et al.* (1991), neither fertilization nor sperm-binding were inhibited in the presence of GalNAc (Togo and Morisawa, unpub. data). Treatment of oocytes with GalNAc-binding lectins (DBA and SBA) also failed to inhibit these processes (Togo and Morisawa, unpub. data). Further studies on the "receptor" prerequisite for the induction of the acrosomal reaction in *Mytilus* will be needed.

Some sperm could undergo an acrosomal reaction and bind to the fertilized oocyte (Fig. 7), although the rate of reaction was reduced in re-inseminated sperm (Fig. 8). Electron microscopic observations showed the acrosomal process of sperm penetrating the oocyte by digesting the vitelline coat with sperm lysin (Fig. 9). However, we could observe neither fusion between the acrosomal process and the oocyte plasma membrane nor formation of the fertilization cone associated with fertilizing sperm (Fig. 9), suggesting that the plasma membrane of the oocyte may change after fertilization. This kind of change would block the sperm-oocyte fusion and has been described in other animals such as the echiuroid *Urechis* (Paul and Gould-Somero, 1976), the nemertean *Cerebratulus* (Kline *et al.*, 1985), mammals (*e.g.*, Horvath *et al.*, 1993), and the surf clam *Spisula* (Ziomek and Epel, 1975; Longo, 1976a). Complete polyspermy block at the plasma membrane was reported in *Spisula:* oocytes from which the vitelline coat had been removed were still monospermic (Ziomek and Epel, 1975). In *M. edulis,* however, polyspermic fertilization occurred even when the vitelline coat was removed by actinase E, suggesting that the oocyte of the species has an incomplete mechanism to block polyspermy at the level of the oocyte plasma membrane (Kyozuka and Osanai, 1994). Changes of the plasma membrane at fertilization was reported by Longo (1976b), who observed a twofold increase in the number of particles on the protoplasmic face of the plasma membrane in freeze-fracture replicas of *Spisula* oocytes. Nevertheless, the relationship between the increase in particles and the block to polyspermy at the oocyte plasma membrane remains obscure.

Bivalves such as *Spisula* (Finkel and Wolf, 1980) and *M. galloprovincialis* (Dufresne-Dubé *et al.*, 1983) are thought to produce a fast polyspermy block by depolarizing the oocyte plasma membrane; the same mechanism was found here in *M. edulis.* Data from re-insemination experiments (Ziomek and Epel, 1975; Longo, 1976a) indicate that a late polyspermy block mechanism is found in *Spisula* as well. As reported here, *M. edulis* clearly shows a complete late block following the electrically mediated fast block. Monospermy is ensured after the fast polyspermy block by the collaboration of the two strategies—suppression of the acrosome reaction of the supernumerary sperm and blockage of sperm entry at the plasma membrane.

Acknowledgments

We thank Drs. H. Nakamura, Akkeshi Marine Biological Station, Hokkaido University, and T. Nawata, College of Medical Sciences, Tohoku University, for their valuable advice and support for the electrophysiological investigations. We also thank the staff of Asamushi Marine Biological Station, Tohoku University, and Misaki Marine Biological Station, University of Tokyo, for supplying the mussels. This work was supported in part by Grants-in-Aid from the Ministry of Education, Science and Culture of Japan to Dr. M. Morisawa (No. 03404004).

Literature Cited

Alliegro, M. C., and D. A. Wright. 1983. Polyspermy inhibition in the oyster, *Crassostrea virginica. J. Exp. Zool.* **227:** 127–137.

Brawley, S. H. 1991. The fast block against polyspermy in fucoid algae is an electrical block. *Dev. Biol.* **144:** 94–106.

Cross, N. L., and R. P. Elinson. 1980. A fast block to polyspermy in frogs mediated by changes in the membrane potential. *Dev. Biol.* **75:** 187–198.

Dufresne-Dubé, L., F. Dubé, P. Guerrier, and P. Couillard. 1983. Absence of a complete block to polyspermy after fertilization of *Mytilus galloprovincialis* (Mollusca, Pelecypoda) oocytes. *Dev. Biol.* **97:** 27–33.

Einsenman, E. A., and M. Alfert. 1982. A new fixation procedure for preserving the ultrastructure of marine invertebrate tissues. *J. Microscop.* **125:** 117–120.

Finkel, T., and D. P. Wolf. 1980. Membrane potential, pH and the activation of surf clam oocytes. *Gamete Res.* **3:** 299–304.

Focarelli, R., D. Rosa, and F. Rosati. 1991. The vitelline coat spikes: A new peculiar structure of *Mytilus galloprovincialis* eggs with a role in sperm-egg interaction. *Mol. Reprod. Dev.* **28:** 143–149.

Goudeau, H., and M. Goudeau. 1989a. A long-lasting electrically mediated block, due to the egg membrane hyperpolarization at fertilization, ensures physiological monospermy in eggs of the crab *Maia squinado. Dev. Biol.* **133:** 348–360.

Goudeau, H., and M. Goudeau. 1989b. Electrical responses to fertilization and spontaneous activation in decapod crustacean eggs: Characteristics and role. Pp. 61–88 in *Mechanisms of Egg Activation,* R. Nuccitelli, G. N. Cherr, and W. H. Clark, Jr., eds., Plenum Press, New York.

Goudeau, H., Y. Depresle, A. Rosa, and M. Goudeau. 1994. Evidence by a voltage clamp study of an electrically mediated block to polyspermy in the egg of the ascidian *Phallusia mammillata. Dev. Biol.* **166:** 489–501.

Gould-Somero, M., L. A. Jaffe, and L. Z. Holland. 1979. Electrically mediated fast polyspermy block in eggs of marine worm, *Urechis caupo. J. Cell Biol.* **82:** 426–440.

Grey, R. D., M. J. Bastiani, D. J. Webb, and E. R. Schertel. 1982. An electrical block is required to prevent polyspermy in eggs fertilized by natural mating of *Xenopus laevis. Dev. Biol.* **89:** 475–484.

Honegger, T. G. 1982. Effect of fertilization and localized binding of lectins in the ascidian, *Phallusia mammillata. Exp. Cell Res.* **138:** 446–451.

Honegger, T. G. 1986. Fertilization in ascidians: Studies on the egg envelope, sperm and gamete interactions in *Phallusia mammillata. Dev. Biol.* **118:** 118–128.

Horvath, P. M., T. Kellom, J. Caulfield, and J. Boldt. 1993. Mechanistic studies of the plasma membrane block to polyspermy in mouse eggs. *Mol. Reprod Dev.* **34:** 65–72.

Iwao, Y. 1989. An electrically mediated block to polyspermy in the primitive urodele *Hynobius nebulosus* and phylogenetic comparison with other amphibians. *Dev Biol* **134:** 438–445.

Jaffe, L. A. 1976. Fast block to polyspermy in sea urchin egg is electrically mediated. *Nature* **261:** 68–71.

Jaffe, L. A. 1980. Electrical polyspermy block in sea urchins: Nicotine and low sodium experiments. *Dev Growth Differ.* **22:** 503–507.

Jaffe, L. A., and M. Gould. 1985. Polyspermy-preventing mechanisms. Pp. 223–250 in *Biology of Fertilization*, Vol. 3, C. B. Metz and A. Monroy, eds. Academic Press, New York.

Kline, D., L. A. Jaffe, and R. P. Tucker. 1985. Fertilization potential and polyspermy prevention in the egg of the nemertean, *Cerebratulus lacteus*. *J. Exp. Zool.* **236:** 45–52.

Kobayashi, W., Y. Baba, T. Shimozawa, and T. S. Yamamoto. 1994. The fertilization potential provides a fast block to polyspermy in lamprey eggs. *Dev. Biol.* **161:** 552–562.

Kyozuka, K., and K. Osanai. 1994. Functions of egg envelope of *Mytilus edulis* during fertilization. *Bull. Mar. Biol. Stn. Asamushi, Tohoku Univ.* **19:** 79–92.

Lambert, C. C. 1986. Fertilization-induced modification of chorion *N*-acetylglucosamine groups blocks polyspermy in ascidian eggs. *Dev. Biol.* **116:** 168–173.

Lambert, C. C. 1989. Ascidian eggs release glycosidase activity which aids in the block against polyspermy. *Development* **105:** 415–420.

Lambert, C. C., and C. A. Goode. 1992. Glycolipid linkage of a polyspermy blocking glycosidase to the ascidian egg surface. *Dev. Biol.* **154:** 95–100.

Longo, F. J. 1976a. Ultrastructural aspects of fertilization in spiralian eggs. *Am. Zool.* **16:** 375–394.

Longo, F. J. 1976b. Cortical changes in *Spisula* eggs upon insemination. *J. Ultrastruct. Res.* **56:** 226–232.

Longo, F. J. 1983. Meiotic maturation and fertilization. Pp. 49–89 in *The Mollusca*, Vol. 3, K. M. Wilbur, ed. Academic Press, New York.

Longo, F. J., L. Mathews, and D. Hedgecock. 1993. Morphogenesis of maternal and paternal genomes in fertilized oyster eggs (*Crassostrea gigas*): Effects of cytochalasin B at different periods during meiotic maturation. *Biol. Bull.* **185:** 197–214.

Matsuura, K., H. Sawada, and H. Yokosawa. 1993. Purification and properties of *N*-acetylglucosaminidase from eggs of the ascidian, *Halocynthia roretzi*. *Eur. J. Biochem.* **218:** 535–541.

Miyazaki, S., and S. Hirai. 1979. Fast polyspermy block and activation potential: Correlated changes during oocyte maturation of a starfish. *Dev. Biol.* **70:** 327–340.

Paul, M., and M. Gould-Somero. 1976. Evidence for a polyspermy block at the level of sperm-egg plasma membrane fusion in *Urechis caupo*. *J. Exp. Zool.* **196:** 105–112.

Reynolds, E. S. 1963. The use of lead citrate at high pH as an electron-opaque stain in electron microscopy. *J. Cell Biol.* **17:** 208–212.

Rosati, F., A. Monroy, and P. DePrisco. 1977. Fine structural study of fertilization in the ascidian, *Ciona intestinalis*. *J. Ultrastruct. Res.* **58:** 261–270.

Rothschild, L., and M. M. Swann. 1952. The fertilization reaction in the sea-urchin. The block to polyspermy. *J. Exp. Biol.* **29:** 469–483.

Vacquier, V. D., D. Epel, and L. A. Douglas. 1972. Sea urchin eggs release protease activity at fertilization. *Nature* **237:** 34–36.

Vacquier, V. D., M. J. Tegner, and D. Epel. 1973. Protease released from sea urchin eggs at fertilization alters the vitelline layer and aids in preventing polyspermy. *Exp. Cell Res.* **80:** 111–119.

Ziomek, C. A., and D. Epel. 1975. Polyspermy block of *Spisula* eggs is prevented by cytochalasin B. *Science* **189:** 139–141.

Reference: *Biol. Bull.* **189**: 340–346. (December, 1995)

In Vivo Effects of Dopamine and Dopaminergic Antagonists on Testicular Maturation in the Red Swamp Crayfish, *Procambarus clarkii*

RACHAKONDA SAROJINI, RACHAKONDA NAGABHUSHANAM, AND MILTON FINGERMAN*

Department of Ecology, Evolution, and Organismal Biology, Tulane University, New Orleans, Louisiana 70118

Abstract. *In vivo*, dopamine (DA) inhibits testicular maturation in the red swamp crayfish, *Procambarus clarkii*. Crayfish given DA injections had a smaller testicular index, smaller testicular lobes, fewer mature sperm, and less-well-developed androgenic glands than did the control crayfish given physiological saline. Males administered 5-hydroxytryptamine (5-HT) or a DA receptor blocker, spiperone or pimozide, showed enhanced testicular maturation and more highly developed androgenic glands than did the control crayfish. When equimolar amounts of 5-HT and DA were co-injected, the actions of DA and 5-HT were found to be antagonistic. These results can be explained by assuming not only that 5-HT triggers release of the gonad-stimulating hormone (GSH) but that DA (a) triggers release of the gonad-inhibiting hormone (GIH), (b) inhibits GSH release, or (c) does both (a) and (b), with GSH and GIH affecting the androgenic glands directly, thereby regulating release of the androgenic gland hormone that has the well-established role of stimulating testicular maturation and spermatogenesis.

Introduction

Biogenic amines function as neurotransmitters in a wide array of animals (Werman, 1966; Gerschenfeld, 1973; Fingerman, 1985). Among the demonstrated roles of at least some of the biogenic amines in crustaceans is regulation of release of neurohormones (Fingerman and Nagabhushanam, 1992; Fingerman *et al.*, 1994).

The presence of the biogenic amines 5-hydroxytryptamine (5-HT) and dopamine (DA) in the nervous systems of crustaceans, including crayfishes, is well established. 5HT-like immunoreactivity in the central nervous system of the red swamp crayfish *Procambarus clarkii*, the species used in the present study, was demonstrated by several investigators (Fujii and Takeda, 1988; Aréchiga *et al.*, 1990; Real and Czternasty, 1990). In addition, 5-HT has been identified and quantitatively measured by high performance liquid chromatography (HPLC) in *Procambarus clarkii* by Kulkarni and Fingerman (1992). Using the crab *Carcinus maenas*, Kerkut *et al.* (1966) provided the first convincing evidence for the existence of DA in the nervous system of a crustacean. Neurons with DA-like immunoreactivity have been visualized in the crayfish *Orconectes limosus* (Elekes *et al.*, 1988), the lobster *Homarus gammarus* (Barthe *et al.*, 1989), and *Procambarus clarkii* (Mercier *et al.*, 1991). By use of HPLC, Elofsson *et al.* (1982) showed the presence of DA in the nervous system of the crayfish *Pacifastacus leniusculus*.

In decapod crustaceans the major neuroendocrine component of the eyestalk, the medulla terminalis X-organ-sinus gland complex, is the source of the gonad-inhibiting hormone (GIH) (Panouse, 1943). In contrast, a gonad-stimulating hormone (GSH) is present in the brain and thoracic ganglia (Otsu, 1960, 1963; Eastman-Reks and Fingerman, 1984). Data from this laboratory provide the basis for the hypothesis that 5-HT triggers release of GSH in both sexes of the fiddler crab *Uca pugilator* (Richardson *et al.*, 1991; Sarojini *et al.*, 1993) and in *Procambarus clarkii* (Kulkarni and Fingerman, 1992; Sarojini *et al.* 1994). On the other hand, DA has so far been found to antagonize the gonad-stimulating action of 5-HT in females of *Procambarus clarkii* (Sarojini *et al.*, 1995a) and in males of *Uca pugilator* (Sarojini *et al.*, 1995b).

Received 8 May 1995; accepted 14 September 1995.
*To whom correspondence should be sent.

In male crustaceans, in addition to the two neurohormones, GSH and GIH, the androgenic gland hormone (AGH) has a major role in the control of spermatogenesis. The function of the androgenic gland in controlling development and maturation of the reproductive system and secondary sexual characteristics in male crustaceans was first described by Charniaux-Cotton (1954). Initiation of spermatogenesis is due to circulating AGH (Payen, 1973). Spermatogenesis stops when the androgenic glands are removed (Charniaux-Cotton, 1964; Puckett, 1964; Nagamine *et al.*, 1980). Removal of both eyestalks, thereby removing the source of GIH, results in hypertrophy of the androgenic glands and precocious spermatogenesis (Meusy, 1965; Demeusy, 1967; Payen *et al.*, 1971). Thus, GIH appears to exert its effect on the testes indirectly, by inhibiting the androgenic glands. On the other hand, a GSH is required to activate the androgenic glands for spermatogenesis to occur (Juchault and Legrand, 1965), a process that Payen (1980) referred to as a positive control of the androgenic glands by a neurohormone. Gupta *et al.* (1989) suggested from their studies of the crab *Paratelphusa hydrodromus* that the inactive phase of the testes is due to an increase in the hemolymph titer of GIH with concomitant decreases in the titers of GSH and AGH.

In view of the facts that 5-HT stimulates gonadal maturation in both male and female *Procambarus clarkii* and DA antagonizes this action of 5-HT in females of this species, this investigation was designed to determine (a) whether DA inhibits testicular maturation in *Procambarus clarkii*, (b) whether 5-HT and DA act antagonistically on gonadal maturation and spermatogenesis in the male crayfish, and (c) whether the androgenic glands will be affected when DA or a dopaminergic receptor blocker is injected. This is the first report that shows injection of DA affects the androgenic glands of any crustacean.

Materials and Methods

Experimental animals

Specimens of the red swamp crayfish, *Procambarus clarkii*, were purchased from a local seafood dealer. In the laboratory they were maintained in freshwater tanks where the water was recirculated constantly through sand filtration units. Male intermolt crayfish with a carapace length of 30–35 mm and a body weight of 11–12 gm were used for these experiments. The crayfish were maintained at a room temperature of 24 ± 2°C, with 12 h of light daily, from 8:00 A.M. to 8:00 P.M., and were fed commercial crayfish food daily.

Drugs

5-HT creatinine sulfate, DA hydrochloride, spiperone, and pimozide were purchased from the Sigma Chemical Company (St. Louis, MO). The drugs were dissolved in crayfish physiological saline (Van Harreveld, 1936). To prepare the stock solution of spiperone a few drops of acetic acid were added to facilitate solubilization. When DA was used 1×10^{-6} mol, 1×10^{-7} mol and 1×10^{-8} mol per crayfish were injected. The amounts of 5-HT, spiperone and pimozide injected were 1×10^{-6} mol per crayfish. The volume injected into each crayfish was 100 μl.

The testicular index (TI) was determined for each crayfish used in these experiments according to the standard formula:

$$\text{TI} = \frac{\text{Weight of the testes}}{\text{Weight of the crayfish}} \times 100$$

The testes and androgenic glands were removed from each of the crayfish used in these experiments after the crayfish were weighed at the time of sacrifice. When these organs were removed the testes were weighed. The testes and androgenic glands were then fixed for 24 h in Bouin's fluid, dehydrated in an alcoholic series, and embedded in paraffin (m.p. 56°–58°C). Sections (7 μm) were cut and stained with Delafield's hematoxylin followed by counterstaining with alcoholic eosin (Bancroft and Stevens, 1982). The diameters of 50 testicular follicles (μm) in the testes of each male were measured by use of a compound microscope fitted with an ocular micrometer. The number of mature sperm per follicle was also determined. The diameters (μm) of 50 cells in each androgenic gland were likewise measured. The experiments were performed twice and the averaged results are presented in the figures where each value represents the mean for 20 crayfish, except for bars IC and SC in Figure 7 which, as we'll explain below, represent the means for 40 crayfish. The data were analyzed by means of Student's *t*-test with significance set at the 95% confidence interval. Standard errors of the means were also calculated.

Results

Effect of DA on the testes

To determine the response of the testes to DA, each time the experiment was done 50 male crayfish were divided into five groups of 10 each. The first group served as the initial control, and this group of crayfish, which received no treatment, was sacrificed on the first day of the experiment. The initial control crayfish were weighed, and then their testes and androgenic glands were dissected out. Then, as stated above, the paired testes were weighed, and the testes and androgenic glands were fixed in Bouin's fluid. A simultaneous control group received only physiological saline in 100 μl doses. The last three groups ran concurrently with the simultaneous control group and

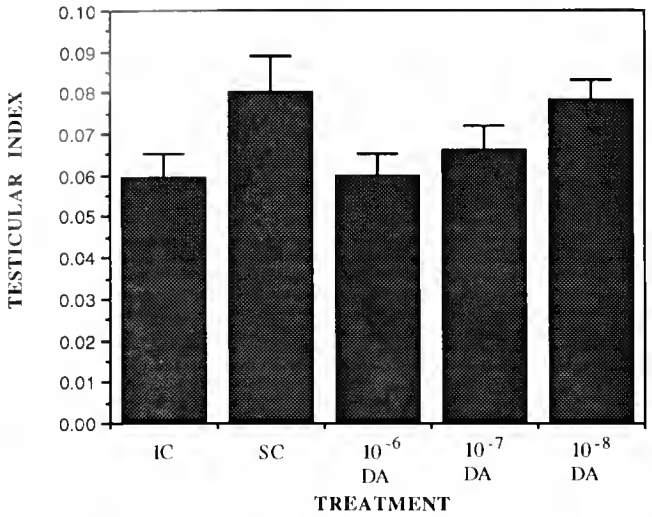

Figure 1. Effect of different doses (1×10^{-8}, 1×10^{-7}, and 1×10^{-6} mol per crayfish) of dopamine (DA) on the mean testicular index of the crayfish, *Procambarus clarkii*. IC, initial control; SC, simultaneous control. Error bars are SEM. Bar SC is significantly ($P < 0.05$) larger than bars IC, 10^{-6} DA, and 10^{-7} DA. Bar 10^{-8} DA is significantly ($P < 0.05$) larger than bar 10^{-6} DA.

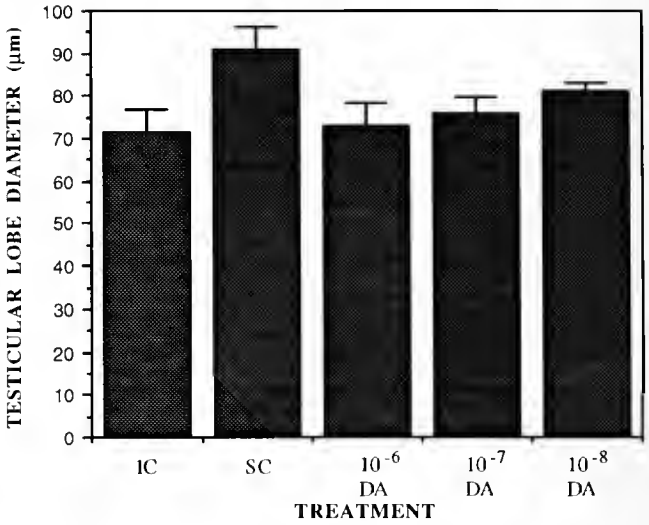

Figure 2. Effect of different doses (1×10^{-8}, 1×10^{-7}, and 1×10^{-6} mol per crayfish) of dopamine (DA) on the mean testicular lobe diameter of the crayfish, *Procambarus clarkii*. IC, initial control; SC, simultaneous control. Error bars are SEM. Bar SC is significantly larger ($P < 0.05$) than bars IC, 10^{-6} DA, and 10^{-7} DA.

received 1×10^{-6} mol, 1×10^{-7} mol, and 1×10^{-8} mol DA per crayfish respectively in 100 μl doses. Injections were administered on the 1st, 5th, and 10th days. The simultaneous control group and those given DA were sacrificed on the 15th day and processed in the same manner as the initial control group.

The TI and mean testicular lobe diameter of the simultaneous control group were significantly larger than the corresponding values of the initial control group, showing that during the 15 days of the experiments the testes were undergoing maturation (Figs. 1, 2). Furthermore, the simultaneous control testes contained mature sperm whereas the initial control testes had none (Fig. 3). The TI and mean testicular lobe diameter of the crayfish that received 1×10^{-6} mol DA injections were significantly smaller than the corresponding values for the simultaneous control crayfish that received only physiological saline. Furthermore, there were no mature sperm in the testicular lobes of the crayfish that received the injections of 1×10^{-6} mol DA in contrast to the simultaneous control crayfish. The crayfish that received injections of the two lower doses of DA (1×10^{-7} mol and 1×10^{-8} mol) also had a smaller TI and mean testicular lobe diameter than the simultaneous control crayfish, but only the difference between the testicular lobe diameter of the simultaneous controls and the crayfish that received injections of 1×10^{-7} mol DA was statistically significant. The testes of the crayfish that received injections of the two lower doses of DA contained mature sperm, but significantly fewer than in the simultaneous control group.

It is evident from Figures 1–3 that DA inhibited testicular maturation. The responses to the three concentrations of DA used strongly suggest that this inhibition is dose-related, as in Figures 1 and 3 where the inhibition produced by 1×10^{-6} mol DA per crayfish is significantly greater than that produced by 1×10^{-8} mol DA per crayfish.

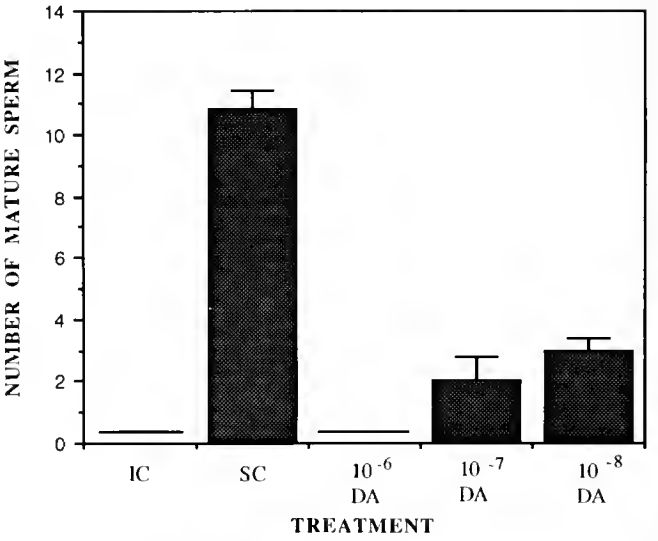

Figure 3. Effect of different doses (1×10^{-8}, 1×10^{-7}, and 1×10^{-6} mol per crayfish) of dopamine (DA) on the mean number of mature sperm per follicle in the testes of the crayfish, *Procambarus clarkii*. IC, initial control; SC, simultaneous control. Error bars are SEM. Bar SC is significantly larger ($P < 0.05$) than bars IC, 10^{-6} DA, 10^{-7} DA, and 10^{-8} DA. Bars 10^{-7} DA and 10^{-8} DA are significantly ($P < 0.05$) larger than bar 10^{-6} DA.

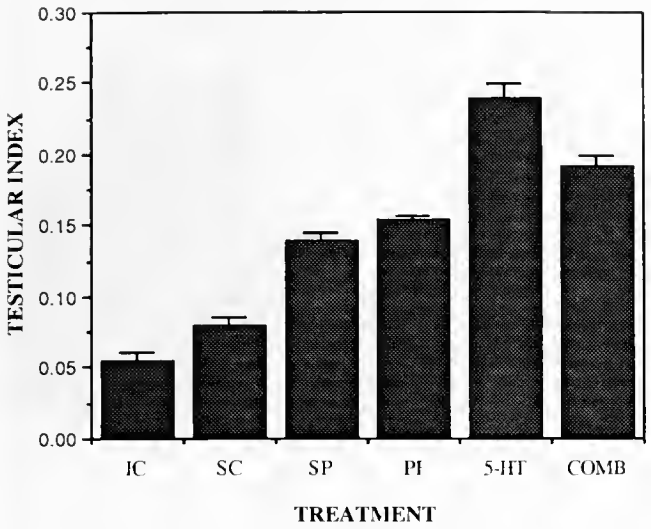

Figure 4. Effect of different treatments on the mean testicular index of the crayfish, *Procambarus clarkii*. IC, initial control; SC, simultaneous control; SP, 1×10^{-6} mol spiperone per crayfish; PI, 1×10^{-6} mol pimozide per crayfish; 5-HT, 1×10^{-6} mol 5-HT per crayfish; COMB, combination of 1×10^{-6} mol DA per crayfish + 1×10^{-6} mol 5-HT per crayfish. Error bars are SEM. Bar SC is significantly ($P < 0.05$) larger than bar IC, but bar SC is significantly ($P < 0.05$) smaller than bars SP, PI, 5-HT, and COMB. Bar 5-HT is significantly ($P < 0.05$) larger than bar COMB.

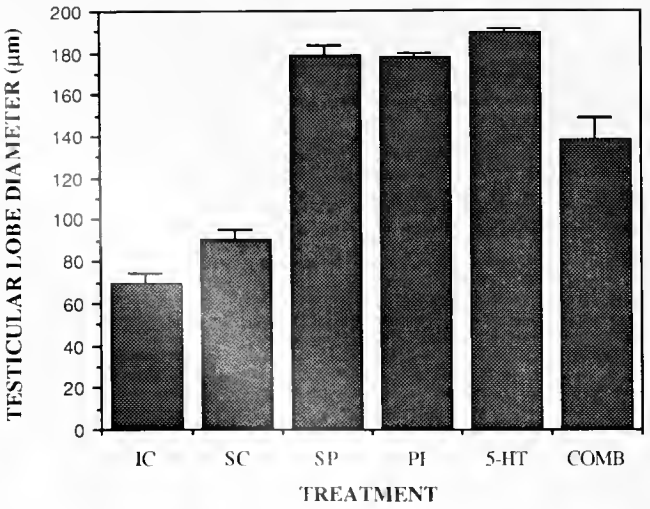

Figure 5. Effect of different treatments on the mean testicular lobe diameter of the crayfish, *Procambarus clarkii*. IC, initial control; SC, simultaneous control; SP, 1×10^{-6} mol spiperone per crayfish; PI, 1×10^{-6} mol pimozide; 5-HT, 1×10^{-6} mol 5-HT per crayfish; COMB, combination of 1×10^{-6} mol DA per crayfish + 1×10^{-6} mol 5-HT per crayfish. Error bars are SEM. Bar SC is significantly ($P < 0.05$) larger than bar IC, but bar SC is significantly ($P < 0.05$) smaller than bars SP, PI, 5-HT, and COMB. Bar 5-HT is significantly ($P < 0.05$) larger than bar COMB.

Effects of the DA receptor blockers spiperone and pimozide, 5-HT alone, and 5-HT in combination with DA on the testes

For each replicate of this set of experiments, 6 groups of 10 crayfish were selected from the stock. One group served as the initial control; the crayfish of this group were treated in the same way as the initial control crayfish of the DA dose-response experiment. The crayfish in the simultaneous control group received physiological saline in 100 μl doses. Two groups received 1×10^{-6} mol of the DA receptor blockers spiperone and pimozide respectively in 100 μl doses. Another group received 1×10^{-6} mol of 5-HT per crayfish in 100-μl doses and the last group received 1×10^{-6} mol DA in 50-μl doses + 1×10^{-6} mol 5-HT in 50-μl doses per crayfish, respectively. Injections were administered on the 1st, 5th, and 10th days. All the crayfish that received injections were sacrificed on the 15th day, and their testes were processed in the same manner as those of the initial control group.

As in the previous experiment, the TI and testicular lobe diameter of the simultaneous control crayfish were significantly larger than the corresponding values for the initial control group (Figs. 4, 5) and, although the initial control testes had no mature sperm, the simultaneous control testes did have some mature sperm (Fig. 6). For the crayfish that each received 100-μl injections of 1×10^{-6} mol of either of the DA receptor blockers (spiperone or

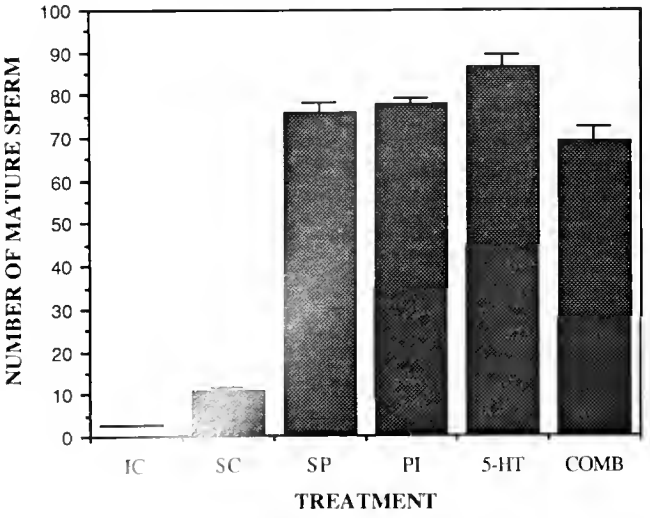

Figure 6. Effect of different treatments on the mean number of mature sperm per follicle in the testes of the crayfish, *Procambarus clarkii*. IC, initial control; SC, simultaneous control; SP, 1×10^{-6} mol spiperone per crayfish; PI, 1×10^{-6} mol pimozide per crayfish; 5-HT, 1×10^{-6} mol 5-HT per crayfish; COMB, combination of 1×10^{-6} mol DA per crayfish + 1×10^{-6} mol 5-HT per crayfish. Error bars are SEM. Bar SC is significantly ($P < 0.05$) larger than bar IC, but bar SC is significantly ($P < 0.05$) smaller than bars SP, PI, 5-HT, and COMB. Bar 5-HT is significantly ($P < 0.05$) larger than bar COMB.

pimozide), the TI and mean testicular lobe diameter were significantly larger than the corresponding values for the simultaneous control crayfish that received physiological saline alone. Furthermore, there was a statistically significant greater number of mature sperm in the testicular follicles of the crayfish that received either spiperone or pimozide than in the simultaneous control crayfish. It is clear from these results that spiperone and pimozide induced testicular maturation.

The TI and mean testicular lobe diameter of the crayfish that received 100 μl of 1×10^{-6} mol 5-HT were significantly larger than the corresponding values for the simultaneous control crayfish (Figs. 4, 5), and the number of mature sperm in the testes of the crayfish given 5-HT was also significantly greater than for the simultaneous control crayfish (Fig. 6). The combination of equimolar amounts of DA and 5-HT produced significant increases in the TI, testicular lobe diameter, and sperm count but significantly less than did 5-HT alone. These results show that DA and 5-HT act antagonistically, but DA was not able to inhibit completely the stimulatory action of 5-HT.

Effects of DA, DA antagonists, 5-HT alone, and 5-HT in combination with DA on the androgenic gland

The androgenic glands of the initial control crayfish consisted of only a few cords of cells closely associated with the vas deferens. These cells had a thin rim of homogeneous cytoplasm around the nucleus. The cells of the simultaneous control crayfish were significantly larger than those in the initial control glands (Fig. 7). The means in Figure 7 for the initial and simultaneous controls represent data from 40 crayfish versus 20 crayfish for the rest of the groups because the means for the initial and simultaneous controls are based on the averages of these controls from the crayfish used in the two sets of experiments that provided the data for Figures 1–3 and 4–6. The cells of the androgenic glands of the crayfish that received injections of 1×10^{-6}, 1×10^{-7}, or 1×10^{-8} mol DA per crayfish were not significantly different in size from those of the initial control group. The cells in the androgenic glands of all the crayfish that received injections of DA, regardless of the dose used, were significantly smaller than the cells in the concurrent control glands. The inhibitory effects of the three concentrations of DA on the androgenic glands do not provide clear evidence of a dose-related response, although the highest concentration produced somewhat more inhibition than did the two lesser doses. The androgenic glands of crayfish that received a DA receptor blocker, spiperone or pimozide, 5-HT alone or 5-HT in combination with DA showed significantly greater development of their androgenic glands over the initial and simultaneous controls. The cytoplasm in these enlarged glands was more dense and granular than in either control group. As with the testes, while the combination of 5-HT and DA produced significant growth of the androgenic glands, this growth was significantly less than that produced by 5-HT alone, additional evidence of antagonistic actions of DA and 5-HT on the reproductive system of male red swamp crayfish.

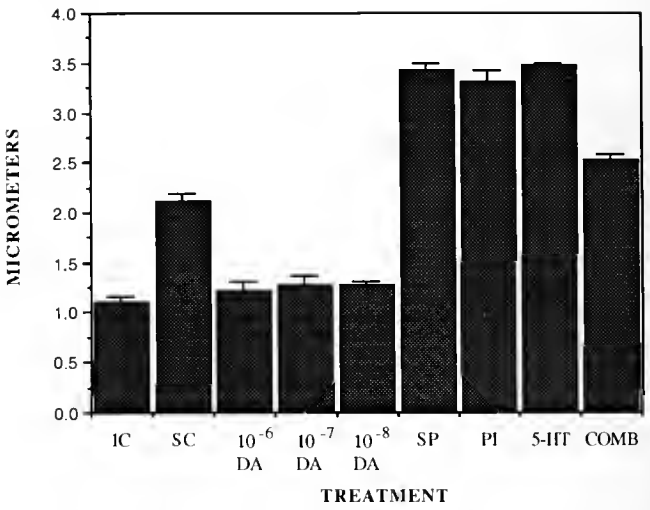

Figure 7. Effect of different treatments on the mean cell size in the androgenic glands of the crayfish, *Procambarus clarkii*. IC, initial control; SC, simultaneous control; 10^{-6} DA, 1×10^{-6} mol DA per crayfish; 10^{-7} DA, 1×10^{-7} mol DA per crayfish; 10^{-8} DA, 1×10^{-8} mol DA per crayfish; SP, 1×10^{-6} mol spiperone per crayfish; PI, 1×10^{-6} mol pimozide per crayfish; 5-HT, 1×10^{-6} mol 5-HT per crayfish; COMB, combination of 1×10^{-6} mol DA per crayfish + 1×10^{-6} mol 5-HT per crayfish. Error bars are SEM. Bar SC is significantly ($P < 0.05$) larger than bars IC, 10^{-6} DA, 10^{-7} DA, and 10^{-8} DA, but bar SC is significantly ($P < 0.05$) smaller than bars SP, PI, 5-HT, and COMB. Bar 5-HT is significantly ($P < 0.05$) larger than bar COMB.

Discussion

The present study demonstrates for the first time in a crayfish an inhibitory action of DA on the testes. Furthermore, this is the first report of the effect of DA and any of its antagonists on the androgenic glands of any crustacean. DA alone inhibited testicular and androgenic gland maturation (Figs. 1–3, 7). On the other hand, 5-HT and the DA receptor blockers spiperone and pimozide induced testicular and androgenic gland maturation (Figs. 4–7).

In *Procambarus clarkii*, as stated above, gonadal maturation is regulated by both stimulatory and inhibitory neurohormones, maturation being stimulated by GSH from the brain and thoracic ganglia and inhibited by GIH from the eyestalk neuroendocrine system. Our previous studies with *Procambarus clarkii* (Sarojini *et al.* 1993, 1994) showed that 5-HT stimulates gonadal maturation in males and females, presumably by stimulating GSH

release and that DA inhibits ovarian development. The evidence for 5-HT and DA presence in the nervous systems of crayfish (Fujii and Takeda, 1988; Aréchiga *et al.* 1990; Real and Czternasty, 1990; Mercier *et al.*, 1991; Kulkarni and Fingerman, 1992) was already demonstrated.

The roles of DA and 5-HT in regulation of gonadal maturation in vertebrates is documented. Goldfish, *Carassius auratus*, fed the DA agonist apomorphine had elevated plasma levels of growth hormone whereas the circulating levels of gonadotropic hormone were reduced (Wong *et al.*, 1993). Long-term feeding of goldfish with apomorphine induced significant increases in both the body weight and length. 5-HT stimulates gonadotropic hormone release in the goldfish (Somoza *et al.*, 1988; Somoza and Peter, 1991). This effect of 5-HT may be due to direct action on the gonadotrophs or to inhibition of DA release from nerve terminals in the pars distalis. DA inhibits release of this gonadotropic hormone (Yu and Peter, 1992). Similarly, DA appears to inhibit luteinizing hormone release in the frog, *Rana temporaria* (Sotowska-Brochocka *et al.*, 1994).

The crayfish that received 5-HT alone had a larger TI and mean testicular lobe diameter and also had more mature sperm in their testicular lobes than did the simultaneous control group (Figs. 4–6) which is consistent with the earlier results of Sarojini *et al.* (1994). The crayfish that received 5-HT in combination with DA had a significantly larger TI and mean testicular lobe diameter, and also a greater number of mature sperm, when compared with the simultaneous controls (Figs. 4–6), but all three values were significantly smaller than the corresponding values of the crayfish given 5-HT alone. The DA in the mixture was not able to antagonize fully the stimulatory action of the 5-HT. This antagonism between the effects produced by 5-HT and DA on the testes is reminiscent of that seen with the erythrophores of *Uca pugilator* where the pigment-dispersing effect of 5-HT and the pigment-concentrating effect of DA were reduced when mixtures of 5-HT and DA were co-injected (Fingerman and Fingerman, 1977).

The data obtained with the DA antagonists used in the present study support the conclusion that DA inhibits testicular maturation. Both spiperone and pimozide produced testicular maturation (Figs. 4–6). Presumably, these blockers prevent the action of endogenous DA, hence leading to precocious testicular maturation.

The inhibitory action of DA on the androgenic glands and testes in *Procambarus clarkii* can be explained as follows: DA has an indirect action on the testes and androgenic glands. We hypothesize that DA either (a) stimulates release of GIH from the eyestalk neuroendocrine system, (b) inhibits release of GSH, or (c) does both (a) and (b). Any of these hypothesized actions of DA would result in reduced AGH in the blood, resulting in at least some inhibition of testicular maturation and spermatogenesis. Experiments are currently in progress to evaluate these suggested modes of action of DA. That DA can have a stimulatory role in the release of a neurohormone was shown for the red pigment-concentrating hormone, as reported by Fingerman and Fingerman (1977) and Quackenbush and Fingerman (1984) who performed *in vivo* and *in vitro* experiments on release of this neurohormone with the fiddler crab, *Uca pugilator*. The concentrations of biogenic amines used in these experiments are quite like those injected by other investigators while studying the same species, *Procambarus clarkii*. Livingstone *et al.* (1980) injected 5.7×10^{-6} mol 5-HT and 6.5×10^{-6} mol octopamine per crayfish, and Aréchiga *et al.* (1990) injected 1×10^{-9} to 1×10^{-3} mol 5-HT per crayfish.

Because DA inhibited testicular maturation in *Procambarus clarkii*, it is worth mentioning the potential application of DA analogues in crayfish farming. Supplementing the crayfish diet with long-lasting DA agonists may slow reproductive activity of crayfish and simultaneously lead to enhanced somatic growth.

Literature Cited

Aréchiga, H., E. Banuelos, E. Frixione, A. Picones, and L. Rodriguez-Sosa. 1990. Modulation of crayfish retinal sensitivity by 5-hydroxytryptamine. *J. Exp. Biol.* **150:** 123–143.

Bancroft, J. D., and A. Stevens. 1982. *Theory and Practice of Histological Techniques*, 2nd Ed. Churchill Livingstone, New York. Pp. 109–121.

Barthe, J. Y., N. Mons, D. Cattaert, M. Geffard, and F. Clarac. 1989. Dopamine and motor activity in the lobster *Homarus gammarus*. *Brain Res.* **497:** 368–373.

Charniaux-Cotton, H. 1954. Découverte chez un Crustacé Amphipode (*Orchestia gammarella*) d'une glande endocrine responsable de la différenciation des caractères sexuels primaires et secondaires mâles. *C. R. Acad. Sci. Paris.* **239:** 780–782.

Charniaux-Cotton, H. 1964. Endocrinologie et génétique du sexe chez les Crustacés supérieurs. *Ann. Endocrinol.* **25:** 36–42.

Demeusy, N. 1967. Modalités d'action du contrôle inhibiteur pédonculaire exercé sur les caractères sexuels externes mâles du Décapode Brachyoure *Carcinus maenus* L. *C. R. Acad. Sci. Paris.* **265D:** 628–630.

Eastman-Reks, S., and M. Fingerman. 1984. Effects of neuroendocrine tissue and cyclic AMP on ovarian growth *in vivo* and *in vitro* in the fiddler crab, *Uca pugilator*. *Comp. Biochem. Physiol.* **79A:** 679–684.

Elekes, K., E. Florey, M. A. Cahill, U. Hoeger, and M. Geffard. 1988. Morphology, synaptic connections and neurotransmitters of the efferent neurons of the crayfish hindgut. *Symposia Biologica Hungarica* **36:** 129–146.

Elofsson, R., L. Laxmyr, E. Rosengren, and C. Hansson. 1982. Identification and quantitative measurements of biogenic amines and DOPA in the central nervous system and hamolymph of the crayfish, *Pacifastacus leniusculus*. *Comp. Biochem. Physiol.* **71C:** 195–201.

Fingerman, M. 1985. The physiology and pharmacology of crustacean chromatophores. *Am. Zool.* **25:** 233–252.

Fingerman, M., and S. W. Fingerman. 1977. Antagonistic actions of dopamine and 5-hydroxytryptamine on color changes in the fiddler crab, *Uca pugilator*. *Comp. Biochem. Physiol.* **58C:** 121–127.

Fingerman, M., and R. Nagabhushanam. 1992. Control of the release of crustacean hormones by neuroregulators. *Comp. Biochem. Physiol.* **102C:** 343–352.

Fingerman, M., R. Nagabhushanam, R. Sarojini, and P. S. Reddy. 1994. Biogenic amines in crustaceans: identification, localization, and roles. *J. Crust. Biol.* **14:** 413–437.

Fujii, K., and N. Takeda. 1988. Phylogenetic detection of serotonin immunoreactive cells in the central nervous system of invertebrates. *Comp. Biochem. Physiol.* **89C:** 233–239.

Gerschenfeld, H. M. 1973. Chemical transmission in invertebrate central nervous systems and neuromuscular junctions. *Physiol. Rev.* **53:** 1–119.

Gupta, N. V. S., K. N. P. Kurup, R. G. Adiyodi, and K. G. Adiyodi. 1989. The antagonism between somatic growth and testicular activity during different phases in intermolt (Stage C_4) in sexually mature freshwater crab, *Paratelphusa hydrodromus. Invert. Reprod. Dev.* **16:** 195–204.

Juchault, P., and J. J. Legrand. 1965. Contribution à l'étude expérimentale de l'intervention des neurohormones dans le changement de sexe d'*Anilocra physodes* (Crustacé, Isopode, Cymothoidae). *C. R. Acad. Sc. Paris.* **260:** 1783–1786.

Kerkut, G. A., C. B. Sedden, and R. J. Walker. 1966. The effect of DOPA, α-methylDOPA and reserpine on the dopamine content of the brain of the snail, *Helix aspersa. Comp. Biochem. Physiol.* **18:** 921–930.

Kulkarni, G. K., and M. Fingerman. 1992. Quantitative analysis by reverse phase high performance liquid chromatography of 5-hydroxytryptamine in the central nervous system of the red swamp crayfish, *Procambarus clarkii. Biol. Bull.* **182:** 341–347.

Livingstone, M. S., R. M. Harris-Warrick, and E. A. Kravitz. 1980. Serotonin and octopamine produce opposite postures in lobsters. *Science.* **208:** 76–79.

Mercier, A. J., I. Orchard, and A. Schmoeckel. 1991. Catecholaminergic neurons supplying the hindgut of the crayfish, *Procambarus clarkii. Can. J. Zool.* **69:** 2778–2785.

Meusy, J. J. 1965. Modifications ultrastructurales des glandes androgènes de *Carcinus maenus* L. (Crustacé Décapode) consécutives à l'ablation des pédoncules oculaires. *C. R Acad Sci Paris* **260:** 5901–5903.

Nagamine, C., A. W. Knight, A. Maggenti, and G. Paxman. 1980. Effects of androgenic gland ablation on male primary and secondary sexual characteristics in the Malaysian prawn *Macrobrachium rosenbergii* (de Man) with first evidence of induced feminization in a non-hermaphroditic decapod. *Gen. Comp. Endocrinol.* **41:** 423–441.

Otsu, T. 1960. Precocious development of the ovaries in the crab, *Potamon dehaani,* following the implantation of the thoracic ganglion. *Annot. Zool. Japon* **33:** 90–96.

Otsu, T. 1963. Bihormonal control of sexual cycle in the freshwater crab, *Potamon dehaani. Embryologia* **8:** 1–20.

Panouse, J. B. 1943. Influence de l'ablation du péndoncle oculaire sur la croissance de l'ovaire chez la Crevette *Leander serratus. C. R. Acad. Sci. Paris* **217:** 553–555.

Payen, G. G. 1973. Etude descriptive des principales étapes de la morphogenèse sexuelle chez un Crustacé Décapode à développement condensé, l'Ecrevisse *Pontastacus leptodactylus leptodactylus* (Eschscholtz, 1823). *Ann. Embryol. Morphog.* **6:** 179–206.

Payen, G. G. 1980. Experimental studies of reproduction in Malacostraca crustaceans. Endocrine control of spermatogenic activity. Pp. 187–196 in *Advances in Invertebrate Reproduction,* W. M. Clark and T. S. Adams, eds. Elsevier/North-Holland, New York.

Payen, G. G., J. D. Costlow, and H. Charniaux-Cotton. 1971. Etude comparative de l'ultrastructure des glandes androgènes de Crabes normaux et pédonculectomisés pendant la vie larvaire ou après la puberté chez les espèces: *Rhithropanopeus harrisii* (Gould) et *Callinectes sapidus* Rathbun. *Gen. Comp. Endocrinol.* **17:** 526–542.

Puckett, D. H. 1964. Experimental studies on the crayfish androgenic gland in relation to testicular function. *Diss. Abstr.* **25:** 3765.

Quackenbush, L. S., and M. Fingerman. 1984. Regulation of the release of chromatophorotropic neurohormones from the isolated eyestalk of the fiddler crab, *Uca pugilator. Biol. Bull.* **166:** 237–250.

Real, D., and G. Czternasty. 1990. Mapping of serotonin-like immunoreactivity in the ventral nerve cord of crayfish. *Brain Res.* **521:** 203–212.

Richardson, H. G., M. Deecaraman, and M. Fingerman. 1991. The effect of biogenic amines on ovarian development in the fiddler crab, *Uca pugilator. Comp Biochem. Physiol.* **99C:** 53–56.

Sarojini, R., R. Nagabhushanam, and M. Fingerman. 1993. *In vivo* evaluation of 5-hydroxytryptamine stimulation of the testes in the fiddler crab, *Uca pugilator:* a presumed action on the neuroendocrine system. *Comp. Biochem. Physiol.* **106C:** 321–325.

Sarojini, R., R. Nagabhushanam, and M. Fingerman. 1994. 5-hydroxytryptaminergic control of testes development through the androgenic gland in the red swamp crayfish, *Procambarus clarkii. Invert. Reprod. Dev.* **26:** 127–132.

Sarojini, R., R. Nagabhushanam, and M. Fingerman. 1995a. *In vivo* inhibition by dopamine of 5-hydroxytryptamine-stimulated ovarian maturation in the red swamp crayfish, *Procambarus clarkii. Experientia.* **51:** 156–158.

Sarojini, R., R. Nagabhushanam, M. Davi, and M. Fingerman. 1995b. Dopaminergic inhibition of 5-hydroxytryptamine-stimulated testicular maturation in the fiddler crab, *Uca pugilator. Comp. Biochem Physiol.* **111C:** 287–292.

Somoza, G. M., K. L. Yu, and R. E. Peter. 1988. Serotonin stimulates gonadotropin release in female and male goldfish, *Carassius auratus* L. *Gen. Comp. Endocrinol.* **72:** 374–382.

Somoza, G. M., and R. E. Peter. 1991. Effects of serotonin on gonadotropin and growth hormone release from *in vitro* perifused goldfish pituitary fragments. *Gen. Comp. Endocrinol.* **82:** 103–110.

Sotowska-Brochocka, J., L. Martyńska, and P. Licht. 1994. Dopaminergic inhibition of gonadotropic release in hibernating frogs, *Rana temporaria. Gen. Comp. Endocrinol.* **93:** 192–196.

Van Harreveld, A. 1936. A physiological solution for freshwater crustaceans. *Proc. Soc. Exp. Biol. Med.* **34:** 428–432.

Werman, R. 1966. Criteria for identification of a central nervous system transmitter. *Comp. Biochem. Physiol.* **18:** 745–766.

Wong, A. O. L., J. P. Chang, and R. E. Peter. 1993. *In vitro* and *in vivo* evidence that dopamine exerts growth hormone-releasing activity in goldfish. *Am. J. Physiol.* **264:** E925–E932.

Yu, K. L., and R. E. Peter. 1992. Adrenergic and dopaminergic regulation of gonadotropin-releasing hormone release from goldfish preoptic-anterior hypothalamus and pituitary *in vitro. Gen. Comp. Endocrinol.* **85:** 138–146.

Reference: *Biol. Bull.* **189**: 347–355. (December, 1995)

A Transient Exposure to Symbiosis-Competent Bacteria Induces Light Organ Morphogenesis in the Host Squid

JUDITH A. DOINO AND MARGARET J. McFALL-NGAI*

Department of Biological Sciences, University of Southern California, Los Angeles, California 90089-0371

Abstract. Recent studies of the symbiotic association between the Hawaiian sepiolid squid *Euprymna scolopes* and the luminous bacterium *Vibrio fischeri* have shown that colonization of juvenile squid with symbiosis-competent bacteria induces morphogenetic changes of the light organ. These changes occur over a 4-day period and include cell death and tissue regression of the external ciliated epithelium. In the absence of bacterial colonization, morphogenesis does not occur. To determine whether the bacteria must be present throughout the morphogenetic process, we used the antibiotic chloramphenicol to clear the light organ of bacteria at various times during the initial colonization. We provide evidence in this study that a transient, 12-hour exposure to symbiosis-competent bacteria is necessary and sufficient to induce tissue regression in the light organ over the next several days. Further, we show that successful entrance into the light organ is necessary to induce morphogenesis, suggesting that induction results from bacterial interaction with internal crypt cells and not with the external ciliated epithelium. Finally, no difference in development was observed when the light organ was colonized by a mutant strain of *V. fischeri* that did not produce autoinducer, a potential light organ morphogen.

Introduction

Prolonged associations with bacterial symbionts are now recognized as important phenomena in the developmental program of many plant and animal hosts (for reviews see Schwemmler, 1989; Hirsch, 1992; Saffo, 1992). In some cases, bacterial symbioses may even be required for normal host development or survival. For example, enteric bacteria provide essential enzymes and vitamins to their mammalian hosts, and associations with bacteria are required for normal development of the mammalian immune system (Gordon and Pesti, 1971). In other cases, though essential only under nutrient-poor conditions, the association is highly beneficial to the host's fitness in its natural environment, such as the symbioses between leguminous plants with nitrogen-fixing bacteria or between the weevil *Sitophilus oryzae* and its associated gram-negative bacteria. In these partnerships, the bacteria provide nutritional metabolites to their host (Nardon and Grenier, 1991) as well as influence its development.

Of the known prokaryote-eukaryote associations, much progress has been made toward the understanding of the development of plant-bacterial symbioses, both because the plant hosts are easily maintained and manipulated in the laboratory and the bacterial symbionts are culturable. An animal-bacterial association offering similar experimental benefits is the highly specific association between the Hawaiian sepiolid squid *Euprymna scolopes* and the bioluminescent bacterium *Vibrio fischeri*. This symbiosis provides an experimental system to study the effect of bacterial symbionts on host animal development (McFall-Ngai and Ruby, 1991; Ruby and McFall-Ngai, 1992). In the host squid, the bacteria are always contained within epithelia-lined crypts inside the light organ, which is housed within the mantle cavity. However, the morphology of the light organ in juvenile squid is much different from that of the adult (McFall-Ngai and Montgomery, 1990), and the light organ undergoes complex de-

Received 6 February 1995; accepted 10 October 1995.

* Corresponding author.

Abbreviations: CEA, ciliated epithelial appendages; CSW, California seawater; Cm, chloramphenicol.

velopmental changes following bacterial colonization (Montgomery and McFall-Ngai, 1994).

Upon hatching, juvenile squid are aposymbiotic (without bacterial symbionts) and normally acquire free-living *V. fischeri* from the surrounding seawater within hours (Wei and Young, 1989; McFall-Ngai and Ruby, 1991). A substantial portion of the juvenile light organ epithelium is microvillous and ciliated, bearing two lateral pairs of appendages (ciliated epithelial appendages; CEA) that appear to facilitate inoculation of bacteria into the light organ (Fig. 1a; McFall-Ngai and Ruby, 1991; Montgomery and McFall-Ngai, 1993). Microscopy and high-speed cinematography have revealed that the two appendages on each side of the light organ form a ring, at the base of which are three pores leading into three independent crypts (Fig. 1b). Beating of the cilia entrains passing seawater within the ring, potentially increasing the probability that symbionts within the water will enter the pores (M. McFall-Ngai and R. Emlet, unpub. results). When the light organ has been successfully colonized by *V. fischeri*, cell death is observed in the CEA and regression of these appendages occurs over a period of four days. Four-day-old squid that are not infected with *V. fischeri* do not show cell death nor regression of the CEA (Montgomery and McFall-Ngai, 1994). Therefore, the presence of symbiosis-competent bacteria somehow induces host tissues that are several cell layers away to initiate light organ morphogenesis. Cell death and the resulting regression of the CEA are the first observable events of light organ morphogenesis and therefore the first developmental evidence that induction has occurred.

In this study we have asked whether the presence of bacteria within the light organ is required continuously for 4 days to induce CEA regression. Additionally, we used noninfective strains of *V. fischeri* to determine whether colonization of the light organ is necessary for induction. Finally, we tested whether *V. fischeri* autoinducer, a cell density-dependent factor secreted by the bacteria and involved in the production of light, is required to induce light organ morphogenesis.

Materials and Methods

Animal care and maintenance

Adult squid were collected at night from Kaneohe Bay, Oahu, HI, with dipnets and were transported back to the University of Southern California, Los Angeles within one week of collection. Animals were maintained in a 265-liter recirculating aquarium at 23°C, and females were mated approximately once a week. Egg clutches, attached to coral rocks or other hard surfaces by the females, were transferred for hatching to smaller temperature-controlled 23°C aquaria. To ensure that juvenile squid did not become prematurely infected with any residual bacteria that might be associated with the egg clutch, squid were transferred immediately upon hatching through three rinses with California coastal seawater (CSW), which does not contain infective strains of *V. fischeri* (McFall-Ngai and Ruby, 1991). Juveniles were used for infection studies within 6 h of hatching.

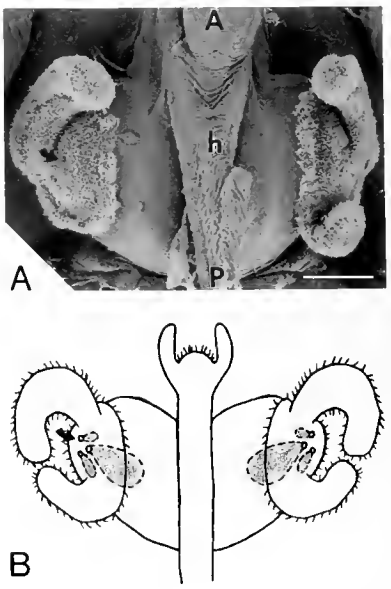

Figure 1. Scanning electron micrograph (A) of a hatchling light organ with complete CEA and a schematic drawing (B) showing the position of the appendages *in vivo* and the three pores in the ciliated epithelium (arrow) with their associated internal crypts (approximated by dashed line). A, anterior; P, posterior; h, hindgut. Scale bar = 100 μm.

Inoculation of squid with V. fischeri *bacteria*

Bacteria were grown to log phase in a seawater-based minimal medium (Ruby and Asato, 1993) and diluted to between 10^3 and 10^5 cells/ml for inoculation of squid. After inoculation, squid were rinsed in CSW and transferred to either CSW or chloramphenicol-treated CSW (as described below). For all experiments, positive (infected) controls were exposed to symbiosis-competent bacteria in CSW for the entire 4 days and negative (uninfected) controls were exposed to CSW alone.

Monitoring bacterial colonization

Because *V. fischeri* is luminous in the light organ, successful colonization of the organ can be monitored by measuring the bioluminescence of the squid with a photomultiplier tube (Luminescence Photometer, Model 3600, Biospherical Instruments, Inc.). For these measurements, individual squid were kept in 5 ml of seawater in glass scintillation vials. Seawater in the vials was changed daily throughout the 4-day experiments, just prior to each luminescence measurement.

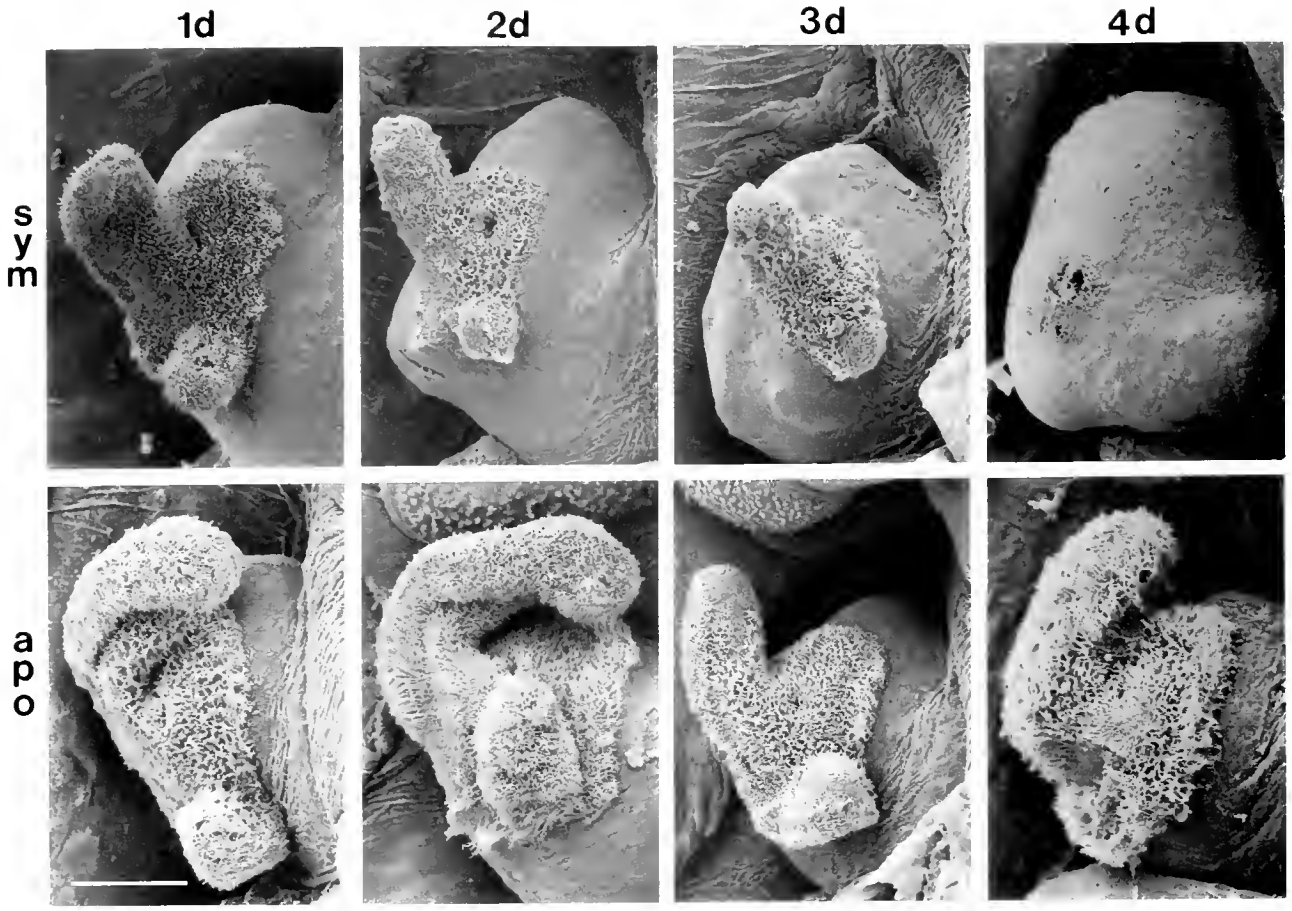

Figure 2. Time series of CEA regression in symbiotic (sym) and aposymbiotic (apo) juvenile squid over 4 days (d). Symbiotic animals were inoculated with ~ 10^4 cells/ml of *V. fischeri* ES114 within 6 h of hatching. The sym-4d panel represents a fully regressed CEA. Only the right half of each light organ is shown. Scale bar = 100 μm. Differences in size reflect individual variation.

Determination of Ciliated Epithelial Appendage (CEA) regression

Regression of the CEA was determined at the end of 4 days for each experiment. Squid were fixed for 24 h in seawater containing either 5% formalin or 2% paraformaldehyde/2% glutaraldehyde. Samples were subsequently rinsed twice for 30 min in 50 m*M* sodium phosphate buffer with 0.45 *M* NaCl (pH 7.2), followed by a dehydration series with 15%–100% ethanol. Samples were critical-point dried with liquid CO_2, or desiccated with hexamethyldisilazane (Polysciences, Inc.). Dried squid were mounted onto aluminum stubs and the ventral portions of the mantle and siphon were dissected away to reveal the juvenile light organs. These samples were then sputter coated with gold and the light organs were examined with a Cambridge 360 scanning electron microscope (SEM). The presence or absence of CEA was scored and recorded, and photomicrographs were taken of representative samples.

CEA regression of symbiotic juveniles was compared to that of aposymbiotic juveniles for 4 days following inoculation with bacteria (Fig. 2). For experiments involving variable exposure times, CEA regression at day 4 was divided into five stages (0, 1, 2, 3, and 4), which correspond to the regression seen at 0 (Fig. 1A), 1, 2, 3, and 4 days of uninterrupted symbiosis (Fig. 2). CEA of light organs were considered regressed if they were at or beyond stage 3. Due to the high variability between individual squid, even within control groups, regression is reported as an E/C index, which is defined as the percentage of experimental animals with regressed CEA divided by that of the symbiotic controls in a given experiment (experimental and control animals for a given experiment were always from the same clutch of eggs).

Manipulation of exposure times and colonization levels

Transient vs. continuous exposure to V. fischeri *strain ES114.* To determine first whether a continuous exposure

to competent bacteria is necessary for initiating morphogenesis of the light organ, we used the bacteriostatic antibiotic chloramphenicol (Cm) to clear the light organ of viable symbionts (Fig. 3a). Squid were exposed to one of two symbiosis-competent strains of *Vibrio fischeri:* ES114, a chloramphenicol-sensitive light organ isolate (Boettcher and Ruby, 1990) or ES114-U2, a spontaneous chloramphenicol-resistant mutant of ES114 (donated by J. Graf). The inoculations were performed for two time periods: (1) continuously for 4 days, or (2) for 12 h. Those exposed continuously were inoculated with *V. fischeri* and then transferred to CSW after 12 h for the remainder of the 4 days (Fig. 3a, top bar). These squid remained infected for the duration of the experiment. Following incubation with *V. fischeri,* squid exposed for only 12 hours were transferred to CSW treated with 10 μg/ml Cm in seawater for the remainder of the experiment (Fig. 3a, second bar). The transient time period of 12 h was chosen because successful colonization of the light organ by bacteria can be confirmed by the appearance of luminescence between 10 and 12 h after exposure. The Cm-resistant strain ES114-U2 was used as a control for any inhibitory pharmacological effects that Cm may have on CEA regression. Squid were monitored for luminescence before exposure to bacteria, every 2 h during initial colonization and every 12 h thereafter. Uninfected controls were exposed to noninfective CSW with or without Cm (Fig. 3a, third and fourth bars) and monitored for luminescence every 12 h.

To insure that Cm treatment was effectively clearing the light organ of viable bacteria, the decrease of both bacteria colony forming units (CFU) and luminescence was monitored in squid treated with 10 μg Cm/ml CSW following exposure to bacteria for 12 h.

Variable exposure times to V. fischeri *strain ES114.* To determine the minimum time period required to induce morphogenesis, hatchling squid were exposed to *V. fischeri* for variable lengths of time (Fig. 3b). At time 0, all squid were placed in a single bowl with of CSW containing $\sim 5 \times 10^3$ ES114 cells/ml. Groups of 10–20 animals were removed from the bowl at 1, 4, 8, and 12 h. Upon removal from the bowl at each time period, half of the squid were rinsed twice and transferred to vials with Cm-treated CSW (Fig. 3b, top), while the other half were transferred to vials with Cm-free CSW (Fig. 3b, bottom). Groups transferred to Cm-free CSW became infected within 12 h. Luminescence was measured immediately before and after exposure to bacteria and once per day thereafter.

Exposure to other strains of V. fischeri

To determine whether colonization of the light organ by the bacteria is necessary to induce CEA regression, squid were exposed to three noninfective strains of *V. fischeri* (M101, MdR12, and MJ1). A fourth strain of *V. fischeri* (MJ11), which is not normally associated with the *E. scolopes* light organ but is capable of colonization, was also tested for its ability to induce morphogenesis. Following the inoculation period, squid were transferred to CSW for the remainder of the 4 days. Possible colonization of squid exposed to noninfective strains was determined by both luminescence measurements and bacterial plate counts. Colonization of positive and negative controls was determined by luminescence only.

Noninfective strains. Strain M101 was produced by transposon (Mu dI-1681) mutagenesis of symbiosis-competent strain ES114, resulting in a nonmotile mutant. Nonmotile mutants of *V. fischeri* have previously been shown to be noninfective in *E. scolopes* (Graf *et al.,* 1994). Squid were exposed to $\sim 10^4$ M101 cells/ml for 12 h. Strain MdR12 is a non-symbiotic wild type isolate from Southern California coastal seawater. Strain MJ1 was originally isolated from the light organ of the Japanese pinecone fish *Monocentris japonica,* but has been in culture for 21 years (Ruby and Nealson, 1976) and does not infect *E. scolopes.* Squid were exposed to $\sim 10^5$ cells/ml of this strain for 24 h.

Infective strain. Strain MJ11 was isolated from the light organ of *M. japonica* in 1992 and is infective to *E. scolopes.* Squid were exposed to $\sim 10^5$ MJ11 cells/ml for 12 h. This strain was of interest because, although it is capable of colonization, bacterial numbers inside the light organ reach only 10% of the levels seen with ES114 (K.H. Lee and E.G. Ruby, pers. comm.).

Exposure to an autoinducer mutant strain of V. fischeri

Symbiont bioluminescence in the *E. scolopes* light organ is induced via a well studied mechanism involving the secreted *V. fischeri* molecule autoinducer (VAI), a homoserine lactone. Normally VAI is expressed constitutively at a low level, but when cell densities become high, such as in the light organ (Boettcher and Ruby, 1990), the build up of VAI in the extracellular medium positively regulates VAI gene expression and in turn activates expression of the *lux* operon, which encodes for those genes responsible for bacterial light production (for review, see Dunlap and Greenberg, 1991). To determine whether VAI was a morphogen of the squid light organ, we used a mutant strain (310Ω) of *V. fischeri* (provided by Kendall Gray) containing an insertion in the autoinducer gene, which renders the cells incapable of making autoinducer.

One-day-old squid were exposed to symbiosis-competent *V. fischeri* strain 310Ω or to ES114 at a concentration of $\sim 10^3$ cells/ml for approximately 20 h. Because the 310Ω strain is nonluminous, successful colonization of the squid could not be monitored with a photometer. Instead, at the end of 4 days, two of the squid that had been

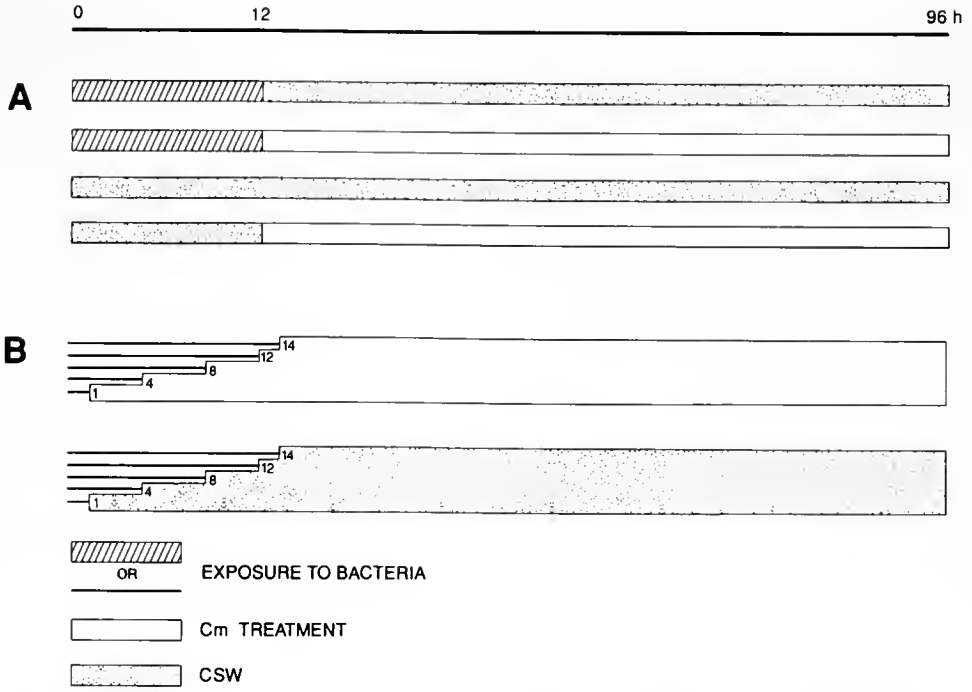

Figure 3. Experimental design for transient and variable exposure to bacteria. n = 5–20 per experiment for each treatment group in A and B. At the end of 4 days (96 h), squid were fixed for SEM to score regression. A. Hatchling squid were exposed to $\sim 10^4$ cells/ml of ES114 or ES114-U2 for 12 h, at which time the bacteria-containing seawater was changed to CSW (top bar) to allow the infection to ensue, or to Cm-treated seawater (second bar) to stop the infection and cure the light organ. Controls were exposed to CSW alone (third bar) or to CSW followed by Cm-treated CSW (fourth bar). B. Hatchling squid were exposed to $\sim 10^4$ cells/ml ES114 for 1, 4, 8, or 12 hours (started at time 0), at which time the bacteria-containing seawater was changed to Cm-treated seawater (top bar) or to CSW (lower bar).

exposed to 310Ω were homogenized and plated to verify that they had been infected. The rest of that group (n = 8) was scored for CEA regression. ES114 and negative control groups were monitored for colonization by measuring luminescence only.

Results

Transient vs. continuous exposure to V. fischeri *strain ES114*

The number of viable bacteria in the light organ declines sharply after only 2 hours in Cm-treated CSW to 487 CFU (approximately 1% of the initial value), concomitant with a decline in luminescence (Fig. 4). After 10 hours of Cm treatment, all of the squid monitored had no viable bacteria detectable in their light organs. Additionally, if the Cm treatment was removed after 4 days and replaced with CSW alone, the light organs of the squid did not become reinfected, confirming that there were no viable *V. fischeri* in the light organ after treatment with Cm for 4 days. Squid exposed to Cm appeared as healthy as those not exposed to Cm and there was no adverse effect on the ability of the squid to infect after a 4-day exposure to Cm; *i.e.*, if the Cm treatment was lifted after 4 days and a new inoculum of *V. fischeri* was introduced into the seawater the squid became luminescent within 24 h, indicating that they were still capable of being infected.

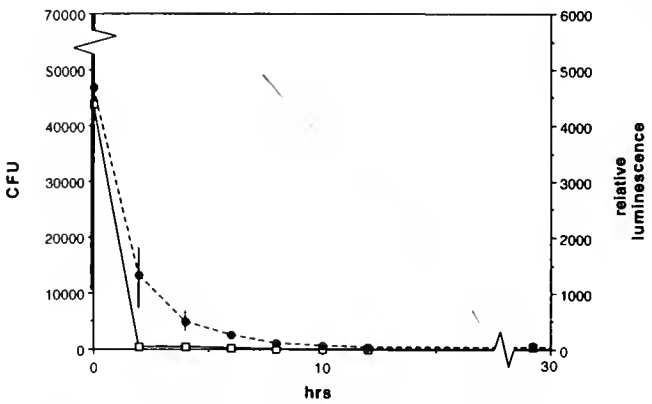

Figure 4. Decrease in colony forming units (CFU) of bacteria per squid (open squares, solid line) and relative luminescence (in photometer units) per squid (closed circles, dashed line) over time following Cm treatment. Squid were exposed to *V. fischeri* bacteria for 12 h prior to Cm treatment (h 0). Data points are the averages from n = 5 squid. Vertical bars represent standard deviations.

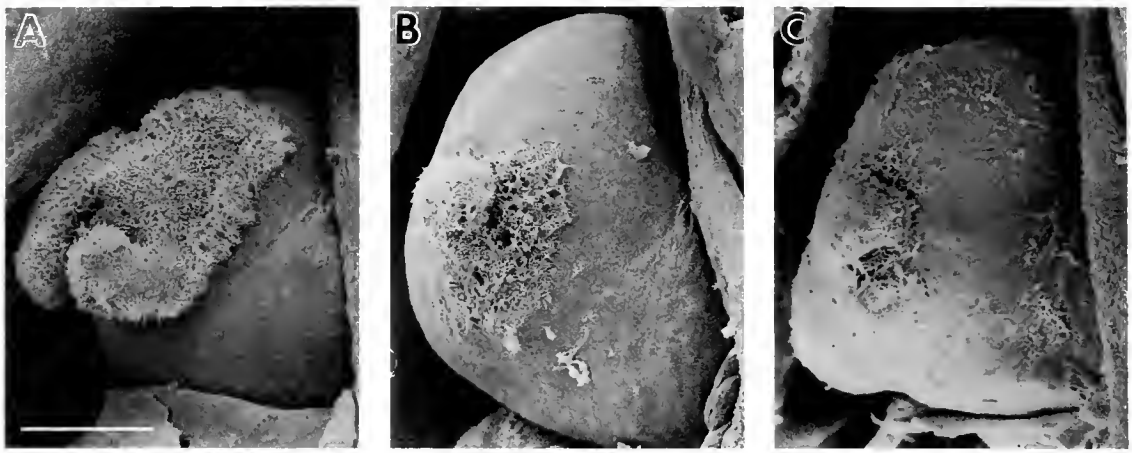

Figure 5. Scanning electron micrographs of light organs (right half only) of 4-day old squid exposed upon hatching to: (A) CSW for 4 days; (B) ES114 for 12 h followed by treatment with Cm for 3.5 days; (C) ES114-U2 (Cm resistant strain) for 12 h followed by treatment with Cm for 3.5 days. See Figure 3A for experimental design. Scale bar = 100 μm.

Squid exposed to *V. fischeri* for 12 h showed regression of the CEA similar to that of squid exposed for 4 days (Fig. 5b). Negative control animals exposed for 4 days to CSW (Fig. 5a) or Cm-treated CSW (not shown) showed no regression of CEA. Additionally, Cm did not have an inhibitory effect on CEA regression, as evidenced by complete regression of CEA from squid infected with the Cm-resistant strain ES114-U2 and treated with Cm (Fig. 5c).

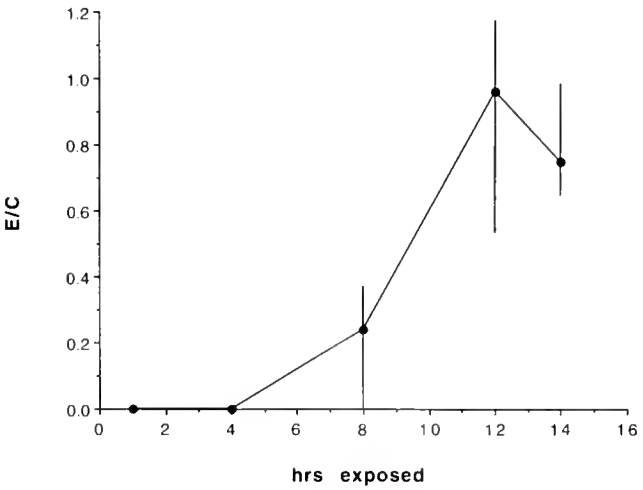

Figure 6. Relative percentage of light organs in 4-day-old squid showing stage 3 regression of the CEA (see text). Hatchling squid were exposed to ES114 for 1, 4, 8, and 12 hours, followed by treatment with Cm (see Fig. 3B for experimental design). Values are reported as E/C, the percentage of Cm-treated squid (experimental) showing regression divided by the percentage of infected controls showing regression. Each point represents values pooled from four separate experiments (see Table 1). Vertical bars represent the full range of data for the four experiments.

Variable transient exposure to V. fischeri *strain ES114*

Exposure of squid to bacteria for 1, 4, 8, 12, or 14 hours to determine the minimum time requirement for induction of CEA regression revealed that only those squid exposed to bacteria for at least 12 h showed CEA regression (E/C = 0.96) comparable to that of continuously exposed control squid (Fig. 6; Table 1). These squid were visibly luminous at the time of Cm treatment. Squid exposed to bacteria for 1 or 4 h were not luminous and showed no CEA regression. Those individuals exposed for 8 h were only occasionally luminous and the E/C ratio was only 0.24. Although some animals died during the experiments, the death rate was not greater than that normally seen in animals 4 days post-hatching (averaging less than 10%) and the incidence of death appeared random with respect to experimental groups. Animals that died were not used in the calculation of CEA regression percentages. The level of infection, measured by plating light organ homogenates after exposure to bacteria, was significantly higher at 12 h

Table 1

Pooled data from four separate experiments as described in Figure 3b. E/C represents ratio of % EXP (Experimental) to % CONT (Control)

H Exposed	Tot. Sample No.		CEA Regression		
	EXP	CONT	% EXP	% CONT	E/C
1	33	48	0	77	0
4	25	43	0	77	0
8	38	50	18	76	0.24
12	23	43	74	77	0.96
14	25	26	72	96	0.75

than at 8 h (Fig. 7). Although CEA regression was higher at 12 h than at 14 h (Fig. 6), the values at 14 h are within the range of values for 12 h. These results suggest that the minimum exposure time for complete regression of the CEA must lie between 8 and 12 h.

Exposure to other strains of V. fischeri

When squid were exposed to the nonmotile strain of *V. fischeri,* M101, neither colonization nor CEA regression was observed, supporting the above evidence that the bacteria must be within the light organ to induce morphogenesis. Additionally, of the natural isolates tested, only the infective strain, MJ11, induced CEA regression (Table II).

Exposure to an autoinducer mutant of V. fischeri

Squid exposed to the autoinducer mutant of *V. fischeri,* 310Ω, were infected and showed complete regression of CEA after 4 days (Table II), thus eliminating the possibility that autoinducer is required for light organ morphogenesis.

Discussion

The results of this study show that light organ morphogenesis of the squid *Euprymna scolopes* in response to the presence of symbiotic bacteria (1) requires only a 12-h exposure to symbiosis-competent bacteria; (2) requires colonization of the light organ by bacteria; (3) does not require *V. fischeri* autoinducer.

The finding that a transient exposure to symbiosis-competent bacteria is sufficient to induce morphogenesis of the squid light organ (*i.e.,* the bacteria are not required throughout the 4-day morphogenetic process) suggests that the signal from the bacteria may trigger an irreversible cascade of events that eventually results in CEA regression. Signal transduction through some host cell surface receptor in the light organ crypts is an attractive model for this type of response. This model is supported by evidence that colonization of the light organ crypts is required to elicit CEA regression (see below), and by the recent finding that cell death and regression events are first seen at the tips of the ciliated appendages, several cell layers away from the crypt epithelium adjacent to the bacteria (Montgomery and McFall-Ngai, 1994). Thus, cells that are in direct contact with the bacteria must somehow pass the signal through several layers of adjacent host cells to effect cell death in the ciliary appendages, presumably through one or more signal transduction pathways.

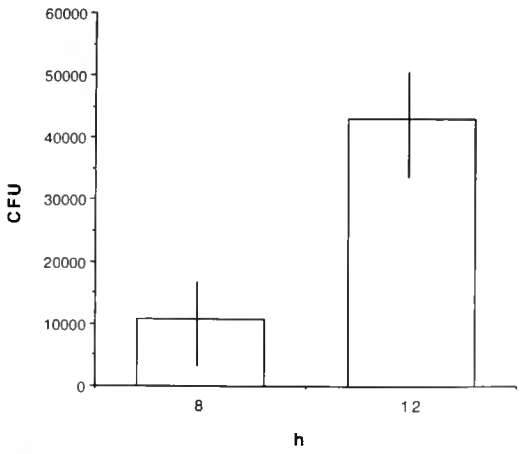

Figure 7. Average colony forming units (CFU) of bacteria per squid after 8 and 12 h of exposure to *V. fischeri.* Vertical bars represent standard deviations ($n = 5$).

Table II

Observed capability of various strains of Vibrio fischeri *to infect* Euprymna scolopes *and induce light organ morphogenesis. n = 5 squid for each strain and all five squid in each group showed the same results*

V.f. Strain	Source	Phenotype	Infection	Morphogenesis
ES114	squid light organ	wildtype	+	+
U2	ES114 derivative	Cm resistant	+	+
M101	ES114 derivative	motility$^-$	−	−
310Ω	ES114 derivative	*lux I*$^-$	+	+
MJ1	fish light organ (1974)	wildtype	−	−
MJ11	fish light organ (1992)	wildtype	+	+
MdR12	seawater isolate	wildtype	−	−

The results of experiments with various strains of *V. fischeri* indicate that noninfective strains are not morphogenic and that the bacteria must enter the light organ to induce morphogenesis. Also, because nonmotile *V. fischeri* are unable to infect the light organ, motility is indirectly required for induction of morphogenesis. Similarly, motility is required for infection and virulence in many pathogenic bacteria, such as *V. cholerae* (Guentznel and Berry, 1975; Yancey *et al.,* 1978), *Pseudomonas* spp. (Drake and Montie, 1988), *Helicobacter pylori* (Eaton *et al.,* 1989; Dunn, 1993), and *Salmonella typhi* (Liu *et al.,* 1988).

The requirement for infection suggests that transduction of the signal occurs through interactions with the light organ crypt epithelial cells, and not through interactions with the external ciliated microvillous cells. Unlike the *Rhizobium*-legume symbiosis, in which a diffusible morphogen excreted by the bacteria induces cell division

and morphological changes in the plant without colonization of the host by the symbiont (Long, 1989; Appelbaum, 1990; Hirsch, 1992), morphogenetic induction in the *Vibrio-Euprymna* symbiosis requires that the bacteria be within the confined space of the light organ. Studies using strain MJ11, which produces a colonization consisting of only about 10% of the typical cell number yet induces morphogenesis, indicate that the actual bacterial volume is probably not exerting a physical pressure or stretching of the light organ to induce morphogenesis. It is unclear at this time whether the signal is secreted from the bacteria into the light organ crypt lumen or the signal is presented directly on the surface of the bacteria. In either case, the observed time window of between 8 and 12 hours necessary to induce CEA regression, may reflect the need for an accumulation of bacteria, or their products, to a critical density within the light organ. If the morphogenic signal is secreted, there are a few possible scenarios: (1) secretion of the morphogen is induced and only occurs within the environment of the light organ, (2) the morphogen is produced constitutively and light organ crypts provide a barrier to diffusion of bacterial products such that within the light organ the signal reaches a critical concentration required for transduction, or (3) the presence of bacteria within the light organ (perhaps through direct cell-cell contact) renders the host cells competent to "accept" the secreted signal from the bacteria.

Rather than secreted, the bacterial signal may be a molecule presented on the bacterial cell surface that interacts directly with a receptor on the animal cell membrane. Direct interactions via glycan-adhesin binding have been implicated in many symbioses and there is evidence for a mannose lectin in *E. scolopes:* when squid are inoculated with bacteria in the presence of mannose, colonization is significantly inhibited (V. Weis, K. Brennan and M. McFall-Ngai, unpub. data). In the *Rhizobium*-legume symbiosis, plant lectins that recognize specific bacterial surface oligosaccharides have been suggested to play a major role in attachment and invasion mechanisms (Dazzo and Truchet, 1983). Further, in pathogenic associations, bacterial adhesins on pili often are involved in recognizing specific sugar receptors on the animal cell surface (Finlay and Falkow, 1989).

Recently it has been shown that various other autoinducer molecules regulate the production of exoenzyme virulence determinants in *Pseudomonas aeruginosa* and *Erwinia carotovora* (Jones *et al.,* 1993). Also, these autoinducers are structural analogs of actinomycetes A-factor, which has been implicated as an autoregulator of cellular differentiation between different *Streptomyces* species (Beppu, 1992). However, the results of this study indicate that *V. fischeri* autoinducer is not required for light organ morphogenesis. Other secreted bacterial molecules such as *Vibrio* spp. endotoxins are known to interact with animal cells (Lin *et al.,* 1993) and may be potential morphogens. For example, cholera toxin has been shown experimentally to induce metamorphosis in certain marine larvae (Hofmann and Brand, 1987). In addition, Reich and Schoolnik recently found that *V. fischeri* carries a gene homologous to *tox*R (1994), which regulates cholera toxin production in *V. cholerae,* and also synthesizes a cholera toxin-like ADP-ribosylating protein (1995). However, while commercially available cholera toxin mimics some aspects of the symbiotic state, by itself it does not cause morphogenesis in *E. scolopes* (Small and McFall-Ngai, 1993), suggesting that if an endotoxin-like molecule is the squid morphogen, it is significantly different from cholera toxin, or that additional molecules (perhaps on the surface of the bacteria) are also required. Other bacterial factors that have been demonstrated to affect metamorphosis or morphogenesis in various host organisms include oligopeptides (Hofmann and Brand, 1987), phorbol esters (Muller, 1985), diacylglycerols (Leitz and Muller, 1987), and lipo-oligosaccharides (Lerouge *et al.,* 1990; van Brussel *et al.,* 1992), any of which may prove important in our system.

In conclusion, we have shown that a transient colonization of *E. scolopes* with symbiosis-competent *V. fischeri* induces morphogenesis of the squid light organ. Transduction of the morphogenic signal requires the presence of the bacteria within the light organ for approximately 12 h. Further investigations are necessary to determine the nature of the bacterial signal, the role of colonization in the generation of the signal, and the transduction pathway within the host squid.

Acknowledgments

We thank Ned Ruby, Mary Montgomery, and Alicia Thompson for technical advice and Angel Lemus for graphics assistance. We thank Jorg Graf and Kendall Gray for their generous donations of mutant *V. fischeri* strains. We also thank Andrea Small, Katie Brennan, Jamie Foster, Wes Toller, and Karen Visick for helpful comments on the manuscript. This is HIMB contribution #991. This work was supported by NSF Grant No. IBN 9220482 (to MM-N and EG Ruby) and ONR Grant No. N00014-91-J-1357 (to MM-N).

Literature Cited

Appelbaum, E. 1990. The *Rhizobium/Bradyrhizobium*-legume symbiosis. Pp. 131–155 in *Molecular Biology of Symbiotic Nitrogen Fixation,* P. M. Gresshoff, ed. CRC Press, Boca Raton, FL.

Beppu, T. 1992. Secondary metabolites as chemical signals for cellular differentiation. *Gene* **115:** 159–165.

Boettcher, K. J., and E. G. Ruby. 1990. Depressed light emission by symbiotic *Vibrio fischeri* of the sepiolid squid *Euprymna scolopes. J. Bacteriol.* **172:** 3701–3706.

Dazzo, F. B., and G. L. Truchet. 1983. Interactions of lectins and their saccharide receptors in the *Rhizobium*-legume symbiosis. *J. Membrane Biol.* **73:** 1–16.

Drake, D., and T. C. Montie. 1988. Flagella, motility and invasive virulence of *Pseudomonas aeruginosa*. *J. Gen. Microbiol.* **134:** 43–52.

Dunlap, P. V., and E. P. Greenberg. 1991. Role of intercellular chemical communication in the *Vibrio fischeri*-monocentrid fish symbiosis. Pp. 219–252 in *Microbial Cell-Cell Interacions*, M. Dworkin, ed. Amer. Soc. Microbiol. Washington, DC.

Dunn, B. E. 1993. Pathogenic mechanisms of *Helicobacter pylori*. *Gastroenterol. Clin. N. Am.* **22:** 43–57.

Eaton, K. A., D. R. Morgan, and S. Krakawa. 1989. *Campylobacter pylori* virulence factors in gnotobiotic piglets. *Infect. Immun.* **57:** 1119–1125.

Finlay, B. B., and S. Falkow. 1989. Common themes in microbial pathogenicity. *Microbiol. Rev.* **53:** 210–230.

Gordon, H. A., and L. Pesti. 1971. The gnotobiotic animal as a tool in the study of host microbial relationships. *Bacteriol. Rev.* **35:** 390–429.

Graf, J., P. V. Dunlap, and E. G. Ruby. 1994. Effect of transposon-induced motility mutations on colonization of the host light organ by *Vibrio fischeri*. *J. Bacteriol.* **176:** 6986–6991.

Guentzel, M. N., and L. J. Berry. 1975. Motility as a virulence factor for *Vibrio cholerae*. *Infect. Immun.* **11:** 890–897.

Hirsch, A. M. 1992. Tansley Review No. 40. Developmental biology of legume nodulation. *New Phytol.* **122:** 211–237.

Hofmann, D. K., and U. Brand. 1987. Induction of metamorphosis in the symbiotic scyphozoan *Cassiopea andromeda:* role of marine bacteria and of biochemicals. *Symbiosis* **4:** 99–116.

Jones, S., B. Yu, N. J. Bainton, M. Birdsall, B. W. Bycroft, S. R. Chhabra, A. J. R. Cox, P. Golby, P. J. Reeves, S. Stephens, M. K. Winson, G. P. C. Salmond, G. S. A. B. Stewart, and P. Williams. 1993. The *lux* autoinducer regulates the production of exoenzyme virulence determinants in *Erwinia carotovora* and *Pseudomonas aeruginosa*. *EMBO J.* **12:** 2477–2482.

Leitz, T., and W. A. Muller. 1987. Evidence for the involvement of PI-signalling and diacylglycerol second messengers in the initiation of metamorphosis in the hydroid *Hydractinia echinata* Fleming. *Dev. Biol.* **121:** 82–89.

Lerouge, P., P. Roche, C. Faucher, F. Maillet, G. Truchet, J. C. Prome, and J. Denarie. 1990. Symbiotic host specificity of *Rhizobium meliloti* is determined by a sulphated and acylated glucosamine oligosaccharide signal. *Nature* **344:** 781–784.

Lin, Z., K. Kumagai, K. Baba, J. J. Mekelanos, and M. Nishibuchi. 1993. *Vibrio parahaemolyticus* has a homolog of the *Vibrio cholerae toxRS* operon that mediates environmentally induced regulation of the thermostable direct hemolysin gene. *J. Bacteriol.* **175:** 3844–3855.

Liu, S., T. Ezaki, H. Miura, K. Matsui, and E. Yabuchi. 1988. Intact motility as a *Salmonella typhi* invasion-related factor. *Infect. Immun.* **56:** 1967–1973.

Long, S. R. 1989. Rhizobium-legume nodulation: life together in the underground. *Cell* **56:** 203–215.

McFall-Ngai, M. J., and Montgomery, M. K. 1990. The anatomy of the adult bacterial light organ of *Euprymna scolopes* Berry (Cephalopoda: Sepiolidae). *Biol. Bull.* **179:** 332–339.

McFall-Ngai, M. J., and E. G. Ruby. 1991. Symbiont recognition and subsequent morphogenesis as early events in an animal-bacterial mutualism. *Science* **254:** 1491–1494.

Montgomery, M. K., and M. J. McFall-Ngai. 1993. Embryonic development of the light organ of the sepiolid squid *Euprymna scolopes* Berry. *Biol. Bull.* **184:** 296–308.

Montgomery, M. K., and M. J. McFall-Ngai. 1994. Bacterial symbionts induce host organ morphogenesis during early postembryonic development of the squid *Euprymna scolopes*. *Development* **120:** 1719–1729.

Muller, W. A. 1985. Tumor promoting phorbol esters induce metamorphosis and multiple head formation in the hydroid *Hydractinia echinata*. *Differentiation* **29:** 216–222.

Nardon, P., and A. M. Grenier. 1991. Serial endosymbiosis theory and weevil evolution: the role of symbiosis. Pp. 153–169 in *Symbiosis as a Source of Evolutionary Innovation*, L. Margulis and R. Fester, eds. MIT Press, Cambridge, MA.

Reich, K. A. and G. K. Schoolnik. 1994. The light organ symbiont *Vibrio fischeri* possesses a homolog of the *Vibrio cholerae* transmembrane transcriptional activator ToxR. *J. Bacteriol.* **176:** 3085–3088.

Reich, K. A., and G. K. Schoolnik. 1995. Purification and characterization of an ADP-ribosyltransferase from the non-pathogenic light organ symbiont, *Vibrio fischeri*. *Am. Soc. Microbiol. Abstr.* **B-199:** 200.

Ruby, E. G., and L. M. Asato. 1993. Growth and flagellation of *Vibrio fischeri* during initiation of the sepiolid squid light organ symbiosis. *Arch. Microbiol.* **159:** 160–167.

Ruby, E. G., and M. J. McFall-Ngai. 1992. A squid that glows in the night: development of an animal-bacterial mutualism. *J. Bacteriol.* **174:** 4865–4870.

Ruby, E. G., and K. H. Nealson. 1976. Symbiotic association of *Photobacterium fischeri* with the marine luminescent fish *Monocentris japonica*: a model of symbiosis based on bacterial studies. *Biol. Bull.* **151:** 574–586.

Saffo, M. B. 1992. Invertebrates in endosymbiotic associations. *Am. Zool.* **32:** 557–565.

Schwemmler, W. 1989. Insect endocytobiosis as a model system for egg cell differentiation. Pp. 37-53 in *Insect Endocytobiosis: Morphology, Physiology, Genetics, Evolution*, W. Schwemmler and G. Gassner, eds. CRC Press, Boca Raton, FL.

Small, A. L., and M. J. McFall-Ngai. 1993. Changes in the oxygen environment of a symbiotic squid light organ in response to infection by its luminous bacterial symbionts. *Am. Zool.* **33:** 61A.

van Brussel, A. A. N., R. Bakhuizen, P. C. van Spronsen, H. P. Spaink, T. Tak, B. J. Lugtenberg, and J. W. Kijne. 1992. Induction of pre-infection thread structure in the leguminous host plant by mitogenic lipo-oligosaccharides of *Rhizobium*. *Science* **257:** 70–72.

Wei, S. L., and Young, R. E. 1989. Development of a symbiotic bacterial bioluminescence in a nearshore cephalopod, *Euprymna scolopes*. *Mar. Biol.* **103:** 541–546.

Yancey, R. J., D. L. Willis, and L. J. Berry. 1978. Role of motility in experimental cholera in adult rabbits. *Infect. Immun.* **22:** 387–392.

Reference: *Biol. Bull.* **189:** 356–362. (December, 1995)

Not All Ctenophores Are Bioluminescent: *Pleurobrachia*

STEVEN H. D. HADDOCK AND JAMES F. CASE

Marine Science Institute, University of California, Santa Barbara, California 93106

Abstract. The traditional view has been that all species of the phylum Ctenophora are capable of producing light. Our inability to elicit luminescence from members of the well-known genus *Pleurobrachia,* as well as a lack of published documentation, led to an effort to determine whether this genus is truly bioluminescent. Physical and chemical assays of several species from the family Pleurobrachiidae produced no evidence of bioluminescence capability, although all other species of ctenophores tested gave positive results. Some of the historical misperception that *Pleurobrachia* can produce light might be attributable to confusion with similar luminous genera.

Introduction

Planktonic marine invertebrates are noted for their ability to produce light (Herring, 1987; Haddock and Case, 1994), but even among these organisms, the phylum Ctenophora is remarkable for the extent of bioluminescence expression. Because there have been no systematic investigations, speculation about the true extent of bioluminescence ability in ctenophores comes mainly from secondary sources. According to Ruppert and Barnes (1994), "Ctenophores are noted for their luminescence, which is characteristic of all species." Others agree that "all ctenophores" (MacGintie and MacGintie, 1968) or "probably all species" (Harvey, 1940) are bioluminescent, and Dahlgren (1916) goes so far as to state that "all the ctenophores have been known for a long time to be light producing."

Pleurobrachia, perhaps the best-known and most studied ctenophore genus, has long been considered capable of bioluminescence (Gadeau de Kerville, 1890; Herring, 1987). However most authors who mention bioluminescence in *Pleurobrachia* proceed to give details of the luminescent system of *Mnemiopsis* or some other species. The published records of luminescent spectra contain no measurements from *Pleurobrachia* (Nicol, 1958; Young, 1981; Herring, 1983; Widder *et al.,* 1983; Latz *et al.,* 1988), even though this genus is one of the most frequently encountered. Despite 'conventional wisdom', we know of no credible accounts of luminescence in the family Pleurobrachiidae—either in the genus *Pleurobrachia* or *Hormiphora.*

It is often difficult to evaluate an early report that a species is bioluminescent. Results can be confounded by the luminescence of a contaminating organism or by external light causing reflection or refraction (Herring, 1987). In some cases the taxonomy of a group of organisms has changed so much that it is not possible to determine which species was investigated by early researchers. Furthermore, once an organism has been reported as luminous, there is considerable resistance to removing it from the list of luminous species (*e.g.,* sponges). To an extent this resistance is understandable, because the ability to luminesce may vary within a population on a sexual, ontogenic, seasonal, or diel basis (Herring, 1987). Variation may also occur between subpopulations, as in the midshipman fish, which is luminous off California but not when found further north (Warner and Case, 1980).

With these caveats in mind, we have attempted to rigorously demonstrate that *Pleurobrachia* is a notable exception to the dogma that all ctenophores are bioluminescent.

Materials and Methods

Various species of *Pleurobrachia* were sampled in the Santa Barbara Channel (*P. bachei,* throughout the year), the Alboran Sea (*P. rhodopis,* spring), the Gulf of Maine (*P. pileus,* summer), at Santa Catalina Island, California (*P. bachei,* summer), and at Friday Harbor, Washington

Received 3 May 1995; accepted 31 July 1995.

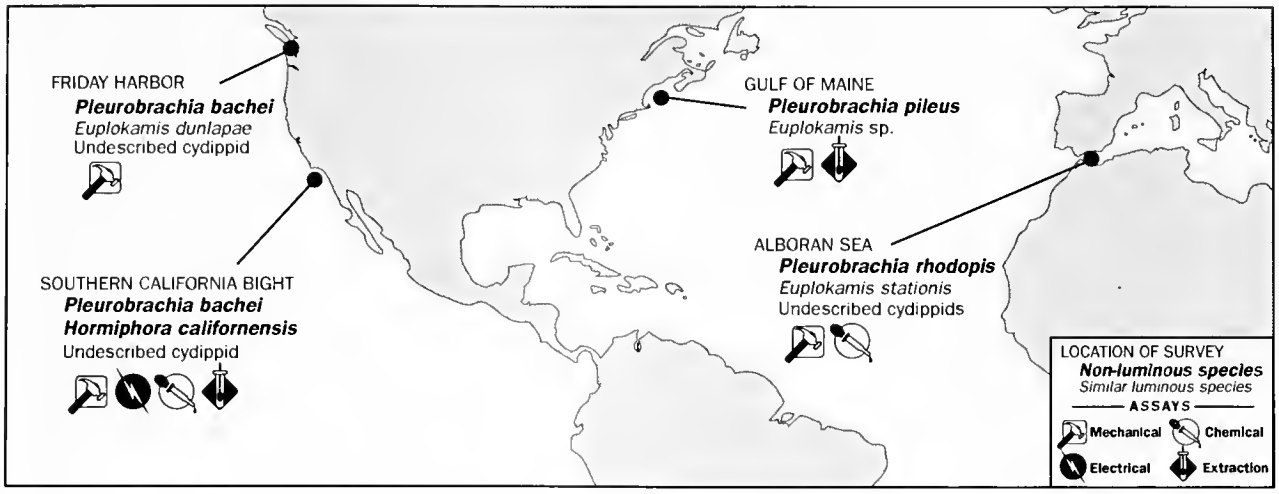

Figure 1. Four types of assays were conducted to determine whether ctenophores were bioluminescent or bore any light-producing chemicals. At each site where specimens were collected, we also found luminous genera which could have been mistaken for *Pleurobrachia*.

(*P. bachei*, fall). To ensure that the ctenophores were not prestimulated or damaged during collection, specimens used in these studies were hand-collected in jars by blue-water divers, except at Friday Harbor, where they were collected from the surface in beakers. Because some ctenophores lose their luminescence upon exposure to light (Ward and Seliger, 1976), specimens were dark-adapted for a minimum of 30 min prior to experiments. After this recovery period, *Pleurobrachia* were subjected to mechanical, electrical, and a variety of chemical stimuli (Fig. 1). To ensure that the assay techniques were effective, we also tested the luminescence of other ctenophore species found at the same locations.

Physical stimulation

The most commonly applied test for luminescence was physical stimulation by a dark-adapted observer. This technique was used at all sites where ctenophores were collected. For quantitative tests of mechanical stimulation, five specimens of *P. pileus* collected in the Gulf of Maine (northwest Atlantic Ocean) were transferred to filtered seawater, allowed to dark-adapt, and stimulated by stirring in a photon-counting chamber for at least five seconds. This test was repeated three times with five or more *P. bachei* collected in the Santa Barbara Channel (eastern temperate Pacific Ocean). For comparison, luminous species were placed in the same apparatus and induced to luminesce by stirring or brief prodding. Because some organisms may be resistant to physical stimulation, additional specimens were exposed to KCl, ddH_2O, $CaCl_2$, and H_2O_2, which can bypass normal control processes and act directly on light-producing cells or chemicals (Herring, 1981).

Photoprotein extraction

Calcium-activated photoproteins have been identified as the light-producing agents in all luminous ctenophores examined (Ward and Seliger, 1974; unpub. results). To test for the presence of active photoproteins in *Pleurobrachia*, dark-adapted specimens were extracted in a Ca^{2+}-chelating buffer as follows.

In the Santa Barbara Channel, five specimens of *Pleurobrachia bachei* were collected at depths between 5 and 20 m on a blue-water dive. Several small ctenophores from three other families (one *Haeckelia beehleri*, one *Beroë cucumis*, and three *Velamen parallelum*) were collected at the same time and used as positive controls. Specimens were sorted into filtered seawater and maintained in the dark for 7 h (until 2100) to allow recovery from potential photodegradation of their luminescence ability (Ward and Seliger, 1976; Anctil and Shimomura, 1984) and to account for the possibility of a diel cycle of luminescence, which is present in some luminous organisms, but has never been reported for ctenophores. These specimens were homogenized in 200 m*M* Tris, 40 m*M* EDTA, pH 8.8, and a 400 μl subsample was assayed by adding 100 μl of 360 m*M* $CaCl_2$.

This experiment was repeated three times using up to 50 *P. bachei* in the extraction, once with *P. bachei* frozen directly in liquid nitrogen, and once using *P. pileus* collected on dives in the Gulf of Maine, with various local luminous species used as positive controls.

Regeneration

To test the hypothesis that *Pleurobrachia* contains an inactive photoprotein but lacks the luciferin necessary to

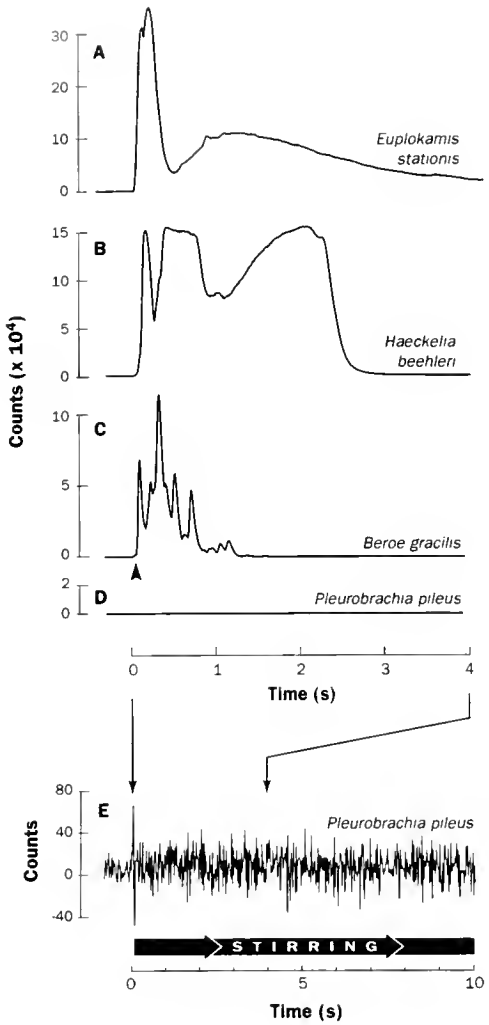

Figure 2. Responses of ctenophores to physical stimulation. Luminous ctenophores produced bright flashes when disturbed (A–C), even if only briefly touched (arrowhead). In contrast, *Pleurobrachia pileus* showed no light emission even during continuous stirring (D, E). The *y*-axis shows counts per 20-ms bin.

produce light, we attempted to regenerate extracts with synthesized coelenterazine (provided by O. Shimomura), the luciferin found in luminous ctenophores and cnidarians (Ward and Cormier, 1975; Shimomura, 1985).

Specimens were homogenized in 100 m*M* Tris, 50 m*M* EDTA, 500 m*M* NaCl, pH 7.5, filtered through a Whatman GF/C glass-fiber filter to remove debris, and centrifuged for 30 min at 35,000 × *g*. Photoprotein present in one ml of supernatant was triggered by the addition of 50 m*M* $CaCl_2$ until no further light was produced (typically 250 μl was sufficient, although no light was emitted by *Pleurobrachia* preparations). This was followed by 250 μl of 200 m*M* EDTA to chelate the added Ca^{2+}, and the solution was saturated with ammonium sulfate to precipitate the reacted protein. For the regeneration, one ml of the saturated solution was centrifuged at 15,000 RPM in an Eppendorf minicentrifuge for 15 min. The pellet of precipitate was resuspended in 200 μl of 10 m*M* Tris, 5 m*M* EDTA, 500 m*M* NaCl, and 5 m*M* β-mercaptoethanol (techniques based on Campbell and Herring, 1990). Each treatment was incubated for 6 h at 4°C with 2 μl methanol either containing coelenterazine or with no luciferin for the negative controls. The light produced upon final addition of $CaCl_2$ indicated the extent of regeneration.

This experiment was conducted using the hydromedusa *Haliscera conica* as a positive control. We replicated this experiment once using *Haliscera*, the hydroid *Obelia* sp., and an undescribed luminous ctenophore; and again using the ctenophores *Beroë cucumis*, *Velamen parallelum*, and *Haeckelia beehleri* with 0.1% gelatin present in the regeneration solution to increase the stability of regenerated photoproteins (Campbell and Herring, 1990).

Results

At no time during these experiments did we detect any bioluminescence produced by *Pleurobrachia* or by the closely related genus *Hormiphora*. Every one of more than forty other ctenophore species tested produced luminescence that was easily detected using our methods.

Physical stimulus

Repeated attempts at mechanical stimulation failed to elicit luminescence from *Pleurobrachia pileus* (Figs. 2D, E). The five specimens run during these trials were negative, as were ten *Pleurobrachia bachei* collected from the Pacific Ocean and run in an identical experiment (not

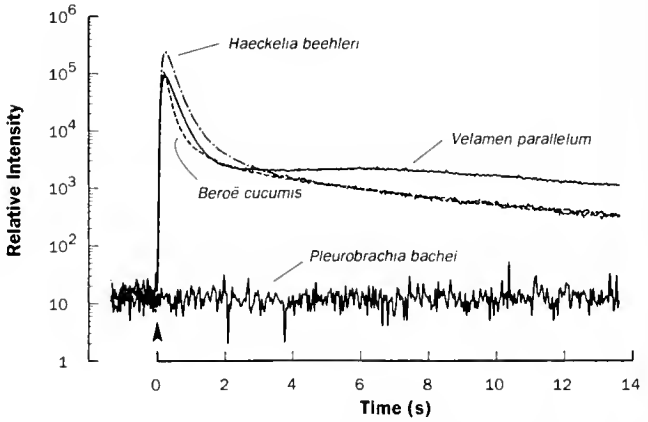

Figure 3. Photoproteins extracted from luminous ctenophores using a calcium-chelating buffer can be triggered to produce light upon the addition of excess calcium. Species from three families shown here illustrate typical flashes produced by extracts of luminous species. In contrast, *Pleurobrachia bachei* and *P. pileus* showed no photoprotein activity in any assays.

shown). Light was not produced by *Pleurobrachia* collected at any of the locations included in this study (Fig. 1). Another member of Pleurobrachiidae, *Hormiphora californensis*, which was collected from the Santa Barbara Channel, also consistently failed to produce light. For comparison, other luminescent ctenophores tested at the same time produced luminescence for the duration of the stirring. Even when given only a single brief stimulus, luminous species produced bright flashes (Fig. 2A–C), with peak intensities of more than 1.75×10^7 counts/s (3.5×10^5 counts in 20 ms).

Chemical extraction

Assays of calcium-free extracts of *Pleurobrachia bachei* from the Santa Barbara Channel (Fig. 3) and *P. pileus* from the Gulf of Maine (not shown) were indistinguishable from the background signal. All extracts of *Pleurobrachia* were inert, while in every case positive control extracts from the ctenophores *Haeckelia beehleri, Beroë cucumis, Velamen parallelum* (Fig. 3), *Bolinopsis infundibulum, Beroë gracilis, Kiyohimea aurita, Bathocyroë fosteri*, and *Bathyctena chuni*, and from the hydrozoans *Haliscera conica* and *Obelia* sp. (not shown), produced light both during extraction and upon the addition of $CaCl_2$, at intensities up to 2.6×10^6 counts/s.

Photoprotein regeneration

Extracts of *Pleurobrachia bachei* incubated with luciferin were not significantly different from those incubated with methanol only, nor were they different from the negative control treatment, which contained only buffer and luciferin (Fig. 4). Regeneration was noted in the positive controls treatments of *Haliscera conica, Haeckelia beehleri*, and *Obelia* sp. However one positive control replicate (*Beroë cucumis*) showed no luminescence activity after the regeneration, and in some replications, the luminous species used as positive controls (undescribed Mertensiid, *Velamen parallelum*) gave inconclusive results, since residual activity remained in luminescent extracts which had been depleted by $CaCl_2$ and then incubated without luciferin.

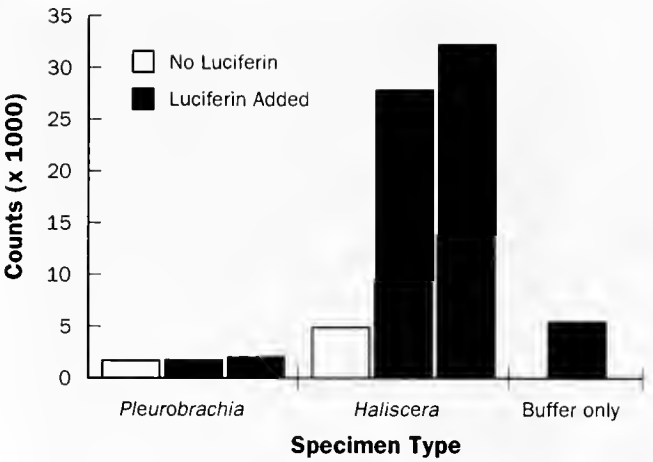

Figure 4. Photoprotein regeneration assays. Even when incubated with an excess of luciferin, extracts of *Pleurobrachia bachei* did not become luminescent, indicating an absence of inactive photoprotein. Extracts from the hydromedusa *Haliscera conica* show the regeneration that typically occurs when an exhausted photoprotein is combined with coelenterazine.

Discussion

Past research

The published record regarding the luminescence of *Pleurobrachia* is sparse, consisting mostly of anecdotal nineteenth-century reports. We have not found any published photographs, spectra, or unequivocal quantitative measurements of bioluminescence from *Pleurobrachia*.

Of the early accounts, the report of Dahlgren (1916) is most explicit in describing bioluminescence in *Pleurobrachia*. Although most of the text concerns *Beroë* and the lobate ctenophore *Mnemiopsis*, there are drawings of *Pleurobrachia* swimming about in "the lighted and unlighted state" (also reproduced in Nicol, 1967). There are also drawings of low-power sections through the gastrovascular canal of a *Pleurobrachia:* one professing to show the "layer of luminous cells covering ovary and testis," and one showing a closer view of the "probable luciferine-secreting cells." Dahlgren supposed that these were luminous cells because of their "highly-vacuolated and glandular nature." Subsequent work on the ultrastructure of the luminous system of *Mnemiopsis leidyi* has shown that these vacuolar cells are not those responsible for light production (Freeman and Reynolds, 1973; Anctil, 1985). Therefore, the cells depicted by Dahlgren are not evidence for light-production in *Pleurobrachia*.

We have found only one quantitative account of *Pleurobrachia* bioluminescence. For this study, Hardy and Kay (1964) placed "a large number of very small *Pleurobrachia*" in unfiltered seawater and left them undisturbed in a light-measuring device to monitor "spontaneous" luminescence. Their records show many brief flashes during several hours of experimentation. To establish that dinoflagellates in the seawater were not producing the flashes, the authors sieved the ctenophores from the container and measured the light again, this time noting no flashes. However, by removing the ctenophores they also removed the stimulation that would have been caused by their actively beating comb plates. The authors themselves noted this effect in a later experiment testing the stimulation of dinoflagellates by mysids. The number and intensity of flashes recorded during the *Pleurobrachia* experiment are more similar to the dinoflagellate

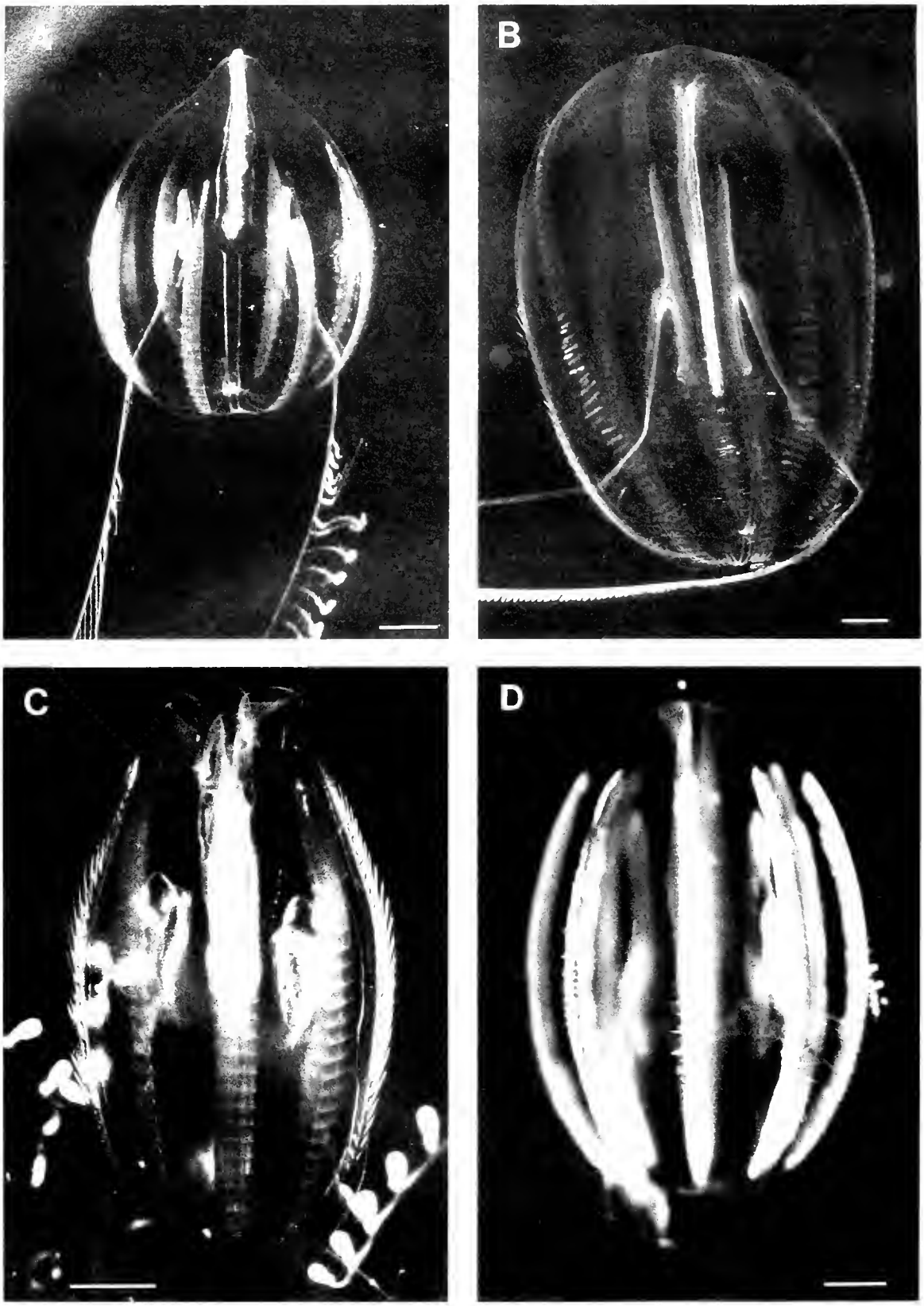

Figure 5. Non-luminous and luminous cydippid ctenophores. Reports of bioluminescence from non-luminous species like *Pleurobrachia bachei* (A) and *Hormiphora californensis* (B) may be attributed to confusion with similar luminous genera *Euplokamis* (C) and other undescribed species (D) are brightly luminescent and are found at the same locations as *Pleurobrachia* (see Fig. 1). Scale bars, 2 mm.

experiments than to a *Beroë* experiment which produced fewer, but brighter, flashes (Hardy and Kay, 1964: figs 1, 2, 14–16). Because the authors did not see the ctenophore luminesce and did not sufficiently rule out the possibility of dinoflagellate flashes, this account of *Pleurobrachia* luminescence remains unconvincing.

Considering that *Pleurobrachia* is one of the most widely distributed and best-known of the ctenophore genera, it is remarkable that we have been unable to find any substantiated reports of its bioluminescence, especially in the recent literature.

Unpublished research

The unpublished observations indicating that *Pleurobrachia* is non-luminous are as convincing as the void in the published literature. In nearly 30 years of observations on luminous plankton, workers from this laboratory have never encountered a luminescent specimen. Similarly, other researchers who have studied bioluminescence in ctenophores from around the world have been unable to observe luminescence in this genus [P. J. Herring, Y. A. Labas (White Sea), B. H. Robison, E. A. Widder, pers. comm.]. Because these negative results have never seen their way into print, apocryphal accounts persist.

Results of our experiments

Because physical stimuli repeatedly failed to elicit light from *Pleurobrachia,* we attempted to determine whether the luminescent chemicals were present either as a calcium-activated photoprotein, or as a luciferin-deficient apophotoprotein. Extractions in calcium-chelating buffers have clearly demonstrated the presence of photoproteins in all other ctenophore species examined (Ward and Seliger, 1974; Shimomura, 1985; unpub. results). Based on the results of Tris-EDTA extractions, *Pleurobrachia* clearly lacks a conventional photoprotein, and because no luminescence was observed during homogenization, there is no evidence that another mechanism is employed.

At the chemical level, failure to detect an active photoprotein could be due to the lack of an appropriate protein, or to a lack of luciferin. Based on the negative results of regeneration experiments, it appears that there is not an apophotoprotein present that merely lacks luciferin. Extracts of *Pleurobrachia* never became luminous in any of the incubations in which coelenterazine was supplied. However, the results of attempted regenerations were sometimes ambiguous, because extracts from luminescent ctenophores used as positive controls could retain high levels of residual activity even after treatment with $CaCl_2$. In *Mnemiopsis* the regeneration of inactive photoproteins was originally found to occur only at pH 9.0 (Anctil and Shimomura, 1984), but it is now thought that the presence of gelatin in the regeneration buffer eliminates this pH sensitivity (Campbell and Herring, 1990; Campbell, pers. comm.). Nonetheless, it would be useful to repeat these experiments using recombinant apophotoprotein, so that discharging and recovering the positive control samples would not be required.

Although we have done most of our rigorous testing on *Pleurobrachia,* we have also been unable to find any luminescence in mechanical assays of *Hormiphora,* suggesting that this closely allied genus, which is abundant at depths around 100 meters off the coast of southern California, may also be unable to produce light.

Identification

Because historically any small cydippid was likely to be called *Pleurobrachia,* anecdotal accounts of luminescence may be due to confusion with similar lesser known genera (Figs. 1, 5). For example, *Euplokamis* (Fig. 5C) is commonly encountered in the north Pacific, the Gulf of Maine, and the Mediterranean Sea, yet this genus was grouped in the family Pleurobrachiidae until recent work by Mills (1987). The luminous species *Euplokamis dunlapae* (Mills) found off the coast of Washington has been alternately described as "*Pleurobrachia pileus*" (Freeman, 1977), "*P. ?pileus*" (Kozloff, 1974), and other *Pleurobrachia* species. (For a complete list, see Mills, 1987.) Prior to Mills's clarification it would not have been possible to know whether a ctenophore that was seen to luminesce was actually *Pleurobrachia.* Similarly, the widespread occurrence and 'pleurobrachioid' appearance (Fig. 5D) of an undescribed midwater ctenophore (Mills and Harbison, in prep.) may have led to other reports of luminescence attributed to *Pleurobrachia.* In light of recent taxonomic revision and the presence of several luminous genera that are easily confused with *Pleurobrachia,* it is not difficult to imagine how erroneous examples of bioluminescence might have been reported, even by knowledgeable researchers.

Conclusions

Pleurobrachia's inability to produce light raises questions about the role of bioluminescence for planktonic organisms: Is this 'deficiency' the handicap that it might seem, given the widespread occurrence of bioluminescence among marine plankton? If bioluminescence is serving a defensive role, it may not be important against non-visual predators such as the ctenophore *Beroë,* which is known to prey upon *Pleurobrachia.* Also of interest is what is missing in *Pleurobrachia* that makes it unable to produce light. Are the homologous genes present but inactive, or are cells equivalent to photocytes lacking altogether? A comparative study of the genetic relationships of ctenophores might help indicate when the ability to bioluminesce arose in this phylum.

The Pleurobrachiidae may not be the only non-luminescent group of ctenophores, because Platyctenida, a small order of non-planktonic ctenophores, has never been reported to be luminescent. However, we have not been able to assay specimens from this rarely studied order.

Despite examining hundreds of specimens of *Pleurobrachia*, collected under ideal conditions at a variety of locations and seasons, we have never observed light production in the genus, while over 40 other species of ctenophores produced luminescence during similar treatment. Furthermore, we have found no substantiated accounts of luminescence in the literature. Therefore, although we cannot say that no *Pleurobrachia* was *ever* luminous, it is clear that this genus is not generally luminescent. The burden of proof should be shifted to those who wish to show that *Pleurobrachia* is bioluminescent.

Acknowledgments

We are grateful to E. A. Widder for opportunities to collect specimens, and to S. Anderson and J. McCullagh for assistance on blue-water dives. O. Shimomura generously provided coelenterazine, synthesized by S. Inoué, which was used in photoprotein regeneration experiments.

Literature Cited

Anctil, M. 1985. Ultrastructure of the luminescent system of the ctenophore *Mnemiopsis leidyi*. *Cell Tissue Res.* **242:** 333–340.

Anctil, M., and O. Shimomura. 1984. Mechanism of photoinactivation and re-activation in the bioluminescence system of the ctenophore *Mnemiopsis*. *Biochem. J.* **221:** 269–272.

Campbell, A. K., and P. J. Herring. 1990. Imidazolopyrazine bioluminescence in copepods and other marine organisms. *Mar. Biol.* **104:** 219–225.

Dahlgren, U. 1916. The production of light by animals. Porifera and Coelenterata. *Franklin Inst. J.* **181:** 243–261.

Freeman, G. 1977. The establishment of the oral-aboral axis in the ctenophore embryo. *J. Embryol. Exp. Morphol.* **42:** 237–260.

Freeman, G., and G. T. Reynolds. 1973. The development of bioluminescence in the ctenophore *Mnemiopsis leidyi*. *Dev. Biol.* **31:** 61–100.

Gadeau de Kerville, H. 1890. *Les animaux et les vegetaux lumineux*. Librairie J.-B. Bailliere et fils, Paris. 327 pp.

Haddock, S. H. D., and J. F. Case. 1994. A bioluminescent chaetognath. *Nature* **367:** 225–226.

Hardy, A. C., and R. H. Kay. 1964. Experimental studies of plankton luminescence. *J. Mar. Biol. Assoc. U.K.* **44:** 435–484.

Harvey, E. N. 1940. *Living Light*. Princeton University Press, Princeton. 328 pp.

Herring, P. J. 1981. Studies on bioluminescent marine amphipods. *J. Mar. Biol. Assoc. U.K.* **61:** 177–191.

Herring, P. J. 1983. The spectral characteristics of luminous marine organisms. *Proc. R. Soc. Lond. B.* **220:** 183–217.

Herring, P. J. 1987. Systematic distribution of bioluminescence in living organisms. *J. Biolum. Chemilum.* **1:** 147–163.

Kozloff, E. N. 1974. *Keys to the marine invertebrates of Puget Sound, the San Juan Archipelago, and adjacent regions*. University of Washington Press, Seattle. 226 pp.

Latz, M. I., T. M. Frank, and J. F. Case. 1988. Spectral composition of bioluminescence of epipelagic organisms from the Sargasso Sea. *Mar. Biol.* **98:** 441–446.

MacGintie, G. E., and N. MacGintie. 1968. *Natural History of Marine Animals*. 2nd ed. McGraw-Hill, New York. 529 pp.

Mills, C. E. 1987. Revised classification of the genus *Euplokamis* Chun, 1880 (Ctenophora: Cydippida: Euplokamidae n. fam.) with a description of the new species *Euplokamis dunlapae*. *Can. J. Zool.* **65:** 2661–2668.

Nicol, J. A. C. 1958. Observations on luminescence in pelagic animals. *J. Mar. Biol. Assoc. U.K.* **37:** 705–752.

Nicol, J. A. C. 1967. *The Biology of Marine Animals*, 2nd ed. Pitman, London. 699 pp.

Ruppert, E. E., and R. D. Barnes. 1994. *Invertebrate Zoology*, 6th ed. Saunders College, Ft. Worth. 1056 pp.

Shimomura, O. 1985. Bioluminescence in the sea: photoprotein systems. Pp. 351–372 in *Society for Experimental Biology, Symposia*, Vol. 39. M. S. Laverack, ed. Cambridge University Press, Cambridge.

Ward, W. W., and M. J. Cormier. 1975. Extraction of Renilla-type luciferin from the calcium-activated photoproteins aequorin, mnemiopsin, and berovin. *Proc. Nat. Acad. Sci.* **72:** 2530–2534.

Ward, W. W., and H. H. Seliger. 1974. Extraction and purification of calcium-activated photoproteins from the ctenophores *Mnemiopsis* sp. and *Beroë ovata*. *Biochemistry* **13:** 1491–1509.

Ward, W. W., and H. H. Seliger. 1976. Action spectrum and quantum yield for the photoinactivation of mnemiopsin, a bioluminescent photoprotein from the ctenophore *Mnemiopsis* sp. *Photochem. Photobiol.* **23:** 351–363.

Warner, J. A., and J. F. Case. 1980. The zoogeography and dietary induction of bioluminescence in the midshipman fish, *Porichthys notatus*. *Biol. Bull.* **159:** 231–246.

Widder, E. A., M. I. Latz, and J. F. Case. 1983. Marine bioluminescence spectra measured with an optical multichannel detection system. *Biol. Bull.* **165:** 791–810.

Young, R. E. 1981. Color of bioluminescence in pelagic organisms. Pp. 72–81 in *Bioluminescence, Current Perspectives*, K. H. Nealson, ed. Burgess Pub. Co., Minneapolis.

Reference: *Biol. Bull.* **189**: 363–369. (December, 1995)

The Life of a Sponge in a Sandy Lagoon

MICHA ILAN AND AVIGDOR ABELSON

Department of Zoology, Tel Aviv University, Tel Aviv 69978, Israel

Abstract. Infaunal soft-bottom invertebrates benefit from the presence of sediment, but sedimentation is potentially harmful for hard-bottom dwellers. Most sponges live on hard bottom, but on coral reefs in the Red Sea, the species *Biemna ehrenbergi* (Keller, 1889) is found exclusively in soft-bottom lagoons, usually in the shallowest part. This location is a sink environment, which increases the deposition of particulate organic matter. Most of the sponge body is covered by sediment, but the chimney-like siphons protrude from the sediment surface. The sponge is attached to the buried beach-rock, which reduces the risk of dislodgment during storms. Dye injected above and into the sediment revealed, for the first time, a sponge pumping interstitial water (rich with particles and nutrients) into its aquiferous system. Visual examination of plastic replicas of the aquiferous system and electron microscopical analysis of sponge tissue revealed that the transcellular ostia are mostly located on the buried surface of the sponge. The oscula, however, are located on top of the siphons; their elevated position and their ability to close combine to prevent the filtering system outflow from clogging. The transcellular ostia presumably remain open due to cellular mobility. The sponge maintains a large population of bacteriocytes, which contains bacteria of several different species. Some of these bacteria disintegrate, and may be consumed by the sponge.

Introduction

Infaunal soft-bottom invertebrates benefit from sediment, which provides a dwelling habitat, shelter from predators, and sometimes a source of nutrition (Lopez and Levinton, 1987; Watling, 1991). In contrast, hard-bottom dwellers can be harmed by sediment—either as a result of abrasion by moving particles or owing to suffocation, shading, and clogging of feeding apparatus by settled particles (*e.g.*, Rogers, 1990).

Sponges, the lowest group of multicellular organisms, are common members of hard-bottom communities (*e.g.*, Schubauer *et al.*, 1990; Soest, 1993). Most sponges are active suspension-feeders that subsist on fine particles such as bacterioplankton and dissolved organic matter (Simpson, 1984). Only a few sponge species inhabit soft-bottom habitats, usually in the deep sea (*e.g.*, Tabachnick, 1991; Werding and Sanchez, 1991), and information on their physiological and morphological adaptation to this environment is scarce. These sponge species may be endangered by two opposing processes in their environment. The first threat is complete burial, resulting from deposition of sediment, which may plug suspension-feeding and respiration channels. The second threat is dislodgment from the substratum, which can occur as a result of the erosive force of moving particles. We may therefore postulate that sponges inhabiting soft-bottom habitats should exhibit specialized adaptations for withstanding effects of cover by sediments and for remaining anchored in place. In addition, they should be able to adjust their feeding mode so that neither burial nor occasional exposure will inhibit their ability to feed.

In the present study, we examined the characteristics of a typical sediment-dwelling sponge species that enable it to survive. In the course of many dives on the reef flat, forereef and deep reef (down to 50 m) of Eilat, Red Sea, and the backreef lagoon to search for sediment-specific sponge communities, we observed that one species, *Biemna ehrenbergi* (Keller, 1889), is confined to the lagoon.

Materials and Methods

Field observations

We studied *Biemna ehrenbergi* in the coral reef lagoon of Eilat, Northern Red Sea (29°30′N; 34°55′E). We sur-

Received 15 March 1995; accepted 18 June 1995.

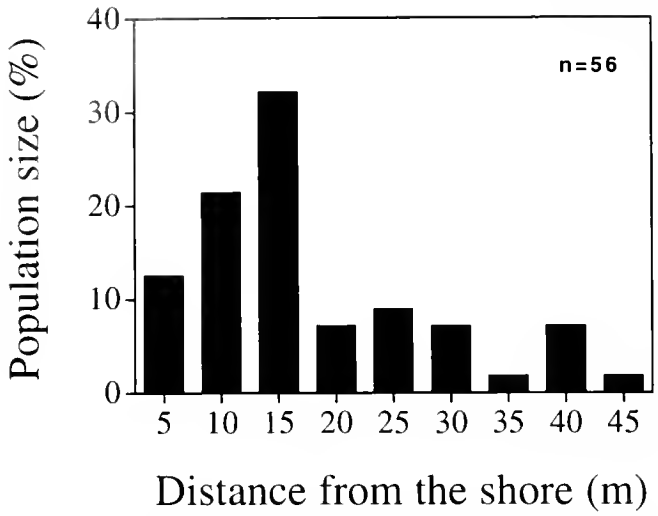

Figure 1. Spatial distribution of *Biemna ehrenbergi* in Eilat, Red Sea, along a belt 150 m long and 40–45 m wide in the inside lagoon of the coral reef.

veyed a belt 150 m in length and 40–45 m in width, recording every sponge within it. The semi-closed lagoon of the Eilat reef encompasses beach-rocks covered with a layer of sediment of various thicknesses, patches of coral heads, and small knolls. A third of its water volume is changed each tidal cycle (Lazar, pers. comm.). The effect of tidal currents and the prevailing northern waves is slight, and the flow regime of the lagoon qualifies it as a 'sink', even for fine-sized particles. To determine grain size distribution, cores (8 cm in diameter) of sediment were taken adjacent to sponges, from the surface down to the beach-rock. Particles were differentiated by size, dried at 80°C for 24 h, and weighed.

Architecture of canal system

Sponge specimens were perfused in the field with a plastic fluid (Batson's 17 Plastic Replica and Corrosion Kit, Polysciences Inc.) that was injected by syringe into the exhalant openings until it leaked out through the inhalant openings. The fluid was allowed to cure for 12 h, then the specimens were transported to the laboratory and immersed in 10% sodium hypochlorite for 24 h. The plastic replicas were then rinsed in tap water and observed under a dissecting microscope (protocol modified from Bavestrello *et al.*, 1988).

Ultrastructure analysis

Sponge samples were fixed (2.5% glutaraldehyde buffered in seawater) for at least 24 h. For transmission electron microscopy (TEM), samples were post-fixed with 1% OsO_4, dehydrated, embedded in Epon 812, sectioned, stained with uranyl acetate and lead citrate, and viewed in a JEOL 1200-EX. Ostia (incurrent openings) diameters were measured on photographs taken with a scanning electron microscope.

Canal flow circulation

Flow direction through the sponge's aquiferous system was recorded by releasing fluorescein dye into the water column near the sponge's "chimneys," or projecting siphons, or by injecting dye into the substratum close to the sponges. When the dye was injected above the sediment, it was difficult to detect currents resulting from the sponge's activity because of background interference. The sponge's siphons were therefore covered with a 1-liter plastic beaker, which was pressed a few centimeters into the sediment. The dye was then injected into the beaker, and its trajectory was followed without the disturbance of external water movements.

Results

Field observations

Biemna ehrenbergi sponges were found exclusively within the inner lagoon of the coral reef in Eilat, Red Sea (depth 0.5–1.8 m). Despite numerous dives from the reef flat through the forereef and down to 50 m, no *B. ehrenbergi* specimen was ever found in other areas. A survey conducted along 150 m of the lagoon (width 40–45 m) revealed 56 individuals. Sixty-six percent of the sponges in this belt were concentrated 5–15 m from the shore (one sponge per 40.5 m^2), with the rest spread out over the lagoon (one sponge per 145 m^2) (Fig. 1). Sponge locations within the lagoon typically had particles of various sizes, but 82.5% of the grains were larger than 500 μm, 13.3%

Table I

Distribution of grain size adjacent to Biemna ehrenbergi *sponges (data taken from 5 cores)*

Grain size (μm)	Average percentage of total grain mass ± SD
X > 2000	28.1 ± 6.4
2000 > X > 1000	27.7 ± 6.1
1000 > X > 500	29.4 ± 7.5
500 > X > 350	4.4 ± 2.4
350 > X > 210	4.0 ± 2.5
210 > X > 105	4.1 ± 2.7
105 > X > 74	0.8 ± 0.5
74 > X > 62	0.3 ± 0.1
62 > X > 53	0.3 ± 0.2
53 > X	1.6 ± 0.7

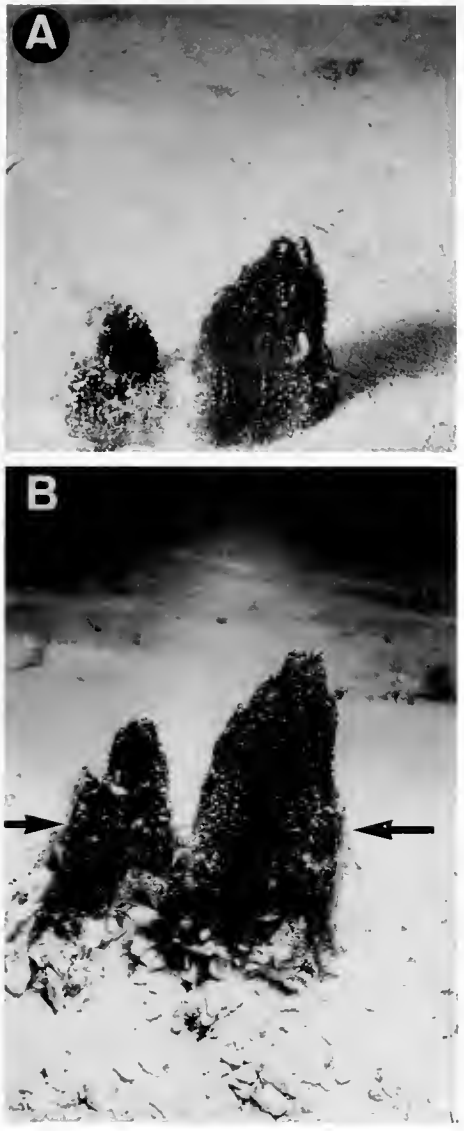

Figure 2. *Biemna ehrenbergi in situ.* (A) The chimney-like siphons, which are above the sediment surface. (B) The sponge after sediments have been removed. Arrows indicate sediment level.

were of medium size, and less than 2% were smaller than 74 μm (Table I).

We found specimens of *B. ehrenbergi* buried to depths of up to 20 cm, with most of the body covered with sand (Fig. 2A). When the buried part was uncovered it was found to be attached to the beach-rock (Fig. 2B). Moreover, the shape of the buried part resembled a conus with a large base bearing several projections (Fig. 2B). Only these projections—the chimney-shaped siphons—extruded (1–7 cm) through the sediment (Fig. 2A). Oscula are located at the uppermost part of the siphons.

The sponge is capable of closing its oscula, and thus probably is able to avoid intake of particles during storms. Observations, using dye injected above and into the sediment 10–15 cm from the siphons, revealed that most of the water pumped into the sponge came through the pores of the buried surfaces; only a minute amount was taken in by pores on the exposed surface of the siphons. Less than a minute after dye was injected into the sediment, it exited from the oscula in a strong flow; but when injected above the sediment surface, only a small amount of dye emerged from the oscula.

Surface structure and morphology

Most of the ostia (inhaling openings) are located on the upper surface of the body and are buried in the sediment (Fig. 3b). The exposed siphons are almost devoid of such openings (Fig. 3a). The average size of the oval pores is 9.4 ± 5.2 μm, with a range of 4–24.7 μm (Fig. 3b). The ostia are transcellular, composed of a single cell (Fig. 3b). The total surface area of the buried parts is extended through processes that protrude from the main central body.

B. ehrenbergi has many small excurrent canals that are accommodated along a central larger canal, leading to the osculum (Fig. 4a). The inhalant canals can be divided into two zones: (a) those of the siphon-like parts of the body, which extend above the substratum surface; and (b) the canals of the body parts that are buried within the sediment. Most of the sponge's soma, which lies beneath the sediment surface, is supported by numerous small incurrent canals and ostia (Figs. 3b, 4b). In contrast, the exposed parts of the body contain few inhalant canals and ostia and a large excurrent canal (Figs. 3a, 4a).

Large quantities of various intracellular bacteria confined within bacteriocytes are a prominent feature in the mesohyl of *B. ehrenbergi* (Fig. 5a–e). These bacteria appear to be contained in a single large vacuole within the cell (Fig. 5e), or immersed in the cytoplasm without being enclosed by a membrane (Fig. 5a–d). No phototrophic bacteria were found (none of the bacteria appeared to contain photosynthetic membranes). Bacteria within some of the bacteriocytes seemed to disintegrate (Fig. 5b–d), whereas bacteria within adjacent cells appeared intact and divided and grew (Fig. 5b, c).

Discussion

Sponge distribution

The distribution of the sediment-buried *B. ehrenbergi* in Eilat is restricted to a narrow belt at the shallower part of the semi-closed back-reef lagoon in Eilat. The possibility of exposure to a non-oxygenated environment is a major problem for sediment-buried sponges. The oxygen level within the sediment is largely dependent on the tidal and

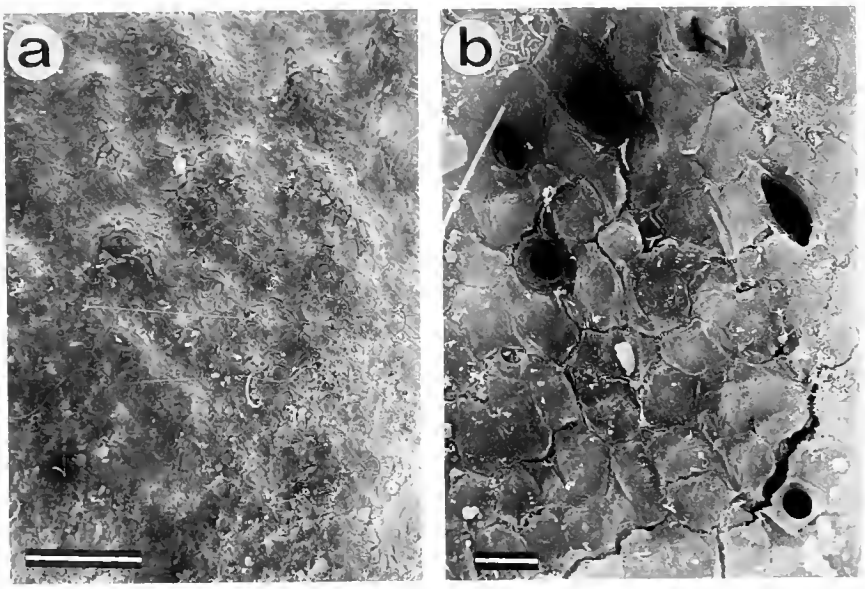

Figure 3. Upper surface architecture of *Biemna ehrenbergi*. (a) SEM photograph of an area of exposed siphon. Scale bar = 100 μm. (b) SEM photograph of an area of the exposed upper surface of the buried parts. Scale bar = 10 μm.

subtidal (wave) pumps (Riedel *et al.*, 1972), as well as on the intensity of the sponge's pumping activity. These two pumps are most effective in shallowest water, at the same depth as *B. ehrenbergi*. We therefore suggest that the sponge's distribution is restricted to an area in which the sediment is mostly oxygenated. Moreover, the large sediment size (small particles are less than 2% of total grain mass) also contribute to the oxygenation of the sponge's vicinity. A sponge inhabiting a soft-substrate, wave-affected environment is also in danger of being uncovered and dislodged. Because closed lagoons, like many other sheltered habitats, are 'sink environments' in which the rate of sediment deposition is higher than the rate of sediment loss, the sponge's chances of remaining covered are enhanced. *B. ehrenbergi* also attaches itself to the buried beach-rock, thus providing anchorage and better ability to maintain an upright position following exposure to storms.

Flow and particle path

The morphology of the canal system of *B. ehrenbergi*, the presence of ostia mostly on the sponge's buried surface, and the observation that the animal can pump in dye injected into the sediment and expel it through the oscula, all provide evidence that this sponge species receives its water supply from the interstitial reservoir. This is a first report of such a pattern of water pumping in sponges. This finding revives and sheds new light on a century-old question: what is the direction of water flow in soft-sediment sponges such as *Disyringa* spp. (Sollas, 1888; Fry and Fry, 1978; Werding and Sanchez, 1991)? On the basis of sponge morphology, it was suggested that *Disyringa* spp., inhabiting a deep, soft-bottom environment, pumps water in from the interstitial reservoir either through a single large pore (Sollas, 1888) or through several small openings buried in the sediment (Fry and Fry, 1978). Werding and Sanchez (1991) found in laboratory experiments that *Oceanapia peltata*, with a body morphology similar to that of *Disyringa* spp., pumps water in from siphons (papillae) projecting above the substrate and discharges it out into the sand. This flow direction is opposite to the one we observed for *B. ehrenbergi*. The fact that sponges are capable of pumping water from the interstitial reservoir, as demonstrated in the present study, suggests that such a direction of water movement may yet be demonstrated in *Disyringa* spp.

Because water is pumped in from the sediment, buried ostia may be clogged by sediment particles. To avoid this problem, the internal anatomy of the sponges is probably frequently reorganized by continuous cell movements, as shown for other sponges (*e.g.*, Bond, 1992). Such plasticity enables the sponges to open new ostia, overcoming any clogging. Due to cell flexibility, a transcellular opening may be easily moved aside or closed, unlike a system of extracellular openings, which requires coordination between many cells.

The conical shape of the chimney-like siphon of *B. ehrenbergi* gives it a high slenderness ratio (SR) [in which

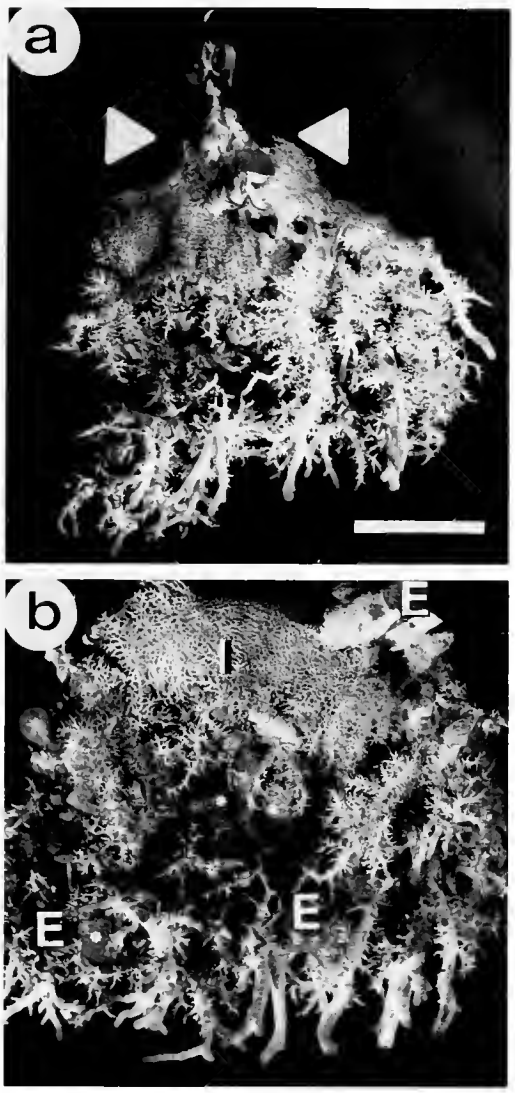

Figure 4. Plastic replica of the aquiferous system of *Biemna ehrenbergi* (SEM photographs). (a) Gross aquiferous system. Arrowheads indicate the point at the surface of the sediment. Scale bar = 5 cm. (b) A portion of the aquiferous system located underneath the surface: I, high density of small incurrent canals; E, zone of many excurrent canals. The "E" at the top of the picture is positioned on a central excurrent canal that leads to the above-surface osculum; * sand particles entrapped within the sponge.

the ratio of the body height to its lowest width is > 1 (Abelson *et al.*, 1993)]. This shape prevents ascension of the near-bed flow, and as a consequence reduces the quantities of bedload particles encountering the siphons. In addition to being relatively high above the sediment surface, the oscula remain unclogged because they can close their entrances during unfavorable conditions. This combination of morphology and behavior gives specimens of this species the twofold advantage of being primarily infaunal organisms, yet having exposure to the water column for waste discharge. The separation of sites for intake and discharge of water ensures that no re-filtration of wastewater occurs.

Feeding modes

B. ehrenbergi appears to possess two feeding modes: one that is common to all sponges—filtering small particles out of the water (either above-surface or interstitial water); and a second based on symbiotic intracellular bacteria.

Symbiotic, usually heterotrophic, bacteria have been observed within many sponge species (*e.g.*, Reiswig, 1974; Vacelet and Donadey, 1977; Wilkinson, 1978). Nutrient translocation between phototrophic symbiotic cyanobacteria and their sponge host has been demonstrated (Wilkinson, 1979). In the sclerosponges *Ceratoporella nicholsoni* and *Stromatospongia norae*, the numerous symbiotic heterotrophic bacteria are spread extracellularly and are phagocytized in some parts of the sponges (Willenz and Hartman, 1989). In *Petrosia ficiformis*, as in *B. ehrenbergi*, symbiotic heterotrophic bacteria are confined intracellularly to bacteriocytes, and no phagocytosis and digestion of these bacteria is observed (Vacelet and Donadey, 1977). The absence of a host membrane around the symbiotic bacteria, as suggested in some of the observed cases, has been considered to indicate a stable association of complex metabolic relationships between the symbiotic partners (Smith, 1979; Saffo, 1990). It may be, however, that even in presence of a vacuole, bacteriocyte cytoplasm had been reduced to a minimum, which would explain its virtual absence in many electron micrographs.

In the present study, transmission electron micrographs provided grounds for suggesting that *B. ehrenbergi* may consume some of its "bacterial farms," while leaving other bacteriocytes intact. Thus there exist, side by side, some bacteriocytes in which the bacteria appear normal and even seem to divide, and others in which the bacteria apparently disintegrate.

In a sink environment (like the reef lagoon), the content of particulate and dissolved organic matter in the sediment is higher than in the water column. For example, dissolved organic carbon is higher in interstitial water than in seawater (Krom and Sholkovitz, 1977), and dissolved free amino acids can be 100 times as concentrated in the interstitial water in the near-surface sediments as they are in the overlaying seawater (Henrichs and Farrington, 1979). We suggest, therefore, that in the lagoon, *B. ehrenbergi* and its symbiotic intracellular bacteria may benefit from interstitial water rich in organic matter (particulate and dissolved), which the sponge pumps through its buried surface.

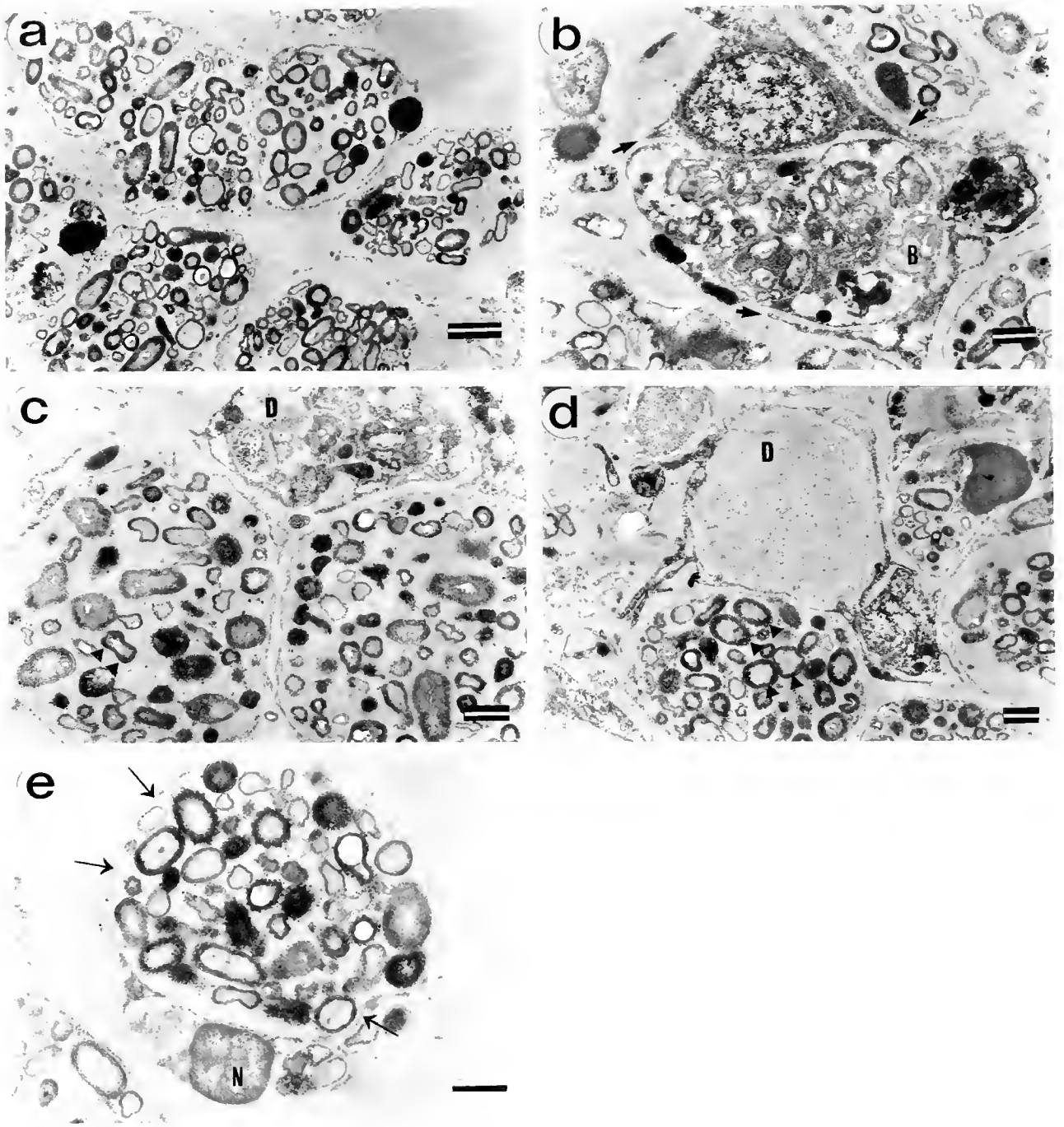

Figure 5. Symbiotic bacteria found in *Biemna ehrenbergi* (TEM photographs). (a) Bacteriocytes—mesohyl cells that are packed with a large number of intracellular bacteria. Scale bar = 2 μm. (b) Partially disintegrated bacteria within a bacteriocyte (B). A sponge cell is attached to the bacteriocyte, engulfing it by projections (arrows). Scale bar = 1 μm. (c) A bacteriocyte in an advanced stage of bacterial disintegration (D), while in two adjacent bacteriocytes the bacterial population seem intact and some bacteria appear to be dividing (arrowheads). Scale bar = 1 μm. (d) A bacteriocyte with proliferating intact bacteria (arrowheads) adjacent to a cell which resembles a bacteriocyte, but in which no bacteria are seen. Scale bar = 1 μm. (e) A bacteriocyte with nucleus (N) and cytoplasm, in which the bacteria appear to be enclosed within a vacuole (arrows). Scale bar = 1 μm.

Acknowledgments

We are indebted to Y. Loya for his invaluable support of this study. Y. Delarea helped with the electron microscopy. An extremely thorough review by B. Rinkevich and helpful suggestions from an anonymous reviewer improved the manuscript immensely. We thank the MBL at Eilat for the hospitality and use of lab facilities.

Literature Cited

Abelson, A., T. Miloh, and Y. Loya. 1993. Flow patterns induced by substrata and body morphologies of benthic organisms, and their roles in determining availability of food particles. *Limnol. Oceanogr.* **38:** 1116–1124.

Bavestrello, G., B. Burlando, and M. Sara. 1988. The architecture of the canal system of *Petrosia ficiformis* and *Chondrosia reniformis* studied by corrosion casts (Porifera, Demospongiae). *Zoomorphology* **108:** 161–166.

Bond, C. 1992. Continuous cell movements rearrange anatomical structures in intact sponges. *J. Exp. Zool.* **263:** 284–302.

Fry, W. G., and P. D. Fry. 1978. Aspects of the functional anatomy and ecological physiology of *Dysyrinx* and some other infaunal tetractinomorph sponges. Coll. Internat. CNRS Biologie des spongiaires. **291:** 335–341.

Henrichs, S. M., and J. W. Farrington. 1979. Amino acids in interstitial waters of marine sediments. *Nature* **272:** 319–322.

Krom, M. D., and E. R. Sholkovitz. 1977. Nature and reaction of dissolved organic matter in the interstitial waters of marine sediments. *Geochim. Cosmochim. Acta* **41:** 1565–1573.

Lopez, G. R., and J. S. Levinton. 1987. Ecology of deposit-feeding animals in marine sediments. *Q. Rev. Biol.* **62:** 235–260.

Reiswig, H. M. 1974. Water transport, respiration and energetics of three tropical marine sponges. *J. Exp. Mar. Biol. Ecol.* **14:** 231–249.

Riedel, R. J., H. Huang, and R. Machan. 1972. The subtidal pump: a mechanism of interstitial water exchange by wave action. *Mar. Biol.* **13:** 210–221.

Rogers, C. R. 1990. Responses of coral reefs and reef organisms to sedimentation. *Mar. Ecol. Prog. Ser.* **62:** 185–202.

Saffo, M. B. 1990. Symbiosis within a symbiosis: intracellular bacteria within the endosymbiotic protist *Nephromyces*. *Mar. Biol.* **107:** 291–296.

Schubauer, J. P., T. P. Burns, and T. H. Richardson. 1990. Population dynamics of five Demospongiae in Jamaica: variation in time and space. Pp. 443–451 in *New Perspectives in Sponge Biology*, K. Rützler, ed. Smithsonian Institution Press, Washington, DC.

Simpson, T. L. 1984. *The Cell Biology of Sponges.* Springer-Verlag, New York.

Smith, D. C. 1990. From extracellular to intracellular: the establishment of symbiosis. *Proc. R. Soc. Lond. B* **204:** 115–130.

Sollas, W. J. 1888. Report on the Tetractinellida collected by HMS "Challenger" during the years 1873–1876. *Rep. Sci. Res. Voyage "Challenger."* **25** i-cixvi: 1–458.

van Soest, R. W. M. 1993. Distribution of sponges on the Mauritanian continental shelf. *Hydrobiologia* **258:** 95–106.

Tabachnick, K. R. 1991. Adaptation of the Hexactinellid sponges to deep-sea life. Pp. 378–386 in *Fossil and Recent Sponges*, J. Reitner and H. Keupp, eds. Springer-Verlag, Berlin.

Vacelet, J., and C. Donadey. 1977. Electron microscope study of the association between some sponges and bacteria. *J. Exp. Mar. Biol. Ecol.* **30:** 301–314.

Watling, L. 1991. The sedimentary milieu and its consequences for resident organisms. *Am. Zool.* **31:** 789–796.

Werding, B., and H. Sanchez. 1991. Life habits and functional morphology of the sediment infaunal sponges *Oceanapia oleracea* and *Oceanapia peltata* (Porifera, Haplosclerida). *Zoomorphology* **110:** 203–208.

Wilkinson, C. R. 1978. Microbial associations in sponges. III. Ultrastructure of the *in situ* associations in coral reef sponges. *Mar. Biol.* **49:** 177–185.

Wilkinson, C. R. 1979. Nutrient translocation from symbiotic cyanobacteria to coral reef sponges. Pp. 373–380 in *Biologie des Spongiaires.* C. Lévi and N. Boury-Esnault, eds. *Coll. Int. C.N.R.S.* **291.**

Willenz, P., and W. D. Hartman. 1989. Micromorphology and ultrastructure of Caribbean sclerosponges. I. *Ceratoporella nicholsoni* and *stromatospongia norae* (Ceratoporellidae: Porifera). *Mar. Biol.* **103:** 387–401.

Reference: *Biol. Bull* **189**: 370–375. (December, 1995)

Interspecific Variations in Adhesive Protein Sequences of *Mytilus edulis, M. galloprovincialis,* and *M. trossulus*

KOJI INOUE[1,*], J. HERBERT WAITE[2], MAKOTO MATSUOKA[3], SATOSHI ODO[1], AND SHIGEAKI HARAYAMA[1]

[1]*Marine Biotechnology Institute, Kamaishi Laboratories, Heita, Kamaishi, Iwate 026, Japan;* [2]*Department of Chemistry and Biochemistry, University of Delaware, Newark, Delaware 19716; and* [3]*Juneau Center, School of Fishery and Ocean Sciences, University of Alaska, Fairbanks, Glacier Highway, Juneau, Alaska 99801*

Abstract. Variation in the adhesive protein gene sequences of *Mytilus edulis, M. galloprovincialis,* and *M. trossulus* collected in Delaware, Kamaishi (Japan), and Alaska, respectively, was analyzed by the polymerase chain reaction (PCR) using two sets of oligonucleotide primers. The first set, Me 13 and Me 14, was designed to amplify the repetitive region. The length of the amplified fragments was highly variable, even among samples of the same species. Another set, Me 15 and Me 16, was designed to amplify a part of the nonrepetitive region. The length of the amplified fragments was uniform in each species and differed interspecifically; 180, 168, and 126 bp for *M. edulis, M. trossulus,* and *M. galloprovincialis,* respectively. The amplified sequence of *M. trossulus* resembled that of *M. edulis.* Mussels from other sites were also examined by PCR using Me 15 and Me 16. Wild mussels from Tromsö (Norway) and cultured mussels from Brittany (France) were identified as *M. edulis.* Cultured mussels from the Mediterranean coast of France and wild mussels from Shimizu (Japan) were identified as *M. galloprovincialis.* Some wild mussels from Hiura (Japan) were identified as a hybrid between *M. galloprovincialis* and *M. trossulus.* Thus, the length of this part (variable region) of the sequence is proposed as a diagnostic marker for these three morphologically similar species and their hybrids.

Received 23 January 1995; accepted 10 August 1995.

The partial nucleotide sequence for *M. trossulus* adhesive protein gene reported in this paper has been submitted to the GenBank/EMBL/DDBJ Data Bank with accession number D50553.

* Address for correspondence: Koji Inoue at present address: Central Research Laboratory, Nippon Suisan Kaisha, Ltd., 559-6 Kitano, Hachioji, Tokyo 192, Japan.

Introduction

Two types of polyphenolic proteins, foot proteins 1 and 2, both of which incorporate 3,4-dihydroxyphenylalanine (DOPA) into their primary structures, have been isolated from the mussel *Mytilus edulis,* and characterized (see Waite, 1992, for a review). Foot protein 1 is an adhesive protein that contains repeats of the decapeptide motif AKPSYP*P*TY*K, where P* and Y* denote hydroxyproline and DOPA, respectively, and the hexapeptide motif AKPTY*K (Waite and Tanzer, 1981; Waite, 1983; Waite *et al.,* 1985). Foot protein 2 is an epidermal growth-factor-like protein that forms the adhesive plaque matrix (Rzepecki *et al.,* 1992; Inoue *et al.,* 1995a). The primary structure of the foot protein 1 has been determined by cDNA or gene cloning. It has been shown that it consists of a relatively short nonrepetitive domain and a long repetitive domain. The repetitive domain contains more than 70 decapeptide repeats and 13 or 14 hexapeptide repeats, but the number and distribution pattern of the motifs are variable even in the same species (Filpula *et al.,* 1990; Laursen, 1992).

We isolated cDNA encoding foot protein 1 from *M. galloprovincialis* sampled in Japan and compared the predicted amino acid sequence to those of *M. edulis* (Inoue and Odo, 1994; Inoue *et al.,* 1995b). The *M. galloprovincialis* sequence also consisted of the nonrepetitive and repetitive domains, but remarkable differences were observed in both. The major difference in the repetitive do-

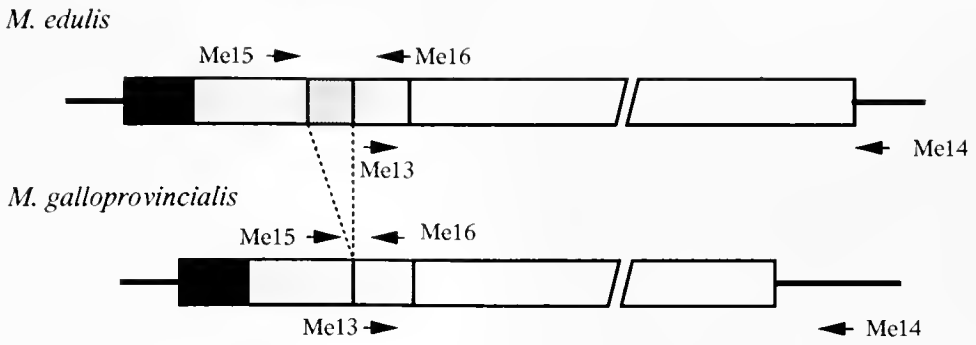

Figure 1. Positions of PCR primers in the adhesive protein genes of *Mytilis edulis* and *M. galloprovincialis*. Adhesive protein genes are shown as cDNA sequences. Position and direction of primers is indicated by arrows. Solid and open boxes indicate the signal peptide and the repetitive region, respectively. Dotted boxes indicate the nonrepetitive region, and the box with dense dots indicates the 18 amino acid sequence found in the *M. edulis* sequence but not in that of *M. galloprovincialis*. Solid lines indicate untranslated region.

main is that the *M. galloprovincialis* sequence contained 62 decapeptide repeats but no hexapeptide motif. In contrast, the nonrepetitive domains differ by a deletion of 18 amino acids observed in the *M. galloprovincialis* sequence.

In this study, we prepared two sets of oligonucleotide primers for polymerase chain reaction (PCR) to amplify the whole repetitive region and a part of the nonrepetitive region. Using these, we have analyzed foot protein 1 sequences of *M. edulis*, *M. galloprovincialis*, and *M. trossulus*. These three species are closely related (Gosling, 1984; Koehn, 1991; Gardner, 1992; Seed, 1992, for reviews) and practically indistinguishable by morphological characteristics only. We report that the length of the fragments amplified from the nonrepetitive region is specific to each species, but the length of the repetitive region is highly variable even within the same species. Thus the nonrepetitive region can be used as a diagnostic marker for identification of the three species.

Materials and Methods

Mussels

M. edulis was collected at Lewes (Delaware, USA); *M. galloprovincialis* and *M. trossulus* were sampled at Kamaishi (Iwate, Japan) and Juneau (Alaska, USA). All these sampling points are "pure sites" of each species where the other two species do not occur (McDonald *et al.*, 1991). Wild mussels were also collected at Tromsö (Norway), Hiura (Hokkaido, Japan), and Shimizu (Shizuoka, Japan). Mussels cultured in Brittany (France) and on the Mediterranean coast of France were obtained at a fish market at Ferney-Valtaire (France).

DNA extraction

A piece of the gill from each mussel, about 0.5 cm^2, was incubated in 500 μl lysis buffer containing 50 m*M* Tris-HCl (pH 7.5), 10 m*M* EDTA, 0.5% SDS, 500 μg/ml Proteinase K at 55°C for 2–4 h. Samples were then extracted twice with equal volumes of saturated phenol and twice with phenol chloroform: isoamyl alcohol (24:24:1). The aqueous phase was precipitated with ethanol and dissolved in 50 μl TE (10 m*M* Tris, 1 m*M* EDTA).

PCR amplification

About 100 ng of DNA was dissolved in 100 μl 1 × Tth buffer (TOYOBO, Japan) containing 6 μg sense primer, 6 μg antisense primer, and 200 μM dNTP. After preheating to 95°C, 1 unit of Tth DNA polymerase (TOYOBO, Japan) was added and 30 cycles of amplification were performed. Each cycle consisted of 30 s at 94°C, 30 s at 56°C, and 90 s at 70°C. The sequences of the primers were Me 13, CCA CTT GCA AAG AAG CTG TCA TCT; Me 14, ACA AAC GTT AAA ATG TGT AGT ACA GTA; Me 15, CCA GTA TAC AAA CCT GTG AAG A; Me 16, TGT TGT CTT AAT AGG TTT GTA AGA. Positions of primers in the foot protein 1 cDNA sequence in *M. galloprovincialis* are shown in Figure 1.

Electrophoresis of amplified products

Ten microliters of PCR product was mixed with the loading dye solution containing bromophenol blue (BPB) and xylene cyanol and subjected to agarose gel electrophoresis. For analysis of PCR products, 4.8% NuSieve 3:1 agarose (FMC) was used for the nonrepetitive region, and 1% LE agarose (FMC) was used for the repetitive region. Electrophoresis on a 4.8% gel was continued until BPB reached the end of the gel.

Sequencing

The fragment amplified from the genome of *M. trossulus* using primers Me 15 and Me 16 was isolated and

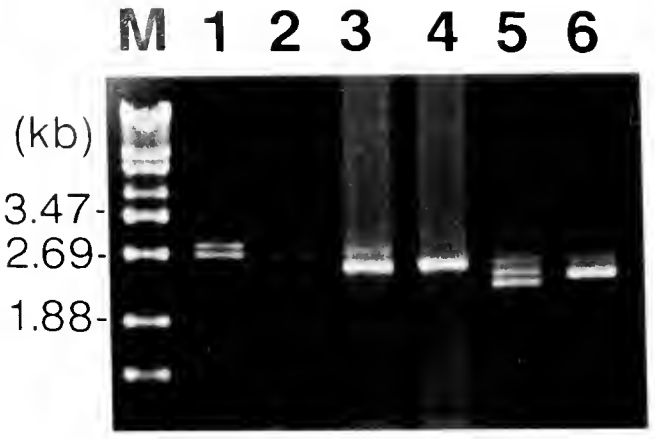

Figure 2. Representative results of amplification of the repetitive region of the adhesive protein gene. Amplified products were electrophoresed on 1% agarose gel. Lanes 1 and 2, *Mytilus edulis;* lanes 3 and 4, *M. trossulus;* lanes 5 and 6, *M. galloprovincialis.* M, molecular marker (lambda DNA digested with *Eco*T 141).

inserted into the *Sma* I site of pUC19. Sequences of both strands of three independent clones were determined using a 373A DNA sequencer (Applied Biosystems Inc.) and a PRISM Dyeterminator Cycle Sequencing Kit (Applied Biosystems Inc.).

Results

Variation in the repetitive region

The primers Me 13 and Me 14 were designed to amplify the repetitive region using the sequences identical to both *M. edulis* and *M. galloprovincialis.* Since the sense primer, Me 13, corresponds to a part of the nonrepetitive region and the antisense primer, Me 14, to a part of the 3′ untranslated region, the whole repetitive region is amplified by PCR. *M. edulis, M. galloprovincialis,* and *M. trossulus* were collected at Delaware, Kamaishi, and Juneau, respectively. These sampling points are known to be "pure sites" at which no other species of the *M. edulis* complex is found (McDonald *et al.,* 1991). We analyzed 8, 16, and 8 individuals of *M. edulis, M. galloprovincialis,* and *M. trossulus,* respectively, using primers Me 13 and Me 14. Since the repetitive region is relatively long and highly repetitive, it was difficult to amplify the whole repetitive region if the template DNA was insufficiently pure and long, but prominent bands were successfully obtained by using well-purified, high molecular weight DNA. Typical results are shown in Figure 2. Sizes of the band ranged from 2.2 to 2.8 kb. The fragments obtained from *M. edulis* were generally larger than those of the other two species. The sizes of bands in *M. trossulus* and *M. galloprovincialis* were similar but, on average, the former were slightly larger. Many individuals had two-banded (heterozygous) patterns, as expected for a highly variable polymorphism. One sample of *M. galloprovincialis* exhibited three bands, which may be a naturally occurring triploid or a mosaic individual that possesses a cell lineage having the differed length of foot protein 1 gene. It is, however, also possible that the third band is a heteroduplex of two different fragments.

Variation in the nonrepetitive region

Another set of primers, Me 15 and Me 16, was also prepared to amplify a part of the nonrepetitive region using sequences perfectly identical between *M. edulis* and *M. galloprovincialis* (Fig. 1). The size of the amplified fragment estimated from sequence data previously reported (Filpula *et al.,* 1990) is 180 bp in *M. edulis.* In *M. galloprovincialis,* the expected size is 126 bp because the sequence of *M. galloprovincialis* contains a deletion of 18 amino acids (Fig. 1; see also Inoue and Odo, 1994). Using these primers, 8, 32, and 16 individuals of *M. edulis, M. galloprovincialis,* and *M. trossulus*—including the same samples used in the analysis of the nonrepetitive region—were examined. PCR analysis indicated that all samples exhibited a single band. Representative results are shown in Figure 3. The position of the band was uniform in each species but differed from species to species. The size of the amplified fragments of *M. edulis* and *M. galloprovincialis* estimated by mobility in agarose agreed with those expected. Fragments from *M. trossulus* were shorter than those of *M. edulis* but longer than those of *M. galloprovincialis.* To determine the length and sequence of the amplified fragment of *M. trossulus,* the band obtained from one sample (Fig. 3, Lane 3) was isolated and se-

Figure 3. Representative results of amplification of the nonrepetitive region of the adhesive protein gene. Amplified products were electrophoresed on 4.8% NuSieve GTG agarose gel (FMC). Lanes 1 and 2, *Mytilus edulis,* lanes 3 and 4, *M. trossulus;* lanes 5 and 6, *M. galloprovincialis.* M, molecular marker (pUC19 DNA digested with *Hap*II).

```
        10         20         30         40         50         60
CCAGTATACAAACCTGTGAAGACAAGTTATTCGTCACCATATAAACCACCAACATACCAA
P  V  Y  K  P  V  K  T  S  Y  S  S  P  Y  K  P  P  T  Y  Q

        70         80         90        100        110        120
CCACTCAAAAAGAAACCGATGGACTATAATAGTTCTCCGCCAACATATGGATCAAAGACA
P  L  K  K  K  P  M  D  Y  N  S  S  P  P  T  Y  G  S  K  T

       130        140        150        160
AACTATCTTGCAAAGAAGCTGTCATCTTACAAACCTATTAAGACAACA
N  Y  L  A  K  K  L  S  S  Y  K  P  I  K  T  T
```

Figure 4. Nucleotide and deduced amino acid sequences of the fragment amplified from the genomic DNA of *Mytilis trossulus* using primers Me15 and Me16. Underlined sequences were derived from primers.

queneed. The sequeneed fragment including the primer sequences was 168 bp, 12 bp shorter than the corresponding region of *M. edulis* (Fig. 4). This difference is small but measurable by mini-electrophoresis, as shown in Figure 3. The nucleotide sequence of the amplified fragment was compared with corresponding sequences of *M. edulis* and *M. galloprovincialis* (Fig. 5). Since the region shown in Figure 5 was especially variable among the three species, this region is hereafter referred to as the "variable region." It seems that variation among the three species was caused by deletion or addition of short sequences, not by base substitutions.

The variable region of mussels cultured in Brittany, those cultured on the Mediterranean coast of France, and the wild mussels collected at Tromsö and Hiura were also examined by PCR using Me 15 and Me 16. Four individuals were examined in each group and representative results are shown in Figure 6. All the wild Tromsö mussels and all the cultured Brittany mussels exhibited the 180-bp fragment and were identified as *M. edulis*. All the cultured Mediterranean mussels and the wild mussels from Shimizu exhibited a 126-bp fragment and were identified as *M. galloprovincialis*. These results are consistent with the distribution map of mussels that was made by using allozyme characters (McDonald *et al.*, 1991). Eight wild mussels of Hiura were also examined using Me 15 and Me 16. Two bands, 126 and 168 bp, were amplified from six individuals (Fig. 6), but only the 126-bp band was amplified from the remainder (data not shown). Hiura is on Hokkaido Island, where both native *M. trossulus* and introduced *M. galloprovincialis* are distributed. The mussels that

```
Mt: CAAGTTATTCGTCACCATATAAACCACCAACATACCAACCACTCAAAAAG
Me: **********G*************************************
Mg: ********-------------------------------------------

Mt: AAACCGATGGACTATAATAGT---------TCTCCGCCAACATATGGATC
Me: ***---G********CG*CC*ACGAAAAGT*A******************
Mg: ---------------CA*CC*ACGAATAGT*A******************

Mt: AAAGACAAACTAT------CTTGCAAAGAAGCTGTCA
Me: **************CTACCA******************
Mg: **************CTGCCA******************
```

Figure 5. Comparison of nucleotide sequences of the variable region of the adhesive protein genes of *Mytilis trossulus*, *M. edulis*, and *M. galloprovincialis*. Sequences of *M. edulis* and *M. galloprovincialis* were according to Filpula *et al.* (1990) and Inoue and Odo (1994), respectively. Asterisks indicate nucleotides identical to those of the *M. trossulus* sequence. Hyphens indicate gaps inserted to align sequences. Mt, *M. trossulus*; Me, *M. edulis*; Mg, *M. galloprovincialis*.

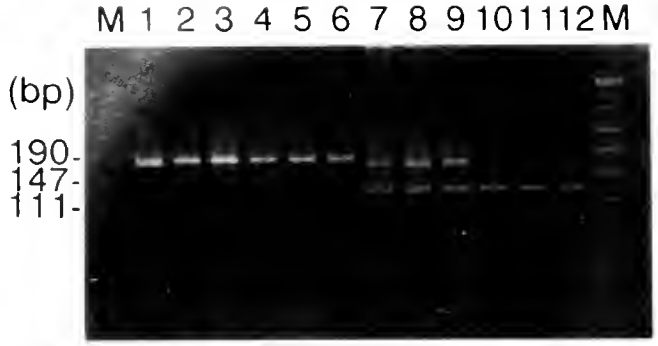

Figure 6. Amplification of the variable region of the adhesive protein gene of wild and cultured mussels. Amplified products were electrophoresed on 4.8% NuSieve GTG agarose gel (FMC). Lanes 1–3, wild mussels collected at Tromsö; Lanes 4–6, mussels cultured in Brittany; Lanes 7–9, wild mussels collected at Hiura; Lanes 10–12, mussels cultured on the Mediterranean coast of France. M, molecular marker (pUC19 DNA digested with *Hap*II).

exhibited two fragments are presumed to be hybrids between the two species.

Discussion

Among the five species of the genus *Mytilus*, *M. edulis*, *M. galloprovincialis*, and *M. trossulus* have been called the "*M. edulis complex*." Since they are morphologically similar and shell shape is often influenced by local environment, it is difficult to identify these species by morphological characteristics. Recently, allozyme characters have been used to clarify the taxonomy of these species (Koehn *et al.*, 1984; McDonald and Koehn, 1988; Varvio *et al.*, 1988; McDonald *et al.*, 1991; Coustau *et al.*, 1991; Viard *et al.*, 1994). These characters are recognized as reliable markers, but data for multiple loci are required for accurate identification of all three species. Identification using mitochondrial DNA (mtDNA) sequences has also been described (Edwards and Skibinski, 1987; Blot *et al.*, 1990; Geller *et al.*, 1993, 1994). Although such attempts were partially successful, it is still difficult to differentiate the three species unambiguously. In this study, we found that differences in a certain "variable region" of a sequence in the nonrepetitive domain of the foot protein 1 agree well with the taxonomic rank of species. It was also shown that the variations can be attributed to differences in the length of the fragments amplified by PCR. Thus the variable region may become an effective diagnostic marker. Because PCR requires only a small amount of DNA as a template, the method may be used for larvae or young individuals that are too small for analysis by other methods. In addition, the PCR system seems effective for the identification of hybrids within the *M. edulis* complex—we could detect hybrids that have the haplotypes of both *M. galloprovincialis* and *M. trossulus* (Fig. 6). This system may become a powerful tool for studying the distribution and genetics of mussels, one of the most cosmopolitan of marine animals.

We also tried to amplify the adhesive protein gene of *M. coruscus*, a mussel species native to Japan, but we were unsuccessful (data not shown). The adhesive protein gene sequence of *M. coruscus* may be considerably different from those of species in the *M. edulis* complex. It seems that other primers are required for analysis of mussels other than the *M. edulis* complex.

In contrast to the nonrepetitive domain, the length of the repetitive domain was highly variable, even in samples collected at the same site. This result is consistent with the fact that repeat patterns observed in three nucleotide sequences encoding foot protein 1 of *M. edulis* reported separately (Strausberg *et al.*, 1989; Filpula *et al.*, 1990; Laursen, 1992) differ from one another. Because the length of this region was partially overlapping among species, it seems inappropriate for use as a marker of species. Many individuals of the three species also have two or more fragments of different length. These results suggest that each species has enormous variability in the patterns of repetitive sequences. Considering that foot protein 1 is a key molecule for adhesion of mussels and thus is essential for their survival, its extensive diversity is intriguing. We suggest that the repetitive domain has been differentiated by a "shuffling" of the repeat pattern as well as by the common base substitution process (Inoue *et al.*, 1995b). Increased diversity may have an important role in mussel survival or evolution.

Acknowledgments

The authors express their sincere thanks to Dr. Shigetoh Miyachi for support in this study, to Drs. Shigeru Nakao and Takashi Noda for valuable advice, to Hiroyuki Kawahara for collecting mussels, and to Sachiko Dobashi for technical assistance. This work was performed as a part of the Industrial Science and Technology Frontier Program supported by New Energy and Industrial Technology Development Organization.

Literature Cited

Blot, M., B. Legendre, and P. Albert. 1990. Restriction fragment length polymorphism of mitochondrial DNA in subantarctic mussels. *J. Exp. Mar. Biol. Ecol.* **141**: 79–86.

Coustau, C., F. Renaud, and B. Delay. 1991. Genetic characterization of the hybridization between *Mytilus edulis* and *M. galloprovincialis* on the Atlantic coast of France. *Mar. Biol.* **111**: 87–93.

Edwards, C. A., and D. O. F. Skibinski. 1987. Genetic variation of mitochondrial DNA in mussel (*Mytilus edulis* and *M. galloprovincialis*) population from South West England and South Wales. *Mar. Biol.* **94**: 547–556.

Filpula, D. R., S-M. Lee, R. P. Link, S. L. Strausberg, and R. L. Strausberg. 1990. Structural and functional repetition in a marine mussel adhesive protein. *Biotechnol. Prog.* **6**: 171–177.

Gardner, J. P. A. 1992. *Mytilus galloprovincialis* (Lmk) (Bivalvia, Mollusca): the taxonomic status of the Mediterranean mussel. *Ophelia* **35:** 219–243.

Geller, J. B., J. T. Carlton, and D. A. Powers. 1993. Interspecific and intrapopulation variation in mitochondrial ribosomal DNA sequences of *Mytilus* spp. (Bivalvia: Mollusca). *Mol. Mar. Biol. Biotechnol.* **2:** 44–50.

Geller, J. B., J. T. Carlton, and D. A. Powers. 1994. PCR-based detection of mtDNA haplotypes of native and invading mussels on the northeastern Pacific coast: latitudinal pattern of invasion. *Mar. Biol.* **119:** 243–249.

Gosling, E. M. 1984. The systematic status of *Mytilus galloprovincialis* in western Europe: a review. *Malacologia* **25:** 551–568.

Inoue, K., and S. Odo. 1994. The adhesive protein cDNA of *Mytilus galloprovincialis* encodes decapeptide repeats but no hexapeptide motif. *Biol. Bull.* **186:** 349–355.

Inoue, K., Y. Takeuchi, D. Miki, and S. Odo. 1995a. Mussel adhesive plaque protein gene is a novel member of epidermal growth factor-like gene family. *J. Biol. Chem.* **270:** 6698–6701.

Inoue, K., Y. Takeuchi, D. Miki, and S. Odo. 1995b. Mussel adhesive protein genes: structure and variations. *J. Mar. Biotechnol.* (in press).

Koehn, R. K. 1991. The genetics and taxonomy of species in the genus *Mytilus*. *Aquaculture* **94:** 125–145.

Koehn, R. K., J. G. Hall, D. J. Innis, and A. J. Zera. 1984. Genetic differentiation in *Mytilus edulis* in eastern North America. *Mar. Biol.* **79:** 117–126.

Laursen, R. A. 1992. Reflections on the structure of mussel adhesive proteins. Pp. 55–74 in *Structure, Cellular Synthesis and Assembly of Biopolymers. Results and Problems in Cell Differentiation*, Vol. 19, S. T. Case, ed. Springer-Verlag, Berlin.

McDonald, J. H., and R. K. Koehn. 1988. The mussels *Mytilus galloprovincialis* and *M. trossulus* on the Pacific coast of North America. *Mar. Biol.* **99:** 111–118.

McDonald, J. H., R. Seed, and R. K. Koehn. 1991. Allozymes and morphometric characters of three species of *Mytilus* in the Northern and Southern Hemispheres. *Mar. Biol.* **111:** 323–333.

Rzepecki, L. M., K. M. Hansen, and J. H. Waite. 1992. Characterization of a cystine-rich polyphenolic protein family from the blue mussel *Mytilus edulis* L. *Biol. Bull.* **183:** 123–137.

Seed, R. 1992. Systematics evolution and distribution of mussels belonging to the genus *Mytilus*: an overview. *Am. Malac. Bull.* **9:** 123–137.

Strausberg, R. L., D. M. Anderson, D. Filpula, M. Finkelman, R. Link, R. McCandliss, S. A. Orndorff, S. L. Strausberg, and T. Wei. 1989. Development of a microbial system for production of mussel adhesive protein. Pp. 453–464 in *Adhesives from Renewable Resources*. ACS Symposium Series 385, R. W. Hemingway and A. H. Conner, eds. American Chemical Society, Washington, DC.

Varvio, S-L., R. K. Koehn, and R. Väinölä. 1988. Evolutionary genetics of the *Mytilus edulis* complex in the North Atlantic region. *Mar. Biol.* **98:** 51–60.

Viard, F., B. Delay, C. Coustau, and F. Renaud. 1994. Evolution of the genetic structure of bivalve cohorts at hybridization sites of the *Mytilus edulis–M. galloprovincialis* complex. *Mar. Biol.* **119:** 535–539.

Waite, J. H. 1983. Evidence for a repeating Dopa and hydroxyproline containing decapeptide in the adhesive protein of *Mytilus edulis*. *J. Biol. Chem.* **258:** 2911–2915.

Waite, J. H. 1992. The formation of mussel byssus: anatomy of a natural manufacturing process. Pp. 27–54 in *Structure, Cellular Synthesis and Assembly of Biopolymers. Results and Problems in Cell Differentiation*, Vol. 19, S. T. Case, ed. Springer-Verlag, Berlin.

Waite J. H., and M. L. Tanzer. 1981. Polyphenolic substance of *Mytilus edulis*. *Science* **212:** 1038–1040.

Waite, J. H., T. J. Housley, and M. L. Tanzer. 1985. Peptide repeats in a mussel glue protein: theme and variations. *Biochemistry* **24:** 5010–5014.

Reference: *Biol. Bull.* **189**: 376–380. (December, 1995)

Flow Cytometric Analysis of Molt-Related Changes in Hemocyte Type in Male and Female *Penaeus japonicus*

TERESA SEQUEIRA[1], MANUEL VILANOVA[2], ALEXANDRE LOBO-DA-CUNHA[3], LUÍS BALDAIA[1], AND MÁRIO ARALA-CHAVES[2]

[1]*Laboratory of General Physiology,* [2]*Laboratory of Immunology,* [3]*Laboratory of Cellular Biology of the "Instituto de Ciências Biomédicas Abel Salazar," Porto, Portugal*

Abstract. Hemocyte cell suspensions obtained from male and female *Penaeus japonicus* were individually analyzed by flow cytometry through forward and side light-scatter parameters. The hemocyte cell suspensions were further characterized after cell sorting. This type of cell analysis has several advantages over microscopy techniques. After staining with phenoloxidase and peroxidase, the hemocytes were classified into the three classic categories of hyaline, semigranular, and granular cells. Significant cyclic differences were detected among the molting stages in both sexes. The hyaline cell population was predominant before and soon after the molt, decreasing over the intermolt. This decrease was, however, more prolonged in females. Thus, the hyaline cell population was dominant in stages B, D0, and D1 in males and only in stages B and D1 in females. Semigranular cells became predominant in females during the D0 stage.

Introduction

Most crustaceans molt throughout their lifetimes, and the periodic replacement of the cuticle is intrinsically linked with their physiology. Although their exoskeleton forms a structural and chemical barrier to parasites, they still need an efficient internal immune system to deal with microorganisms that might enter the hemocoel during ecdysis or through wounds, alimentary tract, or gills. This defense is largely based on the activities of the hemocytes (Söderhäll and Cerenius, 1992). Three types of circulating hemocytes can be distinguished on the basis of morphological criteria and different staining techniques (Bauchau, 1981), and were recently found to have different functions (Söderhäll *et al.*, 1990; Barracco *et al.*, 1991). It is known that hemocytes are affected by microorganisms (De Backer, 1961; Bang, 1971), but few data are available on hemocyte kinetics, particularly throughout the molt cycle (Bauchau and Plaquet, 1973; Tsing *et al.*, 1989). Moreover, the available morphological descriptions are not completely satisfactory because they are based on fixed cells or cells attached to an artificial substrate, resulting in a high percentage of unclassifiable cells.

Flow cytometry is a powerful method of cell analysis because quantitative multiparameter measurements on statistically large numbers of individual cells can be made without the necessity to pool cells from different individuals. Moreover, flow cytometry yields a large number of selected cells in a relatively short time. Furthermore, automation avoids much of the subjectivity inherent in microscopy. Therefore, flow cytometric analysis has been used in invertebrates to detect the DNA content evolution in nematodes (Hoshino *et al.*, 1991), molluscs (Elston *et al.*, 1990; Gerard *et al.*, 1994), insects (Marescalchi *et al.*, 1990), and insect cell lines (Odier *et al.*, 1993). This method has also been used to evaluate hemocyte proliferation upon antigenic stimulation in cockroaches (Ryan and Karp, 1993) and to investigate feeding behavior in molluscs through measurements of plankton cell size (Baldwin, 1991).

In this study, we used flow cytometry to analyze the hemocyte kinetics of a cultured shrimp, *Penaeus japonicus,* throughout its molt cycle.

Received 25 April 1995; accepted 21 September 1995.

Address for correspondence: Prof. Mário Arala-Chaves, Laboratory of Immunology, Instituto de Ciências Biomédicas Abel Salazar, Largo Prof. Abel Salazar, 2, 4 050 Porto, Portugal.

Abbreviations. FSC, forward scatter; SSC, side scatter; H, hyaline; SG, semigranular; G, granular; proPO, prophenoloxidase activating system.

Materials and Methods

Shrimps

Penaeid shrimp for this study were bred in Eurodaqua, Algarve, Portugal. Males (71 animals, 15–25 *g*) and females (83 animals, 20–30 *g*) of *Penaeus japonicus* were maintained in a closed system tank at 12-h light/12-h dark, 3.5% salinity, and 20° ± 2°C and were fed a mixture of fresh mussels and squid three times a week. All shrimp were acclimated at least 1 month prior to use. The molting stages were determined according to Smith and Dall (1990).

Collection of hemolymph and preparation of cell suspensions

From each individual, 0.1–0.3 ml of hemolymph was collected by insertion of a needle syringe into the pericardial cavity. The hemolymph was directly withdrawn into the syringe containing 0.1 ml of anticoagulant buffer 0.2 *M* N-ethylmaleimide in 3% NaCl at 4°C (Martin *et al.*, 1991). Shrimp were bled at the same time of day to avoid possible variations, caused by endogenous rhythm, in the hemocyte populations. For cell size and density analyses, the hemolymph was mixed with 1 ml of 3.5% NaCl. Cells were washed (spun down at 167 × *g* for 10 min) and resuspended in 3.5% NaCl supplemented with 5% fetal calf serum. For cytochemistry, the hemolymph was drawn into a syringe containing 0.5 ml of 1% glutaraldehyde, 1% saccharose in sodium cacodylate buffer (0.2 *M*, pH 7.0). The cells were fixed for 15 min at 4°C, washed once in the cacodylate buffer and twice in the Tris-HCl buffer (0.1 *M*, pH 7.0) at 167 × *g* for 10 min.

Flow cytometry and sorting

Side- and forward-scatter parameters (SSC and FSC) were used for determination of cell granularity and cell size, respectively. SSC and FSC analyses were conducted in a FACScan analyzer (Becton-Dickinson, Mountain View, CA) with a Hewlett Packard computer (HP900) equipped with the LYSYS II analysis program (Becton Dickinson). As cells pass through the focused laser beam, light is scattered in all directions. The amount of light scattered at narrow angles to the axis (FSC parameter) of the laser beam is proportional to the cell size. The laser light scattered at right angles (SSC parameter) relates to the granularity or interior structure of the cell. Dead cells were excluded by propidium iodide (PI) incorporation. PI is a small molecule that binds to nucleic acids; it is very effectively excluded by cells with intact cell membranes, but dead cells become strongly fluorescent and thus are easily distinguished. At least 10,000 cells per sample were always analyzed. Cell sorting was performed in a FACSsort cell sorter (Becton-Dickinson). About 50,000 cells of each population were analyzed with the LYSYS II program.

Hemocyte cytochemistry

The presence of the prophenoloxidase system (proPO) in the hemocytes was determined by the method of Hose *et al.* (1987), incubating the cells in L-dopa (dihydroxyphenylalanine, 1 mg/ml in phosphate buffer 0.1 *M*, pH 7.4) for 16 h at room temperature and then examining them by light microscopy. The hemocyte peroxidase activity was determined by the method of Fahimi (1979). Thus the hemocytes were incubated for 3 h at 30°C in DAB (3,3-diaminobenzidine tetrahydrochloride in Tris-HCl buffer 0.1 *M*, pH 7.0) with 0.003% H_2O_2. The cells were examined by light microscopy. Control incubations were performed with 0.01 *M* sodium azide and 0.05 *M* triazol.

Results

Identification of hemocyte cell populations by flow cytometry

As shown in Figure 1, three hemocyte cell populations can be identified in individual male and female *P. japonicus* when FSC and SSC parameters are used to indicate different cell size and granularity. Hemocytes were analyzed during stages B, C, D0, and D1. After sorting and cytochemically staining each population and analyzing at least 150 cells per sample, it was possible to identify the three basic crustacean cell types. The cell population with low SSC and FSC parameters was considered to be of the hyaline (H) cell type because 98% ± 2% of these cells were both proPO and peroxidase negative (Fig. 2a, b). The cell population with the higher FSC and usually with an intermediate SSC parameter was considered to be semigranular (SG) because the cells were 92% ± 3% proPO positive and 85% ± 4% peroxidase negative (Fig. 2c, d). The cell population with the higher SSC and with FSC similar to H cells was considered to be of the granular (G) cell type. Indeed, strong phenoloxidase activity was detected in this cell population, which was 96% ± 4% positive for proPO and 83% ± 7% positive for peroxidase. Peroxidase activity was confined to the granules and was observed only in these cells (Fig. 2d, e). Furthermore, the intensity of this reaction could be decreased by incubation in sodium azide or triazole, as was reported by Lanz *et al.* (1993) (data not shown).

Changes in relative percentages of H, SG, and G cells during the molting cycle

As shown in Figure 3 and Table I, marked molt-related changes of the pool size of the three hemocyte cell pop-

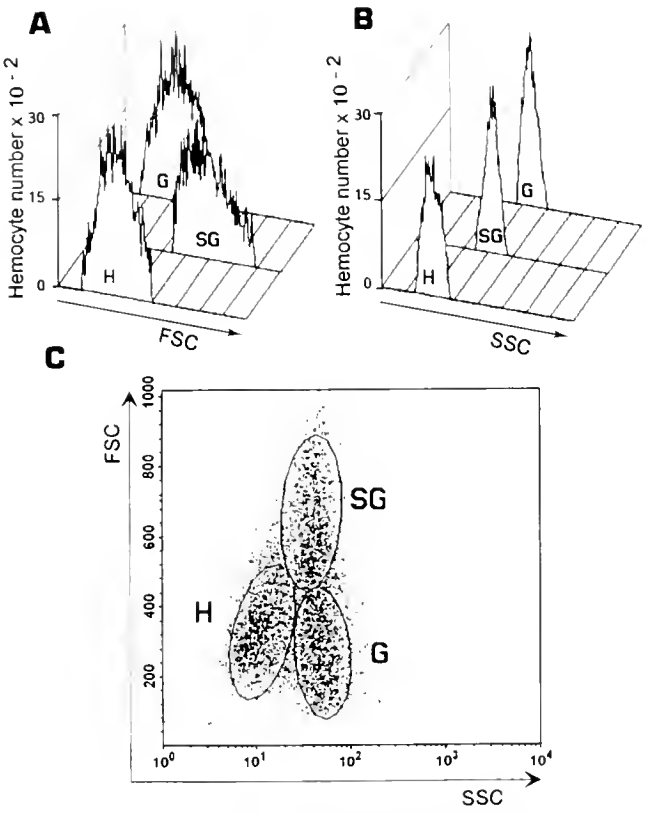

Figure 1. An example of flow cytometric analysis of fresh circulating hemocytes from *Penaeus japonicus* analyzed by forward scatter (FSC), indicating cell size; and side scatter (SSC), indicating cell granularity and structure. Frequency histograms of FSC (A), SSC (B), and a dot plot of both parameters (C) are shown. Hyaline, semigranular, and granular cell populations are designated H, SG, and G, respectively.

ulations were observed in both female and male *P. japonicus*. The patterns of distribution of the H, SG, and G cell populations are identical in both sexes during molt stages B and D1. The H cells are the most abundant (40%–44%), followed by the SG cells (31%–32%) with the G cells lowest (25%–29%). However, the percentages underwent a drastic change from stages B to C in cell type H, SG, and G in females, and in H and G cell types in males. These changes are still present over the D0 stage, but the pattern returned to that found in stage B, near the end of the cycle (stage D1). These intermolting changes, involving a decrease in the percentage of H cells and a subsequent increase in the percentages of SG and G cells, are more marked and more prolonged in females. Thus, the pattern of cell distribution observed in stage D0 is more similar to that observed in stage B in males than that in females. Moreover, the percentage of SG and of G cells has increased slightly from stage B to C to the same number as the H cells in females. In contrast, only the G cell population is increased slightly during the intermolting stage in males, and the number of SG cells is constant over the molting and intermolting stages.

Discussion

These flow cytometric results are in agreement with the general view that three circulating hemocyte populations are present in most crustaceans (Bauchau, 1981). Thus one of the three sorted cell populations totally lacked proPO and was composed of the smallest cells. The features of this cell population fit the H cell category described on the basis of microscopic techniques (Bauchau, 1981; Söderhäll and Smith, 1983; Lanz *et al.*, 1993). Phenoloxidase activity was present in the other two cell populations.

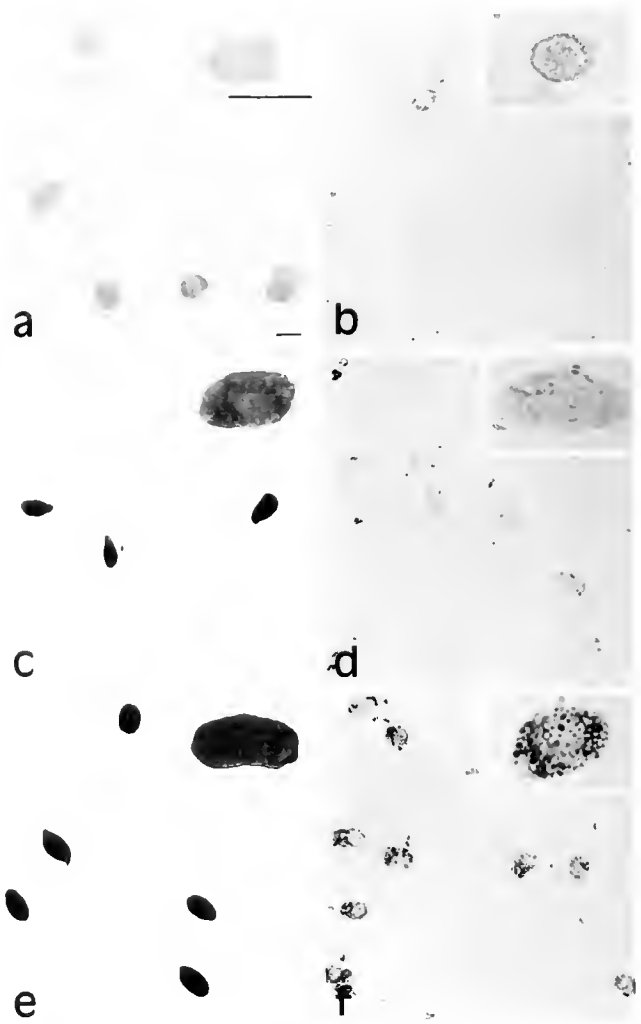

Figure 2. Light microscopy of fixed sorted cell populations stained with proPO (a, c, e) and with peroxidase (b, d, f) revealing hyaline (H) cells, proPO and peroxidase negative (a, b); semigranular (SG) cells, proPO positive and peroxidase negative (c, d); granular (G) cells, proPO and peroxidase positive (e, f). Bar = 10 μm.

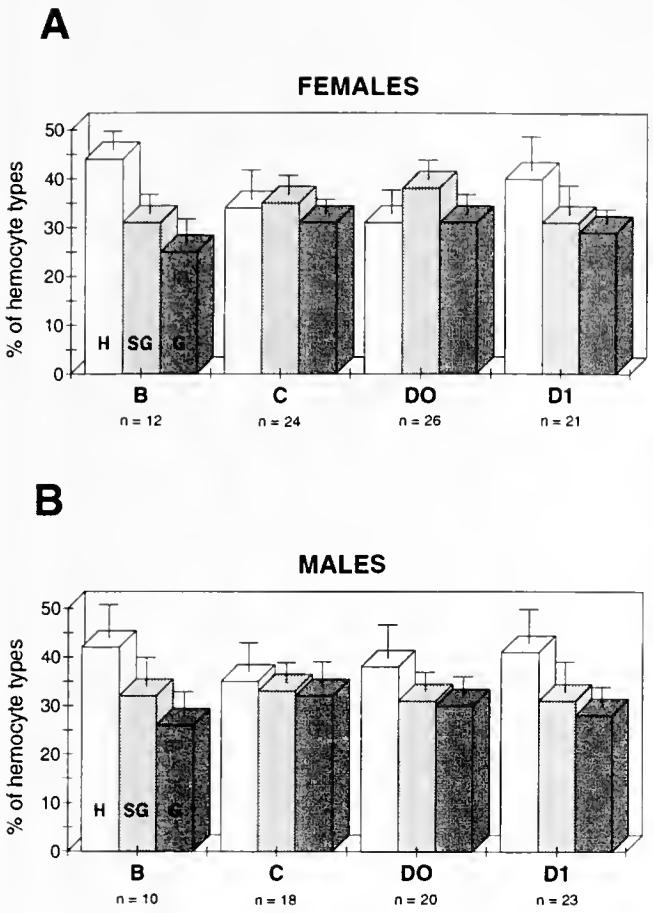

Figure 3. Frequencies of hyaline (H), semigranular (SG), and granular (G) hemocyte cell populations found in *Penaeus japonicus* hemolymph at the indicated stages of the molting cycle in females (A) and males (B). Analyses have been performed with 10,000 cells from each animal; *n* indicates the number of animals used for each value, which is presented as the mean and 1 standard deviation.

Cells of one of these populations were classified as G cells because their peroxidase activity was like that previously observed in similar cells in *Procambarus clarki* (Lanz *et al.*, 1993). When examined by light microscopy, the G cells appear slightly larger than the SG cells, but our flow cytometric results indicate that this may not be the case. This discrepancy might result from analyzing fresh cell suspensions instead of the fixed hemocyte smears used in light microscopy.

This study provides some evidence that the hemocyte cell populations of *P. japonicus* exhibit sex-related variations associated with the molt cycle. In both sexes, the relative percentages of H, SG, and G cells are identical after (stage B) and before (stage D1) ecdysis. Similar results were reported by Bauchau and Plaquet (1973). However, that study, which relied on morphological observations of hemocyte smears, was not directly comparable because SG and G cells could not be identified and were thus counted together, and because the samples were not identified by sex. More recently, Tsing *et al.* (1989) reported that no significant changes of the hemocyte cell populations occurred in *P. japonicus* during the molting stages. However, this study, like the one by Bauchau and Plaquet (1973), pooled male and female samples and was based on smear observations; furthermore, more than 50% of the hemocytes could not be identified. It seems, then, that flow cytometric analysis is a better and more reliable method for studying hemocyte variations than is the traditional technique of morphological observation of smears (Bauchau and Plaquet, 1973; Tsing *et al.*, 1989).

Molt-related changes in hemocyte populations were also demonstrated in insects (Crossley, 1965; Jones, 1967; Hinks and Arnold, 1977). The information about the role of molting hormones in these animals is not yet fully understood, but 20-hydroxyecdysone is known to induce a significant increase in the percentage of circulating phagocytic cells in *Calliphora erythrocephala* (Crossley, 1968). Although insects have somewhat different hemocyte types, the SG and G hemocytes, which may be phagocytic in crustaceans (Hose *et al.*, 1990), also increased in *P. japonicus* coincidentally with elevated ecdysteroid titers described in several crustaceans (Baldaia *et al.*, 1984; Roudy-Cuzin *et al.*, 1989). Tsing *et al.* (1989) also observed an increase in total hemocyte count during these molt stages. Ecdysteroid titers are higher and increase progressively from stages C to D1 in females. The rise of this hormone is considerably smaller in males and it is confined to the D0 stage (Baldaia *et al.*, 1984). Quanti-

Table I

Abundance of hemocyte types throughout the molting cycle of Penaeus japonicus

	H	SG	G
Females	B** > C = D0** < D1 = B	D0* > C* > B = D1	C = D0* > B = D1
Males	B* > C = D0 = D1 = B	B = C = D0 = D1	C = D0* > B = D1

Statistical analysis by paired Student's *t* test of the differences found in the hemocyte cell populations throughout the indicated molting stages. Differences are classified as nonsignificant at $P > 0.05$ (=); significant at $P < 0.05$ (*); and highly significant at $P < 0.01$ (**).

tative differences in ecdysteroids were also reported between the two sexes (Baldaia *et al.*, 1984; Roudy-Cuzin *et al.*, 1989); these may explain the sex-related differences reported here.

Flow cytometry is standardly used in mammalian hematology because it has large advantages over light microscopy. The present report indicates that this tool can also be used advantageously in the study of invertebrate cells such as hemocyte populations. In the future, such study may not only focus on cell size and granularity, but may also include more detailed analysis—for example, the detection of special cell markers using immunofluorescence-specific antibodies or the investigation of cell activation under various immunological stimuli.

Acknowledgments

Teresa Sequeira was supported by a grant from Junta Nacional de Investigação Científica e Tecnológica, Portugal.

Literature Cited

Baldaia, L., P. Porcheron, J. Coimbra, and P. Cassier. 1984. Ecdysteroids in the shrimp *Palaemon serratus*: relation with molt cycle. *Gen. Comp. Endocrinol.* **55:** 437–443.

Baldwin, B. S. 1991. Ingestion of natural plankton by oyster larvae: the relative importance of different cell size fractions. *Am. Zool.* **31:** 7A.

Bang, F. B. 1971. Transmissible disease, probably viral in origin, affecting the amoebocytes of the European shore crab *Carcinus maenas*. *Infect. Immun.* **3:** 617–623.

Barracco, M. A., B. Duvic, and K. Söderhäll. 1991. The β-1,3-glucan–binding protein from the crayfish, *Pacifastacus leniusculus* when reacted with a β-1,3-glucan, induces spreading and degranulation of crayfish granular cells. *Cell Tissue Res.* **266:** 491–497.

Bauchau, A. G., and J. C. Plaquet. 1973. Variation du nombre des hémocytes chez les crustacés brachyoures. *Crustaceana* **24:** 215–223.

Bauchau, A. G. 1981. Crustaceans. Pp. 386–420 in *Invertebrate Blood Cells*. Vol. 2. Academic Press, New York.

Crossley, A. C. 1965. Transformations in the abdominal muscles of the blue blow-fly *Calliphora erythrocephala* (Meig) during metamorphosis. *J. Embryol. Exp. Morphol.* **14:** 375–398.

Crossley, A. C. 1968. The fine-structure and mechanism of break down of larval intersegmental muscles in the blowfly *Calliphora erythrocephala*. *J. Insect Physiol.* **14:** 1389–1407.

De Backer, J. 1961. Rôle joué par les hémocytes dans les réactions tissulaires de défense chez les crustacés. *Ann. Soc. R. Zool. Belgique* **92:** 141–151.

Elston, R. A., A. S. Drum, and S. K. Allen, Jr. 1990. Progressive development of circulating polyploid cells in *Mytilus* with hemic neoplasia. *Dis. Aquat. Org.* **8:** 51–59.

Fahimi, H. D. 1979. An assessment of the DAB methods for cytochemical detection of catalase and peroxidase. *J. Histochem. Cytochem.* **10:** 1365–1366.

Gerard, A., Y. Naciri, J. M. Peignon, C. Ledu, P. Phelipot, C. Noiret, I. Peudenier, and H. Grizel. 1994. Image analysis: a new method for estimation of triploidy in commercial bivalves. *Aquacult. Fish. Manage.* **25:** 697–708.

Hinks, C. F., and J. W. Arnold. 1977. Haematopoiesis in Lepidoptera. II. The role of haematopoietic organs. *Can. J. Zool.* **55:** 1740–1755.

Hose, J. E., G. G. Martin, V. A. Nguyen, J. Lucus, and T. Rosenstein. 1987. Cytochemical features of shrimp hemocytes. *Biol. Bull.* **173:** 178–187.

Hose, J. E., G. G. Martin, and A. S. Gerard. 1990. A decapod classification scheme integrating morphology, cytochemistry, and function. *Biol. Bull.* **178:** 33–45.

Hoshino, K., K. Ohnishi, W. Yoshida, and T. Shinozawa. 1991. Analysis of ploidy in a planarian by flow cytometry. *Turbellarian Biol.* **227:** 175–178.

Jones, J. C. 1967. Effect of repeated haemolymph withdrawals and of ligaturing the head on differential counts of *Rhodnius prolixus* Stal. *J. Insect Physiol.* **13:** 1351–1360.

Lanz, H., V. Tsutsumi, and H. Aréchiga. 1993. Morphological and biochemical characterization of *Procambarus clarki* blood cells. *Dev. Comp. Immunol.* **17:** 389–397.

Marescalchi, O., V. Scali, and M. Zucotti. 1990. Genome size in parental and hybrid species of *Bacillus* (Insecta, Phasmatodea) from southeastern Sicily: A flow cytometric analysis. *Genome* **33:** 789–793.

Martin, G. G., J. E. Hose, S. Omori, C. Chong, T. Hoodbhoy, and N. McKrell. 1991. Localization and roles of coagulogen and transglutaminase in hemolymph coagulation in decapod crustaceans. *Comp. Biochem. Physiol.* **100B:** 517–522.

Odier, F., P. Vago, J. M. Quiot, G. Devauchelle, and J. P. Bureau. 1993. Determination of DNA in densovirus-infected invertebrate cell line by flow cytometry. *J. Invertebr. Pathol.* **62:** 252–256.

Ryan, N. A., and R. D. Karp. 1993. Stimulation of hemocyte proliferation in the American cockroach (*Periplaneta americana*) by the injection of *Enterobacter cloacae*. *J. Insect Physiol.* **39:** 601–608.

Roudy-Cuzin, J., C. Strambi, A. Strambi, and J.-P. Delbecque. 1989. Hemolymph ecdysteroids and molt cycle in males and females of *Siriella armata* M.-Edw. (Crustacea: Mysidacea): possible control by the MI-ME X organ of the eyestalk. *Gen. Comp. Endocrinol.* **74:** 96–109.

Smith, D. M., and W. Dall. 1990. Moult staging in the tiger prawn *Penaeus esculentus*. Second Australian National Prawn Seminar 85–93.

Söderhäll, K., and V. J. Smith. 1983. Separation of the haemocyte populations of *Carcinus maenas* and other marine decapods, and prophenoloxidase distribution. *Dev. Comp. Immunol.* **7:** 229–239.

Söderhäll, K., A. Aspán, and B. Duvic. 1990. The proPO-system and associated proteins; role in cellular communication in arthropods. *Res. Immunol.* **141:** 896–907.

Söderhäll, K., and L. Cerenius. 1992. Crustacean immunity. *Annu. Rev. Fish Dis.* **2:** 3–23.

Tsing, A., J.-M. Arcier, and M. Brehélin. 1989. Hemocytes of penacid and palaemonid shrimps: morphology, cytochemistry, and hemograms. *J. Invertebr. Pathol.* **53:** 64–67.

INDEX

D

E

F

G

H

I

J

K

L

M

N

O

P

Q

R

S

T

U

V

W

Y

Z

CONTENTS